HIGHWAY BRIDGE SUPERSTRUCTURE ENGINEERING

LRFD Approaches to Design and Analysis

Narendra Taly

CRC Press
Taylor & Francis Group

www.EngineeringEBooksPdf.com

Highway Bridge Superstructure Engineering

LRFD Approaches to Design and Analysis

www.EngineeringEBooksPdf.com

Highway Bridge Superstructure Engineering

LRFD Approaches to Design and Analysis

Narendra Taly

CRC Press
Taylor & Francis Group
Boca Raton London New York

CRC Press is an imprint of the
Taylor & Francis Group, an **informa** business

www.EngineeringEBooksPdf.com

CRC Press
Taylor & Francis Group
6000 Broken Sound Parkway NW, Suite 300
Boca Raton, FL 33487-2742

© 2015 by Taylor & Francis Group, LLC
CRC Press is an imprint of Taylor & Francis Group, an Informa business

No claim to original U.S. Government works

Printed on acid-free paper
Version Date: 20140331

International Standard Book Number-13: 978-1-4665-5218-0 (Hardback)

This book contains information obtained from authentic and highly regarded sources. Reasonable efforts have been made to publish reliable data and information, but the author and publisher cannot assume responsibility for the validity of all materials or the consequences of their use. The authors and publishers have attempted to trace the copyright holders of all material reproduced in this publication and apologize to copyright holders if permission to publish in this form has not been obtained. If any copyright material has not been acknowledged please write and let us know so we may rectify in any future reprint.

Except as permitted under U.S. Copyright Law, no part of this book may be reprinted, reproduced, transmitted, or utilized in any form by any electronic, mechanical, or other means, now known or hereafter invented, including photocopying, microfilming, and recording, or in any information storage or retrieval system, without written permission from the publishers.

For permission to photocopy or use material electronically from this work, please access www.copyright.com (http://www.copyright.com/) or contact the Copyright Clearance Center, Inc. (CCC), 222 Rosewood Drive, Danvers, MA 01923, 978-750-8400. CCC is a not-for-profit organization that provides licenses and registration for a variety of users. For organizations that have been granted a photocopy license by the CCC, a separate system of payment has been arranged.

Trademark Notice: Product or corporate names may be trademarks or registered trademarks, and are used only for identification and explanation without intent to infringe.

Library of Congress Cataloging-in-Publication Data

Taly, Narendra.
Highway bridge superstructure engineering : LRFD approaches to design and analysis / author, Narendra Taly.
pages cm
Includes bibliographical references and index.
ISBN 978-1-4665-5218-0 (alk. paper)
1. Bridges--Design and construction. 2. Structural engineering. 3. Load factor design. I. Title.

TG260.T35 2014
624.2'57--dc23 2014011986

Visit the Taylor & Francis Web site at
http://www.taylorandfrancis.com

and the CRC Press Web site at
http://www.crcpress.com

www.EngineeringEBooksPdf.com

To

Trish Taly

For her high-limit states of stress endurance over the years, which made the publication of this book and author's previous books a reality.

And to the memory of my parents, Bhagwan Das and Sundar Bai Taly, who taught me the importance and virtues of academics.

www.EngineeringEBooksPdf.com

www.EngineeringEBooksPdf.com

Contents

Preface xix
Acknowledgments xxiii

Chapter 1 Introduction 1

1.1 Structural Design Philosophies 1
1.2 General Design Concepts 1
1.3 Fundamentals of Structural Design Philosophies 2
1.3.1 Design Philosophies Based on Elastic Behavior: Allowable/Working Stress Design 2
1.3.2 Design Philosophies Based on Inelastic Behavior: Plastic Design Method 3
1.4 Limit States Design Philosophies 8
1.4.1 Concepts of Limit States 8
1.4.1.1 Strength Limit States 9
1.4.1.2 Serviceability Limit States 10
1.4.1.3 Fatigue Limit States 12
1.4.2 Strength Limit States versus Serviceability Limit States 13
1.4.3 Strength Design, Load Factor Design, and Load and Resistance Factor Design 14
1.4.4 Strength Design Philosophy 14
1.4.4.1 Strength Design Concept 14
1.4.4.2 Load Factor Design 15
1.4.4.3 Load and Resistance Factor Design 15
1.5 LRFD Specifications for Highway Bridges 16
1.5.1 Evolution of LRFD Specifications for the Design of Steel Buildings in the United States 16
1.5.2 Evolution of LRFD Specifications for Highway Bridges in the United States 16
1.5.2.1 Why the Change from AASHTO Standard Specifications? 16
1.5.2.2 Why Probability-Based Design Philosophy? 17
1.5.3 Issues and Considerations for the Development of AASHTO LRFD Criteria 18
1.5.4 Probabilistic Basis of AASHTO LRFD Bridge Design Specifications 18
1.5.5 Statistical Nature of Loads and Resistances 19
1.5.5.1 Random Variables, Normal and Lognormal Distributions, and Probability 19
1.5.5.2 Properties and Applications of Normal (Gaussian) Distribution 26
1.5.5.3 Linear Functions of Random Variables: Central Limit Theorem (CLT, Normal Convergence Theorem) 37
1.5.6 Probabilistic Determination of Safety Factors 39
1.5.6.1 Probabilistic Concept of Safety: Limit State Function (Performance Function) 39

www.EngineeringEBooksPdf.com

1.5.6.2 Development of AISC LRFD Criteria 40
1.5.6.3 Development of AASHTO LRFD Criteria 44
1.5.6.4 Calibration Procedure 52
1.5.6.5 Calibration of Load and Resistance Factors 55
1.5.7 AASHTO LRFD Specifications Format of Load and Resistance Relationship 56
1.5.7.1 Loads, Resistance, and Factor of Safety 56
1.6 Differences between Various Design Methods: Summary 63
1.6.1 Difference between the Design Methods Based on the Elastic and Inelastic Material Behavior 63
1.6.2 Difference between Plastic Design, Strength Design, Load Factor Design, and Load and Resistance Factor Design 64
1.7 Historical Review of AASHTO Specifications for Highway Bridges 64
1.8 AASHTO LRFD Highway Bridge Design Specifications and Design Philosophies 65
1.9 AASHTO Interim Specifications 65
1.10 Scope of the AASHTO LRFD Bridge Design Specifications 66
1.11 Commentary to AASHTO LRFD Specifications 67
1.12 General Comments 67
1.A Appendix 68
References 70

Chapter 2 Highway Bridge Superstructure Systems 73

2.1 Introduction 73
2.2 AASHTO LRFD Spec.-Specific Highway Bridge Superstructures 73
2.3 Description and Design Characteristics of Superstructure Systems in Table 2.1 81
2.3.1 RC Deck over Steel Wide Flange Beams of Plate Girders (Type *a*) 81
2.3.2 Spread-Box Beam Superstructure (Type *b*) 83
2.3.3 Open Steel or Precast Concrete Box Superstructure (Type *c*) 83
2.3.4 Cast-in-Place Concrete Multicell Box Girder (Type *d*) 84
2.3.5 Cast-in-Place RC T-Beam Superstructure (Type *e*) 85
2.3.6 Adjacent-Prestressed Concrete Box Superstructure (Type *f*) 85
2.3.7 Adjacent-Prestressed Concrete Box Superstructure with Integral Concrete Deck with or without Transverse Posttensioning (Type *g*) 85
2.3.8 Precast Concrete Channel Sections with Shear Keys and Concrete Overlay (Type *h*) 86
2.3.9 Precast Concrete Double-T Girders with Shear Keys, and with or without Transverse Posttensioning and Integral Concrete Deck (Type *i*) 87
2.3.10 Precast Concrete Single-T Girders with Shear Keys, and with or without Transverse Posttensioning and Integral Concrete Deck (Type *j*) 87
2.3.11 RC Deck over Prestressed I-Beams or Bulb-T Girders (Type *k*) 87
2.3.12 Fiber-Reinforced Polymer Highway Superstructure Systems 89
2.4 Diaphragms 91
2.4.1 Definition of a Diaphragm 91
2.4.2 Diaphragms in Building Structures 91

www.EngineeringEBooksPdf.com

2.4.3 Diaphragms in Bridge Superstructures 91
2.4.3.1 ASSHTO Standard Specifications for Diaphragms 92
2.4.3.2 AASHTO LRFD Specifications for Diaphragms and Cross-Frames 93
2.5 Bridge Site and Geometry 94
2.5.1 Bridge Type, Size, and Location 94
2.5.2 Bridge Width 95
2.5.3 Normal and Skewed Bridges 95
2.6 Deflections 97
2.6.1 Historical Review of Deflection Limitations 97
2.6.2 Purpose of Limiting Bridge Deflections 98
2.6.3 Criteria for Live Load Deflections 99
2.6.4 Optional Criteria for Span-to-Depth Ratios 101
2.6.4.1 Optional Deflection Criteria for Constant Depth Superstructures 101
2.6.4.2 Optional Deflection Criteria for Curved Steel Superstructures 102
2.6.5 Deflections Due to Dead Loads 102
2.6.6 Calculation of Live Load Deflections 103
2.7 Consideration of Future Widening 106
2.8 Constructability 106
2.9 Bridge Esthetics 107
References 107

Chapter 3 Loads on Highway Bridge Structures 109

3.1 Introduction 109
3.2 AASHTO LRFD Highway Bridge Design Philosophy 110
3.2.1 Limit States Concept 110
3.2.2 Loads and Load Designations 114
3.2.3 Load Factors and Load Combinations for Design Loads 114
3.2.4 Selection of Design-Specific Limit States, Load Modifiers, Load Combinations, and Load Factors 120
3.3 Load Factors and Load Combinations for Construction Loads 120
3.3.1 Evaluation at the Strength Limit States 120
3.3.2 Evaluation of Deflection at the Service Limit State 120
3.3.3 Load Factors for Jacking and Posttensioning Forces 121
3.3.3.1 Jacking Forces 121
3.3.3.2 Force for Posttensioning Anchorage Zones 121
3.4 Components of a Highway Bridge Structure 121
3.5 Dead Loads on a Highway Bridge Superstructure 122
3.5.1 General 122
3.5.2 Dead Load Due to Deck Slab 124
3.5.3 Dead Load Due to Girders 124
3.6 Construction Loads 130
3.7 Live Loads on Highway Bridge Superstructures 130
3.7.1 Historical Perspective 130
3.7.2 Development of AASHTO Standard Specifications Live Load Model 131

www.EngineeringEBooksPdf.com

3.7.3 Description of AASHTO LRFD Notional Live Load Model 135
3.7.4 Understanding the Development of AASHTO LRFD Notional Live Load Model 139
3.7.4.1 Concept of Notional Load: What Is It?..... 139
3.7.4.2 Commercial Vehicular Loads 140
3.7.4.3 Development of AASHTO LRFD Notional Live Load: A Brief History 146
3.7.4.4 Permit Loads 156
3.7.5 Application of Design Vehicular Live Loads on Bridge Superstructures 158
3.7.5.1 Position of Live Load on Simple Spans 158
3.7.5.2 Position of Vehicular Live Loads on Continuous Spans 160
3.7.6 Bending Moments and Shears Due to Moving Loads on Simple Spans 160
3.7.6.1 Bending Moments 160
3.7.6.2 Influence Lines for Absolute Maximum Bending Moments in Simple Spans 161
3.7.7 Generalized Expressions for Maximum Moment and Maximum Shear at a Section in a Simple Span Due to HS20 Truck..... 175
3.7.7.1 Maximum Moment and Shear: HS20 Truck Moving from Left to Right 175
3.7.7.2 Maximum Moment and Shear: HS20 Truck Moving from Right to Left 176
3.7.8 Absolute Maximum Bending Moment in Spans Due to Loads Other than AASHTO HS20 Truck 178
3.7.9 Governing Span Lengths for Maximum Live Load Shear in Simple Spans Due to AASHTO LRFD Live Load: HS20 Truck and Tandem 183
3.7.10 Influence Lines for Beams with Other Support Conditions and for Other Types of Structures 184
3.8 Dynamic Effects of Vehicular Live Load 185
3.8.1 General Considerations for Dynamic Force Effects: Dynamic Load Allowance 185
3.8.2 Research on Quantification of Dynamic Load Effects 185
3.8.3 AASHTO LRFD Specifications for Dynamic Load Allowance..... 193
3.8.4 Exceptions to Application of Dynamic Load Effects 197
3.9 Fatigue Loading 198
3.9.1 Fatigue Phenomenon 198
3.9.2 Magnitude and Configuration of Live Load for Fatigue Considerations 198
3.9.3 Formulas for Maximum Moment and Shear for Fatigue Limit State Loading 199
3.9.3.1 Maximum Moment for Fatigue Limit State 199
3.9.3.2 Maximum Shear for Fatigue Limit State..... 202
3.9.4 Frequency of Loading for Fatigue Design Considerations..... 206
3.9.5 Application of $ADTT_{SL}$ for Determination of Fatigue Limit State 209
3.10 Pedestrian Loads 210
3.10.1 Significance of Pedestrian Loading 210
3.10.2 Live Load Due to Sidewalks on Vehicular Bridges 210

www.EngineeringEBooksPdf.com

3.10.3 Live Load on Pedestrian and/or Bicycle Bridges 210
3.11 Application of Design Live Loads on a Bridge Superstructure 212
3.11.1 Design Live Loads for Longitudinal Beams 212
3.11.2 Live Load for Deflection Considerations 214
3.11.3 Design Live Load for Decks, Deck Systems, and Top Slabs of Box Culverts 214
3.11.4 Live Load on Deck Overhangs 215
3.11.5 Force Effects Due to Live Load in Multiple Traffic Lanes: Multiple Presence of Live Load 216
3.12 Design Live Loads in Longitudinal Girders Supporting Bridge Decks 218
3.13 Envelopes for Moment and Shear Values 218
3.14 Tire Contact Area 235
3.14.1 Point Load versus Distributed Load 235
3.14.2 AASHTO LRFD Specifications for Tire Contact Area 245
3.15 Rail Transit Loads 247
3.16 Centrifugal Force (CE) 247
3.17 Braking Force (BR) 251
3.17.1 Magnitude of Braking Force 251
3.17.2 Application of Braking Forces on a Bridge 254
3.18 Vehicular Collision Force (*CT*) 255
3.18.1 Nature, Causes, and Magnitude of Collision Forces 255
3.18.2 Protection of Structures from Vehicular Collision Force, *CT* 256
3.18.3 Protection of Structures from Vessel Collision Force, *CV* 256
3.19 Ice and Snow Loads 259
3.19.1 Ice Loads: General 259
3.19.2 Dynamic Ice Forces on Piers 260
3.19.2.1 Ice Floes and Modes of Failures 260
3.19.2.2 Effective Ice Crushing Strength 260
3.19.2.3 Horizontal Force from Flexing of Moving Ice 261
3.19.2.4 Influence of Directionality of Ice Forces and the Pier Nose Profile on the Magnitude of Forces Acting on the Pier 262
3.19.3 Snow Loads 263
3.20 Wind Loads (*WL* and *WS*) 264
3.20.1 Wind Effects on Structures 264
3.20.2 Magnitude of Horizontal Wind Pressure 265
3.20.3 Variation in Wind Velocity with Height 266
3.20.4 Estimation of Wind Loads 268
3.20.5 Wind Pressure on Structure (*WS*) 270
3.20.6 Wind Pressure on Live Load (*WL*) 271
3.21 Earthquake Forces (EQ) 272
3.21.1 Evolution of Earthquake-Resistant Design Provisions in AASHTO Bridge Design Specifications 272
3.21.2 Philosophy for Design Basis Earthquake Forces 273
3.21.3 Determination of Seismic Forces: Fundamental Concepts 275
3.21.4 AASHTO LRFD Specifications Provisions for Seismic Design of Bridges 277
3.21.4.1 Seismic Design Philosophy 277
3.21.4.2 Site Class Characterization 278
3.21.4.3 Determination of Elastic Seismic Response Coefficient, C_{sm} 278

www.EngineeringEBooksPdf.com

3.21.4.4 Determination of Acceleration Coefficients 280
3.21.4.5 Design Basis Earthquake 284
3.21.4.6 Seismic Hazard Characterization: Design Response Spectrum 285
3.21.4.7 Operational Classification 293
3.21.4.8 Response Modification Factors 294
3.21.5 Application of Earthquake Forces for Design of Structural Members and Connections in Highway Bridges 296
3.21.6 Determination of Design Basis Earthquake Forces 298
3.21.6.1 General 298
3.21.6.2 Single-Span Bridges 298
3.21.6.3 Calculation of Design Connection Forces for Bridges in Various Seismic Zones 300
3.21.7 Determination of Fundamental Period, *T* 305
3.21.7.1 Single-Mode Spectral Analysis Method (SM): Procedure 1 305
3.21.7.2 Other Methods of Analysis 308
3.22 Earth Pressure: *EH, ES, LS,* and *DD* 308
3.22.1 General 308
3.22.2 Determination of Earth Pressure 308
3.22.2.1 Basic Concepts of Earth Pressure 309
3.22.3 Theories and Calculations of Earth Pressures 311
3.22.3.1 Theories of Earth Pressures 311
3.22.3.2 Calculations of Coefficients of Earth Pressures 312
3.22.4 Equivalent-Fluid Method of Estimating Rankine's Lateral Earth Pressures 313
3.22.5 Selection of Backfill Material 313
3.22.6 Effects of Surcharge Loads: *ES* and *LS* 316
3.22.6.1 Nature of Surcharge Loads 316
3.22.6.2 Uniform Surcharge Loads (*ES*) 316
3.22.6.3 Point, Line, and Strip Loads (*ES*) 317
3.22.6.4 Effects of Live Load Surcharge Loads: *LS* 319
3.22.6.5 Downdrag: *DD* 324
3.22.7 Seismic Earth Pressure 324
3.23 Force Effects Due to Superimposed Deformations: *TU*, *TG*, *SH*, *CR*, *SE*, and *PS* 325
3.23.1 General 325
3.23.2 Temperature-Induced Forces 325
3.23.3 Temperature-Induced Forces Due to Uniform Temperature 325
3.23.4 AASHTO LRFD Provisions for Design Unidirectional Thermal Movements 327
3.23.5 Forces Induced by Temperature Gradient 327
3.23.5.1 Nature of Heat Flow Problem: *Thermal Gradient* 327
3.23.5.2 Effect of Nonlinear Temperature Variation 334
3.23.5.3 AASHTO LRFD Provisions for Thermal Gradient Analysis 335
3.24 Miscellaneous Forces for Design Considerations 338
3.25 Friction Forces: *FR* 338
3.A Appendix 339
References 346

www.EngineeringEBooksPdf.com

Chapter 4 Structural Analysis of Highway Bridge Superstructures 353

4.1 Introduction 353
4.2 Load Path in Bridge Structures 354
4.3 Analysis for Dead Load on Bridge Superstructures 356
4.4 Methods of Structural Analysis for Live Load on Bridge Superstructures ... 357
4.5 Approximate Analysis Methods for Live Loads: The Distribution Factor Concept 358
4.6 Considerations for Live Load Distribution Factors for Common Types of Bridge Superstructures 360
4.6.1 General Approach 360
4.6.2 Lever Rule 360
4.6.3 Applicability Criteria for LRFD Live Load Distribution Factors 363
4.6.3.1 Superstructures with Constant Deck Width and Parallel Girders 363
4.6.3.2 Superstructures with Varying Deck Width and Splayed Girders 364
4.6.4 Influence of Multiple Loaded Lanes 365
4.6.4.1 Number of Design or Traffic Lanes on a Bridge 365
4.6.4.2 Influence of Multiple Design/Traffic Lanes on Girders Supporting the Deck 365
4.6.4.3 Position of Wheel Loads on Bridge Deck with Respect to Girders 366
4.7 Calculations of Distribution Factors for Beams/Girders of Typical Superstructures 366
4.7.1 Formulas for Distribution Factors 366
4.7.2 Distribution Factors for Interior Girders 366
4.7.2.1 Bending Moment 366
4.7.2.2 Live Load Distribution Factors for Shear 375
4.7.3 Live Load Distribution Factors for Exterior Girders 375
4.7.3.1 Influence of Diaphragms on Distribution Factors for Exterior Girders 375
4.7.3.2 Distribution Factors for Bending Moment 375
4.7.3.3 Distribution Factors for Shear 377
4.8 Special Analysis for Distribution Factors for Bending Moments and Shears in Exterior Girders 379
4.9 Correction Factors for Bridge Skew 380
4.10 Distribution Factors for Fatigue Limit State 382
4.11 Distribution Factors for Deflection Limit State 382
4.12 Illustrative Examples: Distribution Factors for Bending Moment and Shear 382
4.13 Application of Live Distribution Factors for Design Purposes 417
4.14 Distribution Factors for Special Loads with Other Traffic Loads 421
4.15 Live Load Distribution Factors for Bending Moments and Shear in Transverse Floor Beams 421
4.16 Methods of Refined Analysis 421
4.17 Distribution of Lateral Loads in Multibeam Bridges 422
4.17.1 General 422
4.17.2 Lateral Wind Load Distribution in Multibeam Bridges 422
4.17.2.1 Load Path for Lateral Wind Load 422
4.17.2.2 Determination of Forces and Bending Moments Due to Lateral Wind Load 423

www.EngineeringEBooksPdf.com

4.17.3 Seismic Load Distribution in Multibeam Bridges 424
4.17.3.1 Load Path for Earthquake Forces in Multibeam Bridges 424
4.17.3.2 Design Criteria 425
4.17.3.3 Earthquake Load Distribution 425
4.18 Analysis of Concrete Slabs and Slab-Type Bridges for LRFD Live Loads 425
4.18.1 General 425
4.18.1.1 Slab-Type Bridges 426
4.18.1.2 Concrete Decks 426
4.18.2 Analysis of Slab-Type Bridges 426
4.18.2.1 General 426
4.18.2.2 LRFD Provisions for the Analysis of Slab-Type Bridges: The Approximate Strip Model 430
4.18.3 Analysis of Deck Systems 433
4.18.3.1 General 433
4.18.3.2 Calculation of Force Effects 433
4.18.4 Deflection Analysis of Slab Bridges 434
4.18.4.1 General 434
4.18.4.2 Influence of Cracking of Concrete Sections under Service Loads 435
4.18.4.3 Long-Term Deflections 435
4.A Appendix 436
References 446

Chapter 5 Concrete Bridges 449

5.1 Introduction 449
5.2 Concrete Bridges and Aesthetics 449
5.3 Corrosion of Concrete Bridges 452
5.3.1 Reinforcing Bar Corrosion Problem 452
5.3.2 Mitigation of Corrosion Problem 453
5.3.2.1 Treated Reinforcing Steel 453
5.3.2.2 Concrete Cover for Reinforcing Steel 453
5.3.3 General Protective Requirements 454
5.4 Material Properties 455
5.4.1 Concrete for Bridge Construction 455
5.4.1.1 General 455
5.4.1.2 Normal-Weight and Structural Lightweight Concrete 456
5.4.1.3 Coefficient or Thermal Expansion 458
5.4.1.4 Shrinkage and Creep 458
5.4.1.5 Modulus of Elasticity of Concrete 459
5.4.1.6 Modulus of Rupture 461
5.4.2 High-Strength Concrete and Bridge Span Capabilities 462
5.4.3 Reinforcing Steel (Art. 5.4.3) 462
5.4.3.1 General 462
5.4.3.2 Reinforcing Bars 464
5.4.4 Prestressing Steel: Art. 5.4.4 467
5.4.4.1 General 467
5.4.4.2 Modulus of Elasticity of Prestressing Steels: Art. 5.4.4.2 469
5.4.4.3 Relaxation of Steel 470

www.EngineeringEBooksPdf.com

5.4.5 Strength Limit State ... 471
5.4.5.1 General ... 471
5.4.5.2 Resistance Factors (ϕ-factors) ... 471
5.5 Design Procedures for Flexure in Section 5 of LRFD Specifications ... 473
5.5.1 Assumption for Service and Fatigue Limit States: Art. 5.7.1 ... 476
5.5.2 Assumptions for Strength and Extreme-Event Limit States ... 476
5.5.2.1 General ... 476
5.5.2.2 Rectangular Stress Distribution: Art. 5.7.2.2 ... 478
5.5.3 Flexural Members ... 479
5.5.3.1 General ... 479
5.5.3.2 Nominal Flexural Resistance of Concrete Members with Nonprestressed Reinforcement ... 479
5.5.3.3 Nominal Flexural Resistance of Prestressed Concrete Members ... 481
5.5.3.4 Flexural Resistance: Art. 5.7.3.2 ... 484
5.6 Limits of Reinforcement: Art. 5.7.3.3 ... 485
5.6.1 Provisions for Maximum Reinforcement ... 485
5.6.2 Provisions for Minimum Reinforcement: Art. 5.7.3.3.2 ... 486
5.7 Control of Cracking by Distribution of Reinforcement: Art. 5.7.3.4 ... 487
5.8 Service Limit State ... 488
5.8.1 Service Load Analysis of Reinforced Concrete Sections ... 488
5.8.2 Deformations: Art. 5.7.3.6 ... 490
5.8.2.1 General Requirements ... 490
5.8.3 Deflection and Camber ... 490
5.9 Fatigue Limit State ... 491
5.9.1 General ... 491
5.9.2 Stress Limits for Stresses Due to Fatigue ... 492
5.9.2.1 Reinforcing Bars ... 492
5.9.2.2 Prestressing Tendons ... 492
5.9.2.3 Welded or Mechanical Splices ... 492
5.10 Shear ... 493
5.10.1 General ... 493
5.10.2 Check for Shear near Supports ... 494
5.10.3 Nominal Shear Resistance of a Concrete Section ... 494
5.10.3.1 General ... 494
5.10.3.2 LRFD Procedures for Designing for Shear ... 495
5.10.4 Reinforcement for Shear Resistance: Regions Requiring Transverse Reinforcement ... 497
5.10.5 Minimum Transverse Reinforcement ... 498
5.10.6 Maximum Spacing of Transverse Reinforcement ... 499
5.10.7 Shear Stress on Concrete ... 499
5.10.8 Tensile Capacity of Longitudinal Reinforcement: Art. 5.8.3.5 ... 500
5.11 Estimating the Area of Required Nonprestressed Tensile Reinforcement in Concrete Sections ... 500
5.12 Slab-Type Concrete Bridges and Concrete Decks ... 501
5.13 Concrete Decks ... 503
5.13.1 General ... 503
5.13.2 Minimum Depth and Cover Requirements ... 503
5.13.3 Composite Action between Decks and Supporting Beams ... 505
5.13.4 Skewed Decks ... 507

www.EngineeringEBooksPdf.com

5.13.5 Edge Support Requirements 507
5.13.6 Design of Cantilever Slabs 507
5.13.7 Design Procedures for Deck Slabs 508
5.13.7.1 Empirical Design Method 508
5.13.7.2 Traditional Design Method 513
5.13.8 Empirical Design versus Traditional Design 513
5.14 Design Examples 514
5.15 Design of Reinforced Concrete T-Beam Superstructures 539
5.16 Design of Deck Overhang and Barrier Walls 592
5.16.1 General 592
5.16.2 Traffic Railing Design Forces and Design Criteria 592
5.16.3 Yield Line Analysis for Concrete Traffic Barriers or Parapets 595
5.17 Slab-Precast, Prestressed Concrete Bridges 611
5.17.1 Introduction 611
5.17.2 Characteristics of Prestressed Concrete Bridges 612
5.17.2.1 Use of High-Strength Concrete 612
5.17.2.2 Shapes, Sizes, and Uses of Precast, Prestressed Concrete Girders 612
5.17.3 Concepts of Prestressing 617
5.17.4 Pretensioned and Posttensioned Girders 627
5.17.5 Layout and Location of the Center of Gravity of Multiple Strands in a Prestressed Girder 627
5.17.6 Design of a Prestressed Concrete Girder for a Highway Bridge 630
5.A Appendix 682
References 690

Chapter 6 Slab–Steel Girder Bridges 693

6.1 Introduction 693
6.2 Structural Forms and Characteristics of Steel Bridges 693
6.2.1 Common Forms of Slab–Steel Beam Bridges 693
6.2.2 Orthotropic Steel Bridges 693
6.2.3 Composite Steel Box Girder Bridges 696
6.2.4 Delta Frame Steel Bridges 699
6.3 Corrosion of Steel Bridges 699
6.4 Construction Considerations 702
6.5 Mechanical Properties of Steel for Highway Bridges 703
6.6 Hybrid Steel Girders 704
6.7 Noncomposite and Composite Sections 706
6.7.1 Noncomposite Sections 706
6.7.2 Composite Sections 706
6.7.3 Section Properties of Noncomposite and Composite Sections 706
6.8 Shored and Unshored Construction 707
6.8.1 Sequence of Loading during Construction 707
6.8.2 Shored Construction 707
6.8.3 Unshored Construction 708
6.9 Resistance Factors 708
6.10 Design Provisions for I-Section Flexural Members 709
6.10.1 General 709
6.10.1.1 General Format for LRFD Specifications for Steel Superstructures 709

www.EngineeringEBooksPdf.com

6.10.1.2 Sequence of Loading and Elastic Stresses 714
6.10.1.3 Flange-Strength Reduction Factors 714
6.10.2 Cross-Section Proportion Limits 716
6.10.2.1 Minimum Metal Thickness (LRFD Art. 7.7.3) 716
6.10.2.2 Web Proportion Limits (LRFD 6.10.2.1) 717
6.10.2.3 Flange Proportion (LRFD Art. 6.10.2.2) 717
6.10.3 Constructibility Requirements (LRFD Art. 6.10.3) 718
6.10.3.1 General 718
6.10.3.2 Dead Load Deflection and Camber 719
6.10.3.3 Instability of I-Beams: The Lateral-Torsional-Buckling Phenomenon 719
6.10.3.4 Lateral-Torsional Buckling and Bracing of Beams 721
6.10.3.5 Flange Stresses and Member Bending Moments 721
6.10.3.6 Moment Gradient Modifier, C_b 722
6.10.3.7 Flange Stresses and Member Bending Moments: Critical Stages of Construction 726
6.10.4 Considerations for Service Limit State 729
6.10.4.1 Permanent Deformations 729
6.10.4.2 General 729
6.10.4.3 Flange Stresses 729
6.10.5 Special Fatigue Requirements for Webs 730
6.10.6 Design Requirements for Strength Limit State 731
6.10.6.1 General 731
6.10.6.2 Composite Sections in Positive Flexure 731
6.10.6.3 Composite Sections in Negative Flexure and Noncomposite Sections 732
6.10.7 Flexural Resistance of Composite and Noncomposite Sections in Positive Flexure: Strength Limit State 732
6.10.7.1 Compact Sections in Positive Flexure 732
6.10.7.2 Noncompact Sections 733
6.10.7.3 Ductility Requirements: Art. 6.10.7.3 734
6.10.8 Flexural Resistance: Compact Sections in Negative Flexure and Noncomposite Sections—Strength Limit State 734
6.10.8.1 General Requirements 734
6.10.8.2 Compression Flange Flexural Resistance: Art. 6.10.8.2.1 ... 736
6.10.9 Shear Resistance 739
6.10.9.1 General: Shear Strength of Steel Girders 739
6.10.9.2 Nominal Resistance of Unstiffened Webs 741
6.10.9.3 Nominal Resistance of Stiffened Webs: Interior Panels 743
6.10.9.4 Shear Resistance of End Panels 743
6.10.10 Shear Connectors 743
6.10.10.1 Role of Shear Connectors 743
6.10.10.2 Types and Sizes of Shear Connectors 744
6.10.10.3 Fatigue Limit State: Loads for Fatigue Limit State 746
6.10.10.4 Fatigue Resistance of Shear Connectors: LRFD Art. 6.10.10.2 746
6.10.10.5 Pitch of Shear Connectors (Art. 6.10.10.1.2) 748
6.10.10.6 Design of Shear Connectors for Strength Limit State (Art. 6.10.10.4) 750
6.10.10.7 Strength of Shear Connectors 753
6.10.10.8 LRFD Provisions for Providing Shear Connectors 754

www.EngineeringEBooksPdf.com

6.10.11 Stiffeners ... 766
6.10.11.1 Definitions and Description of Stiffeners ... 766
6.10.11.2 Web Bend-Buckling Resistance ... 768
6.10.11.3 Design of Transverse Stiffeners ... 769
6.10.11.4 Design for Bearing Stiffeners ... 772
6.10.11.5 Design for Longitudinal Stiffeners ... 775
6.10.12 Cover Plates ... 778
6.11 Fatigue and Fracture Considerations ... 779
6.11.1 General ... 779
6.11.2 Classification of Fatigue ... 779
6.11.3 Design for Load-Induced Fatigue ... 779
6.11.3.1 Design Considerations ... 779
6.11.3.2 Design Criteria ... 780
6.11.3.3 Detail Categories ... 780
6.11.3.4 Detailing to Reduce Constraint ... 783
6.11.3.5 Fatigue Resistance ... 783
6.12 Design of Noncomposite Slab–Steel Girder Superstructures ... 785
6.13 Composite Slab–Steel Beam Superstructures ... 812
6.13.1 Introduction to Composite Construction ... 812
6.13.2 Flexural Strength of Composite Sections ... 812
6.13.2.1 Stress Distribution in Composite Beams in Positive Flexure ... 812
6.13.2.2 Stress Distribution in Composite Beams in Negative Flexure ... 815
6.13.2.3 Locating Plastic Neutral Axis of a Composite Section in Positive Flexure ... 815
6.13.3 Effective Flange Width ... 816
6.13.4 AASHTO Procedure for Determining the Plastic Neutral Axis and Plastic Moment Strength of a Composite Section: LRFD Appendix D6, Art. D6.1 ... 817
6.13.5 Examples on Determination of Plastic Moment Strength, M_p ... 825
6.13.5.1 Yield Moment of Noncomposite Sections: LRFD Art. 6.2.1 ... 839
6.13.5.2 Yield Moment of Composite Sections in Positive Flexure: LRFD Art. D6.2.2 ... 839
6.13.5.3 Yield Moment of Composite Sections in Negative Flexure: LRFD Art. D6.2.3 ... 845
6.13.5.4 Yield Moment of Composite Sections with Cover Plates: LRFD Art. D6.2.4 ... 845
6.13.6 Depth of the Web in Compression: LRFD Art. D6.3 ... 846
6.13.6.1 Depth of the Web in Compression in the Elastic Region (D_c): LRFD Art. D6.3.1 ... 846
6.13.6.2 Depth of the Web in Compression at Plastic Moment (D_{cp}): LRFD Art. D6.3.2 ... 848
6.14 Design of Composite Slab-Girder Superstructures ... 849
6.A Appendix ... 906
References ... 922

Index ... 925

www.EngineeringEBooksPdf.com

Preface

> A bridge is more than the sum of stresses and strains: it is an expression of man's creative urge—a challenge and an opportunity to create the beautiful. A bridge is the fulfillment of human dreams and hopes and aspirations…. A bridge is a monument to mankind's indomitable will to achieve. Bridges symbolize the ideals and aspirations of humanity.
>
> **D. B. Steinman and S. R. Watson**
> *Bridges and Their Builders, Putnam, New York, 1957*

> To understand what I don't understand, and to better understand what I do understand, this book has been written.

This book is intended to serve as a source of the state-of-the-art knowledge pertaining to design and analysis of highway bridge superstructures conforming to *AASHTO-LRFD Specifications for Design of Highway Bridges*. The discussion presented herein focuses on the load and resistance design philosophy conforming to *AASHTO LRFD Bridge Design Specifications*. A fairly detailed account of the historical development and design of highway bridges conforming to *AASHTO Standard Specifications for Highway Bridges*, now archived, can be found in the author's 1998 book, *Design of Modern Highway Bridges* (McGraw-Hill, 1998); that topic is not discussed herein.

This book has been designed to serve both as a stand-alone text for a first course in design of highway bridge superstructures and a handy reference for educators and practicing engineers. This is essentially a *how to do* book and has code-connected design focus. A fair amount of undergraduate-level knowledge of structural loads and analyses and exposure to first courses in design of steel and concrete structures are essential for a quick grasp of the material presented herein. Because of the simplicity in style and format, this book can be used as a tool for teaching highway bridge design courses for both undergraduate- and graduate-level classes.

An important reason for the simple formatting of the book is to fill the need of the times. In many civil engineering curricula, highway bridge design course is offered to a class that comprises both graduate- and senior-level students (the author has taught such classes); the latter quite often possess neither the same level of prerequisite knowledge nor the depth of engineering maturity as the former. As such, the format and style of this book, along with many fully solved examples, have been designed to fill that need. Both students as well as design engineers will find this book as an excellent learning resource and a practical guide for engineering practice.

Presented in this book is a detailed discussion, with design examples, of concrete (both reinforced and prestressed) and steel bridge superstructures commonly used for bridges in the short span range. Wood superstructures are not covered in this book as they are built rather infrequently and have limited practical applications.

This book is divided into six chapters as follows.

Chapter 1, Introduction, presents bridge engineering as a discipline of structural design. It begins with a brief discussion of the traditional structural design philosophies, namely, the allowable stress design and the working stress design, which have been around for more than 100 years. This is followed by an introduction of the concepts of limit states design, which form the foundation of modern design philosophies, namely, the strength design used for concrete and masonry structures, the load factor design and the load and resistance factor design (LRFD) used for steel buildings and bridges. This author's 35+ years of teaching bridge engineering have shown that not all students and engineers possess the depth of conceptual understanding of various design philosophies, the lingering confusion about them resulting in design errors. For example, students would correctly determine the required size of a steel beam based on considerations of the strength limit states of

www.EngineeringEBooksPdf.com

LRFD philosophy (using factored loads). But because of a lack of clear understanding of design philosophies, they would incorrectly use the same (factored) loads (instead of using unfactored loads) for a deflection check, only to find that the chosen beam size does not satisfy serviceability criteria. The result would be an abnormally large and overdesigned beam (having a large moment of inertia) just to satisfy deflection criteria. Furthermore, no structure can be designed based on any one design philosophy alone. For example, even though buildings and bridges can be designed by LRFD methods, their serviceability limit states (e.g., restrictions on stresses, deformations, crack width of concrete beams, fatigue, and vibration control) are required to be checked based on allowable stress design philosophy.

Limit states are emphasized in the context of design philosophies for bridges because they are atypical structures when compared with buildings. Generally speaking, for designing buildings based on LRFD methodology, designers have to consider two limit states: the strength limit states (e.g., moment and shear strength requirements for a beam and axial load capacity of a column) and the service limit states (e.g., deflection limitations of a beam). By contrast, when designing a bridge and its components, *four* limit states have to be considered: the strength limit states (more than one, to determine a member's size), the service limit states (to ensure satisfactory performance of the bridge or its components under service loads), the fatigue and fracture limit state (necessitated by the repetitive nature of stress variations caused by the moving loads, not present in buildings) and the extreme event limit state (to ensure survival of a bridge during a major natural disasters, e.g., major earthquakes or wind storms, collisions by vessels, vehicles, or ice flows, or foundation scours caused by extreme floods; some of these are not applicable to buildings).

The most important aspect of the AASHTO LRFD Bridge Design Specifications is that it is, like the AISC's "Load and Resistance Factor Design Specifications," a probabilistic code; calibration (i.e., determination of load and resistance factors) being its most important component. Therefore, considerable space is devoted in Chapter 1 to a brief discussion of the theory of probability with an explanation leading to the calibration process and reliability, which form the basis of load and resistance design specifications. The underlying idea is to engage readers to understand the basis and significance of the *LRFD Specifications*, and appreciate how they are different from the old allowable stress-based design specifications.

The latter part of Chapter 1 introduces the format of *AASHTO LRFD Specifications for Highway Bridges* developed by the American Association of State Highway and Transportation Officials (AASHTO), with a brief narrative of their evolution, and the role of interim specifications that are issued annually by AASHTO in order to keep the Specifications up to date with the state of the art and research. The AASHTO document governs both design and construction of steel, concrete, and wood highway bridges in the United States and elsewhere in the world where this document has been adopted.

A good understanding of the AASHTO LRFD Specifications document is both necessary and important for bridge engineers and designers alike as it represents a legal set of documents since they have been adopted by the departments of transportation of various US states. AASHTO LRFD Specifications are unique in that they specify minimum design loads for highway bridges (analogous to *SEI/ASCE 7: Standard for Minimum Design Loads for Buildings and Other Structures*) as well as design specifications related to specific construction materials (analogous to specifications for steel buildings in AISC's *Manual of Steel Construction*, *ACI 318: Building Code Requirements for Structural Concrete*, AF&PA's *National Design Specification for Design of Wood Structures* (NDS), and the Masonry Society Joint Committee's (MSJC) *Building Code Requirements and Specifications for Masonry*, to name a few). Explained briefly in this chapter are various parts of the Specifications, referred to as sections, as well as the implication and intent of specific words, such as shall, may, and interim, that appear throughout these Specifications.

Chapter 2, Highway Bridge Superstructure Systems, describes the many different types of highway bridge superstructures systems that are used in the United States. Their significance lies in the fact that these also are the types, with some minor variations, most commonly used for short-span

www.EngineeringEBooksPdf.com

highway bridges throughout the world. These superstructures have been selected for discussion in this book because analyses of these types of superstructures are covered in Section 4 of AASHTO LRFD Bridge Design Specifications. These superstructures have two common characteristics: a deck and a number of usually parallel and equally spaced girders that support the deck. The deck is usually constructed from reinforced concrete; the supporting girders may be steel or reinforced or prestressed concrete. Each superstructure is characterized by girders of specific shapes or cross sections.

Also discussed in Chapter 2 is an all-important topic of service limit states and underlying serviceability criteria.

Chapters 3 and 4 form the core of this book.

Chapter 3, Loads on Highway Bridge Structures, presents a detailed discussion of various types of loads that act on bridge superstructures and substructures, which are covered in Section 3 of AASHTO LRFD Bridge Design Specifications. This chapter begins with a brief history of the evolution of live load models for designing highway bridges in the United States. Both gravity and lateral loads are discussed. These include dead and live loads, impact loads, fatigue loads, centrifugal forces on curved bridges, ice loads and flood loads, collision loads, thermal loads, earth pressures, and wind and seismic loads. Considerable space is devoted in this chapter to the discussion of the concept of notional live load model (which is different from the notional live load model specified in the now archived Standard Specifications) that forms the basis for calculating the live load effects in bridge structures. Shears and moments due to live loads—their maximum values in a span as well as their values at critical and/or selected locations in a span (e.g., at supports and at every tenth-point on the span)—are determined from influence lines. Concepts of shear and moment envelopes, which are required for design, are presented along with numerous examples. These examples are presented to help readers develop conceptual understanding of AASHTO LRFD notional live load model and associated calculations. To some readers, a few of these examples might appear to be trivial; nevertheless, they have been provided to answer what if curiosities of the uninitiated. The author feels that a poor understanding of these concepts is a prescription for poor design and ensuing dangerous consequences.

Chapter 4, Structural Analysis of Highway Bridge Superstructures, is devoted to discussion of the methods of analyses of highway bridge superstructures, that is, determining the force effects (moments and shears) required for the design of the deck and the supporting girders. The chapter focuses on the approximate methods of analysis specified in Section 4 of AASHTO LRFD Bridge Design Specifications, which are applicable to the types of superstructures commonly used for short-span bridges (discussed in Chapter 2). A key component of superstructure analysis/design calculations is the determination of the design forces due to the applied loads that cause shears and moments in the deck and the supporting girders. The approximate methods discussed in this chapter use quantities called distribution factors to determine the design forces. The distribution factors are different for shears and moments in the girders of different types of superstructures; they also are different for interior and exterior girders in each case. Several examples are presented to illustrate step-by-step calculations for determining the distribution factors for several different types of bridge superstructures, and their application in the determination of design forces. This all-important chapter is the highlight of the book; it presents the AASHTO-LRFD Specifications' often difficult-to-understand approximate analyses methods in a manner that is easy to grasp, defying their complexity.

Chapters 5 and 6 present discussion on structural designs of concrete and steel highway bridge superstructures. Discussions presented in the previous four chapters serve both as the background as well as essential reading for understanding these two chapters.

Chapter 5, Concrete Bridges, presents discussion of structural design of concrete bridge superstructures conforming to *Section 5: Concrete Structures* and *Section 9: Decks and Deck Systems* of AASHTO LRFD Specifications. These superstructures include reinforced concrete decks, reinforced concrete slab and T-beam bridges, and prestressed concrete bridges. Detailed examples include design of concrete bridge decks supported over steel and concrete girders, design of a slab

www.EngineeringEBooksPdf.com

bridge, design of a T-beam bridge, and design of a prestressed concrete girder bridge. A brief review of reinforced and prestressed concrete design philosophies is presented in this chapter; however, a fair understanding of reinforced and prestressed concrete design principles is a prerequisite to understanding the discussion presented in this chapter.

Chapter 6, the last chapter in this book, presents a discussion of slab-steel girder bridges. This chapter focuses on the design of superstructures that employ reinforced concrete decks supported on steel wide-flange beams conforming to specifications mentioned in *Ch. 6: Steel Structures* of AASHTO LRFD Bridge Design Specifications. Knowledge of the fundamentals of structural steel design is essential to grasp the material presented in this chapter.

All calculations presented in this book are supported by well-known formulas that can be found in texts on mechanics of materials and structural analysis as well as those provided in AASHTO LRFD Bridge Design Specifications. The readers would find that some of these formulas or equations (shown in the right margin) have dual numbering—separated by square brackets; the formula following the square brackets represents the formula as listed in AASHTO LRFD Bridge Design Specifications. This has been done to help present the readers with a quick reference to the corresponding design specification.

In summary, the material presented in this book is not just an academic exercise; rather it presents the state-of-the-art knowledge of highway bridge design practice. A grasp of material presented in this book, with its inherent simplicity and many fully solved design examples, will lead readers to a successful and enriching experience in understanding design of highway bridge superstructures. The author sincerely hopes that readers will find the discussion of various topics presented in the book both instructive and engaging.

Great care has been exercised in organizing and presenting the material in this book, including giving due credit for permissions; any missing credit is inadvertent. However, despite numerous proofreadings, it is inevitable that some errors and omissions will still be found. The author takes complete responsibility for these errors/omissions, and humbly requests the readers to communicate with him (ntaly@calstatela.edu) with helpful suggestions and comments to make necessary corrections in future editions of this book.

www.EngineeringEBooksPdf.com

Acknowledgments

The author is grateful to numerous organizations and professionals for their generous support and permissions to reproduce material from their sources, which has enriched this book. These include American Association of State Highways and Transportation Officials (AASHTO), American Society of Civil Engineers (ASCE), American Concrete Institute (ACI), American Institute of Steel Construction, American Iron and Steel Institute (AISI), Bethlehem Steel Corporation, Concrete Reinforcing Steel Institute (CRSI), Simpson, Gumpertz, and Heger, Inc., Transportation Research Board (National Research Council), U.S. Steel Corporation, and Mr. Bala Sivakumar, Director of Special Projects, Howard, Needles, Tammen & Bergendoff (HNTB), New York, among others.

The author also thanks Taylor & Francis Group's Joseph Clements, the acquisition editor of this book, for his advice, guidance, and continuous support throughout the preparation of the manuscript. His active involvement was key to the progress and successful completion this book project.

The author expresses his gratitude to Taylor & Francis Group associates Marsha Pronin and Joette Lynch, Christine Selvan of SPi Global, India, and many others for their hard work and assistance in completing this book's arduous journey from the author's manuscript to its ultimate destination, the readers.

www.EngineeringEBooksPdf.com

1 Introduction

1.1 STRUCTURAL DESIGN PHILOSOPHIES

Structural engineers use a variety of design methods to ensure that structures perform satisfactorily under prescribed loading conditions—both under service loads (also called working loads) and at ultimate loads. Philosophies for designing structures using members of various materials (concrete, steel, wood, aluminum, composites, etc.) have evolved over a period of decades. Through experimental investigation, research, and experience, prevailing design philosophies have either been modified or superseded by the new ones. For example, for decades the *allowable stress design* (ASD), also called the *working stress design* (WSD) or the *straight line design*, was used for designing steel, concrete, wood, and masonry structures; it is still being used for designing those structures. For concrete structures, WSD was replaced by the *strength design* method in the 1960s.

Design of steel structures began with ASD, which was followed by the *load factor design* (LFD); this was followed by yet another design method—the *load and resistance factor design* (LRFD)—which was introduced in the United States in the 1980s and which has been gaining wider acceptance by structural engineers for design purposes. This chapter presents a brief discussion of fundamentals underlying various structural design philosophies in vogue and their historical background.

1.2 GENERAL DESIGN CONCEPTS

The foundation of every design philosophy is the known stress–strain relationship of the materials. Unless otherwise mentioned, the following assumptions are implied in the context of material properties:

1. The material is homogeneous.
2. The material is isotropic.
3. The material is *Hookean*; that is, it obeys Hooke's law, meaning the material is linearly elastic.

Structural materials do not completely satisfy these assumptions, however. For instance, microscopic examination shows that steel consists of crystals of various kinds and orientations, so the steel is far from being truly homogeneous. Nonetheless, so long as the geometrical dimensions defining the form of a body are very large in comparison to the dimensions of a single crystal, the assumption of homogeneity can be used with great accuracy, and even if the crystals are oriented at random, the material can be treated as isotropic. Experience shows that structural solutions based on the theory of elasticity, which, in turn, is based on the assumptions of homogeneity and isotropy, can be applied to steel for accurately predicting its structural behavior. Structural materials such as concrete and wood are obviously anisotropic. For these materials, design philosophies and methods are somewhat modified. Also, all materials do not behave completely elastically under loads. It is known that materials such as steel and concrete behave inelastically at higher stresses. Accordingly, the design philosophies are essentially based on whether the materials behave elastically or inelastically under given loading conditions.

www.EngineeringEBooksPdf.com

1.3 FUNDAMENTALS OF STRUCTURAL DESIGN PHILOSOPHIES

1.3.1 Design Philosophies Based on Elastic Behavior: Allowable/Working Stress Design

Design philosophies based on the elastic behavior of materials, also known as the elastic design methods, assume that the material is linearly elastic. In the case of materials such as steel and concrete, which exhibit *elastoplastic* behavior, the design is based on the linear portions of the stress–strain curves as shown in Figure 1.1a and b for mild carbon steel and in Figures 1.2 and 1.3 for concrete. For metals such as steel and aluminum, certain fractions of their yield

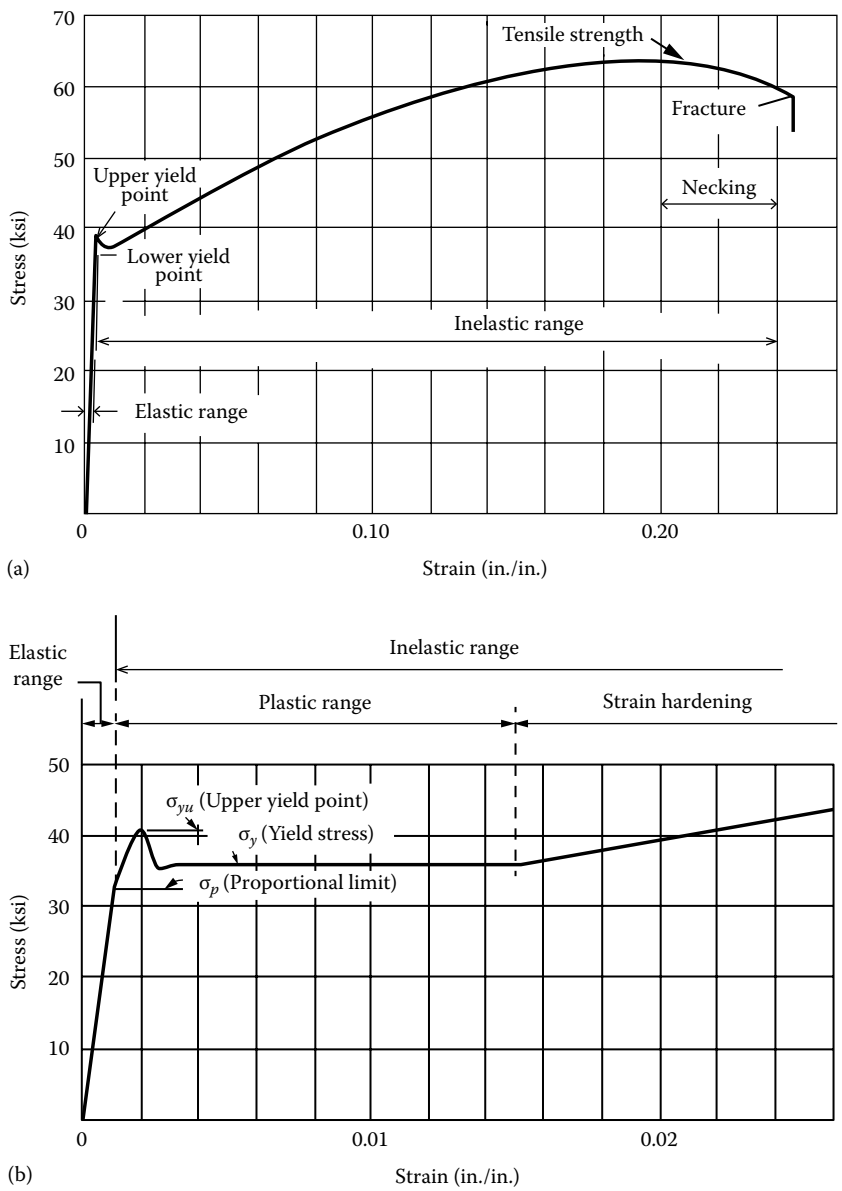

FIGURE 1.1 (a) Typical stress–strain curve for mild carbon steel. (b) Initial portion of the stress–strain curve. (Adapted from McGuire, W., *Steel Structures*, Prentice-Hall, Englewood Cliffs, NJ, 1968.)

www.EngineeringEBooksPdf.com

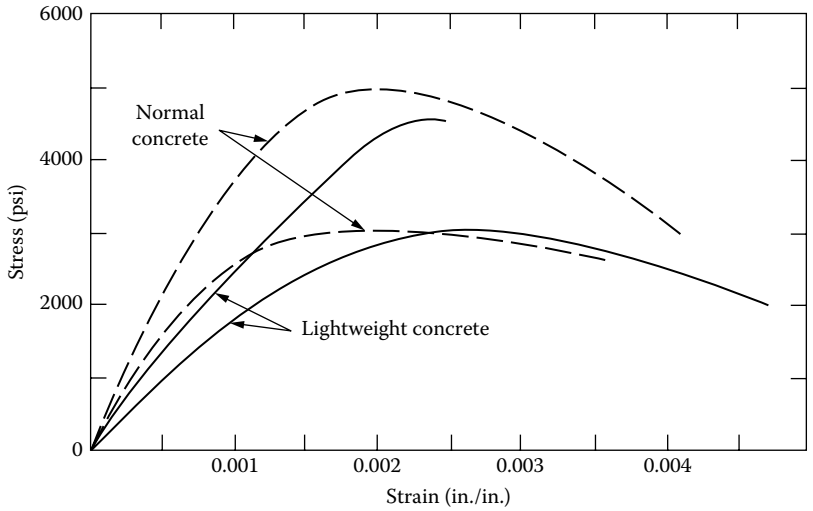

FIGURE 1.2 Stress–strain normal-weight and lightweight concrete. (Reproduced from MacGregor, J.G. and Wight, J.K., *Reinforced Concrete—Mechanics and Design,* 4th ed., Pearson/Prentice Hall, Upper Saddle River, NJ, 2005. With permission; Boris, B., Lightweight aggregate reinforced concrete columns, *Lightweight Concrete*, ACI Pub. SP 29, American Concrete Institute, Detroit, MI, pp. 81–130.)

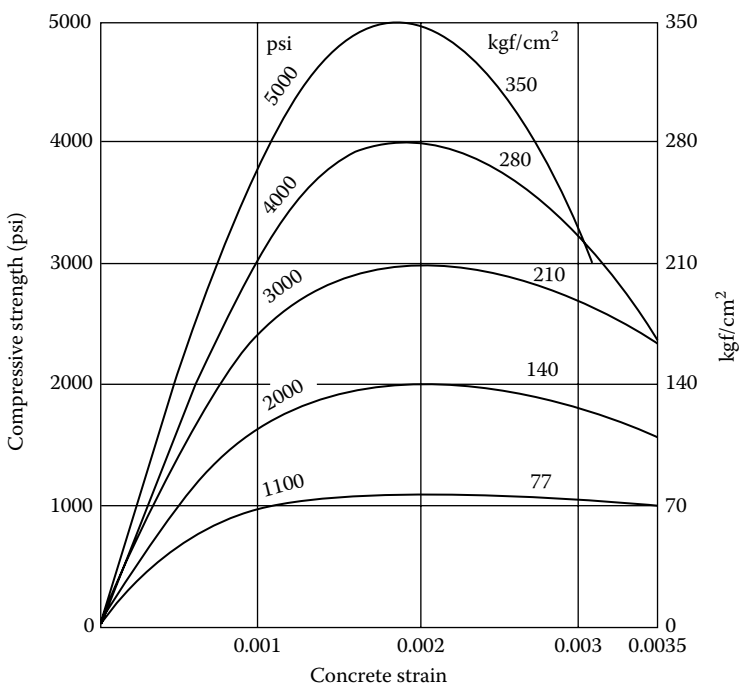

FIGURE 1.3 Representative stress–strain curves for various concrete compressions strengths. (Adapted from Wang, P.T. et al., *ACI J.*, 75, 606, 1978.)

www.EngineeringEBooksPdf.com

strengths (F_y) are specified as allowable stresses. For concrete, the allowable stress is assumed as a fraction of its 28-day compressive strength (f'_c) such that the allowable stress lies on the linear portion of its stress–strain curve. Values of allowable stresses are specified by dividing the material strengths (such as the yield strength of steel and the crushing strength of concrete) by the desired factor of safety, which may be different under different loading conditions (such as flexure, stability, etc.).

Certain materials used in design are brittle and posses very little ductility. Such materials exhibit purely linear behavior; that is, their stress–strain relationship can be represented by straight lines. Glass is an ideal brittle material; it exhibits almost no ductility. Other brittle materials include structural composites such as glass and carbon fiber reinforced polymeric materials (abbreviated, respectively, as GFRP and CFRP) known for their light weight, high strength-to-weight ratios, and corrosion resistance, and composite structural shapes made from glass and carbon fibers. Allowable stresses for such materials are kept at a fraction of their ultimate strengths. Figures 1.4 and 1.5 show stress–strain relationships for GFRP and CFRP

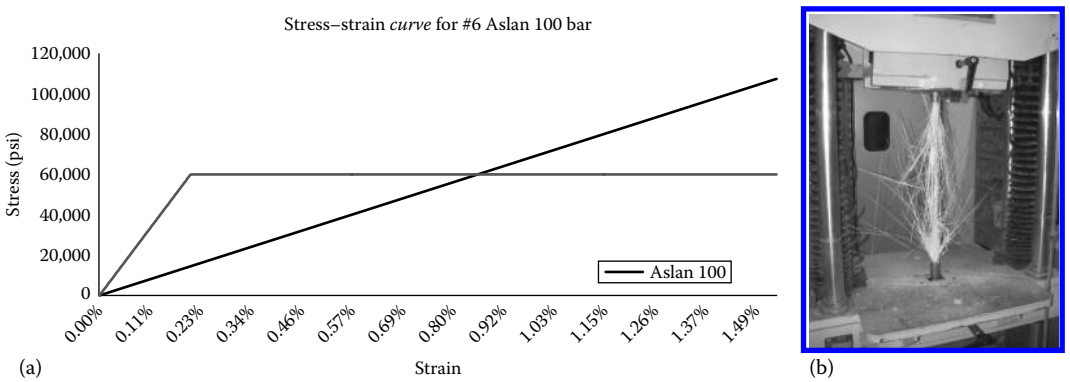

FIGURE 1.4 (a) Stress–strain relationship for GFRP bars (results for Aslan no. 6 GFRP bar shown). The linearity of stress–strain relationship indicates brittle failure and complete lack of ductility. Idealized stress–strain relationship for grade 60 steel reinforcing bar also shown for comparison. (b) Brittle, catastrophic failure of Aslan No. 6 GFRP bar in tensile test. (Photos and illustrations compliments of Doug Gremel, Hughes Brothers, Seward, NE.)

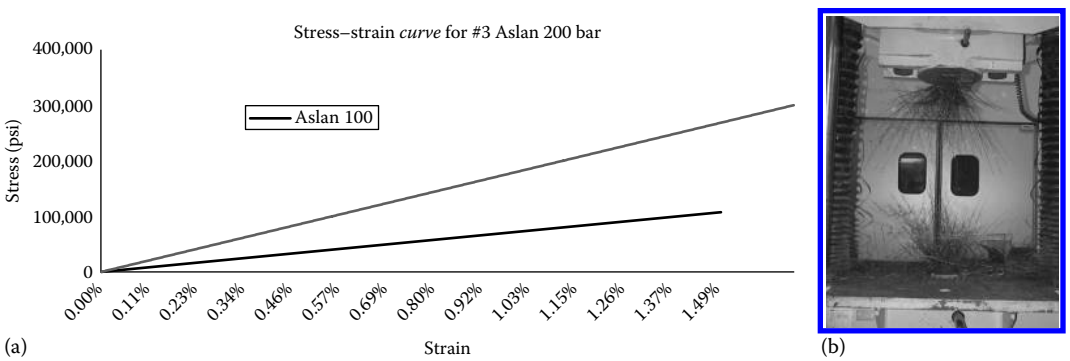

FIGURE 1.5 (a) Stress–strain curve for GFRP and CFRP reinforcing bars. The plot shows results for Aslan 100 (GFRP) and Aslan 200 (CFRP) no. 3 bars; (b) brittle, catastrophic brittle failure of Aslan no. 3 CFRP bar. The linearity of stress–strain relationship indicates brittle failure and complete lack of ductility. (Photos and illustrations compliments of Doug Gremel, Hughes Brothers, Seward, NE.)

www.EngineeringEBooksPdf.com

reinforcing bars. In all cases, the allowable stresses would be located on the linear portion of the stress–strain diagram; deviation of material behavior from elastic behavior is considered undesirable from the viewpoint of safety.

The ASD method is a method of proportioning structural members such that stresses produced in the structural elements subjected to allowable load combinations of working or service loads (as specified in ASCE 7-10, Section 2.4) (ASCE 2010) do not exceed the specified allowable stresses that are kept at fairly low levels in comparison to the material strengths.

Initially, the ASD method was called the working stress design (WSD, or the straight-line design) method as used for reinforced concrete structures from the early 1900s until the early 1960s. Some designers use this method for designing fluid-containing structures, such as water tanks and various sanitary structures, because low levels of allowable stresses used in design keep cracking and subsequent leakage under control, an objective that can also be achieved by using strength design (discussed in Section 1.3.2) and making proper use of crack-control provisions and the strength method as well.

The basic premise of the ASD is that the ultimate limit states are automatically satisfied by basing design on allowable stresses at working load levels. This, however, is not always the case, depending on the variability of loads and material properties. The drawbacks of the ASD and WSD are reported in the literature (MacGregor 1976, Ellingwood et al. 1980).

The allowable stress method is permitted for design of steel structures according to the *AISC Specifications* (AISC 2005), which uses the term *allowable strength method* in lieu of the term *allowable stress method*. This method has been the primary method used for design of structural steel buildings since the first AISC Specification was issued in 1931.

Both wood (AF&PA 2010) and masonry (MSJC 2008) structures, including bridges (AASHTO 2012), have historically been designed based on the ASD philosophies, although both wood structures and bridges can also be designed according to the LRFD philosophy (discussed in Section 1.3.2).

1.3.2 Design Philosophies Based on Inelastic Behavior: Plastic Design Method

Plastic design method, also called *capacity design* method, is applicable for design of steel structures only; the corresponding method of structural analysis is known as *plastic analysis*. The term *plastic* comes from the fact that the maximum load that can be carried by a steel member is calculated from the knowledge of the strength of steel in the *plastic region* of the stress–strain curve (Figure 1.6). This method, referred to as *inelastic design* method in *AISC Specifications* (AISC 2005), is permitted for designing steel structures (using steels having the yield strength not greater than 65 ksi).

According to Beedle (1958), the application of plastic analysis to structural design is attributed to the Hungarian researcher Dr. Gabor Kazinczy, who published the results of his pioneering tests on clamped girders as early as 1914 (Kazinczy 1914). Progress in the field of plastic design theory was made by the works of Van den Broek (1948) in the United States, J.F. Baker and his associates (Baker 1948, Baker et al. 1949) in England, and considerable research conducted at Lehigh University (Luxion and Johnston 1948, Johnston et al. 1953, Beedle et al. 1955). Steel structures designed and built based on plastic design philosophies are reported in the literature (Atkins and Lewis 1951, Estes 1957, Heyman 1957, Wright 1957) and present a discussion of plastic design of portal frames. A comprehensive discussion of the topic of plastic design/analysis can be found in Beedle (1958).

The plastic design method was developed for design of indeterminate steel structures such as continuous beams and frames (not applicable to determinate structures such as simple beams). The method takes advantage of a unique property of structural steel called *ductility* (discussed further in Section 1.5). The maximum load that a structure can carry is based on the structural usefulness just before reaching the collapse condition, which is caused when the applied loads

www.EngineeringEBooksPdf.com

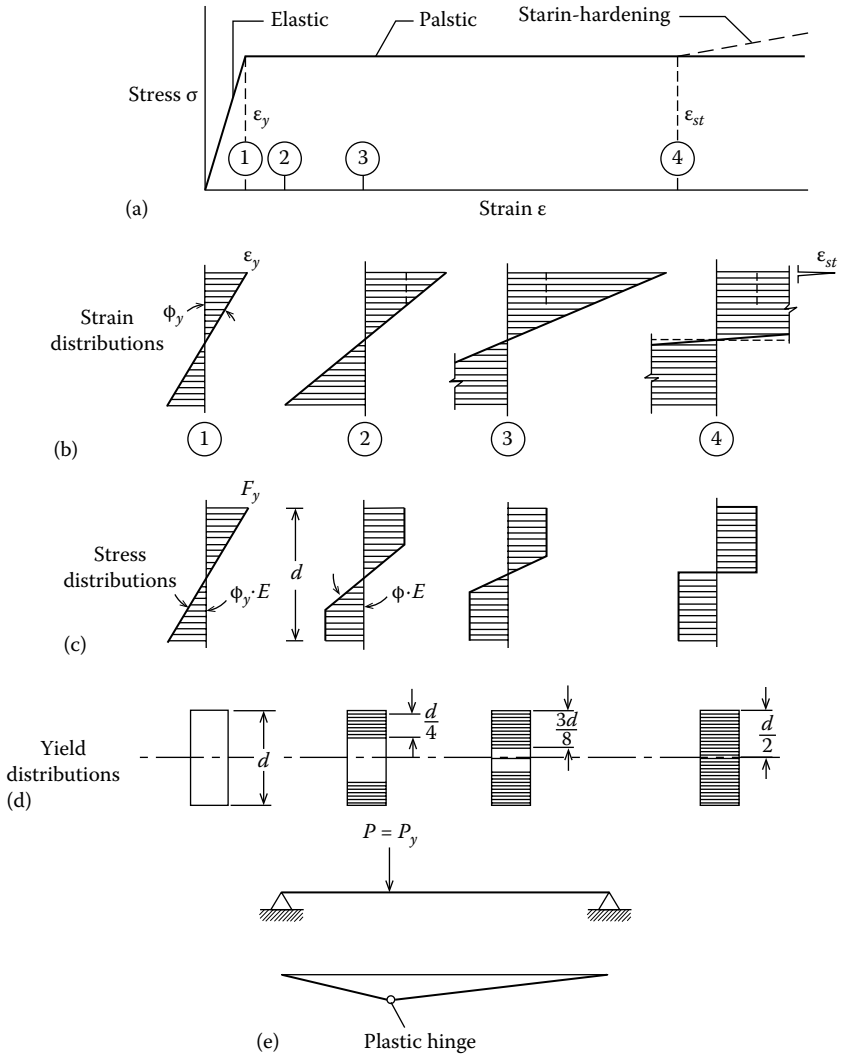

FIGURE 1.6 (a) Idealized stress-strain curve, (b) strain distributions corresponding to loading stages circled in (a), (c) stress distributions corresponding to loading stages circled in (a), (d) yield distributions corresponding to loading stages circled in (a), (e) plastic hinge develops in a simply-supported beam at location of plastic moment. (Adapted from Beedle, Lynn S.: *Plastic Design of Steel Frames*, 1958, John-Wiley & Sons, New York.)

cause one or more hinges to develop in the structure that are required to maintain a stable equilibrium. The hinge so developed is called a *plastic hinge* because the stress across the entire cross section of the loaded member at the hinge is uniform and equal to the yield stress of steel (in the *plastic zone* of the stress–strain curve of steel, Figure 1.6a); the corresponding loads are referred to as *collapse loads*. A structure is said to have become a *collapse mechanism* upon the formation of such a hinge or hinges simply because their formation would lead the structure to collapse.

Figure 1.6 is presented to illustrate the formation of (plastic) hinge in a simply supported steel beam (which is statically determinate) of a rectangular cross section. The beam carries a point load P at the center, which creates the maximum moment equal to $PL/4$ under the load. The stress distribution in the beam under this loading condition is linear, maximum compressive stress in the extreme top fibers and the maximum tensile stress in the extreme bottom fibers. The magnitude of load P is

www.EngineeringEBooksPdf.com

such that flexural stresses in the extreme fibers of the beam at the point of maximum moment are below the yield stress of steel, F_y. Under this loading condition, the maximum flexural stress in the beam can be calculated from the well-known flexural formula expressed as Equation 1.1:

$$f = \frac{M}{S} \tag{1.1}$$

where
f = flexural stress
M = bending moment
S = section modulus of the beam

As the magnitude of load P is gradually increased, we observe the following changes in the behavior of the beam and in the strain and stress patterns in beam cross section at the point of maximum moment (at the center in the present case), as shown in Figure 1.6b and c.

1. The flexural stresses in the beam increase linearly as the load P is increased.
2. As we continue to increase P, a stage is reached when the maximum stress in the extreme fibers of the beam attain the yield stress, F_y, while the stresses in the remaining fibers remain below the yield stress level; the stress distribution in beam remains linear, as shown in Figure 1.6c. The moment corresponding to this loading condition is called the *yield moment,* M_y, which can be calculated from Equation 1.2:

$$M_y = F_y S \tag{1.2}$$

   where
   M_y = yield moment
   F_y = yield stress of steel

   Note that Equation 1.2 is similar to Equation 1.1, albeit somewhat modified.
3. As the load P is increased further, the behavior of steel changes from elastic to plastic, with the result that stresses in the extreme fibers remain constant at the yield stress level as indicated by the plastic range portion of the stress–stain curve corresponding to points circles 1 through 4 in the stress–strain curve (Figure 1.6a), but the stresses in the interior of the beam cross section increase and slowly approach the yield stress level. Flexural stress distribution in the beam under this loading condition is bilinear. The maximum moment in the beam is greater than the plastic moment M_y, and neither Equation 1.1 nor Equation 1.2 is valid for this stress distribution.
4. With further increase of load P, more and more fibers away from the extreme fibers of the beam attain yield stress, F_y. The stresses in other fibers of the beam vary linearly from the yield stress level to zero at the neutral axis.
5. As the load is increased further to a value we would call P_y (Figure 1.6e), the flexural stresses throughout the beam cross section at the point of maximum moment (at mid-span in the present case) attain stress level equal to the yield stress; the corresponding value of the moment is referred to as the *plastic moment*, M_p ($>M_y$ always). At the point of maximum moment, the flexural stresses in the beam attain constant value of yield stress throughout the beam cross section, resulting in rectangular stress distribution; the stress distribution is no longer bilinear. The flexural stress in the entire beam cross section above the neutral axis is compressive and equal to F_y, and that below the neutral axis is tensile and also equal to F_y. Because the stress distribution is no longer linear, the flexural stresses

www.EngineeringEBooksPdf.com

cannot be calculated from Equation 1.1. The plastic moment is the largest value of the moment a beam can carry; its value can be calculated from Equation 1.3:

$$M_p = F_y Z \tag{1.3}$$

where
M_p = plastic moment
Z = plastic section modulus of the beam

Note that since Z is always greater than S, M_p is always greater than M_y. The ratio Z/S is defined as the shape factor (a dimensionless parameter, always >1.0); its value depends on the shape of the member's cross section. For a rectangular shape, its value is 1.5, for a solid circular section, approximately 1.7.

6. The beam cross section at which the stress distribution becomes rectangular (at midspan in our case) is said to have become a hinge with the result that the simple beam that was stable under the load $P < P_y$ has now become a two-bar truss or a mechanism under the load $P = P_y$. The presence of three hinges (two at the supports and one at the midspan) in this simple beam causes it to become unstable, leading it to collapse. It is for this reason that plastic design cannot be used for a determinate beam or structure.

1.4 LIMIT STATES DESIGN PHILOSOPHIES

1.4.1 Concepts of Limit States

It is instructive to understand the concepts of *limit states*, which form the foundations of the strength design, and the LRFD philosophies. Stated simply, *a limit state is a condition which represents the limit of structural usefulness* (AISC 1986). Or, in the context of structural reliability, a limit state can be defined as *a boundary between desired and undesired performance of a structure* (Nowak and Collins 2013).

But how do we define *usefulness*? The term *limit states* refers to a variety of conditions (or states) that must not be violated if a structure, partly or wholly, must retain its ability to perform its intended functions (or usefulness) during its intended service life. The use of plural *limit states* is intentional as there may be, and usually are, many conditions that, if violated, would impair a structure's ability to satisfactorily carry extreme loads. These limit states are owner/designer-driven conditions and their intents are specified in the design codes. *Intended service life* is prescribed in the design codes, usually 50 or 75 years.

To comprehend the concept of limit state, let us say that the deflection of a bridge beam should not exceed $L/800$ (or 1/800th of the span length L); this would form a serviceability limit state for the bridge, which *shall* not be violated. As a second example, let us say that the design load cycles on the bridge should not exceed 2×10^6 cycles for the entire (assumed) service life of the bridge; such a limit would constitute the fatigue limit state for the bridge. As a third example, let us say that the bridge should be safe and remain serviceable when it is subjected to the maximum design load; such a condition would constitute a strength limit state for the bridge. And, so on.

The limit states can be material specific. For example, crushing and cracking, and bond failure are some of the limit states applicable to concrete and masonry structures but not to steel or wood structures. Likewise, buckling of plates and formation of plastic hinges in structural members are conditions (limit states) specific to steel structures, but not to concrete or masonry structures. The condition characterized by the onset of yielding of steel is a limit state that is applicable to both steel structures and steel reinforcement in concrete. Lateral torsional buckling is a condition applicable to both steel and wood beams. Splitting failure is a characteristic of wood members. On the other hand, certain limit states, such as buckling, stability, and bearing failure, are common to structures constructed from all of these three materials. The same holds true for beams of all materials as far as deflections are concerned—excessive deflections, which cause functional problems, must not be permitted.

www.EngineeringEBooksPdf.com

Typical limit states for structures can be classified in the context of (1) safety, (2) damage, and (3) serviceability (Melchers 1999):

1. Safety: This includes collapse of all or part of a structure. Conditions that affect safety of a structure include tipping or sliding, rupture, sudden or progressive collapse, plastic mechanism, instability, corrosion, fatigue, deterioration, fire, etc.
2. Damage: Excessive or premature cracking, deformation or permanent inelastic deformation, collision damage.
3. Serviceability: Disruption of normal use due to excessive deflection, vibrations, local damage, etc.

In structural design codes, generally three kinds of limit states are recognized in relation to the intended functions of a structure:

1. Strength limit states, which relate to safety against some level of predefined loads or extreme loads during the intended life of the structure
2. Serviceability limit states, which relate to the functional requirements of the structure
3. Fatigue limit states, which relate to loss of strength under repeated loads

Design criteria ensure that a limit state is violated only with an acceptably small probability by selecting the load and resistance factors and nominal load and resistance values that will never be exceeded under the design assumptions. Various limit states are discussed in the next two sections.

1.4.1.1 Strength Limit States

Strength limit states are intended to preserve the safety of a structure (including its foundation) and of all of its parts against extreme loads to which a structure might be subjected to during its service life. Behavior of a structure under these loads, which would violate the limit states, is considered unacceptable as it might impair the safety of the structure or its parts (members, joints, etc.). In structural design, each member is designed separately to satisfy all applicable limit states that might vary from member to member; the controlling limit state is the one that would result in the lowest strength. For example, for flexural design of a reinforced concrete beam, some of the possible limit states are flexural strength, shear strength, and development strength of bars (bond strength). Similarly, for rolled steel beams, possible limit states include flexural strength, shear strength, lateral torsional buckling strength, and local buckling strength of flange and the web. As another example, the safety of a bolted joint in a steel structure has to be checked against four limit states: (1) shear strength of bolts, (2) bearing strength of the joint, (3) tension strength of the connected parts, and (4) block shear strength of the gusset plate. The condition that a structure may be damaged but not collapse under the extreme load conditions is a strength limit state applicable to all types of structures. The strength limit states also apply to foundations of structures, which include such concerns as bearing resistance failure, excessive loss of contact, sliding at the base of footing, and loss of overall stability. Design criteria ensure that a limit state is violated only with an acceptably small probability by selecting the load and resistance values that would not be exceeded under the design assumptions.

The overriding concern in defining the strength limit states is to preclude the possibility of a structure or of a structural member losing its load-carrying capacity. A few examples of structural failure modes in this category include the following (Nowak and Collins 2013):

1. Exceeding the flexural capacity of a beam
2. Formation of a plastic hinge
3. Buckling of a flange in a steel beam
4. Buckling of a web in a steel beam
5. Shear failure of the web in a steel beam
6. Weld failure
7. Loss of overall stability
8. Crushing of concrete in compression

www.EngineeringEBooksPdf.com

1.4.1.2 Serviceability Limit States

Serviceability limit states are entirely different from the strength limit states; they address concerns related to the *functional requirements* of a structure or its parts under normal service load conditions. They may or may not be directly related to structural integrity. The basic idea behind serviceability states is to impose design requirements that would ensure and maintain functional ability of a structure during its service life. Serviceability limit states for a structure may vary from one structural member to another; they can be even material specific (e.g., cracking of ceiling or walls, or concrete beams).

The most common limit states include limitations on elastic deflections, span-to-depth ratios for beams, vibrations of a floor, drift of columns or a building, rotation of a connection, etc. The overriding concern is that violations of these limit states could cause an unacceptable level of distress in nonstructural members of a structure (e.g., cracking of plaster of a ceiling, nonstructural damage), and human discomfort due to excessive floor vibrations. Some serviceability limit states are imposed so as to preclude the possibility of structural deterioration due to external causes, which may lead to impairment of structural integrity. The serviceability limit states also apply to functional requirements of foundations, which include such concerns as bearing settlements and lateral displacements.

Designers should exercise good judgment when imposing serviceability states. The following brief description, summarized from Nowak and Collins (2013), is provided to develop an understanding of various service limit states as related to bridges.

1.4.1.2.1 Deflection Limits

Acceptable deflection limits are rather subjective and are often subject to human perception. By themselves, deflections might not be undesirable purely from a structural standpoint; however, they may give public a *perception* of failure. For example, an excessively deflected (sagged) ceiling in a building may pose a perception of failure to the occupants even though the ceiling itself, despite the cracked plaster, may be structurally safe. At the same time, a designer must recognize that a sagged roof ceiling (the one with minimum slope for drainage) is a prescription for *ponding*, which eventually may lead to progressive failure. Additionally, excessive deflection may cause nonstructural damage, which unfortunately is more costly to fix. An excessively deflected floor may interfere with proper function of machines mounted on it. Users (such as pedestrians) may not walk on a deflected bridge because of the perception of impending failure. Typical deflection limits are $L/360$ due to live load in buildings, and $L/800$ for bridge girders. Interestingly, deflection limits, not the strength limit states, may govern the final outcome of a design.

1.4.1.2.2 Excess Vibration

Excessiveness of vibrations is a matter of human perception and, as such, is difficult to quantify. A higher level of vibrations may be acceptable if a bridge does not carry pedestrian traffic. In buildings, vibrations may cause discomfort to its occupants; hence, they are considered undesirable and unacceptable beyond certain level (defined by MHz of frequency) (Witchey 1997). Design for vibration control requires a complex dynamic analysis. For the sake of simplicity in design, codes often specify static deflection limits, which indirectly mitigates vibration problem.

1.4.1.2.3 Permanent Deformations

This is condition of exceedance of elastic limit. Accumulations of permanent deformations over time may lead to serviceability problems. Unfortunately, this situation is often not addressed in all design codes. An example of occurrence of a permanent deformation in a continuous steel beam is illustrated in Figure 1.7a. Each time the stress in the beam exceeds the yield stress, the strain also exceeds the yield strain, which is permanent as shown in Figure 1.7b. Over time, such events accumulate permanent strains, which eventually cause the formation of a *kink* (Figure 1.7c).

1.4.1.2.4 Cracking

The phenomenon of cracking is related to reinforced concrete structures: slabs, beams, and columns. Cracks in concrete by themselves are not detrimental to strength, but they progress to

www.EngineeringEBooksPdf.com

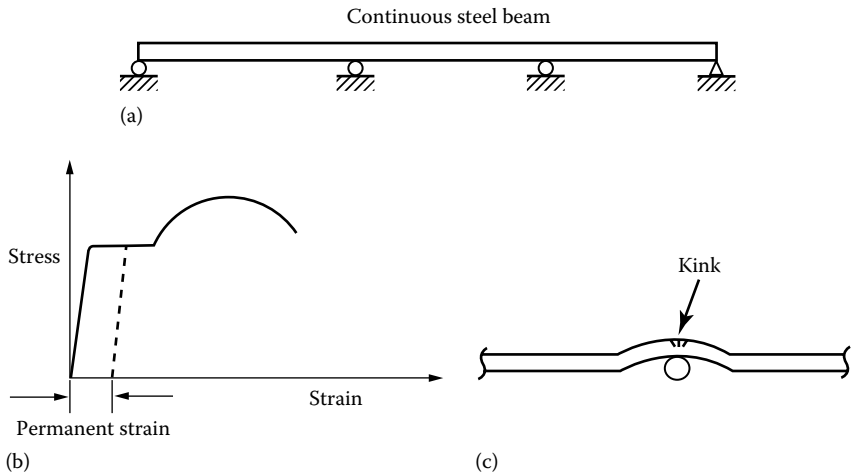

FIGURE 1.7 Permanent deformation in a continuous steel beam due to accumulated permanent strains: (a) a continuous steel beam, (b) stress–strain curve for steel showing permanent strain, and (c) a permanent *kink* in the beam. (Adapted from Nowak, A.S. and Collins, K.R., *Reliability of Structures*, CRC Press, Boca Raton, FL, 2013.)

FIGURE 1.8 Severe and extensive corrosion of tensile reinforcing bars and spalling of concrete at the bottom of a deck slab.

affect the strength rather indirectly. Increased crack widths permit ingress of moisture, which leads to corrosion of reinforcing bars causing spalling, eventually impairing structural integrity of the concrete members. In many cases, the corrosion of reinforcing bars is so severe and extensive (Figures 1.8 and 1.9) that replacement of the structure is the only option left. In bridges, penetration of deicing chemicals in concrete members is a major problem. One way to mitigate this problem is to limit the crack widths, a code-prescribed practice. Permissible crack width depends on many factors. These include members' exposure: interior or exterior, exposed to saline environment (proximity to the sea or toxic facilities), type of structure (a bridge or a building), type of reinforcement (uncoated, coated, fiber-reinforced polymer reinforcement, etc.).

www.EngineeringEBooksPdf.com

FIGURE 1.9 Severe corrosion of reinforcing bars and spalling of concrete in the bents of a reinforced concrete bridge.

1.4.1.3 Fatigue Limit States

Fatigue can be broadly defined as a phenomenon of reduced material resistance under fluctuating stresses; it is related to loss of a member's strength under repeated loading. What is interesting about fatigue is the fact that failure can occur under well below the ultimate loads if a member is subjected to a repetitive loading. Therefore, *fatigue limit* can be defined as the maximum stress that can be repeated indefinitely without causing fatigue failure when applying fluctuating loads.

Fatigue was discovered during the development of railroads in Europe as a result of failures of the axles of railroad cars. This phenomenon was first described in 1839 by J. V. Poncelet (1788–1867), who presented it in his book *Industrial Mechanics* (Poncelet 1870). He stated that under the action of alternating tension and compression, the most perfect spring may fail in fatigue. A much more complete description of this phenomenon was made later by A. Wohler (1819–1914), who initiated the first scientific investigation of fatigue failures. The close relationship between the failures of metal parts (failures of axles of railroad cars were a major problem at the time) was amply recognized by McConnell (1849), who made an exhaustive study of the failure of axles of railroad cars. Based on this study, the French engineers recommended a careful inspection of coach axles after 70,000 km of service to avoid problems of sudden fracturing. Now, fatigue is believed to be responsible for a large percentage of failures in connecting rods and crank shafts of engines, steam or gas turbine blades, connections or supports of bridges, and railroad wheels and axles.

The mechanism of fatigue failure is believed to begin at the surface of a member where there are microscopic imperfections (present at the time of fabrication), which act as stress raisers. As a result, the stress at this location becomes much greater than the average stress acting over the cross section. As this higher stress is repeated, it leads to the formation of minute cracks. Occurrence of these cracks causes reduction in the member cross section at those locations (at tips or boundaries of members such as eye bars), which results in increased stresses. This, in turn, causes further propagation of the cracks into the material as the stress continues to be cycled. Eventually, as the propagation of cracks continues, the member cross section is reduced over time to such an extent that it can no longer sustain the load, and the member *suddenly* fractures—this is called *fatigue failure*. In the process, the material believed to be ductile behaves as if it were brittle. Two infamous bridge failures (December 15, 1967, failure of Pt. Pleasant Bridge, West Virginia, and

www.EngineeringEBooksPdf.com

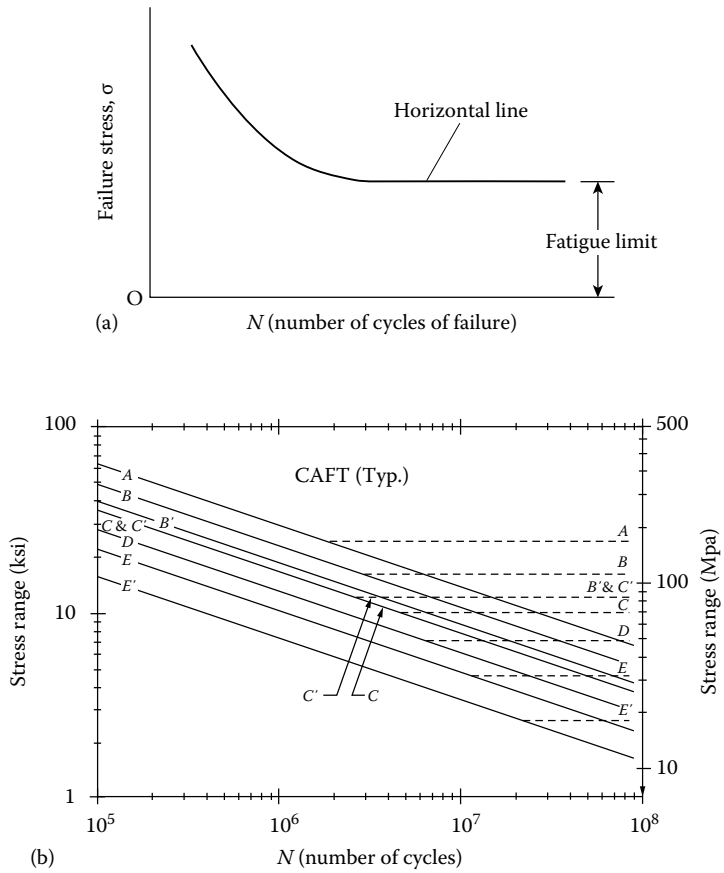

FIGURE 1.10 (a) Endurance (or S–N) curve showing fatigue limit (vertical scale is linear, the horizontal scale is logarithmic). The curve shows that the smaller the stress, the larger the number of stress cycles to produce failure. Horizontal line indicates that infinite number of stress cycles can be run if the fatigue limit is not exceeded. (b) S–N curve used for practical design, for example, for highway bridges. CAFT = constant-amplitude fatigue threshold. B, B′, C, C′ refer to detail category as listed in Table 6.2-2.4. (Refer to Section 6.11 for design considerations for *fatigue*.)

August 1, 2007, failure of the Mississippi River Bridge over I-35W in Minneapolis, Minnesota, among others) were ascribed to fatigue failure.

Fatigue failures have been reported in eye bars and gusset plates of steel truss bridges, in reinforcing bars of concrete beams that are in tension, and prestressing strands of posttensioned concrete bridges.

In order to preclude the possibility of fatigue failure of metallic member, it is necessary to determine a stress limit below which no signs of failure can be detected after applying a number of load cycles. This limiting stress is called the *endurance* or *fatigue limit*; the corresponding number of cycles is a threshold that must not be exceeded during the service life of the member. Both the magnitude of load and the number of load cycles play a role in arriving at the fatigue limit. Figure 1.10a shows the endurance limit (or the *S–N* diagram) showing fatigue limit; Figure 1.10b shows the relationship between the failure stress (as percent of ultimate tensile stress) to number of cycles to failure for steel and aluminum.

1.4.2 Strength Limit States versus Serviceability Limit States

Design engineers should have a clear understanding of the relative importance of strength limit states and serviceability limit states. The strength limit states define safety against the maximum as well as extreme loads that a structure is expected to experience during its intended service life,

www.EngineeringEBooksPdf.com

whereas the serviceability limit states focus on functional requirements. The primary concern and overriding emphasis of structural design codes is on the safety for the life, limb, and property of the public, which makes the strength limit states relatively more important. This is not to say that the serviceability states are not important; it is just that serviceability limit states permit designers to exercise more judgment. On the other hand, minimum considerations of safety are not permitted to be a matter of individual judgment; they must be ensured. This is the reason why design codes dwell more on the strength limit states than on the serviceability limit states.

It is noteworthy that either the strength limit state or the serviceability limit state might govern a design. In some cases, the serviceability limit states, not the strength limit states, might govern a design, which may sound a bit odd. For example, as mentioned earlier, the current bridge design specifications require that deflections of bridge girders not exceed $L/800$, where L = span length; this deflection limit often governs the girder design.

1.4.3 Strength Design, Load Factor Design, and Load and Resistance Factor Design

The limit states design philosophy is generally practiced for all types of structures, including buildings and bridges. In design codes for structures, the limit states design philosophy is referred to somewhat differently. AASHTO Standard Specifications (AASHTO 1996, 2002) refer to strength design and LFD synonymously in the context of both concrete and steel bridges. AASHTO 1996 (Article [Art.] 10.42) defines the load factor method as *an alternate methods for design of simple and continuous beam and girder structures of moderate length. It is a method of proportioning structural members for multiples of design loads.* AASHTO 2002 has modified the foregoing statement to simply *a method proportioning structural members for multiples of design loads* (but the intent of the specifications remained the same).

In the United States, the limit states design philosophy is used in two forms: strength design (SD) for concrete and masonry structures, and the LFD and LRFD for steel structures and for highway bridges. These are briefly described in the next section.

1.4.4 Strength Design Philosophy

1.4.4.1 Strength Design Concept

The strength design method, formerly called the *ultimate strength design* method (the word *ultimate* now dropped), is the modern method of designing both reinforced and prestressed concrete structures according to the *ACI Code* (ACI 2008); it is also being used for the designing reinforced masonry structures according to the *MSJC Code* (MSJC 2008). Essentially, it is a method of proportioning structural elements such that the calculated forces produced in elements by the factored load combinations do not exceed the factored element strengths. The modern analytical approach to calculating the moment strength of a reinforced concrete beam is said to have been developed by F. Stussi in 1932 (Janney et al. 1956).

Strength design philosophy is based on the condition of the member at the ultimate loads level when the member is at the point of incipient failure manifested by cracking of concrete in the compression zone and/or yielding of reinforcement in the tension zone of the beam. For reinforced concrete structures, this failure condition is defined to have been reached when the member stresses at critical locations reach predefined threshold levels: compressive strain of 0.003 in concrete and yield stress (f_y) in the reinforcing bars. At that stage, the concrete in the compression zone is assumed to have attained an average maximum stress of 0.85 times its 28-day compressive strength (i.e., $0.85f'_c$). Similarly, for reinforced masonry structures, the failure condition is defined to have been reached when the member stresses at critical locations reach compressive strain of 0.0025 in concrete masonry, or 0.003 in clay masonry, and yield stress (f_y) in the reinforcing bars. At that stage, the masonry in the compression zone is assumed to have an average maximum stress of 0.80 times its 28-day compressive strength (i.e., $0.80f'_m$). The stress distribution

www.EngineeringEBooksPdf.com

in compression zone is assumed to be rectangular for both concrete and masonry structures. A general discussion on material failure can be found in Collins (1981).

According to the strength design method, the structure is analyzed by the methods of elastic analyses using factored loads. Then the cross section of the structural member is proportioned for those factored loads. The emphasis is on the load-carrying capacity of a member at the ultimate load conditions rather than on the stress in the member at the service loads.

In strength design for concrete and masonry buildings, load factors are both load type specific and load combination specific; that is, the load factor assigned to the same load may be different in different load combinations. For example, according to ASCE 7-10 (ASCE 2010) for design of buildings, the load factor for the dead load is 1.4 for load combination 1, whereas the load factor for the dead load is 1.2 and the load factor for the live load is 1.6 for load combination 2, and so on. Equally important is the fact that *the load factors for use in design are specified by specific design codes, and are different for design of buildings and bridges*. This is because of the differences in calibration procedures used in accounting for probability, reliability, and many uncertainties in design (see discussion in Section 1.5.3).

1.4.4.2 Load Factor Design

The LFD method and the strength design methods were developed for designing steel highway bridges along the same general principles as reinforced and prestressed concrete bridges designed by the strength method. This design methodology is specified in the AASHTO *Standard Specifications* (AASHTO 1996, 2002) wherein the LFD is defined as *a design method in which safety provisions are incorporated by separately accounting for uncertainties relative to load and resistance* (AASHTO 2002, Art. 4.9).

1.4.4.3 Load and Resistance Factor Design

LRFD, the modern design philosophy used for buildings and bridges, is a probability-based design methodology. The term *resistance* refers to the load-carrying capacity of a structural member. The method aims at proportioning structural members for multiples of working loads such that no applicable limit states (or chosen limits of structural usefulness) are exceeded when the structure is subjected to variously defined load combinations. According to AISC (1986), *load and resistance factor design is an improved approach to the design of structural steel buildings (this design philosophy had not yet been developed for bridges). It involves explicit consideration of limit states, multiple load factors and resistance factors, and implicit probabilistic determination of reliability.* Some engineers also use the term *limit states design* (as in Canada and most European countries) in the same general context and include methods commonly referred to as strength design and LFD discussed earlier. A discussion on limit states design has been provided by Allen (1976).

In the LRFD philosophy, loading conditions at failure are predefined. These failure conditions may include situations in which a member, a connection, or the entire structure may cease to perform its intended function. Each failure condition is referred to as a *limit state*. Failure is deemed to have occurred when any of these predefined limit states is reached. Both the LRFD and ASD methods are presently used for design of steel and wood structures (AF&PA 2010, AISC 2011), but only the LRFD method as specified in *AASHTO LRFD Bridge Design Specifications* (AASHTO 2012) is used for design of highway bridges.

What constitutes limit states depends on the type of structures under consideration as well as designers' intent. The two commonly recognized limit states for structural design are (1) the *serviceability limit state* and (2) the *strength limit state*. The first refers to a condition in which a structure or component is judged to be no longer useful for its intended function, whereas the second limit state refers to a condition of unsafe structure from the standpoint of both strength and stability. Serviceability limit states include conditions under the service loads, such as deflection, vibrations, permanent deformation, and cracking. Strength limit states, on the other hand, include conditions such as plastic strength, stability, buckling, and fracture. For bridges, two additional limit states are recognized: (3) the *fatigue and fracture limit state* and (4) the *extreme event limit state*. This is because bridges are intended to carry entirely different kinds of loads than buildings. Because of

www.EngineeringEBooksPdf.com

the moving loads (vehicular loads), bridge structural members are subjected to repetitive stresses or stress reversals, for which case fatigue and fracture limit states must be considered in design. Generally speaking, moving loads are not present in buildings (other than parking structures, industrial buildings, and warehouses); consequently, fatigue and fracture limit states do not merit consideration for building structures. The *extreme event limit states* considered for bridges refer to their survivability during a major earthquake or flood, or during collisions by a vessel, vehicle, or ice flow. Although safety of a building during an earthquake or flood must be considered as one of the limit states, collision by a vessel or ice flow obviously do not constitute design limit states for buildings.

The LRFD method uses multiple *load factors* (discussed in Chapter 3 as pertinent to highway bridge design) for various types of loads as determined by the probabilistic methods. Because all design loads cannot be predicted with the same degree of certainty, different load factors are used for different loads to arrive at the ultimate load conditions. For example, the load factors for dead load and live load are different. Likewise, because the material strengths also cannot be predicted with the same degree of certainty, different resistance factors, by which the material strengths are multiplied, are used to arrive at the usable (or ultimate) strength of a member cross section. For example, the *strength reduction factors* are different for flexure, shear, bearing, etc. Load factors for design of highway bridges are discussed in Chapter 3; the strength reduction factors of concrete and steel bridges are discussed in Chapters 5 and 6, respectively.

1.5 LRFD SPECIFICATIONS FOR HIGHWAY BRIDGES

1.5.1 Evolution of LRFD Specifications for the Design of Steel Buildings in the United States

The LRFD method is based on the theory of statistical probability. In the United States, the LRFD methodology was extensively researched, and proposed and codified first by the American Institute of Steel Construction (AISC) for the design of steel buildings. The summary of this research has been reported in the many issues of *Structural Journal of the American Society of Civil Engineers* (Bjorvde et al. 1978, Cooper et al. 1978, Fisher et al. 1978, Galambos and Ravindra 1978, Hansell et al. 1978, Ravindra and Galambos 1978, Ravindra et al. 1978, Yura et al. 1978, Galambos et al. 1982). These eight papers describe the early fundamental work in the development of LRFD criteria for AISC (1986) publication (the first edition of AISC LRFD Specifications). A discussion of the probabilistic concepts that form the basis of LRFD is beyond the scope of this book. For a complete background of these concepts, readers should refer to those references; a brief summary can be found in AISC (1986, 1998) and in texts on steel design (Engelkirk 1994, Vinnakota 2006, Charles et al. 2009, Segui 2012).

1.5.2 Evolution of LRFD Specifications for Highway Bridges in the United States

1.5.2.1 Why the Change from AASHTO Standard Specifications?

LRFD Specifications for highway bridges in the United States, written in the 1980s, represented a quantum leap for designers. The pre-LRFD Specifications for highway bridges, known as AASHTO Standard Specifications, were initially written in the 1930s. Since then, the body of knowledge of designing highway bridges had grown enormously. At the same time, the state-of-the-art knowledge of various branches of bridge engineering had advanced considerably, and it continues to do so. Since their advent in 1931, the Standard Specifications had gone through many changes and adjustments at different times through interim revisions, essentially a piecemeal development process, causing gaps and inconsistencies. This problem was compounded by the fact that a comprehensive commentary on the specifications to clarify the intent and record the origin of key provision was not available. Some of the specifications' shortcomings were corrected by complete revision of the specifications in 1984.

That was not all. Many new types of superstructures, along with new analytical and design methodologies including computer-based methods, had been developed. Research had advanced

www.EngineeringEBooksPdf.com

the knowledge related to the understanding of the properties of materials, in improved materials, in more rational accurate analysis of structural behavior, and in the study of external events representing specific hazards to bridges such as earthquakes and stream scour, and many other areas. It was also realized that the ASD and LFD methods specified in the AASHTO Standard Specifications did not provide consistent and uniform safety level for various groups of bridges; those specifications had simply become outdated. Additionally, the theory of code writing had advanced during the many years since the 1930s. The idea of a probabilistic code was put forth by Cornell (1969); many contributions in this field are summarized in the literature (Collins 1969, Nowak and Lind 1979, Ellingwood et al. 1980, Madesn et al. 1986, Melchers 1999, Nowak and Collins 2013). Much research had already been done to understand the structural behavior of steel buildings, leading to codification of LRFD philosophy for steel buildings (as alluded to in Section 1.5.1), and culminating in the publication of the *first* edition of *AISC Manual of Steel Construction-LRFD* (AISC 1986). While the variability in loads and material properties was considered to a limited extent in the LFD, the proposed LRFD Specifications considered these variabilities in an explicit manner. The rewriting of highway bridge design specifications and embracing the LRFD philosophy for bridges was only a logical step that followed.

1.5.2.2 Why Probability-Based Design Philosophy?

Everyone is familiar with a typical weather forecast: *Today's high is going to be X°F (or C), the low as Y°F (or C), and the chance of precipitation as Z percent*. This statement implies that the forecast temperatures indicate merely a *probability*, not a certainty, of their occurrence, and the forecast of precipitation is clearly stated as a mere *chance*. The whole idea is that neither the high and low temperatures for the day nor the precipitation can be stated with any degree of certainty, but just that there is a probability of their occurrence; variation in the forecast figures is clearly implied. This is so because the weather (temperature variation and precipitation) are random phenomena, which can only be predicted with some degree of uncertainty. Likewise, there is a degree of uncertainty associated with all phenomena with which civil engineers must work. Observed phenomena such as traffic demands, total annual rainfalls, measured properties such as compressive strength of concrete, yield strength of steel, specific gravity or densities of materials, the roughness coefficients of surfaces, etc., are examples that would never have the same values in repeated measurements. A comparison of the measured cross-sectional dimensions of a piece of lumber, say, a 2 × 4, at 1 ft intervals of a 10 ft long piece, would convince one of the variability of data (measured values). In general, engineering problems involve phenomena that inherently suffer from a scatter of data, which must be accounted for in design. *When the element of uncertainty, owing to* natural variation or incomplete professional knowledge*, is to be considered explicitly, the models derived are probabilistic and subject to analysis by the rules of probability theory* (Benjamin and Cornell 1970). It is this aspect that forms a compelling reason for the use of the theory of probability in design. Acknowledgment of this reasoning led to the development of probabilistic limit states design embodied in the current AASHTO LRFD Specifications.

The principal advantages of probabilistic limit states design are as follows (excerpted from Ellingwood et al. 1980):

1. More consistent reliability is attained for different design situations because the different variabilities of various strengths and loads are considered explicitly.
2. The reliability level can be chosen to reflect the consequences of failure.
3. It gives the designer a better understanding of the fundamental structural requirements and the behavior of the structure in meeting those requirements.
4. It simplifies the design process by encouraging the same design philosophy and procedures to be adopted for all materials of construction.
5. It is a tool for exercising judgment in nonroutine situations.
6. It provides a tool for updating standards in rational manner.

www.EngineeringEBooksPdf.com

It is interesting to note that although LRFD codification for steel building in the United States had been accomplished by 1986, the same had not been done for highway bridge design as the related research was in progress (Kulicki and Mertz 1993). For one thing, the AISC LRFD Specifications for steel buildings could not be applied in their as-is form for designing highway bridges. A very important reason for this was the many issues related to bridges (see Section 1.5.3), not pertinent to buildings, that needed to be addressed and accounted for in writing what was to become the AASHTO LRFD Bridge Design Specifications. The advent of these new specifications gave the bridge engineers discretion of using any of the two different sets of design specifications, the long-standing *AASHTO Standard Bridge Design Specifications* and the newly written and adopted *AASHTO LRFD Bridge Design Specifications* and its companions. (*AASHTO LRFD Bridge Construction Specifications* and *AASHTO LRFD Movable Highway Bridge Design Specifications*.) Subsequently, the Federal Highway Administration (FHWA) and various states established a goal that LRFD Standards be incorporated in all new bridge designs after 2007.

1.5.3 Issues and Considerations for the Development of AASHTO LRFD Criteria

AASHTO LRFD Specifications for Highway Bridges were developed based on considerations of many issues of interest to bridge engineers as discussed in Nowak (1995, 1999) and Nowak et al. (1993) and summarized by Kulicki (1999); a summary from these references follows:

1. Expected service life of a structure.
2. The degree to which future maintenance should be assumed to preserve the original resistance of the structure or should be assumed to be relatively nonexistent.
3. The ways brittle behavior can be avoided.
4. How much redundancy and ductility are needed?
5. The degree to which analysis is expected to represent accurately the force effects actually experienced by the structure.
6. The extent to which loads are thought to be understood and predictable.
7. The degree to which the designer's intent will be upheld by rigorous material-testing requirements and thorough inspection during construction.
8. The balance between the need for high precision during construction in terms of alignment and positioning compared with allowing for misalignment and compensating for it in design.
9. The basis for establishing safety in the design specifications.

Items 1 through 8 relate to the many uncertainties encountered in structural design process, whereas item 9 relates to the acceptable level of safety. Whereas all of the aforementioned considerations are important design issues, item 9 is by far the most fundamental criterion for establishing an acceptable design philosophy. Stated differently, an acceptable design philosophy must provide an acceptable reliability of the outcome (i.e., the design). That leads us to the question of how to determine that desirable or acceptable value of the reliability index. It is here that probability-based reliability analysis comes in the picture. This indeed is why, like other modern design codes such as the Ontario Highway Bridge Design Code (OHBDC 1994) and the Canadian Highway Bridge Design Code (CSA 1998), the level of safety provided for in AASHTO LRFD Bridge Design Specifications is based on probability-based reliability analysis. This aspect is discussed in the following section.

1.5.4 Probabilistic Basis of AASHTO LRFD Bridge Design Specifications

Two important tasks in the development of the AISC LRFD Specifications for steel buildings involved calibration process and reliability analysis. The calibration process (i.e., determining load and resistance factors) was necessary to ensure that the safety of buildings designed according to

www.EngineeringEBooksPdf.com

the new code would be at a preselected target level. Structural performance is measured in terms of reliability or probability of failure. The specifications provisions are so formulated that structures designed using them have consistent and uniform safety level. For bridges, this calibration process meant developing load and resistance factors, and reliability index, so that the safety of bridges designed according to the LRFD philosophy would be at a preselected target level, a major task in the development of LRFD Specifications for highway bridges. The major analytical tool used in the development of LRFD Specifications, for both buildings and bridges, was reliability analysis procedure to develop reliability index. What is meant by *reliability index*? *The Manual for Bridge Evaluation* (AASHTO 2011) defines *reliability index* as *a computed quantity defining the relative safety of a structural element or structure expressed as the number of standard deviations that the mean of the margin of safety falls on the safe side*. A discussion on reliability analysis can be found in several textbooks (Thoft-Christensen and Baker 1982, Melchers 1999, Gatty 2005, Nowak and Collins 2013). The methods vary with regard to accuracy, required input data, computational effort, and special features.

The most challenging task in the development of LRFD bridge design criteria was the calibration process (calculation of load and resistance factors) and the reliability analysis as discussed in Ellingwood et al. (1980). A complete discussion of these topics and pertinent research is beyond the scope of this book; that information can be found in the literature (Hwang and Nowak 1991, Tabsh and Nowak 1991, Ting and Nowak 1991a,b, Nowak 1993a,b, 1995, Nowak et al. 1993, Melchers 1999, Nowak and Collins 2013). A summary of calibration procedure is presented by Nowak (1995); a complete discussion on the same topic is presented in Nowak (1999). A summary from these references follows.

1.5.5 Statistical Nature of Loads and Resistances

1.5.5.1 Random Variables, Normal and Lognormal Distributions, and Probability

1.5.5.1.1 Representation of Engineering Data

For understanding the calibration process, it is necessary to have conceptual knowledge of elements of theory of probability, such as random variables, normal distribution, and probability distribution. The following discussion is intended to provide readers a brief overview of these concepts. The discussion presented herein aims at the characteristic normal distribution (standard normal distribution and lognormal distribution); other types of distributions, for example, gamma, exponential, chi-square, Poisson, and Weibull distributions, are not discussed. A detailed discussion on this topic can be found in many textbooks on the subject (Benjamin and Cornell 1970, Meyer 1975, Melchers 1999, Gatty 2005, Walpole et al. 2005, Johnson 2011).

What is a random variable? According to *Webster's Dictionary*, a *random variable*, a term in *statistics*, is simply a variable whose numerical values are determined by the results of a chance experiment. *Normal distribution*, a related term, is defined as a theoretical frequency distribution for a set of variable data, usually represented by a bell-shaped curve symmetrical about the *mean*.

In the context of topic under discussion, a random variable can be defined as a quantity that assumes different numerical values as the outcome of an observation or measurements. The term *probability* is used in the context of a random event. According to Laplace (1812), the probability of a random event is the ratio of the number of cases that favor it to the total number of all possible cases when nothing leads us to believe that one of these cases ought to occur more readily than the others. We say that all of these cases are *equally likely* (Laplace 1951). As such, a probability function is defined by a set of events.

Most civil engineering problems, specifically in structural engineering, deal with quantitative measures. In the context of the familiar deterministic formulations of engineering problems, the concepts of mathematical variables (e.g., loads on a beam) and functions of variables (e.g., shear and moment caused by the loads, which are functions of the loads and their positions on the beam)

www.EngineeringEBooksPdf.com

have proved to be useful substitutes for less precise qualitative characterizations. Such is the case in probabilistic models, a variable is referred to as a *random variable*.

At the outset, one should recognize that all measured physical or mechanical properties of materials are subject to certain amount of *variability*; the same holds for measurement of loads, especially live loads and environmental loads such as earthquakes, wind, and snow. This is just the intrinsic nature of data sampling. This variability is due primarily to two factors (Young et al. 1998):

1. Intrinsically, no materials are perfect in their composition; that is, they all have some kind of imperfections. Therefore, no two samples of material are truly identical.
2. In common material testing environment in a laboratory, regardless of quality control, it is virtually impossible to reproduce precisely the same test conditions over a large number of tests.

The variations in observed dada can be relatively small or large. A few examples would help clarify this statement. Figure 1.11 from Collins (1981) shows a plot of stress-cycle data as might be collected by laboratory fatigue testing. It shows that smallest the number of N (number of cycles to failure) is about 100, whereas the largest number is about 10,000. Thus, the ratio of largest value of N (100) to the smallest value of N (10,000) is 100, which is quite large. Figure 1.11 also shows the median fatigue life curve. Noting that about 50 percent of the specimens fail below the median fatigue life, the median fatigue life curve is not very useful for design purposes. Instead, a statistical approach is taken to establish a satisfactory basis for selecting a design value in practice. One way of doing this is to look at the distribution of the fatigue data as shown in Figure 1.12. This figure shows a histogram, a plot of the number of specimen failures under identical loading conditions versus the *logarithm of the number of cycles to failure*. The solid lines in this figure represent a frequency histogram of the test results. It is found that the histogram can be closely approximated by a bell-shaped curve (shown by a dotted line) called *normal* distribution; the function represented by the curve is a symmetric normal function.

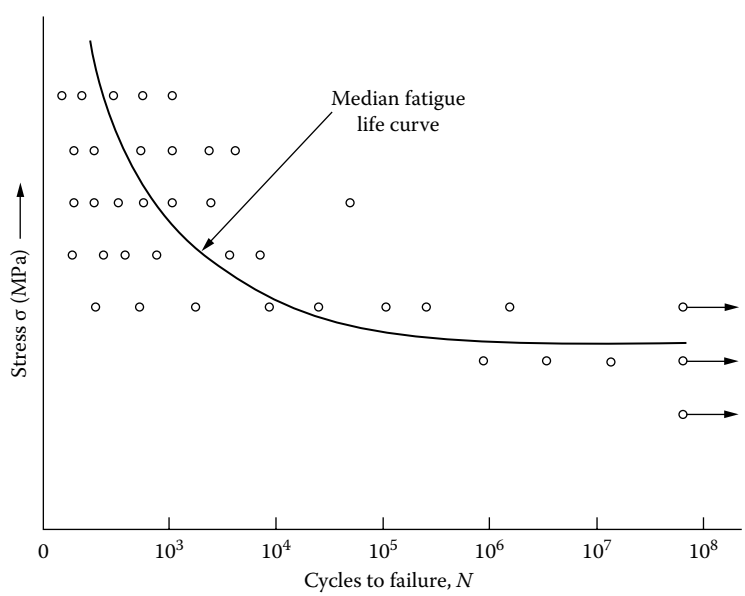

FIGURE 1.11 Plot of stress–cycle (S–N) data as might be collected by a laboratory fatigue testing of a material. (Adapted from Collins, J.A., *Failure of Materials in Mechanical Design*: *Analysis, Prediction, Prevention*, John Wiley, 1981; Young, J.F. et al., *The Science and Technology of Engineering Materials*, Prentice Fall, Upper Saddle River, NJ, 1998.)

www.EngineeringEBooksPdf.com

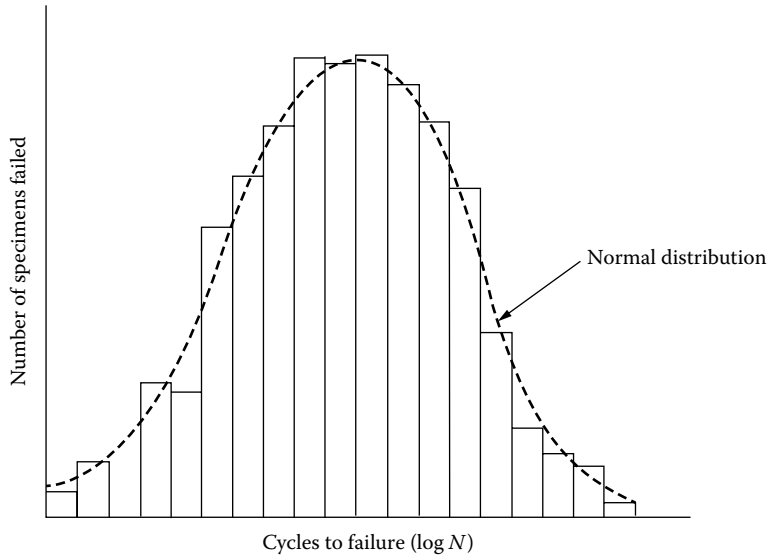

FIGURE 1.12 Distribution of fatigue specimens failed at a constant stress level as a function of logarithm of the number of stress cycles to failure (life). (Adapted from Collins, J.A., *Failure of Materials in Mechanical Design*: *Analysis, Prediction, Prevention*, John Wiley & Sons, 1981.)

The normal distribution, discussed heretofore, arose from the sum of many small effects. Often it becomes necessary to consider the distribution of a phenomenon that arises as a result of multiplicative mechanism. Figure 1.12 shows that the fatigue data can be represented as having *lognormal distribution* (a transformation of normal distribution function, in which the variables are expressed as the *logarithms* of N instead of N itself, where n = number of cycles to failure) (Young et al. 1998). The lognormal distribution occurs when the distribution of data is nonsymmetrical, that is, when a random variable is such that its logarithm, rather than the variable itself, has a normal distribution. See further discussions in Sections 1.5.6.2 and 1.5.6.3.

The characteristic bell-shaped curve shown in Figure 1.12 is called *normal curve* or *normal distribution* or *normal probability density* (the words *distribution* and *density* are often used interchangeably in the literature of applied statistics). It is considered to be the most important *continuous probability distribution* in the entire field of statistics and is commonly used to describe the distribution of many, many sets of data in nature, industry, and research. It was first studied in the eighteenth century when scientists observed an astonishing degree of regularity in errors of measurements, which they found to closely approximate a continuous distribution. This distribution, attributed to *laws of chance*, was called *normal curve of errors*. The mathematical equation of this curve was developed in 1733 by DeMoivre. The normal distribution is also referred to as *Gaussian* distribution in honor of mathematician Carl Gauss (1777–1855), who also independently derived its equation from a study of errors in repeated measurements of the same quantity.

Interestingly, for most physical properties (e.g., yield strengths, compressive strength of concrete, resistances of materials, modulus of elasticity, etc.), the variations in the repeated measurements are relatively small, which makes it possible for an average value based on a small number of test data to fairly represent the property in question. For example, for wood, which is the most variable of structural engineering materials, bending test results on clear small specimens would be expected to lie between ±50 percent of the mean value so that the ratio of the highest to the lowest measured strengths would be 3:1 (= (100 + 50/(100 − 50))). Consider, for example, the histogram shown in Figure 1.13, which shows laboratory measurements of moment

www.EngineeringEBooksPdf.com

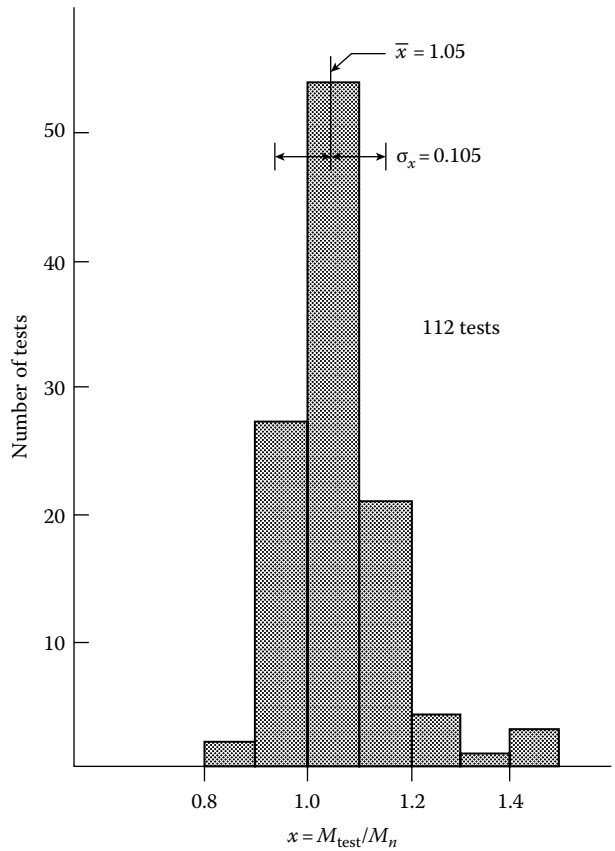

FIGURE 1.13 Comparison of measured and computed failure moments, based on all data for reinforced concrete beams with $f'_c > 2000$ psi. (Reproduced from MacGregor, J. and White, J.K., *Reinforced Concrete—Mechanics and Design,* 4th ed., Pearson/Prentice Hall, Upper Saddle River, NJ, 2005. With permission; Mattock, A.H. et al., *ACI J. Proc.*, 57(8), 875, 1961.)

strengths of 112 reinforced concrete test beams. The ratio of the smallest value of the random variable M_{test}/M_n is 1.875:1 (= 1.5/0.8).

A variable that can be represented by the bell-shaped distribution shown in Figure 1.14 is called a *normal random variable*. The mathematical equation for the probability distribution of the continuous normal variable depends on two parameters: its mean, μ, and standard deviation, σ, which are mathematically defined. Once μ and σ are specified, the normal curve is completely determined.

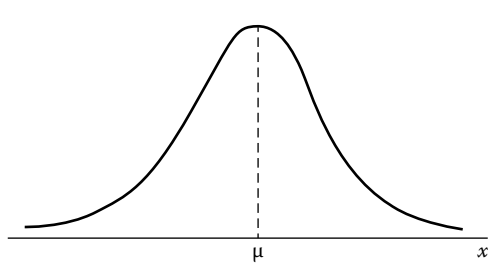

FIGURE 1.14 Normal distribution curve. Note the characteristic bell shape of the curve.

www.EngineeringEBooksPdf.com

1.5.5.1.2 Moments of Random Variables

1.5.5.1.2.1 Mean of Expected Value (First Moment) In probability analysis, the measured property is considered a random variable. The *sample mean* (or *mean*) or the average of several similar random variables in a group, commonly referred to as *weighted average* (essentially an arithmetic mean), is calculated by summing up the measured values and dividing by the total number n. The result can be expressed by Equation 1.4:

$$\bar{x} = \frac{1}{n}\sum_{i=1}^{n} x_i \tag{1.4a}$$

where

$\bar{x}$ = mean

$x_i = x_1, x_2, x_3, \ldots x_n$ are the measured values (random variables of size n)

n = number of measurements

Equation 1.4a applies to discrete random variables. For continuous variables, the value of mean can be expressed by Equation 1.4b:

$$E(X) = \mu_x = \int_{-\infty}^{\infty} x f_x(x)dx \tag{1.4b}$$

In both cases, the result is called the *first moment* since it is the first moment of *area* of the probability density function (PDF) about the origin. The mean μ_x is analogous to the centroidal distance of the cross section for a beam (Melchers 1999). The mean is the single most helpful number associated with a set of data.

The most probable measured value is called *mode*. If n measurements have been made, the mode is the value that appeared most often. The *median* is defined as the middle value in an ordered list of data—it is the middle value if n is odd, or the average of two middle values if the n is even.

1.5.5.1.2.2 Variance and Standard Deviation (Second Moment) When dealing with a set of observed data, it is desirable to be able to summarize numerically the variability of data such as the *range* of data and the *scatter* of data. The range is the difference between the maximum and minimum values in the data, but this description ignores the bulk of the data; those extreme values could very well be the result of experimental errors! To summarize the data more meaningfully, two *calculated numbers* are frequently used: standard deviation and variance.

The measure of dispersion or scatter of data is given by *sample variance* (or simply *variance*). This number is analogous to the moment of inertia of a cross section in that it deals with the squares of distances from the center of gravity, which is simply the sample mean. The variance, expressed as σ^2, is given by Equation 1.5:

$$\sigma^2 = \frac{1}{n-1}\sum_{i=1}^{n}\left(x_i - \bar{x}\right)^2 \tag{1.5}$$

The absolute value of the difference between a particular measurement and some value, usually the average, is called *deviation*. The dispersion of the data can be measured from the sample *standard deviation* (also called *root-mean-square deviation*) σ (it is analogous to the radius

www.EngineeringEBooksPdf.com

of gyration of a cross section); its value is given by the positive square root of the variance, which is expressed by Equation 1.6:

$$\sigma = \sqrt{\frac{(x_1-\bar{x})^2+(x_2-\bar{x})^2+(x_3-\bar{x})+(x_4-\bar{x})^2+\cdots+(x_n-\bar{x})^2}{n-1}} \tag{1.6}$$

where

σ = standard deviation

σ^2 = sample variance

We can also state that the standard deviation is the positive square root of the variance; accordingly Equation 1.5 can be expressed in the form of more useful computational formula given by Equation 1.7:

$$\sigma^2 = \frac{1}{n(n-1)}\left[n\sum_{i=1}^{n} x_i^2 - \left(\sum_{i=1}^{n} x_i\right)^2\right] \tag{1.7}$$

Note that in both Equations 1.5 and 1.6, the divisor is $(n - 1)$ rather than n because for $n = 1$, the value of the divisor would be zero, rendering both equations meaningless.

The units for the standard deviation are the same as those of the data. It is an important property of the data in the sense that, roughly speaking, the smaller the standard deviation of the sample data, the more clustered about the mean is the data and less frequent are the large variations from the average value (Benjamin and Cornell 1970).

The standard deviation is related to the average error of each measurement. If one makes a frequency distribution of the values x_i, the standard deviation is related to the shape (especially the *width*) of the distribution. If the means of two distributions are equal, they would be centered at the same positions on the horizontal axis. However, if their standard deviations are unequal, their spreads (widths) would be different (discussed later in this section).

The standard deviation divided by the value of the mean is called the *coefficient of variation* (COV) V, a *nondimensional* quantity, which is expressed by Equation 1.8:

$$V = \frac{\sigma}{\bar{x}} \tag{1.8}$$

The variance is always taken as a positive quantity even though the mean may be negative. The ratio of mean value divided by the nominal value is called *bias factor*, denoted by λ, as given by Equation 1.9:

$$\lambda = \frac{\bar{x}}{x_i} \tag{1.9}$$

1.5.5.1.2.3 Skewness γ_1 (Third Moment) The data may or may not be symmetrical about the mean. Skewness is a measure of the lack of symmetry of data about the mean; it is given by the third central moment about the mean.

www.EngineeringEBooksPdf.com

1.5.5.1.2.4 Coefficient γ_2 of Kurtosis (Fourth Moment) The measure of the flatness of a distribution is given by the fourth central moment. Sections 1.5.5.1.2.3 and 1.5.5.1.2.4 are not discussed further in this book.

Example 1.1 illustrates the application of Equations 1.4 through 1.8.

Example 1.1

The following 25 length measurements were made of an object where the measurements were made (in cm) to the *nearest half inch*: 4.7, 4.4, 4.1, 4.6(5), 4.5(5), 4.3, 4.1(5), 4.5, 4.4, 4.6, 4.8, 5.1, 4.9, 4.4(5) 4.5, 4.8(5), 4.5, 4.5, 4.7, 4.5(5), 4.7, 4.5, 4.9, 4.7, 4.6. For this set of measurements, (a) plot the frequency histogram and calculate (b) mean, (c) standard deviation, (d) variance, and (e) coefficient of variation. Plot a suitable normal curve for the frequency histogram.

Solution

It is convenient to tabulate the given data of measurements and make other calculations. It is easily done on an excel spread sheet as shown in Table 1.1.

a. The frequency histogram is shown in Figure 1.15.
b. The mean is given by Equation 1.4,

$$\bar{x} = \frac{1}{n}\sum_{i=1}^{n} x_i = \frac{1}{25}(114.6) = 5.58$$

c and d. The standard deviation is given by Equation 1.6. First calculate variance from Equation 1.5:

$$\sigma^2 = \frac{1}{n-1}\sum_{i=1}^{n}(x-\bar{x})^2 = \frac{1}{25-1}(1.10) = 0.04583$$

Therefore, by definition, the standard deviation is $\sigma = \sqrt{0.04583} = 0.214$.

A suitable normal distribution curve is plotted in Figure 1.15.

TABLE 1.1
Measurements for Example 1.1

Measured Value x (in.)	Number of Occurrences n	nx	$(x-\bar{x})$	$(x-\bar{x})^2$
4.1	1	4.1	−0.5	0.25
4.2	1	4.2	−0.4	0.16
4.3	1	4.3	−0.3	0.09
4.4	3	13.2	−0.2	0.04
4.5	5	22.5	−0.1	0.01
4.6	5	23.0	0.0	0.0
4.7	4	18.8	0.1	0.01
4.8	2	9.6	0.2	0.04
4.9	2	9.8	0.3	0.09
5.0	0	0.0	0.4	0.16
5.1	1	5.1	0.5	0.25
Σ	25	114.6	4.2	1.10

www.EngineeringEBooksPdf.com

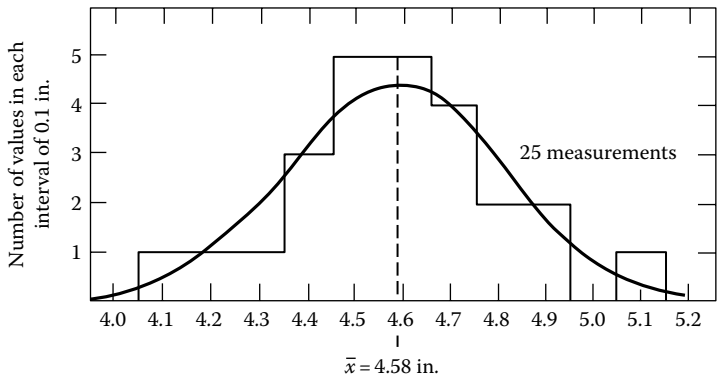

FIGURE 1.15 Histogram and normal distribution curve for Example 1.1.

1.5.5.2 Properties and Applications of Normal (Gaussian) Distribution

Normal (or Gaussian) distribution has many applications in practice. Some important properties of normal (or normal distribution) curves should be noted (Walpole and Myers 1978):

1. The mode, which is the point on the horizontal axis where the curve is a maximum, occurs at $x = \mu$.
2. The curve is symmetric about a vertical axis through the mean μ.
3. The normal curve approaches the horizontal axis asymptotically as one proceeds in either direction from the mean.
4. The total area under the curve and above the horizontal axis is equal to 1.
   In addition, the normal distribution curves have the following characteristics:
5. The normal distribution curve need not be centered at the origin.
6. The *area* under the normal distribution curve bounded by the ordinates a and b represents the *probability* that the variable X assumes a value between a and b as shown in Figure 1.16.

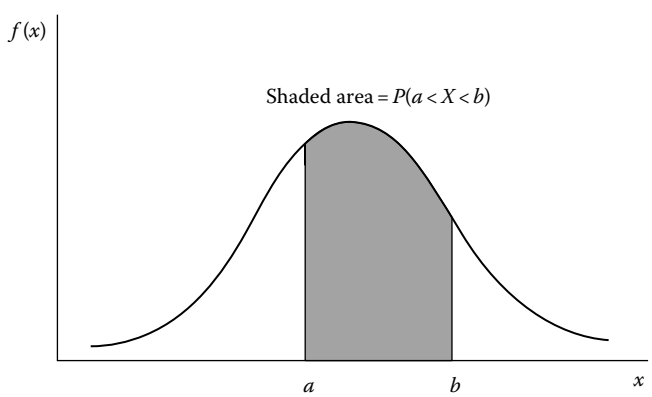

FIGURE 1.16 Area under the normal curve bounded by the ordinates $x = a$ and $x = b$ represents $P(a < X < b)$. (Adapted from Walpole, R.E. and Meyers, R.H., *Probability and Statistics for Engineers and Scientists*, Macmillan Publishing Company, New York, 1978. With permission.)

www.EngineeringEBooksPdf.com

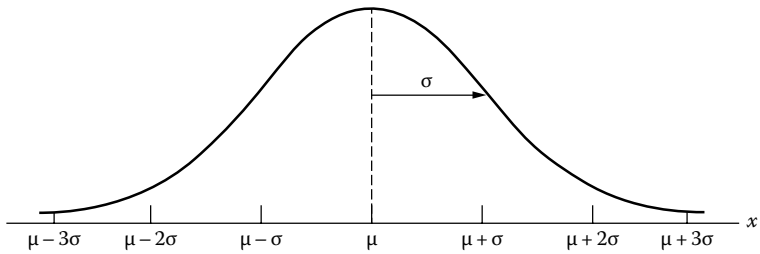

FIGURE 1.17 Normal probability density curve showing ordinates at the intervals of $\pm\sigma$, $\pm 2\sigma$, and $\pm 3\sigma$ from the mean.

7. The *areas* included between the ordinates erected on each side of the center of the normal distribution curve at distances of σ (standard deviation), 2σ (two times the standard deviations), and 3σ (three times the standard deviations) as shown in Figure 1.17 are 68.26 percent, 95.44 percent, and 99.74 percent, respectively (see Example 1.5). *This is an important property of a normal distribution curve.*

Figure 1.18 illustrates cases of normal curves that represent normal PDFs, which are characterized by values of the mean and the standard deviation. As noted earlier, Figure 1.14 shows a normal

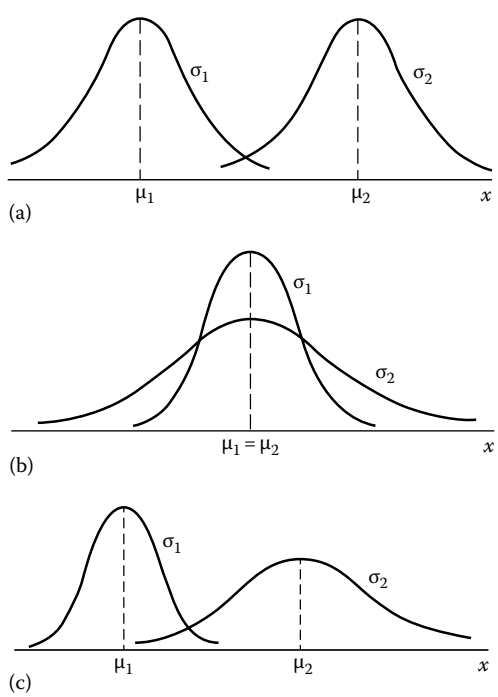

FIGURE 1.18 Profiles of normal distribution curves having different means and standard deviations. (a) Normal curves with $\mu_1 < \mu_2$ and $\sigma_1 = \sigma_2$. Note that $\mu_1 < \mu_2$ so the two curves are centered at different positions on the horizontal axis; but $\sigma_1 = \sigma_2$, so their spread (width) is the same. (b) Normal curves with $\mu_1 = \mu_2$ and $\sigma_1 < \sigma_2$. Because the means of the two distributions are equal, the two curves are centered at the same position on the horizontal axis; but their standard deviations are unequal, so their spreads (widths) are different. (c) Normal curves with $\mu_1 < \mu_2$ and $\sigma_1 < \sigma_2$. Because the means of the two distributions are unequal, they centered at different positions on the horizontal axis; but their standard deviations also are unequal, so their spreads (widths) are different.

www.EngineeringEBooksPdf.com

curve having a mean value μ. Figure 1.18a shows two normal curves that have different means ($\mu_1 < \mu_2$) but the same standard deviations ($\sigma_1 = \sigma_2$). Consequently, the two curves are identical in form but are centered at different positions on the horizontal axis because their *mean* values are different. Figure 1.18b shows two normal curves that have the same means (so they are centered at the same positions on the horizontal axis), but their standard deviations are different, which makes their spreads different from each other. Figure 1.18c shows two normal curves both of which have different means ($\mu_1 < \mu_2$, so they are centered differently on the horizontal axis) and different standard deviations ($\sigma_1 < \sigma_2$). Note that in all cases the curves spread asymptotically on both sides of the mean.

It is important to recognize that the distributions need not be centered at the origin. Figure 1.19 illustrates several probability density curves that are positioned differently with respect to vertical axis through the origin. Note that the positions of normal curves depend on the values of their *means*,

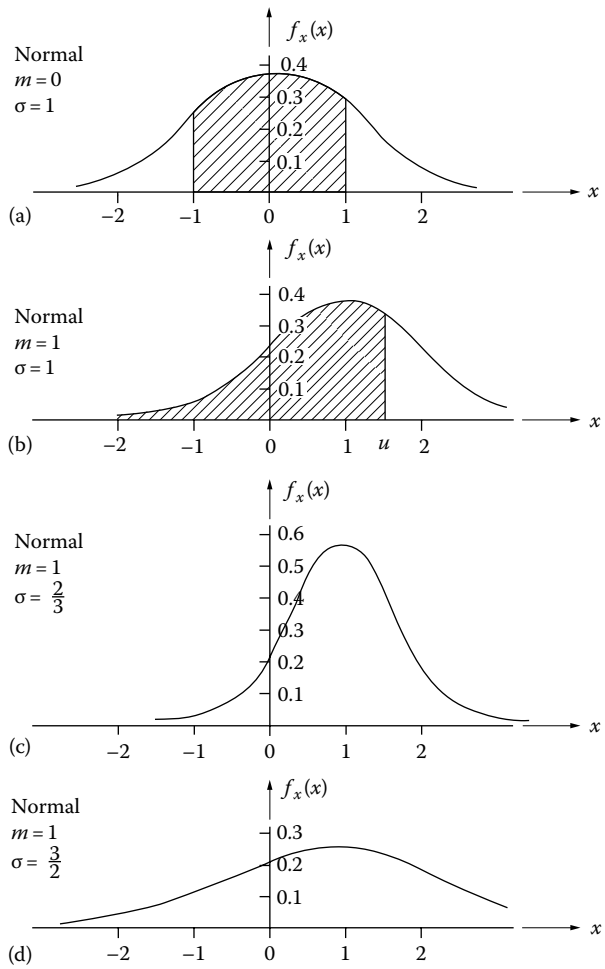

FIGURE 1.19 Normal density functions showing effects of changes in m (mean) and σ (standard deviation); in all cases the plots are symmetrical about the mean. (a) $m = 0$ and $\sigma = 1$, (b) $m = 1$, $\sigma = 1$, (c) $m = 1$, $\sigma = 2/3$, (d) $m = 1$, $\sigma = 3/2$. Figures (c) and (d) show the effect of changes in σ even though m is same. (Reproduced from Benjamin, J.R. and Cornell, C.A., *Probability, Statistics and Decisions for Civil Engineers*, McGraw Hill Co., New York, 1970. With permission.)

www.EngineeringEBooksPdf.com

whereas their spreads depend on the standard deviations (the larger the standard deviation, the wider the spread). Depending on the observed data, a part of the probability density curve may lie to the left of the origin, which represents a *negative* area.

A normal distribution function associated with the PDF is the cumulative density function (CDF) $F(x)$ defined by Equation 1.10:

$$F(x) = P\left(X \le x\right) = \int_{-\infty}^{+\infty} f(t)dt \tag{1.10}$$

Figure 1.20 shows both the PDF and the CDF of a normal random variable. As for the PDF, there is no closed-form solution for the CDF. However, tables have been prepared for the special case in which $\mu = 0$ and $\sigma = 1$.

Referring back to Figures 1.14 and 1.18, it is noted that once the value of the means μ and the standard deviations σ are specified, the normal curve is completely determined from Equation 1.11:

$$n(x;\mu,\sigma) = \frac{1}{\sigma\sqrt{2\pi}}\exp\left[-\frac{1}{2}\left(\frac{x-\mu}{\sigma}\right)^2\right] \tag{1.11}$$

For example, if $\mu = 50$ and $\sigma = 5$, then the ordinates $n(x; 50, 5)$ can be easily computed and the normal curve drawn. As shown in Figure 1.16, the area bounded by the two ordinates $x = a = x_1$ and

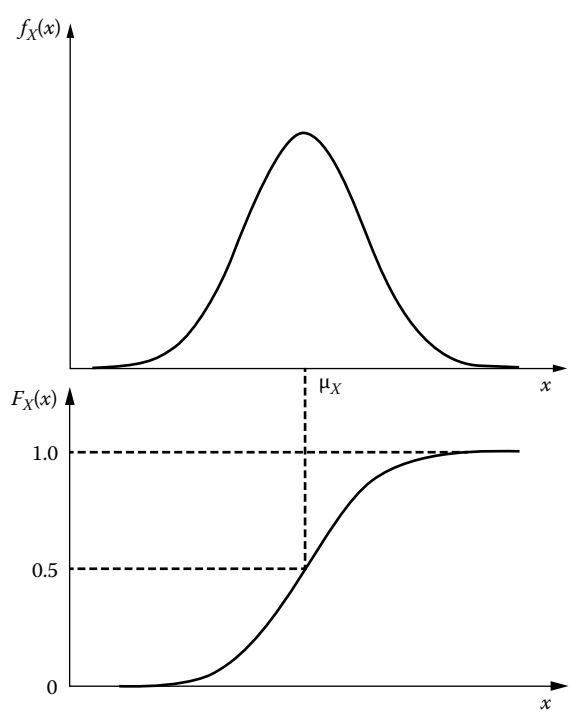

FIGURE 1.20 (Top) PDF and (bottom) CDF of a normal random variable.

www.EngineeringEBooksPdf.com

$x = b = x_2$ equals the probability that the random variable X assumes a value between $x = x_1$ and $x = x_2$. The shaded area in Figure 1.16 is determined from Equation 1.12 (Walpole and Myers 1978):

$$P\left(x_1 < X < x_2\right) = \int_{x_1}^{x_2} n(x;\mu,\sigma)dx$$

$$= \frac{1}{\sqrt{2\pi}\sigma}\int_{x_1}^{x_2} e^{-\left(\frac{1}{2}\right)\left[\frac{x-\mu}{\sigma}\right]^2} dx \tag{1.12}$$

Lognormal distribution was alluded to earlier in this section (see Figure 1.12). If $Y = \ln(x)$ is normally distributed, then x is said to be lognormal. Its probability density is given by Equation 1.13:

$$P\left(\ln x_1 < X < \ln x_2\right) = \int_{\ln x_1}^{\ln x_2} n(\ln x;\mu,\sigma)dx$$

$$= \frac{1}{\sqrt{2\pi}\sigma}\int_{\ln x_1}^{\ln x_2} e^{-\left(\frac{1}{2}\right)\left[\frac{\ln x-\mu}{\sigma}\right]^2} dx \tag{1.13}$$

Figure 1.21 shows two normal distribution curves identified as (distribution) I and (distribution) II, which have different *mean* values (μ) and different standard deviations (σ); however, the two curves are so centered on the horizontal axis that *they partially overlap each other by a small amount*. This happens when some random variables in distribution II have smaller values than some random variables in distribution I. Accordingly, this figure has two shaded regions corresponding to $P(x_1 < x < x_2)$ for the two distributions having two different *means*. The $P(x_1 < x < x_2)$, where X is the random variable describing (distribution) I, is indicated by the lines in the shaded area sloping *up* to the right. But if x is the random variable describing distribution II, then $P(x_1 < x < x_2)$ is indicated by the lines in the shaded area sloping *down* to the right. *Because the two shaded areas are different, the probability associated with each distribution is different.*

The integral in Equation 1.11 cannot be evaluated in the closed form between every pair of limits between x_1 and x_2; solution can be simplified by using tables, however. But preparing tables for each conceivable value of mean μ and standard deviation σ would be a huge task. This difficulty is overcome by transforming all the observations of any normal random variable X to a new, nondimensional variable Z (sometimes called *reduced variable*) with mean zero and variance 1. The reduced variable Z can be expressed by Equation 1.14:

$$Z = \frac{X-\mu}{\sigma} \tag{1.14}$$

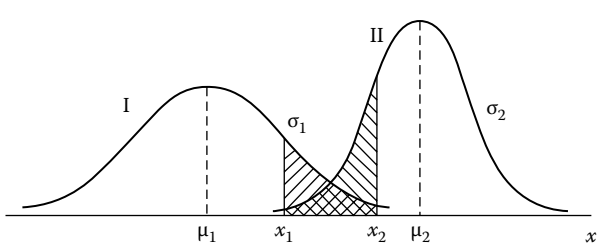

FIGURE 1.21 $P(x_1 < X < x_2)$ for different normal curves.

www.EngineeringEBooksPdf.com

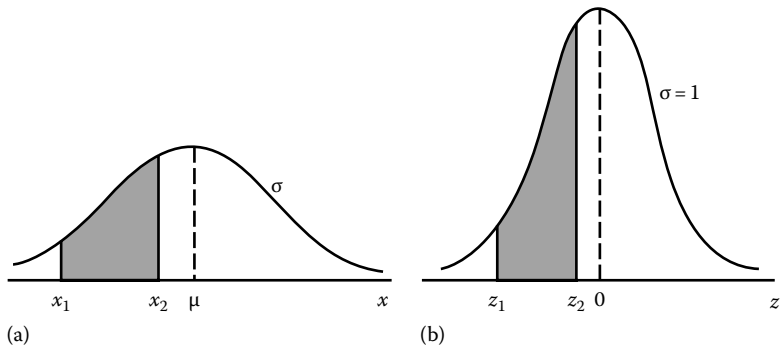

FIGURE 1.22 (a) Original and (b) transformed normal distributions.

When X assumes a value x, the corresponding value of Z becomes $z = (x - \mu)/\sigma$. Figure 1.22 shows the original and transformed distributions. It follows that if X falls between $x = x_1$ and $x = x_2$, the random variable Z would fall between $z_1 = (x_1 - \mu)/\sigma$ and $z_2 = (x_2 - \mu)/\sigma$ as shown in Figure 1.22. With these substitutions, we can rewrite Equation 1.11 in the form of Equation 1.15 (Walpole and Myers 1978):

$$P\left(x_1 < X < x_2\right) = \frac{1}{\sqrt{2\pi}\sigma}\int_{x_1}^{x_2} e^{-\left(\frac{1}{2}\right)\left[\frac{x-\mu}{\sigma}\right]^2} dx$$

$$= \frac{1}{\sqrt{2\pi}}\int_{z_1}^{z_2} e^{-\frac{z^2}{2}} dz$$

$$= \int_{z_1}^{z_2} n(z;0,1)dz = P(z_1 < Z < z_2) \tag{1.15}$$

where Z is seen to be normal random variable with mean zero and variance 1.

Equation 1.15 (normal probability density) cannot be integrated in closed form between every pair of limits a and b (Figure 1.16). Therefore, probabilities relating to normal distributions are obtained from special tables such as Table 1.A.1 (at the end of the chapter). This table pertains to the *standard normal distribution* (normal distribution with $\mu = 0$ and $\sigma = 1$) for values of $z = -5.0$ to $z = 5.0$. These two values (–5.0 and 5.0) are intentionally chosen because for $z < -5.0$, the value in the table is 0.0000003 (≈0), and of $z = 5.0$, the value in the table is 0.9999997 (≈1.0), this being the case because of the asymptotic nature of the normal distribution curve. The use of this table is quite straightforward. Suppose we wish to find the probability that Z is less than 2.25. First, we locate a value of z equal to 2.2 in the left column of Table 1.A.1, and then we move across the row to column under 0.05, and read 0.9878. Example 1.2 explains the use of Table 1.A.1. Examples 1.3 through 1.5 illustrate transformation of the given random variables x_i to transformed variables z_i and use of Table 1.A.1 to calculate probabilities. Note that use of this table requires values of only the mean and the standard deviation.

A very important use of Table 1.A.1 is its use for determining the probability of failure for a given reliability index or vice versa, as explained in Section 1.5.6.

www.EngineeringEBooksPdf.com

Example 1.2

A data of random variable X having normal distribution have mean $\mu = 60$ and standard deviation $\sigma = 12$. Find the probability that the variable X assumes a value between 45 and 72.

Solution

Here, $x_1 = 45$ and $x_2 = 72$. The z-values corresponding to x_1 and x_2 are determined from Equation 1.14:

$$z_1 = \frac{45-60}{12} = -1.25$$

$$z_2 = \frac{72-60}{12} = 1.00$$

Therefore,

$$P(45 < X < 72) = P(-1.25 < Z < 1.0)$$

Therefore, from Equation 1.14 and Table 1.A.1,

$$\begin{aligned} P(45 < X < 72) &= P(-1.25 < Z < 1.00) \\ &= P(Z < 1.00) - P(Z < -1.25) \\ &= 0.8413 - 0.1056 \\ &= 0.7375 \end{aligned}$$

This means that there is 73.75 percent probability that X would have a value between 45 and 72.

Example 1.3

In a laboratory, 250 measurements, which are recorded to the nearest tenth, follow approximately a normal distribution with a mean of 2.2 and a standard deviation of 0.75. How many of these measurements can be expected to have a value between 2.4 and 3.4 if the averages are computed to the nearest tenth?

Solution

Figure 1.23 shows the normal curve corresponding to the distribution of 250 measurements. Because the measurements are recorded to the nearest tenth, we need to calculate the area

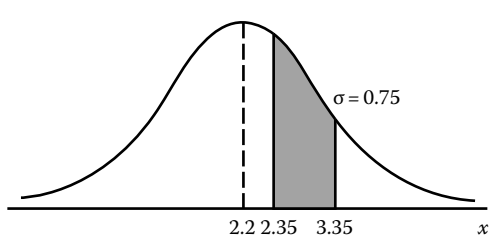

FIGURE 1.23 Probability density curve and area under the curve for Example 1.3.

www.EngineeringEBooksPdf.com

under the distribution (normal curve) between $x_1 = 2.35$ and $x_2 = 3.35$ as shown in Figure 1.23. From Equation 1.14, we have

$$z_1 = \frac{2.35 - 2.2}{0.75} = 0.20$$

$$z_2 = \frac{3.35 - 2.2}{0.75} = 1.53$$

Therefore, from Equation 1.14 and Table 1.A.1,

$$\begin{aligned} P(2.35 < X < 3.45) &= P(0.20 < Z < 1.53) \\ &= P(Z < 1.53) - P(Z < 0.20) \\ &= 0.9370 - 0.5973 \\ &= 0.3397 \end{aligned}$$

which is the shaded area under the normal curve. This means that 33.97 percent or $0.3397 \times 250 = 84.9 \approx 85$ of the 250 measurements would have values between 2.4 and 3.4.

Many engineering tests or sampling data can be closely approximated by normal distribution. Example 1.4 presents such a case.

Example 1.4

Figure 1.24 shows the histogram of the test results of uniaxial compression tests of 176 concrete cylinders. For this set of 176 tests, the mean and the standard deviation have been calculated to be 3940 and 615 psi, respectively. The design strength of concrete was 4000 psi. Determine the following:

a. Coefficient of variation
b. Number of cylinders that can be expected to have compressive strength between 4000 and 5000 psi
c. Number of cylinders that can be expected to have compressive strength between 2500 and 4000 psi
d. Number of cylinders that can be expected to have compressive strength between 3000 and 4000 psi
e. The bias factor
f. Check the validity of your calculations

Solution

Note the familiar bell-shaped curve (normal distribution) that is used to approximate the histogram in Figure 1.17; the mean and the standard deviation are also shown in the figure. Therefore, Equations 1.9 through 1.14 can be used here. From the given data, we have mean $\bar{x} = 3940$ psi, standard deviation $\sigma = 615$ psi.

a. Coefficient of variation (Equation 1.8), COV: $V = \frac{\sigma}{\bar{x}} = \frac{615}{3940} = 0.1561$ or 15.61 percent.
b. $x_1 = 4000$ psi, $x_2 = 5000$ psi.
From Equation 1.14,

$$z_1 = \frac{4000 - 3940}{615} = 0.10$$

$$z_2 = \frac{5000 - 3940}{615} = 1.72$$

www.EngineeringEBooksPdf.com

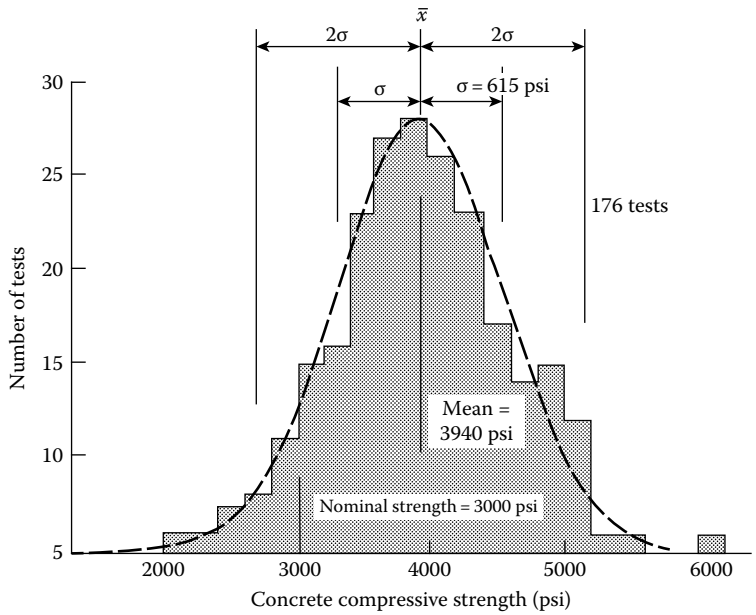

FIGURE 1.24 Distribution of concrete strengths for Example 1.4. (Reproduced from MacGregor, J. and White, J.K., *Reinforced Concrete—Mechanics and Design*, 4th ed., Pearson/Prentice Hall, Upper Saddle River, NJ, 2005. With permission.)

From Equation 1.14 and Table 1.A.1,

$$\begin{aligned} P(4000 < X < 5000) &= P(0.10 < Z < 1.72) \\ &= P(Z < 1.72) - P(Z < 0.10) \\ &= 0.9573 - 0.5398 \\ &= 0.4175 \text{ or } 41.75 \text{ percent} \end{aligned}$$

Therefore, $0.4166 \times 176 \approx 73$ cylinders can be expected to have compressive strength between 4000 and 5000 psi.

c. $x_1 = 2500$ psi, $x_2 = 4000$ psi.
From Equation 1.14,

$$z_1 = \frac{2500 - 3940}{615} = -2.34$$

$$z_2 = \frac{4000 - 3940}{615} = 0.10$$

From Equation 1.14 and Table 1.A.1,

$$\begin{aligned} P(2500 < X < 4000) &= P(-2.34 < Z < 0.10) \\ &= P(Z < 0.10) - P(Z < -2.34) \\ &= 0.5398 - 0.0096 \\ &= 0.5302 \text{ or } 53.02 \text{ percent} \end{aligned}$$

Therefore, $0.5302 \times 176 \approx 93$ cylinders can be expected to have compressive strength between 2500 and 4000 psi.

www.EngineeringEBooksPdf.com

d. x_1 = 3000 psi, x_2 = 4000 psi.
From Equation 1.14,

$$z_1 = \frac{3000 - 3940}{615} = -1.53$$

$$z_2 = \frac{4000 - 3940}{615} = 0.10$$

From Equation 1.14 and Table 1.A.1,

$$\begin{aligned} P(3000 < X < 4000) &= P(-1.53 < Z < 0.10) \\ &= P(Z < 0.10) - P(Z < -1.53) \\ &= 0.5398 - 0.0630 \\ &= 0.4768 \text{ or } 47.68 \text{ percent} \end{aligned}$$

Therefore, 0.4768 × 176 = 83.92 ≈ 84 cylinders can be expected to have compressive strength between 4000 and 5000 psi.

e. Bias factor is determined from Equation 1.9. The mean cylinder strength, $\bar{x}$ = 3640 psi, nominal cylinder strength, x_n = 4000 psi. Therefore, the bias factor is

$$\lambda = \frac{\bar{x}}{x_n} = \frac{3640}{4000} = 0.985$$

f. To check the validity of the aforementioned calculations, determine the number of cylinders that can be expected to have compressive strength between 2020 and 6090 psi as stated in the problem statement (it should be all 176 cylinders).
x_1 = 2020 psi, x_2 = 6090 psi. From Equation 1.14,

$$z_1 = \frac{2020 - 3940}{615} = -3.12$$

$$z_2 = \frac{6000 - 3940}{615} = 3.50$$

From Equation 1.14 and Table 1.A.1,

$$\begin{aligned} P(2020 < X < 6090) &= P(-3.12 < Z < 3.50) \\ &= P(Z < 3.50) - P(Z < -3.12) \\ &= 0.9998 - 0.0009 \\ &= 0.9989 \text{ or } 99.89 \approx 100 \text{ percent} \end{aligned}$$

Therefore, all 176 cylinders can be expected to have compressive strength between 2020 and 6090 psi as stated in the example statement, which proves the validity of the above mentioned calculations.

www.EngineeringEBooksPdf.com

Example 1.5

For the data given in Example 1.4, calculate the number of test cylinders that can be expected to have compressive strength between (a) the mean and ± one standard deviation ($\mu \pm \sigma$), (b) the mean and ± two standard deviations ($\mu \pm 2\sigma$), and (c) the mean and ± three standard deviations ($\mu \pm 3\sigma$).

Solution

a. $x_1 = (\mu + \sigma)$, $x_2 = (\mu - \sigma)$.
From Equation 1.14,

$$z_1 = \frac{(\mu + \sigma) - \mu}{\sigma} = +1.00$$

$$z_2 = \frac{(\mu - \sigma) - \mu}{\sigma} = -1.00$$

From Equation 1.14 and Table 1.A.1,

$$\begin{aligned} P(1.0 < Z < 0.100) &= P(Z < 0.10) - P(Z < -1.00) \\ &= 0.8413 - 0.1587 \\ &= 0.6826 \text{ or } 68.26 \text{ percent} \end{aligned}$$

Therefore, 176 × 0.6826 = 120 cylinders can be expected to have compressive strengths between the mean and ± one standard deviation ($\mu \pm \sigma$).

b. $x_1 = (\mu + 2\sigma)$, $x_2 = (\mu - 2\sigma)$.
From Equation 1.14,

$$z_1 = \frac{(\mu + 2\sigma) - \mu}{\sigma} = +2.00$$

$$z_2 = \frac{(\mu - 2\sigma) - \mu}{\sigma} = -2.00$$

From Equation 1.14 and Table 1.A.1,

$$\begin{aligned} P(2.00 < Z < -2.00) &= P(Z < 2.00) - P(Z < -2.00) \\ &= 0.9772 - 0.0228 \\ &= 0.9544 \text{ or } 95.44 \text{ percent} \end{aligned}$$

Therefore, 176 × 0.9544 = 168 cylinders can be expected to have compressive strengths between the mean and ± two standard deviations ($\mu \pm 2\sigma$).

c. $x_1 = (\mu + 3\sigma)$, $x_2 = (\mu - 3\sigma)$.
From Equation 1.14,

$$z_1 = \frac{(\mu + 3\sigma) - \mu}{\sigma} = +3.00$$

$$z_2 = \frac{(\mu - 3\sigma) - \mu}{\sigma} = -3.00$$

www.EngineeringEBooksPdf.com

From Equation 1.14 and Table 1.A.1,

$$P(3.00 < Z < -3.00) = P(Z < 3.00) - P(Z < -3.00)$$
$$= 0.9987 - 0.0013$$
$$= 0.9987 \text{ or } 99.9 \text{ percent}$$

Therefore, 176 × 0.999 = 176 cylinders (i.e., almost all) can be expected to have compressive strengths between the mean and ± three standard deviations ($\mu \pm 3\sigma$). This result is in conformity with the statement made earlier.

1.5.5.3 Linear Functions of Random Variables: Central Limit Theorem (CLT, Normal Convergence Theorem)

1.5.5.3.1 Sum of Random Variables

The sum or difference of several random variables, n, can be used to model certain quantities in engineering that are of like nature but have arbitrary distributions. Consider a function Y as a sum of random variables X_i (i = 1, 2, 3, … n). Assume that variables X_i are independent and have arbitrary probability distributions. According to the *central limit theorem* (also known as *normal convergence theorem*, first partially obtained by deMoiver in the eighteenth century and completed by Laplace some 60–70 years later), as the number n of the random variables approaches infinity, the sum of these independent random variables also approaches a normal probability distribution function even if the random variables X_i themselves are not normally distributed, provided that none of the random variables tend to dominate the function. This is, in fact, one of the most important results of theory of probability that *under very general conditions, as the number of variables in the sum becomes large, the distribution of the sum of random variables will approach the normal distribution* (Benjamin and Cornell 1970). Stated differently, if a function can be defined as the sum of a large number of random variables, the sum can reasonably be expected to have normal distribution.

Many situations are encountered in structural engineering for which the CLT can be used as a powerful tool for representing the sum (or difference) of different functions as random variables. For example, total gravity load, Q, on a structure can be expressed as a linear function as the *sum* of dead load, D, live load, L, and snow load, S, each of which is an independent random variable. Mathematically, Q can be expressed as Equation 1.16:

$$Q = D + L + S \tag{1.16}$$

According to the CLT, it can be stated that Q is *approximately* normally distributed even if D, L, and S are not normal. The mean of the *sum* Q of the three functions, D, L, and S, can be expressed as the sum of individual means of D, L, and S, as given by Equation 1.17:

$$\mu_Q = \mu_D + \mu_L + \mu_S \tag{1.17}$$

The variance of Q can be expressed as Equation 1.18:

$$\sigma_Q^2 = \sigma_D^2 + \sigma_L^2 + \sigma_S^2 \tag{1.18}$$

The CLT can be used also to express the *difference* of the functions of two variables. For example, consider two functions R (load-carrying capacity or resistance) and Q (load effect or demand),

www.EngineeringEBooksPdf.com

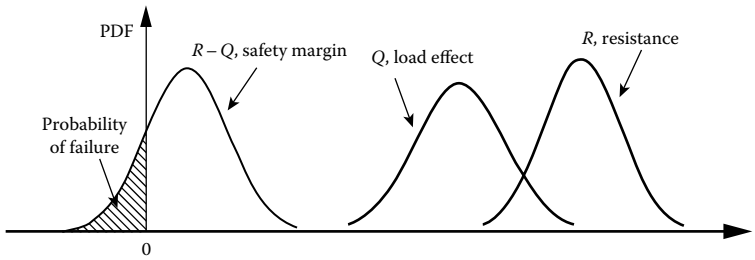

FIGURE 1.25 Probability distribution functions of load, resistance, and safety margin. (Reproduced from Nowak, A.S. and Collins, K.R., *Reliability of Structures*, CRC Press, Boca Raton, FL, 2013. With permission.)

both of which have normal probability distributions as shown in Figure 1.25. The *difference* of these two functions, g (marked as $R - Q$, *safety margin* in Figure 1.25), can be expressed as Equation 1.19:

$$g(R, Q) = R - Q \tag{1.19}$$

This function $g(R, Q)$ is called the *performance function* or the *limit state function* (Nowak and Collins 2013). Now, according to the CLT, the mean of the difference of the two functions can be expressed by Equation 1.20 and the variance by Equation 1.21:

$$\mu_{R-Q} = \mu_R - \mu_Q \tag{1.20}$$

$$\sigma^2_{(R-Q)} = \sigma^2_R + \sigma^2_Q \tag{1.21}$$

Application of properties expressed by Equations 1.20 and 1.21 is discussed in the next section.

1.5.5.3.2 Product of Random Variables: The Lognormal Distribution

Sometimes, a product of two statistically independent variables is used to model quantities. An example of such a quantity is the resistance of a structural member, which is the product of two random variables—cross-sectional area and the material strength. In such cases, the variables can be approximated as lognormal variables. Consider a function Y as a product of statistically independent variables $X_1, X_2, X_3, \ldots X_n$, which can be expressed by Equation 1.22:

$$Y = X_1 X_2 X_3 \ldots X_n \tag{1.22}$$

Taking natural logarithm on both sides, we obtain

$$\ln Y = \ln X_1 + \ln X_2 + \ln X_3 + \cdots + \ln X_n \tag{1.23}$$

The right-hand side of Equation 1.23 can be interpreted as the sum of random variables $\ln X_i$. The function $\ln Y$ approaches a normal distribution as the number of random variable approaches infinity (see Figures 1.11 and 1.12). Since the X_i are random variables, the functions $\ln X_i$ are also random variables. Calling upon the CLT, one may predict that the sum of a number of these variables will be approximately normally distributed. In this case, we expect $\ln Y$ to be normally distributed. It follows that if $\ln Y$ is normal, then Y must be lognormal. This means that if we have a product of many independent random variables, the product approaches a lognormal distribution as the

www.EngineeringEBooksPdf.com

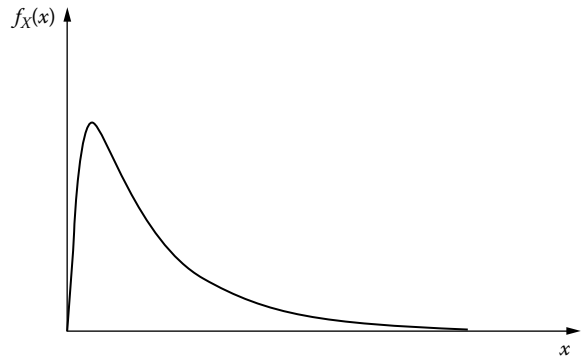

FIGURE 1.26 Plot of the PDF of a lognormal random variable.

number of random variables approaches infinity (Nowak and Collins 2013). A random variable Y whose logarithms are normally distributed is said to have the *logarithmic normal* or *lognormal* distribution. This principle also applies to a function of the *quotient* of several statistically independent variables.

One of the many applications of lognormal distribution is in structural reliability analyses as discussed in Section 1.5.6.2. Figure 1.26 shows the plot of the PDF of a lognormal random variable.

1.5.6 Probabilistic Determination of Safety Factors

1.5.6.1 Probabilistic Concept of Safety: Limit State Function (Performance Function)

It is intuitive to think that for a structure, for example, a beam, to be safe, the requirement would be that resistance is greater than the load effect: $R \geq Q$. Obviously, the beam would fail if $R < Q$. This concept is illustrated in Figure 1.27 in which the PDF of load effects S (= Q, e.g., bending moments) that a structure is expected to experience during its lifetime is plotted on the vertical axis and the PDF of the resistance R is plotted on the horizontal axis. For consistency, it is convenient to express both the resistance and the load effects in terms of a quantity such as bending moment. The 45° line in Figure 1.27 corresponds to $S = R$; that is, load effect is equal to the resistance. It also represents a transition between

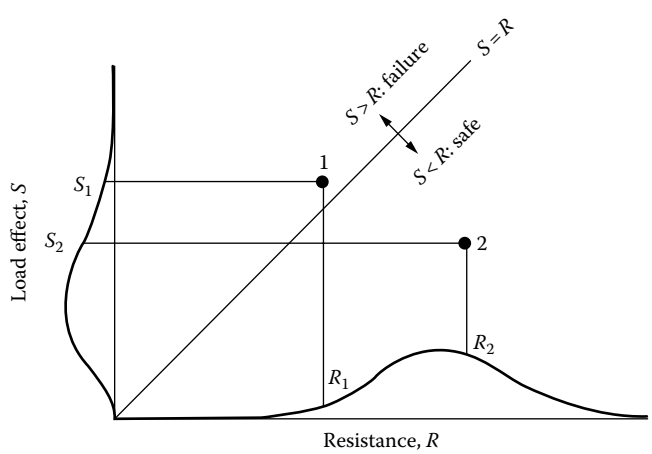

FIGURE 1.27 Safe and unsafe combinations of loads and resistances. (Reproduced from MacGregor, J.G. and White, J.K., *Reinforced Concrete Mechanics and Design*, 4th ed., Pearson/Prentice Hall, Upper Saddle River, NJ, 2005. With permission; MacGregor, J.G., *Can. J. Civil Eng.*, 3(4), 484, December 1976.)

www.EngineeringEBooksPdf.com

the unsafe and safe combination of R and S. Combinations falling below the 45° line represent the condition $S < R$; that is, the load effect (or demand) S is smaller than the resistance R. Accordingly, this represents a *safe* condition. Combinations that are above the 45° line represent the condition $S > R$; that is, the load effect (or demand) is greater than the resistance; therefore, this condition represents failure. For example, the load effect S_1 acting on a structure having resistance R_1 (point 1 in Figure 1.27) indicates failure or unsafe combination of S and R. On the other hand, a load effect S_2 acting on a structure having resistance R_2 (point 2 in Figure 1.27) represents a safe combination of S and R.

As explained in Section 1.4.1, a limit state can be defined as a boundary between the desired and the undesired performances of a structure. For example, the desired and the undesired performances can be explained in the context of a beam having resistance (flexural capacity) R, and the load effect (moment demand) Q. Accordingly, a *limit state function* or *performance function* can be defined as expressed earlier by Equation 1.19* (Nowak and Collins 2013):

$$g(R, Q) = R - Q \tag{1.19}$$

Evidently, the condition $g = 0$ represents the limit between the desired and the undesired performance. The condition $g \geq 0$ represents the desired performance ($R - Q \geq 0$, i.e., the structure is safe), whereas the condition $g < 0$ represents the undesired performance ($R - Q < 0$, i.e., the structure is not safe).

1.5.6.2 Development of AISC LRFD Criteria

1.5.6.2.1 Development of Reliability Index Concept

The concepts of normal distributions and probability discussed in preceding paragraphs can be used to determine *reliability index* (safety factors). AISC's development of reliability indexes for the LRFD of steel structures preceded the development of the same for the LRFD of highway bridges in the United States as specified in the post-2000 AASHTO LRFD Bridge Specifications. A discussion on this important topic can be found in the literature (Fredunthal et al. 1966, Cornell 1969, Ang and Cornell 1974, MacGregor 1976, Ravindra and Galambos 1978, Ellingwood et al. 1980, 1982, Melchers 1999, Nowak and Collins 2013) and is briefly summarized in (AISC 1986, 1998, Nowak 1995, MacGregor and Wight 2013). The following brief summary is based on these references.

Figure 1.28 shows a plot of frequency distributions of resistances R (e.g., axial strength, flexural strength, etc.) of a group of similar structures, having the mean R_m, along the horizontal axis.

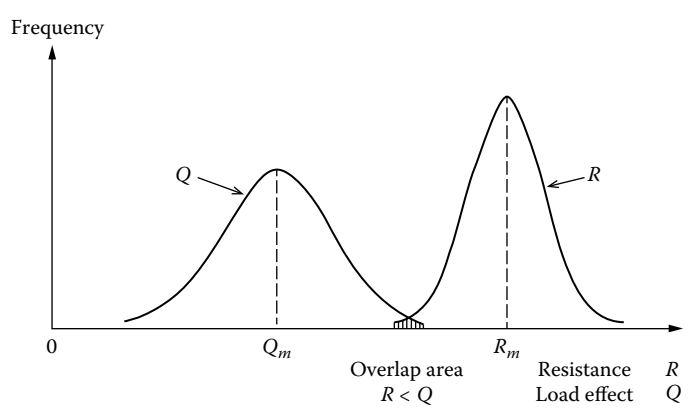

FIGURE 1.28 Frequency distribution of load effect Q and resistance R. (Adapted from American Institute of Steel Construction, 1986. With permission.)

* All equations in this book are numbered to indicate the chapter number followed by the number of equation in that chapter. For example, Equation 3.60 represents equation number 60 in Chapter 3. After the original appearance of an equation it may be referenced in the original chapter or other chapters. When this occurs, it is not a problem.

www.EngineeringEBooksPdf.com

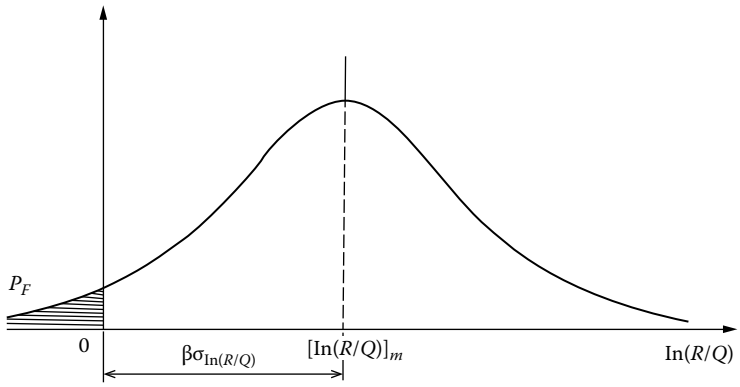

FIGURE 1.29 Illustration of the reliability index, β. (After Ellingwood, B. et al., Development of Probability-Based Load Criterion for American National Standard A58. NBS Special Publication 577, National Bureau of Standards, Department of Commerce, Washington, DC, 1980.)

Also shown on the same axis but centered at a different position (somewhat similar to Figure 1.21) is the distribution of load effects Q (e.g., axial loads, bending moments, etc.), having the mean Q_m, that those structures are expected to experience during their lifetimes. For consistency, it is convenient to express both the resistance (load-carrying capacity) and the load effects (demand) in terms of a quantity such as bending moment. It is easy to see that as long as the resistance R is greater than the load effect Q, a margin of safety for a particular limit state exists. For resistance R to be greater than the load effect Q, the distribution of R must be to the right of distribution of Q; that is, the curve representing R must be centered to the right of the center of the curve representing Q. However, because both Q and R are random variables, there exists a probability that the resistance R may be less than the load effect Q (i.e., probability exists that $R < Q$). In Figure 1.28, this is shown by the small shaded area where the two distributions overlap each other.

Alternatively, the distributions of R and Q can be combined into one function, $R - Q$, according to the CLT as stated earlier, so that these two curves can be transformed into a single-frequency curve as shown in Figure 1.29. Note that the expression $R < Q$ (which represents failure) has been divided by Q (or normalized with respect to Q), and the result expressed logarithmically (i.e., as lognormal distribution), the result being a single-frequency distribution curve that combines the uncertainties of both random variables, the load effect Q and the resistance R; the mean of this lognormal curve is shown as $(\ln(R/Q))_m$. The lognormal, rather than standard normal, distribution was used because the former better represented the distribution of observed data of loads and resistances. Note that some data of this combined distribution are shown to the left of the origin (i.e., negative); it represents the case where $(R - Q)$ may be negative (load effect being greater than the resistance).

Evidently, positive values of $R - Q$ correspond to survival; its negative values correspond to failure. Alternatively, the quotient R/Q can be thought of as a safety factor, and we can make the following statements:

$$\text{Resistance } R \geq \text{load effect } Q \rightarrow R/Q \geq 1.0 \rightarrow \text{Safe}$$
$$\text{Resistance } R < \text{load effect } Q \rightarrow R/Q < 1.0 \rightarrow \text{Failure}$$

Thus, the probability of failure is the probability that R/Q is less than 1.0, which can be mathematically expressed by Equation 1.24:

$$P_f = \text{Prob}\left[\left(\frac{R}{Q}\right) < 1\right] \tag{1.24}$$

www.EngineeringEBooksPdf.com

Taking the natural logarithm of both sides of Equation 1.24, we obtain Equation 1.25:

$$P_f = \text{Prob}\left[\ln\left(\frac{R}{Q}\right) < \ln 1\right] = \text{Prob}\left[\ln\left(\frac{R}{Q}\right) < 0\right] \tag{1.25}$$

Equation 1.25 states that the probability of attaining a limit state ($R < Q$) is equal to the probability that $\ln(R/Q) < 0$ and is represented by the shaded area under the frequency curve to the left of the vertical axis. In other words, *probability of failure*, P_f, is defined as the chance that a particular combination of R and Q would give $\ln(R/Q)$ a negative value (area under the curve to the left of vertical axis) as shown in Figure 1.28. This shaded area (probability of failure) is of concern for it should be less than or equal to what would be acceptable to a code-writing body. Accordingly, a designer's objective is to minimize the shaded area in Figure 1.29 and thus increase reliability (safety). This can be done in one of the two ways (AISC 1986):

1. Move the mean, $[\ln(R/Q)]_m$, to the right (so that the distribution would shift to the right and be centered to a new position to the right of the position shown in Figure 1.29); consequently, this would reduce the shaded area and thus reduce the probability of failure.
2. Reduce the spread (width) of the curve for a given position of the mean relative to the origin (which would also reduce the shaded area and thus reduce the probability of failure).

It is convenient to define the two aforementioned approaches by defining the position of the mean in terms of the standard deviation of the distribution curve, $\sigma_{\ln(R/Q)}$. In Figure 1.29, this position is defined by the distance β times $\sigma_{\ln(R/Q)}$ (or $\beta\sigma_{\ln(R/Q)}$); the factor β is called the *reliability index* or *safety index*. While this approach is simple, it is not amenable to easy solution because the quantity $R - Q$, and hence, quantity $\ln(Q/R)$ is not explicitly known. As discussed in Ellingwood et al. (1980), the distribution shape of each of the many variables (such as materials, loads, etc.) has an influence on the shape of the distribution of $\ln(R/Q)$. While much is known about the variations in loads by themselves and resistances by themselves, the difference between these two has not yet been quantified. However, it is known from the theory of probability that if load and resistance are both random variables, the standard deviation of the difference is given by the CLT, Equation 1.26 (modified from Equation 1.21):

$$\sigma_{(R-Q)} = \sqrt{\sigma_R^2 + \sigma_Q^2} \tag{1.26}$$

where σ_R^2 and σ_Q^2 are, respectively, standard deviations of the frequency distributions of R and Q. Referring to Figure 1.29, Equation 1.26 can be expressed as Equation 1.27 (Ravindra and Galambos 1978, AISC 1998):

$$\beta\sigma_{\ln\left(\frac{R}{Q}\right)} \cong \beta\sqrt{V_R^2 + V_Q^2} \le \ln\left(\frac{R_m}{Q_m}\right) \tag{1.27}$$

Note that in Equation 1.27, the standard deviation, $\sigma_{\ln(R/Q)}$, has been replaced by the approximation $\sqrt{V_R^2 + V_Q^2}$, where

β = reliability index
$V_R = \sigma_R/R_m$ = COV for distribution of resistance R
$V_Q = \sigma_Q/Q_m$ = COV for distribution of load effects Q
σ_R, σ_Q = standard deviations for resistance and load effects, respectively
R_m, Q_m = mean values of the resistance and load effects, respectively

www.EngineeringEBooksPdf.com

It can be shown that for structural elements having usual resistance R_m, load effect Q_m, the coefficients of variation, V_R and V_Q, respectively, for resistance and load effects, can be estimated. Accordingly, the value of reliability index determined from Equation 1.27 and expressed by Equation 1.28 will give a comparative value of the measure of the reliability of a structure or a component (Ravindra and Galambos 1978):

$$\beta = \frac{\ln\left(R_m/Q_m\right)}{\sqrt{V_R^2 + V_Q^2}} \tag{1.28}$$

The importance of the reliability index (or safety index), β, can be seen from Figure 1.29. Note that the larger the value of β, the farther to the right the position of the mean of the probability density function, the smaller the shaded area marked P_F, and, consequently, the smaller the probability of failure. Note that β is a function of both the load effect Q and the resistance R. Therefore, use of the same value of β for all types of members subjected to the same type of loading results in members having relatively uniform strength.

1.5.6.2.2 Target Reliability Indexes for AISC LRFD Specifications

A design code is formatted to cover many situations that a designer may encounter in practice. Its general objective is to ensure that the structures designed according to the provisions of the code would provide a specified, minimum level of safety. Accordingly, acceptable safety levels must be established first so as to serve as a basis for the development of design criteria (Lind 1971). The values of the reliability index, β, accepted by a code-writing body is called *target reliability index* and is expressed by symbol β_T.

Selection of target reliability index is a complex task for it involves many considerations and decision making. It is a multidisciplinary task that involves structural safety analysis, economic analysis, and even the considerations of political decisions. While reliability indexes lower than the target reliability index are generally considered unacceptable, lower values may be justified in exceptional cases (e.g., for simplicity of code format). In some cases, reliability index higher than the target reliability index may be used when design conditions warrant it. For example, a beam designed for flexure may have a reliability index for shear much larger than the target reliability index. Economic ramifications of reliability index become evident when one considers safety in various structures and parts. For example, increasing the safety level in beam connections costs less than increasing the same in the beam itself. Connections are known to fail in a brittle, catastrophic manner; for this reason, the reliability index for connections must be relatively higher (Nowak and Collins 2013).

For the development AISC LRFD criteria (AISC 1986), the values of the target reliability indexes, β_T, were selected as recommended by Ravindra and Galambos (1978), which are shown in Table 1.2.

TABLE 1.2
Target Values of Reliability Index, β_T, for AISC LRFD Specifications

	Loading Conditions		
Type of Component	***D* + (*L* or *S*)**	***D* + *L* + *W***	***D* + *L* + *E***
Members	3.0	2.5	1.75
Connections	4.5	4.5	4.5

Note: D = dead load; L = live load; S = snow load; W = wind load; E = earthquake load.

www.EngineeringEBooksPdf.com

These β_T values were also used in developing Equation 1.29 (Ravindra and Galambos 1978) used for calculating the load and resistance factors, ϕ:

$$\phi = \frac{R_m}{R_n} e^{-0.55\beta V_R} \tag{1.29}$$

Equation 1.29 was developed for establishing reliability indexes for AISC LRFD criteria for steel structures; a discussion of a more refined method for the same has been presented by Ellingwood et al. (1980).

1.5.6.3 Development of AASHTO LRFD Criteria

1.5.6.3.1 Development of Reliability Index Concept

A complete report on the calibration of LRFD Bridge Code is provided by Nowak (1993a) and is summarized in Nowak (1995); the general principles used in this development are discussed in Nowak and Collins (2013) from which the following summary is presented.

For calibration of AASHTO LRFD Bridge Design Specifications, relationships for standard normal distribution (rather than the lognormal distribution) were used as shown in Figure 1.30, so the standard deviation for the distribution of $(R - Q)$ can be expressed by Equation 1.26. With these changes, the reliability index, β, can be expressed by Equation 1.30:

$$\beta = \frac{\bar{R} - \bar{Q}}{\sqrt{\sigma_R^2 + \sigma_Q^2}} \tag{1.30}$$

In Equation 1.30, $\bar{R}$ and $\bar{Q}$ are mean values of R and Q, respectively; σ_R and σ_Q are standard deviations. For a given distribution of loads, probability of failure can be reduced by increasing the distribution of resistances. In Figure 1.30, this would correspond to shifting the distribution of resistances to the right. In general, to ensure safety, the resistance R must be greater than the load effect Q. To explore the probability of failure, let g be the performance function, a function of random variables R and Q expressed by Equation 1.31:

$$g(R, Q) = R - Q \tag{1.31}$$

Probability of failure, P_f, is defined as the chance that a particular combination of R and Q would give $R - Q$ a negative value (which is the area under the curve to the left of vertical axis) as expressed by Equation 1.32:

$$P_f = \text{Prob}(R - Q < 0) = \text{Prob}(g < 0) \tag{1.32}$$

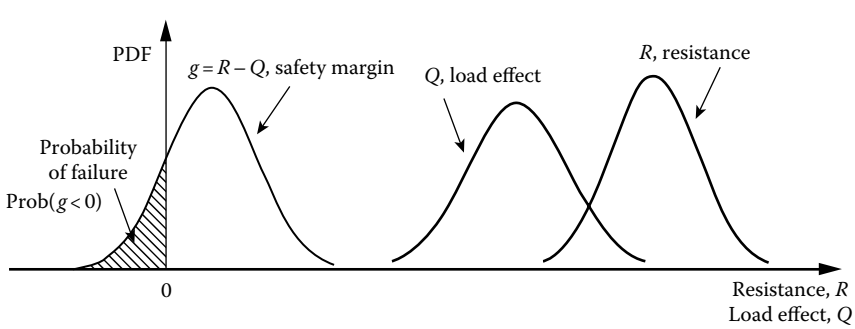

FIGURE 1.30 PDFs of load effect (Q), resistance (R), and safety margin. (After Nowak, A.S. and Collins, K.R., *Reliability of Structures*, CRC Press, Boca Raton, FL, 2013.)

www.EngineeringEBooksPdf.com

Equation 1.32 states that a structure is safe if $g > 0$; the structure fails if $g < 0$. The reliability index β can be calculated by using the principle of transforming the basic variables R (resistance) and Q (load effect) to new, nondimensional variables Z_R and Z_Q (Nowak and Collins 2013) (see Equation 1.14 for the transformation of variables). These transformations are expressed by Equations 1.33 and 1.43:

$$Z_R = \frac{R - \mu_R}{\sigma_R} \tag{1.33}$$

$$Z_R = \frac{Q - \mu_Q}{\sigma_Q} \tag{1.34}$$

Equations 1.33 and 1.34 can be simplified and expressed in terms of R and Q:

$$R = \mu_R + Z_R\sigma_R \tag{1.35}$$

$$Q = \mu_Q + Z_Q\sigma_Q \tag{1.36}$$

Substitution of Equations 1.35 and 1.36 in Equation 1.31 results in Equation 1.37:

$$g(R, Q) = g(Z_R, Z_Q) = (\mu_R - \mu_Q) + Z_R\sigma_R - Z_Q\sigma_Q \tag{1.37}$$

Equation 1.37 expresses the function $g(R, Q)$ in terms of the reduced variables, Z_R, Z_Q; it is referred to as the *limit state function* and expressed as $g(Z_R, Z_Q)$. It represents a straight line for any specific values of $g(Z_R, Z_Q)$ in the space of reduced variables Z_R and Z_Q as shown in Figure 1.31. As shown by Hasofer and Lind (1974), the reliability index, β, is defined as the *shortest* distance from the origin of the reduced variables to the line $g(Z_R, Z_Q)$, shown as line OC in Figure 1.31.

The value of β (distance OC) can be determined from the geometry of Figure 1.31. Let angle OBA = θ. From ΔOCB, we obtain

$$\beta = \left(\frac{\mu_R - \mu_Q}{\sigma_R}\right)\sin\theta \tag{1.38}$$

From ΔOAB, we obtain

$$AB = \sqrt{OB^2 + OA^2} = \sqrt{\left(\frac{\mu_R - \mu_Q}{\sigma_R}\right)^2 + \left(\frac{\mu_R - \mu_Q}{\sigma_Q}\right)^2} \tag{1.39}$$

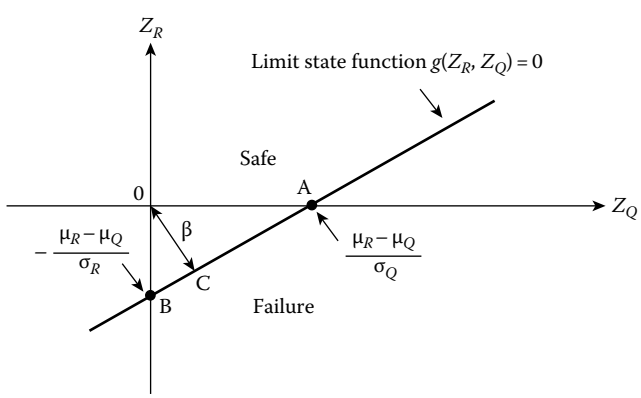

FIGURE 1.31 Reliability index defined as the shortest distance in the space of reduced variable. (Adapted from Nowak, A.S. and Collins, K.R., CRC Press, Boca Raton, FL, 2013; Ellingwood, B. et al., J. *Struct. Div.*, 108, 978, 1982.)

www.EngineeringEBooksPdf.com

Also, from ΔOAB, we obtain

$$\sin\theta = \frac{AO}{AB} = \frac{\left(\mu_R - \mu_Q/\sigma_Q\right)}{AB} \tag{1.40}$$

Substitution for AB from Equation 1.39 and for sin θ from Equation 1.40 into Equation 1.38 yields Equation 1.41:

$$\beta = \frac{\left(\frac{\mu_R - \mu_Q}{\sigma_R}\right)\left(\frac{\mu_R - \mu_Q}{\sigma_Q}\right)}{\sqrt{\left(\frac{\mu_R - \mu_Q}{\sigma_R}\right)^2 + \left(\frac{\mu_R - \mu_Q}{\sigma_Q}\right)^2}} \tag{1.41}$$

Equation 1.41 can be simplified to yield Equation 1.42:

$$\beta = \frac{\mu_R - \mu_Q}{\sqrt{\sigma_R^2 + \sigma_Q^2}} \tag{1.42}$$

$$\beta = \frac{\bar{R} - \bar{Q}}{\sqrt{\sigma_R^2 + \sigma_Q^2}} \tag{1.30}$$

Note that Equation 1.42 is the same as Equation 1.30, in which the mean $\mu_R = \bar{R}$ and the mean $\mu_Q = \bar{Q}$. The format of Equation 1.30 is used for further discussion later in this section.

1.5.6.3.2 Relationship between the Reliability Index and Probability of Failure

It is noted from the preceding discussion that the reliability index, β, is directly related to the probability of failure, P_f. That relationship can be expressed by Equation 1.43:

$$\beta = -\Phi^{-1}\left(P_f\right) \tag{1.43}$$

where Φ^{-1} = inverse standard distribution function.

Conversely, Equation 1.43 can be expressed as Equation 1.44:

$$P_f = \Phi(-\beta) \tag{1.44}$$

Values of the reliability index corresponding to a chosen probability of failure can be read directly from Table 1.A.1 by using the principle of reduced variables as discussed in Section 1.5.5.1 (refer to Equation 1.14). Since the total area under a normal curve = 1.0, knowing the distance βσ as shown in Figure 1.32, the value of P_f can be read directly from Table 1.A.1. See Example 1.6, which illustrates reading the values of β corresponding to a chosen value of P_f. Equation 1.43 is presented in a tabular from in Table 1.3 for selected values of β. Table 1.4 (Nowak and Collins 2013) presents a relationship between the reliability index and the probability of failure.

We can now define the reliability, S, as expressed by Equation 1.45:

$$S = 1 - P_f \tag{1.45}$$

Substitution for P_f from Equation 1.44 into Equation 1.45 yields Equation 1.46:

$$S = \left[1 - \left\{\Phi\left(-\beta\right)\right\}\right] \tag{1.46}$$

Table 1.5 shows the relationship between the reliability index (β), reliability (S), and the probability of failure (P_f).

www.EngineeringEBooksPdf.com

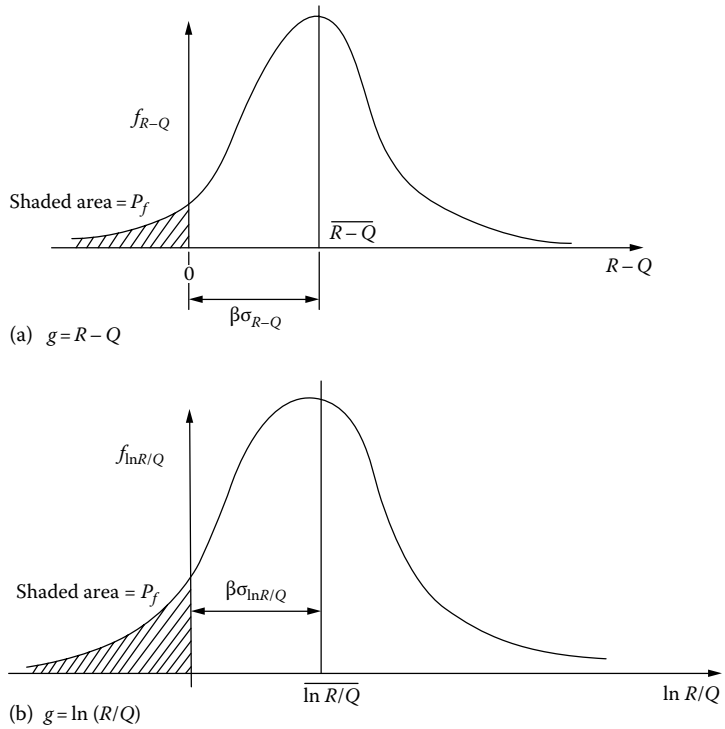

FIGURE 1.32 Probability of failure and reliability index: (a) standard normal distribution and (b) lognormal distribution. The shaded areas represent probability of failure.

TABLE 1.3
Reliability Index and Probability of Failure (Equation 1.43)

Reliability Index, β	Probability of Failure, $P_f = \Phi(-\beta)$
0.5	3.09 (10^{-1})
1.0	0.16 (10^{-1})
1.5	0.07 (10^{-1})
2.0	0.23 (10^{-2})
2.5	0.62 (10^{-2})
3.0	1.30 (10^{-3})
3.5	2.00 (10^{-4})
4.0	3.00 (10^{-5})
5.0	3.00 (10^{-7})

Now that we have established a relationship between the reliability index, reliability, and the probability of failure, Table 1.A.1 can be used to obtain important information. For example, $\beta = 2.0$ (under the z-column) corresponds to area under the curve = 0.9772; that is, 97.72 percent of the values are included under the normal distribution curve, or stated differently, only 2.3 of 100 values are not included. But if β is increased to 3.5, the corresponding area under the curve increases to 0.9998 (or 0.999767 as shown in Table 1.5), that is, 99.98 percent values are included under the normal distribution curve, or stated differently, only two values out of approximately 10,000 are *not* included. More precisely, as shown in Table 1.5, $\beta = 3.5$ means that the probability of failure is 233 out of one million (or approximately 2 in 10,000). This illustrates the significance of establishing the target reliability index, β_T.

www.EngineeringEBooksPdf.com

TABLE 1.4
Probability of Failure and Reliability Index (Equation 1.44)

Probability of Failure, P_f	Reliability Index, β
10^{-1}	1.28
10^{-2}	2.33
10^{-3}	3.09
10^{-4}	**3.71**
10^{-5}	**4.26**
10^{-6}	**4.75**
10^{-7}	**5.19**
10^{-8}	**5.62**
10^{-9}	**5.99**

Source: Nowak, A.S. and Collins, K.R., *Reliability of Structures*, CRC Press, Boca Raton, FL, 2013.

Note: The values in bold cannot be read from Table 1.A.1 because of the tabulated values at 0.01 intervals are cutoff at –3.409. Extended values can be found in handbooks.

TABLE 1.5
Reliability Index, Reliability, and Probability of Failure

Reliability Index, β	Reliability, $S = 1 - P_f$	Probability of Failure, P_f
0.0	0.500	$0.500 \times 10^{+0}$
0.5	0.691	$0.309 \times 10^{+0}$
1.0	0.841	$0.159 \times 10^{+0}$
1.5	0.933 2	0.668×10^{-1}
2.0	0.977 2	0.228×10^{-1}
2.5	0.993 79	0.621×10^{-2}
3.0	0.998 65	0.135×10^{-2}
3.5	0.999 767	0.233×10^{-3}
4.0	0.999 968 3	0.317×10^{-4}
4.5	0.999 996 60	0.340×10^{-5}
5.0	0.999 999 713	0.287×10^{-6}
5.5	0.999 999 981 0	0.190×10^{-7}
6.0	0.999 999 999 013	0.987×10^{-9}
6.5	0.999 999 999 959 8	0.402×10^{-10}
7.0	0.999 999 999 998 72	0.128×10^{-11}
7.5	0.999 999 999 999 998 1	0.319×10^{-13}
8.0	0.999 999 999 999 999 389	0.317×10^{-15}

Example 1.6

From Table 1.A.1, determine the reliability index, β, corresponding to probability of failure of (a) 1 in 10 (or $P_f = 10^{-1}$), (b) 1 in 100 (or $P_f = 10^{-2}$), and (c) 1 in 1000 (or $P_f = 10^{-3}$).

Solution

Note that the area under a standard normal distribution curve = 1.0. The negative values in Table 1.A.1 represent negative areas, which represent the probability of failure, P_f. Note that $z = \beta\sigma$ as shown in Figure 1.32. For a probability density curve, mean $\mu = 0$ and the standard deviation $\sigma = 1.0$; therefore, as shown in Figure 1.32, $z = \beta\sigma = \beta$ (= reliability index).

www.EngineeringEBooksPdf.com

a. In Table 1.A.1, find the value $F(z) = 10^{-1}$ or 0.1000; the value closest to it is seen to be 0.1003, for which $z = -1.28$. Therefore, $\beta = 1.28$.
b. In Table 1.A.1, find the value $F(z) = 10^{-2}$ or 0.0100; the value closest to it is seen to be 0.0099, for which $z = -2.33$. Therefore, $\beta = 2.33$.
c. In Table 1.A.1, find the value $F(z) = 10^{-3}$ or 0.0010; this value corresponds to $z = -3.08$ or -3.09. Therefore, $\beta = 3.08$ or 3.09.

Note: A *very approximate* value of β corresponding to $P_f = 10^{-4}$ (= 0.0001) can be calculated using straight-line interpolation of values for $z = -3.5$ (for $\beta = 0.0002$) and $z = -4.0$ (for $\beta = 0.00003$) shown in Table 1.A.1; the approximate value is calculated to be 3.79, which is close to the correct value of 3.71 shown in Table 1.3. In practice, such interpolations should *not* be used because of the asymptotic nature of the bell curve. Values of reliability indexes corresponding to smaller probabilities can be read directly from the tables found in handbooks.

Equation 1.42 can be modified for the general case of n variables where the variables are *uncorrelated* (Nowak and Collins 2013). A simple example of such a case would be a beam subjected to two variables—a uniform load and a concentrated load, which are not correlated. The reliability index for such cases, called the Hasofer–Lind reliability index, can be determined by considering a limit state function $g(X_i)$ as a function of several random, uncorrelated variables $X_1, X_2, X_3, \ldots X_n$:

$$g\left(X_i\right) = g\left(X_1, X_2, X_3, \ldots X_n\right) \tag{1.47}$$

For variables $X_1, X_2, X_3, \ldots X_n$, we can define reduced variables $Z_1, Z_2, Z_3, \ldots Z_n$ as defined earlier by Equation 1.33:

$$Z_i = \frac{X_i - \mu_{x_i}}{\sigma_{x_i}} \tag{1.48}$$

The limit state function given by Equation 1.47 can now be expressed in terms of reduced variables as follows:

$$Z_1 = \frac{X_1 - \mu_{x_1}}{\sigma_{x_1}} \tag{1.49}$$

$$Z_2 = \frac{X_2 - \mu_{x_2}}{\sigma_{x_2}} \tag{1.50}$$

$$Z_3 = \frac{X_3 - \mu_{x_3}}{\sigma_{x_3}} \tag{1.51}$$

and so on. The reliability index for this case, β, is defined as the *shortest* distance from the origin in the n-dimensional space of the reduced variables to the curve described by $g(Z_1, Z_2, Z_3, \ldots Z_n)$.

A concept related to reliability index is *first-order second-moment (FOSM) reliability index* for *linear* limit state function of the form given by Equation 1.52 (see discussion in Melchers 1999, Ch. 4):

$$g\left(X_i\right) = g\left(X_1, X_2, X_3, \ldots X_n\right) = a_0 + a_1X_1 + a_2X_2 + a_3X_3 + \cdots + a_nX_n \tag{1.52}$$

where $a_1, a_2, a_3 \ldots a_n$ are constants. Equation 1.52 can be expressed in a compact as Equation 1.53:

$$g\left(X_i\right) = a_0 + \sum_{i=1}^{n} a_iX_i \tag{1.53}$$

www.EngineeringEBooksPdf.com

Following the earlier-described procedure, the reliability index can be expressed by Equation 1.54:

$$\beta = \frac{a_0 + \sum_{i=1}^{n} a_i \mu_{x_i}}{\sqrt{\sum_{i=1}^{n} \left(a_i \sigma_{x_i}\right)^2}} \tag{1.54}$$

An important property of Equation 1.54 is that the reliability index, β, depends only on the values of the means and the standard deviations. The value of β given by Equation 1.54 is called a *second-moment* measure of structural safety because only the first moments (mean and variance) are required to calculate β. Example 1.7 illustrates the application of Equation 1.54 for calculating reliability index of a simple beam.

Example 1.7

A simply supported WF steel beam spanning 20 ft carries a uniform load w = 2.4 kip/ft and a concentrated load P = 16 kip at the midspan (see Figure 1.33). The plastic section modulus, Z, of the beam is 60 in.^{3} and F_y = 50 ksi. The loads are random variables. Assume that P, w, and the yield stress F_y are random quantities. The length L and the plastic modulus, Z, are deterministic and precisely known.

The distribution parameters loads (P and w) and the yield stress (F_y) are as follows:

Nominal (design) value of $w = w_n$ = 2.4 kip/ft = 0.20 kip/in.
  Bias factor for $w = \lambda_w$ = 1.0 (= ratio of mean value divided by the nominal value)
  $\mu_w = \lambda_w w_n$ = (1.0) kip/ft = 0.20 kip/in.
  V_w = 10 percent ⇒ $\sigma_w = V_w \mu_w$ = 0.24 kip/ft = 0.02 kip/in.
Nominal design of $P = p_n$ = 16.0 kip
  Bias factor for $P = \lambda_p$ = 0.85
  $\mu_p = \lambda_p p_n$ = 0.85(16.0) = 13.6 kip
  V_p = 11 percent ⇒ $\sigma_p = V_p \mu_p$ = (0.11)(13.6) = 1.496 ≈ 1.5 kip
Nominal design value of $F_y = f_y$ = 50 ksi
  Bias factor for $F_y = \lambda_F$ = 1.12
  $\mu_F = \lambda_F f_y$ = 1.12(50) = 56.0 ksi
  V_F = 11.5 percent ⇒ $\sigma_F = (V_F)(\mu_F)$ = (0.115)(56.0) = 6.44 ksi
Calculate the reliability index.

Solution

The limit state function for beam bending can be expressed as

$$g\left(P, w, F_y\right) = F_y Z - \frac{PL}{4} - \frac{wL^2}{8}$$

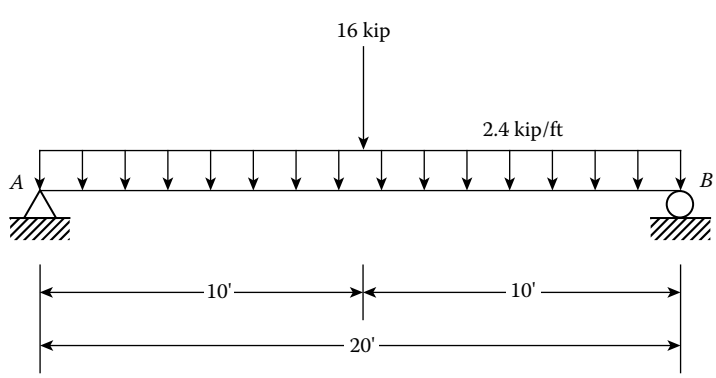

FIGURE 1.33 Beam for Example 1.7.

www.EngineeringEBooksPdf.com

Substituting F_y = 6.44 ksi, L = 20 ft in the aforementioned equation and converting all units to inches, the limit state function can be rewritten as

$$g\left(P,w,F_y\right)=60F_y-60P-7200w$$

Since the limit state function is linear, Equation 1.54 can be used to determine the reliability index β:

$$\beta=\frac{a_o+\sum_{i=1}^{n}a_i\mu x_1}{\sqrt{\sum_{i=1}^{n}\left(a_ix_i\right)^2}}=\frac{60(56.0)-60(13.6)-7200(0.2)}{\sqrt{\left[(60)(6.44)\right]^2+\left[(-60)(1.5)\right]^2+\left[(-7200)(0.02)\right]^2}}$$

$$=\frac{1104}{422.07}=2.62$$

Reliability index, β = 2.78.

So, what is the significance of β = 2.62? From Table 1.A.1, the value of $Pf(=F(z)$ in Table 1.A.1) corresponding *to* $z=-2.62$ is 0.0044; that is, the probability of failure is 44 in 10,000, or approximately 1 in 227.

1.5.6.3.3 Reliability Indexes and Load and Resistance Factors for AASHTO LRFD Specifications

As was mentioned earlier, use of normal and lognormal distributions for the purpose of determining the reliability index depends on the nature of data, that is, whether data can be represented by normal or lognormal distribution. Based on the nature of distribution, the load Q was considered as a normal random variable, whereas the resistance R was considered as a lognormal random variable for the calibration of AASHTO LRFD Specifications (Nowak 1993a). The expression for the reliability index corresponding to these distributions is given by Equation 1.55 (Nowak 1993a):

$$\beta=\frac{R\left(1-kV_R\right)\left[1-\ln\left(1-kV_R\right)\right]-Q}{\sqrt{\left[\sigma_RV_R\left(1-kV_R\right)\right]^2+\sigma_Q^2}} \tag{1.55}$$

Equation 1.55 can be expressed in terms of given data (R_n, λ_R, V_R, $\bar{Q}$, and σ_Q) as given by Equation 1.56:

$$\beta=\frac{R_n\lambda_R\left(1-kV_R\right)\left[1-\ln\left(1-kV_R\right)\right]-Q}{\sqrt{\left[R_nV_R\lambda_R\left(1-kV_R\right)\right]^2+\sigma_Q^2}} \tag{1.56}$$

where

R_n = nominal (design) value of resistance
λ_R = bias factor for resistance (= mean value/nominal value, Equation 1.9)
k = parameter whose value depends on the design point (in practice, k = 2)

AASHTO LRFD Specifications represent an overhaul of its predecessor, the AASHTO Standard Specifications, which had been used successfully for many years. Bridges designed according to the provisions of Standard Specifications have served very well. Therefore, as a guide to the selecting target reliability indexes for highway bridges to be designed according to the provisions of the LRFD Specifications, the past performance of the bridges served as a valuable guide. The reliability indexes of many old bridges were calculated and used for comparison purposes.

www.EngineeringEBooksPdf.com

Equation 1.30 (or Equation 1.42) makes the starting point for the calibration process for LRFD code. The basic design relationship can be expressed by Equation 1.57, which states that the factored resistance must be equal to or greater than the factored loads:

$$\phi R \geq Q = \sum \gamma_i x_i \tag{1.57}$$

where

ϕ = resistance factor (or the strength reduction factor)
γ_i = load factor for an arbitrary load

Alternatively, R can be expressed in terms of factored load and the resistance factor:

$$R \geq \frac{1}{\phi} \sum \gamma_i x_i \tag{1.58}$$

From Equation 1.30, $\bar{R}$ can be expressed in terms of $\bar{Q}$ and the square root of the sum of the squares of the standard deviations for R and Q, as given by Equation 1.59:

$$\bar{R} = \bar{Q} + \beta\sqrt{\sigma_R^2 + \sigma_Q^2} = \lambda R \tag{1.59}$$

where λ = bias factor = ratio of mean value divided by the nominal value (see Equation 1.9). Substitution of R from Equation 1.58 into 1.59 yields

$$\bar{R} = \lambda R = \frac{1}{\phi} \lambda \sum \gamma_i x_i \tag{1.60}$$

Equating the values of $\bar{R}$ from Equations 1.59 and 1.60, we obtain the following result:

$$\frac{1}{\phi} \lambda \sum \gamma_i x_i = \bar{Q} + \beta\sqrt{\sigma_R^2 + \sigma_Q^2} \tag{1.61}$$

The value of ϕ, the resistance factor (or the strength reduction factor), can be expressed by Equation 1.62 by rearranging Equation 1.61:

$$\phi = \frac{\lambda \Sigma \gamma_i x_i}{Q + \beta\sqrt{\sigma_R^2 + \sigma_Q^2}} \tag{1.62}$$

Equation 1.62 can be used to calculate the values of the resistance factors ϕ. Clearly, Equation 1.62 cannot be solved in the form shown because it contains *three* variables: the resistance factor, ϕ, the reliability index, β, and the load factors, γ. However, Equation 1.61 can be solved if we begin with a target value of the reliability index, β_T, as discussed in the next section.

1.5.6.4 Calibration Procedure

AASHTO LRFD Specifications are based on the assumption that both loads and resistances are normal random variables, each of which can be represented by a bell-shaped curve (normal or Gaussian distribution). A complete discussion of the calibration procedure used for the development of AASHTO LRFD Specifications is beyond the scope of this book. Pertinent information is reported in Nowak (1993) and summarized elsewhere (Nowak 1993a,b, 1995, 1999, Kulicki 1999);

www.EngineeringEBooksPdf.com

the relevant procedures are discussed in Nowak and Collins (2013). The calibration involved a multistep procedure summarized briefly as follows.

Step 1. Using the experience with design of bridges based on 1992 Standard Specifications (AASHTO 1992), a database of their reliability indexes was created as reported in Nowak (1993). This database consisted of some 200 bridges from various geographical regions of the United States to represent a full range of materials, types, and spans, which were characteristic of the region. Emphasis was placed on current and future trends instead of very old bridges. This was done by sending questionnaires to various departments of transportation asking them to identify the future trends (i.e., types of bridges being considered for future construction). For each selected bridge, load effects were calculated for various components; also load-carrying capacities were calculated.

Step 2. A statistical database for load (Q) and resistance (R) parameters was established. This included available data on load components including surveys and other measurements. Truck survey data and weigh-in-motion (WIM) data were used for modeling live load. Field data on dynamic load were scant; so a numerical procedure was developed to simulate the dynamic bridge behavior. Statistical data for resistance included material tests, component tests, and field measurements. Numerical procedures were developed for simulating the behavior of large components and systems.

Step 3. Development of load (Q) and resistance (R) models: As discussed earlier, loads and resistance were treated as random variables. Their variation was described by cumulative distribution function (CDFs) and correlations. The live load model (discussed in Chapter 3) included multiple presence of trucks in one lane and in the adjacent lanes. The dynamic load was modeled for two cases: (1) a single truck and (2) two trucks, side-by-side. Resistance models were developed for girder bridges (Collins and Mitchell 1991, Zokaie et al. 1991, Nowak et al. 1993). Simulations were used to determine the variation of the ultimate strength.

Step 4. Development of reliability analysis procedure: Structural performance was measured in terms of probability of failure (P_f) as discussed in the preceding sections. Reliability was measured in terms of the reliability (or safety) index as discussed earlier by using an iterative procedure.

Step 5. Selection of target reliability index, β_T (defined in the preceding section): Reliability indexes were calculated for a wide variety of bridges designed according to AASHTO Standard Specifications (AASHTO 1992). The performance of existing bridges was evaluated to determine the adequacy of their reliability level. A comparison of reliability indexes for bridges designed according to 1989 AASHTO Standard Specifications (not substantially different from 1992 AASHTO Standard Specifications) and for the proposed AASHTO LRFD Specifications is presented in Figure 1.34 from Kulicki (1999). A target reliability index, $\beta_T = 3.5$, was selected based

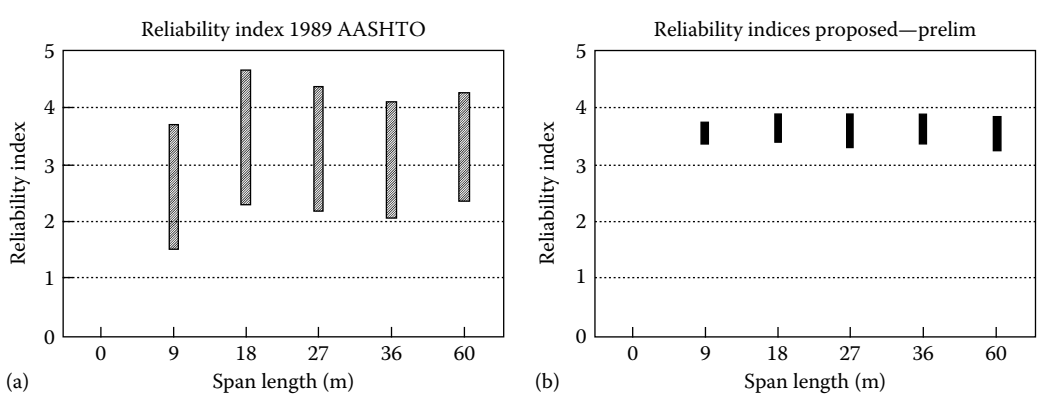

FIGURE 1.34 Reliability indexes inherent in (a) 1989 AASHTO Standard Specifications and (b) AASHTO LRFD Specifications. (From Kulicki, J., Design philosophies for highway bridges, in *Bridge Engineering Handbook*, W.-F. Chen and L. Duan, ed., CRC Press, Boca Raton, FL, 1999.)

www.EngineeringEBooksPdf.com

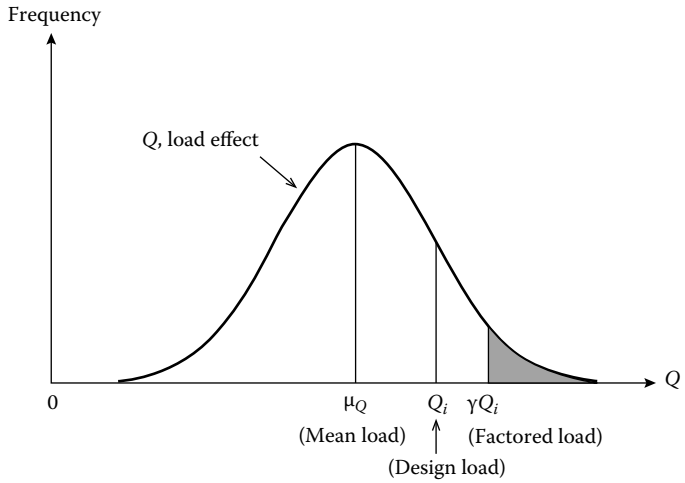

FIGURE 1.35 Relationships among nominal load, mean load, and factored load. (From Nowak, A.S. and Collins, K.R., *Reliability of Structures*, CRC Press, Boca Raton, FL, 2013.)

on the fact that (1) it was used for the Ontario Highway Bridge Design Code (OHBDC), (2) it was under consideration for other reliability-based specifications, and (3) it was representative of the past LFD. A discussion on the sensitivity of the reliability index to probability of failure was presented in the preceding section.

Step 6. Calculation of load and resistance factors: Load factors, γ, were calculated such that the factored loads had a predetermined probability of being exceeded. Figure 1.35 shows the relationship between the mean load, design load, and the factored load. Likewise, Figure 1.36 shows the relationship between reduced resistance, design resistance, and the mean resistance. Resistance factors, ϕ, are calculated so that the structural reliability is close to the target value β_T (see discussion in Section 1.5.6.2.2).

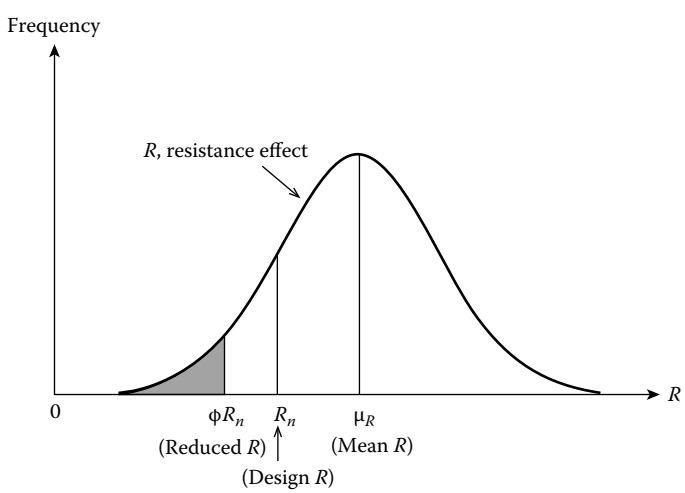

FIGURE 1.36 Relationships among nominal resistance, mean resistance, and factored (reduced) resistance. (From Nowak, A.S. and Collins, K.R., *Reliability of Structures*, CRC Press, Boca Raton, FL, 2013.)

www.EngineeringEBooksPdf.com

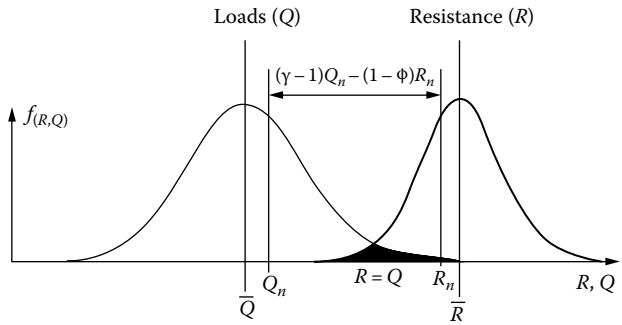

FIGURE 1.37 Separation of loads and resistance. (*Note*: $\bar{Q}$ is the mean value of load; $\bar{R}$ is the mean value of resistance; Q_n is the nominal value of load; R_n is the nominal value of the resistance.) (From Kulicki, J., Design philosophies for highway bridges, in *Bridge Engineering Handbook*, W.-F. Chen and L. Duan, ed., CRC Press, Boca Raton, FL, 1999.)

Figure 1.37 shows a combined distribution of the probability function, $R - Q$, in which a second value for both the load and the resistance, called the nominal load and resistance values, Q_n and R_n, respectively, is shown. These values are somewhat offset from the mean values of load and resistance, $\bar{Q}$ and $\bar{R}$, respectively. As defined by Equation 1.9, the ratio of mean value divided by the nominal value ($\bar{Q}/Q_n$ or $\bar{R}/R_n$) is called *bias*. The overlap area in this figure represents cases where the resistance is smaller than the load effect, an undesirable condition. The objective of calibration is to separate the distribution of load from the distribution of resistance in such a way that the area of overlap is as small as possible. To achieve this objective, the load and resistance factors were so developed that the overlap area was small enough to be acceptable by the code-writing body.

1.5.6.5 Calibration of Load and Resistance Factors

Referring to Equation 1.58, it is noted that once the target value of the reliability index, β_T (= β in Equation 1.58) has been established, both the load and resistance factors must be found, which depend on each other. Therefore, it becomes necessary to first select one of the factors in order to the value of the other. A practice used by several code-writing bodies (OHBDC 1994, AASHTO 1996, CSA 1998) was to first select load factors and then calculate the resistance factors. The steps used in this procedure have been reported by Kulicki (1999) as follows:

1. The factored loads are defined as the average value of load, x_i, plus some number (parameter k in Equation 1.63) times the standard deviations of the load, $k\sigma_i$, as expressed by Equation 1.63:

$$\gamma_i x_i = \bar{x}_i + k\sigma_i \tag{1.63}$$

where k = a constant that is determined based on the target exceedance probability of the load (Nowak and Collins 2013). From Equation 1.8, the variance, $V = \sigma\bar{x}$, so that $\sigma = V\bar{x}$, substitution of which in Equation 1.63 results in Equation 1.64:

$$\gamma_i x_i = \bar{x}_i + kV_i\bar{x}_i = \bar{x}_i(1 + kV_i) \tag{1.64}$$

www.EngineeringEBooksPdf.com

TABLE 1.6
Parameters of Bridge Load Components

Load Component	Bias Factor, λ	Coefficient of Variation, V_i	Load Factor, γ_i		
			$k = 1.5$	$k = 2.0$	$k = 2.5$
Dead load, shop built	1.03	0.08	1.15	1.20	1.24
Dead load, field built	1.05	0.10	1.20	1.25	1.30
Dead load, asphalt and utilities	1.00	0.25	1.375	1.50	1.65
Live load (with impact)	1.10–1.20	0.18	1.40–1.50	1.50–1.60	1.60–1.70
Final value of load factor for live load (with impact) adopted				1.75	

Source: After Nowak, A.S., Calibration of LRFD bridge design code, NCHRP Project 12-33, Report 368, University of Michigan, Ann Arbor, MI, 1993a.

Noting that the ratio of mean value divided by the nominal value, $\bar{x}_i/x_i = \lambda$ = bias factor (Equation 1.9), Equation 1.64 can be rearranged and expressed as Equation 1.65:

$$\gamma_i = \lambda(1 + kV_i) \tag{1.65}$$

Equation 1.65 expresses load factor in terms of the bias and the variance. It states that load factors can be defined so that all loads have the same probability of being exceeded during the design life. The underlying idea is not to say that all load factors are identical; rather, it is that probability of loads being exceeded is the same. Table 1.6 (Nowak 1993a,b) summarizes parameters of bridge load components and various sets of load factors corresponding to different values of the parameter k in Equation 1.65. Recommended values of load factors correspond to $k = 2$.

2. By using Equation 1.65 for a given set of load factors, the value of resistance factors was assumed for various types of structural members and for various load components (bending moments, shear, etc.). Computer simulation was used to yield a large number of values for the reliability indexes.
3. Reliability indexes were compared with the target reliability index. A close clustering of results indicated that a suitable combination of load and resistance factors had been obtained.
4. If the computer simulation did not result in close clustering, a new trial set of load factors was used and process repeated until the reliability indexes did cluster around, and acceptably close to, the target reliability index.

1.5.7 AASHTO LRFD Specifications Format of Load and Resistance Relationship

1.5.7.1 Loads, Resistance, and Factor of Safety

In design, irrespective of the design philosophy adopted, providing safety is the primary objective. When following the ASD, the generalized design equation, sometimes referred to as *equation of sufficiency* (Kulicki 1999), can be expressed in the form of Equation 1.66:

$$\sum Q_i = \frac{R_E}{FS} \tag{1.66}$$

where
Q_i = a load
R_E = the elastic resistance
FS = the factor of safety

www.EngineeringEBooksPdf.com

A generalized equation for LRFD can be written in a slightly different form of Equation 1.66, which can be expressed as Equation 1.67:

$$\phi R \geq \sum \gamma_i Q_i \tag{1.67}$$

where

γ_i = load factor, a statically based multiplier on force effects
Q_i = a load
R = resistance
ϕ = resistance (or modification) factor; a statistically based multiplier applied to nominal resistance as specified in various AASHTO LRFD Specifications Sections 5, 6, 7, 8, 10, 11, and 12 (these sections deal with material-specific designs)
≤ 1.0

Equation 1.67 is the standard format of LRFD Specifications that had been derived in the early 1980s (AISC 1986, Equation C-A5-1, p. 6-143) for the design of steel buildings. It states that the modified capacity (or the modified resistance, ϕR) of a structural member must be greater than or equal to the sum of effects of all loads acting on the member ($\Sigma\gamma_i Q_i$). In the calibration process, the load and resistance factors were selected with a view that $\beta = \beta_T = 3.5$. A design situation involves starting with the design load and the factored load (calculated values), and coming up with a design to provide factored resistance (i.e., modified load-carrying capacity) having an acceptable level of reliability and safety indexes.

For LRFD of highway bridges, Equation 1.67 is expressed slightly differently, as Equation 1.68 (AASHTO LRFD Art. 1.3.3.1)*:

$$\sum \eta_i \gamma_i Q_i \leq \phi R_n = R_r \tag{1.68}$$ [AASHTO LRFD 1.3.2.1-1]

The left side of Equation 1.68 represents the required resistance determined from structural analyses based on the assumed loads, whereas the right side represents a limiting load-carrying capacity provided by the selected members. In LRFD as in LFD, a designer essentially compares the effects of factored loads (left side of Equation 1.68) to the strength (or resistance) actually provided (the right side of Equation 1.68); an acceptable design must satisfy Equation 1.68.

In Equation 1.68, η_i = a load modifier, a factor relating to ductility, redundancy, and operational importance (discussed later in this section); it is the product of three load modifiers representing those attributes and is expressed as Equation 1.69:

$$\eta_i = \eta_D \, \eta_R \, \eta_I \tag{1.69}$$

In Equation 1.69, the value of η_i is prescribed as follows:

1. For loads for which a maximum value of γ_i is appropriate:

$$\eta_i = \eta_D \, \eta_R \, \eta_I \geq 0.95 \tag{1.70}$$ [AASHTO LRFD 1.3.2.1-2]

* Frequently, equations will have double numbers followed by AASHTO LRFD Specifications in square brackets. For example, Equation 4.8 [A5.4.2.4-10] indicates Equation 4.8 in Chapter 4; the number A5.4.2.4-10 indicates equation number from AASHTO LRFD Specifications (alphabet A is used to reference AASHTO). Likewise, Equation 4.9 [AC5.4.2.4-1] indicates Equation 4.9 in Chapter 4; the number AC5.4.2.4-1 indicates Equation C5.4.2.4-1 from AASHTO Commentary (alphabet C is used to reference to the Commentary section of AASHTO LRFD Specifications).

www.EngineeringEBooksPdf.com

2. For loads for which a minimum value of γ_i is appropriate:

$$\eta_i = \frac{1}{\eta_D \, \eta_R \, \eta_I} \leq 1.0 \qquad (1.71) \text{ [AASHTO LRFD 1.3.2.1-2]}$$

where
η_i = load modifier
η_D = a factor relating to ductility
η_R = a factor relating to redundancy
η_I = a factor relating to operational importance
Q_i = nominal force effect, a deformation, stress or stress resultant
R_n = nominal resistance, based on the dimension shown on the plans and on the permissible stresses, deformations, or specified strength of materials
R_r = factored resistance = ϕR_n

In LRFD, Equation 1.68 is to be applied to each component and connection to be designed as appropriate for each limit state under consideration. Recognize that the influence of η_i on design is to increase (when $\eta_i > 1.0$) or decrease (when $\eta_i < 1.0$) the load effects, the latter having a beneficial effect on design (because the member or the connection to be designed has to resist a smaller force).

An important clarification about the load modifier η, which is grouped on the load side of Equation 1.68, and which is intended to take into account ductility, redundancy, and operational importance, should be noted. The first two of these factors are directly related to the physical strength and performance of the bridge, the last is related to the consequences of the bridge being out of service. According to AASHTO (2012, Com. 1.3.2.1), grouping of these factors on the left side of Equation 1.68 is arbitrary; *it represents as the first effort of codification*. In the absence of more precise information, effects of each of these factors, except that for fatigue and fracture, are estimated as ±5 percent accumulated geometrically. Future research into quantification of ductility, redundancy, and operational importance and their interaction with system reliability may lead to changes in Equation 1.68.

It is important to recognize the *whys* and the significance of the resistance factor ϕ (referred to as strength reduction factor in concrete and masonry design codes), a statistically based multiplier applied to nominal resistance as specified in various sections of AASHTO LRFD Highway Bridge Design Specifications. First, note that (1) the resistance, R, is a random variable, and (2) $\phi \leq 1.0$ always because there is always the possibility that actual resistance may be less than the nominal resistance, R_n, as determined from the LRFD formulas. For uniform reliability, the greater the scatter in the test data for a given nominal resistance, the lower the resistance factor will be. The ϕ-factor essentially accounts for uncertainties in predicting the resistance of a structural element. The randomness of resistance, R, results from a number of factors as described in the design codes (AISC 1986, AASHTO 2012, ACI 318-08, MSJC-08 Code), which include the following (not a complete list):

1. Variability inherent in the mechanical properties of materials such as yield and ultimate strength of structural steel, compressive strength of concrete and masonry (design strength and actual strength of as-poured concrete and masonry prism), yield and ultimate strength of reinforcing steel and prestressing tendons
2. Resistance of connectors and anchors
3. Variations in geometrical properties introduced by fabrication, and construction and erection tolerances
4. Assumptions used in determining design models
5. Using approximations for theoretically exact formulas

www.EngineeringEBooksPdf.com

6. Making assumptions such as ideal elasticity and ideal plasticity, using beam theory instead of theory of elasticity
7. Importance of the member in the structure (resistance factor for a column is smaller than for a beam because of the greater importance of a column than that of a beam in a structure)

The ACI 318 Code (ACI 2008) summarizes the following as reasons for including the ϕ-factor (strength reduction factor) in its design equations:

1. To allow for the probability of under-strength due to variations in material strength and dimensions
2. To allow for inaccuracies in the design equations
3. To reflect the degree of ductility and required reliability of the member under the load effects being considered
4. To reflect the importance of the member in the structure

Similarly, the γ-factors (load factors) reflect the fact that loads and load effects (computed forces and moments in structural elements) can be determined only to imperfect degree of accuracy.

Let us now turn our attention to other foretasted items. It is instructive to note that a safe design is not necessarily one that merely ensures adequate sizing of a structural member or a connection; the safety and performance of the entire bridge as structure under prescribed limit states are equally important. It is here that considerations of ductility, redundancy, and operational importance become relevant. Whereas ductility and redundancy considerations are directly related to the physical behavior of the bridge, that of operational importance is related to consequences of the bridge being out of service (such as inconvenience to public, loss of business revenue, inordinate delays that affect public health and safety).

1.5.7.1.1 Ductility and Ductile Behavior

Ductility refers to a material property that enables it to withstand large deformations beyond deformations at yield. A structural member is called ductile when it can sustain postyield (inelastic) deformation. Brittle materials are so called because they do not posses ductility. A member built from a brittle material such as plain concrete would fail suddenly when loaded beyond the elastic limit, without giving any signs of failure (such as cracking or deflections). For this reason, plain concrete is not to be used for structural applications. Reinforced and prestressed concrete members have to be designed as *under-reinforced* so that they would exhibit *tension control mode* when loaded to capacity (i.e., exhibit ductile behavior). A condition of impending failure of such members would be exhibited by cracking, followed by large deflections. It is for this reason that reinforced and prestressed concrete members are not permitted to be designed as *over-reinforced* for structural applications because such members would fail in *compression control mode* (tension reinforcement would not yield) with a sudden loss of capacity, a structurally undesirable situation. Similarly, in the case of structural steel members, an impending failure would be exhibited by flaking mill scale (indicating yielding) and increasing deflections.

Ductility is one of the most desirable properties for structures to posses, particularly when they are subjected to strength and extreme event limit states because it gives them postelastic energy dissipation capability. For these reasons, AASHTO LRFD Art. 1.3.3 requires that *the structural system of a bridge shall be proportioned and detailed to ensure the development of significant and visible inelastic deformations at the strength and extreme event limit states*. Readers familiar with building codes would note that structures are required to be *detailed* for seismic resistance even if the design is governed by load combinations that do not include earthquake loads (e.g., a load combination with wind loads might govern strength design), the idea being to force the structure to exhibit ductile behavior (ASCE 7-10, Section 11.1.1).

www.EngineeringEBooksPdf.com

How do we quantify ductility or express it mathematically? Ductility can be expressed as displacement ductility or curvature ductility. For design purposes, displacement ductility, often referred to as displacement ductility factor, is quantified as the ratio of displacement at the maximum design-level loads to displacement at yield, as expressed by Equation 1.72:

$$\mu_\Delta = \frac{\Delta_m}{\Delta_y} \tag{1.72}$$

where
μ_Δ = displacement ductility factor
Δ_m = maximum displacement at the maximum design load level
Δ_y = displacement at yield

If desired, Equation 1.72 can be expressed as the ratio of displacement at the ultimate loads, Δ_u, to displacement at yield; thus,

$$\mu_\Delta = \frac{\Delta_u}{\Delta_y} \tag{1.73}$$

Likewise, curvature ductility is expressed as the ratio of the attained postyield curvature to curvature at yield, which can be expressed as Equation 1.74:

$$\mu_\phi = \frac{\phi_p + \phi_y}{\phi_y} \tag{1.74}$$

where
μ_ϕ = curvature ductility
ϕ_p = postyield component of curvature
ϕ_y = curvature at yield = the angle change between the original and deformed positions of the end sections of a unit-length element

It is instructive to recognize that curvature is directly proportional to applied moment and inversely proportional to flexural stiffness (EI) of a member. As shown in Figure 1.38, since for small angles, $\tan\phi = \phi$, we have

$$\phi = \frac{\varepsilon}{d/2} \tag{1.75}$$

where
ϕ = curvature
ε = extreme fiber strain due to the applied moment M
d = depth of the flexural member

Since, from Hooke's law, strain $\varepsilon = f/E$, Equation 1.75 can be rewritten as Equation 1.76:

$$\phi = \frac{f}{E(d/2)} \tag{1.76}$$

where
f = flexural stress
E = modulus of elasticity
d = depth of the member with a symmetrical cross section

www.EngineeringEBooksPdf.com

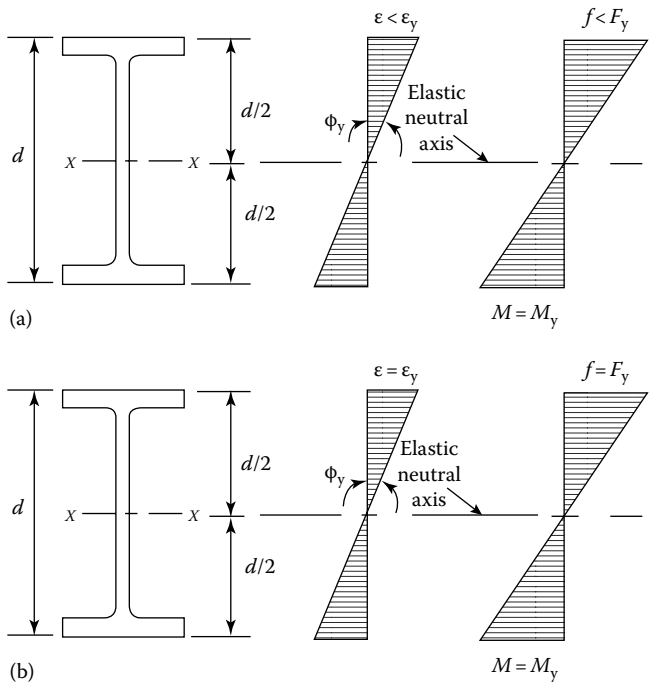

FIGURE 1.38 Elastic and inelastic behavior of a steel wide flange beam. (a) Stress and strain distribution under elastic conditions. (b) Stress and strain distribution at yield.

Knowing that the flexural stress $f = Mc/I$ (where I = moment of inertia of the member cross section) and $c = d/2$ for a member symmetrical about the axis of bending, Equation 1.76 can be expressed as Equation 1.77:

$$\phi = \frac{M(d/2)}{EI(d/2)} = \frac{M}{EI} \tag{1.77}$$

Equation 1.77 represents the classical definition of curvature. An $M - \phi$ curve is commonly used to study the experimental behavior flexure members (since EI is constant, M, rather than M/EI, is shown on the plot). Alternatively, since $M = F_yS$, Equation 1.77 can also be expressed as Equation 1.78:

$$\phi = \frac{F_yS}{EI} \tag{1.78}$$

It follows from the foregoing discussion that ductile behavior is characterized by significant inelastic deformation, that is, deformation past the elastic limit of the material. This is a highly desirable and preferred attribute for structural response because it gives ample warning of loss of load-carrying capacity of a structure and of an impending failure. Under cyclic loads, large reversed cycles of inelastic deformation dissipate energy and have a beneficial effect on structural response. It is unlike the behavior of brittle materials that suddenly lose their load-carrying capacity when loaded beyond their elastic limit, an undesirable attribute.

Ductile behavior is not necessarily limited to members and connections made from metals such as steel. Concrete is an example of a brittle material but, when properly reinforced and/or prestressed, it can exhibit a ductile behavior. This is accomplished by designing concrete members such that the reinforcement would yield significantly (i.e., they would fail in tension-controlled mode) and thereby provide some level of ductility; in such cases, members and connections can be considered as ductile.

www.EngineeringEBooksPdf.com

In some cases, a structural member or connection may exhibit ductile behavior under static loads, but not under dynamic loads; such behaviors should be avoided. Examples of such behaviors are shear and bond failures in concrete members and loss of composite action in flexural members (Kulicki 1999).

As explained in AASHTO (2012) Commentary C1.1.3, in all cases, the key design consideration is that a structure exhibits inelastic behavior. To achieve it, a structural system should have a sufficient number of ductile members, and either

1. Joints and connections that are also ductile and can provide energy dissipation without loss of capacity or
2. Joints and connections that have sufficient excess strength so as to assure that the inelastic response occurs at the locations designed to provide ductile energy absorbing response

Now that we have understood the beneficial effects of ductility, it is easy to see how its effect is included in LRFD philosophy. AASHTO LRFD Specifications (2012, Art. 1.3.3) specify the following values of the ductility related factor, η_D:

1. For the strength limit state of all members, and for the fatigue and fracture limit state for fracture-critical members,
   η_D = a factor relating to ductility (see Equation 1.69)
   ≥ 1.05 for nonductile members and connections
   $= 1.00$ for conventional design and details complying with these specifications
   ≥ 0.95 for components and connections for which additional ductility-enhancing measures have been specified beyond those required by these specifications
2. For all other limit states: $\eta_D = 1.00$

1.5.7.1.2 Redundancy

The Manual for Bridge Evaluation (AASHTO 2011 C6A.4.2.4) defines bridge redundancy as *the capability of a bridge structural system to carry loads after damage to or the failure of one or more of its members*. An indeterminate structure is an example of a redundant structure—it has more restraints (reactions) than are necessary to satisfy equilibrium. Continuous beams and rigid frames are examples of redundant structures—they have more restraints than are necessary to maintain equilibrium. Redundant structures can be described as multiple-load path structures and behave differently as compared with single-load path structures. Structural redundancy is a highly desirable attribute from the viewpoint of safety. AASHTO (2012) Art. 1.3.4 *requires that multiple-load path and continuous structures should be used unless there are compelling reasons not to use them*.

The purpose of providing redundant structures is to ensure that failure of one component or a structural member would *not* lead to the failure of the entire structure. Such a structural behavior is possible because structural members of a bridge do not behave independently, but interact with each other to form one structural system; that is, a redistribution of load occurs in redundant structures when one of its load-carrying element fails.

Nonredundancy in a bridge is highly undesirable. Several examples may be mentioned to develop a clearer understanding of redundancy in a bridge. A single-span slab bridge is a nonredundant structure because the collapse of the slab would mean the collapse of the entire bridge. A pedestrian bridge supported by either only one or two parallel single- or double-tee beams is a nonredundant structure because the collapse of the beam would mean the collapse of the entire footbridge. Single-cell box girder bridges and single-column bents are also nonredundant structures. In the latter case, the collapse of the single-column bent would result in the collapse of the structure. A truss bridge is also a nonredundant structure because the failure of one of its load-carrying members (e.g., a floor beam), or of a joint, would result in the loss of equilibrium, and consequently, lead to partial or complete collapse of the truss. Several redundancy measures have been proposed by Frangopol and Nakib (1991).

System reliability encompasses redundancy by considering the system of interconnected components and members so that rupture or yielding of individual component may or may not mean

www.EngineeringEBooksPdf.com

collapse of the whole structure or system (Nowak and Collins 2013). Research to establish correlation between ductility, redundancy, and member continues.

AASHTO LRFD Specifications (2012) require additional resistance in order to reduce the probability of loss of nonredundant component and to provide additional resistance to accommodate load distribution. Stated differently, members in nonredundant structures are penalized because they have to be sized to carry loads larger than conventional loads. AASHTO (2012) Art. 1.3.4 specifies the following values of the redundancy related factor, η_R (see Equation 1.69):

1. For the strength limit state:
   η_R = a factor relating to redundancy (see Equation 1.69)
   ≥ 1.05 for nonredundant members
   $= 1.00$ for conventional level of redundancy
   ≥ 0.95 for exceptional levels of redundancy beyond girder continuity and a closed torsionally closed cross section
2. For all other limit states: $\eta_D = 1.00$

1.5.7.1.3 Operational Importance

In many situations involving strength and extreme event limit states, it may be necessary to ensure that a bridge is operational. Such bridges are classified as *critical* or *essential*; the classification is based on social/survival and/or security/defense requirements. Such classification should be done by personnel responsible for the affected transportation network, and knowledgeable of its operational needs. The bridge owner may declare a bridge or any structural component and connection thereof to be of operational priority. AASHTO (2012) Commentary C1.3.5 provides the following guidelines for classifying critical or essential bridges:

1. Bridges that are required to be open to all traffic once inspected after the design event and are usable by emergency vehicles and for security, defense, economic, or secondary life safety purposes immediately after the event
2. Bridges that should, as a minimum, be open to emergency vehicles, and to vehicles for security, defense, or economic purposes, after the design event, and be open to all traffic within days after the design event

AASHTO LRFD Specifications (2012) Art. 1.3.5 specifies the following value of the operational importance factor, η_D, as follows:

1. For the strength limit state:
   η_D = a factor relating to operational importance (see Equation 1.69)
   ≥ 1.05 for critical or important bridges
   $= 1.00$ for typical bridges
   ≥ 0.95 for relatively less important bridges
2. For all other limit states: $\eta_D = 1.00$

1.6 DIFFERENCES BETWEEN VARIOUS DESIGN METHODS: SUMMARY

1.6.1 Difference between the Design Methods Based on the Elastic and Inelastic Material Behavior

A striking difference between the design methods based on the elastic behavior (allowable stress and WSD methods) and the inelastic behavior (strength design and the LRFD methods) should be noted. The former is a *stress*-based design at working loads. The emphasis is on the allowable *stresses*; the calculated stresses must not exceed the allowable stresses. On the other hand, the methods based on the inelastic behavior are *strength*-based methods; the emphasis is on the *strength* or

www.EngineeringEBooksPdf.com

the load-carrying capacity of a structural member at incipient failure, which must not be less than the applicable load combinations. Stated differently, when using methods based on the inelastic behavior of material, we deal with various combinations of maximum loads that may act on a structure during its service life, and the strength (maximum load-carrying capacity) of the structural members rather than allowable stresses as used in conventional working or ASD.

1.6.2 Difference between Plastic Design, Strength Design, Load Factor Design, and Load and Resistance Factor Design

It is instructive to recognize the fundamental difference between the plastic design method and all other methods of design. Whereas all four design methods have a similarity in that factored loads are used to analyze and design a structure, the significant difference lies in the *methods* used for analyzing the subject structure. In plastic design, a basic assumption is made in analysis that the structure has undergone inelastic deformation at the hinges, a condition for which the conventional methods of elastic analysis are not applicable. The plastically deformed structure is analyzed by special methods based on the formation of plastic hinges as the structure nears a collapse condition. In contrast, the other design methods (the strength method, the LFD method, and the LRFD) employ elastic analyses in which the fundamental assumption is that the structure (and all members) remains *elastic*. More importantly, the LRFD Specifications for highway bridges are based on modern probabilistic concepts.

1.7 HISTORICAL REVIEW OF AASHTO SPECIFICATIONS FOR HIGHWAY BRIDGES

The year 1921 marked the genesis of highway bridge design specifications in the United States; the current form of specifications has evolved over the past 92 years (as of 2012). The first complete set of specifications was available in 1926, which was revised in 1928, and appeared in print in 1931 as the first edition of AASHO's *Standard Specifications for Highway Bridges* (it was then entitled as *Standard Specifications for Highway Bridges and Incidental Structures*). Published by the American Association of State Highway Officials (AASHO), it was the first document that was widely recognized as national standard for the design and construction of highway bridges in the United States. Soon came along the automobile, and highway departments (now commonly known as the Departments of Transportation or DOTs) were established in all of the American states. The design, construction, and maintenance of most US bridges became the responsibility of these departments, with the State Bridge Engineer within each department as engineer-in-charge. These engineers, acting collectively as the AASHO (now AASHTO) Highway Subcommittee on Bridges and Structures (hereafter referred to as *Subcommittee*), would become the author and guardian of this first bridge design standard.

AASHO's first publication quickly became the *de facto* national standard; it was adopted and used by not only the state highway departments but also other bridge-owning authorities and agencies in the United States and several other countries. At some time, the last three words of the original title (*and incidental structures*) were dropped, and *Standard* has been reissued in consecutive editions typically in 4-year cycles ever since as *AASHTO Standard Specifications for Highway Bridges,* with the final 17th edition appearing in 2002. These specifications have since been archived and replaced by the current *AASHTO LRFD Bridge Design Specifications*, which first became available in 1997.

Since the first publication of bridge design specifications in 1931, research and experience has added enormously to the body of knowledge related to the design of highway bridges, which continues.

Many design theories and practices (discussed earlier in this chapter) have evolved reflecting advances through research in understanding the properties of materials and their improvements, and in more rational and accurate analysis of structural behavior. The advent of computers and rapidly advancing computer technology, and modeling techniques have been particularly helpful in recent years in the study of external events representing particular hazards to bridges such as wind and seismic events, stream scour, and in many other areas.

www.EngineeringEBooksPdf.com

To accommodate this growing body of knowledge and experience in bridge engineering, the Subcommittee on Bridges and Structures has been granted authority under AASHTO's governing documents to approve and issue Bridge *Interims* each year, not only with respect to the Specifications but also to incrementally modify and enhance the many bridges' and structures' engineering-related documents that are under its guidance and sponsorship.

1.8 AASHTO LRFD HIGHWAY BRIDGE DESIGN SPECIFICATIONS AND DESIGN PHILOSOPHIES

The Standard Specifications were developed based on the philosophy of ASD or WSD. As a result of considerable research beginning about 1940s, and experience from the performance of bridges in the United States and Canada, a need was felt to reassess the US bridge design specifications, to review foreign design specifications and codes, to consider design philosophies alternative to those underlying the Standard Specifications, and to consider recommendations based on these investigations. This effort began in 1986, with a request by the Subcommittee to the AASHTO Standing Committee on Research to undertake an assessment of the past design practices as embodied in *Standard Specifications*. Canada and some countries in Europe had already switched their design philosophies from ASD and WSD to limit states design. This investigation was accomplished under the National Cooperative Highway Research Program (NCHRP) directed by the ASSHTO Standing Committee on Research and administered by the Transportation Research Board (TRB) on behalf of AASHTO. Completed in 1987, it concluded that the Standard Specifications had drawbacks—discernible gaps, inconsistencies, and even some conflicts, which needed to be fixed.

Historically, beginning in the early 1970s, ASD began to be adjusted to reflect the variable predictability of certain load types, such as vehicular loads and wind forces, through adjusting design factors, a design philosophy referred to as LFD. Starting in the 1990s, AASHTO Specifications included both ASD (and WSD) and LFD; they are included in AASHTO 2002. A better understanding of the variability in the properties of structural elements and loads led to the development of a design philosophy called LRFD, which takes into account the variability in the behavior of structural elements in an explicit manner. While relying on the extensive use of statistical methods, the LRFD philosophy sets forth the results in a manner readily usable by bridge designers and analysts.

The design philosophy behind the LRFD Specifications for highway bridges was introduced in several sections in this chapter earlier. However, it should not be construed that Standard Specifications did not serve their intended purpose or were substandard in any way or form. Indeed, those specifications represent historical basis of highway bridge design in the United States. Several thousand bridges designed using the Standard Specifications, both in the United States and elsewhere in the world, have stood the test of time and continue to serve well. But then why change those specifications? The simple answer is that neither the ASD nor the follow-up LFD, both of which formed the basis of Standard Specifications, had a mathematical basis for establishing safety and reliability (these concepts were not rationally defined). It is this aspect of design philosophy that gave bridge design engineers impetus to develop LRFD Specifications, which are based on much better-understood design philosophies of safety and reliability (very important) with a clear understanding of the type of safety inherent in the system. This became possible when statistically based probability methods became available in the 1980s, leading to work on developing the LRFD Specifications in the later years and culminating in 1997 when the first set of AASHTO LRFD Specifications for Highway were proposed and approved. (This author was present in the 1997 annual meeting of the AASHTO Subcommittee on Bridges and Structures in Denver, Colorado, when this historic event took place.)

1.9 AASHTO INTERIM SPECIFICATIONS

With the intent to keep bridge designers and analysts informed of the state of the art, AASHTO publishes Interim Specifications (called Interims). They are usually published in the middle of the calendar year, and a revised edition of the Specifications is generally published every 4 years.

www.EngineeringEBooksPdf.com

The Interim Specifications have the same status as AASHTO standards, but they are tentative in the sense that these revisions have been approved by at least two-thirds of the subcommittee. Later, these revisions are voted on by the AASHTO member departments prior to the publication of each new edition. If approved by at least two-thirds of the members, these Interims are included in the new edition of AASHTO LRFD Bridge Design Specifications.

As a matter of standing policy, AASHTO membership consists of the 50 State Highway or Transportation Departments, the District of Columbia, and Puerto Rico; each member has one vote, with the U.S. Department of Transportation (USDOT) being a nonvoting member.

1.10 SCOPE OF THE AASHTO LRFD BRIDGE DESIGN SPECIFICATIONS

The provisions of these AASHTO LRFD Specifications apply, as the Standard Specifications did before them, to the design, evaluations, and rehabilitation of both fixed and movable highway bridges. Mechanical, electrical, and special vehicular and pedestrian safety aspects of movable bridges, however, are not covered by these provisions. Also, these provisions do not apply to bridges used solely for railway, rail transit, or public utilities. For bridges not fully covered in these provisions, these specifications may be applied, as augmented with additional design criteria where required.

It is very important to recognize that these specifications state only the *minimum* requirement necessary to provide for public safety; they are not substitutes for proper training or the exercise of judgment by the designer. *The owner or the designer may require the sophistication of design or the quality of materials and construction to be higher than the minimum requirements.* The concepts of safety through redundancy and ductility and of protection against scour and collision are emphasized by these specifications.

The design provisions of these specifications employ the LRDS methodology. The factors have been developed from the theory of reliability based on current statistical knowledge of loads and structural performance. Methods of analysis other than those included in previous specifications and the modeling techniques inherent in them are included, and their use is encouraged.

Pertinent references have been made to AASHTO LRFD Specifications throughout this book. This document is divided into 15 sections (similar to *chapters* in other codes); each section is divided into several subsections, which are called *articles* (similar to *sections* in other codes). Unlike its predecessor, Standard Specifications, the AASHTO LRFD is written in a two-column format; the left side contains various articles (specifications), and the right side contains commentary on the specifications and pertinent references.

The following are the various *sections* listed in 2012-AASHTO LRFD Bridge Design Specifications:

1. Introduction
2. General design and location features
3. Loads and load factors
4. Structural analysis and evaluation
5. Concrete structures
6. Steel structures
7. Aluminum structures
8. Wood structures
9. Decks and deck systems
10. Foundations
11. Abutment, piers, and walls
12. Buried structures and tunnel liners

www.EngineeringEBooksPdf.com

13. Railings
14. Joints and bearings
15. Design of sound barriers (new to the 6th edition)
    Index

Detailed Tables of Contents precede each section. The last article of each section is a list of references displayed alphabetically by author.

1.11 COMMENTARY TO AASHTO LRFD SPECIFICATIONS

An important part of AASHTO LRFD Bridge Design Specifications is the accompanying *Commentary.* The commentary is not intended to provide a complete historical background concerning the development of these or previous specifications, nor is it intended to provide a detailed summary of the studies and research data reviewed in formulating the provisions of the specifications. However, references to some of the research data are provided for those who wish to study the background material in depth.

The commentary directs attention to other documents that provide suggestions for carrying out the requirements and intent of these specifications. However, those documents and this commentary are *not* intended to be a part of these specifications.

Construction specifications consistent with these design specifications are the *AASHTO LRFD Bridge Construction Specifications.* Unless otherwise specified, the Material Specifications referenced therein are the AASHTO *Standard Specifications for Transportation Material and Methods of Sampling and Testing.*

Curved girders are not fully covered and were not part of the calibration database.

The term *notional* is often used in these specifications to indicate an idealization of the physical phenomenon, as in *notional load* or *notional resistance.* The use of this term strengthens the separations of an engineer's *notion* or perception of the physical world in the context of design from the physical reality itself.

The specifications intentionally use the words such as *shall*, *may*, *should*, etc., throughout the document. Their intent is as follows:

The term *shall* (as differentiated from *may*) denotes a requirement for compliance with these specifications.

The term *should* indicates a strong preference for a given criterion.

The term *may* indicates a criterion that is usable, but other local and suitably documented, verified, and approved criteria may also be used in a manner consistent with the LRFD approach to bridge design.

1.12 GENERAL COMMENTS

Bridge designers should be aware that bridges, as a matter of general practice, are designed according to applicable codes/specifications, which may be different in different countries. Although established principles of structural design and analysis are universally applicable to bridge design, design loads must be determined in accordance with the provisions of applicable codes and specifications. In this book, design calculations are based on AASHTO LRFD Bridge Design Specifications (AASHTO 2012), which are used for designing highways in the United States. Readers are advised to have a copy of the latest AASHTO LRFD Specifications handy for a quick reference and easy understanding of the material presented in this book.

As a fundamental principle of structural design, it should be recognized at the very outset that all structures, irrespective of the occupancy type, must be designed for a combination of loads (i.e., loads that may be expected to occur concurrently). This important topic is covered in Chapter 3. It is noted that loads discussed in Chapter 3 are unfactored or service loads. These loads would need to be multiplied by appropriate load factors to determine design loads to be used for LRFD.

www.EngineeringEBooksPdf.com

1.A APPENDIX

TABLE 1.A.1
Standard Normal Distribution Function

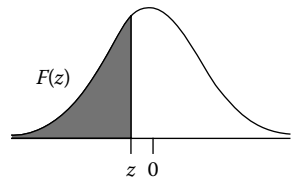

$$F(z) = \frac{1}{\sqrt{2\pi}} \int_{-\infty}^{z} e^{-t^2/2} dt$$

z	0.00	0.01	0.02	0.03	0.04	0.05	0.06	0.07	0.08	0.09
–5.0	0.0000003									
–4.0	0.00003									
–3.5	0.0002									
–3.4	0.0003	0.0003	0.0003	0.0003	0.0003	0.0003	0.0003	0.0003	0.0003	0.0002
–3.3	0.0005	0.0005	0.0005	0.0004	0.0004	0.0004	0.0004	0.0004	0.0004	0.0003
–3.2	0.0007	0.0007	0.0006	0.0006	0.0006	0.0006	0.0006	0.0005	0.0005	0.0005
–3.1	0.0010	0.0009	0.0009	0.0009	0.0008	0.0008	0.0008	0.0008	0.0007	0.0007
–3.0	0.0013	0.0013	0.0013	0.0012	0.0012	0.0011	0.0011	0.0011	0.0010	0.0010
–2.9	0.0019	0.0018	0.0018	0.0017	0.0016	0.0016	0.0015	0.0015	0.0014	0.0014
–2.8	0.0026	0.0025	0.0024	0.0023	0.0023	0.0022	0.0021	0.0021	0.0020	0.0019
–2.7	0.0035	0.0034	0.0033	0.0032	0.0031	0.0030	0.0029	0.0028	0.0027	0.0026
–2.6	0.0047	0.0045	0.0044	0.0043	0.0041	0.0040	0.0039	0.0038	0.0037	0.0036
–2.5	0.0062	0.0060	0.0059	0.0057	0.0055	0.0054	0.0052	0.0051	0.0049	0.0048
–2.4	0.0082	0.0080	0.0078	0.0075	0.0073	0.0071	0.0069	0.0068	0.0066	0.0064
–2.3	0.0107	0.0104	0.0102	0.0099	0.0096	0.0094	0.0091	0.0089	0.0087	0.0084
–2.2	0.0139	0.0136	0.0132	0.0129	0.0125	0.0122	0.0119	0.0116	0.0113	0.0110
–2.1	0.0179	0.0174	0.0170	0.0166	0.0162	0.0158	0.0154	0.0150	0.0146	0.0143
–2.0	0.0228	0.0222	0.0217	0.0212	0.0207	0.0202	0.0197	0.0192	0.0188	0.0183
–1.9	0.0287	0.0281	0.0274	0.0268	0.0262	0.0256	0.0250	0.0244	0.0239	0.0233
–1.8	0.0359	0.0351	0.0344	0.0336	0.0329	0.0322	0.0314	0.0307	0.0301	0.0294
–1.7	0.0446	0.0436	0.0427	0.0418	0.0409	0.0401	0.0392	0.0384	0.0375	0.0367
–1.6	0.0548	0.0537	0.0526	0.0516	0.0505	0.0495	0.0485	0.0475	0.0465	0.0455
–1.5	0.0668	0.0655	0.0643	0.0630	0.0618	0.0606	0.0594	0.0582	0.0571	0.0559
–1.4	0.0808	0.0793	0.0778	0.0764	0.0749	0.0735	0.0721	0.0708	0.0694	0.0681
–1.3	0.0968	0.0951	0.0934	0.0918	0.0901	0.0885	0.0869	0.0853	0.0838	0.0823
–1.2	0.1151	0.1131	0.4112	0.4093	0.1075	0.1056	0.4038	0.4020	0.4003	0.0985
–1.1	0.1357	0.1335	0.4314	0.4292	0.1271	0.1251	0.4230	0.1210	0.1190	0.4170
–1.0	0.1587	0.1562	0.1539	0.1515	0.4492	0.1469	0.4446	0.4423	0.1401	0.1379
–0.9	0.1841	0.1814	0.4788	0.1762	0.4736	0.1711	0.1685	0.1660	0.4635	0.1611
–0.8	0.2319	0.2090	0.2061	0.2033	0.2005	0.1977	0.4949	0.1922	0.4894	0.4867
–0.7	0.2420	0.2389	0.2358	0.2327	0.2296	0.2266	0.2236	0.2206	0.2177	0.2148
–0.6	0.2743	0.2709	0.2676	0.2643	0.2611	0.2578	0.2546	0.2514	0.2483	0.2451
–0.5	0.3085	0.3050	0.3015	0.2981	0.2946	0.2912	0.2877	0.2843	0.2810	0.2776
–0.4	0.3446	0.3409	0.3372	0.3336	0.3300	0.3264	0.3228	0.3192	0.3156	0.3121
–0.3	0.3821	0.3783	0.3745	0.3707	0.3669	0.3632	0.3594	0.3557	0.3520	0.3483
–0.2	0.4207	0.4168	0.4129	0.4090	0.4052	0.4013	0.3974	0.3936	0.3897	0.3859
–0.1	0.4602	0.4562	0.4522	0.4483	0.4443	0.4404	0.4364	0.4325	0.4286	0.4247
–0.0	0.5000	0.4960	0.4920	0.4880	0.4840	0.4801	0.4761	0.4721	0.4681	0.4641

(*Continued*)

www.EngineeringEBooksPdf.com

TABLE 1.A.1 (*Continued*)
Standard Normal Distribution Function

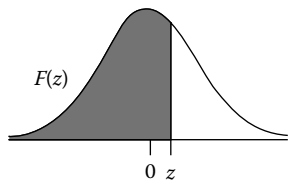

$$F(z) = \frac{1}{\sqrt{2\pi}} \int_{-\infty}^{z} e^{-t^2/2} dt$$

z	0.00	0.01	0.02	0.03	0.04	0.05	0.06	0.07	0.08	0.09
0.0	0.5000	0.5040	0.5080	0.5120	0.5160	0.5199	0.5239	0.5279	0.5319	0.5359
0.1	0.5398	0:5438	0.5478	0.5517	0.5557	0.5596	0.5636	0.5675	0.5714	0.5753
0.2	0.5973	0.5832	0.5871	0.5910	0.5948	0.5987	0.6026	0.6064	0.6103	0.6141
0.3	0.6179	0.6217	0.6255	0.6293	0.6331	0.6368	0.6406	0.6443	0.6480	0.6517
0.4	0.6554	0.6591	0.6628	0.6664	0.6700	0.6736	0.6772	0.6808	0.6844	0.6879
0.5	0.6915	0.6950	0.6985	0.7019	0.7054	0.7088	0.7123	0.7157	0.7190	0.7224
0.6	0.7257	0.7291	0.7324	0.7357	0.7389	0.7422	0.7454	0.7486	0.7517	0.7549
0.7	0.7580	0.7611	0.7642	0.7673	0.7704	0.7734	0.7764	0.7794	0.7823	0.7852
0.8	0.7881	0.7910	0.7939	0.7967	0.7995	0.8023	0.8051	0.8078	0.8106	0.8133
0.9	0.8159	0.8186	0.8212	0.8238	0.8264	0.8289	0.8315	0.8340	0.8365	0.8389
1.0	0.8413	0.8438	0.8461	0.8485	0.8508	0.8531	0.8554	0.8577	0.8599	0.8621
1.1	0.8643	0.8665	0.8686	0.8708	0.8729	0.8749	0.8770	0.8790	0.8810	0.8830
1.2	0.8849	0.8869	0.8888	0.8907	0.8925	0.8944	0.8962	0.8980	0.8997	0.9015
1.3	0.9032	0.9049	0.9066	0.9082	0.9099	0.9115	0.9131	0.9147	0.9162	0.9177
1.4	0.9192	0.9207	0.9222	0.9236	0.9251	0.9265	0.9279	0.9292	0.9306	0.9319
1.5	0.9332	0.9345	0.9357	0.9370	0.9382	0.9394	0.9406	0.9418	0.9429	0.9441
1.6	0.9452	0.9463	0.9474	0.9484	0.9495	0.9505	0.9515	0.9525	0.9535	0.9545
1.7	0.9554	0.9564	0.9573	0.9582	0.9591	0.9599	0.9608	0.9616	0.9625	0.9633
1.8	0.9641	0.9649	0.9656	0.9664	0.9671	0.9678	0.9686	0.9693	0.9699	0.9706
1.9	0.9713	0.9719	0.9726	0.9732	0.9738	0.9744	0.9750	0.9756	0.9761	0.9767
2.0	0.9772	0.9778	0.9783	0.9788	0.9793	0.9798	0.9803	0.9808	0.9812	0.9817
2.1	0.9821	0.9826	0.9830	0.9834	0.9838	0.9842	0.9846	0.9850	0.9854	0.9857
2.2	0.9861	0.9864	0.9868	0.9873	0.9875	0.9878	0.9881	0.9884	0.9887	0.9890
2.3	0.9893	0.9896	0.9898	0.9901	0.9904	0.9906	0.9909	0.9911	0.9913	0.9916
2.4	0.9918	0.9920	0.9922	0.9925	0.9927	0.9929	0.9931	0.9932	0.9934	0.9936
2.5	0.9938	0.9940	0.9941	0.9943	0.9945	0.9946	0.9948	0.9949	0.9951	0.9952
2.6	0.9953	0.9955	0.9956	0.9957	0.9959	0.9960	0.9961	0.9962	0.9963	0.9964
2.7	0.9965	0.9966	0.9967	0.9968	0.9969	0.9970	0.9971	0.9972	0.9973	0.9974
2.8	0.9974	0.9975	0.9976	0.9977	0.9977	0.9978	0.9979	0.9979	0.9980	0.9981
2.9	0.9981	0.9982	0.9982	0.9983	0.9984	0.9984	0.9985	0.9985	0.9986	0.9986
3.0	0.9987	0.9987	0.9987	0.9988	0.9988	0.9989	0.9989	0.9989	0.9990	0.9990
3.1	0.9990	0.9991	0.9991	0.9991	0.9992	0.9992	0.9992	0.9992	0.9993	0.9993
3.2	0.9993	0.9993	0.9994	0.9994	0.9994	0.9994	0.9994	0.9995	0.9995	0.9995
3.3	0.9995	0.9995	0.9995	0.9996	0.9996	0.9996	0.9996	0.9996	0.9996	0.9997
3.4	0.9997	0.9997	0.9997	0.9997	0.9997	0.9997	0.9997	0.9997	0.9997	0.9998
3.5	0.9998									
4.0	0.99997									
5.0	0.9999997									

Sources: NBS, *Tables of Normal Probability Functions*, Applied Mathematics Series 23, National Bureau of Standards (NBS), Washington, DC, 1953; Hald, A., *Statistical Tables and Formulas*, John Wiley & Sons, Inc., New York, 1952.

www.EngineeringEBooksPdf.com

REFERENCES

AASHTO. 1992. *Standard Specifications for Highway Bridges*, American Association of State Highway and Transportation Officials (AASHTO), Washington, DC.

AASHTO. 1996. *Standard Specifications for Highway Bridges*, 15th ed., American Association of State Highway and Transportations, Washington, DC.

AASHTO. 2002. *Standard Specifications for Highway Bridges*, 17th ed., American Association of State Highways and Transportation Officials, Washington, DC.

AASHTO. 2011. *Manual for Bridge Evaluation*, American Association of State Highways and Transportation Officials, Washington, DC, 2011.

AASHTO. 2012. *AASHTO LRFD Specifications for Highway Bridges*, 6th ed., American Association of State Highway and Transportation Officials, Washington, DC.

ACI Code. 2008. *Building Code Requirements for Structural Concrete* (ACI 318-08) *and Commentary* (ACI 318R-08), American Concrete Institute, Farmington, MO.

AF&PA. 2010. *ASD/LRFD National Design Specification for Wood Construction*, ANSI/AF&PA NDS-2010, American Forest and Paper Association (AF&PA), American Wood Council, Washington, DC.

AISC. 1986. *Manual of Steel Construction*: *Load and Resistance Factor Design*, American Institute of Steel Construction, Chicago, IL, 1986. This is the first edition of *AISC's Manual of Steel Construction: Load and Resistance Factor Design*.

AISC. 1998. *Manual of Steel Construction*: *Load and Resistance Factor Design*, vol. I, 2nd ed., American Institute of Steel Construction, Chicago, IL.

AISC. 2005. *Steel Construction Manual*, 13th ed., American Institute of Steel Construction (AISC), Chicago, IL.

Allen, D.E. 1976. "Limit state design—A probabilistic study", *Canadian Journal of Civil Engineering*, 2 (1), 36–49.

Ang, A.H. and Cornell, C.A. 1974. "Reliability basis of structural safety and design", *Journal of Structural Division*, *ASCE*, 100 (ST9), Proceedings Paper 10777, 1755–1769.

ASCE. 2010. *Minimum Design Loads for Building and Other Structures*, ASCE Standard ASCE/SEI 7-10, American Society of Civil Engineers, New York.

Atkins, W.S. and Lewis, E.M. 1951. "Developments of design and fabrication in recent British structures", *Transactions of the Institute of Welding*, 14, 74–84.

Baker, J.F. 1948. "A review of recent investigations into the behavior of steel frames in plastic design", *Journal of Institute of Civil Engineers*, 31 (3), 185–240.

Baker, J.F., Horne, M.R., and Heyman, J. 1949. *The Steel Skeleton*, *Vol. II: Plastic Behavior and Design*, Cambridge University Press, Cambridge, MA.

Beedle, L.S. 1958. *Plastic Design of Steel Frames*, John Wiley & Sons, Inc., New York.

Beedle, L.S., Thurliman, B., and Ketter, R.L. 1955. *Plastic Design in Structural Steel*, Lehigh University, Bethlehem, PA, and American Institute of Steel Construction.

Benjamin, J.R. and Cornell, C.A. 1970. *Probability, Statistics, and Decision for Civil Engineers*, McGraw-Hill Co., New York.

Bjorhovde, R., Galambos, T.V., and Ravindra, M.K. 1978. "LRFD criteria for steel beams and columns", *Journal of the Structural Division*, *ASCE*, 104 (ST9), 1371–1387.

Boris, B. 1970. Lightweight aggregate reinforced concrete columns, *Lightweight Concrete*, ACI Publication SP 29, American Concrete Institute, Detroit MI, pp. 81–130.

Charles, S.G., Johnson, J.E., and Malhas, F.A. 2009. *Steel Structures*: *Design and Behavior*, 5th ed., Pearson Education, Inc., Pearson-Prentice Hall, Upper Saddle River, NJ.

Collins, J.A. 1981. *Failure of Materials in Mechanical Design*: *Analysis, Prediction, Prevention*, John Wiley & Sons.

Collins, M.P. and Mitchell, D. 1991. *Prestressed Concrete Structures*, Prentice-Hall, Inc., Englewood Cliffs, NJ.

Cooper, P.B., Galambos, T.V., and Ravindra, M.K. 1978. "LRFD criteria for plate girders", *Journal of the Structural Division*, *ASCE*, 104 (ST9), 1389–1407.

Cornell, C.A. 1969. "A probability-based structural code", *Journal of the American Concrete Institute, Proceedings*, 66 (12), December 1969, 974–985.

CSA. 1998. *Highway Bridge Design Code*, Canadian Standards Association, Toronto, Ontario, Canada.

Ellingwood, B., Galambos, T.V., MacGregor, J.G., and Cornell, C.A. 1980. Development of Probability-Based Load Criterion for American National Standard A58. NBS Special Publication 577, National Bureau of Standards, Department of Commerce, Washington, DC, June.

Ellingwood, B., McGregor, J.C., Galambos, T.V., and Cornell, A.S. 1982. "Probability-based load criteria: Load factors and load combinations", *Journal of the Structural Division*, 108 (5), 978–997.

www.EngineeringEBooksPdf.com

Englekirk, R. 1994. *Steel Structures*: *Controlling Behavior through Design*, John Wiley & Sons, New York.
Estes, E.R. Jr. 1957. "Plastic design of warehouse saves steel", *Civil Engineering*, 27 (9), 608.
Fisher, J.W., Galambos, T.V., Kulak, G.L., and Ravindra, M.K. 1978. "Load and resistance criteria for connections", *Journal of the Structural Division*, *ASCE*, 104 (ST9), 1427–1441.
Frangopol, D.M. and Nakib, R. 1991. Redundancy in highway bridges, *Engineering Journal*, 28 (1), 45–50.
Fredunthal, A.M., Garrelts, J., and Shinozuka, M. 1966. "The analysis for structural safety", *Journal of the Structural Division*, *ASCE*, 92 (ST1), Proceedings Paper 4682, 267–325.
Galambos, T.V., Ellingwood, B., MacGregor, J.G., and Cornell, C.A. 1982. "Probability-based load criteria: Assessment of current design practice", *Journal of the Structural Division, ASCE*, 108 (ST5), May, pp. 959–977.
Galambos, T.V. and Ravindra, M.K. 1978. "Properties of steel for use in LRFD", *Journal of the Structural Division*, *ASCE*, 104 (ST9), 1459–1468.
Gatty, P.L. 2005. *Probability Theory and Mathematical Statistics for Engineers*, CRC Press, Spon Press, London, U.K.
Gere, J.M. and Goodno, B.J. 2009. *Mechanics of Materials*, 7th ed., Cengage Learning, Mason, OH.
Hald, A. 1952. *Statistical Tables and Formulas*, John Wiley & Sons, Inc., New York.
Hansell, W.C., Galambos, T.V., Ravindra, M.K., and Viest, I.V. 1978. "Composite beam criteria in LRFD", *Journal of the Structural Division*, *ASCE*, 104 (ST9), 1409–1426.
Hasofer, A.M. and Lind, N. 1974. "An exact and invariant first-order reliability format", *Journal of Engineering Mechanics*, 100 (EM1), February, 111–121.
Heymen, J. 1957. *Plastic Design of Steel Frames*, Cambridge University Press, Cambridge, MA.
Hwang, E.S. and Nowak, A.S. 1991. "Simulation of dynamic load for bridges", *Journal of Structural Engineering, ASCE*, 117 (5), 1413–1434.
Janney, J.R., Hognestad, E., and McHenry, D. 1956. "Ultimate strength of prestressed and conventionally reinforced beams", *ACI Journal, Proceedings*, 52, 601–620.
Johnson, R.A. 2011. *Miller and Freund's Probability and Statistics for Engineers*, 8th ed., Prentice Hall, Upper Saddle River, NJ.
Johnston, B.G., Yang, C.H., and Beedle, L.S. 1953. "An evaluation of plastic analysis as applied to structural design", *Welding Journal*, 32 (5), 224-s.
Kazinczy, G. 1914. "Kiserletek Befalzott Tartokkal ("Experiments with clamped girders")", *Betonszemle*, 2 (4), 68; 2 (5), 83; 2 (7), 101.
Kulicki, J. 1999. Design philosophies for highway bridges, in *Bridge Engineering Handbook*, W.-F. Chen and L. Duan, ed., CRC Press, Boca Raton, FL.
Kulicki, J.M. and Mertz, D.R. 1993. Development of comprehensive bridge specifications and commentary, Final Report, NCHRP 12-33, Modjeski and Masters, Harrisburg, PA.
Laplace, P.S. de. 1951. *A Philosophical Essay on Probabilities*, Dover, New York.
Lind, N.S. 1971. "Consistent partial safety factors", *Journal of Structural Division, ASCE*, 97 (ST6), Proceedings Paper 8166, June, 1651–1669.
Luxion, W.W. and Johnston, B.G. 1948. "Plastic behavior of wide flange beams", *Welding Journal*, 27 (11), 538-s–554-s.
MacGregor, J.G. 1976. "Safety and limit states design for reinforced concrete", *Canadian Journal of Civil Engineering*, 3 (4), 484–513.
MacGregor, J.G. and Wight, J.K. 2005. *Reinforced Concrete—Mechanics and Design*, Prentice Hall, Upper Saddle River, NJ.
Madsen, H.O., Krenk, S., and Lind, N.C. 1986. *Methods of Structural Safety*, Prentice-Hall, Inc., Englewood Cliffs, NJ.
Mattock, A.H., Kriz, L.B., and Hognested, E. 1961. "Rectangular concrete stress distribution in ultimate strength design", *ACI Journal Proceedings*, 57(8), 875–928.
McConnell, J.E. 1849. On railway axles, *Proceedings of the Institute of Mechanical Engineers*, London, U.K., pp. 1847–1849.
Melchers, R.E. 1999. *Structural Reliability Analysis and Prediction*, John Wiley & Sons, New York.
Meyer, S. 1975. *Data Analysis for Scientists and Engineers*, John Wiley & Sons, New York.
MSJC. 2008. Building Code requirements for Masonry Structures (TMS 402-08/ACI 530-08/ASCE 5-08) and Specification for Masonry Structures (TMS 602-08/ACI 530.1-08/ASCE 6-08), Reported by the Masonry Standards Joint Committee, American Concrete Institute, Farmington Hills, MI; Structural Engineering Society of the American Society of Civil Engineers, Reston, VA; and the Masonry Society, Boulder, CO.
NBS. 1953. *Tables of Normal Probability Functions*, Applied Mathematics Series 23, National Bureau of Standards (NBS), Washington, DC.

www.EngineeringEBooksPdf.com

Nowak, A.S. 1993a. Calibration of LRFD bridge design code, NCHRP Project 12-33, Report 368, University of Michigan, Ann Arbor, MI.

Nowak, A.S. 1993b. Calibration of LRFD bridge design code, Department of Civil and Environmental Engineering Report 92-65, University of Michigan, Ann Arbor, MI.

Nowak, A.S. 1993. "Live load model for highway bridges", *Journal of Structural Safety*, 13 (1&2), 53–66.

Nowak, A.S. 1995. "Calibration of LRFD bridge code", *Journal of Structural Engineering*, *American Society of Civil Engineers*, August 1995, 121 (8), 1245–1251.

Nowak, A.S. 1999. Calibration of LRFD bridge code, NCHRP Report 368, Transportation Research Board, National Research Council, Washington, DC.

Nowak, A.S. 2012. Personal communication.

Nowak, A.S. and Collins, K.R. 2013. *Reliability of Structures*, CRC Press, Boca Raton, FL.

Nowak, A.S. and Lind, N.C. 1979. "Practical bridge code calibration", *Journal of Structural Division*, ASCE, 105(12), 2497–2510.

Nowak, A.S., Yamani, A.S., and Tabsh, S.W. 1993. "Probabilistic models for resistance of concrete bridge girders", *ACI Structural Journal,* 91 (3), 269–276.

OHBDC. 1994. *Ontario Highway Bridge Design Code*, Ontario Ministry of Transportation and Communications (OMTC), Toronto, Ontario, Canada.

Poncelet, J.V. 1870. *Introduction a la Mecanique industrielle*, 3rd ed., Paris, France, p. 317.

Ravindra, M.K., Cornell, C.A., and Galambos, T.V. 1978. "Wind and snow load factors for use in LRFD", *Journal of the Structural Division*, *ASCE*, 104 (ST9), 1443–1457.

Ravindra, M.K. and Galambos, T.V. 1978. "Load and resistance factor design for steel", *Journal of the Structural Division*, *ASCE*, 104 (ST9), 1337–1353.

Salmon, C.G., Johnson, J.E., and Malhas, F.A. 2009. *Steel Structures—Design and Behavior*, 5th ed., Pearson Education, Inc., Pearson-Prentice Hall, Upper Saddle River, NJ.

Segui, W.T. 2012. *Steel Design*, 4th ed., Thomson Publishing, Toronto, Ontario, Canada, pp. 26–31.

Tabsh, S.W. and Nowak, A.S. 1991. "Reliability of highway girder bridges", *Journal of Structural Engineering, ASCE*, 117 (8), 2373–2388.

Thoft-Christensen, P. and Baker, M.J. 1982. *Structural Reliability Theory and its Applications,* Springer-Verlag Inc., New York.

Ting, S.-C. and Nowak, A.S. 1991a. Effect of tendon area loss on flexural behavior of P/C beam, *Journal of Structural Engineering, ASCE*, 117 (4), 1127–1143.

Ting, S.-C. and Nowak, A.S. 1991b. Effect of rebar area loss on flexural behavior of R/C beams, *ACI Structural Journal*, 88 (3), 309–314.

Van den Broek, J.A. 1948. *Theory of Limit Design*, John Wiley & Sons, New York.

Vinnakota, S. 2006. *Steel Structures*: *Behavior and LRFD*, McGraw-Hill Companies, New York.

Walpole, R.E. and Myers, R.H. 1978. *Probability and Statistics for Engineers and Scientists*, 2nd ed., Macmillan Publishing Co., New York.

Walpole, R.E., Myers, R.H., Myers, S.L., and Keying, Y. 2005. *Probability and Statistics for Engineers and Scientists*, 9th ed., Prentice Hall Co., New York.

Wang, P.T., Shah, S.P., and Naaman, A.E. 1978. "Stress–strain curves of normal and lighweight concrete in compression", *ACI Journal Proceedings*, 75 (11), 603–611, November.

Witchey, R. 1997. *Applied Principles and Analysis of Human Movement*, McGraw-Hill Companies, New York.

Wright, D.T. 1957. "Plastic design is used successfully", *Engineering News-Record*, 158 (15), 59.

Young, J.F., Sidney, M., Gray, R.J., and Bentur, A. 1998. *The Science and Technology of Civil Engineering Materials*, Prentice Hall, Upper Saddle River, NJ.

Yura, J.A., Galambos, T.V., and Ravindra, M.K. 1978. "The bending resistance of steel beams", *Journal of the Structural Division*, *ASCE*, 104 (ST9), 1355–1370.

Zokaie, T., Osterkamp, T.A., and Imbsen, R.A. 1991. Distribution of wheel loads on highway bridges, Final Report, NCHRP 12-26(11), Transportation Research Board, Washington, DC.

www.EngineeringEBooksPdf.com

2 Highway Bridge Superstructure Systems

2.1 INTRODUCTION

All types of bridge structures—highway, railroad, and pedestrian—consist of two basic structural parts: superstructure and substructure. The superstructures provide a means to cross space between two points; the substructure supports the superstructure and transfers all forces acting on it to the ground. Short-span bridges, which are typically single-span structures, consist of a superstructure and a substructure; the latter consists of abutments with bearing pads on top, which supports the superstructure, and the wingwalls (on its both sides), which retain the embankments of the connecting roadway. Multispan bridges may consist of several single-span bridges, which are supported by additional supports such as column bents and piers.

Highway bridge superstructures can have a variety of structural forms (cross sections). All must have a deck to support the traffic, with traffic barriers on both sides. Decks can be built from a variety of materials—reinforced concrete (RC), steel, wood, and composites. Typically, they are supported over longitudinal beams (oriented parallel to the centerline of the roadway), which in turn are supported on the abutments. Additionally, decks are provided with a half-inch (or more) of concrete-wearing surface so as to preserve the structural thickness of RC decks from being worn out. Decks and deck systems are discussed in Chapter 5.

Superstructures of medium- and long-span bridges, such as truss, arch, cable-stayed, and suspension types, comprise additional elements. For example, a truss bridge comprises a deck (there are several types discussed in Chapter 5) supported over the longitudinal beams called *stringers*, which in turn are supported over the transversely spanning floor beams that transfer all loads to truss joints on either sides. The trusses then transfer all loads to the abutments. Similarly, arch bridges have arches; cable-stayed bridges have stay cables and pylons; suspension bridges have towers, suspension cables and hangers, and so on. In addition to these bridges, which are stationary, there are *movable bridges* that are built over navigable waterways. Figures 2.1 through 2.10 depict several types of highway bridges and their structural components.

2.2 AASHTO LRFD SPEC.-SPECIFIC HIGHWAY BRIDGE SUPERSTRUCTURES

Several types of structural forms and construction materials can be used to build bridge superstructures. Table 2.1 (AASHTO LRFD Spec. Table 4.6.6.2.2.1-1) (AASHTO 2012) lists the cross sections of several typical superstructures that are commonly used worldwide for highway bridges. Table 2.1 has a three-column format: the first column describes the types of supporting components, the second describes the type of deck, and the third presents 11 typical cross sections identified as Types *a*, *b*, *c*… *k*. This chapter presents their description and important design-specific characteristics. They are cross-referenced in AASHTO LRFD Spec. Articles [Art.] 4.6.2.2.2, 4.6.2.2.3, and Table 4.6.2.2.2, which designers must use to calculate live load distribution factors (discussed in Chapter 4) that are required to determine live load design forces acting on superstructures.

Understanding the format of information presented in Table 2.1 is important. Several types of superstructures that possess similar design features are grouped together in this table for the convenience of designers. For example, a slab-beam type of superstructure may consist of a variety of

www.EngineeringEBooksPdf.com

FIGURE 2.1 A typical single-span highway bridge. (Photo by author.)

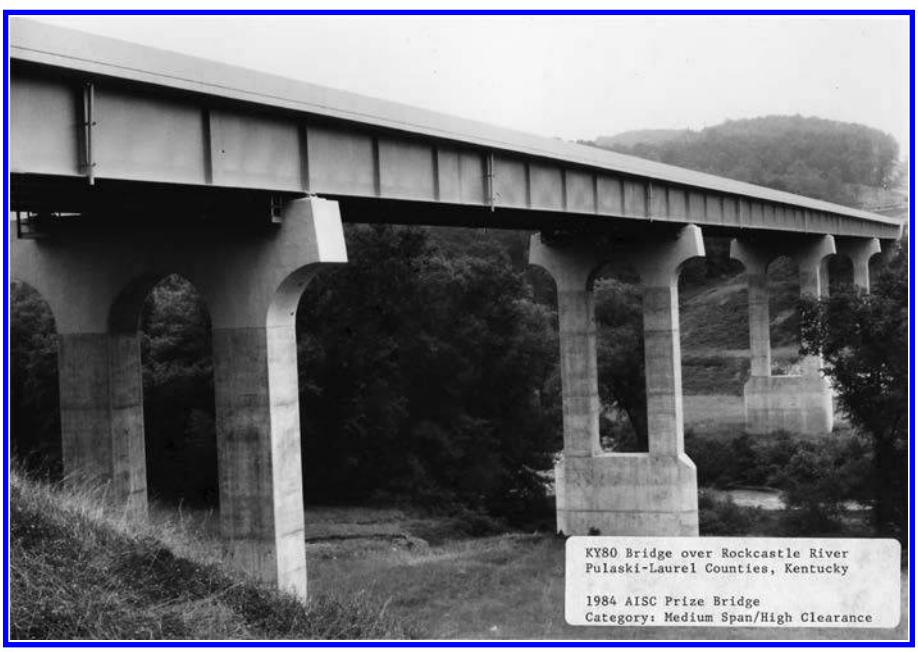

FIGURE 2.2 A multispan bridge (a typical plate girder bridge). Photo: KY80 Bridge over Rockcastle River, Pulaski-Laurel Counties, KY. (Courtesy of AISC, Chicago, IL.)

www.EngineeringEBooksPdf.com

FIGURE 2.3 A steel truss bridge. Photo: The Newburgh-Beacon Bridge No. 1, Newburgh, New York; the center span is a through-truss bridge; the end spans are deck-truss bridges. (Courtesy of AISC, Chicago, IL.)

FIGURE 2.4 The Eads Bridge, St. Louis, MO. Built by James Eads (1820–1887) and opened to traffic on July 4, 1878, the construction of this bridge was a milestone in the history of bridge engineering. This triple-arch bridge (502-520-502 ft) carries two railroad tracks on its lower deck and highway traffic on the upper deck. The three arches are fixed ended, and thus indeterminate. When built, these arches were the first ever to span distances of over 500 ft. The arches marked the first ever use of steel in bridge building, as well as the first ever use of tubular steel members for chords. See Taly (1998) for more on this great bridge. (Courtesy of AISC, Chicago, IL.)

www.EngineeringEBooksPdf.com

(a)

(b)

FIGURE 2.5 The New River Gorge Arch Bridge, WVA. The longest in the world and spanning 1700 ft, the construction of this scenic two-hinged steel deck arch bridge was completed in 1977; it carries four lanes of highway US 19. (a) Construction of the approach span and steel column bents and (b) construction of the arch beginning from the hinged end. (*Continued*)

www.EngineeringEBooksPdf.com

(c)

(d)

(e)

FIGURE 2.5 (*Continued*) The New River Gorge Arch Bridge, WVA. The longest in the world and spanning 1700 ft, the construction of this scenic two-hinged steel deck arch bridge was completed in 1977; it carries four lanes of highway US 19. (c) The arch under construction and (d and e) the completed arch. (Photos by author.)

www.EngineeringEBooksPdf.com

deck types supported and spanning transversely over steel wide flange beams or plate girders (see typical sketch in column 3 of Table 2.1). The decks are designed to act in unison with the supporting beams to act as composite systems under live load. Because of this similarity, these types of superstructures are grouped together and identified as Type *a* in Table 2.1. Another very common type of superstructure consists of cast-in-place or precast RC decks supported over prestressed concrete I-beams or bulb-T beams. The deck is designed to act compositely with the supporting beams/girders under live load. This type of superstructure is identified as Type *k*. An RC T-beam

(a)

(b)

FIGURE 2.6 (a) A cable-stayed bridge at Tacoma Narrows, State of Washington; (b) a view of the cable anchor at the deck level. (*Continued*)

www.EngineeringEBooksPdf.com

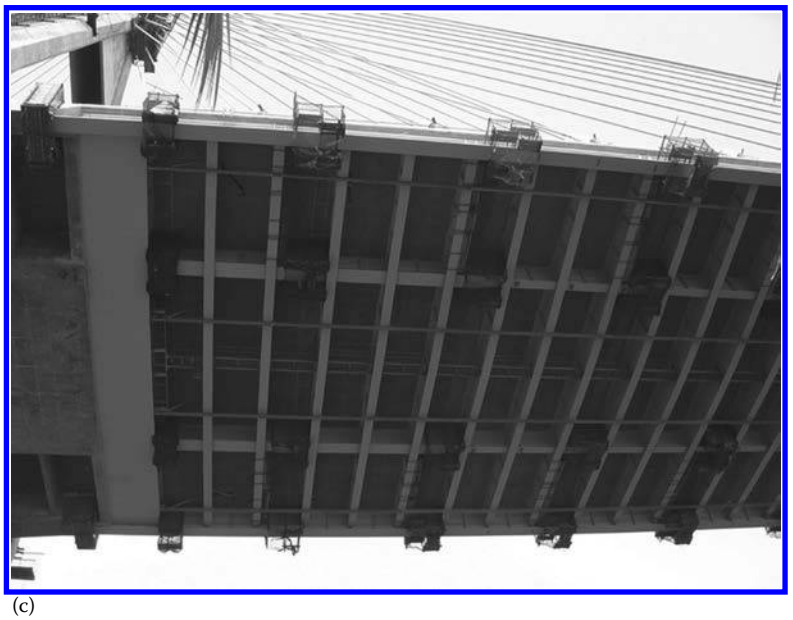

(c)

FIGURE 2.6 (*Continued*) (c) The underside of the deck of a cable-stayed bridge under construction in Bangkok. The deck slab spans longitudinally over the floor beams; each floor beam is supported by cable stays, one at each end. (Photos by author.)

FIGURE 2.7 A suspension bridge (right: Tacoma Narrow Bridge 2 completed in 1950, left: Tacoma Narrow Bridge 3, under construction in 2007). (Photo by author.)

superstructure, which consists of several monolithically cast-reinforced concrete T-beams, behaves differently from those described earlier; accordingly, it is identified separately as Type *e*. By contrast, a superstructure consisting of a wood deck consisting of planks supported transversely over glued-laminated beams acts as a noncomposite system under live load; therefore, it is identified separately as Type *l*.

www.EngineeringEBooksPdf.com

FIGURE 2.8 A utility-cum-pedestrian bridge. (Photo by author.)

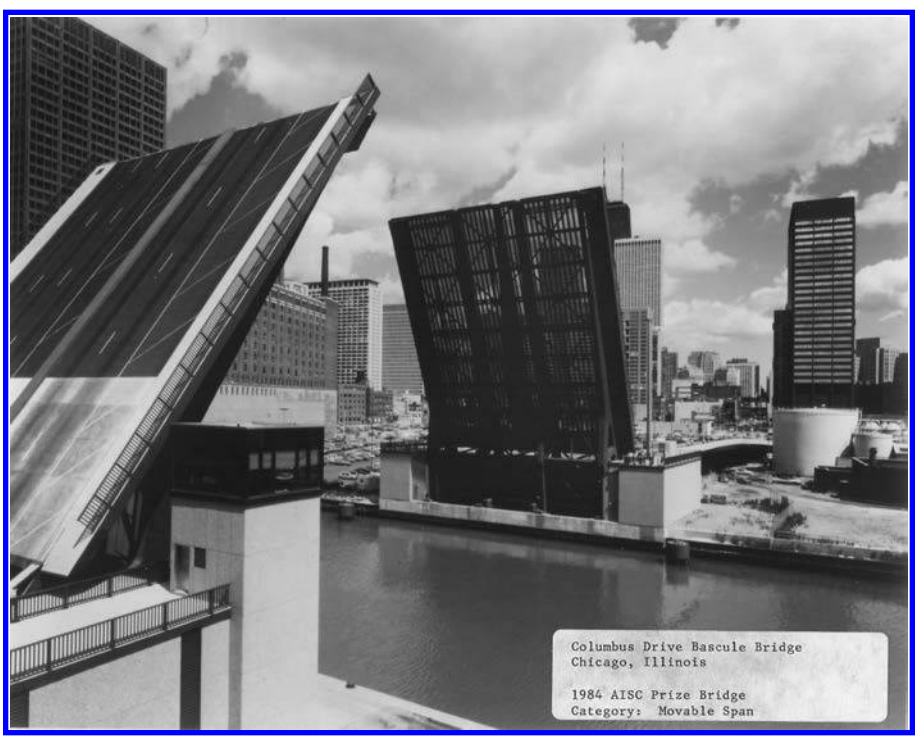

FIGURE 2.9 A bascule bridge (a type of movable bridge). Photo: The Columbus Drive bascule bridge Chicago, IL. (Courtesy of AISC, Chicago, IL.)

www.EngineeringEBooksPdf.com

FIGURE 2.10 A lift bridge (a type of movable bridge).

A brief description of superstructure systems listed in Table 2.1 follows. A comprehensive discussion of this topic can be found in Taly (1998). Any of the listed systems can be used at designers' discretion. However, it is noted that these are not the only systems that can be used or are considered suitable per se for highway bridge superstructures. As a matter of fact, any system comprising suitably arranged structural members that can perform satisfactorily conforming to AASHTO LRFD Specifications and that can be analyzed and/or designed based on principles of structural mechanics can be used; innovation is the key to successful designs. It is just that the state of the art of the current AASHTO LRFD Specifications covers only the systems listed in Table 2.1, which are commonly used worldwide for the purpose of calculating load distribution factors by the approximate method (discussed in Chapter 4); hence, these systems are discussed in this chapter. In addition, satisfactory performance of these systems has been proven by research and experience from the many, many as-built highway bridges.

2.3 DESCRIPTION AND DESIGN CHARACTERISTICS OF SUPERSTRUCTURE SYSTEMS IN TABLE 2.1

2.3.1 RC Deck over Steel Wide Flange Beams of Plate Girders (Type *a*)

This type of superstructure (Figure 2.11) has the following characteristics:

1. A cast-in-place RC deck that spans transversely as a continuous slab supported over longitudinally spanning, usually equally spaced, steel beams or plate girders.
2. The deck is designed for both the dead and live loads.
3. The beams/girders are designed as noncomposite elements to support dead load due to the deck and their self-weight. They are designed and built to act compositely with the RC deck under live load.

www.EngineeringEBooksPdf.com

TABLE 2.1
Types of Highway Bridge Superstructure Systems

Supporting Components	Type of Deck	Typical Cross Section
Steel beam	Cast-in-place concrete slab, precast concrete slab, steel grid, glued/spiked panels, stressed wood	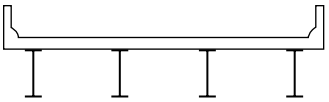 (a)
Closed steel or precast concrete boxes	Cast-in-place concrete slab	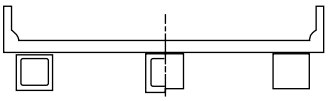 (b)
Open steel or precast concrete boxes	Cast-in-place concrete slab, precast concrete deck slab	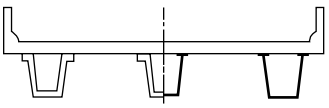 (c)
Cast-in-place concrete multicell box	Monolithic concrete	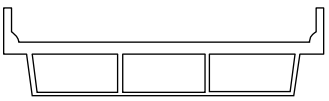 (d)
Cast-in-place concrete T-beam	Monolithic concrete	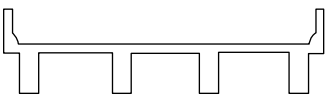 (e)
Precast solid, voided or cellular concrete boxes with shear keys	Cast-in-place concrete overlay	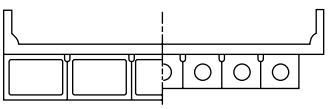 (f)
Precast solid, voided, or cellular concrete box with shear keys and with or without transverse posttensioning	Integral concrete	(g)
Precast concrete channel sections with shear keys	Cast-in-place concrete overlay	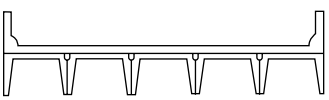 (h)
Precast concrete double-T section with shear keys and with or without transverse posttensioning	Integral concrete	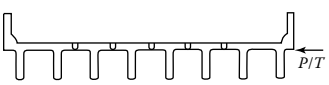 (i)
Precast concrete T-section with shear keys and with or without transverse posttensioning	Integral concrete	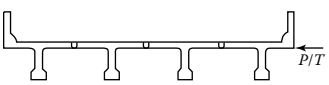 (j)

(*Continued*)

www.EngineeringEBooksPdf.com

TABLE 2.1 (*Continued*)
Types of Highway Bridge Superstructure Systems

Supporting Components	Type of Deck	Typical Cross Section
Precast concrete I or bulb-T sections	Cast-in-place concrete, precast concrete	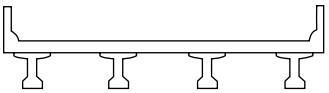 (k)
Wood beams	Cast-in-place concrete or plank, glued/spiked panels or stressed wood	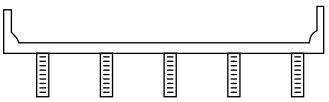 (l)

Source: *AASHTO LRFD Specifications for Highway Bridges*, 6th ed., Copyright 2012, by the American Association of State Highway and Transportation Officials, Washington, DC. Used by permission.

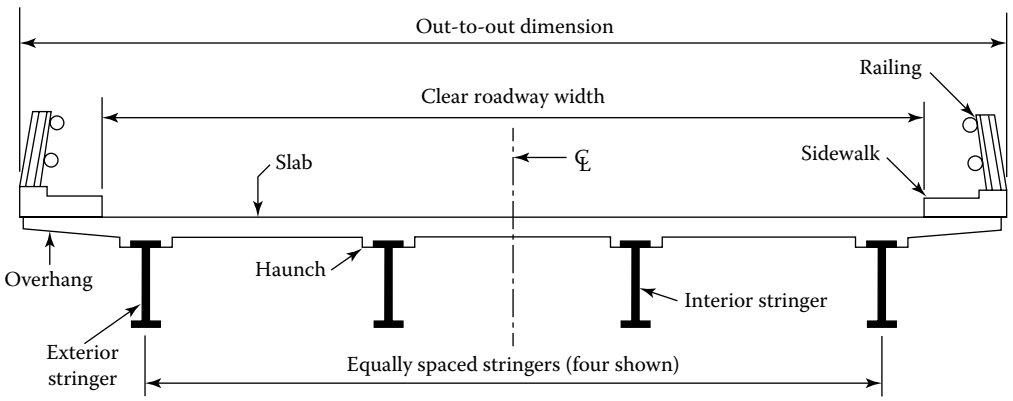

FIGURE 2.11 Superstructure Type *a*: cross section of slab-steel beam bridge. The cast-in-place concrete deck is built to act compositely with the WF steel beams or plate girders.

4. Composite action between the RC deck and the supporting beams/girders is developed by providing steel shear connectors welded to the top flanges of beams/girders and embedded sufficiently into the deck to prevent interfacial slip.

2.3.2 Spread-Box Beam Superstructure (Type *b*)

This type of superstructure (Figure 2.12) consists of a continuous cast-in-place RC deck supported over several equally spaced steel or concrete box beams that span longitudinally and supported over the abutments. The deck is designed to support both the dead and live loads, and to act compositely with the beams.

2.3.3 Open Steel or Precast Concrete Box Superstructure (Type *c*)

This type of superstructure (Figure 2.13) consists of either *open* steel or precast concrete girders. The deck supported over the steel girders is a cast-in-place concrete slab that is designed to act compositely with the girders under live load. The deck supported by precast concrete girders consists of precast concrete slab.

www.EngineeringEBooksPdf.com

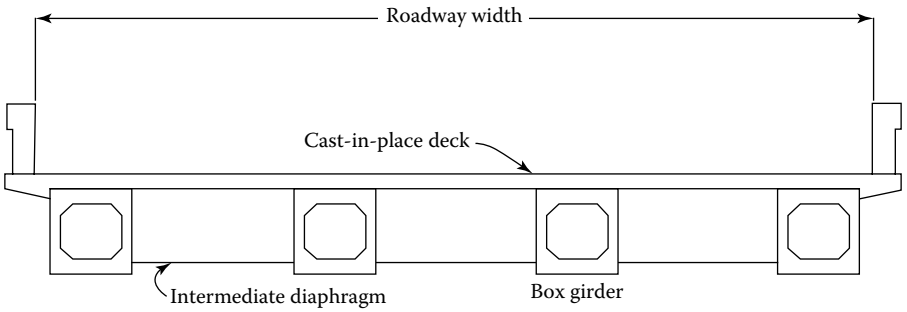

FIGURE 2.12 Superstructure Type *b*: typical cross section of a spread box beam bridge. The deck slab, cast to act compositely with the box girders, spans transversely over the precast, prestressed concrete box beams. Diaphragms are provided between the box girders. The number of box beams can be increased as necessary to provide for the required bridge width.

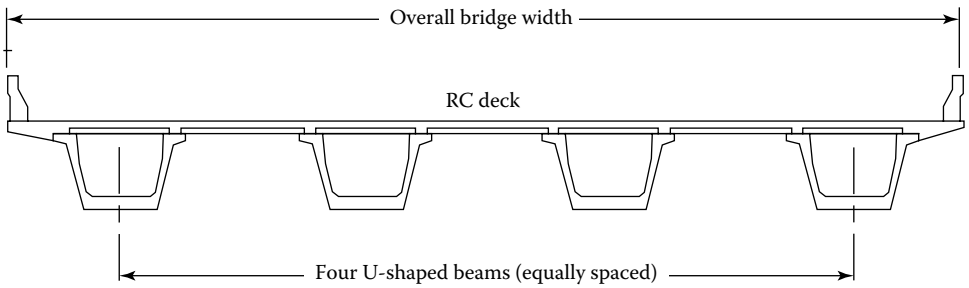

FIGURE 2.13 Superstructure system Type *c*: *open* steel or precast concrete girders.

2.3.4 Cast-in-Place Concrete Multicell Box Girder (Type *d*)

This type of superstructure (Figure 2.14) is very commonly used for highway bridges because of its high torsional stiffness. It consists of a single, monolithic, multicell, cast-in-place reinforced or prestressed concrete girder having a box-shaped cross section. Its exterior webs are either vertical or slightly inclined (for esthetics). The deck, spanning transversely over the

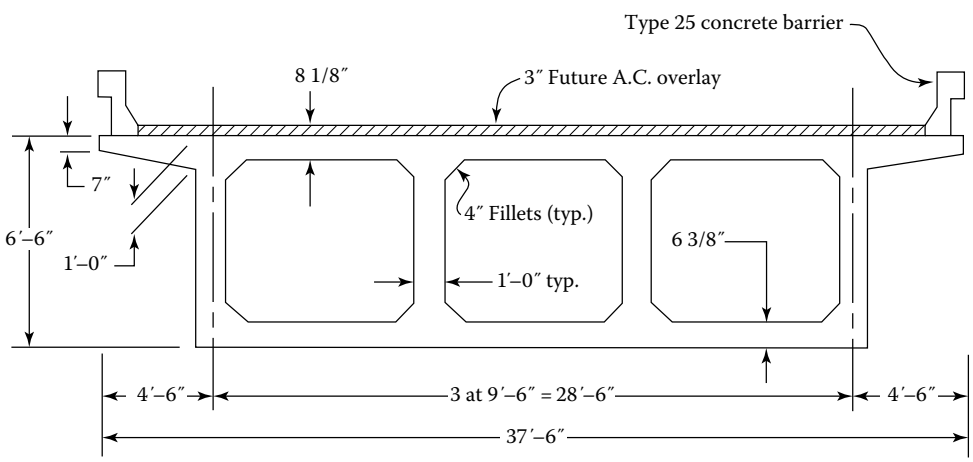

FIGURE 2.14 Superstructure Type *d*: a cast-in-place box girder. (*Note*: dimensions shown are for illustrative purposes only; cross-sectional dimensions may vary depending on the number of design lanes.)

www.EngineeringEBooksPdf.com

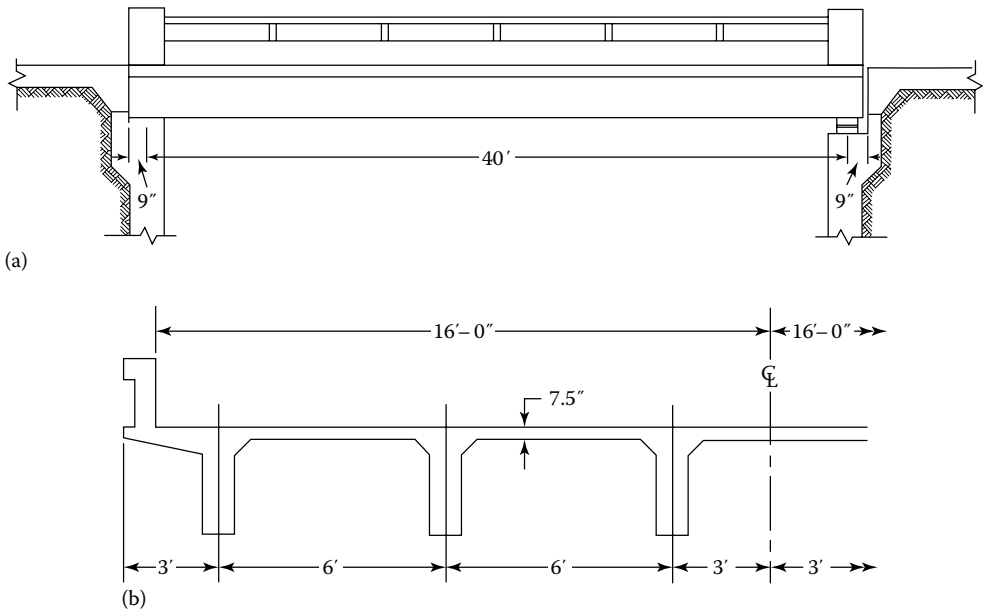

FIGURE 2.15 Superstructure Type *d*: a cast-in-place T-beam bridge. (a) Elevation and (b) cross section. (*Note*: dimensions shown are for illustrative purposes only; cross-sectional dimensions may vary depending on the number of design lanes.)

webs and cast monolithically with them and the bottom flange, is designed to independently carry both dead and live loads.

2.3.5 Cast-in-Place RC T-Beam Superstructure (Type *e*)

This type of superstructure system (Figure 2.15) consists of an RC deck that is cast in place with longitudinal RC beams, which act as stems of the T-beams. In contrast to superstructure Types *c* and *d* , the entire superstructure is designed to support both the dead *and* live loads.

2.3.6 Adjacent-Prestressed Concrete Box Superstructure (Type *f*)

As the name implies, this superstructure system (Figure 2.16) consists of several adjacently placed prestressed concrete box girders, which may be cellular or voided. Shear keys are provided in the webs of the girders, which are grouted and (supposedly) help transfer shear (but not bending moment) from one girder to the other. The top flanges of the box girders are designed to independently resist both dead *and* live loads. The girders are designed to span longitudinally between the abutments. Each girder is designed to carry its share of dead and live loads. The entire top surface provided by the top flanges of the girders is covered with cast-in-place concrete overlay after the shear keys between them are grouted.

2.3.7 Adjacent-Prestressed Concrete Box Superstructure with Integral Concrete Deck with or without Transverse Posttensioning (Type *g*)

This type of superstructure (Figure 2.17) is almost similar in appearance to Type *f*, except that the concrete deck is cast integrally with the box girders. Composite action between the deck and the box girders is developed by providing stirrups that project from the top flanges of the girders and

www.EngineeringEBooksPdf.com

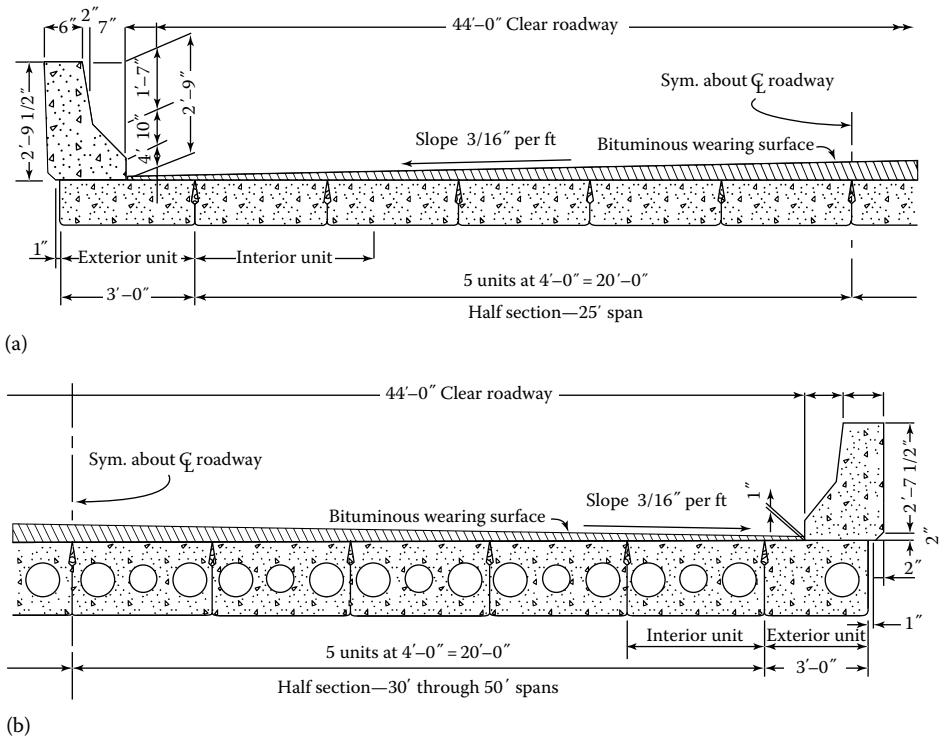

FIGURE 2.16 Superstructure system Type *f*: adjacent prestressed concrete box girders: (a) adjacent solid box girders and (b) adjacent voided box girders. (*Note*: dimensions shown are for illustrative purposes only; cross-sectional dimensions may vary depending on the number of design lanes.)

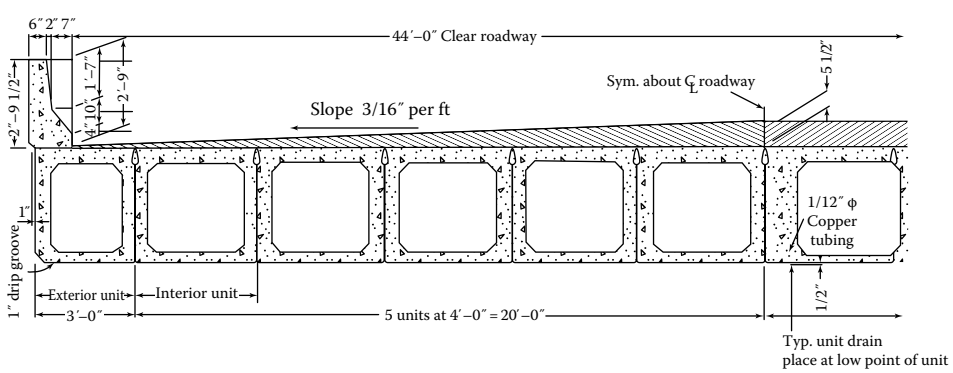

FIGURE 2.17 Superstructure system Type *g*: adjacent-prestressed concrete box girder superstructure with integral concrete deck with or without transverse posttensioning. (*Note*: dimensions shown are for illustrative purposes only; cross-sectional dimensions may vary depending on the number of design lanes.)

embedded in the slab. Additionally, the box girders might be transversely posttensioned at certain intervals, which help the entire superstructure to act as one tight unit.

2.3.8 Precast Concrete Channel Sections with Shear Keys and Concrete Overlay (Type *h*)

This type of superstructure (Figure 2.18) consists of inverted precast, prestressed concrete channel sections with shear keys and cast-in-place concrete overlay.

www.EngineeringEBooksPdf.com

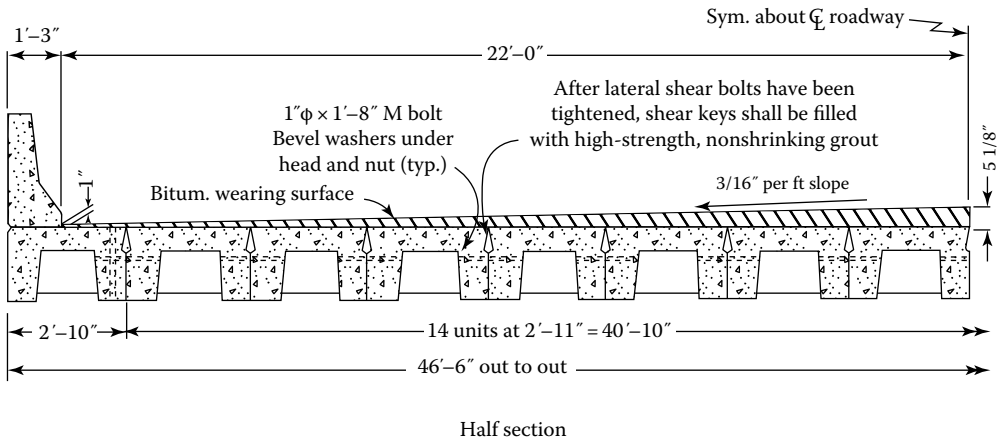

FIGURE 2.18 Superstructure system Type *h*: precast concrete channel sections with shear keys and concrete overlay. (*Notes*: cross-sectional dimensions shown are for illustrative purposes only and may vary depending on the number of design lanes. Fill dowel sleeves with grout at fixed end and bitumen at exp. end.)

2.3.9 Precast Concrete Double-T Girders with Shear Keys, and with or without Transverse Posttensioning and Integral Concrete Deck (Type *i*)

This superstructure system (Figure 2.19) consists of prestressed concrete double-T girders with their flanges abutting each other. Longitudinal shear keys are provided at the ends of flanges, which are grouted to enable girder-to-girder shear (but not bending moment) transfer. An integral concrete overlay is provided to serve as a deck. The girders might (or might not) be posttensioned transversely at certain intervals.

2.3.10 Precast Concrete Single-T Girders with Shear Keys, and with or without Transverse Posttensioning and Integral Concrete Deck (Type *j*)

This type of structure (Figure 2.20) is identical to Type *i* , except that the girders are single-Ts instead of double-Ts.

2.3.11 RC Deck over Prestressed I-Beams or Bulb-T Girders (Type *k*)

This type of superstructure (Figure 2.21) has the following characteristics:

1. A cast-in-place RC deck that spans transversely as a continuous slab supported over longitudinally spanning, usually equally spaced, prestressed I-beams or bulb-T girders. (I-beams are doubly symmetric sections, whereas the bulb-T girders, singly symmetric sections and have top flanges that are much wider than the bottom flanges.)
2. The deck is designed for both the dead and live loads.
3. The beams/girders are designed as noncomposite elements to support dead load due to the deck and their self-weight. They are designed and built to act compositely with the RC deck under live load.
4. The composite action between the RC deck and the prestressed beams or bulb-T girders is developed by providing shear stirrups extending from the top of the prestressed beams/girders and embedded sufficiently into the deck to prevent interface slip.

www.EngineeringEBooksPdf.com

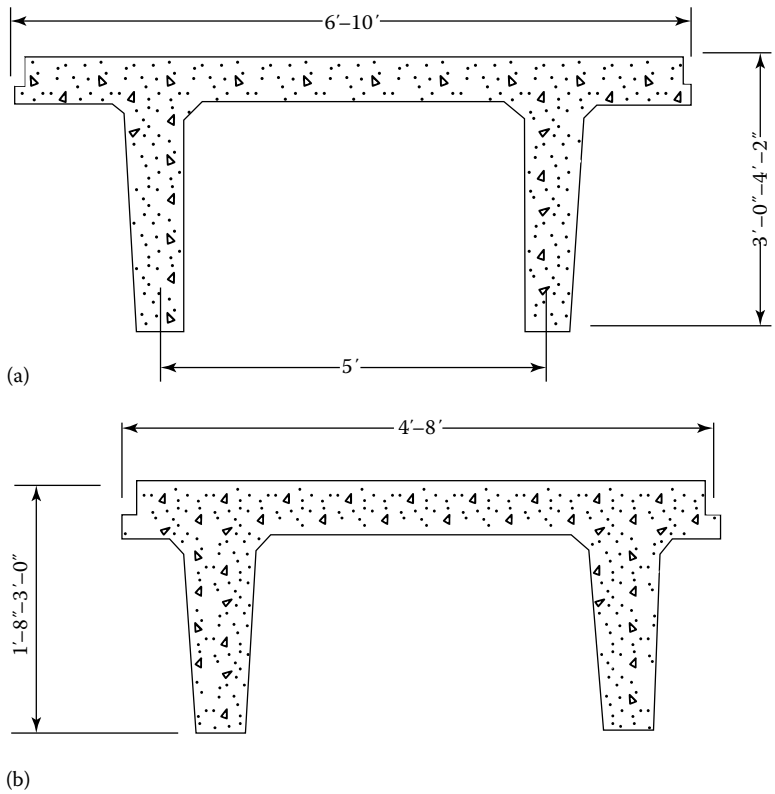

FIGURE 2.19 Superstructure system Type *i*: precast concrete double-T girders with shear keys, and with or without transverse posttensioning, and integral concrete deck. Continuous grouted shear keys are provided between the flanges of adjacent double-T beams. (a) Span range 50′–80′ large double T and (b) span range 25′–70′ small double T.

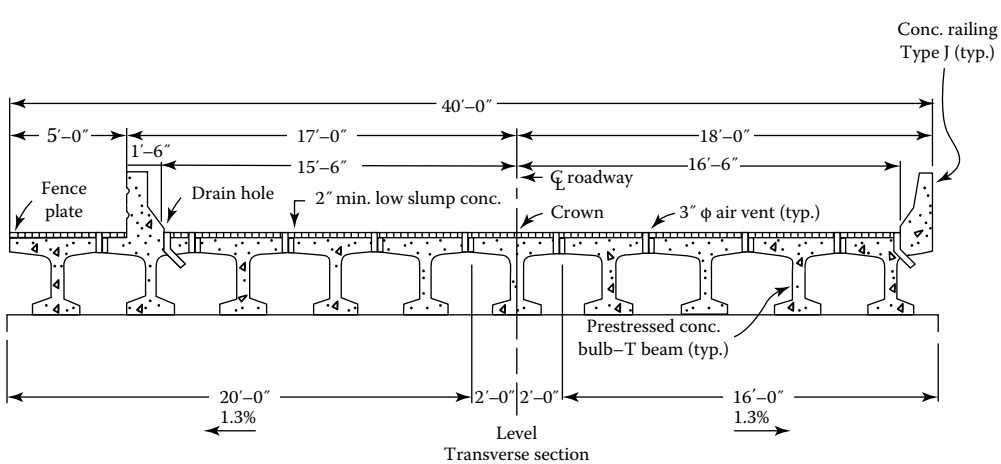

FIGURE 2.20 Superstructure system Type *j*: precast concrete single-T girders with shear keys, and with or without transverse posttensioning, and integral concrete deck.

www.EngineeringEBooksPdf.com

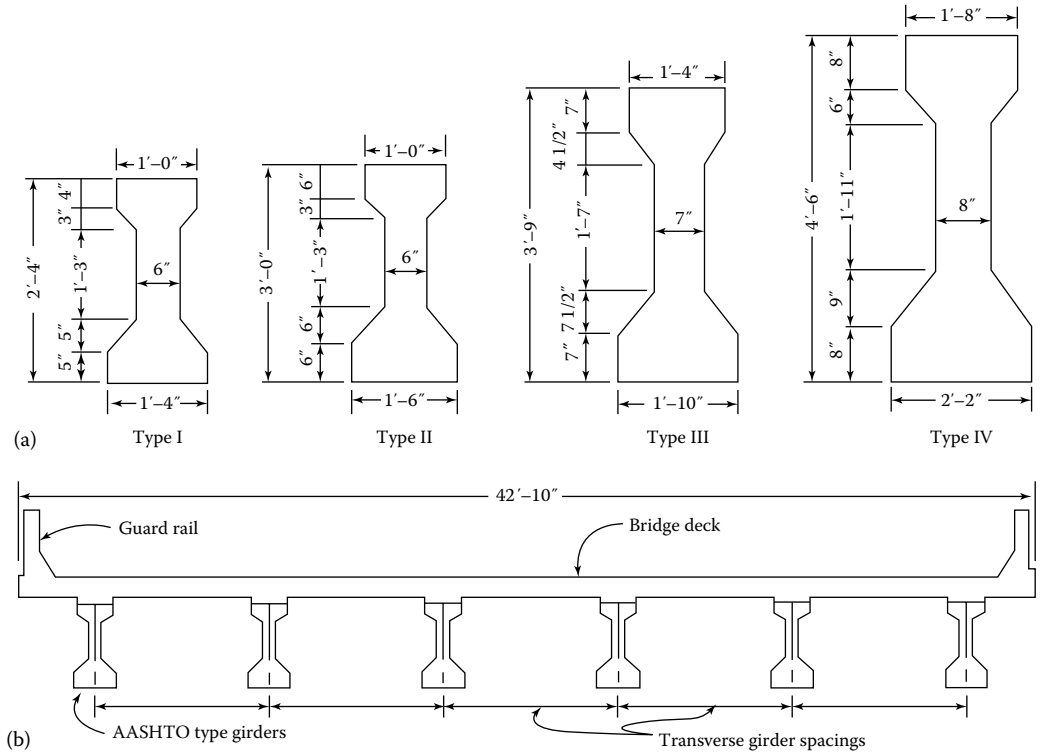

FIGURE 2.21 (a) Typical standardized prestressed concrete I-shaped girders, (b) cross section of a superstructure system *Type k*: RC deck supported on prestressed concrete I-beams (shown) or bulb-T girders (not shown). The deck is designed to act compositely with the supporting girders. The dimensions shown are for illustrative purposes only.

2.3.12 Fiber-Reinforced Polymer Highway Superstructure Systems

A new type of highway bridge superstructure system, consisting of advanced composite materials (so called because of their superior strength), has emerged relatively recently (since the 1990s) in the United States and elsewhere in the world, notably in Japan. These are called fiber-reinforced polymer (FRP) deck systems, which are fabricated from glass or carbon fiber fabrics with polymer binders. While presently very limited in use, mostly experimental and under monitoring by research institutions, FRP bridge deck systems are significantly lighter than conventional superstructures; first-generation FRP decks weigh only about 25 lb/ft^2 to about 135 lb/ft^2 for a comparable 9 in. thick concrete deck, including the wearing surface. FRP desk systems are durable and less maintenance intensive, resulting in low lifecycle costs. Their modular characteristics lend them as suitable, and often preferred, alternatives for rapid installation/erection leading to savings in construction costs. These qualities notwithstanding, these types of superstructure systems are not covered in the current AASHTO LRFD Specifications (AASHTO 2012) owing to the lack of data, experience, and sufficient research.

Two examples of FRP superstructure deck systems are shown in Figures 2.22 through 2.24. Figure 2.22 illustrates two units of prefabricated FRP deck modules placed adjacently. A highway superstructure deck system comprises several such units (Figure 2.23). Figure 2.24 shows a pedestrian truss bridge built from prefabricated (pultruded) FRP structural elements.

The FRP superstructure systems are not discussed further in this book.

www.EngineeringEBooksPdf.com

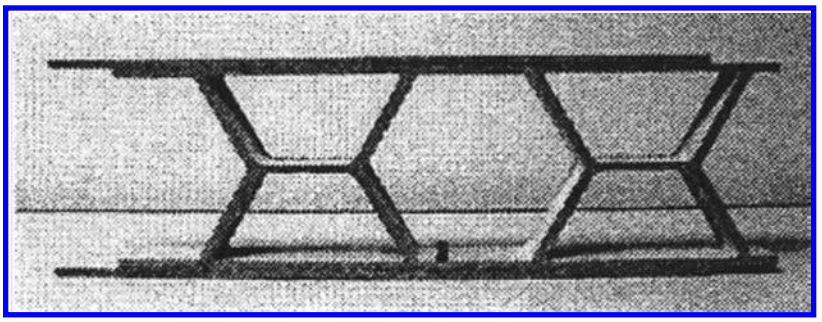

FIGURE 2.22 Two modular units of prefabricated FRP deck modules of placed adjacently.

FIGURE 2.23 An FRP highway bridge superstructure deck system built from pultruded units shown in Figure 2.22. These units are clearly visible underneath the sidewalk on the left. (Market Street Bridge, Wheeling, West Virginia, nearing completion.) (Photo by author.)

FIGURE 2.24 A pedestrian FRP bridge built from pultruded structural shapes. (FRP bridge in Tujunga, CA. Photo by author.)

www.EngineeringEBooksPdf.com

2.4 DIAPHRAGMS

2.4.1 Definition of a Diaphragm

The term *diaphragm* refers to a structural element that resists *in-plane* forces (as different from the *out-of-plane* forces or forces perpendicular to it). Diaphragms are used in both buildings and bridges; however, they are used to serve different purposes in these two types of structures. Because of the importance of their function and influence on structural behavior, this section presents a brief discussion on diaphragms in the context of their usage in both types of structures.

2.4.2 Diaphragms in Building Structures

In buildings, *diaphragms* act as structural elements that serve to transfer lateral forces, such as wind or earthquakes, to the ground. Lateral forces acting perpendicular to walls of box-like structures are transferred as in-plane forces to horizontal elements (floors and roofs, which also support gravity loads) present in the building. This structural action is called the *diaphragm action*, and the participating floors and roofs are called *horizontal diaphragms* (roof diaphragms and floor diaphragms). These elements (horizontal diaphragms) transfer their in-plane forces to the supporting walls in the form of horizontal reactions through the connections between them. The walls, in turn, receive these forces as in-plane forces and transfer them to the ground. For this structural action, the walls are called *vertical diaphragms* or shear panels (in wood buildings) or shear walls (in steel, concrete, and masonry buildings). Horizontal and vertical diaphragms constitute two very important components of lateral force resisting systems (LFRS) in wood buildings, whose function, in addition to resisting gravity loads, is to transfer lateral loads to the ground. A discussion on this topic can be found in Taly (2003).

2.4.3 Diaphragms in Bridge Superstructures

Interestingly, in bridge structures, the term *diaphragms* is used in a different context, and they also look quite different from the horizontal (roofs and floors) and vertical diaphragms (walls); as such their definition depends on the usage. Essentially, diaphragms as used in highway bridge superstructures can be characterized as short structural elements positioned transversely to and in between adjacent girders that support the deck slab. Depending on the type of superstructure, the diaphragms can be of concrete, steel, or wood.

Diaphragms are provided to ensure lateral distribution of live loads from the bridge deck to the adjacent girders supporting it, which depends on both the stiffness of the diaphragms relative to the girders and the method of connectivity. However, the extent of this structural action has not been quantified (Decastro and Kostem 1975, Degenkolb 1977, Kostem 1984). The diaphragm action comes into play when a load is placed on the desk and applied *at* the diaphragm location, a condition seldom realized in practice. Research shows that a diaphragm under the load lessens the load carried by the girder immediately under the girder by transferring portions of it to adjacent girders; remote diaphragms do not participate in distributive action. For full effectiveness (i.e., more uniform transverse distribution of the live load) under highway or railway loadings, several closely spaced diaphragms should be provided; this would cause the deck to act as a two-way slab. However, this distributive action does not develop unless the diaphragm spacing is as close as the girder spacing, and if so provided, the structure would be uneconomical (Degenkolb 1977).

In both concrete and steel box girders, diaphragms are vertical elements placed within the girders at the span ends (called the *end diaphragms*) and also at intervals (called *intermediate diaphragms*); they are intended to act as stiffeners whose function is to maintain the cross-sectional shape of the girders by providing torsional rigidity. In typical slab-girder-type superstructures, diaphragms are vertical elements that are placed vertically in between the girders at the span ends (over the abutments) and also at intervals as required by the specifications. At the abutments, the diaphragms are

www.EngineeringEBooksPdf.com

intended to transfer horizontal forces from the superstructure to the substructure (abutments). The intermediate diaphragms are intended to provide torsional stiffness to the entire superstructure.

Diaphragms have historically been part of the highway bridge superstructures since the early days. Both the AASHTO Standard Specifications (AASHTO 2002) and the AASHTO LRFD Specifications (AASHTO LRFD 2012) call for providing both the end and the intermediate diaphragms. In the ASSHTO Standard Specifications (AASHTO 2002), the diaphragms and their spacing were arbitrarily set based on experimental research (DeCastro and Kostem 1975, Zellin et al. 1975a,b, Degenkolb 1977, Kostem 1984), but this arbitrary requirement has been removed in the current AASHTO LRFD Specifications (AASHTO 2012). It is noteworthy that the questionable effectiveness of diaphragms in straight girder superstructures notwithstanding, diaphragms and bracings constitute very important load-carrying components of curved girder bridges.

2.4.3.1 ASSHTO Standard Specifications for Diaphragms

2.4.3.1.1 Reinforced and Prestressed Concrete Superstructures

AAHTO Standard Specifications (AASHTO 2002, Art. 8.12 for reinforced concrete girder bridges, and Art. 9.10 for prestressed concrete girder bridges) mandate the following requirements for diaphragms. These requirements are rather arbitrary as they are apparently based on experience and past practices.

For reinforced and prestressed concrete T- and box-girder bridges, diaphragms should be provided, except that they may be omitted where tests or structural analysis show adequate strength without them.

For T-beams, diaphragms or other means are required to be placed at span ends to strengthen the free edge of the slab and to transmit lateral forces to the substructure. Intermediate diaphragms are to be placed in between the beams at points of maximum moment for spans over 40 ft.

For cast-in-place box girders, diaphragms or other means shall be used at span ends to resist lateral forces and to maintain section geometry. Intermediate diaphragms are not required for bridges with an intermediate radius of curvature 800 ft or greater.

For precast box multibeam bridges, diaphragms are required only if necessary for slab-end support or to contain or resist transverse tension ties.

For all types of prestressed boxes in bridges with an inside radius of curvature less than 800 ft, intermediate diaphragms may be required; the spacing and strength of these diaphragms shall be given special consideration in the design of the structure.

2.4.3.1.2 Steel Girder Bridge Superstructures

AASHTO 2002 Art. 10.20 specifies the requirements for diaphragms for steel girder bridge superstructures as follows:

1. Rolled beam and plate girder spans to be provided with cross-frames or diaphragms at each support.
2. Intermediate diaphragms or cross-frames to be provided in all bays at intervals not exceeding 25 ft.
3. Diaphragms for rolled beams to have at least one-third and preferably half the beam depth.
4. Diaphragms for plate girders to have at least half and preferably three-fourths the girder depth.
5. Cross-frames, when provided, to be as deep as possible.
6. Intermediate cross-frames preferably to be of the cross-type or V-type.
7. End cross-frames or diaphragms to be proportioned to adequately transmit all the lateral forces to the bearings.
8. Intermediate diaphragms or cross-frames to be placed normal to girders when the supports are skewed more than 20°.

www.EngineeringEBooksPdf.com

2.4.3.2 AASHTO LRFD Specifications for Diaphragms and Cross-Frames

AASHTO LRFD Specifications (AASHTO 2012) have replaced the AASHTO Standard Specifications' arbitrary requirement for diaphragms to be placed at not more than 25 ft by a requirement for a rational analysis that will often result in the elimination of fatigue-prone attachment details. Diaphragms and cross-frames may be provided at the ends of the bridge superstructure, across interior supports, and intermittently along the span.

Art. 6.7.4 of AASHTO 2012 specifies that the need for diaphragms or cross-frames in steel girder superstructures be investigated for all stages of assumed construction procedures and then final condition. This investigation should include, but not limited to, the following:

1. Transfer of lateral wind loads from the bottom of the girder to the deck and from the deck to the bearings.
2. Stability of the top flange in compression prior to curing of the deck. (This is the typical case when the girder is under positive moment as in simply supported spans. Metal stay-in-place deck forms should not be assumed to provide adequate stability to the top flange in compression prior to the curing of the deck.)
3. Stability of the bottom flange for all loads when it is in compression. (This would happen when the girder is subjected to negative moment.)
4. Consideration of any flange lateral bending effects.
5. Distribution of vertical dead and live loads applied to the structure.

Investigation for item 5 is very important when analyzing a beam-slab-type bridge superstructure for determining design forces in the exterior girders. The presence of diaphragms in such a superstructure calls for *additional* investigation when calculating the *live load distribution factors* for the exterior girders (discussed in Chapter 4). Art. 4.6.2.2.2d (AASHTO 2012) specifies

> In beam slab bridge cross sections with diaphragms or cross frames, the distribution factor for the exterior beam shall not be taken to be less than that would be obtained by assuming that the cross section deflects and rotates as a rigid cross section. The provisions of Art. 3.6.1.1.2 shall apply.

Art. 3.6.1.1.2 specifies consideration of *multipresence factors*, discussed in Chapter 4

This additional investigation is required because the distribution factor for girders in a multigirder cross section, Types *a*, *e*, and *k* in Table 2.1 (AASHTO Table 4.6.2.2.1-1, discussed in Chapter 4), was determined without the consideration of diaphragm or cross-frames. An exact analytical method for the determination of distribution factors for the exterior girders in multigirder bridges with diaphragms or cross-frames is not specified in AASHTO 2012; however, *Commentary C4.6.2.2.2d* (AASHTO 2012) recommends an interim procedure that is similar to the conventional approximation for loads on piles (discussed in Chapter 4).

When diaphragms are provided in steel girder bridges, Art. 6.7.4 (AASHTO 2012) specifies the following general requirements for providing them:

1. Intermediate diaphragms or cross-frames should be provided at nearly uniform spacing in most cases for efficiency of structural design, for constructability, and/or to allow simplified methods of analysis for calculating flange lateral bending stresses. Closer spacings may be necessary adjacent to interior piers, in the vicinity of skewed supports, and, in some cases, near midspan.
2. For effectiveness, diaphragms for rolled beams and cross-frames should be as deep as practicable, but as a minimum should be at least one-half of beam depth for rolled beams and three-fourth of the depth for plate girders. Cross-frames in horizontally curved bridges should contain diagonals and top and bottom chords.

www.EngineeringEBooksPdf.com

3. At the end of the bridge and intermediate points where the continuity of the slab is broken, the edges of the slab are broken, and the edges of the slab are required to be supported by diaphragms or other suitable means (refer to Art. 9.4.4 for details).
4. Where supports are not skewed, intermediate diaphragms or cross-frames should be placed in contiguous lines normal to girders.
5. Where supports are not skewed more than 20°, intermediate diaphragms or cross-frames may be placed in contiguous lines normal to the girders.
6. Where supports are skewed more than 20°, diaphragms or cross-frames should be placed in contiguous lines or in staggered patterns.
7. Diaphragms or cross-frames are not required along skewed interior supports if diaphragms or cross-frames normal to the girders are provided at bearings that resist lateral forces.
8. If the end diaphragm or cross-frame is skewed, the effect of the tangential component of force transmitted by the skewed unit on the girder shall be considered.

Art. 6.7.4 specifies the following requirements for design of diaphragms and cross-frames:

1. End diaphragms shall be designed for forces and distortion transmitted by the deck and deck joint.
2. End moments in diaphragms shall be considered in the design of the connection between the longitudinal component and the diaphragm.
3. Diaphragms with depth-to-span ratio greater than 4.0 may be designed as beams.
4. Shear deformation shall be considered in the design of diaphragms having a span-to-depth ratio of less than 4.0.
5. In the case of box girder bridges, diaphragms are required to be provided within the box sections at each support to resist cross-sectional distortion of the box and are to be designed to resist torsional moments in the box and transmit vertical and lateral forces from the box to the bearings.

As a rule, diaphragms and cross-frames are designed as secondary members. In contrast, diaphragms and cross-frames in curved girder bridges (also called *horizontally curved* bridges, not discussed in this book) resist forces that are critical to the proper functioning of those bridges. Because they transmit forces necessary to maintain equilibrium, diaphragms and cross-frames in curved girder bridges are to be designed as primary members.

Readers are encouraged to read the commentary to Art. 6.7.4 (AASHTO 2012) for a comprehensive understanding of the requirements for design and placement of diaphragms and cross-frames.

2.5 BRIDGE SITE AND GEOMETRY

2.5.1 Bridge Type, Size, and Location

The first step of planning, designing, and building a highway bridge is to decide on its *type*, *size*, and *location* (commonly referred to as the TSL of a bridge); AAHTO LRFD Specifications (AASHTO 2012) Section 2 Art. 2.3–2.4 provide specifications for this aspect of a bridge design project. The location of and alignment of the bridge should be selected to satisfy both on-bridge and under-bridge traffic requirements. The choice of the bridge location should be decided after a careful investigation and should be supported by analyses of alternatives with considerations given to economic, engineering, social, and environmental concerns. Lifecycle costs of a bridge should form an important consideration for the TSL consideration for a bridge. As such, costs of maintenance and inspection associated with a bridge should be considered as well during the planning phase.

www.EngineeringEBooksPdf.com

A bridge should be designed and built for the near-term needs but with a vision for the future. Due consideration should be given to future variations in alignment or width of the waterway, highway, or railway to be spanned by the bridge. Prospects of future addition of mass-transit facilities or bridge widening should be considered where appropriate. Future bridge widening has implications in the design of bridge structures, which designers should be aware of. AASHTO Art. 2.5.2.7 mandates that *unless future widening is virtually inconceivable, the load-carrying capacity of the exterior beams shall not be less than the load-carrying capacity of an interior beam* (more discussion on this topic in Chapter 4). Future widening and increased loading should be carefully investigated and assessed, and adequate provisions should be made in the design of both the superstructure and the substructure.

Where a highway bridge is to span a waterway, it would be necessary to make complete *hydraulic* and *hydrologic* investigations and assessments of bridge sites (not discussed in this book; refer to AASHTO 2012 Art. 2.6 for detailed requirements and guidance) as a part of preliminary plan development to ensure that sufficient waterway and overhead clearance are provided. Art. 2.6 requires mandatory evaluation of bridge design alternatives involving considerations of stream stability, backwater, flow stabilization, stream velocities, scour potential, flood hazards tidal dynamics where appropriate, and consistency with established criteria for the National Flood Insurance (refer to the commentary C2.6.1 of AASHTO 2012 for details on National Flood Insurance Program). Permission to build a bridge over a navigable waterway must be obtained from the US Coast Guard and/or other agencies having jurisdiction. Navigational clearances, both horizontal and vertical, as established in cooperation with the US Coast Guard, are required to be provided.

2.5.2 Bridge Width

The width of a bridge is the starting point for determining the configuration of its cross section, viz., the number of girders required to support the deck and the width of the overhang on each side of the deck. AASHTO 2012 Art. 2.3.2.2.3 requires that the geometric standards of a highway bridge should satisfy the requirements of the AASHTO publication *A Policy on geometric Design of Highways and Streets* (AASHTO 2011) unless exceptions can be justified. The width of shoulders and geometry of traffic barriers should meet the specifications of the owner. Art. 2.3.3.3 mandates that the bridge width shall not be less than that of the approach roadway section, including shoulders or curbs, gutter, and sidewalks. Some bridges, particularly the long-span bridges, such as arch, cable-stayed, and suspension type, carry highways that provide for two-way traffic, might have a center median (traffic separator), which should be included when determining the overall bridge width.

The number of traffic lanes to be permitted on a bridge plays a major factor in deciding its clear roadway width (i.e., the width between the curbs and/or barriers) available for traffic. Two terms are used in conjunction with the highway traffic—*traffic lane* and *design lane*—and both have different meanings. The term *traffic lane* is used by the traffic engineer to accommodate lanes of vehicular traffic on a bridge (e.g., x number of traffic lanes) and is typically 12 ft wide. The term *design lane*, also referred to as standard design lane, is used by designers for the live load placement on the bridge deck for structural analyses of the superstructure (discussed in Chapter 4). For a bridge of given width, w, the number of design lanes is taken as the integer part of the ratio $w/12$ (Art. 3.6.1.1.1). Whenever possible, bridges should be built to accommodate the standard design lanes and appropriate shoulders.

2.5.3 Normal and Skewed Bridges

From a geometric viewpoint (in plan), bridges can be described as *normal* (or *right*) or *skewed* (Figure 2.25). The *longitudinal axis* of a bridge is defined as the axis of symmetry of the bridge deck that is oriented parallel to the direction of the flow of traffic; the other axis of symmetry is

www.EngineeringEBooksPdf.com

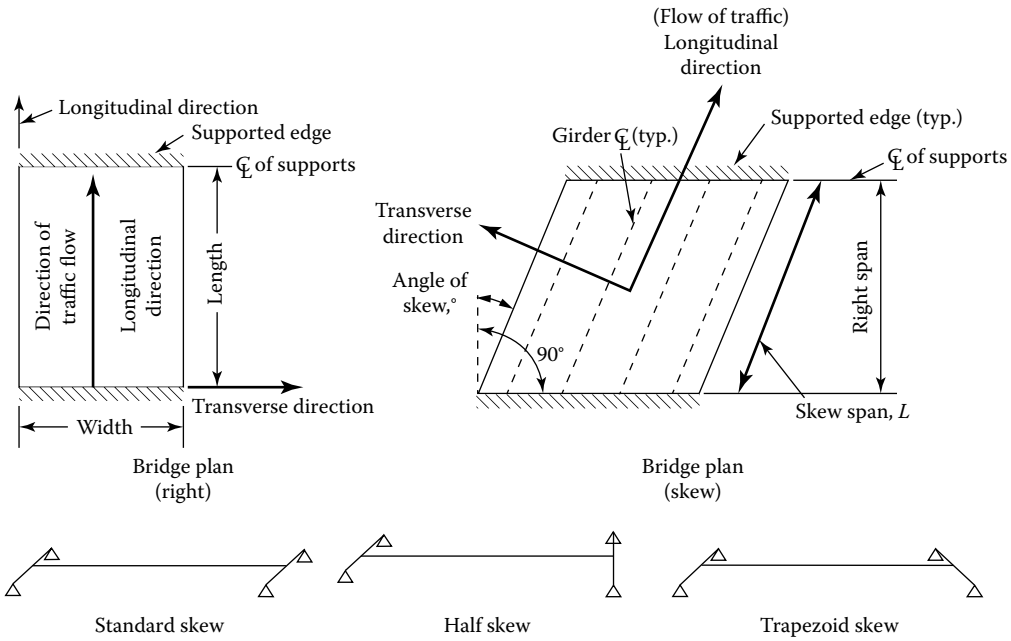

FIGURE 2.25 Definition of right and skew bridges.

called *transverse axis*. A normal bridge is one that has its longitudinal axis perpendicular to the supporting abutments and piers (when present). Generally, with a few exceptions, the longitudinal axis of a bridge would also align with the longitudinal axis of the connecting roadway. In a normal bridge, the deck and the supporting girders are oriented and placed symmetrically with respect to the centerline of the bridge, which is the same as its longitudinal axis. Such an arrangement is ideal and highly desirable because it simplifies both analysis and construction of the bridge, resulting in an economical structure.

Occasionally, it is not feasible to build a bridge with a normal configuration because of human-created obstacles, complex intersections and interchanges, space limitations, mountainous terrain, etc. In such a case, the bridge must be built with its longitudinal axis at an angle to the centerlines of the supports; the result is a *skewed* bridge (or a skewed span). By definition, a *skewed* bridge, simple or continuous, is characterized by its longitudinal axis (i.e., the axis parallel to the girders) forming an acute angle, instead of right angles (as in a normal bridge), with the centerlines of the supports.

Skew angle (or *angle of skew*) is defined as the angle between the centerlines of the support and the longitudinal axis of the bridge (Figure 2.25). The skew angles at the two end supports might not be the same. Skewed bridge geometry with the end supports having the same centerlines is called *standard skew*. Bridge geometry with only one support normal to the longitudinal to the axis of the deck and the other at an angle to it is called *half skew*. When the slew angles are different at both end supports, the bridge geometry is called *trapezoidal skew*.

Presence of skew in a bridge causes analytical and construction implications, and the result is a more costly bridge. Skew angle forms an important consideration in the determination of design loads for the superstructure (deck as well as the supporting girders). It has been suggested that for skew angles *not* exceeding 20° (30° for slab-beam bridges), bridges may be safely designed as normal or right bridges. However, it has been shown that for larger skew angles, torsional moments, which are not included in the approximate analyses, are large and would invalidate the results from such analyses. The specifications (AASHTO 2012 Art. 4.6.2.2.2e) provide for *correction factors* (see AASHTO 2012 Tables 4.6.2.2.2e-1 and 4.6.2.2.3c-1) that must be used in conjunction with the

www.EngineeringEBooksPdf.com

live load distribution factors when the line supports are skewed and the difference between the skew angles of adjacent supports does not exceed 10°. This topic is discussed further in Chapter 4.

2.6 DEFLECTIONS

2.6.1 Historical Review of Deflection Limitations

Functional considerations are the very reason for creating a structure. Structural design can be considered optimal if it can simultaneously satisfy the requirements of function, safety, economy, and esthetics (Kuzmanovic and Willems 1983). Although all of these requirements are important, the functionality and safety, in that order, carry the most weight. Toward that end, designers provide highway bridges not merely with adequate strength but also with service lives uninterrupted by fatigue damage, durable riding surfaces, and comfortable crossings for pedestrians and occupants of moving vehicles. Deflection and fatigue are the two elements of the design matrix that are related to the performance of the bridge. Together, they from a part of overall design criteria known as *serviceability criteria*.

Limiting the *deflection-to-span* and *depth-to-span* ratios (slenderness) had been recognized early on by both railroad and highway engineers as the key to providing bridges with durable riding surfaces as well as comfort to the occupants of the moving vehicles. However, how these criteria contribute to those qualities is not very clear (Wright and Walker 1971).

There exists a long and interesting history of the developments of deflection limitations for both railroad and highway bridges.

Both the deflection-to-span and depth-to-span ratio limitations have evolved over more than 100 years. During the early years, because of the widespread use of railroad and the much heavier loadings involved, railroad engineers took the lead in establishing the two limitations. In the United States, evolutions of deflection limitations can be traced back to the 1870s. According to the 1958 landmark study on deflection limitations of bridges (ASCE 1958), the first serious effort in this regard appears to be that of the Phoenix Bridge Company, which, in 1871, limited the deflection due to the passage of a train and locomotive at 30 miles per hover to 1/1200 of the span. In 1905, the American Railroad Engineers Association (AREA) specifications provided that pony trusses and plate girders shall preferably have a depth not less than 1/10 of the span and the rolled beams and channels used as girders shall preferably have not less than 1/12 of the span. When these ratios are decreased, proper increases shall be made to the flange section.

Historically, it appears that the purpose of limiting depth-to-span ratios was to limit the live load deflection. In the case of railroad bridges, deflection was limited to avoid excessive vibration of the structure in resonance with the recurring hammer blows of the locomotive drive wheels and also to avoid objectionable oscillation of the rolling stock induced when the deflections of successive spans tended to set up a harmonic excitation of the sprung weight.

Early highway bridge specifications followed the lead of AREA specifications for railroad bridges that existed. It was not until the early 1930s that a distinctive limitation tailored to a distinctive problem for highway bridges was developed. The limiting depth-to-span ratios specified by AREA were modified from time to time as shown in Table 2.2 (ASCE 1958).

Early highway bridge specifications soon followed, with minor modifications from time to time, the lead of AREA specifications as shown in Table 2.3.

These modifications were quite possibly set and modified arbitrarily because no record exists to any basis for a particular value for them. In fact, in 1905, the AREA Committee explained the somewhat ambiguous wording of their provisions for design, which reduced depths, as follows:

> We established the rule because we could not agree on any. Some of us in designing a girder that is very shallow in proportion to its length decrease the unit stress or increase section according to some rule which we guess at. We put it there so that a man would have a warrant for using whatever he pleased.

www.EngineeringEBooksPdf.com

TABLE 2.2
Development of Depth-Span Limitations for Railroad Bridges

Years	Trusses	Plate Girders	Rolled Beams
1913, 1924	1/10	1/12	1/12
1931	1/10	1/12	1/12
1935, 1941, 1949, 1953	1/10	1/12	1/15

Source: Adapted from Deflection limitation on bridges, progress report of committee on deflection limitations of bridges of the structural division, in *Proceedings of Paper 1633, Journal of Structural Division,* American Society Civil Engineers, May 1958. (This report cites 108 references, 1958.)

TABLE 2.3
Development of Depth-Span Limitations for Highway Bridges

Years	Trusses	Plate Girders	Rolled Beams
1913, 1924	1/10	1/12	1/20
1931	1/10	1/15	1/20
1935, 1941, 1949, 1953	1/10	1/25	1/25

Source: Adapted from Deflection limitation on bridges, progress report of committee on deflection limitations of bridges of the structural division, in *Proceedings of Paper 1633*, *Journal of Structural Division,* American Society Civil Engineers, May 1958. (This report cites 108 references, 1958.)

2.6.2 Purpose of Limiting Bridge Deflections

The ASCE Committee (ASCE 1958) considered the following reasons for limiting deflections in highway bridges:

1. To avoid undesirable structural effects, including
   a. Excessive deformation stresses in secondary members or connections resulting from the deflection itself or from induced rotations at joints or supports
   b. Excessive dynamic stresses of the type considered in design by the use of conventional *impact factors*
   c. Fatigue effects resulting from excessive vibrations
2. To avoid undesirable psychological reactions by
   a. Pedestrians, whose reactions are clearly a consequence of the motion of the bridge alone
   b. Passengers in vehicles, whose reactions are affected by the resultant motion of the vehicle in combination with the bridge or by the motion of the bridge when the vehicle is at rest on the span

Following extensive studies, the ASCE Committee (ASCE 1958) stated that *Neither the reasons for these changes nor the original basis for the limitation on depth-span ratios have been determined by the Committee*. Unable to reach a consensus for any recommendations for limiting deflections, it concluded: *The Committee has been forced to conclude, therefore, that the information*

www.EngineeringEBooksPdf.com

now available is not sufficient to warrant any recommendations regarding either what constitutes objectionable deflection or vibration or how best to limit them.

Little has changed in the understanding of the purpose of deflection limitations since the ASCE 1958 report. A flexible bridge (i.e., one with a relatively large deflection) should not be construed to be an unsafe bridge. Quite interestingly, in summarizing the purposes of deflection limitations for highway bridges, the ASCE Committee stated: *…it should be noted that the safety of structure is not involved, even to the extent that more flexible bridges may be adequate to carry the live load with safety.* This line of thought was echoed in the *Commentary C2.5.2.6.1* in 1994 AASHTO LRFD Specifications: *…service load deformations may cause deterioration of wearing surfaces and local cracking in concrete slabs and in metal bridges which could impair serviceability and durability, even if self limiting and not a potential cause of collapse.* (Engineers familiar with building codes-imposed live deflections limitation of $L/360$ for floors would recognize that this limitation is set to prevent cracking of the ceiling plaster rather than to prevent any structural damage.)

In retrospect, it should be noted that when the first limitations were proposed, the standard floor was plank; the supporting members were either simple beams, pony trusses, or pin-connected through trusses; and questions concerning effects of vibrations centered on individual members. Fortunately, these questions were largely eliminated with the advent of more substantial members, riveted and bolted joints, and later, welded connections and composite construction.

Along with the changes in design and construction practices, there were changes in highway design live loads from time to time. At the turn of the twentieth century, the heaviest loading was a road roller. With the development of motor trucks, design loadings were first based on 10- and 15-ton trucks. This was followed by the introduction of 20-ton trucks in 1924 for bridges on which heavy traffic was anticipated during their service life. Three years later, the Conference Committee representing AASHO and AREA introduced the truck train—a heavy truck preceded and followed by trucks having three-fourths its weight—which appeared in 1927 *Specifications for Steel Highway Bridges*. This was superseded in 1941 by the equivalent lane loading, which was first used as an optional loading in the 1931 AASHO Bridge Specifications. Later, HS20 S16-44 was introduced in 1941; the current highway live loading being HL-93 loading. The evolution of highway live loading is discussed in Chapter 3.

2.6.3 Criteria for Live Load Deflections

Although deflections are caused by both dead loads and live loads, the deflection limitations have historically been linked to live loads. Deflections due to dead loads can be taken care of by providing camber in the girders.

The AASHTO LRFD criteria for live load deflections of bridges are specified in Art. 2.5.2.6.2. It is important to note that these criteria are to be considered *optional*, except for the following:

1. The provisions for orthotropic decks shall be considered mandatory.
2. The provisions in Art. 12.14.5.9 for precast reinforced concrete three-sided structures shall be considered mandatory.
3. Metal grid decks and other lightweight metal and concrete bridge decks shall be subject to the serviceability provisions of Art. 9.5.2.

AASHTO LRFD Commentary C2.5.2.6.2 provides the basis for calling these criteria as optional:

> These provisions permit, but do not encourage, the use of past practice for deflection control. Designers were permitted to exceed these limits at their discretion in the past. Calculated deflections of structures have often been found to be difficult to verify in the field due to numerous sources of stiffness not accounted for in calculations. The desire (of designers) for availability of continued guidance often stated during the development of these Specifications has resulted in the retention of optional criteria.

www.EngineeringEBooksPdf.com

Deflection is a serviceability issue, not a strength issue; accordingly service live loads (i.e., unfactored live loads) should be considered in calculating deflections. In applying these criteria, the vehicular load shall include the dynamic load allowance (*DLA*) as discussed in Section 3.8.3.

Owners may specify stricter deflection criteria. If an owner chooses to invoke deflection control, the following principles may be applied:

1. When investigating the maximum absolute deflection for straight girder systems, all design lanes shall be loaded, and all supporting components should be assumed to deflect equally. For a multibeam bridge, this is equivalent to saying that the distribution factor for deflection is equal to the number of design lanes divided by the number of beams.
2. For composite design, the stiffness of the design cross section used for the determination of deflection should include the entire width of the roadway and the structurally continuous portions of the railings, sidewalks, and median barriers. This indeed is the essence of composite construction.
3. For straight girder systems, the composite bending stiffness of an individual girder may be taken as the stiffness determined as specified earlier, divided by the number of girders.
4. For curved steel box and I-girder systems, the deflection of each girder should be determined individually based on its response as part of a system.
5. When investigating maximum relative displacements, the number and position of loaded lanes should be selected to provide the worst differential effect.
6. The live load portion of Load Combination Service I of AASHTO LRFD Table 3.4.1-1 should be used, including the dynamic load allowance, IM.
7. The live load shall be taken from *Art. 3.6.1.3.2: Loading for Optional Live Load Deflection Evaluation*. It requires that the deflection should be taken as the larger of the following:
   a. That resulting from design truck alone
   b. That resulting from 25 percent of the design truck taken together with the design lane load
8. The provisions of Art. 3.6.1.1.2 with regard to the multiple presence of live load should apply as discussed in Section 3.11.5.
9. For skewed bridges, a right cross section may be used, and for curved and cured skewed bridges, a radial cross section may be used.

In the absence of other criteria, the deflection limits may be considered for steel, aluminum, and/or concrete vehicular bridges as shown in Table 2.4.

For steel I-shaped beams and girders, and for steel box and tub girders, the provisions of Art. 6.10.4.2 and 6.11.4, respectively, regarding the control of permanent deflections through flange stress controls, shall apply. For pedestrian bridges, that is, bridges whose primary function is to carry

TABLE 2.4
Deflection Criteria for Steel, Aluminum, and/or Concrete Vehicular Bridges

Type of Live Load	Deflection Limit
Vehicular load, general	$L/800$
Vehicular and pedestrian loads	$L/1000$
Vehicular load on cantilever arms	$L/300$
Vehicular and pedestrian loads on cantilever arms	$L/375$

Note: L = span.

www.EngineeringEBooksPdf.com

pedestrians, bicyclists, equestrians, and light maintenance vehicles, the provisions of Section 5 of AASHTO's *LRFD Guide Specifications for the Design of Pedestrian Bridges* shall apply.

In the absence of other criteria, the following deflection limits may be considered for wood construction:

1. Vehicular and pedestrian loads: span/425
2. Vehicular load on wood planks and panels (extreme relative deflection between adjacent edges): 0.10 in.

The following provisions *shall* apply to orthotropic plate decks:

1. Vehicular load on deck plate: span/300
2. Vehicular load on ribs of orthotropic metal decks: span/1000
3. Vehicular load on ribs of orthotropic metal decks (extreme relative deflection between adjacent ribs): 0.10 in.

2.6.4 Optional Criteria for Span-to-Depth Ratios

2.6.4.1 Optional Deflection Criteria for Constant Depth Superstructures

AASHTO LRFD Art. 2.5.2.6.3 provides *optional* deflection criteria in terms of span-to-depth ratios as shown in Table 2.5. These provisions represent traditional *constant depths*, for constant depth superstructures. With some modifications, they are carried over from the previous editions of AASHTO *Standard Specifications for Highway Bridges*. These provisions may be used, at the discretion of owners/designers, when no specific deflection criteria are available (hence referred to as optional).

TABLE 2.5
Traditional Minimum Depths for Constant Depth[a] Superstructures

Superstructure		Minimum Depth (Including Deck)[a]	
Material	**Type**	**Simple Spans**	**Continuous Spans**
Reinforced concrete	Slabs with main reinforcement parallel to traffic	$\frac{1.2S+10}{30}$	$\frac{S+10}{30} \geq 0.54\,\text{ft}$
	T-beams	$0.070L$	$0.065L$
	Box beams	$0.060L$	$0.055L$
	Pedestrian structure beams	$0.035L$	$0.033L$
Prestressed concrete	Slabs	$0.030L \geq 6.5$ in.	$0.027L \geq 6.5$ in.
	CIP box beams	$0.045L$	$0.040L$
	Precast I-beams	$0.045L$	$0.040L$
	Pedestrian structure beams	$0.033L$	$0.030L$
	Adjacent box beams	$0.030L$	$0.025L$
Steel	Overall depth of composite I-beam	$0.040L$	$0.032L$
	Depth of I-beam portion of composite beam	$0.033L$	$0.027L$
	Trusses	$0.1000L$	$0.100L$

Source: Adapted from AASHTO, *AASHTO LRFD Specifications for Highway Bridges*, 6th ed., American Association of State Highway and Transportation Officials, Washington, DC, 2012, Table 2.5.2.6.3-1.

Note: S, span of slab (ft); L, length of span (ft).

[a] These limits apply to the overall depth of the superstructure. Where variable depth members are used, the values shown in the table may be adjusted to account for the changes in relative stiffness of positive and negative moment sections.

www.EngineeringEBooksPdf.com

2.6.4.2 Optional Deflection Criteria for Curved Steel Superstructures

For curved steel girder systems, the deflection limitation is specified in terms of the span-to-depth ratio, L_{as}/D, of each steel girder. This ratio should not exceed 25, subject to the following stipulations:

1. When the specified minimum yield strength of the girder in regions of positive flexure is 50.0 ksi or less
2. When the specified minimum yield strength of the girder is 70.0 ksi or less in regions of negative flexure
3. When hybrid sections satisfying the provisions of Art. 6.1.1.3 are used in regions of negative flexure

For all other curved steel girder systems, L_{as}/D of each steel girder should not exceed the limit given by Equation 2.1:

$$\frac{L_{as}}{D} \leq \sqrt{\frac{50}{f_{yt}}} \qquad (2.1)\ [A2.5.2.6.3\text{-}1]$$

where

f_{yt} = specified minimum yield strength of the compression flange (ksi)
D = depth of steel girder (ft)
L_{as} = an arc girder length defined as follows (ft):
= Arc span for simple span
= 0.9 times the arc span for continuous end spans
= 0.8 times the arc span for continuous interior spans

2.6.5 Deflections Due to Dead Loads

In the preceding paragraphs, discussion was focused on deflection limitations for the live load. Of course, there would be deflections due to dead load as well, but no limitation is set for it in the AASHTO LRFD Specifications (there was none in the AASHTO *Standard Specifications*).

It is generally agreed that perceptibly deflected beams are unsightly and give the appearance of inherent weakness to passing motorists. Perhaps, it might give some a feeling of impending failure! If the thickness of the concrete deck is kept constant over the supporting girders, the resulting flooring would also have an undesirable deflected profile. Consequently, the beam dead load deflections must be accommodated during the placement of concrete deck.

It has been found that the most cost-effective method of accommodating dead load deflections is *cambering* (forming them with an initial upward deflection) of beams supporting the deck slab. In addition, the resulting relatively straight profile of the girders also adds to the overall esthetic appeal. Prestressed concrete beams automatically develop camber during the prestressing process.

Steel structures should be cambered during fabrication to compensate for dead load deflection and vertical alignment. Dead load deflections include those due to the dead weight of steel, concrete deck (including stay-in-place forms), and that due to the future wearing surface (typically 25–35 lb/ft^2 of the deck area). AASHTO LRFD Art. 6.7.2 provides guidance regarding dead load camber; it mandates: *Vertical camber shall be specified to account for the computed dead load deflection*. When staged construction (i.e., superstructures are built in separate longitudinal units with a longitudinal joint, e.g., superstructures Types *g*, *i*, and *j*) is specified, the sequence of load application should be considered when considering camber.

When longitudinal steel girders are used to support the concrete deck, the construction may be shored or unshored. In unshored construction, the girders alone (not the composite section)

www.EngineeringEBooksPdf.com

would have to support the dead load of the poured concrete, which would cause the girders to deflect. If the girders are shored before placement of concrete, they would not deflect due to the dead weight of concrete. When the concrete hardens, both dead load and live load deflections would be resisted by the composite section. These construction aspects should be accounted for in design. AASHTO LRFD Commentary C6.7.2 provides more information pertinent to dead load camber.

2.6.6 Calculation of Live Load Deflections

Live load deflections should be computed for the governing loading conditions—HL-93 design truck and lane (Figure 2.26)—by the usual methods of computing deflections. For composite beams, the moment of inertia of the composite section, I_c, with a modular ratio n, should be used. Because of the usually large moment of inertia of composite beam, deflections seldom control the design of composite beams; however, deflections may be critical or even a controlling factor for noncomposite beams.

Deflections due to LRFD live load are calculated for one-lane loaded case (the lane is loaded with both the design truck *and* the lane load). In the case of the design truck loading, it is difficult, although theoretically possible, to determine the exact positions of the three axles that will result in maximum deflection. As a practical matter, however, one may calculate deflection by placing the design truck on the span in certain positions, which make it possible to use formulas for deflections due to typical positions of concentrated loads as given in texts on mechanics of materials, structural analysis, handbooks on structural engineering, and various editions of the *AISC Manual of Steel Construction*. Two such design truck positions are discussed here; the formulas for deflections due to these concentrated loads can be found in the *AISC Manual* (AISC 2011).

1. Method 1: The middle 32-kip load is placed at the midspan and the other two loads are placed at 14 ft apart elsewhere on the span.

   This load case can be split into two separate cases: (a) load case 7 for the centrally placed point load and (b) load case 8 for point load placed off the midspan (AISC 2011) (Figure 2.27).

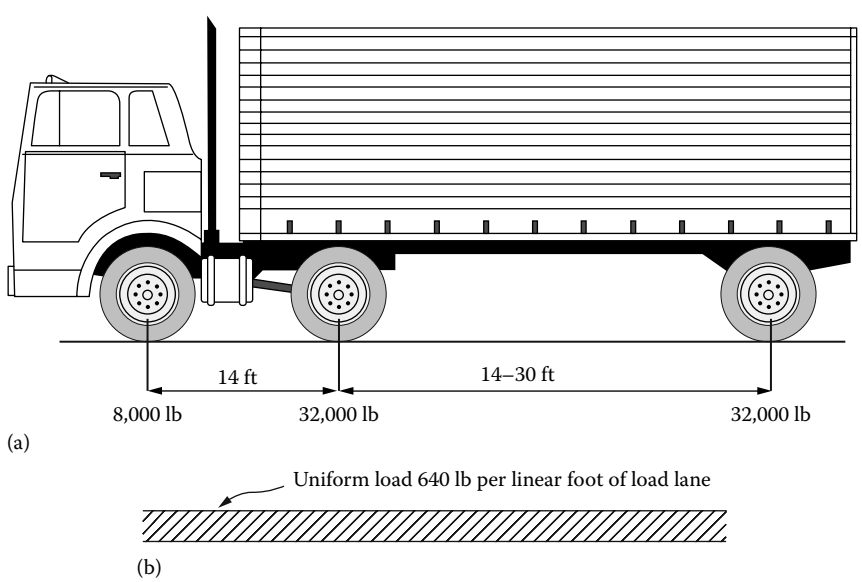

FIGURE 2.26 HL-93 live loads: (a) design truck and (b) lane load.

www.EngineeringEBooksPdf.com

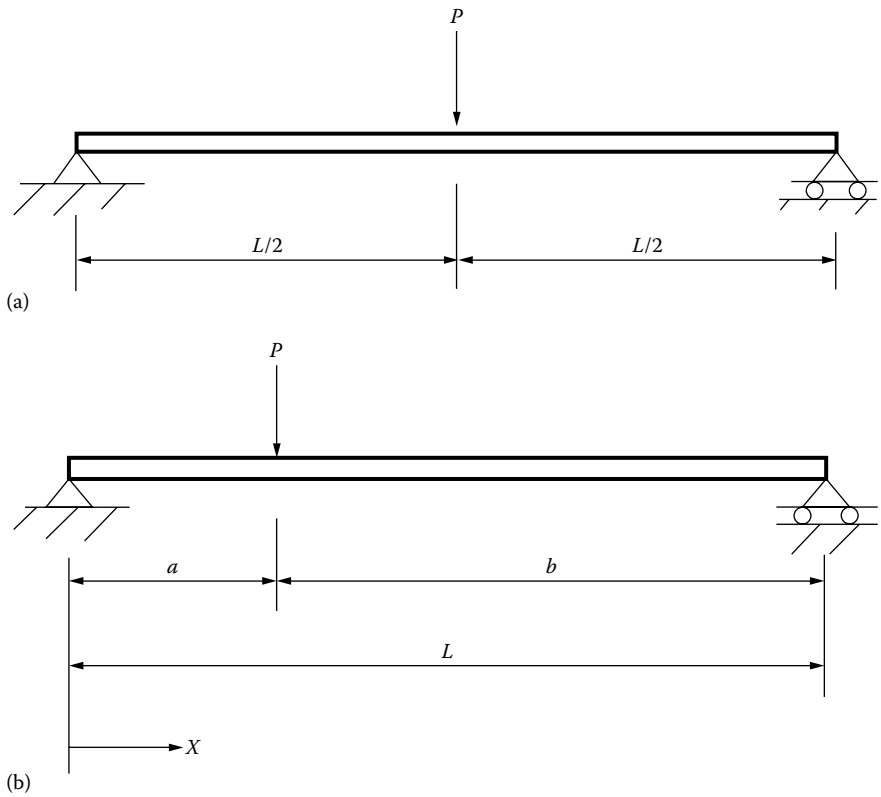

FIGURE 2.27 (a) Point load at midspan and (b) point load off midspan.

For load case 7 (centrally placed point load P, Figure 2.27a), the maximum deflection occurs at the center, which can be calculated from Equation 2.2:

$$\Delta_c = \frac{PL^3}{48EI} \tag{2.2}$$

where

Δ_c = deflection at midspan (in.) due to point load
L = span
E = modulus of elasticity
I = moment of inertia

For load case 8 (off-center point load P placed at a distance a from the left support, Figure 2.27b), the deflection at a distance x (when $x < a$) from the left support can be calculated from Equation 2.3:

$$\Delta_x = \frac{Pbx\left(L_2 - b^2 - x^2\right)}{6EIL} \tag{2.3}$$

Equation 2.3 can be used to calculate deflections due to the two off-center point loads (separately for the 8- and 32-kip loads). The total deflection due to the design truck can be calculated as the sum of the deflections due to the center load and the two off-center loads.

www.EngineeringEBooksPdf.com

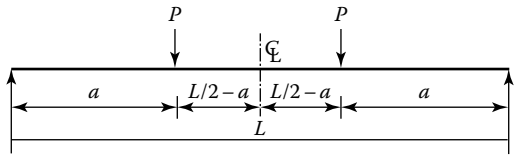

FIGURE 2.28 Two-point loads placed symmetrically about the midspan.

2. Method 2. Symmetrically placing the two 32-kip loads (the heaviest loads) about the center line of the girder (Figure 2.28); the 8-kip load can be placed at 14 ft away from one of the 32-kip loads, if it can be placed on the span at all (depending on the span length) (Figure 2.27b).

   For the two equal, symmetrically placed loads P on a simple span, each placed at a distance a from the supports, load case 9 (AISC 2011) applies. The maxim deflection occurs at the center as given by Equation 2.4:

$$\Delta_{max} = \frac{Pa}{24EI}\left(3L^2 - 4a^2\right) \tag{2.4}$$

   For the special case of HL-93 design truck, $a = (L/2 - 7)$ ft.

The deflection due to the third load, which is placed off-center, can be calculated from Equation 2.3. The total deflection due to the design truck can be calculated as the sum of deflections given by Equations 2.3 and 2.4.

Reference (AISC 1986) gives Equation 2.5 for computing midspan deflections of a continuous composite girder due to HL-93 design truck loading:

$$\Delta_{truck} = \frac{324}{E_s I_c}\left[P_T\left(L^3 - 555L + 4780\right) - \frac{1}{3}\left(M_R + M_L\right)L^2\right] \tag{2.5}$$

where

Δ_{truck} = deflection at midspan (in.) due to HL-93 truck
P_T = weight of one front axle (kip)
I_c = moment of inertia (in.^{4}) of the composite section with modular ratio n, computed at point of maximum positive moment
L = span (ft)
M_L = moment at the left support
M_R = moment at the right support

For a simple span, $M_R = M_L = 0$, so Equation 2.5 simplifies to Equation 2.6:

$$\Delta_{truck} = \frac{324P_T}{E_s I_c}\left(L^3 - 555L + 4780\right) \tag{2.6}$$

Substitution of E_s = 29,000 ksi in Equation 2.6 yields Equation 2.7:

$$\Delta_{truck} = \frac{P_T}{90I_c}\left(L^3 - 555L + 4780\right) \tag{2.7}$$

www.EngineeringEBooksPdf.com

For deflection of a noncomposite girder, the moment of inertia of the composite girder, I_c, should be replaced by the moment of inertia of the noncomposite section, I:

$$\Delta_{truck} = \frac{P_T}{90I}\left(L^3 - 555L + 4780\right) \tag{2.8}$$

For the case of lane loading (uniform load), the maximum deflection can be calculated from Equation 2.9 (Case 1, AISC 2011):

$$\Delta_{lane} = \frac{5wL^4}{384EI} \tag{2.9}$$

where
w = 0.64 kip/ft
L = span

In all cases, the following should be noted:

1. The design truck loads (i.e., point loads in Equations 2.1 through 2.7) should be modified by the dynamic load allowance, that is, multiply by (1 + IM), where IM = 0.33.
2. The dynamic load allowance is not applicable to the lane load.
3. Total calculated deflection as discussed in Section 2.6.3 (Art. 3.6.1.3.2) should be multiplied by the live load distribution factor for deflection to get the live load deflection of the girder; this is the live load deflection that should be compared against the allowable live load deflection.

2.7 CONSIDERATION OF FUTURE WIDENING

The possibility of future widening of bridges exists as a real possibility for a majority of bridges, particularly those that serve centers of commerce and industry and growing neighborhoods. Therefore, this possibility should be considered during the planning stages of designing bridge superstructures as this would affect the design of exterior girders of multibeam superstructures (Table 2.1). For this reason, unless future widening is virtually inconceivable, *the load carrying capacity of exterior beams shall not be less than the load carrying capacity of an interior beam* (Art. 2.5.2.7). This provision applies to any longitudinal flexural members traditionally considered to be stringers, beams, or girders.

2.8 CONSTRUCTABILITY

Constructability is a real issue to be concerned with during the construction phase of all kinds of structures, buildings, bridges, water tanks, stadiums, etc. Constructability issues include considerations of deflection, strength of steel, and stability during critical stages of construction, and others as might be necessary. In general, bridges should be designed in such a manner that fabrication and erection can be performed without undue difficulty or distress and that locked-in construction force effects are within tolerable limits. Climate and hydraulic conditions that may affect the construction of the bridge shall be considered.

Construction sequences (e.g., unshored construction) have important bearing on stresses due to dead load that might be induced during construction. Such conditions should be defined in the contract documents.

The issue of constructability is addressed by Art. 2.5.3. Whereas a bridge designer is not required to educate a contractor on how to build a bridge, it is to be expected that a contractor possesses the necessary expertise to build the bridge. Contractors can also freely use innovative construction methods to their own advantage over the competitors.

www.EngineeringEBooksPdf.com

2.9 BRIDGE ESTHETICS

> It so happens that the work which is likely to be foremost a durable monument, and convey some knowledge of us to the most remote posterity, is a work of bare utility, not a shrine, not a fortress, not a palace, but a bridge.
>
> **(Schuyler 1983)**

So wrote Montgomery Schuyler, one of the greatest art critics of his time, in *Harper's Weekly*, No. 27, May 24, 1883. The Brooklyn Bridge (New York) and the Golden Gate Bridge (San Francisco) stand as glaring and enduring testimonies to this statement.

From a structural standpoint, a bridge is a utilitarian structure built for the safe passage of traffic in space from a point A to a point B, a very simple statement. However, bridges form an important part of human-built environment that would last for decades; consequently, their appearances make lasting visual statements. As such, their architectural design—their appearance and appeal to human eye—is important. While bridges should present the appearance of strength commensurate with their function, they should also appear to be graceful in form and harmonize with their surroundings. The application of extraordinary and nonstructural embellishment solely for creating a pleasing appearance should be considered unnecessary and should be avoided. These considerations for designing bridges constitute *bridge esthetics*.

The topic of bridge esthetics is worthy of a book by itself. Discussion of comprehensive guidelines for designing and building bridges that would be considered beautiful is beyond the scope of this book; readers should look up pertinent literature on this subject such as Fritz Leonhardt's *Bridges-Aesthetics and Design* (Leonhardt 1984), the most detailed study and one of the best guides on the esthetics of bridges, Transportation Research Board's *Bridge Architecture Around the World* (TRB 1991), a compendium of 23 papers from well-known engineers, authors, and designers of distinctive bridges from 16 countries, including an annotated bibliography of 254 references on bridge esthetics (Burke and Teach 1991, Gottemoeller 2004), to name a few. A comprehensive summary of (TRB 1991) and other literature on bridge esthetics can be found in (Taly 1998, Chapter 11).

Architectural design of bridges attains much greater importance when they are long-span structures, such as truss, arch, cable-stayed, and suspension types, and multispan bridges, because their substructures (abutments, piers and bents, pylons of cable-stayed bridges, and towers of suspension bridges) are massive and attract the attention of human eye. A bridge with a pleasing appearance can result from judicious and coordinated planning and esthetic thinking during the initial phase of the design project; experience can be helpful in achieving this goal. A bridge designer should think of himself/herself as a structural artist.

AASHTO 2012 Art. 2.5.5 provides a few general guidelines for bridge esthetics. For spanning deep ravines, arch-type structures should be preferred. For multispan bridges, alternative bridge designs without piers or with fewer piers should be studied during the TSL considerations and refined during the preliminary design stage. Abutments and piers constitute parts of the substructure and are not discussed in this book.

REFERENCES

AASHTO. 2002. *Standard Specifications for Highway Bridges*, 17th ed., American Association of State Highway and Transportation Officials, Washington, DC.

AASHTO. 2011. *A Policy on Geometric Design of Highways and Streets* (*The Green Book*), 6th ed., American Association of State Highways and Transportation Officials, Washington, DC.

AASHTO. 2012. *AASHTO LRFD Specifications for Highway Bridges*, 6th ed., American Association of State Highway and Transportation Officials, Washington, DC.

AISC. 1986. *Highway Structures Design Handbook*, vols. I and II, AISC Marketing, Inc., Pittsburgh, PA.

AISC. 2011. *Steel Construction Manual*, 14th ed., American Institute of Steel Construction, Chicago, IL.

www.EngineeringEBooksPdf.com

ASCE. 1958. "Deflection limitation on bridges, progress report of committee on deflection limitations of bridges of the structural division", in *Proceedings of Paper 1633, Journal of Structural Division,* American Society Civil Engineers. (This report cites 108 references.)

Burke, M.P. and Teach, A. 1991. Annotated bibliography of bridge aesthetics, *Bridge Aesthetics around the World*, Committee on General Structures, Subcommittee on Bridge Aesthetics, Transportation Research Board, National Research Council, Washington DC.

DeCastro, E.S. and Kostem, C.N. 1975. Load distribution in skewed beam-slab highway bridges, Report No. 378A.7, Fritz Engineering Laboratory, Lehigh University, Bethlehem. PA.

Degenkolb, O.H. 1977. *Concrete Box Girder Bridges*, American Concrete Institute, Detroit, MI.

Gottemoeller, F. 2004. *Bridgescape: The Art of Designing Bridges*, 2nd ed., John Wiley & Sons, New York.

Kostem, C.N. 1984. Lateral live load distribution in prestressed concrete highway bridges, in *Analysis and Design of Bridges*, C. Yilmitaz and S. Tanvir Wasti, eds., NATO ASI Series, Martinus Nijhoff, Publishers, Boston, MA, pp. 213–224.

Kuzmanovic, B.O. and Willems, N. 1983. *Steel Design for Structural Engineers*, 2nd ed., Prentice Hall, Englewood Cliffs, NJ.

Leonhardt, F. 1984. *Bridges—Aesthetics and Design*, MIT Press, Cambridge, MA. (This edition is combined with the original version of this book, *Brucken—Aesthetic und Gestaltung,* Deutsche Verlags-Anstalt GmbH DVA, Stuttgart, Germany.)

Schuyler, M. 1883. The bridge as monument, *Harper's Weekly*, No. 27, May 24.

Taly, N. 1998. *Design of Modern Highway Bridges*, McGraw-Hill Cos., New York.

Taly, N. 2003. *Loads and Load Paths in Buildings: Principles of Structural Design*, International Code Council (ICC), Country Club Hills, IL.

TRB. 1991. *Bridge Aesthetics around the World*, Committee on General Structures, Subcommittee on Bridge Aesthetics, Transportation Research Board, National Research Council, Washington, DC.

Wright, R.N. and Walker, W.H. 1971. Criteria for deflection of steel bridges, AISI Bulletin No. 19, American Iron and Steel Institute, November 1971, 45pp. (This report discusses findings from 45 references cited in the report.)

Zellin, M.A., Kostem, C.N., and Kulicki, J.M. 1975a. *Lateral Load Distribution of Live Load in Prestressed Concrete I-Beam Bridges*, Report No. 387.2A, Fritz Engineering Laboratory, Lehigh University, Bethlehem, PA.

Zellin, M.A., Kostem, C.N., and Kulicki, J.M. 1975b. *Live Load Distribution Factors for Prestressed Concrete I-Beam Bridges*, Report No. 387.B, Fritz Engineering Laboratory, Lehigh University, Bethlehem, PA.

www.EngineeringEBooksPdf.com

3 Loads on Highway Bridge Structures

3.1 INTRODUCTION

Bridges constitute important links in the ground transportation systems worldwide. It is the primary responsibility of an engineer to design bridges that are safe and durable. American Association of Highway and Transportation Officials (AASHTO) Load and Resistance Factor Design (LRFD) Bridge Design Specifications provide *minimum* requirements to ensure structural safety of bridges as conveyances. The philosophy of designing bridges having adequate structural safety is outlined in 2012 *AASHTO LRFD Bridge Design Specifications* (AASHTO 2012) Article (Art.) 1.3 and is discussed in Section 3.2.

Throughout the discussion in this chapter, references would be made to various editions of *AASHTO* (previously called American Association of State Highway Officials [AASHO]) *Standard Specifications for Highway Bridges* and *AASHTO LRFD Bridge Design Specifications*. For brevity, they would be referred to, respectively, as *AASHTO Standard* and *AASHTO LRFD*.

Thinking of structures immediately brings building and bridges to one's mind. Both types of structures have to be designed to safely resist the many different kinds of loads/forces that might act on them, singly or in combinations with one another. These loads can be classified into two broad categories:

1. Gravity loads
2. Lateral loads

Gravity loads act vertically downward and include such loads as the dead weight of the structure and the live load on the bridge. Lateral loads are assumed to act horizontally and include such loads as wind and seismic, braking forces, thermal forces, earth pressure, water pressure, ice pressure, debris forces, and collision forces. Of these, certain loads are classified as *permanent* loads because they are always present on the bridge; others, such as live loads (vehicular and pedestrian loads), are classified as *transient* loads.

All types of loads that might act on highway bridges and details pertaining to their magnitudes are presented in Chapter 3 of the specifications (AASHTO 2012) and discussed in this chapter beginning Section 3.3. While readers follow the following discussion, they should bear in mind the two important considerations in determining the load effects on the bridge structure:

1. The loads discussed in Section 3 of AASHTO LRFD Specifications specifies *minimum* requirements for loads and forces, the limits of their application, load factors, and load combinations used for the design of *new* bridges. However, these load provisions may also be used for the structural evaluation of *existing* bridges (Art. 3.1).
2. In regard to the load combinations, commentary to Art. 3.4.1 (see C3.4.1) states that "all relevant subsets of the load combinations be investigated. For each load combination, every load that is indicated to be taken into account and that is germane to the component being designed, including all significant effects due to distortion, shall be multiplied by the appropriate load factor and multiple presence factor specified in Art. 3.6.1.1.2, if applicable."

www.EngineeringEBooksPdf.com

3.2 AASHTO LRFD HIGHWAY BRIDGE DESIGN PHILOSOPHY

3.2.1 Limit States Concept

The philosophy that forms the core of AASHTO LRFD Specifications (AASHTO 2012) is based on the concept of *limit states* (see discussion in Chapter 1), which sets it apart from AASHTO Standard Specifications (AASHTO 2002). *Limit state* is defined as a condition beyond which a bridge or its component ceases to satisfy the provisions for which it was designed. Concepts of limit states applicable to highway bridge design are specified in Specifications Art. 1.3.2 and are briefly described as follows.

In structural design, typically, two types of limit states are recognized:

1. *Strength limit states*: These include limit states relating to strength and stability during the service life. They are intended to ensure that a bridge is capable of providing both local and global strength and stability to resist the specified statistically significant load combinations that it is expected to experience during its design life. The specifications recognize five subsets of strength limit state as listed in Table 3.1.

   Strength limit states take into account the strength and stability of each structural element, including splices and connections; if the demand exceeds their resistance (capacity), it is assumed that the resistance of the bridge has been exceeded. But this does not mean that the bridge has failed in a strictly physical sense (as if it had collapsed) as far as design is concerned. This is because typical multigirder bridge cross sections (discussed in Chapter 2) are assumed to possess significant elastic reserve capacity beyond such a load level because the live load cannot be positioned to simultaneously maximize the force effects in all its parts. This being the case, "the flexural resistance of the bridge cross section typically exceeds the resistance required for the total live load that can be placed on the number of traffic lanes available. Extensive distress and structural damage may occur under strength limit state, but overall integrity is expected to be maintained" (AASHTO 2012 *Commentary* C1.3.2.4).
2. *Service limit states*: Limit states relating to stress, deformation, and cracking under regular operating conditions. It provides for certain experience-related provisions that cannot always be derived solely from strength or statistical considerations. AASHTO LRFD Specifications recognize four service limit states as listed in Table 3.2.

   Because of the importance of bridges as parts of public transportation infrastructure, they are also subject to the provisions of two additional limit states typically not considered explicitly for design of conventional buildings.

TABLE 3.1
Strength Limit States

Load Combination Designation		Details of Load Combination
1	Strength I	Basic load combination relating to the normal vehicular use of the bridge *without wind*
2	Strength II	Load combination relating to the use of the bridge by owner-specified special design vehicle, evaluation permit vehicles, or both *without wind*
3	Strength III	Load combination relating to the bridge exposed to wind velocity exceeding 55 mph
4	Strength IV	Load combination relating to very high dead-load-to-live-load force effect ratios
5	Strength V	Load combination relating to normal vehicular use of the bridge with wind of 55 mph velocity

www.EngineeringEBooksPdf.com

TABLE 3.2
Service Limit States

Load Combination Designation		Details of Load Combination
1	Service I	Load combination relating to the normal operational use of the bridge with a 55 mph wind and all loads taken at their nominal values. Also related to deflection control in buried metal structures, tunnel liner plate, and thermoplastic pipe, to control crack width in reinforced concrete structures, and for transverse analysis relating to tension in concrete segmental girders. This load combination should also be used for the investigation of slope stability.
2	Service II	Load combination intended to control yielding of steel structures and slip of slip-critical connections due to vehicular live load.
3	Service III	Load combination for longitudinal analysis relating to tension in prestressed concrete superstructures with the objective of crack control and to principal tension in the webs of segmental concrete girders.
4	Service IV	Load combination relating only to tension in prestressed concrete columns with the objective of crack control.

TABLE 3.3
Fatigue and Fracture Limit States

Load Combination Designation		Details of Load Combination
1	Fatigue I	Fatigue and fracture load combination related to infinite fatigue-induced life.
2	Fatigue II	Fatigue and fracture load combination related to finite load-induced fatigue life.

3. *Fatigue and fracture limit states*: These are related, respectively, to the stress range as a result of a single design truck occurring at the number of expected stress range cycles and the material toughness requirements of AASHTO material specifications. The intent of this limit state is to limit crack growth under repetitive loads to prevent fracture during the design life of the bridge. The specifications recognize two fatigue and fracture limit states as listed in Table 3.3.
4. *Extreme event limit states*: Provisions for these limit states are intended to ensure structural survival of bridge during a major earthquake or a flood or when collided by a vehicle, vessel, or ice flow, possibly under scoured conditions. These limit states are considered to be unique occurrences whose return period may be significantly greater than the design life of the bridge (75 years). The specifications recognize two extreme event limit states as listed in Table 3.4. It should be recognized that the recurrence intervals of extreme events (I and II) are thought to exceed design life; however, the joint probability of these events is very low. Therefore, events are specified to be applied separately.

There are many reasons for classifying various strength limit states as listed in Table 3.1. Fortunately, not all bridge superstructures have to be designed for all limit states. As summarized in Table 3.1, Strength I Limit State is the *basic* strength limit state—*without wind* or any extreme event limit states. This is the strength limit state for which most superstructures are designed.

Limit State II entails live load due to owner-specified special design vehicle and evaluation permit vehicles, but *without of wind*. Bridges are commonly designed for HL-93 live load that causes

www.EngineeringEBooksPdf.com

TABLE 3.4
Extreme Event Limit States

Load Combination Designation		Details of Load Combination
1	Extreme event I	Load combination including earthquake.
2	Extreme event II	Load combination relating to ice load, collision by vessels and vehicles, check floods, and certain hydraulic events with a reduced live load other than that which is part of the vehicular collision load, *CT*. The cases of check floods shall not be combined with *CV*, *CT*, or *IC*.

force effects different from those caused by owner-specified vehicles or evaluation permit vehicles. The latter vehicles might be heavier than HL-93 live loading, but they would be driven on the bridge under controlled conditions, such as only a single vehicle of that type on the bridge and no other vehicles in the other lanes and slow speed so that dynamic load effects are very small. Under these controlled conditions, a superstructure designed for Strength I Limit State may not be too overstressed under Strength II Limit State conditions.

Strength III Limit State entails design loads that involve wind velocity exceeding 55 miles per hour (mph) (90 km/h). Under such high wind load conditions, no live load is assumed to be present on the bridge.

Strength IV Limit State is a special case that involves very high dead-load-to-live-load ratio. This load condition may be critical for certain members when the bridge has a long span or for a bridge under construction.

Strength V Limit State involves normal live load, similar to Strength I Limit State, with one exception: it includes wind load corresponding to a high wind velocity of 55 mph. In other words, this load combination involves gravity loads (permanent load and live load) *and* wind load that is a lateral load. The probability of a bridge superstructure to be subjected to full live load as well a maximum lateral force due to wind is very low. Accordingly, full load values of both loads are not used in design. For example, the γ-factor (load factor) for the live load corresponding to Strength V Limit State is 1.35 as compared with 1.75 for live load corresponding to Strength I Limit State (see Table 3.7).

Art. 1.3.1 requires that highway bridges be "designed for specified limit states to achieve the objectives of constructability, safety, and serviceability, with due regard to issues of inspectability, economy, and aesthetics" (Specifications Art. 2.5). All limit states are to be considered of equal importance.

As a sound design objective, regardless of the analysis used, it is required that each component and connection of a bridge be designed to satisfy Equation 3.1 for each limit state, unless otherwise specified. For service and extreme event limit states, the resistance factor shall be taken as 1.0 except for bolts for which provisions of Art. 6.5.5 apply and for concrete columns in Seismic Zones 2, 3, and 4, for which provisions of Art. 5.10.11.3 and 5.10.11.4.1b shall apply (see Chapter 1 for a complete discussion of Equations 3.1 through 3.3):

$$\sum \eta_i \gamma_i Q_i \leq \phi R_n = R_r \qquad (3.1)\ [A1.3.2.1\text{-}1]$$

where

η_i = load modifier; a factor related to ductility, redundancy, and operational classification
γ_i = load factor, a statistically based multiplier applied to force effects
Q_i = force effect
ϕ = resistance factor; a statistically based multiplier applied to nominal resistance
R_n = nominal resistance
R_r = factored resistance = ϕR_n

www.EngineeringEBooksPdf.com

In Equation 3.1, the load modifier η_i is a function of three factors as given by Equation 3.2 and 3.3, respectively:

For loads for which a maximum value of γ_i is appropriate,

$$\eta_i = \eta_D \eta_R \eta_I \geq 0.95 \qquad (3.2)\ [A1.3.2.1\text{-}2]$$

For loads for which a minimum value of γ_i is appropriate,

$$\eta_i = \frac{1}{\eta_D \eta_R \eta_I} \leq 1.0 \qquad (3.3)\ [A1.3.2.1\text{-}3]$$

where
η_D = factor related to ductility
η_R = factor related to redundancy
η_I = factor related to operational classification

To provide sufficient ductility, the bridge shall be proportioned and detailed to ensure that significant and visible inelastic deformations occur at the strength and extreme event limit states. The value of η_D for various limit states is specified in Specifications Art. 1.3.3:

a. For the strength limit state,
   $\eta_D \geq 1.05$ for nonductile components and connections
   = 1.0 for conventional designs and details complying with the specifications
   ≥ 0.95 for components and connections for which additional ductility-enhancing measures have been specified beyond those required by the specifications
b. For all other limit states, $\eta_D = 1.0$.

To provide redundancy in bridges, multiple load path and continuous structures should be used unless there are compelling reasons for not using them. The value of η_R for various limit states is specified in the Specifications Art. 1.3.4:

a. For the strength limit state,
   $\eta_R \geq 1.05$ for nonredundant members
   = 1.0 for conventional levels of redundancy and foundation elements where ϕ already accounts for redundancy as specified in AASHTO LRFD Specifications Art. 10.5
   ≥ 0.95 for exceptional levels of redundancy beyond girder continuity and a torsionally closed cross section
b. For all other limit states, $\eta_R = 1.0$.

Factor η_I is related to the operational importance of a bridge meaning if it is essential or critical. Such classification would depend on the operational priority of a bridge, which may differ from owner to owner. The specifications provide the following guidelines for classifying critical or essential bridges (AASHTO 2012 *Commentary* C1.3.5):

1. Bridges that are required to be open to all traffic once inspected after the design event and are useable by emergency vehicles and for security, defense, economic, or secondary life safety purposes immediately after the design event.
2. Bridges that should, as a minimum, be open to emergency vehicles and for security, defense, or economic purposes after the design event and open to all traffic within days after the design event.

www.EngineeringEBooksPdf.com

The value of η_l for various limit states is specified in LRFD Art. 1.3.5 as follows:

a. For the strength limit state,
   $\eta_l \geq 1.05$ for critical or essential bridges
   $= 1.0$ for typical bridges
   ≥ 0.95 for relatively less important bridges
b. For all other limit states, $\eta_l = 1.0$.

3.2.2 Loads and Load Designations

Art. 3.3.2 of the specifications classifies various design loads into two groups: (1) permanent loads and (2) transient loads, which are designated as follows (these abbreviations are used throughout this chapter). These loads are listed (alphabetically in order of notations), respectively, in Tables 3.5 and 3.6.

3.2.3 Load Factors and Load Combinations for Design Loads

Development of load and resistance factors and load combinations was a huge effort in the calibration of highway bridge design specifications as discussed by Nowak (1993a,b). The total load effect in highway bridge members is taken as a combined effect of all loads, permanent and transient (see Tables 3.6 and 3.7), that are likely to act on the bridge. The distribution of joint effects is based on Turkstra's rule. Turkstra and Madson (1980) observed that a combination of several load components reaches its extreme value when only one of the components takes an extreme value while other components take *arbitrary-point-in-time* (APT) value. Structural members are designed for a total load that is less than the sum of the peak loads. This concept is based on the hypothesis that if a structure is subject to the effects of two loads that separately have the probabilities p_a and p_b, the probability $p = p_a \times p_b$ for those two loads acting simultaneously would be less than either of the possibilities p_a and p_b (CTBUH 1980, p. 36). This is obvious because each of the two probabilities is less than one.

Interestingly, the philosophy of load combinations for highway bridge design is based on considerable research on probability-based criteria that had been conducted for the development of ANSI 58 Standard (ANSI 1982) for design of buildings. This research had been conducted prior to the development of AASHTO LRFD Bridge Design Specifications and reported in the literature (Borges and Castanheta 1971, Larrabe and Cornell 1979, Chalk and Corotis 1980, Ellingwood et al. 1980, Turkstra and Madsen 1980, Ellingwood et al. 1982a,b, NKB 1987, Eurocode No. 1 1990, summarized in Taly 2003). This research was deemed applicable for design of highway bridge

TABLE 3.5
Permanent Loads on Bridge Structures

Notation	Load Designation
CR	Force effects due to creep
DD	Downdrag force
DC	Dead load of structural components and nonstructural attachments
DW	Dead load of wearing surfaces and utilities
EH	Horizontal earth pressure load
EL	Miscellaneous locked-in force effects resulting from the construction process, including the jacking apart of cantilevers in segmental construction
ES	Earth surcharge load
EV	Vertical pressure from dead load of earth fill
PS	Secondary forces from posttensioning
SH	Force effects due to shrinkage

www.EngineeringEBooksPdf.com

TABLE 3.6
Transient Loads on Bridge Structures

Notation	Load Designation
BL	Blast loading
BR	Vehicular braking force
CE	Vehicular centrifugal force
CT	Vehicular collision force
CV	Vessel collision force
EQ	Earthquake load
FR	Friction load
IC	Ice load
IM	Vehicular dynamic load allowance
LL	Vehicular live load
LS	Live load surcharge
PL	Pedestrian live load
SE	Force effect due to settlement
TG	Force effect due to temperature gradient
TU	Force effect due to uniform temperature
WA	Water load and stream pressure
WL	Wind on live load
WS	Wind load on structure

members and used, with necessary modifications, in the calibration of LRFD procedure for highway bridge design specifications; as such no specific research for load combinations was done for highway bridges (Nowak 1993). A discussion on the calibration of AASHTO LRFD Specifications is presented in Chapter 1.

Several aspects of codification of loads and LRFD load combinations are noteworthy. These load combinations are

1. Material independent; consequently, they are applicable to structures built from conventional materials such as steel, concrete, masonry, and wood
2. Applicable to all geographic regions in the United States
3. Applicable to LRFD design philosophy

Load factors and load combinations are specified in Specifications Art. 3.4.1. Like building structures, bridges are also subjected to several forces simultaneously. Therefore, load factors assigned to different loads depend on load combinations as well as limit states under consideration; these are listed in Tables 3.7 through 3.9 (AASHTO 2012, Tables 3.4.1-1 through 3.4.1-3). *In all cases, all structures including bridges must be designed to resist the most critical effects from any of the applicable load combinations*. Additionally, irrespective of the design philosophy and construction material used, a cardinal design principle is that effects of one or more loads *not* acting must also be investigated.

The total factored force effect shall be taken as given by Equation 3.4:

$$Q = \sum n_i \gamma_i Q_i \qquad (3.4)\ [A3.4.1\text{-}1]$$

where

n_i = load modifier specified in Specifications Art. 1.3.2
Q_i = force effects from loads specified herein
γ_i = load factors specified in Tables 3.7 through 3.9

www.EngineeringEBooksPdf.com

TABLE 3.7
Load Combinations and Load Factors

Load Combination Limit State	*DC* *DD*[a] *DW* *EH* *EV* *ES* *EL* *PS* *CR* *SH*	*LL* *IM* *CE* *BR* *PL* *LS*	*WA*	*WS*	*WL*	*FR*	*TU* *CR* *SH*	*TG*	*SE*	Use One of These at a Time *EQ*	*BL*	*IC*	*CT*	*CV*
Strength I (unless noted)	γ_p	1.75	1.00	—	—	1.00	0.50/1.20	γ_{TG}	γ_{SE}	—	—	—	—	
Strength II	γ_p	1.35	1.00	—		1.00	0.50/1.20	γ_{TG}	γ_{SE}	—	—	—	—	
Strength III	γ_p	—	1.00	1.40		1.00	0.50/1.20	γ_{TG}	γ_{SE}	—	—	—	—	
Strength IV	γ_p	—	1.00	—		1.00	0.50/1.20	—	—	—	—	—	—	
Strength V	γ_p	1.35	1.00	0.40	1.0	1.00		γ_{TG}	γ_{SE}	—	—	—	—	
Extreme event I	γ_p	γ_{EQ}	1.00	—		1.00	—	—	—	1.00	—	—	—	
Extreme event II	γ_p	0.50	1.00	—		1.00	—	—	—	—	1.00	1.00	1.00	1.00
Service I	1.00	1.00	1.00	0.30	1.0	1.00	1.00/1.20	γ_{TG}	γ_{SE}	—	—	—	—	
Service II	1.00	1.30	1.00	—		1.00	1.00/1.20	—	—	—	—	—	—	
Service III	1.00	0.80	1.00	—		1.00	1.00/1.20	γ_{TG}	γ_{SE}	—	—	—	—	
Service IV	1.00	—	1.00	0.70		1.00	1.00/1.20	—	1.0	—	—	—	—	
Fatigue I—*LL*, *IM*, and *CE* only	—	1.5		—	—	—	—	—	—	—	—	—	—	
Fatigue II—*LL*, *IM*, and *CE* only	—	0.75	—	—	—	—	—	—	—	—	—	—	—	

Source: From *AASHTO LRFD Bridge Design Specifications*, Copyright © 2012 by American Association of State Highway and Transportation Officials, Washington, DC. Used by permission.

[a] Downdrag, *DD*. The term *downdrag* refers to a downward acting force exerted on piles or drilled shafts due to soil movement around them (refer to LRFD Art. 3.11.8 for details of this force).

www.EngineeringEBooksPdf.com

TABLE 3.8
Load Factors for Permanent Loads (AASHTO LRFD 2012 Table 3.4.1-2)

Type of Load, Foundation Type, and Method Used to Calculate Downdrag	Load Factor Maximum	Load Factor Minimum
DC: Component and attachments	1.25	0.90
DC: Component and attachments—Strength IV only	1.50	0.90
DD: Downdrag pile, α Tomlinson method	1.4	0.25
Piles, λ method	1.05	0.30
Drilled shafts, O'Neill and Reese (1999) method	1.25	0.35
DW: Wearing surfaces and utilities	1.5	0.65
EH: Horizontal earth pressure	1.50	0.90
Active	1.35	0.90
At rest		
EL: Locked-in erection stresses	1.00	1.00
EV: Vertical earth pressure		
Overall stability	1.00	N/A
Retaining walls and abutments	1.35	1.00
Rigid buried structure	1.30	0.90
Rigid frames	1.35	0.90
Flexible buried structures		
Metal box culverts and structural plate culverts with deep corrugations	1.5	0.9
Thermoplastic culverts	1.3	0.9
All others	1.95	0.9
ES: Earth surcharge	1.50	0.75

Source: From *AASHTO LRFD Bridge Design Specifications*, Copyright © 2012 by American Association of State Highway and Transportation Officials, Washington, DC. Used by permission.

TABLE 3.9
Load Factors for Permanent Loads due to Superimposed Deformations, γ_p

Bridge Component	*PS*	*CR, SH*
Structures—segmental	1.0	See γ_p for *DC* Table 3.8
Concrete substructures supporting segmental superstructures (see AASHTO LRFD Art. 3.12.4, 3.12.5)		
Concrete structures—nonsegmental	1.0	1.0
Substructures supporting nonsegmental structures		
Using I_g	0.5	0.5
Using $I_{effective}$	1.0	1.0
Steel substructures	1.0	1.0

Source: From *AASHTO LRFD Bridge Design Specifications*, Copyright © 2012 by American Association of State Highway and Transportation Officials, Washington, DC. Used by permission.

www.EngineeringEBooksPdf.com

Tables 3.7 through 3.9 provide considerable information on loads, load factors, limit states, and associated load combinations. This information is grouped as follows:

Table 3.7: Load Combinations and Load Factors (AASHTO 2012, Table 3.4.1-1)
Table 3.8: Load Factors for Permanent Loads, γ_p (AASHTO 2012, Table 3.4.1-2)
Table 3.9: Load Factors for Permanent Loads due to Superimposed Deformations, γ_p (AASHTO 2012, Table 3.4.1-3)

Applicable load combinations for different limit states and corresponding load factors are listed in Table 3.7; it lists load factors for permanent loads in the second column (see Section 3.2) by the symbol, γ_p, the numerical values of which are given in Table 3.8. Table 3.9 lists load factors for permanent loads due to superimposed deformations, γ_p. The background information on load factors specified in the specifications can be found in Nowak (1993a,b, 1995).

Good engineering judgment should be exercised when selecting load factors from Table 3.7. These factors should be selected to produce total extreme factored force effects. For each load combination, both positive and negative extremes should be investigated. Readers should thoroughly review Art. 3.4 and associated commentary (C3.4.1) in the specifications in order to develop a sound understanding of applying appropriate load factors for the different limit states listed in Table 3.7. The following brief should be helpful in using the information provided in Table 3.7:

1. All subsets of limit states are listed in the first column of Table 3.7. For each limit state, various loads to be considered in the load combination are listed horizontally. Under each load are given the associated load factors; a zero load factor under a load indicates that it is not to be considered in the load combination.
2. All of the permanent loads (see Table 3.5) are grouped together in the second column of Table 3.7. For strength and extreme event limit states, load factors for these loads are designated by the symbol γ_p, the values of which are given in Table 3.8. For the four service limit states, the load factor for the permanent loads, γ_p, is taken as 1.0. Because the permanent loads do not cause stress change cycles, the load factors for these loads do not apply.
3. For each of the permanent loads listed in Table 3.7, two values of γ_p, separated by a slash, are listed; the load factor that results in more critical combination should be applied to the load combination. The intent of providing these dual values is to permit a designer to apply the smaller value when it would produce the more critical load combination.

   As listed in Table 3.7, each limit state comprises a combination of several specific loads; applying appropriate load factors to those loads is the most crucial step in design calculations. In considering load combinations, the minimum value of a force should be considered for design if it reduces the total stabilizing force effects. For permanent force effects, the load factor that produces the more critical combination should be selected from Table 3.8. The philosophy underlying the selection of appropriate load factors is that where the permanent load increases the stability or load-carrying capacity of a component or bridge, the minimum value of that permanent load should be selected.

   For example, gravity loads acting on an abutment offset some of the sliding force at its base and also the abutment overturning moment caused by active earth pressure. In such case, the load factor (γ_p) for the permanent loads (dead load of the abutment, which contributes resistance to sliding and overturning) should be taken as 0.9 (the minimum value shown in Table 3.8 for *DC*: Component and attachment), whereas the load factor for the active earth pressure should be taken as 1.5 (the maximum value shown in Table 3.8 for *EH*: horizontal earth pressure).

   As a second example, consider the load factors for the permanent load due to components and attachments, wearing surface and utilities, and live load (listed in Table 3.7, respectively, as *DC* and *DW* and as *LL* and *IM* in column 3 of Table 3.7). When considering the load

www.EngineeringEBooksPdf.com

combination Strength I Limit State for a simple-span bridge, the load factors for *DC* and *DW* should be, respectively, 1.25 and 1.5 (both are maximum values for these loads) and 1.75 for *LL* and *IM* because simultaneous actions of all these three types of loads would produce maximum force effects in the bridge (e.g., reactions and shears and moments in the deck slabs and girders); therefore, the load combination would be $1.25DC + 1.50DW + 1.75(LL + IM)$. However, these load factors would be different if one were to investigate uplift in a *continuous* bridge. Where a permanent load *produces* uplift, that load should be multiplied by the *maximum* load factor, regardless of the span where it is located. If another permanent load *reduces* uplift, that load should be multiplied by the *minimum* load factor regardless of the span where it is located (so that the net result is *maximum* uplift). Again, for the Strength I Limit State, where the permanent load reaction is positive and the live load can cause a negative reaction, the load combination would be $0.9DC + 0.65DW + 1.75(LL + IM)$. Note that 0.9 and 0.65 are, respectively, the *minimum* load factor values for *DC* and *DW*, listed in Table 3.8, and 1.75 is the load factor listed for *LL* and *IM* in Table 3.7. If both reactions were negative, the load combination would be $1.25DC + 1.5DW + 1.75(LL + IM)$, where 1.25 and 1.5 are, respectively, the *maximum* values for *DC* and *DW* listed in Table 3.8.

4. Load factor γ_{EQ} applicable to the live load in Extreme Event I Limit State: This load factor is listed in column 3 of Table 3.7. Its value is to be determined on project-specific basis.
5. Load factor for *TU* (the force effect due to uniform temperature): Under this column in Table 3.7, the load factors for the strength and service limit states are denoted simply by the symbol γ_{TG}; numerical values are not given. This is because its values are to be selected on a project-specific basis, based on the type of structure, and the limit state under consideration. In lieu of project-specific information to the contrary, the values of γ_{TG} may be taken as follows (LRFD Specifications Art. 3.4.1):
   γ_{TG} = 1.0 at the service limit state when live load is not considered
   = 0.5 at the service limit state when live load is considered
   = 0.0 at the strength limit states
   = 0.0 at the extreme event limit states
6. Load factors for *SE* (force effect due to settlement): Under this column in Table 3.7, the load factor is denoted by the symbol γ_{SE} (no numerical values are given). Its values are to be selected on a project-specific basis, based on the type of structure, and the limit state under consideration. In lieu of project-specific information to the contrary, the value of γ_{SE} may be taken as 1.0 (LRFD Specifications Art. 3.4.1).
7. Not all forces are considered as acting simultaneously on a bridge structure. The basic idea of a load combination scheme is that in addition to the permanents loads, one of the transient loads in the combination is given APT value (Cornell and Larrabe 1977, Larrabe and Cornell 1979). Accordingly, as shown in the heading of the last column of Table 3.7, *only one* of the four transient loads—earthquake (*EQ*), ice (*IC*), vehicular collision (*CT*), and vessel collision (*CV*) forces—is to be considered in any given load combination. Additionally, Table 3.7 shows that some forces such as those related to live load on the bridge are not required for design consideration for selected strength limit states. For example, the load factor for wind load on live load (*WL*) for Strength III Limit State is zero; this limit state applies when the wind velocity exceeds 55 mph. This is because of the observation that vehicles tend to become unstable at higher (assumed >55 mph) wind velocities and, in all likelihood, would not be present on the bridge. However, a high value of load factor (1.4) applies to wind forces on the structure (*WS*) in Strength III Limit State. Likewise, the load factor for both transient forces—*WS* (wind load on structure) and *WL* (wind load on live load)—is set to zero for Strength IV Limit State because this limit state involves high dead-load-to-live-load force effect ratios (i.e., live load effect is relatively small). On the other hand, for this limit state, the load factor for permanent loads (*DC* and *DW* components of the loads) is 1.5, much higher than for all other loads.

www.EngineeringEBooksPdf.com

Where prestressed components are used in conjunction with steel girders, the force effects from the following sources shall be considered as construction loads (locked-in erection stresses), *EL*:

1. In conjunction with longitudinal prestressing of a precast deck prior to making the deck sections composite with the girders, the friction between the precast deck sections and the steel girders
2. When longitudinal posttensioning is performed after the deck becomes composite with the girders, the additional forces induced in the steel girders and shear connectors
3. The effects of differential creep and shrinkage of the concrete
4. The Poisson effect

In spite of the detailed information about load factors and load combinations for various limit states presented later in the chapter in Tables 3.7 through 3.9, situations may arise that are not covered in these tables. In such cases, extreme caution should be exercised in applying appropriate load factors. Engineering judgment shall be exercised when applying blast loadings and when combining them with other loads.

For segmentally constructed bridge, the following combination shall be investigated at the service limit state:

$$DC + DW + EH + ES + WA + CR + SH + TG + EL + PS \qquad (3.5)\ [A3.4.1\text{-}2]$$

3.2.4 Selection of Design-Specific Limit States, Load Modifiers, Load Combinations, and Load Factors

Load and resistance factor design methodology requires careful consideration and selection of limit states, load modifiers, load combinations, and load factors specific for bridge design at hand. Seldom, all bridges are required to be designed for all limit states. To ensure that all appropriate design requirements are met, applicable limit states, load modifiers, load combinations, and load factors to be used in design should be clearly defined at the beginning of a design document.

3.3 LOAD FACTORS AND LOAD COMBINATIONS FOR CONSTRUCTION LOADS

3.3.1 Evaluation at the Strength Limit States

Construction loads are discussed in Section 3.4. Load factors for construction loads are not listed in Tables 3.7 through 3.9. Art. 3.4.2 specifies the following requirements whenever construction loads are considered:

1. *Load factors*: When investigating load combinations for Strength Limits I, III, and V during construction, the load factors for both the weight of the structure and appurtenances (*DC* and *DW*) shall be not less than 1.25.
2. Unless otherwise specified by the owner, the load factor for construction loads and for any associated dynamic effects shall be not less than 1.5 in Strength I Limit State load combination. The load factor for wind in Strength III Limit State load combination shall be not less than 1.25.

3.3.2 Evaluation of Deflection at the Service Limit State

In the absence of special provisions to the contrary, where evaluation of construction deflections is required by the contract documents, load Combination Service I shall apply. Construction dead loads

www.EngineeringEBooksPdf.com

shall be considered as part of the permanent load and construction transient loads considered as part of the live load. The associated permitted deflections shall be included in the contract documents.

3.3.3 Load Factors for Jacking and Posttensioning Forces

3.3.3.1 Jacking Forces

Unless otherwise specified by the owner, the design forces for jacking in service shall be not less than 1.3 times the permanent load reaction at the bearing, adjacent to the point of jacking.

Where the bridge will not be closed to traffic during the jacking operation, the jacking load shall also contain a live load reaction consistent with the maintenance of traffic plan, multiplied by the load factor for live load.

3.3.3.2 Force for Posttensioning Anchorage Zones

The design force for posttensioning anchorage zones shall be taken as 1.2 times the maximum jacking force.

3.4 COMPONENTS OF A HIGHWAY BRIDGE STRUCTURE

A bridge structure, irrespective of the type and span length, consists of two major structural parts: *superstructure* and *substructure*. The superstructure includes the following:

1. Bridge deck (on which the vehicles ride) including the sidewalk(s), traffic barriers, and railings.
2. Horizontal framing, which consists of longitudinal and transverse beams and girders that support the deck. The deck-supporting girders can be of steel, reinforced or prestressed concrete, wood, or of composite materials.
3. Bearing pads, which support the ends of longitudinal beams and girders over the abutments and piers (or bents, when they are present, as in the case of continuous bridges).

Practically speaking, a bridge deck is an extension, albeit not structurally, of the roadway it connects. To provide for safety to vehicles moving on the bridge, traffic barrier systems (also referred to as bridge parapets), running parallel to the traffic lanes, are provided on both sides of the bridge. A bridge parapet typically consists of a short concrete wall having an inside sloping face, which is provided with protective railings on its top (see AASHTO LRFD Section 13 for the design of traffic barrier systems). Figure 3.1 shows a typical slab–girder bridge, characterized by a reinforced concrete deck supported over steel girders (or beams).

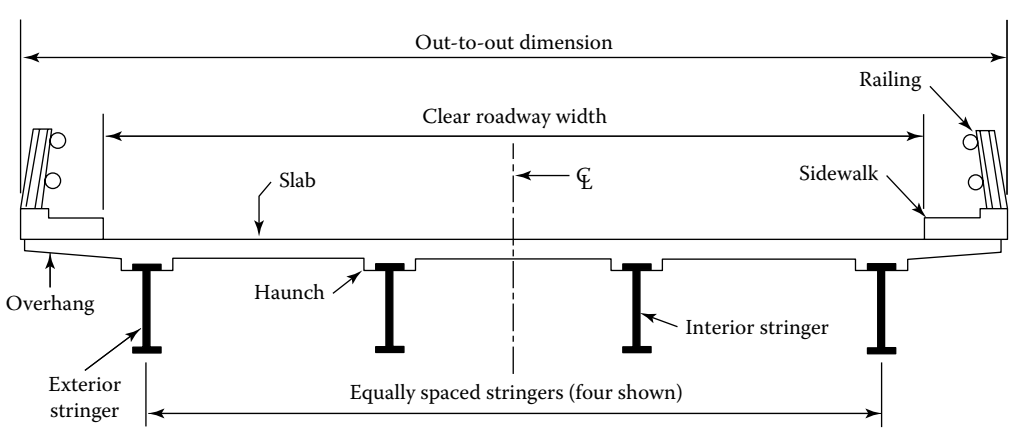

FIGURE 3.1 Cross section of a typical slab–steel girder bridge.

www.EngineeringEBooksPdf.com

All other structural elements of the bridge—abutments, wing walls, piers, and footings—comprise the substructure. All of these bridge elements are subjected to many different forces, both gravity and lateral, which are listed in Section 3.2.2 and are discussed in the remainder of this chapter. It is incumbent on a bridge designer to understand clearly the origin and nature of all forces acting on each and every element of the bridge and, based on the load path (discussed in Chapter 4), ensure that all forces are accounted for in design.

3.5 DEAD LOADS ON A HIGHWAY BRIDGE SUPERSTRUCTURE

3.5.1 General

Dead loads on a highway bridge superstructure include the following:

1. Weight of all components and structure appurtenances, *DC*
2. Weight of wearing surfaces and utilities, *DW*

Determination of dead loads, which are *permanent loads*, on a bridge structure is an important step in design. Underestimation of dead load can be dangerous as it can impair safety of the bridge. This is particularly true when permanent loads reduce the effects of transient loads such as wind, earthquake, and collision loads, because the permanent loads tend to counteract the effects of overturning caused by the transient loads.

Underestimation of dead loads was one of the contributory causes of the catastrophic collapse of the famous Quebec Bridge, Canada, on August 29, 1907, which killed 75 workers and injuring 11 others (the second failure of the bridge occurred on September 11, 1916, during rebuilding). This 3300 ft long bridge (including the end viaducts) consists of two 500 ft cantilever spans and an 800 ft suspended span (total main span 1800 ft long) is the longest double-cantilever bridge in the world. As it turned out, the main span was initially designed for 1600 ft, and later modified to 1800 ft, but the engineers had mistakenly used 1660 ft span length for calculating the dead load; it proved to be a disastrous modification resulting on overstressing the truss members (Steinman and Watson 1957, Gies 1963, Virola 1969).

Even under ordinary dead and live loads, the safety of a bridge can be seriously compromised as happened in the case of I-35W Mississippi River Bridge, Minneapolis, MN, which collapsed on August 1, 2007, amid evening rush hour traffic, killing 13 and injuring 145 people. The National Transportation Safety Board (NTSB) cited in its collapse investigation report that a design flaw (underdesigned gusset plates of the truss) was the likely cause of the collapse and asserted that *additional weight on the bridge at the time of the collapse contributed to the catastrophic failure.* This extra weight (dead load) consisted of 2 in. of concrete that was added to the road surface over the years, increasing the dead load by 20 percent, and the extraordinary weight of construction equipment and material resting on the bridge just above its weakest point at the time of the collapse, which was estimated at 578,000 pounds consisting of sand, water, and vehicles.

Dead load includes the weight of structural components and the attached appurtenances and utilities, earth cover, wearing surface, future overlays, and planned or anticipated widening of the bridge. When designing a bridge superstructure, it may be wise to make a provision for 25–35 lb/ft^2 of dead weight for future overlays. Attached appurtenances include elements such as traffic barriers and railings. Most bridge owners prefer certain types of traffic barriers and railings. Designers should obtain the necessary information regarding their dead weight from the owners, vendors, or fabricators.

Dead load calculations are based on the unit weights of materials; their values can be found in design handbooks. For consistency, unit weight of materials as recommended by the specifications (see Table 3.10) should be used. The weight of granular materials depends on the degree of

www.EngineeringEBooksPdf.com

TABLE 3.10
Unit Weight of Materials

Material	Unit Weight (kcf)
Aluminum alloys	0.175
Bituminous wearing surfaces	0.140
Cast iron	0.450
Cinder filling	0.060
Compacted sand, silt, or clay	0.120
Concrete	
Lightweight	0.110
Sand lightweight	0.120
Normal weight with $f'_c \leq 5.0$ ksi	0.145
Normal weight with $5.0 < f'_c \leq 15.0$ ksi	$0.140 + 0.001\ f'_c$
Loose sand, silt, or gravel	0.100
Soft clay	0.100
Rolled gravel, macadam, or ballast	0.140
Steel	0.490
Stone masonry	0.170
Wood	
Hard	0.060
Soft	0.050
Water	
Fresh	0.0624
Salt	0.0640
Item	Weight per unit length (klf)
Transit rails, ties, and fastening per track	0.200

Source: From *AASHTO LRFD Bridge Design Specifications*, Copyright © 2012 by American Association of State Highway and Transportation Officials, Washington, DC. Used by permission.

compactness and water content. The unit weight of (plain) concrete depends primarily on the unit weight of the aggregate (which varies with geographical location) and the type of concrete (such as lightweight, normal weight, and heavy weight) and increases with its compressive strength. The unit weight of reinforced concrete is generally taken as 150 lb/ft^3, 5 lb/ft^3 greater than that of plain concrete (145 lb/ft^3), which accounts for the weight of steel reinforcement. The values provided for the unit weight of wood include the weight of mandatory preservatives. The weight of transit rails is to be used only for preliminary design.

Calculations for the dead loads are routinely required for designing the deck slab and supporting girders. The discussion of dead loads in this section is limited to the common slab–girder-type bridge superstructures, which are the majority type as discussed in Chapter 2. These are characterized by bridge decks supported by a series of parallel, usually equally spaced beams or girders (the term *beams* is used synonymously with *girders* throughout this book), which transmit their loads in the form of reactions to the abutments and/or piers. Dead load calculations for a bridge superstructure consist of two parts: (1) dead load due to the deck slab and (2) dead load due to the girders supporting the deck. The deck and the girder may be of different materials. For example, the deck may be of reinforced concrete, steel grid (open or filled), or wood; the girders may be of steel, reinforced concrete or prestressed concrete, or wood. In all cases, the dead weight of components can be determined from their section properties and the unit weight of their materials.

www.EngineeringEBooksPdf.com

3.5.2 Dead Load due to Deck Slab

The deck slab has to support its own dead weight plus the live load. In the case of typical slab–girder-type bridges, the dead weight of deck slab depends on its thickness, which, in turn, depends on the girder spacing. The total or *overall thickness* of the deck slab, which should be used for dead load calculations, is *greater* than its *structural thickness*; the latter is used for strength calculations. The overall thickness of the slab includes integral wearing surface, which is typically ½ in. thick.

When designing a bridge for a given span length and width, neither the deck slab thickness nor the sizes and spacing of girders are known *a priori*. Therefore, it becomes necessary to use an iterative design procedure. For starters, the thickness of the deck slab and the size and the spacing of the supporting girders are guessed (or assumed) based on the span length, and their dead weight used in design as a first iterative step. The structural thickness of the deck slab typically varies between 7½ in. and 12 in. depending on the spacing of the girders supporting it; an 8 or 9 in. thickness may be assumed for dead load calculations. This is within 4–12 in. thickness limits for the slab for which the approximate live load distribution method permitted by AASHTO Specifications (discussed in Chapter 4) is valid. Concrete decks are generally topped with an integral wearing surface. Therefore, the overall thickness of the slab, which includes integral wearing surface, is used for calculating the dead weight of the slab. Both the deck slab thickness and the girder sizes (and their dead weights) might need to be revised for the final design after their load-carrying capacities have been checked for bridge live load.

3.5.3 Dead Load due to Girders

When using multigirder cross sections (Chapter 2, Table 2.1; AASHTO 2012, Table 4.6.2.2.1-1), a variety of girders, differing both in materials and forms, are used to support bridge decks. For a preliminary design, it can be assumed that all girders in such cross sections are of the same size and equally spaced. A bridge girder has to support its own deadweight as well as the dead weight of the tributary area of the deck slab it supports. In addition, the girder also has to support the dead weight of some essential items that might not be obvious to the uninitiated. Typically, a girder, as a minimum, should be designed to support dead load from following items:

1. Tributary area of the deck slab (including the wearing surface).
2. Future wearing surface, typically, 25–35 lb/ft^2 of the deck surface area.
3. Girder (including the haunch).
4. Traffic barriers or bridge parapets (including railing) on each side of the bridge. The dead weight of traffic barriers may be distributed equally to the supporting girders if they are cast after the deck concrete has hardened (an acceptable assumption).
5. Permanent (or stay-in-place) deck forms required for supporting concrete slab during construction; these would be left on the girder permanently as a part of the deck slab.
6. Diaphragms, cross frames, etc. (as applicable), which would be required to connect the girders transversely at designated intervals and at the supports (abutments and piers).
7. Intermediate and bearing stiffeners for steel (built-up) girders when used.
8. Construction loads.

Dead weights due to items 1 and 2 are known once the deck has been designed. The dead weight of the girders is easily determined from their section properties and/or from information supplied by the vendors. When W-shaped steel girders are used, their dead weight can be found from information in AISC's *Steel Construction Manual* (AISC 2011). If built-up steel girders are used, their dead weight can be determined from their section properties (using unit weight of steel as 490 lb/ft^3). In the case of reinforced and prestressed concrete girders, the dead weight can be determined from

www.EngineeringEBooksPdf.com

their section properties (using unit weight of concrete as 150 lb/ft^3). When prestressed concrete or glued-laminated (wood) girders are used, the information about their self-weight can be found from the suppliers' data sheets.

A *haunch* is a part of dead load to be carried by the girder (item 3 earlier). The bridge deck is not perfectly flat; rather, it is sloped to facilitate drainage. Instead of the bridge deck sitting directly atop the supporting longitudinal girders, a haunch, typically a 2–4 in. thick layer of concrete, is provided between the bottom of the concrete deck slab and the top of the supporting girders. Its function is to adjust the geometry of the bridge deck and facilitate maintaining the required thickness of the deck slab across its entire width. The haunch is considered a nonstructural element, is assumed to not act compositely with the girder, and, thus, is ignored when calculating the section properties of the composite girder.

The dead weight of items 5–7 is generally not known until the preliminary bridge cross section is established. Therefore, it is common practice to use an estimated value for these dead loads and lump with the dead weight of the girder (i.e., distribute over the length of the girder). Finalizing girder sizes requires a few iterative steps.

Construction loads (item 8) should be carefully estimated, preferably, in consultation with owner/builder, prior to engaging in design calculations. Generally speaking, both steel and prestressed concrete girders are installed as *unshored* girders (i.e., without any temporary supports along their length during construction). Thus, the girders alone have to support all permanent loads before the deck concrete hardens and acts compositely with the girders.

An important nature of permanent loads should be recognized by designers. It has been observed that *permanent loads are likely to be greater than the nominal value than to be less than this value*. This becomes an important design consideration where the permanent load reduces the effects of transient loads.

For design purposes, the dead weight to be carried by a girder is expressed in terms of weight per unit length (i.e., per linear foot). It is determined as the sum of the self-weight of the girder and all structural attachments (expressed as per linear foot) and the dead weight of the tributary area of the deck (*DC*). For strength design calculations, different load factors (γ factors) are applied to the combined dead weight of deck concrete and the girder (*DC*) and the combined dead load due to the wearing surface and utilities (*DW*) to arrive at the *factored* loads. Therefore, these dead loads (referred to as *unfactored* loads) should be calculated separately, to be used later for calculating the factored loads.

The following two examples present itemized dead load calculations for typical slab–girder-type short-span bridge superstructures (discussed in Chapter 2). Bridge cross sections and other pertinent information are given in both examples. Example 3.1 presents calculations for a bridge with a concrete deck supported on steel girders (Table 2.1, cross section Type (a)); Example 3.2 presents calculations for a similar bridge but with prestressed concrete girders (Table 2.1, cross section Type (k)). These examples are used again in Chapter 4 to illustrate and preserve completeness for live load and total design load calculations for designing the girders. The dead weight of the traffic barrier is 353 lb/ft.

Example 3.1

Figure 3.2 shows the cross section of a simple-span concrete deck–steel girder bridge spanning 75 ft on an urban highway. The 8½ in. thick deck slab, which includes ½ in. thick integral wearing surface, is cast from 4500 psi concrete. The deck is supported by four steel girders of Gr. 50 steel, built to act compositely with deck slab using 4 in. long, ¾ in. diameter headed shear studs (F_y = 50 ksi, F_u = 60 ksi), which would be welded to the girder. The girders are spaced at 10 ft on centers. Calculate the gravity loads for designing an interior girder. Assume the dead weight due to stay-in-place forms (to support concrete during construction), cross frames, and detailing as 200 lb/ft of girder length, and the dead weight of future wearing surface as 25 lb/ft^2 of the deck.

www.EngineeringEBooksPdf.com

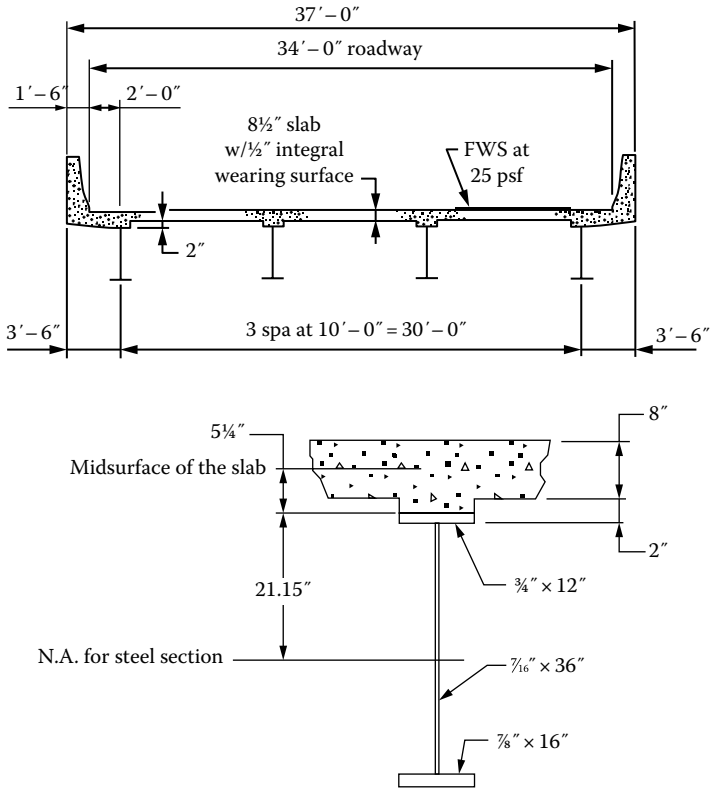

FIGURE 3.2 Bridge cross section for Example 3.1.

Solution

Commentary: The only information required determining gravity loads is the bridge cross section and the unit weight of materials. Other information provided in the example statement would be used in examples in Chapter 4.

The following unit weight would be used to calculate the dead loads in this example:

$$\text{Reinforced concrete: unit weight} = 150 \text{ lb/ft}^3$$

$$\text{Steel: unit weight} = 490 \text{ lb/ft}^3$$

Calculations are presented for an *interior* girder of the bridge.

Calculations for element loads: Gravity loads are calculated separately as dead loads *DC* and *DW* because different load factors might be assigned to them for calculating limit state loads.

1. *Deck slab*:

$$\text{Slab thickness} = 8.5 \text{ in. (including ½ in. thick integral wearing surface)}$$

$$\text{Tributary width of slab} = \text{spacing between the girders} = 10 \text{ ft}$$

$$\text{Dead weight of slab, } w_s = \left(\frac{8.5}{12}\right)(10)(0.15) = 1.063 \text{ kip/ft}$$

2. Future wearing surface per girder (tributary width of slab = 10 ft):

$$w_{ws} = (25 \text{ lb/ft}^2)(10 \text{ ft}) = 0.25 \text{ kip/ft}$$

www.EngineeringEBooksPdf.com

3. *Haunch*: Thickness of haunch = 2 − 0.75 = 1.25 in.

$$\text{Weight of concrete haunch, } w_h = \left(\frac{1.25\times 12}{144}\right)(0.15) = 0.016 \text{ kip/ft } (DC)$$

4. *Traffic barriers*:

$$\text{Dead weight of traffic barrier, } w_p = 0.353 \text{ kip/ft}$$

$$\text{Dead weight due to traffic barriers per girder} = \frac{2(0.353)}{4\,girders} = 0.177 \text{ kip/ft}$$

5. *Steel girder*: Calculate its self-weight based on cross-sectional area and unit weight 490 lb/ft^3.

$$\text{Area of top flange} = (0.75(12) = 9.0 \text{ in.}^2$$

$$\text{Area of web} = (0.4375)(36) = 15.75 \text{ in.}^2$$

$$\text{Area of bottom flange} = (0.875)(16) = 14 \text{ in.}^2$$

$$\text{Total cross-sectional area} = 9 + 15.75 + 14 = 38.75 \text{ in.}^2$$

$$\text{Dead weight of girder} = w_g = \left(\frac{38.75}{144}\right)(1)(0.490) = 0.132 \text{ kip/ft}$$

6. Estimated dead weight of stay-in-place forms, stiffeners, cross frames, and detailing:

$$w_{misc} = 0.20 \text{ kip/ft}$$

Total dead weight *DC*:

$$\begin{aligned} w_{DC} &= w_s + w_h + w_p + w_g + w_{misc} \\ &= 1.063 + 0.016 + 0.177 + 0.132 + 0.20 \\ &= 1.59 \text{ kip/ft} \end{aligned}$$

Total dead weight *DW* (due to wearing surface):

$$w_{DW} = 0.25 \text{ kip/ft}$$

Dead load shears in girders:

$$\text{Span} = 75 \text{ ft}$$

Maximum dead load shear = support reaction

$$V_{DC} = (w_{DC})(L/2) = (1.59)(75/2) = 59.63 \text{ kip}$$

$$V_{DW} = (w_{DW})(L/2) = (0.25)(75/2) = 9.38 \text{ kip}$$

Dead load moments in girders:

$$M_{DC} = \frac{w_{DC}L^8}{8} = \frac{(1.59)(75)^2}{8} = 1118 \text{ kip-ft}$$

$$M_{DW} = \frac{w_{DW}L^2}{8} = \frac{(0.25)(75)^2}{8} = 176 \text{ kip-ft}$$

Commentary: In AASHTO LRFD Specifications, load factors for *permanent* loads are given a symbol γ_p, which are different for different limit states (strength and service limit states, see Table 3.5). For Strength I Limit State, γ_p = 1.25 for *DC* (to be applied to M_{DC} = 1118 kip-ft in

www.EngineeringEBooksPdf.com

this example) and γ_p = 1.5 for *DW* (to be applied to M_{DW} = 175.8 kip-ft in this example). See Table 3.7 and 3.8 for AASHTO load factor values for different loads on highway bridges. See Example 4.9 for calculations for design live load loads for the interior girders of this bridge.

Example 3.2

Figure 3.3 shows the cross section of a highway bridge having a single span of 85 ft. It consists of an 8½ in. thick reinforced concrete deck (including ½ in. thick integral wearing surface) cast from 4500 psi concrete. The deck is supported on and acts compositely with AASHTO–PCI Type IV precast, prestressed concrete girders having a compressive strength of 6000 psi, which spaced at 7 ft 8 in. on centers. The cross-sectional area of each girder is 789 in^2. The parapets weigh 353 lb per linear ft. Assume the dead load due to future wearing surface (FWS) as 35 lb/ft^2. Calculate the gravity loads for design of an interior girder of the bridge.

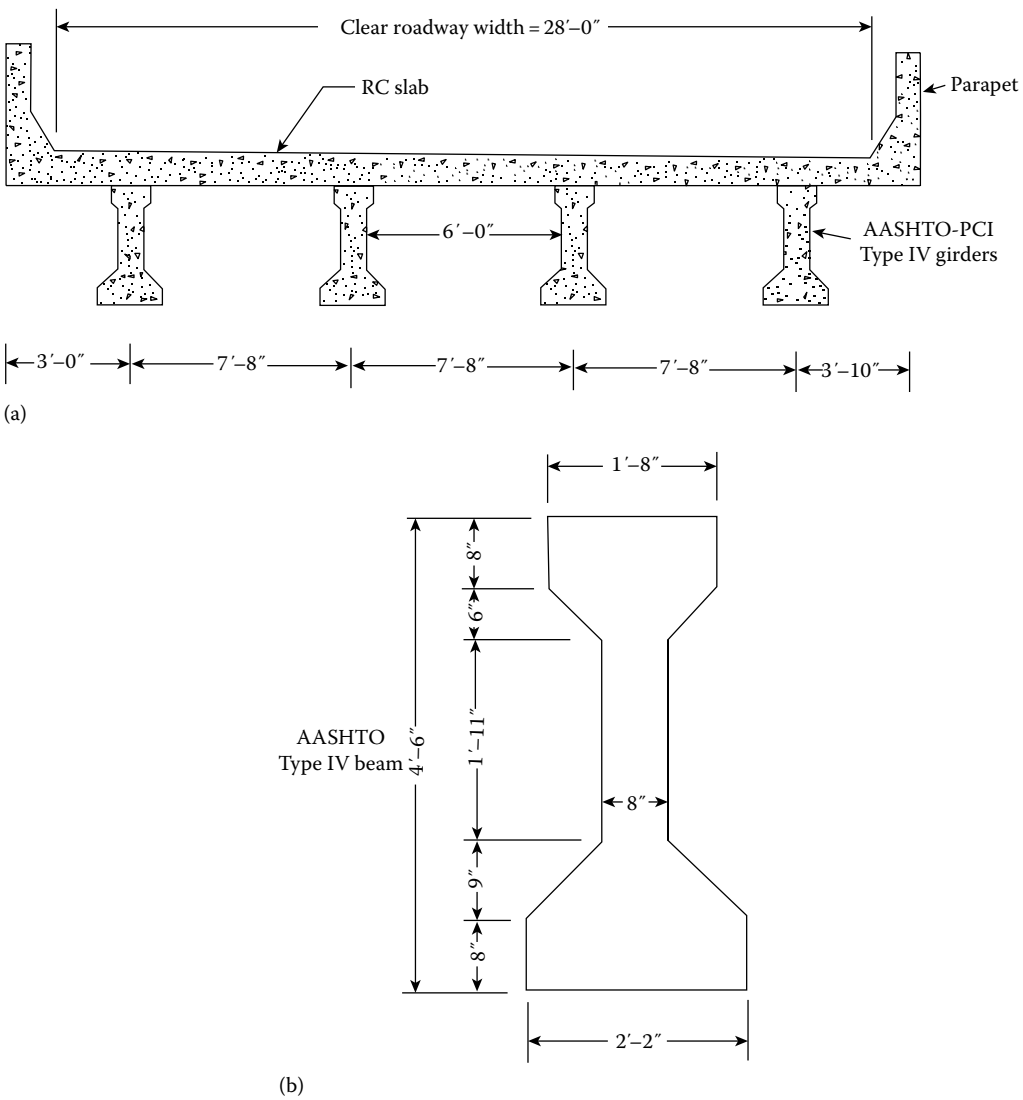

FIGURE 3.3 Bridge cross section for Example 3.2. (a) Bridge cross section and (b) cross section of prestressed concrete girder bridge for Example 3.2.

www.EngineeringEBooksPdf.com

Solution

Calculations are presented for an *interior* girder of the bridge.

Calculations for element loads: Gravity loads are calculated separately as dead loads DC and DW because different load factors may be assigned to them for calculating limit state loads.

1. Deck slab:

$$\text{Slab thickness} = 8.5 \text{ in.}$$

$$\text{Tributary width of slab} = \text{spacing between the girders} = 7 \text{ ft } 8 \text{ in.} = 7.67 \text{ ft}$$

$$\text{Dead weight of slab} = \left(\frac{8.5}{12}\right)(7.67)(0.15) = 0.815 \text{ kip/ft}$$

$$\text{Cross-sectional area of girder} = 789 \text{ in.}^2 \text{ (given)}$$

$$\text{Dead weight of girder} = \left(\frac{789}{144}\right)(1.0)(0.15) = 0.822 \text{ kip/ft}$$

Dead weight of integrally cast traffic barriers (parapets) = 0.353 kip/ft (see Example 3.1)

The dead weight of two traffic barriers is distributed over four girders:

$$\text{Dead weight due to traffic barriers} = \left(\frac{2(0.353)}{4}\right) = 0.177 \text{ kip/ft}$$

$$\text{Total dead load, } DC = 0.815 + 0.822 + 0.177 = 1.814 \text{ kip/ft}$$

$$w_{DC} = 1.81 \text{ kip/ft}$$

$$\text{Dead load due to future wearing surface} = 34 \text{ lb/ft}^2$$

$$\text{Tributary width of girder} = 7.67 \text{ ft}$$

$$\text{Dead load on girder due to the future wearing surface} = (0.035)(7.67) = 0.268 \text{ kip/ft}$$

$$w_{DW} = 0.268 \text{ kip/ft}$$

Maximum dead load shears in girders:

$$\text{Span} = 85 \text{ ft}$$

$$\text{Maximum dead load shear} = \text{support reaction}$$

$$V_{DC} = (w_{DC})(L/2) = (1.81)(85/2) = 76.93 \text{ kip}$$

$$V_{DW} = (w_{DW})(L/2) = (0.268)(85/2) = 10.5 \text{ kip}$$

Maximum dead load moments in girders:

$$M_{DC} = \frac{w_{DC}L^8}{8} = \frac{(1.81)(85)^2}{8} = 1635 \text{ kip-ft}$$

$$M_{DW} = \frac{w_{DW}L^2}{8} = \frac{(0.268)(85)^2}{8} = 242 \text{ kip-ft}$$

www.EngineeringEBooksPdf.com

3.6 CONSTRUCTION LOADS

Construction loads are considered as permanent loads. These loads act on a bridge during construction only and do not form a part of the completed bridge superstructure. The type of construction equipment used during bridge construction might vary depending on the bridge type and location. Examples of construction loads include the weight of equipment such as deck finishing machines and loads applied through false work or other temporary supports. In the case of continuous bridges, the construction equipment might include cranes to be used for building adjacent spans.

Generally speaking, construction loads are not known at the time of design; nevertheless, those loads need to be correctly estimated for design purposes. For example, when *unshored* construction is used for building a composite girder (prestressed concrete), the girder alone should be adequate to support all loads (dead load of the deck and construction equipment) before the deck concrete hardens. The composite action of the girder comes into play only after the deck concrete hardens. The magnitude and location of construction loads should be noted on construction drawings.

3.7 LIVE LOADS ON HIGHWAY BRIDGE SUPERSTRUCTURES

3.7.1 Historical Perspective

When we think of live loads on bridges, we intuitively think of the many different types of vehicles—from military tanks to big trucks to small cars to motorcycles and pedestrians—that we see crossing a bridge. These loads are classified as *moving* or *transient loads* (i.e., loads that are not stationary with respect to time). It is this nature of the live load that sets bridge structures apart from building structures.

Highway bridge live loads are rather complex from analytical standpoint because at any given time, a bridge deck may be loaded randomly with a multitude of vehicles, of different configurations (distance between various axles) and axle weights. The effect of live load on a bridge is a function of several parameters, such as the gross vehicle weight (GVW), magnitude and configuration of axle loads, span length, position (longitudinal and transverse) of the vehicles on the deck, number of traffic lanes (referred to as *multipresence* of vehicles in Chapter 4), and the number of vehicles in them, speed of the vehicles (impact or dynamic effect considerations), bridge geometry (straight, skewed, and curved, which causes centrifugal force), and stiffness characteristics. Together, these parameters introduce analytical complexity and influence the force distribution in the supporting structures and its components. Live load distribution in various elements of a bridge superstructure (i.e., structural analysis of superstructure) is discussed in Chapter 4.

From a historical perspective, the genesis of highway design live loads has a long and interesting history that goes back to the mid-nineteenth century. The first live load procedure for highway bridge design was proposed and used by Squire Whipple in 1846. In his *Essay no.* 2, he regarded it "proper to consider the whole area of the roadway covered with men, which is about 100 lb to the square foot, as the greatest load to which the bridge can be exposed," and this standard continued to be in use for many years. However, after many bridge failures, the American Society of Civil Engineers (ASCE) created a committee to determine "the most practical means of averting bridge accidents." This committee, in its March 3, 1875, report, made recommendations for both the railroad and highway bridge loadings. It divided highway bridges into the following three categories (Edwards 1959):

1. City and suburban bridges and those over large rivers, where great concentration of weight is possible
2. Highway bridges in manufacturing districts or on level, well-ballasted roads
3. County road bridges, where roads are unballasted and the loads hauled are consequently light

For these bridges, design loads were recommended as shown in Table 3.11.

www.EngineeringEBooksPdf.com

TABLE 3.11
Early Classifications of Highway Bridges and Design Live Load

	Load per Square Foot of the Deck Area, lb		
Length of Span	**A**	**B**	**C**
60 ft and under	100	100	70
60–100 ft	90	75	60
100–200 ft	75	60	50
200–400 ft	60	50	40

The provision for concentrated loads was made in view of the then-commonly used single-axle ox carts by these recommendations:

> City bridges 6 tons; turnpikes 5 tons; country roads 4 tons.
>
> **(Edwards 1959)**

At the turn of the century, the heaviest highway loading was a road roller, which continued to be used as a model for describing design live loads for highway bridges. The first American practice specifying a definite concentrated axle load for highway traffic is reported to have evolved in July 1877 through *General Specifications for Railway and Highway Bridge Combined over the Wisconsin River at Kilburn City, Wisconsin*, on the Chicago, Milwaukee, and St. Paul Railroad, proposed by D. J. Whitmore (Edwards 1959). In 1895, the Phoenix Bridge Company issued *Standard Specifications of the Phoenix Bridge Company for Steel and Iron Railway and Highway Structures*, Edwards (1959), in which a road roller weighing 16 tons was specified with this configuration:

> 6 tons concentrated on two front rolls spaced 2 ft 6 in. center to center, 10 tons on the rear rolls spaced 6 ft center to center, and axles spaced 11 ft center to center.

A more complete description of the road rollers to be used in the design of highway bridges was contained in *General Specifications for Steel and Iron Bridges and Viaducts* issued in 1896 by the Canadian Department of Railways and Canals:

> Road roller of 32,000 pounds weight distributed as follows: on forward axle 16,000 pounds on a wheel 4 feet 2 inches wide, on rear axle 11 feet 2 inches from forward axle 8,000 pounds on each of two wheels spaced 5 feet 8 inches centers and 20 inches wide.
>
> **(Edwards 1959)**

3.7.2 Development of AASHTO Standard Specifications Live Load Model

The first serious effort to quantify highway live loads was made by the U.S. Department of Agriculture, Office of Public Roads, through its Circular No. 100 of August 19, 1913: *Typical Specifications for the Fabrication and Erection of Steel Highway Bridges.* It contained a provision for a 15-ton road roller loading for the computation of live load stresses. On July 1, 1919, the Office of Public Roads became the Bureau of Public Roads, which prepared and issued a revised specification (Edwards 1959).

With the beginning of industrial revolution came motorcars and trucks, which grew heavier and bigger with time and necessitated new live load specifications for designing highway bridges. Design live loads were first based on 10- and 15-ton trucks, followed in 1924 by a 20-ton truck. These trucks came to be known as H10, H15, and H20 trucks, respectively (the letter *H* stands for highway, and the number following specifies total truck weight in tons). The total weight of H10 truck was specified to be 50 percent of the H20 truck, whereas that of H15 truck was specified to be 75 percent of the H20 truck. In each of these trucks, the front axle carried 20 percent of the total truck weight and the rear axle carried 80 percent of the total weight (Figure 3.4). Thus evolved the first *notional*

www.EngineeringEBooksPdf.com

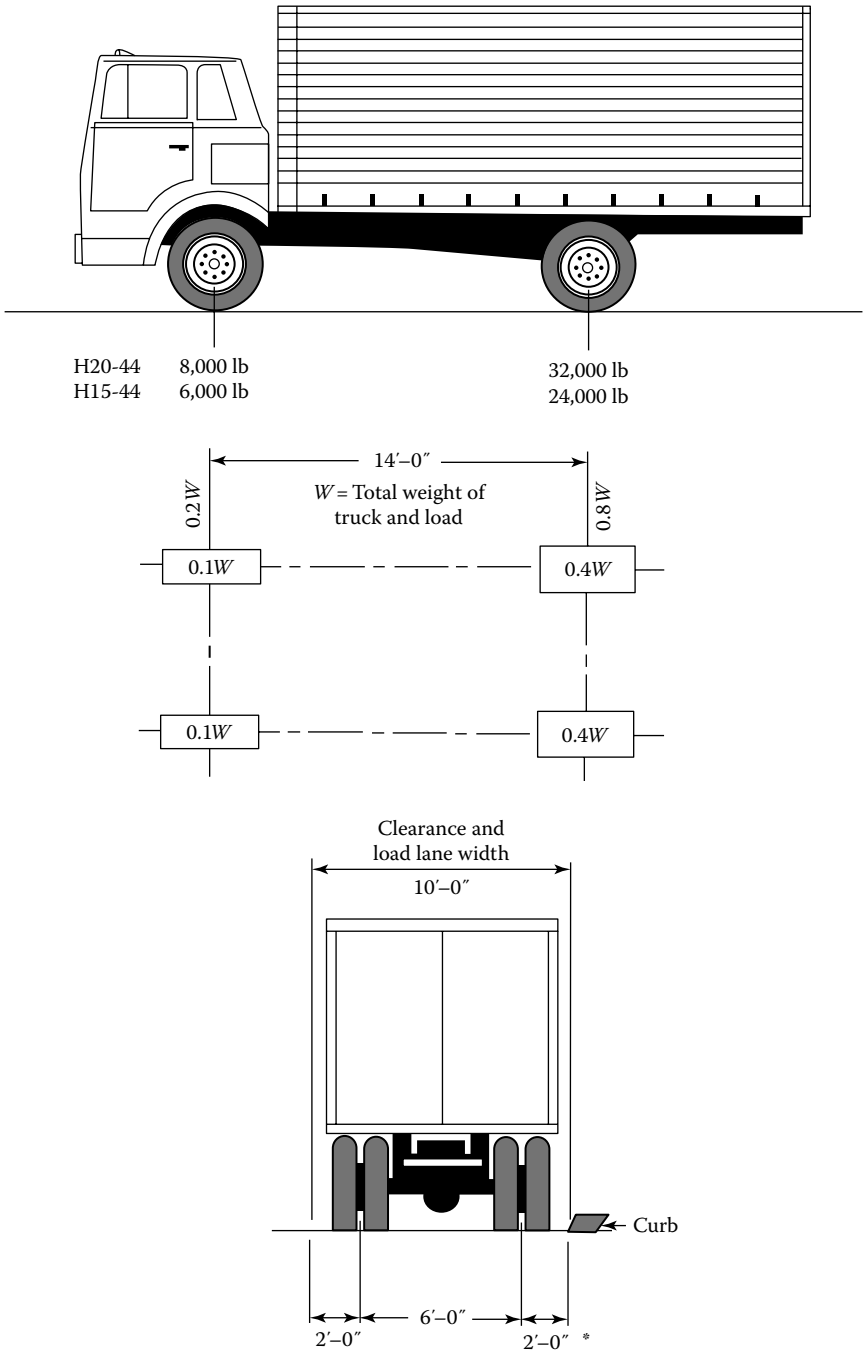

*For slab design, the centerline of the wheel shall be assumed to be 1 ft from the face of curb.

FIGURE 3.4 AASHTO H15 and H20 trucks. Axle loads of H15 truck are three-fourths of HS 20 truck.

www.EngineeringEBooksPdf.com

model to represent highway bridge design live load specification; it is referred to as *notional* because these trucks did not represent physical configuration of or similarity to any particular type of truck or trucks in existence. The second *notional* model, currently in use, evolved in the 1990s when the current AASHTO LRFD Specifications were developed (discussed in the next section).

The AASHO, the predecessor of the AASHTO, was created on December 12, 1914. In July 1922, it formed a special committee, *Committee on Bridges and Allied Structures*, which studied the problem of highway live loads. The committee's *final report* on specification for design and construction of steel highway bridge superstructure was presented at the spring meeting of the ASCE on April 9, 1924 (Seaman 1924). In 1927, the conference committee representing AASHO and the American Railway Engineers Association (AREA) introduced the truck train—a heavy truck preceded and followed by trucks having three-fourths of its weight—as shown in Figure 3.5. The primary idea of train of wheel loads was apparently based on the Cooper E-72 loading for railroads (Figure 3.6, used for design of railroad bridges, originally devised by Theodore Cooper in 1894), derived from L. E. Moore's discussion of Hussey's paper (Hussey 1924, Edwards 1959). AASHO's *first* edition of *Specifications*

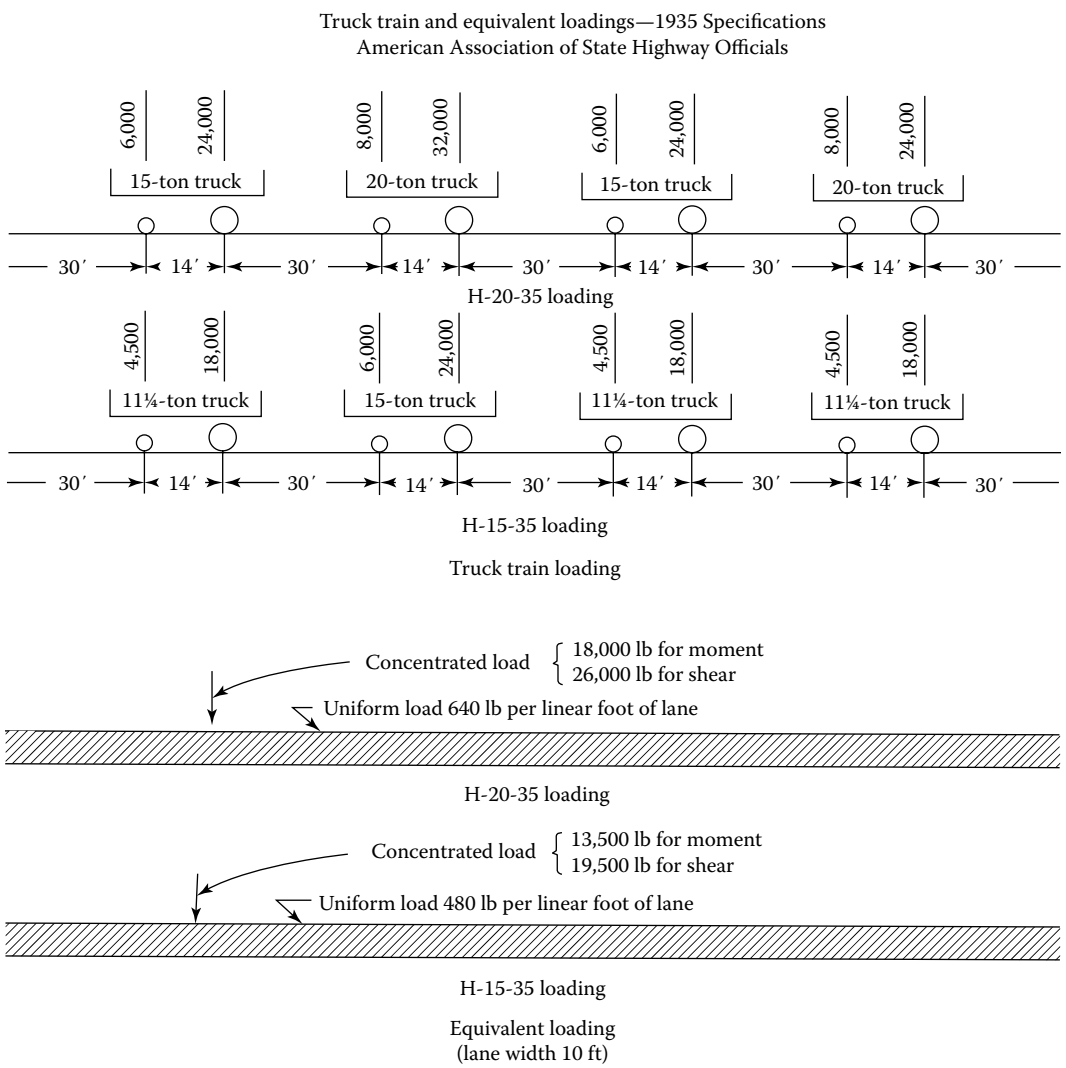

FIGURE 3.5 The 1935 AASHO Standard Specifications for highway live load. (From ASCE, *Proceedings, ASCE*, 84(ST3), 1631-1–1633-19, paper no. 1633, May 1958.)

www.EngineeringEBooksPdf.com

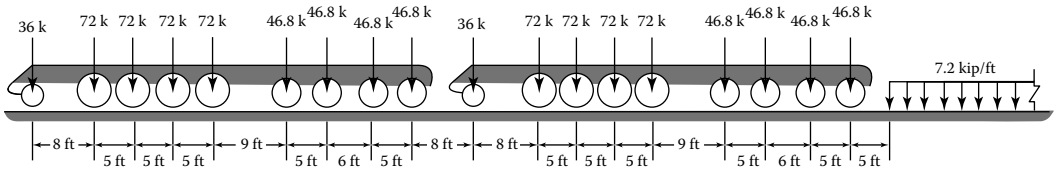

FIGURE 3.6 Cooper E-72 loading (AREA).

for Design of Highway Bridges was published in 1931. In November 1932, AASHO adopted its first policy concerning maximum dimensions, weights, and speeds of motor vehicles (AASHTO 1991). These specifications were first published in the 1935 AASHO Specifications (ASCE 1958).

The system of truck train loadings was superseded in 1941 by the equivalent lane loading, which was first used as an optional loading in the 1931 AASHO Standard. The Public Roads Administration, an agency of the US government, developed the new or modified live load model. It was based on the AASHO Standard, then in practice, to meet conditions created by movement of military equipment. The changes in the then-existing load model, H15 loading and H20 loading, were necessitated by the loads imposed by heavy tanks and the need for greater roadway width to permit military convoys over the highways without interference with the normal traffic (ENR 1941, ASCE 1958). In the early 1940s, this led to the introduction of H20-S16 loading, a system of truck and lane loading (Figure 3.5) that served as the live load model for AASHTO Standard Specifications (AASHTO 2002). The H20-*S*16 truck, briefly called HS20 truck, consists of a single steering axle weighing 16 kip and two axles that support a semitrailer, each weighing 32 kip (GVW = 8 + 32 + 32 = 72 kip). The spacing between the front and the adjacent axle is maintained at 14 ft, whereas the spacing between the middle axle and the rear axles is kept as variable between 14 and 30 ft. In this load designation, letter *H* stands for highway and *S* for semitrailer. These live load models were formalized and first published in the 1944 AASHO Standard Specifications and came to be known as H15-44, H20-44, HS15-44, and HS20-44 loadings, characterized as follows:

1. H15 loading is three-fourths or 75 percent of H20 loading.
2. The number 44 indicates the year 1944.
3. The difference between H and HS trucks is that the latter carries a two-axle semitrailer (32 kip per axle); HS15 truck carries a two-axle semitrailer (24 kip/axle).

The geometric configuration of an HS20 truck (i.e., distance between the axles and distribution of loads on them) is described in the next section.

In addition to the design *truck* load, a design *lane* load was also specified as a part of the AASHO live load model. It was developed to better model highway loading on long spans where the load due to a string of vehicles might be critical. The lane load model consisted of a combination of a uniform load *and* a concentrated load (different for moment and shear) specified as follows (Figure 3.7):

H20 loading: A combination of (1) uniform load of 640 lb/ft over the entire span (spread over a width of 10 ft in a traffic lane) *and* (2) a concentrated load of 18 kip for determining moment (only) and a concentrated 26 kip load for shear (only), to be placed on the span to cause maximum force effects; the two concentrated loads are *not* to be used concurrently. For example, when maximum moment is to be determined in a simple span, the 18 kip concentrated load would be placed at the midspan along with a uniform 640 lb/ft load over the entire span. Likewise, when maximum shear is to be determined in a simple span, the 26 kip concentrated load would be placed near the support, along with the uniform load on the entire span.

H15 loading: The values were set at three-fourths of those for H20 loading configuration, that is, 480 lb/ft for uniform load (spread over a width of 10 ft in a traffic lane), and 13.5 and 19.5 kip, respectively, for moment and shear.

www.EngineeringEBooksPdf.com

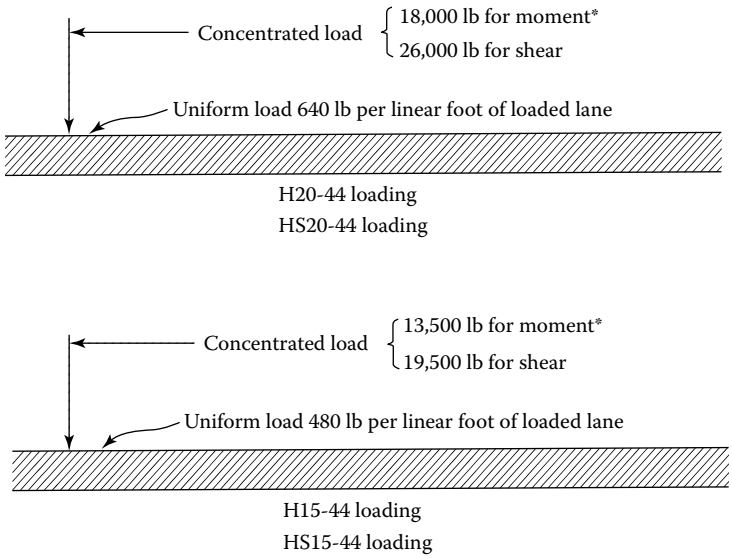

FIGURE 3.7 AASHTO Standard lane loading (AASHTO 2002). Concentrated loads are placed on the span so as to create critical force effects. Asterisks indicate that these loads should be placed *on* the span (as opposed to *at the end of the span*) to create maximum load effects (moment) in the span.

The standard specifications *required* design moments and shears, as well as any other forces, to be determined separately as caused by the truck *and* the lane loading, and the *larger* of the two values to be used for design.

Industrial growth in the United States following after World War II created a demand for yet heavier loads to be carried on nation's highway bridges. As a result, several states mandated to design their highway bridges for HS25 loading, defined as 25 percent heavier than HS20 trucks, which resulted in each axle load being 25 percent heavier than those of HS20 trucks.

3.7.3 Description of AASHTO LRFD Notional Live Load Model

The AASHTO LRFD notional model for live load on American highway bridges, designated as HL-93, is a modification of notional live load model that had been specified in standard specifications (AASHTO 2002). It was developed to represent moments and shears produced by a group of vehicles routinely permitted on highways of various states under *grandfather* exclusions to weight laws. The vehicles considered to be representative of these *exclusions* were based on a study by the Transportation Research Board (TRB) (Cohen 1990) (discussed later in this section). This live notional load model is based on truck surveys and weigh-in-motion (WIM) data that were collected in the 1990s for modeling the live load for use in developing AASHTO LRFD Specifications (Nowak and Hong 1991, Nowak 1993a,b, 1995); its modeling is discussed in Nowak and Collins (2013). A brief discussion on this topic can be found in the literature (Kulicki and Mertz 1991, 2006).

The notional design live load model specified in AASHTO LRFD represents a stark deviation from its predecessor, *Standard* Specifications (AASHTO 2002), both in designation and magnitude (live load effects), as follows:

1. The design vehicular live load in AASHTO LRFD is referred to as HL-93 loading (the letters *HL* mean *highway loading*).
2. The number 93 indicating the year 1993 when this new loading was officially approved by AASHTO at its annual meeting in Denver, Colorado.

www.EngineeringEBooksPdf.com

3. The HL-93 design live load consists of a *combination* load (this is the important part) placed *concurrently* in each design lane as follows; *the more critical of these two load combinations should be chosen as the design basis*:
   a. The design truck (concentrated loads, Figure 3.8) combined with the design lane load (uniform load, Figure 3.10).
   b. The design tandem (concentrated loads, Figure 3.9) *and* the design lane load (uniform load, Figure 3.10). The tandem load, also known as the *alternate military loading,* is specified to simulate military loading and typically governs design of spans approximately shorter than 40 ft (discussed later). Tandem loading is defined as two closely spaced axles, usually connected to the same undercarriage, by which the equalization of load between the axles is enhanced.

These combination vehicular live load models are shown in Figure 3.11. In each case, the concentrated loads are to be positioned so as to create the maximum load effects in the span. Furthermore, the lane load is *not* to be interrupted to provide space for the axle sequences of the design truck or the design tandem; interruption is needed only for the patch loading patterns to produce maximum load effects tandem.

In addition to the aforementioned, ASSHTO LRFD Art. 3.6.1.3.1 specifies the vehicular live load model for continuous spans as shown in Figure 3.12. Note that all loads should be positioned as shown in the figure, and their magnitudes should be reduced to 90 percent.

Specifications for vehicular live load are covered in AASHTO LRFD Art. 3.6.1.2. The design truck specified therein is the same as the AASHTO HS20 truck specified in the standard specifications; however, it is now referred to as HL-93 design truck (Figure 3.8) and configured as follows:

1. It consists of three axle loads: a front 8 kip axle load, an intermediate 32 kip axle load, and a rear 32 kip axle load due to a semitrailer, a total of 72 kip (= 8 + 32 + 32).
2. The distance between the front and the next (or intermediate) axle of the truck is kept fixed at 14 ft, whereas the distance between the intermediate and the rear axles is kept as variable—between 14 ft (minimum) and 30 ft (maximum) to produce extreme load effects. The long spacing would control when the trucks are placed individually on two adjacent, structurally continuous spans.
3. The transverse spacing between the centerlines of the wheel loads is fixed at 6 ft.
4. The minimum distance between the centerlines of the exterior truck wheel and the interior face of the curb is kept as 2 ft for design of girders, and 1 ft for design of deck overhang (discussed later).
5. Dynamic load allowance (DLA) (referred to as *impact* in AASHTO Standard Specifications) is to be applied as specified in AASHTO LRFD Art. 3.6.2 (discussed in Section 3.6) to account for the dynamic effects caused by the vehicular traffic.

The HL-93 design tandem (Figure 3.9) is defined as follows:

1. It consists of a pair of 25 kip axle loads (slightly heavier from 2002 AASHTO *Standard* Specifications, which had 24 kip axle loads).
2. The axles are spaced 4 ft apart longitudinally.
3. The transverse spacing of the centerlines of wheels on the axles is 6 ft.
4. DLA is to be applied as specified in Art. 3.6.2.

The design lane load (Figure 3.10) is defined as follows:

1. A load of 640 lb/ft distributed uniformly in the longitudinal direction.
2. Transversely, the design lane load is assumed distributed uniformly over a width of 10 ft.
3. DLA is *not* applicable to the design lane load.

www.EngineeringEBooksPdf.com

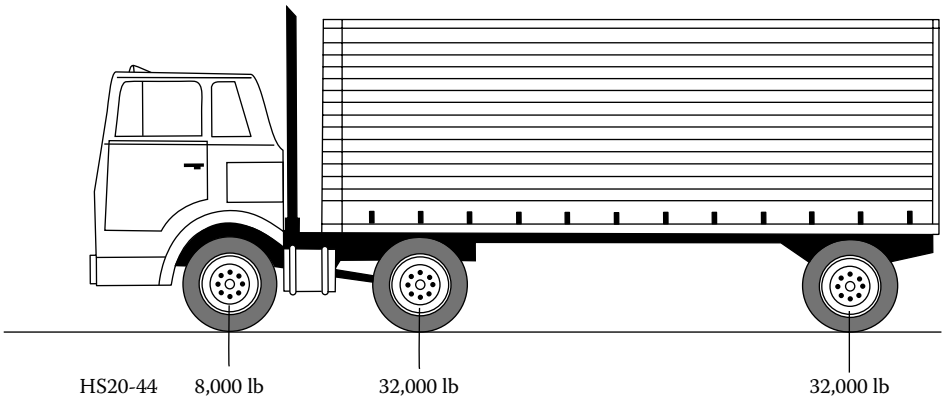

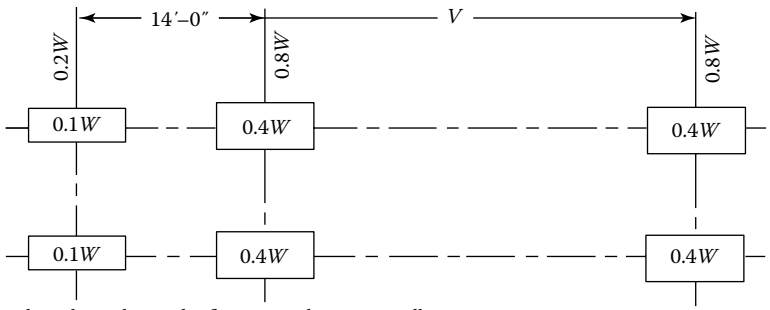

W = Combined weight on the first two axles = 40,000 lb
V = Variable spacing—14–30 ft, inclusive. Spacing to be used is that which produces maximum stresses.

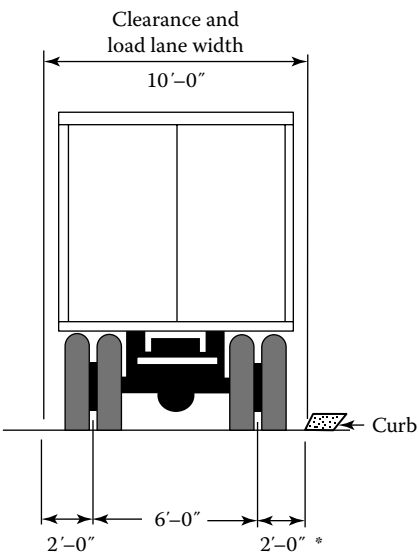

*1 ft from the face of the curb or railing; 2 ft from the edge of the design lane for all other components.

FIGURE 3.8 Configuration of HL-93 design truck. This same truck was designated as HS20 in AASHTO Standard Specifications.

www.EngineeringEBooksPdf.com

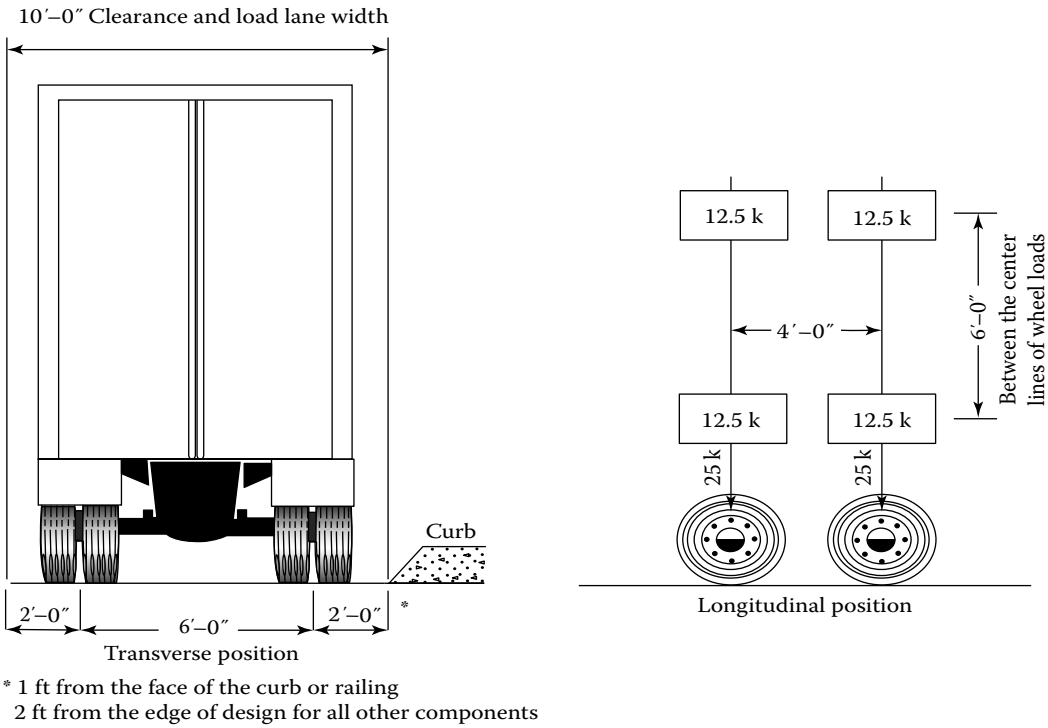

FIGURE 3.9 HL-93 design tandem configuration. Each axle weighs 25 kip.

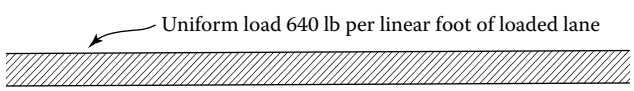

FIGURE 3.10 HL-93 design lane load.

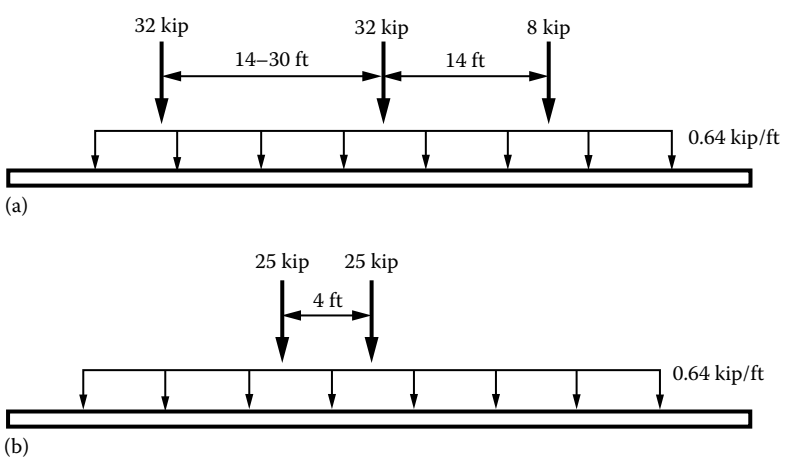

FIGURE 3.11 AASHTO LRFD HL-93 live load models: (a) HS20 truck *plus* lane load and (b) tandem *plus* lane load. Note that tandem consists of two 25 kip axles spaced 4 ft apart (which is different from AASHTO Standard HS20 alternative live load model that had two 24 kip axle loads).

www.EngineeringEBooksPdf.com

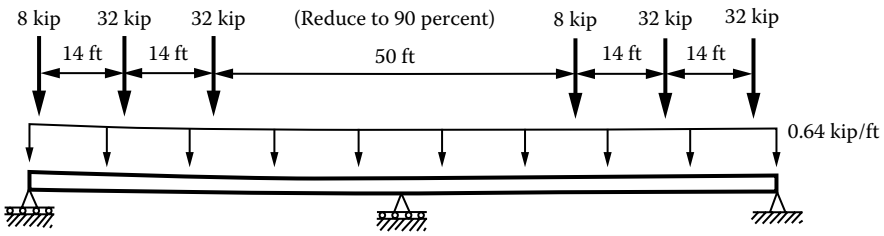

FIGURE 3.12 HL-93 loading for negative moments at intermediate supports in continuous spans (AASHTO LRFD Art. 3.6.1.3.1). Reduce loads to 90 percent. The 50 ft distance is to be maintained between the lead axle of one truck and the rear axle of the other truck.

The combination live loading would be referred to as HL-93 loading in discussions throughout this book.

From the foregoing discussion, it should be apparent that the HL-93 live load model is quite different from its AASHTO Standard model, which consisted of only *one* of the following, and the critical one selected for design:

1. An HS20-44 truck (same as HL-93 truck, Figure 3.8)
2. A tandem load (two 24 kip axles 4.0 ft apart)
3. A uniform load over the entire span, with a concentrated load (different for moment and shear) positioned to produce the maximum load effects (Figure 3.7).

The design load is always an axle load; single wheel loads should not be considered. For multiple lane bridges, it is assumed that the design live load is the same in all lanes, either combination of HL-93 truck and uniform load or combination of tandem and uniform loads. Although, theoretically, it is possible that an extreme live load effect could result from a 32.0 kip axle in one lane and 50.0 kip tandem in a second lane, such sophistication is not warranted in design.

3.7.4 Understanding the Development of AASHTO LRFD Notional Live Load Model

3.7.4.1 Concept of Notional Load: What Is It?

It was stated earlier that the live load model specified in AASHTO LRFD Specifications was developed as a *notional model* to represent moments and shears produced by a group of vehicles routinely permitted on highways of various states under *grandfather* exclusions (discussed later in this section) to weight laws. The word *notional* is used as a qualifier for the *model* because, in a physical sense, it does not represent any particular truck configuration(s) that traverse nation's highways. The HS20 truck and the uniform 640 lb/ft lane load discussed earlier, in a physical sense, are not representative of any real vehicular traffic that one sees on highways; rather, they are conceptual, an idealization, intended to convey merely an *idea* of vehicular loads. More importantly, the notional live load, based on the results of extensive, continuing research and studies, represents *spectra* of many different vehicular loads and associated load effects. This notional live load concept is similar to the live load model used for the design of buildings for which uniform and concentrated loads, which have no physical resemblance to actual loads, are used for design of floors (Taly 2003).

The AASHTO LRFD notional live load model raises several important questions. Why use a *notional* model? What necessitated the change from the AASHTO Standard live load model? What does it mean to designers? A clear answer to these questions is important to understanding the notional live load model. A discussion on this important topic has been provided by Cohen (1990) and Kulicki and Mertz (1991, 2006); a summary from these references follows.

For the time being, let us forget the notional model. Since the AASHTO Standard live load model was developed in the early 1940s, the nature of commercial traffic has changed considerably

www.EngineeringEBooksPdf.com

and in many ways. In 1944 Standard Specifications, the HS20 truck (a truck with two axles and a semitrailer) was extended into a tractor-trailer combination called HS20-S16-44 (known as HS20 truck for simplicity). Strictly, from the *loads* point of view, a basic truck may be thought of as a body supported on two axles (i.e., four-wheel loads). With industrial growth came the demand for heavier-load-carrying trucks, which led to the development of truck tractor and tractor-trailer configurations. Today, there exists a multitude of vehicular configurations having widely varying load-carrying capacities (GVWs) and axle configurations (i.e., spacing between the adjacent axles) that crisscross the highways. Other configurations include truck tractor and tractor-trailer combinations, varying in their load-carrying capacities and axle spacing. Then there are escorted permit loads of various states in the United States that also have many different configurations, and illegal overloads, or short-duration special-permit loads (discussed in the next section). For design purposes, it would be necessary to calculate live load force effects from all of these vehicular loads and select the largest values, a formidable task. To simplify this daunting task, notional live load model is used; it provides an extremely simple model that provides *spectra* of many different vehicular loads and associated load effects.

As the bridge engineers started realizing the ill effects (overstressing) of ever-increasing weight and volume of vehicular live load on highway bridges, they responded by making adjustments to this new reality. In the 1970s and 1980s, some states started designing bridges for the increased live load, simply by increasing the HS20 truck to an HS25, which resulted in to a 90 kip gross weight truck, a 25 percent increase over the HS20 truck that had a 72 kip GVW (it was done by proportionally increasing all axle weights while maintaining the same axle spacing). Some states also increased 25 percent in the lane load and possibly the same increase in the military loading; there was no uniformity. Although it was a step in the right direction, it did not satisfactorily address the problem of bridge overstressing and the multitude of commercial truck configurations using the highways. This indeed was the problem that precipitated the development of the current notional live load model.

In the initial development of the notional load, no attempt was made to relate to the load effects of these many different vehicle types. The moment and shear effects were subsequently compared to the truck weight studies (Csagoly and Knobel 1981, Nowak 1992), selected data from WIM studies (which obtain truck weight data using passive weighing techniques unbeknown to the operator that the truck weight is being monitored), and the 1991 Ontario Highway Bridge Design Code (OHBDC) bridge live load model (Harman 1985). Bridges are instrumented to obtain the required data. Such studies include Hwang and Nowak (1991a,b) and Moses and Ghosen (1983, 1985); their results were confirmed by Kulicki and Mertz (2006) and Nowak (1993a). Under continuing monitoring, researchers, as of this writing (2012), have amassed WIM data on over 40 million trucks! These studies indicated that the notional live load could be scaled by appropriate load factors to be representative of these other load spectra.

3.7.4.2 Commercial Vehicular Loads

The truck weight limits and their configuration (lengths and widths) are regulated by the government (state and federal). From the perspective of commercial vehicular loads, the wide variety of them traversing the interstate and state highways can be classified as follows:

1. Legal loads
2. Exclusion vehicles
3. Overweight (permit) vehicles (Section 3.7.4.4)

3.7.4.2.1 Legal Loads

There are federal legal loads and state legal loads. The GVW and axle configurations of commercial vehicles permitted on interstate highways are described in Federal Highway Administration (FHWA) (1995). Figure 3.13 from AASHTO (1991) shows the silhouettes of most commercial vehicle types in use; a few of these legal loads are depicted pictorially in Figure 3.14. These vehicle types are described variously as *long combination vehicles* (LCVs) and *short hauling vehicles* (SHVs) (such as solid waste

www.EngineeringEBooksPdf.com

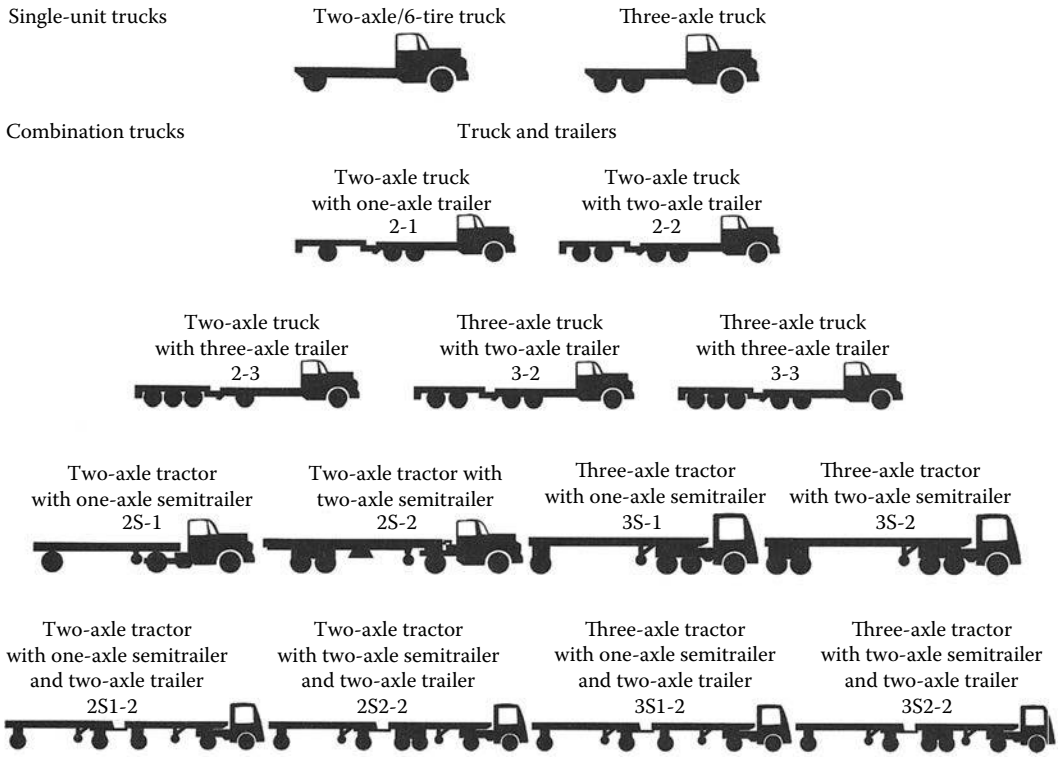

FIGURE 3.13 Typical commercial vehicle types (based on axle arrangements) in regular operation on highways. *Note*: *S* = semitrailer. The digit following *S* indicates the number of axles on the semitrailer. Any digit other than the first in a combination, when not preceded by an *S*, indicates a trailer and the number of axles. *Example*: The designation 3S1-2 indicates a three-axle truck with tandem rear axles, a semitrailer with a single axle and a trailer with two axles.

disposal trucks, dump trucks, and concrete mixers). The term LCV refers to one of the following three types of vehicles (Farris 1991):

1. A truck tractor pulling three 28 or 28.5 ft trailers (triples)
2. Tractor trailer combinations involving two 48 or 45 ft trailers (turnpike doubles)
3. Double 48s or tractor-trailer combinations involving one 48 or 45 ft trailer and one 28 or 29 ft trailer (Rocky Mountain doubles)

The SHVs include dump trucks, construction vehicles, solid waste trucks, and other hauling trucks (Figure 3.15).

The maximum permissible axle loads and their configurations are as follows (AASHTO 1991, FHWA 2006a). Various weight-related definitions used in this context are as follows:

Single-axle weight: The total weight on one or more axles whose centers are spaced not more than 40 in. apart. The federal single-axle weight limit on the interstate system is 20,000 lb, including any and all weight tolerances.

Tandem-axle weight: The total weight on two or more consecutive axles whose centers are spaced more than 40 in. apart but not more than 96 in. apart. The federal tandem-axle weight limit on the interstate system is 34,000 lb, including any and all weight tolerances.

GVW: The weight of a vehicle or vehicle combination and any load thereon. As trucks grew heavier in the 1950s and 1960s, something had to be done to protect bridges. The solution was to link

www.EngineeringEBooksPdf.com

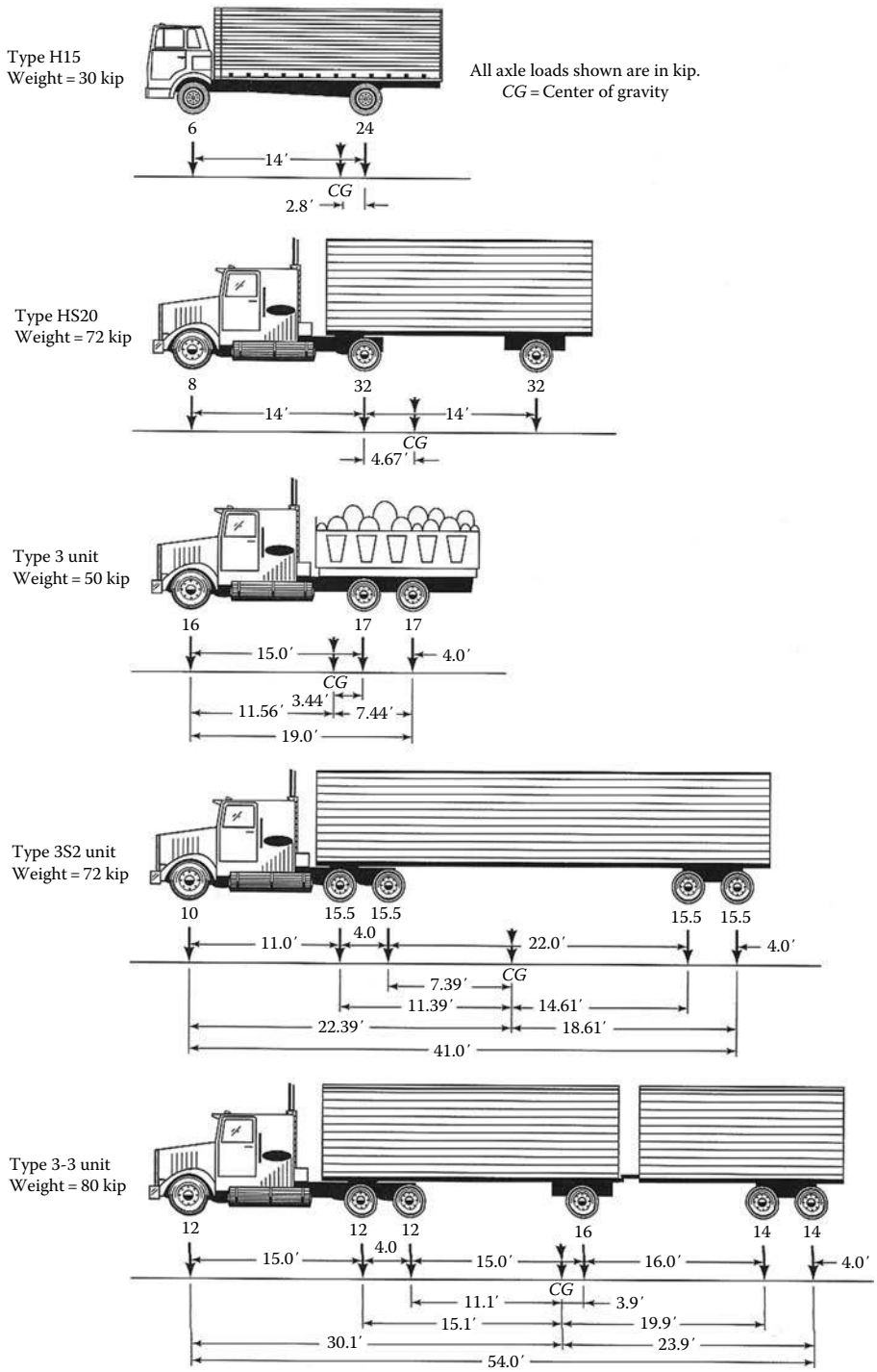

FIGURE 3.14 Examples of legal live loads (trucks and truck-trailer units, known as AASHTO rating vehicles) used for posting of highway bridges. Figures show axle loads, their relative positions, and the center of gravity of wheel loads, which can be used for determining shears and moments in bridge superstructures. (From AASHTO, *The Manual for Bridge Evaluation*, 2nd ed., American Association of State Highway and Transportation Officials (AASHTO), Washington, DC, 2011.)

www.EngineeringEBooksPdf.com

FIGURE 3.15 Example of a specialized hauling vehicle (SHV). (Courtesy of Bala Sivakumar, Director of Special Bridge Projects, HNTB, New York.)

allowable weights to the number and spacing of axles. The federal gross weight limit on the interstate system is 80,000 lb unless the bridge formula, Equation 3.6 (FHWA 2006a), dictates a lower weight limit:

$$W = 500\left(\frac{LN}{N-1} + 12N + 36\right) \tag{3.6}$$

where

W = maximum weight in pounds, carried on any group of two or more axles, computed to the nearest 500 lb

L = distance, in feet, rounded off to the nearest foot, between the extremes of any group of two more consecutive axles

N = number of axles in the group under consideration

The U.S. Congress enacted the bridge formula in 1975 to limit the weight-to-length ratio of a vehicle crossing a bridge. This is accomplished either by spreading weight over additional axles or by increasing the distance between axles. Compliance with bridge formula weight limits is determined by using the following formula.

The development of Equation 3.6 was based on the premise that the actual stresses must not exceed the allowable stress for bridges designed (in the past) for HS20 and HS15 trucks by more than 5 percent and 30 percent, respectively. Interstate system weight limits in some states may be higher than the figures noted earlier due to *grandfather* rights. This is so because, historically, in 1956, the U.S. Congress legislated maximum axle weights, GVW, and width limits for trucks on interstate highways based on limits recommended by AASHO (now AASHTO) as follows:

18,000 lb on a single axle
32,000 lb on a tandem axle
73,280 lb GVW

Readers should refer to FHWA (2006a) to develop a clear understanding of application of bridge weight formula (Equation 3.6). For simplicity, FHWA (2006a) provides examples of application of the

www.EngineeringEBooksPdf.com

bridge weight formula, as well as a user-friendly table for the permissible gross weight for vehicles having a variety of axle configurations and truck lengths, which can be used without the need for calculations. An exhaustive discussion on various aspects of commercial vehicles can be found in TRB (2002).

3.7.4.2.2 Exclusion Vehicles

Exclusion vehicles (Figures 3.16 and 3.18) are trucks that exceed federal weight limits. They are legal based on state weight regulations. They are not allowed on interstate highways but can operate

FIGURE 3.16 Exclusion truck. (Courtesy of Bala Sivakumar, Director of Special Bridge Projects, HNTB, New York.)

FIGURE 3.17 A specialized hauling vehicle (SHV, 7 axles). (Courtesy of Bala Sivakumar, Director of Special Bridge Projects, HNTB, New York.)

www.EngineeringEBooksPdf.com

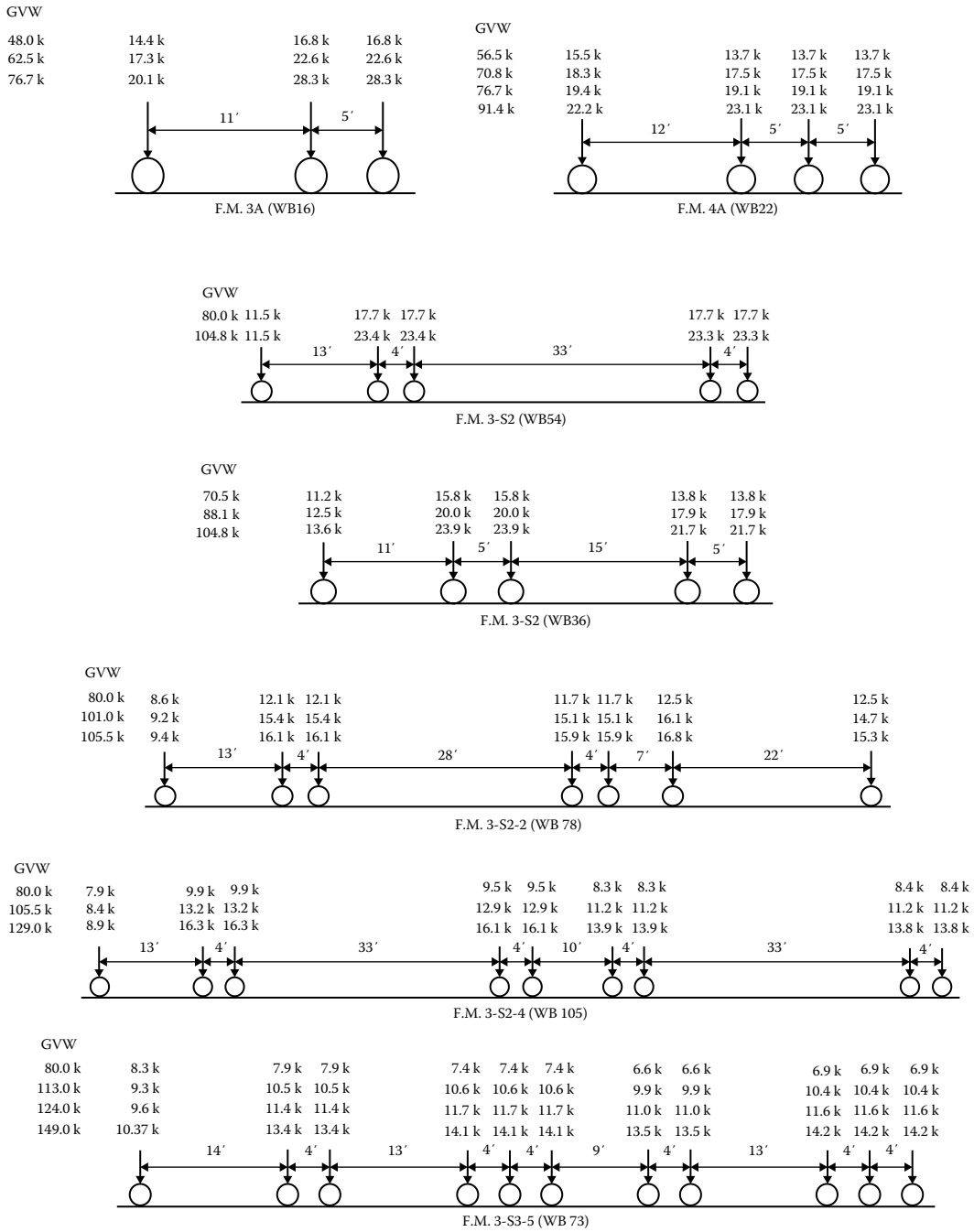

FIGURE 3.18 Exclusion vehicles (schematics). (Reproduced with permission from TRB. *50 Years of Interstate Structures—Past, Present, and Future*, Transportation Research Circular E-C104, Transportation Research Board, National Academies, Washington D.C., September 2006, 145pp., 2006.)

www.EngineeringEBooksPdf.com

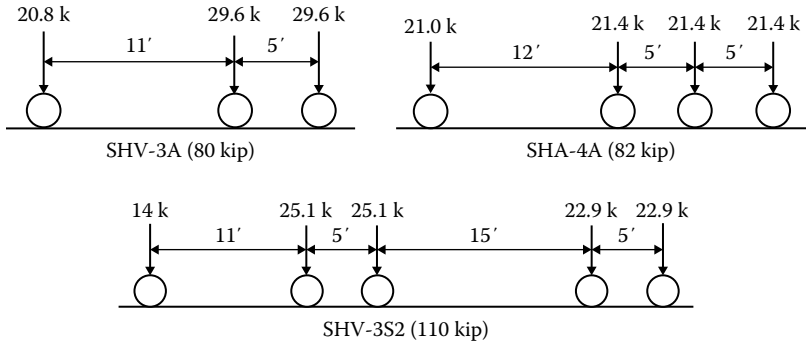

FIGURE 3.19 NTWAC special hauling vehicles (schematics).

on state and local roads. *The exclusion vehicles also are the vehicles that induce the highest load effects on bridges; this was the main reason for developing the new live load model.*

In 1956, the U.S. Congress legislated maximum axle weights, GVW, and width limits for trucks operating on interstate highways based on limits recommended in 1946 by AASHO (now AASHTO): 18,000 lb on a single axle, 32,000 lb on a tandem axle, and 73,280 lb GVW. The federal law also authorized states to allow operation of heavier vehicles on interstate highways, but only if such operation was legal in the state prior to July 1956. Because of these stipulations, this provision came to be known as the *grandfather right* or *grandfather clause* and the vehicles as *grandfathered trucks* or *exclusion vehicles*. There are three different grandfather clauses in Section 127, Title 23, U.S.C. (U.S. Govt. 1975) adopted at different times as follows:

1. The first was enacted in 1956; it deals with axle weights, gross widths, and permit practices.
2. The second was adopted in 1975, which deals with bridge formula and the axle spacing tables as mentioned earlier.
3. The third was adopted in 1991, which ratified state practices with respect to LCVs (discussion follows).

Figures 3.18 through 3.23 present many different vehicle configurations including exclusion vehicles (TRB 2006).

3.7.4.3 Development of AASHTO LRFD Notional Live Load: A Brief History

As stated earlier, by the early 1970s, it was being realized that the vehicular traffic on the interstate highways was causing load effects on bridges greater than those that could be determined theoretically based on the notional live load model of AASHTO Standard (Figure 3.24). Stated differently, the AASHTO Standard live load model was not representative of the actual traffic on the highways. This drawback and disparity in the live load effects (see Figures 3.37 and 3.38 later in this section) called for a change in the existing live load model. Another reason that prompted a need for the change in the existing live load model was the advancement in design philosophies, notably the state-of-the-art LRFD philosophy, which structural engineers had embraced and was being used for design of buildings; bridge engineers felt that it was time for it to be incorporated in bridge design specifications. The notional live load model of AASHTO Standard already existed; therefore, it was used as the starting point for the development of the new notional live load model that came to be known as AASHTO LRFD live load model, referred to as HL-93, now in use.

It is easy to see that a bridge designer's task of calculating force effects due to the plethora vehicles (Figures 3.14 through 3.23) traversing highway bridges and determining the governing force effects can be both tedious and overwhelming. In order to develop a simple solution to this problem, an extensive research was conducted by AASHTO's LRFD development group that involved

www.EngineeringEBooksPdf.com

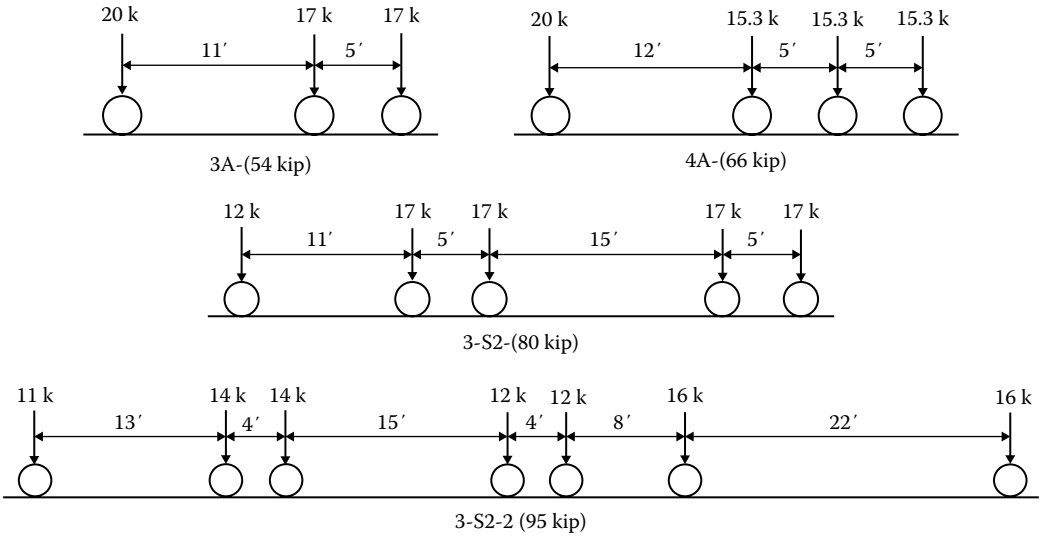

FIGURE 3.20 Modified TTI formula vehicles (schematics). (Reproduced with permission from TRB. *50 Years of Interstate Structures—Past, Present, and Future*, Transportation Research Circular E-C104, Transportation Research Board, National Academies, Washington D.C., September 2006, 145pp., 2006.)

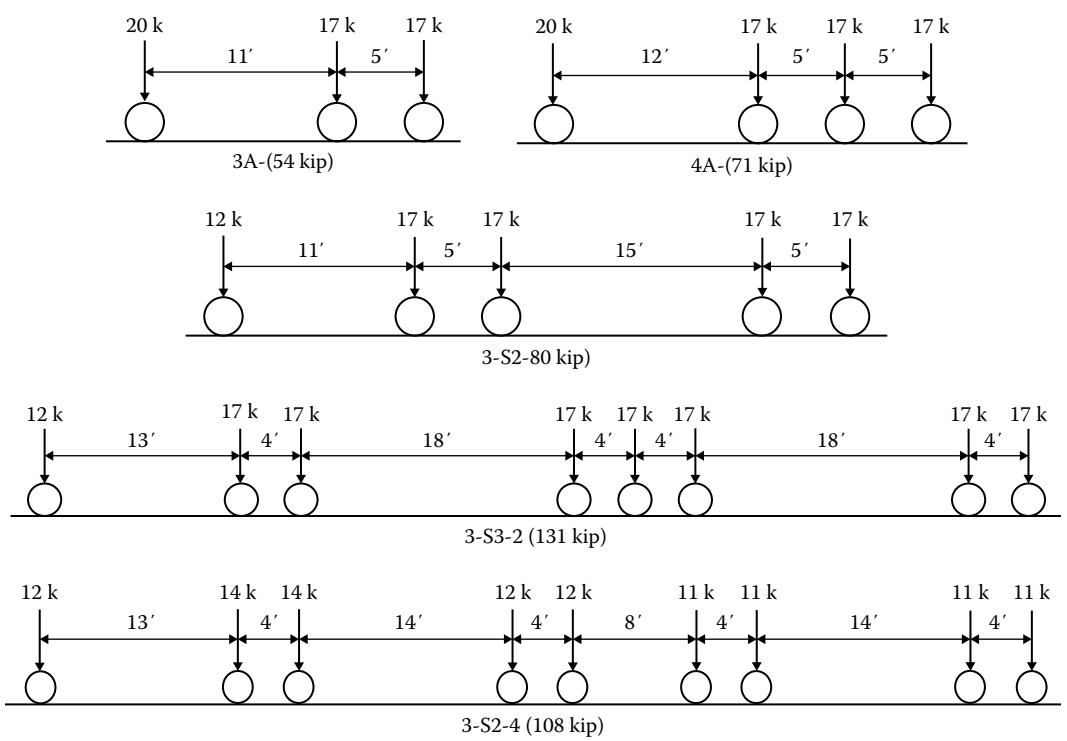

FIGURE 3.21 Canadian interprovincial load vehicles (schematics).

www.EngineeringEBooksPdf.com

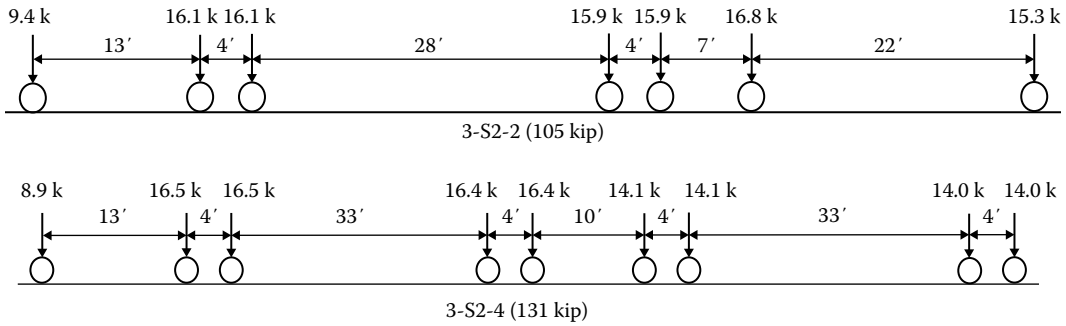

FIGURE 3.22 Extended bridge formula vehicles (schematics). (Reproduced with permission from TRB. *50 Years of Interstate Structures—Past, Present, and Future*, Transportation Research Circular E-C104, Transportation Research Board, National Academies, Washington D.C., September 2006, 145pp., 2006.)

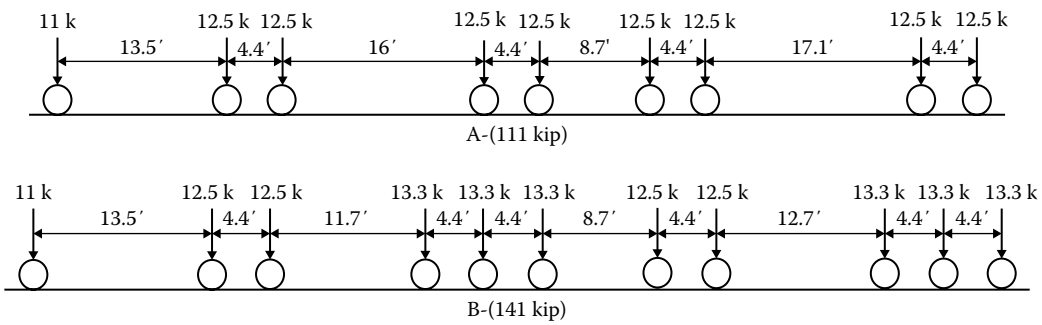

FIGURE 3.23 Turner trucks (schematics).

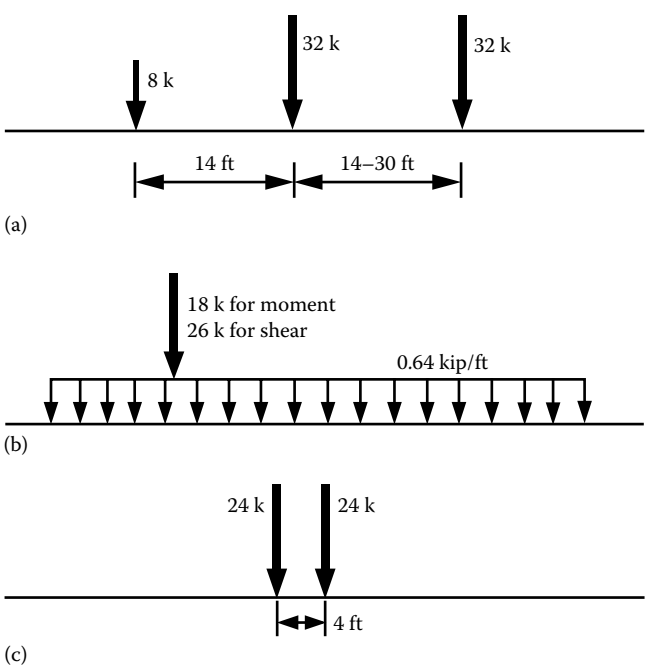

FIGURE 3.24 AASHTO Standard notional live load model. (a) HS20 truck, (b) HS20 lane, and (c) HS20 tandem.

www.EngineeringEBooksPdf.com

studying the force effects of one lane loaded (i.e., without distribution) on bridge superstructures due to these families of vehicles by calculating the envelope of force effects from each of the representative vehicles in a family as follows:

1. Centerline moment of a simply supported beam (not the absolute maximum moment)
2. Positive and negative moments at the 0.4L point of a two-span continuous girder with equal spans
3. Positive and negative end shears ($+V_{ab}$, $-V_{ab}$) and shear at the interior support ($-V_{ba}$) of a two-span continuous girder with equal spans
4. Negative moment at the interior support of two-span continuous girder with equal spans

Plots of the force effects caused by the HS20 truck, the National Truck Weight Advisory Committee (NTWAC) trucks, the Turner trucks, the Texas Transportation Institute (TTI) trucks, the extended bridge formula trucks (EXTBRFOR), and the exclusion trucks (EXCL) for various span lengths are presented in Figures 3.25 through 3.31. The force effects of AASHTO rating vehicles (Figure 3.14)

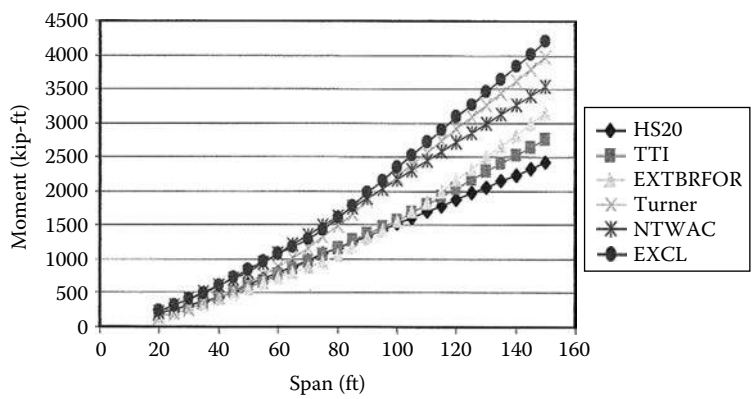

FIGURE 3.25 Centerline moments for simple spans. (From Kulicki, J.M. and Mertz, D.R., Evolution of vehicular live load models during the interstate design era and beyond, in *50 Years of Interstate Structures: Past, Present, and Future*, Transportation research Circular, E-C104, Transportation Research Board, National Research Council, Washington, DC, 2006.)

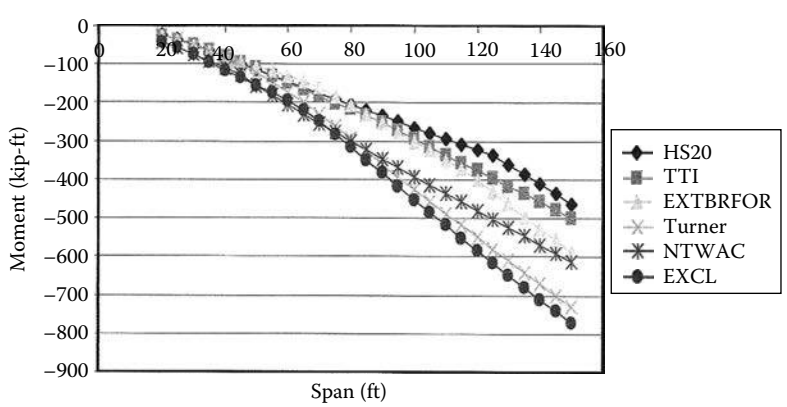

FIGURE 3.26 Negative moments at 0.4L. (From Kulicki, J.M. and Mertz, D.R., Evolution of vehicular live load models during the interstate design era and beyond, in *50 Years of Interstate Structures: Past, Present, and Future*, Transportation research Circular, E-C104, Transportation Research Board, National Research Council, Washington, DC, 2006.)

www.EngineeringEBooksPdf.com

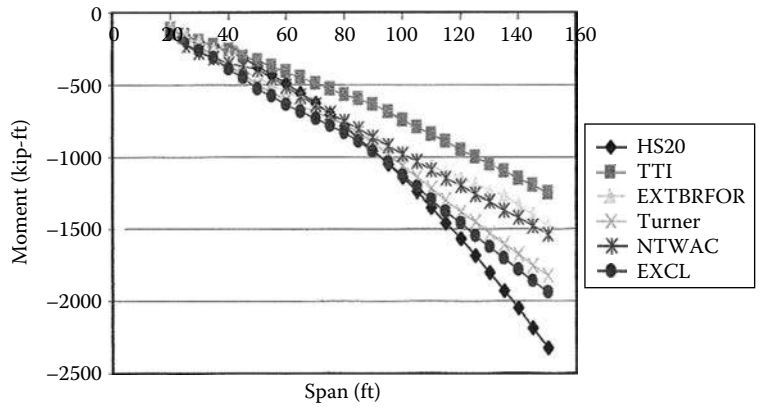

FIGURE 3.27 Negative moments at support. (From Kulicki, J.M. and Mertz, D.R., Evolution of vehicular live load models during the interstate design era and beyond, in *50 Years of Interstate Structures: Past, Present, and Future*, Transportation research Circular, E-C104, Transportation Research Board, National Research Council, Washington, DC, 2006.)

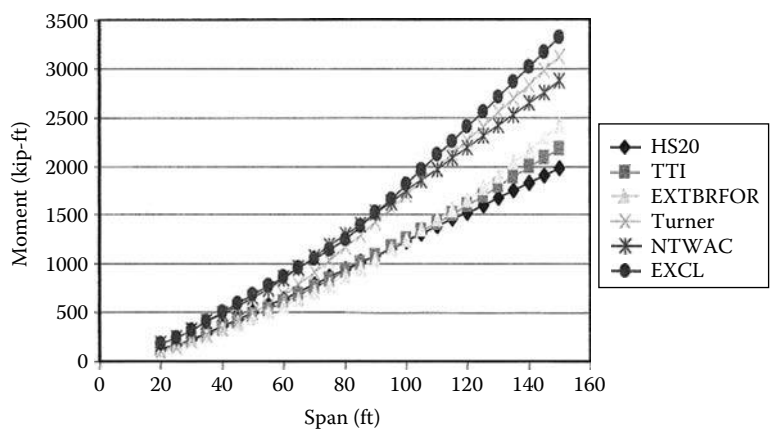

FIGURE 3.28 Positive moments at 0.4*L*. (From Kulicki, J.M. and Mertz, D.R., Evolution of vehicular live load models during the interstate design era and beyond, in *50 Years of Interstate Structures: Past, Present, and Future*, Transportation research Circular, E-C104, Transportation Research Board, National Research Council, Washington, DC, 2006.)

were found not to govern these conditions and have not been plotted in these figures. These figures indicated predominance of load effects due to the *exclusion vehicles. For this reason, these loads were selected as the basis of the development of new national notional design load*. An exception to this conclusion is seen in Figure 3.26 that indicates that HS20 truck load dominates the load effects (negative moments at support of two-span continuous girders); this load effect was considered in the final selection of the notional design load. For Figures 3.25 through 3.31 and 3.36 through 3.41 (later in the chapter), the following legend applies:

M POS 0.4L = positive moment at 0.4*L* in either span.
M NEG 0.4L = negative moment at 0.4*L* in either span.
M Support = moment at the interior support.
V_{ab} = shear adjacent to either exterior support.
Vab = shear adjacent to interior support.
M_{ss} = midspan moment in a simply supported beam.

www.EngineeringEBooksPdf.com

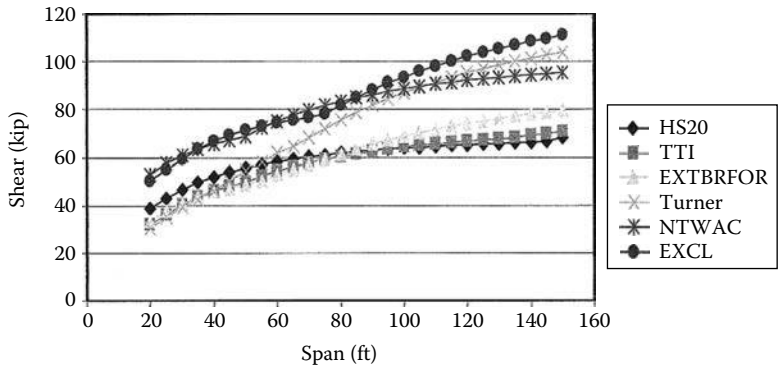

FIGURE 3.29 Positive moments at $+V_{ab}$. (From Kulicki, J.M. and Mertz, D.R., Evolution of vehicular live load models during the interstate design era and beyond, in *50 Years of Interstate Structures: Past, Present, and Future*, Transportation research Circular, E-C104, Transportation Research Board, National Research Council, Washington, DC, 2006.)

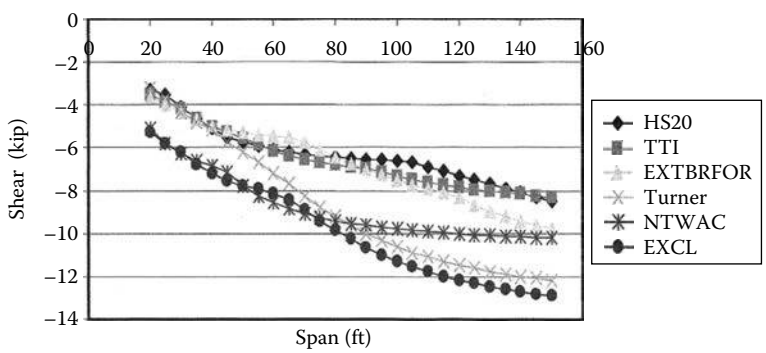

FIGURE 3.30 Negative shear at $-V_{ab}$. (From Kulicki, J.M. and Mertz, D.R., Evolution of vehicular live load models during the interstate design era and beyond, in *50 Years of Interstate Structures: Past, Present, and Future*, Transportation research Circular, E-C104, Transportation Research Board, National Research Council, Washington, DC, 2006.)

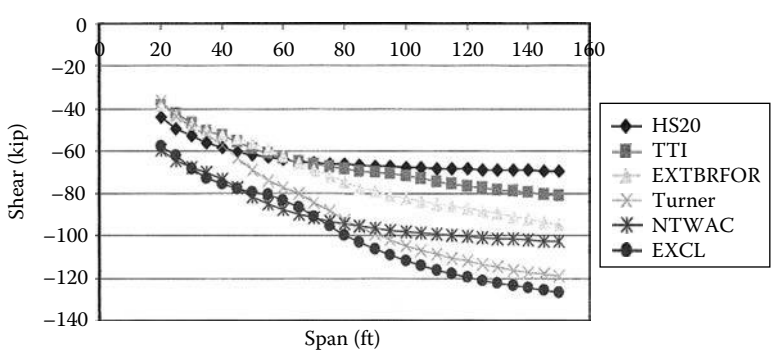

FIGURE 3.31 Negative shear at $-V_{ba}$. (From Kulicki, J.M. and Mertz, D.R., Evolution of vehicular live load models during the interstate design era and beyond, in *50 Years of Interstate Structures: Past, Present, and Future*, Transportation research Circular, E-C104, Transportation Research Board, National Research Council, Washington, DC, 2006.)

www.EngineeringEBooksPdf.com

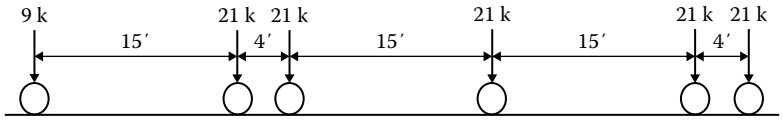

FIGURE 3.32 The HTL-57 (114 kip). (From Kulicki, J.M. and Mertz, D.R., Evolution of vehicular live load models during the interstate design era and beyond, in *50 Years of Interstate Structures: Past, Present, and Future*, Transportation research Circular, E-C104, Transportation Research Board, National Research Council, Washington, DC, 2006.)

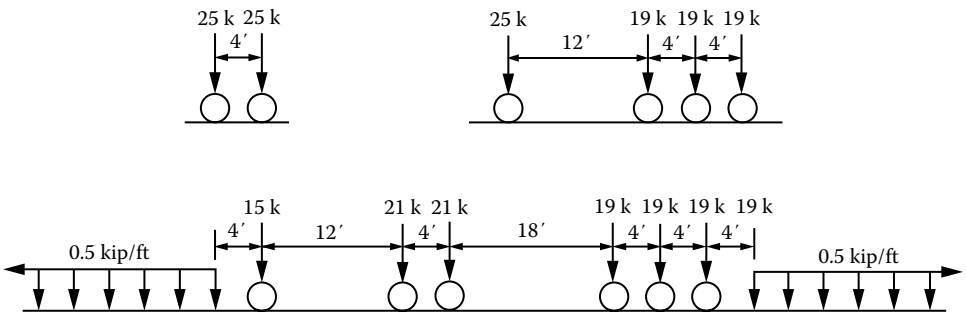

FIGURE 3.33 Family of three loads. (From Kulicki, J.M. and Mertz, D.R., Evolution of vehicular live load models during the interstate design era and beyond, in *50 Years of Interstate Structures: Past, Present, and Future*, Transportation research Circular, E-C104, Transportation Research Board, National Research Council, Washington, DC, 2006.)

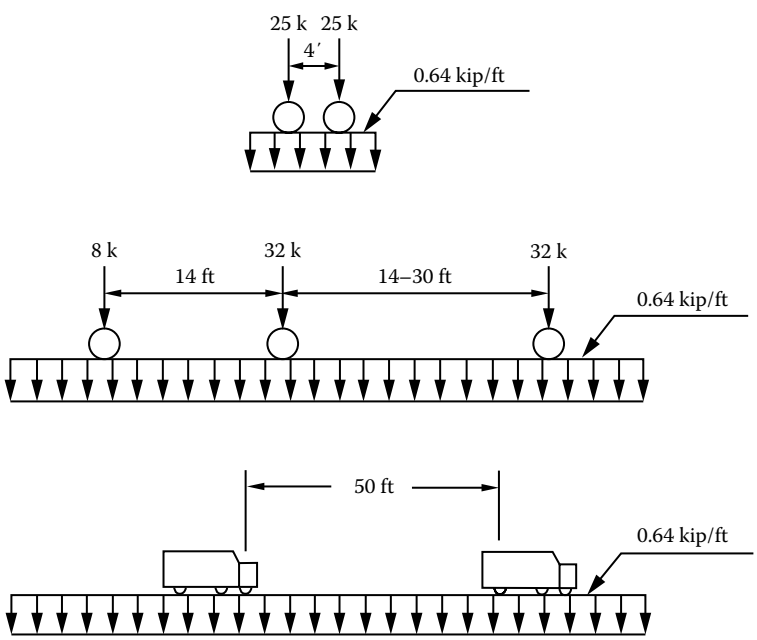

FIGURE 3.34 HL-93 design live load. (From Kulicki, J.M. and Mertz, D.R., Evolution of vehicular live load models during the interstate design era and beyond, in *50 Years of Interstate Structures: Past, Present, and Future*, Transportation research Circular, E-C104, Transportation Research Board, National Research Council, Washington, DC, 2006.)

www.EngineeringEBooksPdf.com

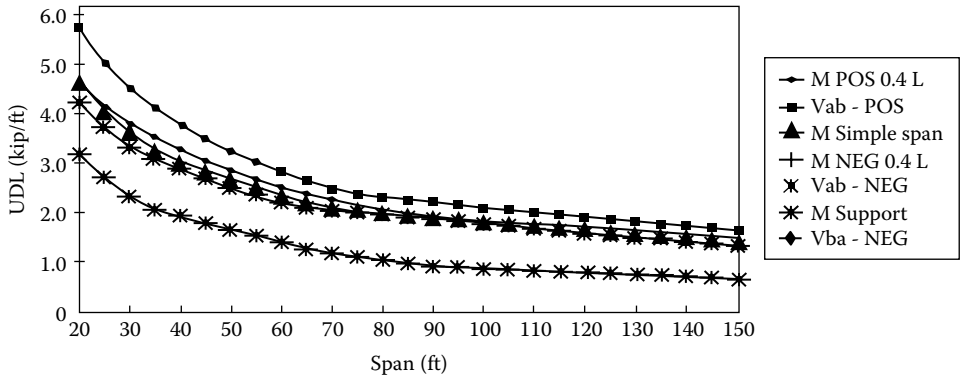

FIGURE 3.35 Equivalent uniform load. (From Kulicki, J.M. and Mertz, D.R., Evolution of vehicular live load models during the interstate design era and beyond, in *50 Years of Interstate Structures: Past, Present, and Future*, Transportation research Circular, E-C104, Transportation Research Board, National Research Council, Washington, DC, 2006.)

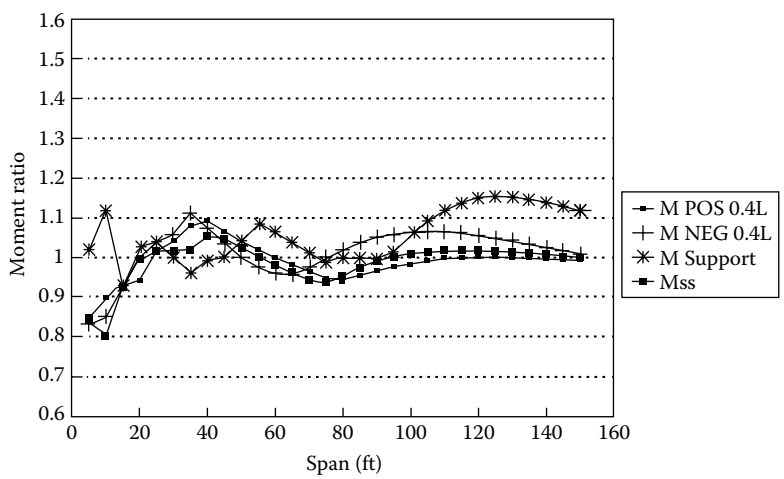

FIGURE 3.36 Comparison of the load effects of the exclusion vehicles to the load effects of the AASHTO LRFD combination load model, *moment ratios* (AASHTO LRFD 2010 Figure C3.6.1.2.1-3). (From *AASHTO LRFD Bridge Design Specifications*, Copyright © 2012 by American Association of State Highway and Transportation Officials, Washington, DC. Used by permission.)

Based on the aforementioned study, the LRFD development group identified five notional live load models in the search of a new notional love load model as follows (Kulicki and Mertz 2006):

1. A single vehicle similar to the design vehicle specified in the 1983 and 1991 editions of the *OHBDC* (1983, 1991). As shown in Figure 3.32, this vehicle, called the HTL57, is a six-axle single unit with fixed wheel base and fixed axle spacing and a total weight of 114 kip.
2. A family of three loads (Figure 3.33): (a) a tandem, (b) a four-axle single unit, with a tridem rear combination, and a 3-S-2 axle configuration *and* a uniform load of 0.5 kip/ft preceding and following the axle grouping.
3. A design family (Figure 3.34) called HL-93 consisting of combinations of a design tandem similar to that shown in Figure 3.32: (a) a design tandem and a uniform load of 0.64 kip/ft of lane (Figure 3.11b), (b) the HS20 design truck and a uniform load of 0.64 kip/ft of lane (Figure 3.11a), and (c) an extension of the loading (b) to include 90 percent of the two

www.EngineeringEBooksPdf.com

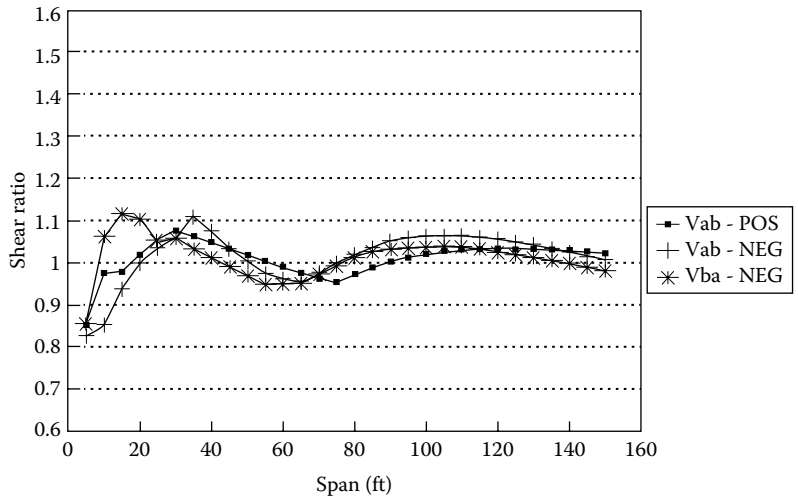

FIGURE 3.37 Comparison of the load effects of the exclusion vehicles to the load effects of the AASHTO LRFD combination load model, *shear* ratios (AASHTO LRFD 2010 Figure C3.6.1.2.1-4). (From *AASHTO LRFD Bridge Design Specifications*, Copyright © 2012 by American Association of State Highway and Transportation Officials, Washington, DC. Used by permission.)

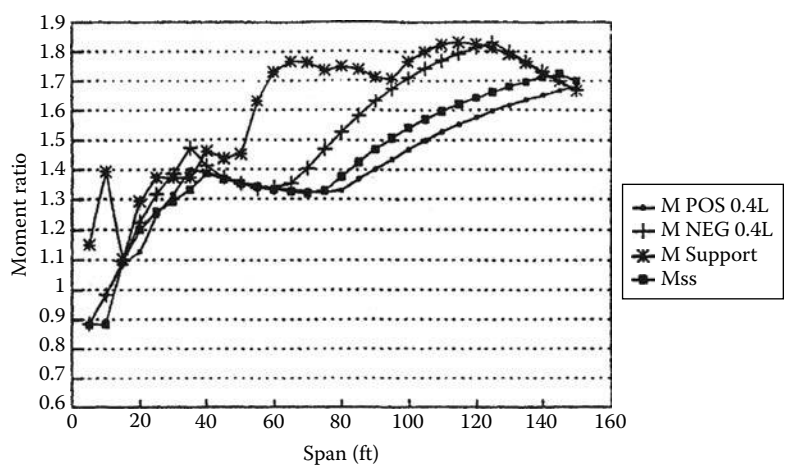

FIGURE 3.38 Comparison of the load effects produced by the exclusion vehicles to the traditional HS20 load effects, *moment ratios* (AASHTO LRFD 2010 Figure C3.6.1.2.1-1). (From *AASHTO LRFD Bridge Design Specifications*, Copyright © 2012 by American Association of State Highway and Transportation Officials, Washington, DC. Used by permission.)

HS20 trucks and 90 percent of the uniform load to investigate for negative moments near the supports and interior reactions of continuous spans greater than 50 ft (Figure 3.12).

4. An equivalent uniform load in kip/ft of lane required to produce the same force effect as the envelope of the exclusion vehicles for various span lengths (Figure 3.35).
5. An HS25 truck load, preceded and followed by a uniform load of 0.48 kip/ft of lane, with the uniform load interrupted for the HS25 vehicle. (The HS25 vehicle [GW = 90 kip] is 125 percent of HS20 vehicle [GW = 72 kip], axle loads being 25 percent heavier than those of the HS20 vehicle.)

www.EngineeringEBooksPdf.com

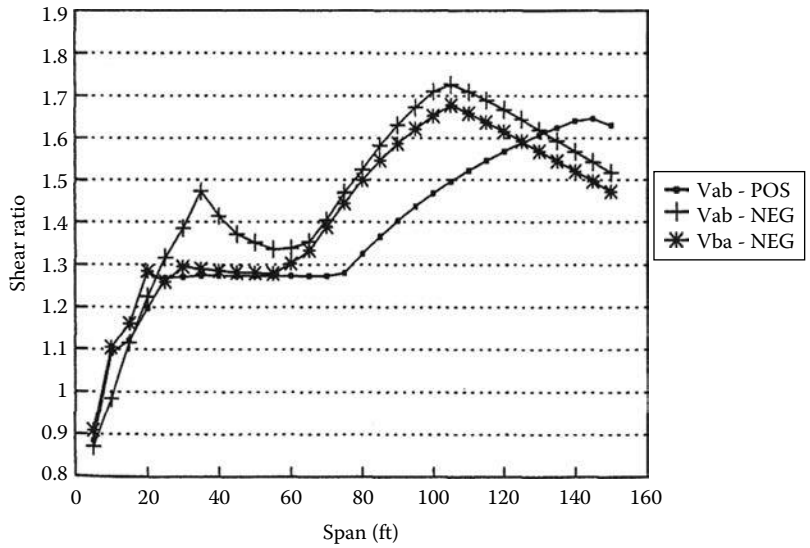

FIGURE 3.39 Comparison of the load effects produced by the exclusion vehicles to the traditional HS20 load effects, *shear* ratios (AASHTO LRFD 2010 Figure C3.6.1.2.1-2). (From *AASHTO LRFD Bridge Design Specifications*, Copyright © 2012 by American Association of State Highway and Transportation Officials, Washington, DC. Used by permission.)

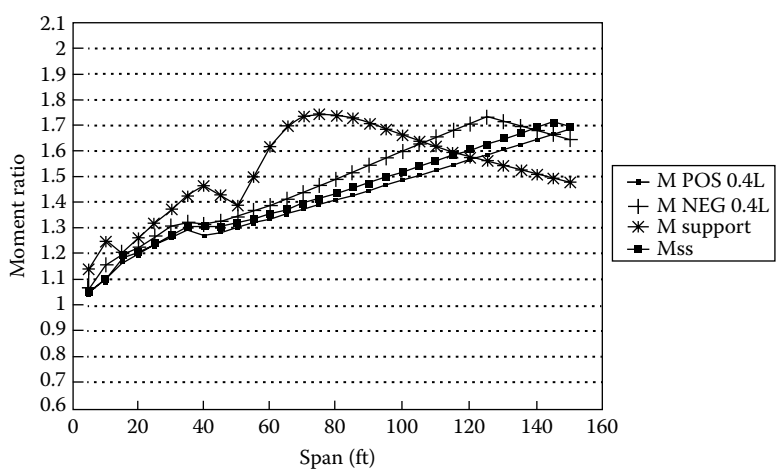

FIGURE 3.40 Comparison of the load effects produced by the notional model to HS20 (truck or lane) or two 24.0 kip axles at 4.0 ft, *moment ratios* (AASHTO LRFD 2010 Figure C3.6.1.2.1-5). (From *AASHTO LRFD Bridge Design Specifications*, Copyright © 2012 by American Association of State Highway and Transportation Officials, Washington, DC. Used by permission.)

An influence line analysis of the aforementioned loads indicated that model 3 seemed to produce the best fit to the load effects due to the exclusion vehicles as indicated by Figures 3.36 and 3.37. Figure 3.36 is a plot of the ratios of the load effects (moments) due to the exclusion vehicles to those due to the HL-93 live load model (no. 3 given earlier). Likewise, Figure 3.37 is a plot of the ratios of the load effects (shears) due to the exclusion vehicles to those due to the HL-93 live load model (no. 3). In both these plots, it is seen that data are tightly clustered and very parallel and form bands of data that are essentially horizontal. For this reason, the live load model 3 was chosen as the final LRFD notional live load model (shown earlier as Figures 3.11 and 3.12). A discussion on

www.EngineeringEBooksPdf.com

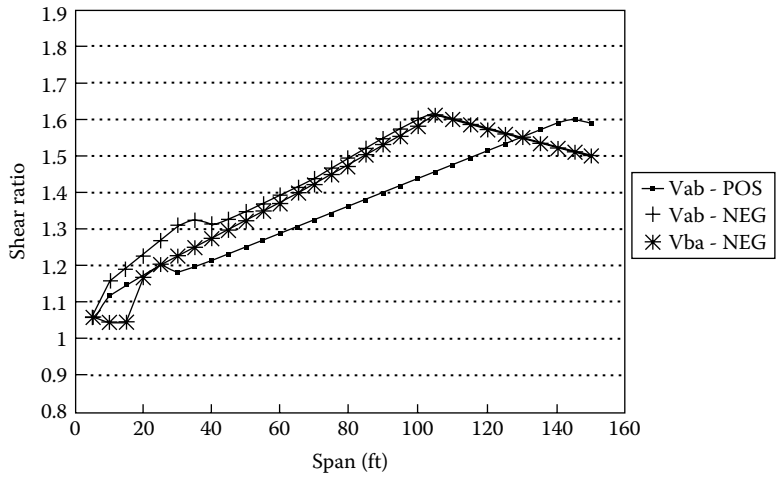

FIGURE 3.41 Comparison of the load effects produced by the notional model to HS20 (truck or lane) or two 24.0 kip axles at 4.0 ft, *shear* ratios (AASHTO LRFD 2010 Figure C3.6.1.2.1-6). (From *AASHTO LRFD Bridge Design Specifications*, Copyright © 2012 by American Association of State Highway and Transportation Officials, Washington, DC. Used by permission.)

the development of AASHTO LRFD live models can be found in the literature (Kulicki and Mertz 1991, 2006, Nowak and Hong 1991, Nowak 1993b).

It was stated earlier that the AASHTO Standard (or the traditional) live model had become outdated because it was no longer representative of the actual highway traffic live load effects. This disparity is shown in Figures 3.38 and 3.39, which show, respectively, the moment ratios and shear ratios of the load effects due to the 22 exclusion vehicles and the AASHTO Standard live load model. These figures show that most ratios are greater than 1, which indicates that the load effects (shear and moment) caused by the exclusion vehicles are *greater* than those caused by the AASHTO Standard live load model (traditional HS20 loading), which indicates an unconservative situation. This was the main justification for the change to the new, probability-based LRFD live load model. And, finally, Figures 3.40 and 3.41 show, respectively, the plots of the ratios of moments and shears due to the LRFD notional live load model to those due to the AASHTO Standard live load model. Again, these figures indicate that most ratios are greater than 1, which indicates that the load effects (shear and moment) caused by the LRFD notional live load model are *greater* than those caused by the AASHTO Standard live load model (traditional HS20 loading), which indicates obsolescence of the later model.

While the notional live load model selected as discussed earlier satisfied LRFD Specification requirement, it still needed to be shown to have a reasonable/acceptable fit to a statistically projected live load because the LRFD Specification is both a reliability-based specification and a structural code. The process of developing the statistically projected load and the determination of load and resistance based in part on both the notional live load and statistically projected live load is described in Nowak (1993b, 1995, 1999) and Nowak and Hong (1991). A discussion on calibration of the AASHTO LRFD code has been provided by Nowak (1993a,b, 1995, 1999). A discussion pertinent to reliability of the LRFD bridge code can be found in Nowak and Collins (2013) and a brief summary in Chapter 1.

3.7.4.4 Permit Loads

Permit loads are heavier and wider than the HS20 truck. These modifications are permitted by state departments of transportation to accommodate the needs of commercial, industrial, and logging areas. Permit loads induce load effects on bridges, which are greater than those induced by the notional live load model. Therefore, owners of these heavier-load-carrying vehicles are required to obtain special permits to operate on highways. Examples of a permit loads from a few states are shown in Figures 3.42 through 3.45. Nutt et al. (1988) provide configurations of operating vehicles for several US states.

www.EngineeringEBooksPdf.com

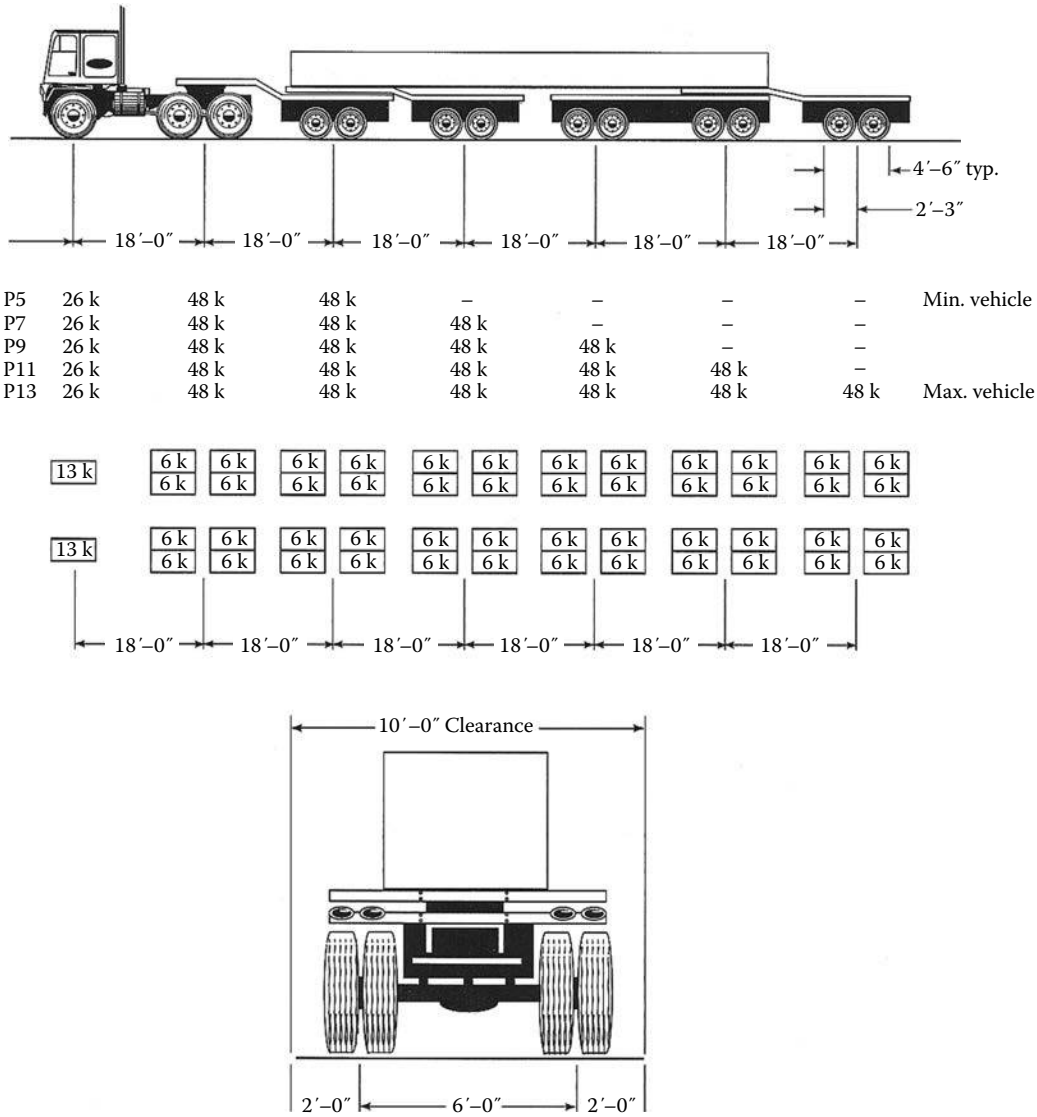

FIGURE 3.42 Permit live load for the state of California. Load occupies standard 10 ft wide lanes. The transverse wheel configuration is the same as HS20 truck. (From CALTRANS, *Bridge Design Practice Manual*, California Department of Transportation, Sacramento, CA, 1992.)

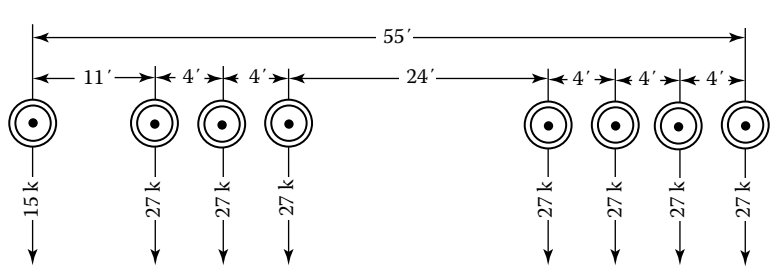

FIGURE 3.43 The 204 kip eight-axle Pennsylvania permit load (P-820). *Note*: Load occupies standard 10 ft wide lane. Transverse wheel location is the same as in HS vehicle. (From PennDOT, *Design Manual Part 4*, Pennsylvania Department of Transportation, Harrisburg, PA, 1993.)

www.EngineeringEBooksPdf.com

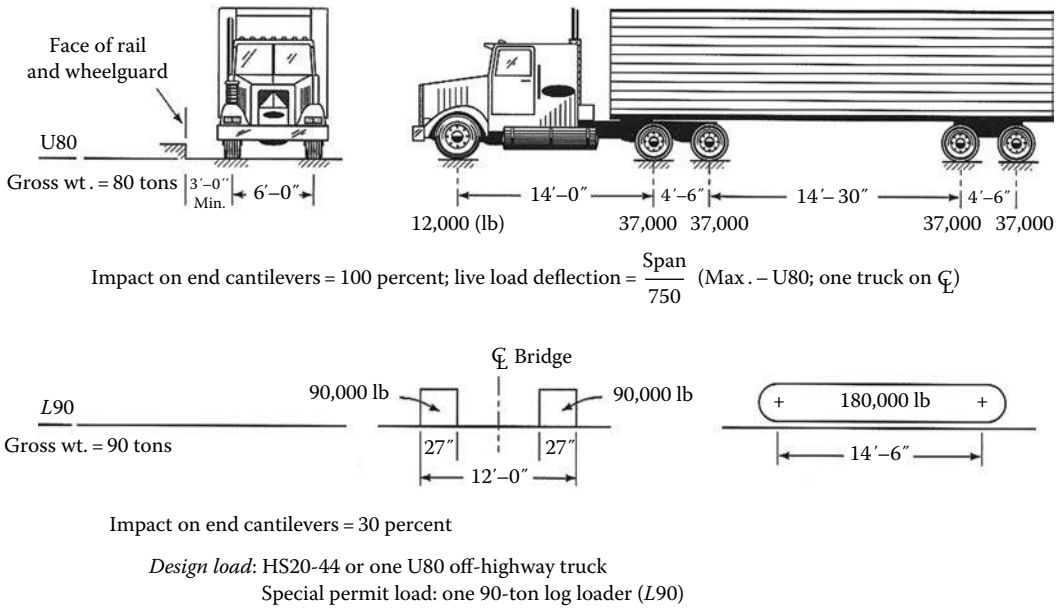

FIGURE 3.44 State of Alaska permit loads. (From USS, Nine steel bridges for forest development roads, South Tongass National Forest, Alaska, Bridge Structural Report, ADUSS 88-5973-02, U.S. Steel, Pittsburg, PA, 1975.)

3.7.5 Application of Design Vehicular Live Loads on Bridge Superstructures

3.7.5.1 Position of Live Load on Simple Spans

Reference is made to Figures 3.11 and 3.12 that show, respectively, HL-93 design live loads for simple and continuous spans. Figure 3.11a shows a simple span with HS20 truck (the axle load placement with variable spacing of 14–30 ft between the rear axles), concurrently loaded with a uniform load of 0.64 kip/ft over the entire span. Figure 3.11b shows a simple span loaded with tandem concurrently loaded with a uniform load of 0.64 kip/ft over the entire span. The larger force effects produced by loads shown in either Figure 3.11a or b should be used for designing the superstructure.

Because the AASHTO LRFD vehicular live load model calls for a *combination* of design HS20 truck *and* the design lane load, or tandem *and* the design lane load, it is important to recognize that the positions of both the truck and the tandem (being concentrated loads) on a given span are different for causing the maximum shear and moment. For simple spans, it means the following:

1. The entire span is loaded with the design lane load (uniform load of 0.64 kip/ft of lane) so as to produce both maximum shear and moment in the span. The lane load is assumed to be continuous over the entire span length, end to end; it is *not* interrupted to produce space for the axle sequences of the design truck or the design tandem.
2. The truck or the tandem (both are treated as concentrated loads) is so positioned on the span that they produce the maximum force effects, noting that their positions on the span would be different for maximum shear and maximum moment.
3. The governing force effects, induced either by the truck or the tandem, are to be *superimposed with those of the lane load effects* in order to obtain extreme load effects on the bridge structure. Which of the two concentrated load models—the design truck (Figure 3.11a) or the design tandem (Figure 3.11b)—would cause maximum shear or moment in the span depends on the span length. As illustrated in Example 3.9, the moments due to the design truck or the tandem are the same for a span length of 40.27 ft. The design truck governs for the maximum moment for spans longer than 40.27 ft; for shorter spans, the design tandem results in the larger moment.

www.EngineeringEBooksPdf.com

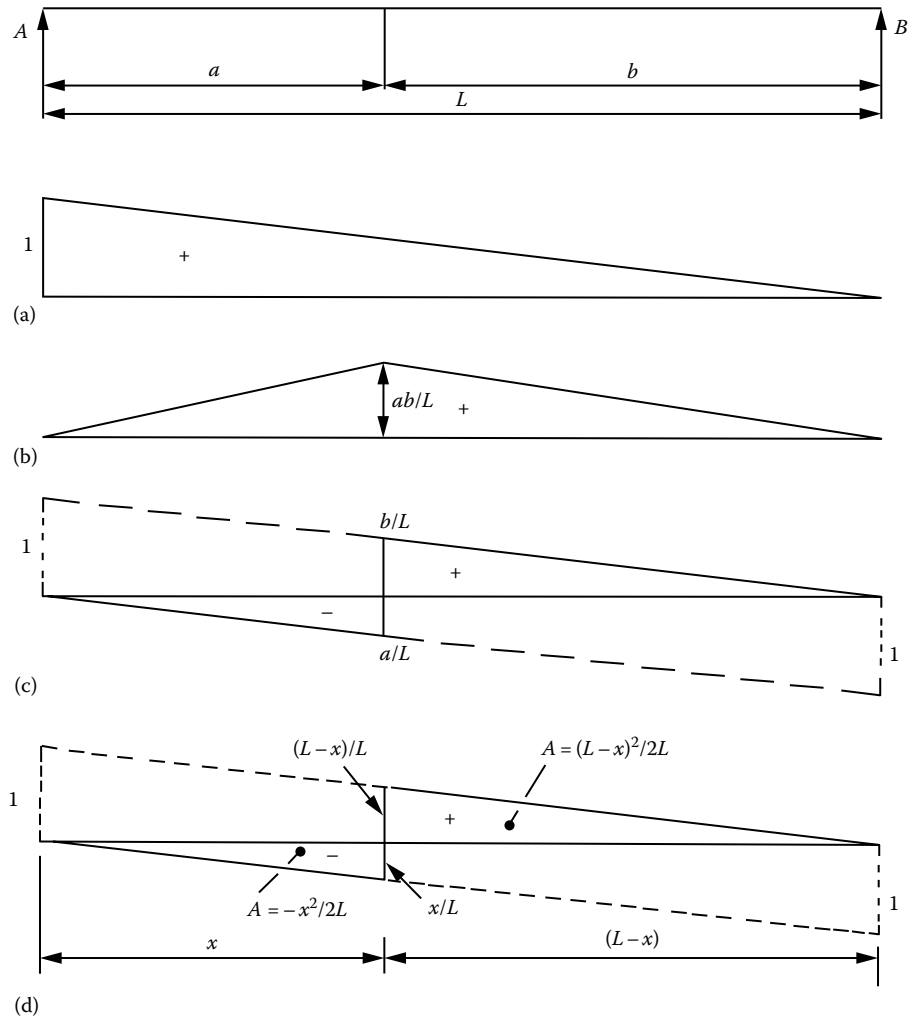

FIGURE 3.45 Typical influence line diagrams for (a) reaction at A, (b) bending moment at a section at a distance a from the left support, (c) shear at a section located at a distance a from the left support, and (d) positive and negative areas under the influence line diagram for shear at a distance x from the left support.

For design purposes, the live load effects (moment and shear) are to be augmented to account for the dynamic effects of the moving loads, referred to as *DLA* (discussed in Section 3.9), and is applied as follows:

1. The DLA is applied to *only* the force effects due to the truck or the tandem; *it is not applied to the force effects due to the lane load*. Thus, the total live load (*LL*) effects (shear and moment) including the dynamic load effects can be determined from Equation 3.7:

$$LL_{total} = (LL_{truck\ or\ tandem})(1 + IM) + (LL_{lane}) \tag{3.7}$$

   where IM = DLA (expressed as a fraction or percentage).
2. For fatigue limit state, only the HS20 truck load is to be used on the span; the lane load need not be considered (see Section 3.9). DLA is applicable to the fatigue loading.

www.EngineeringEBooksPdf.com

3.7.5.2 Position of Vehicular Live Loads on Continuous Spans

On simple spans, design live loads (either truck *or* tandem, accompanied by the lane load) can be placed, often intuitively in most cases, to produce the extreme load effects. Such, however, is not the case for the structurally continuous spans because they are subjected to negative moments over the supports and have points of contraflexure within in the span. For such cases, AASHTO LRFD Art. 3.6.1.3.1 stipulates a third live load model so as to produce extreme live load force load effects as shown in Figure 3.12:

> For negative moment between points of contraflexure under a uniform load on all spans, and reaction at the interior piers only, 90 percent of the effect of two design trucks spaced a minimum of 50 ft between the lead axle of one truck and rear axle of the other truck, combined with 90 percent of the lane load. The distance between the 32-kip axles shall be 14 ft.

Lastly, it should be recognized that in some situations, the actual loading on the bridge might be more critical than that produced by the notional HL-93 live loading. In such cases, consideration should be given to site-specific modification to the design truck, design tandem, and/or the design lane load when the following conditions warrant (AASHTO 2012 Com. C3.6.1.2.1):

1. The legal load of a given jurisdiction is significantly greater than typical.
2. The roadway is expected to carry exceptionally high percentages of truck traffic.
3. Traffic flow control, such as a stop sign, traffic signal, or tollbooth, causes trucks to collect on certain areas of a bridge or not to be interrupted by rail traffic.
4. Special industrial loads are common due to the location of the bridge.

3.7.6 Bending Moments and Shears due to Moving Loads on Simple Spans

3.7.6.1 Bending Moments

In design of bridge superstructures, it is necessary to have the following information:

1. Magnitudes and locations of maximum moment and shear in a span.
2. Moments and shears at certain specified locations along the span. The values of these forces are required for determining several design parameters such as follows:
   a. Cutoff points and development lengths for reinforcement in reinforced and prestressed concrete girders
   b. Shear reinforcement in reinforced and prestressed concrete girders
   c. Cutoff points of cover plates for steel built-up beams and plate girders
   d. Spacing of shear connectors in steel–concrete composite beams

Determination of force effects due to live load (i.e., shears, moments, and deflections) in longitudinal girders supporting the deck is a complex analytical problem because the live load is transferred to these girders through the medium of the deck slab. However, this problem, commonly referred to as *live load distribution* in bridge superstructures, is simplified considerably by following the approximate method specified in Section 4 of the AASHTO LRFD Specifications (see Chapter 4). In general, this method can be summarized as a two-step procedure:

Step 1: It is assumed that the loads act directly on one of the girders (even though, in reality, they act on the bridge deck supported over several girders). The load effects (moments and shears) in the girder are determined by idealizing (1) the uniform load as a line load over the entire span and (2) the truck axle loads as point loads positioned so as to cause extreme force effects in the girder. Determination of these load effects is discussed in this chapter.

Step 2: The force effects in individual longitudinal girders supporting the deck are determined by multiplying the force effects determined in step 1 with dimensionless numbers called *distribution*

www.EngineeringEBooksPdf.com

factors (*DF*s), which are discussed in Chapter 4. The latter depend on such parameters as the type and geometry of the superstructure, position of the member under the deck (e.g., the interior or the exterior girder), and the number of design lanes. These load effects would be the forces to be used for design purposes.

Moments and shears in bridge beams and girders involve force effects caused by the dead loads and the moving loads (both uniform and concentrated, acting together). Determination of dead load effects along with examples was presented in Section 3.5.2. For moving loads, the *influence lines* offer a convenient method for determining the force effects. This is a topic discussed in texts on structural analysis and not discussed here in detail. However, because of the importance of the topic for bridge design, a few general comments are made in this section.

3.7.6.2 Influence Lines for Absolute Maximum Bending Moments in Simple Spans

Influence lines can be drawn easily using the *Muller-Breslau principle* (discussed in texts on structural analysis). Determination of influence lines for simple and cantilevered spans is simple but that for continuous beams is analytically tedious and is best suited for computers. Influence lines for shears and moments for continuous beams can be determined also from the tables of influence line coefficients published by the American Institute of Steel Construction (AISC 1989).

Generally speaking, when a span is subjected to a series of moving, concentrated loads, a designer needs to have the following information for design purposes:

1. Position of the moving loads on the span that would cause absolute maximum moment and shear in the span, and their magnitudes and locations in the span at which they occur.
2. Position of moving loads on the span that would cause maximum shear and moment at a given point. Typically, for designing a longitudinal beam, these quantities are required to be determined for every one-tenth of span (i.e., at every tenth point on the span or at every $0.1L$ point, typically, for $x/L = 0.1$, 0.2, 0.3, 0.4, and 0.5).

Determination of maximum moments and shears due to uniform load on a span is a trivial exercise; they will be caused when the entire span is loaded. These forces can be determined either analytically or from influence lines. However, influence lines offer a more convenient way for determining moments and shears in a beam when analyzing a series of moving concentrated loads (idealized wheel loads) on a span or when a span is partially loaded with a uniform load. A brief overview of influence lines follows:

1. The influence lines are drawn to determine the force effects of loads (support reactions, moments, shears, and deflections) *at a specific location of a beam for any position of the moving loads on the beam*.
2. An influence line is drawn for a *unit load* as it *moves* across the span from the left support to the right support (this is the convention). *Therefore, it is independent of the type of actual load on the beam such as one or more concentrated loads, distributed loads, or a combination of both*. By contrast, the moment and shear diagrams give the values of moment and shears, respectively, for all locations in a beam, produced by the *fixed* positions of given loads.

Typical influence line diagrams for moment and shear are shown in Figure 3.45. These have the following general characteristics:

1. Influence line for reactions
   a. The influence line for reaction at the *left support* consists of a sloping line having an ordinate of +1 at the left support and zero at the right support (Figure 3.45a). The influence line for reaction at the *right support* consists of a sloping line having an ordinate of +1 at the right support and zero at the left support.

www.EngineeringEBooksPdf.com

b. The magnitude of support reaction R due *concentrated load* on a span is given by the sum of the products of the loads and the influence line ordinates under the respective loads:

$$R = \Sigma P_i y_i \tag{3.8a}$$

where
P_i = ith load on the span, $i = 1, 2, 3, \ldots, n$
y_i = influence line ordinate under the ith load $y_1, y_2, y_3, \ldots, y_n$

If a number of moving concentrated loads $P_1, P_2, P_3, \ldots, P_n$ are present on a span, which have the influence line ordinates for reaction, respectively, as $y_1, y_2, y_3, \ldots, y_n$, then from Equation 3.8b,

$$R = P_1 y_1 + P_2 y_2 + P_3 y_3 + \cdots P_n y_n \tag{3.8b}$$

c. The magnitude of the support reaction R due to a *uniform load* on a span is given by the product of the load intensity and the area under the influence line diagram:

$$R = w \text{ (area under the influence line diagram)} \tag{3.9}$$

where w is the intensity of uniformly distributed load on the span.

2. Influence lines for bending moment
   a. The influence line for moment at a section in a simple span, irrespective of the type of loading (concentrated or distributed), always consists of two straight lines that form a triangle with apex under the point on the beam for which the influence line is drawn (Figure 3.45b).
   b. The influence line ordinate under the point (i.e., the height of the apex of the triangle) always equals ab/L (Figure 4.45b), where a = distance of the section from the left support and b = distance of the section from the right support (so $a + b = L$).
   c. The moment at the selected section due to a group of moving concentrated loads on the span is given by the sum of the products of the individual concentrated loads and the corresponding influence line ordinates, which can be expressed as follows:

$$M = \Sigma P_i y_i \tag{3.10}$$

If a number of moving concentrated loads $P_1, P_2, P_3, \ldots, P_n$ are present on a span, which have the influence line ordinates for moment, respectively, as $y_1, y_2, y_3, \ldots, y_n$, then from Equation 3.10,

$$M = P_1 y_1 + P_2 y_2 + P_3 y_3 + \cdots P_n y_n \tag{3.11}$$

   d. The moment, M_{xw}, at a selected point due to a uniform load w, is given by the product of the load intensity and the area under the influence line diagram drawn for that location:

$$M_{xw} = w \text{ (area under the influence line diagram)} \tag{3.12}$$

Alternatively, moment, M_x, at any section distant x from the *left* support can be determined analytically from Equation 3.13:

$$M_x = \frac{wx(L - x)}{2} \tag{3.13}$$

www.EngineeringEBooksPdf.com

3. Influence lines for shear at a location on the span
   a. The IL for shear at a location on a span consists of two parallel, sloping lines having ordinates equal to +1 at the left support and −1 at the right support and joined by a vertical line under the point of interest on the span (Figure 3.45c). The ordinates to the right of this line are considered positive, those to the left as negative.
   b. For obtaining the values of maximum positive shear at a section in a span, the moving loads should be positioned over the segment of span for which the influence line ordinates are positive. Similarly, for obtaining the values of maximum negative shear, the moving loads should be positioned over the segment of span for which the influence line ordinates are negative.
   c. Shear at the selected location distant x from the left support due to a series of concentrated loads is given by the *sum of the product of the concentrated loads and the corresponding influence line ordinates under those loads*. To determine positive shear at a section of a beam, all loads should be positioned over the segment of the span for which the influence line ordinates are positive. Likewise, to determine negative shear at a section of a beam, all loads should be positioned over the segment of the span for which the influence line ordinates are negative. In general, shear at a selected location is determined from Equation 3.14:

$$V_x = \Sigma P_i y_i \tag{3.14}$$

   where P_i and y_i were defined earlier. Consider a moving load group comprising several concentrated loads $P_1, P_2, P_3, \ldots, P_n$. To obtain maximum positive shear at the selected section of the beam due to this load group, all loads should be placed on the segment of the span for which the influence line ordinates are positive. If the influence line ordinates under these load are, respectively, as $y_1, y_2, y_3, \ldots, y_n$, then the positive shear at that section is given by Equation 3.15:

$$V_x = +\left(P_1 y_1 + P_2 y_2 + P_3 y_3 + \cdots P_n y_n\right) \tag{3.15}$$

   Likewise, to obtain maximum negative shear at the selected section of the beam due to this load group, all loads should be placed on the segment of the span for which the influence line ordinates are negative. If the influence line ordinates under these load are, respectively, as $y_1, y_2, y_3, \ldots, y_n$, then negative shear at that section is given by Equation 3.16:

$$V_x = -\left(P_1 y_1 + P_2 y_2 + P_3 y_3 + \cdots P_n y_n\right) \tag{3.16}$$

   d. Shear at the selected location distant x from the left support due to a uniform load, w (e.g., lane load), is given by the product of the intensity of the uniform load and the area under the influence line diagram (Equation 3.17). *For maximum positive shear, the distributed load should be placed only on that segment of the beam for which the area under the influence line is positive, not on the entire span. Likewise, for negative shear, the uniform load should be placed only on that segment of the span for which the influence line area is negative, not on the entire span* (Figure 3.45c):

$$\pm V_{xw} = w(\pm \text{ area under the influence line diagram}) \tag{3.17}$$

   Alternatively, shear, the positive and the negative shears, V_x, at any section distant x from the *left* support can be determined analytically, respectively, from Equations 3.18 and 3.19:

$$V_x = \frac{w\left(L - x\right)^2}{2L} \tag{3.18}$$

www.EngineeringEBooksPdf.com

$$V_x = -\frac{wx^2}{2L} \tag{3.19}$$

The right-hand side quantities in Equations 3.18 and 3.19 are simply the products of uniform load w and the positive and negative areas under the IL diagrams (Figure 3.45d).

For a preliminary design of a beam section, it is necessary to first determine the maximum moment in the beam. The AASHTO design truck (HS20 truck) consists of a group of three axle (moving) loads, which, for design purposes, are assumed as knife-edge loads. Generally speaking, when a simply supported beam is subjected to a group of unequal moving point loads, the associated absolute maximum moment in the span and the corresponding load positions cannot be determined by inspection because we do not intuitively know under which load the maximum moment would occur. However, the problem can be solved analytically. See Example 3.3.

In the case of shear, it is necessary to determine both positive *and* negative shear at a section (typically at one-tenth span points) in the beam; these values are required for design for fatigue (discussed in Section 3.12); Equation 3.15 through 3.19 should be used for that purpose.

Example 3.3

Determine the absolute maximum bending moment due to a series of concentrated loads on a simple span.

Solution

Consider a simply supported span subjected to moving concentrated loads P_1, P_2, and P_3 placed as shown in Figure 3.46. It is established that moment diagram for a beam subjected to several concentrated loads consists of straight-line segments having peaks under each force, and the maximum moment would occur under one of these forces. It is assumed that the resultant P_R of the load group lies between loads P_2 and P_3 at a distance $\bar{x}$ to the right of P_2 and that the maximum moment occurs under load P_2. Letting the distance between the load P_2 and the center line of the beam be x, the relationship between x and $\bar{x}$ can be determined as follows. Taking moments about the right support B,

$$R_A = \frac{1}{L}\left(P_R\right)\left[\frac{L}{2} - (\bar{x} - x)\right]$$

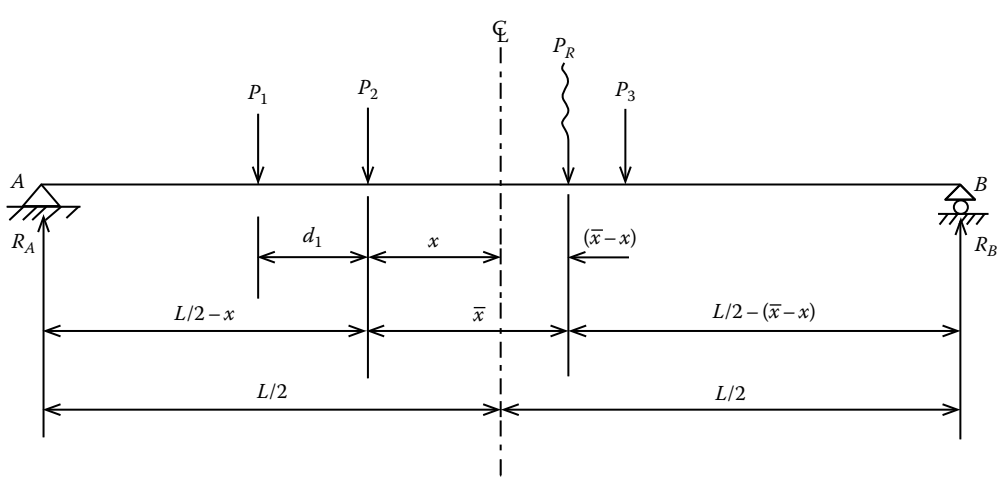

FIGURE 3.46 Determination of absolute maximum bending moment due to several moving concentrated loads on a simple span.

www.EngineeringEBooksPdf.com

The moment under load P_2 can be expressed as (Figure 3.46)

$$M_2 = R_A\left(\frac{L}{2} - x\right) - P_1 d_1$$

$$= \frac{1}{L}(P_R)\left[\frac{L}{2} - (\bar{x} - x)\right]\left(\frac{L}{2} - x\right) - P_1 d_1$$

$$= \frac{P_R L}{4} - \frac{P_R \bar{x}}{2} - \frac{P_R x^2}{L} + \frac{P_R x \bar{x}}{L} - P_1 d_1$$

For maximum value of M_2, we must have $dM_2/dx = 0$. Thus,

$$\frac{dM_2}{dx} = -\frac{2P_R x}{L} + \frac{P_R \bar{x}}{L} = 0$$

$$\text{where } x = \bar{x}/2$$

Thus, it is concluded that the absolute maximum moment in a span due to a group of moving concentrated loads occurs under one of those loads when the loads are so placed that this load and the resultant of the load group are placed equidistant from the centerline of the span (i.e., the centerline of the span bisects the distance $\bar{x}$). However, it is neither intuitive nor apparent as to under which of the two loads (on either side of the resultant of the load group) would the maximum moment occur. It, therefore, becomes necessary to determine the maximum moment that would occur under each of the two loads nearest the resultant of the load group, and the larger of the two values taken as the absolute maximum moment in the span. As a general rule, however, the absolute maximum moment often occurs under the largest load nearest the resultant of the moving load system. See Example 3.4.

Example 3.4: Absolute Maximum Bending Moment in a Span due to a Group of Moving Concentrated Loads

Determine the absolute maximum bending moment in the span due to a group of moving concentrated loads shown in Figure 3.47a.

Solution

Determine the resultant of the load group from statics. Taking moments of all loads about the exterior 4 kip load, we obtain

$$\text{Resultant of all loads} = \Sigma P_i = 4 + 12 + 4 + 8 = 28 \text{ kip}$$

$$\bar{x} = \frac{12(3) + 4(7) + 8(13)}{28} = 6 \text{ ft}$$

Thus, the resultant of the load group lies 6 ft to the right of the exterior 4 kip load (or 3 ft to the right of the 12 kip load and 1 ft to the left of the interior 4-kip load) as shown in Figure 3.47b. Now, consider two cases:

Case 1: Assume that the absolute maximum moment occurs under the 4 kip load that is nearest the resultant of the load group. This case requires the loads to be so placed that the centerline of span bisects the distance between the resultant of the load group and the adjacent 4 kip load (see Figure 3.47b). For this position of the load group, the reaction at support A is determined from statics by taking moments about B:

$$R_A = \frac{1}{40}\left[4(26.5) + 12(23.5) + 4(19.5) + 8(13.5)\right] = 14.35 \text{ kip}$$

www.EngineeringEBooksPdf.com

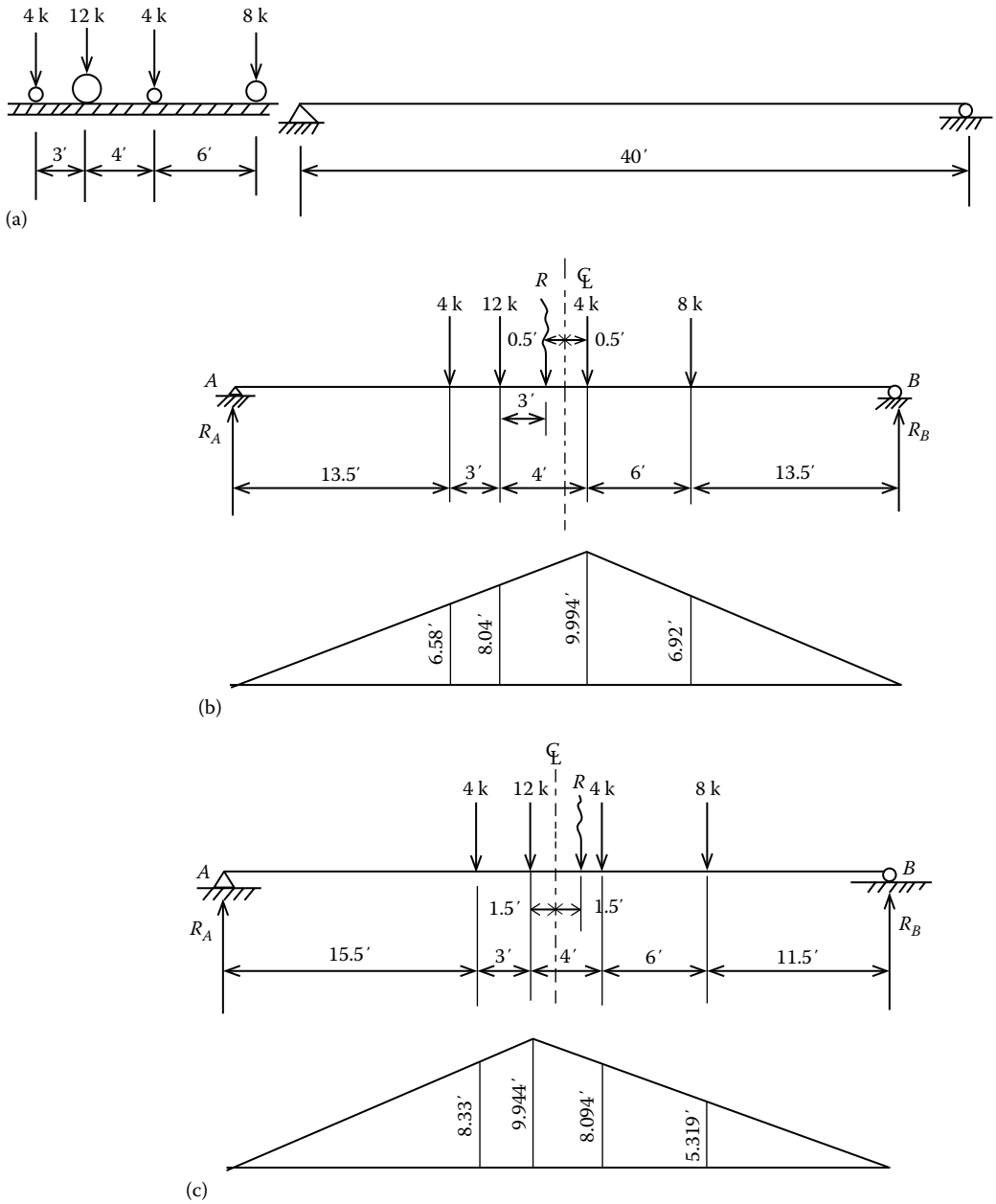

FIGURE 3.47 (a) Group of moving loads for Example 3.4. (b) Influence line for maximum bending moment under the interior 4 kip load. (c) Influence line for maximum bending moment under the 12 kip load.

The moment under the 4 kip load (nearest the centroid) is calculated to be

$$M = 14.35(20.5) - 4(7.0) - 12(4) = 218.2 \text{ kip-ft}$$

Alternatively, the moment under the same 4 kip load can be determined also from the *influence lines* (Figure 3.47b) as being equal to the sum of the products of the individual loads and the respective influence line ordinates:

$$M_{max} = 4(6.58) + 12(8.04) + 4(9.994) + 8(6.92) = 218.2 \text{ kip-ft}$$

www.EngineeringEBooksPdf.com

Case 2: Assume that the absolute maximum moment occurs under the 12 kip load, the larger load that is nearest the resultant of the load group. For this case, the loads are so placed that the centerline of span bisects the distance between the resultant of the loads and the 12 kip load (Figure 3.47c). For this position of the load group, the reaction at support *A* is determined by taking moments about *B*:

$$R_A = \frac{1}{40}\left[4(24.5) + 12(21.5) + 4(17.5) + 8(11.5)\right] = 12.95 \text{ kip}$$

The bending moment under the 12 kip load (nearest the centroid) is calculated as

$$M = 12.95(18.5) - 4(3.0) = 227.6 \text{ kip-ft} > 218.2 \text{ kip-ft}.$$

Alternatively, the bending moment under the 12 kip load can be determined also from the influence lines (Figure 3.47c) as being equal to the sum of the products of individual loads and respective influence line ordinates:

$$M_{max} = 4(8.33) + 12(9.944) + 4(8.094) + 8(5.319) = 227.6 \text{ kip-ft}$$

Thus, the absolute maximum bending moment in the span is 227.6 kip-ft; it occurs under the 12 kip load, *which is the larger of the two loads nearest the resultant of the load group.*

In the case of HS20 truck, the axle configuration is such that the absolute maximum bending moment in a simple span always occurs under the interior 32 kip axle load when this load and the resultant of the load group are placed equidistant from the centerline of the span (Figure 3.48). In this book, this method is referred to as the *exact* method in the following discussion (see Examples 3.5 and 3.6). Interestingly, for HS20 truck, the absolute maximum bending moment in a simple span can also be determined, without appreciable error, by placing the intermediate 32 kip axle at the midspan (see Example 3.7). Similarly, the absolute maximum bending moment due to AASHTO design tandem can be obtained by placing one of the 25 kip axles at the midspan (see Example 3.8). These latter methods, which are simpler, may be used for determining the values of the absolute maximum bending moments in simple spans caused by AASHTO truck or tandem loads. The difference between the moment values obtained by the two methods is inconsequential and can be ignored for all practical purposes.

Simpler expressions for determining shear and bending moment due to HS20 truck are derived in the latter examples. However, it is noted that these approximate methods are to be used specifically

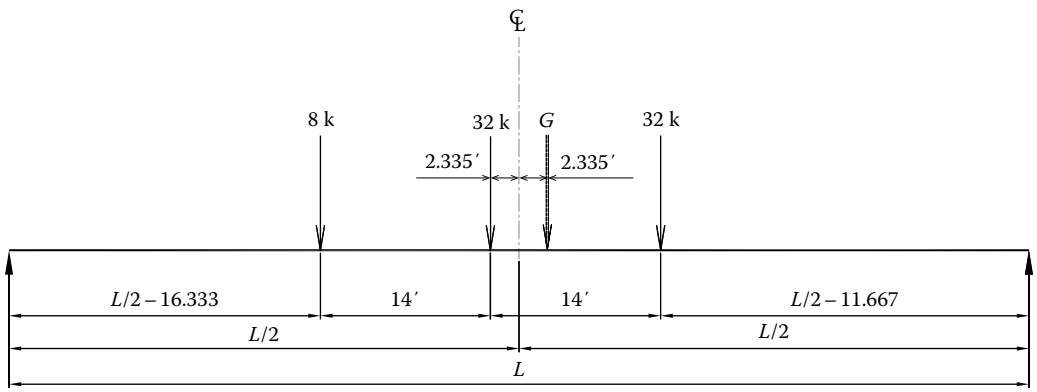

FIGURE 3.48 Position of AASHTO HS20 truck for absolute maximum bending moment in a simple span. *G* is the resultant of the load group, which is located at 4.67 ft right of the middle 32 kip axle load. The center line of the span bisects the distance between the 32 kip axle load and *G*. Maximum moment occurs under the middle 32-axle load.

www.EngineeringEBooksPdf.com

for the AASHTO HS20 truck or tandem load configuration; they are not applicable for load groups having different load configurations.

Influence lines can also be used for determining maximum bending moment and shear anywhere in a span produced by the moving loads. For example, it is established that the maximum bending moment in a span due to uniform load occurs when the entire span is loaded; its magnitude equals the product of the load intensity and the area under the influence line diagram (Equation 3.12).

Example 3.5

Derive an expression for the exact value of the absolute maximum bending moment in a simple span due to AASHTO HS20 truck.

Solution

Figure 3.49 shows the position of AASHTO HS20 truck that would cause absolute maximum moment in a simple span. Reaction at B can be obtained by summing up moments about A. Thus,

$$\Sigma M_A = 0$$

$$R_B = \frac{1}{L}\left[8\left(\frac{L}{2} - 2.335 - 14\right) + 32\left(\left(\frac{L}{2} - 2.335\right) + \left(\frac{L}{2} + 14 - 2.335\right)\right)\right]$$

$$= \frac{1}{L}(36L + 167.88) \text{ kip}$$

The absolute maximum moment in span occurs under the middle 32-kip axle and equals

$$M_{max,truck} = R_B\left(\frac{L}{2} + 2.335\right) - 32(14)$$

$$= \frac{1}{L}(36L + 167.88)\left(\frac{L}{2} + 2.335\right) - 448$$

$$= \left(18L - 280 + \frac{392}{L}\right) \text{ kip-ft} \tag{3.20}$$

Equation 3.20 can be used to determine absolute maximum moment in a simple span due to HS20 truck. As noted earlier, *this expression is applicable for the configuration of HS20 truck only and may not be used for a group of moving concentrated loads having different configuration*. This is because Equation 3.20 has been derived based on axle loads of 8, 32, and 32 kip, spaced 14 ft apart.

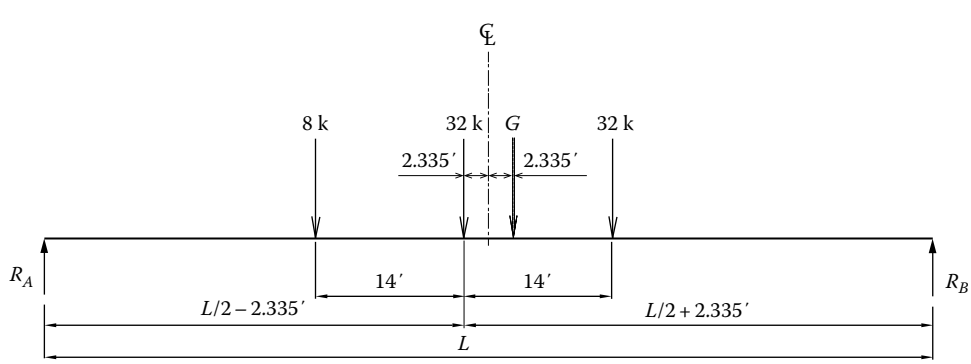

FIGURE 3.49 Position of HS20 truck for absolute maximum bending moment in a simple span.

www.EngineeringEBooksPdf.com

Example 3.6: Influence Lines for the Absolute Maximum Moment in Simple Spans due to AASHTO HL-93 Loading

Determine, from influence lines, the maximum moment due to HL-93 loading HS20 truck (plus the lane load) in a simple span of 84 ft.

Solution

The HL-93 loading consists of two concurrent loadings: AASHTO HS20 truck and a uniform load of 0.64 kip/ft over the entire span. The maximum moments due to these two types of loadings are calculated separately from the influence lines.

a. Absolute Maximum Bending Moment in Span due to the HS20 Truck
For the HS20 design truck, the resultant of the three-load group (8, 32, and 32 kip) is determined to lie at 4.67 ft to the right of the intermediate 32 kip axle (reader to verify the position of the resultant). For this load group, the absolute maximum moment in the span occurs when the intermediate 32 kip load is placed such that the centerline of span bisects the distance between it and the resultant of load group (Figure 3.50).

The maximum moment occurs under the 32 kip axle load nearest the centerline, which is located at a = 39.665 ft from the left support and at b = 44.335 ft from the right support. Therefore, the influence line ordinates are

$$\text{Under the middle 32-kip axle load, } y_1 = \frac{ab}{L} = \frac{(39.665)(44.335)}{84} = 20.935 \text{ ft}$$

The IL ordinates y_2 and y_3 are determined from similar triangles:

$$\text{Under the rear 32-kip axle load, } y_2 = \left(\frac{30.335}{44.335}\right)(20.935) = 14.324 \text{ ft}$$

$$\text{Under the front 8-kip axle load, } y_3 = \left(\frac{25.665}{39.665}\right)(20.935) = 13.546 \text{ ft}$$

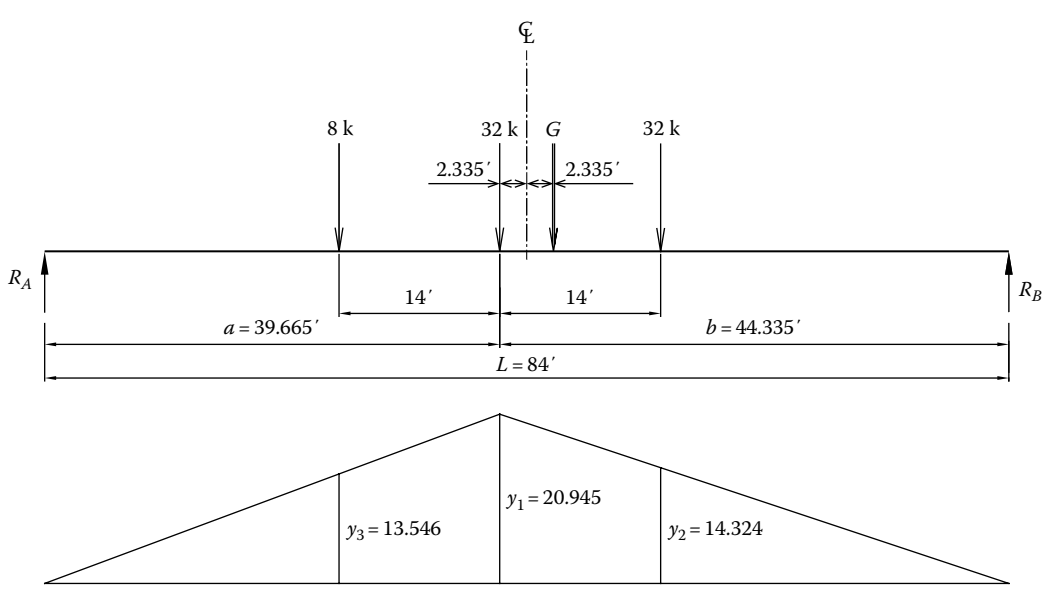

FIGURE 3.50 Influence line for bending moment in simple span of Example 3.6.

www.EngineeringEBooksPdf.com

The magnitude of the maximum moment in the span is determined as being equal to the sum of the products of the axle loads and the respective influence line ordinates:

$$M_{max} = \Sigma P_i y_i = 8(13.546) + 32(20.935 + 14.324) = 1236.66 \text{ kip-ft}$$

The aforementioned result can be verified from Equation 3.14 by substituting L = 84 ft:

$$\begin{aligned} M_{x,truck} &= \left(18L - 280 + \frac{392}{L}\right) \\ &= 18(84) - 280 + \frac{392}{84} \\ &= 1236.66 \text{ kip-ft} \end{aligned}$$

b. Absolute Maximum Bending Moment in Span due to Lane Loading
The moment due to the uniform load of 0.64 kip/ft can be calculated as the product of the load intensity and the area under the influence line diagram (Equation 3.12). Before proceeding to calculations, it is pointed out that the maximum moment due to a uniform load on span would occur at the midspan. However, in this problem, the maximum moment is determined at the same location where the absolute maximum moment occurs due to concentrated loads (AASHTO HS20 truck), that is, at 2.335 ft right of the middle 32 kip axle; the influence line ordinate under this point is determined as follows:

From Figure 3.50, a = 39.665 ft, b = 44.335 ft:

$$\frac{ab}{L} = \frac{(39.665)(44.335)}{84} = 20.935 \text{ ft}$$

$$M = w\left(\frac{1}{2} y_1 L\right) = (0.64))(0.5)(20.935)(84) = 562.73 \text{ kip-ft}$$

(By comparison, the midspan moment due to the uniform load of 0.64 kip/ft is found to be

$$M = \frac{wL^2}{8} = \frac{(0.64)(84)^2}{8} = 564.48 \text{ kip-ft}$$

Note that the aforementioned two values of moments are very close to each other.

The preceding examples illustrate how to determine design moments due to a group of moving concentrated loads on simple spans by using influence lines.

Finally, it is noted that the maximum moment in a span equals the sum of moments due to the design truck *or* tandem (whichever is greater) *and* the lane load, with appropriate DLA for moment due to truck or tandem (but *not* for lane load) as given by Equation 3.7. It also should be noted that *the design truck governs for maximum moment for spans greater than 40.27 ft; for smaller spans, the design tandem gives larger moment* See Example 3.7.

Example 3.7: Absolute Maximum Bending Moment due to AASHTO HS20 Truck by the Approximate Method

Derive a general expression for maximum bending moment due to AASHTO HS20 truck on a simple span by the approximate method. Calculate the maximum bending moment in a span of 84 ft and compare this value with the result obtained in Example 3.6.

www.EngineeringEBooksPdf.com

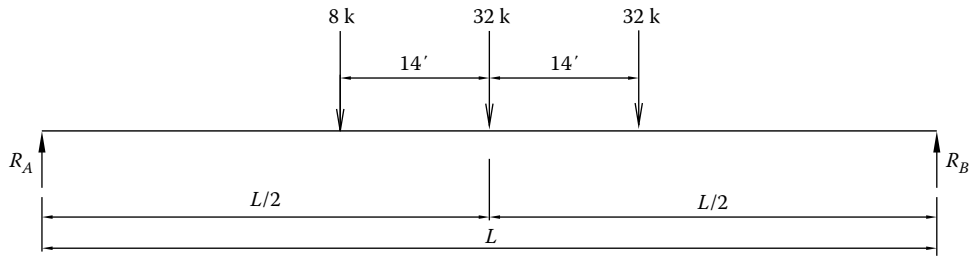

FIGURE 3.51 Approximate position of AASHTO design truck for maximum bending moment in a simple span. The interior 32 kip load is placed at the midspan.

Solution

Figure 3.51 shows the *approximate* load position of the AASHTO HS20 truck for maximum bending moment in a simple span, with the interior 32 kip axle placed at the midspan. Note that in this specific case, the positions of the 8 kip and the rear 32 kip axles are interchangeable.

The reaction at the right support, R_B, is determined by taking moments about the left support A:

$$R_B = 0.5(32) + (32)\left(\frac{L/2+14}{L}\right) + (8)\left(\frac{L/2-14}{L}\right)$$
$$= \left(36 + \frac{336}{L}\right)\text{kip}$$

The maximum bending moment occurs under the interior 32 kip load:

$$M_{max,truck,apx} = R_B(L/2) - 32(14)$$
$$= \left(36 + \frac{336}{L}\right)\left(\frac{L}{2}\right) - 32(14)$$
$$= 18L - 280 \text{ kip-ft} \tag{3.21}$$

For L = 84 ft, $M_{max,truck,apx}$ = 18(84) − 280 = 1232 kip-ft.

By the exact method illustrated in Example 3.6, M_{max} = 1236.66 kip-ft, which is only 4.66 kip-ft or 0.38 percent (negligible) greater than the value obtained by the approximate method.

Discussion: It is instructive to compare the results obtained from Equations 3.20 and 3.21 and select the appropriate equation for calculation of absolute maximum moment due to the AASHTO design truck on a simple span:

$$M_{max,truck} = 18L - 280 + 392/L \text{ kip-ft} \tag{3.20}$$

$$M_{max,truck,apx} = 18L - 280 \text{ kip-ft} \tag{3.21}$$

It is seen that the difference between the two values of the maximum moments is 392/L kip-ft. Evidently, as L increases, the difference between the two values of the maximum moment given by Equations 3.20 and 3.21 decreases. For example, for a simple span of 55 ft, the difference between the two values of the maximum moments is about 1 percent; for a simple span of 100 ft, the difference is less than 0.3 percent. Such minor differences are insignificant from a practical point of view. Therefore, because of its simplicity, Equation 3.21 can be used for all practical purposes.

Example 3.8: Absolute Maximum Bending Moment due to AASHTO Tandem by the Approximate and the Exact Methods

Derive a general expression for maximum bending moment due to AASHTO tandem on a simple span by the approximate method. Calculate the maximum moment in a span of 84 ft from influence lines and compare this value with the approximate value of the maximum bending moment.

www.EngineeringEBooksPdf.com

Solution

Exact Method

Because the two axle loads are equal, the resultant of the load group lies midway between them. Figure 3.52a shows the influence line for maximum moment in the span. For a span of 84 ft, the influence line ordinates are as follows:

$$\text{Under the 25-kip axle right of midspan, } y_1 = \frac{ab}{L} = \frac{(43)(41)}{84} = 20.988 \text{ ft}$$

$$\text{Under the 25-kip axle left of midspan, } y_2 = \left(\frac{39}{43}\right)(20.99) = 19.036 \text{ ft}$$

$$M_{max} = \Sigma P_i y_i = 25(20.988 + 19.036) = 1000.6 \text{ kip-ft}$$

Alternatively, the absolute maximum bending moment in span can be determined by the exact method once the load position is fixed as shown in Figure 3.52a. For a length of span L in the aforementioned figure, the left 25 kip axle is positioned at $(0.5L - 1)$ ft to the right of the left

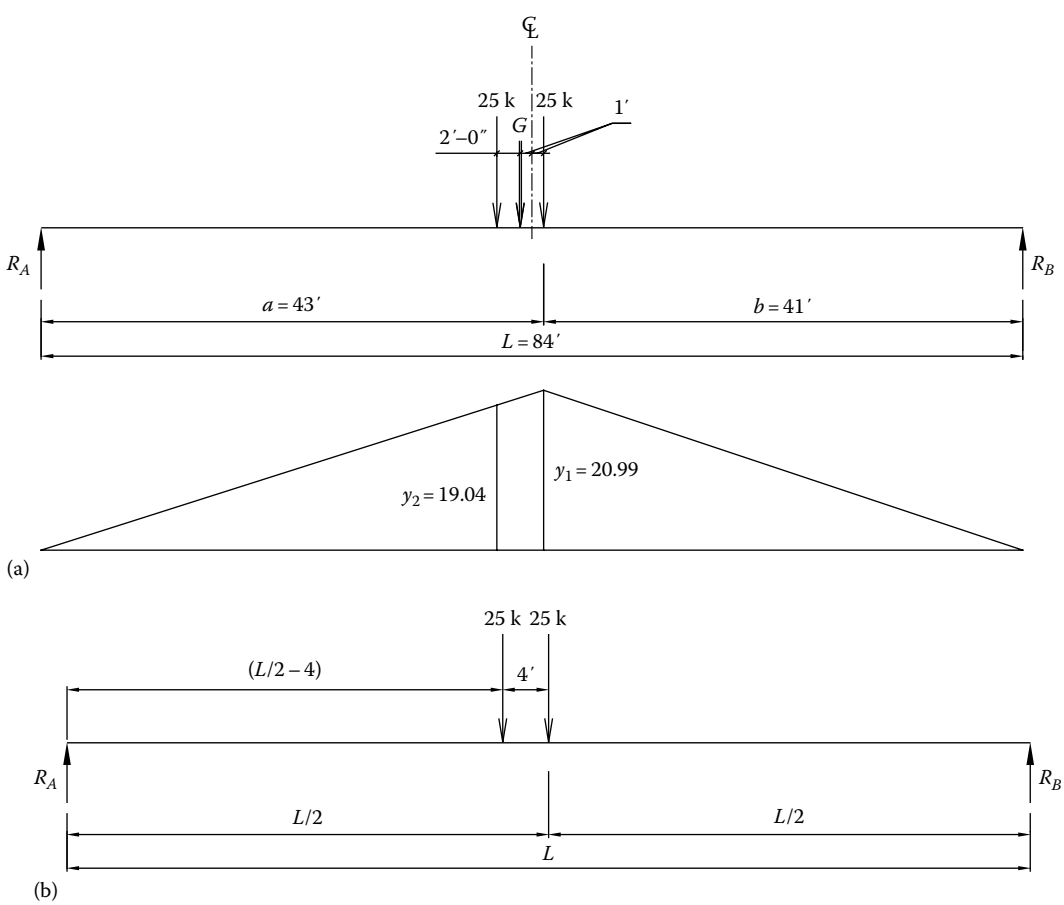

FIGURE 3.52 (a) Position of AASHTO tandem for maximum bending moment in a simple span (exact method). (b) Position of AASHTO tandem for absolute maximum bending moment in a simple span (approximate method).

www.EngineeringEBooksPdf.com

support (support A) or 1.0 ft left of the center line of the span, and the right 25 kip axle is positioned at $(0.5L - 3)$ ft left of the right support (support B). Reaction R_A is determined by taking moments about the right support B:

$$R_A = \frac{1}{L}(25L - 50)\text{ kip}$$

The absolute maximum bending moment occurs under the left 25 kip axle and is given by

$$M_{max,tandem.apx} = R_A\left(\frac{L}{2} - 1\right) = \frac{1}{L}(25L - 50)\left(\frac{L}{2} - 1\right)$$
$$= \left(12.5L - 50 + \frac{50}{L}\right)\text{ kip-ft} \tag{3.22}$$

a. Approximate Method
Figure 3.52b shows the load position of the AASHTO tandem for maximum bending moment in a simple span; one of the 25 kip axles is placed at the midspan.

The reaction at the right support, R_B, is determined by taking moments about the left support A:

$$R_B = 0.5(25) + 25\left(\frac{L/2 - 4}{L}\right) = \left(25 - \frac{100}{L}\right)\text{ kip}$$

The maximum bending moment at the midspan occurs under the 25 kip load at the midspan:

$$M_{max,tandem} = R_B\left(\frac{L}{2}\right) = \left(25 - \frac{100}{L}\right)\left(\frac{L}{2}\right)$$
$$= 12.5L - 50\text{ kip-ft} \tag{3.23}$$

For $L = 84$ ft,

$$M_{max,tandem} = 12.5(84) - 50 = 1000\text{ kip-ft}$$

The aforementioned value of the moment is almost the same as obtained by the exact method; the difference of 0.6 kip-ft between the two values of the moment is insignificant by comparison.

Example 3.8 shows that the difference between the two values of the maximum moments is $50/L$ kip-ft, which decreases with increasing span lengths. For a span of 100 ft, this difference amounts to 0.5 kip-ft, which is negligible. Therefore, Equation 3.23 should be used wherever necessary.

When determining the absolute maximum bending moments in a span for design, it is necessary to determine which of the two live load types (AASHTO design truck and the tandem loads) will result in a larger bending moment. It can be shown that for simple spans <40.27 ft, the AASHTO *tandem* gives larger bending moment; for $L > 40.27$ ft, AASHTO *design truck* gives larger bending moment. For $L = 40.27$ ft, the maximum bending moment is the same for both types of loads. See Example 3.9. Note that there are no such limiting lengths for the lane load because the lane load is assumed distributed uniformly over the entire span, continuously end to end.

www.EngineeringEBooksPdf.com

Example 3.9: Determination of Limiting Span Lengths for Governing AASHTO HS20 Design Truck and Tandem for Absolute Maximum Bending Moment in a Simple Span

Expressions for maximum bending moments due to AASHTO HS20 truck and tandem loads were derived in Examples 3.7 and 3.8 (see Equations 3.15 and 3.17, respectively).

For HS20 truck,

$$M_{max,truck} = 18L - 280 + \frac{392}{L} \text{ kip-ft} \tag{3.20}$$

For *tandem*,

$$M_{max,tandem} = 12.5L - 50 + \frac{50}{L} \text{ kip-ft} \tag{3.22}$$

Equating the aforementioned two expressions, we obtain

$$18L - 280 + \frac{392}{L} = 12.5L - 50 + \frac{50}{L}$$

Or L = 40.274 ft, say 40.27 ft

The aforementioned result means that *for L = 40.27 ft, the absolute maximum bending moment in span due to HS20 truck and tandem would be the same. HS20 truck would govern for spans greater than 40.27 ft, whereas design tandem would govern for spans smaller than 40.27 ft*. See Example 3.10.

Example 3.10

Determine the absolute maximum bending moment in a simple span due to HS20 truck or tandem when (a) L = 40 ft, (b) L = 50 ft. Indicate the governing load

Solution

Equations 3.20 and 3.22 would be used.

a. L = 40 ft
For HS20 truck,

$$M_{max,truck} = 18L - 280 + 392/L = 18(40) - 280 + 392/40 \approx 450 \text{ kip-ft}$$

For AASHTO tandem,

$$M_{max,tandem} = 12.5L - 50 + 50/L$$
$$= 12.5(40) - 50 + 50/40 \approx 452 \text{ kip-ft} > 450 \text{ kip-ft}$$

Thus, for L = 40 ft, AASHTO *tandem* controls; M_{max} = 452 kip-ft

b. L = 50 ft
For HS20 truck,

$$M_{max,truck} = 18L - 280 + 392/L = 18(50) - 280 + 392/50 \approx 628 \text{ kip-ft}$$

www.EngineeringEBooksPdf.com

For AASHTO tandem,

$$M_{max,tandem} = 12.5L - 50 + 50/L$$
$$= 12.5(50) - 50 + 50/50 = 576 \text{ kip-ft} < 628 \text{ kip-ft}$$

Thus, for L = 50 ft, HS20 *truck* controls; M_{max} = 628 kip-ft.

3.7.7 Generalized Expressions for Maximum Moment and Maximum Shear at a Section in a Simple Span due to HS20 Truck

As was mentioned earlier, in bridge design, it is necessary to determine maximum bending moments and shears at several points in a span, typically at tenth points, that is, at 0.1L intervals. This section presents general equations, based on influence lines, which can be used for this purpose.

At the outset, it should be understood *that in bridge design, because of the specific design loading, it is required to determine the maximum design forces only for one-half of the span (typically the left half) because the design forces for the other half span are considered to be identical. Therefore, the following equations are valid for a range of $x/L \leq 0.5$.* Also, to develop general equations that are valid for the entire range of $x/L \leq 0.5$, it is necessary to position the HS20 truck in two different positions: the truck moving (1) from the left to the right and (2) from the right to the left. This is discussed in the next section.

3.7.7.1 Maximum Moment and Shear: HS20 Truck Moving from Left to Right

Figure 3.53 shows the position of the HS20 truck as it moves across the span from left to right. The rear 32 kip axle is positioned at a distance x from the left support, for which influence lines are also shown in the figure. The influence line ordinates for the three axle loads are determined as follows:

$$y_1 = \frac{x(L-x)}{L}$$

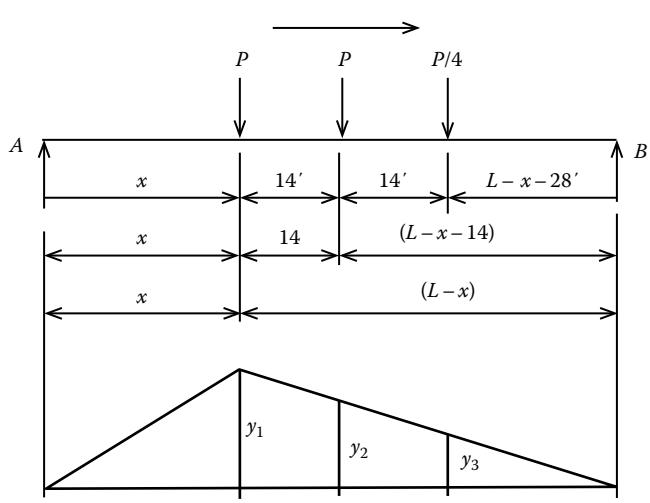

FIGURE 3.53 Position of the HS20 truck for maximum moment and shear at any point in a simple span when it moves from left to right.

www.EngineeringEBooksPdf.com

$$y_2 = y_1\left(\frac{L-x-14}{L-x}\right) = \left(\frac{x(L-x)}{L}\right)\left(\frac{L-x-14}{L-x}\right) = \left(\frac{x(L-x-14)}{L}\right)$$

$$y_3 = y_1\left(\frac{L-x-28}{L-x}\right) = \left(\frac{x(L-x)}{L}\right)\left(\frac{L-x-28}{L-x}\right) = \left(\frac{x(L-x-28)}{L}\right)$$

From Equation 3.11,

$$M_x = P_1y_1 + P_2y_2 + P_3y_3$$

Substitution for y_1, y_2, and y_3 from above and $P_1 = P_2 = P$, and $P_3 = P/4$ in Equation 3.11 yields

$$M_x = P\left(\frac{x}{L}\right)(L-x) + P\left(\frac{x}{L}\right)(L-x-14) + \frac{P}{4}\left(\frac{x}{L}\right)(L-x-28)$$

$$= \frac{Px}{L}(2.25L - 2.25x - 21)$$

Substitution of $P = 32$ kip in the aforementioned equation yields Equation 3.24:

$$M_x = \frac{72x}{L}(L-x-9.33) \tag{3.24}$$

Because of the selected axle positions in Figure 3.53, Equation 3.24 is valid for the span range $0 < x/L \leq 0.333$ and for a minimum values of $x = 14$ ft and $L = 28$ ft. Also, because Equation 3.24 gives maximum moment at a distance x from the left support, the reaction at A, and hence the maximum shear at x from the left support can be expressed as given by Equation 3.25:

$$V_x = \frac{72}{L}(L-x-9.33) \tag{3.25}$$

Note that Equation 3.25 is valid for the span range $0 < x/L \leq 0.500$.

3.7.7.2 Maximum Moment and Shear: HS20 Truck Moving from Right to Left

Now, consider the position of HS20 truck on the span as it moves from right to left. Figure 3.54 shows the position of the HS20 truck as it moves across the span from right to left. The middle

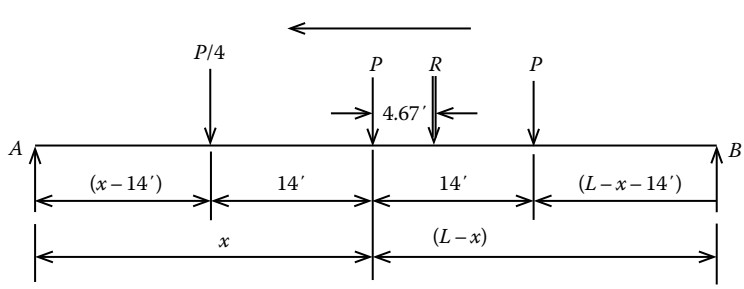

FIGURE 3.54 Position of the HS20 truck for maximum moment and shear at any point in a simple span when the truck moves from right to left.

www.EngineeringEBooksPdf.com

32 kip axle is positioned at a distance x from the left support, for which influence lines are also shown in the figure. The influence line ordinates for the three axle loads are determined as follows:

$$y_1 = \frac{x(L-x)}{L}$$

$$y_2 = y_1\left(\frac{x-14}{x}\right) = \left(\frac{x(L-x)}{L}\right)\left(\frac{x-14}{x}\right) = \frac{(L-x)(x-14)}{L}$$

$$y_3 = y_1\left(\frac{L-x-14}{L-x}\right) = \left(\frac{x(L-x)}{L}\right)\left(\frac{L-x-14}{L-x}\right) = \left(\frac{x(L-x-14)}{L}\right)$$

From Equation 3.11,

$$M_x = P_1y_1 + P_2y_2 + P_3y_3 = P\left(y_1 + \frac{y_2}{4} + y_3\right)$$

where $P_1 = P_3 = P$ and $P_2 = P/4$.

Substitution for y_1, y_2, and y_3 in the aforementioned expression and simplifying yields to Equation 3.26:

$$M_x = \frac{2.25Px}{L}(L-x-4.67) - 3.5P \tag{3.26}$$

Substitution of $P = 32$ kip in Equation 3.26 gives Equation 3.27:

$$M_x = \frac{72x}{L}(L-x-4.67) - 112 \tag{3.27}$$

Equation 3.27 is valid for the span range $0.333 \le x/L \le 0.500$ and $L_{min} = 42$ ft.

We can verify the validity of Equation 3.27 by calculating the maximum moment for a span of 84 ft (Examples 3.6 and 3.7). For $L = 84$ ft and $x = 42$ ft (i.e., at midspan, $x/L = 0.500$), Equation 3.27 gives $M_{max} = 1231.88$ kip-ft ≈ 1232 kip-ft, same as calculated in Example 3.7, and only slightly less than 1236.66 kip-ft (the exact value) calculated in Example 3.6.

Equation for the maximum shear at a distance x from the left support can be determined by calculating the reaction at A, R_A. The resultant R of all the axle loads acts at 4.67 ft to the right of the middle axle load or at $x + 4.67$ ft from support A. Then,

$$R_A = R\left(\frac{L-x-4.67}{L}\right) = 2.25P\left(\frac{L-x-4.67}{L}\right)$$

Shear V_x just to the left of the middle 32 kip axle load is given by Equation 3.28:

$$V_x = R_A - \frac{P}{4} = 2.25P\left(\frac{L-x-4.67}{L}\right) - 0.25P \tag{3.28}$$

www.EngineeringEBooksPdf.com

TABLE 3.12
Maximum Bending Moment in Simple Spans Due to HS20 Truck Loading (Strength Limit States)

		Minimum		
x/L	**Formula for Maximum Bending Moment (kip-ft)**	***x*, ft**	***L*, ft**	**Equation No.**
0–0.333	$M_x = \frac{72x}{L}\left[\left(L-x\right)-9.33\right]$	0	28	3.24
0.333–0.5000	$M_x = \frac{72x}{L}\left[\left(L-x\right)-4.67\right]-112$	14	42	3.27

Note: x, distance from the left support to the section being considered, ft.

TABLE 3.13
Maximum Shear in Simple Spans Due to HS20 Truck Loading (Strength Limit States)

		Minimum		Maximum	
x/L	**Formula for Maximum Shear (kip)**	***x*, ft**	***L*, ft**	***L*, ft**	**Equation No.**
0–0.500	$V_x = \frac{72}{L}\left(L-x-4.67\right)-8$	14	28	42	3.29
0–0.500	$V_x = \frac{72}{L}\left(L-x-9.33\right)$	0	42	—	3.25

Note: x, distance from the left support to the section being considered, ft.

Substitution of $P = 32$ kip in Equation 3.28 results in Equation 3.29:

$$V_x = \frac{72}{L}\left(L-x-4.67\right)-8 \tag{3.29}$$

Equation 3.24 is valid for $x_{min} = 0$ ft, $L_{min} = 28$ ft.

The aforementioned results are summarized in Tables 3.12 and 3.13. Example 3.18 illustrates application of Equations 3.24, 3.25, 3.27, and 3.29.

3.7.8 Absolute Maximum Bending Moment in Spans Due to Loads Other than AASHTO HS20 Truck

While designing a bridge superstructure, it is often necessary to determine the maximum bending moment and moments at other locations (e.g., at $0.1L$ intervals) in a span caused by vehicles having length and weight configurations (but not the width between the wheels of an axle) that are different from the AASHTO HS20 truck. Such vehicles are referred to variously as *exclusion* vehicles and *permit vehicles* as discussed in Section 3.7.4.2. Practically speaking, there are many trucks of varying load configurations (magnitude of axle loads and the distance between them, see Figures 3.13 through 3.23) for which a designer may have to determine maximum bending moment in a span.

Example 3.11 illustrates calculations for determining the absolute maximum bending moment in a simple span due to a Type 3-3 Unit (see Figure 3.14). This type of computational exercise becomes

www.EngineeringEBooksPdf.com

a necessity when one has to determine if a truck-trailer, which is different from HL-93 design load, can be permitted to safely cross a bridge. This is a very important consideration bridge owner agencies because a majority of the old bridges had been designed years ago conforming to the older specifications when the highway loads were much lighter.

Determination of maximum bending moment in a span caused by such vehicles is relatively simple if the span is long enough to concurrently accommodate all axles of the truck-trailer on it. However, if the load configuration (i.e., the distance between the front and the rear axles) is such that it is physically impossible to concurrently place all axles on the span, it would be necessary to first determine the load group (i.e., the group of adjacent axles) that should be placed on span for obtaining maximum bending moment. However, unless the load group is symmetrical, which of the adjacent loads would form such a load group is not quite apparent (intuition would not help either). In such cases, a trial-and-error approach would be necessary as illustrated in Example 3.11.

Example 3.11: Absolute Maximum Bending Moment in a Span Due to Permit Trucks

Figure 3.55a shows a vehicle configuration known as Type 3-3 unit that is permitted to cross a simple span of 50 ft. Determine (a) maximum bending moment in span and (b) maximum bending moment at 10 ft from the left support.

Solution

a. Maximum Bending Moment in Span
It is observed that the truck comprises six axles, and the length of the load (i.e., the distance between the front and the rear axle), 54 ft, is 4 ft longer than the span length (50 ft). This implies that not all axles (i.e., the entire truck) can be placed on the span simultaneously; either the front axle (12 kip load) or the rear axle (14 kip load) must be excluded from the span. If we exclude the rear axle (14 kip load) from the span, the distance between the front and the fifth axle is 50 ft. With these five axles on the span, the truck would occupy

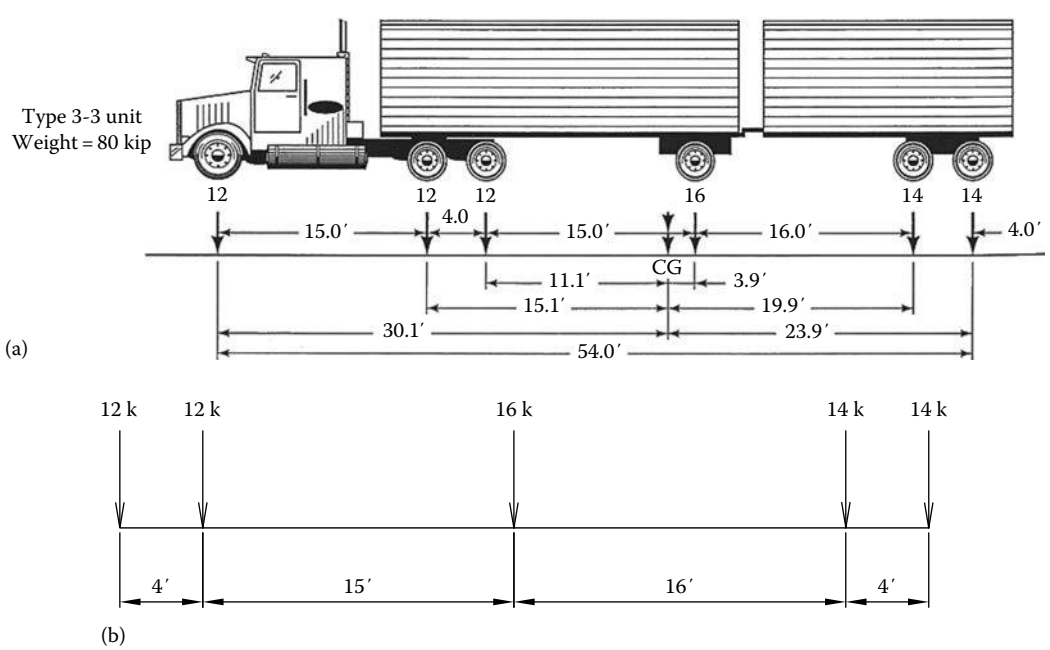

FIGURE 3.55 (a) Vehicle configuration of a Type 3-3 Unit. (b) Load group for maximum moment in span. (*Continued*)

www.EngineeringEBooksPdf.com

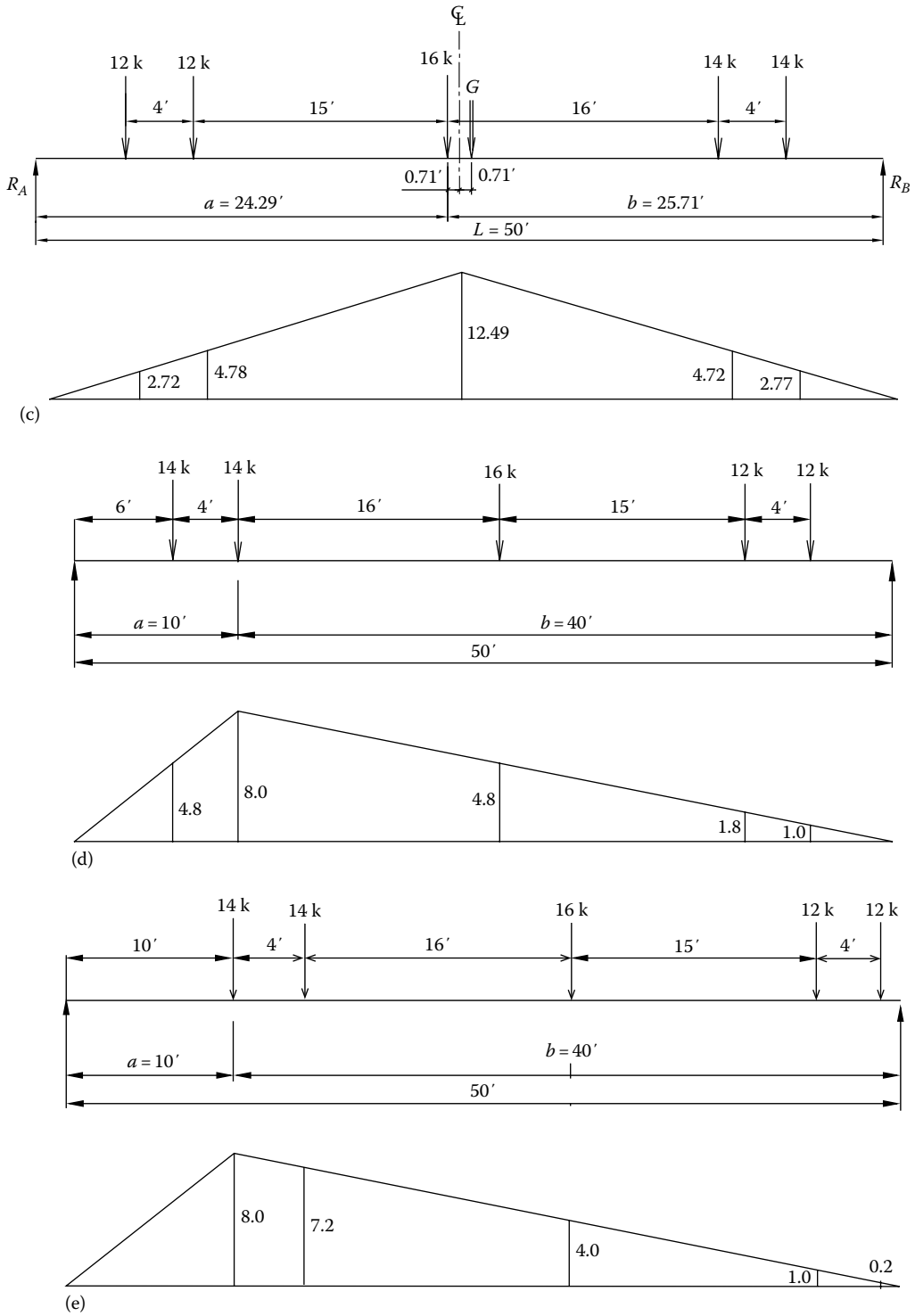

FIGURE 3.55 (*Continued*) (c) Load position and influence line for maximum moment in span. (d) Load position 1 and influence line for maximum moment at 10 ft from the left support. (e) Load position 2 and influence line for maximum moment at 10 ft from the left support.

www.EngineeringEBooksPdf.com

the whole span, with the front and the rear axles positioned directly over the supports. However, with this load position, the front and the rear axles would not contribute any moment (or shear) in the span. We should, therefore, position the truck in such a way that the front axle (which is lighter than the rear axle) is off span; Figure 3.55b shows the selected load group.

Determine the resultant of the load group (five axles, excluding the front axle). Distance $\bar{x}$ of the resultant from the second 12 kip axle is calculated as

$$\bar{x} = \frac{12(4)+16(19)+14(35)+14(39)}{(12+12+16+14+14)} = 20.41\,\text{ft}$$

Thus, the resultant of the load group is located at 20.41 ft from the second 12 kip axle or 1.41 ft to the right of the 16 kip axle. For maximum bending moment on span due to this load group, it is required to position the 16 kip axle and the resultant of the load group equidistant from the centerline of span, that is, at 0.71 ft off of the centerline. These load positions as well as the IL for maximum bending moment, which occurs under the 16 kip axle, are shown in Figure 3.55c. The influence line ordinates corresponding to the selected axle positions are calculated (from similar triangles) as follows:

$$a = 24.29\text{ ft}, \quad b = 25.71\text{ ft}, \quad L = 50\text{ ft}.$$

$$\text{Under the 16-kip axle, } y_1 = \frac{ab}{L} = \frac{(24.29)(25.71)}{50} = 12.49$$

$$\text{Under the left end 12-kip axle, } y_2 = \left(\frac{5.29}{24.29}\right)(12.49) = 2.72\text{ ft}$$

$$\text{Under the interior 12-kip axle, } y_3 = \left(\frac{9.29}{24.29}\right)(12.49) = 4.78\text{ ft}$$

$$\text{Under the interior 14-kip axle, } y_4 = \left(\frac{9.71}{25.71}\right)(12.49) = 4.72\text{ ft}$$

$$\text{Under the rear 14-kip axle, } y_5 = \left(\frac{5.71}{25.71}\right)(12.49) = 2.77\text{ ft}$$

$$M_{max} = \Sigma P_i y_i = 12(2.72) + 12(4.78) + 16(12.49) + 14(4.72 + 2.77) = 394.7\text{ kip-ft}.$$

b. Maximum Bending Moment at 10 ft from the Left Support

The IL line for maximum bending moment at 10 ft (point D in Figure 3.55d) from the left support consists of two inclined lines forming a triangle with its apex at 10 ft from the left support. The load group selected for part (a) should be placed suitably on span. The influence lines for moment at point D are shown in Figure 3.55d. From inspection, the position of loads that would cause maximum bending moment at D is not quite obvious. Therefore, two load positions are considered when the truck moves from left to right: (1) the rear 14 kip axle is at 6 ft from the left support and the adjacent 14 kip axle is at the 10 ft from the left support and (2) the rear 14 kip axle is at 10 ft from the left support. These two load positions and the corresponding IL for maximum bending moment at 10 ft from the left support are shown in Figure 3.55d and e. The IL ordinates and the corresponding moment at 10 ft from the support are calculated as follows:

$$a = 10\text{ ft}, \quad b = 40\text{ ft}, \quad L = 50\text{ ft}.$$

www.EngineeringEBooksPdf.com

i. Load position 1: The rear 14 kip load at 6 ft from the left support

Under the 14-kip axle at 10 ft from the left support, $y_1 = \frac{ab}{L} = \frac{(10.0)(40.0)}{50} = 8.0$ ft

Under the 14-kip axle at 6 ft from the left support, $y_2 = \left(\frac{6.0}{10.0}\right)(8.0) = 4.8$ ft

Under the 16-kip axle, $y_3 = \left(\frac{24.0}{40.0}\right)(8.0) = 4.8$ ft

Under the intermediate 12-kip axle, $y_4 = \left(\frac{9.0}{40.0}\right)(8.0) = 1.8$ ft

Under the front 12-kip axle, $y_5 = \left(\frac{5.0}{40.0}\right)(8.0) = 1.0$ ft

$$M_{max} = \Sigma P_i y_i = 14(4.8 + 8) + 16(4.8) + 12(1.8 + 1.0) = 289.6 \text{ kip-ft.}$$

ii. Load position 2: The rear 14-kip load at 10 ft from the left support

Under the rear 14-kip axle (at 10 ft from the left support), $y_1 = \frac{ab}{L} = \frac{(10.0)(40.0)}{50} = 8.0$ ft

Under the intermediate 14-kip axle (at 4 ft from the rear axle), $y_2 = \left(\frac{36.0}{40.0}\right)(8.0) = 7.2$ ft

Under the 16-kip axle, $y_3 = \left(\frac{20.0}{40.0}\right)(8.0) = 4.0$ ft

Under the intermediate 12-kip axle, $y_4 = \left(\frac{5.0}{40.0}\right)(8.0) = 1.0$ ft

Under the front 12-kip axle, $y_5 = \left(\frac{1.0}{40.0}\right)(8.0) = 0.2$ ft

$$M_{max} = \Sigma P_i y_i = 14(8 + 7.2) + 16(4.0) + 12(1.0 + 0.2) = 291.2 \text{ kip-ft} > M = 289.6 \text{ kip-ft.}$$

Therefore, the maximum bending moment at 10 ft from the left support is equal to 291.2 kip-ft.

Discussion: We could have determined the position of loads for maximum bending moment in span without performing the given calculations. The change in bending moment at point *D* as loads move from left to right and the rear 14 kip axle occupies position at point *D* can be obtained from the slope of the influence line for maximum bending moment at point *D*. Note that the slope of the left sloping line is 8/10 and that of the right sloping line is 8/40. As the loads move 4 ft to the right, so that the rear 14 kip axle occupies position at point *D*, the change in moment can be expressed as

$$\Delta M = 14\left(\frac{8}{10}\times 4\right) - 14\left(\frac{8}{40}\times 4\right) - 16\left(\frac{8}{40}\times 4\right) - 12\left(\frac{8}{40}\times 4\right) - 12\left(\frac{8}{40}\times 4\right) = 1.6 \text{ kip-ft}$$

www.EngineeringEBooksPdf.com

When the loads are moved further to the right, inspection of the influence line diagram shows that the change in the bending moment at point D would be negative (because the slope of the influence line diagram between points D and B is negative, −8/40). Therefore, the maximum moment at D occurs when the 14 kip axle is placed at point D. For this position of loads, $M_{D,max}$ = 291.2 kip-ft. Note the difference between bending moments at D calculated earlier for the two load positions is 291.2 − 289.6 = 1.6 kip-ft, which is the value of ΔM calculated earlier.

3.7.9 Governing Span Lengths for Maximum Live Load Shear in Simple Spans Due to AASHTO LRFD Live Load: HS20 Truck and Tandem

The preceding discussion focused on determination of maximum bending moments in simple spans produced by HS20 truck and other types of trucks. The following examples illustrate determination of governing span lengths for maximum shear in simple spans due to AASHTO LRFD live load: HS20 truck and tandem loads.

Example 3.12

Derive an expression for the governing live load vehicles, truck or tandem, that would cause maximum shear in a simple span.

Solution

Maximum shear in a simple span would occur at one of the supports (left support chosen in this example). Figure 3.56 shows the influence line for maximum reaction at the left support. For maximum reaction at the left support, obviously, the rear 32 kip axle (in the case of HS20 truck) and the 25 kip axle (in the case of HL-93 tandem) should be positioned directly over the support. These load positions are shown in Figure 3.56.

Maximum shear at A, $V_A = R_A$

Let P_{tr} = 32-axle load of HS20 truck

P_{tm} = 25-axle load of HL-93 tandem

Calculate reaction at A due to HS20 truck. Assuming that $L > 28$ ft, all three axles of the truck can be placed on the span. From the influence line for reaction at A (Figure 3.56),

$$R_{A,tr} = P_{tr}\left(1+\frac{L-14}{L}+\frac{L-28}{4L}\right)$$

$$= P_{tr}\left(2.25-\frac{21}{L}\right)\text{kip} \tag{3.30}$$

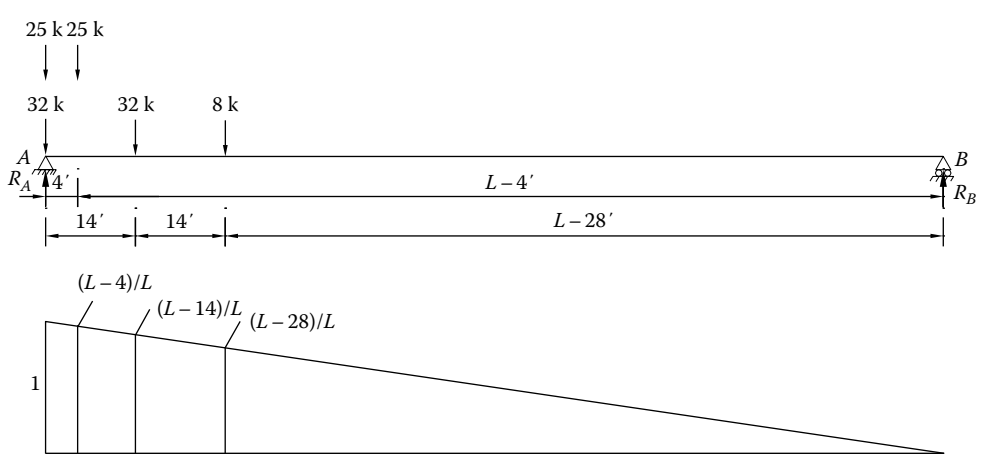

FIGURE 3.56 Influence line for reaction and maximum shear at the left support.

www.EngineeringEBooksPdf.com

TABLE 3.14
Liming Span Lengths for Maximum Moments and Shears in Simple Spans Due to HS20 Truck and Tandem

Force Effects	HS 20 Truck (ft)	Tandem (ft)
Moment	$L > 40.27$	$L < 40.27$
Shear	$L > 26$	$L < 26$

Calculate reaction at A due to HL-93 tandem. Assuming $L > 4$ ft so that both axles of the tandem can be placed on the span, from the influence line shown in Figure 3.56,

$$R_{tn} = P_{tn}\left(1 + \frac{L-4}{L}\right) = P_{tn}\left(\frac{2L-4}{L}\right) \tag{3.31}$$

Dividing Equation 3.30 by Equation 3.31, we obtain Equation 3.32:

$$\frac{R_{A,tr}}{R_{A,tn}} = \frac{P_{tr}}{P_{tn}}\left(\frac{2.25L-21}{2L-4}\right) \tag{3.32}$$

Substituting $P_{tr} = 32$ kip and $P_{tn} = 25$ kip in Equation 3.32, we obtain

$$\begin{aligned}\frac{R_{A,tr}}{R_{A,tn}} &= \frac{32}{25}\left(\frac{2.25L-21}{2L-4}\right)\\ &= \frac{2.88L-26.88}{2L-4}\end{aligned} \tag{3.33}$$

For maximum shear at the left support due to both the truck and the tandem to be the same, it is required that $R_{A,tr} = R_{tn}$, which, when substituted in Equation 3.33, yields

$$2.88L - 26.88 = 2L - 4$$

$$L = 26 \text{ ft}$$

Thus, for $L = 26$ ft, maximum shear at A will be same due either to the truck or tandem. For $L < 26$ ft, the tandem would cause greater shear at A; for $L > 26$, the truck would cause greater shear at A. Table 3.14 gives a summary of governing simple-span lengths for moment and shears.

Commentary: Note that these results are different than those for maximum moments in the span. In earlier discussion (Example 3.8), it was noted that for the *absolute maximum moment* in a simple span, HS20 truck controls when $L > 40.27$ ft, and the tandem controls when $L < 40.27$ ft. For $L = 40.27$ ft, both the truck and tandem give the same value of the absolute maximum moment in span.

3.7.10 Influence Lines for Beams with Other Support Conditions and for Other Types of Structures

The preceding discussion focused on methods of determining maximum moments and shear values due to a group of moving loads on beams that were simply supported. In practice, longitudinal beams may be supported in ways other than the simply supported as discussed earlier, for which

www.EngineeringEBooksPdf.com

influence lines would need to be drawn. Influence lines are also useful in determining maximum force effects such as maximum moment, shear, and reactions in floor beams and arches, maximum axial forces in truss members, etc. Calculations for influence lines for these members, as well as for continuous beams, tend to be monotonous, tedious, and time intensive; one should resort to computers for such calculations.

3.8 DYNAMIC EFFECTS OF VEHICULAR LIVE LOAD

3.8.1 General Considerations for Dynamic Force Effects: Dynamic Load Allowance

DLA is defined as the ratio of dynamic deflection to static deflection at midspan (similar to *dynamic load factor*, as defined in classic texts on structural dynamics). Dynamic loads are characterized by the suddenness of their application. If the fundamental period (T) of a structure is considerably shorter than the time taken by the applied load to reach its final value, that load is considered as *gradually applied* or *static* load. On the other hand, if the fundamental period of a structure is greater than the period of application of the load, the load is said to be dynamic. If the fundamental periods (or the natural frequencies, $f = 1/T$) of the structure and the applied load are close to being equal, the load is characterized as *resonant*. Resonant loads can have undesirable consequences on structures such as excessive vibrations that can cause human discomfort, among others.

Dynamic loads can be *oscillatory* (e.g., due to wind and earthquakes) or *impulsive* (e.g., due to impact, nuclear or bomb blasts, and sonic booms); dynamic load effects on bridge superstructures generated by vehicular traffic are of the later type. Furthermore, dynamic loads can be external or *exogenous* (e.g., those due to wind and earthquakes) or *internal*; dynamic loads generated by vehicular motion, commonly known as *impact* loads (referred to as such in all AASHTO Specifications) are of the later type. AASHTO LRFD uses the term *dynamic load allowance* or *DLA* for impact (Art. 3.6.2.1).

All bridge superstructures are subjected to the dynamic effects induced by the fast moving vehicular traffic, which must be accounted for in design. Both in buildings and bridges, dynamic effects are considered as equivalent static loads for design purposes. Effects of dynamic loads are typically accounted for in design as equivalent static loads and contextually referred to by terms such as *DLA*, *dynamic load factors* (DLFs), and *impact factors* (IM).

3.8.2 Research on Quantification of Dynamic Load Effects

Early studies on dynamic effects of moving loads were conducted in England and Germany in the beginning late eighteenth century. Concerns about the dynamic action of moving loads evolved in the eighteenth century in the context of studying strength of bridges. Much of the earlier work related to impact focused on railway bridges. It was later that attention shifted to highway bridges as their spans became larger and the loads of highway vehicles increased. Historically speaking, Thomas Young (1773–1829), through his studies of prismatic beams, was the first to show the importance of dynamical effects of loads. J. V. Poncelet (1788–1867), influenced by contemporary suspension bridges, made a more detailed study of dynamic action. Dynamic tests on beams by Willis, James, and Galton during the 1850s showed that deflections increased with increase in speeds and that dynamic deflections two to three times the static deflections were obtained at higher speeds (Barlow 1851). However, experimental investigation of actual bridges did not show the effects of speed in such a marked way. Considering only the fundamental mode of vibration, G. G. Stokes (1819–1903) was the first to show that the magnitude of dynamic deflection depended on the ratio of period of beam's first mode of vibration to the time taken by the moving force to cross the span. Progress in this field was by Homersham Cox, who concluded in 1949 from energy considerations that dynamic deflection was limited to twice the static deflection. Work to improve the knowledge of dynamic

www.EngineeringEBooksPdf.com

action continued both in England and Germany, where deflection of cast-iron bridges on the Baden Railroad was measured for various speed of locomotives.

In the United States, until 1900, although it was known that loadings moving at varying speeds subjected highway bridges to dynamic action—vibration and oscillation, commonly termed *impact*—no special effort had been made to quantify its intensity. Even the highway bridge specifications did not contain any empirical formulas to provide for the impact. During the early years, owing to the lack of understanding of the impact phenomenon made it somewhat customary to post, even on new and sturdy bridges, signboards warning traffic to cross at a walking pace. Signs worded "Warning! Walk your horses. Penalty: $5.00 fine" or "$5.00 fine for crossing faster than a walk" were common (Edwards 1959).

The dynamic response of a bridge superstructure to moving loads is a complex phenomenon that involves many variables: vehicle types and load, vehicle speed, bridge type, span length, number of spans, surface roughness, and stiffness of superstructure. The dynamic load effects may be attributed to several sources:

1. Hammering effect resulting from vehicle assemblies riding over the surface discontinuities, such as potholes, cracks, deck joints, and delaminations
2. Dynamic response of the bridge as a whole to moving vehicles, which may be due to long undulations in the roadway pavement, such as those caused by settlement or fill
3. Resonant excitation as a result of similar frequencies of vibration between the bridge superstructure and the vehicle

The first systematic research dealing with highway bridge impact forces was carried out at the Civil Engineering Department of the University of Illinois. Based on this research, the first American scientific paper on highway impact forces appears to be one entitled *Some Experiments on Highway Bridges under Moving Loads* by Prof. F. O. Daffer, presented at the Western Society of Civil Engineers in 1913 (Edwards 1959).

Considerable research and numerous field studies were conducted in this area in the late 1900s (Huang 1976, Page 1976, Harmon and Davenport 1979, Billing 1980, Gupta 1980, Cantieni 1984, O'Connor and Prichard 1985, Honda et al. 1986, Hwang and Nowak 1991a,b, Paultre et al. 1992). These studies have indicated that the dynamic behavior of a bridge is function of three major factors (Hwang and Nowak 1991b):

1. Dynamic properties of the bridge structure (span, mass, support types, material, geometry)
2. Road roughness (approach, roadway, cracks, potholes)
3. Dynamic properties of the vehicle (mass, suspension, axle configuration, tires, speed)

Research and field studies suggested that the most accurate indicator of the dynamic response of a bridge superstructure is its natural frequency (Shephard and Aves 1973, Schilling 1982, Cantieni 1984, Chan and O'Connor 1990a,b, Schelling et al. 1990, Huang et al. 1992). The first natural frequency (or the fundamental frequency), f, of a bridge considered as a simple beam is given by Equation 3.34:

$$f = \frac{\pi}{2L^2}\sqrt{\frac{EI_x}{m}} \tag{3.34}$$

where

L = span length
I_x = moment of inertia of the structural element considered
m = mass of the structural element considered

www.EngineeringEBooksPdf.com

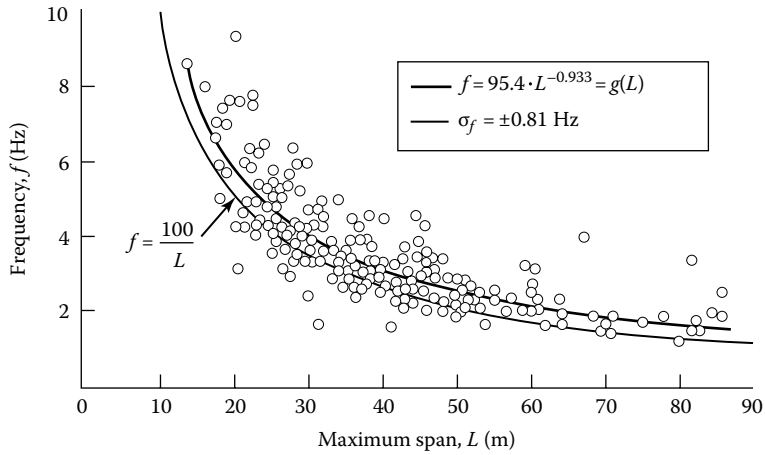

FIGURE 3.57 Natural frequency–span relationship (Cantieni 1984, Chan and O'Connor 1990a). (Reprinted with permission from ASCE, Reston, VA.)

The most significant aspect of Equation 3.34 is that the first natural frequency, and consequently, dynamic response based on this equation, is span-dependent.

Evaluation of the natural frequency from Equation 3.34 requires *a priori* the knowledge of the flexural stiffness, EI_x, of the superstructure. However, it is difficult to estimate this quantity because it depends on the flexural stiffness of the girders as well as the transverse flexibility of the slab and the diaphragms (Hwang and Nowak 1991b). Research, based on the results obtained by the Concrete Structures Section of the Swiss Federal Laboratories for Materials Testing and Research (EMPA) through static and standardized tests on 226 slab- and slab-and-beam-type highway bridges conducted from 1958 to 1981, suggested a fundamental frequency–span (m) relationship given by Equation 3.35 (Cantieni 1984):

$$f = 95.4L^{-0.933} \tag{3.35}$$

where L = span in meters.

A plot of Equation 3.35 is shown in Figure 3.57. It is seen that a curve defined by $Lf = 100$ also fits the data points and approximates Equation 3.35. A study (Chan and O'Connor 1990a) shows that characteristic curves bearing the relationship Lf = constant can be drawn for various types of superstructures (constant = 60, 90, 120, and 150), as shown in Figure 3.58.

In recognition of the significant influence of the natural frequency of the bridge superstructure (i.e., its dynamic characteristics), the 1983 edition of OHBDC (OHBDC 1983) specified values of dynamic allowance based on first flexural frequency of the bridge (Figure 3.59). However, this provision was revised and replaced in the 1993 OHBDC by the values of DLA as given in Table 3.15.

A major study (Nowak 1993a) undertaken at the University of Michigan for calibration of AASHTO LRFD code included research on the dynamic load effects of highway loadings on simply supported bridges, which considered the following three major factors as its basis (Hwang and Nowak 1991a,b):

1. Dynamic properties of the vehicle (mass, suspension, axle configuration, tires, speed)
2. Road roughness (approach, roadway, cracks, potholes, waves)
3. Dynamic properties of the bridge structure (span, mass, support types, material, geometry)

This research studied a variety of vehicle configurations (Figure 3.60): tractor with or without trailer(s), different axle loads, and axle spacings. The four most common vehicle types were

www.EngineeringEBooksPdf.com

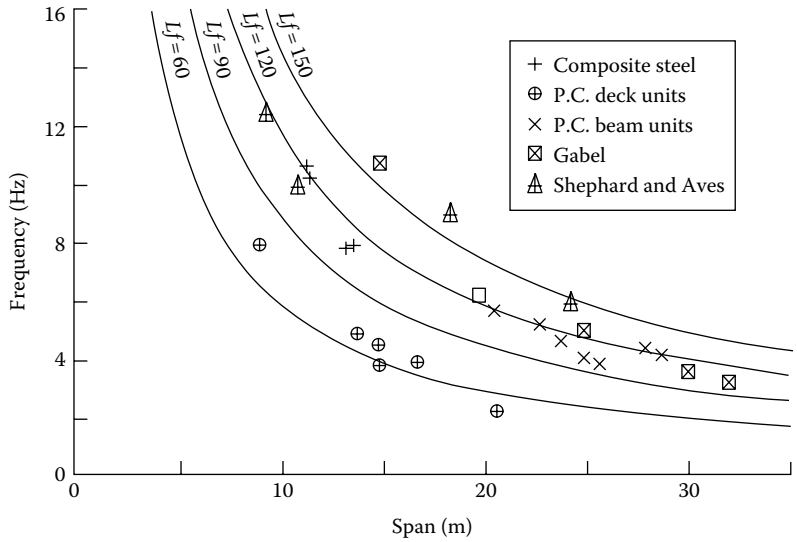

FIGURE 3.58 Natural frequency–span relationship for various superstructure types (Chan and O'Connor 1990). (Reprinted with permission from ASCE, Reston, VA.)

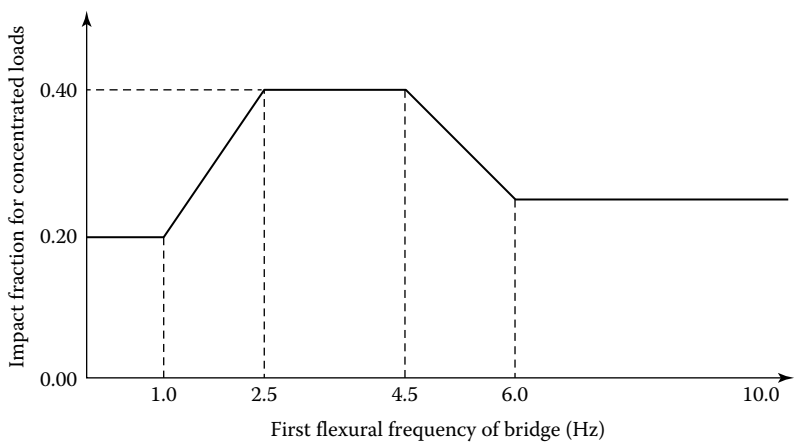

FIGURE 3.59 DLA according to the OHBDC.

TABLE 3.15
Dynamic Load Allowance

Number of Axles	DLA
1	0.4
2	0.3
3 or more	0.25

Source: OHBDC, *Ontario Highway Bridge Design Code*, 3rd ed., Ontario Ministry of Transportation, Downsview, Ontario, Canada, 1983.

www.EngineeringEBooksPdf.com

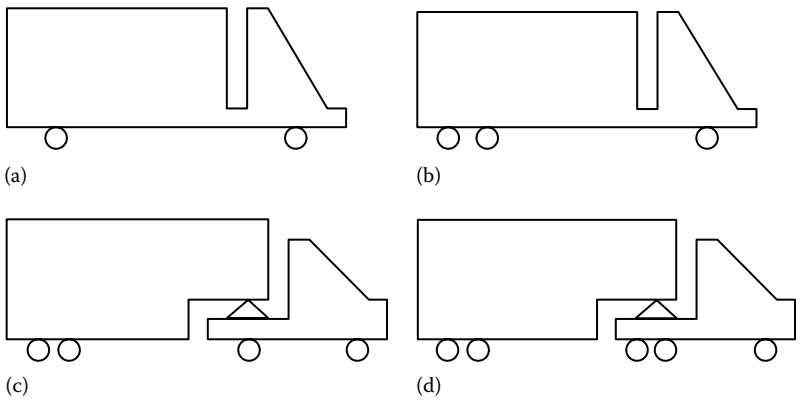

FIGURE 3.60 Trucks used in the Hwang and Nowak study (Hwang and Nowak 1991b). (a) Two-axle single truck (*S*2), (b) three-axle single truck (*S*3), (c) four-axle tractor-trailer (*T*4), and (d) five-axle tractor-trailer (*T*5). (Reprinted with permission from Transportation Research Board, Washington, DC.)

TABLE 3.16
Weight Distribution and Axle Distances

	Weight Distribution (percent)			
Truck Type	**Front**	**Middle**	**Rear**	**Axle Distances (ft)**
S2	40		60	16.0
S3	31		69	18.2
T4	24	39	37	12.0, 29.7
T5	18	47	35	14.0, 33.1

Source: Reprinted with permission from TRB, *50 Years of Interstate Structures—Past, Present, and Future*, Transportation Research Circular E-C104, Transportation Research Board, National Academies, Washington, D.C., September 2006, 145pp, 2006.

considered: two single trucks, namely, S2 and S3, and two semitractor trailers, namely, T4 and T5 (loads and spacing configurations listed in Table 3.16). Typically, the truck was modeled as a rigid body mounted on wheels with tires and multileaf leap spring type suspension and represented as a trapezoidally distributed mass (Figure 3.61) with a constant density subjected to rigid body motions. Tires were treated as linear elastic springs, and the leaf springs as nonlinear devices that dissipated energy during each cycle of oscillation (Hwang and Nowak 1991b). The characteristics of the tires and suspension system were modeled as suggested by Fancher et al. (1980) and Fancher and Ervin (1986).

Figure 3.62 shows cross sections of the slab–girder-type bridge cross sections that were used in this study. Figures 3.63 and 3.64 show typical static and dynamic live load responses of trucks of different weights versus various span lengths. Note that static response increases linearly (elastic response) with truck weights, whereas the dynamic response remains almost unchanged with increase in truck weights. Figures 3.65 and 3.66 show, for various span lengths, correlationships between the truck weights and dynamic load factor. Both figures indicate independence of load factors with increasing spans lengths. Figure 3.67 shows a plot of time history for midspan-static and midspan-dynamic deflections, which shows that dynamic deflection is only a small percentage of static deflection. Table 3.17 summarizes the dynamic load factors for various truck types listed in Table 3.16.

www.EngineeringEBooksPdf.com

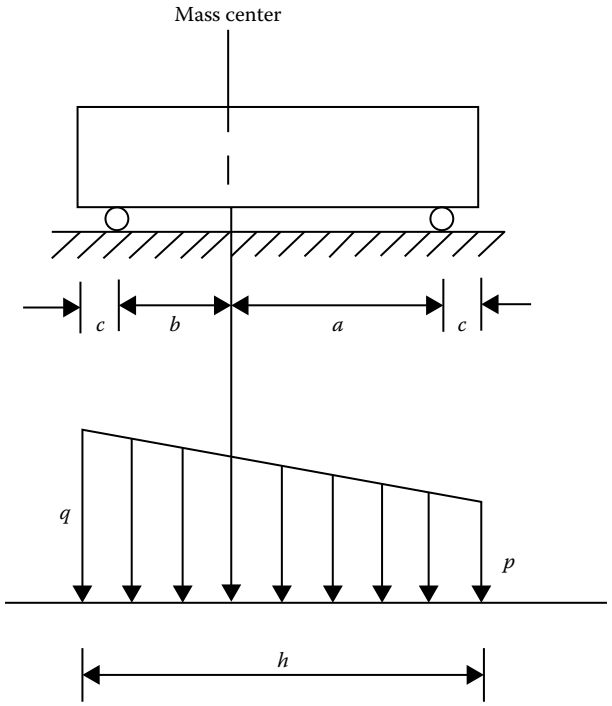

FIGURE 3.61 Truck body model used in Hwang and Nowak study (Hwang and Nowak 1991b). (Reprinted with permission from Transportation Research Board, Washington, DC.)

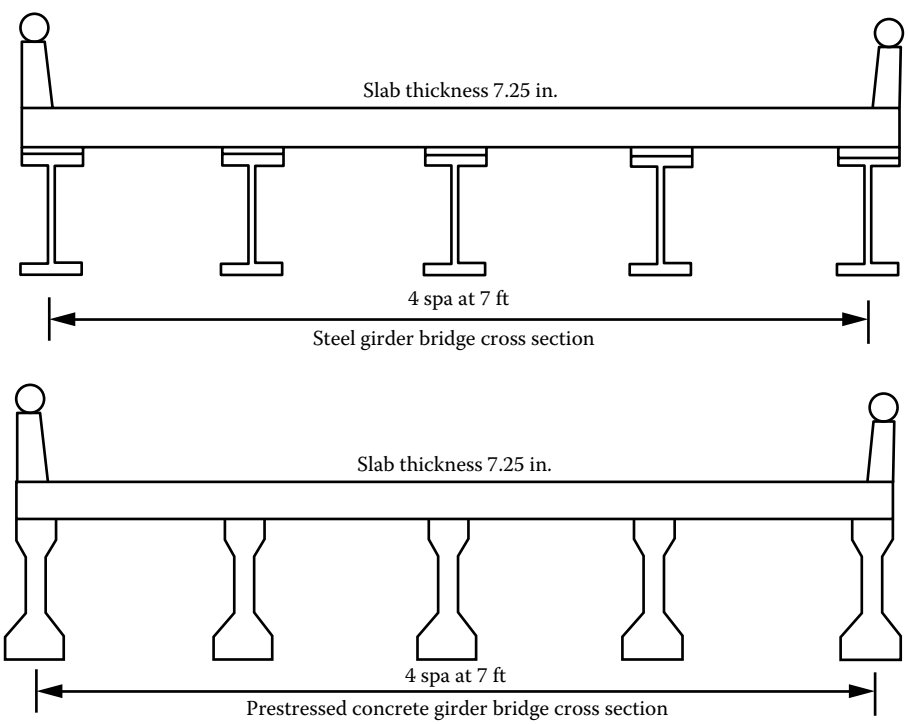

FIGURE 3.62 Bridge cross sections used in the University of Michigan's DLA study (Nowak 1993a). (Reprinted with permission from Transportation Research Board, Washington, DC.)

www.EngineeringEBooksPdf.com

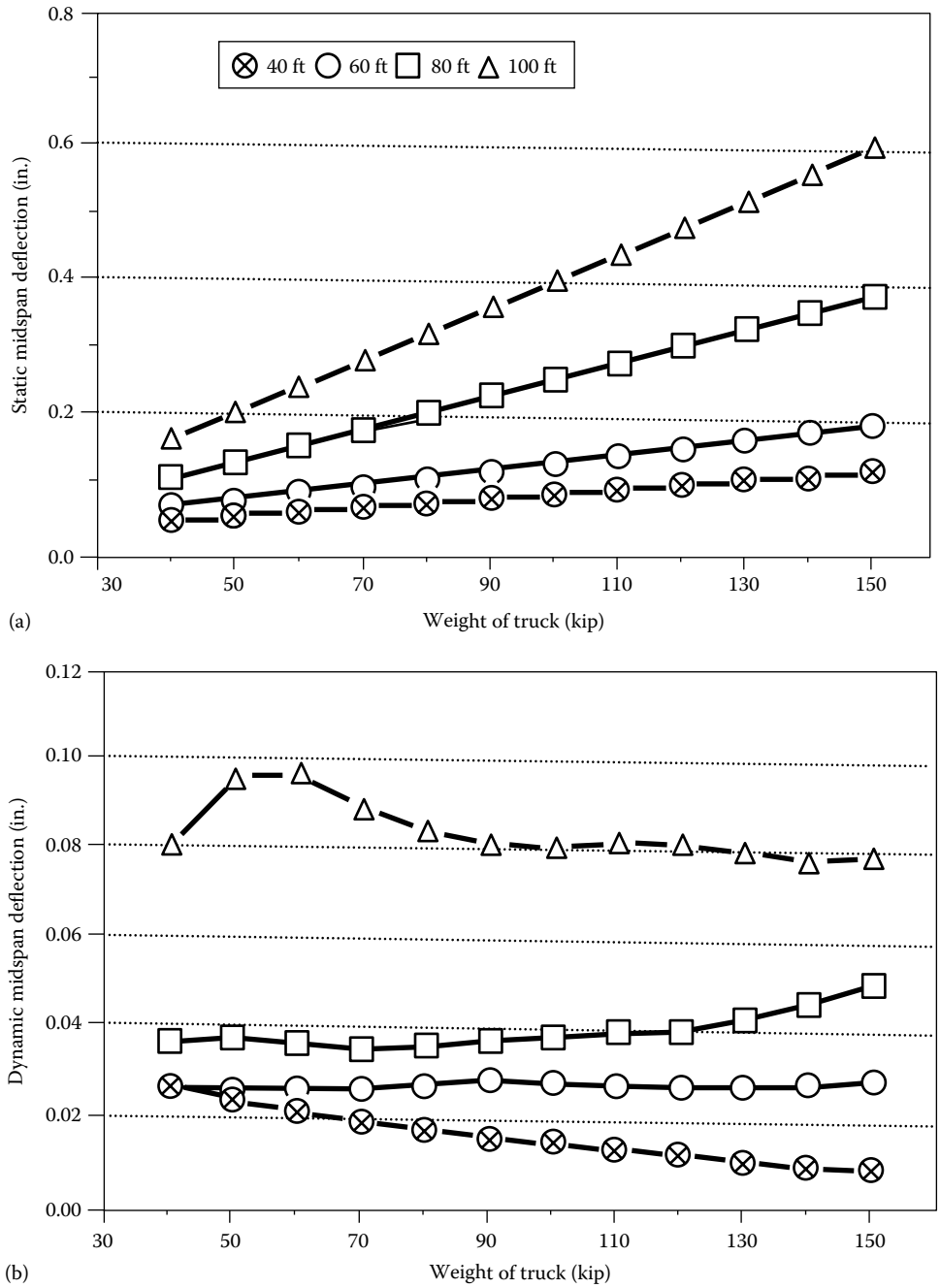

FIGURE 3.63 Live load response (of bridge cross sections shown in Figure 3.62) for various truck weights and spans. (a) Static response increases linearly with truck weights, whereas (b) the dynamic response remains almost unchanged with increase in truck weights (Nowak 1993a). (Reprinted with permission from Transportation Research Board, Washington, DC.)

www.EngineeringEBooksPdf.com

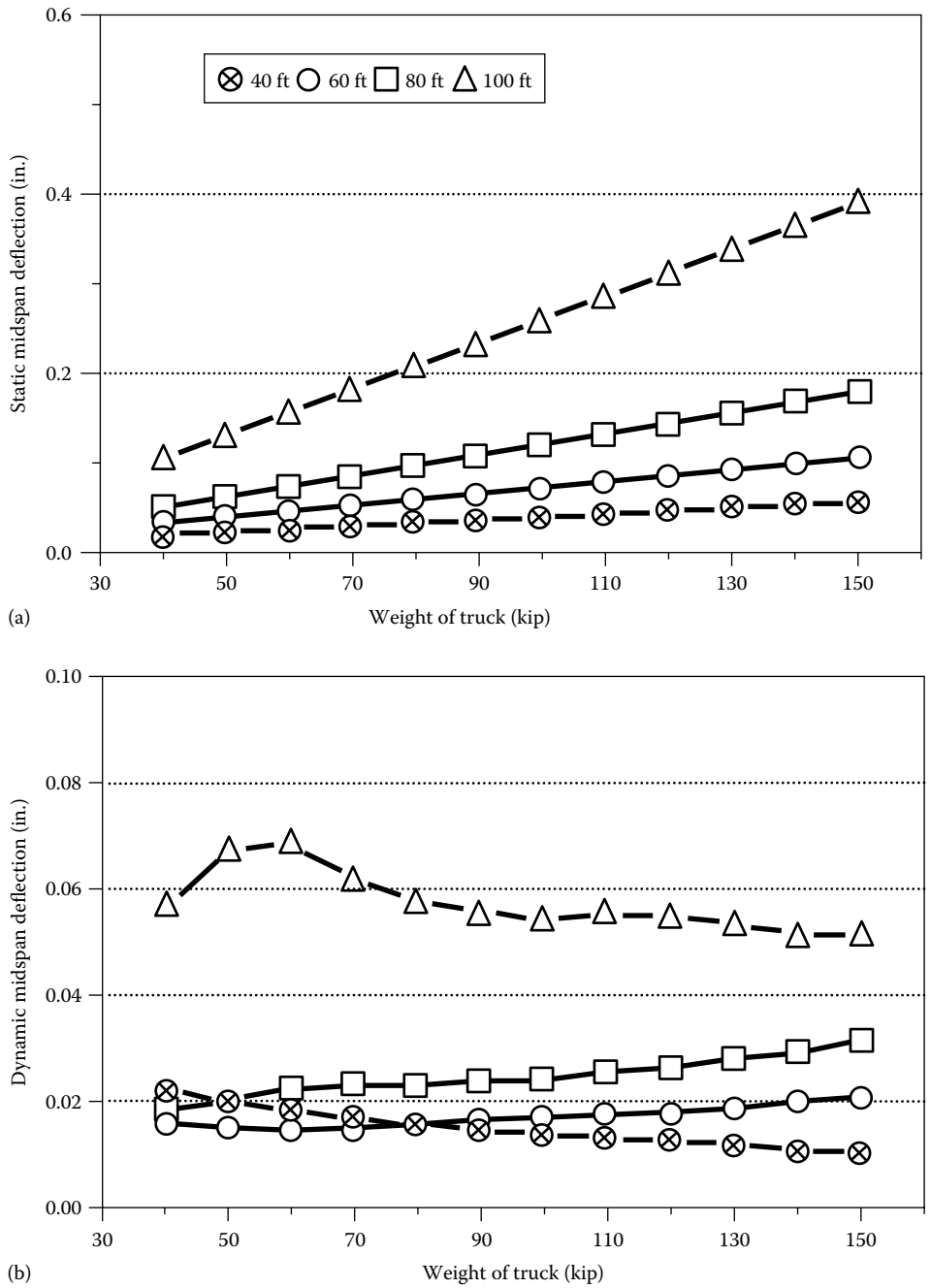

FIGURE 3.64 Typical live load response (of bridge cross sections shown in Figure 3.62) for various truck weights and spans. (a) Static response increases linearly with truck weights, whereas (b) the dynamic response remains almost unchanged with increase in truck weights (Nowak 1993a). (Reprinted with permission from Transportation Research Board, Washington, DC.)

www.EngineeringEBooksPdf.com

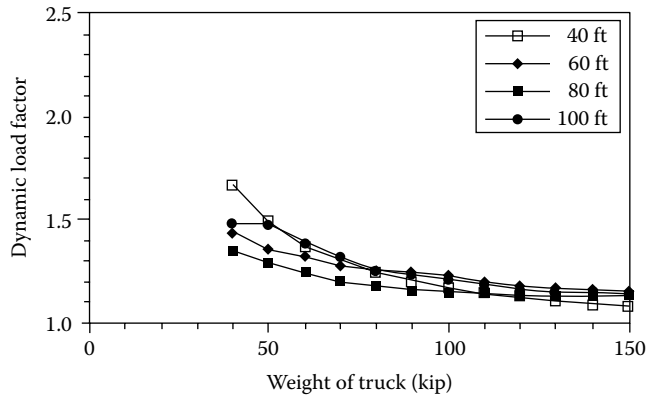

FIGURE 3.65 Relationship between truck weights and the dynamic load factor (Nowak 1993a). (Reprinted with permission from Transportation Research Board, Washington, DC.)

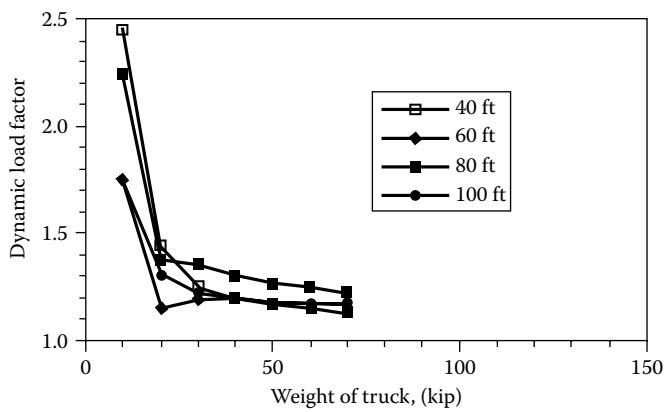

FIGURE 3.66 Relationship between truck weights and the dynamic load factor (Nowak 1993a). (Reprinted with permission from Transportation Research Board, Washington, DC.)

The worldwide research on dynamic load effects notwithstanding and inconsistencies in the definitions of dynamic load effects, expressed variously as *DLA*, DLF (ratio of dynamic midspan deflection to static deflection), and *impact* (IM), make the use of the end results difficult for uniform application in design (Bakth and Pinjarkar 1991, Paultre et al. 1992). A review of impact factors in highway bridge design codes worldwide can be found in a 1998 National Cooperative Highway Research Program (NCHRP) Report (NCHRP Synthesis 266). Figure 3.68 presents an overview of DLA–fundamental frequency relationship used by selected countries. This suggests DLA being span dependent because the natural frequency depends on span length, *L*.

3.8.3 AASHTO LRFD Specifications for Dynamic Load Allowance

AASHTO LRFD Art. 3.6.2.1 (AASHTO LRFD 2012) specifies that static load effects be increased by a factor called *DLA*, which is defined as "an increment to be applied to the static wheel load to account for wheel load impact from moving vehicles." Typically, all bridge design codes account for the dynamic effects of vehicular loads by incrementing the static load effects by a load factor (called the *IM* in AASHTO Standard).

www.EngineeringEBooksPdf.com

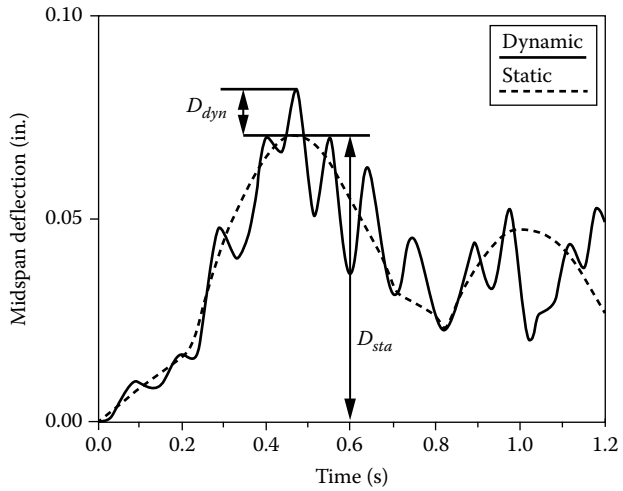

FIGURE 3.67 Time history of midspan-static and midspan-dynamic live load responses for typical slab–girder bridge cross sections (Nowak 1993a). (Reprinted with permission from Transportation Research Board, Washington, DC.)

TABLE 3.17
Dynamic Load Factors (DLF[a]) for Various Truck Types

Truck Type	Mean DLF	Standard Deviation
S2	1.288	0.184
S3	1.249	0.168
T4	1.179	0.096
T5	1.271	0.171

Source: Reprinted with permission from Hwang, E.S. and Nowak, A.S., *Dynamic Analysis of Girder Bridges*, Transportation Research Record 1223, National Research Council, Washington, DC, 1991b.

[a] DLF = dynamic deflection/static deflection.

Field tests indicate that in the majority of highway bridges, the dynamic component of the response does not exceed 25 percent of the static response to vehicles. This is the basis for the DLA included in the AASHTO LRFD Specifications, except for the deck joints. However, the specified live load combination of design truck and lane load represents a group of exclusion vehicles that are 4/3 of those caused by the design truck alone on short- and medium-span bridges. The 33 percent value of *IM* in Table 3.24 is the product of 4/3 and the basic 25 percent value ($25 \times 4/3 \approx 33$). Thus, the dynamic effects of vehicular load are treated as equivalent static loads.

One may wonder as to dynamic load effects on a bridge due to the presence of multiple loaded lanes. It is noted that the dynamic effects are moderated as follows:

1. As the weight of the vehicle goes up, the apparent amplification goes down.
2. Multiple vehicles produce a lower dynamic amplification than a single vehicle.
3. More axles result in a lower dynamic amplification.

Dynamic effects of vehicular live load are taken into account by applying to the static effects of design truck or tandem (but not to the effects of lane load) factors referred to as *DLA* or *IM* factors

www.EngineeringEBooksPdf.com

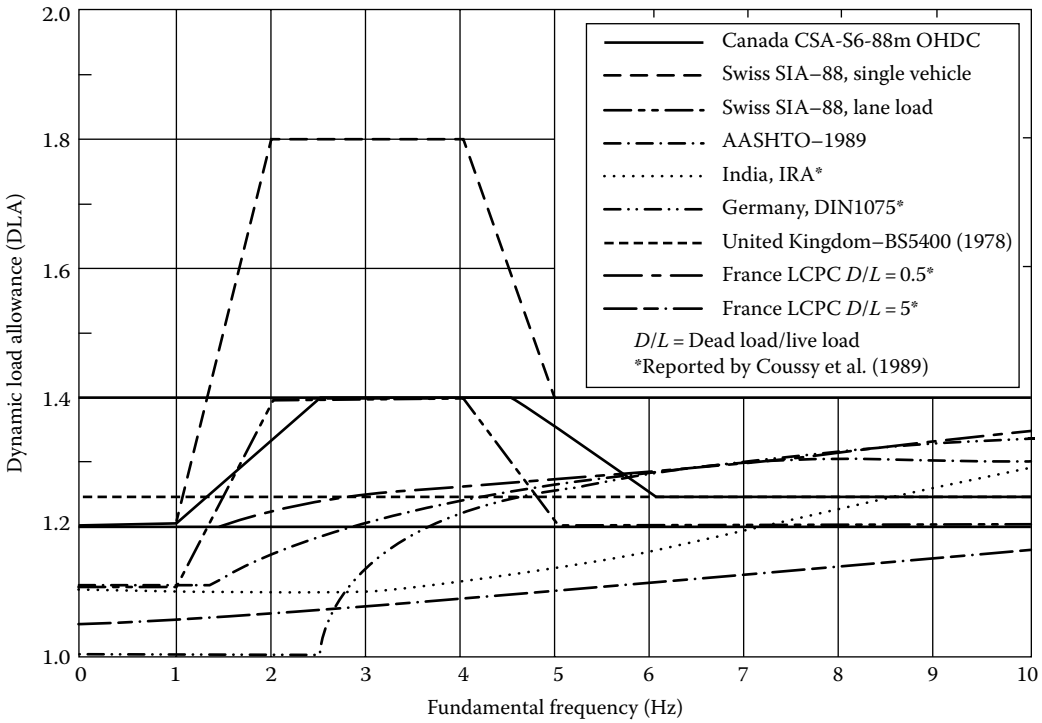

FIGURE 3.68 DLA used for highway bridge design by selected countries. (From Paultre, P. et al., *Canadian Journal of Civil Engineering*, 19, 260, 1992. Reprinted with permission from Canadian Association of Civil Engineers, Westmount, Quebec, Canada.)

TABLE 3.18
Dynamic Load Allowance (*IM*)

Components	*IM*
Deck joints—all limit states	75 percent
All other components	
Fatigue and fracture limit states	15 percent
All other limit states	33 percent

listed in Table 3.18 (AASHTO LRFD Table 3.6.2.1-1). The obvious simplicity of using AASHTO LRFD approach versus using frequency–DLA relationship (Figure 3.68) can hardly be emphasized.

The factor to be applied to the static load effects is to be taken as (1 + *IM*/100). Thus, the *total* live load effects from HL-93 loading (i.e., including the DLA) are obtained from Equation 3.36:

$$Q_{HL\text{-}93} = (Q_{truck} \text{ or } Q_{tandem})(1 + IM) + Q_{lane} \tag{3.36}$$

As indicated by the last term in Equation 3.36, DLA is *not* applicable to the design lane load. Table 3.24 shows that in order to account for the dynamic effects of live load on a bridge superstructure, shears and moments in beams and girders caused by HS20 truck or tandem (whichever governs) would need to be increased by 33 percent, and added to the corresponding force effects caused by the lane load (without increasing it for dynamic load influence). See Examples 3.13 and 3.14.

www.EngineeringEBooksPdf.com

The discussion in the preceding text notwithstanding, it must be recognized these specifications are applicable to only the superstructure types discussed in Chapter 2. DLA factors for any other types of superstructures, such as fiber-reinforced polymer (FRP) composite bridges, must be evaluated experimentally and substantiated by field tests as for practical applications (Paultre et al. 1992, Aluri et al. 2005).

Example 3.13

Determine the maximum design moment in a simple span of 84 ft due to AASHTO LRFD live load.

Solution

From Example 3.6, the following moment values are obtained for L = 84 ft:

$$M_{tr} = 1236.66 \text{ kip-ft}$$

$$\text{DLA, } IM = 33 \text{ percent (Table 3.24)}$$

$$M_{tr} \text{ incl. DLA} = (1236.66)(1 + 0.33) = 1644.76 \text{ kip-ft}$$

$$M_{lane} = 564.48 \text{ kip-ft}$$

$$M_{total} = 1644.76 + 564.48 = 2209.24 \text{ kip-ft}$$

(**Note:** DLA is *not* applied to moment due to the lane load.)

Example 3.14

Determine the maximum reaction at the left support for the single-span bridge of Example 3.13 including the DLA.

Solution

The reaction at the left support is determined from Equation 3.25 for x = 0:

$$V_x = \frac{72}{L}\left(L - x - 9.33\right) \tag{3.25}$$

$$R_L = \frac{72}{84}\left(84 - 0 - 9.33\right) = 64 \text{ kip}$$

$$R_{A,tr} = 64.0 \text{ kip}$$

DLA, IM = 33 percent
Including the DLA, $R_A = (64.0)(1.33) = 85.12$ kip

$$R_{A,lane} = \tfrac{1}{2}wL = 0.5(0.64)(84) = 26.88 \text{ kip}$$

Therefore, the maximum reaction at the left support, including the DLA, is

$$R_A = 85.12 + 26.88 = 112 \text{ kip}$$

(**Note:** DLA is *not* applied to reaction due to lane load.)

www.EngineeringEBooksPdf.com

Commentary: It is interesting to note that AASHTO LRFD-DLA applies to superstructures *irrespective of their span lengths*, a significant change from AASHTO Standard. In this context, two important differences in the values of DLA as compared to those specified in AASHTO Standard (AASHTO 2002, now archived) are noteworthy. First, called the *IM* (same as DLA in the *LRFD* version), the AASHTO Standard specified a value given by Equation 3.37, subject to an upper limit of 0.3 (i.e., 30 percent of the live load effects). Second, the IM (in the standard specification) was applied to *both* the truck and the lane load (truck or tandem only in AASHTO LRFD:

$$I = \frac{50}{L+125} \leq 0.3 \tag{3.37}$$

where L = span (ft).

Equation 3.37 implies that any span longer than 41.67 ft would have IM less than 0.3, whereas all spans smaller than 41.67 ft would have IM equal to 0.3. Of course, according to AASHTO LRFD, the DLA (same as IM) would be 0.33 for all span lengths for the case of strength limit states.)

A major drawback of Equation 3.37 was that it did not correlate well with the measured dynamic amplification, hence the need for change.

3.8.4 Exceptions to Application of Dynamic Load Effects

The DLA is *not* to be applied to the following loads and structural components:

1. Design lane load (see Equation 3.36)
2. Pedestrian loads
3. Incidental vehicles (e.g., snow removal and maintenance vehicles that may have access to sidewalks)
4. Retaining walls not subject to vertical reactions from the superstructure
5. Foundation components that are entirely below ground level
6. Wood components

Wood structures are excluded from the effects of DLA because they are known to exhibit reduced dynamic load response due to internal friction between the components and the dampening characteristics of wood. As for buried components, it is recognized that the soil cover provides a damping effect on a buried structure or a component such as a footing. To qualify for relief from dynamic effects of moving loads, it is required that the entire structure be buried under the soil. For the purposes of this relief provision, retaining walls are considered as buried to the top of the fill and not subject to DLA (i.e., $IM = 0$). However, the abutments are not exempt from dynamic load effects because of the presence of the vertical reactions from the superstructure.

The DLA for culverts and other buried structures (specified in AASHTO LRFD Specifications Section 12), in percent, is given by Equation 3.38:

$$IM = 33(1.0 - 0.125D_E) \geq 0 \text{ percent} \tag{3.38}$$

where D_E = the minimum depth of earth cover (ft) above the structure.

Equation 3.38 shows that a structure or a component under 8 ft or greater depth of soil cover would be free from the dynamic effects of moving loads (i.e., $IM = 0$ for $D_E \geq 8$ ft). Note that the value of *IM* cannot be negative.

www.EngineeringEBooksPdf.com

3.9 FATIGUE LOADING

3.9.1 Fatigue Phenomenon

The *fatigue* phenomenon and its importance in bridge design were briefly discussed in Chapter 1. AASHTO LRFD deals with *fatigue* as one of the four limit states for design of superstructures, the other three being strength, extreme event, and service limit states.

Fatigue must be considered whenever a structure or any of its components is subjected to cyclic loading, resulting in alternating stresses (stress change from compression to tension or *vice versa*) or fluctuation in tensile stresses (from some low value when the live load is not present to some high value when full live load is present). The effect of alternating stresses can be best observed by unbending and bending a paper clip several times; after a few cycles of unbending and bending, the clip snaps into two pieces. This happens because under cyclic load conditions, the stress level that fractures a material can be significantly below its normal yield strength. Because of the presence of moving loads on a bridge, elements of its superstructure (such as beams and girders, truss members) are subjected to cyclic loading, which causes cyclic stress changes in structural members. Therefore, in order to preclude the possibility of fatigue failure, one must know the threshold value of stress cycles N, which must not be exceeded during the service life of a bridge structure. Discussion of AASHTO LRFD methodology of determining N follows. A brief discussion on evolution of fatigue phenomenon can be found in Taly (1998).

3.9.2 Magnitude and Configuration of Live Load for Fatigue Considerations

AAASHTO LRFD Art. 3.6.1.4 specifies the following criteria for determining the fatigue load for bridge superstructures; its magnitude and configuration are illustrated in Figure 3.69:

1. The fatigue load consists of one design truck or axles thereof; tandem or the lane load is *not* to be considered. The reasoning behind this specification is the fact that HL-93 live model is somewhat conservative in that it is based on exclusion vehicles to estimate the live load force effects. But a majority of trucks do not exceed the legal limits. In recognition of this reality, it is considered unduly conservative to use the full live load force effects for the purpose of calculating the stress range for fatigue design. For fatigue design, one has to consider the stress range and the number of stress cycles under service load conditions (see discussion in Chapter 1). Therefore, a lesser load is considered reasonable to estimate the force effects for fatigue design.

   Two levels of fatigue limit state are recognized: Fatigue I and Fatigue II.

   The load factor for Fatigue I Limit State is 1.5, which reflects load levels found to be representative of the maximum stress range of the truck population for infinite fatigue life

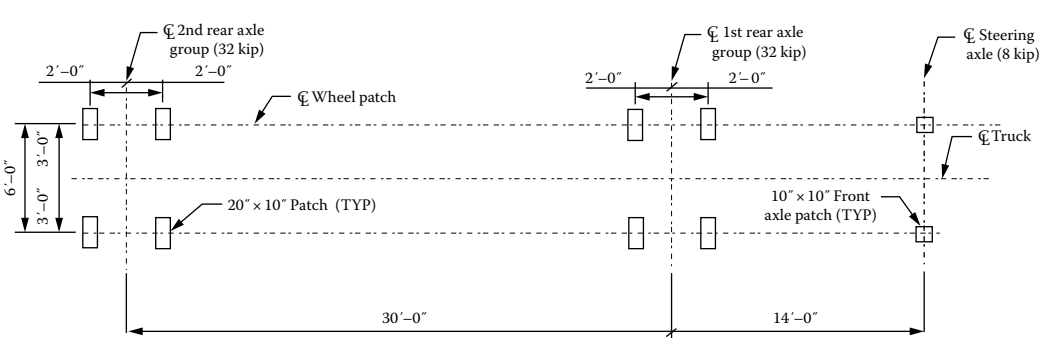

FIGURE 3.69 Refined design truck footprint for fatigue design. (From *AASHTO LRFD Bridge Design Specifications*, Copyright © 2012 by American Association of State Highway and Transportation Officials, Washington, DC. Used by permission.)

www.EngineeringEBooksPdf.com

design. This factor was chosen on the assumption that maximum stress range in the random variable spectrum is twice the stress range caused by Fatigue II Load Combination.

The load factor for Fatigue II Limit State is 0.75. It reflects load levels found to be representative of the effective stress range of the truck population with respect to a small number stress range cycles and to their cumulative effects in steel elements, components, and connections for finite fatigue life.

2. In both Fatigue Limit States (I and II), the loading consists of a single design truck with the constant spacing between the two 32 kip axles of 30 ft.
3. The DLA (1.15) is applicable to fatigue load (*IM* = 15 percent for fracture and fatigue limit state, Table 3.18).
4. Live load distribution factors (discussed in Chapter 4) are applicable to fatigue loading.
5. The multiple presence factor (discussed earlier) is *not* applicable to loads for fatigue limit state; only one traffic lane occupied by HS20 truck is to be considered for design for fatigue load regardless of the number of traffic lanes (AASHTO LRFD Art. 3.6.1.1.2) on a bridge. The (approximate) equations for live load DFs (discussed in Chapter 4) include the multiple presence factor of 1.2 for one design lane loaded case. Therefore, the calculated live load DF for one lane loaded case should be divided by 1.2 before applying it to the fatigue loading.
6. For the design of orthotropic decks and wearing surfaces on orthotropic decks, the loading pattern shown in Figure 3.69 shall be used. Specifically, AASHTO LRFD *Commentary C3.6.1.4.1* calls for the middle and rear 16 kip wheel loads to be modeled in more detail as two closely spaced 8 kip wheel loads 4 ft apart to more accurately reflect modern tractor-trailer with tandem rear axles. These wheel loads should be distributed over the specified contact area (20 in. wide × 10 in. long) for rear axles and 10 in.^{2} (100 in.^{2}) for front axles. Because of the smaller patch area, the front wheels can be controlling loads for fatigue design for many orthotropic deck details. *Furthermore, this loading should be positioned both longitudinally and transversely on the bridge deck, ignoring the striped lanes, to create the worst stress or deflection, as applicable.*

3.9.3 Formulas for Maximum Moment and Shear for Fatigue Limit State Loading

3.9.3.1 Maximum Moment for Fatigue Limit State

Similar to the discussion in Section 3.7.7 pertaining to determination of maximum live load bending moment in a simple span due to HL-93 truck, this section presents derivations of expressions that can be used to determine maximum bending moment in simple spans due to fatigue loading.

Figure 3.70 shows the position of HL-93 truck as it moves from left to right on a simple span. Note that the distance between the front (lead axle) and the middle axles is 14 ft whereas the distance between the middle and the rear axles is kept as 30 ft constant (*not* as variable between 14 and 30 ft as in Section 3.7.7). The formula for maximum moment for this position of HL-93 truck can be determined from the influence line (Figure 3.70) for the rear 32 kip axle load. The influence line ordinates corresponding to the three axle loads are determined as follows:

x = distance from the left support to the rear axle load:

$$y_1 = \frac{x(L-x)}{L}$$

$$y_2 = y_1\left(\frac{L-x-30}{L-x}\right) = \left(\frac{x(L-x)}{L}\right)\left(\frac{L-x-30}{L-x}\right) = \left(\frac{x(L-x-30)}{L}\right)$$

$$y_3 = y_1\left(\frac{L-x-44}{L-x}\right) = \left(\frac{x(L-x)}{L}\right)\left(\frac{L-x-44}{L-x}\right) = \left(\frac{x(L-x-44)}{L}\right)$$

www.EngineeringEBooksPdf.com

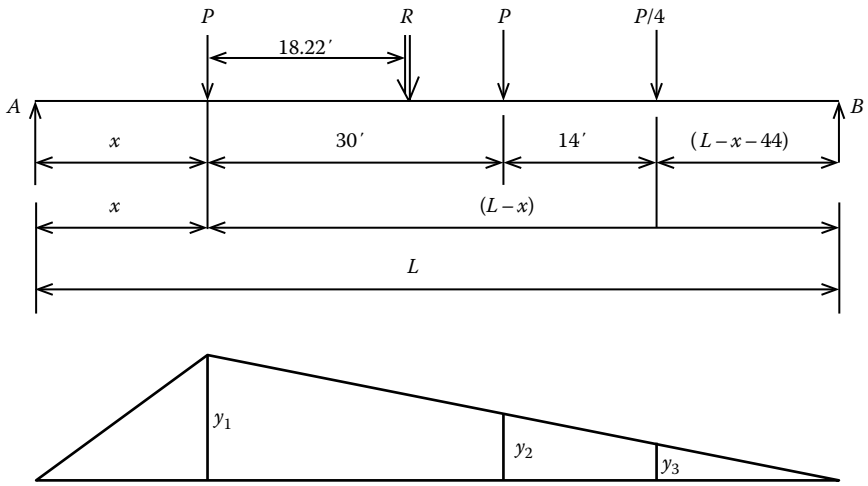

FIGURE 3.70 Position of the HS20 truck for maximum moment in a simple span for fatigue limit state loading when the truck moves from left to right.

From Equation 3.10,

$$M_x = P_1 y_1 + P_2 y_2 + P_3 y_3$$

Substitution for y_1, y_2, and y_3 from earlier and $P_1 = P_2 = P$ and $P_3 = P/4$ in Equation 3.10 yields

$$M_x = P\left(\frac{x}{L}\right)(L-x) + P\left(\frac{x}{L}\right)(L-x-30) + \frac{P}{4}\left(\frac{x}{L}\right)(L-x-44)$$

$$= \frac{Px}{L}(2.25L - 2.25x - 41)$$

Substitution of $P = 32$ kip in the aforementioned equation yields Equation 3.39:

$$M_x = \frac{72x}{L}(L - x - 18.22) \tag{3.39}$$

Because of the selected axle positions in Figure 3.70, Equation 3.39 is valid for the span range $0 < x/L \leq 0.241$ and for a minimum values of $x = 0$ ft and $L = 44$ ft.

Now, consider the position of HS20 truck on the span as it moves from right to left. Figure 3.71 shows the position of the HS20 truck as it moves across the span from right to left. The middle 32 kip axle is positioned at a distance x from the left support, for which influence lines are also shown in the figure. The influence line ordinates corresponding to the three axle loads are calculated as follows:

x = distance from the left support to the middle axle load:

$$y_1 = \frac{x(L-x)}{L}$$

$$y_2 = y_1\left(\frac{L-x-30}{L-x}\right) = \left(\frac{x(L-x)}{L}\right)\left(\frac{L-x-30}{L-x}\right) = \frac{x(L-x-30)}{L}$$

www.EngineeringEBooksPdf.com

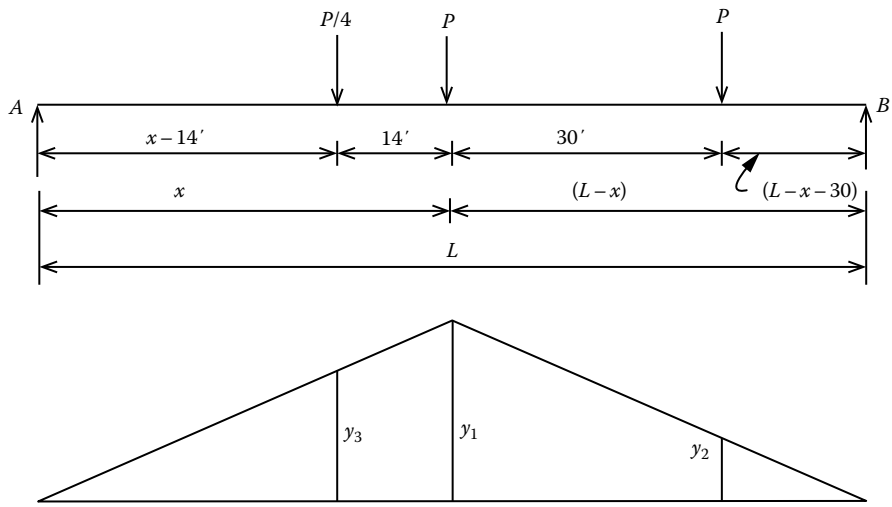

FIGURE 3.71 Position of the HS20 truck for maximum moment at any point in a simple span when the truck moves from right to left.

$$y_3 = y_1\left(\frac{L-14}{x}\right) = \left(\frac{x(L-x)}{L}\right)\left(\frac{x-14}{x}\right) = \left(\frac{(L-x)(x-14)}{L}\right)$$

From Equation 3.10,

$$M_x = P_1y_1 + P_2y_2 + P_3y_3 = P\left(y_1 + y_2 + \frac{y_3}{4}\right)$$

where $P_1 = P_2 = P$ and $P_3 = P/4$.

Substitution for y_1, y_2, and y_3 in the aforementioned expression yields the following expression:

$$M_x = \frac{P}{L}\left[x(L-x) + x(L-x-30) + \frac{1}{4}(L-x)(x-44)\right]$$

Simplifying the aforementioned expression yields Equation 3.40:

$$M_x = \frac{2.25Px}{L}(L-x-11.78) - 3.5P \tag{3.40}$$

Substitution of $P = 32$ kip in Equation 3.40 yields Equation 3.41:

$$M_x = \frac{72x}{L}(L-x-11.78) - 112 \tag{3.41}$$

Equation 3.41 is valid for the span range $0.241 \le x/L \le 0.500$ and $x_{min} = 14$ ft and $L_{min} = 42$ ft.

The foregoing results are summarized in Table 3.19.

Example 3.16 illustrates the application of Equations 3.39 and 3.41.

www.EngineeringEBooksPdf.com

TABLE 3.19
Maximum Bending Moment in Simple Spans Due to Fatigue Limit State Loading

		Minimum		
x/L	Formula for Maximum Bending Moment (kip-ft)	*x*, ft	*L*, ft	Equation No.
0–0.241	$M_x = \frac{72x}{L}(L - x - 18.22)$	0	44	3.39
0.241–0.500	$M_x = \frac{72x}{L}(L - x - 11.78) - 112$	14	28	3.41

Note: *x*, distance from the left support to the section being considered, ft.

3.9.3.2 Maximum Shear for Fatigue Limit State

Figure 3.72a shows the various positions of HS20 truck and corresponding influence lines for maximum shear in a simply supported beam. Maximum positive shear at the left support equals maximum reaction at that support, which occurs when the truck is moving from left to right and rear 32 axle is positioned on it. From Figure 3.72a,

$$R_A = 32\left[1 + \left(\frac{L-30}{L}\right)\right] + 8\left(\frac{L-44}{L}\right)$$

$$V_A = R_A = 72 - \frac{1312}{L} \tag{3.42}$$

Positive shear at a distance x from the left support is obtained from the IL for shear at that location. The IL ordinates under the loads are (Figure 3.72b)

$$y_1 = \frac{L-x}{L}, \quad y_2 = \frac{L-x-30}{L}, \quad y_3 = \frac{L-x-44}{L} \tag{3.43}$$

$$V_x = 32\left[\left(\frac{L-x}{L}\right) + \left(\frac{L-x-30}{L}\right)\right] + 8\left(\frac{L-x-44}{L}\right)$$

$$V_x = 72\left(1 - \frac{x}{L}\right) - \frac{1312}{L} \tag{3.44}$$

Equation 3.44 is valid for $0 < x \le (L - 44)$ ft. For $x > (L - 44)$ ft, the lead 8 kip axle is off span, so the positive shear is obtained from the IL as shown in Figure 3.72c. The IL ordinates under the two 32 kip axles are calculated to be as given by Equation 3.45:

$$y_1 = \frac{L-x}{L}, \quad y_2 = \frac{L-x-30}{L} \tag{3.45}$$

The positive corresponding to Equation 3.45 is obtained from the IL line ordinates:

$$V_x = 64\left(1 - \frac{x}{L}\right) - \frac{960}{L} \tag{3.46}$$

www.EngineeringEBooksPdf.com

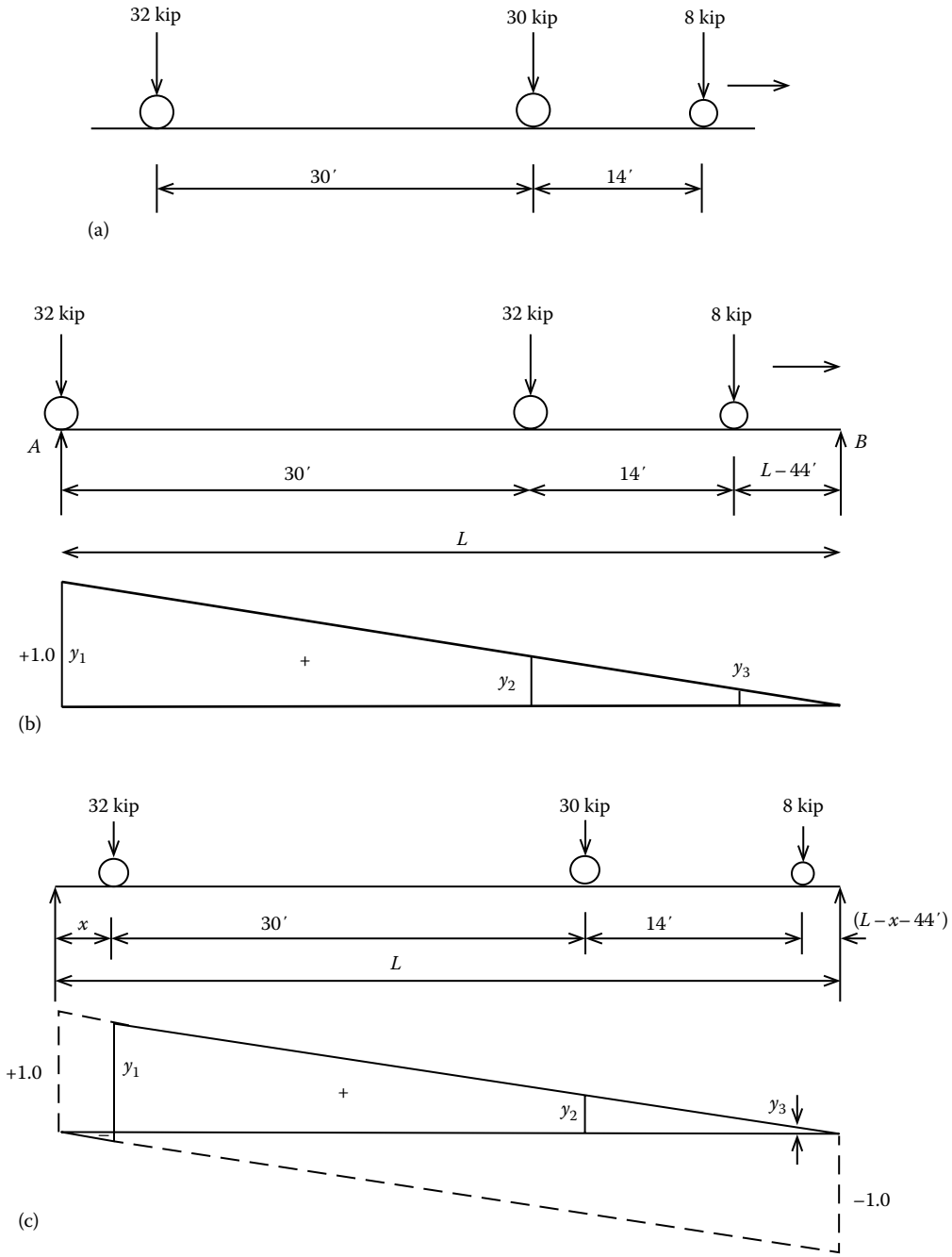

FIGURE 3.72 Position of the HL-93 fatigue truck and influence lines for maximum shear at any point in a simple span when the fatigue truck moves from left to right: (a) fatigue truck configuration; (b) influence line for maximum shear in the span with all three axles on span; (c) influence line for shear at a section distant x from the left support, with all three axles on span. (*Continued*)

www.EngineeringEBooksPdf.com

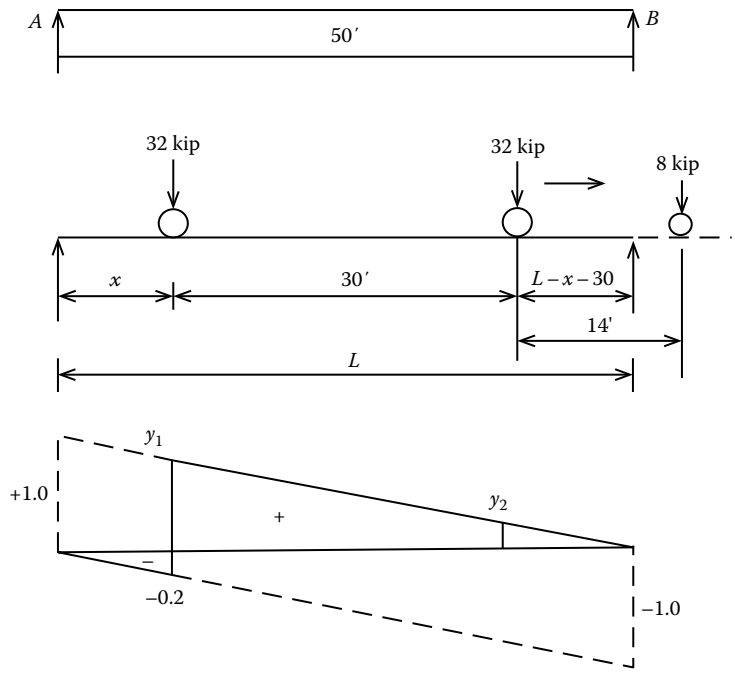

(d)

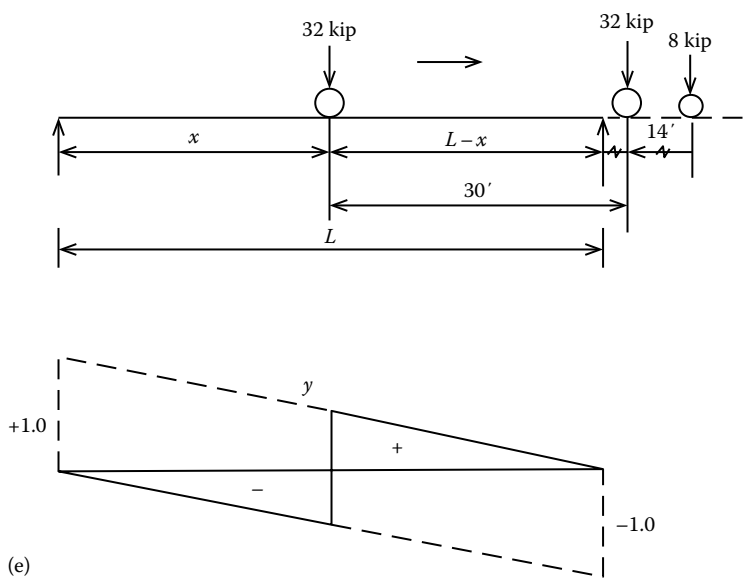

(e)

FIGURE 3.72 (*Continued*) Position of the HL-93 fatigue truck and influence lines for maximum shear at any point in a simple span when the fatigue truck moves from left to right: (d) influence line for maximum shear at a section distant x from the left support, with only the two 32 kip axles on span and the 8 kip axle off span; and (e) influence line for maximum shear at a section distant x from the left support, with only the rear 32 kip axle on span and the middle 32 kip and the 8 kip axles off span.

www.EngineeringEBooksPdf.com

Equation 3.46 is valid for $0 < x\ (L - 30)$ ft. For $x > (L - 30)$ ft, both the lead 8 kip axle and the middle 32 kip axles are off span, so the positive shear is obtained from the IL as shown in Figure 3.72d. The IL ordinate under the rear 32 kip axle is calculated to be as given by Equation 3.47:

$$y_1 = \frac{L - x}{L} \tag{3.47}$$

The positive shear corresponding to Equation 3.47 is given by Equation 3.48:

$$V_x = 32\left(1 - \frac{x}{L}\right) \tag{3.48}$$

Calculations for design for shear require determination of stress range at selected beam cross sections. Therefore, at every one-tenth point on span (at every $0.1L$), both positive and negative shear values are required. The values of positive shear can be calculated from Equations 3.43 through 3.48; those of negative at these points can be determined from the principle of antisymmetry. Applications of Equations 3.39 through 3.48 are illustrated in Example 3.18.

Example 3.15 illustrates application of equations derived in the preceding discussion for determining moments and shear due to AASHTO LRFD fatigue loading in simply supported spans.

Example 3.15

Determine (a) moment at mid-span, (b) maximum shear in the span due to AASHTO LRFD fatigue loading in a simple span of 84 ft.

Solution

(a) Moment at mid-span
For the stated case, Equation 3.41 applies:

$$M_x = \frac{72x}{L}(L - x - 11.78) - 112$$

For $L = 84$ ft, $x/L = 0.5$, $x = 42$ ft, the above equation gives

$$M_x = \frac{72x}{L}(L - x - 11.78) - 112$$

$$= 72(0.5)(84 - 42 - 11.78) - 112$$

$$= 976 \text{ kip-ft}$$

(b) Maximum shear in span
For the stated case, the maximum shear in span is given by Equation 3.42:

$$V_{max} = 72 - \frac{1312}{L} = 72 - \frac{1312}{84} = 56.38 \text{ kip}$$

Discussion: It is instructive to compare mid-span moment and maximum shear in a simple span due to AASHTO fatigue truck with those due to the conventional HL-93 truck. Moment at mid-span due to conventional HL-93 truck is obtained from Equation 3.27:

$$M_x = \frac{72x}{L}(L - x - 4.67) - 112$$

www.EngineeringEBooksPdf.com

For the stated case, L = 84 ft, x = 42 ft, x/L = 0.5, which gives

$$M_{x=0.5L} = 72(0.5)(84-42-4.67)-112 = 1231.88 \text{ kip-ft}$$

The maximum shear in span due to conventional HL-93 truck is given by Equation 3.25:

$$V_{max} = R_{max} = \frac{72}{L}(L-x-9.33)$$

For L = 84 ft and x – 42 ft, the above equation gives

$$V_{max} = \frac{72}{84}(84-0-9.33) = 64.00 \text{ kip}$$

Note that, as expected, both the moment and shear due to AASHTO fatigue truck are smaller than those due to conventional HL-93 truck. This, of course, is due to the fact that the distance between the 32-kip axles of the fatigue truck is 30 ft as compared to a distance of 14 ft for the conventional HL-93 truck.

3.9.4 Frequency of Loading for Fatigue Design Considerations

Fatigue failure depends on the magnitude of load as well as the number of stress range cycles. Therefore, fatigue and fracture limit state is defined in terms of both the frequency of load occurrence and the accumulated stress range cycles. This section presents a discussion on the relationship between the traffic across a bridge and the stress range cycles (N).

The number of accumulated stress range cycles due to traffic crossing a bridge depends on the *single-lane average daily truck* traffic ($ADTT_{SL}$) (subscript *SL* stands for *single lane*). In the context of fatigue loading, a *truck* is defined as any vehicle with more than either two axles or four wheels. The $ADTT_{SL}$ refers to the truck traffic (in one direction) in the lane in which the majority of the truck traffic crosses the bridge.

The number of stress range cycles that must be determined to evaluate the fatigue and fracture limit states depends on three interrelated traffic parameters as follows:

1. Average daily traffic (ADT): This is the total number of vehicles of all kinds (cars and trucks) that is expected to cross a bridge in any one direction. Research has shown that ADT is physically limited to about 20,000 vehicles per lane per day under normal conditions. This limiting value of traffic should be considered as the default value when estimating the ADTT.
2. ADTT: The number of trucks crossing (in one direction) a bridge daily depends on the *class* of highway such as rural interstate, urban interstate, other rural, and other urban. In the absence of site-specific traffic data, ADTT can be determined by multiplying the ADT by a fraction, p_{TT} (Equation 3.49) as shown in Table 3.20 (AASHTO LRFD *Commentary C3.6.1.4.2*):

$$ADTT = (p_{TT})(ADT) \tag{3.49}$$

3. $ADTT_{SL}$: This is the number of trucks that can be expected in a single traffic lane in one direction. It is logical to think that the more the number of traffic lanes available to the

www.EngineeringEBooksPdf.com

TABLE 3.20
Fraction of Trucks in Traffic, p_{TT}

Class of Highway	Fraction of Truck Traffic, p_{TT} $ADTT = p_{TT}(ADT)$
Rural interstate	0.20
Urban interstate	0.15
Other rural	0.15
Other urban	0.10

truck, the less would be the number of trucks in a single lane. On a typical bridge, with no nearby entrance or exit ramps, the shoulder lane carries most of the traffic. However, because of the uncertainty of the future traffic patterns, the frequency of the fatigue load for a single lane is assumed for all lanes. The fraction of truck traffic in a single can be determined from Equation 3.50:

$$ADTT_{SL} = (p)(ADTT) \tag{3.50}$$

where
$ADTT$ = number of trucks per day in one direction averaged over design life
$ADTT_{SL}$ = number of trucks per day in a single lane averaged over the design life
p = fraction of truck traffic in a single lane (Table 3.21)

Thus, it is seen that of the three traffic parameters defined earlier, the $ADTT_{SL}$ is the defining parameter for evaluating the fatigue and fracture limit state of a highway bridge superstructure. The $ADTT_{SL}$ is related to the ADTT, which, in turn, is related to the ADT. The value of $ADTT_{SL}$ is required to determine the threshold number of stress cycles, N (discussion following Example 3.16), which, in turn, is required to determine the fatigue limit state design of load-carrying components.

In summary, a designer needs to estimate the number of trucks that can be expected to be in a single traffic lane on a bridge, $ADTT_{SL}$, the main parameter required to determine the threshold number of stress cycles N, which is determined as follows:

1. Find the ADT from the available data (traffic study); use 20,000 if traffic data are not available.
2. Calculate the ADTT (Equation 3.49), by multiplying ADT with the percentage of daily truck traffic (p_{TT}) given in Table 3.20.
3. Determine the number of traffic lanes available (designated) to truck traffic on the bridge (from traffic data).

TABLE 3.21
Fraction of Truck Traffic in a Single Lane, p

Number of Traffic Lanes Available to Trucks	p
1	1.00
2	0.85
3 or more	0.80

www.EngineeringEBooksPdf.com

TABLE 3.22
Number of Cycles per Truck Passage, *n* (AASHTO LRFD Table 6.6.1.2.5-2)

	Span Length	
Longitudinal Members	**>40 ft**	**≤40 ft**
Simple-span girders	1.0	2.0
Continuous girders		
Near interior support	1.5	2.0
Elsewhere	1.0	2.0
Cantilever girders	5.0	
Trusses	1.0	
	Spacing	
Transverse Members	**>20 ft**	**≤20 ft**
	1.0	2.0

Source: From *AASHTO LRFD Bridge Design Specifications*, Copyright © 2012 by American Association of State Highway and Transportation Officials, Washington, DC. Used by permission.

4. Based on the number of traffic lanes on the bridge available to truck traffic, find the fraction of truck traffic for single lane (p) from Table 3.21.
5. Calculate the $ADTT_{SL}$ by multiplying ADTT with p (Equation 3.50).
6. Find the number of stress cycles per truck passage, n, from Table 3.22.
7. Calculate the threshold number of stress cycles N from Equation 3.51 (Section 3.9.5).

Example 3.16 illustrates the use of information presented earlier.

Example 3.16: Determination of $ADTT_{SL}$ for a Highway Bridge

It is required to determine the $ADTT_{SL}$ for two bridges that carry a four-lane interstate highway in a large metropolitan area. One of the bridges is located in the commercial and industrial area for which the site-specific study shows that the trucks account for about 25 percent of the traffic and that two traffic lanes are available for truck traffic. The other bridge is located in a rural area where three traffic lanes are allowed to truck traffic. Determine the average $ADTT_{SL}$ for these bridges. The ADT for an interstate highway may be taken as 20,000 for a 75-year design life.

Solution

1. Bridge in the commercial/industrial area

$$ADTT = (p_{TT})(ADT)$$

$$ADT = 20{,}000 \text{ vehicles per day}$$

Fraction of trucks in traffic p_{TT} = 25 percent = 0.25 (site-specific study)

$$ADTT = (p_{TT})(ADT) = (0.25)(20{,}000) = 5000 \text{ trucks per day}$$

For two lanes available to truck traffic, $p = 0.85$ (Table 3.21)

$$ADTT_{SL} = p(ADTT) = (0.85)(5000) = 4250 \text{ trucks}$$

www.EngineeringEBooksPdf.com

Had the site-specific traffic study not been available, the bridge would be considered as being in an urban interstate highway, for which $p_{TT} = 0.2$ (Table 3.20). Thus,

$$ADTT = (p_{TT})(ADT)$$

$$ADT = 20{,}000 \text{ vehicles per day}$$

Fraction of trucks in traffic, $p_{TT} = 0.20$ (Table 3.20)

$$ADTT = (p_{TT})(ADT) = (0.20)(20{,}000) = 4000 \text{ trucks}$$

For three lanes available to truck traffic, $p = 0.80$ (Table 3.21)

$$ADTT_{SL} = (p)(ADTT) = (0.80)(4000) = 3200 \text{ trucks}$$

2. Bridge in the rural area

$$ADTT = (p_{TT})(ADT)$$

$$ADT = 20{,}000 \text{ vehicles per day}$$

Fraction of trucks in traffic, $p_{TT} = 0.20$ (Table 3.20)

$$ADTT = (p_{TT})(ADT) = (0.20)(20{,}000) = 4000$$

For three lanes available to truck traffic, $p = 0.80$ (Table 3.21)

$$ADTT_{SL} = (p)(ADTT) = (0.80)(4000) = 3200 \text{ trucks}$$

3.9.5 Application of $ADTT_{SL}$ for Determination of Fatigue Limit State

The value of $ADTT_{SL}$ is used to determine the stress range cycles N during the service life of a bridge, which, in turn, is required to determine the design loads for the fatigue limit state design of load-carrying components of a bridge. The value of N can be determined from Equation 3.51:

$$N = (365)(\text{service life in years})(n)(ADTT_{SL}) \tag{3.51}$$

where n = number of stress range cycles per truck passage as listed in Table 3.22 (AASHTO LRFD Table 6.6.1.2.5-2). Values of n are different for slab–beam type of bridges having simple and continuous spans of different lengths:

1. For spans exceeding 40 ft in length,
   a. For simple spans, $n = 1.0$.
   b. For continuous spans, $n = 1.5$ near interior support and 1.0 for other portions of the span.
      For continuous spans, a distance equal to one-tenth of span on each side of an interior support is considered as being *near*.
2. For spans less than or equal to 40 ft long, $n = 2$.

Because of the uncertainty of traffic patterns on a bridge, the frequency of fatigue load for a single lane is assumed to apply to all lanes.

Example 3.17 presents the use of the information given earlier.

www.EngineeringEBooksPdf.com

Example 3.17: Calculation of Number of Stress-Range Cycles, *N*, for a Highway Bridge

Calculate the number of stress cycles, *N*, for the two bridges described in Example 3.16. Assume that for both bridges the span is longer than 40 ft.

1. Bridge in industrial/commercial area
   For a bridge spanning longer than 40 ft, having a service life of 75 years, and $ADTT_{SL}$ of 4250 (as calculated earlier), $n = 1$ (from Table 3.22). Therefore,

$$N = (365)(75)(1)(4250) = 116{,}343{,}750 \text{ stress cycles}$$

2. Bridge in the rural area
   For a bridge spanning longer than 40 ft and having a service life of 75 years and $ADTT_{SL}$ of 3200 (as calculated earlier), $n = 1$ (from Table 3.22). Therefore,

$$N = (365)(75)(1)(3200) = 87{,}600{,}000 \text{ stress cycles}$$

3.10 PEDESTRIAN LOADS

3.10.1 Significance of Pedestrian Loading

Highway bridges may also be provided with a sidewalk for pedestrian traffic as is generally the case with those in the city areas. However, not all bridges are designed for pedestrian loads. For example, bridges on highways in rural areas may not be required to carry pedestrian traffic, whereas those in the urban areas may necessarily be required to carry it.

Typically, long-span bridges, such as arch, cable-stayed, and suspension bridges, as well as bridges over waterways, are provided with pedestrian traffic as these bridges are popular tourist attractions, some of them being iconic and examples of engineering awe and aesthetic grandeur. Bridges that are designed with sidewalks are required to be designed for pedestrian traffic.

3.10.2 Live Load due to Sidewalks on Vehicular Bridges

Bridges intended for only pedestrian, equestrian, light maintenance vehicle, and/or bicycle traffic are to be designed in accordance with the provisions of AASHTO's *LRFD Guide Specifications for Design of Pedestrian Bridges* (AASHTO 2009a).

For design purposes, pedestrian loads (on sidewalks) are considered as *static loads* as specified in AASHTO LRFD Art. 3.6.1.6:

1. For bridges with sidewalks wider than 2 ft, a pedestrian load of 75 lb/ft^2 is to be used and considered simultaneously with the vehicular design live load in the vehicle lane.
2. Where vehicles can mount the sidewalk, the sidewalk pedestrian load need not be considered concurrently; however, the sidewalk must be designed for the truck load.
3. The pedestrian load shall not be considered to act concurrently with vehicles.
4. The DLA need not be considered for vehicles.

3.10.3 Live Load on Pedestrian and/or Bicycle Bridges

Bridges may often be designed solely for pedestrians (footbridges) and/or bicycle traffic, such as pedestrian bridges over highways. Such bridges are to be designed for a uniform live load of 85 lb/ft^2.

As specified in Specifications Art. 13.8.2 and 13.9.3, the railing for pedestrian and/or bicycle traffic must be designed for a load of 50 lb/ft, acting both vertically and transversely on each longitudinal element in the railing system. In addition, the railing must be designed to sustain

www.EngineeringEBooksPdf.com

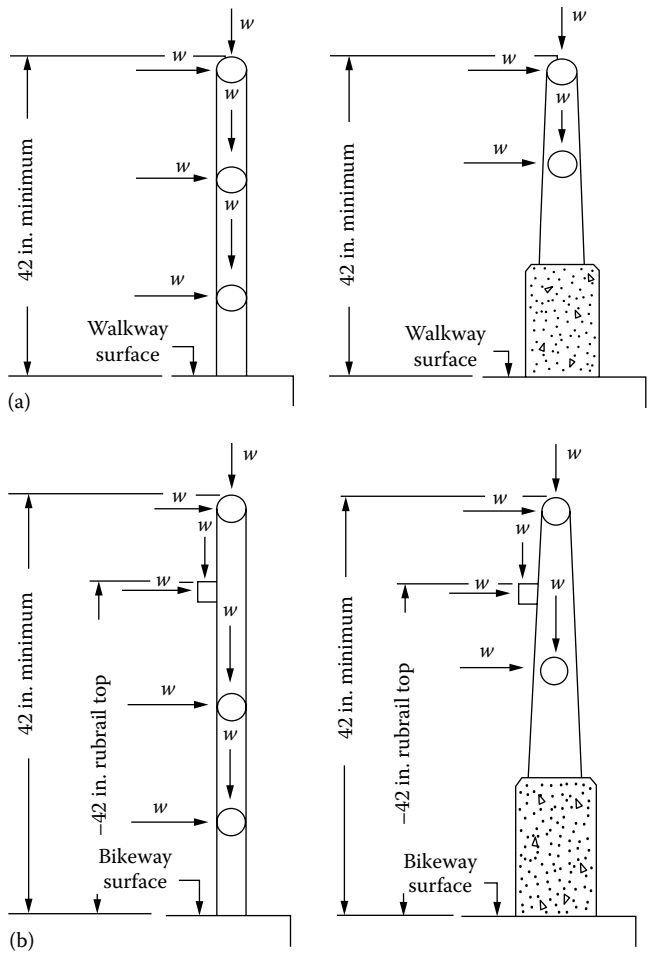

FIGURE 3.73 Loads on railing systems for pedestrian and bicycle bridges. Refer to LRFD Art. 13.8 and 13.9 for details. (a) Pedestrian railing loads. (b) Bicycle railing loads. (From *AASHTO LRFD Bridge Design Specifications*, Copyright © 2012 by American Association of State Highway and Transportation Officials, Washington, DC. Used by permission.)

a single concentrated load of 200 lb applied to the top of the rail at any location and in any direction (Figure 3.73).

Although the magnitude of pedestrian loads on a highway bridge is significantly smaller than the vehicular loading, its effect on the bridge can be disastrous under certain extraordinary conditions, particularly for long- and medium-span bridges. Notoriety of pedestrian and other bridges under the influence of lateral pedestrian excitation is well documented in the literature.

For example, London's Millennium Bridge (London's only bridge solely for pedestrians), a shallow three-span (81, 144, 108 m) suspension bridge, with vertically and horizontally curved suspension cables supporting a 4 m wide, lightweight, steel and aluminum deck, was opened to traffic on June 10, 2000. Unexpected excessive lateral vibrations of the bridge occurred when a large number of pedestrians were on the affected spans. The bridge was closed on June 12, 2000 for investigation (Dallard et al. 2001a,b). Other examples include the first Bosporus suspension bridge (Istanbul, Turkey, main span 3524 ft, completed in 1973); Auckland Harbour Road Bridge (a two-lane section was closed to vehicles and crossed by 2000–4000 demonstrators); Alexandra Bridge in Ottawa, Pont du Solferino in Paris; and NEC Bridge in Birmingham and Queen's Park Bridge in Chester, England (Roberts 2005).

www.EngineeringEBooksPdf.com

TABLE 3.23
Bridge Frequency–Human Discomfort Relationship

Number of Cycles per Second (Hz)	Type of Discomfort
0.25–1	Motion sickness
2	Head resonance, motion sickness
4–6	Major resonance of the whole body
7–9	Abdominal resonance
10–12	Unspecified trunk resonances

Source: Leonard, D.R., Human tolerance levels for bridge vibrations, RRL Report No. 34, Ministry of Transport, Road Research Laboratory, Harmondsworth, England, 1966.

Walking across a pedestrian bridge produces a complex dynamic response involving different modes of vibration as well as motion due to time variation of static deflection. People jumping up and down at a frequency close to the fundamental frequency of the bridge would cause resonance. A larger group of people walking across a bridge produces a dynamic loading. In the past, it was common practice for soldiers to break up step when marching across bridges to avoid large and potentially dangerous vibrations or resonance. The normal walking rate of people varies up to 2.3 paces per second or 2.3 Hz (about 4 mph), which is also considered the upper limit of a marching infantry. Undesirable bridge vibrations from marching armies have been reported in the literature (Leonard 1966). Foot bridges are particularly susceptible to human-induced vibrations, and special measures are sometimes required to avoid resonant frequencies (Leonard 1966, Bachman 1992). Table 3.23 presents bridge frequency–human discomfort relationship.

Vibrations can be longitudinal or lateral. There can also be synchronization of pedestrian lateral motion with that of the footbridge (Roberts 2003). An analysis for lateral pedestrian excitation of foot bridges can be found in Roberts (2005).

Designers should consider all effects of vibration-induced forces when designing footbridges. AASHTO LRFD Specifications for bridges for pedestrian and/or bicycle traffic require that "the frequency of footfall in either vertical or transverse direction shall not resonate with the natural frequencies of the structure." This conservatism reflects the unpredictable nature of pedestrian loads, which gains significance where it becomes a primary load. The frequency of footfall has been estimated to have a frequency of 2 Hz in the vertical direction and 0.67 Hz in the lateral transverse direction. Therefore, in order to avoid resonance, the fundamental frequency of the structure should be a minimum of 3 Hz in the vertical direction and 1.3 Hz in the lateral transverse direction.

3.11 APPLICATION OF DESIGN LIVE LOADS ON A BRIDGE SUPERSTRUCTURE

3.11.1 Design Live Loads for Longitudinal Beams

This topic remains as one of the least understood and difficult and also as one of the most researched in the area of bridge superstructures design. The analysis of live load distribution in highway bridge superstructures is compounded by the following facts of simultaneous occurrences:

1. A bridge superstructure is occupied by a number of many different types (configurations) of vehicles.
2. Vehicles move randomly in several lanes (i.e., there are no specifically designated lanes based on vehicle configurations).
3. Vehicles often change or crisscross lanes while moving (overtaking) on the bridge.
4. Vehicles move at different speeds and can apply brakes suddenly while in motion.

www.EngineeringEBooksPdf.com

Design of a bridge superstructure entails structural design of several individual elements:

1. Deck
2. Longitudinal beams
3. Floor beams (when present, e.g., in a truss, arch, and other types of superstructures)
4. Bearings at supports, such as abutments and piers

Determination of design forces (shear and moment) in the superstructure elements is a complex analytical problem. In spite of considerable research conducted during the past, there is little agreement on any universally acceptable analyses that can be considered exact. This uncertainty remains because of the many such factors as follows:

1. Flexibility of the superstructure system: The vehicular loads (wheel loads) are first applied on the deck, which is a flexible structural element. The deck transmits its load to several supporting longitudinal beams, which also are flexible.
2. Position of live load on the deck: The vehicular traffic, at the discretion of the drivers, can occupy any position, longitudinally or transversely relative to the position of the longitudinal girders supporting the deck. This uncertainty of the live load position on the superstructure results in unknown distribution of forces in the supporting girders.
3. Simultaneous presence of live load in multiple traffic lanes: In the case of a common multilane decks, uncertainty with respect to the presence of live load in two or more traffic lanes simultaneously.

To simplify determination of design forces in various elements of a bridge superstructure (deck, longitudinal beams, floor beams, etc.), specific requirements are specified in AASHTO LRFD Art. 3.6.1.3 with regard to the position of the design truck or design tandem (along with uniform load on the entire span), both transversely and longitudinally, which form the basis for calculating extreme force effects. Separate provisions are specified for simple and structurally continuous span superstructures as follows:

1. The design truck or tandem is assumed to occupy a design lane width of 12 ft irrespective of whether a span is simple or continuous.
2. For simple-span superstructures, the extreme force effects are to be taken as the larger of the effects caused by the following loading conditions:
   a. Each design lane under consideration occupied by the following:
      i. One design truck with the fixed spacing of 14 ft between the front (8-kip axle) and the middle 32 kip axle and a variable axle spacing (14–30 ft between the two 32 kip axles; see Figure 3.8), combined with the effect of the design lane load (Figure 3.10).
      ii. The design tandem (Figure 3.9) combined with the effects of design lane load.
      In case (i) given earlier, the variable spacing implies that the spacing used should cause extreme load effects.
   b. For structurally continuous spans, for both the negative moment between points of contraflexure due to uniform load on all spans and reaction at interior piers only, 90 percent of the effects of two design trucks spaced a minimum of 50 ft between the lead axle of one truck and the rear axle of the other truck, combined with 90 percent of the effect of the design lane load (Figure 3.12). The distance between the 32 kip axles of each truck is to be kept as 14 ft. The two design trucks shall be placed in the adjacent spans to produce maximum force effects.
   c. Axles that do not contribute to the extreme load effects shall be ignored (i.e., no negative force effects considerations).

www.EngineeringEBooksPdf.com

3. The loads (truck, tandem, and lane) are assumed to occupy 10 ft transversely within a design lane.
4. Transversely, the design truck or tandem is placed in a design lane so as to produce extreme load effects. The positions of the center line of the wheel loads are subject to the following provisions (Figures 3.8 and 3.9):
   a. For design of deck overhang: no closer than 1 ft from the face of the curb or railing
   b. For the design of all other components: no closer than 2 ft from the edge of the design lane
5. Unless otherwise specified, the lengths of design lanes or parts thereof that contribute to the extreme force effects under consideration shall be loaded with the design lane load.
6. Where a sidewalk is not separated from the roadway by a crashworthy traffic barrier, consideration should be given to the possibility that vehicles can mount the sidewalk. This consideration may be important for bridges in urban areas, which may be rehabilitated by future widening or by addition of a traffic lane.

With regard to item 2 given earlier, it is clarified that an axle sequence (i.e., design truck or tandem) *and* the lane load are *superposed* to obtain extreme load effects. This is a stark deviation from AASHTO Standard live load model in which either a truck, tandem, or the lane load with an additional concentrated load was used to determine extreme load effects.

3.11.2 Live Load for Deflection Considerations

The foregoing discussion presents loading criteria for the *strength design* of superstructure elements. For bridge superstructures that need to conform to the *optional* live load deflection criteria specified in AASHTO LRFD Art. 2.5.2.6.2, the deflection is to be taken as the larger of the following:

1. Deflection resulting from the design truck alone
2. Deflection resulting from 25 percent of the design truck combined with design lane load

Deflection of bridge superstructures is a *serviceability limit state*; criteria for deflection limits are discussed in Chapter 2.

3.11.3 Design Live Load for Decks, Deck Systems, and Top Slabs of Box Culverts

Selection of live loads for the design of superstructures of slab-type bridges, decks, deck systems, and top slabs of box culverts depends on the span lengths and the direction of the slab. When the approximate strip method (AASHTO LRFD Art. 3.6.1.3.3) is used to analyze decks and top slabs of box culverts, force effects are required to be determined as follows:

1. When the slab spans primarily in the *transverse* direction, only the axles of the design truck (HS20 truck) or the axles of design tandem are to be applied to deck slab or the top slab of box culverts.
2. When the slab spans primarily in the *longitudinal* direction, two cases need to be considered:
   a. For top slabs of box culverts of all spans and for all other cases including slab bridges where the *span does not exceed 15 ft*, only the axles of the design truck (HS20 truck) or the axles of design tandem are to be applied.
   b. For all other cases including slab-type bridges (but *excluding* the top slabs of box culverts) where the *span exceeds 15 ft*, all of the loads specified in Specifications Art. 3.6.1.2 all of the loads specified in AASHTO LRFD Art. 3.6.1.2 (i.e., both, either the design truck *or* design tandem, *and* the lane load) must be used.

www.EngineeringEBooksPdf.com

3. When the refined methods are used for the analysis of slabs, the deign loads are determined based on the primary direction (transverse or longitudinal) of the slab:
   a. When the slab spans primarily in the *transverse* direction, only the axles of the design truck (HS20 truck) or the axles of design tandem are to be applied.
   b. When the slab spans primarily in the *longitudinal* direction (including slab-type bridges), all of the loads specified in AASHTO LRFD Art. 3.6.1.2 (i.e., both, either the design truck *or* design tandem, *and* the lane load) are to be used.

      Both wheels of an axle unit shall be assumed to be equal within an axle unit (i.e., both wheels share equal loads, no unbalanced wheel loads). Amplification of wheel loads due to centrifugal and braking forces need *not* be considered for design of decks.

It is possible that an extreme force effect could result in a slab from placing a 32 kip axle in one lane and 50 kip tandem in a second lane, but such sophistication is not warranted in practical design of deck systems (AASHTO LRFD *Commentary C3.6.1.3.3*).

3.11.4 Live Load on Deck Overhangs

It is common practice to build bridge decks that overhang the exterior girders of a slab–girder-type bridge superstructure. Live load for the design of a deck overhang is specified in AASHTO LRFD Art. 3.6.1.3.4. It requires that for the design of deck overhangs with a cantilever not exceeding 6 ft from the centerline of the exterior girder to the face of a structurally continuous concrete railing, the outside row of the wheel loads may be replaced with a uniformly distributed line load of 1.0 kip per linear foot intensity, located 1 ft from the face of the railing (Figure 3.28). The 1.0 kip/ft uniform load is based on the following assumptions (AASHTO LRFD *Commentary C3.6.1.3.4*):

1. There is a *structurally continuous* barrier at the end of the overhang (e.g., a parapet without any joints (Figure 3.74). Structurally discontinuous traffic barriers consist of several individually precast segments placed contiguously on the edge of deck).
2. The 25.0 kip (half the weight of a design tandem) is distributed over a longitudinal length of 25 ft. This results in a uniform load of 1 kip/ft.
3. There is a cross beam or other appropriate component at the end of the bridge supporting the barrier, which is designed for one-half the tandem weight.

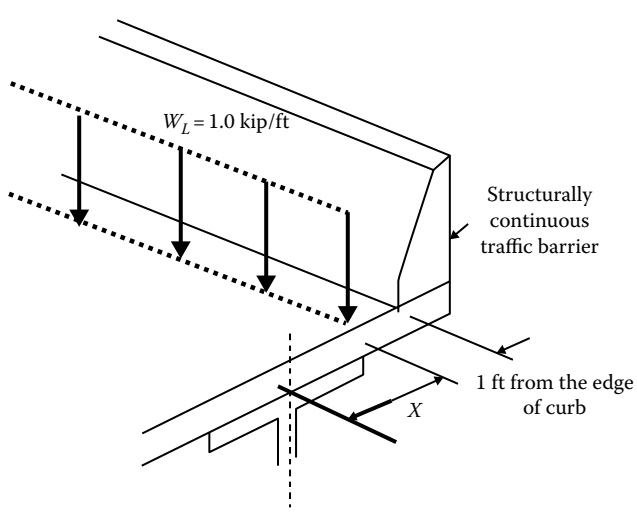

FIGURE 3.74 Design live load for a deck overhang.

www.EngineeringEBooksPdf.com

The 1.0 kip/ft load for the design of the overhang as stated earlier is, in reality, a replacement for the tandem wheel load. Therefore, a multiple presence factor of 1.2 (discussed in the next section) is applicable to the load effect. For example, if a load W_L (= 1.0 kip/ft) were placed at a distance X from the center of an exterior girder, the design moment (per unit length in the longitudinal direction) for the overhang would be given by Equation 3.52:

$$M_L = 1.2(W_L)(X) \tag{3.52}$$

The condition of structural continuity in barriers (item 1 earlier) must be satisfied in design because it is the *structurally continuous* (Figure 3.74) barriers that have been found to be effective in distributing wheel loads in the overhang. The aforementioned stated design provision does not apply if the barrier is not structurally continuous; in such a case, the load should be distributed over a shorter (<25 ft) distance.

Horizontal loads on the overhang resulting from vehicle collision with traffic barriers are to be determined as specified in Section 13 of the AASHTO LRFD.

3.11.5 Force Effects Due to Live Load in Multiple Traffic Lanes: Multiple Presence of Live Load

Multiple presence of live load refers to the presence of live load in several design lanes of a bridge. How to account for the force effects caused by the simultaneous occupation by live load in all design lanes of multilane bridges (e.g., four- or six-lane bridges, common on interstate highways traversing through large metropolitan cities) has been a topic of concerted research effort for many years. The fundamental question is as follows: What are the design loads (shears and moments) in beams and girders supporting the deck when vehicular traffic is present in one or more lanes on a bridge? In spite of many studies, this problem continues to defy an exact analytical solution that would be simple for designers' use. Analytical methods specified in AASHTO Standard had been a subject of debate and uncertainty for many years. Readers should refer to AASHTO LRFD *Commentary C3.6.1.1.2* for a brief discussion of this very important topic.

The force effects in the girders of multigirder superstructures are determined by the approximate method—using live load DFs presented in Section 4 of AASHTO LRFD (see Tables 4.6.2.2 and 4.6.2.3). An interesting, and important, feature of this method is its simplicity: *the effects of single and multiple loaded lanes are already included in the expressions for load* DF*s*. Therefore, the multiple presence factors (Table 3.24, discussed in the next paragraph) are *not* to be used in conjunction with the approximate *live load distribution method* specified in AASHTO LRFD Art. 4.6.2.2 and 4.6.2.3 (discussed in Chapter 4). However, this provision is subject to the following exceptions, that is, the multiple presence factors *must be used* when considering the force effects (shears and moments in beams and girders, centrifugal force, and braking force) in the following cases:

1. When the lever rule (discussed in Chapter 4) is used
2. When special requirements for the exterior beams in slab–beam bridges, specified in AASHTO LRFD Art. 4.6.2.2.2d are used

For the aforementioned two cases, AASHTO LRFD Art. 3.6.1.1.2 specifies a method that uses *multiple presence factors* to account for the *probability of coincidental loading* (presence of vehicular traffic in more than one design lane) on a bridge deck. It requires, where applicable, that extreme live load force effects be determined by considering each possible combination of loaded lanes multiplied by a corresponding multiple presence factor to account for the probability of simultaneous lane occupation by full HL-93 design live load. Multiple presence factors, m, to be used for single or multiple lanes loading condition are listed in Table 3.24.

www.EngineeringEBooksPdf.com

TABLE 3.24
Multiple Presence Factors, *m* (AASHTO LRFD 2012 Art. 3.6.1.1.2)

Number of Loaded Lanes	Multiple Presence Factor, *m*
1	1.2
2	1.00
3	0.85
>3	0.65

Source: Adapted from *AASHTO LRFD Bridge Design Specifications*, Copyright © 2012 by American Association of State Highway and Transportation Officials, Washington, DC. Used by permission.

Notes:

1. The aforementioned values are for ADTT of 5000 trucks in one direction.
2. The multiple presence factors listed in Table 3.23 are *not* to be used in conjunction with the approximate *live load distribution method* specified in AASHTO LRFD Art. 4.6.2.2 and 4.6.2.3 because the effects of single and multiple loaded lanes are already included in the expressions for load DFs.
3. Multiple presence factors *must be used* when considering the force effects (shears and moments in beams and girders, centrifugal force, and braking force) in the following cases:
   a. When the lever rule is used
   b. When special requirements for the exterior beams in slab–beam bridge (AASHTO LRFD Art. 4.6.2.2.2d) are used

If a bridge carries pedestrian loads in addition to the design lanes, multiple presence factors apply by considering additional design lanes. For the purpose of determining the number of lanes when the loading condition includes pedestrian loads (AASHTO LRFD Art. 3.6.1.6, discussed in Section 3.11) combined with one or more lanes of vehicular live load, the pedestrian loads may be taken to be one loaded lane. This consideration is based on the assumption that simultaneous occupancy by a dense loading of people combined with a 75-year design load is remote.

To reiterate, the multiple presence factors are applied rather selectively; they are *not* applicable in all cases. The following restrictions apply:

1. As noted earlier, the multiple presence factors listed in Table 3.24 are *not* to be used in conjunction with the approximate *live load distribution method* specified in AASHTO LRFD Art. 4.6.2.2 and 4.6.2.3 (in specifications Section 4, discussed in Chapter 4). This is because the effects of single and multiple loaded lanes are already included in the expressions for load DFs.
2. The multiple presence factors are *not* applicable to design for *fatigue limit state* (discussed later) for which only one design truck is used, regardless of the number of design lanes (AASHTO LRFD Art. 3.6.1.1.2) on the bridge. Therefore, when using tabularized expressions (listed in specifications Section 4, discussed in Chapter 4) for DFs for one lane loaded in the *fatigue limit state check*, the 1.2 multiple presence factor for one lane loaded (listed in Table 3.24) must be divided out of the calculated live load DF.
3. The multiple presence factor of 1.2 does not apply to pedestrian loads (it applies to vehicular loads only).
4. Multiple presence factors are to be used specifically where
   a. *Lever rule*, the special requirement for exterior beams in beam–slab bridges assuming rigid-body rotation of the cross section (as specified in AASHTO LRFD Art. 4.6.2.2.2d, discussed in Chapter 4), is used. See examples in Chapter 4.
   b. Refined analysis (e.g., finite element) methods are used for determination of live load DFs.
5. Multiple presence factors are applicable to centrifugal and braking forces (both discussed later in this chapter).

www.EngineeringEBooksPdf.com

TABLE 3.25
Reduced Multiple Presence Factors (*m*) for ADTT < 5,000 Trucks

Range of ADTT	Force Effects Reduction (percent)
$100 \leq \text{ADTT} \leq 1000$	95
ADTT < 100	90

The multiple presence factors shown in Table 3.24 were developed on the basis of ADTT_{SL} of 5000 trucks in one direction. The ADTT_{SL} refers to the traffic lane in which the majority of the truck traffic crosses the bridge.

The extreme force effects resulting from the appropriate number of lanes may be adjusted (reduced) for sites with lower ADTT as shown in Table 3.25. This adjustment is based on the reduced probability of attaining the design event during 75-year design life with reduced truck traffic.

The foretasted adjustment is based on the reduced probability of attaining the design event during a 75-year design life with reduced traffic volume.

3.12 DESIGN LIVE LOADS IN LONGITUDINAL GIRDERS SUPPORTING BRIDGE DECKS

It must be recognized that the value of the live load bending moment determined in Example 3.16 and that of live load reaction in Example 3.17 (using Equation 3.36) are *not* the values of *design* forces for those girders. In general, to obtain the values of design forces (bending moment, shear, reactions) in longitudinal girders supporting a bridge deck, the force values obtained from Equation 3.36 must be multiplied by the following two quantities:

1. Applicable load factor for live load (pertinent to the limit state considered, γ_L)
2. Appropriate DF

Thus, the values of *design* live load forces for longitudinal girders are obtained from Equation 3.52:

$$Q_{design} = (Q_{HL\text{-}93})(\gamma_L)(DF) \tag{3.52}$$

where $Q_{HL\text{-}93}$ = live load force from Equation 3.36.

The topic of *DFs* is discussed fully in Chapter 4. Note that the DFs are different for

1. Bending moment and shear in the interior girders
2. Bending moment and shear in the exterior girders

Examples on calculations for design loads for longitudinal girders are presented in Chapter 4.

3.13 ENVELOPES FOR MOMENT AND SHEAR VALUES

In practice, in addition to the absolute maximum bending moment in the span, maximum shear and bending moment values at selected points along the entire span (typically at $0.1L$, one-tenth of span intervals) are required for design purposes. These values can be determined as illustrated in the preceding examples. For simple spans only, calculations need to be performed for only half the span because of the symmetry about the centerline of span (the other half would be similar). For other girder support arrangements (e.g., cantilevered beams), calculations would be required for all selected points along the span. In any case, it is common practice to plot values of maximum design

www.EngineeringEBooksPdf.com

moments and shears at 0.1L intervals in the span; these plots are called the *envelopes* of maximum moment and shears in the span due to the live load. As mentioned earlier, these calculations can be monotonously tedious if done by hand; a computer solution would be desirable. Example 3.18 illustrates envelopes for moments and shear for a simple-span bridge.

Example 3.18

Figure 3.75a shows the cross section and the framing plan of typical composite slab–steel girder bridge spanning 161 ft. The bridge cross section consists of four steel plate girders spaced equally at 13 ft, which supports 10 in. thick RC slab including ½ in. thick integral wearing surface (t_s = 9.5 in.). The deck overhangs are 4 ft 3 in. each. Each abutment is skewed a positive 35°. Plot the moment envelopes for moments and shear for a typical interior girder of this bridge. The *DFs*, including the skew effects, for live load moment and shear in an interior girder for strength and fatigue limit states have been calculated as follows:

1. Strength limit state
   Moment: DF = 0.801
   Shear: End support, DF = 1.284
   In span, DF = 1.145

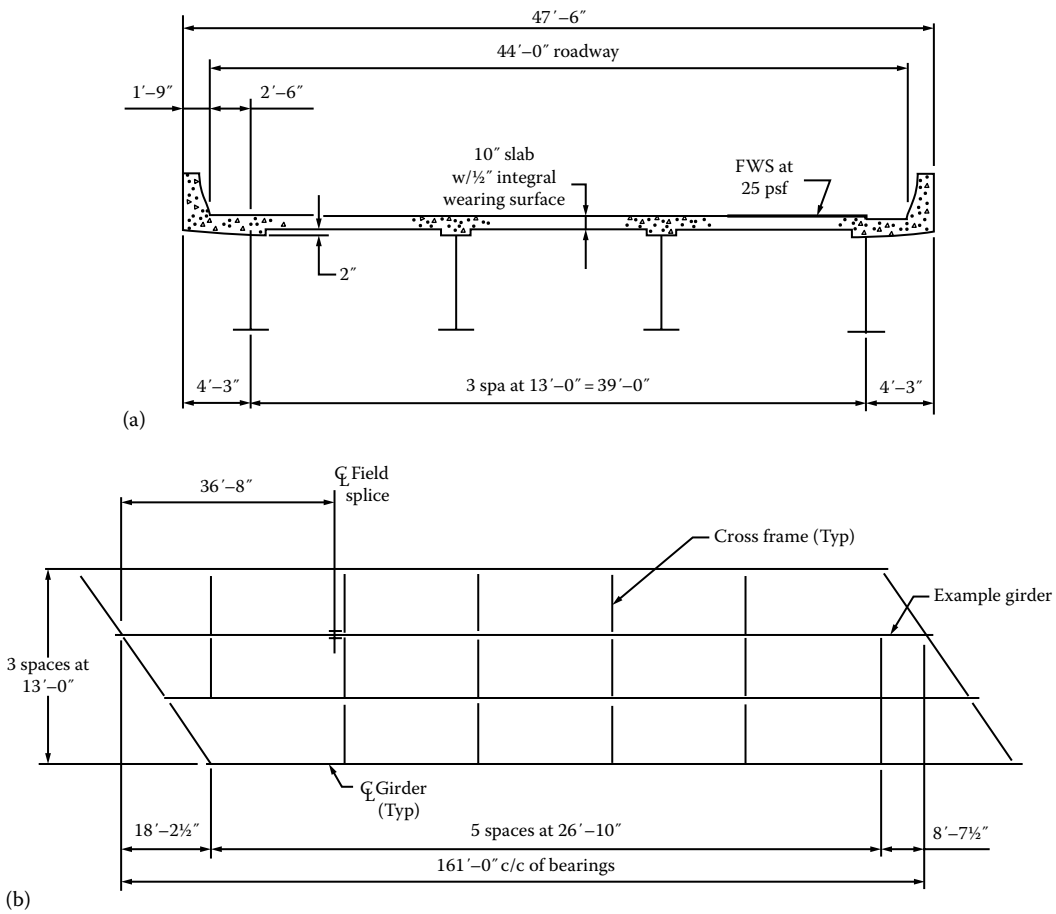

FIGURE 3.75 (a) Bridge cross section and (b) framing plan for Example 3.18. (Courtesy of American Iron and Steel Institute, New York.)

www.EngineeringEBooksPdf.com

2. Fatigue limit state
   Moment: $DF = 0.428$
   Shear: End support, $DF = 0.822$
   In span, $DF = 0.733$

Solution

Plotting moment and shear envelopes for simple span involve a lot of different calculations; these are explained step by step as follows. These calculations are for the *unfactored* loads. It is only necessary to calculate the force effects for the left half of the span; the right half span would have similar force effects because of the symmetry. Calculations are for every one-tenth of span for the left half span (i.e., $0.1L$–$0.5L$).

Step 1: Calculate dead loads on the span.
The following data have been used for the plotting moment and shear envelopes for the interior girder for the bridge in this example.

Dead load:

$$DC_1 = \text{dead load acting on noncomposite section}$$

$$DC_2 = \text{dead load acting on the long-term composite section}$$

$$\text{Dead weight of concrete} = 150\ \text{lb/ft}^3$$

$$\text{Slab (including integral wearing surface)} = \left(\frac{10}{12}\right)(13)(0.15) = 1.625\ \text{kip/ft}$$

$$\text{Concrete haunch} = \left(\frac{2}{12}\right)\left(\frac{22}{12}\right)(0.15) = 0.046\ \text{kip/ft}$$

$$\text{Steel girder, cross frames, and details} = 0.069\ \text{kip/ft}$$

$$\text{Stay-in-place forms} = 0.078\ \text{kip/ft}$$

$$\text{Total dead load } DC_1 = 1.625 + 0.046 + 0.369 + 0.078 = 2.118\ \text{kip/ft}$$

For DC_2, assume that each barrier weighs 505 lb per linear foot and the resulting load is distributed equally to each girder:

$$\text{Dead load due to barriers, } DC_2 = \frac{0.505 \times 2}{4} = 0.253\ \text{kip/ft}$$

Dead load due to the wearing surface (*DW*): This load is carried in full by the long-term composite sections and assumed distributed equally to all four girders:

$$\text{Wearing surface load, } DW = \left(\frac{0.025 \times 44}{4}\right) = 0.275\ \text{kip/ft}$$

Step 2: Dead load moments in span.
These moments are calculated from Equation 3.13:

$$M_x = \frac{wx(L - x)}{2} \tag{3.13}$$

www.EngineeringEBooksPdf.com

Moments due to dead loads DC_1, DC_2, and DW are calculated separately.

Moments due to DC_1:

$$M_{0.1L} = \frac{(2.118)(16.1)(161-16.1)}{2} = 2471\,\text{kip-ft}$$

$$M_{0.2L} = \frac{(2.118)(32.2)(161-32.2)}{2} = 4392\,\text{kip-ft}$$

$$M_{0.3L} = \frac{(2.118)(48.3)(161-48.3)}{2} = 5765\,\text{kip-ft}$$

$$M_{0.4L} = \frac{(2.118)(64.4)(161-64.4)}{2} = 6588\,\text{kip-ft}$$

$$M_{0.5L} = \frac{(2.118)(80.5)(161-80.5)}{2} = 6863\,\text{kip-ft}$$

Moments due to DC_2:

$$M_{0.1L} = \frac{(0.253)(16.1)(161-16.1)}{2} = 295\,\text{kip-ft}$$

$$M_{0.2L} = \frac{(0.253)(32.2)(161-32.2)}{2} = 525\,\text{kip-ft}$$

$$M_{0.3L} = \frac{(0.253)(48.3)(161-48.3)}{2} = 689\,\text{kip-ft}$$

$$M_{0.4L} = \frac{(0.253)(64.4)(161-64.4)}{2} = 787\,\text{kip-ft}$$

$$M_{0.5L} = \frac{(0.253)(80.5)(161-80.5)}{2} = 820\,\text{kip-ft}$$

Moments due to DW:

$$M_{0.1L} = \frac{(0.275)(16.1)(161-16.1)}{2} = 321\,\text{kip-ft}$$

$$M_{0.2L} = \frac{(0.275)(32.2)(161-32.2)}{2} = 570\,\text{kip-ft}$$

$$M_{0.3L} = \frac{(0.275)(48.3)(161-48.3)}{2} = 748\,\text{kip-ft}$$

www.EngineeringEBooksPdf.com

$$M_{0.4L} = \frac{(0.275)(64.4)(161-64.4)}{2} = 855 \text{ kip-ft}$$

$$M_{0.5L} = \frac{(0.275)(80.5)(161-80.5)}{2} = 891 \text{ kip-ft}$$

Step 3: Moments and shears due to live loads.
The first thing to determine is which of the two live load combinations would govern the design of girders for a simple span of 161 ft: (1) HS20 truck *plus* lane load or (2) tandem *plus* lane load. From Table 3.14, we note that for a simple span of 161 ft, the governing live load combination is HL-93 truck *plus* lane load. So, for a span of 161 ft, we need to calculate moments and shears at 0.1*L* intervals (i.e., every one-tenth point on the span). These moment and shear values are calculated separately for the HL-93 truck and the lane load. Moments and shears due to HS20 truck are calculated from the governing equations given in Tables 3.12 and 3.13. Moments due to the lane load are calculated from Equation 3.13, and shears due to the lane load are calculated from Equations 3.18 and 3.19. These calculations are easily performed on an excel spreadsheet. The total live load effects are then calculated from Equation 3.6.

Moment at the one-tenth span points: Use Equation 3.24 for x/L = 0.1, 0.2, and 0.3:

$$M_x = \frac{72x(L-x-9.33)}{L} \tag{3.24}$$

$$M_{0.1L} = \frac{72(16.1)(161-16.1-9.33)}{161} = 976 \text{ kip-ft}$$

$$M_{0.2L} = \frac{72(32.2)(161-32.2-9.33)}{161} = 1720 \text{ kip-ft}$$

$$M_{0.3L} = \frac{72(48.3)(161-48.3-9.33)}{161} = 2233 \text{ kip-ft}$$

Moment at the one-tenth span points: Use Equation. 3.27 for x/L = 0.4 and 0.5:

$$M_x = \frac{72x(L-x-4.67)}{L} - 112 \tag{3.27}$$

$$M_{0.4L} = \frac{72(64.4)(161-64.4-4.67)}{161} - 112 = 2536 \text{ kip-ft}$$

$$M_{0.5L} = \frac{72(80.5)(161-80.5-4.67)}{161} - 112 = 2618 \text{ kip-ft}$$

Moments at one-tenth span points due to the lane load of 0.64 kip/ft: Use Equation 3.13:

$$M_x = \frac{wx(L-x)}{2} \tag{3.13}$$

$$M_{0.1L} = \frac{(0.64)(16.1)(161-16.1)}{2} = 747 \text{ kip-ft}$$

www.EngineeringEBooksPdf.com

$$M_{0.2L} = \frac{(0.64)(32.2)(161-32.2)}{2} = 1327 \text{ kip-ft}$$

$$M_{0.3L} = \frac{(0.64)(48.3)(161-48.3)}{2} = 1742 \text{ kip-ft}$$

$$M_{0.4L} = \frac{(0.64)(64.4)(161-64.4)}{2} = 1991 \text{ kip-ft}$$

$$M_{0.5L} = \frac{(0.64)(80.5)(161-80.5)}{2} = 2074 \text{ kip-ft}$$

Step 4: Total live load moments, including the DLA or impact.
These moments are calculated from Equation 3.6. Note that DLA (*IM*) is applied to the moments due to HS20 truck only:

$$LL_{total} = (LL_{truck})(1 + IM) + (LL_{lane}) \tag{3.6}$$

With $IM = 0.33$ for all strength limit states (discussed in Section 3.8), Equation 3.6 is expressed as follows:

$$LL_{total} = 1.33(LL_{truck}) + (LL_{lane})$$

Total live load moments at the tenth point are calculated as follows:

$$(M_{0.1L})_{total} = 1.33(976) + 747 = 2045 \text{ kip-ft}$$

$$(M_{0.2L})_{total} = 1.33(1720) + 1327 = 3615 \text{ kip-ft}$$

$$(M_{0.3L})_{total} = 1.33(2233) + 1742 = 4712 \text{ kip-ft}$$

$$(M_{0.4L})_{total} = 1.33(2536) + 1991 = 5364 \text{ kip-ft}$$

$$(M_{0.5L})_{total} = 1.33(2618) + 2074 = 5556 \text{ kip-ft}$$

Step 5: Design live load moments.
The *unfactored* design *live load moments* are obtained by multiplying the total live moments by the *DF* (discussed in Chapter 4). For an interior girder of this superstructure, *DF* has been calculated to be 0.801 (see sample calculations in examples in Chapter 4). The resulting design live load moments are determined to be as follows (note that moment at the support is zero):

$$(M_{0.0l}) = 0$$

$$(M_{0.1L})_{design} = 2045(0.801) = 1638 \text{ kip-ft}$$

$$(M_{0.2L})_{design} = 3615(0.801) = 2896 \text{ kip-ft}$$

$$(M_{0.3L})_{design} = 4712(0.801) = 3774 \text{ kip-ft}$$

$$(M_{0.4L})_{design} = 5364(0.801) = 4297 \text{ kip-ft}$$

$$(M_{0.5L})_{design} = 5556(0.801) = 4450 \text{ kip-ft}$$

www.EngineeringEBooksPdf.com

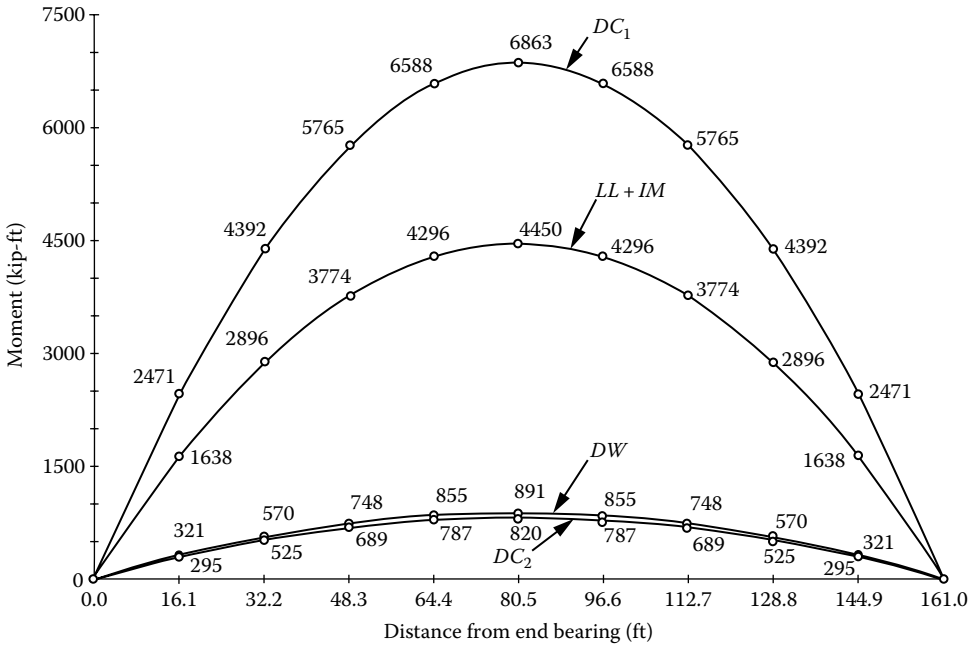

FIGURE 3.76 Dead and live load moment envelopes. (Courtesy of American Iron and Steel Institute, New York.)

Envelopes of moments due to DC_1, DC_2, DW, and HL-93 live load as calculated earlier are shown separately in Figure 3.76.

Step 6: Shears—maximum shear due to dead loads.
These are calculated as for a simple span:

$$V_x = w(L/2 - x) \tag{3.14b}$$

Shears due to DC_1:

$$V_{0.0L} = 2.118(161/2 - 0.0) = 171 \text{ kip}$$

$$V_{0.1L} = 2.118(161/2 - 16.1) = 136 \text{ kip}$$

$$V_{0.2L} = 2.118(161/2 - 32.2) = 102 \text{ kip}$$

$$V_{0.3L} = 2.118(161/2 - 48.3) = 68 \text{ kip}$$

$$V_{0.4L} = 2.118(161/2 - 64.4) = 34 \text{ kip}$$

$$V_{0.5L} = 2.118(161/2 - 80.5) = 0 \text{ kip}$$

From antisymmetry,

$$V_{0.6L} = -34 \text{ kip}$$

$$V_{0.7L} = -68 \text{ kip}$$

www.EngineeringEBooksPdf.com

$$V_{0.8L} = -102 \text{ kip}$$

$$V_{0.9L} = -136 \text{ kip}$$

$$V_{1.0L} = -171 \text{ kip}$$

Shears due to DC_2:

$$V_{0.0L} = 0.253(161/2 - 0.0) = 20 \text{ kip}$$

$$V_{0.1L} = 0.253(161/2 - 16.1) = 16 \text{ kip}$$

$$V_{0.2L} = 0.253(161/2 - 32.2) = 12 \text{ kip}$$

$$V_{0.3L} = 0.253(161/2 - 48.3) = 8 \text{ kip}$$

$$V_{0.4L} = 0.253(161/2 - 64.4) = 4 \text{ kip}$$

$$V_{0.5L} = 0.253(161/2 - 80.5) = 0 \text{ kip}$$

From antisymmetry,

$$V_{0.6L} = -4 \text{ kip}$$

$$V_{0.7L} = -8 \text{ kip}$$

$$V_{0.8L} = -12 \text{ kip}$$

$$V_{0.9L} = -16 \text{ kip}$$

$$V_{1.0L} = -20 \text{ kip}$$

Shears due to DW:

$$V_{0.0L} = 0.275(161/2 - 0.0) = 22 \text{ kip}$$

$$V_{0.1L} = 0.275(161/2 - 16.1) = 18 \text{ kip}$$

$$V_{0.2L} = 0.275(161/2 - 32.2) = 13 \text{ kip}$$

$$V_{0.3L} = 0.275(161/2 - 48.3) = 9 \text{ kip}$$

$$V_{0.4L} = 0.275(161/2 - 64.4) = 4 \text{ kip}$$

$$V_{0.5L} = 0.275(161/2 - 80.5) = 0 \text{ kip}$$

From antisymmetry,

$$V_{0.6L} = -4 \text{ kip}$$

$$V_{0.7L} = -9 \text{ kip}$$

www.EngineeringEBooksPdf.com

$$V_{0.8L} = -13 \text{ kip}$$

$$V_{0.9L} = -18 \text{ kip}$$

$$V_{1.0L} = -22 \text{ kip}$$

Step 7: Shear at the one-tenth span points due to HS20 truck.
Shear at the one-tenth span points: Use Equation 3.20 for all values of x/L, from 0 to 1.0:

$$V_x = \frac{72(L - x - 9.33)}{L} \tag{3.25}$$

$$V_{0.0L} = \frac{72(161 - 0.0 - 9.33)}{161} = 68 \text{ kip}$$

$$V_{0.1L} = \frac{72(161 - 16.1 - 9.33)}{161} = 61 \text{ kip}$$

$$V_{0.2L} = \frac{72(161 - 32.2 - 9.33)}{161} = 53 \text{ kip}$$

$$V_{030L} = \frac{72(161 - 48.3 - 9.33)}{161} = 46 \text{ kip}$$

$$V_{0.4L} = \frac{72(161 - 64.4 - 9.33)}{161} = 39 \text{ kip}$$

$$V_{0.5L} = \frac{72(161 - 80.5 - 9.33)}{161} = 32 \text{ kip}$$

$$V_{0.6L} = \frac{72(161 - 96.6 - 9.33)}{161} = 25 \text{ kip}$$

$$V_{0.7L} = \frac{72(161 - 112.7 - 9.33)}{161} = 17 \text{ kip}$$

$$V_{0.8L} = \frac{72(161 - 128.8 - 9.33)}{161} = 10 \text{ kip}$$

$$V_{0.9L} = \frac{72(161 - 144.9 - 9.33)}{161} = 3 \text{ kip}$$

$$V_{1.0L} = 0 \text{ kip}$$

www.EngineeringEBooksPdf.com

Step 8: Positive shear at the one-tenth span points due to the lane load.
Use Equation 3.18:

$$V_x = \frac{w(L-x)^2}{2L} \tag{3.18}$$

$$V_{0.0L} = \frac{0.64(161-0)^2}{2(161)} = 52 \text{ kip}$$

$$V_{0.1L} = \frac{0.64(161-16.1)^2}{2(161)} = 42 \text{ kip}$$

$$V_{0.2L} = \frac{0.64(161-32.2)^2}{2(161)} = 33 \text{ kip}$$

$$V_{0.3L} = \frac{0.64(161-48.3)^2}{2(161)} = 25 \text{ kip}$$

$$V_{0.4L} = \frac{0.64(161-64.4)^2}{2(161)} = 19 \text{ kip}$$

$$V_{0.5L} = \frac{0.64(161-80.50)^2}{2(161)} = 13 \text{ kip}$$

$$V_{0.6L} = \frac{0.64(161-96.6)^2}{2(161)} = 8 \text{ kip}$$

$$V_{0.7L} = \frac{0.64(161-112.7)^2}{2(161)} = 5 \text{ kip}$$

$$V_{0.8L} = \frac{0.64(161-128.8)^2}{2(161)} = 2 \text{ kip}$$

$$V_{0.9L} = \frac{0.64(161-144.9)^2}{2(161)} = 1 \text{ kip}$$

$$V_{1.0L} = \frac{0.64(161-161)^2}{2(161)} = 0 \text{ kip}$$

www.EngineeringEBooksPdf.com

Step 9: Negative shear at the one-tenth span points due to the lane load.
Use Equation 3.19:

$$V_x = \frac{wx^2}{2L} \tag{3.19}$$

$$V_{0.0L} = \frac{w(0)^2}{2(161)} = 0 \text{ kip}$$

$$V_{0.1L} = -\frac{0.64(16.1)^2}{2(161)} = -1 \text{ kip}$$

$$V_{0.2L} = -\frac{0.64(32.2)^2}{2(161)} = -2 \text{ kip}$$

$$V_{0.3L} = -\frac{0.64(48.3)^2}{2(161)} = -5 \text{ kip}$$

$$V_{0.4L} = -\frac{0.64(64.4)^2}{2(161)} = -8 \text{ kip}$$

$$V_{0.5L} = -\frac{0.64(80.5)^2}{2(161)} = -13 \text{ kip}$$

$$V_{0.6L} = -\frac{0.64(96.6)^2}{2(161)} = -19 \text{ kip}$$

$$V_{0.7L} = -\frac{0.64(112.7)^2}{2(161)} = -25 \text{ kip}$$

$$V_{0.8L} = -\frac{0.64(128.2)^2}{2(161)} = -33 \text{ kip}$$

$$V_{0.9L} = -\frac{0.64(144.9)^2}{2(161)} = -42 \text{ kip}$$

$$V_{1.0L} = -\frac{0.64(161.0)^2}{2(161)} = -52 \text{ kip}$$

Step 10: Total unfactored positive and negative live load shear is obtained from Equation 3.6.
$IM = 0.33$ is applied to live load shear due to HS20 truck:

$$LL_{total} = 1.33(LL_{truck}) + (LL_{lane})$$

$$V_{0.0L} = 1.33(68) + 52 = 142 \text{ kip}$$

www.EngineeringEBooksPdf.com

$$V_{0.1L} = 1.33(61) + 42 = 123 \text{ kip}$$

$$V_{0.2L} = 1.33(53) + 33 = 103 \text{ kip}$$

$$V_{0.3L} = 1.33(46) + 25 = 86 \text{ kip}$$

$$V_{0.4L} = 1.33(39) + 19 = 71 \text{ kip}$$

$$V_{0.5L} = 1.33(32) + 13 = 56 \text{ kip}$$

$$V_{0.6L} = 1.33(25) + 8 = 41 \text{ kip}$$

$$V_{0.7L} = 1.33(17) + 5 = 28 \text{ kip}$$

$$V_{0.8L} = 1.33(10) + 2 = 15 \text{ kip}$$

$$V_{0.9L} = 1.33(4) + 1 = 6 \text{ kip}$$

$$V_{1.0L} = 1.33(0) + 0 = 0 \text{ kip}$$

Values of negative live load shear are obtained from the aforementioned values from antisymmetry:

$$-V_{0.0L} = 0 \text{ kip}$$

$$-V_{0.1L} = -6 \text{ kip}$$

$$-V_{0.2L} = -15 \text{ kip}$$

$$-V_{0.3L} = -28 \text{ kip}$$

$$-V_{0.4L} = -41 \text{ kip}$$

$$-V_{0.5L} = -56 \text{ kip}$$

$$-V_{0.6L} = -71 \text{ kip}$$

$$-V_{0.7L} = -86 \text{ kip}$$

$$-V_{0.8L} = -103 \text{ kip}$$

$$-V_{0.9L} = -123 \text{ kip}$$

$$-V_{1.0L} = -142 \text{ kip}$$

Step 11: Calculate unfactored design live load shear.
Apply DF of 1.284 to shear at support and 1.145 to shear in span. The resulting shears are as follows:

$$V_{0.0L} = 142(1.284) = 182 \text{ kip}$$

$$V_{0.1L} = 123(1.145) = 141 \text{ kip}$$

www.EngineeringEBooksPdf.com

$$V_{0.2L} = 103(1.145) = 118 \text{ kip}$$

$$V_{0.3L} = 86(1.145) = 98 \text{ kip}$$

$$V_{0.4L} = 71(1.145) = 81 \text{ kip}$$

$$V_{0.5L} = 56(1.145) = 64 \text{ kip}$$

$$V_{0.6L} = 41(1.145) = 47 \text{ kip}$$

$$V_{0.7L} = 28(1.145) = 32 \text{ kip}$$

$$V_{0.8L} = 15(1.145) = 17 \text{ kip}$$

$$V_{0.9L} = 6(1.145) = 7 \text{ kip}$$

$$V_{1.0L} = 0(1.145) = 0 \text{ kip}$$

From antisymmetry,

$$-V_{0.0L} = 0 \text{ kip}$$

$$-V_{0.1L} = -7 \text{ kip}$$

$$-V_{0.2L} = -17 \text{ kip}$$

$$-V_{0.3L} = -32 \text{ kip}$$

$$-V_{0.4L} = -47 \text{ kip}$$

$$-V_{0.5L} = -64 \text{ kip}$$

$$-V_{0.6L} = -81 \text{ kip}$$

$$-V_{0.7L} = -98 \text{ kip}$$

$$-V_{0.8L} = -118 \text{ kip}$$

$$-V_{0.9L} = -141 \text{ kip}$$

$$-V_{1.0L} = -182 \text{ kip}$$

Envelopes of shear due to DC_1, DC_2, DW, and HL-93 live load as calculated earlier are shown separately in Figure 3.77.

Step 12: Moments for the fatigue limit state.
For fatigue limit state, dead loads (static loads) are ignored. For live load, only HS20 truck is considered; lane load is ignored. Use Equation 3.39 for $x/L = 0 - 0.241$ and Equation 3.41 for $x/L = 0.241 - 0.5$:

$$M_x = \frac{72(x)\left[(L-x)-18.22\right]}{L} \tag{3.39}$$

www.EngineeringEBooksPdf.com

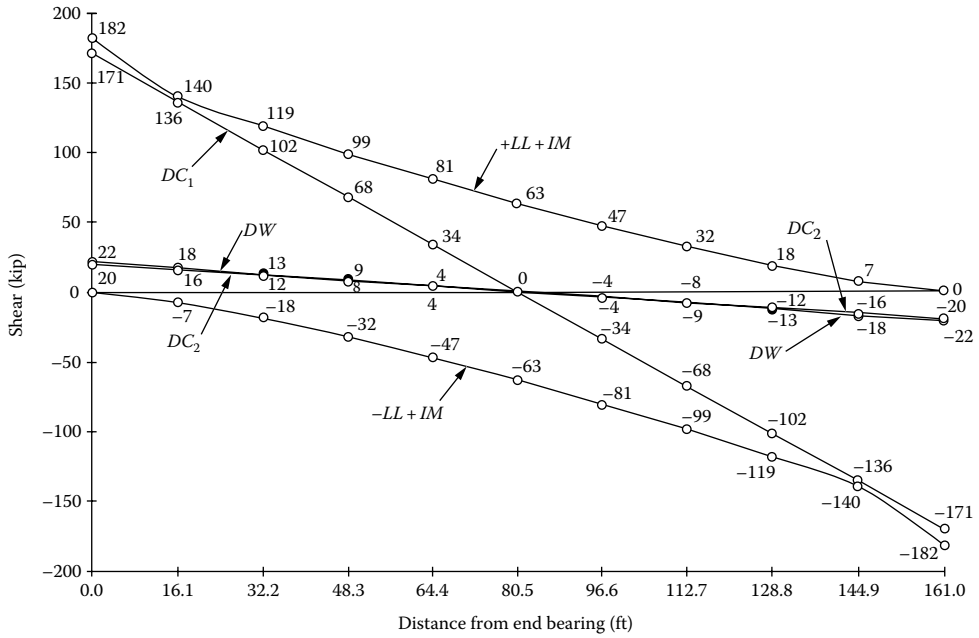

FIGURE 3.77 Shear envelopes. (Courtesy of American Iron and Steel Institute, New York.)

$$M_{0.0L} = 0 \text{ (at left support)}$$

$$M_{0.1L} = 72(0.1)\ [(0.9)(161) - 18.22] = 912 \text{ kip-ft}$$

$$M_{0.2L} = 72(0.2)\ [(0.8)(161) - 18.22] = 1592 \text{ kip-ft}$$

$$M_{0.3L} = 72(0.3)\ [(0.7)(161) - 11.78] - 112 = 2068 \text{ kip-ft}$$

$$M_{0.4L} = 72(0.4)\ [(0.6)(161) - 11.78] - 112 = 2331 \text{ kip-ft}$$

$$M_{0.5L} = 72(0.5)\ [(0.5)(161) - 11.78] - 112 = 2362 \text{ kip-ft}$$

For fatigue limit state, $IM = 0.15$ and $DF = 0.428$. So, *unfactored* fatigue live load moments, including impact and DF, are as follows (*note*: lane load force effects are not considered for fatigue limit state):

$$M = M_x(1 + 0.15)(0.428) = M_x(0.4922) \text{ kip-ft}$$

$$M_{0.0L} = 0 \text{ at support}$$

$$M_{0.1L} = 912(0.4922) = 449 \text{ kip-ft}$$

$$M_{0.2L} = 1592(0.4922) = 784 \text{ kip-ft}$$

$$M_{0.3L} = 2068(0.4922) = 1018 \text{ kip-ft}$$

www.EngineeringEBooksPdf.com

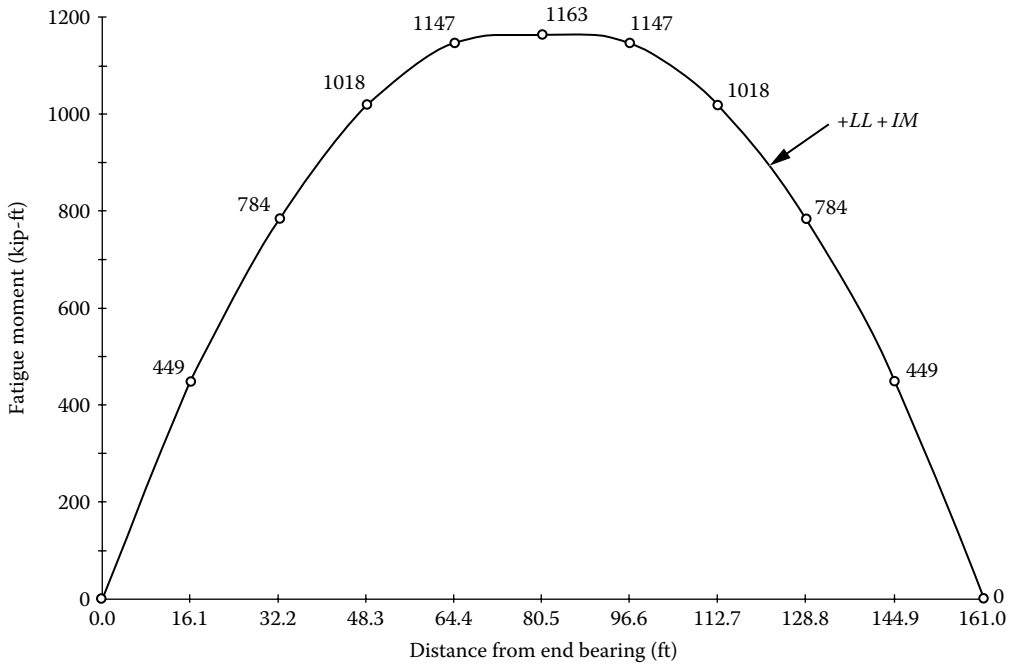

FIGURE 3.78 Fatigue load moments. (Courtesy of American Iron and Steel Institute, New York.)

$$M_{0.4L} = 2331(0.4922) = 1147 \text{ kip-ft}$$

$$M_{0.5L} = 2362(0.4922) = 1163 \text{ kip-ft}$$

Figure 3.78 shows the envelope for fatigue load moments.

Step 13: Shears for fatigue limit state.
Reference is made to Figure 3.72 for calculating (unfactored) shears for the fatigue limit state. Required shear values are calculated from Equations 3.39 and 3.48.

Maximum live load shear at the left support due to HS20 truck equals maximum reaction when the rear 32 kip axle is placed at that support. For L = 161 ft,

$$V_{0.0L} = R_{A,max} = 72 - \frac{1312}{L} = 72 - \frac{1312}{161} = 64 \text{ kip}$$

For x/L = 0.1 to 0.7, the positive shears are given by Equation 3.44:

$$V_x = 72\left(1 - \frac{x}{L}\right) - \frac{1312}{L} \tag{3.44}$$

$$V_{0.1L} = 72(1 - 0.1) - \frac{1312}{161} = 57 \text{ kip}$$

$$V_{0.2L} = 72(1 - 0.2) - \frac{1312}{161} = 49 \text{ kip}$$

$$V_{0.3L} = 72(1 - 0.3) - \frac{1312}{161} = 42 \text{ kip}$$

www.EngineeringEBooksPdf.com

$$V_{0.4L} = 72(1-0.4) - \frac{1312}{161} = 35 \text{ kip}$$

$$V_{0.5L} = 72(1-0.5) - \frac{1312}{161} = 28 \text{ kip}$$

$$V_{0.6L} = 72(1-0.6) - \frac{1312}{161} = 21 \text{ kip}$$

$$V_{0.7L} = 72(1-0.7) - \frac{1312}{161} = 13 \text{ kip}$$

For $x/L = 0.8$ and 0.9, the positive shears are given by Equations 3.46 and 3.48, respectively:

$$V_x = 64\left(1-\frac{x}{L}\right) - \frac{960}{L} \tag{3.46}$$

$$V_{0.8L} = 64(1-0.8) - \frac{960}{161} = 9 \text{ kip}$$

$$V_{0.9L} = 32\left(1-\frac{x}{L}\right) = 32(1-0.9) = 3 \text{ kip} \tag{3.48}$$

For $x/L = 1.0$,

$$V_x = 32\left(1-\frac{x}{L}\right) = 0.0 \text{ kip} \tag{3.48}$$

Maximum negative shears due to HS20 truck at $0.1L$ points are obtained from antisymmetry:

$$-V_{0.0L} = 0 \text{ kip}$$

$$-V_{0.1L} = -3 \text{ kip}$$

$$-V_{0.2L} = -7 \text{ kip}$$

$$-V_{0.3L} = -13 \text{ kip}$$

$$-V_{0.4L} = -21 \text{ kip}$$

$$-V_{0.5L} = -28 \text{ kip}$$

$$-V_{0.6L} = -35 \text{ kip}$$

$$-V_{0.7L} = -42 \text{ kip}$$

www.EngineeringEBooksPdf.com

$$-V_{0.8L} = -49 \text{ kip}$$

$$-V_{0.9L} = -57 \text{ kip}$$

$$V_{1.0L} = -64 \text{ kip}$$

Both positive and negative shears calculated earlier are multiplied by 1.15 to account for DLA (IM = 0.15 for fatigue) and DF = 0.822 for the shear at support and 0.733 for shear in span. The resulting values of unfactored live load shears are as follows:

$$V_{0.0L} = 64(1.15)(0.822) = 60 \text{ kip}$$

$$V_{0.1L} = 57(1.15)(0.733) = 48 \text{ kip}$$

$$V_{0.2L} = 49(1.15)(0.733) = 41 \text{ kip}$$

$$V_{0.3L} = 42(1.15)(0.733) = 35 \text{ kip}$$

$$V_{0.4L} = 35(1.15)(0.733) = 29 \text{ kip}$$

$$V_{0.5L} = 28(1.15)(0.733) = 23 \text{ kip}$$

$$V_{0.6L} = 21(1.15)(0.733) = 18 \text{ kip}$$

$$V_{0.7L} = 13(1.15)(0.733) = 11 \text{ kip}$$

$$V_{0.8L} = 7(1.15)(0.733) = 6 \text{ kip}$$

$$V_{0.9L} = 3(1.15)(0.733) = 2 \text{ kip}$$

$$V_{1.0L} = 0(1.15)(0.822) = 0 \text{ kip}$$

The values of negative shears are obtained from antisymmetry:

$$-V_{0.0L} = 0 \text{ kip}$$

$$-V_{0.1L} = -2 \text{ kip}$$

$$-V_{0.2L} = -6 \text{ kip}$$

$$-V_{0.3L} = -11 \text{ kip}$$

$$-V_{0.4L} = -18 \text{ kip}$$

$$-V_{0.5L} = -23 \text{ kip}$$

$$-V_{0.6L} = -29 \text{ kip}$$

$$-V_{0.7L} = -35 \text{ kip}$$

www.EngineeringEBooksPdf.com

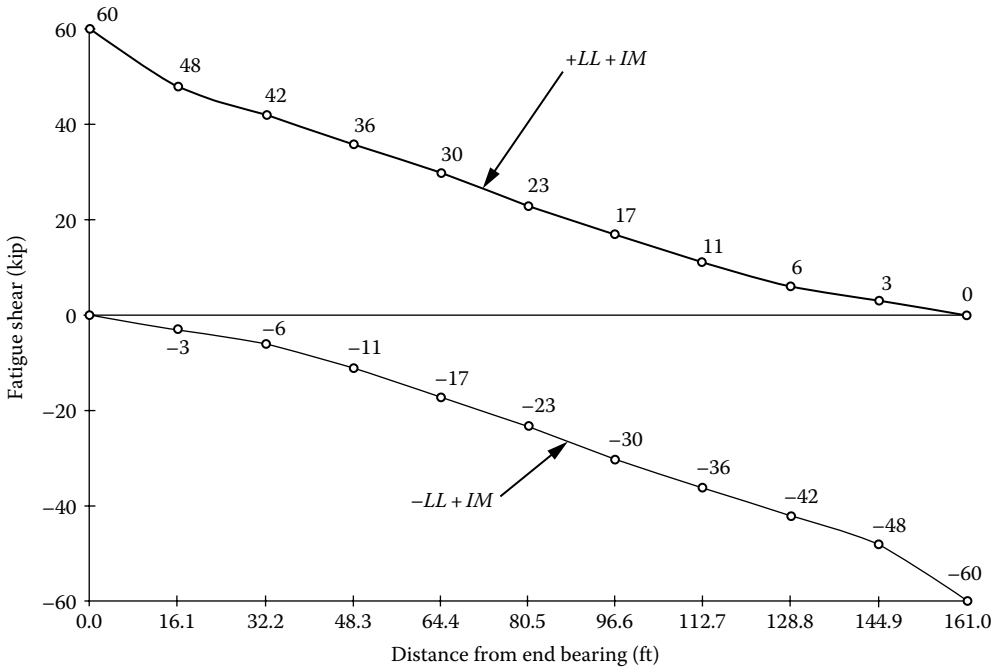

FIGURE 3.79 Fatigue load shear. (Courtesy of American Iron and Steel Institute, New York.)

$$-V_{0.8L} = -41 \text{ kip}$$

$$-V_{0.9L} = -48 \text{ kip}$$

$$-V_{1.0L} = -60 \text{ kip}$$

Figure 3.79 shows the envelope for fatigue load shears.

The aforementioned typical calculations illustrate the extent of numerous, lengthy, albeit simple, calculations required to draw moment and shear envelopes for girder design of a highway bridges. Note that these calculations are for the interior girder; similar calculations would need to be performed for the exterior girder as well. In practice, it is advisable that such calculations be performed on a spreadsheet to save time.

It is important to recognize that the aforementioned calculations are for unfactored loads; these moments and shears would need to be multiplied by appropriate load factors (γ-factors) to obtain the design forces for load and resistance factor design of the girders. Tables 3.26 through 3.29 present a summary of all calculations for the interior girder, including those for factored loads. Table 3.25 also shows moments due to the design tandem (for completeness); however, they are for illustrative purpose only as they do not govern for L = 161 ft (tandem load governs only for spans approximately 40 ft).

3.14 TIRE CONTACT AREA

3.14.1 Point Load versus Distributed Load

Although for design purposes, the wheel loads are assumed as knife-edge (or point) loads, in reality, they are applied over a certain contact area between the tires and the road surface. This contact area is called the *footprint* area and can sometimes be a design consideration for bridge decks and for road surfaces.

www.EngineeringEBooksPdf.com

TABLE 3.26
Moments (Unfactored) for Interior Girder

	Unfactored Live Load Moments (kip-ft) due to the Design Truck									
	Pointed toward 1.0*L* Rear-Axle Spacing				Pointed toward 0.0*L* Rear-Axle Spacing				Governing Design-Truck Moments	
	14 ft		30 ft		14 ft		30 ft			
x/L	*M+*	*M–*	*M+*	*M–*	*M+*	*M–*	*M+*	*M–*	*M+*	*M–*
0.00	0	0	0	0	0	0	0	0	0	0
0.10	976	0	912	0	909	0	858	0	976	0
0.20	1720	0	1592	0	1676	0	1573	0	1720	0
0.30	2233	0	2041	0	2221	0	2068	0	2233	0
0.40	2513	0	2257	0	2536	0	2331	0	2536	0
0.50	2618	0	2362	0	2618	0	2362	0	2618	0
0.60	2536	0	2331	0	2513	0	2257	0	2536	0
0.70	2221	0	2068	0	2233	0	2041	0	2233	0
0.80	1675	0	1573	0	1720	0	1592	0	1720	0
0.90	909	0	858	0	976	0	912	0	976	0
1.00	0	0	0	0	0	0	0	0	0	0

www.EngineeringEBooksPdf.com

	Unfactored Live Load Moments (kip-ft)												
	Vehicle Moments				Governing				1.33 × Vehicle Moment Plus Lane Moment (HL-93)			Governing Unfactored and Distributed *LL* + *IM* Moments	
	Design Truck		Design Tandem		Vehicle Moments		Design Lane						
x/L	*M+*	*M−*	*M+*	*M−*	*M+*	*M−*	*M+*	*M−*	*M+*	*M−*	D.F.	*M+*	*M−*
0.00	0	0	0	0	0	0	0	0	0	0	0.801	0	0
0.10	976	0	714	0	976	0	747	0	2045	0	0.801	1638	0
0.20	1720	0	1268	0	1720	0	1327	0	3615	0	0.801	2896	0
0.30	2233	0	1660	0	2233	0	1742	0	4712	0	0.801	3774	0
0.40	2536	0	1892	0	2536	0	1991	0	5364	0	0.801	4297	0
0.50	2618	0	1963	0	2618	0	2074	0	5556	0	0.801	4450	0
0.60	2536	0	1892	0	2536	0	1991	0	5364	0	0.801	4297	0
0.70	2233	0	1660	0	2233	0	1742	0	4712	0	0.801	3774	0
0.80	1720	0	1268	0	1720	0	1327	0	3615	0	0.801	2896	0
0.90	976	0	714	0	976	0	747	0	2045	0	0.801	1638	0
1.00	0	0	0	0	0	0	0	0	0	0	0.801	0	0

Source: Courtesy of American Iron and Steel Institute, New York.

www.EngineeringEBooksPdf.com

TABLE 3.27
Moments (Factored) for Interior Girder

	Calculation of Total Factored Moments (kip-ft) for Strength I Load Combination											Total Factored and Distributed Strength I Moments		
	Distributed *LL* + *IM*					1.25	1.25	1.5	Factored 1.75 (*LL* + *IM*)					
x/L	*DC*1	*DC*2	*DW*	*M*+	*M*−	*DC*1	*DC*2	*DW*	*DL*	*M*+	*M*−	η	*M*+	*M*−
0.00	0	0	0	0	0	0	0	0	0	0	0	0.95	0	0
0.10	2471	295	321	1638	0	3089	369	482	3940	2867	0	0.95	6,467	3,743
0.20	4392	525	570	2896	0	5490	656	855	7001	5068	0	0.95	11,466	6,651
0.30	5765	689	748	3774	0	7206	861	−1122	9189	6605	0	0.95	15,004	8,730
0.40	6588	787	855	4297	0	8235	984	1283	10502	7520	0	0.95	17,121	9,977
0.50	6863	820	891	4450	0	8579	1025	1337	10941	7788	0	0.95	17,793	10,394
0.60	6588	787	855	4297	0	8235	984	1283	10502	7520	0	0.95	17,121	9,977
0.70	5765	689	748	3774	0	7206	861	LI22	9189	6605	0	0.95	15,004	8,730
0.80	4392	525	570	2896	0	5490	656	855	7001	5068	0	0.95	11,466	6,651
0.90	2471	295	321	1638	0	3089	369	482	3940	2867	0	0.95	6,467	3,743
1.00	0	0	0	0	0	0	0	0	0	0	0	0.95	0	0

www.EngineeringEBooksPdf.com

Calculation of Total Factored Moments (kip-ft) for Fatigue Load Combination

	Fatigue Truck Moments				Governing Moments		*LL + IM* (*IM* = 1.15)		Governing Unfactored and Distributed Fatigue Moments			Governing Factored and Distributed Fatigue Moments (*LF* = 0.75)	
	Toward 1.0*L*		Toward 0.0*L*										
x/L	*M+*	*M–*	*M+*	*M–*	*M+*	*M–*	*M+*	*M–*	D.F.	*M+*	*M–*	*M+*	*M–*
0.00	0	0	0	0	0	0	0	0	0.428	0	0	0	0
0.10	912	0	858	0	912	0	1049	0	0.428	449	0	337	0
0.20	1592	0	1573	0	1592	0	1831	0	0.428	784	0	588	0
0.30	2041	0	2068	0	2068	0	2378	0	0.428	1018	0	764	0
0.40	2257	0	2331	0	2331	0	2681	0	0.428	1147	0	860	0
0.50	2362	0	2362	0	2362	0	2716	0	0.428	1162	0	872	0
0.60	2331	0	2257	0	2331	0	2681	0	0.428	1147	0	860	0
0.70	2068	0	2041	0	2068	0	2378	0	0.428	1018	0	764	0
0.80	1573	0	1592	0	1592	0	1831	0	0.428	784	0	588	0
0.90	858	0	912	0	912	0	1049	0	0.428	449	0	337	0
1.00	0	0	0	0	0	0	0	0	0.428	0	0	0	0

Source: Courtesy of American Iron and Steel Institute, New York.

www.EngineeringEBooksPdf.com

TABLE 3.28
Shears (Unfactored) for Interior Girder)

	Unfactored Live Load Shears (kip) due to the Design Truck									
	Pointed toward 1.0*L* Rear-Axle Spacing				Pointed toward 1.0*L* Rear-Axle Spacing				Governing Design-Truck Shears	
	14 ft		30 ft		14 ft		30 ft			
x/L	*V*+	*V*–	*V*+	*V*–	*V*+	*V*–	*V*+	*V*–	*V*+	*V*–
0.00	68	0	64	0	64	0	60	0	68	0
0.10	61	–4	57	–3	56	–4	53	–3	61	–4
0.20	53	–10	49	–7	49	–10	46	–7	53	–10
0.30	46	–16	42	–13	42	–17	39	–13	46	–17
0.40	39	–23	35	–20	36	–25	32	–21	39	–25
0.50	32	–29	28	–26	29	–32	26	–28	32	–32
0.60	25	–36	21	–32	23	–39	20	–35	25	–39
0.70	17	–42	13	–39	16	–46	13	–42	17	–46
0.80	10	–49	7	–46	10	–53	6	–49	10	–53
0.90	4	–56	3	–53	3	–61	3	–57	4	–61
1.00	0	–63	0	–60	0	–68	0	–64	0	–68

www.EngineeringEBooksPdf.com

	Unfactored Live Load Shears (kip)											Governing Unfactored and Distributed *LL* + *IM* Shears	
	Vehicle Shears				Governing				1.33 × Vehicle Shear Plus Lane Shear (HL-93)				
	Design Truck		Design Tandem		Vehicle Shears		Design Lane						
x/L	*V*+	*V*−	*V*+	*V*−	*V*+	*V*−	*V*+	*V*−	*V*+	*V*−	D.F.	*V*+	*V*−
0.00	68	0	49	0	68	0	52	0	142	0	1.284	182	0
0.10	61	−4	44	−4	61	−4	42	−1	123	−6	1.145	141	−7
0.20	53	−10	39	−9	53	−10	33	−2	103	−15	1.145	118	−17
0.30	46	−17	34	−14	46	−17	25	−5	86	−28	1.145	98	−32
0.40	39	−25	28	−19	39	−25	19	−8	71	−41	1.145	81	−47
0.50	32	−32	24	−24	32	−32	13	−13	56	−56	1.145	64	−64
0.60	25	−39	19	−28	25	−39	8	−19	41	−71	1.145	47	−81
0.70	17	−46	14	−34	17	−46	5	−25	28	−86	1.145	32	−98
0.80	10	−53	9	−39	10	−53	2	−33	15	−103	1.145	17	−118
0.90	4	−61	4	−44	4	−61	1	−42	6	−123	1.145	7	−141
1.00	0	−68	0	−49	0	−68	0	−52	0	−142	1.284	0	−182

Source: Courtesy of American Iron and Steel Institute, New York.

www.EngineeringEBooksPdf.com

TABLE 3.29
Shears (Factored) for Interior Girder

	Calculation of Total Factored Shears (kip) for Strength I Load Combination											Total Factored and Distributed Strength I Shears		
	Distributed *LL + IM*					1.25	1.25	1.5	Factored 1.75 (*LL + IM*)					
x/L	*DC*1	*DC*2	*DW*	*V*+	*V*−	*DC*1	*DC*2	*DW*	*DL*	*V*+	*V*−	η	*V*+	*V*−
0.00	171	20	22	182	0	214	25	33	272	319	0	0.95	561	258
0.10	136	16	18	141	−7	170	20	27	217	247	−12	0.95	441	195
0.20	102	12	13	118	−17	128	15	20	163	207	−30	0.95	352	126
0.30	68	8	9	98	−32	85	10	14	109	172	−56	0.95	267	50
0.40	34	4	4	81	−47	43	5	6	54	142	−82	0.95	186	−27
0.50	0	0	0	64	−64	0	0	0	0	112	−112	0.95	106	−106
0.60	−34	−4	−4	47	−81	−43	−5	6	−54	82	−142	0.95	27	−186
0.70	−68	−8	−9	32	−98	−85	−10	−14	−109	56	−172	0.95	−50	−267
0.80	−102	−12	−13	17	−118	−128	−15	−20	−163	30	−207	0.95	−126	−352
0.90	−136	−16	−18	7	−141	−170	−20	−27	−217	12	−247	0.95	−195	−441
1.00	−171	−20	−22	0	−182	−214	−25	−33	−272	0	−319	0.95	−258	−561

www.EngineeringEBooksPdf.com

Calculation of Total Factored Shears (kip) for Fatigue Load Combination

	Fatigue Truck Shears												
	Toward 1.0*L*		Toward 0.0*L*		Governing Shears		*LL* + *IM* (*IM* = 1.15)		Governing Unfactored and Distributed Fatigue Shears			Governing Factored and Distributed Fatigue Shears (*LF* = 0.75)	
x/*L*	*V*+	*V*–	*V*+	*V*–	*V*+	*V*–	*V*+	*V*–	D.F.	*V*+	*V*–	*V*+	*V*–
0.00	64	0	60	0	64	0	74	0	0.822	61	0	46	0
0.10	57	–3	53	–3	57	–3	66	–3	0.733	48	–2	36	–2
0.20	49	–6	46	–6	49	–6	56	–7	0.733	41	–6	31	–5
0.30	42	–13	39	–13	42	–13	48	–15	0.733	35	–11	26	–8
0.40	35	–20	32	–21	35	–21	40	–24	0.733	29	–18	22	–14
0.50	28	–26	26	–28	28	–28	32	–32	0.733	23	–23	17	–17
0.60	21	–32	20	–35	21	–35	24	–40	0.733	18	–29	14	–22
0.70	13	–39	13	–42	13	–42	15	–48	0.733	11	–35	8	–26
0.80	7	–46	6	–49	7	–49	8	–56	0.733	6	–41	5	–31
0.90	3	–53	3	–57	3	–57	3	–66	0.733	2	–48	2	–36
1.00	0	–60	0	–64	0	–64	0	–74	0.822	0	–61	0	–46

Source: Courtesy of American Iron and Steel Institute, New York.

www.EngineeringEBooksPdf.com

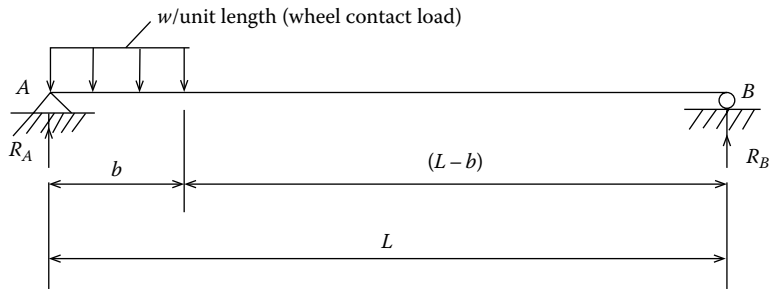

FIGURE 3.80 Position of wheel contact load for maximum shear.

For short spans, modeling wheel contact area loads as point loads (as assumed in all previous examples) results in overly conservative design. Instead, the wheel load can be modeled as a uniform load over the tire contact surface.

Generally speaking, the span length would be longer than the length of the tire footprint area. In such case, the position of the uniform load on span would be different for maximum shear and maximum moment. In both cases, the span is only partially uniformly loaded.

Figure 3.80 shows the load position for maximum shear condition, which occurs when the distributed load is at one end of the span. The maximum shear in the span, V_{max}, equals the reaction at the left support, R_L, which can be expressed as given by Equation 3.53:

$$V_{max} = R_L = \frac{wb}{2L}(2L - b) \tag{3.53}$$

Likewise, Figure 3.81 shows load position of the partial uniform load for maximum moment in the span, which occurs when the load is positioned at the midspan. The maximum moment in the span is given by Equation 3.54:

$$M_{max} = \frac{wb}{4}\left(L - \frac{b}{2}\right) \tag{3.54}$$

For longer spans, the designer must consider as many wheel load contact areas as possibly can be placed on the span simultaneously (i.e., two- or three-wheel load in the case of HL-93 truck and two wheel loads in the case of tandem load).

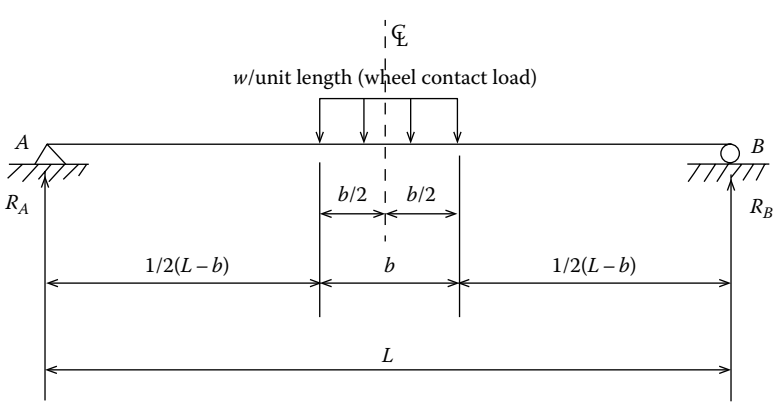

FIGURE 3.81 Position of wheel contact load for maximum moment.

www.EngineeringEBooksPdf.com

3.14.2 AASHTO LRFD Specifications for Tire Contact Area

The tire contact area of a wheel (of AASHTO design truck or tandem) consisting of one or two tires is assumed to be a 20 in. wide × 10 in. long rectangular footprint. The tire pressure is assumed distributed over this contact area as follows (AASHTO LRFD Art. 3.6.1.2.5):

1. On continuous surfaces, uniformly over the specified contact area
2. On interrupted surfaces, uniformly over the actual contact area within the footprint with the pressure increased in the ratio of the specified to actual area (ratio > 1.0)

The aforementioned provisions apply to the design truck and tandem only. For other trucks or design vehicles, the tire contact area should be determined by the designer. As a guide, the tire contact area (in.^{2}) may be determined from the following dimensions:

$$\text{Tire width} = P/0.8 \tag{3.55}$$

$$\text{Tire length} = 6.4\gamma[1 + 0.01(IM)] \tag{3.56}$$

where
γ = load factor
IM = DLA (or impact factor)
P = design wheel load (kip)

Example 3.19 illustrates applications of Equations 3.53 and 3.54. Example 3.20 illustrates applications of Equations 3.55 and 3.56.

Example 3.19

(a) Calculate, based on the tire contact area, the maximum shear and moment due to HL-93 truck and (b) compare these results with maximum shear and moment calculated assuming the wheel loads as point loads.

Solution

a. Maximum shear and moment in the decking based on the tire contact area
Convert the wheel load (concentrated load) into distributed load. The wheels of the HL-93 truck are spaced 6 ft apart laterally. Therefore, we can place only one wheel on the 72 in. span of the decking element:

$$\text{Wheel load, } P = 16{,}000 \text{ lb}$$

$$\text{Tire contact area} = (10)(20) = 200 \text{ in.}^2$$

$$\text{Average contact pressure, } p = \frac{\textit{wheel load}}{\textit{tire contact area}} = \frac{16{,}000}{200} = 80 \text{ lb/in.}^2$$

$$\text{Load per unit length on each decking element, } w = p(\text{element width})$$

$$= (80)(12) = 960 \text{ lb/in. in 10 in. length}$$

To obtain maximum shear in the decking element, the distributed load of 960 lb/in. should be placed near the left support as shown in Figure 3.80. Referring to that figure, we now

www.EngineeringEBooksPdf.com

have w = 960 lb/in., b = 10 in., and L = 72 in. The maximum shear in the decking element is obtained from Equation 3.53:

$$V_{max} = R_A = \frac{wb}{2L}(2L - b) = \frac{(960)(10)}{2(72)}(2\times 72 - 10) = 8933 \text{ lb (or 8.93 kip)}$$

Maximum moment is obtained when the distributed load is placed at the midspan as shown in Figure 3.81. Referring to that figure, the maximum moment in the span is obtained from Equation 3.54:

$$M_{max} = \frac{wb}{4}\left(L - \frac{b}{2}\right) = \frac{(960)(10)}{4}\left(72 - \frac{10}{2}\right) = 160{,}800 \text{ lb-in.} = 13.4 \text{ kip-ft}$$

b. Maximum shear and moment in the decking due to the concentrated wheel load
For maximum shear in span, the concentrated wheel load should be placed as close to the support as possible. For this load position,

$$V_{max} = 16 \text{ kip}$$

By comparison, V_{max} = 8.93 kip based on distributed load criterion.

For maximum moment in the span, the wheel load should be placed at the center of the span. For this load position,

$$M_{max} = PL/4 = (16)(72)/4 = 288 \text{ kip-in.} = 24 \text{ kip-ft}$$

By comparison, M_{max} = 13.4 kip-ft based on distributed load criterion.

Conclusion: The distributed load criterion results in much smaller forces, just slightly over 50 percent of the forces based on the wheel load criterion, a huge design advantage. Therefore, the lower value (13.4 kip-ft) may be used for design.

Example 3.20

Calculate the maximum shear and moment in a decking element due to 20 kip wheel load of a loader equipment. The decking element spans 72 in. and is 12 in. wide. Information about the tire contact area is not available.

Solution

$$P = 20 \text{ kip}$$

Tire contact area information is not available. So, use Equations 3.55 and 3.56 to estimate the tire contact area. From Equations 3.55,

$$\text{Tire width} = P/(0.8) = 20/(0.8) = 25 \text{ in.}$$

The length of the tire contact area, b, is given by Equations 3.56:

$$\text{Tire length} = 6.4\gamma[1 + 0.01(IM)]$$

For the Strength I Limit State, the load factor for live load is

$$\gamma = 1.75 \text{ (Table 3.7/AASHTO LRFD Table 3.7.1-1)}$$

www.EngineeringEBooksPdf.com

$$IM = 33 \text{ percent (for all other elements, specifications Table 3.6.2.1-1)}$$

$$\text{Tire length} = 6.4\gamma[1 + 0.01(IM)] = (6.4)(1.75)[1 + 0.01(33)] = 14.9 \text{ in., say 15 in.}$$

$$b = 15 \text{ in.}$$

$$\text{Tire contact area} = (\text{length})(\text{width}) = (15)(25) = 375 \text{ in.}^2$$

$$\text{Average contact pressure, } p = \frac{\textit{wheel load}}{\textit{tire contact area}} = \frac{20{,}000}{375} = 53.33 \text{ lb/in.}^2$$

Calculate the distributed load, w, on the decking element:

$$W = p(\text{element width}) = (53.33)(12) = 640 \text{ lb/in.}$$

Calculate the maximum shear in the decking element from Equation 3.53 (refer to Figure 3.80):

$$V_{max} = R_L = \frac{wb}{2L}(2L - b) = \frac{(640)(15)}{2(72)}(2 \times 72 - 15) = 8600 \text{ lb}$$

By comparison, as a concentrated load, $V_{max} = 20$ kip.

Calculate the maximum moment in the decking element from Equation 3.54 (refer to Figure 3.81):

$$M_{max} = \frac{wb}{4}(L - b/2) = \frac{(640)(15)}{4}\left(72 - \frac{15}{2}\right) = 154{,}800 \text{ lb-in.} = 12.9 \text{ kip-ft}$$

By comparison, as point load, $M_{max} = PL/4 = (20)(72)/4 = 360$ kip-in. = 30 kip-ft.

3.15 RAIL TRANSIT LOADS

In some situations, a bridge may have to be designed to carry both the highway traffic and railroad-transit vehicles. Many such bridges exist all over the world. For these multiple-use bridges, the highway bridge deck and the railroad tracks may be at the same level or at different levels. For example, in some double-deck bridges, the rail-transit vehicles use one deck and the highway traffic the other. For design of a combined highway–railroad bridge, design specifications and transit load characteristics should be obtained from the bridge owner. The latter may include loads, load distribution, load frequency, DLA, and dimensional requirements (AASHTO LRFD Art. 3.6.1.5).

If the rail transit is designed to occupy an exclusive lane, transit loads should be included in the design, but in no case the bridge may be designed for strength less than if it had been designed as a highway bridge of the same width. This is a very important consideration because of the possibility of relocation of railroad tracks.

3.16 CENTRIFUGAL FORCE (CE)

Bridges that are *curved* in plan must be designed for *centrifugal force*, which results from the dynamics of the moving vehicle. In general, when a particle of mass m moves along a constrained curved path with a constant velocity, there is a normal force exerted on the particle by the constraint. It is caused by the *centripetal* (meaning *toward the center of rotation*) acceleration and acts perpendicular to the tangent to the path. For equilibrium, an equal and opposite force, called the

www.EngineeringEBooksPdf.com

centrifugal force, is transferred to the path. Based on the theory of particle dynamics, the magnitude of this force can be determined from Equation 3.57:

$$F = \frac{mv^2}{R} \tag{3.57}$$

Alternatively, Equation 3.57 can be expressed as given by Equation 3.58:

$$F = \left(\frac{W}{g}\right)\frac{v^2}{R} \tag{3.58}$$

where

$m = W/g$ = mass of the particle
W = weight of the particle
v = particle velocity, ft/sec
R = instantaneous radius of curvature of the path
g = acceleration due to gravity (32.2 ft/s^2)

The centrifugal force, thus, originates from the dynamics of the vehicle motion along a curved path and is transmitted to the path itself, in this case, the bridge deck. Because this force is inversely proportional to the radius of curvature, the sharper the curve, the larger the centrifugal force. Equation 3.58 shows that the magnitude of this force equals the product of the weight of the moving vehicle and the quantity v^2/gR. If the speed of the vehicle is expressed in V mph, Equation 3.58 can be expressed as Equation 3.59:

$$F = \left(\frac{W}{32.2}\right)\left(\frac{5280}{3600}V\right)^2\left(\frac{1}{R}\right) \tag{3.59}$$

Equation 3.59 is simplified and expressed as given by Equation 3.60:

$$\frac{F}{W} = 0.0668\left(\frac{V}{R}\right)^2 \tag{3.60}$$

The right side of Equation 3.60 represents the magnitude of the centrifugal force in terms of a fraction of the vehicle weight. It can be also expressed in terms of the percentage of the weight of the vehicle (W) in motion:

$$\frac{F}{W} = 6.68\left(\frac{V^2}{R}\right) \tag{3.61}$$

For computational simplicity, AASHTO LRFD suggests neglecting the presence of lane load in calculating the centrifugal force assuming the spacing of vehicles at high speeds to be large, which results in a low density of vehicles following and/or preceding the design truck. The specified combination of design truck and the lane load, however, represents a group of exclusion vehicles that produce force effects of at least 4/3 times of those caused by the design truck alone on short- and medium-span bridges (AASHTO LRFD *Commentary C3.6.3*). In view of this assumption, the right

www.EngineeringEBooksPdf.com

side of Equation 3.57 is multiplied by a factor 4/3 (factor f in Equation 3.66, shown later) so that the centrifugal force is expressed as given by Equation 3.62:

$$F = \frac{4}{3}\left(\frac{mv^2}{R}\right) = \frac{4}{3}\left(\frac{W}{g}\right)\frac{v^2}{R} \tag{3.62}$$

Accordingly, Equation 3.61 can be written as given in Equation 3.63:

$$\frac{F}{W} = \frac{4}{3}\left[6.68\left(\frac{V^2}{R}\right)\right] = 8.91\left(\frac{V^2}{R}\right) \tag{3.63}$$

For simplicity, Equation 3.63 can be rewritten as given Equation 3.64:

$$F = CW \tag{3.64}$$

where

$$C = \frac{8.91V^2}{R} \tag{3.65}$$

ASHTO LRFD Specification suggests Equation 3.65 in the form of Equation 3.66:

$$C = f\frac{v^2}{gR} \tag{3.66}$$

where f = 4/3 for load combinations other than fatigue
= 1.0 for fatigue

Equation 3.66 is the same as AASHTO LRFD Equation 3.6.3-1. The centrifugal force is calculated as the product of coefficient C and the weight of the axles and is assumed to act horizontally at a distance of 6.0 ft above the road surface.

AASHTO LRFD Specification suggests applying Equation 3.66 only to truck load and *not* to the lane load. Therefore, the centrifugal force so determined would be an approximation of the actual centrifugal force that would be exerted on a curved bridge deck as the provision (Art. 3.6.3) does not explicitly account for the presence of the lane load. However, this convenient representation is considered acceptable in view of the uncertainty of centrifugal force from random traffic patterns.

Multiple presence factors listed in Table 3.24 (discussed earlier) apply to the centrifugal force.

Care should be exercised in determining centrifugal forces due to trucks moving in different traffic lanes of a multilane bridge deck. This is because the radius R in Equation 3.66 refers to the curvature of the path traversed by the *centroid* of the moving load, which would be different for the vehicles moving in different traffic lanes of the same curved deck; the farther the lane from the center of curve, the larger the radius R.

As a practical matter, it is noted that centrifugal force is directly proportional to the *square* of velocity (or the speed) of the moving vehicle—the larger the speed, the larger the centrifugal force. Driving faster than the posted safe speed limit on the curved highway or a bridge can be very dangerous, which can lead to overturning of the vehicles. This is especially true for entrance or exit ramps for freeways.

www.EngineeringEBooksPdf.com

In order to determine the centrifugal force exerted by a vehicle on the deck, coefficient C should be determined from Equation 3.65, which when multiplied by the weight of a single truck would give the centrifugal force (Equation 3.64).

Example 3.21 presents the calculations for the centrifugal forces on single-span curved bridge.

Example 3.21

Figure 3.82 shows the plan and cross section of a single-span, two-lane curved, slab–girder bridge. Calculate the centrifugal force on the bridge according to AASHTO LRFD Specifications. Assume that the safe speed along the curve is limited to 35 mph.

Solution

Commentary: Positioning the wheel loads correctly on the bridge deck to produce maximum force effect is the sole consideration here. In Figure 3.82, one HS20 truck is placed in each of the two 12 ft wide lanes, with wheels of the trucks placed to produce the maximum effect on both girders G_2 and G_3. Note also that the radii of girders G_2 and G_3 are shorter than the radius of girder G_1, which is positioned farthest from the center of the curved girders. Thus, the two trucks have been so positioned in their respective lanes that their centroids travel on curves with the shortest radii. Because the centrifugal force is inversely proportional to the radius (radius R appears in the

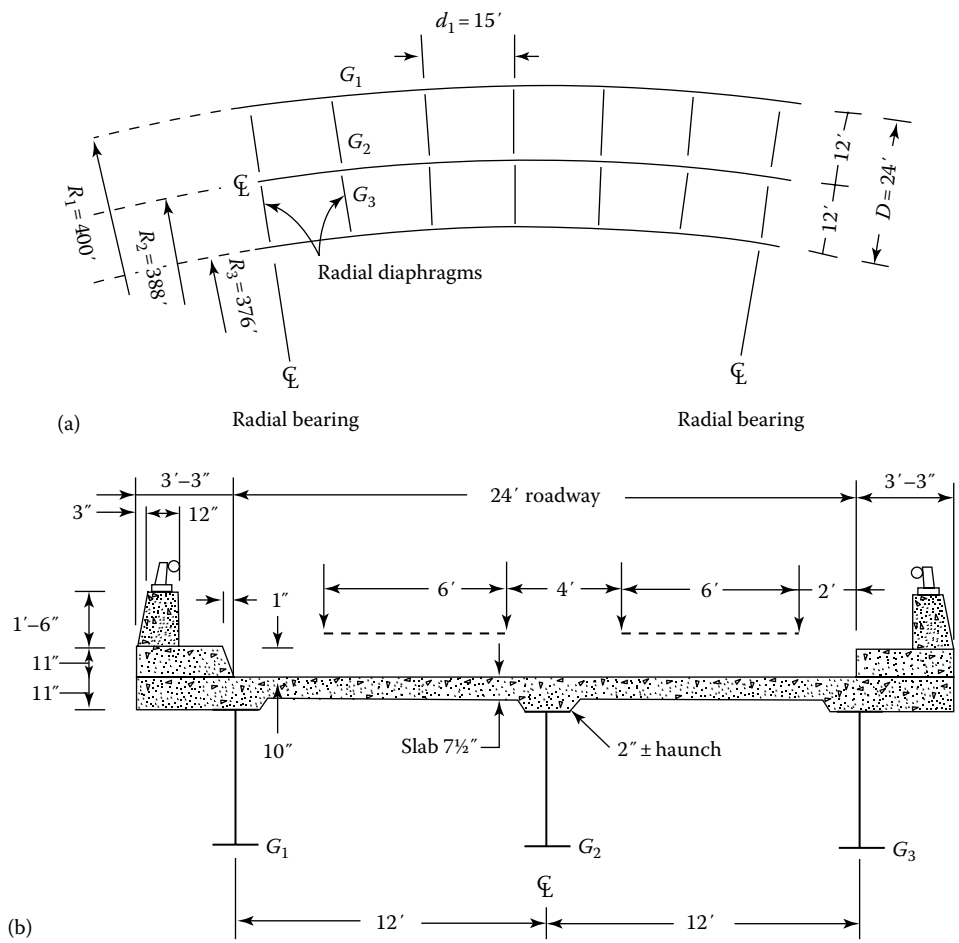

FIGURE 3.82 (a) Plan and (b) cross section of the curved bridge for Example 3.21.

www.EngineeringEBooksPdf.com

denominator of Equation 3.65 or its variations), the shorter the radius, the large the centrifugal force. Note that the two trucks can also be positioned in their respective lanes so as to have maximum effect on girders $G1$ and G_2. However, in this position, the centroids of both trucks will be moving along curves with larger radii, which would develop smaller centrifugal force.

For placement of the trucks in the most critical position, it is noted that the radius of the right exterior girder is 376 ft. The centroid of the truck in the right lane would be located at 5 ft from the curb (closest distance). The centroid of the truck in the left lane would be at a distance of 10 ft (= 3 + 4 + 3 ft) from the centroid of the truck in the right lane. From the position of the curved girders shown in Figure 3.82, and we obtain the radii of the girders G_2 and G_3 as follows:

$$R_1 = 376 + 5 = 381 \text{ ft}$$

$$R_2 = 381 + 10 = 391 \text{ ft}$$

From Equation 3.65, we obtain the value of coefficient C as follows:

$$\text{For the right truck, } C = \frac{8.91V^2}{R_1} = 8.91\left(\frac{(35)^2}{381}\right) = 28.65 \text{ percent of } W$$

$$\text{For the left truck, } C = \frac{8.91V^2}{R_2} = 8.91\left(\frac{(35)^2}{391}\right) = 27.91 \text{ percent of } W$$

Thus, for each of the rear 32 kip axles, the centrifugal force, F_c, would be

$$\text{Right truck: } F_c = 0.2865(32) = 9.17 \text{ kip}$$

$$\text{Left truck: } F_c = 0.2791(32) = 8.93 \text{ kip}$$

For front 8 kip axle, the centrifugal force, F_c, would be

$$\text{Right truck: } F_c = 0.2865(8) = 2.29 \text{ kip}$$

$$\text{Left truck: } F_c = 0.2791(8) = 2.23 \text{ kip}$$

Total centrifugal force: Apply multipresence factor = 1.0 (for two lanes)

$$\text{Right truck, } F_c = (1.0)\ [2(9.17) + 2.29] = 20.63 \text{ kip}$$

$$\text{Left truck, } F_c = (1.0)\ [2(8.93) + 2.23] = 20.09 \text{ kip}$$

These forces act horizontally at 6 ft above the road surface.

3.17 BRAKING FORCE (BR)

3.17.1 Magnitude of Braking Force

Braking force is produced when brakes are suddenly applied to a moving vehicle. Research indicates that braking forces for short- and medium-span bridges can be much higher than those specified in AASHTO Standard, provisions that date back almost to 1940s and had remained unchanged to address the improved braking capacity of modern trucks. AASHTO LRFD provides for design

www.EngineeringEBooksPdf.com

braking forces that are significantly larger than those specified by AASHTO Standard. Figure 3.83 shows a comparison of braking forces provided for in other bridge design codes; braking forces according to AASHTO Standard seem to be much smaller for short- and medium-span bridges. The sloping portions of the curves in Figure 3.83 represent the braking forces that include a portion of the lane load. Readers should refer to *AASHTO LRFD Commentary C3.6.4* for a brief discussion on this topic.

AASHTO LRFD Art. 3.6.4 specifies a prescriptive method to calculate the magnitude of this force as related to bridge design. The braking force is calculated as a function of vehicle weight, which depends on the following two parameters:

1. Velocity of the vehicle, v
2. The length (distance) over which the vehicle decelerates, a

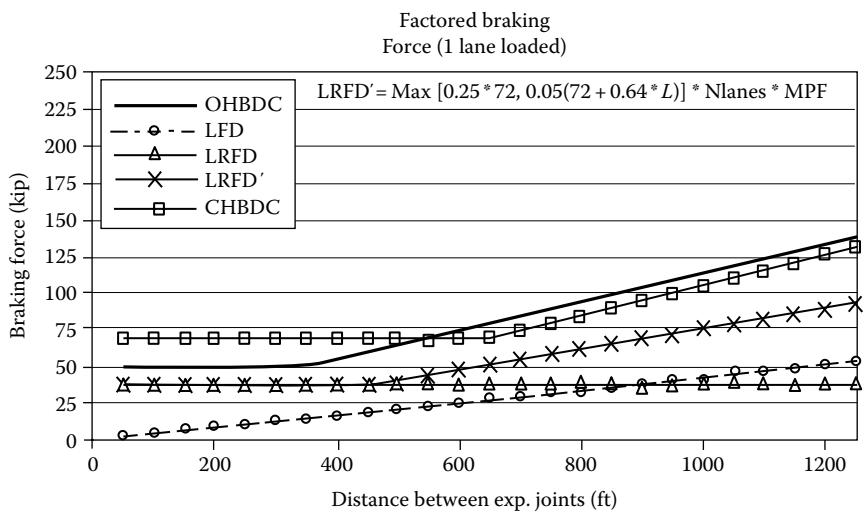

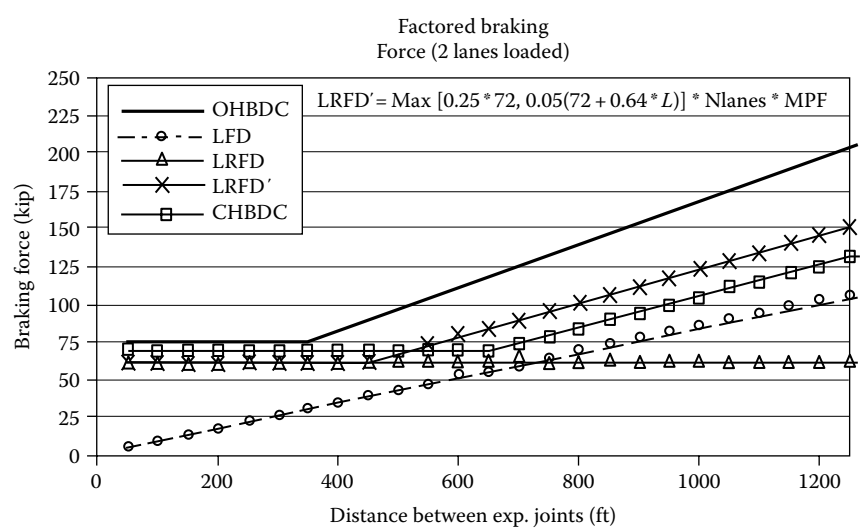

FIGURE 3.83 Comparison of braking force models. (From *AASHTO LRFD Bridge Design Specifications*, Copyright © 2012 by American Association of State Highway and Transportation Officials, Washington, DC. Used by permission.) (*Continued*)

www.EngineeringEBooksPdf.com

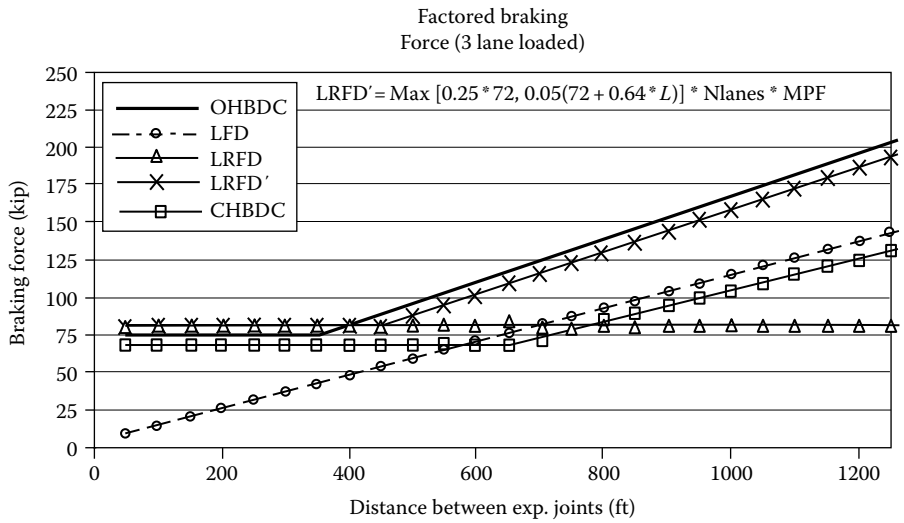

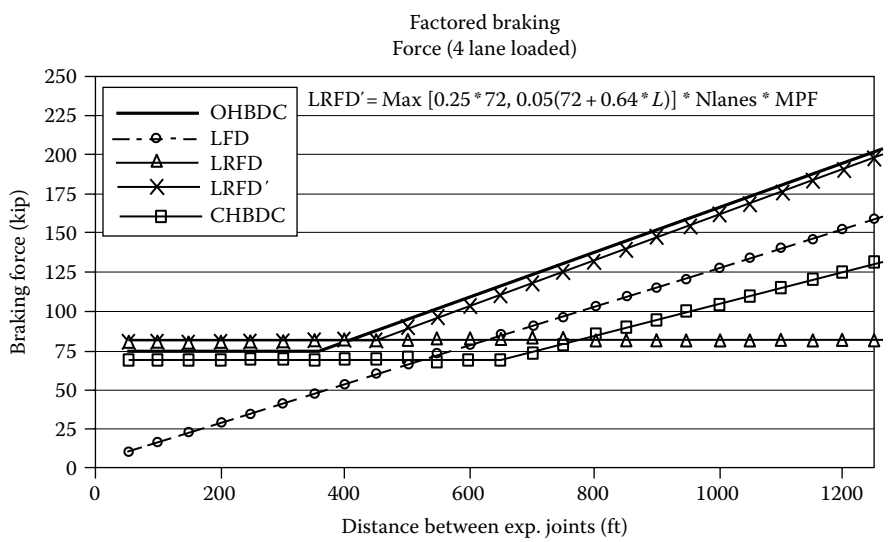

FIGURE 3.83 (*Continued*) Comparison of braking force models. (From *AASHTO LRFD Bridge Design Specifications*, Copyright © 2012 by American Association of State Highway and Transportation Officials, Washington, DC. Used by permission.)

Assuming a uniform deceleration produced by braking, the induced braking force can be expressed as a fraction of the vehicle weight by Equation 3.67:

$$b = \frac{v^2}{2ga} \tag{3.67}$$

where

b = fraction of the vehicle weight
v = velocity of the vehicle, ft/s
a = length of uniform deceleration

www.EngineeringEBooksPdf.com

According to AASHTO LRFD, the braking force is to be as the greater of the following:

1. 25 percent of the axle weights of the design truck or the design tandem.
2. 5 percent of the design truck plus lane load or 5 percent of design tandem and the lane load.

Although the 25 percent value specified in items 1 and 2 given earlier appears to be prescriptive, it has been derived based on energy principles. These forces are calculated for one design lane only; the total braking force would be obtained by multiplying the aforementioned force by the number of design lanes. Braking forces are transferred to bearings on the supports; they are used for design of bearings and for stability analysis and design of abutments. For design, braking force on one bearing would be obtained by dividing the total braking force by the number of bearings.

3.17.2 Application of Braking Forces on a Bridge

The following specifications apply with respect to application of the braking force:

1. The braking force is to be applied in *all* design lanes that are considered loaded (as discussed earlier) and carrying traffic headed in the same direction.
2. The braking forces are assumed to act horizontally, 6 ft above the roadway surface, in *either* direction to produce maximum force effects.
3. All design lanes shall be assumed loaded simultaneously for bridges likely to become one-directional in the future.
4. The multiple presence factors (Table 3.14) apply to the braking force to account for the simultaneous loading of all design lanes.
5. Dynamic load allowance (*IM*) is *not* applied to braking force.

Braking force does not affect the design of superstructure elements directly. However, the superstructure transfers this force to the substructure (abutments and piers) through girder bearings. *Because the braking force can act in either direction, it should be ignored if it counteracts the worst-case scenario.* For example, its effect on the abutment should be considered as producing overturning moment, which would be additive to overturning moment due to earth pressure, that is, its direction should be the same as that of the active pressure acting on the abutment.

Example 3.22 illustrates application of Equation 3.67.

Example 3.22: Calculation of Braking Force

Calculate braking force on a two-lane highway bridge spanning 100 ft according to AASHTO LRFD. Assume the vehicle velocity as 55 mph and that it can decelerate over a distance of 400 ft. The bridge deck is supported over four longitudinal girders supported on bearings.

Solution

Length of uniform deceleration, a = 400 ft
Vehicle velocity, V = 55 mph
The fraction of the vehicle weight, b, is calculated from Equation 3.67 as follows:

$$b = \frac{v^2}{2ga} = \left(\frac{55 \times 5280}{3600}\right)^2 \frac{(1)}{2(32.2)(400)} = 0.2526 \ \textit{or} \ 25 \text{ percent of vehicle weight}$$

www.EngineeringEBooksPdf.com

Calculate the braking force. The braking force is to be as the greater of the following:

1. 25 percent of the axle weights of the design truck:

$$BR = 0.25(8 + 32 + 32) = 0.25(72) = 18 \text{ kip (governs)}, \quad \text{or}$$

25 percent of the axle weights of the design tandem:

$$BR = 0.25(25 + 25) = 0.25(50) = 12.5 \text{ kip} < 18 \text{ kip}$$

2. 5 percent of the design truck plus lane load:

$$BR = 0.05(72) + 0.05(0.64 \times 100) = 6.8 \text{ kip}, \quad \text{or}$$

5 percent of the design tandem plus the lane load:

$$BR = 0.05(50) + 0.05(0.64 \times 100) = 5.7 < 6.8 \text{ kip}$$

Therefore, BR = 18 kip per lane (the largest of the aforementioned values)

$$\text{For two lanes, } BR = 2(18) = 36 \text{ kip}$$

$$\text{Number of bearings} = 4$$

$$BR = 36/4 = 9 \text{ kip per bearing}$$

Apply the multiple presence factor (from Table 3.14).
For two loaded lanes, multiple presence factor = 1.0

$$BR = (9)(1.0) = 9 \text{ kip per bearing}$$

3.18 VEHICULAR COLLISION FORCE (*CT*)

3.18.1 Nature, Causes, and Magnitude of Collision Forces

All over the world, many bridges or parts thereof are either severely damaged or destroyed as a result of collision with other objects. The collision forces may be caused by vehicular or other traffic smashing into the bridge. The damage may be caused to the superstructure, the substructure, or both, which can be catastrophic.

Superstructures of overhead bridges may be hit by vehicles passing under them because of insufficient overhead clearances, essentially caused by negligent drivers who ignore posted overhead clearance limits. Accidental collisions of heavy vehicles with bridge piers or bent columns are yet another cause of damage to bridge substructures. These collision forces are called *vehicular collision forces* (denoted by abbreviation *CT*). Several examples of such accidents have been reported in the literature (NTSB 1993, ENR 2003). Bridges over waterways may be hit by ships and barges causing damage to abutments, piers, or bents. Collision by floating ice is yet another possible cause of damage to bridges over water. Forces causing such damage are referred to as *vessel collision forces* (denoted by abbreviation *CV*). Bridges over waterways may also be hit by floating ice; the causative forces are referred to as *ice loads* (abbreviated as *IC*).

AASHTO LRFD presents design requirements to guard against collision forces in separate articles as follows:

1. *Art. 3.6.5*: Vehicular collision force, *CT*, for land-based bridges (a subarticle under Art. 3.6: live loads). The provisions of this article apply to land-based bridges that may be subjected to collisions from approaching vehicles.

www.EngineeringEBooksPdf.com

2. *Art. 3.14*: Vessel collision force, *CV*. The provisions of this article apply to the accidental collision between a vessel and a bridge over a navigable water way.
3. *Art. 3.9*: Ice loads, *IC* (discussed in Section 3.19).

3.18.2 Protection of Structures from Vehicular Collision Force, *CT*

AASHTO LRFD (2012) Art. 3.6.5.1 specifies requirements for protection of structures from vehicular collision force that have been revised from those in its previous edition. Under these provisions, unless the site conditions indicate otherwise, the owner is obligated (it is mandatory) to investigate the possibility of collision by an errant vehicle with abutments and piers located within a distance of 30 ft to the edge of roadway. The aim should be to provide safe passage to vehicles on or under a bridge.

When warranted, adequate means of minimizing the impact from collision is to be provided. This can be addressed by one of the following choices:

1. Providing structural resistance
2. By redirecting or absorbing the collision forces

When the choice is to provide structural resistance, abutments, piers, and column bents are required to be designed to resist an equivalent static force of 600 kip, assumed to act in a direction of zero to 15° with the edge of the pavement in a horizontal plane, at a distance of 5 ft above the ground. The 600 kip force design requirement is based on the information from full-scale crash tests of rigid columns impacted by 80.0 kip tractor-trailers at 50 mph. For individual column shafts, the 600 kip force should be considered a point load. Field tests indicate that shear failures are the primary mode of failure for individual columns, and columns that are 30 in. in diameter and smaller are the most vulnerable (AASHTO LRFD *Commentary C3.6.5.1*). An investigative study of impact behavior of bridge piers has been presented by El-Tawil et al. (2005).

When the design choice is to redirect or absorb the collision force, the protection systems should consist of one of the following:

1. An embankment
2. A structurally independent (i.e., if it does not transmit loads to the bridge) crashworthy, ground-mounted 54.0 in. high barrier, located within 10 ft from the component being protected
3. A 42 in. high barrier located at more than 10 ft from the component being protected

Such barriers must be structurally and geometrically capable of surviving the crash test for *Test Level 5* as specified in AASHTO LRFD, Section 13: Railings.

AASHTO LRFD *Commentary C3.6.5.1* provides a method (based on the annual frequency of impact from heavy vehicles) to determine whether site conditions qualify for the exemption from the aforementioned discussed protection systems.

3.18.3 Protection of Structures from Vessel Collision Force, *CV*

Bridges over navigable waterways are particularly vulnerable to colliding with the approaching traffic. A variety of causes are responsible for collision damage of bridge substructures (Mastaglio 1997):

1. Inadequate attention given to waterborne traffic in relation to the waterway between the adjacent piers. Many bridges over navigation channels are not wide enough to safely accommodate today's ships and barge tows that regularly exceed 800 ft in length and 100 ft in width.

www.EngineeringEBooksPdf.com

2. Narrow waterways permit little margin of pilot error, and the risk is compounded when high winds or difficult water current conditions create a challenging environment in steering.
3. Bridges too close to tricky bends or turns in the navigation channel or too close to docks, where berthing maneuvers can be dangerous to the safety of a bridge.
4. Over time, a greater number of merchant ships are making more frequent trips under more bridges. Since 1960, the number of US bridges that cross major waterways at coastal ports has reportedly increased 33 percent, while the number of vessels in the world fleet has increased threefold.

Many collisions with bridge substructures have occurred as a result of the waterborne traffic (ships and barges) colliding with the piers supporting a bridge over a navigable waterway. In some cases, the entire bridge span(s) collapsed, some spectacularly, which necessitated complete rebuilding. Bridge collisions can be catastrophic. The infamous 1980-collapse of the Sunshine Skyway Bridge in Florida took 35 lives and cost $250 million for replacement. By comparison, the value of the ship *MV Summit Venture* that caused the accident was only $13 million. Similarly, the 1993-vessel collision with an Amtrak Bridge in Alabama cost 47 lives and millions of dollars in replacement/repairs and other costs. Table 3.30 lists but a few of the world's major collisions between 1960 and 2003 (Mastaglio 1997, Gucma 2009).

While the impact of a vessel with a bridge can be powerful, its magnitude is difficult to estimate as a number of factors influence it. According to one report, the impact force caused by a 30,000-ton deadweight vessel traveling at 10 knots (1 knot = 1 nautical mile/h = 6080 ft/h) when hitting a bridge would be equivalent to a fully loaded 747 airplane crashing into a building at a speed of 120 knots (compare it with New York's World Trade Center collapse on September 11, 2001, which was hit by a 747 airplane). The impact energy released during a 100,000-ton deadweight ship moving at 10 knots would be equivalent to four 747s smashing simultaneously into the same spot.

In order to prevent mishaps and extreme damages to bridge superstructure elements, it is now common practice to provide protective barriers to piers and abutment of bridges over navigable water crossings. A number of protection systems that can absorb impact due to collisions are

TABLE 3.30
Selected Major Ship Collisions

Location	Year	Lives Lost
Severn River railway Bridge, United Kingdom	1960	5
Lake Pontchartrain, United States	1964	6
Sidney Lanier Bridge	1972	10
Lake Pontchartrain, United States	1974	3
Tasman Bridge, Australia	1975	15
Pass Manchaca Bridge, United States	1976	1
Torn Bridge, Sweden	1980	8
Sunshine Skyway Bridge, United States	1980	35
Lorraine pipeline Bridge, France	1982	7
Santos Aerial Tramway, China	1983	7
Volga River Railroad Bridge, Russia	1983	176
Claiborne Avenue (Judge Seeker) Bridge, United States	1993	1
CSX/Amtrak Railroad Bridge, United States	1993	47
Port Isabel, United States	2001	8
Webber Falls, United States	2002	12

Sources: Mastaglio, L., Bridge bashing, Civil Engineering, American Society of Civil Engineers, Washington, DC, April 1997; Gucma, L., Methods of ship-bridge collision safety evaluation, gnedenko.forum.org/Journal/2009/0222009/RATA_2_2009–05.pdf, 2009.

www.EngineeringEBooksPdf.com

FIGURE 3.84 Dolphins protection system for the Dam Point cable-stayed bridge near Jacksonville, Florida. (Courtesy of Florida Department of Transportation, Jacksonville, FL.)

in vogue. One such alternative is fenders (either wood or rubber), which can be affixed to piers. Freestanding, pile-supported structures provide another means of absorbing collision impact. Protective islands and dolphins are yet another class of protection systems that are highly effective in absorbing collision impact. Protective islands typically consist of sand or a rock core. This type of design provides for surface layers of heavy rock, which acts as armor against wave, current, or ice deformation. Dolphins are circular cells, generally 33–36 ft in diameter, constructed of driven sheet piling and filled with rock or concrete (Figure 3.84). They can be also cast offsite and floated to their final position. Dolphins are capped with concrete, and driven piles are sometimes incorporated into the cell design. Some protection systems adopt a combination of both the protective islands around the piers and the dolphins close to the islands (Figure 3.85).

FIGURE 3.85 Sunshine Skyway Bridge, Florida, uses a combination of protective islands and dolphins as protection system for its piers. (Courtesy of Florida Department of Transportation, Jacksonville, FL.)

www.EngineeringEBooksPdf.com

No one type of collision prevention system can work for all types of bridges. For bridges over waterways, collision prevention systems must be designed on individual basis. Major factors influencing the selection of collision prevention system are the sources and types of collisions that are likely to occur. In general, the selection of the type of collision prevention system for bridges over navigable waterways depends on many factors such as, but not limited to, follows:

1. Width of the waterway
2. Height of the substructure elements (piers and bents)
3. Distance between intermediate piers or bents
4. Type of ships and barges (height, width, and dead weight) using the waterway facility
5. Velocity of ships and barges using the waterway
6. Depth of the waterway
7. Nature and velocity of water current in the waterway

Vehicular collision forces are not discussed further as they affect substructures, which are not covered in this book. AASHTO LRFD Art. 3.14 provides extensive coverage for design for vessel collision forces, including those from intentional collisions (Art. 3.14.16).

3.19 ICE AND SNOW LOADS

3.19.1 Ice Loads: General

Ice loads affect piers and column bents of continuous (structurally or piecewise) bridges over waterways, which form parts of substructure, a topic not discussed in this book. Therefore, the topic of ice loads is only briefly discussed in this section. For comprehensive information, readers should refer to Section 3.9 and accompanying commentary in AASHTO LRFD (2012).

Provisions for design for both ice and snow loads are specified in AASHTO LRFD refer only to freshwater ice in rivers and lakes. Ice loads from seawater should be determined from site-specific studies made by specialists. In general, much of the design-related information comes from research in *ice engineering* and related findings presented in Cold Regions Specialty Conferences (Neill 1976, 1981, Montgomery et al. 1980, 1984, Montgomery and Lispett 1980) and design provisions in CSA (1988, 2000).

Ice loads are a matter of concern to designers of bridges over bodies of water. Bridge piers may be subjected to severe forces due to ice flowing in a stream or river; those forces may be static or dynamic. Static ice pressure is created by thermal movements of continuous stationary ice sheets on large bodies of water or from ice jams. Dynamic pressure is caused as a result of moving ice sheets and ice floes carried by stream flow, wind, or currents. AASHTO LRFD Art. 3.9.1 requires ice forces on piers to be determined with regard to site conditions and expected modes of ice action as follows:

1. Dynamic pressure due to moving sheets or floes of ice being carried by stream flow, wind, or currents
2. Static pressure due to thermal movements of ice sheets
3. Pressure resulting from hanging dams or jams of ice
4. Static uplift or vertical load resulting from adhering ice in waters of fluctuating level

The thickness of ice has a major influence on the magnitude of force that it can exert, which also happens to be the greatest unknown in the determination of ice forces on piers. The *expected thickness* of ice, the direction of its movement, and the height of its action are unknowns that shall be investigated and/or determined by field investigations, review of public records, aerial surveys, or other suitable means.

www.EngineeringEBooksPdf.com

3.19.2 Dynamic Ice Forces on Piers

3.19.2.1 Ice Floes and Modes of Failures

The forces imposed on the piers by ice floes are functions of (1) size of the floe, (2) the strength and thickness of ice, and (3) the geometry of the pier (described by the shape of pier's nose, e.g., angular, semicircular). The design of piers for ices forces should be based on the extreme, not average, thickness of ice floes.

Piers are subjected to dynamic ice forces; as a consequence, ice floes fail (from reaction force from the pier). The following types of ice failure modes have been recognized due to Montgomery et al. (1984):

1. *Crushing*: The ice floe fails by local crushing across the width of a pier.
2. *Bending*: Vertical reaction component acts on the ice floe impinging on a pier with an inclined nose.
3. *Splitting*: A relatively small floe strikes a pier and is split into smaller parts by stress cracks propagating from the pier.
4. *Impact*: A small floe is brought to halt by impinging on the nose of the pier before it has crushed over the full width of the pier, bent, or split.
5. *Buckling*: Compressive forces cause a large floe to fail by buckling in front of the nose of a very wide pier.

A designer has to make a judgment about which of the aforementioned failure modes to consider as governing for design. For bridge piers of usual proportions on larger bodies of water, crushing and bending failures usually govern the magnitude of design dynamic ice force. On the smaller streams, which cannot carry larger floes, impact failure can be the governing mode.

3.19.2.2 Effective Ice Crushing Strength

Estimation of effective ice crushing strength defies computational science; only crude approximations can be made. It depends on how the ice floe breaks up, which, in turn, depends on a variety of unknowns, including the thickness and size of ice, its structural integrity, and melting temperatures. The strength is greatest when the ice floe is large, internally sound (i.e., not disintegrated), and the ice temperature, averaged over its depth, is measurably below the melting point. Effective ice strength depends mostly on its grain size and temperature.

In the absence of precise information, AASHTO LRFD suggests the effective ice crushing strengths as shown in Table 3.31. This advisory notwithstanding, designers should be aware that

TABLE 3.31
Effective Ice Strength (AASHTO LRFD Art. 3.9.2.1)

Ice Breakup Mode	Effective Ice Crushing Strength, kip/ft^2
Breakup occurs at melting temperatures, and ice structure is substantially disintegrated.	8.0
Breakup occurs at melting temperatures, and ice structure is somewhat disintegrated.	16.0
Breakup or major ice movement occurs at melting temperatures, but the ice moves in large pieces and is internally sound.	24.0
Breakup or major ice movement occurs when the ice temperature, averaged over its depth, is measurably below the melting point.	32.0

Source: Adapted from *AASHTO LRFD Bridge Design Specifications*, Copyright © 2012 by American Association of State Highway and Transportation Officials, Washington, DC. Used by permission.

www.EngineeringEBooksPdf.com

regional climate conditions have a significant bearing on the crushing strength of ice, and information in Table 3.31 should be used prudently. Effective ice strengths up to 57.6 kip/ft^2 (or 400 lb/in.^{2}, a large force) have been used in the design of some bridges in Alaska (Haynes 1995).

3.19.2.3 Horizontal Force from Flexing of Moving Ice

Horizontal force resulting from crushing (see Section 3.19.2.4 for the influence of the pier nose profile on the forces acting on the pier) and flexing of moving ice acts dynamically on piers. Its magnitude, F, a function of pier width to ice thickness ratio (w/t) as suggested by Lispett and Gerard (1980), is calculated as follows (AASHTO LRFD Art. 3.9.2.2):

1. If $w/t \leq 6.0$, then F = lesser of either F_c or F_b when ice failure by flexure is considered applicable (i.e., when $\alpha > 15°$) (see exception 1).
2. If $w/t \geq 6.0$, then $F = F_c$

Forces F_c and F_b are calculated as given by Equations 3.68 through 3.71:

$$F_c = C_a ptw \tag{3.68}$$

$$F_b = C_n pt^2 \tag{3.69}$$

$$C_a = \left(\frac{5t}{w} + 1\right)^{0.5} \tag{3.70}$$

$$C_n = \frac{0.5}{\tan(\alpha - 15)} \tag{3.71}$$

where

t = thickness of ice (ft)
α = inclination of nose to vertical
p = effective ice crushing strength as specified in Table 3.31 (kip/ft^2)
w = pier width at level of ice action (ft)
F_c = horizontal ice force caused by ice floes that fail by crushing over the full width of the pier (kip)
F_b = horizontal ice force caused by ice floes that fail flexure as they ride up the inclined pier nose (kip)
C_a = coefficient accounting for the effect of the w/t ratio where the ice floe fails by crushing
C_n = coefficient accounting for the inclination of the pier nose with respect to a vertical

Exceptions

1. Where $\alpha \leq 15°$, ice failure by flexure shall not be considered to be a possible ice failure mode for the purpose of calculating the horizontal force, F, in which case $F = F_c$.
2. On small streams, not conducive to formation of large ice floes, the forces F_b and F_c may be reduced, but under no circumstances, by more than 50 percent (AASHTO LRFD Art. 3.9.2.3). Refer to AAHTO LRFD Commentary C3.9.2.3 for more information on this topic.

www.EngineeringEBooksPdf.com

TABLE 3.32
Suggested Values of Coefficient α in Equation 3.73

Local Conditions	Coefficient α
Windy lakes without snow	0.8
Average lake with snow	0.5–0.7
Average river with snow	0.4–0.5
Sheltered small river with snow	0.2–0.4

Source: Neill, C.R. ed., *Ice Effects on Bridges*, Road and Transportation Association of Canada, Ottawa, Ontario, Canada, 1981.

In the aforementioned formulas for the forces on piers from the moving ice floes, the ice thickness is the greatest and the most important unknown. Equations can be used for estimating ice thickness. For design purposes, the preferred method of establishing the thickness of ice, t, is to base it on measurements of maximum thickness, taken over a period of several years at potential bridge sites. For situations in which such information is not available, Neill (1981) suggests an empirical method to determine t, which is based on Equation 3.72:

$$t = 0.0830\alpha\sqrt{S_f} \tag{3.72}$$

where
α = coefficient for local conditions, normally less than 1.0*
S_f = freezing index, being the algebraic sum, $\Sigma(32\text{-}T)$, summed from the date of freeze-up to date of interest, in degree days
t = mean daily temperature (°F)

3.19.2.4 Influence of Directionality of Ice Forces and the Pier Nose Profile on the Magnitude of Forces Acting on the Pier

The horizontal ice forces F (i.e., F_b or F_c) are to be taken as acting along the longitudinal axis of the pier. This is based on the assumption that ice movement is only in one direction, and the pier is approximately aligned with that direction; however, such may not always be the case. Therefore, two design cases are required to be considered as follows (Montgomery et al. 1984):

1. A longitudinal force equal to F combined with a transverse force equal to $0.15F$.
2. A longitudinal force equal to $0.5F$ combined with a transverse force equal to F_t (Figure 3.86). The magnitude of transverse force, F_t, is a function of F and is given by Equation 3.73.

Both the longitudinal and transverse forces are assumed to act at the pier nose.

$$F_t = \frac{F}{2\tan\left(0.5\beta + \theta_f\right)} \tag{3.73}$$

where
β = nose angle in a horizontal plane for a round nose taken as 100°
θ_f = friction angle (degrees) between ice and pier nose

* As a guide, values of α given in Table 3.32 are suggested by Neill (1981).

www.EngineeringEBooksPdf.com

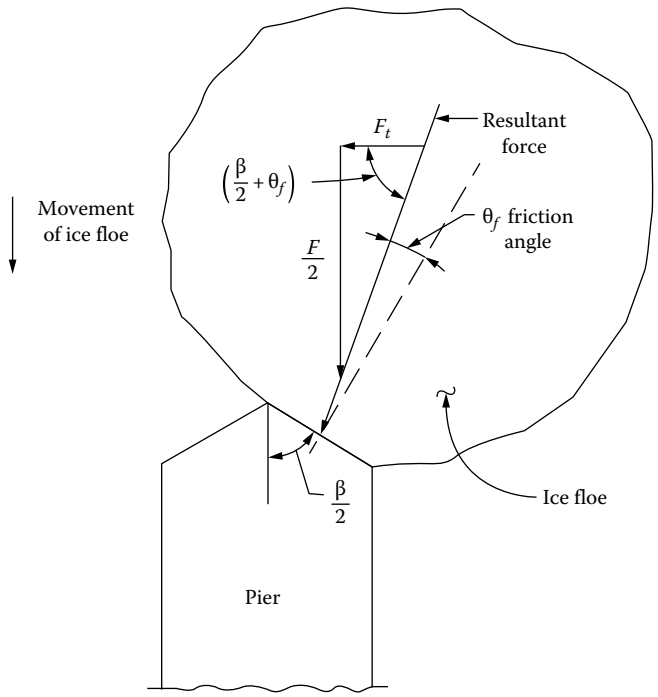

FIGURE 3.86 Transverse ice force where a floe fails over a portion of a pier. (From *AASHTO LRFD Bridge Design Specifications*, Copyright © 2012 by American Association of State Highway and Transportation Officials, Washington, DC. Used by permission.)

3.19.3 Snow Loads

Snow loads warrant superstructure design considerations only for bridges in areas of potentially heavy snowfall. Such snow conditions generally occur at high elevations in mountainous areas with large seasonal accumulations. In the United States, the following geographical information is pertinent to the snowfall:

1. Snow loads are normally negligible in areas that are (a) below 2000 ft elevation and east of longitude 105° W and (b) below 1000 ft elevation and west of longitude 105° W.
2. In other areas of the country, snow loads as large as 0.7 kip/ft^2 may be encountered in mountainous locations.

Information regarding snow and ice loads (including ice accretions) in various parts of the United States can be found in ASCE (2010). In some cases, site-specific studies may be necessary. From a design perspective, the following considerations are warranted:

1. The effects of snow loads are assumed offset by an accompanying decrease in the vehicular live load; the effect of impact would be also negligible because of the very low vehicle speeds in the snowed areas.
2. The aforementioned assumption is valid for most structures, but is not realistic in areas of significant snowfall. This is because prolonged winter closure of a road makes snow removal impossible resulting in heavy snow accumulations or stockpiling of plowed snow, both of which can cause force effects greater than those due to vehicular live load. In such cases, designers need to make judgment about the applicability and the magnitude of the snow loads.

www.EngineeringEBooksPdf.com

3.20 WIND LOADS (*WL* AND *WS*)

3.20.1 Wind Effects on Structures

The body of knowledge about wind is known as *wind science*. *Wind engineering* refers to aspects of wind science that are related to engineering design of structures, namely, the forces exerted by wind on structures including bridges, which are discussed in this section.

Wind as a cool breeze on a sultry day can be very pleasant. Occasionally, when in the form of hurricanes, twisters, and tornadoes, it can be mildly damaging to catastrophic. Fortunately, wind effects on short-span bridges of slab–girder types, which form the bulk of the most common types, are not significant as they possess large in-plane stiffness.

History is replete with examples, some spectacular, of severe structural damage/failures caused by wind.

Charles Ellet's record-breaking 1010 ft (main span) suspension bridge over the Ohio River at Wheeling, West Virginia (United States), the world's first long-span wire-cable suspension bridge and completed in 1849, was destroyed by wind on May 17, 1854, due to lack of aerodynamic stability. The bridge was repaired and strengthened in the same year and later reconstructed by John Roebling in 1861 (Tyrell 1911). This bridge disaster had remarkable resemblance to that of Tacoma Narrows suspension bridge that would occur 86 years later on November 7, 1940 (Steinman and Watson 1957). Another catastrophic, wind-caused disaster to follow was the collapse of the famed Tay Bridge in Scotland on December 28, 1879, which killed all 75 people riding on a train that, along with the collapsed bridge spans, plunged into the water below. As the most notable example of the twentieth century, the 2800 ft (main span) long Tacoma Narrows suspension bridge, the third longest at the time, which opened to traffic on July 1, 1940, was completely destroyed four months later in November as a result of lateral-torsional vibrations (Figures 3.87 and 3.88) that were induced by a mere 35–42 mph moderate wind (the bridge, known as the second Tacoma Narrows suspension bridge, was rebuilt in 1950). The cause was found to be aerodynamic instability caused by wind. As it turned out, this bridge had been built to withstand a static wind force of 50 lb/ft^2, but not for its aerodynamic effects!

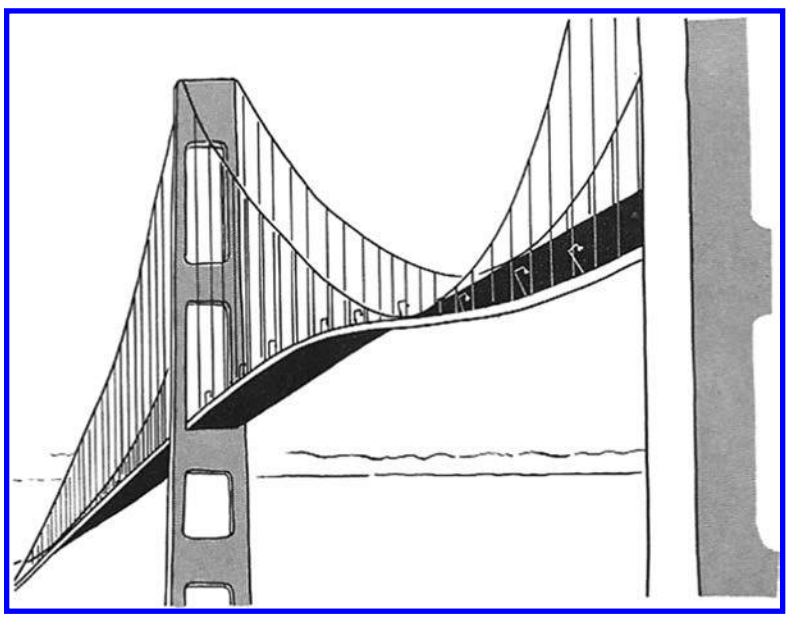

FIGURE 3.87 Aerodynamic vibrations of Tacoma Narrows suspension bridge that led to its failure in November 1940. (Reproduced with permission from Salvadori, M. and Heller, R., *Structure in Architecture—The Building of Buildings*, 2nd edition, Prentice-Hall, Englewood Cliffs, NJ, 1975.)

www.EngineeringEBooksPdf.com

FIGURE 3.88 Collapse of Tacoma Narrows Bridge (November 7, 1940) due to wind loads. (From Smith, D., A case study and analysis of the Tacoma Narrows Bridge failure, 99.497 Engineering Project, Department of Mechanical Engineering, Carleton University, Ottawa, Ontario, Canada, March 29, 1974.)

This spectacular bridge failure led to a herculean, worldwide research on the effects of wind forces on suspension bridges, which resulted in major developments in their analyses and design practices. A discussion of early wind-induced failures of suspension bridges has been provided by Finch (1941); a brief history of wind-related bridge disasters has been provided by Taly (1998, 2003).

Wind is a transient lateral force. In bridge design, two components of wind loads are to be considered simultaneously:

1. Wind load on live load (*WL*). This refers to wind forces acting perpendicular to the vehicles (live load) that might be present on the bridge.
2. Wind load on structure (*WS*). This refers to wind forces acting perpendicular to bridge's structural and nonstructural components such as parapets, traffic barriers, railings, deck, girders, and diaphragms (under the deck).

In both cases, wind loads are calculated in terms of pressures on the structure or on the live load. Because of the omnipresence of wind, the wind pressure (*WS*) is always acting on a bridge structure. The effect of wind load on live load (*WL*) is considered only when vehicles are present on the bridge. In both cases, wind pressures are determined based on the base design wind velocity of 100 mph.

The analysis for wind loads on short-span bridge structures is rather simple. Wind loads, along with all other applicable lateral loads, must be accounted for in design; however, they usually do not govern for short-span bridges. Wind loads influence significantly the behavior of medium- and long-span and/or tall bridges and constitute one of the major design considerations (the other being earthquake force for bridges located in regions of high seismicity). For such bridges, effects of wind loads based on local wind conditions need to be investigated and properly accounted for in design. Examples of medium- and long-span and/or tall bridges include truss bridges, arch bridges, cable-stayed bridges, and suspension bridges. Design wind pressures for such bridges are usually obtained from wind tunnel tests.

3.20.2 Magnitude of Horizontal Wind Pressure

Wind is defined as the flow or movement of air in the atmosphere that occurs because of atmospheric pressure differentials caused by solar radiation. These pressure differentials rise above the surface of the earth, and the air flows from the high-pressure areas to the low-pressure areas.

www.EngineeringEBooksPdf.com

Wind will exert pressure on any object that it encounters in its flow path. Wind loads are calculated from knowing pressure q that would be caused by the wind moving at a velocity V. The pressure exerted by wind on an object is calculated from the principles of fluid mechanics. According to Bernoulli's theorem, when an ideal fluid strikes an object, the increase in static pressure equals the decrease in dynamic pressure, which is given by Equation 3.74:

$$q = 0.5\rho V^2 \tag{3.74}$$

where

q = dynamic or velocity pressure on the object
ρ = mass density of air (specific weight, $w = 0.07651$ lb/ft^3 at sea level and 15°C)
V = wind velocity, ft/s

Pressure exerted on structures is influenced by many factors such as terrain characteristics, size and shape of structure, and speed, direction, and gustiness of wind (accounted for in Equation 3.75 by pressure coefficient C_D). Accordingly, Equation 3.74 is modified as given by Equation 3.75:

$$q = 0.5\rho V^2 C_D \tag{3.75}$$

where C_D = drag, shape, or pressure coefficient.

The drag or shape factor, C_D, has significant effect on the magnitude of wind pressure on objects of different shapes. A mathematical discussion of the basic shape factors is presented by Sach (1978).

If V is expressed in mph, Equation 3.75 can be expressed as given by Equation 3.76:

$$q = 0.5\left(\frac{0.07651}{32.2}\right)\left(\frac{5280V}{3600}\right)^2 C_D, \quad \text{or} \quad q = 0.00256V^2 C_D \tag{3.76}$$

Because of the weakness of wind pressure, the units used to express it are pounds per square foot (lb/ft^2 or psf) rather than the customary units of pounds per square inch (lb/in.^{2} or psi). Equation 3.76 therefore expresses wind pressure in pounds per square foot. For example, for $V = V_B$ (base wind velocity) = 100 mph, the wind pressure $q = 25.6C_D$ lb/ft^2. This is called *wind stagnation pressure*.

3.20.3 Variation in Wind Velocity with Height

Characteristically, the velocity of wind increases with height—from zero at the ground surface to some maximum value at a height of approximately half to one kilometer above the ground. This height is called the *gradient height*, which varies with terrain roughness (e.g., open space over the oceans vs. forest areas and urban areas). The gradient height is essentially a region of turbulent wind called the *atmospheric boundary layer* (ABL). To account for wind effects on ground-based structures, the height of the ABL is taken as approximately 1200 ft from the ground; this is also the practical height within which the wind speed is affected by topography. The atmosphere above the boundary layer is called *free atmosphere*. This is the region of free air in which wind velocity is fairly constant and unaffected by topography; the velocity of this free air is known as the *gradient velocity*. This characterization of atmospheric wind velocity is shown schematically in Figure 3.89.

At the gradient height, the pressure gradient is said to be dynamically balanced against its two components arising from centrifugal force, one due to the rotation of the earth and the other due to the curvature of the wind path. This forms the basis of calculation of gradient velocity (ASCE 1961).

The wind and the atmospheric conditions above the ABL are of special interest to flight and aeronautical engineers, climatologists, and meteorologists. Wind in the ABL is the source of one

www.EngineeringEBooksPdf.com

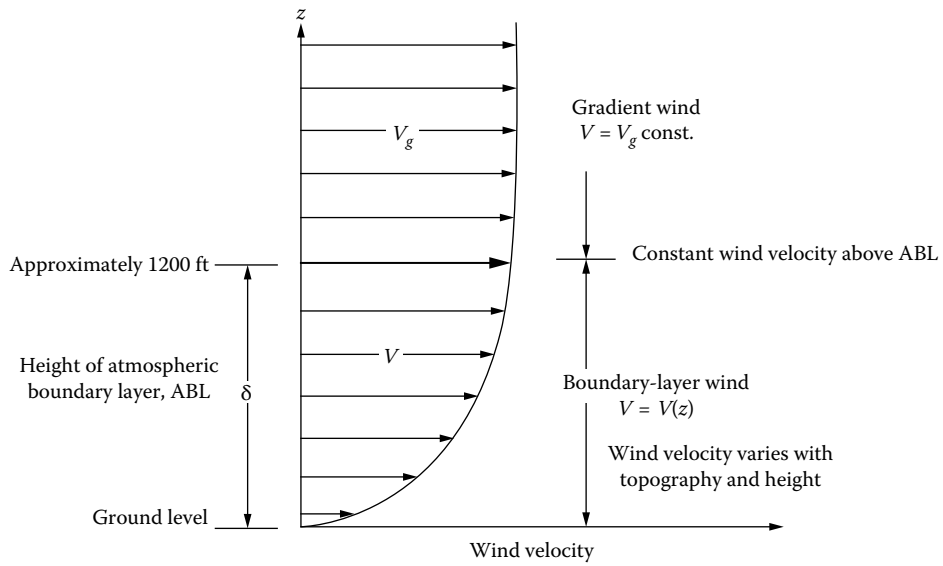

FIGURE 3.89 Variation in atmospheric of wind velocity over the height. (Adapted from Liu, H., *Wind Engineering: A Handbook for Structural Engineers*, Prentice-Hall, Englewood Cliffs, NJ, 1991.)

of the principal environmental loads, called *wind-induced* loads, acting on aboveground structures. This aspect of wind is of paramount interest to structural engineers and is discussed in detail in this chapter. (Wind itself cannot be discerned as a load such as dead or live loads, which can be physically identified. Consequently, the term *wind-induced loads*, rather than *wind loads*, is used in this introductory paragraph. However, for convenience, the term *wind loads* is used in this chapter.)

The velocity of wind is practically zero at the surface of the earth. The transition from the surface velocity to the gradient velocity is referred to as the variation of wind velocity with height. The variation in wind speed with height is logarithmic up to approximately 300 ft above the ground, beyond which the variation in wind speed is insignificant. Ground roughness and man-made obstructions together retard the movement of air close to the ground surface; the rougher the terrain, the greater the retardation. This retardation causes a reduction in wind speed. Above the gradient height (700–1500 ft), the movement of air is independent of ground obstructions and completely free.

Below the gradient height, wind speed varies; the variation is strongly influenced by ground surface roughness, which is the cumulative drag effect of any obstacle to the free movement of wind. Surface roughness is characterized by the density, size, and height of buildings, trees, vegetation, and rocks. Because of these obstructions, surface roughness will be maximum over a large city and minimum over the ocean (or water). These surface characteristics are grouped by design codes as *exposure categories*.

Within the ABL, the wind speed profile can be expressed by mathematical models or relationships based on the fundamental equations of continuum mechanics. Historically, the first representation of the mean wind profile in horizontally homogenous terrain, called the *power law* (Equation 3.77), was proposed by Hellman (1916):

$$V(z) = V_g\left(\frac{z}{z_g}\right)^{1/\alpha} \tag{3.77}$$

where

$V(z)$ = wind velocity at height z aboveground
V_g = wind velocity at any reference height z_g aboveground, usually 10 m
α = power law exponent that depends on the terrain characteristics

www.EngineeringEBooksPdf.com

Another model used to approximate the wind profile is the *logarithmic law*, which is expressed by Equation 3.78:

$$V(z) = \frac{1}{\kappa} V^* \ln\left(\frac{z}{z_g}\right) \tag{3.78}$$

where

V^* = shear velocity or friction velocity
= $\sqrt{\tau_0/\rho}$ where τ_0 = stress of wind at ground level and ρ = air density = 0.07651 lb/ft^3 (1.2256 kg/m^3) at sea level (760 mm of mercury) and 15°C

κ = von Karman constant = 0.4 approximately, based on experiments in wind tunnels and in the atmosphere

With $\kappa = 0.4$, Equation 3.78 can be expressed as Equation 3.79:

$$V(z) = 2.5V^* \ln\left(\frac{z}{z_g}\right) \tag{3.79}$$

Equations 3.77 and 3.79 are empirical formulas for variation in wind speed over flat areas. The *logarithmic law* is regarded by meteorologists as the more accurate representation of wind profile in the lower atmosphere; consequently, the *power law* is not used in micrometeorological practice. However, because of its simplicity in use for wind pressure calculations, the power law formula, rather than the logarithmic law, has historically been used in model building codes. A discussion on the applications of the power law formula for building structures can be found in Simiu and Scanlan (1986).

3.20.4 Estimation of Wind Loads

The following assumptions are made in estimating the wind forces:

1. Wind force is assumed to be uniformly distributed on the area of the bridge structure exposed to wind.
2. The exposed area is taken as the sum of areas of all components, including floor system, traffic barrier and/or parapets, and railing, as seen in elevation, taken perpendicular to the assumed wind direction.
3. The direction of the wind is to be varied to determine the extreme force effects on the structure and its components.
4. Pressures on windward and leeward sides are to be taken as acting simultaneously in the assumed direction of the wind.
5. Areas that do not contribute to the extreme force effects under consideration may be neglected in analysis.
6. Shielding effects of girders are to be ignored.

Typically, a bridge structure should be examined separately under wind pressures from two or more different directions in order to ascertain windward, leeward, and side pressures producing the most critical loads on the structure.

Wind load provisions for highway bridge design are specified in AASHTO LRFD Art. 3.8 (wind loads: *WL* and *WS*). Wind pressures depend on the wind velocity (and exposure conditions surrounding the bridge location). Wind velocity data for a particular bridge location can be obtained

www.EngineeringEBooksPdf.com

from the National Weather Service, which maintains wind data for the Unites States. These data give wind velocity at a standard height of 30 ft (V_{30}). For bridges or its parts located more than 30 ft above the ground level or water level, the design wind velocity, V_{DZ}, is determined from Equation 3.80 (a variation of logarithmic law, Equation 3.79):

$$V_{DZ} = 2.5V_0\left(\frac{V_{30}}{V_B}\right)\ln\left(\frac{Z}{Z_0}\right) \tag{3.80}$$

where

V_{DZ} = design wind velocity at design elevation, Z (mph)
V_{30} = wind velocity at 30 ft above low ground or above the design water level (mph)
V_B = base wind velocity of 100 mph at 30 ft height yielding pressures
Z = height of the structure at which wind loads are being calculated as measured from low ground or from water level >30 ft
V_0 = friction velocity (mph), a meteorological wind characteristic taken as in Table 3.33 for various upwind surface characteristics
Z_0 = friction length (ft) of upstream fetch, a meteorological wind characteristic taken as in Table 3.33

The friction velocity, V_0, may be established from the following:

1. Fastest-mile-of-wind charts available in ASCE 7-88 (ASCE 7-88) for various recurrence intervals
2. Site-specific wind surveys
3. In the absence of better criterion, the assumption that $V_{30} = V_B = 100$ mph

It must be noted that wind load provisions of ASCE 7-88 are 26 years old (as of 2014). Although wind load provisions for structural design have changed significantly since 1988 and reported in ASCE 7-10 (ASCE 7-10), corresponding changes have not yet been incorporated in 2012-AASHTO LRFD Specifications. Designers should note that the fact that wind loads specified in 2012-AASHTO LRFD Specifications are *allowable stress design-level* (ASD-level) forces, whereas the earthquake

TABLE 3.33
Values of V_0 and Z_0 for Various Upstream Conditions (AASHTO LRFD 2012 Table 3.8.1.1-1)

Condition	Open Country[a]	Suburban[b]	City[c]
V_0, mph	8.2	10.9	12.0
Z_0, ft	0.23	3.28	8.2

Source: Adapted from *AASHTO LRFD Bridge Design Specifications*, Copyright © 2012 by American Association of State Highway and Transportation Officials, Washington, DC. Used by permission.

[a] Refers to open terrain with scattered obstructions having generally less than 30.0 ft. This category includes flat open country and grasslands.

[b] Refers to urban and suburban areas, wooded areas, or other terrain with numerous closely spaced obstructions having the size of single-family or larger dwellings. Use of this category shall be limited to those areas for which representative terrain prevails in the upwind direction at least 1500 ft.

[c] Refers to large city centers with at least 50 percent of the buildings having a height of 70.0 ft. Use of this category shall be limited to those areas for which representative terrain prevails in the upwind direction at least one-half mile. Possible channeling effects of increased velocity pressures due to the bridge or structure's location in the wake of adjacent structures shall be taken into account.

www.EngineeringEBooksPdf.com

forces are the *strength-level* forces. Because of this difference, designers are cautioned to use these forces appropriately when making a comparison for determining the governing design forces. It is for this reason that load factor (γ in Table 3.7) for *WS* is 1.4 when designing for Strength III Limit State (wind velocity exceeding 55 mph). Note also that the load factor for *WS* is zero for Strength I and II Limit States because significant wind is not assumed to be present.

3.20.5 Wind Pressure on Structure (*WS*)

In some cases, if justified by local conditions, a different base design wind velocity may be selected for load conditions not involving wind on live load (*WL*). The direction of design wind is assumed to be horizontal. In the absence of more precise data, design wind pressure may be determined from Equation 3.81:

$$P_D = P_B\left(\frac{V_{DZ}}{V_B}\right)^2 = P_B\left(\frac{V_{DZ}^2}{10{,}000}\right) \tag{3.81}$$

where

V_B = 100 mph

P_B = base wind pressure specified in Table 3.34

The design wind pressures shown in Table 3.34 are based on the assumption that wind direction is horizontal. If such is not the case, the wind pressure, P_B, for various angles of wind direction may be taken as specified in Table 3.35 with the following stipulations:

1. The wind pressure shall be applied to the centroid of a single plane of exposed area.
2. The skew angle is to be taken as measured from a perpendicular to the longitudinal axis.
3. The wind direction for design shall be that which produces the extreme effect on the component under investigation.
4. The transverse and longitudinal pressures shall be applied simultaneously.
5. For the usual girder and slab bridges having an individual span length of not more than 125 ft and a maximum height of 30 ft above the ground or water level, the following wind loading may be used:
   a. 0.05 kip/ft^2 transverse
   b. 0.012 kip/ft^2 longitudinal

TABLE 3.34
Base Pressures, P_B, Corresponding to Equation 3.69

Superstructure Component	Windward Pressure,[c] kip/ft^2	Leeward Pressure, kip/ft^2
Trusses, columns, and arches[a]	0.050	0.025
Beams[b]	0.050	NA
Large flat surfaces	0.040	NA

Source: Adapted from *AASHTO LRFD Bridge Design Specifications*, Copyright © 2012 by American Association of State Highway and Transportation Officials, Washington, DC. Used by permission.

[a] The total wind loading shall not be taken less than 0.30 klf in the plane of a windward chord and 0.15 klf in the plane of the leeward chord on truss and arch components.

[b] Wind loading shall be not less than 0.30 klf on beams and girder spans.

[c] The wind stagnation pressure corresponding to 100 mph base wind velocity is 0.0256 ksf, which is significantly less than values shown in the table; the difference reflects the effects of gusting combined with some tradition of long-time usage.

www.EngineeringEBooksPdf.com

TABLE 3.35
Basic Wind Pressures, P_B, or Various Angles of Attack and V_B = 100 mph (AASHTO LRFD Table 3.8.1.2.2-1)

Skew Angle of Wind (Degrees)	Trusses, Columns, and Arches		Girders	
	Lateral Load, kip/ft²	Longitudinal Load, kip/ft²	Lateral Load, kip/ft²	Longitudinal Load, kip/ft²
0	0.075	0.000	0.050	0.000
15	0.070	0.012	0.044	0.006
30	0.065	0.028	0.041	0.012
45	0.047	0.041	0.033	0.016
60	0.024	0.050	0.017	0.019

Source: From *AASHTO LRFD Bridge Design Specifications*, Copyright © 2012 by American Association of State Highway and Transportation Officials, Washington, DC. Used by permission.

Both the aforementioned forces are to be applied simultaneously. These forces are not to be used in determining wind loads on sound barriers (refer to AASHTO LRFD Art. 15.8.2, not discussed herein).

3.20.6 Wind Pressure on Live Load (*WL*)

The following specifications apply when determining wind loads on vehicles present on the bridge:

1. When vehicles are present on the bridge, wind pressures are applied to *both* the structure and vehicles as follows:
   a. Wind pressure on vehicles is represented by an interruptible, moving force of 100 lb/ft acting normal to and 6 ft above the roadway.
   b. This force shall be transmitted to the structure.
2. When wind is not taken as acting normal to the structure, its normal and parallel components may be taken as shown in Table 3.36; the skew angle is taken as referenced normal to the surface. Alternatively, for the usual slab–girder-type bridges, having an individual span length of not more than 125 ft and a maximum height of 30 ft above low ground level, the following wind loads may be used:
   Transverse: 0.1 kip per linear ft (or 100 lb per linear ft)
   Longitudinal: 0.04 kip per linear ft (or 40 lb per linear ft)
   Both wind loads are to be applied simultaneously.

TABLE 3.36
Wind Components on Live Load (AASHTO LRFD Table 3.8.1.3-1)

Skew Angle (Degrees)	Normal Component (klf)	Parallel Component (klf)
0	0.100	0.000
15	0.088	0.012
30	0.082	0.024
45	0.066	0.032
60	0.034	0.038

Source: Adapted from *AASHTO LRFD Bridge Design Specifications*, Copyright © 2012 by American Association of State Highway and Transportation Officials, Washington, DC. Used by permission.

www.EngineeringEBooksPdf.com

AASHTO LRFD *Commentary C3.8.1.3* provides important insight into the intent and understanding of wind load provisions specified therein.

The 0.10 klf wind load corresponding to 0 degree skew angle (in Table 3.32) is based on a long row of randomly sequenced passenger cars, commercial vans, and trucks exposed to the 55 mph design wind load. This horizontal live load, similar to the design lane load, is to be applied only to the tributary areas producing force effect of the same kind (i.e., it should not be used to counteract other force effects).

The 55 mph wind velocity is considered as a threshold value because experience indicates that maximum live loads are not expected to be present on the bridge when this velocity is exceeded. This is the basis considered in Strengths III and V Limit States (see Table 3.1).

The load factor (γ in Table 3.7) corresponding to wind load on structure only (WS) in Load Combination Strength III Limit State would be $(55/100)^2(1.4) = 0.42$ (with reference to $V_B = 100$ mph), which has been rounded off to 0.40 load factor. This load factor corresponds to 0.3 for the Service I Limit State.

3.21 EARTHQUAKE FORCES (EQ)

3.21.1 Evolution of Earthquake-Resistant Design Provisions in AASHTO Bridge Design Specifications

AASHTO LRFD Specifications prescribe certain mandatory requirements that must be complied with in order to account for earthquake-induced forces (denoted as EQ) in the design of bridges regardless of where they are located. A discussion of this topic follows.

Although highway bridges were designed in the United States as early as the eighteenth century, the provisions for including earthquake effects in designing highway bridge structures were not included in specifications before 1950s. The 1949 AASHO Specifications (AASHO 1949) did not incorporate any earthquake-related specifications. Later, provisions for seismic design of high bridges evolved gradually and in empirical form. The 1969 AASHO Specifications (AASHO 1969) included the following empirical provisions for including earthquake forces in design.

1.2.20—Earthquake Stresses

In regions where earthquakes may be anticipated, provision shall be made to accommodate lateral forces from earthquakes as follows:

$$EQ = CD$$

where

EQ = lateral force applied horizontally in any direction at center of gravity of the weight of the structure

D = dead load of structure

C = 0.02 for structures founded on spread footings on material rated as 4 tons or more per square foot

= 0.04 for structures founded on spread footings on material rated as less than 4 tons per square foot

= 0.06 for structures founded on piles

Live load may be neglected.

The aforementioned simplistic specification states that the lateral force due to earthquake shall be taken arbitrarily, although based on overall condition of the foundation soil quality, as being equal to 2 percent–6 percent of the dead weight of the structure.

www.EngineeringEBooksPdf.com

The seismic design provisions in the AASHTO LRFD Specifications (AASHTO 2012) have evolved over time. The 1992 AASHTO Standard Specifications (AASHTO 1992) incorporated detailed seismic analysis provisions, which have been expanded considerably in AASHTO LRFD Specifications (AASHTO 2012); a summary of these seismic provisions is presented in this section. A discussion on the evolution of AASHTO seismic design provisions can be found in the literature (ATC 1978, AASHTO 1992 (Division I-A), Rojahn et al. 1997). The terms *earthquake forces* and *seismic forces* are used synonymously throughout this section.

3.21.2 Philosophy for Design Basis Earthquake Forces

Bridges continue to be serious structural casualties of earthquakes, often catastrophic, resulting in severe structural damage or complete collapses, which necessitate replacements. Several spectacular occurrences are shown in Figures 3.90 through 3.94.

The fundamental premise in designing highway bridges for earthquake resistance is to minimize their susceptibility to damage. Needless to say that bridges designed in accordance with these specifications would not be earthquake proof (no structures are); rather, they will be earthquake tolerant (as most structures are designed). The development of AASHTO LRFD specifications for the design of earthquake-resistant bridges evolved based on the following premise (Rojahn et al. 1997):

1. Realistic seismic ground motion intensities and forces should be used in design procedures.
2. Small-to-moderate earthquakes should be resisted within the elastic range for structural components without significant damage.
3. Exposure to shaking from large earthquakes should not cause collapse of all or part of the bridge.
4. Where possible, damage that does occur should be readily detectable and accessible for inspection and repair.

In all cases, bridge owners have the leeway to design their bridges for higher level of performance at their discretion.

FIGURE 3.90 Complete collapse of bridge carrying Interstate 10 (Santa Monica Freeway) in Los Angeles during the 1994 Northridge earthquake.

www.EngineeringEBooksPdf.com

FIGURE 3.91 Spectacular collapse of the double-deck Cypress Viaduct during the Magnitude 7.1 1989 Loma Prieta, California, earthquake. A large portion of this viaduct collapsed during the earthquake killing 41 people. (From The Governor's Board of Inquiry on the 1989 Loma Prieta Earthquake, *Competing against Time*: *Report to Governor George Deukmejian from the Governor's Board of Inquiry on the 1989 Loma Prieta Earthquake*, State of California, Office of Planning and Research, San Francisco, CA, 1990.)

FIGURE 3.92 Collapse of the Struve Slough Bridge, Watsonville (California), with concrete support columns punching through the bridge deck like toothpicks, during the October 17, 1989, M 7.1 Loma Prieta (California) earthquake.

www.EngineeringEBooksPdf.com

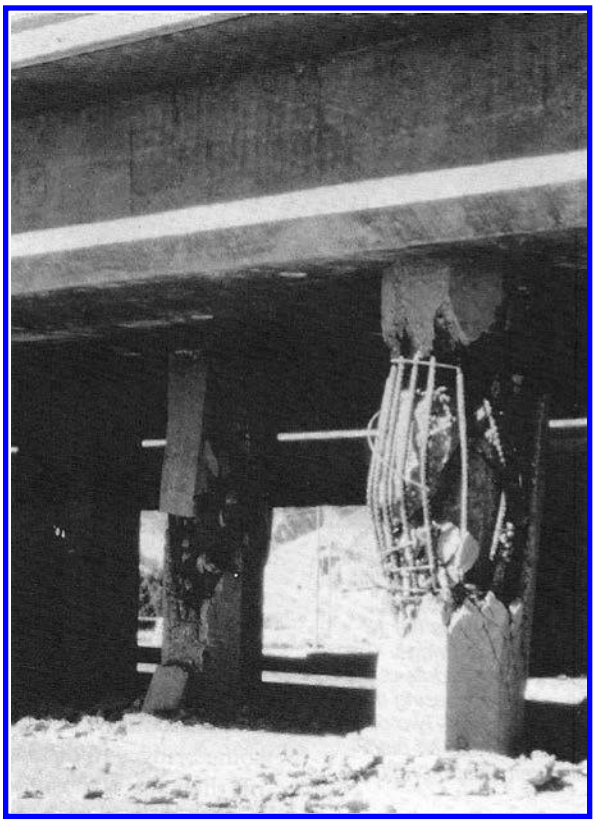

FIGURE 3.93 Shear failure of concrete bridge columns in the February 8, 1971, M 6.6 San Fernando (California) earthquake. The dramatic failure was typical of many bridge failures in October 4, 1994, M 6.4 Northridge (California) earthquake.

3.21.3 Determination of Seismic Forces: Fundamental Concepts

The determination of earthquake effects is based on the fundamental principle commonly known as Newton's second law of motion: *force equals mass times acceleration*, which can be expressed by Equation 3.82:

$$F = ma \tag{3.82}$$

where

F = force due to earthquake
m = mass of the structure = W/g
W = weight of the structure
g = acceleration due to gravity = 32.2 ft/s^2
a = ground acceleration due to earthquake

www.EngineeringEBooksPdf.com

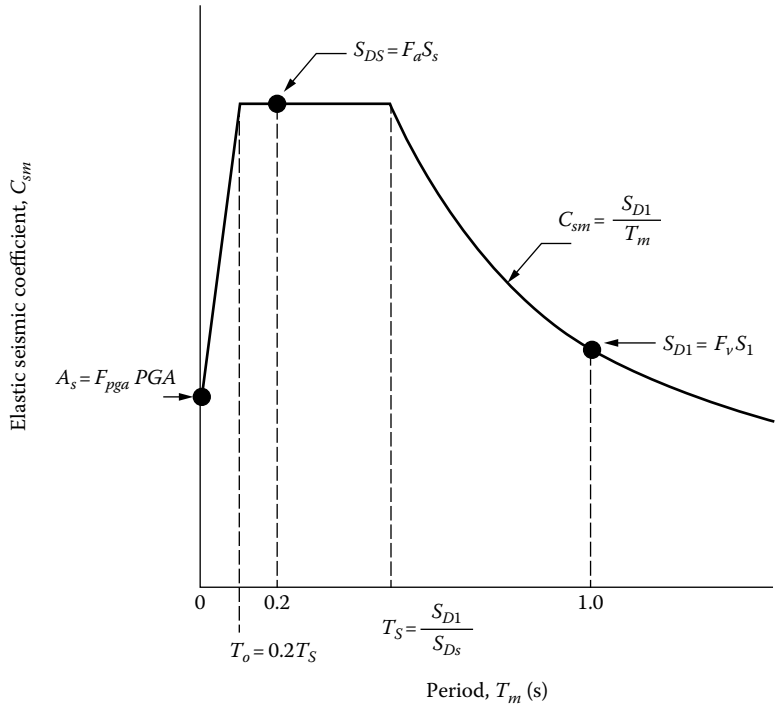

FIGURE 3.94 Design response spectrum. (Adapted from *AASHTO LRFD Bridge Design Specifications*, Copyright © 2012 by American Association of State Highway and Transportation Officials, Washington, DC. Used by permission.)

Substitution of the aforementioned notations in Equation 3.82 yields to Equation 3.83:

$$F = \left(\frac{W}{g}\right)a$$

$$= \left(\frac{a}{g}\right)W \tag{3.83}$$

Equation 3.83 is the fundamental equation used to determine the earthquake forces induced in bridge structures. It simply states that the earthquake force, F, induced in a structure can be determined by multiplying its seismic weight W by the quantity (a/g), which is commonly referred to as the *elastic seismic response coefficient* and denoted by C_{sm}:

$$C_{sm} = \frac{a}{g} \tag{3.84}$$

Equations 3.83 and 3.84 are combined and expressed in a more general form as follows:

$$F = C_{sm}W \tag{3.85}$$

Equation 3.85 is used to calculate *elastic* seismic forces which a bridge structure might experience. C_{sm}, the elastic seismic response coefficient (for the mth mode of vibration), is clearly a function of ground acceleration a; determination of this parameter is the focus of discussion in this section.

www.EngineeringEBooksPdf.com

Earthquakes are random phenomena; the ground acceleration, a, and therefore C_{sm}, is always an unknown quantity. The ground accelerations generated by earthquakes are a complex phenomena, which depend on the *ground acceleration coefficient*, A_s, which, in turn, depends on the soil properties of the foundation (AASHTO LRFD Section 3.10.4.2). These concepts are discussed in the following sections.

3.21.4 AASHTO LRFD Specifications Provisions for Seismic Design of Bridges

3.21.4.1 Seismic Design Philosophy

For the purposes of seismic design, bridges may be classified as having (1) conventional forms and (2) nonconventional forms (Table 3.37); the design provisions of AASHTO LRFD are intended to apply to bridges of conventional forms, generally with spans not exceeding 500 ft. For bridge superstructures of other types and for those exceeding 500 ft spans, design specifications need to be specifically approved by the owner agency. Unless otherwise specified by the owner, these specifications are not intended to be applied to buried structures.

Many perplexing questions arise when considering design of structures for earthquake resistance. What magnitude of seismic force a structure should be designed for? What should be the defining parameters for determining earthquake forces that a structure must resist? The simple answer is as follows: Based on the state-of-the-art knowledge, seismic design of structures is based on *ground motion characteristics* (discussed in the next section) rather than on a specific earthquake magnitude, that is, the earthquake-induced force is recognized and determined as a function of ground motion characteristics.

AASHTO LRFD *Commentary C3.10.1* presents an important caveat in regard to the seismic design procedures to be used for highway bridges. As stated in the previous paragraph, AASHTO LRFD provisions for seismic design are *force based* wherein a bridge is designed to have adequate strength (capacity) to resist earthquake forces (demands). A recent trend is to use the so-called *displacement-based* procedures wherein a structure is designed to have adequate displacement capacity to accommodate earthquake demands. The main reason for this trend is that displacement-based procedures are believed to more reliably identify the limit states that cause damage leading to collapse and that in some cases produce more efficient design against collapse. The commentary advises that displacement capacity of bridges located in high seismic zones be checked using displacement-based procedures. Details of displacement-based design procedures can be found in AASHTO (2009b).

In AASHTO LRFD Specifications, the provisions for seismic design of highway bridges are not given in any specific section, rather they are scattered in many different sections, notably in Sections 3 and 4. This section presents a summary of these specifications as they pertain to

TABLE 3.37
Conventional and Nonconventional Bridge Superstructures and Substructures

Bridge Types	Superstructure/Substructure Types
Conventional	Slab, slab–beam, box girder, and truss types
	Single- or multiple-column piers
	Wall-type piers
	Pile-bent substructures
Nonconventional	Cable stayed
	Suspension
	Arch
	Bridges with truss towers or hollow piers for substructures

www.EngineeringEBooksPdf.com

seismic forces. The background information pertaining to these specifications can be found in the literature (NCHRP 2002, 2006, MCEER/ATC 2003, FHWA 2006).

3.21.4.2 Site Class Characterization

Seismic forces are generated from ground motion (acceleration); as such, the behavior of a structure during a seismic event is strongly influenced by the soil characteristics at site. As stated earlier, the value of the elastic seismic response coefficient, C_{sm} (Equation 3.84), is a function of ground acceleration, which is influenced by soil characteristics.

To account for them in structural design, soils are classified into six categories, which are referred to as *site classes* designated *A* through *F* (Table 3.38). Site classes are characterized by their stiffness, which is determined by the shear wave velocity in the upper 100 ft layer of the soil. Standard penetration tests (SPTs), blow counts, and undrained shear strengths of soils are also used to determine a site class. Relationship between these soil characteristics and the site classes are presented in Table 3.38. Procedures for site classification are described in Table C3.10.3.1-1 (AASHTO 2012). *Where the soil properties are not known in sufficient detail to determine a site class, a site investigation shall be undertaken sufficient to determine site class. Site classes E or F should not be assumed unless the authority having jurisdiction determines that site classes E or F could be present at the site or in the event that site classes are established by technical data.*

3.21.4.3 Determination of Elastic Seismic Response Coefficient, C_{sm}

This section presents procedure for determining the value of the elastic seismic response coefficient, C_{sm} (defined by Equation 3.84), as specified in AASHTO LRFD Section 3.10.4.2 (ASSHTO 2012). (Readers to note: related provisions in AASHTO 2012 are changed completely from the 2010 edition).

TABLE 3.38
Site Class Classification

Site Class	Soil Type and Profile
A	Hard rock with measured shear wave velocity, $\bar{v}_s > 5000$ ft/s
B	Rock with 2500 ft/s $< \bar{v}_s <$ 5000 ft/s
C	Very dense soil and soil rock with 1200/ft $< \bar{v}_s <$ 2500 ft/s or with either $\bar{N} > 50$ blows/ft, or $\bar{s}_u > 2$ kip/in.^{2}
D	Soil with 600 ft/s $< \bar{v}_s <$ 1200 ft/s, or with either $\bar{N} < 15$ blows/ft, or $1.0 < \bar{s}_u < 2$ kip/in.^{2}
E	Soil with $\bar{v}_s < 600$ ft/s, or with either $\bar{N} < 15$ blows/ft or $\bar{s}_u < 1$ ksf, or any profile with more than 10 ft of soft clay defined as soil with $PI > 20$, $W > 40$ percent and $\bar{s}_u < 0.5$ ksf.
F	Soils requiring site-specific evaluations, such as 1. Peats or highly organic clays ($H > 10$ ft of Peat or highly organic clay where H = thickness of soil) 2. Very high plasticity clays ($H > 25$ ft with $PI > 75$) 3. Very thick soft/medium stiff clays ($H > 120$ ft)
Exceptions	Where the soil properties are not known in sufficient detail to determine site class, a site investigation shall be undertaken sufficient to determine site class. Site classes E or F should not be assumed unless the authority having jurisdiction determines that site classes E or F could be present at the site or in the event that site classes are established by technical data.

Source: Adapted from *AASHTO LRFD Bridge Design Specifications*, Copyright © 2012 by American Association of State Highway and Transportation Officials, Washington, DC. Used by permission.

Notes: $\bar{v}_s$ = average shear wave velocity for the upper 100 ft of soil profile; $\bar{N}$ = average STP blow count (blows/ft) (ASTM D1586) for the upper 100 ft of the soil profile; $\bar{s}_u$ = average undrained shear strength in ksf (ASTM D2166 or ASTM D2850) for the upper 100 ft of soil profile; PI = plasticity index (ASTM D4318); W = moisture content (ASTM D2216).

www.EngineeringEBooksPdf.com

An earthquake is a random vibratory phenomenon, which may excite several modes of vibration. Therefore, it is necessary to determine the elastic response coefficient for each relevant mode. The value of C_{sm} is determined with reference to certain characteristic periods, T_m, T_s, and T_o, defined as follows. These parameters are used to plot the design response spectrum described in Section 3.21.4.6.

Typically, a structure possesses several modes of vibration. The *m*th mode period of vibration, T_m, is determined from the following classical equation:

$$T_m = 2\pi\sqrt{\frac{W}{Kg}} \tag{3.86}$$

where

W = weight of the structure
g = acceleration due to gravity = 32.2 ft/s^2
K = flexural stiffness of the structure
T_S = corner period at which spectrum changes from being independent of period to being inversely proportional to period, defined by Equation 3.87:

$$T_S = \frac{S_{D1}}{S_{DS}} \tag{3.87}$$

T_o = reference period used to define spectral shape:

$$T_o = 0.2T_S \tag{3.88}$$

The dimensionless elastic response coefficient C_{sm} is determined with reference to characteristic periods T_m, T_S, and T_o as follows:

1. For periods less than or equal to T_o, the dimensionless elastic response coefficient C_{sm} for the *m*th mode is given by Equation 3.89:

$$C_{sm} = A_S + \left(S_{DS} - A_S\right)\left(\frac{T_m}{T_0}\right) \quad \text{(3.89) [AASHTO LRFD Equation 3.10.4.2-1]}$$

where

$$A_S = F_{pga}PGA \quad \text{(3.90) [AASHTO LRFD Equation 3.10.4.2.2]}$$

$$S_{DS} = F_a S_S \quad \text{(3.91) [AASHTO LRFD Equation 3.10.4.2-3]}$$

F_{pga} = site factor at zero period on acceleration spectrum (Table 3.40)
PGA = peak ground acceleration coefficient on rock (site class B)
S_{DS} = five percent, damped horizontal response spectral acceleration coefficient at 0.2 s period on rock (site class B)
F_a = site factor for short-period range of acceleration spectrum (Table 3.41)
S_S = horizontal response spectral acceleration coefficient at 0.2 s period on rock (site class B)

www.EngineeringEBooksPdf.com

2. For periods greater than or equal to T_o and less than or equal to T_S ($T_o \leq T_m \leq T_S$), the elastic response coefficient C_{sm} for the mth mode is given by Equation 3.92:

$$C_{sm} = S_{DS} \qquad (3.92) \text{ [AASHTO LRFD Equation 3.10.4.4-4]}$$

3. For periods greater than T_S ($T_m > T_S$), the elastic response coefficient for the mth mode C_{sm} is determined from Equation 3.93:

$$C_{sm} = \frac{S_{D1}}{T_m} \qquad (3.93) \text{ [AASHTO LRFD Equation 3.10.4.2-5]}$$

where

$$S_{D1} = F_v S_1 \qquad (3.94) \text{ [AASHTO LRFD Equation 3.10.4.2-6]}$$

S_{D1} = five percent, damped horizontal response spectral acceleration coefficient at 1.0 s period on rock (site class B)
F_v = site factor for long-period range of acceleration spectrum (Table 3.42)
S_1 = horizontal response spectral acceleration coefficient at 1.0 s period on rock (site class B)

In essence, in order to determine the elastic seismic response coefficient C_{sm} for a bridge located at a given site, one needs to determine the fundamental period T_m from Equation 3.86 and then determine C_{sm} from Equations 3.89, 3.92, or 3.93 as applicable. Examples 3.26 through 3.29 present applications of Equations 3.86 through 3.94 for bridges located in different seismic regions of the United States.

The value of S_{D1} (Equation 3.94) is used to determine seismic performance zones as defined in Table 3.39; each bridge shall be assigned to one of the four seismic performance zones. These seismic zones reflect the variation in seismic risk across the United States and are used to permit different requirements for methods of analysis, minimum support lengths, column design details, and foundation and abutment design procedures. Additionally, the value of S_{D1} is used to define the descending portion of *design response spectrum*, which characterizes a seismic hazard (discussed in Section 3.21.4.5).

3.21.4.4 Determination of Acceleration Coefficients

The site factors, F_{pga}, F_a, and F_v, identified, respectively, in Equations 3.90, 3.91, and 3.94, bear certain relationships to site classes A through E (described in Table 3.38); these relationships are shown in Tables 3.40 through 3.42. They are used in the zero-period, short-period, and the long-period range of the design response spectrum (discussed in the next section); their values are determined using the site classes and the mapped values of acceleration coefficients shown in AASHTO LRFD seismic hazard maps Figures 3.10.2.1-1 through 3.10.2.1-21 (Figures 3.10.2.1-1 through 3.10.2.1-3 are shown in Appendix 3.A to this chapter as Figures 3.A.1 through 3.A.3). Specifically, these hazard maps

TABLE 3.39
Definition of Seismic Performance Zones

Acceleration Coefficient, S_{D1}	Seismic Performance Zone
$S_{D1} \leq 0.15$	1
$0.15 < S_{D1} \leq 0.30$	2
$0.30 < S_{D1} \leq 0.50$	3
$0.50 < S_{D1}$	4

Source: From *AASHTO LRFD Bridge Design Specifications*, Copyright © 2012 by American Association of State Highway and Transportation Officials, Washington, DC. Used by permission.

www.EngineeringEBooksPdf.com

TABLE 3.40
Values of Site Factor, F_{pga}, at Zero-Period on Acceleration Spectrum

	Peak Ground Acceleration (F_{pga})[a]				
Site Class	***PGA* < 0.10**	***PGA* = 0.2**	***PGA* = 0.30**	***PGA* = 0.40**	***PGA* > 0.50**
A	0.8	0.8	0.8	0.8	0.8
B	1.0	1.0	1.0	1.0	1.0
C	1.2	1.2	1.1	1.0	1.0
D	1.6	1.4	1.2	1.1	1.0
E	2.5	1.7	1.2	0.9	0.9
F[b]	*	*	*	*	*

Source: From *AASHTO LRFD Bridge Design Specifications*, Copyright © 2012 by American Association of State Highway and Transportation Officials, Washington, DC. Used by permission.

Note: Asterisks indicate that these loads should be placed *on* the span (as opposed to *at the end of the span*) to create maximum load effects (moment) in the span.

[a] Use straight-line interpolation for intermediate values of *PGA*.

[b] Site-specific geotechnical investigation and dynamic site response analysis should be performed for all site class F.

TABLE 3.41
Values of Site Factor, F_a, for Short-Period Range of Acceleration Spectrum

	Spectral Acceleration Coefficient at Period 0.20 s (S_S)[a]				
Site Class	**S_S < 0.25**	**S_S = 0.50**	**S_S = 0.75**	**S_S = 1.0**	**S_S = 1.25**
A	0.8	0.8	0.8	0.8	0.8
B	1.0	1.0	1.0	1.0	1.0
C	1.2	1.2	1.1	1.0	1.0
D	1.6	1.4	1.2	1.1	1.0
E	2.5	1.7	1.2	0.9	0.9
F[b]	*	*	*	*	*

Source: From *AASHTO LRFD Bridge Design Specifications*, Copyright © 2012 by American Association of State Highway and Transportation Officials, Washington, DC. Used by permission.

Note: Asterisks indicate that these loads should be placed *on* the span (as opposed to *at the end of the span*) to create maximum load effects (moment) in the span.

[a] Use straight-line interpolation for intermediate values of S_S.

[b] Site-specific geotechnical investigation and dynamic site response analysis should be performed for all site class F.

provide the following seismic coefficients with *seven percent probability of exceedance in 75 years (approximately 1000-year return period* [in the form of contours]) for all parts of the United States:

1. *PGA*: Peak ground acceleration for site class B (theoretically, the PGA is the maximum acceleration experienced by a small particle attached to the earth during the course of an earthquake motion). The maximum contour value of PGA is 1.0*g*, indicated by a contour of 100.
2. S_{DS}: Five percent, damped horizontal response spectral acceleration coefficient at 0.2 s period on rock (site class B). The maximum value of S_{DS} shown is 3.0*g*, indicated by a contour of 300.
3. S_{D1}: Five percent, damped horizontal response spectral acceleration coefficient at 1.0 s period on rock (site class B). The maximum value of S_{D1} shown in 1.0*g*, indicated by a contour of 100.

www.EngineeringEBooksPdf.com

TABLE 3.42
Values of Site Factor, F_v, for Long-Period Range of Acceleration Spectrum

	Spectral Acceleration Coefficient at Period 0.10 s (S_1)[a]				
Site Class	$S_1 < 0.1$	$S_1 = 0.2$	$S_1 = 0.3$	$S_1 = 0.4$	$S_1 > 0.5$
A	0.8	0.8	0.8	0.8	0.8
B	1.0	1.0	1.0	1.0	1.0
C	1.7	1.6	1.5	1.4	1.3
D	2.4	2.0	1.8	1.6	1.5
E	3.5	3.2	2.8	2.4	2.4
F[b]	*	*	*	*	*

Source: From *AASHTO LRFD Bridge Design Specifications*, Copyright © 2012 by American Association of State Highway and Transportation Officials, Washington, DC. Used by permission.

[a] Use straight-line interpolation for intermediate values of S_1.

[b] Site-specific geotechnical investigation and dynamic site response analysis should be performed for all site class F.

These maps provide the following information for various parts of the United States. These site factor values are also available on the *United States Geological Survey (USGS) 2007 Seismic Parameters CD*, which is included with the 2012 AASHTO LRFD documents. Coefficients are given by the location (longitude and latitude) of the bridge site, as well as its zip code. The electronic versions of these maps are available at the National Seismic Hazard website: http://eqhazmaps.usgs.gov. Note that these maps are periodically updated by the USGS:

1. *Figure 3.10.2.1-1*: Horizontal *PGA* for the *conterminous United States*, with seven percent probability of exceedance in 75 years (approximately 1000-year return period).
2. *Figure 3.10.2.1-2*: Horizontal response spectral acceleration coefficient for the *conterminous United States* at period of 0.2 s (S_S), with seven percent probability of exceedance in 75 years (approximately 1000-year return period) and five percent of critical damping.
3. *Figure 3.10.2.1-3*: Horizontal response spectral acceleration coefficient for the *conterminous United States* at period of 1.0 s (S_1), with seven percent probability of exceedance in 75 years (approximately 1000-year return period) and five percent of critical damping.
4. *Figure 3.10.2.1-4*: Horizontal *PGA* for *Region 1*, with seven percent probability of exceedance in 75 years (approximately 1000-year return period).
5. *Figure 3.10.2.1-5*: Horizontal response spectral acceleration coefficient for the *Region 1* at period of 0.2 s (S_S), with seven percent probability of exceedance in 75 years (approximately 1000-year return period) and five percent of critical damping.
6. *Figure 3.10.2.1-6*: Horizontal response spectral acceleration coefficient for *Region 1* at period of 1.0 s (S_1), with seven percent probability of exceedance in 75 years (approximately 1000-year return period) and five percent of critical damping.
7. *Figure 3.10.2.1-7*: Horizontal *PGA* for *Region 2*, with seven percent probability of exceedance in 75 years (approximately 1000-year return period).
8. *Figure 3.10.2.1-8*: Horizontal response spectral acceleration coefficient for the *Region 2* at period of 0.2 s (S_S), with seven percent probability of exceedance in 75 years (approximately 1000-year return period) and five percent of critical damping.
9. *Figure 3.10.2.1-9*: Horizontal response spectral acceleration coefficient for *Region 2* at period of 1.0 s (S_1), with seven percent probability of exceedance in 75 years (approximately 1000-year return period) and five percent of critical damping.
10. *Figure 3.10.2.1-10*: Horizontal *PGA* for *Region 3*, with seven percent probability of exceedance in 75 years (approximately 1000-year return period).

www.EngineeringEBooksPdf.com

11. *Figure 3.10.2.1-11*: Horizontal response spectral acceleration coefficient for *Region 3* at period of 0.2 s (S_S), with seven percent probability of exceedance in 75 years (approximately 1000-year return period) and five percent of critical damping.
12. *Figure 3.10.2.1-12*: Horizontal response spectral acceleration coefficient for *Region 3* at period of 1.0 s (S_1), with seven percent probability of exceedance in 75 years (approximately 1000-year return period) and five percent of critical damping.
13. *Figure 3.10.2.1-13*: Horizontal *PGA* for *Region 4*, with seven percent probability of exceedance in 75 years (approximately 1000-year return period).
14. *Figure 3.10.2.1-14*: Horizontal response spectral acceleration coefficient for *Region 4* at periods of 0.2 s (S_S) and 1.0 s (S_1), with seven percent probability of exceedance in 75 years (approximately 1000-year return period) and five percent of critical damping.
15. *Figure 3.10.2.1-15*: Horizontal *PGA* for *Hawaii*, with seven percent probability of exceedance in 75 years (approximately 1000-year return period).
16. *Figure 3.10.2.1-16*: Horizontal response spectral acceleration coefficient for *Hawaii* at periods of 0.2 s (*Ss*) and 1.0 s (S_1), with seven percent probability of exceedance in 75 years (approximately 1000-year return period).
17. *Figure 3.10.2.1-17*: Horizontal *PGA* for *Alaska*, with seven percent probability of exceedance in 75 years (approximately 1000-year return period).
18. *Figure 3.10.2.1-18*: Horizontal response spectral acceleration coefficient for *Alaska* at period of 0.2 s (S_S), with seven percent probability of exceedance in 75 years (approximately 1000-year return period) and five percent of critical damping.
19. *Figure 3.10.2.1-19*: Horizontal response spectral acceleration coefficient for *Alaska* at period of 1.0 s (S_1), with seven percent probability of exceedance in 75 years (approximately 1000-year return period) and five percent of critical damping.
20. *Figure 3.10.2.1-20*: Horizontal *PGA* for *Puerto Rico*, *Culebra*, *Vieques*, *St. Thomas*, *St. John*, and *St. Croix*, with seven percent probability of exceedance in 75 years (approximately 1000-year return period).
21. *Figure 3.10.2.1-21*: Horizontal response spectral accelerations coefficient (*PGA*) for *Puerto Rico*, *Culebra*, *Vieques*, *St. Thomas*, *St. John*, and *St. Croix* at periods of 0.2 s (S_S) and 1.0 s (S_1), with seven percent probability of exceedance in 75 years (approximately 1000-year return period).

Values of the ground coefficients *PGA* and the spectral coefficients, S_S and S_1, are shown in the form of contours (expressed in percent) in Figures 3.10.2.1-1 through 3.10.2.1-21 (AASHTO 2012); numerical values are obtained by dividing those values by 100. Local maxima and minima are shown inside the highest and lowest contours for a given region. Linear interpolation can be used for sites located between a contour line and a local maximum or minimum. Alternatively, these values can be obtained from the owner-approved state ground motion maps. Values of these coefficients are also available on the *USGS 2007 Seismic Parameter CD* included in the 2012 AASHTO LRFD document. Coefficients are given by longitude and latitude of the bridge site or by the zip code of the bridge site.

The following information should be noted with reference to Tables 3.40 through 3.42:

1. The values of site factors F_{pga}, F_a, and F_v for site class B are 1.0 in all cases. This is because site class B has been chosen as a reference site class for the USGS and NEHRP ground shaking maps.
2. Site classes A, C, D, and E have separate set of site factors. Note that these site factors generally increase as the stiffness of the soil decreases (i.e., soil profile becomes softer, from site class A to site class E).
3. Except for site class A, the site factors also decrease as the ground motion level increases, due to the strongly nonlinear behavior of the soil.
4. Site factors for site class F are not given because they are required to be determined from site-specific investigations as specified in AASHTO LRFD Art. 3.10.2.2.

www.EngineeringEBooksPdf.com

3.21.4.5 Design Basis Earthquake

For earthquake-resistant design, it is convenient to use *design basis earthquake* (DBE) or *design earthquakes* established/specified by codes. The fundamental premise in establishing a DBE is that it has *low* probability of exceedance during the normal life expectancy of the structure. For highway bridges, the DBE is defined as one having seven percent probability of exceedance in 75 years. Such earthquakes have a return period of 1000 years (AASHTO LRFD *Commentary C3.10.2.1*). It is expected that bridges designed and detailed in accordance with these provisions may suffer some damage but will have a low probability of collapse due to earthquake-induced ground shaking. It has been shown that larger earthquakes (having a return period of 2500 years) than that implied by a return period of 1000 years have a finite probability of occurrence throughout the United States.

The site factors are based on a uniform risk model of seismic hazard. The probability that a coefficient will not be exceeded at a given location during a 75-year period is estimated to be 93 percent, that is, a seven percent probability of exceedance. The probability that mapped coefficients would not be exceeded at a given location during a 75-year period (assumed as the useful life of a bridge) is estimated to be 93 percent (i.e., seven percent probability of exceedance in 75 years). The 75-year useful life of a bridge is merely an arbitrary convenience used for analytical purposes; it does not imply that all bridges have 75-year useful life.

Earthquakes larger than the DBE are sometimes referred to in the context of design. These earthquakes, variously referred to as *maximum probable earthquakes* or *maximum considered earthquakes* (MCEs) or *maximum credible earthquakes*, are characterized by a return period of 2500 years and have a three percent probability of exceedance in 50 years. PGAs for these larger earthquakes would be higher than those shown in the AASHTO seismic risk maps. Equation 3.95 is frequently used to establish the mathematical relationship between the probability of exceedance of an event and the return period:

$$P\left(a_{max} > a\right) = 1 - e^{-T/R} \tag{3.95}$$

where

$P(a_{max} > a)$ = probability that a given acceleration or response spectrum will be exceeded
T = time frame in which the probability is expressed (e.g., design life of 75 years, 100 years, etc.)
R = return period

Equation 3.95 is quite general and can be used to determine the probability of exceeding an earthquake with a specified return period as illustrated by Examples 3.23 and 3.24.

Example 3.23

Show that (a) the probability of exceedance of the DBE (a 1000-year return period event) once in 75 years (assumed design life of a bridge) is 7 percent and (b) the probability of exceedance of the MCE (a 2500-year return period event) once in 75 years is three percent.

Solution

a. T = 75 years, R = 1000 years

$$\begin{aligned} P\left(a_{max} > a\right) &= 1 - e^{-T/R} \\ &= 1 - e^{(-75/1000)} \\ &= 0.07 \textit{ or } 7 \text{ percent} \end{aligned}$$

www.EngineeringEBooksPdf.com

TABLE 3.43
Return Period and Probability of Exceedance (Equation 3.92)

	Probability of Exceedance		
Return Period (Years)	**In 50 Years Design Life (Percent)**	**In 75 Years Design Life (Percent)**	**In 100 Years Design Life (Percent)**
25	86	95	98
50	63	78	86
75	49	63	74
100	39	53	63
150	28	39	48
200	22	31	39
300	15	22	28
400	12	17	22
500	10	14	18
1,000	05	07	10
2,000	02	04	05
2,500	02	03	04
4,000	01	02	02
10,000	—	<01	01

b. $T = 75$ years, $R = 2500$ years

$$P\left(a_{max} > a\right) = 1 - e^{-T/R}$$
$$= 1 - e^{(-75/2500)}$$
$$= 0.03 \textit{ or } 3 \text{ percent}$$

Example 3.24

What is the probability of exceeding an earthquake with a return period of 500 years if the useful life of a bridge is 75 years?

Solution

$T = 75$ years, $R = 500$ years

$$P\left(a_{max} > a\right) = 1 - e^{-T/R}$$
$$= 1 - e^{(-75/500)}$$
$$= 0.1393 \textit{ or } 14 \text{ percent}$$

If the design life of a bridge were to be 100 years, the probability of exceedance of a 2500-year return period event will be four percent, and so on. For comparison, Table 3.43 presents relationships between several arbitrarily chosen return periods of an event and probabilities of exceedance in 50, 75, and 100 years.

3.21.4.6 Seismic Hazard Characterization: Design Response Spectrum

Figure 3.94 shows the five percent damped design response spectrum specified in AASHTO LRFD 2012 Section 3.10.4. It is a plot of earthquake response (represented by the elastic seismic response

www.EngineeringEBooksPdf.com

coefficient, C_{sm}) on the y-axis and period T_m on the x-axis. This shape is based on recent studies (NCHRP 2002, 2006, MCEER/ATC 2003, FHWA 2006) and is revised from previous AASHTO LRFD publications.

The design response spectrum is plotted for a specific site using mapped PGAs and spectral coefficients from AASHTO Figures 3.10.2.1-1 through 3.10.2.1-21, scaled by zero-, short-, and long-period site factors F_{pga}, F_a, and F_v, respectively (Tables 3.40 through 3.42). It consists of three parts:

1. Short-period response spectrum, indicated by an inclined straight line between $T = 0$ to $T = T_o = 0.2T_s$ (short period, Equation 3.88). Note that for $T_o = 0$, $A_S = F_{pga}PGA$ (Equation 3.90).
2. A horizontal line between $T = T_o$ and $T = T_S$ (Equation 3.87).
3. Long-period response spectrum, indicated by a curve beyond $T > T_S$ (Equation 3.93).

Note that the long-period portion of the response spectrum shown in Figure 3.90 is different from the previous version of AASHTO LRFD in that it is inversely proportional to the period, T, rather than being proportional to $T^{2/3}$ (as in the previous edition). This change reflects consistency with the observed characteristics of response spectra calculated from observed ground motions. There are two consequences resulting from this change: for the same ground acceleration and soil type, the spectral accelerations are (1) smaller than previously specified at periods greater than 1.0 s and (2) greater than previously specified for period less than 1.0 s but greater than T_S.

Example 3.25 illustrates the application of Equations 3.85 through 3.93 for calculating the response spectrum for a given site. Examples 3.26 through 3.29 present calculations for determining the value of seismic coefficient, C_{sm}, for a two-span highway bridge located in various seismic regions of the United States.

Example 3.25

Calculate and plot the response spectrum for a site classified as *site class B* and located at approximately *latitude* 35° N and *longitude* 119.5° W. The fundamental period for the proposed bridge structure has been estimated to be 0.36 s. Show all calculations step by step.

Solution

Step 1: The following information is obtained from USGS hazard maps:

PGA = peak ground acceleration = 0.9g (Figure A3.10.2.1.1)

S_S = horizontal response spectral acceleration coefficient at 0.2 s period on rock (site class B)
= 2.2g (Figure A3.10.2.1-2)

S_1 = horizontal response spectral acceleration coefficient at 1.0 s period on rock (site class B)
= 1.0g (Figure A3.10.2.1-3)

Step 2: Determine seismic coefficients F_{PGA}, F_a, and F_v:

For PGA = 0.9g (>0.5g), F_{PGA} = 1.0 (Table 3.40)

For S_S = 2.2g (>1.25g), F_a = 1.0 (Table 3.41)

For S_1 = 1.0g (>0.5g), F_v = 1.3 (Table 3.42)

www.EngineeringEBooksPdf.com

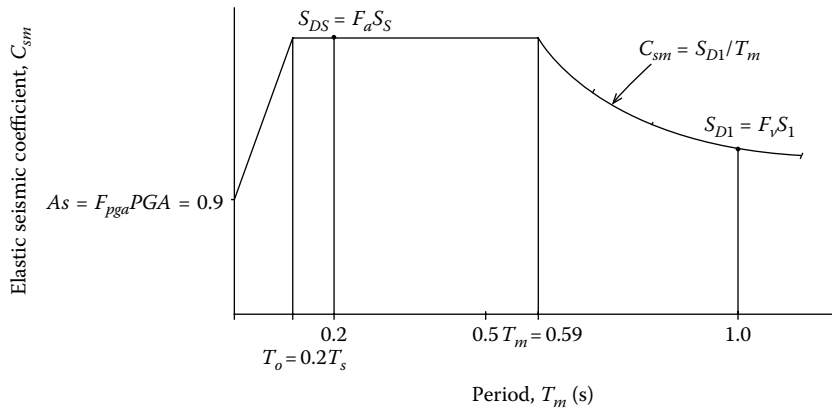

FIGURE 3.95 Response spectrum for Example 3.25.

Step 3: Calculate C_{sm} from Equations 3.89, 3.92, or 3.93 as applicable. First, check if $T_o \le T_m \le T_S$ to determine the applicable equation:

$$T_m = 0.36 \text{ s (estimated)}$$

$$T_S = S_{D1}/S_{DS} \text{ (Equation 3.87)}$$

$$S_{D1} = F_v S_1 \text{ (Equation 3.94)}$$
$$= (1.3)(1.0) = 1.3g$$

$$S_{DS} = F_a S_S \text{ (Equation 3.91)}$$
$$= (1.0)(2.2) = 2.2g$$

$$T_S = S_{D1}/S_{DS} = 1.3/2.2 = 0.59 \text{ s} > T_m = 0.36 \text{ s}$$

$$T_o = 0.2T_S \text{ (Equation 3.88)}$$
$$= (0.2)(0.59) = 0.12 \text{ s} < T_m = 0.36 \text{ s}$$

For $T_o \le T_m \le T_S$, C_{sm} is given by Equation 3.92:

$$C_{sm} = S_{DS} = 2.2g$$

Figure 3.95 illustrates the required response spectrum. The descending branch of this response spectrum is defined by Equation 3.93.

Example 3.26

A two-span highway bridge shown in Figure 3.96 having a central reinforced concrete column is located in an area having an approximate location of *latitude* 35° N, *longitude* 120° W (Region 1). The bridge is located on a strategic route. The geological report indicates that the *site class is C*. Assume that the column is fixed at the top and the bottom. The following data are given:

Moment of inertia of column	40 ft^4
Modulus of elasticity of column concrete	3000 kip/in.^{2}
Weight of the superstructure and the tributary substructure	8 kip/ft

www.EngineeringEBooksPdf.com

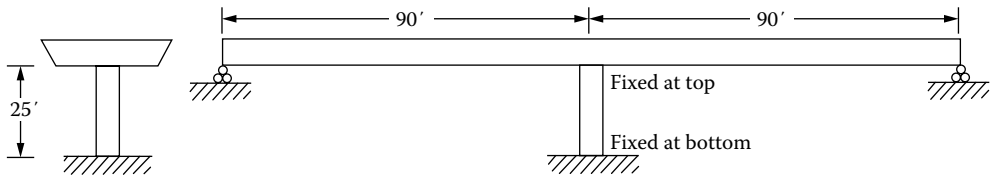

FIGURE 3.96 Bridge elevation for Example 3.26.

For this bridge, determine the following:

a. The fundamental period of the structure
b. The elastic seismic response coefficient, C_{sm}
c. Seismic zone

Solution

a. Fundamental period

$$W = 8(2)(90) = 1440 \text{ kip}$$

The stiffness of the column (fixed at top and bottom) is

$$K_c = \frac{12EI}{h^3} = \frac{12(3{,}000)(144)(40)}{(25)^3} = 13{,}271 \text{ kip/ft}$$

Therefore, the longitudinal stiffness of the bridge is

$$K = 13{,}271/12 = 1105 \text{ kip/in.}$$

From Equation 3.86, the fundamental period of the bridge is

$$T_m = 2\pi\sqrt{\frac{W}{Kg}} = (0.32)\sqrt{\frac{1440}{1105}} = 0.37 \text{ s}$$

b. Seismic response coefficient, C_{sm}
For the given location, the following information is obtained from the USGS hazard maps:

PGA = peak ground acceleration = 1.0g (Figure A3.10.2.1-1)

S_S = horizontal response spectral acceleration coefficient at 0.2 s period on rock (site class B)
= 0.80 (Figure A3.10.2.1-2)

S_1 = horizontal response spectral acceleration coefficient at 1.0 s period on rock (site class B)
= 0.4g (Figure A3.10.2.1-3)

Determine seismic coefficients F_{PGA}, F_a, and F_v for *site class C*:

For PGA = 1.0g (>0.5g), F_{PGA} = 1.0 (Table 3.40)

www.EngineeringEBooksPdf.com

For $S_S = 0.80g$ (>0.75g but <1.0g), $F_a \approx 1.1$ (Table 3.41)

For $S_1 = 0.4g$, $F_v = 1.4$ (Table 3.42)

Calculate C_{sm} from Equations 3.89, 3.92, or 3.93 as applicable. First, check if $T_m < T_S$, $T_o \leq T_m \leq T_S$, or $T_m > T_S$ to determine the applicable equation:

$$T_m = 0.37 \text{ s}$$

$$T_S = S_{D1}/S_{DS} \text{ (Equation 3.87)}$$

$$S_{D1} = F_v S_1 \text{ (Equation 3.94)}$$
$$= (1.4)(0.4g) = 0.56g$$

$$S_{DS} = F_a S_S \text{ (Equation 3.91)}$$
$$= (1.1)(0.8) = 0.88g$$

$$T_S = S_{D1}/S_{DS} = 0.56/0.88 = 0.64 \text{ s} > T_m = 0.37 \text{ s}$$

$$T_o = 0.2T_S \text{ (Equation 3.88)}$$
$$= (0.2)(0.64) = 0.13 \text{ s} < T_m = 0.37 \text{ s}$$

For $T_o \leq T_m \leq T_S$, C_{sm} is given by Equation 3.92:

$$C_{sm} = S_{DS} = 0.88g$$

Therefore, $C_{sm} = 0.88$.

c. Seismic zone
From Table 3.39, it is seen that for $S_{D1} > 0.50$, the assigned seismic zone would be Zone 4. For the subject bridge, $S_{D1} = 0.56g > 0.50g$; so the seismic zone is Zone 4.

Various seismic parameters used in calculations for Example 3.26 should be determined with due diligence because the elastic seismic response coefficient is quite sensitive to these parameters. Example 3.37 presents calculations for a bridge similar to one shown in Example 3.26 with some differences in span lengths and column height.

Example 3.27

Determine the elastic seismic response coefficient for the bridge shown in Figure 3.96 with the following changes:

Geographical location of the bridge: 39° N latitude, 123° W longitude (Region 1)

Span lengths: 120 ft each span

Column height: 26 ft

Solution

a. Fundamental period

$$W = 8(2)(120) = 1920 \text{ kip}$$

www.EngineeringEBooksPdf.com

The stiffness of the columns (fixed at top and bottom) is

$$K_c = \frac{12EI}{h^3} = \frac{12(3{,}000)(144)(40)}{(26)^3} = 11{,}798 \text{ kip/ft}$$

The longitudinal stiffness of the bridge, K = 11,798/12 = 983 kip/in., is

$$T_m = 2\pi\sqrt{\frac{W}{Kg}} = 0.32\sqrt{\frac{W}{K}} = 0.32\sqrt{\frac{1920}{983}} = 0.45 \text{ s}$$

b. Seismic response coefficient, C_{sm}
For the given location (39° N latitude, 123° W longitude), the following information is obtained from the USGS hazard maps:

PGA = peak ground acceleration = 0.50g (Figure A3.10.2.1-1)

S_S = horizontal response spectral acceleration coefficient at 0.2 s period on rock (site class B)
= 1.25 (Figure A3.10.2.1-2)

S_1 = horizontal response spectral acceleration coefficient at 1.0 s period on rock (site class B)
= 0.70g (Figure A3.10.2.1-3)

Determine seismic coefficients F_{PGA}, F_a, and F_v for *site class C*:

For $PGA = 0.50g$, $F_{PGA} = 1.0$ (Table 3.40)

For $S_S = 1.25g$, $F_a = 1.0$ (Table 3.41)

For $S_1 = 0.70g$, $F_v = 1.3$ (Table 3.42)

Calculate C_{sm} from Equations 3.89, 3.92, or 3.93 as applicable. First, check if $T_m < T_S$, $T_o \le T_m \le T_S$, or $T_m > T_S$ to determine the applicable equation:

$$T_m = 0.45 \text{ s}$$

$$T_S = S_{D1}/S_{DS} \text{ (Equation 3.87)}$$

$$S_{D1} = F_v S_1 \text{ (Equation 3.94)}$$
$$= (1.3)(0.70) = 0.91g$$

$$S_{DS} = F_a S_S \text{ (Equation 3.91)}$$
$$= (1.0)(1.25) = 1.25g$$

$$T_S = S_{D1}/S_{DS} = 0.91/1.25 = 0.73 \text{ s} > T_m = 0.45 \text{ s}$$

$$T_o = 0.2T_S \text{ (Equation 3.88)}$$
$$= (0.2)(0.73) = 0.15 \text{ s} < T_m = 0.45 \text{ s}$$

www.EngineeringEBooksPdf.com

For $T_o \leq T_m \leq T_S$, C_{sm} is given by Equation 3.92:

$$C_{sm} = S_{DS} = 1.25g$$

Therefore, $C_{sm} = 1.25$.

Example 3.28

Determine the elastic seismic response coefficient for the bridge shown in Figure 3.96 with the following changes:

Geographical location of the bridge: 36° N latitude, 91.4° W longitude (Region 3)

Span lengths: 120 ft each span

Column height: 26 ft

Solution

a. Because there are no changes in the dimensions of the bridge, $T_m = 0.45$ s
b. Seismic response coefficient, C_{sm}

For the given location (36° N latitude, 91.4° W longitude), the following information is obtained from USGS hazard maps:

PGA = peak ground acceleration = $0.25g$ (Figure A3.10.2.1-1)

S_S = horizontal response spectral acceleration coefficient at 0.2 s period on rock (site class B)
= 0.5 (Figure A3.10.2.1-2)

S_1 = horizontal response spectral acceleration coefficient at 1.0 s period on rock (site class B)
= $0.14g$ (Figure A3.10.2.1-3)

Determine seismic coefficients F_{PGA}, F_a, and F_v for *site class C*:

For $PGA = 0.25g$, $F_{PGA} = 1.15$ (Table 3.40)

For $S_S = 0.5g$, $F_a = 1.2$ (Table 3.41)

For $S_1 = 0.14g$, $F_v = 1.65$ (Table 3.42)

Calculate C_{sm} from Equations 3.89, 3.92, or 3.93 as applicable. First, check if $T_m < T_S$, $T_o \leq T_m \leq T_S$, or $T_m > T_S$ to determine the applicable equation:

$$T_m = 0.45 \text{ s}$$

$$T_S = S_{D1}/S_{DS} \text{ (Equation 3.87)}$$

$$S_{D1} = F_v S_1 \text{ (Equation 3.94)}$$
$$= (1.65)(0.14) = 0.23g$$

www.EngineeringEBooksPdf.com

$$S_{DS} = F_a S_S \text{ (Equation 3.91)}$$
$$= (1.2)(0.5) = 0.60g$$

$$T_S = S_{D1}/S_{DS} = 0.23/0.60 = 0.38 \text{ s} < T_m = 0.45 \text{ s}$$

$$T_o = 0.2T_S = 0.2(0.38) = 0.08 \text{ s}$$

For $T_m > T_S$, C_{sm} is given by Equation 3.93:

$$C_{sm} = \frac{S_{D1}}{T_m} = \frac{0.23g}{0.45} = 0.51g$$

Therefore, $C_{sm} = 0.51$.

For $S_{D1} = 0.23g$, seismic zone is Zone 2.

Example 3.29

Determine the elastic seismic response coefficient for the bridge shown in Figure 3.96 with the following changes:

Geographical location of the bridge: 39° N latitude, 123° W longitude (Region 1), same as in Example 3.27

Weight of tributary area of superstructure = 6 kip/ft

Span lengths: 90 ft each span

Column height: 13.5 ft

Modulus of elasticity of concrete = 3600 kip/in.^{2}

Solution

a. Fundamental period

$$W = 6(2)(90) = 1080 \text{ kip}$$

The stiffness of the columns (fixed at top and bottom) is

$$K_c = \frac{12EI}{h^3} = \frac{12(3{,}600)(144)(40)}{(13.5)^3} = 101{,}136 \text{ kip/ft}$$

The longitudinal stiffness of the bridge, $K = 101{,}136/12 = 8428$ kip/in.

$$T_m = 2\pi\sqrt{\frac{W}{Kg}} = 0.32\sqrt{\frac{W}{K}} = 0.32\sqrt{\frac{1080}{8428}} = 0.11\text{s}$$

b. Seismic response coefficient, C_{sm}
For the given location (39° N latitude, 123° W longitude), the following information is obtained from the USGS hazard maps:

$$PGA = \text{peak ground acceleration} = 0.50g \text{ (Figure A3.10.2.1-1)}$$

www.EngineeringEBooksPdf.com

S_S = horizontal response spectral acceleration coefficient at 0.2 s period on rock (site class B)
= 1.25 (Figure A3.10.2.1-2)

S_1 = horizontal response spectral acceleration coefficient at 1.0 s period on rock (site class B)
= 0.70*g* (Figure A3.10.2.1-3)

Determine seismic coefficients F_{PGA}, F_a, and F_v for site *class C*:

$$\text{For } PGA = 0.50g, \quad F_{PGA} = 1.0 \text{ (Table 3.40)}$$

$$\text{For } S_S = 1.25g, \quad F_a = 1.0 \text{ (Table 3.41)}$$

$$\text{For } S_1 = 0.70g, \quad F_v = 1.3 \text{ (Table 3.42)}$$

Calculate C_{sm} from Equations 3.89, 3.92, or 3.93 as applicable. First, check if $T_m < T_S$, $T_o \leq T_m \leq T_S$, or $T_m > T_S$ to determine the applicable equation:

$$T_m = 0.11 \text{ s}$$

$$T_S = S_{D1}/S_{DS} \text{ (Equation 3.87)}$$

$$S_{D1} = F_v S_1 \text{ (Equation 3.94)}$$
$$= (1.3)(0.70) = 0.91g$$

$$S_{DS} = F_a S_S \text{ (Equation 3.91)}$$
$$= (1.0)(1.25) = 1.25g$$

$$T_S = S_{D1}/S_{DS} = 0.91/1.25 = 0.73 \text{ s} > T_m = 0.11 \text{ s}$$

$$T_o = 0.2T_S \text{ (Equation 3.88)}$$
$$= (0.2)(0.73) = 0.15 \text{ s} > T_m = 0.11 \text{ s}$$

For $T_m < T_o$, C_{sm} is given by Equation 3.89:

$$C_{sm} = A_S + (S_{DS} - A_S)(T_m/T_o)$$

$$A_S = F_{PGA}PGA = (1.0)(0.5) = 0.5$$

$$C_{SM} = 0.5 + (1.25 - 0.5)(0.11/0.15) = 1.05$$

Therefore, $C_{sm} = 1.05$.

3.21.4.7 Operational Classification

Operational classification refers to prioritization of bridges that should be useable *after* a seismic event has occurred. The basis of classification must include social/survival and defense/security requirements. In earlier versions of AASHTO LRFD Specifications, this classification

www.EngineeringEBooksPdf.com

was referred to as *importance classification*, but the new classification is now tied to the return periods of seismic events.

For the purposes of seismic analysis and design, highway bridges are required to be classified in one of the three categories:

1. Critical bridges
2. Essential bridges
3. Other bridges

1. *Critical Bridges*: Some bridges must remain open to all traffic after the design earthquake and be useable by emergency vehicles and for national security/defense purposes immediately after a large earthquake, such as a 2500-year return period event. Such bridges are classified as critical bridges.
2. *Essential bridges*: Bridges in this category are generally those that, as a minimum, are useable by emergency and security/defense purposes immediately after the occurrence of the design earthquake (i.e., a 1000-year event).
3. *Other bridges*: All bridges that are not classified as either critical or essential are classified as *other* bridges.

3.21.4.8 Response Modification Factors

One of the fundamental, and often highly debatable, questions in dealing with seismic design of structures is the level of earthquake forces that should be considered. This indeed is a multifaceted, complex question that continues to be researched for answers. Should we consider for design the *elastic* force levels to which a structure will be subjected during the occurrence of a *design earthquake* (a 1000-year return period event) or during the occurrence of the *MCE* (a 2500-year return period event)? Should we design a bridge (or any structure, in general) in such a way that stresses caused by earthquake forces in its various elements would not exceed the elastic limit (of the materials)? It has long been recognized that it is uneconomical to design a bridge to resist large earthquakes elastically, that is, to design the structure in such a way that stresses in various components of the bridge would remain in the elastic range during the earthquake's occurrence. Obviously, such a design philosophy would result in a very heavy structure and, therefore, uneconomical. The following is excerpted from the ATC-3-06 Report (ATC 1978) to answer these questions, which forms the rationale for establishing design earthquake forces:

> It must be emphasized at the outset that the specification of earthquake ground motion cannot be achieved solely by following a set of scientific principles. First, the causes of earthquakes are not still well understood and experts do not fully agree as to how available knowledge should be interpreted to specify ground motion for use in design. Second, to achieve workable bridge designs provisions, it is necessary to simplify enormously complex matter of earthquake occurrence and ground motions. Finally, any specification of a design ground shaking involves balancing the risk of that motion occurring against the cost to society of requiring the structures be designed to withstand that motion. Hence, judgment, engineering experience, and political wisdom are as necessary as scientific knowledge. In addition, it must be remembered that design ground shaking alone does not determine how a bridge will perform during a future earthquake; there must be balance of the specified shaking with the rules used to assess structural resistance to shaking.

Accordingly, the seismic design loading of a bridge component is determined by the lesser of the following:

1. The elastic response force divided by a response modification factor, R
2. The maximum force that can be produced by the development of the plastic hinging in the columns

www.EngineeringEBooksPdf.com

TABLE 3.44
Response Modification Factors for Substructures (AASHTO LRFD Table 3.10.7.1-1)

	Operational Category		
Substructure	**Critical**	**Essential**	**Other**
Wall-type piers—larger dimension	1.5	1.5	2.0
Reinforced concrete bent piles			
Vertical piles only	1.5	2.0	3.0
With batter piles	1.5	1.5	2.0
Single columns	1.5	2.0	3.0
Steel or composite steel and concrete pile bents			
Vertical piles only	1.5	3.5	5.0
With batter piles	1.5	2.0	3.0
Multiple-column bents	1.5	3.5	5.0

Source: From *AASHTO LRFD Bridge Design Specifications*, Copyright © 2012 by American Association of State Highway and Transportation Officials, Washington, DC. Used by permission.

Table 3.44 lists response modifications factors, R, for *substructures* of bridges based on their operational classification. Elastic design forces are used for axial and shear forces, unless the values corresponding to the plastic hinging are smaller in which case then smaller values are to be used.

Table 3.45 gives R-values for *connections between components of a bridge structure*. It would be noted that R-values for connections (Table 3.45) are smaller (1.0 or less) than those for substructure (1.5 or greater, Table 3.44). Because R is a divisor, the result is greater design forces to be used for connections. This is considered necessary for preserving integrity of the bridge under extreme (seismic) loads. For expansion joints within the superstructure and connections between the superstructure and the abutment, the application of R-factor results in force effect magnification.

A notable observation in Table 3.44 is the much greater values of the response modification factor assigned for *multiple-column bents* as compared to those for the single substructure (except for the bridges in the *critical* category). These higher values of R (and therefore, considerably reduced design earthquake forces) are permitted because of the redundancy present in a multiple-column bent as compared to that in a single-column bent (it has none).

Example 3.30 presents application of determination of elastic seismic forces and information provided in Table 3.44.

TABLE 3.45
Response Modification Factors for Connections (AASHTO LRFD Table 3.10.7.1-2)

Connection	**All Operational Categories**
Superstructure to abutment	0.8
Expansion joints within a span of the superstructure	0.8
Columns, piers, or pile bents to cap beam or superstructure	1.0
Columns or piers to foundations	1.0

Source: From *AASHTO LRFD Bridge Design Specifications*, Copyright © 2012 by American Association of State Highway and Transportation Officials, Washington, DC. Used by permission.

www.EngineeringEBooksPdf.com

Example 3.30

A two-span bridge shown in Figure 3.96 (see Example 3.26) has a central reinforced concrete column and is located at a site where the elastic seismic ground acceleration coefficient C_{sm} has been determined to be 0.88. The bridge is located on a strategic route. Assume that the column is fixed at the top and the bottom. The following data are given:

Moment of inertia of column	40 ft^4
Modulus of elasticity of column concrete	3000 kip/in.^{2}
Weight of the superstructure and the tributary substructure	8 kip/ft

For this bridge, determine (a) the elastic moment in the column, (b) the reduced design moment in the column, and (c) the reduced design moment in the column if the bridge were to be located on a nonessential route.

Solution (Note: This example is an extension of Example 3.26)

a. Elastic moment in the column
The dead weight, W, and the maximum value of the elastic seismic response coefficient for the stated structure were determined, respectively, to be 1440 kip and 0.88 in Example 3.26. Therefore, the total elastic seismic shear is

$$V = C_{sm}W = 0.88(1440) \approx 1267 \text{ kip}$$

The elastic moment in the column is given by

$$M_E = Vh/2 = (0.5)(1267)(25) \approx 15{,}838 \text{ kip-ft}$$

b. Reduced design moment
From Table 3.44 (see next section), a bridge on a strategic rout is classified as having critical operational importance. For a bridge of this classification, the response modification factor R is 1.5 for both single-column and multiple-column bents.
The bridge is located on a strategic route; therefore, it is classified as *critical*, for which the response modification for single-column substructure, R, is 1.5 (Table 3.25). Thus, the reduced design moment is

$$M_{red} = 15{,}838/1.5 \approx 10{,}559 \text{ kip-ft}$$

c. Reduced design moment if the bridge was located on a nonessential route
This bridge falls in the *other* operational category. The response modification factor R for a single column is 3.0. Therefore,

$$M_{red} = 15{,}838/3.0 \approx 5279 \text{ kip-ft}$$

3.21.5 Application of Earthquake Forces for Design of Structural Members and Connections in Highway Bridges

Directional uncertainty of earthquake forces requires assumption that the calculated elastic design earthquake forces may act in any lateral direction. For analytical purposes, the elastic forces and displacements are determined along two orthogonal axes. It is convenient to choose the two orthogonal axes as the longitudinal and transverse axes of the bridge; however, the selection of

www.EngineeringEBooksPdf.com

TABLE 3.46
Percentage *N* by Seismic Zone, Acceleration Coefficient, and the Soil Types (AASHTO LRFD Table 4.7.4.4-1)

Zone	Acceleration Coefficient, A_S	Percent *N*
1	<0.05	≥75
1	≥0.05	100
2	All applicable	150
3	All applicable	150
4	All applicable	150

Source: From *AASHTO LRFD Bridge Design Specifications*, Copyright © 2012 by American Association of State Highway and Transportation Officials, Washington, DC. Used by permission.

the axes is left to the designer's discretion. In the case of a curved bridge, the longitudinal axis may be taken as the chord joining the two abutments. Wall-type columns may be treated as wide columns in the strong direction provided that the *R*-factor in this direction is used. Note that these calculated forces are elastic forces and are to be modified by appropriate *R*-factors as listed in Tables 3.45 and 3.46.

The elastic seismic force effects along each of the principal axes of a component resulting from analyses in two orthogonal directions are to be combined to form two load cases as follows:

Load case 1: 100 percent of the absolute value of the force effects in one of the perpendicular directions (F_L) combined with 30 percent of the absolute value of the force effects in the second perpendicular direction (F_T).

Load case 2: 100 percent of the absolute value of the force effects in the second perpendicular direction (F_T) combined with 30 percent of the absolute value of the force effects in the first perpendicular direction (F_L).

Considering longitudinal and lateral directions as the chosen axes (it is convenient to do so), the aforementioned two load cases can be expressed by Equations 3.96 and 3.97:

$$\text{Load case 1: } 1.0F_L + 0.3F_T \tag{3.96}$$

$$\text{Load case 2: } 1.0F_T + 0.3F_L \tag{3.97}$$

Exception: Where foundation and/or column connection forces (shear and moment) are determined from plastic hinging of columns (specified in AASHTO LRFD Art. 3.10.9.4.3), the resulting force effects may be determined without consideration of the fore-stated load combinations.

The modified seismic forces determined from the aforementioned procedures apply to the following:

1. The superstructure, its expansion joints, and the connection between the superstructure and the supporting substructure
2. The supporting substructure down to the base of the columns and piers but not including the footing, pile caps, or piles
3. Components connecting the superstructure to the abutment

Finally, the seismic loads determined from applicable seismic analysis procedures are to be combined with other forces acting on the structure that form 12 load combinations (discussed in Section 3.2.3).

www.EngineeringEBooksPdf.com

Of these, the load combination that involves seismic forces is the *Extreme Event I* Load Combination, U_{EEI} (Table 3.7), which can be expressed by Equation 3.98:

$$U_{EEI} = \gamma_p \left(DC + DD + DW + EH + EV + ES + EL\right) + \gamma_{EQ}\left(LL + IM + CE + BR + PL + LS\right) + WA + FR + EQ \tag{3.98}$$

The values of the load factor γ_p are listed in Table 3.8. The load factor for live load, γ_{EQ}, is to be determined on project-specific basis.

When combining other design loads with the seismic loads, it is important to remember that, like wind-induced forces, seismic forces are reversible (positive and negative); accordingly, proper sign should be considered to result in critical design loads.

3.21.6 Determination of Design Basis Earthquake Forces

3.21.6.1 General

One of the most important considerations for seismic designs of bridges, as for all structures generally, is to provide a continuous load path for lateral seismic forces. The lateral forces generated by the inertia of the superstructure must be properly transferred to the supporting ground through adequate connections between the superstructure and the substructure (abutments and/or column bents as applicable). Methods to be used for the determination of these seismic forces are specified in AASHTO LRFD Specifications Art. 3.10.9, which refers to superstructure effects carried into the substructure. These specifications are different for different seismic zones and for bridges of different types (single span, multispan, etc.). AASHTO LRFD Art. 3.10.9 specifies analysis procedures for bridges that depend on the type of seismic zones of their location. The methods of dynamic (seismic) analyses are specified in AASHTO LRFD Art. 4.7.

This book presents analysis and design of simple-span bridges that are mostly single-span types. *AASHTO LRFD does not require any seismic analysis for such bridges, only certain prescriptive requirements are specified for such bridges*. Therefore, only a limited discussion of seismic analysis of bridges is presented in this section.

3.21.6.2 Single-Span Bridges

AASHTO LRFD Specifications specify prescriptive requirements for *single-span bridges* regardless of the seismic zones in which they are located. These bridges are the common types; they are characterized by a superstructure supported on two abutments, without any intermediate piers or bents. Connections between the superstructures and abutments of such bridges are required to be designed for the minimum force effects in the restrained direction, which may not be less than the product of the site coefficient, the acceleration coefficient, and the tributary permanent load.

In general, single-span bridges are exempt from any seismic analysis requirements. The following provisions are noted:

1. "Bridges in Seismic Zone 1 need not be analyzed for seismic loads, regardless of their operational classification and geometry. However, the minimum requirements, as specified in Art. 4.7.4.4 and 3.10.9, shall apply" (AASHTO LRFD Art. 4.7.4.1).
2. "Seismic analysis is not required for single-span bridges regardless of the seismic zone. Connections between the bridge superstructure and the abutments must be designed for the minimum force requirements specified in Art. 3.10.9. Minimum support length requirements shall be satisfied at each abutment as specified in Art. 4.7.4.4" (AASHTO LRFD Art. 4.7.4.2).

www.EngineeringEBooksPdf.com

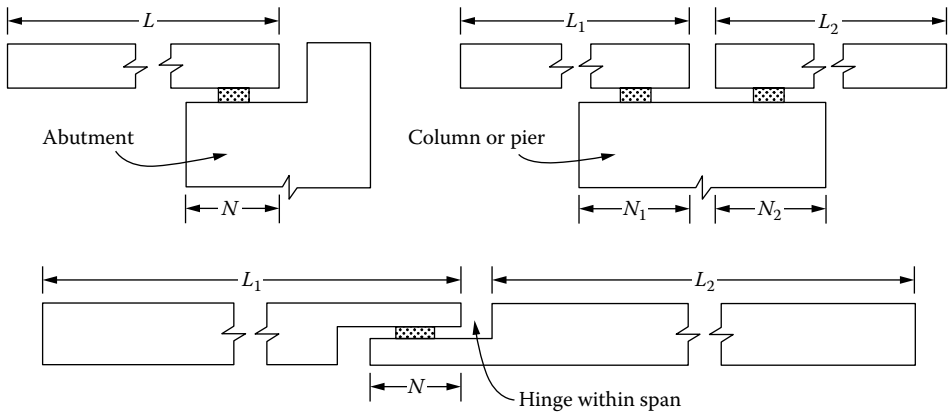

FIGURE 3.97 Definition of length L to be used in Equation 3.99.

However, for single-span bridges, minimum seat width requirements per Equation 3.99 must be satisfied as specified empirically in Art. 4.7.4.4 as given in Equation 3.99:

$$N = (8 + 0.02L + 0.08H)(1 + 0.000125S^2) \quad (3.99)\ \text{[AASHTO LRFD Equation 4.7.4.4-1]}$$

where

N = minimum support length measured normal to the centerline of bearing (in.)
L = length of the bridge deck to the adjacent expansion joint, or to the end of the bridge deck or the sum of the distances to either side of the hinge for hinges within a span
L = the length of the bridge deck (ft) for single-span bridges
H is defined differently for different bridge components as follows:

For single-span bridges, $H = 0.0$
For abutments, H = average height of columns supporting the bridge deck to the next expansion joint (ft)
For columns and piers, H = column or pier height (ft)

S = skew of support measured from line normal to span (degrees)

Definitions of length L for various span configurations are shown in Figure 3.97.

It is further required that length N be modified by the percentages as shown in Table 3.46 corresponding to the listed seismic zones, acceleration coefficient (A), and the soil type.

Example 3.31 presents the application of Equation 3.99.

The purpose of providing a minimum bridge seat width (support length) is to ensure that maximum displacement of the deck during an earthquake would be accommodated safely, without the danger of the deck sliding off the abutment and piers as had been experienced in many past earthquakes. Figures 3.98 through 3.100 show examples of some of the spectacular bridge failures caused because of the insufficient support lengths over the supports (abutments and piers).

Example 3.31

A single-span bridge spanning 80 ft is located in Los Angeles County, California. Determine the minimum required support width over the abutment if the bridge is designated as (a) critical, (b) essential structure, and (c) other.

www.EngineeringEBooksPdf.com

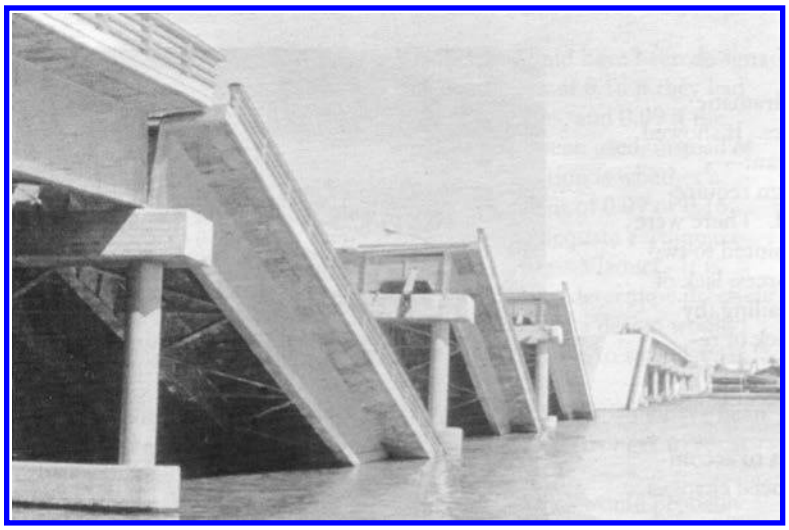

FIGURE 3.98 Collapse of the Showa Bridge during the 1964 Niigata, Japan, earthquake. Two piers in the middle of the river failed, causing three spans to drop (front of the photo). Two other spans slipped off piers that remained upright (back of the photo).

Solution

For single-span bridges, the support width requirements are the same for bridges in all operational categories.

For the given bridge, $L = 80$ ft, $H = 0$ (single-span bridge), $S = 0$ (no skew). Substitution of these values in Equation 3.99 yields

$$N = (8 + 0.02L + 0.08H)(1 + 0.000125S^2) = (8 + 0.02 \times 80) = 9.6 \text{ in.}$$

The support length N needs to be increased as shown in Table 3.47.

1. If $A_S < 0.05$, $N_{min} = 9.6 \times (1 + 0.75) = 16.8$ in., say 17 in.
2. If $A_S \geq 0.05$, $N_{min} = 9.6 \times (1 + 1) = 19.2$ in., say 19.5 in.

3.21.6.3 Calculation of Design Connection Forces for Bridges in Various Seismic Zones

3.21.6.3.1 General Provisions

AAAHTO LRFD Art. 3.10.9 specifies methods of calculating seismic forces for bridges in various seismic zones as defined in Table 3.39. For single-span bridges, regardless of their seismic zones, it is required that the minimum design connection force, $F_{SC,min}$, be calculated from Equation 3.100:

$$F_{SC,min} \geq F_{PGA} PGA(A_T) \tag{3.100}$$

where

A_T = tributary permanent load

F_{PGA} and PGA were defined earlier

3.21.6.3.2 Seismic Zone 1

Seismic Zone 1 is defined (Table 3.39) as the region in which the five percent damped spectral acceleration for 1 s period is less than 0.15 (i.e., $S_{D1} \leq 0.15$).

AASHTO LRFD Art. 4.7.4.4 specifies minimum support length requirements as discussed earlier (Equation 3.97 and Figure 3.97). Art. 3.10.9 specifies minimum force requirements for providing

www.EngineeringEBooksPdf.com

restraint at the bearings (on the abutments), which are based on the soil classification of the bridge site (specified in Art. 3.10.9.2) as follows:

1. For bridge sites where the acceleration coefficient, A_S, is less than 0.05, the horizontal design connection force in the restrained directions shall not be taken less than 0.15 times the vertical reaction due to tributary permanent load and the tributary live loads assumed existing during the earthquake.
2. For all other sites in Seismic Zone 1, the horizontal design connection force in the restrained directions shall not be taken less than 0.25 times the vertical reaction due to tributary permanent load and the tributary live loads assumed existing during the earthquake. The horizontal design connection force shall be addressed from the point of application through the substructure and into the foundation elements, that is, follow a logical load path.
3. The elastomeric bearings and its connection to the masonry and sole plates shall be designed to resist the horizontal seismic design forces transmitted through the bearing. For all bridges in Seismic Zone 1 and all single-span bridges, these seismic forces shall not be less than connection forces as specified in items 1 and 2 mentioned earlier.

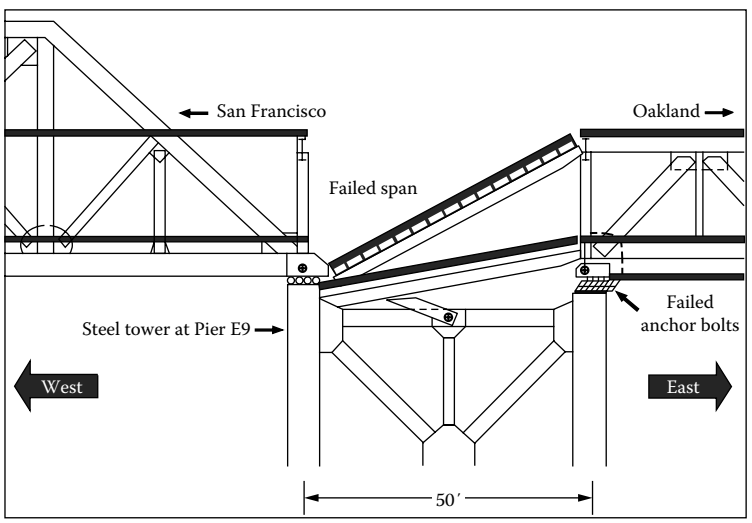

(a)

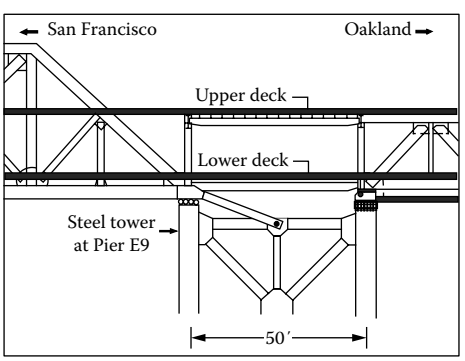

(b)

FIGURE 3.99 Collapse of the upper and lower decks of the East Bay Bridge, San Francisco, during the October 17, 1989, M 7.1 Loma Prieta earthquake: (a) positions of the upper and lower decks at Pier E9 after the earthquake and (b) as built positions of the upper and the lower decks. (*Continued*)

www.EngineeringEBooksPdf.com

(c)

FIGURE 3.99 (*Continued*) Collapse of the upper and lower decks of the East Bay Bridge, San Francisco, during the October 17, 1989, M 7.1 Loma Prieta earthquake: (c) aerial view of the collapsed upper and lower decks.

(a)

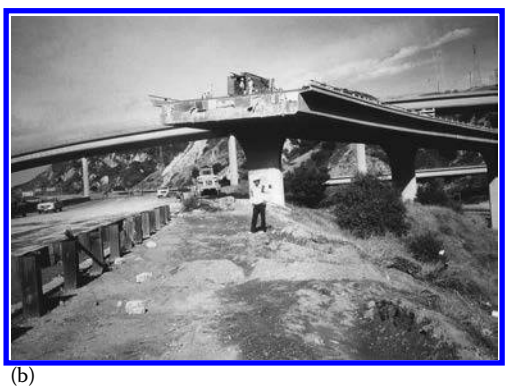

(b)

(c)

FIGURE 3.100 Collapse of highway bridges during the January 17, 1994, M 6.7-Northridge, California, earthquake. (a) Typical cantilever span support span (right side of the joint) for the suspended span (left side of the joint). Due to the longitudinal movement of the bridge during the earthquake, the joint widened causing sliding away of the suspended span and thus losing support, resulting in the collapse of the suspended spans, (b) the suspended span has collapsed (removed by the crew), and (c) suspended spans collapsed (removed by the crew).

www.EngineeringEBooksPdf.com

TABLE 3.47
Minimum Analysis Requirements for Seismic Effects (AASHTO LRFD Table 4.7.4.3.1-1)

Seismic Zone	Single-Span Bridges	Multispan Bridges: Other Bridges, Regular	Other Bridges, Irregular	Essential Bridges, Regular	Essential Bridges, Irregular	Critical Bridges, Regular	Critical Bridges, Irregular
1	No seismic analysis required	None	None	None	None	None	None
2	No seismic analysis required	SM/UL	SM	SM/UL	MM	MM	MM
3	No seismic analysis required	SM/UL	MM	MM	MM	MM	TH
4	No seismic analysis required	SM/UL	MM	MM	MM	TH	TH

Source: From *AASHTO LRFD Bridge Design Specifications*, Copyright © 2012 by American Association of State Highway and Transportation Officials, Washington, DC. Used by permission.

Notes: UL, uniform load elastic method; SM, single-mode elastic method; MM, multimode elastic method; and TH, time-history method.

3.21.6.3.3 Seismic Zone 2

Seismic Zone 2 is defined as the region in which the five percent damped spectral acceleration for 1 s period is between 0.15 and 0.30 (i.e., $0.15 < S_{D1} \leq 0.30$).

Seismic forces for bridges in this zone are required to be determined based on minimum analysis requirements as specified in Art. 4.7.4.1 (referred to earlier) and 4.7.4.3, which specifies the analysis methods required for *multispan* bridges having different importance categories (critical, essential, and other) as described earlier. Table 3.47 presents a list of these analysis methods; readers are referred to AASHTO LRFD Art. 4.7.4.3 for the detailed description of these methods.

For analytical purposes, bridges in Table 3.48 are classified as *regular* and *irregular*. *Regular* bridges are defined as those that satisfy the requirements of Table 3.48; all other bridges should be considered *irregular*.

A flow chart summarizing the earthquake provisions of AASHTO LRFD Specifications is presented in the appendix to this chapter.

Note that Table 3.48 makes no mention of *curved* bridges. In reality, curved bridges may consist of multiple simple-span straight bridges that appear to be curved because of the curved deck profile.

TABLE 3.48
Regular Bridge Requirements (AASHTO LRFD Table 4.7.4.3.1-2)

Parameter	Value				
Number of Spans	2	3	4	5	6
Maximum subtended angle for a curved bridge	90°	90°	90°	90°	90°
Maximum span length ratio from span to span	3	2	2	1.5	1.5
Maximum bent/pier stiffness ratio from span to span, excluding abutments	—	4	4	3	2

Source: From *AASHTO LRFD Bridge Design Specifications*, Copyright © 2012 by American Association of State Highway and Transportation Officials, Washington, DC. Used by permission.

www.EngineeringEBooksPdf.com

TABLE 3.49
Approximate Values of Relative Movements Required to Reach Active and Passive Pressure Conditions

	Values of Δ/H	
Type of Backfill	**Active**	**Passive**
Dense sand	0.001	0.01
Medium dense sand	0.002	0.02
Loose sand	0.004	0.04
Compacted silt	0.002	0.02
Compacted lean clay	0.010	0.05
Compacted fat clay	0.010	0.05

Source: Adapted from Clough, G.W. and Duncan, J.M., Earth pressures, in: *Foundation Engineering Handbook*, 2nd ed., H.Y. Fang, ed., Van Nostrand Reinhold, New York, 1991, Chapter 6.

However, some bridges may have a curved geometry. Art. 4.7.4.3 specifies the following provisions for seismic analysis of bridges that are curved in plan:

1. Curved bridges comprised of multiple simple spans shall be considered as *irregular* if the subtended angle in plan is greater than 20°. Such bridges are required to be analyzed by either the *multimode elastic method* or the *time-history method*.
2. A curved, continuous-girder bridge may be analyzed as if it were straight, provided that *all* of the following requirements are satisfied:
   a. The bridge is regular as defined in Table 3.49, except that for a two-span bridge, the maximum span length ratio from span to span must not exceed 2.
   b. The subtended angle in plan is not greater than 90°.
   c. The span lengths of the equivalent straight bridge are equal to arc lengths of the curved bridge.

If all of the aforementioned requirements are not satisfied, then curved continuous-girder bridges must be analyzed using the actual curved geometry.

It is noted that rigorous methods of analysis are required for (1) critical bridges (described earlier), (2) bridges that are geometrically complex, and (3) bridges that are located in close proximity of active faults. AASHTO LRFD recommends the use of time-history methods of analysis for such bridges, provided care is taken with both the modeling of the bridge and the selection of the input time histories of ground acceleration.

3.21.6.3.4 Seismic Zones 3 and 4

Seismic Zone 3 is defined as the region in which the five percent damped spectral acceleration for 1 s period is between 0.30 and 0.50 (i.e., $0.30 < S_{D1} \leq 0.50$); regions in which $S_{D1} > 0.5$ are classified as Seismic Zone 4. Bridge structures in these zones are required to be analyzed as specified in Table 3.48. The design forces for bridge components (such as columns, column bents, and their foundation and connections) are to be taken as *lesser* of the following:

1. *Provisions of Art. 3.10.9.4.2*: Require design forces to be determined as specified in Art. 3.10.9.3, except that the *R*-factor is to be taken as 1.0 for the foundation.
2. *Provisions of Art. 3.10.9.4.3*: Require determination of forces that would cause inelastic hinges in columns.

www.EngineeringEBooksPdf.com

Readers should refer to Art. 3.10.9 4 for further details for determination of seismic forces on bridges in Seismic Zones 3 and 4.

3.21.7 Determination of Fundamental Period, *T*

Each of the four analysis methods listed in Table 3.48 requires determination of the fundamental period *T* for bridge vibration in both longitudinal and transverse directions. The single-mode elastic method (SM) assumes that the first (or the fundamental) mode of vibration is predominant as the structure vibrates (as an inverted pendulum), a reasonable assumption for all *regular* structures (as in the case of regular buildings). In reality, a structure may vibrate randomly in any direction. For analytical purposes, it is assumed that a bridge (or any structure) can vibrate longitudinally (i.e., along the length) or transversely (i.e., perpendicular to the longitudinal axis). Different techniques are used to determine the fundamental periods of vibration in these two directions. Various analysis methods are briefly described as follows.

3.21.7.1 Single-Mode Spectral Analysis Method (SM): Procedure 1

The single-mode spectral analysis method (SM) described in the following steps may be used for both transverse and longitudinal earthquake motions (AASHTO LRFD Art. 4.7.4.3.2). Examples illustrating its application can be found in AASHTO 1992 (see *Commentary* to Division IA of this reference). The following summary is provided based on AASHTO 1992 and AASHTO LRFD 2012 and AASHTO LRFD *Commentary C4.7.4.3.2b.*

Step 1. Calculate the static displacements $v_s(x)$ due to an assumed uniform loading P_o as shown in Figure 3.101. Abutment stiffness, if desired, can be incorporated by the procedure outlined in Art. C5.3 of the Commentary in AASHTO 1992. The uniform loading, P_o, is applied over the length of the bridge; it has units of force/unit length and is arbitrarily set equal to 1 for computational convenience. The static displacement, $v_s(x)$, has units of length.

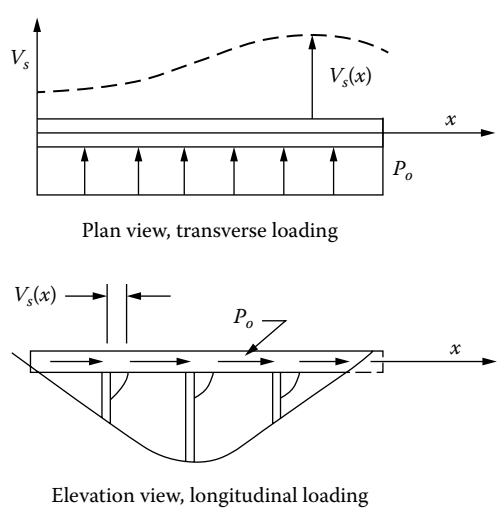

FIGURE 3.101 Bridge deck subjected to assumed transverse and longitudinal loading. (From *AASHTO LRFD Bridge Design Specifications*, Copyright © 2012 by American Association of State Highway and Transportation Officials, Washington, DC. Used by permission.)

www.EngineeringEBooksPdf.com

Step 2. Calculate factors α, β, and γ from the following expressions:

$$\alpha = \int v_s(x)dx \tag{3.101}$$

$$\beta = \int w(x)v_s(x)dx \tag{3.102}$$

$$\gamma = \int w(x)v_s^2(x)dx \tag{3.103}$$

where the quantity $w(x)$ is the weight of the dead load of the bridge superstructure and tributary substructure (force/unit length). The computed factors α, β, and γ have units of (ft^2), (kip-ft), and (kip-ft^2), respectively.

The weight $w(x)$ should take into account structural elements and other relevant loads including, but not limited to, pier caps, abutments, columns, and footings. Other loads such as live loads may be included. Generally, the inertial effects of live loads are not included in the analysis; however, the design of bridges having high live to dead load ratios, such as those located in metropolitan areas where traffic congestion is likely to occur, should consider the probability of large live load being present on the bridge during an earthquake.

Equations 3.101 through 3.103 simplify considerably if it is assumed that the weight of the tributary superstructure and the substructure is constant (as may often be the case) and the displacement profile is constant (see Figure 3.101). Under these assumptions, $w(x) = w$ and $v_s(x) = v_s$, both of which are constant, and Equations 3.99 through 3.101 can be rewritten, respectively, as Equation 3.104 through 3.106:

$$\alpha = v_s L \tag{3.104}$$

$$\beta = w v_s L \tag{3.105}$$

$$\gamma = w v_s^2 L \tag{3.106}$$

Step 3. Calculate the period of the bridge from Equation 3.107:

$$T_m = 2\pi\sqrt{\frac{\gamma}{p_o g \alpha}} \tag{3.107}$$

where g = acceleration due to gravity (ft/s^2). Substitution in Equation 3.107 for α and γ from Equations 3.104 and 3.106, respectively, yields

$$T_m = 2\pi\sqrt{\frac{w v_s}{p_o g}} \tag{3.108}$$

Multiplying by L both the numerator and denominator under the radical sign in Equation 3.108 yields to Equation 3.109:

$$T_m = 2\pi\sqrt{\frac{w L v_s}{p_o L g}} \tag{3.109}$$

www.EngineeringEBooksPdf.com

Substitution of the following in Equation 3.109 yields to Equation 3.110:

$W = wL$ = weight of the tributary superstructure and the substructure
$P_o = p_oL$ = total applied virtual load
$g = 32.2$ ft/s^2 = 386.4 in./s^2

$$T_m = 0.32\sqrt{\frac{Wv_s}{P_o}} \tag{3.110}$$

In Equation 3.110, the quantity P_o/v_s can be expressed as the force required to cause unit displacement, that is, the total stiffness of the structure, K. With this substitution, Equation 3.110 can be expressed as given by Equation 3.111:

$$T_m = 0.32\sqrt{\frac{W}{K}} \tag{3.111}$$

Note that Equation 3.111 is the same as Equation 3.86 (constant $2\pi/\sqrt{g}$ in Equation 3.86 equals 0.32 in Equation 3.111). Again, expressing $W/K = \Delta_w$ = longitudinal displacement (in.) due to total dead weight acting longitudinally, Equation 3.111 can be expressed as given by Equation 3.112:

$$T_m = 0.32\sqrt{\Delta_w} \tag{3.112}$$

Step 4. Using T_m from Equation 3.111, calculate the equivalent static earthquake loading $p_e(x)$ from Equation 3.113:

$$p_e(x) = \frac{\beta C_{sm}}{\gamma} w(x) v_s(x) \tag{3.113}$$

where

C_{sm} = the dimensionless elastic seismic response coefficient given by Equation 3.89
$p_e(x)$ = intensity of the equivalent static seismic loading applied to represent the primary mode of vibration (kip/ft)

Substitution for β and γ from Equations 3.105 and 3.106 in Equation 3.113 and noting as before that $w(x) = x$ and $v_s(x) = v_s$, Equation 3.113 is simplified and expressed as given by Equation 3.114:

$$p_e(x) = wC_{sm} \tag{3.114}$$

Step 5. Apply loading $p_e(x)$ to the structure as shown in Figure 3.101 and determine the resulting member forces and displacements for design purposes.

It is noted that determination of these response parameters is not required for the types of short-span bridge superstructures described in Chapter 2; as such, this topic is not discussed further in this book. Readers should refer to the Commentary to AASHTO LRFD Specifications for further details on this topic.

www.EngineeringEBooksPdf.com

3.21.7.2 Other Methods of Analysis

AASHTO LRFD Art. 4.7.3 specifies other methods for multispan bridges. These include uniform load method (UM), multimode spectral analysis method (MM), and time-history method. The multimode response spectrum analysis (MM) should be performed with a suitable space frame linear dynamic analysis computer program. Currently available computer programs are included in AASHTO LRFD *Commentary C4.7.4.3b*. These methods and computer are not discussed here; readers should refer to the commentary for details.

Flow charts for seismic design and detailing (Figures 3.A.4 and 3.A.5) are provided in Appendix 3.A.

3.22 EARTH PRESSURE: *EH, ES, LS,* AND *DD*

3.22.1 General

Forces due to earth pressure do not act on bridge superstructures. As such, this topic is not discussed in detail in this book. However, for completeness of the topic of loads, introductions to various aspects of forces caused earth pressure are discussed in this section.

Earth, when retained by an object at angles steeper than its angle of repose, exerts lateral pressure against the retaining object. Such objects are called retaining walls. Bridge abutments, wing walls, and basement walls in buildings are examples of retaining walls. In the context of bridges, abutments and wing walls are the two structural components that are subjected to earth pressure. In addition, bridge abutments are subjected to gravity loads from the superstructure as well as additional lateral loads due to live load surcharge (Figure 3.102). Similarly, basement walls are subjected to lateral earth pressure as well as gravity loads from the walls supported above them.

In AASHTO LRFD (2012), specifications for earth pressure are covered in Art. 3.11. This article covers forces related to retained earth as follows:

1. *EH*: Lateral (or horizontal) earth pressure
2. *ES*: Surcharge loads
3. *LS*: Live load surcharge
4. *DD*: Downdrag

3.22.2 Determination of Earth Pressure

Earth pressure shall be considered as a function of the following parameters:

1. Type and unit weight of earth
2. Water content
3. Soil creep characteristics

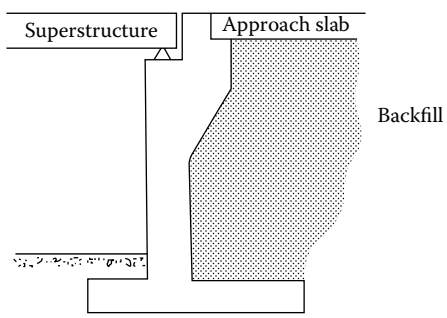

FIGURE 3.102 A typical bridge abutment.

www.EngineeringEBooksPdf.com

4. Degree of compaction
5. Location of groundwater table
6. Earth-structure interaction
7. Amount of surcharge
8. Earthquake effects
9. Back slope angle
10. Wall interaction

3.22.2.1 Basic Concepts of Earth Pressure

If a retaining wall were built against a solid rock face, the wall will not be subjected to any lateral pressure from the rock. This is because rock is a rigid material and, unless subjected to external force, will retain its form and shape. The principle forces acting on retaining structures arise from retaining loose materials, such as earth and grains or liquids, which are not capable of supporting or retaining themselves in a desired stable shape. In the absence of supporting walls, these materials will simply flow and spread into their natural shape. For example, loose earth, sand, and grains, if not retained by a wall, will simply spread in a pyramid shape. Liquids will simply flow. Consequently, the principal force that retaining walls have to resist is the pressure exerted on them by the retained materials. All walls that retain materials or liquids are designed based on the same general principles, that is, they must be able to resist lateral pressure exerted by the materials they support. For example, basement walls in buildings, subterranean walls in buried structures, and underground parking structures must be designed to resist earth pressure.

From an engineering perspective, it is appropriate to introduce the concept of strain in soils. Loose soil poured on a flat surface will spread into a heap of pyramid shape freely because of the unlimited strain it can have. When the same soil is retained by a wall, the amount of strain (expansion or contraction) the soil can have is severely limited. The amount and distribution of lateral pressure due to the retained soil depends largely on the relative lateral strain it can have, which, in turn, depends on the rigidity of the retaining structure.

Retained soil can cause three types of lateral pressures. If a retaining structure is unyielding or rigid, it will be subjected to lateral pressure referred to as *earth pressure at rest*. Lateral pressure against basement walls is generally in this category. On the other hand, if a retaining wall is permitted to yield (i.e., move away from the retained soil) allowing a lateral expansion of the soil, the earth pressure decreases with increasing expansion. This continues until a stage is reached when further expansion causes a shear failure of the soil, characterized by a sliding wedge moving forward (toward the wall) and downward with respect to the original position (Figure 3.103a). At this stage of failure, the value of lateral pressure on the wall is the smallest; additional deformation in the soil does not cause any further reduction in lateral pressure. This minimum earth pressure is called *active earth pressure*.

A situation may exist where the retaining structure may have a mass of soil in the front, which will be pushed as the wall moves away from the retained soil. In that case, the retained soil is pushed

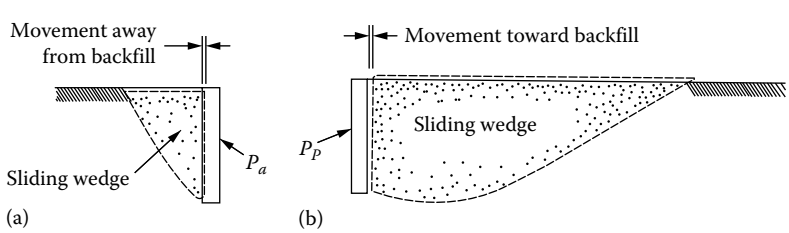

FIGURE 3.103 Concept of lateral earth pressure: (a) active pressure and (b) passive pressure.

www.EngineeringEBooksPdf.com

causing it to contract laterally. A larger force is required to move the soil behind the retaining structure. This soil movement continues until a stage is reached when further contraction causes a shear failure of the soil, characterized by a sliding wedge moving backward and upward with respect to its original position (Figure 3.103b). The lateral pressure experienced by the wall at this stage is the largest; and no additional force is required to cause further movement of the wedge. This maximum lateral pressure is called *passive pressure*.

In the event of an earthquake, the retaining walls would be subjected to additional (lateral) earth pressure referred to as *seismic* or *dynamic* earth pressure.

Movement of a retaining wall, however slight, is required to develop active or passive pressures. Relatively larger movements, as much as five to ten times larger, are required to attain passive pressures as compared to active pressures. Table 3.49 gives approximate values of relative movements required to reach active or passive earth pressure conditions (Clough and Duncan 1991).

Several methods of estimating pressure due to backfill are in use, all of which are associated with some degree of approximations and uncertainty. Ten important factors that can cause these uncertainties were described in the previous section. As a result, accurate determination of earth pressure is difficult, and often, it can be estimated for only specific conditions of backfill material and assumptions.

Methods of determining earth pressures on retaining walls based on classical earth-pressure theories. The following is a brief overview of current practices of determining earth pressures on retaining walls.

Various methods of determining earth pressures on retaining walls are based on the following three assumptions:

1. The pressure in the pore water of the backfill is negligible.
2. The soil properties appearing in the earth-pressure equations have definite values that can be determined reliably.
3. The wall can yield by tilting, deforming, or sliding through a distance sufficient to develop the full shearing resistance of the backfill.

These assumptions are important in that if not satisfied, the calculated earth pressures would be invalid. For example, if the first and the second assumptions are not satisfied, the retaining wall will be acted upon by agents and forces beyond the scope of any earth pressure theory. Properties of loosely deposited or inadequately drained backfill change from season to season so that the backfill passes through states of partial or total saturation alternating with states of drainage or even partial desiccation. Changes in earth pressures caused by these phenomena are not accounted for in the classical earth pressure theories. Pressure cell measurements on the back of a 10 m high retaining wall by McNary (1925) indicated that within one year, the pressure varied from the average value by ± 30 percent (Terzaghi et al. 1996).

The third assumption is extremely significant because its implications continue to lead to considerable confusion among designers. This involves uncertainties regarding the movements of retaining walls when acted upon by the earth pressure. These uncertainties were first investigated by Terzaghi through model tests (Terzaghi 1920, 1934a,b, 1936). His findings indicated that neither the small-scale nor the large-scale tests or even filed measurements could furnish consistent results unless the walls moved far enough to establish the active state. For granular soils placed under controlled conditions, the required movements were relatively small. Therefore, it was concluded "that most conventional walls, if not restrained at their tops, could move far enough without objectionable consequences to reduce the earth pressure to the active value and that the stability of the walls could, therefore, properly be investigated on the basis of that pressure." This conclusion is subject to several limitations not always realized by designers (Terzaghi et al. 1996; see Art. 45.4 for a detailed discussion on this important subject).

www.EngineeringEBooksPdf.com

3.22.3 Theories and Calculations of Earth Pressures

3.22.3.1 Theories of Earth Pressures

Irrespective of the type of retaining wall used, two basic requirements must be satisfied:

1. The retaining wall must be stable and have an adequate factor of safety against sliding, overturning, and settlement.
2. The retaining wall must provide sufficient strength to resist forces to which it is subjected (i.e., structural design must be adequate).

These two requirements are sometimes referred to, respectively, as *external stability* and *internal stability*.

The magnitude and direction of earth pressure on a retaining wall depends on many factors, chiefly on the nature of the backfill and other factors (e.g., wall movements) that cannot be determined with the same degree of certainty as the gravity loads. Although the distribution of pressure on the back of the retaining wall is complex, for simplicity, it is common to assume hydrostatic or linear pressure distribution so that the earth pressure increases linearly with the height of the wall. Accordingly, the lateral pressure, p, at any height of wall is a function of wall height z below the surface of the backfill and the unit weight of soil γ_s is taken as linearly proportional to the depth of earth and is expressed by Equation 3.115:

$$p = k\gamma_s z \qquad (3.115)\ \text{[AASHTO LRFD 3.11.5.1-1]}$$

where

p = lateral earth pressure (ksf)
k = coefficient of lateral earth pressure
γ_s = unit weight of soil (kcf)
z = depth below the surface (ft)

Coefficient k is calculated as follows based on the conditions applicable to wall movements:

k_o = coefficient of at-rest lateral earth pressure for wall that do not move
k_a = coefficient of active lateral earth pressure (for walls that deflect or move sufficiently to reach minimum active conditions)
k_p = coefficient of passive lateral earth pressure (for walls that deflect or move sufficiently to reach passive conditions)

The resultant of the lateral pressure is assumed to act at $H/3$ above the base of the wall, where H is the total height of the wall measured from the surface of the ground at the back of the wall to the bottom of the footing of the wall.

The value of coefficient k in Equation 3.115 depends on the physical properties of soil, varying from about 0.3 for loose granular soil (e.g., dry sand) to about 1.0 for cohesive soils such as wet clays. Both active and passive pressures against a retaining wall are assumed to have linear distribution. The nature of the backfill plays a defining role in the distribution of pressure. Noncohesive, granular materials such as dry sand behave differently from cohesive materials such as clay, silt, or any soil containing these soils as constituents. When the backfill consists of dry granular material, the assumption of hydrostatic or linear distribution of earth pressure is fairly satisfactory. However, cohesive soils or saturated sands behave in nonlinear manner, which is not well defined. For this reason, it is common practice to specify granular material, such as dry sand, as backfill material and to also provide adequate means for the drainage of water from the back of the wall so that linear pressure distribution can be justifiably used.

The two most commonly used theories for computing earth pressures are known as Rankine's theory and Coulomb's theory. These theories are described in texts on *soil mechanics* and not discussed here. Both theories are based on the three assumptions discussed in the previous section. Another method to calculate earth pressures, called the *log spiral method*, was developed by Ohde (1938) and is discussed in Terzaghi et al. (1996).

www.EngineeringEBooksPdf.com

3.22.3.2 Calculations of Coefficients of Earth Pressures

3.22.3.2.1 At-Rest Lateral Earth Pressure Coefficient, k_o

1. For normally consolidated soils, vertical wall, and level ground, the coefficient of at-rest lateral earth pressure, k_o, is given by Equation 3.116:

$$k_o = 1 - \sin\phi'_f \qquad (3.116)\ [\text{AASHTO LRFD } 3.11.5.2\text{-}1]$$

   where ϕ'_f = effective angle of internal friction of soil.
2. For overconsolidated soils, vertical wall, and level ground, the coefficient of at-rest lateral earth pressure, k_o, is a function of overconsolidation ratio (*OCR*) and is given by Equation 3.117:

$$k_o = \left(1 - \sin\phi'_f\right)\left(OCR\right)^{\sin\phi'_f} \qquad (3.117)\ [\text{AASHTO LRFD } 3.11.5.2\text{-}2]$$

3.22.3.2.2 Active Lateral Earth Pressure Coefficient, k_a

The coefficient of active lateral pressure, k_a, based on Coulomb's earth pressure theory, is given by Equation 3.118:

$$k_a = \frac{\sin^2\left(\theta + \phi'_f\right)}{\Gamma\left[\sin^2\theta\,\sin\left(\theta - \delta\right)\right]} \qquad (3.118)\ [\text{AASHTO LRFD } 3.11.5.3\text{-}1]$$

where

$$\Gamma = \left[1 + \sqrt{\frac{\sin\left(\phi'_f + \delta\right)\sin\left(\phi'_f - \beta\right)}{\sin\left(\theta - \delta\right)\sin\left(\theta + \beta\right)}}\right]^2 \qquad (3.119)\ [\text{AASHTO LRFD } 3.11.5.3\text{-}2]$$

δ = friction angle between fill and wall taken as specified in AASHTO LRFD Table 3.11.5.3-1 (degrees, Figure 3.104)
β = angle of fill to the horizontal (degrees, Figure 3.104)
θ = angle of the back face of wall to the horizontal (degrees, Figure 3.104)
ϕ'_f = effective angle of internal friction of soil (degrees, Figure 3.104)

Values of friction angle for various types of soils are given AASHTO LRFD Table 3.11.5.31-1.

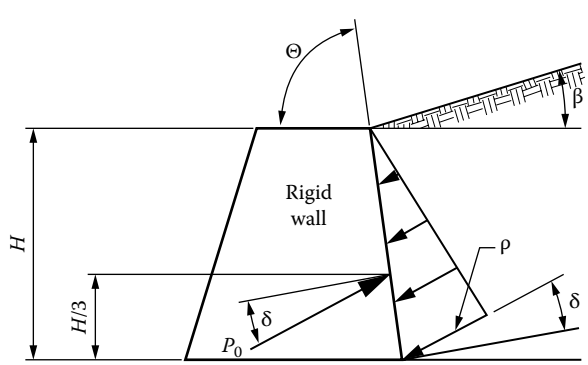

FIGURE 3.104 Notations for Equations 3.118 and 3.119.

www.EngineeringEBooksPdf.com

3.22.3.2.3 Passive Lateral Earth Pressure Coefficient, k_p

Passive lateral earth pressures due to noncohesive soils and cohesive soils are calculated differently:

1. *Noncohesive soils*: Passive lateral earth pressure due to noncohesive soils for the case of sloping or vertical walls supporting a horizontal backfill is determined from Figure 3.105. Passive lateral pressure due to a sloping backfill is determined from Figure 3.106.
2. *Cohesive soils*: The passive lateral pressure due to cohesive soils is calculated from Equation 3.120:

$$p_p = k_p \gamma_s z + 2c\sqrt{k_p} \qquad (3.120)\ [\text{AASHTO LRFD } 3.11.5.4\text{-}1]$$

where
p_p = passive lateral earth pressure (ksf)
γ_s = unit weight of soil (kcf)
z = depth of soil below the surface
c = cohesion coefficient (ksf)
k_p = coefficient of passive earth pressure specified in Figures 3.105 and 3.106 as appropriate

3.22.4 Equivalent-Fluid Method of Estimating Rankine's Lateral Earth Pressures

The equivalent-fluid method may be used where the Rankine earth pressure is applicable. "The equivalent-fluid method shall only be used where the backfill is free draining." "If this criterion cannot be satisfied, the provisions of AASHTO LRFD Art. 3.11.3, 3.11.5.1 and 3.11.5.3 shall be used to determine horizontal earth pressure" (AASHTO LRFD Art. 3.11.5.3), that is, Equations 3.115 through 3.119 should be used. When the equivalent-fluid method is used, the basic earth pressure, p (ksf), may be calculated from Equation 3.121:

$$p = \gamma_{eq} z \qquad (3.121)\ [\text{AASHTO LRFD } 3.11.5.4\text{-}1]$$

where
γ_{eq} = equivalent-fluid unit weight of soil, not less than 0.030 (kcf)
z = depth of soil below the ground surface

The resultant lateral earth pressure due the weight of the backfill is assumed to act at a height of $H/3$ above the base of the wall, where H is the height of the wall from the surface of the ground to the bottom of the footing. Typical values for equivalent-fluid weights for design of a wall may be taken from Table 3.50.

3.22.5 Selection of Backfill Material

Care should be exercised in the selection of the backfill material for retaining walls and basement walls. Generally speaking, the requirements specified for backfill materials specified for retaining walls also apply to basement walls. Most backfill materials can be assigned to one of the following five categories (Terzaghi et al. 1996):

1. Coarse-grained soil without admixture of fine soil particles, very permeable (clean sand or gravel)
2. Coarse-grained soil of low permeability due to admixture of particles of silt size
3. Residual soil with stones, fine silty sand, and granular materials with conspicuous clay content
4. Very soft or soft clay, organic silts, or silty clays
5. Medium or stiff clay

www.EngineeringEBooksPdf.com

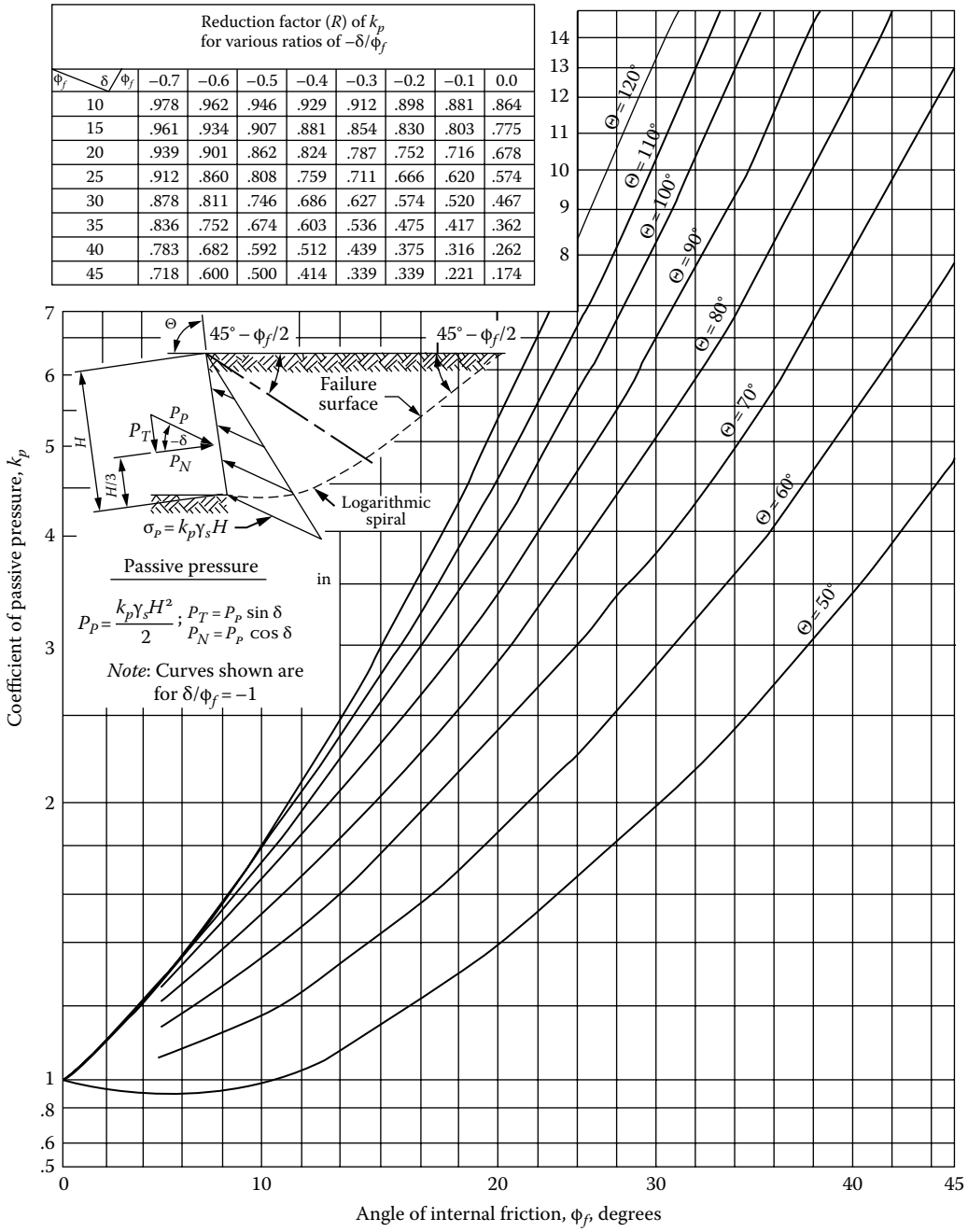

Reduction factor (R) of k_p for various ratios of $-\delta/\phi_f$

ϕ_f \ δ/ϕ_f	−0.7	−0.6	−0.5	−0.4	−0.3	−0.2	−0.1	0.0
10	.978	.962	.946	.929	.912	.898	.881	.864
15	.961	.934	.907	.881	.854	.830	.803	.775
20	.939	.901	.862	.824	.787	.752	.716	.678
25	.912	.860	.808	.759	.711	.666	.620	.574
30	.878	.811	.746	.686	.627	.574	.520	.467
35	.836	.752	.674	.603	.536	.475	.417	.362
40	.783	.682	.592	.512	.439	.375	.316	.262
45	.718	.600	.500	.414	.339	.339	.221	.174

FIGURE 3.105 Computational procedure for passive pressures for vertical and sloping walls with *horizontal* backfill. (From U.S. Department of Navy, Foundations and earth structures, Technical Report, NAVFAC DM-7.1 and DM-7.2, Naval Facilities Command, U.S. Department of Defense, Washington, DC, p. 244, 1982.)

www.EngineeringEBooksPdf.com

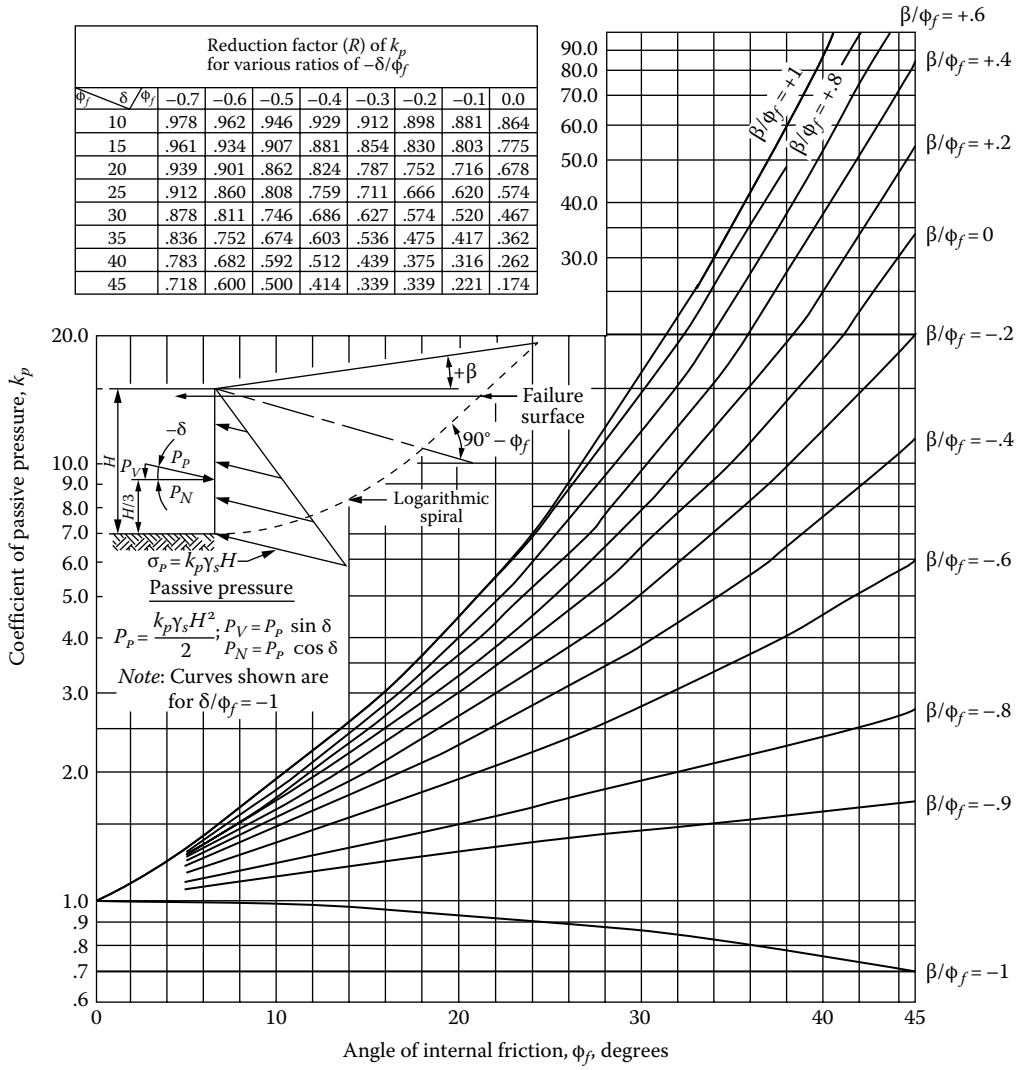

Reduction factor (R) of k_p for various ratios of $-\delta/\phi_f$

ϕ_f \ δ/ϕ_f	−0.7	−0.6	−0.5	−0.4	−0.3	−0.2	−0.1	0.0
10	.978	.962	.946	.929	.912	.898	.881	.864
15	.961	.934	.907	.881	.854	.830	.803	.775
20	.939	.901	.862	.824	.787	.752	.716	.678
25	.912	.860	.808	.759	.711	.666	.620	.574
30	.878	.811	.746	.686	.627	.574	.520	.467
35	.836	.752	.674	.603	.536	.475	.417	.362
40	.783	.682	.592	.512	.439	.375	.316	.262
45	.718	.600	.500	.414	.339	.339	.221	.174

FIGURE 3.106 Computational procedure for passive pressures for vertical and sloping walls with *sloping* backfill. (From U.S. Department of Navy. 1982. Foundations and earth structures, Technical Report, NAVFAC DM-7.1 and DM-7.2, Naval Facilities Command, U.S. Department of Defense, Washington, DC, p. 244, 1982.)

Backfill material should preferably be free-draining soil without large stones, construction debris, organic materials, and frozen earth. The most favorable backfill materials are coarse-grained soils, preferably with little or no silt or clay content. Design codes/specifications commonly provide general specifications for the selection of a suitable backfill such as follows (AASHTO 1992):

> The backfill material behind all retaining walls shall be free draining, nonexpansive, noncorrosive material and shall be drained by weep holes with French drains, placed at suitable intervals and elevations….Silts and clays shall not be used for backfill unless suitable design procedures are followed and construction control measures are incorporated in the construction documents to account for their presence.

However, such ideal backfill materials may be either unavailable or too expensive. Use of less suitable materials is associated with large earth pressures and increases the cost of the wall.

www.EngineeringEBooksPdf.com

TABLE 3.50
Typical Values for Equivalent-Fluid Unit Weights of Soils

	Level Backfill		Backfill with β = 25°	
	At Rest	Active $\Delta/H = 1/240$	At Rest	Active $\Delta/H = 1/240$
Type of Soil	γ_{eq} (kcf)	γ_{eq} (kcf)	γ_{eq} (kcf)	γ_{eq} (kcf)
Loose sand or gravel	0.055	0.040	0.065	0.050
Medium dense sand or gravel	0.050	0.350	0.060	0.045
Dense sand or gravel	0.045	0.030	0.055	0.040

Source: From *AASHTO LRFD Bridge Design Specifications*, Copyright © 2012 by American Association of State Highway and Transportation Officials, Washington, DC. Used by permission.

Notes: Δ = movement of top of wall to reach minimum active or passive pressure by tilting or lateral translation (ft); H = height of wall; β = angle of fill to horizontal.

For example, backfill materials such as soft clays, silty clays, or organic silts can be expected to lead to large pressures and progressive wall movements. Stiff clays, as a rule, should not be used. This is because they are certain to experience an increase in water content over the years and to exert *swelling pressures* that may greatly exceed the lateral resistance of the wall. At the very least, it should be ensured that the properties of the selected backfill material match as closely as possible the soil properties used in design. Saturated backfill material, such as saturated clays, should be avoided as the wet backfill materials significantly increase the hydrostatic pressure on the walls.

3.22.6 Effects of Surcharge Loads: *ES* and *LS*

3.22.6.1 Nature of Surcharge Loads

Often the surface of the backfill in the vicinity of a retaining wall is subjected to various types of vertical loads. The presence of this loading is referred to as *surcharge*, and it induces additional pressure on the back of the wall. Two common examples of surcharge loads are the surface of the backfill behind a bridge abutment that is always subjected to vehicular loading (i.e., vehicular live load) and load due to vehicles on an embankment (e.g., parking area) that is supported by a retaining wall. Surcharge loads can be uniform or concentrated (*ES*), or they may be due to live load (*LS*). Provisions for surcharge loads are covered in AASHTO LRFD Art. 3.11.6.

3.22.6.2 Uniform Surcharge Loads (*ES*)

Lateral earth pressure due to uniform surcharge is calculated as a constant horizontal earth pressure, which is added to the basic earth pressure (at rest or active). This constant earth pressure is calculated from Equation 3.122:

$$\Delta_p = k_s q_s \qquad (3.122)\ \text{[AASHTO LRFD 3.11.6.1-1]}$$

where

Δ_p = constant horizontal pressure due to uniform surcharge (ksf)
k_s = coefficient of earth pressure due to surcharge
= k_a for active earth pressure conditions
= k_o for at-rest conditions
= intermediate values (between k_a and k_o) appropriate for the type of backfill and wall movement

www.EngineeringEBooksPdf.com

3.22.6.3 Point, Line, and Strip Loads (*ES*)

Two cases are considered: (1) wall restrained from movement and (2) flexible walls.

3.22.6.3.1 Walls Restrained from Movement

3.22.6.3.1.1 Surcharge due to Uniformly Loaded Strip The horizontal pressure, Δ_{ph} (ksf), on a wall resulting from a *uniformly loaded strip parallel to the wall* may be calculated from Equation 3.123:

$$\Delta_{ph} = \frac{2p}{\pi}\left[\delta - \sin\delta\cos(\delta + 2\alpha)\right] \qquad (3.123)\ [\text{AASHTO LRFD } 3.11.6.2\text{-}1]$$

where

p = uniform load intensity on strip parallel to wall
α = angle specified in Figure 3.107 (rad.)
δ = angle specified in Figure 3.107 (rad.)

3.22.6.3.1.2 Surcharge due to a Point Load The horizontal pressure Δ_{ph} (ksf) on a wall resulting from a *point load* is calculated from Equation 3.124:

$$\Delta_{ph} = \frac{P}{\pi R^2}\left[\frac{3ZX^2}{R^3} - \frac{R(1-2\nu)}{R+Z}\right] \qquad (3.124)\ [\text{AASHTO LRFD } 3.11.6.2\text{-}2]$$

where

P = point load (kip)
R = radial distance from point of load application to a point on the wall as specified in Figure 3.108 where $R = (X^2 + Y^2 + Z^2)^{0.5}$ (ft)
X = horizontal distance from back of wall to point of load application
Y = horizontal distance from point on the wall under consideration to a plane, which is perpendicular to the wall and passes through the point of load application measured along the wall (ft)
Z = vertical distance from point of load application to elevation of a point on the wall under consideration (ft)
ν = Poisson's ratio

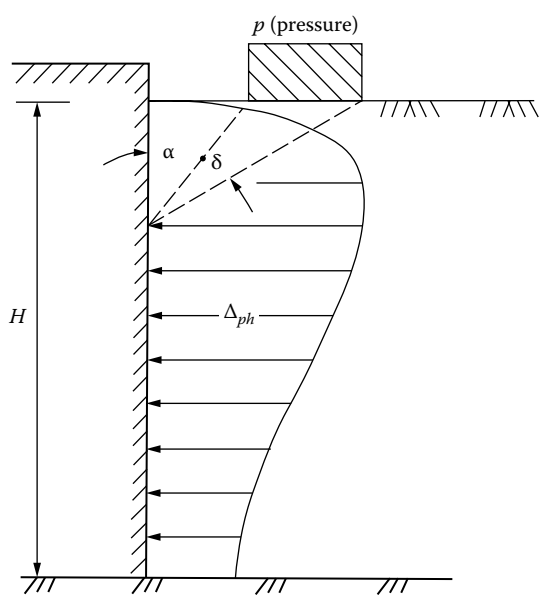

FIGURE 3.107 Horizontal pressure on wall caused by a uniformly loaded strip (AASHTO LRFD 2012 Figure 3.11.6.2-1). (From *AASHTO LRFD Bridge Design Specifications*, Copyright © 2012 by American Association of State Highway and Transportation Officials, Washington, DC. Used by permission.)

www.EngineeringEBooksPdf.com

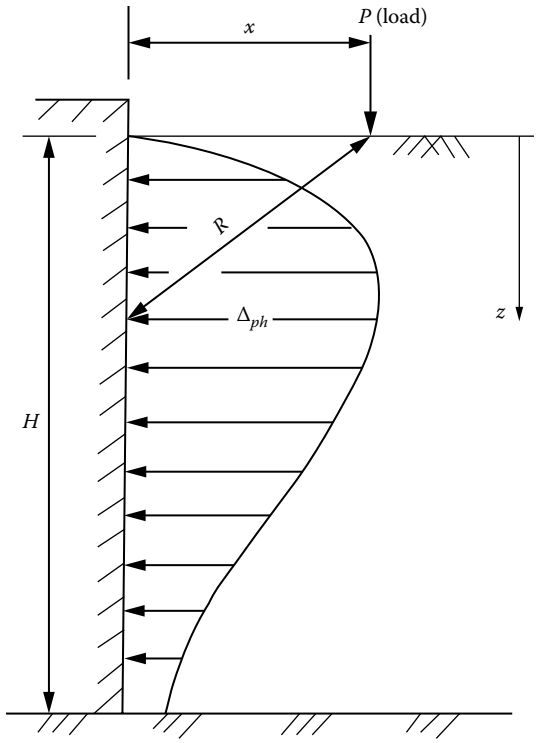

FIGURE 3.108 Horizontal pressure on wall caused by a point load (AASHTO LRFD 2012 Figure 3.11.6.2-2). (From *AASHTO LRFD Bridge Design Specifications*, Copyright © 2012 by American Association of State Highway and Transportation Officials, Washington, DC. Used by permission.)

3.22.6.3.1.3 Surcharge due to an Infinitely Long Line Load Parallel to Wall The horizontal pressure Δ_{ph} (ksf), due to an infinitely long line load parallel to a wall, can be calculated from Equation 3.125:

$$\Delta_{ph} = \frac{4Q}{\pi}\frac{X^2 Z}{R^4} \qquad (3.125)\ [\text{AASHTO LRFD } 3.11.6.2\text{-}3]$$

where Q = load intensity, kip/ft, and all other notations are the same as defined earlier and shown in Figure 3.109.

3.22.6.3.1.4 Surcharge Due to a Finite Long Line Load Perpendicular to Wall The horizontal pressure distribution, Δ_{ph} (ksf), on a wall resulting from a finite line load perpendicular to a wall can be determined from Equation 3.126:

$$\Delta_{ph} = \frac{Q}{\pi Z}\left[\frac{1}{A^3} - \frac{1-2\nu}{A+\dfrac{Z}{X_2}} - \frac{1}{B^3} + \frac{1-2\nu}{B+\dfrac{Z}{X_1}}\right] \qquad (3.126)\ [\text{AASHTO LRFD } 3.11.6.2\text{-}4]$$

where

$$A = \sqrt{1+\left(\frac{Z}{X_2}\right)^2} \qquad (3.127)\ [\text{AASHTO LRFD } 3.11.6.2\text{-}5]$$

www.EngineeringEBooksPdf.com

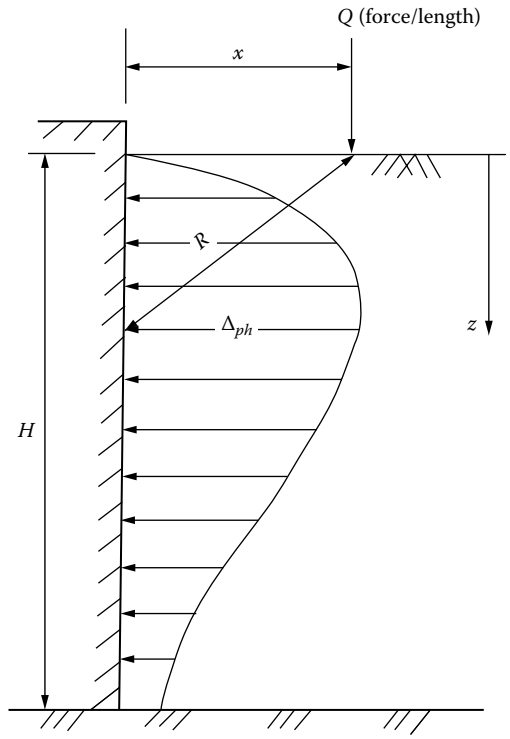

FIGURE 3.109 Horizontal pressure on wall caused by an infinitely long line load parallel to wall (AASHTO LRFD 2012 Figure 3.11.6.2-3). (From *AASHTO LRFD Bridge Design Specifications*, Copyright © 2012 by American Association of State Highway and Transportation Officials, Washington, DC. Used by permission.)

$$B = \sqrt{1 + \left(\frac{Z}{X_1}\right)^2} \qquad (3.128)\ [\text{AASHTO LRFD } 3.11.6.2\text{-}6]$$

where

X_1 = distance (ft) from the back of the wall to the start of the line load as specified in Figure 3.110
X_2 = length of the lone load (ft)
Z = depth (ft) from the ground surface to a point on the wall under consideration
ν = Poisson's ratio

3.22.6.3.2 Flexible Walls: Strip Loads

Figure 3.111 shows a concentrated dead load *supported on a footing*. How is this load dispersed through the underlying foundation soil is subject to uncertainty. For design purposes, this load shall be incorporated into the internal and external stability design by using a simplified distribution of 2 vertical to 1 horizontal (approximately 63.43°) to determine the vertical component of stress with depth within the reinforced soil mass as shown in Figure 3.111. Concentrated horizontal loads *at the top of the wall* shall be distributed within the reinforced soil as shown in Figure 3.112. If concentrated dead loads are located *behind the reinforced mass*, they shall be distributed in the same way as would be done within the reinforced soil mass.

3.22.6.4 Effects of Live Load Surcharge Loads: *LS*

Effects of live load surcharge are to be accounted for in design whenever a vehicular load is expected to act on the surface of the backfill within a distance equal to one-half the wall height behind back

www.EngineeringEBooksPdf.com

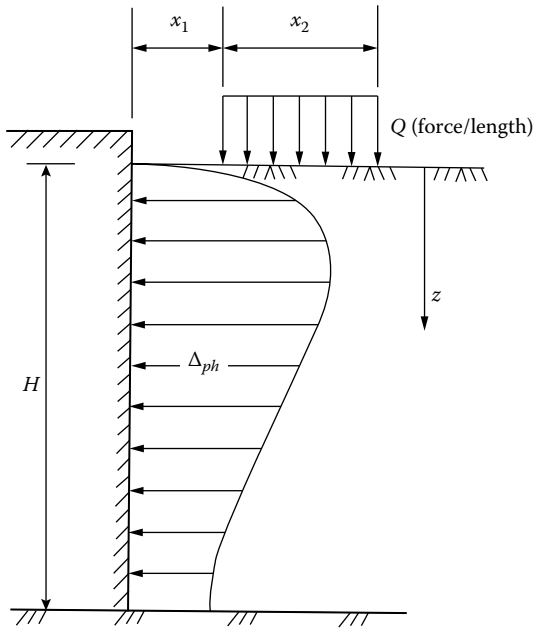

FIGURE 3.110 Horizontal pressure on wall caused by a finite line load perpendicular to the wall (AASHTO LRFD 2012 Figure 3.11.6.2-4). (From *AASHTO LRFD Bridge Design Specifications*, Copyright © 2012 by American Association of State Highway and Transportation Officials, Washington, DC. Used by permission.)

face of the wall. This is always the case for a bridge abutment. When the surcharge live load is for a highway, the intensity of load should be consistent with AASHTO LRFD Art. 3.6.1.2: Design Vehicular Live Load. If the surcharge is due to other than a highway, the required information about the loads should be obtained from the bridge owner.

When live surcharge loads are applied, earth pressures are calculated by substituting the actual load by an equivalent surcharge layer, h_{eq} (AASHTO LRFD Art. 3.11.6.4). The earth pressure due to vehicular live load surcharge can be determined from Equation 3.129:

$$\Delta_p = k\lambda_s h_{eq} \qquad (3.129)\ \text{[AASHTO LRFD 3.11.6.4-1]}$$

where

Δ_p = constant horizontal earth pressure due to live load surcharge
γ_s = unit weight of soil
k = coefficient of lateral earth pressure
= k_o for walls that do not deflect or move
= k_a for walls that deflect or move sufficiently to reach minimum active conditions
h_{eq} = equivalent height of soil for vehicular load

Figure 3.113 shows earth pressure distribution from uniform surcharge load close to the wall subjected to active earth pressure conditions.

Magnitudes of surcharge loads are often specified by applicable design codes/specifications. For highway bridge abutments and retaining walls, AASHTO LRFD specifies equivalent heights of soil for vehicular loading on abutments (perpendicular to traffic) and retaining walls (parallel to traffic) as listed in Table 3.51. In both cases, the wall height is taken as the distance between the surface of the backfill and bottom of the footing along the pressure surface being considered.

www.EngineeringEBooksPdf.com

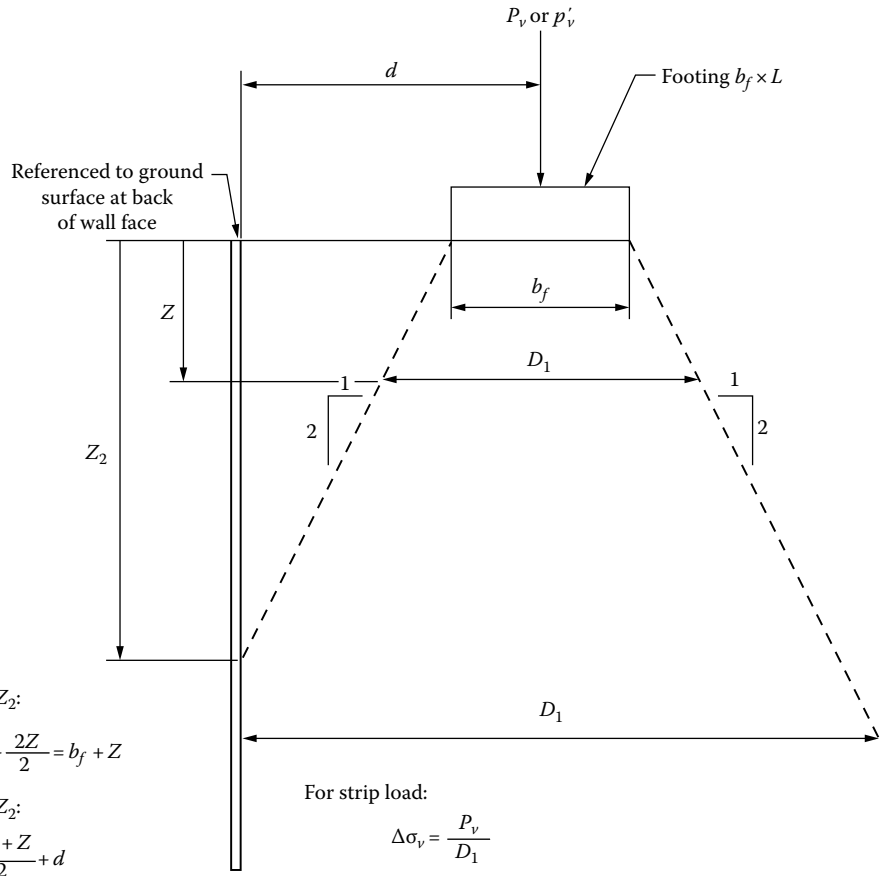

For $Z \le Z_2$:

$$D_1 = b_f + \frac{2Z}{2} = b_f + Z$$

For $Z > Z_2$:

$$D_1 = \frac{b_f + Z}{2} + d$$

For strip load:

$$\Delta\sigma_v = \frac{P_v}{D_1}$$

For isolated footing load:

$$\Delta\sigma_v = \frac{P'_v}{D_1(L+Z)}$$

For point load:

$$\Delta\sigma_v = \frac{P'_v}{D_1^2} \text{ with } b_f = 0$$

where

D_1 = effective width of applied load at any depth, calculated as shown earlier

b_f = width of applied load. For footings that are eccentrically loaded (e.g., bridge abutment footings), set b_f equal to the equivalent footing width B' by reducing it by $2e'$, where e' = eccentricity of the footing load (i.e., $b_f - 2e'$)

L = Length of footing

P_v = Load per linear foot of strip footing

P'_v = Load on isolated rectangular footing or point load

Z_2 = Depth where effective width intersects back of wall face = $2d - b_f$

d = Distance between the centroid of the concentrated vertical load and the back of the wall face

Assume the increased vertical stress due to the surcharge load has no influence on stresses used to evaluate internal stability if the surcharge load is located behind the reinforced soil mass. For external stability, assume the surcharge has no influence if it is located outside the active zone behind the wall.

FIGURE 3.111 Distribution of stress from concentrated vertical load P_v for internal and external stability (AASHTO LRFD 2012 Figure 3.11.6.3-1). (From *AASHTO LRFD Bridge Design Specifications*, Copyright © 2012 by American Association of State Highway and Transportation Officials, Washington, DC. Used by permission.)

www.EngineeringEBooksPdf.com

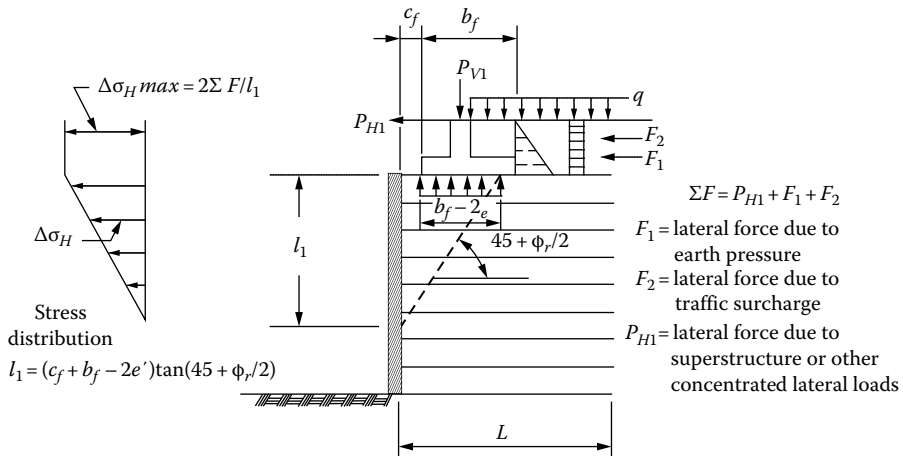

e' = eccentricity of load on footing (see Figure 11.10.10.1–1 for an example of how to calculate this)

(a)

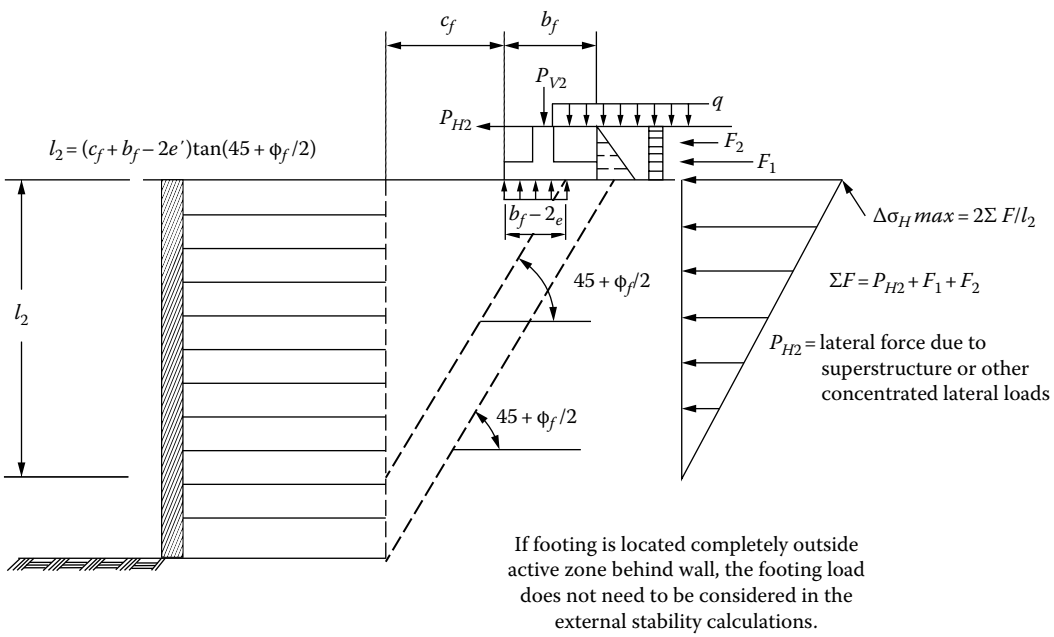

(b)

FIGURE 3.112 Distribution of stress from concentrated horizontal loads (AASHTO LRFD 2012 Figure 3.11.6.3-2). (a) Distribution of stress for internal stability calculations. (b) Distribution of stress for external stability calculations. (From *AASHTO LRFD Bridge Design Specifications*, Copyright © 2012 by American Association of State Highway and Transportation Officials, Washington, DC. Used by permission.)

In the case of retaining walls, the earth pressure due to live load surcharge depends the distance from the wall back face to the edge of the traffic. Note that the magnitude of h_{eq} is greater for an abutment than for a retaining wall due to the proximity and closer spacing of wheel loads to the back of an abutment compared to a wall. (Readers should note that these equivalent heights are greater than previous versions of AASHTO Specifications that required h_{eq} = 2 ft regardless of

www.EngineeringEBooksPdf.com

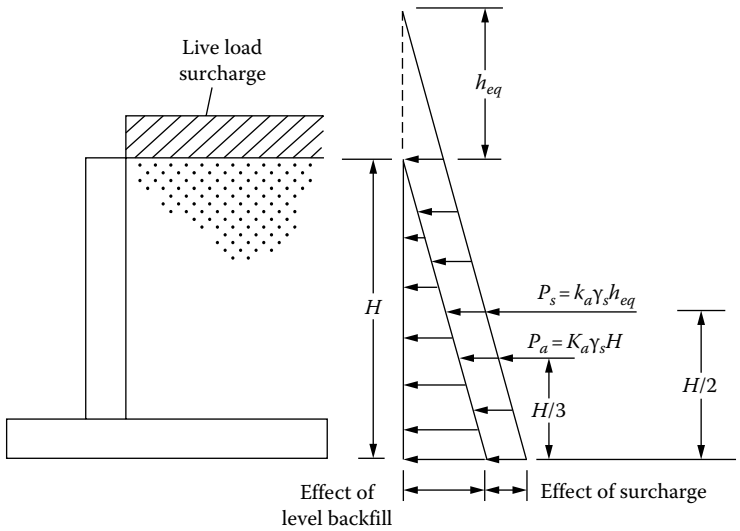

FIGURE 3.113 Earth pressure distribution due to live load surcharge in conjunction of active earth pressure. The resultant of earth pressure due to surcharge acts at $H/2$ from the bottom of the footing; the resultant of active earth pressure act at $H/3$ from the bottom of the footing.

TABLE 3.51
Equivalent Height of Soil, h_{eq}, for Vehicular Loading on Highway Bridge Abutments and Retaining Walls

	Equivalent Height of Soil, h_{eq} (ft)		
		Retaining Walls	
		Distance from Wall Back Face to Edge of Traffic	
Abutment or Retaining Wall Height	Abutment	0.0 ft	1.0 ft or Further
5.0	4.0	5.0	2.0
10.0	3.0	3.5	2.0
≥20 ft	2.0	2.0	2.0

Source: Adapted from *AASHTO LRFD Bridge Design Specifications*, Copyright © 2012 by American Association of State Highway and Transportation Officials, Washington, DC. Used by permission.

the heights [as specified in AASHTO Standard 2000 Art. 3.20.3]. The reason for this discrepancy is the fact that these lower values of h_{eq} corresponded to H10 truck rather than HS 20 truck [Peck et al. 1974]).

Another factor akin to surcharge that may cause increased lateral pressure is the effect of compacting backfill in confined areas behind retraining walls. As a result of backfill compaction in the vicinity of the wall, lateral pressures greater than active or at-rest values may develop. Such possibilities should be properly accounted for in design.

www.EngineeringEBooksPdf.com

3.22.6.5 Downdrag: *DD*

The term *downdrag* is used to describe negative friction on piles or shafts used for foundations. It has long been recognized that when end-bearing piles are situated in a consolidating soil mass, a *downward* force (hence the term *negative friction*) is induced in the pile because of the downward movement of the soil relative to the pile.

Provisions for accounting for evaluation of downdrag are specified in AASHTO LRFD Art. 3.11.8. Possible development of downdrag on piles or shafts is required when the following conditions are present:

1. Sites are underlain by compressible materials such as clays, silts, or organic soils.
2. Fill will be or has recently been placed adjacent to the piles or shafts. Such is frequently the case for bridge approach fills.
3. The groundwater is substantially lowered.
4. Liquefaction of loose sandy soil can occur.

Downdrag forces do not affect design of superstructures; as such, they are not discussed further in this chapter.

3.22.7 Seismic Earth Pressure

In seismic events, the backfill behind a retaining wall responds dynamically, resulting in additional lateral pressure called seismic earth pressure. Several studies have been carried out to study the response of cantilever retaining walls. These studies may be classified into two groups:

1. Elastic analysis in which the wall is considered to be fixed against both deflection and rotation at the base and the backfill is presumed to respond as a linearly elastic or viscoelastic material.
2. Limit state analyses in which the wall is considered to displace sufficiently at the base mobilize the full shearing strength of the backfill.

The most frequently used methods for estimating seismic active and passive pressures are based on the pseudostatic approach developed in 1920s by Mononabe (Mononabe and Matsuo 1929) and Okabe (1924) commonly known as the Mononabe–Okabe (M-O) analysis. It is based on an extension of the Coulomb sliding wedge theory taking into account horizontal and vertical inertia forces acting on the soil. However, the effects of wall inertia are neglected in the analysis. A detailed discussion on this method has been provided by Seed and Whitman (1970) and summarized by Elms and Martin (1979). The M-O analysis or methodology is now a part of AASHTO LRFD Specification, which is summarized as follows. The following assumptions are made in the M-O analysis:

1. The abutment is free to move sufficiently so that the soil strength will be mobilized. If the abutment is rigidly fixed and unable to move, the soil forces will be very much higher than those predicted by the M-O analysis.
2. The backfill is cohesionless, with a friction angle of ϕ.
3. The backfill is unsaturated and thus, not subject to liquefaction.

Further discussion of seismic earth pressure is not presented in this book. Readers should refer to AAHTO LRFD Section 11 Art. 11.6.5 for details of seismic earth pressures on abutments and retaining walls.

www.EngineeringEBooksPdf.com

3.23 FORCE EFFECTS DUE TO SUPERIMPOSED DEFORMATIONS: *TU*, *TG*, *SH*, *CR*, *SE*, AND *PS*

3.23.1 General

In addition to the permanent and transient loads described in the preceding sections, there are forces due to superimposed deformations that act on superstructures. These forces are as follows:

1. Force effect due to uniform temperature, *TU*
2. Force effect due to temperature gradient, *TG*
3. Force effect due to shrinkage, *SH*
4. Force effect due to creep, *CR*
5. Force effect due to settlement, *SE*
6. Secondary forces from posttensioning, *PS*

3.23.2 Temperature-Induced Forces

Temperature-induced forces are environmental loads that are generated by solar radiation and act on all structures. Effects of seasonal as well as daily temperature changes are well known—they cause thermal changes (expansion and contraction) in structural members, which must be accounted for in design in order to avoid distress.

Broadly speaking, thermal effects in a bridge superstructure can be three dimensional: (1) along the length, (2) along the width, and (3) along the depth. The superstructure is unrestrained along the width, so thermal movement in the width direction is not of any concern. The two components of thermal effects of consequence are (1) the uniform change (i.e., the entire superstructure undergoing the same temperature change longitudinally [discussed in Section 3.23.3]) and (2) temperature gradient (i.e., gradually reduced temperatures through the depth of the superstructure), which occurs because the top of the superstructure is exposed to direct radiation from the sun while the bottom is not (discussed in Section 3.23.6).

3.23.3 Temperature-Induced Forces due to Uniform Temperature

Unidirectional displacements due to change in temperature (expansion or contraction) is the most commonly observed thermal phenomenon. Thermal movement, ΔL, due to uniform temperature change can be predicted by the thermal-displacement relationship:

$$\Delta L = \alpha L(\Delta T) \tag{3.130}$$

where
α = coefficient of thermal expansion
L = length of the element or member
ΔT = range of change in temperature

If movement is restrained, the thermal deformation given by Equation 3.130 would induce an axial force P, which can be calculated from Hooke's law as given by Equation 3.131:

$$P = \frac{(\Delta L)AE}{L} \tag{3.131}$$

where
A = cross-sectional area of member
E = modulus of elasticity

www.EngineeringEBooksPdf.com

Note that in Equation 3.131, the quantity $\Delta L/L = \varepsilon$ (strain), so Equation 3.131 can be rewritten as follows:

$$P = \varepsilon AE \tag{3.132}$$

Equation 3.132 can be used to calculate thermally induced stress, σ:

$$\sigma = \frac{P}{A} = \frac{(\Delta L)E}{L} \tag{3.133}$$

Thermal movements form the basis for the design of expansion joints and bearings. Examples 3.32 and 3.33 illustrate the significance of the thermally induced forces and their importance in design.

Example 3.32

A 10 ft long steel rod ($\alpha = 6.5 \times 10^{-6}$/°F) having an area of 1 in.^{2} is subjected to a temperature variation of +50°F from the ambient temperature. Calculate the stress in the rod if it is restrained from movement.

Solution

From Equation 3.130, the change in length of the rod is calculated as

$$\Delta L = \alpha L(\Delta T) = (6.5 \times 10^{-6})(10 \times 12)(50) = 0.039 \text{ in.}$$

The thermal stress σ can be calculated from Equation 3.133:

$$\sigma = \frac{(\Delta L)E}{L} = \frac{(0.039)(29{,}000)}{(10 \times 12)} = 9.425 \text{ ksi}$$

Discussion: A small movement of 0.039 in. (or 1 mm) might appear to be insignificant at first glance. But if restrained, the temperature change would subject the rod to a stress of 9.425 kip/in.^{2} (or 18.85 percent of the yield strength 50 kip/in.^{2}) in addition to stresses due to other loads on the member, which would be disastrous if not accounted for in the design.

Example 3.33

A highway bridge spanning 160 ft consists of concrete deck supported over four built-up steel girders spaced at 13 ft on center. The cross-sectional area of each girder is 106 in.^{2} Calculate the movement of the girder that must be accommodated at the expansion joint at the support. Assume a temperature variation of 50°F from the ambient conditions.

Solution

The change in length of the girder is calculated from Equation 3.130:

$$\Delta L = \alpha L(\Delta T) = (6.5 \times 10^{-6})(160 \times 12)(50) = 0.624 \text{ in.}$$

In practice, specifications may require the design thermal movement to be taken as 1½ times the calculated value as it is not practical to install the bearing pads at the ambient temperatures assumed in design. This would require that a girder movement of 1 in. (0.624 × 1.5) must be accommodated at the expansion joint. Restraining this 1 in. movement at the support would cause an axial stress σ in the girder, which is calculated from Equation 3.133:

$$\sigma = \frac{(\Delta L)E}{L} = \frac{(1.0)(29{,}000)}{(160 \times 12)} = 15.1 \text{ ksi}$$

This 15.1 kip/in.^{2} stress would be in addition to the tensile stress in the girder; the combined stress may very well be greater than the yield stress. Clearly, if this movement is not accommodated, the result would be disastrous.

www.EngineeringEBooksPdf.com

TABLE 3.52
***Procedure A* Temperature Ranges (AASHTO LRFD Table 3.12.2.1-1)**

Climate	Steel or Aluminum	Concrete	Wood
Moderate	0°F–120°F	10°F–80°F	10°F–75°F
Cold	−30°F–120°F	0°F–80°F	0°F–75°F

Source: From *AASHTO LRFD Bridge Design Specifications*, Copyright © 2012 by American Association of State Highway and Transportation Officials, Washington, DC. Used by permission.

3.23.4 AASHTO LRFD Provisions for Design Unidirectional Thermal Movements

Although temperature changes in a bridge do not occur uniformly, it is common practice to design bridges for a uniform temperature change. To accommodate thermal movements associated with a uniform temperature change in design, two procedures are specified (Art. 3.12.2): (1) *Procedure A* and (2) *Procedure B*.

1. *Procedure A*: Procedure A is a simplified procedure that specifies Equation 3.134 (a modified form of Equation 3.130) to calculate thermal movements:

$$\Delta L = \alpha L(T_{MaxDesign} - T_{MinDesign}) \tag{3.134}$$

   where L = expansion length (in.)

$$T_{MaxDesign} - T_{MinDesign} = \Delta T$$

   The range of temperature specified in Equation 3.134 is shown in Table 3.52. The difference between the extended lower or upper boundary and the base construction temperature assumed in design should be used to calculate the range of temperature ΔT ($=T_{MaxDesign} - T_{MinDesign}$).
2. *Procedure B*: This procedure requires determination of maximum and minimum design temperatures from $T_{MaxDesign}$ and $T_{MinDesign}$ contour maps of the United States. Separate maps are provided for (a) concrete girder bridges with concrete decks (Figures 3.114 and 3.115) and (b) steel girder bridges with concrete decks (Figures 3.116 and 3.117). It is a calibrated procedure that was developed on the basis of a report by Roeder (2002). However, it does not cover all types of bridges. The temperatures provided in Figures 3.114 through 3.117 are extreme bridge design temperatures. They are based on statistical data for an average history of 70 years with a minimum of 60-year data for locations throughout the United States. The design values of temperatures for locations between the contours should be determined by linear interpolation. Alternatively, it is permissible to use the largest adjacent contour to define $T_{MaxDesign}$ and the smallest adjacent contour to define $T_{MinDesign}$. Both the maximum and minimum design temperatures should be noted on the drawings for girders, expansion joints, and bearings.

3.23.5 Forces Induced by Temperature Gradient

3.23.5.1 Nature of Heat Flow Problem: *Thermal Gradient*

When a body is subjected to heat or cold, temperature variations occur throughout the body in all directions. All bodies, such as bridges, are exposed to heat from solar radiation. As a rule, a structure's outer surface that is exposed to direct sunshine is at a higher temperature than its inner portion that is not directly exposed to sunshine. In the case of bridge superstructure, the top surface is at a higher

www.EngineeringEBooksPdf.com

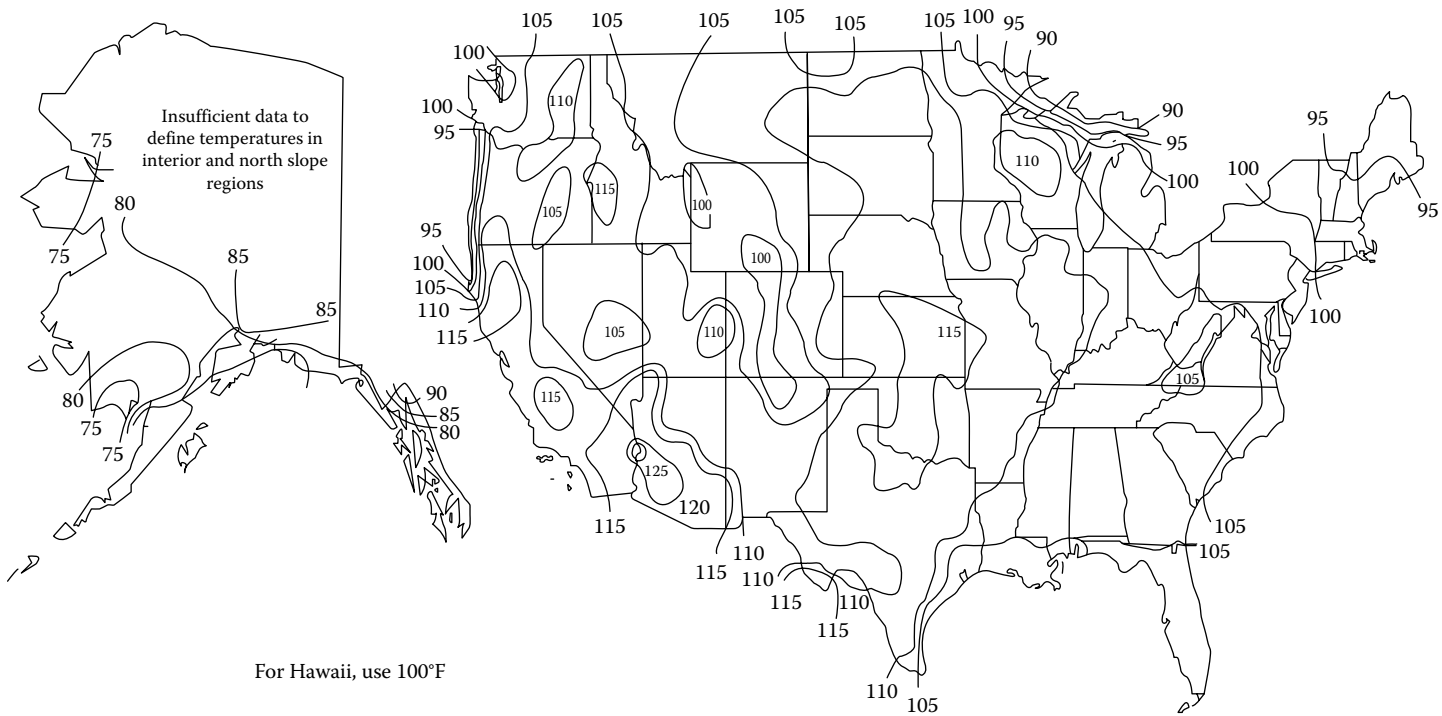

FIGURE 3.114 Contour map of the United Stated for $T_{MaxDesign}$ for concrete girder bridges with concrete decks (AASHTO LRFD 2012 Figure 3.12.2.2-1). (From *AASHTO LRFD Bridge Design Specifications*, Copyright © 2012 by American Association of State Highway and Transportation Officials, Washington, DC. Used by permission.)

www.EngineeringEBooksPdf.com

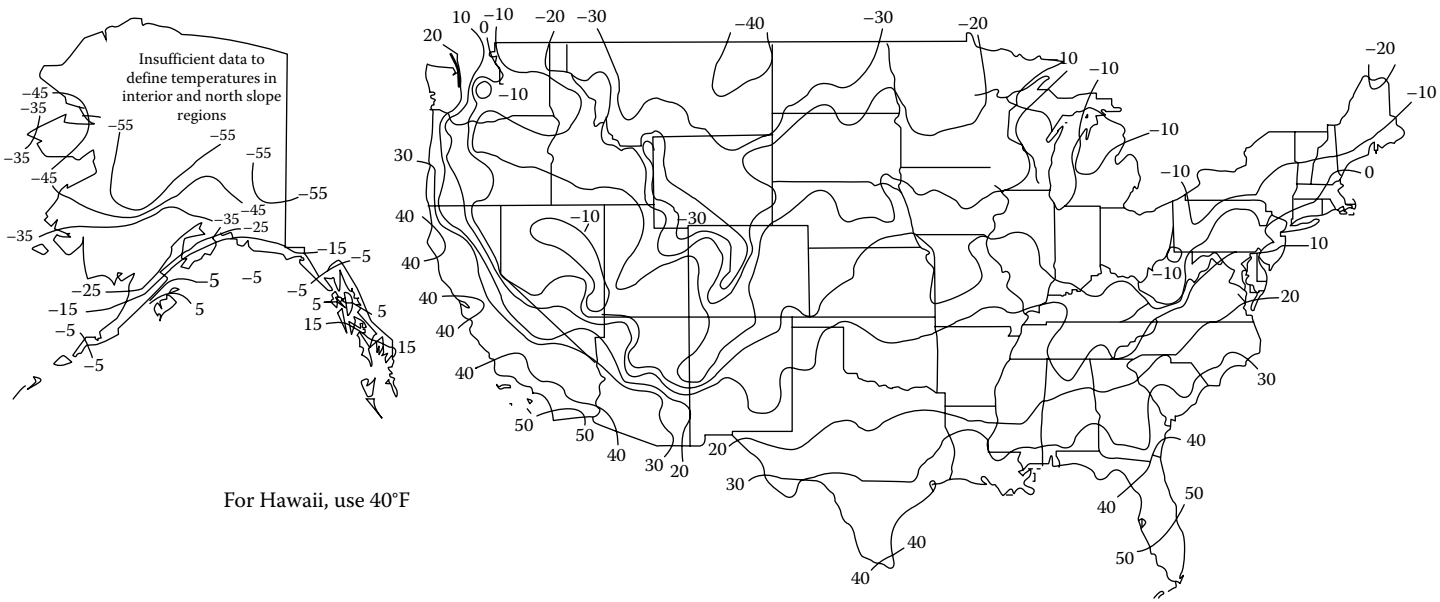

FIGURE 3.115 Contour map of the United Stated for $T_{MinDesign}$ for concrete girder bridges with concrete decks (AASHTO LRFD 2012 Figure 3.12.2.2-2). (From *AASHTO LRFD Bridge Design Specifications*, Copyright © 2012 by American Association of State Highway and Transportation Officials, Washington, DC. Used by permission.

www.EngineeringEBooksPdf.com

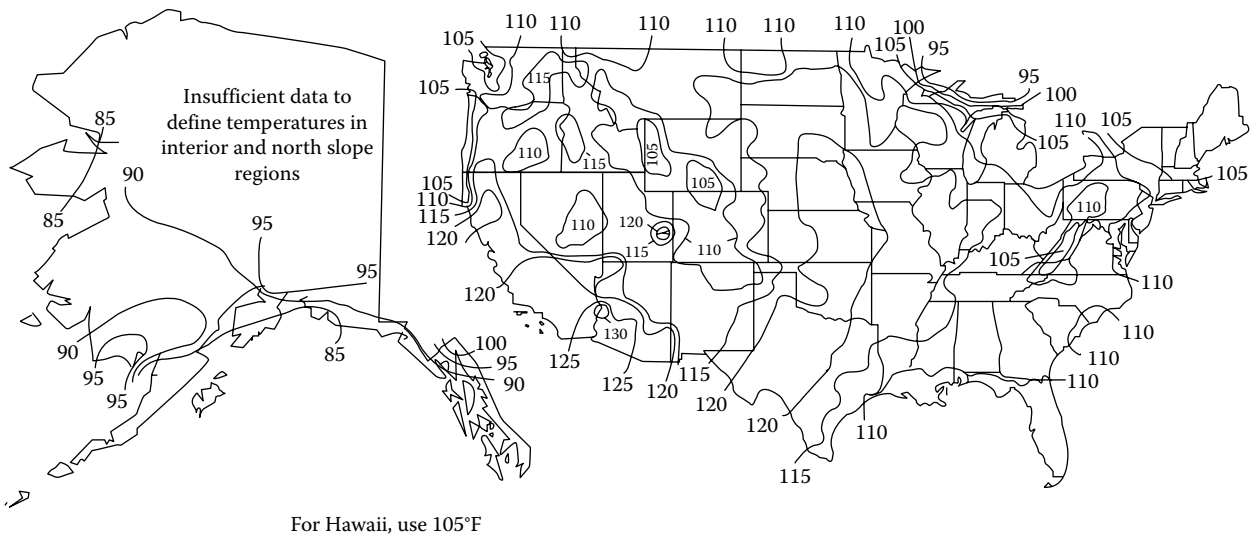

FIGURE 3.116 Contour map of the United Stated for $T_{MaxDesign}$ for steel girder bridges with concrete decks (AASHTO LRFD 2012 Figure 3.12.2.2-4). (From *AASHTO LRFD Bridge Design Specifications*, Copyright © 2012 by American Association of State Highway and Transportation Officials, Washington, DC. Used by permission.)

www.EngineeringEBooksPdf.com

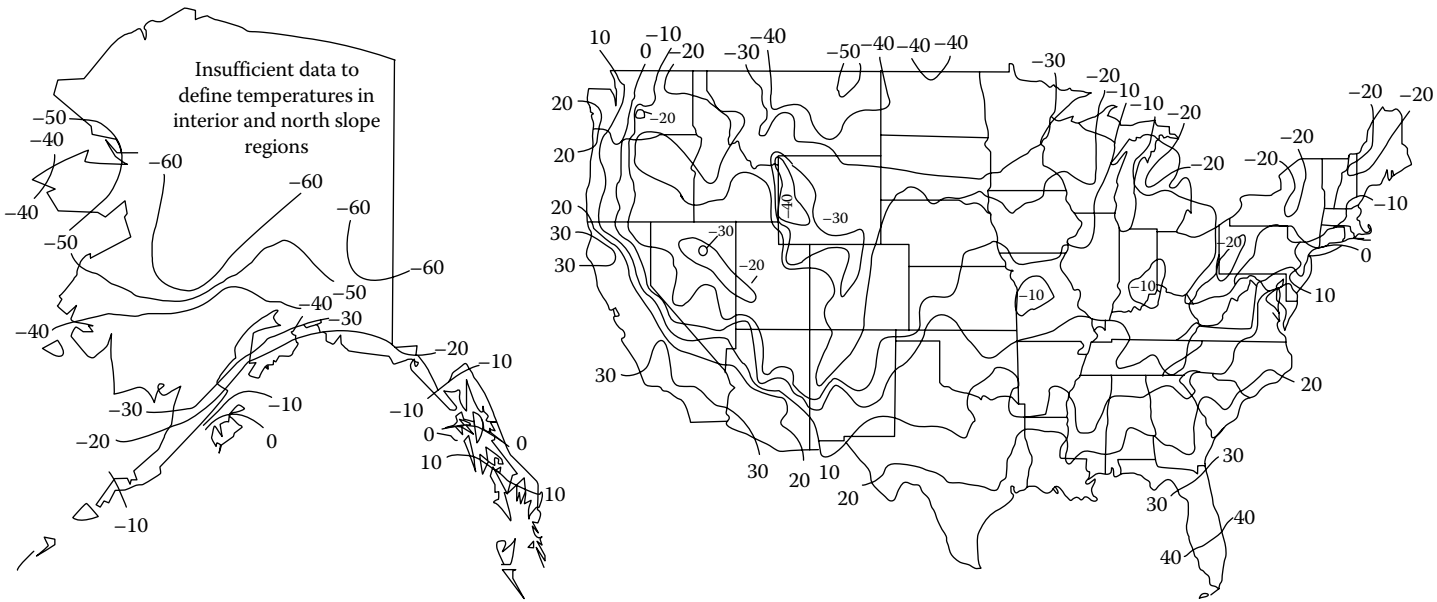

FIGURE 3.117 Contour map of the United Stated for $T_{MinDesign}$ for steel girder bridges with concrete decks (AASHTO LRFD 2012 Figure 3.12.2.2-4). (From *AASHTO LRFD Bridge Design Specifications*, Copyright © 2012 by American Association of State Highway and Transportation Officials, Washington, DC. Used by permission.)

www.EngineeringEBooksPdf.com

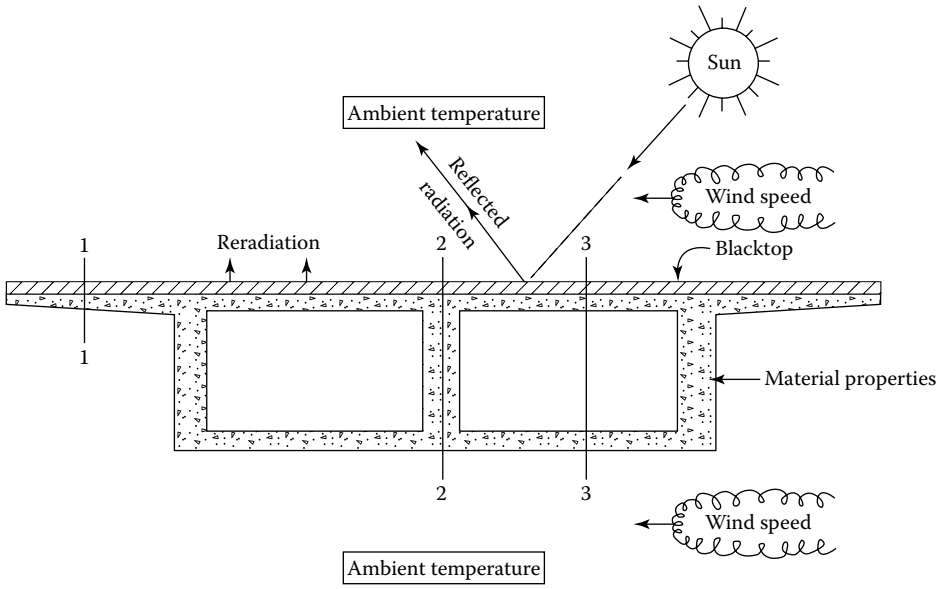

FIGURE 3.118 Factors affecting thermal response of superstructures (Priestley 1976). (Reproduced with permission from American Concrete Institute, Farmington Hills, MI.)

temperature than the inner portion of its body. This is referred to as *temperature gradient*. Because of the temperature gradient, the exterior surfaces of the superstructure (top and bottom) experience different thermal strains and, hence, different thermal stresses. These are internal stresses that need to be accounted for in design. By convention, a positive gradient is defined as a condition in which the temperature of the top deck is higher than the temperature of the webs. A negative gradient exists when the temperature of the web is warmer than that of the top deck.

Sunshine temperature change caused by solar radiation is a very complex phenomenon because of the numerous influencing factors. These include direct solar radiation, ground reflection, air temperature changes, wind speed and geographic latitude, orientation, and the terrain conditions where bridges are stationed. Therefore, as a rule, the surface and inner temperature changes of the superstructure due to sunshine temperature change follow a complex random function that is not amenable to a direct solution. Figure 3.118 shows schematically factors affecting the thermal response of a typical two-cell concrete girder bridge superstructure (Priestley 1978).

Historically, the thermoelastic analysis of problem of heat flow was first presented by Fourier (1811) in the form of a three-dimensional equation. It was improved upon by Duhamel by including the effects of deformations produced by temperature changes (not considered by Fourier). Duhamel was the first to suggest that total stresses in a body could be obtained by superposition (Timoshenko 1953). The governing equation for the flow of heat in a solid, assumed linear, is expressed as a three-dimensional equation given by Equation 3.135:

$$\frac{\partial}{\partial x}\left(k_x \frac{\partial T}{\partial x}\right)+\frac{\partial}{\partial y}\left(k_y \frac{\partial T}{\partial y}\right)+\frac{\partial}{\partial z}\left(k_z \frac{\partial T}{\partial z}\right)=c\rho\frac{\partial T}{\delta t} \tag{3.135}$$

where

x, y, z = Cartesian coordinates
t = time
c = coefficient of specific heat of the medium
ρ = density of the medium
k_x, k_y, k_z = thermal conductivity corresponding to the x, y, and z Cartesian coordinate axes, respectively

www.EngineeringEBooksPdf.com

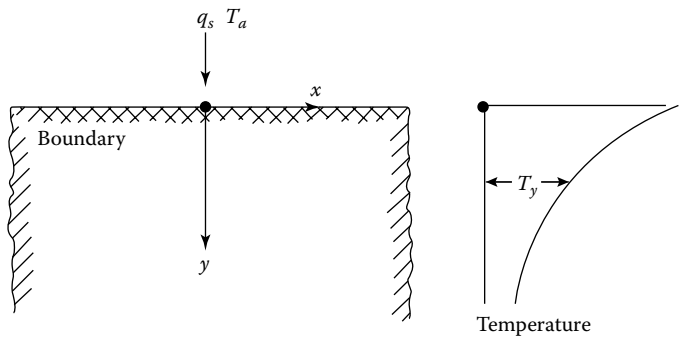

FIGURE 3.119 Coordinate definition for transient heat flow analysis (Priestley 1978). (Reproduced with permission from American Concrete Institute, Farmington Hills, MI.)

Equation 3.135 is the Fourier thermal conduction differential equation. For a bridge subjected to solar radiation, it is assumed that there are no thermal variations along the longitudinal direction, z. For the material-independent properties, with $k/c\rho$ (in Equation 3.135) replaced with K, the diffusivity of the medium, Equation 3.135 is reduced to a two-dimensional heat flow problem as defined in Figure 3.119 and expressed by Equation 3.136:

$$\frac{\partial^2 T}{\partial x^2} + \frac{\partial^2 T}{\partial y^2} = \frac{1}{K}\frac{\partial T}{\partial t} \tag{3.136}$$

with the following boundary conditions:

1. *Heat flow*: Heat flow input at specific points of a body, that is, the boundary heat flow, q_s, as expressed by Equation 3.137:

$$q_s = k_n \frac{\partial T}{\partial n} \tag{3.137}$$

   where k_n is the median thermal conductivity in a direction normal to the surface n (i.e., along the depth of the superstructure)
2. *Convection*: Due to convection flow to and from the surrounding air as a result of temperature differences between the bridge surface and the air:

$$q_s = h\left[T_a - T_o(t)\right] \tag{3.138}$$

   where
   T_a = environmental temperature
   T_o = solid boundary temperature, that is, the surface temperature of the body in contact with air
   h = boundary heat transfer coefficient or convection coefficient (a variable mainly dependent on the speed of the air across the boundary)
   n = direction normal to the boundary

The two boundary conditions expressed by Equations 3.137 and 3.138 can be jointly written as given by Equation 3.139:

$$k_n \frac{\partial T}{\partial n} + q + h\left(T_a - T_o\right) = 0 \tag{3.139}$$

www.EngineeringEBooksPdf.com

Research has indicated that for most bridges, the transverse heat flow is insignificant. Consequently, Equation 3.139 reduces to a one-dimensional equation that can be expressed as given by Equation 3.140:

$$\frac{k_n}{\rho c}\frac{\partial^2\theta}{\partial y^2} = \frac{\partial\theta}{\partial t} \tag{3.140}$$

Further discussion of this topic can be found in the literature (Priestley 1978, Imbsen et al. 1985, Ho and Liu 1989); a summary can be found in Taly (1998). Research in this field continues (Cheng and Zhang 2011).

3.23.5.2 Effect of Nonlinear Temperature Variation

As a result of solar radiation, the temperature rise along the length of bridge superstructure is fairly uniform but along the cross section, it is generally nonlinear. Figure 3.120 shows schematically distribution of temperature due to solar radiation across the depth of a bridge girder. Characteristically, the temperature rise is maximum at the surface of the girder, reduces nonlinearly along the depth of the cross section, and increases slightly toward the bottom fibers of the cross section.

Analytically, a bridge girder may be determinate (e.g., simply supported) or indeterminate (e.g., continuous). In a statically determinate beam of homogeneous material (such as in Figure 3.120a), no stresses are produced when the temperature variation is linear because the thermal expansion occurs freely, without restraint. But when the temperature variation along the depth of the member is nonlinear, each fiber being attached to the adjacent fibers is restrained from undergoing full expansion, which induces stresses. In a statically determinate structure, these induced stresses must be self-equilibrating. The *self-equilibrating stresses* caused by nonlinear temperature variation over the cross section of statically determinate frame are sometimes referred to as *eigenstresses*. The following discussion due to Ghali et al. (2009).

The self-equilibrating stresses in a simple beam referred to in the preceding paragraph can be determined from Hooke's law. If each fiber were free to expand, the hypothetical strain that would occur in each fiber can be expressed in the form of Equation 3.141:

$$\varepsilon_f = \alpha T \tag{3.141}$$

where

ε_f = strain in fiber
α = coefficient of thermal expansion
$T = T(y)$ = temperature rise in any fiber at a distance y below the centroid O

If the expansion given by Equation 3.141 is artificially prevented, the stress in the restrained condition can be also determined from Hooke's law as given by Equation 3.142 (Ghali et al. 2009):

$$\sigma_r = -E\varepsilon_f \tag{3.142}$$

where

σ_r = stress in the restrained condition
E = modulus of elasticity

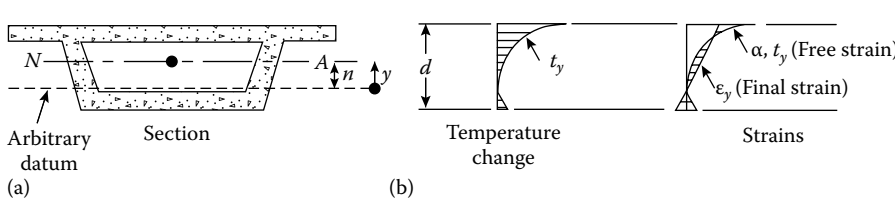

FIGURE 3.120 Nonlinear temperature variation along the depth of a bridge girder. (a) Girder cross section. (b) Variation in temperature and strains with depth of girder.

www.EngineeringEBooksPdf.com

The resultant of σ_r can be represented by a normal force N (positive when tensile) at the centroid O and a moment M (considered positive when producing tension in the bottom fibers; the corresponding curvature is positive) about the horizontal axis at O given by Equations 3.143 and 3.144, respectively:

$$N = \int \sigma_r \, da \tag{3.143}$$

$$M = \int \sigma_r y \, da \tag{3.144}$$

To eliminate the artificial restraint, apply force N and moment M in the opposite directions. The corresponding changes in the strain and the curvature are given, respectively, by Equations 3.145 and 3.146:

$$\varepsilon_0 = -\frac{N}{EA} \tag{3.145}$$

$$\psi = -\frac{M}{EI} \tag{3.146}$$

where

A = area of cross section of the girder
I = second moment of area about the horizontal axis through centroid O
ψ = curvature = $1/R$
R = radius of curvature

The corresponding stress and strain of any fiber are obtained, respectively, from Equations 3.147 and 3.148:

$$\varepsilon = \varepsilon_o + y\psi \tag{3.147}$$

$$\Delta\sigma = E(\varepsilon_o + y\psi) \tag{3.148}$$

The sum of σ_r and $\Delta\sigma$ gives the self-equilibrating stress due to temperature, which is obtained by combining Equations 3.141, 3.142, and 3.148 and expressed as given by Equation 3.149:

$$\sigma_s = E(-\alpha T + \varepsilon_o + y\psi) \tag{3.149}$$

The changes in axial strain and curvature due to temperature can be derived from the aforementioned equations and expressed as follows:

$$\varepsilon_o = \frac{\alpha}{A} \int T(y) \, dA \tag{3.150}$$

$$\psi = \frac{\alpha}{I} \int T(y) y \, dA \tag{3.151}$$

Further discussion can be found in Ghali et al. (2009).

3.23.5.3 AASHTO LRFD Provisions for Thermal Gradient Analysis

In 1985, the NCHRP published Report 276, *Thermal Effects in Concrete Bridge Superstructures* (Imbsen et al. 1985), which provided guidelines for the consideration of thermal gradients in

www.EngineeringEBooksPdf.com

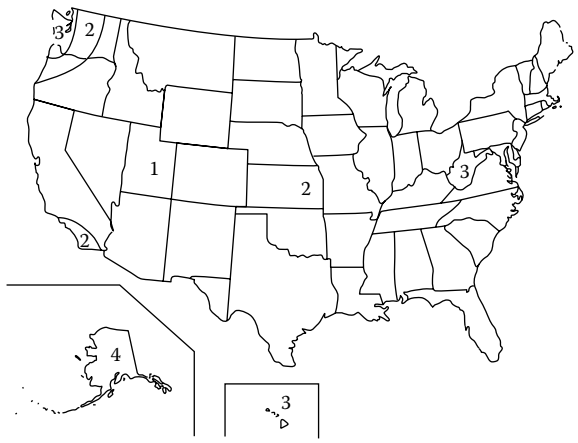

FIGURE 3.121 Solar radiation zones of the United States (AASHTO LRFD 2012 Figure 3.12.3-1). (From *AASHTO LRFD Bridge Design Specifications*, Copyright © 2012 by American Association of State Highway and Transportation Officials, Washington, DC. Used by permission.)

the design of concrete bridges. This report formed the basis for provisions for considering the effects of thermal gradient in highway bridges, first incorporated in the 1989 AASHTO Standard Specifications (AASHTO 1989).

AASHTO LRFD Art. 3.12.3 specifies procedures for accounting for the effects of temperature gradient in design of superstructures. Essentially, these provisions are due to Imbsen et al. (1985), which were developed for concrete structures. The addition for steel structures is patterned after the Australian bridge specifications (AUSTROADS 1992). For design convenience, the entire United States is divided into four solar radiation zones (Figure 3.121). Table 3.53 shows the basis for vertical temperature gradients. For thermal gradient analysis, the following procedure is followed for selecting temperatures:

1. Positive temperature values for various solar radiation zones shall be taken for various deck surface conditions as shown in Table 3.53.
2. Negative temperature values shall be obtained by multiplying the tabulated values by (a) −0.3 for plain concrete and (b) −0.2 for decks with asphalt overlay.
3. Vertical temperature gradient in concrete and steel superstructures with concrete decks may be taken as a multilinear gradient shown in Figure 3.122.

Temperature gradient in bridge superstructure causes axial extension, flexural deformation, and internal stresses. AASHTO LRFD Art. 4.6.6 (Commentary C4.6.6) provides a methodology for the

TABLE 3.53
Basis for Temperature Gradients (AASHTO LRFD 2012 Table 3.12.3-1)

Zone	T_1 (°F)	T_2 (°F)
1	54	14
2	46	12
3	41	11
4	38	9

Source: From *AASHTO LRFD Bridge Design Specifications*, Copyright © 2012 by American Association of State Highway and Transportation Officials, Washington, DC. Used by permission.

www.EngineeringEBooksPdf.com

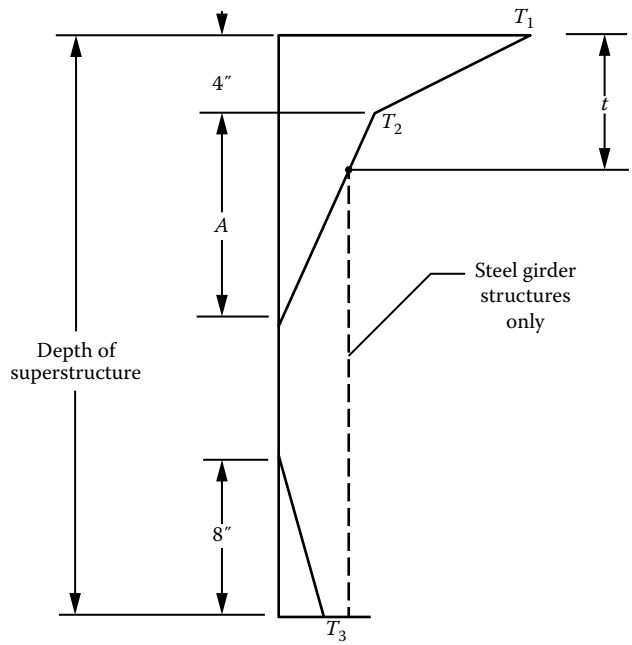

Dimension A (AASHTO LRFD 2012 Art. 3.12.3)

Superstructure type	Depth of superstructure	Dimension A, in.
Concrete	16 in. or more	12 in.
Concrete	Shallower than 12 in.	4 in. less than actual depth
Steel	Any depth	12 in., t = depth of concrete deck
Note: Temperature T_3 shall be taken as 0.0°F, unless a site-specific study is made to determine appropriate value, but it shall not exceed 5°F.		

FIGURE 3.122 Positive vertical temperature gradient in concrete and steel superstructures (AASHTO LRFD 2012 Figure 3.12.3-2). (From *AASHTO LRFD Bridge Design Specifications*, Copyright © 2012 by American Association of State Highway and Transportation Officials, Washington, DC. Used by permission.)

determination of response of a structure to temperature gradient. This response can be divided into three effects as follows:

1. *Axial expansion*: This deformation is due to uniform component of the temperature distribution that should be considered simultaneously with that discussed in Section 3.23.4. The combined effect may be calculated from Equation 3.152:

$$T_{UG} = \frac{1}{A_c} \iint T_G \, dwdz \qquad (3.152)\ [AC4.6.6\text{-}1]$$

where
T_{UG} = temperature averaged across the cross section
T_G = temperature gradient (Δ°F)
w = width of the element cross section (in.)
z = vertical distance from the center of gravity of cross section (in.)

The thermal strain due to combined temperature change ($T_{UG} + T_U$) can be calculated from Equation 3.130, which can be expressed as given by Equation 3.153:

$$\varepsilon = \alpha(T_{UG} + T_U) \qquad (3.153)$$

www.EngineeringEBooksPdf.com

2. *Flexural deformation*: Assuming that plane sections remain plane (a fundamental assumption in the theory of flexure), a curvature is imposed on the superstructure to accommodate the linearly variable component of the temperature gradient higher at the top and decreasing downwardly. The rotation per unit length corresponding to this curvature, ϕ, may be determined from Equation 3.154:

$$\phi = \frac{\alpha}{I_c} \iint T_G z \, dwdz = \frac{1}{R} \tag{3.154}$$

where R = radius of curvature.

When a superstructure is unrestrained, that is, simply supported or cantilevered, it can deform freely so no external force effects are developed due to this superimposed deformation. An expanded discussion with examples can be found in the literature (Ghali et al. 2009, Barker and Puckett 2013).

3. *Internal stresses*: Internal stresses in addition to those corresponding to restrained axial expansion and/or rotation may be calculated from Equation 3.155:

$$\sigma_E = E[\alpha T_G - \alpha T_{UG} - \phi z] \qquad (3.155)\ [\text{AC4.6.6-6}]$$

In Equations 3.152 through 3.155, the following notations are used:

T_G = temperature gradient (Δ°F)
T_{UG} = temperature averaged across the cross section (°F)
T_u = uniform specified temperature

3.24 MISCELLANEOUS FORCES FOR DESIGN CONSIDERATIONS

In addition to the loads and forces described in the preceding sections, the following forces are indirect forces that need to be considered in design where appropriate (AASHTO LRFD Art. 3.12.4–3.12.7):

1. *Differential shrinkage*: Differential shrinkage strains between concretes of different age and composition and between concrete and steel or wood should be accounted for in design. Relevant provisions for considerations are specified in AASHTO LRFD Section 5.
2. *Creep*: This is a time-dependent phenomenon that affects concrete and wood structures. Relevant provisions for determination of effects of creep are given in AASHTO LRFD Section 5.
3. *Settlement*: Force effects due to extreme values of differential settlements among substructures and within individual substructure units should be considered in design according to the provisions of Art. 10.7.2.3.
4. *Secondary forces from posttensioning*: These forces result from applying posttensioning forces on a continuous structure, which produces reactions at the supports and internal forces (collectively called secondary forces). These should be accounted for in design where appropriate.

3.25 FRICTION FORCES: *FR*

Frictional forces occur whenever sliding surfaces are encountered. Examples include design of sliding bearings at supports and pretensioning and posttensioning operations for prestressed concrete structures. Frictional forces should be established on the basis of extreme values of the friction coefficients between the sliding surfaces (AASHTO LRFD Art. 3.13). Values of low and high frictions may be obtained from the textbooks. Where necessary, these values may be established from tests.

www.EngineeringEBooksPdf.com

3.A APPENDIX

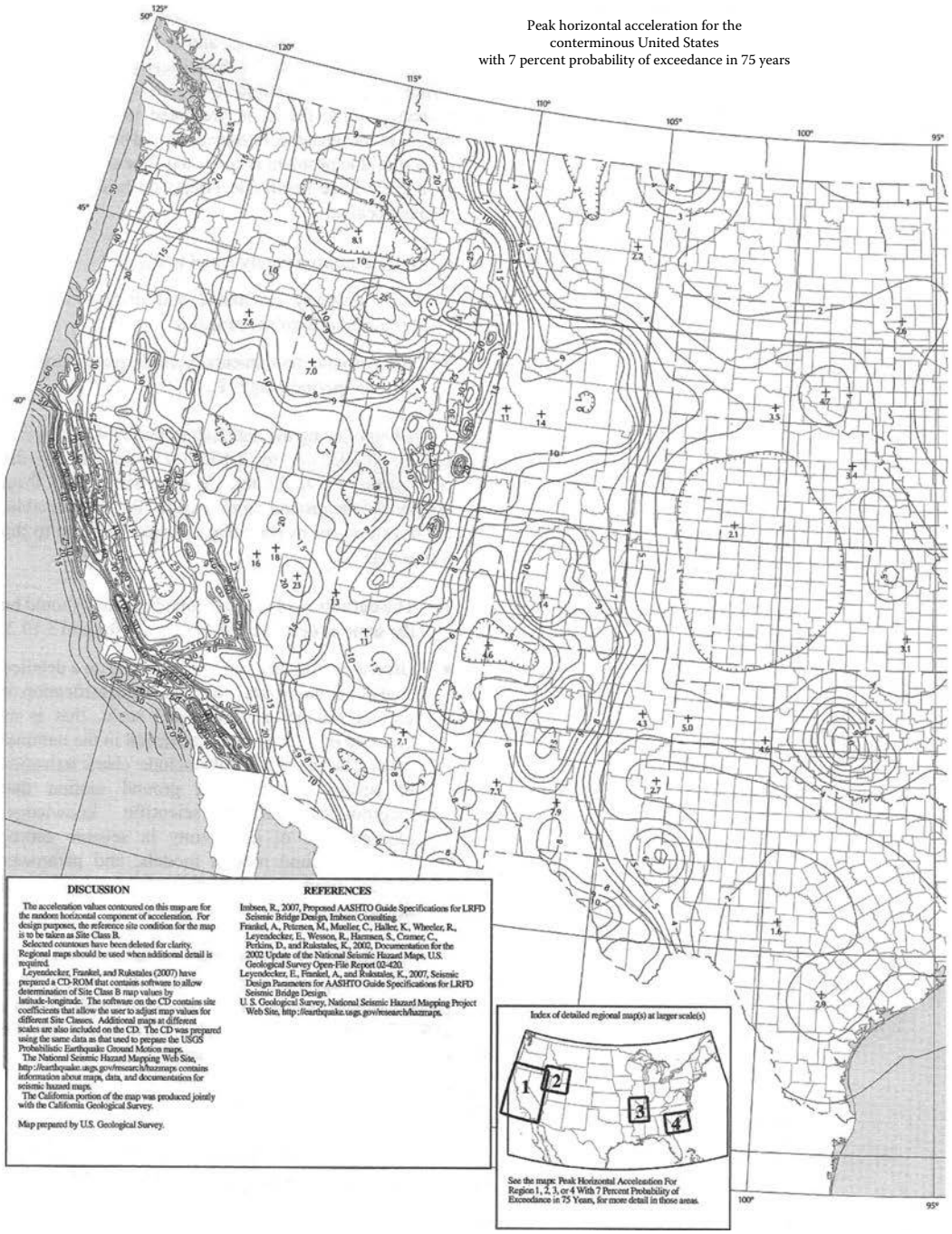

FIGURE 3.A.1 Horizontal PGA for the conterminous United States (*PGA*) with seven percent probability of exceedance in 75 years (approximately 1000-year return period). AASHTO LRFD 2012 Figure 3.10.2.1-1. (*Continued*)

www.EngineeringEBooksPdf.com

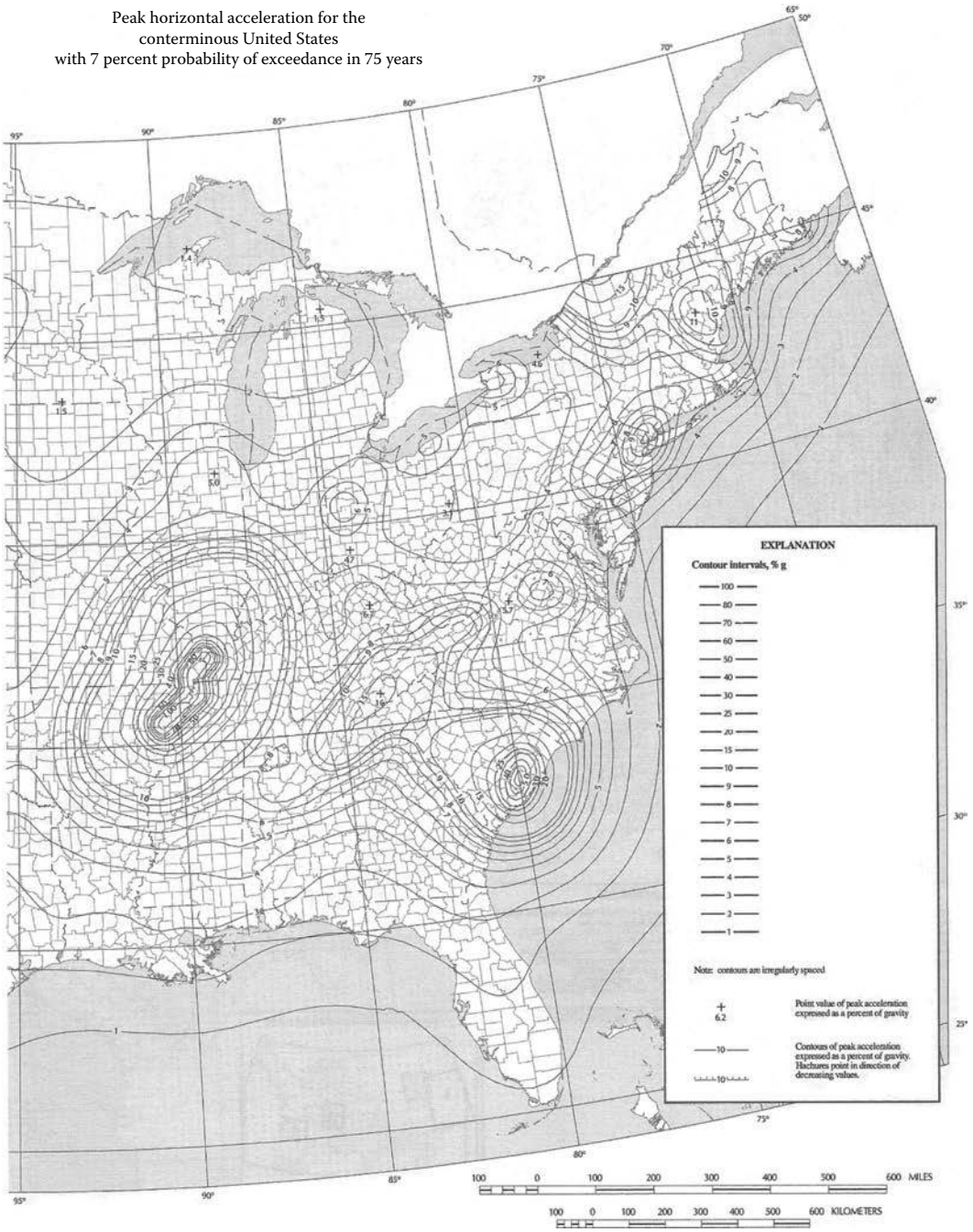

FIGURE 3.A.1 (*Continued*) Horizontal PGA for the conterminous United States (*PGA*) with seven percent probability of exceedance in 75 years (approximately 1000-year return period). AASHTO LRFD 2012 Figure 3.10.2.1-1. (From *AASHTO LRFD Bridge Design Specifications*, Copyright © 2012 by American Association of State Highway and Transportation Officials, Washington, DC. Used by permission.)

www.EngineeringEBooksPdf.com

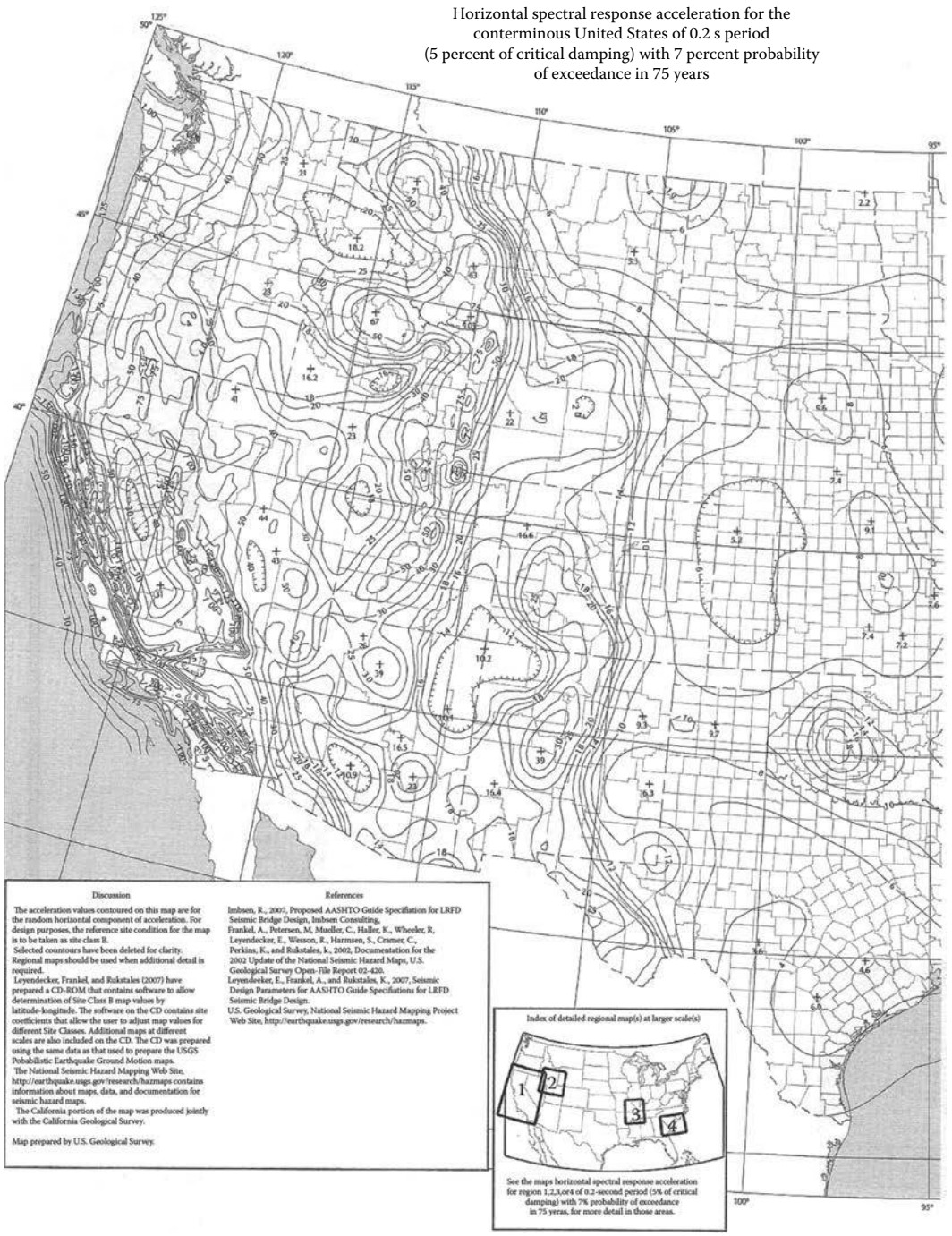

FIGURE 3.A.2 Horizontal response spectral acceleration coefficient for the conterminous United States at period of 0.2 s (S_S) with seven percent probability of exceedance in 75 years (approximately 1000-year return period). AASHTO LRFD 2012 Figure 3.10.2.1-2. (*Continued*)

www.EngineeringEBooksPdf.com

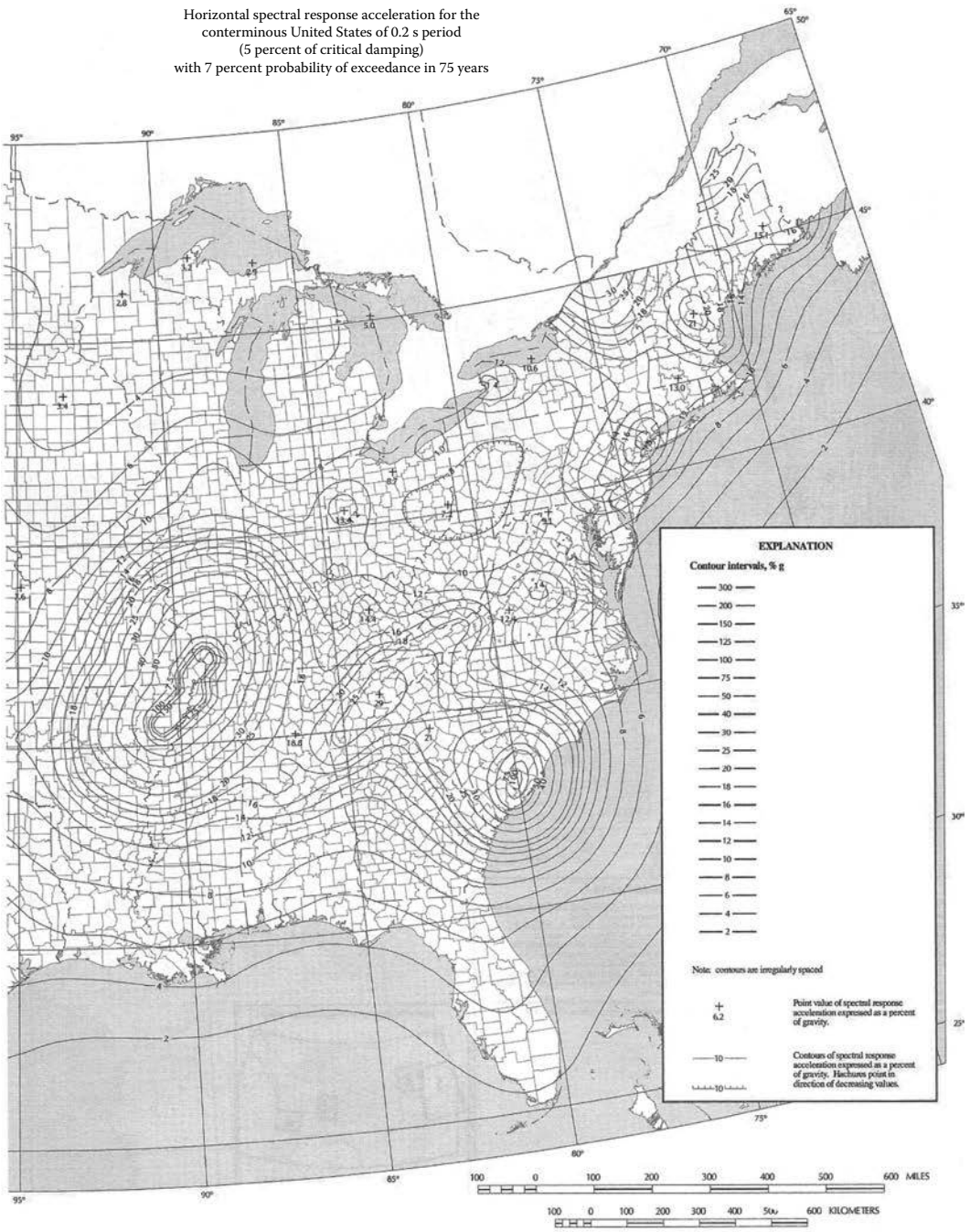

FIGURE 3.A.2 (*Continued*) Horizontal response spectral acceleration coefficient for the conterminous United States at period of 0.2 s (S_S) with seven percent probability of exceedance in 75 years (approximately 1000-year return period). AASHTO LRFD 2012 Figure 3.10.2.1-2. (From *AASHTO LRFD Bridge Design Specifications*, Copyright © 2012 by American Association of State Highway and Transportation Officials, Washington, DC. Used by permission.)

www.EngineeringEBooksPdf.com

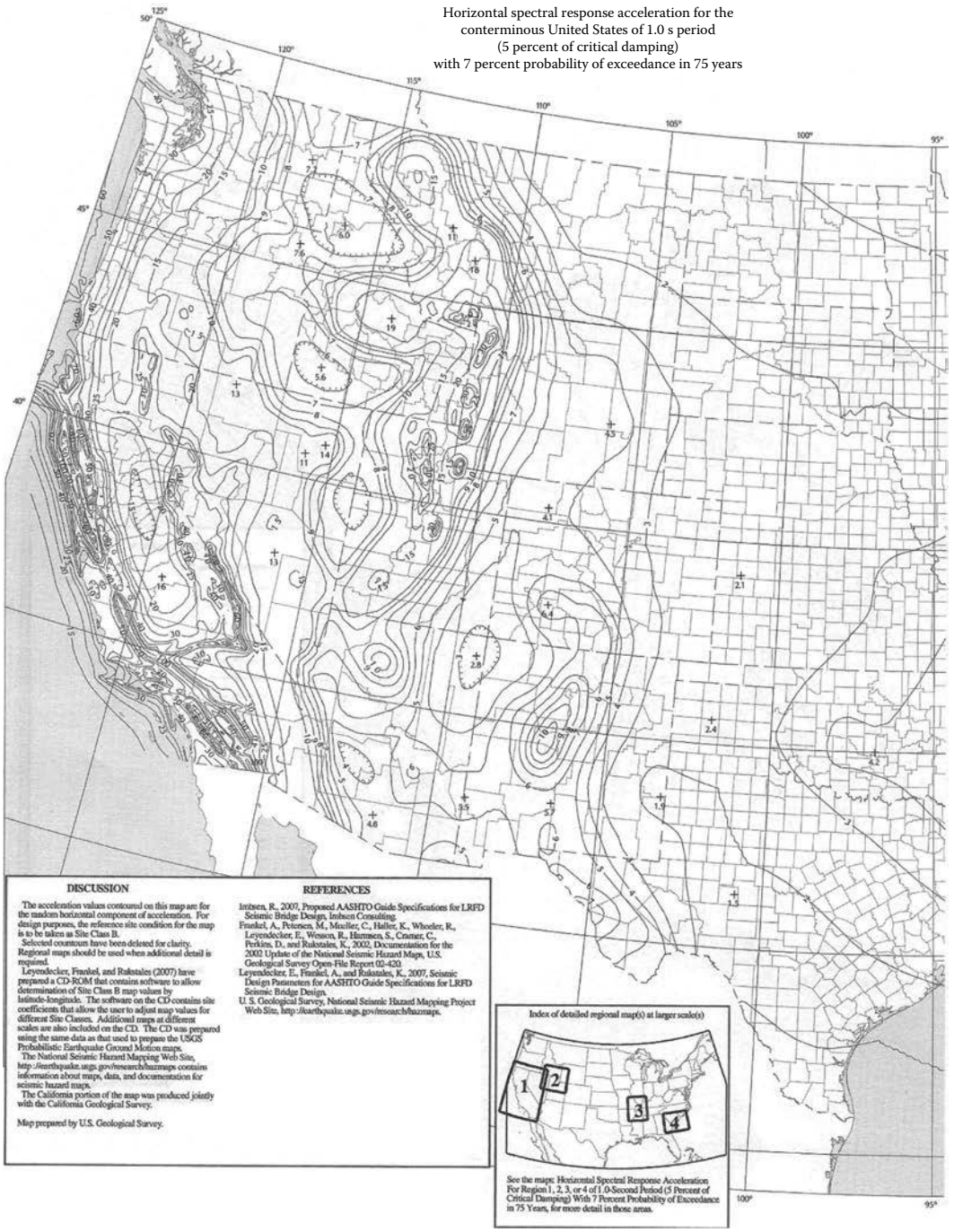

FIGURE 3.A.3 Horizontal response spectral acceleration coefficient for the conterminous United States at period of 1.0 s (S_1) with seven percent probability of exceedance in 75 years (approximately 1000-year return period). AASHTO LRFD 2012 Figure 3.10.2.1-3. (*Continued*)

www.EngineeringEBooksPdf.com

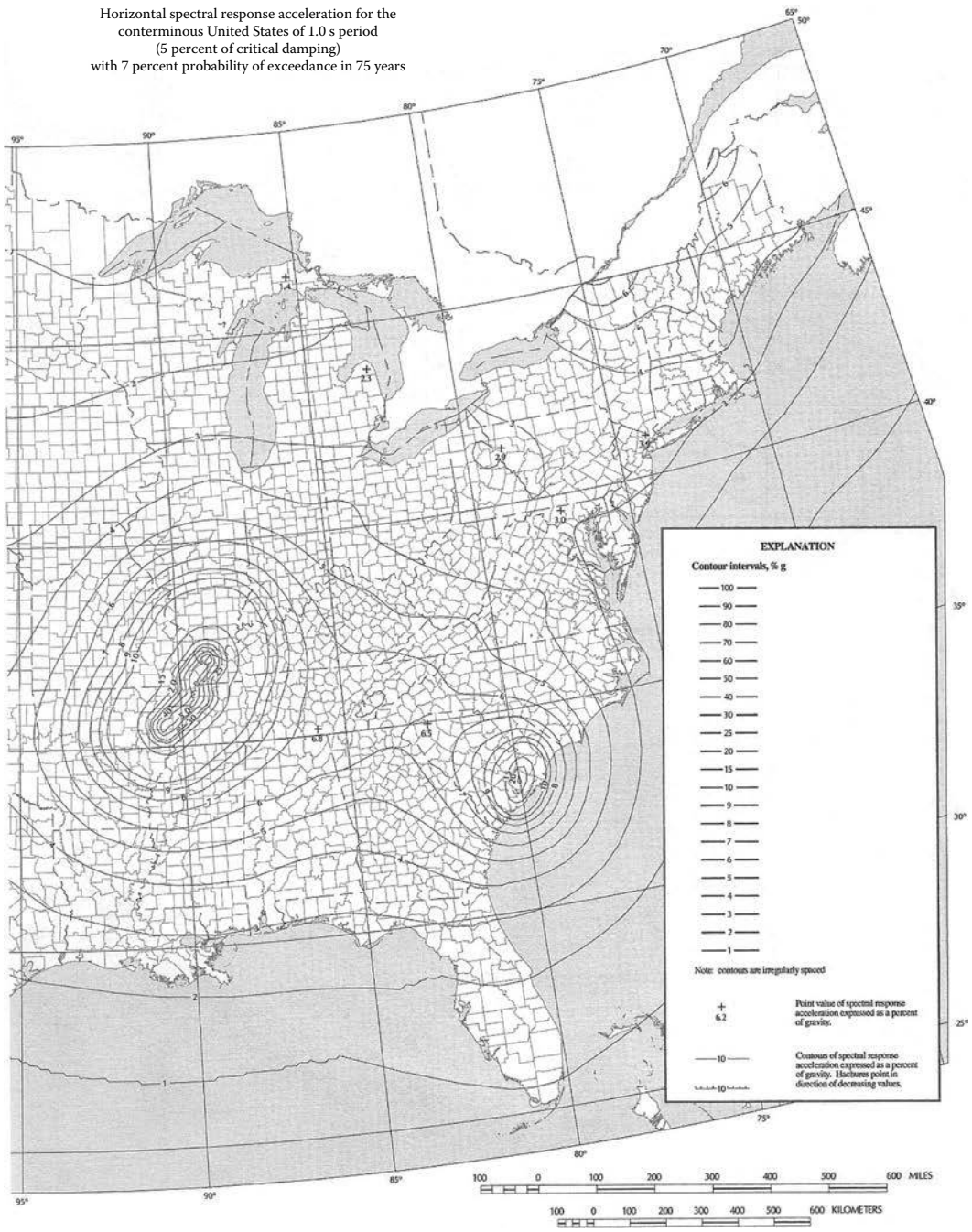

FIGURE 3.A.3 (*Continued*) Horizontal response spectral acceleration coefficient for the conterminous United States at period of 1.0 s (S_1) with seven percent probability of exceedance in 75 years (approximately 1000-year return period). AASHTO LRFD 2012 Figure 3.10.2.1-3. (From *AASHTO LRFD Bridge Design Specifications*, Copyright © 2012 by American Association of State Highway and Transportation Officials, Washington, DC. Used by permission.)

www.EngineeringEBooksPdf.com

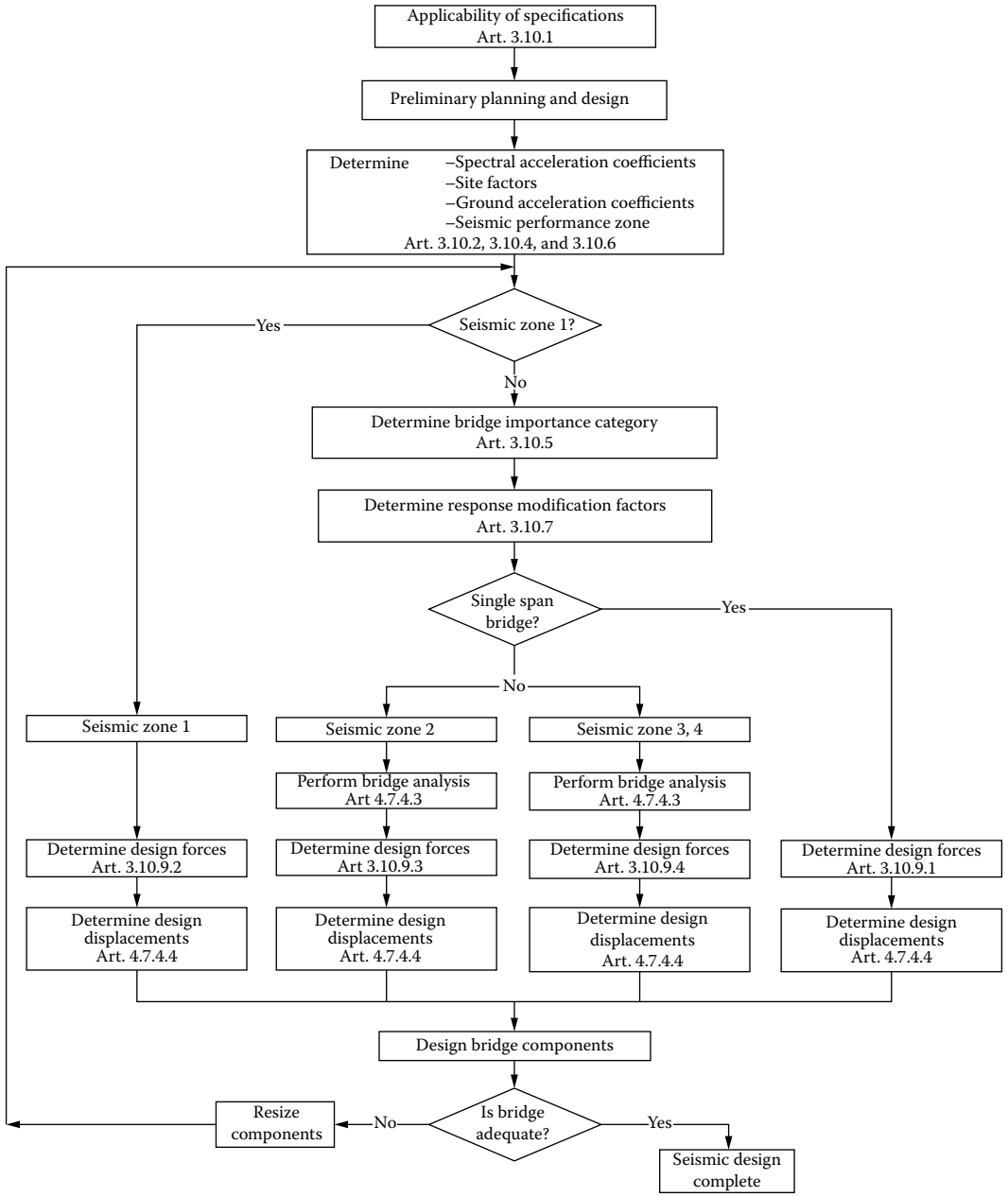

FIGURE 3.A.4 Seismic design procedure flowchart. (From *AASHTO LRFD Bridge Design Specifications*, Copyright © 2012 by American Association of State Highway and Transportation Officials, Washington, DC. Used by permission.)

www.EngineeringEBooksPdf.com

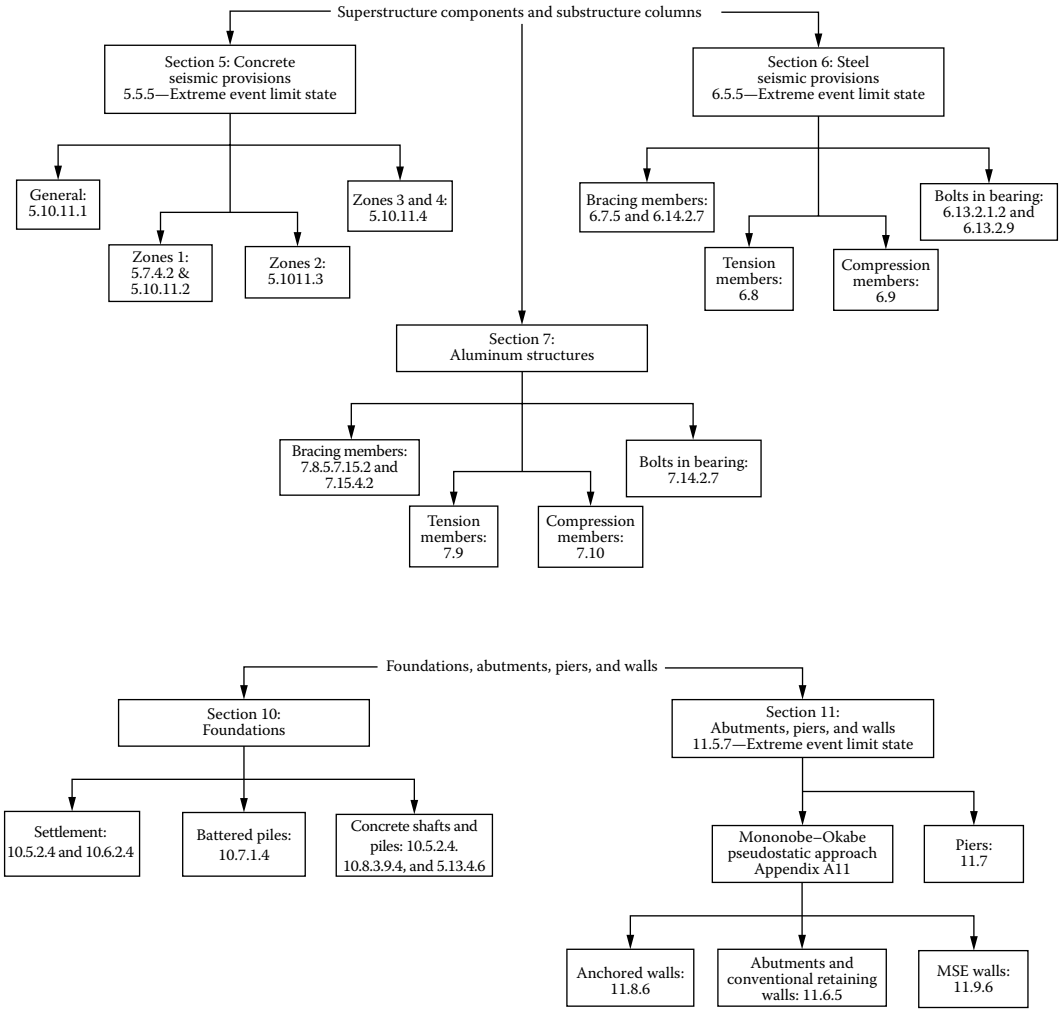

FIGURE 3.A.5 Seismic detailing and foundation design procedure flow chart. (From *AASHTO LRFD Bridge Design Specifications*, Copyright © 2012 by American Association of State Highway and Transportation Officials, Washington, DC. Used by permission.)

REFERENCES

AASHO. 1949. *Standard Specifications for Highway Bridges*, American Association of State Highways and Transportation Officials (AASHTO), Washington, DC.

AASHO. 1969. *Standard Specifications for Highway Bridges*, American Association of State Highways and Transportation Officials (AASHTO), Washington, DC, p. 26.

AASHTO. 1989. *Standard Specifications for Highway Bridges*, American Association of State Highways and Transportation Officials (AASHTO), Washington, DC.

AASHTO. 1991. *Guide for Maximum Dimensions and Weights of Motor Vehicles and for the Operation of Nondivisible Load Oversize and Overweight Vehicles, Revised 1991*, American Association of State Highways and Transportation Officials (AASHTO), Washington, DC.

AASHTO. 1992. *Standard Specifications for Highway Bridges*, American Association of State Highways and Transportation Officials (AASHTO), Washington, DC.

AASHTO. 2002. *Standard Specifications for Highway Bridges*, 17th ed., American Association of State Highways and Transportation Officials (AASHTO), Washington, DC.

www.EngineeringEBooksPdf.com

AASHTO. 2009a. *LRFD Guide Specifications for Design of Pedestrian Bridges*, American Association of State Highways and Transportation Officials (AASHTO), Washington, DC.

AASHTO. 2009b. *Guide Specifications for LRFD Seismic Design*, American Association of State Highways and Transportation Officials (AASHTO), Washington, DC.

AASHTO. 2011. *The Manual for Bridge Evaluation*, 2nd ed., American Association of State Highway and Transportation Officials (AASHTO), Washington, DC.

AASHTO. 2012. *AASHTO LRFD Bridge Design Specifications*, American Association of State Highways and Transportation Officials (AASHTO), Washington, DC.

AISC. 1989. *Moments, Shears and Reactions for Continuous Highway Bridges*, American Institute of Steel Construction, Chicago, IL.

AISC. 2011. *Steel Construction Manual*, 14th ed., American Institute of Steel Construction, Chicago, IL.

Aluri, S., Jinka, C., and GangaRao, H.V.S. 2005. "Dynamic response of three fiber reinforced polymer composite bridges", *Journal of Bridge Engineering, ASCE*, Vol. 10, No. 6, 722–730.

ANSI. 1982. *Minimum Design Loads for Buildings and Other Structures: ANSI A58.1*, American National Standard Institute, New York.

ASCE. 1958. Deflection limitations of bridges—Progress report of the ASCE committee on deflection limitations of bridges, *Proceedings, ASCE*, 84 (ST3), paper no. 1633, 1631-1–1633-19.

ASCE. 1961. Task committee on wind forces, "Wind Forces on Structures—Final Report," *Transactions, ASCE*, 26 (III), 1124–1198.

ATC-2-06. 1978. Tentative provisions for the development of seismic regulations for new buildings, Report ATC-3-06, Applied Technology Council, Berkeley, CA.

AUSTROADS. 1992. *Bridge Design Code*, Austroads, Haymarket, New South Wales, Australia.

Bachman, H. 1992. "Case studies of structures with man-induced vibrations", *Journal of Structural Engineering, ASCE*, 118 (3), 631–647.

Bakth, B. and Pinjarkar, S.G. 1991. *Dynamic Testing of Highway Bridges—A Review*, Transportation Research Record 1223, National research Council, Washington, DC.

Barker, R.M. and Puckett, J.A. 2013. *Design of Highway Bridges—An LRFD Approach*, John Wiley & Sons, Inc., New York.

Barlow, P. 1851. *A Treatise on the Strength of Timber*, J. Weale, London, U.K. (The Willis report describing the experiments by Prof. R. Willis, Capt. H. James, and Lt. D Dalton can be found in the appendix of this book.)

Billing, J.R. 1980. *Dynamic Tests of Bridges in Ontario*, Research and Development Reports, Vol. 26, Ministry of Transportation and Communications, Downsview, Ontario, Canada, 1982.

Borges, J.F. and Castanheta, M. 1971. Statistical definition and combination of loads, in *Probabilistic Design of Reinforced Concrete Building*, ACI Publication SP-31, American Concrete Institute, Farmington Hills, MI.

CALTRANS. 1992. *Bridge Design Practice Manual*, California Department of Transportation, Sacramento, CA.

Cantieni, R. 1984. Dynamic load tests on highway bridges in Switzerland, Report 211, Swiss Federal Laboratories of Materials Testing and Research, Dübendorf, Switzerland, 1983; Civil Engineers, New York.

Chalk, P.L. and Corotis, R.B. 1980. "Probability models for design live loads", *Journal of Structural Division*, 106 (ST10), 2017–2033.

Chan, T.H.T. and O'Connor, C. 1990a. "Vehicle model for highway bridge impact", *Journal of Structural Engineering, ASCE*, 116 (7), 1772–1793.

Chan, T.H.T. and O'Connor, C. 1990b. "Wheel loads from highway bridge strains", *Journal of Structural Engineering, ASCE*, 116 (7), 1751–1771.

Cheng, C. and Zhang, K. 2011. "Research on temperature field and temperature stress of prestressed concrete girders", *International Journal of Intelligent Systems and Applications*, 25–32.

Clough, G.W. and Duncan, J.M. 1991. Earth pressures, *Foundation Engineering Handbook*, 2nd ed., H.Y. Fang, ed., Van Nostrand Reinhold, New York, Chapter 6.

Cohen, H. 1990. Special Report 225: Truck weight limits: Issues and options, TRB, National Research Council, Washington, DC.

Cornell, C.A. and Larrabe, R.D. 1977. Representation of loads for code purposes, in *Proceedings*, *ICOSSAR*, Munich, Germany, pp. 135–148.

CSA. 1988. *Design of Highway Bridges*, CAN/CSA-S6-88, Canadian Standard Association, Rexdale, Ontario, Canada.

CSA. 2000. *Canadian Highway Bridge Design Code*, CAN/CSA-S6-00, Canadian Standard Association International, Sec. 3, Loads, Rexdale, Ontario, Canada.

Csagoly, P.F. and Knobel, Z. 1981. *The Survey of Commercial Weights in Ontario*, Ontario Ministry of Transportation and Communication, Toronto, ON.

www.EngineeringEBooksPdf.com

CTBUH. 1980. "Tall building criteria and loading," *Monograph on Planning and Design of Tall Buildings*, Council on Tall Buildings and Urban Habitat, ASCE, New York.

Dallard, P., Fitzpatrick, A.J., Flint, A., Le Bourva, S., and Ridsill-Smith, R.M. 2001a. "The London Millennium foot bridge: Problems and solutions", *Structural Engineer*, 79 (8), 15–17.

Dallard, P., Fitzpatrick, A.J., Flint, A., "Le Bourva, S., Ridsill-Smith, R.M., and Willford, M. 2001b. "The London Millennium foot bridge", *Structural Engineer*, 9 (22), 17–33.

Edwards, L.N. 1959. *A Record of History and Evolution of Early American Bridges*, University Press, Orono, MD.

Ellingwood, B., Galambos, T.V., MacGregor, J.G., and Cornell, C.A. 1980. *Development of a Probability-Based Load Criterion for American National Standard A58*, NBS 577, U. S. Department of Commerce, National Bureau of Standards, Washington, DC.

Ellingwood, B., Galambos, T.V., MacGregor, J.G., and Cornell, C.A. 1982a. "Probability-based load criteria, assessment of current practice", *Journal of Structural Division, ASCE*, 108 (ST5), 959–997.

Ellingwood, B., Galambos, T.V., MacGregor, J.G., and Cornell, C.A., 1982b. "Probability-based load criteria, load factors and load combinations", *Journal of Structural Division, ASCE*, 108 (ST5), 978–997.

Elms, D.G. and Martin, G.R. 1979. Factors involved in the seismic design of bridge abutments, in *Proceedings of a Workshop on Earthquake Resistance of Highway Bridges*, Applied Technology Council (ATC), Palo Alto, CA, December 29–31.

El-Tawil, S., Severion, E., and Fonseca, P. 2005. "Vehicle collision with bridge piers", *Journal of Bridge Engineering, ASCE*, 10 (3), 345–353.

ENR. 1941. New specifications issued for defense highway design, *Engineering News Record*, McGraw-Hill Co., New York, March 13, 1941, 71–73.

ENR. 2003. Nebraska overpass will be built with fewer piers, *Engineering News Record*, June 9, 2005, 25.

Eurocode No. 1. 1990. *Common Rules Unified Rules Different Types of Construction and Material*, Commission of the European Communities, Brussels, Belgium.

Fancher, P.S. and Ervin, R.D. 1986. A component factbook for straight and articulated heavy trucks, Report UMTRI-86-12, University of Transportation Institute, Ann Arbor, MI.

Fancher, P.S., Ervin, R.D., MacAdam, C.C., and Winkler, C.B. 1980. *Measurements and Representation of the Mechanical Properties of Truck Leaf Springs*, Technical Paper Series 800905, Society of Automotive Engineers, Warrendale, PA.

Farris, R.E. 1991. *Should the Federal Government Allow the States to Increase Truck-Size Limits?* Cato Review of Business and Government, The Cato Institute, Washington, DC.

FHWA. 1995. Comprehensive truck size and weight study, summary report for phase I—Synthesis of truck size and weight (TS & W) studies and issues, U.S. Department of Transportation, Washington, DC.

FHWA. 2006a. *Bridge Formula Weights*, *Circular* No. FHWA-HOP-06-105, Office of Freight Management and Operations, FHWA, U.S. Department of Transportation, Washington, DC.

FHWA. 2006b. Seismic retrofitting manual for highway structures, part 1—Bridges, FHWA Report No. FHWA-HRT-06-032, Federal Highway Administration, U.S. Department of Transportation, Washington, DC.

Finch, J.K. 1941. Wind failures of suspension bridges, *Engineering News Record,* March 13, pp. 74–79.

Ghali, A., Neville, A.M., and Brown, T.G. 2009. *Structural Analysis: A Unified Classical and Matrix Approach*, 6th ed., Taylor & Francis, New York.

Gies, J. 1963. *Bridges and Men*, Grosset and Dunlap, New York.

Gucma, L. 2009. Methods of ship-bridge collision safety evaluation, gnedenko.forum.org/Journal/2009/0222009/RATA_2_2009–05.pdf (February 2, 2009).

Gupta, R.K. 1980. Dynamic loading of highway bridges, *Journal of the Engineering Mechanics Division, ASCE*, 106 (EM2), 377–393.

Harman, D.J. and Davenport, A.G. 1979. "A statistical approach to traffic loading on highway bridges," *Canadian Journal of Civil Engineering*, 6, 494–513.

Harman, D.J. 1985. Survey of commercial vehicles weights 1978 to 1982, Report RR 236. Ministry of Transportation and Communications, Downsview, Ontario, Canada.

Haynes, F.D. 1995. *Bridge Pier Design for Ice Forces*, Ice Engineering, Army Cold Regions Research and Engineering Laboratory, Hanover, NH. (AASHTO LRFD p. 3–161 also references Haynes (1996) as "Private Communication.")

Hellman, G. 1916. Úber die Bewegung der luft in denundersten Schichtender Atmosphere, *Meteor.* Z, 34, 273.

Ho, D. and Liu, C.-H. 1989. "Extreme thermal loadings in highway", *ASCE Journal of Structural Engineering*, 115 (7), 1681–1697.

Honda, H., Kobori, T., and Yamada, Y. 1986. Dynamic factor for highway steel girder bridges, *Proceedings of the International Association of Bridge and Structural Engineering, p. 98/86*, Zurich, Switzerland, pp. 57–75.

www.EngineeringEBooksPdf.com

Huang, D., Wang, T., and Shahawy, M. 1992. "Impact analysis of continuous multigirder bridges due to moving vehicles", *Journal of Structural Engineering, ASCE*, 118 (12), 3427–3443.

Huang, T. 1976. Vibration of bridges, *Shock and Vibration Digest*, 8 (3), 61–76.

Hussey, H.D. 1924. Proposed loads on highway bridges, *Transactions*, 87, 414, American Society of Civil Engineers, paper no. 1536.

Hwang, E.S. and Nowak, A.S. 1991a. "Simulation of dynamic load for bridges", *Journal of Structural Engineering, ASCE*, 117 (5), 1413–1434.

Hwang, E.S. and Nowak, A.S. 1991b. *Dynamic Analysis of Girder Bridges*, Transportation Research Record 1223, National Research Council, Washington, DC.

Imbsen, R.A., Vandershaf, D.E., Schamber R.A., and Nutt, R.V. 1985. Thermal effects in concrete bridge superstructures, NCHRP Report 276, Transportation research Board, National research Council, Washington, DC.

Kulicki, J.M. and Mertz, D.R. 1991. A new live load modal for bridge design, in *Proceedings of the Eighth Annual International Bridge Conference*, Pittsburgh, PA, June, pp. 238–246.

Kulicki, J.M. and Mertz, D.R. 2006. Evolution of vehicular live load models during the interstate design era and beyond, in *50 Years of Interstate Structures: Past, Present, and Future*, Transportation Research Circular, E-C104, Transportation Research Board, National Research Council, Washington, DC.

Larrabe, R.D. and Cornell, C.A. 1979. "A combination procedure for wide class of loading processes," *ASCE Proceedings of the Spealty Conference on Probabilistic Mechanics and Structural Reliability*, Tucson, AZ, January 1979.

Leonard, D.R. 1966. Human tolerance levels for bridge vibrations, RRL Report No. 34, Ministry of Transport, Road Research Laboratory, Harmondsworth, England.

Lispett, A.W. and Gerard, R. 1980. Field measurements of ice forces on bridge piers 1973–1979, Report SWE 80-3, Alberta Research Council, Edmonton, Alberta, Canada.

Liu, H. 1991. *Wind Engineering: A Handbook for Structural Engineers*, Prentice-Hall, Englewood Cliffs, NJ.

Mastaglio, L. 1997. Bridge bashing, Civil Engineering, American Society of Civil Engineers, Washington, DC.

MCEER/ATC. 2003. Recommended LRFD guidelines for seismic design of highway bridges, Special Publication No. MCEER-03-SP03, Multidisciplinary Center for Earthquake Engineering, Buffalo, NY.

McNary, J.V. 1925. "Earth pressure against abutment walls measured with soil pressure cells", *Public Roads*, 6, 102–106.

Mononabe, N. and Matsuo, H. 1929. "On the determination of earth pressures during earthquakes", in *Proceedings, World Engineering Congress*, Tokyo, Japan, Vol. 9, paper no. 388.

Montgomery, C.T., Gerard, R., Huiskamp, W.J., and Korlensen, R.W. 1984. Application of ice engineering to bridge design standards, in *Proceedings of the Cold Regions Engineering Specialty Conference*, Canadian Society of Civil Engineering, Montreal, Quebec, Canada, April 4–6, 1984, pp. 795–810.

Montgomery, C.T., Gerard, R., and Lispett, A.W. 1980. "Dynamic response of bridge piers to ice forces", *Canadian Journal of Civil Engineering*, NRC Research Press, Ottawa, Ontario, Canada, 7 (2), 345–356.

Montgomery, C.T. and Lispett, A.W. 1980. "Dynamic tests and analysis of a massive pier subjected to ice forces", *Canadian Journal of Civil Engineering*, NRC Research Press, Ottawa, Ontario, Canada, 7 (3), 432–441.

Moses, F. and Ghosen, M. 1983. Instrumentation of weighing trucks-in-motion for highway bridge loads, Final Report, FHWA-OH-83-001, FGWA, U.S. Department of Transportation, Washington, DC.

Moses, F. and Ghosen, M. 1985. A comprehensive study of bridge loads and reliability, Final Report, FHWA/OH-85/005, U.S. Department of Transportation, Washington, DC.

National Cooperative Highway Research Program (NCHRP). 1998. Dynamic impact factors for bridges, *Synthesis 266*, National Academy Press, Washington, DC.

National Transportation Safety Board (NTSB). 1993. Tractor-semitrailer collision with bridge columns on Interstate 65, Evergreen, Alabama, Highway Accident Report, NTSB No. HAR-94-2, NTIS No. PB94-916202, National Technical Information Service, Springfield, VA.

NCHRP. 2002. Comprehensive design specifications for seismic design of bridges, NCHRP Report 472, Transportation Research Board, National Research Council, Washington, DC.

NCHRP. 2006. Recommended seismic guidelines for design specifications for seismic design of highway bridges, Draft Report NCHRP Project 20-07, Task 193, TRC Imbsen & Associates, Sacramento, CA.

Neill, C.R. 1976. Dynamic ice forces on piers and piles: An assessment of design guidelines in the light of recent research, *Canadian Journal of Civil Engineering*, NRC Research Press, Ottawa, Ontario, Canada, 3 (2), 305–341.

Neill, C.R., ed. 1981. *Ice Effects on Bridges*, Road and Transportation Association of Canada, Ottawa, Ontario, Canada.

NKB. 1987. Guidelines for loading and safety regulations for structural design, Nordic Committee on Building Regulations, Report No. 55E, Copenhagen, Denmark.

www.EngineeringEBooksPdf.com

Nowak, A.S. 1992. *Calibration of LRFD Bridge Design Code*, NCHRP Project 12-33, University of Michigan, Ann Arbor, MI.

Nowak, A.S. 1993a. Calibration of LRFD bridge design code, NCHRP Project 12-33, NCHRP Report 368, University of Michigan, Ann Arbor, MI.

Nowak, A.S. 1993b. "Live load models for highway bridges", *Journal of Structural Safety*, 13 (1 + 2), 53–66.

Nowak, A.S. 1995. "Calibration of LRFD bridge design code", *Journal of Structural Engineering, ASCE*, August 1995, Vol. 121, No. 6, 1245–1251.

Nowak, A.S. 1999, Calibration of LRFD bridge design code, NCHRP Report 368, Transportation Research Board, National Research Council, Washington, DC.

Nowak, A.S. and Collins, K.R. 2013. *Reliability of Structures*, CRC Press, Boca Raton, FL.

Nowak, A.S. and Hong, Y.-K. 1991. "Bridge live load models", *Journal of Structural Engineering, ASCE*, 117 (9), 2757–2767.

Nutt, R.V., Schamber, R.A., and Zokaie, T. 1988. Distribution of wheel loads on highway bridges, Final Report No. 183, Imbsen & Associates, Sacramento, CA.

O'Connor, C. and Prichard, R.W. 1985. "Impact studies on small composite girder bridge", *Journal of the Structural Engineering Division, ASCE*, 111 (3), 641–653

O'Neill, M.W. and Reese, L.C. 1999. *Drilled Shafts: Construction Procedures and Design*, Federal Highway Administration, Washington, DC.

OHBDC. 1983. *Ontario Highway Bridge Design Code*, 3rd ed., Ontario Ministry of Transportation, Downsview, Ontario, Canada.

OHBDC. 1991. *Ontario Highway Bridge Design Code*, 3rd ed., Ontario Ministry of Transportation, Downsview, Ontario, Canada.

Ohde, J. 1938. "Zur Theorie des Erddruckes unter besonderer Berucksichtigung der Erdruck Verteilung (On earth Pressure with Special Consideration to Earth Pressure Distribution)", *Bautechnik*, 16, 150–159, 176–180, 241–245, 331–335, 480–487, 570–571, 753, 671.

Okabe, S. 1924. "General theory of earth pressure and seismic stability of retaining wall and dams", *Journal of Japanese Society of Civil Engineers*, Tokyo, Japan, 12 (1).

Page, J. 1976. *Dynamic Wheel Load Measurements on Motorway Bridges*, Transportation and Road Research Laboratory, Report No. 722, Crowthorne, Berkshire, United Kingdom.

Paultre, P., Challal, O., and Proulx, J. 1992. "Bridge dynamics and dynamic amplification factors: A review of analytical and experimental findings", *Canadian Journal of Civil Engineering*, 19 (2), 260–278.

Peck, R.B., Hanson, W.E., and Thornburn, T.H. 1974. *Foundation Engineering*, 2nd ed., John Wiley and Sons, New York.

PennDOT. 1993. *Design Manual Part 4*, Pennsylvania Department of Transportation, Harrisburg, PA.

Priestley, M.J.N. 1976. "Ambient thermal stresses in circular prestressed concrete tanks", *Journal of American Concrete Institute*, 73 (10), 553–560.

Priestley, M.J.N. 1978. "Design of concrete bridges for temperature gradient", *Journal of American Concrete Institution*, 75 (5), 209–217.

Roberts, T.M. 2003. "Synchronization pedestrian excitation of footbridges", *Proceedings of the Institute of Civil Engineers, Bridge Engineering*, 156 (4), 155–160.

Roberts, T.M. 2005. "Lateral pedestrian excitation of footbridges", *Journal of Bridge Engineering, ASCE*, 10 (1), 107–112.

Roeder, C.W. 2002. Thermal design procedure for steel and concrete bridges, Final Report, NCHRP 20-07/106, Transportation research Board, National Research Council, Washington, DC.

Rojahn, C., Mayes, R., Anderson, D.G., Clark, J., Hom, J.H., Nutt, R.V., and O'Rourke, M.J. 1997. Seismic design criteria for bridges and other highway structures, Technical Report, NCEER-97-0002, National Center for Earthquake Engineering Research, April 30, 1997, Buffalo, NY.

Sach, P. 1978. *Wind Forces in Engineering*, 2nd ed., Pergamon Press, New York.

Salvadori, M. and Heller, R. 1975. *Structure in Architecture—The Building of Buildings*, 2nd ed., Prentice-Hall, Inc., Englewood Cliffs, NJ.

Schelling, D.R., Galdos, N.H., and Sahin, M.A. 1990. "Evaluation of impact factors for horizontally curved bridges", *Journal of Structural Division, ASCE*, 118 (11), 3203–3221.

Schilling, G.C. 1982. "Impact factors for fatigue design", *Journal of Structural Division, ASCE*, 108 (9), 2034–2044.

Seaman, H.R. 1924. Final report on specifications for design and construction of steel highway superstructures, *Transactions, ASCE*, Reston, VA, 1924.

www.EngineeringEBooksPdf.com

Seed, H.B. and Whitman, R.V. 1970. "Design of earth retaining structures for dynamic loads," *Proceedings of the ASCE Spealty Conference on Lateral Stresses in the Ground and Design of Earth Retaining Structures*, ASCE, pp. 103–147.

Shephard, R. and Aves, R.J. 1973. "Impact factors for simple concrete bridges", *Proceedings of the Institution of Civil Engineers*, part 2, 55, 191–210.

Simiu, E. and Scanlan, R. 1986. *Wind Effects on Structures*, 2nd ed., John Wiley & Sons, Inc., New York.

Smith, D. 1974. A case study and analysis of the Tacoma Narrows Bridge failure, 99.497 Engineering Project, Department of Mechanical Engineering, Carleton University, Ottawa, Ontario, Canada, March 29, 1974.

Steinman, D.B. and Watson, S.R. 1957. *Bridges and Their Builders*, Dover Publications, New York.

Taly, N. 1998. *Design of Modern Highway Bridges*, McGraw-Hill Co., New York.

Taly, N. 2003. *Loads and Load Paths in Buildings—Principles of Structural Design*, International Code Council, Inc., Country Club Hills, IL.

Terzaghi, K. 1920. Old earth pressure theories and new test results, *Engineering News Record*, September 30, 1920, 632–637.

Terzaghi, K. 1934a. "Large retaining wall tests", *Engineering News Record*, 112, 136–140.

Terzaghi, K. 1934b. "Retaining walls for fifteen miles dam", *Engineering News Record*, May 17, 1934b, 532–536.

Terzaghi, K. 1936. "A fundamental fallacy in earth pressure computations", *Journal of Boston Society of Civil Engineers*, 23, 71–88.

Terzaghi, K., Peck, R.B., and Mesri, G. 1996. *Soil Mechanics in Engineering Practice*, 3rd ed., John Wiley & Sons, Inc., New York.

The Governor's Board of Inquiry on the 1989 Loma Prieta Earthquake. 1990. *Competing against Time: Report to Governor George Deukmejian from the Governor's Board of Inquiry on the 1989 Loma Prieta Earthquake*, State of California, Office of Planning and Research, San Francisco, CA.

Timoshenko, S. 1953. *History of Strength of Materials*, McGraw-Hill Co., New York.

TRB Committee for the Truck Weight. 1990. Truck weight limits: Issues and options, Special Report 225, Transportation Research Board, National Research Council, Washington, DC.

TRB. 2002. *Regulation of Weights, Lengths, and Widths of Commercial Motor Vehicles*, TRB Special report 267, Committee for the Study of the Regulation of Weights, Lengths, and Widths of Commercial Motor Vehicles, Transportation Research Board, National Research Council, Washington, DC, 2002, 267pp.

TRB. 2006. *50 Years of Interstate Structures—Past, Present, and Future*, Transportation Research Circular E-C104, Transportation Research Board, National Academies, Washington, DC, September 2006, 145pp.

Turkstra, C.J. and Madsen, H. 1980. "Load combinations for codified structural design", *Journal of Structural Division, ASCE*, 106 (12), 2527–2543.

Tyrell, H.G. 1911. *History of Bridge Engineering*, H.G. Tyrell, Chicago, IL.

U.S. Department of Navy. 1982. Foundations and earth structures, Technical Report, NAVFAC DM-7.1 and DM-7.2, Naval Facilities Command, U.S. Department of Defense, Washington, DC, p. 244.

U.S. Govt. 1975. 23 USC 127—Sec. 127, Vehicle weight limitations—Interstate System.

USS. 1975. Nine steel bridges for forest development roads, Couth Tongass National Forest, Alaska, Bridge Structural Report, ADUSS 88-5973-02, U.S. Steel, Pittsburg, PA.

Virola, J. 1969. "The world's greatest cantilever bridges", *Acier–Stahl–Steel*, (4), 164–170.

www.EngineeringEBooksPdf.com

4 Structural Analysis of Highway Bridge Superstructures

4.1 INTRODUCTION

Load distribution in bridge superstructures is used as a synonym for *structural analysis* of a bridge superstructure. It involves determination of load effects in the bridge deck and the supporting beams/girders, which are required for design purposes. These load effects, such as shear, bending moment, and deflection, are caused by dead and live loads applied to the bridge superstructure, the effects of which can be determined based on the principles of structural mechanics and *load path* considerations.

The dead load effects in beams and girders supporting a bridge deck can usually be determined based on tributary or influence areas, the same way they are determined for gravity loads–sharing components in buildings (viz., floor, floor beams, girders, columns, and walls). Although the same general principle is used to determine also the live load effects in building components (viz., beams, girders, and columns), it cannot be used to determine live load effects in bridge superstructures (i.e., deck, beams, and girders supporting the bridge deck). This is because of the fundamental differences between the live load in buildings and the live load on bridge superstructures. In the case of buildings, the live load is expressed generally as a *uniform load* over the tributary (or influence) area of the component of interest. By contrast, in the case of bridge deck, the live load consists of *moving* load (traffic consisting of many different types of vehicles), which can occupy *any position* on the bridge deck (longitudinally and transversely) and which can reverse the direction of movement. It is the uncertainty of the nature and position of live load on the bridge deck that warrants a need for special analytical tools for determining force effects in the components of a bridge superstructure. These methods, as applicable to beams/girders supporting a bridge deck and specified in 2012 AASHTO LRFD Specifications (referred to hereinafter as LRFD Specifications) (AASHTO LRFD 2012), are discussed in this chapter. For the purpose of discussion, the terms *beams* and *girders* are used interchangeably throughout this book.

In a general sense, designing a bridge is analogous to designing a building—both involve structural analysis and design. In both cases, a designer needs to proceed as follows:

1. Identify and determine various loads acting on the structure
2. Identify various load-sharing components in the structure
3. Determine the load path to ensure that all of the loads acting on the structure are safely transferred to the ground

Component forces can be determined based on the load path, which form the basis for structural analysis/design.

As discussed in Chapter 2, a variety of bridge superstructure types, identified as Types (a) through (l) (discussed in Chapter 2 and shown in Table 4.A.1), can be used for highway bridges depending on designer/owner preferences, which might be based on a number of considerations such as feasibility, economics, durability, aesthetics, environmental, and others. These are the superstructure types covered for analytical purposes in Section 4 of LRFD Specifications. However, by far the most common types of bridge superstructures fall in the category of multibeam (also called slab-beam

www.EngineeringEBooksPdf.com

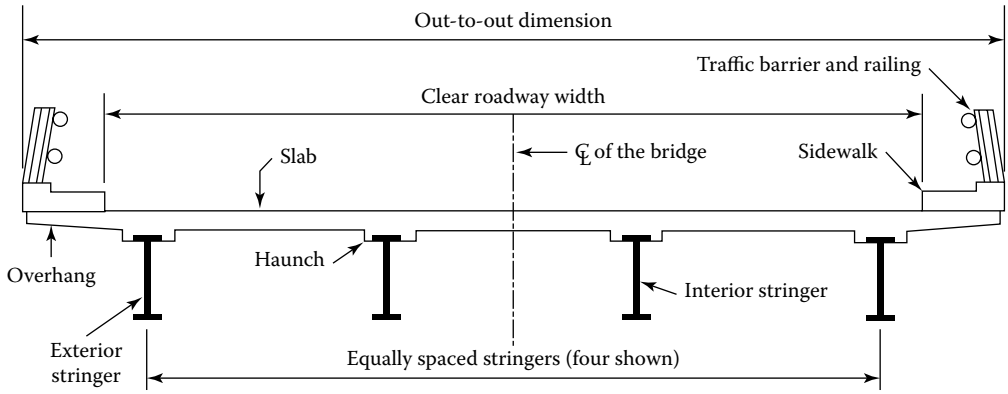

FIGURE 4.1 Typical cross section of a slab-girder bridge with sidewalks.

or slab-girder) type superstructures (Figure 4.1) and box-girder superstructures. Therefore, in this chapter, major emphasis is placed on structural analyses of these types of superstructures. These are the *basic* types of structures that form either complete structures by themselves (such as simple and continuous span bridges) or parts of other types of bridge structures, such as truss, arch, cable-stayed, and suspension bridges.

This chapter presents a discussion of determination of service live load effects on bridge superstructures of a few selected types. In the context of *load and resistance design* (LRFD), these loads are referred to as *unfactored* live loads. These load effects, in conjunction with other applicable load effects (such as dead loads and impact), can be used for the following purposes:

1. Structural design based on *allowable stress design* (ASD) philosophy
2. To check serviceability limit state (LRFD)
3. To check fatigue and fracture limit states (LRFD)

To satisfy the strength limit states (LRFD), these loads are multiplied by appropriate load factors; the resulting loads are called the *factored* loads. Various kinds of loads that act on bridge structures and the applicable load factors are discussed in Chapter 3.

4.2 LOAD PATH IN BRIDGE STRUCTURES

Loads are shared in a structure by several interconnected components in a hierarchical manner, which constitutes the load path. Identification of a load path is a fundamental requirement in structural design. Analytically speaking, a bridge is essentially a horizontally spanning structure; by contrast, a building acts as a vertically spanning (cantilevered) structure.

All structures are acted upon by gravity as well as lateral loads. A clear, continuous load path must be provided for both types of loads. These load paths must be clearly articulated and designed to transmit all loads from their origin to the foundation. The principles of transmitting loads through various components and connections are similar for both buildings and bridges. A comprehensive discussion on loads paths for gravity and lateral loads in buildings can be found in Taly (2003). This section presents a discussion on load paths for gravity loads in bridges. Discussion on load paths for lateral loads (wind and seismic) is presented in Section 4.17.

Unlike buildings, a bridge has two major parts that share the load path, the superstructure and the substructure, *in that order*. The bridge roadway and supporting elements (e.g., beams, cables in cable and suspension bridges, etc.) are considered as part of the superstructure; the remaining portion of the bridge, which supports the superstructure, constitutes the substructure.

www.EngineeringEBooksPdf.com

Load path in bridge structures, as in buildings, depends on the *structural form* of the bridge under consideration, viz., slab-beam bridges, truss bridges, arch bridges, cable-stayed bridges, and suspension bridges. Although these bridges appear to be strikingly different, they share many commonalities with slab-beam bridges, which can be easily identified:

1. All bridges must provide a roadway (in the form of a bridge deck), which may consist of many different types of (bridge) floors (material selection). Source loads are transferred directly to the bridge floor.
2. Typically, the bridge floor is supported on a series of longitudinal beams; the bridge floor transfers its loads to these beams. An exception to this load path is a slab bridge in which, typically, the roadway consists solely of a concrete slab.
3. Longitudinal beams (deck slab in the case of a slab bridge) are supported on rigid supports on either side of the bridge. For a simple span bridge, these supports would simply be abutments on either side; a continuous bridge would have intermediate supports (variously called piers, column bents, etc.) also between the abutments.
4. Beams are seated (or supported) on bearings provided on top of supports (abutments and piers). Bridge bearings receive loads from beams in the form of reactions, both vertical and horizontal. Here begins the substructure of the bridge.
5. Bearings transfer reactions to the support on which they are seated.
6. The supports (abutments and piers) transfer their loads to the ground below.

Items 1–6 are common to all types of bridges. Items 1–3 pertain to superstructures, and items 3–6 to substructures. This chapter focuses on the load path in the superstructure. Figure 4.2 shows load path in a typical slab-girder bridge.

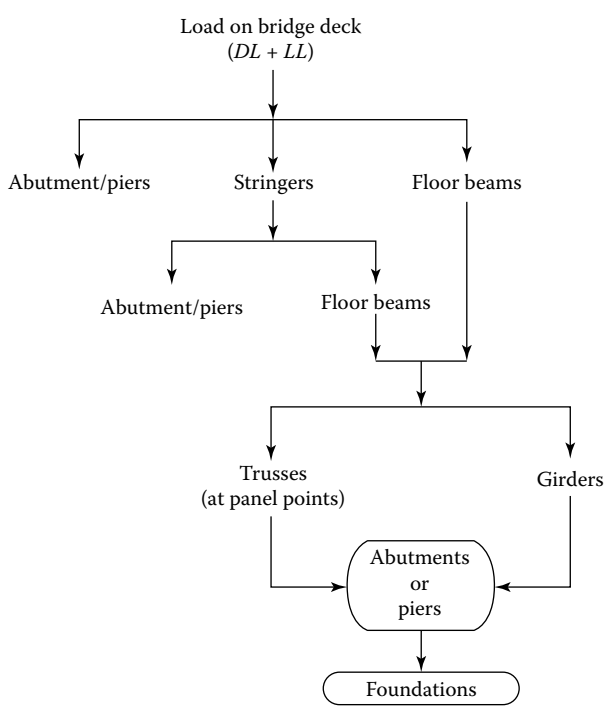

FIGURE 4.2 Load path in a typical slab-beam bridge.

www.EngineeringEBooksPdf.com

Differences in the superstructure load paths become evident when one observes bridges other than simple beam-slab bridges. In such cases, a complete system can be identified for load path purposes. For example,

1. The superstructure of a truss bridge consists of several identical basic beam-slab units, which are supported on floor beams attached to the truss joints. The floor beams transfer loads to truss joints in the form of reactions. Joints loads are then shared by various truss members. The truss is supported on abutments (substructure). The same is true for steel arch bridges.
2. In cable-stayed bridges, the bridge deck is supported by cables attached to the bridge deck at intervals (instead of rigid supports underneath), which are attached to towers (called cable stays). The cables act as flexible supports (in tension, in contrast to piers that act in compression). The towers transfer bridge loads partly to the abutments and partly to the ground.
3. In suspension bridges, the basic beam-slab unit is supported on floor beams, which transfer bridge loads to the suspension cable(s) via hanger cables attached to them. The hangers act as load-transferring links between the basic slab-beam roadway units and the suspension cables, which carry the entire bridge load to towers and abutments.

All load-sharing bridge components can be designed once the load path is identified.

4.3 ANALYSIS FOR DEAD LOAD ON BRIDGE SUPERSTRUCTURES

The dead load, referred to as permanent load, on a bridge deck typically consists of the following components (Figure 4.1):

1. Deck (concrete, wood, open or filled steel deck, fiber-reinforced polymer composite, etc.)
2. Wearing surface over the deck and future wearing surface
3. Traffic barriers/curbs and railing
4. Sidewalk
5. Beams/girders supporting the deck

Dead load due to these components can be determined based on material unit weights (Table 3.10), which is a trivial computational exercise. In most cases, the girders are equally spaced. Regardless of their spacing, dead load to be carried by these girders can be determined on tributary width basis. It is common practice to consider a weight of 25–35 lb/ft^2 of deck as the dead weight due to the future wearing surface or overlay. Practices in this regard vary from one bridge owner agency to another. Traffic barriers (parapet/curbs) are typically cast after the deck has hardened, and railings are installed thereafter. These elements are typically located on the overhang portion of the deck and act as heavy line loads.

Practices for distributing permanent loads, including the line loads, to the girders vary. One approach assumes that after the deck has hardened, it acts as a rigid element and distributes these loads equally to all the girders supporting the deck (except in the case of curved I-girder bridges). LRFD Article (Art.) 4.6.2.2.1 states as follows: *Where bridges meet the conditions specified herein, permanent loads of and on the deck may be distributed uniformly among beams and/or stringers.* Most common types of superstructures meet this condition. Accordingly, this approach has been followed in this book.

However, this is a conservative approach for the interior girders but may result in underestimation of dead load on the exterior girders. The other approach is based on the premise that these line loads are positioned on the overhang portion of the deck, and as such they are much closer to the exterior girders. Accordingly, this approach distributes these line loads to the exterior girder and the first interior girder based on the principle of the *lever rule* (see Section 4.6.2).

www.EngineeringEBooksPdf.com

4.4 METHODS OF STRUCTURAL ANALYSIS FOR LIVE LOAD ON BRIDGE SUPERSTRUCTURES

Determination of live load effects (shear, bending moment, and deflection) in girders supporting highway bridge decks forms a key step in the design calculations for a bridge superstructure. Referred to as *live load distribution* in bridge superstructures, the topic has been researched extensively over many years throughout the world. Analytically speaking, a bridge deck may be considered a large plate stiffened by the supporting beams or girders that are oriented in the direction of traffic and typically supported on two perpendicular sides, viz., abutments and/or piers. Accordingly, it could be modeled as a stiffened plate supported along the short edges and free along the long edges (Figure 4.3). This plate (i.e., the bridge deck) can be built from a variety of materials such as concrete, steel, and wood. Likewise, the supporting girders can also be built from different materials such as steel, reinforced concrete, prestressed concrete, wood, and composites. The girders can have a variety of cross sections such as W-shape or box-shape steel beams, reinforced or prestressed concrete beams in the shape of I, single-T, double-T, or box, or rectangular wood beams. Compounding the problem is the fact that the stiffened plate (i.e., the bridge deck) can be built from a combination of these elements. For example, a concrete deck can be supported over steel or concrete (reinforced or prestressed) beams of many different shapes, and the construction can be noncomposite or composite. The deck can consist of wood planks supported on steel or wood beams, and so on. While the flexibility in selecting the type of deck and supporting beams is great for designers, it presents complexity in analysis of the superstructure.

Analysis of bridge superstructures for live loads is described in Section 4 of LRFD Specifications. These methods are classified as follows:

1. Approximate methods (LRFD Art. 4.6 2)
2. Refined methods (LRFD Art. 4.6.3)

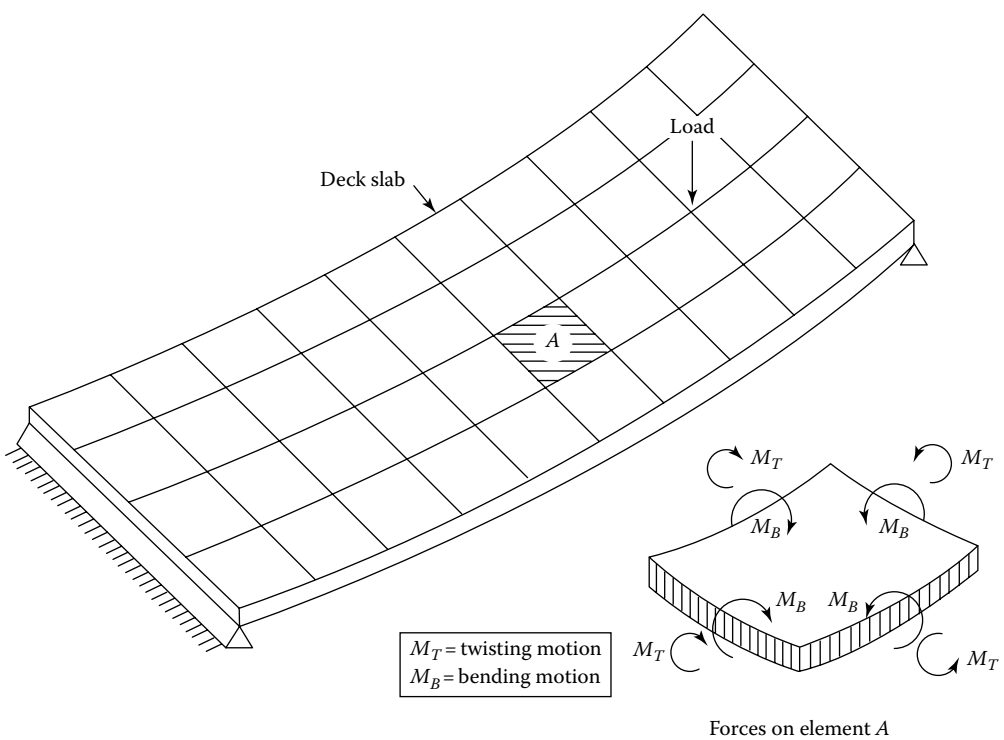

FIGURE 4.3 Bridge deck as a large stiffened plate supported along the short edges and free along the long edges.

www.EngineeringEBooksPdf.com

Because of their simplicity, it is common practice to use the *approximate methods* for designing short- and medium-span bridge superstructures; accordingly, these are described in great detail in this chapter. *Refined methods*, although more accurate, are cumbersome and time intensive. Availability of fast and efficient computational methods and computers has made use of these analytical methods somewhat easier than in the past. These methods are described in detail in the current specification document (LRFD 2012, Art. 4.6.3) and are discussed briefly in Section 4.16. For details and background information on both methods, readers should refer to the *commentary* to Section 4 of LRFD Specifications.

At the heart of the approximate methods lies the concept of *live load distribution factors* (hereinafter simply referred to as *distribution factors* or *DF*), which is described in the next section. Essentially, this method is a simple analytical tool to apportion the live load effects (bending moment, shear, and deflection) in the beams or girders supporting the bridge deck.

The approximate methods, developed in early 1940s and based on the research conducted at University of Illinois at Urbana–Champaign, continued to be included in AASHTO Standard Specifications (AASHTO 2002). Many efforts have been made over the years to refine these methods in order to gain better understanding and improved accuracy. A major study of live load distribution in highway bridges was published in 1970 as *NCHRP Report 83* (Sanders and Elleby 1970, with 297 citations), which was the basis of changes in the live load distributions in AASHTO *Standard* Specifications (referred to hereinafter as AASHTO Standard). The distribution factors specified in the LRFD Specifications are based on later studies (Nutt et al. 1988, Zokaie et al. 1991a, 1991b), which are very different from their counterparts specified in AASHTO Standard Specification (AASHTO 1996). These studies notwithstanding, interest in further research for simplification of live load distribution in highway bridge superstructures continues. A discussion on simplified methods for lateral distribution factors for live load bending moment and shear in common types of highway bridge superstructures can be found in the literature (Bakth and Jaeger 1992, Elbeido and Kennedy 1996, TDOT 1996, Mabsout et. al. 1997, Huo et al. 2003, 2004, 2005, Kocsis 2005).

4.5 APPROXIMATE ANALYSIS METHODS FOR LIVE LOADS: THE DISTRIBUTION FACTOR CONCEPT

All structural engineers are familiar with the concept of *distribution factors* as used in the method of *bending moment distribution* in structural analysis. But the concept of distribution factors as used in structural analysis of bridge superstructures is entirely different.

Method *of live load distribution factors* is an approximate, but simple and convenient, method specified in LRFD Specifications for analyzing force effects (shear, bending moment, deflection) in beams/girders supporting a bridge deck. This method involves a three-step procedure:

Step 1: The live load effects (bending moment and shear) are determined by considering a predefined load system, in our case the AASHTO HL-93 truck (referred to hereinafter as the design truck) *or* tandem (assumed as knife-edge loads as discussed in Chapter 3) combined with a uniform load, in our case the AASHTO lane load of 0.64 kip/ft, *moving* on a beam or girder, by rational methods (i.e., methods based on principles of structural mechanics) as described in Chapter 3. This step is performed regardless of the number of design lanes on the bridge. The type of the deck system, the type of girders (e.g., steel, reinforced concrete, prestressed concrete, wood, or composite), and their number and profiles (cross-sectional types) have no influence on the outcome of this step.

Step 2: The live load effects (i.e., magnitude of shear and bending moment) in a girder supporting a deck are determined by multiplying the force effect determined in step 1 by a dimensionless quantity called *distribution factor* (*DF*). The distribution factors (*DF*s) are calculated separately as

www.EngineeringEBooksPdf.com

follows (suffixes *m* and *v* stand for bending moment and shear, respectively; *i* and *e* stand for interior and exterior girders, respectively):

1. *DF* for bending moment in the interior girders (g_{mi})
2. *DF* for shear in the interior girders (g_{vi})
3. *DF*s for bending moments in the exterior girders (g_{me})
4. *DF*s for shear in the exterior girders (g_{ve})

Step 3: The distribution factors calculated in step 2 are valid for a bridge superstructure that is aligned perpendicular to the supports (abutments and/or piers, bent caps), that is, for a bridge without a *skew* (see Section 2.5.3). When the supports are skewed (i.e., when their layout is not perpendicular to the superstructure they support), *skew correction factors* are calculated and used to modify the calculated distribution factors.

In order to use the live load distribution factors, the following rules should be borne in mind:

1. Distribution factors are applied to the live load effects only; they are not applicable to the permanent load effects (which are calculated on the basis of tributary areas).
2. Live load effects include load effects from HL-93 truck *or* tandem (as applicable) multiplied by the dynamic load allowance (1 + *IM*), *and* the effects from the lane load (see Equation 3.1). The lane load is *not* multiplied by the dynamic load allowance (1 + *IM*).
3. The distribution factors are applied to the unfactored live load effects (often called the service live load effects), which is the sum of effects of design truck (or tandem, whichever governs) load including dynamic load effects, and lane load effects (without dynamic load effects); appropriate load factors are applied later to determine the limit state loads.
4. For the limit states design, LRFD specifies different numerical values of load factors (γ_p) for different types of permanent loads and for live load as follows:
   a. Dead load of the deck and the girder including structural components attachments (specified as *DC*)
   b. Dead load due to the wearing surface and utilities (specified as *DW*)
   c. Live load (specified as *LL* + *IM*) (distribution factors are applied to this live load component as stated in item 1)

   Refer to Tables 3.7 through 3.9. For example, the following load factors are used for Strength Limit State I (typically used for design of girders):

$$\gamma_p = 1.25 \text{ for } DC$$

$$\gamma_p = 1.5 \text{ for } DW$$

$$\gamma = 1.75 \text{ for } LL(1 + IM)$$

   Accordingly, Strength I Limit State state load combination is expressed as follows:

$$\text{Strength I Limit Strength: } 1.25DC + 1.5DW + 1.75[(LL + IM)(DF)] \tag{4.1}$$

5. The lateral load distribution factors obtained for simple spans are also considered applicable to continuous spans.

Several examples are presented in this chapter to illustrate calculations for distribution factors for shear and bending moment in both interior and exteriors girders, as well as calculations for correction factors where applicable (Examples 4.3 through 4.7). Also presented are examples of their application to determining load values for the applicable limit states (required for designing bridge bearings and substructure), shear and bending moments in girders (Example 4.8).

www.EngineeringEBooksPdf.com

From structural mechanics standpoint, the entire superstructure (i.e., the deck and supporting girders) acts as a giant stiffened plate (beam/girders act as longitudinal stiffeners). The distribution factor takes into consideration the distributive property of the deck in transferring the live load from itself to the supporting girders. This distributive property is difficult to define with mathematical precision because of the many variables that influence it, some of which are as follows:

1. Type of deck (e.g., concrete deck, open or filled steel deck, orthotropic deck, wood, composite)
2. Material of construction of the girders (steel, concrete, wood, composite, etc.)
3. Number of girders supporting the deck and the manner in which they are interconnected transversely along the span
4. Geometry of the girder section (W-shape box steel girders, reinforced or prestressed concrete T- or box-beams, etc.)
5. Position of the girder (interior or exterior)
6. Number of design lanes on the bridge deck (single or multiple)
7. Position of wheel loads with respect to the position of girders
8. Bridge geometry (e.g., superstructures with or without a skew, curved, continuous)

4.6 CONSIDERATIONS FOR LIVE LOAD DISTRIBUTION FACTORS FOR COMMON TYPES OF BRIDGE SUPERSTRUCTURES

4.6.1 General Approach

The most common types of highway bridge superstructures consist of concrete decks supported on and built to act compositely with parallel steel or concrete girders. These are generally referred to as *beam-slab* bridges (LRFD Art. 4.6.2.2). Typical examples include concrete deck, filled grid, partially filled grid, or unfilled grid deck composite with reinforced concrete slab on steel or concrete beams; concrete T-beams, T- and double-T-sections (as listed in LRFD Table 4.6.2.2.2b-1, column 1).

Referred to as approximate methods, expressions for distribution factors for bending moment and shear in interior girder and exterior girders are specified in LRFD Art. 4.6.2.2. Conditions for applicability of approximate methods are specified in LRFD Art. 4.6.2.2.1. LRFD Table 4.6.2.2.1-1 lists 12 different types of bridge cross sections (beam-slab, box girder, etc.), which are identified as Types (a) through (l) (illustrated in Table 4.A.1 in the Appendix, discussed in detail in Chapter 2). They represent common types of superstructures used in the United States and elsewhere in the world. Expressions for determining distribution factors for bending moments and shears in interior and exterior beams supporting a bridge deck are given in separate tables (see Appendix). Formulas are given for one-design lane load case, and two or more design loaded case. The expressions listed in these tables apply to bridge superstructures without a skew. Correction factors (given in LRFD tables) are provided for superstructures that have skew.

4.6.2 Lever Rule

In addition to the formulas for distribution factors given in LRFD tables, the use of *lever rule* is suggested for a few selected types of superstructures and for specific conditions. *What is lever rule?* The lever rule is a computational procedure (analytical tool) analogous to determining the reaction at the supports of a simple beam with or without a loaded overhang. It involves simple statics—summing bending moments about one support to determine the reaction at another support assuming that the supported component is hinged at the interior support. Example 4.1 illustrates this simple concept.

www.EngineeringEBooksPdf.com

Example 4.1: Lever Rule Concept

Use lever rule to determine the reactions due to wheel loads of a truck in the exterior and the interior girders of a slab-beam type superstructure shown in Figure 4.4.

Solution

Figure 4.5 shows the partial superstructure from Figure 4.4. The design truck (shown by two concentrated loads representing wheel loads) is shown in the exterior lane of the deck. The exterior wheel is placed at 2 ft (minimum prescribed distance) from the face of the curb. The resultant of the wheel loads (each equal to *P*) is indicated by *R*.

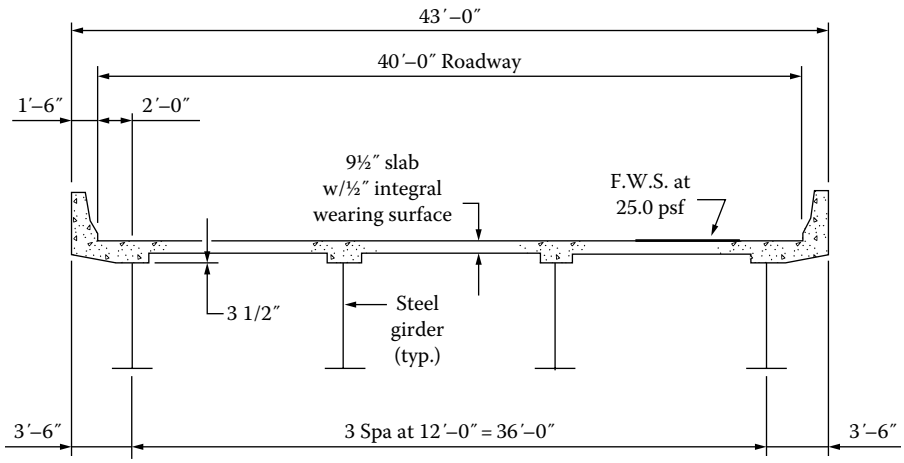

FIGURE 4.4 A slab-beam type superstructure (Type (a)). (Courtesy of AISI.)

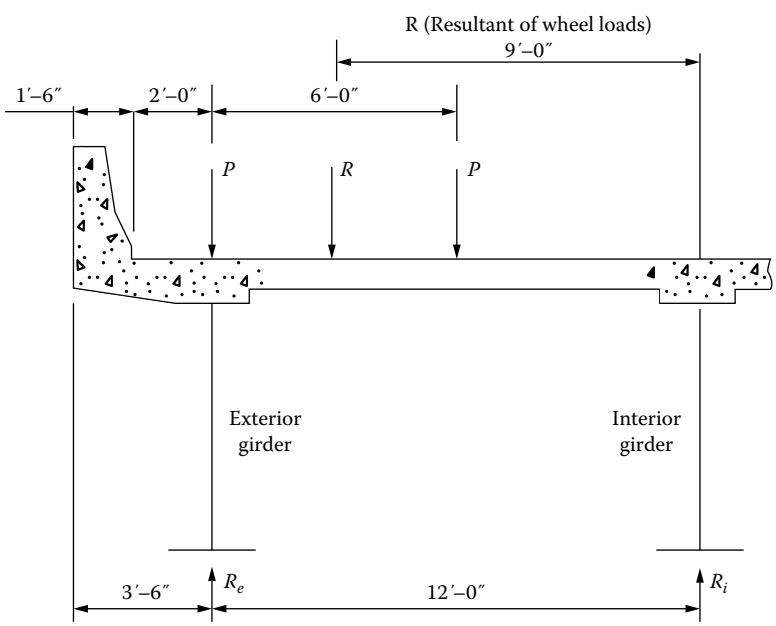

FIGURE 4.5 Determination of load effects in the exterior girder by the lever rule. (Courtesy of AISI.)

www.EngineeringEBooksPdf.com

From statics, taking moments about the interior girder, we obtain the value of reaction at the exterior girder, R_e, in terms of the resultant R:

$$R_e = \frac{9}{12}R$$

Alternatively, we can determine the reaction R_e by taking the moments of wheel loads, P, about the interior girder:

$$R_e = P + \frac{P}{2} = \frac{3P}{2} = \frac{3}{4}R$$

This result means that when only one lane is loaded by the design truck, three-fourths of the load effect is shared by the exterior girder. This also means that the reaction at the interior girder is $R_i = ¼R$, that is, the interior girder shares one-fourth of the truck load.

Lever rule is *that* simple!

In the case of curved I-girder bridges, AASHTO LRFD *Commentary C4.6.1.2.4b* specifically recommends that heavier line loads such as parapets, sidewalks, barriers, or sound walls should not be distributed equally to the girders. Engineering judgment must be used in determining the distribution of these loads. Often the largest portion of the loads on the overhang is assigned to the exterior girder or to the exterior girder and the first interior girder. The exterior girder on the outside of the curve is often critical in curved girder bridges.

LRFD Table 4.6.2.2.2d-1 specifies using the lever rule for determining distribution factors for both bending moments and shears in interior and exterior girders selectively as shown in LRFD Tables 4.6.2.2.2b-1 through 4.6.2.2.3b-1 (see these tables in Appendix 4.A).

When using the lever rule on the exterior girder of a bridge that is being supported by three or more girders, the supported element is assumed simply supported over the exterior girder and the adjacent interior girder (Figure 4.6). It is a *notional* model that is simple and convenient for determination of distribution factor for the exterior girders (LRFD Com. C4.6.6.1). Moments should be taken about the assumed or notional hinge in the deck over the middle girder to find the reaction on the exterior girder.

It is important to understand the background of development of the specifications for distribution factors for bending moment and shear in bridge superstructures of the types listed in LRFD tables. Some of these superstructures are posttensioned, supposedly, in order to develop integral action between the units. LRFD Specifications recommend a minimum of 0.25 ksi prestress to accomplish this objective.

Several of these superstructure types (Types (f), (g), (h), (i), and (j) [Appendix 4.A, Table A.4.1]) use precast units that employ longitudinal joints between them. This type of construction is assumed to act as a monolithic unit if sufficiently interconnected. LRFD Art. 5.14.4.3 identifies a fully interconnected joint as a shear joint. This type of interconnection is enhanced by either transverse posttensioning of the aforementioned intensity or by a reinforced structural overlay (specified in Art. 5.14.4.3.3f), or both. *The use of transverse mild steel rods secured by nuts or similar unstressed dowels should not be considered effective to achieve full transverse continuity unless demonstrated by testing or experience*. In general, posttensioning is thought to be more effective than a structural overlay if the aforementioned prestress intensity is achieved.

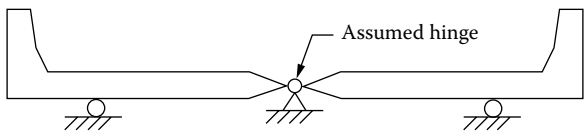

FIGURE 4.6 Notional model for applying *lever rule* to three-girder bridges.

www.EngineeringEBooksPdf.com

4.6.3 Applicability Criteria for LRFD Live Load Distribution Factors

4.6.3.1 Superstructures with Constant Deck Width and Parallel Girders

Most of the equations for distribution factors were derived for superstructures having constant deck width and parallel girders. In addition, there are other parametric limitations that form the basis of the analytical model used in the development of these equations. Fortunately, these parameters, such as deck slab thickness, and length and numbers of parallel beams supporting the deck, cover a wide range of values encountered in practice. These limitations are listed as the *range of applicability* in various LRFD Tables 4.6.2.2.2 and 4.6.2.2.3 (last column of these tables), which list equations for distribution factors for different superstructure types. These limitations are different for

1. Different superstructure types
2. Bending moments in interior and exterior girders
3. Shear in interior and exterior girders

Consider, for example, a reinforced concrete bridge deck of constant width and supported by a few parallel steel or concrete girders, concrete T-beams, and double-T-sections (superstructures Types (a), (e), (k), (i), and (j), see Table 4.1). The *range of applicability* column in LRFD Table 4.6.2.2.2b-1 lists the following limitations for calculating distribution factor for bending moment in the interior girders:

1. $3.5\ S \leq 16.0$ (i.e., the spacing, S, between adjacent girders should be between 3.5 and 16 ft)
2. $4.5 \leq t_s \leq 12$ (i.e., the slab thickness, t_s, should be between 4.5 and 12 in.)
3. $20 \leq L \leq 240$ (i.e., the span, L, should be between 20 and 240 ft)
4. $N_b \geq 4$ (i.e., the number of beams, N_b, supporting the deck must be at least four)
5. $10{,}000 \leq K_g \leq 7{,}000{,}000$ (K_g = longitudinal stiffness parameter, defined in the next section)

All of these limitations must be satisfied if a designer wishes to use the tabulated equations for distribution factors for bending moment in the interior girders. Somewhat similar limitations are also specified for determining distribution factors for shear in the interior girders. Range of applicability parameters are also given for distribution factors for bending moment and shear in the exterior girders. In cases where superstructures are outside these limitations, the tabulated expressions may not be used without modifications.

The following provisions are made in the LRFD Specifications (AASHTO 2012):

1. The listed expressions are valid for LRFD design truck/lane load in one or more lanes. If one lane is loaded with a special vehicle or evaluation permit loads, the design force effect per girder resulting from the mixed traffic may be determined as specified in Art. 4.6.2.2.5 (discussed in Section 4.13).
2. For the beam spacing exceeding the aforementioned range of applicability ($S > 16$ ft) as specified in LRFD Tables 4.6.2.2.2 and 4.6.2.2.3, the live load on each beam shall be the reaction of loaded lanes based on the lever rule unless specified otherwise in Section 4 of LRFD Specifications (Section 4.6.2.2.1).

TABLE 4.1
Multiple Presence Factors, *m*

Number of Loaded Lanes, N_L	Multiple Presence, m
1	1.2
2	1.00
3	0.85
>3	0.65

www.EngineeringEBooksPdf.com

3. Attention should be paid to the limitations of deck slab thickness of item 2 listed in the range of applicability column, which specifies the range of slab thickness between 4.5 and 12 in. *The lower limits on the slab thickness in this item are not intended to override the lower limit (i.e., minimum) of slab thickness of 7 in. specified in LRFD Art. 9.7.1.1* (Unless approved by the owner, the depth of a concrete deck, excluding any provisions for grinding, grooving, and sacrificial surface, should not be less than 7.0 in.). The range of lower limits on slab thickness shown in item 2 is meant only to reflect the range of slab thickness that was used in research for deriving expressions for the distribution factors.
4. Another item pertinent to the development of equations for distribution factors is diaphragms. The bridge superstructures considered in the development of the equations had interior end diaphragms only (i.e., no interior diaphragms within the spans, and no exterior diaphragms between the boxes). If interior or exterior diaphragms are provided within the span, the transverse load distribution characteristics of the bridge would be improved to some degree. This improvement can be evaluated using acceptable analysis methods specified in Art. 4.4. These include methods of analysis that satisfy the requirements of equilibrium and compatibility and uses stress–strain relationships for the proposed materials to be used including, but not limited to, the following:
   a. Classical force and displacement method
   b. Finite difference method
   c. Finite element method
   d. Folded plate method
   e. Finite strip method
   f. Grillage analogy method
   g. Series or other harmonic methods
   h. Methods based on formation of plastic hinges
   i. Yield line method

Many computer programs are available for analysis of bridge superstructures, which cater to the many analytical tools ranging from simple formulae to detailed finite element procedures. All computer programs are based on specific engineering assumptions embedded in their codes, which might not be applicable to the specific case being considered. It is further cautioned that computer programs are only tools, that the users/designers bear the responsibility for ensuring the accuracy and interpretation of the generated results. It is highly recommended that the results of computer programs be verified against the results obtained by other means such as (1) universally accepted closed-form solutions, (2) other previously verified computer programs, and (3) physical reasoning (the most important in the author's opinion).

4.6.3.2 Superstructures with Varying Deck Width and Splayed Girders

As noted earlier, the LRFD tabulated expressions for distribution factors are based on the assumption of a deck having a constant width. In some cases, a bridge deck may have varying width and supported over *splayed* girders. Where moderate deviations from a constant deck width or parallel beams exist, a rational approach may be used to extend LRFD provisions (Art. 4.6.2.2) for determining the distribution factors. According to LRFD *Commentary C4.6.2.2.1*, the distribution factors for live load at any point along the span may be calculated by setting the girder spacing in the equations of this article equal to half the sum of center-to-center distance between the girder under consideration and the two girders to either side. This will result in a variable distribution factor along the length of the girder. However, it is cautioned that when cross-checking this value of distribution factor by another method (such as computer programs discussed in the preceding paragraph), it may not be always possible to compare this value of distribution factor as the latter may only allow a constant value of distribution factor.

www.EngineeringEBooksPdf.com

4.6.4 Influence of Multiple Loaded Lanes

4.6.4.1 Number of Design or Traffic Lanes on a Bridge

The terms *design lane* and *traffic lane* were introduced in Section 2.5.2 in the context of defining *bridge width*. There are two questions that always concern a bridge designer/analyst when dealing with live load on a bridge deck: (1) How many design or traffic lanes should be considered to be simultaneously present on a bridge deck? (2) How to distribute live load due to these multiple design/traffic lanes to the girders supporting a deck? The specification provided by LRFD Art. 3.6.1.1.1 should be followed in this regard:

1. Ideally, the standard width of a design lane is to be 12 ft. Wherever possible, bridges should be built to accommodate the standard design lane and appropriate shoulders. The number of design lanes (N_L) on a bridge deck is obtained by dividing the clear roadway width (w, ft) between curbs and/or barriers by 12 and taking the integer part of the ratio $w/12$.
2. Where the traffic lanes are less than 12 ft wide, the following stipulations apply:
   a. In cases where the traffic lanes are less than 12 ft wide, the number of design lanes is to be taken as equal to the number of actual traffic lanes and width of the design lane as equal to the width of the actual traffic lane.
   b. In the case of roadway widths from 20 to 24 ft, two design lanes, each equal to one-half the roadway width, should be assumed for analysis.

4.6.4.2 Influence of Multiple Design/Traffic Lanes on Girders Supporting the Deck

Most bridges are built to accommodate at least two design/traffic lanes; those in the urban areas and at the interchanges for more than two. Bridges connecting interstate highways near large metropolitan areas might carry 4–6 design/traffic lanes. All of these design lanes may or may not be simultaneously loaded (i.e., occupied by vehicular traffic). To account for the presence of live load in one design/traffic lane only, or simultaneously in two or more lanes, expressions for distribution factors are listed (in a tabular form, see Tables 4.A.3 through 4.A.6) in LRFD Specifications for two load cases: (1) one design lane loaded and (2) two or more design lanes loaded. The tabularized expressions were derived with due consideration for the effects for coincidental loading in one or more design/traffic lanes. In other words, the LRFD expressions for distribution factors are based on the evaluation of several combinations of loaded lanes with their appropriate multiple presence factors and represent the worst-case scenario. Therefore, when using the tabularized expressions for distribution factors, the following rules (LRFD Art. 3.6.1.1.2) should be observed:

1. The multiple presence factors are *not* to be applied to distribution factors calculated from these tabularized expressions (LRFD Art. 4.6.2.2.1). Distribution factors should be calculated for both loading conditions and the more critical of the two values should be used for design.
2. The multiple presence factors (Table 4.1) are to be applied when using (i) the lever rule (Section 4.6.2), (ii) the special requirements for the exterior girders assuming rigid body rotation of the bridge cross section (LRFD Art. 4.6.2.2.2d), and (iii) refined analysis. Readers should refer to LRFD *Commentary C3.6.1.1.2* for more discussion on this topic.
3. The multiple presence factors are *not* be applied when calculating distribution factors for investigating fatigue limit loads. This is because the fatigue limit loads are determined for one lane only loaded condition for which the multiple presence factor is 1.2. Because the tabularized *DF* expressions for one lane–loaded condition have 1.2 factor embedded in them, it should be removed from the expression (by dividing by 1.2) for the purpose of fatigue investigation (discussed further in Section 4.10).
4. It is noted that the distribution factor for the case of two design lanes loaded is usually greater than that for more than two design lanes loaded. Therefore, the influence of more than two loaded lanes on distribution factors is nongoverning.

www.EngineeringEBooksPdf.com

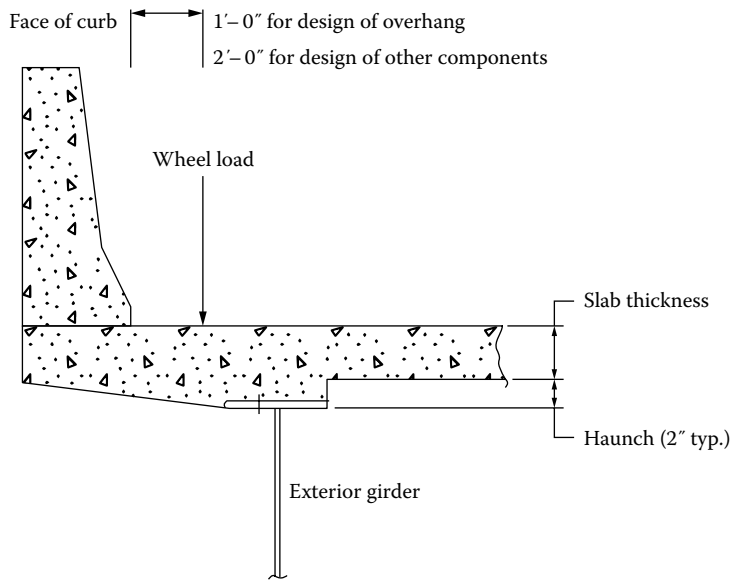

FIGURE 4.7 Specific positions of wheel loads on a bridge deck for design of the overhang and other components.

4.6.4.3 Position of Wheel Loads on Bridge Deck with respect to Girders

The design live load for a bridge deck overhang or a supporting girder is influenced by the position of the wheel loads of the exterior truck relative to the distance from the traffic barrier and the position of the girder. The distribution factors listed in LRFD Specifications are based on the following fixed positions (see Figure 4.7) of exterior wheel load of the design truck on the deck (LRFD Art. 3.6.1.3.1):

1. Design of deck overhang: 1.0 ft from the face of the curb or railing
2. Design of all other components: 2 ft from the face of the curb or railing

4.7 CALCULATIONS OF DISTRIBUTION FACTORS FOR BEAMS/GIRDERS OF TYPICAL SUPERSTRUCTURES

4.7.1 Formulas for Distribution Factors

LRFD Specifications provide the following tables of formulas for distribution factors for bending moment and shear in the interior and exterior girders and for the skew correction factors. These tables are referred to in the discussion in the remainder of this chapter; they are reproduced at the end of this chapter for ready reference.

4.7.2 Distribution Factors for Interior Girders

Distribution factors for bending moment and shear in the interior girders are determined from the following procedures.

4.7.2.1 Bending Moment

4.7.2.1.1 Slab-Beam-Type Superstructures

Superstructure Types (a), (e), (k), and also Types (i) and (j) (if sufficiently connected to act as a single unit) are called slab-beam (or slab-girder) type superstructures. Expressions for distribution

www.EngineeringEBooksPdf.com

factors for bending moments in interior girders (g_{mi}) are given in LRFD Table 4.6.2.2.2b-1; those with corrugated steel plank decks are given in LRFD Table 4.6.2.2.2c. These tables make a cross-reference to the typical bridge superstructures shown in LRFD Table 4.6.2.2.2-1. Distribution factors are listed for two load cases:

1. One design lane loaded
2. Two or more design lanes loaded

It is important to recognize that in most cases of superstructures having a deck supported by a group of parallel girders, the distribution factors are functions of several variables including the span. This is a significant deviation from distribution factors specified in AASHTO Standard in which the distribution factors were not functions of the span (they were functions of average spacing between the adjacent beams). For uniformity in interpretation and application, LRFD Art. C4.6.2.2.1 defines the span length, L, as listed in Table 4.2.

Expressions for distribution factors specified in LRFD Art. 4.6.2.2.2 (for bending moment) and Art. 4.6.2.2.3 (for shear) have been derived based on the following assumptions (LRFD Art. 4.6.2.2.1):

1. The bridge cross section conforms to one of the superstructure types shown in LRFD Table 4.6.2.2.2-1.
2. The bridge deck has *constant* width.
3. There are at least *four* beams supporting the deck.
4. Beams are parallel and have approximately the same stiffness (EI).
5. The roadway part of the overhang, d_e (distance between the inside face of the curb and the centerline of the exterior web of the *exterior* girder), does not exceed 3.0 ft.
6. Curvature in plan is less than the limit specified in LRFD Art. 4.6.12.

It is to be noted that equal spacing of parallel girders is not one of the requirements for using the approximate methods discussed in this chapter. However, it is common practice to support the deck over equally spaced parallel girders; this simplifies both design and detailing.

LRFD Table 4.6.2.2.2-1 lists 12 different types of bridge superstructure systems (several combinations of *deck* types and the *beam* types) that are commonly used for highway bridges in the United States and elsewhere in the world. These are discussed in Table 2.1. These expressions are subject to certain limitations as suggested by the *range of applicability* of various tabulated expressions

TABLE 4.2
Span Length, *L* (ft), for Use in Expressions for Live Load Distribution Factor

Force Effect	Length, *L* (ft)
Positive bending moment	The length of span for which bending moment is being calculated
Negative bending moment—near interior supports of continuous spans from point of contraflexure to point of contraflexure under a uniform load on all spans	The average length of two adjacent spans
Negative bending moment—other than near interiors supports of continuous spans	The length of span for which bending moment is being calculated
Shear	The length of span for which bending moment is being calculated
Exterior reaction	The length of the exterior span
Interior reaction of continuous span	The average length of two adjacent spans

www.EngineeringEBooksPdf.com

(listed in the tables). However, there may be practical situations where the aforementioned requirements are not met. In cases where moderate deviations from a constant width or parallel beams exist, LRFD Art. 4.6.2.2.1 recommends the following:

1. Varying the distribution factor at selected locations along the span
2. Using expressions in tables of distribution factors in conjunction with a suitable value for beam spacing

For example, Equations 4.2 and 4.3 are expressions for distribution factors for bending moments in the interior girder of superstructures Types (a), (e), (k), etc. (characterized as typical slab-beam bridges):

One design lane loaded:

$$g_{mi1} = 0.06 + \left(\frac{S}{14}\right)^{0.4} \left(\frac{S}{L}\right)^{0.3} \left(\frac{K_g}{12Lt_s^3}\right)^{0.1} \tag{4.2}$$

Two or more design lanes loaded:

$$g_{mi2} = 0.075 + \left(\frac{S}{14}\right)^{0.6} \left(\frac{S}{L}\right)^{0.2} \left(\frac{K_g}{12Lt_s^3}\right)^{0.1} \tag{4.3}$$

where

g_{mi1} = distribution factor for bending moment for the interior girder for one lane loaded case
g_{mi2} = distribution factor for bending moment for the interior girder for two lanes loaded case
S = average spacing between the parallel girders supporting the deck (ft)
L = span (ft)
t_s = thickness of concrete deck (in.) *not* including the integral wearing surface
K_g = longitudinal stiffness parameter (in.^{4} units)

The value of K_g is given by Equation 4.4:

$$K_g = n\left(I + Ae_g^2\right) \tag{4.4 [A4.6.2.2.1-1]}$$

where

$n = E_B/E_D$
E_B = modulus of elasticity of the beam material (ksi)
E_D = modulus of elasticity of the deck material (ksi)
A = area of cross section of the noncomposite girder (in.^{2})
I = bending moment of inertia of noncomposite girder (in.^{4})
e_g = girder eccentricity
= distance between the middle surface of deck slab and the centroidal axis of the noncomposite girder (see Figure 4.8)
= 0 for noncomposite construction

Parameters A and I in Equation 4.4 are for the noncomposite section of the beam. The distance e_g is measured from the centroidal axis of the basic beam to the (geometric) middle surface of the

www.EngineeringEBooksPdf.com

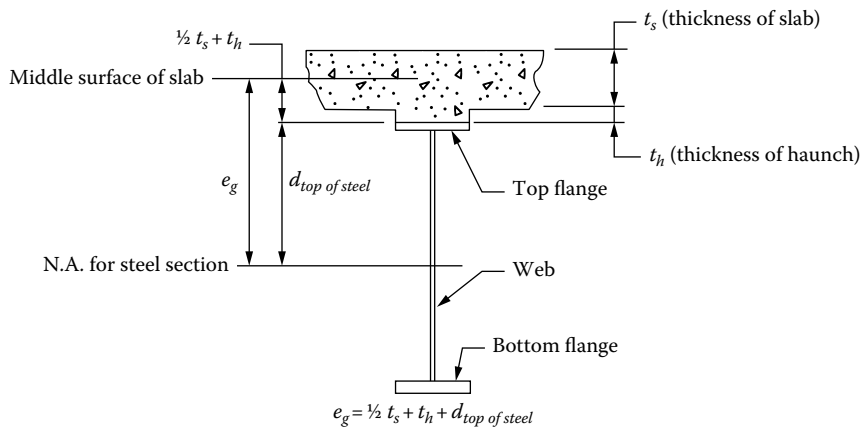

FIGURE 4.8 Definition of e_g in Equation 4.4. For noncomposite construction, $e_g = 0$.

slab (not including the thickness of the wearing surface of any kind); contribution of the wearing surface, even if integral, is ignored for the purpose of structural calculations.

Attention should be paid to units used for various parameters in the last parenthetical quantity in Equations 4.2 and 4.3, which contains the longitudinal stiffness parameter, K_g, defined by Equation 4.4 (its units are in.[4]). Note that the units of K_g and the deck slab thickness (t_s) are in inches, whereas the units of span length (L) are in feet; the multiplier 12 in the denominator of this term converts L from feet to inches.

The expressions containing the longitudinal stiffness parameter, K_g, similar to the last parenthetical quantity in Equations 4.2 and 4.3 (the stiffness term), appear in expressions for distribution factors for several superstructure types (LRFD cross-sectional Types (a), (e), (k), and also (i) and (j), if sufficiently connected as a unit) in the form of $K_g \big/ \left(12.0Lt_s^3\right)$. Note that the value of this parameter depends on the section properties of the deck slab and the girder, so a preliminary superstructure cross section must be assumed for the determination of K_g. Because the stiffness of the girder is not known *a priori*, older LRFD Specifications (Art. 4.6.2.2.2b) permitted assuming the value of the terms containing K_g as unity for preliminary design. This provision was deleted from later editions. Instead, Art. 4.2.2.2.1, with the owner's concurrence, permits the use of constant values of these terms as shown in Table 4.3.

The value of K_g given by Equation 4.4 raises some interesting questions when a designer is faced with the following conditions:

1. Bridges in which the girder section is not constant for the entire span
2. Continuous span bridges when spans are unequal but girder sections are constant in all spans
3. Continuous bridges when spans are unequal and girder sections are not constant in all spans

In the case of a single-span bridge, one option is to calculate the value of K_g for the maximum positive bending moment region in the span. In the case of simple or continuous span bridges, when the girder sections are not constant, one option would be to calculate separate values of K_g for each span based on the average or weighted average of properties along each span in the positive bending moment region. The other option would be to calculate K_g based on the actual section properties of the girder at each change of section, which would result in a variable value of

www.EngineeringEBooksPdf.com

TABLE 4.3
Constant Values of the Term $K_g/\left(12.0Lt_s^3\right)^x$ for Use in Equations for Distribution Factors

		Simplified Value			
		Superstructure Type			
Equation Parameters	**AASHTO LRFD Table Reference**	***a***	***e***	***k***	***f, g, i, j***
$\left(\frac{K_g}{12.0Lt_s^3}\right)^{0.1}$	4.6.2.2.2b-1	1.02	1.05	1.09	—
$\left(\frac{K_g}{12.0Lt_s^3}\right)^{0.25}$	4.6.2.2.2e-1	1.03	1.07	1.15	—
$\left(\frac{K_g}{12.0Lt_s^3}\right)^{0.3}$	4.6.2.2.3c-1	0.97	0.93	0.85	—
$\frac{I}{J}$	4.6.2.2.2b-1 4.6.2.2.3a-1	—	—	—	$0.54\left(\frac{d}{b}\right)+0.16$

Source: From *AASHTO LRFD Bridge Design Specifications*, Copyright © 2012 by American Association of State Highway and Transportation Officials, Washington, DC. Used by permission.

distribution factor along each span. However, it is found that the distribution factor is generally not very sensitive to the value of K_g that is assumed in such cases.

It is noteworthy that Equation 4.4 was developed for composite sections. For noncomposite design, it may be justifiable to use the bending moment of inertia of the basic girder, I, instead of the stiffness parameter $n\left(I+Ae_g^2\right)$, because the effective value of the term e_g in a noncomposite cross section is zero (Nutt et al. 1988, p. 136, E-27).

Equation 4.4 is a function of the modular ratio, n, which is defined by Equation 4.5:

$$n=\frac{E_{beam\ material}}{E_{deck\ material}}=\frac{E_B}{E_D} \tag{4.5}$$

For the most common slab-girder type superstructures, the bridge deck consists of reinforced concrete so that n can be defined by Equation 4.6:

$$n=\frac{E_B}{E_c} \tag{4.6}$$

For most common slab-steel girder-type superstructures, the bridge consists of reinforced concrete deck and steel girders, so n can be defined by Equation 4.7:

$$n=\frac{E_s}{E_c} \tag{4.7}$$

where

E_B = modulus of elasticity of beam material, ksi
E_D = modulus of elasticity of deck material, ksi
E_c = modulus of elasticity of concrete, ksi
E_s = modulus of elasticity of steel = 29,000 ksi

www.EngineeringEBooksPdf.com

TABLE 4.4
Values of Short-Term Modular Ratio, *n*, for a Range of f'_c Values

Range of f'_c Values, ksi	Short-Term[a] Modular Ratio, *n*
$2.4 \le f'_c \le 2.9$	10
$2.9 \le f'_c \le 3.6$	9
$3.6 \le f'_c \le 4.6$	8
$4.6 \le f'_c \le 6.0$	7
$6.0 \le f'_c$	6

[a] For long-term effects from loads, the value of n is taken as $3n$ to account for *creep*.

The value of the modulus of elasticity of concrete, E_c, may be determined from Equation 4.8:

$$E_c = 33{,}000 K_1 w_c^{1.5} \sqrt{f'_c} \qquad (4.8)\ [A5.4.2.4\text{-}10]$$

where

K_1 = correction factor for source of aggregate, to be taken as 1.0 unless determined from physical tests and approved by jurisdiction
w_c = unit weight of concrete
= 0.145 kip/ft^3 for normal weight concrete
f'_c = 28-day compressive strength of concrete, ksi

For normal weight concrete, w_c = 0.145 kip/ft^3; the value of E_c for such concrete can be determined from Equation 4.9 by substituting this value in Equation 4.7 resulting in Equation 4.8 (the number 1820 results from rounding off the actual value 1822.07).

$$E_c = 1820\sqrt{f'_c}\ \text{ksi} \qquad (4.9)\ [AC5.4.2.4\text{-}1]$$

When beams/girders are made from steel, $E_B = E_s$ = 29,000 ksi. It is often permissible to round-off the value of the modular ratio, n (Equation 4.7), to the nearest integer without any appreciable error. LRFD Art. 6.10.1.1.1b-1 permits using integer values of the short-term modular ratio, n, for various values of f'_c as shown in Table 4.4.

Example 4.2 presents calculations for determination of quantities e_g and K_g appearing in Equation 4.4.

Example 4.2

Figure 4.9a shows the bridge cross section of Type (a) (slab-beam type) superstructure. Calculate quantities e_g and K_g for this superstructure. Assume a 2 in. typical haunch over the girder, f'_c = 4000 psi.

Solution

Figure 4.9b shows the typical girder cross section taken from the superstructure shown in Figure 4.9a. First, determine the elastic neutral axis of the steel section. These calculations are shown in Table 4.5. The datum is chosen at the bottom of the steel section.

$$y_{bot\ of\ steel} = \frac{654.3}{44.75} = 14.62\ \text{in.}$$

$$y_{top\ of\ steel} = 0.75 + 36.0 + 1.25 - 14.62 = 23.38\ \text{in.}$$

www.EngineeringEBooksPdf.com

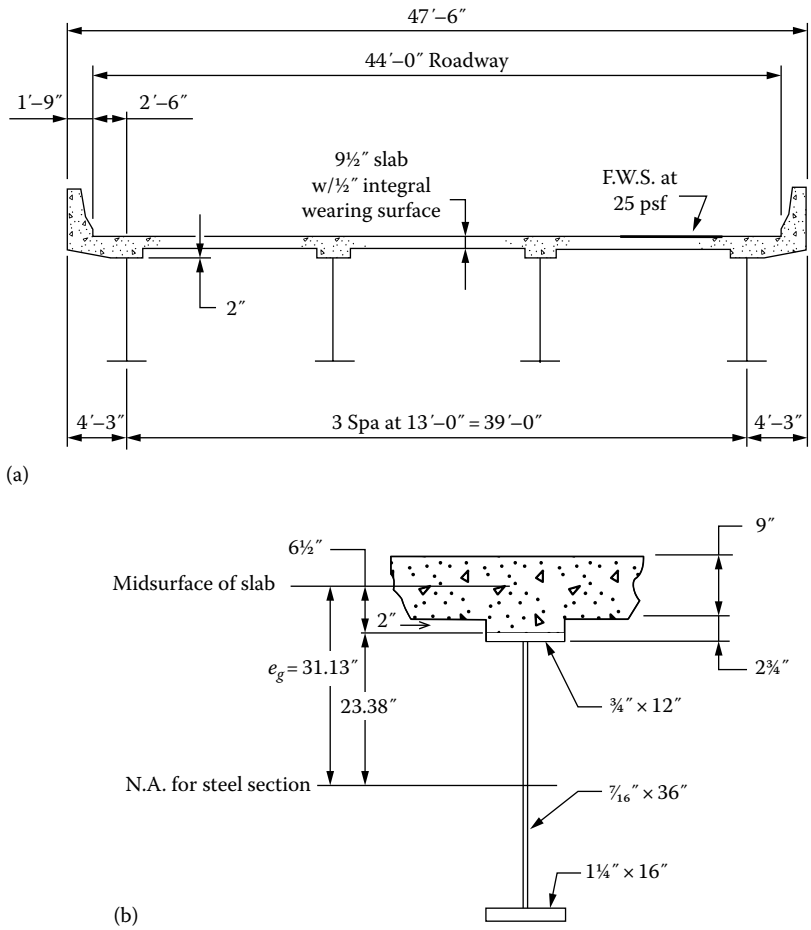

FIGURE 4.9 (a) Bridge cross section for Example 4.2. (b) Girder cross section for Example 4.2. (Courtesy of AISI.)

TABLE 4.5
Calculations for the Elastic Neutral Section for Steel Section for Example 4.2

Component	A, in.^{2}	y, in.	Ay, in.^{3}	$\bar{y}$, in.	$A\bar{y}^2$, in.^{4}	I_o, in.^{4}	I, in.^{4}
Top flange 3/4″ × 12″	9.0	37.625	338.6	23.005	4763	—	4,763
Web 7/16″ × 36″	15.75	19.25	303.2	4.63	338	1701	2,039
Bottom flange 1 1/4 × 16″	20.0	0.625	12.5	13.995	3917	3	3,920
Σ	44.75		654.3		9018	1704	10,722

$\bar{y}$ = distance between the centroid of the composite section and the centroid of the element
e_g = distance between the centers of gravity of the deck and the basic beam
= distance between the mid-surface of the slab to the elastic neutral axis of the steel section
= ½ × 9.0 + 2.75 + 23.38 = 30.63 in.

Distance e_g is shown in Figure 4.10.
Calculate the longitudinal stiffness parameter, K_g. For f'_c = 4000 psi, n = 8 (Table 4.4).

$$K_g = n\left(I + Ae_g^2\right) = 8\left[10{,}722 + 44.75\left(30.63\right)^2\right] = 421{,}650 \text{ in.}^4$$

www.EngineeringEBooksPdf.com

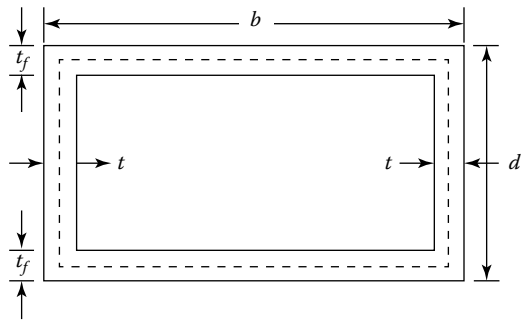

FIGURE 4.10 St. Venant torsion constant, *J*, for thin-walled box beams.

4.7.2.1.2 Superstructures with Torsionally Stiff Cross Sections

Multibeam deck superstructures such as Types (f) and (g) (if sufficiently connected to act as a single unit) represent torsionally stiff superstructures. The quantity *I/J* appears in the expressions for the distribution factors for the beams of these superstructures as given by Equations 4.10 and 4.11:

For one design lane loaded:

$$DF = k\left(\frac{b}{33.3L}\right)^{0.5}\left(\frac{I}{J}\right)^{0.25} \tag{4.10}$$

For two or more design lanes loaded:

$$DF = k\left(\frac{b}{305L}\right)^{0.65}\left(\frac{b}{12.0L}\right)\left(\frac{I}{J}\right)^{0.25} \tag{4.11}$$

where

$k = 2.5(N_b)^{-0.2} \geq 1.5$ (LRFD Table 4.6.2.2.2b-1)
N_b = number of breams supporting the bridge
J = St. Venant's torsional bending moment of inertia (or polar bending moment of inertia)

In lieu of more refined analysis, the St. Venant torsional bending moment of inertia, *J*, may be evaluated from the following expressions as suggested by Kollbrunner and Basler (1969):

For thin-walled open sections:

$$J = \frac{1}{3}\sum bt^3 \qquad \text{(4.12) [AC4.6.2.2.1-1]}$$

For stocky open sections, for example, prestressed I-beams, T-beams, etc., and solid sections:

$$J = \frac{A^4}{40.0I_p} \qquad \text{(4.13) [AC4.6.2.2.1-2]}$$

www.EngineeringEBooksPdf.com

For closed thin-walled sections, the value of torsional constant is given by Bredt's formula, which is expressed as Equation 4.14:

$$J = \frac{4A_o^4}{\oint \frac{ds}{t(s)}} \tag{4.14}$$

where $\oint \frac{ds}{t(s)}$ = contour integral along the centerline of s of the reciprocal value of the wall thickness $t(s)$.

If the hollow cross section is built up of n parts, each with a constant thickness t_i (e.g., a rectangular hollow section), then the integral may be replaced by the sum given by Equation 4.15:

$$\oint \frac{ds}{t} = \sum_{i=1}^{n} \frac{s_i}{t_i} \tag{4.15}$$

For the case of a constant wall thickness t all along the circumference of length u, the value of integral given by Equation 4.15 becomes

$$\oint \frac{ds}{t} = \frac{u}{t} \tag{4.16}$$

Substitution of Equation 4.15 into 4.14 results in Equation 4.17:

$$J = \frac{4A_o^2}{\sum \frac{s}{t}} \qquad \text{(4.17) [AC4.6.2.2.1-1]}$$

where

I = bending moment of inertia of beam (in.^{4})
b = width of placement (in.)
t = thickness of plate-like element (in.)
A = area of cross section (in.^{2})
I_p = polar bending moment inertia (in.^{4})
A_o = area enclosed by centerlines of elements (in.^{2})
s = length of a side element (in.)

For closed, thin-walled, rectangular sections (e.g., box beams), area A_o can be determined with reference to Figure 4.10 as follows:

$$\begin{aligned} A_o &= (\text{Average width})(\text{Average depth}) \\ &= (b-t)(d-t_f) \end{aligned} \tag{4.18}$$

$$\begin{aligned} \sum \frac{s}{t} &= 2\left[\left(\frac{b-t}{t_f}\right)+\left(\frac{d-t_f}{t}\right)\right] \\ &= 2\left(\frac{bt+dt_f-t^2-t_f^2}{tt_f}\right) \end{aligned} \tag{4.19}$$

www.EngineeringEBooksPdf.com

Substitution of Equations 4.18 and 4.19 in Equation 4.17 in Equation 4.14 yields Equation 4.20:

$$J = \frac{4tt_f(b-t)^2(d-t_f)^2}{\left(bt + dt_f - t^2 - t_f^2\right)} \tag{4.20}$$

For preliminary design, the value of quantity (I/J) in Equations 4.10 and 4.11 may be taken as unity (LRFD Art. 4.6.2.2.2b).

In addition to the aforementioned limitations, LRFD Art. 4.6.2.2.2b requires providing deep, rigid, *end* diaphragms in superstructures consisting of concrete deck and concrete girders to ensure proper load distribution laterally. Essentially, the provision of diaphragms, which connect parallel beams at certain intervals, is made to ensure that the entire superstructure acts as an integral unit so that the supporting beams participate collectively in receiving the load from the deck.

4.7.2.2 Live Load Distribution Factors for Shear

Expressions for the distribution factors for shear in the interior beams of different types of superstructures are given in LRFD Table 4.6.2.2.3a (see Appendix for these tables). As in the case of bending moment, expressions are given for the two load cases: (1) one design lane loaded and (2) two or more design lanes loaded. A general discussion presented in the preceding paragraph applies also to the distribution factors for shear.

For interior beams not listed in LRFD Table 4.6.2.2.3a-1, lateral distribution of the wheel or axle adjacent to the end span shall be that produced by the lever rule (Art. 4.6.2.2.3).

For concrete box beams used in multibeam decks, if the values of I and J do not comply with the limitations in Table 4.6.2.2.3a-1, the distribution factor for shear may be taken as that for bending moment (Art. 4.6.2.2.3).

4.7.3 Live Load Distribution Factors for Exterior Girders

4.7.3.1 Influence of Diaphragms on Distribution Factors for Exterior Girders

The concept of *diaphragms* was introduced in Section 2.4. As a general construction practice, end diaphragms or cross-frames would be provided when any of the multigirder cross sections (Types (a), (e), and (k), in LRFD Table 4.6.2.2.1-1 or Table 2.1) are used for superstructures. The procedure presented in this section was developed for the determination of distribution factors for shear and bending moment in the exterior girders without considering the presence of end diaphragms or cross-frames. Therefore, an additional investigation is required for determining distribution factors for the exterior girders of cross-sectional Types (a), (e), and (k). This procedure, often referred to as *special analysis* and presented in Section 4.8, is recommended until further research becomes available.

4.7.3.2 Distribution Factors for Bending Moment

Provisions for determining *DF*s for bending moments in exterior girders (g_{me}) are specified in LRFD Art. 4.6.2.2.2d. Expressions for distribution factors for the different superstructure types are listed in LRFD Table 4.6.2.2.2d-1 (see Appendix for these tables).

The distribution factor for live load bending moment in an exterior girder for selected superstructure types may be obtained by adjusting the distribution factor for interior girder, g_{mi} (for the same load case), specified in the table. The *adjustment factor* is designated e, which is a function of the overhang distance d_e. The distribution factor for bending moment in an exterior girder is obtained by multiplying g_{mi} (distribution factor for the interior girder) with the adjustment factor e. For some superstructure types ((a), (b), (c), (e), (k), and (i) and (j) if sufficiently connected to act as a single unit that they usually are), the adjustment factor is applicable for two or more lanes loaded case only while for other Types ((f) and (g)), it is applicable for both cases—one lane loaded and two or more lanes loaded.

www.EngineeringEBooksPdf.com

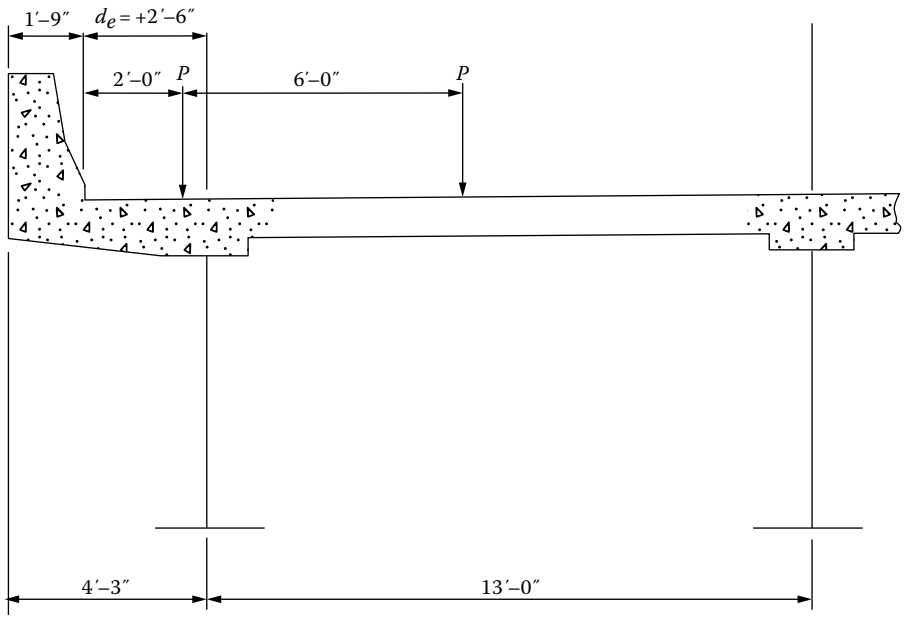

FIGURE 4.11 Definition of distance d_e; it is the distance between the edge of the curb or the traffic barrier and the web of the exterior girder. d_e is positive in this figure as the web of the exterior girder is inboard of the edge of the curb or traffic barrier. (d_e would be negative if the exterior girder web would be outboard of the curb or the traffic barrier.) Note that the exterior wheel of the exterior lane is placed at 2 ft (minimum distance) from the inside edge of the curb or the traffic barrier.

For a given bridge cross section, distance d_e is a fixed distance. It is defined as the horizontal distance from the centerline of the exterior web of the exterior girder at the deck level to the interior edge of the curb or traffic barrier (Figure 4.11). It may be taken as positive or negative, depending on the position of the edge of the exterior lane with respect to the centerline of the exterior girder:

1. Positive if the edge of the exterior lane is outside of the (centerline of) exterior girder (as in the examples presented in this chapter).
2. Negative if the edge of the exterior lane is to the interior side of the exterior girder.

For example, for distribution factors for bending moment in the exterior longitudinal girders in bridge superstructure Types (a), (e), (k), etc., LRFD Table 4.6.2.2.d-1 lists the following for the two or more design lanes loaded case:

$$g = eg_{interior} \tag{4.21}$$

where

$$e = 0.77 + \frac{d_e}{9.1} \tag{4.22}$$

where d_e = horizontal distance from the centerline of the exterior web of the exterior girder to the interior edge of the curb or traffic barrier (Figure 4.11); it is subject to a range of

$$-1.0 \le d_e \le 5.5 \text{ ft} \tag{4.23}$$

www.EngineeringEBooksPdf.com

LRFD Table 4.6.2.2.2d-1 specifies using *lever rule* (described earlier) for determining the distribution factors for the exterior girders for certain superstructure types. When using the lever rule on the exterior girder of a bridge that is being supported by three or more girders, the supported element is assumed simply supported over the exterior girder and the adjacent interior girder (Figure 4.4). It is a notional model that is simple and convenient for the determination of distribution factor for the exterior girders (LRFD *Commentary C4.6.6.1*).

It is important to recognize that bridges may be widened in the future to provide for additional traffic lanes, a real possibility. If that happens, the exterior girder of the existing superstructure would become an interior girder. For this reason, LRFD Art. 2.5.2.7.1 and 4.6.2.2.1 require that *the load carrying capacity of the exterior girders of multibeam bridge superstructures, irrespective of the methods of analyses (approximate or refined) used, be not less than the load carrying capacity of the interior girders. Accordingly, the distribution factors for the exterior beams may not be smaller than those for the interior beams.*

4.7.3.3 Distribution Factors for Shear

Provisions for determining live load distribution factors for shear in exterior girders of superstructures are specified in LRFD Art. 4.6.2.2.2d. Expressions for distribution factors for different superstructure types are listed in LRFD Table 4.6.2.2.3b-1 (see Appendix for these tables).

As for the case of distribution factor for bending moment, the distribution factor for shear in an exterior girder for the *two or more design lanes loaded* case may be obtained by adjusting the distribution factor for bending moment for the interior girder, g (for the same load case), specified in LRFD tables. Several of these expressions also contain the quantity (distance), d_e (discussed in the preceding paragraph and which has different applicable range for different types of superstructures), required to calculate the *adjustment factor e*, to be applied to the calculated value of g (distribution factor for the interior girder). Discussion on the adjustment factor, e, in the preceding paragraph applies to the distribution factor for shear also.

For example, for the distribution factors for shear in the exterior longitudinal girders in bridge superstructure Types (a), (e), (k), etc., Table 4.6.2.2.d-1 (see Table 4.A.1) specifies Equation 4.22 for the two or more design lanes loaded case:

$$g = eg_{interior} \tag{4.24}$$

where

$$e = 0.6 + \frac{d_e}{10} \tag{4.25}$$

where

e = distribution correction factor

d_e = horizontal distance from the centerline of the exterior web of the exterior girder to the interior edge of the curb or traffic barrier (Figure 4.11) and is subject to a range of

$$-1.0 \le d_e \le 5.5 \text{ ft} \tag{4.26}$$

An interesting but important observation is to be made in the context of the expressions for the distribution factors for bending moment and shear in the exterior beams of the superstructure Type (g) (concrete box beams used in multibeam decks, also called *adjacent box beam decks*). Distribution factors for bending moment in the exterior girder of this type of superstructure

www.EngineeringEBooksPdf.com

are to be calculated from Equation 4.22, where the value of the adjustment factor e is to be calculated as follows:

1. One design lane loaded:

$$e = 1.125 + \frac{d_e}{30} \geq 1.0 \tag{4.27}$$

2. Two design lanes loaded:

$$e = 1.04 + \frac{d_e}{25} \geq 1.0 \tag{4.28}$$

Similarly, the distribution factor for shear in the exterior girder of this type of superstructure is to be calculated from Equation 4.24, where the value of the adjustment factor e is to be calculated as follows:

1. One design lane loaded:

$$e = 1.25 + \frac{d_e}{20} \geq 1.0 \tag{4.29}$$

2. Two design lanes loaded:

$$g = eg_{interior}\left(\frac{48}{b}\right) \tag{4.30}$$

where it is stipulated that

$$\frac{48}{b} \leq 1.0 \tag{4.31}$$

$$e = 1 + \left(\frac{d_e + \frac{b}{12} - 2.0}{40}\right)^{0.5} \geq 1.0 \tag{4.32}$$

Equation 4.31 limits the width of box beams to not greater than 48 in. (or 4 ft) because of the practical limitations of box beam sizes (i.e., wider box beams are not used in practice). Equations 4.27 through 4.29 and 4.32 stipulate that the value of the adjustment factor, e, be equal to or greater than 1 ($e \geq 1.0$). This requirement has a very important and significant implication: it implies that *the distribution factors for bending moment and shear in the exterior girder may not be less than those for the interior girder.* Stated differently, this means that the load-carrying capacity of the exterior girder may not be smaller than that of the interior girder. In general, this statement is valid for the exterior girders of all types of superstructures.

The LRFD expressions for the distribution factors for live load shear in multibeam bridges (Types (a), (c), (k), (i), and (j)) are noteworthy in the sense that they are functions of only the spacing of beams supporting the deck, S; they are not functions of the stiffness of beams or the span of the bridge. This means that distribution factors for live load shear in steel or concrete beams, concrete T-beams and double-T-beams supporting concrete decks would be the same if their spacing is the same.

www.EngineeringEBooksPdf.com

4.8 SPECIAL ANALYSIS FOR DISTRIBUTION FACTORS FOR BENDING MOMENTS AND SHEARS IN EXTERIOR GIRDERS

When beam-slab bridge cross sections are provided with diaphragms or cross-frames, their torsional rigidity is sufficiently improved. In such cases, the distribution factor for bending moment and shear in the *exterior girders* shall not be taken less than that which would be obtained by assuming that the bridge cross section deflects and rotates a rigid cross section. Multiple presence factors specified in LRFD Art. 3.6.1.1.2 shall apply to distribution factors so determined.

This additional investigation is required because the distribution factor for girders in a multi-girder cross section (e.g., Types (a), (e), and (k) in LRFD Table 4.6.2.2.1-1) was determined without the consideration of end diaphragms or cross-frames. This procedure, often referred to as *special analysis*, is recommended until further research becomes available.

A special analysis for the determination of the distribution factors for the *exterior girder* is performed on the assumption that the entire cross section rotates as a rigid body about the longitudinal centerline of the bridge. It is a two-step procedure:

1. The reaction R on the exterior girder is calculated in terms of design lanes for one or more design lanes (in increments of one lane) loaded simultaneously as given by Equation 4.33

$$R = \frac{N_L}{N_b} + \frac{X_{ext} \sum^{N_L} e}{\sum^{N_b} x^2} \qquad (4.33)\ [\text{AC}4.6.2.2.2\text{d-}1]$$

where

N_L = number of loaded lanes (discussed earlier)

N_b = number of beams supporting the deck

X_{ext} = eccentricity of the exterior girder from the center of gravity of the pattern of girders (i.e., horizontal distance from the center of gravity of the pattern of girders to the exterior girder)

e = eccentricity of the design truck or a design lane load from the center of gravity of the pattern of girders (ft), *positive* when to the left of the center of gravity of the pattern of girders, *negative* when to the right of center of gravity of the pattern of girders

x = horizontal distance from the center of gravity of pattern of girders to each girder

For clarity, Figure 4.12 illustrates the definitions of terms X_{ext}, e, and x as defined earlier. In the case of a superstructure supported by a symmetrical pattern of girders, the center of gravity of the pattern of girders would be the same as the centerline of the bridge. Also, in Equation 4.33, R is to be calculated separately for cases of *one* and *two or more* design lanes loaded. Note that $N_L = 1$ when only one lane is loaded; $N_L = 2$ when two lanes are loaded; $N_L = 3$ when three lanes are loaded; and so on. See Examples 4.3, 4.4, and 4.8 for application details.

For calculating the distribution factors for the exterior girders according to the aforementioned procedure, the live load should be placed within the roadway width in a manner specified in AASHTO LRFD Art. 3.6.1.1.1.

1. The live loads occupying their individual lane widths are to be placed within their design lanes.
2. The design lanes are to be placed within the roadway width to maximize the wheel load reaction at the exterior girder, with the condition that *a wheel load cannot be placed closer than 2 ft from the edge of a curb or a barrier* (LRFD 3.6.1.3.1).

www.EngineeringEBooksPdf.com

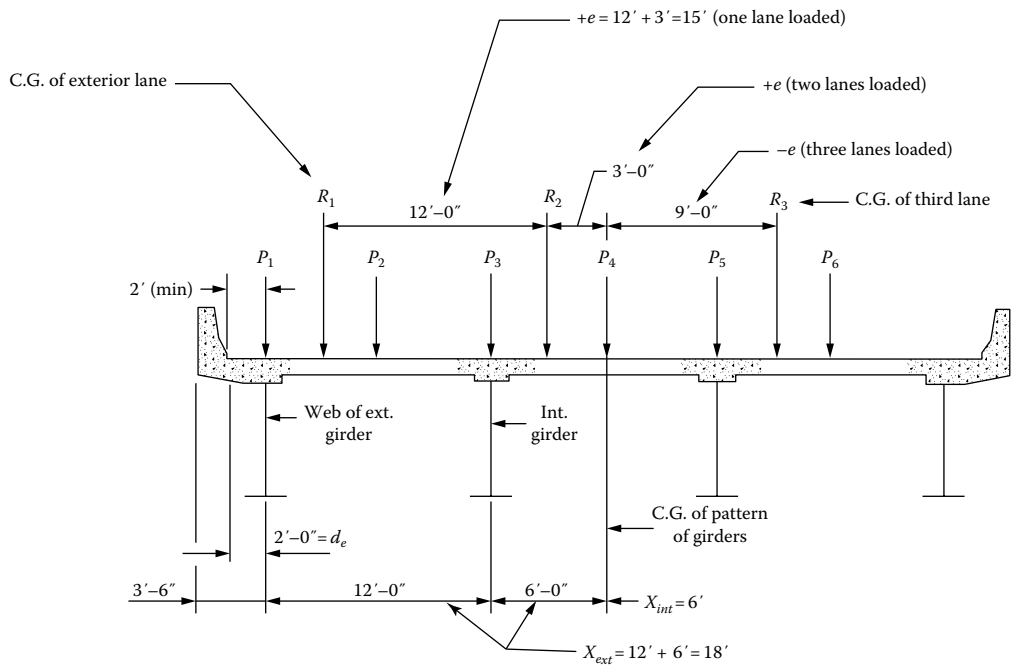

FIGURE 4.12 Definition of various parameters used in Equation 4.27 (AASHTO LRFD Eq. C4.6.2.2.2d-1). For illustrative purposes, girders in this three-lane bridge cross section are spaced equally at 12′–0″ on centers. As shown in this figure, the number of lanes, $N_L = 3$, number of beams, $N_b = 4$. Distance d_e (= 2 ft) is measured from the face of the curb or traffic barrier to the center of the exterior girder. Distance e is the eccentricity of a lane from the center of gravity of the pattern of girders. In this figure, e = 12 + 3 = 15 ft for the exterior lane, e = 3 ft for the middle lane, and e = –9 ft for the right lane. Distance x is the horizontal distance from the center of gravity of pattern of girders to each girder (= 12 ft for the exterior girder, 6 ft for the adjacent interior girder). X_{ext} is the distance from the center of gravity of the pattern of girders to the exterior girder (= 12′ + 6′).

In special analysis, design trucks (or tandems) on a deck are assumed to be placed centrally within their 12-ft-wide design lanes. While the actual transverse positions of vehicles in various design lanes can vary from this assumption of fixed spacing, a limited study has found that live load distribution factors are relatively insensitive to different vehicle spacings for both interior and exterior girders (Patrick et al. 2006).

4.9 CORRECTION FACTORS FOR BRIDGE SKEW

The expressions for calculating the distribution factors for bending moment and shear in the longitudinal girders as listed in LRFD tables are for *normal* (or *right*) bridge superstructures. Normal superstructures are those in which the longitudinal axes of the deck and those of the supporting girders are perpendicular to the orientation of supports (abutments and piers). When the longitudinal axes of the girders are not perpendicular to the orientation of supports (abutments and/or piers), the bridge is said be on a *skew*. *Angle of skew* (or *skew angle*) is defined as the acute angle between the longitudinal axes of the supporting girders and the normal to orientation of supports (see discussion in Section 2.5.3, Figure 2.25). The skew angles at the two ends of the bridge may not be the same. Bridge superstructures with longitudinal girder axes perpendicular to abutment (and/or pier) at one end but at a skew at the other end are referred to be on *half skew*; those with different skew angles at the two supports are referred to be on *trapezoidal skew*.

Skew angle is an important parameter that affects the analysis of a bridge superstructure—it can have a meaningful effect on shear and bending moments in girders supporting the deck. It has

www.EngineeringEBooksPdf.com

been suggested that for skew angles not exceeding 20° (30° for slab-beam bridges), bridges can be safely designed as normal bridges. For larger skew angles, the torsional bending moments, which are not calculated directly in simplified analysis, are large and may invalidate the results from the simplified analysis.

Effects of skew angles on distribution factors for bending moments and shear in longitudinal beams can be calculated from the expressions listed in LRFD Tables 4.6.2.2.2e-1 and 4.6.2.2.3c-1, respectively. For both bending moment and shear, the range of applicability is specified. For example, for cross-sectional Type (a), the following correction factor is specified for *DF* for bending moment:

$$\text{Correction factor} = 1 - c_1(\tan\theta)^{1.5} \tag{4.34}$$

where

$$c_1 = 0.25\left(\frac{K_g}{12.0Lt_s^3}\right)^{0.5}\left(\frac{S}{L}\right)^{0.5} \tag{4.35}$$

Equations 4.34 and 4.35 are subject to the following limitations:

If $\theta < 30°$, then $c_1 = 0$ (so that the correction factor = 1.0)
If $\theta > 60°$, then use $\theta = 60°$

The range of applicability for the aforementioned correction factor is as follows:

$$30° \le \theta \le 60°$$

$$3.5 \le S \le 16.0 \text{ ft}$$

$$20 \le L \le 240 \text{ ft}$$

$$N_b \ge 4 \text{ beams}$$

Similarly, the correction factor for *DF* for support shear at the *obtuse* corner of the bridge is given by Equation 4.36:

$$\text{Correction factor} = 1.0 + 0.20\left(\frac{12.0Lt_s^3}{K_g}\right)^{0.3}\tan\theta \tag{4.36}$$

The range of applicability for Equation 4.36 is the same as for the correction factor for the bending moment for Type (a) cross section. As noted earlier, the values of the parenthetical terms in the aforementioned equations containing the longitudinal stiffness parameter, K_g, may be taken as unity for preliminary design purposes.

The following observations are made from LRFD Tables 4.6.2.2.2e-1 and 4.6.2.2.3c-1:

1. For bending moment due to live load, the effect of skew is to *reduce* the distribution factors.
2. For shear due to live load, the effect of skew is to *increase* the distribution factors for the end shear in the exterior girder at the *obtuse* corner of the bridge. For investigating a case involving uplift in the exterior girder at the *acute* corner of the bridge, the second term in the correction factor (in LRFD Tables 4.6.2.2.2e-1 and 4.6.2.2.3c-1) should be taken as negative (LRFD C4.6.2.2.3c).
3. In all cases, the correction factors are valid for skew angle $\theta \le 60°$.

www.EngineeringEBooksPdf.com

4.10 DISTRIBUTION FACTORS FOR FATIGUE LIMIT STATE

Distribution factors are also required for fatigue limit state. For the purposes of checking the effects of fatigue on a bridge girder, the fatigue load is placed in a *single* lane.

As stated in Art. 3.6.1.1.2, multiple presence factors are not to be used for the fatigue load limit check for which only one design truck lane is used. Therefore, the distribution factors for the fatigue load limit are obtained by dividing the distribution factors for bending moment and shear for one lane loaded case by 1.2 (because the multiple presence factor for one lane loaded case = 1.2 is embedded in those expressions). If the supports are skewed, the distribution factors for fatigue should be multiplied by appropriate distribution factor for live load deflection.

4.11 DISTRIBUTION FACTORS FOR DEFLECTION LIMIT STATE

Distribution factors are also required for calculating live load deflection in beams and girders supporting a deck. But these distribution factors are *different* than those used for bending moment, shear, and fatigue limit state discussed earlier. LRFD Art. 2.5.2.6.2 requires that all design lanes be loaded when investigating absolute live load deflection of a girder supporting the deck, and that all supporting elements be assumed to deflect equally. This means that for multigirder bridges, the distribution factors for calculating the live load deflection would be equal to the number of lanes divided by the number of girders supporting the deck. Also, as stated in Art. 2.5.2.6.2, appropriate multiple presence factors from Art. 3.6.1.1.2 shall apply. Thus, the distribution factor for absolute maximum live load deflection, DF_{Δ}, can be expressed by Equation 4.37:

$$DF_{\Delta} = m\frac{N_L}{N_b} \tag{4.37}$$

Examples 4.3 through 4.8 illustrate the application of Equations 4.11 through 4.37.

4.12 ILLUSTRATIVE EXAMPLES: DISTRIBUTION FACTORS FOR BENDING MOMENT AND SHEAR

Several examples are presented as follows to illustrate the procedures for determining distribution factors for live load effects in interior and exterior girders of the most commonly used types of superstructures. Examples are presented for two-, three-, and four-lane bridges, having different girder geometries and span lengths. In all cases, it should be ensured that

1. The superstructure under consideration is one of the types listed in LRFD Table 4.6.2.2.1-1
2. The superstructure is within the range of applicability listed in applicable LRFD tables (included at the end of this chapter)

Readers should take note that formulas listed in these tables are algebraically complex equations. Due diligence should be exercised in using them for calculations.

The following is a brief summary of the examples presented in this chapter:

Example 4.3: Calculations are presented in a step-by-step format in order to clarify the intent of the LRFD Specifications in the determination of the live distribution factors for both the interior girders and the exterior girders of a straight (no skew), two-lane slab-beam bridge (superstructure Types (a), (e), and (k)). The superstructure consists of a concrete deck supported on five rolled wide flange steel beams. Also presented are calculations for the distribution factors for both fatigue and deflection limit states.

www.EngineeringEBooksPdf.com

Example 4.4: A four-lane superstructure supported on four-plate girders, having a longer span than that in Example 4.1 and also having a skew. Calculations are presented for the distribution factors for bending moment and shear in both interior and exterior girders along with skew correction factors. Also presented in this example are calculations for the distribution factors for both fatigue and deflection limit states.

Example 4.5: Calculations for the distribution factors for bending moment and shear in the interior girder of a bridge superstructure consisting of a concrete deck supported over precast–prestressed concrete I-girders (superstructure Types (a), (e), and (k)). The bridge has no skew.

Example 4.6: Calculations for a bridge superstructure consisting of AASHTO Type BIII-48 precast–prestressed adjacent box beams (superstructure Type (g)) with no skew.

Example 4.7: Calculations for distribution factors for a cast-in-place multicell concrete box beam superstructure (superstructure Type (d)) with no skew.

Example 4.8: This example is the highlight of this book. It is a three-lane superstructure supported on four-plate girders (which is the minimum number of girders specified in applicability criteria). The bridge has a skew. Calculations are presented for distribution factors for bending moment and shear in both interior and exterior girders along with skew correction factors, as well as distribution factors for fatigue and deflection. It is a special example in that it has been designed to illustrate complete design of the superstructure. Bending moments and shear, including bending moment and shear envelopes, for this bridge are calculated in great detail in Example 3.18. A complete structural design of this bridge is presented in Chapter 6.

Example 4.9: Complete calculations for distribution factors and their application to design live load bending moment for the interior girder of a slab-steel beam bridge (superstructure Types (a), (e), and (k)).

In the following calculations, letter g is used as a general notation to denote distribution factor; subscripts are used as follows to denote bending moment (m) and shear (v) in interior (i) and exterior (e) girders due to one lane (1) or two or more lanes (2) loaded:

g_{mi1} = distribution factor for bending moment in the interior girder, one design lane loaded
g_{mi2} = distribution factor for bending moment in the interior girder, two design lanes loaded
g_{vi1} = distribution factor for shear in the interior girder, one design lane loaded
g_{vi2} = distribution factor for shear in the interior girder, two design lanes loaded
g_{me1} = distribution factor for bending moment in the exterior girder, one design lane loaded
g_{me2} = distribution factor for bending moment in the exterior girder, two design lanes loaded
g_{ve1} = distribution factor for shear in the exterior girder, one design lane loaded
g_{ve2} = distribution factor for shear in the exterior girder, two design lanes loaded

Example 4.3: Distribution Factors for a Two-Lane Highway Bridge Having a Concrete Deck Supported over Wide Flange (W-Shape) Steel Girders

Figure 4.13 shows the cross section of a two-lane composite bridge for a simple span of 50 ft. The concrete deck is supported over five W30 × 90 wide flange beams spaced at 7 ft 6 in. on centers. The concrete deck is 8 in. thick including a ½ in. thick integral wearing surface (Figure 4.14). Assuming f'_c = 4000 psi, a 2 in. haunch and composite construction, determine the live load distribution factors for the following:

a. Bending moment and shear for interior and exterior girders
b. For fatigue limit state
c. Absolute maximum live load deflection

www.EngineeringEBooksPdf.com

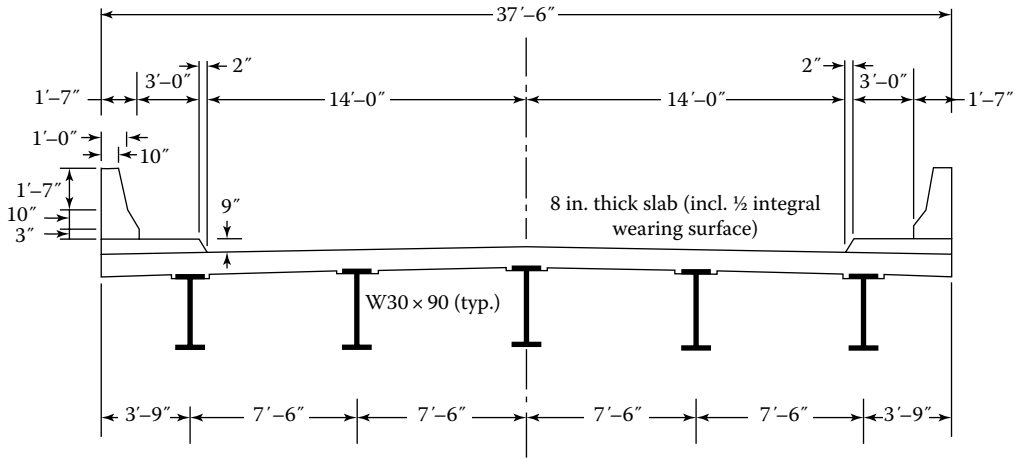

FIGURE 4.13 Cross section of slab-WF steel beam bridge.

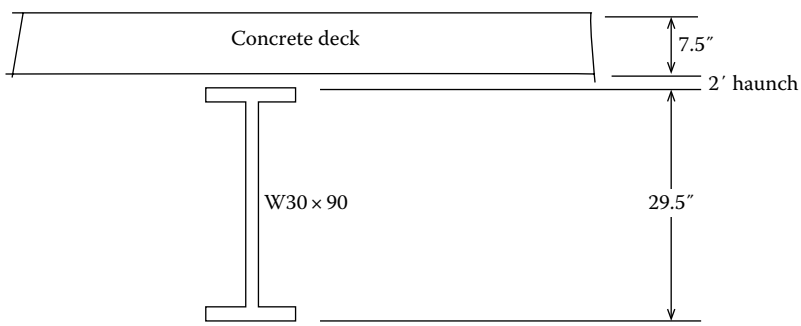

FIGURE 4.14 Details of the girder cross section.

The following calculations are presented in a step-by-step format:

a. Interior girder

1. Distribution factors for bending moment

Step 1: Check if the superstructure type conforms to one of the types listed in LRFD Table 4.6.2.2.1-1.

The given superstructure has cross section of Type (a) listed in LRFD Table 4.6.2.2.1-1. Hence, the expressions for distribution factors listed in LRFD Table 4.6.2.2.2b-1 can be used.

Step 2: Check the range of applicability in LRFD Table 4.6.2.2.2b-1.

Girder spacing, $S = 7.5$ ft	$3.5 \le S \le 16.0$ ft, OK
Slab thickness, $t_s = 8.0 - 0.5 = 7.5$ in.	$4.5 \le t_s \le 12.0$ in., OK
Span = 50 ft	$20 \le L \le 240$ ft, OK
Number of beams, $N_b = 5$	$N_b \ge 4$, OK
$K_g = 151{,}899$ in.^{4} (see step 4)	$10{,}000 \le 117{,}300 \le 7{,}000{,}000$, OK

The range of applicability is satisfied.

Step 3: Calculate the number of traffic design lanes, N_L.

$$\text{Clear roadway width, } w = 28 \text{ ft}$$

$$N_L = \text{integer part of } w/12 = 28/12 = 2.33, \text{ use } N_L = 2$$

www.EngineeringEBooksPdf.com

Step 4: Calculate the value of the longitudinal stiffness parameter, K_g.
Thickness of slab excluding the integral wearing surface = 8.0 − 0.5 = 7.5 in.

Calculate the distance from the mid-plane of deck slab to centroidal line of noncomposite steel girder, e_g.

Thickness of haunch = 2 in. above the top flange

For W30 × 90, depth of steel section: d = 29.5 in.

Area of cross section: A = 26.3 in.^{2}

Distance from the mid-surface of the slab to the neutral axis of steel section:

$$\begin{aligned} e_g &= 0.5d + t_h - t_f - 0.5t_s \\ &= 0.5(29.5) + 2 + 0.5(7.5) \\ &= 20.5 \text{ in.} \end{aligned}$$

For f'_c = 4000 psi, n = 8 (Table 4.4)

$$K_g = n\left(I + Ae_g^2\right) = 8\left[3610 + 26.3\left(20.5\right)^2\right] = 117{,}300 \text{ in.}^4$$

$$10{,}000 < 117{,}300 < 7{,}000{,}000, \text{ OK}$$

Interior girder

Step 5. Calculate the distribution factors for bending moment for the interior girder, g_{mi}:

$$S = 7.5 \text{ ft}, \quad L = 50 \text{ ft}, \quad t_s = 7.5 \text{ in.}$$

Case 1: One design lane loaded: g_{mi1}

$$\begin{aligned} g_{mi1} &= 0.06 + \left(\frac{S}{14}\right)^{0.4}\left(\frac{S}{L}\right)^{0.3}\left(\frac{K_g}{12Lt_s^3}\right)^{0.1} \\ &= 0.06 + \left(\frac{7.5}{14}\right)^{0.4}\left(\frac{7.5}{50}\right)^{0.3}\left(\frac{117{,}300}{12(50)(7.5)^3}\right)^{0.1} \\ &= 0.468 \text{ lane/girder} \end{aligned}$$

Case 2: Two or more design lanes loaded: g_{mi2}

$$\begin{aligned} g_{mi2} &= 0.075 + \left(\frac{S}{9.5}\right)^{0.6}\left(\frac{S}{L}\right)^{0.2}\left(\frac{K_g}{12Lt_s^3}\right)^{0.1} \\ &= 0.075 + \left(\frac{7.5}{9.5}\right)^{0.6}\left(\frac{7.5}{50}\right)^{0.2}\left(\frac{117{,}300}{12(50)(7.5)^3}\right)^{0.1} \\ &= 0.625 \text{ lane} > g_{mi1} = 0.467 \text{ lane/girder} \end{aligned}$$

Therefore, g_{mi2} = 0.625 lane/girder (governs).

Step 6. Calculate the distribution factors for shear for the interior girder, g_{vi}:

Case 1: One design lane loaded: g_{vi1}

$$g_{vi1} = 0.36 + \frac{S}{25.0} = 0.36 + \frac{7.5}{25.0} = 0.66 \text{ lane/girder}$$

www.EngineeringEBooksPdf.com

Case 2: Two or more design lanes loaded: g_{vi2}

$$g_{vi2} = 0.2 + \frac{S}{12} - \left(\frac{S}{35}\right)^2$$

$$= 0.2 + \frac{7.5}{12} - \left(\frac{7.5}{35}\right)^2$$

$$= 0.779 \text{ lane} > g_{vi1} = 0.66 \text{ lane/girder}$$

Therefore, $g_{vi2} = 0.779$ lane/girder governs

Exterior girder

Step 7. Calculate the distribution factors for bending moment in the exterior girder. Two methods are used:

1. Using expressions in LRFD Table 4.6.2.2.2d-1
2. Special analysis as recommended in LRFD Commentary C4.6.2.2.2d

Method 1. Using expressions in LRFD Table 4.6.2.2.2d-1

Case 1: One lane loaded: use lever rule (refer to Example 4.1)
The exterior wheel of the design truck is placed at 2 ft (minimum distance) from the interior face the curb. From the geometry of the bridge cross section, the distance between the center of the exterior truck lane and the centerline of first interior girder = 3.75 + 7.5 − 1.75 − 2.0 − 3.0 = 4.50 ft. Therefore, by lever rule (Figure 4.15).

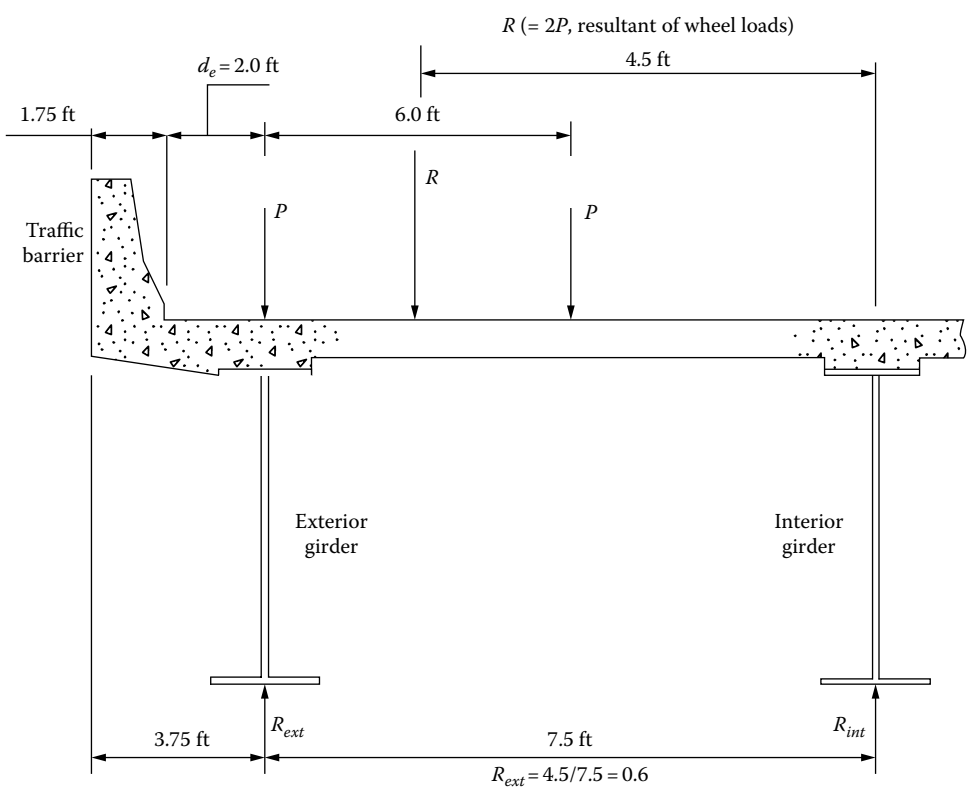

FIGURE 4.15 Lever rule for live load distribution factor for the exterior girder: one design lane loaded.

www.EngineeringEBooksPdf.com

$$\text{Fraction of the lane to the exterior girder, } R_{ext} = \frac{4.50}{7.5} = 0.60$$

$$\text{Multipresence factor, } m = 1.2$$

$$g_{me1} = m(R_{ext}) = 1.2(0.60) = 0.72 \text{ lane/girder}$$

Case 2: Two or more design lanes loaded
Modify the distribution factor for the interior girder by the adjustment factor, e. Determine d_e, the distance between the centerline of the exterior web of the exterior girder and the face of the curb. Referring to Figure 4.15,

$$d_e = 3.75 - 1.75 = 2.00 \text{ ft}$$

$$-1.0 \leq (d_e = 2.00 \text{ ft}) \leq 5.5 \text{ ft, O.K.}$$

$$\begin{aligned} e &= 0.77 + \frac{d_e}{9.1} \\ &= 0.77 + \frac{2.0}{9.1} \\ &= 0.99 \end{aligned}$$

$$\begin{aligned} g_{me2} &= e g_{interior} \\ &= (0.99)(0.625) = 0.62 \text{ lane/girder} \end{aligned}$$

Method 2. Special analysis
Refer to Figure 4.16 showing loaded lanes on the bridge cross section.

$$N_L = w/12 = 28/12 = 2.33, \text{ use } N_L = 2 \text{ lanes}$$

a. Bending moment

$$R = \frac{N_L}{N_b} + \frac{X_{ext} \sum^{N_L} e}{\sum^{N_b} x^2} \qquad (4.33)\ [\text{AC}4.6.2.2.2\text{d-}1]$$

$$\text{Number of design lanes, } N_L = 2$$

$$\text{Number of beams, } N_b = 5$$

The multiple lane factors are

$$\begin{aligned} &1 \text{ design lane} \quad m_1 = 1.2 \\ &2 \text{ design lanes} \quad m_2 = 1.0 \end{aligned}$$

For determining the eccentricity of a truck lane from the center of gravity of the pattern of girders, the truck is placed centrally within its 12 ft wide traffic lane. Refer to Figure 4.16 for various distances.

www.EngineeringEBooksPdf.com

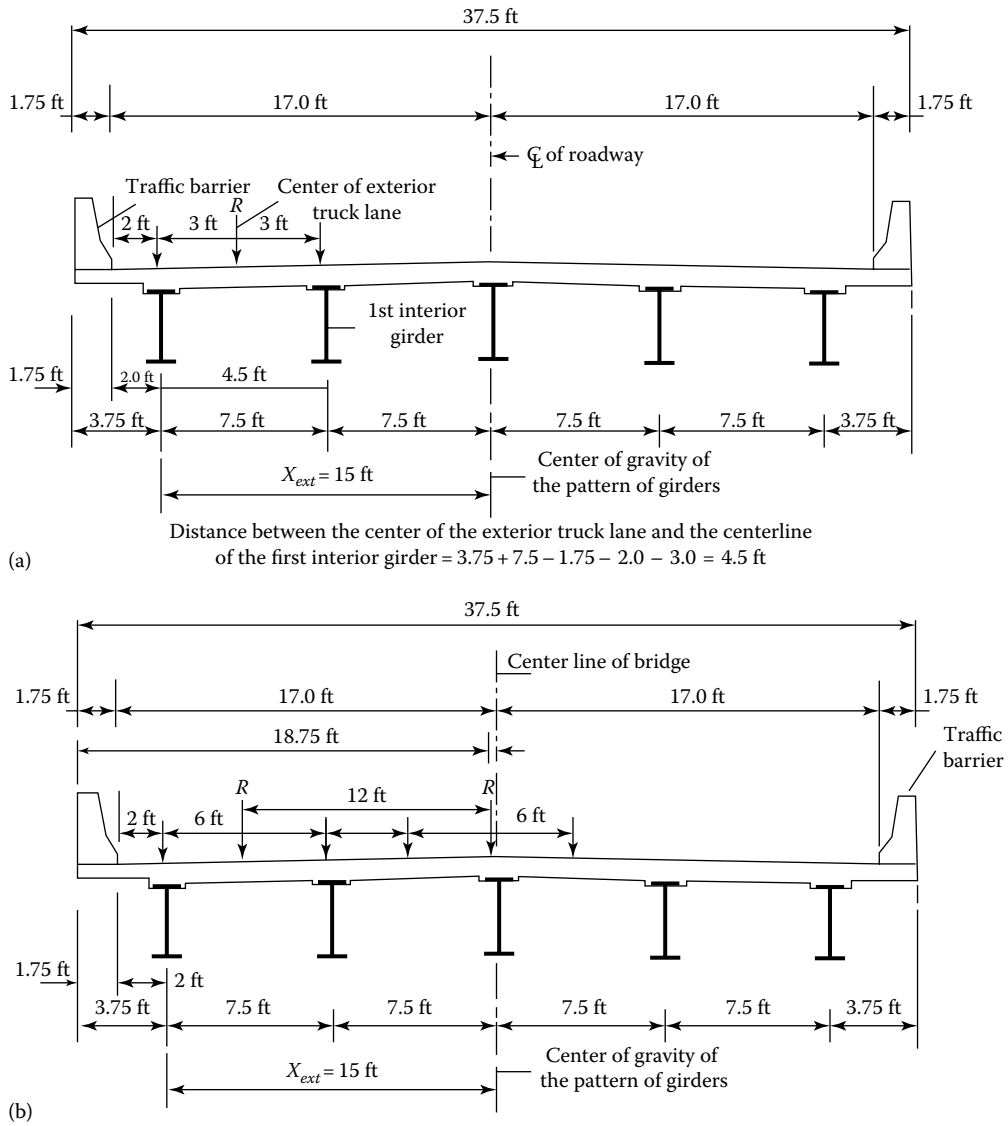

FIGURE 4.16 Schematics showing loaded lanes on bridge cross section for special analysis. (a) Position of HL-93 truck for one design lane loaded case. (b) Position of HL-93 trucks for two design lanes loaded case.

Case 1: One lane design loaded: $N_L = 1$, $N_b = 5$

X_{ext} = eccentricity of the exterior girder from the center of gravity of the pattern of girders
= distance between the centerline of the exterior girder to centerline of the bridge
= 7.5 + 7.5 = 15 ft

e = eccentricity of the extreme truck lane from the center of gravity of the pattern of girders
= 12 + 0.0 = 12.0 ft

x = horizontal distance from the center of gravity of pattern of girders to each girder
= 15 ft for the exterior girder
= 7.5 ft for the interior girder

$$R_1 = \frac{1}{5} + \frac{15(12+0.0)}{2(15^2+7.5^2)} = 0.52$$

$$m_1 R_1 = (1.2)(0.52) = 0.624 \text{ lane/girder}$$

www.EngineeringEBooksPdf.com

Case 2: Two design lanes loaded: $N_L = 2$, $N_b = 5$

$$R_2 = \frac{2}{5} + \frac{15(12.0 + 0.0)}{2(15^2 + 7.5^2)} = 0.72$$

$$m_2 R_2 = (1.0)(0.72) = 0.72 \text{ lane/girder}$$

b. Shear

Step 8. Calculate the distribution factors for shear in the exterior girder.

Case 1: One lane loaded. Use lever rule (LRFD Table 4.4.2.2.3b-1)

$$g_{ve1} = 0.72 \text{ (see previous calculations)}$$

Case 2: Two lanes loaded: modify the interior girder factor by e

$$e = 0.6 + \frac{d_e}{10}$$

$$= 0.6 + \frac{2.0}{10}$$

$$= 0.80$$

For the interior girder (from previous calculations), $g_{vi2} = 0.779$

Therefore, $g_{ve2} = (0.80)(0.779) = 0.623$.

Special analysis

The distribution factors calculated for the bending moment are also used for shear. From previous calculations, these distribution factors are

One design lane loaded: 0.624 lane/girder

Two or more design lanes loaded: 0.720 lane/girder

The values of the governing distribution factors for both bending moment and shear in interior as well as exterior girders are taken as the largest of all the values calculated earlier. A summary of these factors is presented in Table 4.6.

c. Distribution factors for fatigue limit state

Step 9. Calculate the distribution factors for fatigue limit state.

The distribution factors for fatigue limit state are determined for only one lane–loaded case for interior girders and exterior girders.

The distribution factors for the interior girder for one design lane loaded case were calculated earlier. The distribution factors for the fatigue limit state are obtained by dividing the distribution factors for bending moments and shear by 1.2 (multipresence factor for one design lane loaded) to obtain the distribution factors for fatigue limit state.

Bending moment: 0.468/1.2 = 0.390 lane/girder

Shear: 0.66/1.2 = 0.55 lane/girder

TABLE 4.6
Summary of Distribution Factors for Superstructure in Example 4.3

Force	Interior Girder	Exterior Girder
Bending moment	0.625	0.72
Shear	0.779	0.779[a]

[a] Value governed by the requirement that the distribution factor for the exterior girder be not less than that for the interior girder.

www.EngineeringEBooksPdf.com

TABLE 4.7
Distribution Factors for Fatigue Limit State

	Interior Girder (Lane)	Exterior Girder (Lane)
Bending moment	0.39	0.60
Shear	0.55	0.60

The distribution factors for the *exterior* girder for one design lane loaded case were calculated earlier. The distribution factors for the fatigue limit state are obtained by dividing the distribution factors for bending moments and shear by 1.2 (multipresence factor for one design lane loaded case) to obtain the distribution factors for fatigue limit state:

Bending moment: 0.80/1.2 = 0.667 lane/girder

Shear: 0.779/1.2 = 0.649 lane/girder

Table 4.7 shows distribution factors for the fatigue limit state for interior and exterior girders.

Step 10. Calculate the distribution factors for absolute maximum live load deflection.
For this two-lane bridge, the multipresence factor, $m = 1.0$. Also, $N_L = 2$, $N_b = 5$. From Equation 4.15,

$$g_{\Delta max} = m\left(\frac{N_l}{N_b}\right) = 1.0\left(\frac{2}{5}\right) = 0.4$$

Example 4.4: Distribution Factors for a Four-Lane Highway Bridge Having a Concrete Deck over Steel Girders

Figure 4.17 shows the cross section of a four-lane highway bridge spanning 165 ft and a skew of 30°. The superstructure consists of a concrete slab supported over five steel plate girders spaced at 11 ft 6 in. on centers. The concrete slab is 9 in. thick, including a ½ in. integral wearing surface, and has a 2 in. thick haunch. Each steel girder is built from a 1¼ × 24 in. top flange, a ½ × 72 in. web, and a 2 × 24 in. bottom flange (Figure 4.18). Assume f'_c = 4000 psi, F_y = 50 ksi, and composite construction. Calculate the distribution factors for bending moment and shear for interior and exterior girders of this bridge, including the correction factor for skew.

Solution

Check if the given superstructure type conforms to one of the types listed in AASHTO LRFD Table 4.6.2.2.1-1.

The given superstructure has cross section of Type (a) listed in AASHTO LRFD Table 4.6.2.2.1-1. Hence, the expressions for *DF*s listed in AASHTO LRFD Table 4.6.2.2.2b-1 can be used. Check the range of applicability in AASHTO LRFD Table 4.6.2.2.2b-1.

Girder spacing, S = 11.5 ft,	$3.5 \le S \le 16.0$ ft, OK
Slab thickness, t = 9 in.,	$4.5 \le t \le 12.0$ in., OK
Number of beams, $N_b > 4$,	$N_b \ge 4$, OK
Span = 165 ft,	$20 \le L \le 240$ ft, OK

Determine the bending moment of inertia of the steel girder. Datum is chosen at the bottom of the steel section. The required calculations are shown in Table 4.8.

$\bar{y}$ = distance between the centroid of the element and elastic neutral axis of the steel section

www.EngineeringEBooksPdf.com

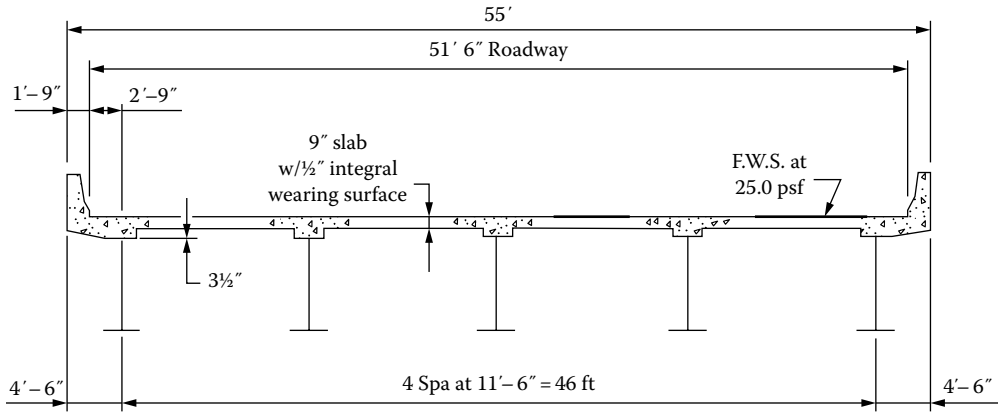

FIGURE 4.17 Bridge cross section for Example 4.2.

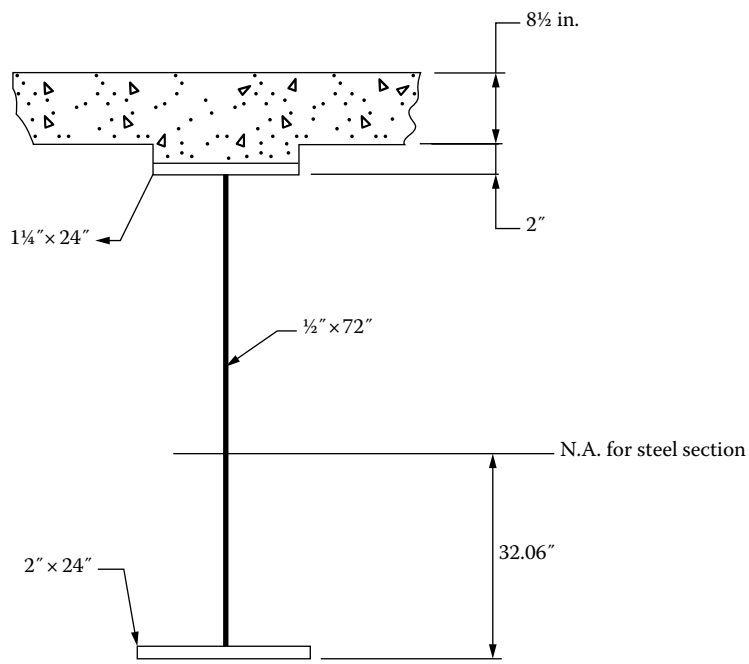

FIGURE 4.18 Details of bridge girder cross section.

TABLE 4.8
Elastic Section Properties of Girder

Component	A, in.^{2}	y, in.	Ay, in.^{3}	$\bar{y}$, in.	$A\bar{y}^2$, in.^{4}	I_o, in.^{4}
Top flange 1¼ × 24	30	74.625	2239	42.565	54,353	4.0
Web ½ × 72	36	38.0	1368	5.94	1,270	15,552
Bot. Flange 2 × 24	48	1.0	48	31.06	46,307	16
Total	114		3655		101,930	15,572

www.EngineeringEBooksPdf.com

From the aforementioned calculations, the distance of the centrodial axis of the steel section from the bottom of steel flange is given by

$$d_{bot\ of\ steel} = \frac{3655}{114} = 32.06 \text{ in.}$$

$$d_{top\ of\ steel} = 1.25 + 72.0 + 2.0 - 32.06 = 43.19 \text{ in.}$$

The bending moment of inertia about the centrodial axis of the steel section is calculated to be

$$I_{NA} = 101{,}930 + 15{,}572 = 117{,}502 \text{ in.}^4$$

Calculate K_g. Thickness of slab excluding the integral wearing surface = 9 − 0.5 = 8.5 in.

The distance from the centroidal line of concrete slab to the center of gravity of the steel section, e_g, is given by

$$e_g = 8.5/2 + 2 + 43.19 - 1.25 = 48.19 \text{ in.}$$

For f'_c = 4000 psi, n = 8 (Table 4.4)

$$\begin{aligned} K_g &= n\left(I + Ae_g^2\right) \\ &= 8\left[117{,}502 + (114.0)(48.19)^2\right] \\ &= 3.058 \times 10^6 \text{ in.}^4 \end{aligned}$$

a. Interior girder

Distribution factor for bending moment

Case 1: One design lane loaded

$$\begin{aligned} g_{m1} &= 0.06 + \left(\frac{S}{14}\right)^{0.4}\left(\frac{S}{L}\right)^{0.3}\left(\frac{K_g}{12Lt_s^3}\right)^{0.1} \\ &= 0.06 + \left(\frac{11.5}{14}\right)^{0.4}\left(\frac{11.5}{165}\right)^{0.3}\left(\frac{3.058(10^6)}{12(165)(8.5)^3}\right)^{0.1} \\ &= 0.06 + (0.924)(0.587)(1.097) \\ &= 0.516 \text{ lane} \end{aligned}$$

Case 2: Two or more design lanes loaded

$$\begin{aligned} g_{m2} &= 0.075 + \left(\frac{S}{9.5}\right)^{0.6}\left(\frac{S}{L}\right)^{0.2}\left(\frac{K_g}{12Lt_s^3}\right)^{0.1} \\ &= 0.075 + \left(\frac{11.5}{9.5}\right)^{0.6}\left(\frac{11.5}{165}\right)^{0.2}\left(\frac{3.058(10^6)}{12(165)(8.5)^3}\right)^{0.1} \\ &= 0.075 + (1.121)(0.587)(1.097) \\ &= 0.797 \text{ lane (governs)} \end{aligned}$$

www.EngineeringEBooksPdf.com

Distribution factor for shear

Case 1: One design lane loaded

$$g_{v1} = 0.36 + \frac{S}{25} = 0.25 + \frac{11.5}{25} = 0.82 \text{ lane}$$

Case 2: Two or more design lanes loaded

$$g_{v2} = 0.2 + \frac{S}{12} - \left(\frac{S}{35}\right)^2 = 0.2 + \frac{11.5}{12} - \left(\frac{11.5}{35}\right)^2 = 1.05 \text{ lanes (governs)}$$

b. Exterior girder

Distribution factor for bending moment
Three methods will be used as described in AASHTO LRFD Specifications. The largest value will be selected as the *DF*.

Method 1. Use the lever rule
From the geometry of the bridge cross section, the distance d_e (the distance between the face of curb and the centerline of the exterior girder) is determined to be 2.75 ft so the distance between the center of the exterior truck lane from the centerline of first interior girder = 11.5 + 0.75 − 3 = 9.25 ft. Therefore, by lever rule (Figure 4.19):

Fraction of the lane to the exterior girder, $g = \frac{9.25}{11.5} = 0.804$

Multipresence factor, m = 1.2

$$g_{me1} = 0.804(1.2) = 0.965 \text{ lane (governs)}$$

Method 2. Two or more design lanes loaded: modify the *DF* for the interior girder factor by e

$$e = 0.77 + \frac{d_e}{9.1} = 0.77 + \frac{2.75}{9.1} = 1.072$$

$$g_{me2} = 0.797(1.072) = 0.854 \text{ lane}$$

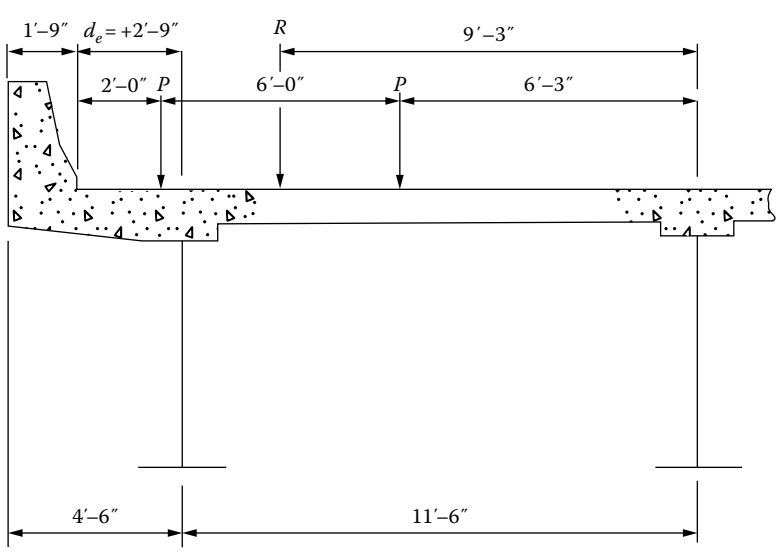

FIGURE 4.19 Exterior girder distribution factor—lever rule for Example 4.4.

www.EngineeringEBooksPdf.com

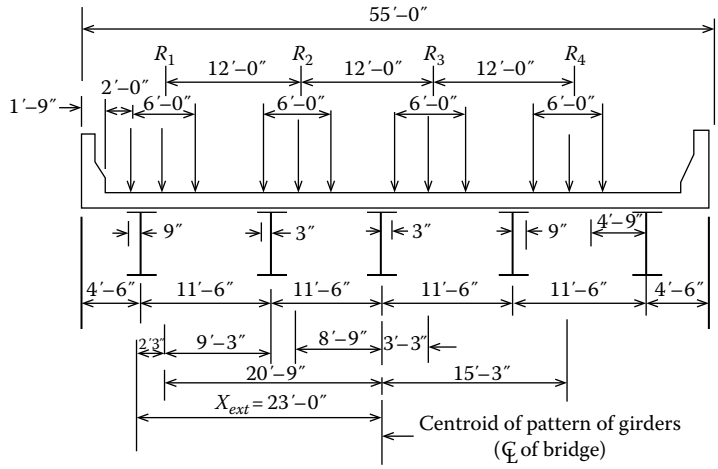

FIGURE 4.20 Exterior girder distribution factor—special analysis for Example 4.4.

Method 3. Special analysis
Refer to Figure 4.20 for position of wheel loads for special analysis. The centers of gravity truck of the loads in the four lanes are shown as R_1, R_2, R_3, and R_4.

$$R = \frac{N_L}{N_b} + \frac{X_{ext}\sum^{N_L} e}{\sum^{N_b} x^2}$$

$$N_L = \frac{\text{Roadway width}}{12} = \frac{51.5}{12} = 4.29 \qquad (4.33)\ [\text{AC}4.6.2.2.2\text{d-}1]$$

Use $N_L = 4$ (integer part of 4.29).
Number of lanes, $N_L = 4$, number of beams, $N_b = 5$
The multiple lane factors are

1 lane	$m_1 = 1.2$
2 lanes	$m_2 = 1.0$
3 lanes	$m_3 = 0.85$
> 3 lanes	$m_4 = 0.65$

The distance e is measured as the eccentricity of a truck lane from the center of gravity of the pattern of girders. For this purpose, each truck is placed centrally within its 12 ft wide traffic lane.

Case 1: One design lane loaded

$$N_L = 1, \quad N_b = 5$$

X_{ext} = eccentricity of the exterior girder from the center of gravity of the pattern of girders
= distance between the centerline of the exterior girder to centerline of the bridge
= 11.5 + 11.5 = 23 ft
e = eccentricity of the extreme truck lane from the center of gravity of the pattern of girders
= 23 − (3 − 0.75) = 20.75 ft

www.EngineeringEBooksPdf.com

x = horizontal distance from the center of gravity of pattern of girders to each girder
= 2(11.5) = 23 ft for the exterior girder
= 11.5 ft for the interior girder

$$R_1 = \frac{1}{5} + \frac{23(20.75)}{2\left[(11.5\times 2)^2 + (11.5)^2\right]} = 0.561$$

$$m_1R = (1.2)(0.561) = 0.673 \text{ lane}$$

Case 2: Two or more design lanes loaded

$$N_L = 2, \quad N_b = 5$$

Eccentricity of the extreme truck lane from the center of gravity of the pattern of girders,

$$e = 20.75 \text{ ft (calculated earlier)}$$

Eccentricity e of the interior truck lane from the center of gravity of the pattern of girders (each truck is placed within its 12 ft wide design lane),

$$e = 8.75 \text{ ft}$$

x = horizontal distance from the center of gravity of pattern of girders to each girder
= 2(11.5) = 23 ft for the exterior girder
= 11.5 ft for the interior girder

$$R_2 = \frac{2}{5} + \frac{23(20.75+8.75)}{2\left[(23)^2 + (11.5)^2\right]} = 0.913$$

$$m_2R = (1.0)(0.913) = 0.913 \text{ lane}$$

Case 3: Three design lanes loaded
When three lanes are loaded, the centroid of the third lane is positioned 3.25 ft to the right of the center of gravity of the pattern of girders (all three trucks are placed within their 12 ft wide traffic lanes), so e is assigned a *negative* sign; thus,

$$e = -3.25 \text{ ft}$$

$$R_3 = \frac{3}{5} + \frac{23(20.75+8.75-3.25)}{2\left[(23)^2 + (11.5)^2\right]} = 1.0565$$

$$m_3R = (0.85)(1.0565) = 0.898 \text{ lane}$$

Case 4: Four design lanes loaded
When four lanes are loaded, the centroid of the fourth lane is positioned 15.25 ft to the right of the center of gravity of the pattern of girders (all four trucks are placed within their 12 ft wide traffic lanes), so e is assigned a *negative* sign; thus,

$$e = -15.25 \text{ ft}$$

$$R_4 = \frac{4}{5} + \frac{23(20.75+8.75-3.25-15.25)}{2\left[(23)^2 + (11.5)^2\right]} = 0.9913$$

$$m_4R = (0.65)(0.9913) = 0.644 \text{ lane}$$

www.EngineeringEBooksPdf.com

Distribution factor for shear

Case 1: One design lane loaded: use the lever rule
g_{ve1} = 0.804 lane (calculated earlier)

Case 2: Two or more design lanes loaded
Modify the distribution factor for shear for the interior girder for the two lanes loaded case by factor e calculated as follows:

$$e = 0.6 + \frac{d_e}{10} = 0.6 + \frac{2.75}{10} = 0.875$$

$$g_{ve2} = 0.875(1.05) = 0.92 \text{ (governs)}$$

Case 3: Special analysis
The distribution factors calculated for bending moment are also used for shear.
One design lane loaded: g_{ve1} = 0.673 lane
Two design lanes loaded: g_{ve2} = 0.913 lane
Three design lanes loaded: g_{ve3} = 0.898 lane
Four design lanes loaded: g_{ve4} = 0.644 lane

c. Skew correction factors
Correction factor for bending moment (AASHTO LRFD Table 4.6.2.2.2e-1):

$$C_1 = 0.25\left(\frac{K_g}{12Lt_s^3}\right)^{0.25}\left(\frac{S}{L}\right)^{0.5}$$

$$= 0.25\left(\frac{3.058\times10^6}{12(165)(8.5)^3}\right)^{0.25}\left(\frac{11.5}{165}\right)^{0.5}$$

$$= 0.083$$

$$\text{Correction factor} = 1 - C_1(\tan\theta)^{1.5} = 1 - 0.083(\tan 30°)^{1.5} = 0.964$$

Correction factor for shear (AASHTO LRFD Table 4.6.2.2.3c-1):

$$\text{Correction factor} = 1.0 + 0.2\left(\frac{12.0Lt_s^3}{K_g}\right)^{0.3}\tan\theta = 1.0 + 0.2\left(\frac{12(165)(8.5)^3}{(3.058)(10^6)}\right)^{0.3}\tan 30° = 1.088$$

The final values of the distribution factors for bending moment and shear in interior and exterior girders are shown in Table 4.9. Note that the shears in both the interior and exterior girders away from the skewed support are not modified by the skew correction factors.

TABLE 4.9
Distribution Factors for Bending Moments and Shear

	Interior Girder (Lane)	Exterior Girder (Lane)
Bending moment, g_m	0.797(0.964) = 0.768	0.965(0.964) = 0.93
Shear: end support, g_v	1.05(1.088) 1.142	0.965(1.088) = 1.049
Shear: in span, g_v	1.05	0.965

www.EngineeringEBooksPdf.com

TABLE 4.10
Distribution Factors for Fatigue Limit State

	Interior Girder (Lane)	Exterior Girder (Lane)
Bending moment, g_{mf}	0.415	0.775
Shear: end support, g_{vf}	0.743	0.875
Shear: in span, g_{vf}	0.683	0.804

d. Distribution factors for fatigue limit state

The distribution factors for fatigue limit state are determined for only one lane loaded case.

The distribution factors for the interior girder for one lane loaded case were calculated earlier. The skew correction factors for bending moment and shear were calculated, respectively, to be 0.964 and 1.088. The following distribution factors, calculated earlier for the interior girder, are multiplied by the appropriate skew correction factors and divided by 1.2 (multipresence factor for one lane loaded) to obtain the *DF*s for fatigue limit state:

Bending moment: $g_{mf} = 0.516\ (0.964)/1.2 = 0.415$
Shear: End support: $g_{vf} = 0.82\ (1.088)/1.2 = 0.743$
Shear: In span: $g_{vf} = 0.82/1.2 = 0.683$

The distribution factors for the exterior girder for one lane loaded case were calculated earlier. The skew correction factors for bending moment and shear were calculated, respectively, to be 0.964 and 1.088. The distribution factors for the fatigue limit state are obtained by multiplying the distribution factors for bending moments and shear by the appropriate skew correction factors and dividing by 1.2 (multipresence factor for one lane loaded) to obtain the distribution factors for fatigue limit state:

Bending moment: $g_{mf} = 0.965\ (0.964)/1.2 = 0.775$
Shear: End support: $g_{vf} = 0.965\ (1.088)/1.2 = 0.875$
Shear: In span: $g_{vf} = 0.965/1.2 = 0.804$

These results are shown in Table 4.10.

e. Distribution factors for absolute maximum live load deflection

For this four-lane bridge, the multipresence factor, $m = 0.65$. Also, $N_L = 4$, $N_b = 5$. From Equation 4.9,

$$g_{\Delta max} = m\left(\frac{N_L}{N_b}\right) = 0.65\left(\frac{4}{5}\right) = 0.52$$

Example 4.5: Concrete Slab over Precast–Prestressed Concrete Girders

Figure 4.21 shows the cross section of a highway bridge having a simple span of 85 ft. It consists of an 8.5 in. thick R.C. deck (including ½ in. thick integral wearing surface) supported on and composite with AASHTO Type IV prestressed concrete girders that are spaced at 7′-8″ on centers. Assuming composite construction, determine the distribution factors for an interior girder (a) for live load bending moment and (b) live load shear. The following data are given:

Cross-sectional area of girder, $A_g = 789$ in.^{2}
Bending moment of inertia of girder, $I_g = 260{,}730$ in.^{4}
Neutral axis from the extreme bottom fibers, $y_b = 24.73$ in.
Compressive strength of concrete: Deck: $f'_c = 4500$ psi
Girder: $f'_c = 6000$ psi

Solution

Check if the superstructure type conforms to one of the types listed in AASHTO LRFD Table 4.6.2.2.1-1.

The given superstructure has cross section similar to Type (k) listed in AASHTO LRFD Table 4.6.2.2.1-1. Hence, the expressions for *DF*s listed in AASHTO LRFD Table 4.6.2.2.2b-1 can be used.

www.EngineeringEBooksPdf.com

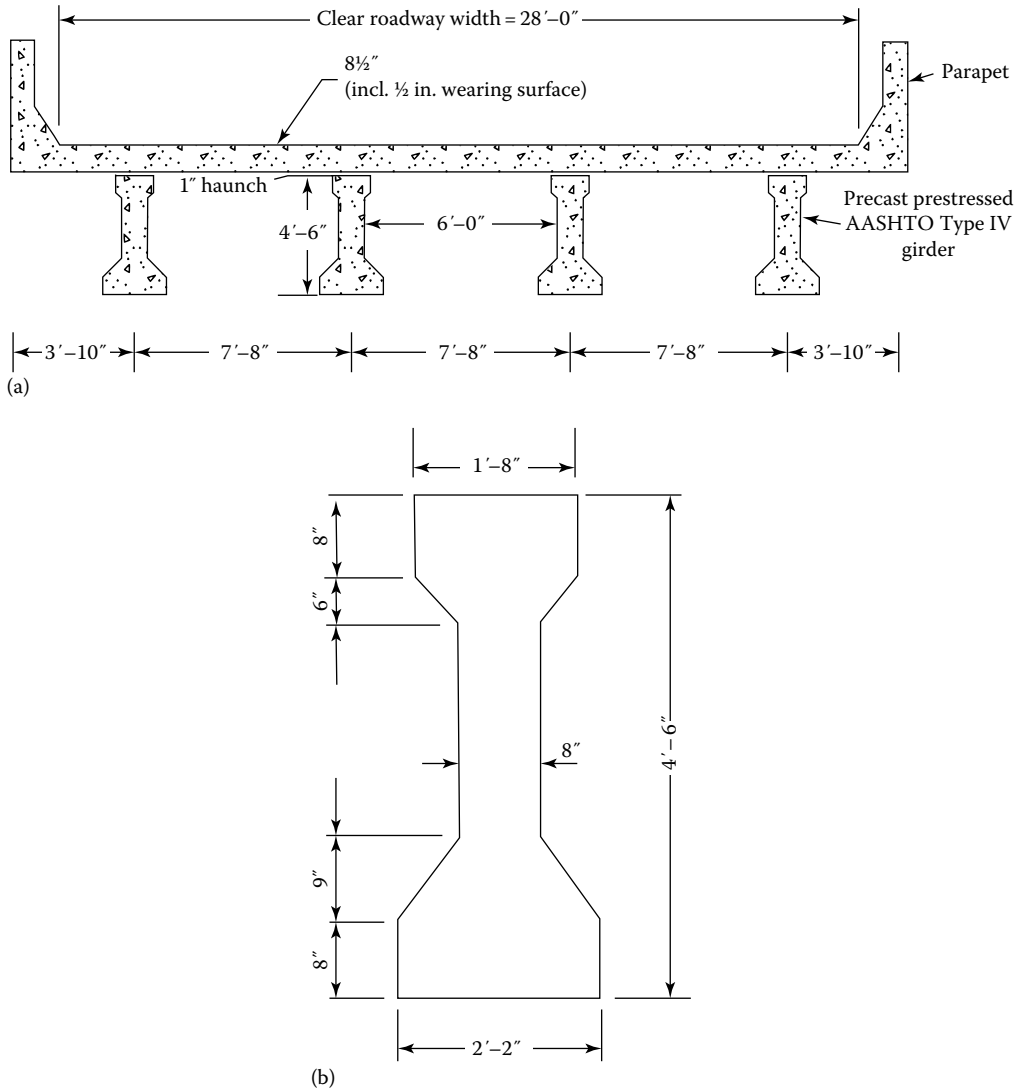

FIGURE 4.21 (a) Cross section of bridge with AASHTO Type IV prestressed concrete girders. (b) Cross section of AASHTO-PCI precast–prestressed concrete Type IV girder.

Check the range of applicability in AASHTO LRFD Table 4.6.2.2.2b-1.

Girder spacing, S = 7′-8″ = 7.67 ft,	$3.5 \le S \le 16.0$ ft, OK
Slab thickness, t_s = 8.5 – 0.5 = 8 in.	$4.5 \le t_s \le 12.0$ in., OK
Span = 85 ft,	$20 \le L \le 240$ ft, OK
Number of beams, N_b = 4,	$N_b \ge 4$, OK
K_g = 1,309,849 in.^{4} (calculated later)	$10{,}000 \le K_g \le 7{,}000{,}000$ in.^{4}, OK

The range of applicability is satisfied. Calculate the number of design traffic lanes, N_L.

Clear roadway width, w = 28 ft

N_L = integer part of $w/12 = 28/12 = 2.33$, use $N_L = 2$

www.EngineeringEBooksPdf.com

a. Distribution factor for bending moment:
Calculate the longitudinal stiffness parameter, K_g:

$$K_g = n\left(1 + Ae_g^2\right)$$

The concrete compressive strengths of concrete are

$$\text{Deck: } f_c' = 4500 \text{ psi}$$

$$\text{Girder: } f_c' = 6000 \text{ psi}$$

For the deck:

$$E_c = 33{,}000\left(w_c^{1.5}\right)\sqrt{f_c' \text{ ksi}} = 33{,}000\left(0.15\right)^{1.5}\sqrt{4.5 \text{ ksi}} = 4{,}067 \text{ ksi}$$

For the beam:

$$E_c = 33{,}000\left(w_c^{1.5}\right)\sqrt{f_c' \text{ ksi}} = 33{,}000\left(0.15\right)^{1.5}\sqrt{6 \text{ ksi}} = 4{,}696 \text{ ksi}$$

$$n = \frac{E_B}{E_D} = \frac{4696}{4067} = 1.155$$

The following girder properties are given:

Cross-sectional area of girder, $A_g = 789$ in.^{2}
Bending moment of inertia of girder, $I_g = 260{,}730$ in.^{4}

Calculate e_g (Figure 4.22).

$$e_g = 29.27 + 1 + (1/2)(8) = 34.27 \text{ in.}$$

$$\begin{aligned} K_g &= n\left(1 + Ae_g^2\right) \\ &= 1.155[260{,}730 + (789)(34.27)^2] \\ &= 1.371 \times 10^6 \text{ in.}^4 \end{aligned}$$

$$S = 7 \text{ ft–8 in.} = 7.667 \text{ ft}, \quad L = 85 \text{ ft}, \quad t_s = 8 \text{ in.}$$

Case 1: One design lane loaded: g_{mi1}

$$\begin{aligned} g_{mi1} &= 0.06 + \left(\frac{S}{14}\right)^{0.4}\left(\frac{S}{L}\right)^{0.3}\left(\frac{K_g}{12Lt_s^3}\right)^{0.1} \\ &= 0.06 + \left(\frac{7.667}{14}\right)^{0.4}\left(\frac{7.667}{85}\right)^{0.3}\left(\frac{1.371 \times 10^6}{12(85)(8)^3}\right)^{0.1} \\ &= 0.481 \text{ lane/girder} \end{aligned}$$

www.EngineeringEBooksPdf.com

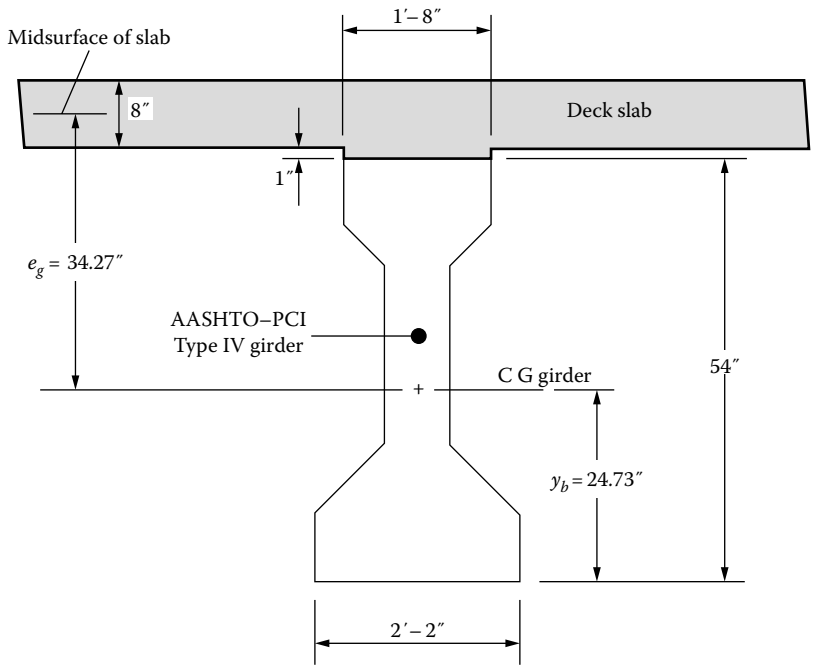

FIGURE 4.22 Calculation of e_g for Example 4.5.

Case 2: Two or more design lanes loaded: g_{mi2}

$$g_{mi2} = 0.075 + \left(\frac{S}{9.5}\right)^{0.6}\left(\frac{S}{L}\right)^{0.2}\left(\frac{K_g}{12Lt_s^3}\right)^{0.1}$$

$$= 0.075 + \left(\frac{7.667}{9.5}\right)^{0.6}\left(\frac{7.667}{85}\right)^{0.2}\left(\frac{1.371\times10^6}{12(85)(8)^3}\right)^{0.1}$$

$$= 0.674 \text{ lane} > g_{mi1} = 0.481 \text{ lane/girder}$$

Therefore, g_{mi2} = 0.674 lane/girder (governs).

b. Distribution factor for shear for the interior girder:

Case 1: One design lane loaded: g_{vi1}

$$g_{vi1} = 0.36 + \frac{S}{25.0} = 0.36 + \frac{7.667}{25.0} = 0.667 \text{ lane/girder}$$

Case 2: Two or more design lanes loaded: g_{vi2}

$$g_{vi2} = 0.2 + \frac{S}{12} - \left(\frac{S}{35}\right)^2$$

$$= 0.2 + \frac{7.667}{12} - \left(\frac{7.667}{35}\right)^2$$

$$= 0.791 \text{ lane} > g_{vi1} = 0.667 \text{ lane/girder}$$

Therefore, g_{vi2} = 0.791 lane/girder governs.

www.EngineeringEBooksPdf.com

Example 4.6: Distribution Factors for a Two-Lane Precast–Prestressed Adjacent Box Beam Superstructure

Figure 4.23 shows the cross section of a 90 ft span precast–prestressed adjacent box beam bridge that consists of seven AASHTO Type BIII-48 box girders. A 3 in. bituminous surfacing would be placed on the beams as wearing surface. The beams are posttensioned transversely through 8 in. thick full-depth diaphragms provided at quarter points so as to develop integral action between them. Calculate the distribution factors for bending moment and shear in the interior girder and exterior girders of this superstructure. There is no skew in the bridge. The following information is provided:

Area of cross section of box beam, A = 813 in.^{2}
h is the overall depth of precast beam = 39 in.
I is the bending moment of inertia about the centroidal axis of beam = 168,367 in.^{4}
Dead weight of girder = 847 lb/ft

Solution

Live load distribution factors for a typical interior beam.

Check if the superstructure type conforms to one of the types listed in LRFD Table 4.6.2.2.1-1.

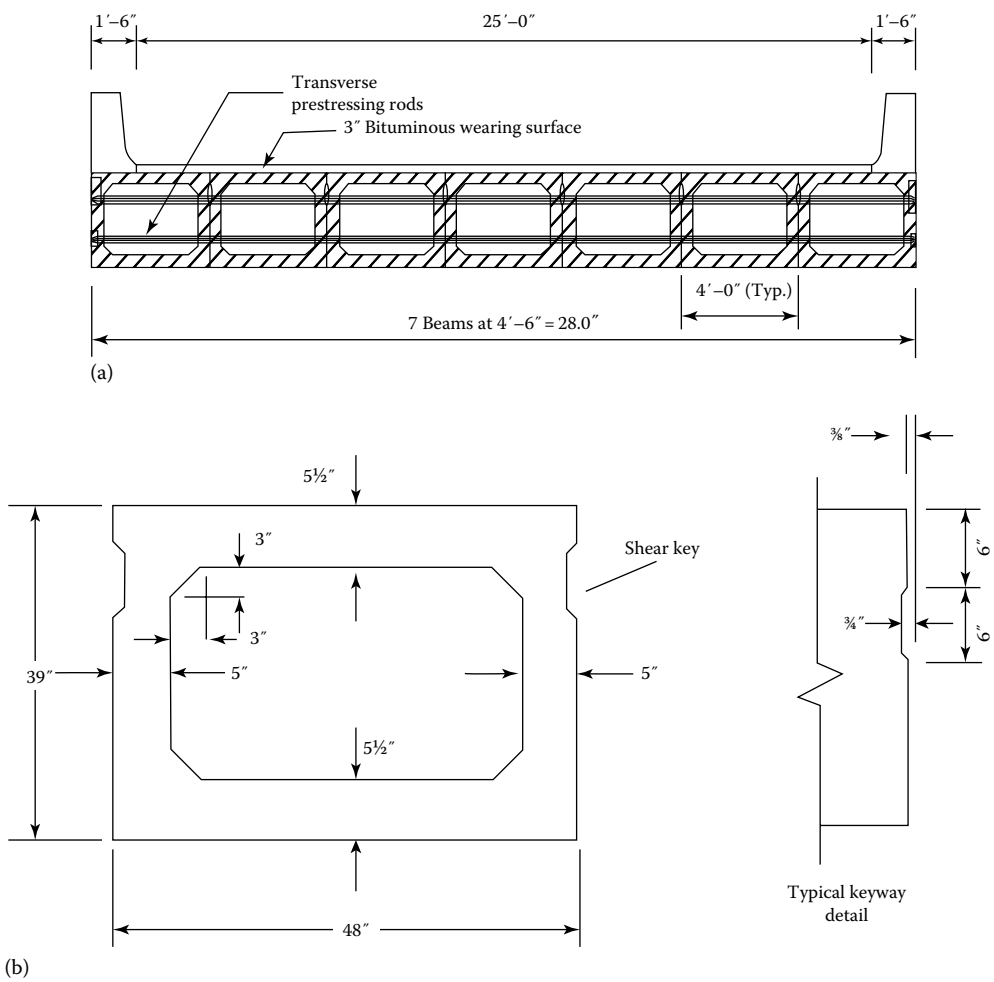

FIGURE 4.23 (a) Prestressed adjacent box beam bridge cross section. (Adapted from Prestressed Concrete Institute, *Precast Prestressed Concrete Bridge Design Manual*, Chicago, IL, 2003.) (b) Cross section of AASHTO-PCI BIII-48 box beam.

www.EngineeringEBooksPdf.com

The given superstructure has cross section similar to Type ((precast cellular concrete box with shear keys and with or without transverse posttension) listed in LRFD Table 4.6.2.2.1-1. Hence, expressions for distribution factors for interior beams listed in LRFD Table 4.6.2.2.2b-1 can be used if the following conditions are satisfied (LRFD Art 4.6.2.2.1):

Width of slab is constant OK.
Number of beams, $N_b \geq 4$ ($N_b = 7$) OK.
Beams are parallel and approximately of the same stiffness OK.
The roadway part of the overhang, $d_e \leq 2.0$ ft. ($d_e = 0.0$) OK.
Curvature in plan is less than 5° (AASHTO LRFD Table 4.6.1.2.1-1) (Curvature = 0.0°) OK.
Calculate the number of design lanes, N_L.
Number of design lanes, N_L = integer part of the ratio $w/12$, where w is the clear roadway width (ft) between the curbs (AASHTO LRFD Art 3.6.1.1.1)
From Figure 4.23, $w = 25$ ft

$$N_L = \text{Integer part of } (25/12) = 2 \text{ lanes}$$

1. Interior girder

a. Distribution factor for bending moment

For all limit states except fatigue limit state:
Check the range of applicability:

35 in. $\leq b \leq$ 60 in.	b = 48 in.	OK
20 ft $\leq L \leq$ 120 ft	L = 90 ft	OK
$5 \leq N_b \leq 20$	N_b = 7 beams	OK

Case 1: One design lane loaded, if members are sufficiently connected to act as a unit

$$g_{mi1} = k\left(\frac{b}{33.3 \times L}\right)^{0.5}\left(\frac{I}{J}\right)^{0.25} \quad \text{(LRFD Table 4.6.2.2.2b-1)}$$

where
g_{mi1} = distribution factor for bending moment for the interior girder
b = beam width = 48 in.
L = beam span = 90 ft
I = bending moment of inertia of the beam = 168,367 in.^{4}
$k = 2.5(N_b)^{-0.2} \geq 1.5$: $2.5(7)^{-0.2} = 1.694 > 1.5$, OK
J = St. Venant torsional constant for closed, thin-walled shapes, in.^{4}

where

$$J \approx \frac{4A_o^2}{\sum \frac{s}{t}} \quad (4.17)\ [\text{AC4.6.2.2.1-3}]$$

where
A_o = area enclosed by centerlines of the elements of the beam
= (48 − 5)(39 − 5.5) = 1440.5 in.^{2}
s = length of an element of the beam
t = thickness of an element of the beam

Calculate the St. Venant's torsional constant, J, from Equation 4.17:

$$J = \frac{4(1440.5)^2}{2\left(\frac{48-5}{5.5}\right)+2\left(\frac{39-5.5}{5}\right)} = 285{,}854 \text{ in.}^4$$

www.EngineeringEBooksPdf.com

$$g_{mi1} = k\left(\frac{b}{33.3\times L}\right)^{0.5}\left(\frac{I}{J}\right)^{0.25}$$

$$= 1.694\left(\frac{48}{33.3\times 90}\right)^{0.5}\left(\frac{168,367}{285,854}\right)^{0.25}$$

$$= 0.188 \text{ lane/beam}$$

Case 2: Two or more design lanes loaded if members are sufficiently connected to act as a unit

$$g_{mi2} = k\left(\frac{b}{305}\right)^{0.6}\left(\frac{b}{12.0L}\right)^{0.2}\left(\frac{I}{J}\right)^{0.06} \quad \text{(AASHTO LRFD Table 4.6.2.2.2b-1)}$$

$$g_{mi2} = 1.694\left(\frac{48}{305}\right)^{0.6}\left(\frac{48}{12.0\times 90}\right)^{0.2}\left(\frac{168,367}{285,854}\right)^{0.06} = 0.290 \text{ lane/beam}$$

Thus, the case of two or more lanes loaded controls, g_{mi} = 0.290 lane/beam.

Fatigue limit state:
LRFD Art. 3.4.1 states that for fatigue limit state, a single design truck should be used. Therefore, the distribution factor for one design lane loaded should be used as previously calculated. However, the live load distribution factors given in LRFD Art 4.6.2.2 take into consideration the multiple presence factors, *m*. LRFD Art. 3.6.1.1.2 states that the multiple presence factor, *m*, for one design lane loaded is 1.2. The distribution factor for fatigue limit state is

DF for fatigue limit state, g_{mf} = 0.188/1.2 = 0.157 lane/beam

b. Distribution factor for shear:
Check if the superstructure type conforms to one of the types listed in LRFD Table 4.6.2.2.1-1.
The given superstructure conforms to the superstructure Type (g), OK.
Check the range of applicability:

35 in. $\le b \le$ 60	b = 48 in.	OK
20 ft $\le L \le$ 120 ft	L = 90 ft	OK
$5 \le N_b \le 20$	N_b = 7 beams	OK
25,000 $\le J \le$ 610,000	J = 285,854 in.^{4}	OK
40,000 $\le I \le$ 610,000	I = 168,367 in.^{4}	OK

1. One design lane loaded:

$$g_{Vi1} = \left(\frac{b}{130L}\right)^{0.15}\left(\frac{I}{J}\right)^{0.05}$$

$$= \left(\frac{48}{130\times 90}\right)^{0.15}\left(\frac{168,367}{285,854}\right)^{0.05} \quad \text{(LRFD Table 4.6.2.2.3a-1)}$$

$$= 0.427 \text{ lane/beam}$$

2. Two or more design lanes loaded:

$$g_{Vi2} = \left(\frac{b}{156}\right)^{0.4}\left(\frac{b}{12.0L}\right)^{0.1}\left(\frac{I}{J}\right)^{0.05} \quad \text{(LRFD Table 4.6.2.2.3a-1)}$$

www.EngineeringEBooksPdf.com

$$g_{Vi2} = \left(\frac{48}{156}\right)^{0.4}\left(\frac{48}{12.0\times 90}\right)^{0.1}\left(\frac{168,367}{285,854}\right)^{0.05} = 0.445 \text{ lane/beam}$$

Thus, the case of two design lanes loaded controls, $g_{vi} = 0.445$.

2. Exterior girder

a. Distribution factor bending moment:

Case 1: One design lane loaded

$$g = eg_{interior}$$

$$e = 1.125 + \frac{d_e}{30} \geq 1.0$$

From the cross section of the superstructure, it is observed that

d_e = distance between the edge of the curb and the centerline of the exterior web of the exterior girder
= width of the traffic barrier at the deck level – ½(exterior web thickness)
= –[18 in. – ½ (5.0 in.)] = –15.5 in. (negative because the centerline of the exterior web is outboard of the edge of the curb)
= –1.292 ft

Check the applicability criteria: $d_e \leq 2.0$ ft.

$$-1.292 \text{ ft} < 2.0 \text{ ft, OK}$$

$$e = 1.125 + \frac{-1.292}{30} = 1.082 > 1.0$$

Therefore, use $e = 1.082$.

$$g_{me1} = eg_{interior} = (1.082)(0.188) = 0.203 \text{ lane/girder}$$

Case 2: Two or more design lanes loaded

$$g = eg_{interior}$$

$$e = 1.04 + \frac{d_e}{25} \geq 1.0$$

$$e = 1.04 + \frac{-1.292}{25} = 0.988 < 1.0$$

Therefore, use $e = 1.0$.

$$g_{me2} = eg_{interior} = (1.0)(0.290) = 0.290 \text{ lane/girder}$$

$$g_{me} = 0.29 \text{ lane/girder governs.}$$

b. Distribution factor for shear:

Check applicability criteria:

$$d_e \leq 2.0 \text{ ft: } -15.5 \text{ in.} < 24 \text{ in. } (=2.0 \text{ ft}), \text{ OK}$$

$$35 \leq b \leq 60 \text{ in.: } 35 \leq 48 \text{ in.} \leq 60 \text{ in., OK}$$

www.EngineeringEBooksPdf.com

Applicability criteria are satisfied.

Case 1: One design lane loaded

$$g = eg_{interior}$$

$$e = 1.25 + \frac{d_e}{20} \geq 1.0$$

$$e = 1.25 + \frac{-1.292}{20} = 1.185 > 1.0$$

Therefore, use e = 1.185.

$$g_{ve1} = eg_{interior} = (1.185)(0.427) = 0.506 \text{ lane/girder}$$

Case 2: Two or more design lanes loaded

$$g = eg_{interior}$$

Check that $\frac{48}{b} \leq 1.0$.

$$\frac{48}{48} = 1.0, \text{ OK}$$

$$e = 1 + \left(\frac{d_e + \frac{b}{12} - 2.0}{40} \right)^{0.5} \geq 1.0$$

$$e = 1 + \left(\frac{-1.292 + \frac{48}{12} - 2.0}{40} \right)^{0.5} = 1.133 > 1.0$$

Therefore, use e = 1.133.

$$g_{ve2} = eg_{interior} = (1.133)(0.445) = 0.504 \text{ lane/girder}$$

$$g_{ve} = 0.504 \text{ lane/girder governs.}$$

A summary of distribution factors for bending moment and shear for both the interior and exterior girders is presented in Table 4.11.

TABLE 4.11
Summary of Distribution Factors for Bending Moment and Shear

	Interior Girder	Exterior Girder
Bending moment	0.290	0.290
Shear	0.445	0.504

www.EngineeringEBooksPdf.com

Example 4.7: Distribution Factors for a Multicell, Cast-in-Place, Concrete Box Girder Superstructure

Figure 4.24 shows the cross section of cast-in-place multicell concrete box beam superstructure. The girder webs are spaced at 9 ft 6 in. on centers. The span is 100 ft. Calculate the distribution factors for this bridge. The bridge has no skew.

Solution

Commentary: For the purposes of calculating distribution factors, each web of a multicell box beam is treated as a separate beam—interior webs as interior beams and exterior webs as exterior beams. Accordingly, the expressions for distribution factors for bending moment and shear given in LRFD Tables 4.6.2.2.2b-1, 4.6.2.2.2d-1, 4.6.2.2.3a-1, and 4.6.2.2.3b-1 would be used.

Distribution factors for the interior girder:

1. Identify the superstructure type.
   The superstructure cross section qualifies as Type (d) superstructure in LRFD Table 4.6.2.2.2-1.
2. Check the range of applicability (LRFD Table 4.6.2.2.2b-1)

$7.0 \le S \le 13.0$ ft,	$S = 9.5$ ft, OK
$60 \le L \le 240$ ft,	$L = 100$ ft, OK
$N_c \ge 3$	$N_c = 3$ cells, OK
$W_e \le S$	W_e = half the web spacing, plus the total overhang $= ½(9.5) + 4.5 - 0.5 = 8.75$ ft $< S = 9.5$ ft, OK

Therefore, formulas for distribution factors from LRFD Table 4.6.2.2.2b-1 (for interior beams) and Table 4.6.2.2.2d-1 (for exterior beams) can be used.

3a. Distribution factor for bending moment:

Case 1: One design loaded

$$g_{mi1} = \left(1.75 + \frac{S}{3.6}\right)\left(\frac{1}{L}\right)^{0.35}\left(\frac{1}{N}\right)^{0.45}$$

$$= \left(1.75 + \frac{9.5}{3.6}\right)\left(\frac{1}{100}\right)^{0.35}\left(\frac{1}{3}\right)^{0.45} = 0.534 \text{ lane/web}$$

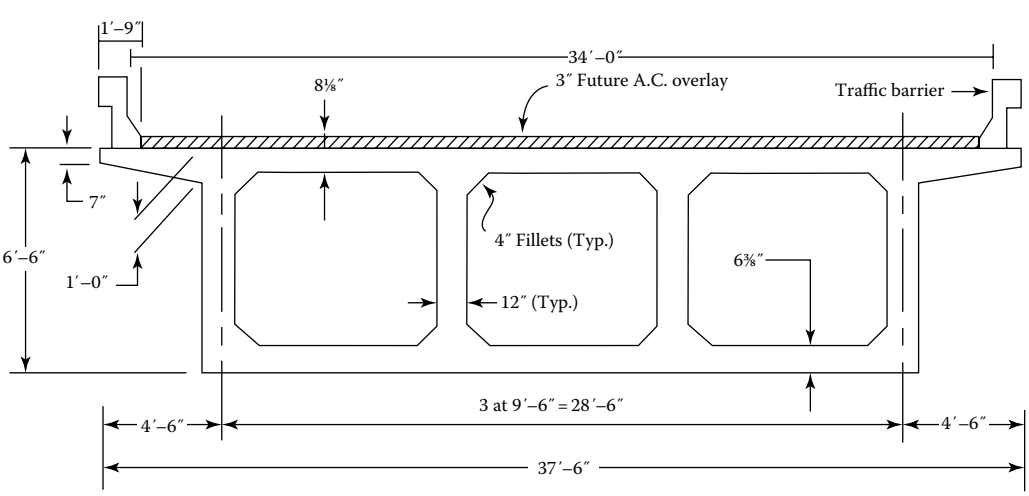

FIGURE 4.24 Cast-in-place multicell concrete box beam superstructure.

www.EngineeringEBooksPdf.com

Case 2: Two or more design lanes loaded

$$g_{mi2} = \left(\frac{13}{N_c}\right)^{0.3}\left(\frac{S}{5.8}\right)\left(\frac{1}{L}\right)^{0.25}$$

$$= \left(\frac{13}{3}\right)^{0.3}\left(\frac{9.5}{5.8}\right)\left(\frac{1}{100}\right)^{0.25} = 0.804 \text{ lane/web}$$

Therefore, g_{mi2} = 0.804 lane/web for bending moment in the interior girder (governs).

3b. Distribution factor for shear

Check the range of applicability (LRFD Table 4.6.2.2.3a-1).

$6.0 \le S \le 13.0$ ft,	$S = 9.5$ ft, OK
$20 \le L \le 240$ ft,	$L = 100$ ft, OK
$35 \le d \le 110$,	$d = 78$ in., OK
$N_c \ge 3$	$N_c = 3$ cells, OK

The range of applicability is satisfied.

Case 1: One design lane loaded

$$g_{vi1} = \left(\frac{S}{9.5}\right)^{0.6}\left(\frac{d}{12.0L}\right)^{0.1}$$

$$= \left(\frac{9.5}{9.5}\right)^{0.6}\left(\frac{78}{(12.0)(100)}\right)^{0.1} = 0.761 \text{ lane/web}$$

Case 2: Two or more design lanes loaded

$$g_{vi2} = \left(\frac{S}{7.3}\right)^{0.9}\left(\frac{d}{12.0L}\right)^{0.1}$$

$$= \left(\frac{9.5}{7.3}\right)^{0.9}\left(\frac{78}{(12.0)(100)}\right)^{0.1} = 0.964 \text{ lane/web}$$

Therefore, g_{vi2} = 0.964 lane/web for shear in the interior girder (controls).

4. Distribution factors for the exterior girder

4a. Distribution factor for bending moment (LRFD Table 4.6.2.2.2d-1)

Check the range of applicability: $W_e \le S$

$$W_e = \text{half the web spacing plus the total overhang}$$

$$= 1/2(9.5) + 4.5 - 0.5$$

$$= 8.75 \text{ ft} \le S = 9.5 \text{ ft, OK}$$

The range of applicability is satisfied.

Case 1: One design lane loaded

$$g_{me1} = \frac{W_e}{14} = \frac{9.5}{14} = 0.679 \text{ lane/web}$$

www.EngineeringEBooksPdf.com

Case 2: Two or more design lanes loaded

$$g_{me2} = \frac{W_e}{14} = \frac{9.5}{14} = 0.679 \text{ lane/web}$$

$$g_{me2} = 0.679 \text{ lane/web} < g_{mi2} = 0.804 \text{ (governs)}$$

4b. Distribution factor for shear (LRFD Table 4.6.2.2.3b-1):
Check the range of applicability: $-2.0 \le d_e \le 5.0$
From Figure 4.24,
Distance between the outside and inside edges of the traffic barrier = 1′–9″ (=1.75 ft)
d_e = distance between the inside edge of the traffic barrier and the centerline of the exterior web
= 4.5 − 1.75 = +2.75 ft, OK
The range of applicability is satisfied.

Case 1: One design lane loaded
Use lever rule. Figure 4.25 shows the free-body diagram of the multicell box girder for using lever rule. Supports at A and B represent, respectively, the exterior and adjacent interior webs of the girder. Calculate reaction R_A:

$$\Sigma M_B = 0$$

$$\frac{P}{2}(10.25) + \frac{P}{2}(4.25) - R_A(9.5) = 0$$

$$R_A = 0.763P$$

$$g = 0.763 \text{ lane}$$

Apply multipresence factor, $m = 1.2$

$$g_{ve1} = 1.2(0.763) = 0.916 \text{ lane/web}$$

$$g_{ve1} = 0.916 \text{ lane/web}$$

Case 2: Two or more design lanes loaded

$$g = e(g_{interior})$$

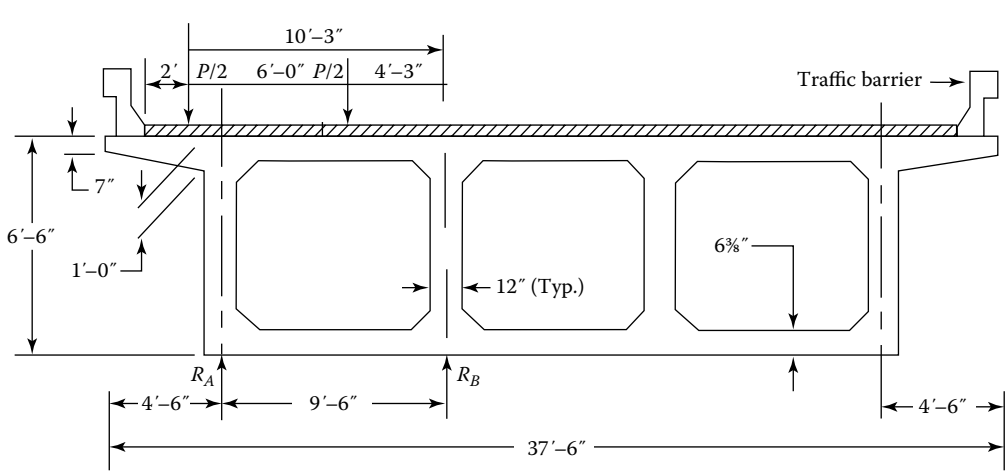

FIGURE 4.25 Lever rule for cast-in-place multicell box girder bridge of Example 4.7.

www.EngineeringEBooksPdf.com

TABLE 4.12
Summary of Distribution Factors for Example 4.7

	Distribution Factor	
Girder Position	**Bending Moment (Lane)**	**Shear (Lane)**
Interior	0.804	0.964
Exterior	0.804[a] (0.679)	0.964[a] (0.829)

[a] Values selected because the distribution factors for the exterior beam may not be smaller than those for the interior beam. Calculated values are shown in the parentheses.

Calculate the adjustment factor *e*.

$$e = 0.64 + \frac{d_e}{12.5} = 0.64 + \frac{2.75}{12.5} = 0.86$$

DF for shear in the interior girder, $g_{interior} = 0.964$ (Table 4.12)

$$e(g_{interior}) = (0.86)(0.964) = 0.829$$

$$g_{ve2} = 0.829 \text{ lane/web} < g_{ve1} = 0.916 \text{ lane/web}$$

$$g_{ve1} = 0.916 \text{ lane/web} < g_{vi2} = 0.964$$

$$g_{ve2} = 0.964 \text{ (governs)}$$

Example 4.8: Live Load Distribution Factors for Three-Lane Steel Plate Girder Bridge with a Skew

Figure 4.26 shows the typical cross section and framing plan of a three-lane highway bridge having a simple span of 161 ft between centers of bearings. The cross section consists of four steel plate girders spaced equally at 13 ft on centers with 4 ft-3 in. overhangs and a 44 ft roadway width. Each steel girder is built from a 1¼ × 22 in. top flange, a ½ × 69 in. web, and a 2 × 22 in. bottom flange (Figure 4.26c). The concrete deck is 10 in. thick, which includes a ½ in. integral wearing surface. Provisions should be made for a dead load of 25 lb/ft^2 in design. The abutments are skewed a 35° positive.

Calculate (1) the distribution factors for bending moment and shear for interior and exterior girders of this bridge, including the correction factor for skew, (2) the distribution factors for fatigue for both interior and exterior girders, and (3) the distribution factors for deflection.

Solution

Check if the superstructure type conforms to one of the types listed in LRFD Table 4.6.2.2.1-1.

The given superstructure has cross section similar to Type (a) listed in LRFD Table 4.6.2.2.1-1. Hence, the expressions for distribution factors listed in LRFD Table 4.6.2.2.2b-1 can be used.

Check the range of applicability in LRFD Table 4.6.2.2.2b-1.

Girder spacing, $S = 13$ ft,	$3.5 \le S \le 16.0$ ft, OK
Slab thickness, $t = 9.5$ in.,	$4.5 \le t \le 12.0$ in. OK
Number of beams, $N_b > 4$,	$N_b \ge 4$, OK
Span = 161 ft,	$20 \le L \le 240$ ft, OK

www.EngineeringEBooksPdf.com

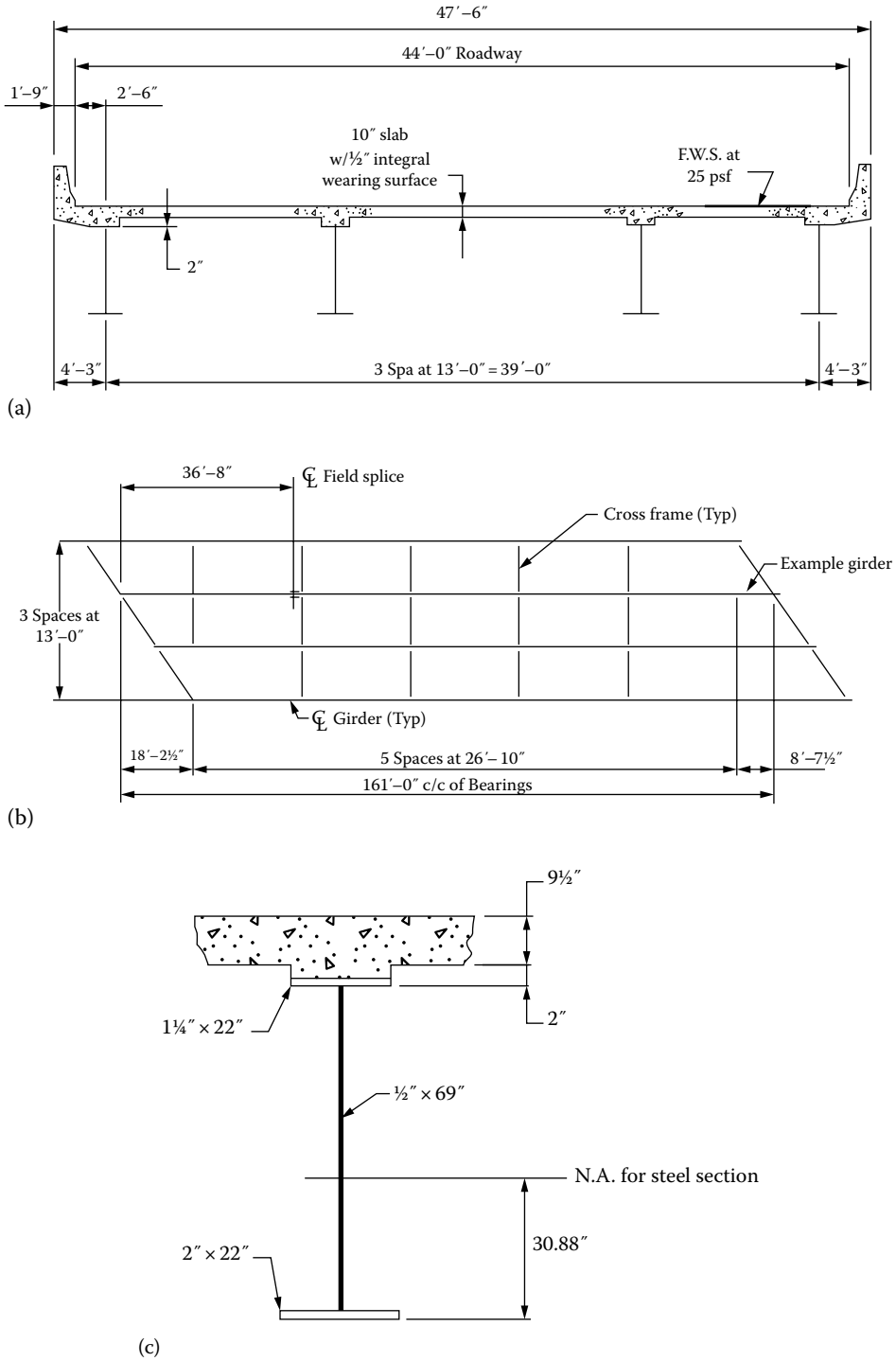

FIGURE 4.26 (a) Bridge cross section, (b) framing plan, and (c) girder cross section for Example 4.8. (Courtesy of American Iron and Steel Institute, Washington, DC.)

www.EngineeringEBooksPdf.com

TABLE 4.13
Calculation of Section Properties for Plate Girder of Example 4.8

Component	A, in.	y, in.	Ay, in.^{4}	$\bar{y}$, in.	$A\bar{y}^2$, in.^{4}	I_o, in.^{4}	I_x, in.^{4}
Top flange 1¼″ × 22	27.50	71.625	1970	40.75	45,665	4	
Web ½″ × 69′	34.50	36.50	1259	5.62	1,090	13,688	
Bottom flange 2″ × 22″	44.00	1.00	44	29.88	39,284	15	
Total	106.0		3273	—	86,039	13,707	99,746

Determine the bending moment of inertia of the steel girder. The required calculations are shown in Table 4.13.

Determine the neutral axis (NA) of steel section (see Figure 4.26c). The above calculations are performed with reference to the bottom of the steel section as datum (Table 4.13).

$\bar{y}$ = distance between the centroidal axis of the section and the centroid axis of the element.

$$y_{bot\ of\ steel} = \frac{3273}{106} = 30.88 \text{ in.}$$

$$y_{top\ of\ steel} = 1.25 + 69 + 2 - 30.88 = 41.37 \text{ in.}$$

The bending moment of inertia about the centrodial axis of the steel section is calculated to be

$$I_{NA} = 99{,}746 \text{ in.}^4$$

Calculate the longitudinal stiffness parameter, K_g. First, calculate distance e_g.

Thickness of slab excluding the integral wearing surface = 10 − 0.5 = 9.5 in.

The distance from the mid-surface of concrete slab to the centroid of steel section, e_g, is given by

$$e_g = \frac{9.50}{2} + 2.0 + 41.37 - 1.25 = 46.87 \text{ in. (see Figure 4.27).}$$

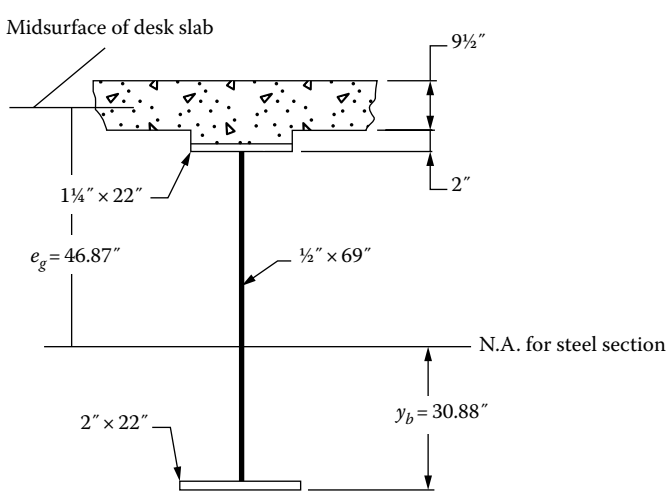

FIGURE 4.27 Determination of distance e_g.

www.EngineeringEBooksPdf.com

For f'_c = 4000 psi, n = 8 (Table 4.4)

$$K_g = n\left(\mathrm{I} + Ae_g^2\right)$$
$$= 8\left[99{,}746 + (106.0)(46.87)^2\right] = 2.661\times 10^6 \text{ in.}^4$$

a. Interior girder

Distribution factor for bending moment

Calculate the distribution factors for bending moment for the interior girder, g_{mi}:

$$S = 13 \text{ ft}, \quad L = 161 \text{ ft}, \quad t_s = 9.5 \text{ in.}$$

Case 1: One design lane loaded: g_{mi1}

$$g_{mi1} = 0.06 + \left(\frac{S}{14}\right)^{0.4}\left(\frac{S}{L}\right)^{0.3}\left(\frac{K_g}{12Lt_s^3}\right)^{0.1}$$
$$= 0.06 + \left(\frac{13.0}{14}\right)^{0.4}\left(\frac{13.0}{161}\right)^{0.3}\left(\frac{2.661\times 10^6}{12(161)(9.5)^3}\right)^{0.1}$$
$$= 0.538 \text{ lane/girder}$$

Case 2: Two or more design lanes loaded: g_{mi2}

$$g_{mi2} = 0.075 + \left(\frac{S}{9.5}\right)^{0.6}\left(\frac{S}{L}\right)^{0.2}\left(\frac{K_g}{12Lt_s^3}\right)^{0.1}$$
$$= 0.075 + \left(\frac{13.0}{9.5}\right)^{0.6}\left(\frac{13.0}{161}\right)^{0.2}\left(\frac{2.661\times 10^6}{12(161)(9.5)^3}\right)^{0.1}$$
$$= 0.84 \text{ lane} > g_{mi1} = 0.538 \text{ lane/girder}$$

Therefore, g_{mi2} = 0.84 lane/girder (governs).

Distribution factor for shear

Case 1: One design lane loaded: g_{vi1}

$$g_{vi1} = 0.36 + \frac{S}{25.0} = 0.36 + \frac{13.0}{25.0} = 0.880 \text{ lane/girder}$$

Case 2: Two or more design lanes loaded: g_{vi2}

$$g_{vi2} = 0.2 + \frac{S}{12} - \left(\frac{S}{35}\right)^2$$
$$= 0.2 + \frac{13.0}{12} - \left(\frac{13.0}{35}\right)^2$$
$$= 1.145 \text{ lanes} > g_{vi1} = 0.88 \text{ lane/girder}$$

Therefore, g_{vi2} = 1.145 lanes/girder (governs).

www.EngineeringEBooksPdf.com

b. Exterior girder

Distribution factor for bending moment
Two methods will be used as described in LRFD Specifications. The largest value will be selected as the distribution factor.

Method 1. LRFD Table 4.6.2.2.2c-1

Case 1: One design lane loaded: use the lever rule
The centerline of the exterior wheel of the exterior lane is placed at 2 ft (minimum distance) from the face of the curb (Art. 3.6.1.3.1). From the geometry of the bridge cross section, the distance d_e (the distance between the face of curb and the centerline of the exterior girder) is determined to be 2.75 ft so the distance between the center of the exterior truck lane from the centerline of first interior girder = 13.0 + 4.25 − 1.75 − 2.0 − 3.0 = 10.5 ft. Therefore, by lever rule (see Figure 4.28).

Fraction of the lane to the exterior girder, $g_{me1} = \dfrac{10.5}{13.0} = 0.808$
Apply multipresence factor, $m = 1.2$
$g_{me1} = 0.808(1.2) = 0.970$ lane (governs).

Case 2: Two or more design lanes loaded
Modify the distribution factor for the interior girder by adjustment factor e. Factor e is determined from distance d_e, the horizontal distance from the centerline of the web of the exterior beam at deck level to the interior edge of the curb or traffic barrier (ft). From the geometry of the cross section, d_e = +2.5 ft

$$e = 0.77 + \frac{d_e}{9.1} = 0.77 + \frac{2.5}{9.1} = 1.045$$

$$g_{mi2} = 1.045(0.840) = 0.878 \text{ lane}$$

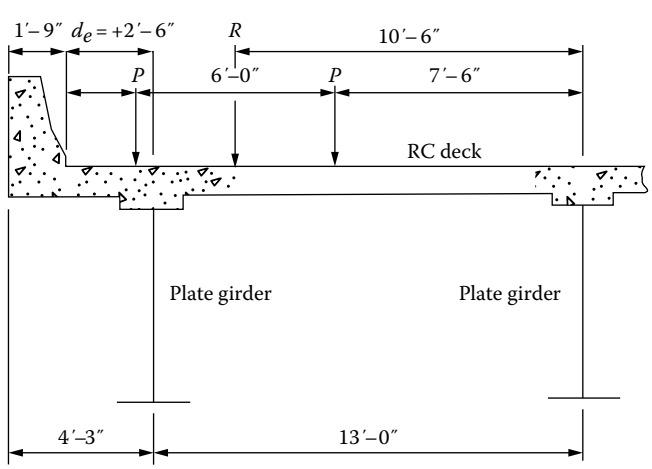

FIGURE 4.28 Exterior girder distribution factor—lever rule. The exterior wheel of the lane is placed at 2.0 ft (required minimum distance) from the face of the curb. Distance d_e = +2.5 ft (measured from the face of the curb to the center of the web of the exterior girder).

www.EngineeringEBooksPdf.com

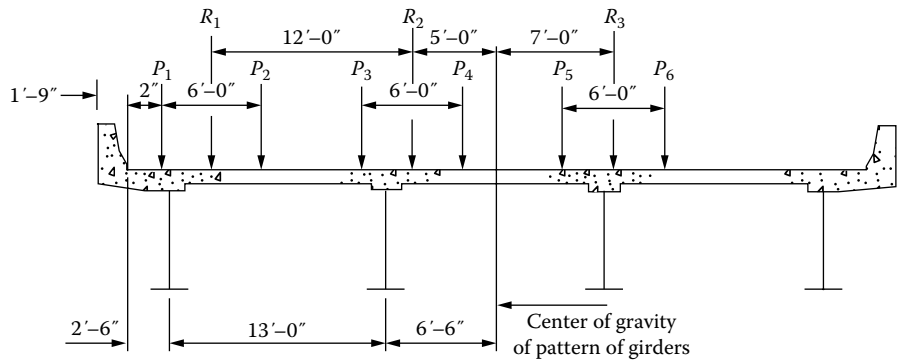

FIGURE 4.29 Schematics showing loaded lanes on bridge cross section for special analysis for Example 4.8. Note that the exterior wheel of the exterior lane is placed at 2 ft (minimum distance) from the edge of the curb.

Method 2. Special analysis
Refer to Figure 4.29 showing loaded design lanes on the bridge cross section

$$N_L = w/12 = 44/12 = 3.66, \text{ use } N_L = 3 \text{ lanes}$$

$$R = \frac{N_L}{N_b} + \frac{X_{ext}\sum^{N_L} e}{\sum^{N_b} x^2} \qquad (4.33)\ [AC4.6.2.2.2d\text{-}1]$$

Number of design lanes, $N_L = 3$, number of beams, $N_b = 4$
The multiple lane factors are

1 lane	$m_1 = 1.2$
2 lanes	$m_2 = 1.0$
3 lanes	$m_3 = 0.85$

For determining the eccentricity of a truck lane from the center of gravity of the pattern of girders, the truck is placed centrally within its 12 ft wide design lane.

Case 1: One design lane loaded: refer to Figure 4.29 for various distances

$$N_L = 1, \quad N_b = 4$$

X_{ext} = eccentricity of the exterior girder from the center of gravity of the pattern of girders
= distance between the centerline of the exterior girder to centerline of the bridge
= 13.0 + 6.5 = 19.5 ft
e = eccentricity of the extreme truck lane from the center of gravity of the pattern of girders
= 12 + 5 = 17 ft
x = horizontal distance from the center of gravity of pattern of girders to each girder
= 19.5 ft for the exterior girder
= 6.5 ft for the interior girder

$$R_1 = \frac{1}{4} + \frac{(13.0+6.5)(12.0+5.0)}{2\left(19.5^2+6.5^2\right)} = 0.642$$

Apply multiple presence factor for one loaded lane, $m_1 = 1.2$

$$m_1 R_1 = (1.2)(0.642) = 0.770 \text{ lane/girder}$$

www.EngineeringEBooksPdf.com

Case 2: Two design lanes loaded: $N_L = 2$, $N_b = 4$

$$R_2 = \frac{2}{4} + \frac{19.5(12.0 + 5.0 + 5.0)}{2\left(19.5^2 + 6.5^2\right)} = 1.008$$

Apply multiple presence factor for two loaded lanes, $m_2 = 1.0$

$$m_2R_2 = (1.0)(1.008) = 1.008 \text{ lanes/girder}$$

Case 3: Three design lanes loaded: $N_L = 3$, $N_b = 4$

$$R_3 = \frac{3}{4} + \frac{19.5(12.0 + 5.0 + 5.0 - 7.0)}{2\left(19.5^2 + 6.5^2\right)} = 1.096$$

Apply multiple presence factor for three loaded lanes, $m_3 = 0.85$

$$m_2R_3 = (0.85)(1.096) = 0.932 \text{ lanes/girder}$$

The largest calculated value of the distribution factor is 1.008 lanes/girder (governs).

Distribution factor for shear

Case 1: One lane loaded: use the lever rule

$$g_{v1} = 0.970 \text{ lane (calculated earlier)}$$

Case 2: Two or more lanes loaded

Modify the distribution factor for bending moment by factor e calculated as follows:

$$e = 0.6 + \frac{d_e}{10}$$

$$= 0.6 + \frac{2.5}{10}$$

$$= 0.85$$

$$g_{ve2} = 0.85(1.145) = 0.973$$

Case 3: Special analysis
The distribution factors calculated for bending moment are also used for shear.
One design lane loaded: $g_{ve1} = 0.770$ lane
Two design lanes loaded: $g_{ve2} = 1.008$ lane
Three design lanes loaded: $g_{ve3} = 0.932$

c. Skew correction factors
Correction factor for bending moment (AASHTO LRFD Table 4.6.2.2.2e-1):

$$c_1 = 0.25\left(\frac{K_g}{12Lt_s^3}\right)^{0.25}\left(\frac{S}{L}\right)^{0.5}$$

$$= 0.25\left(\frac{2.661\times10^6}{12(161)(9.5)^3}\right)^{0.25}\left(\frac{13.0}{161.0}\right)^{0.5}$$

$$= 0.080$$

Correction factor = $1 - c_1(\tan\theta)^{1.5} = 1 - 0.080(\tan 35)^{1.5} = 0.953$

www.EngineeringEBooksPdf.com

TABLE 4.14
Distribution Factors for Bending Moment and Shear for Example 4.8

	Interior Girder (Lane)	Exterior Girder (Lane)
Bending moment, g_m	0.801	0.961
Shear: end support, g_v	1.284	1.130
Shear: in span, g_v	1.145	1.008

Correction factor for shear (LRFD Table 4.6.2.2.3c-1):

$$\text{Correction factor} = 1.0 + 0.20\left(\frac{12Lt_s^3}{K_g}\right)^{0.3} \tan\theta$$

$$= 1.0 + 0.20\left(\frac{12(161)\,(9.5)^3}{2.661 \times 10^6}\right)^{0.3} \tan 35$$

$$= 1.121$$

The final values of distribution factors for bending moment and shear in interior and exterior girders, modified by appropriate corrections factors, are shown in Table 4.14. Note that the shears in both the interior and exterior girders away from the skewed support are not modified by the skew correction factors.

d. Distribution factors for fatigue limit state

Distribution factors for fatigue limit state are determined for only one lane loaded case.

The distribution factors for the interior girder for one lane loaded case were calculated earlier. The skew correction factors for bending moment and shear were calculated, respectively, to be 0.953 and 1.121. The distribution factors for the fatigue limit state are obtained by multiplying the distribution factors for bending moment and shear by the appropriate skew correction factors and dividing by 1.2 (multipresence factor for one lane loaded):

a. Interior girder:
   Bending moment: g_{mif} = 0.538 (0.953)/1.2 = 0.427
   Shear: End support: g_{vif} = 0.88 (1.121)/1.2 = 0.822
   Shear: In span: g_{vif} = 0.88/1.2 = 0.733
b. Exterior girder:
   Bending moment: g_{mef} = 0.97 (0.953)/1.2 = 0.770
   Shear: End support: g_{vef} = 0.97 (1.121)/1.2 = 0.906
   Shear: In span: g_{vef} = 0.97/1.2 = 0.808

The aforementioned results are shown in Table 4.15.

e. Distribution factors for absolute maximum live load deflection

For this three-lane bridge, the multipresence factor, $m = 0.85$. Also, $N_L = 3$, $N_b = 4$. From Equation 4.9,

$$g_{\Delta max} = m\left(\frac{N_L}{N_b}\right) = 0.85\left(\frac{3}{4}\right) = 0.638 \text{ lane}$$

TABLE 4.15
Distribution Factors for Fatigue Limit State

	Interior Girder (Lane)	Exterior Girder (Lane)
Bending moment, g_{mf}	0.427	0.770
Shear: end support, g_{vf}	0.822	0.906
Shear: in span, g_{vf}	0.733	0.808

www.EngineeringEBooksPdf.com

4.13 APPLICATION OF LIVE DISTRIBUTION FACTORS FOR DESIGN PURPOSES

Examples 4.3 through 4.8 presented the procedures for determining distribution factors for bending moment and shear in longitudinal girders of slab-beam bridges. These distribution factors are to be used as multipliers to the bending moment and shear in a span (as discussed in Chapter 3) in order to obtain (unfactored) design loads. The resulting force values are then multiplied with appropriate load factors to obtain force values for use in load and resistance factor design of the girders. Example 4.9 presents this procedure.

Example 4.9

Figure 4.30 shows the cross section of a single-span concrete deck steel girder bridge spanning 75 ft on an urban highway. The 8½ in. thick deck slab, which includes ½ in. thick integral wearing surface, is cast from 4500 psi concrete. The deck is supported by four steel girders (F_y = 50 ksi) built to act compositely with deck slab using 4 in. long, ¾ in. diameter headed shear studs (F_y = 50 ksi, F_u = 60 ksi), which would be welded to the girders. The girders are spaced at 10 ft on centers. Assume the dead weight due to stay-in-place forms (to support concrete during construction), cross-frames, and detailing as 200 lb/ft of girder length. For this bridge superstructure, calculate

a. The distribution factors for bending moment and shear
b. The design bending moment in an interior girder due to live load

Solution

Commentary: This example bridge was presented in Example 3.1 for illustrating the calculations for bending moment and shear in an interior girder of the bridge due to dead load. This example presents the calculations for bending moment due to live load in an interior of the same bridge. To preserve completeness of calculations, the solution is presented in four parts:

a. Calculations for bending moment due to dead loads
b. Calculations for bending moment in span due to live load
c. Calculation of the distribution factors for bending moment and shear in an interior girder
d. Application of distribution factor to live load bending moment
e. Calculation of maximum design bending moment for Strength Limit State I.

Note: *The following calculations are for unfactored loads.*

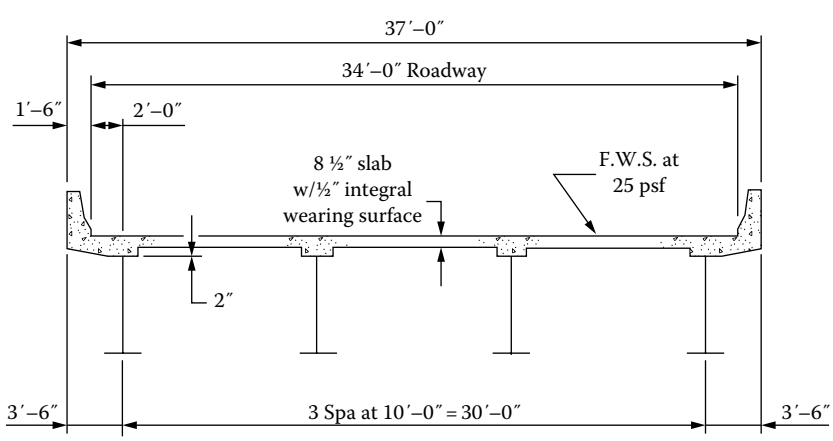

FIGURE 4.30 Bridge cross section for Example 4.9.

www.EngineeringEBooksPdf.com

a. Calculate bending moment in the girder due to dead load:
From Example 3.1, the following information is obtained:

$$M_{DC} = 1118 \text{ kip/ft}$$

$$M_{DW} = 176 \text{ kip/ft}$$

b. Calculate live load bending moment in span: $L = 75$ ft
Due to the design (HL-93) truck,

$$\begin{aligned} M_{truck} &= 18L - 280 + \frac{392}{L} \lim_{x \to \infty} \\ &= 18(75) - 280 + \frac{392}{75} \\ &= 1075.2 \text{ kip-ft} \end{aligned}$$

Dynamic load allowance: $IM = 0.33$ (truck load only)

$$M_{LL}\,(1 + IM) = (1075.2)(1 + 0.33) = 1430 \text{ kip/ft}$$

Due to lane load: The influence line ordinate is (refer to Example 3.5b for procedure)

$$\frac{ab}{L} = \frac{(37.5 - 2.335)(37.5 + 2.335)}{75} = 18.677 \text{ ft}$$

$$\begin{aligned} M_{lane} &= (0.64)\left(\frac{1}{2}\right)(L)\left(\frac{ab}{L}\right) \\ &= (0.64)(0.5)(75)(18.677) \\ &= 448.3 \text{ kip-ft} \end{aligned}$$

Total bending moment due to live load,

$$M_{LL+IM} + M_{lane} = 1430 + 448.3 = 1878.3 \text{ kip/ft}$$

Distribution factor would be applied to $(M_{LL+IM} + M_{lane}) = 1878.3$ kip/ft

c. Calculate the distribution factors for bending moment in the interior girder:
   1. The bridge cross section is Type (a)
   2. Check the range of applicability criteria for LRFD distribution factors:

$3.5 \text{ ft} \le S \le 16 \text{ ft}$	$S = 10$ ft,	OK
$4.5 \le t_s \le 12$ in.	$t_s = 8.5 - 0.5 = 8$ in.,	OK
$N_b \ge 4$,	$N_b = 4$ beams,	OK
$20 \text{ ft} \le L \le 240 \text{ ft}$	$L = 75$ ft,	OK
$10{,}000 \le K_g \le 7{,}000{,}000 \text{ in.}^4$	$K_g = 290{,}282 \text{ in.}^4$ (calculated later)	OK

   3. Calculate the bending moment inertia of the steel girder:
      y is the distance from bottom flange to centroid of each element
      $\bar{y}$ is the distance from the centroid of the steel section to centroid of each element (Table 4.16)

$$\bar{y}_{bot\ of\ steel} = \frac{638.66}{38.75} = 16.48 \text{ in. (Figure 4.31)}$$

www.EngineeringEBooksPdf.com

TABLE 4.16
Calculations for the Bending Moment of Inertia of the Girder

Component	A, in.^{2}	y, in.	Ay, in.^{2}	$\bar{y}$, in.	$A\bar{y}^2$, in.^{4}	I_o, in.^{4}
Top flange ¾ × 12	9.0	37.25	335.25	20.77	3882.5	0.4
Web 7/16 × 36	15.75	18.875	297.28	2.395	90.3	1701
Bottom flange ⅞ × 16	14.0	0.4375	6.13	16.043	3603.3	0.9
Total	38.75		638.66		7576.1	1702.3

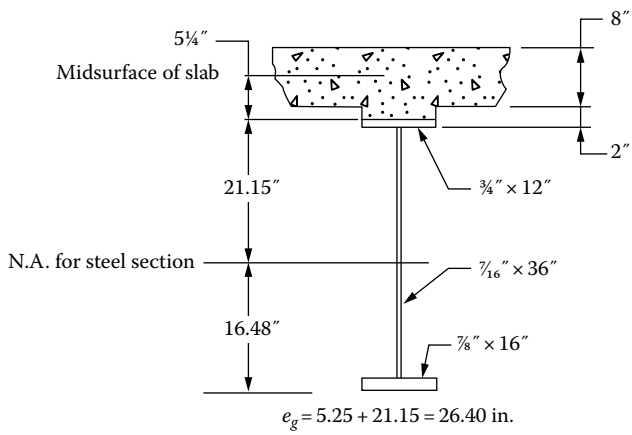

FIGURE 4.31 Determination of e_g for girder section of Example 4.9. (Adapted from American Iron and Steel Institute, *Four Design Examples of Steel Highway Bridges*, New York, 1997.)

$$\bar{y}_{top\ of\ steel} = 0.875 + 36 + 0.75 - 16.48 = 21.145 \text{ in.} \approx 21.15 \text{ in.}$$

$$I = I_0 + A\bar{y}^2 = 1702.3 + 7576.1 = 9278 \text{ in.}^4$$

e_g = perpendicular distance between the midsurface of the deck and the centroid of the steel section

= ½ × 8 + 2 − 0.75 + 21.15

= 26.4 in. (Figure 4.31)

$$K_g = n\left(I + Ae_g^2\right)$$

For f'_c = 4.5 ksi, n = 8 (Table 4.4)

$$K_g = 8\left[9278 + 38.75(26.4)^2\right] = 290{,}282 \text{ in.}^4$$

Check: 10,000 ≤ K_g = 290,282 ≤ 7,000,000 in.^{4}, OK

www.EngineeringEBooksPdf.com

Calculate the distribution factor for bending moment in an interior girder:

Case 1: One design lane loaded

$$g_{mi1} = \left(\frac{S}{14}\right)^{0.4}\left(\frac{S}{L}\right)^{0.3}\left(\frac{K_g}{12Lt_s^3}\right)^{0.1}$$

$$= 0.06 + \left(\frac{10}{14}\right)^{0.4}\left(\frac{10}{75}\right)^{0.3}\left(\frac{290,282}{(12)(75)(8)^3}\right)^{0.1}$$

$$= 0.516 \text{ lane}$$

Case 2: Two or more design lanes loaded

$$g_{mi2} = 0.075 + \left(\frac{S}{9.5}\right)^{0.6}\left(\frac{S}{L}\right)^{0.2}\left(\frac{K_g}{12Lt_s^3}\right)^{0.1}$$

$$= 0.075 + \left(\frac{10}{9.5}\right)^{0.6}\left(\frac{10}{75}\right)^{0.2}\left(\frac{290,282}{(12)(75)(8)^3}\right)^{0.1}$$

$$= 0.733 \text{ lane (governs)}$$

Calculate the distribution factor for shear in an interior girder:

Case 1: One design loaded

$$g_{vi1} = 0.36 + \frac{S}{25} = 0.36 + \frac{10}{25} = 0.76$$

Case 2: Two or more design lanes loaded

$$g_{vi2} = 0.2 + \frac{S}{12} - \left(\frac{S}{35}\right)^2 = 0.2 + \frac{10}{12} - \left(\frac{10}{35}\right)^2 = 0.952$$

d. Apply the distribution factor to total live load bending moment.

$$(M_{design\ LL})(g_{mi2}) = (1878.3)\ (0.733) = 1377 \text{ kip/ft } (LL + IM)$$

Design live load bending moment = 1377 kip/ft (unfactored)

e. Calculation of maximum bending moments in the girder for Strength Limit State I.
The bending moments calculated above are due to *unfactored* loads. The maximum bending moments due to *factored* loads for various strength limit states are calculated by multiplying the unfactored loads by the appropriate load factors (γ factors) as discussed in Chapter 3. For Strength Limit State I, the γ factors are as follows:

$$M_{DC}\ \gamma = 1.25$$

$$M_{DW}\ \gamma = 1.50$$

$$M_{LL+IM}\ \gamma = 1.75$$

Therefore, the maximum design bending moment (for LRFD) for Strength Limit State I is calculated as follows:

$$\Sigma\gamma_i M_i = 1.25(1118) + 1.5(176) + 1.75(1377) = 4071 \text{ kip/ft}$$

$$M_u = 4071 \text{ kip/ft}$$

For strength design purposes, $M_u \leq \phi M_n$.

www.EngineeringEBooksPdf.com

4.14 DISTRIBUTION FACTORS FOR SPECIAL LOADS WITH OTHER TRAFFIC LOADS

Provision for determining distribution factor when special (heavy) loads are combined with other traffic on a bridge deck is made in LRFD Art. 4.6.2.2.5. Force effects resulting from heavy vehicles in one lane with routine traffic in adjacent lanes, such as might be considered with load combination strength II (see Chapter 3), may be determined from Equation 4.38:

$$G = G_p\left(\frac{g_I}{Z}\right) + G_D\left(g_m - \frac{g_I}{Z}\right) \tag{4.38}$$

where

G = final force effect applied to a girder (kip or kip-ft)
G_p = force effect due to overload truck (kip or kip-ft)
g_I = single lane live load distribution factor
G_D = force effects due to design loads (kip or kip-ft)
g_m = multiple lane live load distribution factor
Z = modification factor
= 1.2 where the lever rule was not utilized
= 1.0 where the lever rule was used for single lane live load distribution factor

Equation 4.38 cannot be applied for cases where

1. The lever rule has been specified for both single lane and multiple lane loadings
2. The special requirement for exterior girders of slab-beam bridge cross sections with diaphragms specified in LRFD Art. 4.6.2.2.2d has been utilized for analysis

4.15 LIVE LOAD DISTRIBUTION FACTORS FOR BENDING MOMENTS AND SHEAR IN TRANSVERSE FLOOR BEAMS

The preceding discussion on the determination of live load distribution factors focused on the slab-beam type of bridge superstructures. These bridge types typically consist of a deck slab supported on longitudinal beams that are themselves supported on the abutments. These may be situations where the deck is supported directly by transverse floor beams. In such cases, the floor beams may be designed for loads determined in accordance with LRFD Table 4.6.2.2.2f-1 (see Table 4.A.7). The distribution factors are listed in the form of *S over*… fractions, where S = spacing of floor beams.

LRFD Art. 4.6.2.2.2f specifies the methodology for using Table 4.6.2.2.2f-1. The fractions provided in this table are to be used in conjunction with the 32.0-kip design axle load alone. For spacing of floor beams outside the given range of applicability, all of the design live load shall be considered, and the lever rule may be used.

4.16 METHODS OF REFINED ANALYSIS

It is noted that the method of live load distribution factors for determining bending moments and shear in the interior and exterior girders of slab-beam types of bridges as noted in the preceding discussion is simple to use, but they have some drawbacks. While bridges using the approximate method result in safe design, it is an approximate method nevertheless. Furthermore, this method is applicable for only the specified types of bridge superstructures meeting specified range of bridge parameters. When these parameters exceed the range of applicability of these expressions, LRFD Specifications require that refined methods of analysis such as grillage analogy or finite element analysis be performed to determine live load effects in the superstructure. In some cases, refined

www.EngineeringEBooksPdf.com

methods may be even desirable for analyzing bridge superstructures having complex geometrics. A refined analysis may be desirable, for example, for highly skewed bridges, where cross-frame forces can become significant due to large differential deflections. As a general rule, refined methods are used when closed-form solutions are not available.

From an analytical perspective, any method that satisfies the requirements of equilibrium and compatibility and utilizes stress–strain relationships for the proposed materials (i.e., any method based on the principles of applied mechanics) may be used. Some of the refined methods that may be used for analyses (Art. 4: Acceptable Methods of Analysis) were discussed in Section 4.6.3.1.

LRFD Art. 4.6.3 provides guidance on applications of refined methods for several types of superstructures. These methods are outside the scope of this book and not discussed further. A discussion of refined methods can be found in the literature (Hendry and Jaeger 1956, Kerfoot and Ostapenko 1967, Bares and Massonet 1968, Sanders and Elleby 1970, Jaeger and Bakth 1982). A brief summary of several refined methods has been provided by Taly (1998) and Barker and Puckett (2013).

4.17 DISTRIBUTION OF LATERAL LOADS IN MULTIBEAM BRIDGES

4.17.1 General

In bridges as in all types of structures, continuous load paths must be provided for gravity as well as lateral loads so that they are transmitted from their origin to the foundations. The load path for gravity loads on bridge substructures was discussed in Section 4.2. For gravity loads, a clear and visual, and often obvious, link is easily established for component-to-component force transfer through a vertically oriented support system as illustrated in Figure 4.2. But for lateral loads (wind or seismic) acting on the superstructure, a continuous load path to transmit them from their origin to the foundation is not as obvious. Therefore, it is critical to establish and provide a viable load path to transmit lateral loads to the foundation based on the stiffness characteristics of various components of the superstructure, viz., the deck, diaphragms, cross-frames, and lateral bracings. Distribution of wind and seismic loads on multibeam bridge superstructures is presented in this section.

4.17.2 Lateral Wind Load Distribution in Multibeam Bridges

4.17.2.1 Load Path for Lateral Wind Load

All of the previous discussion was focused on distribution of vehicular live load to various types of structures as shown in Table 4.A.1. Of course, all of these superstructures as well as all other types of bridges are subjected to lateral loads, wind load among them. This section presents a discussion on the distribution of wind loads in *multibeam bridges*.

In all cases, wind load acting transverse to the superstructures must be transmitted to the supports and finally to the foundation through a load path. In multibeam bridges, the load path for lateral loads due to wind is provided as follows:

1. In bridges with composite decks, noncomposite decks with concrete haunches, and other decks that can provide horizontal action (i.e., decks act as horizontal diaphragms), wind load on the upper half of the exterior beam, the deck, vehicles, barriers, and appurtenances shall be assumed to be directly transmitted to the deck as a lateral diaphragm carrying this load to supports.
2. Wind load on the lower half of the beam shall be assumed to be applied directly to the lower flange of the beam. As a result, the beam would have a tendency to bend about its weak (or minor axis) causing a lateral flange bending stress, f_ℓ (discussed in Chapter 6).
3. Precast concrete planks, plank decks, and timber decks are not considered as solid diaphragms. For such bridges, the lever rule shall apply for the distribution of wind load to the top and bottom flanges of the exterior beam. This action would cause lateral bending of the beam causing lateral flange-bending stress, f_ℓ (discussed in Chapter 6).

www.EngineeringEBooksPdf.com

4. Bottom and top flanges subjected to lateral wind load shall be assumed to carry that load to adjacent bracing points by flexural action. Such bracing points occur at wind bracing nodes, or at cross-frames and diaphragm locations.
5. The lateral forces applied at brace points by the flanges shall be transmitted to the supports by one of the following load paths:
   a. Truss action of horizontal wind bracing in the plane of the flange.
   b. Frame action of the cross-frames or diaphragms transmitting the forces into the deck or the wind bracing in the plane of the other flange, and then by diaphragm action of the deck, to the supports.
   c. In some cases, the deck cannot provide horizontal diaphragm action, and there is no wind bracing in the plane of the flange. In such cases, load path is provided by lateral bending of the flange subjected to the lateral forces and all other flanges in the same plane, thus transmitting the forces to the ends of the span.

4.17.2.2 Determination of Forces and Bending Moments Due to Lateral Wind Load

Determination of forces and bending moments in structural members that participate in the load path in transmitting lateral wind load should be determined by methods based on the principles of structural mechanics. Unfortunately, because of the interconnectivity of various members in the load path (exterior beam, intermediate diaphragms, end diaphragms and cross-frames, wind bracing, etc.), a mathematical analysis of this problem is not easy. Simplifying assumptions must be made in order to calculate member forces and stresses for design purposes.

LRFD Commentary C4.7.2.7.1 provides a simplified procedure for the distribution of lateral wind load to multibeam bridges. This procedure may also be used for other types of bridges.

The wind force, W (Equation 4.39), may be applied to the flanges of exterior beams of composite members and noncomposite members with cast-in-place concrete or orthotropic steel decks, W, need not be applied to the top flange:

$$W = \frac{\eta_i \gamma P_D d}{2} \qquad (4.39)\ [\text{AC4.6.2.7.1-1}]$$

where

W = factored wind force per unit length applied to the flange (kip/ft)
P_D = design horizontal wind pressure, ksf (Art. 3.8.1)
d = depth of member (ft)
β = load factor as specified in LRFD Table 3.4.1-1 for the particular group loading combination AQ16
η_i = load modifier relating to ductility, redundancy, and operational importance as specified in Art. 1.3.2.1

For the first two load paths described in the preceding section (items 5a and 5b), the maximum wind bending moment on the loaded flange is determined from Equation 4.40:

$$M_w = \frac{WL_b^2}{10} \qquad (4.40)\ [\text{AC4.6.2.7.1-2}]$$

where

M_w = maximum lateral bending moment in the flange due to the factored wind loading (kip-ft)
W = factored wind force per unit length applied to the flange (kip/ft)
L_b = spacing of bracing points (ft)

www.EngineeringEBooksPdf.com

For the third path (item 5c), the maximum wind bending moment on the loaded flange may be determined from Equation 4.41:

$$M_w = \frac{WL_b^2}{10} + \frac{WL^2}{8N_b} \quad (4.41)\ [AC4.6.2.7.1\text{-}3]$$

where
N_b = number of longitudinal members
L = span length (ft)

Equation 4.41 is based on the assumption that cross-frames and diaphragms act as struts in distributing the wind force on the exterior flange to adjacent flanges. If there are no cross-frames or diaphragms, the first term in Equation 4.41 should be taken as zero, and N_b should be taken as 1.0, resulting in Equation 4.42:

$$M_w = \frac{WL^2}{8} \quad (4.42)$$

Note that Equation 4.42 is simply an expression for bending moment in a uniformly loaded simple beam.

The horizontal wind force applied to each brace point may be calculated based on the tributary area as given by Equation 4.43:

$$P_w = WL_b \quad (4.43)\ [A4.6.2.7.1\text{-}4]$$

Lateral bracing systems required to support both flanges due to transfer of wind loading through diaphragms or cross-frames should be designed to resist an axial force of $2P_w$ at each brace point.

Application for the earlier-described procedure is illustrated in Chapter 6.

4.17.3 Seismic Load Distribution in Multibeam Bridges

4.17.3.1 Load Path for Earthquake Forces in Multibeam Bridges

A discussion on the determination of earthquake forces and related LRFD provisions was presented in Section 3.21. This section presents an overview of the distribution of earthquake forces in multibeam bridges. Just as a continuous load path must be provided for transferring gravity loads from the superstructure to the substructure, and eventually, to the foundation, a clear, continuous load path must be provided to also transfer earthquake forces acting on the superstructure to the substructure, and eventually to the foundation.

An important difference between the distribution of wind loads in multibeam bridges and the distribution of seismic load must be recognized. The wind loads are lateral loads that act externally on the superstructure just as they act externally on the shell of a building, whereas the earthquake forces are inertia forces (force = mass *times* acceleration) that are generated as a result of ground motion (discussed in Section 3.21). The general principles of transferring inertia forces from a bridge superstructure to its foundation are similar as those applicable to buildings and discussed by Taly (2003).

A difficulty associated with the transmission of earthquake forces, which essentially are inertia forces, is that a load path for these forces is not as readily recognized and defined as the one for gravity loads. This is because in multibeam bridges, the major source of earthquake force is the deck (generated by its inertia). For resisting the earthquake force, the deck acts as a horizontal diaphragm (just as floors act as horizontal diaphragms in buildings, the force generating mechanism being similar as in bridges). Both are discussed here.

www.EngineeringEBooksPdf.com

For design purposes, the United States is divided into four seismic zones. The design provisions for various seismic zones in the United States are covered in LRFD Specifications as follows:

Seismic zone 1	Art. 3.10.9.2
Seismic zone 2	Art. 3.10.9.3
Seismic zones 3 and 4	Art. 3.10.9.4

A comprehensive discussion on various seismic zones and pertinent LRFD provisions has been provided in Section 3.21.

4.17.3.2 Design Criteria

In all cases, it must be ensured that a clear, straightforward, continuous load path exists, by design, to transmit earthquake forces from superstructure to the bearings at abutments and/or piers, and then to the foundation. All components and connections that comprise the links of the load path must be properly designed. The flow of forces in assumed load path must be accommodated through all the affected components and details. Diaphragms, cross-frames, lateral bracings, bearings, and substructure elements are parts (or links) of a seismic force resisting system (SFRS). The performance of these elements is affected by the strength and stiffness characteristics of the other elements of the bridge. Experience from the past earthquakes has shown that when one of these elements responded in a ductile manner or allowed some movement, the damage was limited. The underlying assumption on designing the SFRS is that plastic hinging in the substructure is the primary source of energy dissipation.

Members of diaphragms and cross-frames identified by the designer as part of the SFRS for carrying the earthquake forces from the superstructure to the bearings are to be designed and detailed to remain elastic based on the gross area criteria, under all design earthquakes, regardless of the types of bearings used.

4.17.3.3 Earthquake Load Distribution

The distribution of earthquake forces discussed herein is limited to the slab-on-girder types of bridges. Typically, these bridges fall into one of the following two categories:

1. Bridges with concrete decks that can provide horizontal diaphragm action or bridges that have horizontal bracing system in the plane of the top flange
2. Bridges that cannot provide horizontal diaphragm action and have no lateral bracings in the plane of the top flange

In the first category of bridges, the loads applied to the deck (which acts as a horizontal diaphragm) are assumed to be transmitted directly to the bearings through the end diaphragms or cross-frames. Concrete decks, by virtue of their mass, possess significant rigidity in their horizontal plane; as a result, in short- and medium-span bridges, their responses approach rigid body motion. For this reason, the lateral loading of the intermediate diaphragms and cross-frames is minimal.

In the second category of bridges, the lateral load applied to the deck is to be distributed through the intermediate diaphragms and cross-frames to the bottom lateral bracings or the bottom flange, and then to the bearings, and through the end diaphragms and cross-frames, in proportion to their relative rigidity and respective tributary mass of the deck.

4.18 ANALYSIS OF CONCRETE SLABS AND SLAB-TYPE BRIDGES FOR LRFD LIVE LOADS

4.18.1 General

Analysis methods presented in this chapter thus far focused on the analysis of interior and exterior girders of multibeam bridges that constitute the most common types of modern short-span highway bridges. This section presents a discussion on the analysis of two structural components of highway bridges not

www.EngineeringEBooksPdf.com

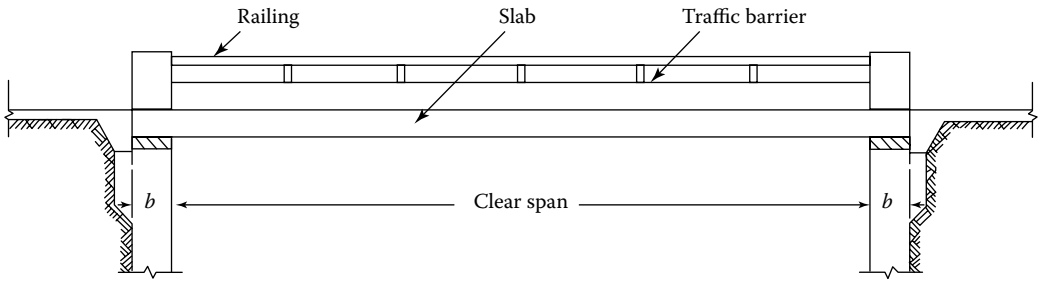

FIGURE 4.32 Typical reinforced concrete slab bridge. The slab is supported between the abutments; the longitudinal reinforcement is oriented *parallel* to the direction of traffic.

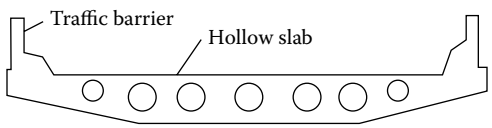

FIGURE 4.33 Cross section of a hollow slab bridge (with circular holes).

discussed earlier, viz., slab-type bridges and concrete decks. Concrete slabs constitute the most commonly used type of decks for all types of bridges—reinforced concrete as well as steel bridges. Both are discussed here.

From a structural perspective, slabs are used for highway bridges in two ways, distinguished by the direction of main reinforcement with respect to the direction of traffic: (1) slab-type bridges and (2) concrete decks.

4.18.1.1 Slab-Type Bridges

In many cases, short-span bridges consist of simply supported concrete slabs (reinforced or prestressed) that span primarily between the abutments and/or piers. These bridges are called slab-type bridges and are characterized by their primary (or main) reinforcement that is oriented *parallel* to the direction of the traffic (Figure 4.32). In some long-span steel girder bridges, the longitudinally spanning slab is supported over transverse floor beams, which themselves are framed into longitudinally spanning plate girders; the primary reinforcement in such slabs also is parallel to traffic (discussed in Chapter 5).

Generally speaking, slab bridges are not economical for spans exceeding 50 ft or so because of the excessive dead weight resulting from the depth requirements (see Example 5.1). Hollow concrete slabs were developed to overcome this problem by incorporating circular or rectangular cross section placed symmetrically about the neutral axis for analytical simplicity (Figure 4.33).

4.18.1.2 Concrete Decks

A deck is a structural component, with or without wearing surface, which directly supports wheel loads. Concrete decks (reinforced or prestressed) are supported and span transversely over parallel beams in multibeam highway bridges. The main reinforcement in concrete decks is oriented *perpendicular* to the direction of traffic that is different from the slab-type bridges in which the main reinforcement is oriented *parallel* to the direction of traffic. Several deck systems and deck arrangements are shown in Figures 4.34 through 4.36.

4.18.2 Analysis of Slab-Type Bridges

4.18.2.1 General

Several methods are available to analyze live load force effects (or live load distribution) in bridges (including slab-type bridges) as discussed in Section 4.16. While these methods are not discussed herein, a brief overview of the structural behaviors concrete slabs is presented.

www.EngineeringEBooksPdf.com

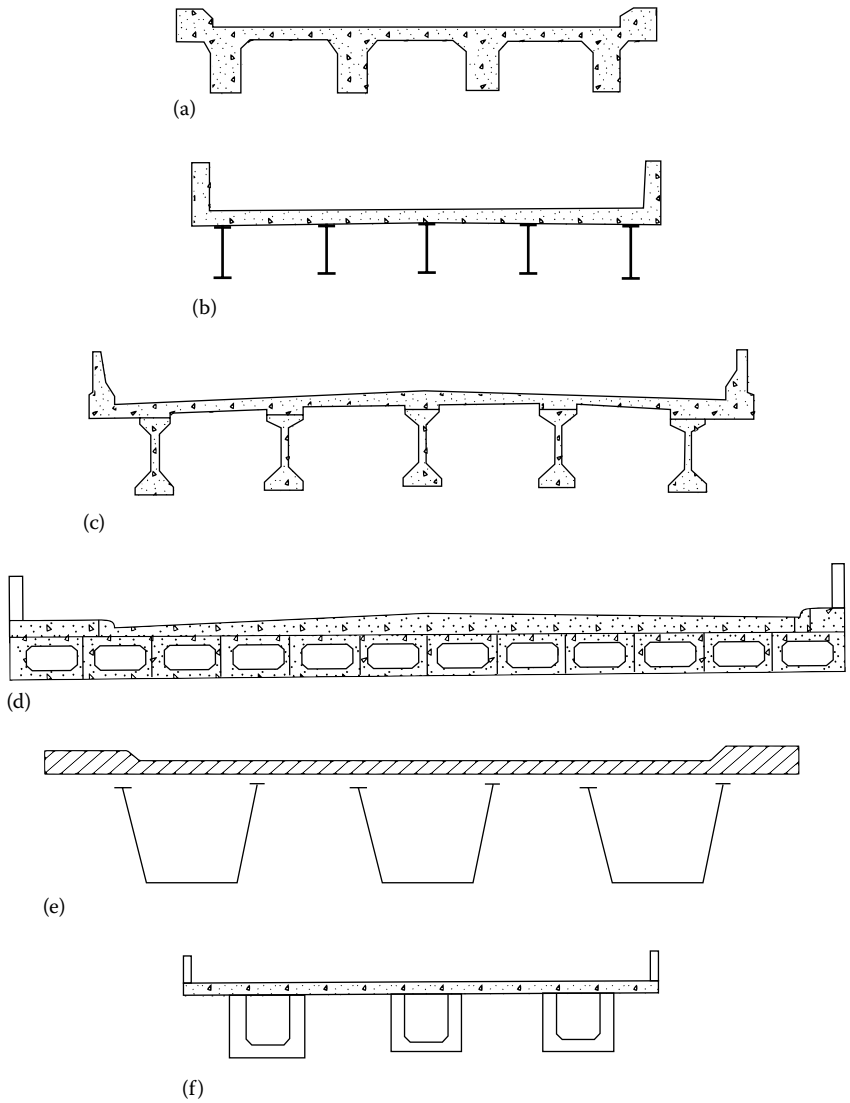

FIGURE 4.34 Concrete deck systems: (a) T-beam bridge, (b) slab on steel beams, (c) slab on prestressed concrete I-beams, (d) contiguous prestressed box beam and slab deck, (e) multispine deck with steel box beams, and (f) multispine deck with concrete U-beams. All decks shown have one characteristic in common—the primary or main reinforcement is oriented *perpendicular* to traffic.

A concrete slab essentially acts as a giant plate that has a small aspect ratio (i.e., ratio of span to width) that bends longitudinally between the supports, as well as transversely. Theoretically speaking, its load-carrying mechanism is analogous to that of a plate, which is characterized by its ability to transfer bending and twisting in its own plane owing to continuity in all directions. The physical behavior of a rectangular plate simply supported on two parallel edges and free on the other two parallel edges is illustrated in Figure 4.37a, which shows the slab divided into several rectangular elements; Figure 4.37b shows the free-body diagram of an arbitrary rectangular element.

As a two-dimensional solution, the governing equation for the lateral deflection of uniformly loaded plate, developed by S. D. Poisson (1781–1840), with boundary conditions modified by

www.EngineeringEBooksPdf.com

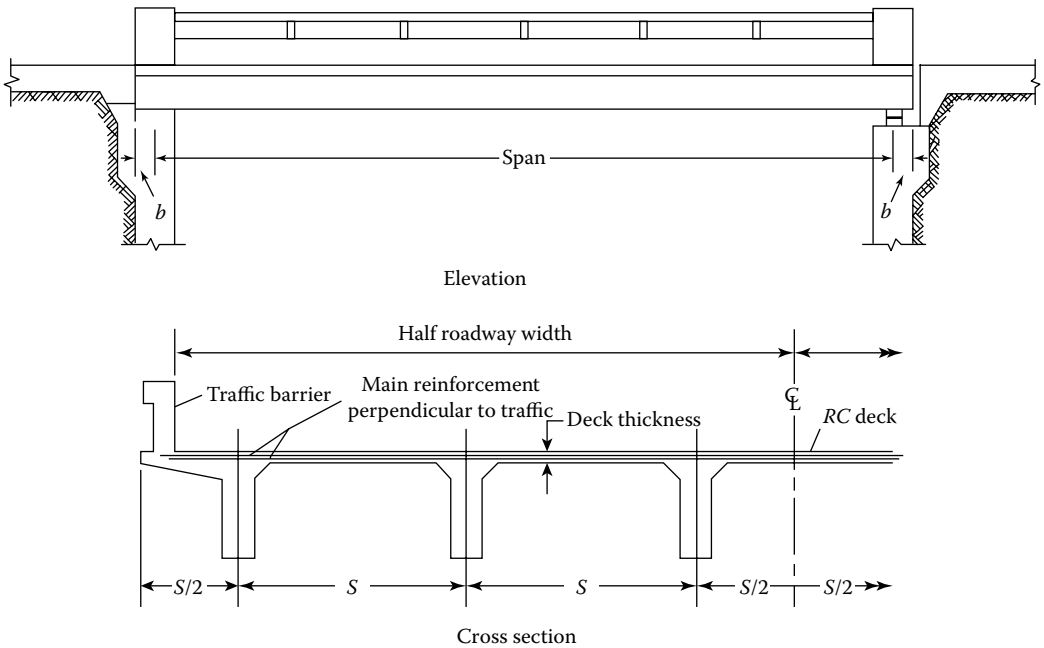

FIGURE 4.35 A typical reinforced concrete T-beam bridge. The concrete deck is cast monolithically with the stems. The main reinforcement in the concrete deck slab runs *perpendicular* to the direction of traffic.

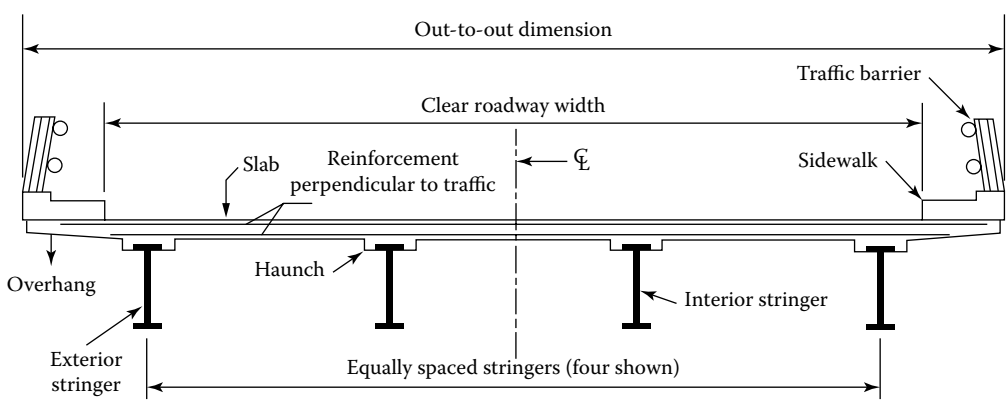

FIGURE 4.36 A typical slab-steel beam bridge. The reinforcement in the deck slab runs *perpendicular* to traffic.

G. R. Kirchhoff (1824–1887) (Timoshenko 1953, Timoshenko and Woinowsky-Krieger 1959) can be expressed by Equation 4.44:

$$D\left(\frac{\partial^4 w}{\partial x^4}+2\frac{\partial^4 w}{\partial x^2 \partial y^4}+\frac{\partial^4 w}{\partial y^4}\right)=q \tag{4.44}$$

where

w = deflection of the plate

q = intensity of uniform load

www.EngineeringEBooksPdf.com

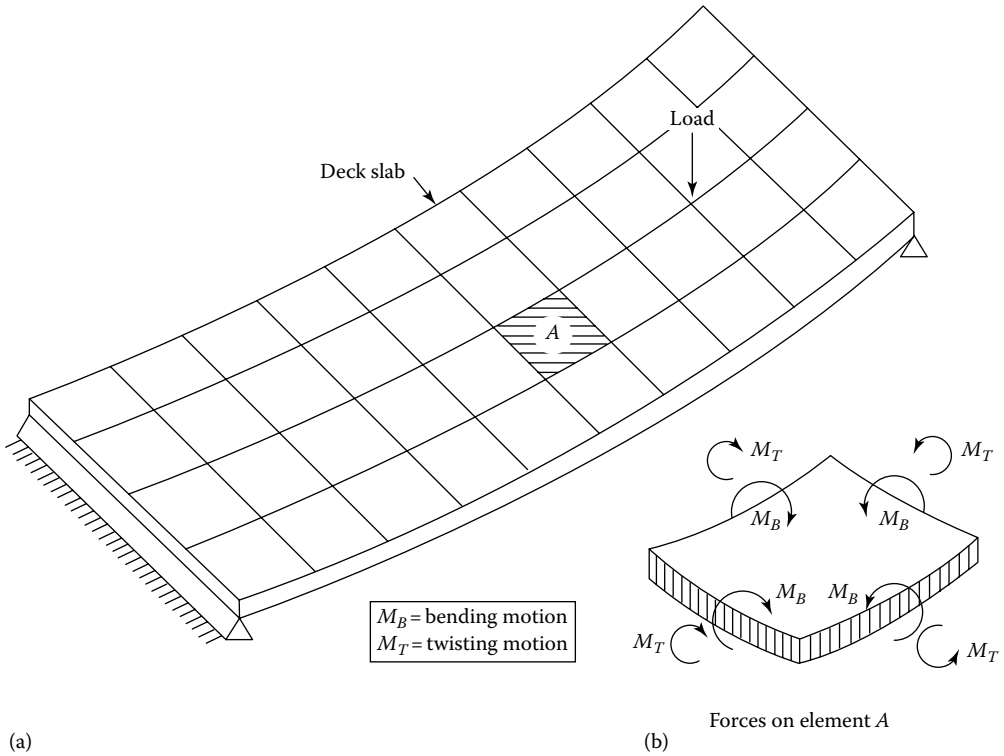

FIGURE 4.37 (a) Plate action in a slab and (b) free-body of a rectangular element showing distribution of forces by bending and twisting in two directions.

D = flexural rigidity of the plate as expressed by Equation 4.45:

$$D = \frac{Eh^3}{12(1-\nu^2)} \tag{4.45}$$

where
E = modulus of elasticity of the material
h = thickness of the plate
ν = Poisson ratio

In the absence of a closed-form solution of Equation 4.44 for a real deck, approximate solutions have been developed (Chaudhary 1978). One of these is the grillage method, wherein, for analytical purposes, real continuous plated structure (slab) is idealized by a series of discrete, orthogonally intersecting beams (Figure 4.38). Details of these methods can be found in the literature (Kerfoot and Ostapenko 1967, Bares and Massonet 1968, Bakth and Jaeger 1985, Jaeger and Bakth 1989, Hambly 1991).

Another method for analysis of slabs is the method of influence surfaces, which uses design charts. These charts have been prepared for various shapes and support conditions by Pucher (1964), and for *skew* simply supported slabs by Rusch and Hergenroder (1961), and Balas and Hanuska (1964). For orthotropic slabs, charts prepared by Morice and Little (1954, 1955, 1956) and described by Rowe (1962), and charts of Cusens and Pama (1975) are available.

www.EngineeringEBooksPdf.com

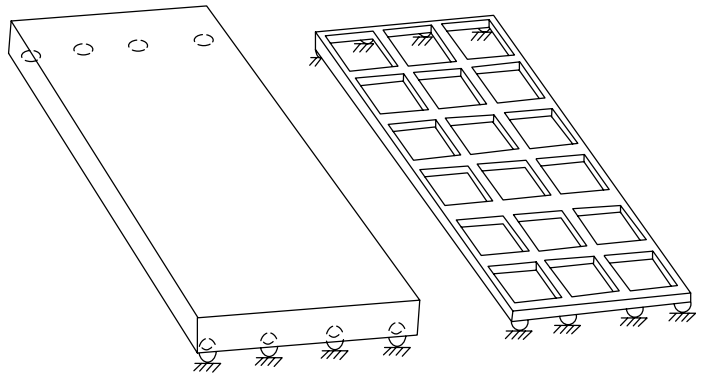

FIGURE 4.38 Grillage analysis of a slab: (a) prototype slab and (b) equivalent grillage. (After Hambly, E.C., *Bridge Deck Behavior*, 2nd ed., E & FN Spon, London, U.K., 1991.)

Yet another method, the application of the line solution technique to the general solution of reinforced concrete decks, has been described by Coull and Rao (1969). Applicable to both right and skew bridge slabs, this method reduces the partial differential equation of the plate theory to a set of differential equations by replacing the derivatives in one direction by their finite difference equivalents. Analysis of decks formed from contiguously placed hollow beams with longitudinal shear keys (Figure 4.34d, superstructure Type (f) in LRFD Table 4.6.2.2.1-1) can be found in the literature (Newmark 1938, Cusens and Pama 1965, Nasser 1965, Pool et al. 1965).

4.18.2.2 LRFD Provisions for the Analysis of Slab-Type Bridges: The Approximate Strip Model

4.18.2.2.1 General

The methods of live load distribution factors applicable to multigirder bridges (slab-beam bridges) discussed in the previous sections of this chapter are referred to as *approximate methods of analysis* (Art. 4.6.2). Approximate methods of analysis for decks are specified in Art 4.6.2.1, which specifies analysis methods for slab-type bridges and for concrete decks. Art. 4.6.2.1.2 specifies that *for slab bridges and concrete slabs spanning more than 15 ft and which span primarily in the direction of traffic, provisions of Art. 4.6.2.3 shall apply*, which is discussed next.

The analysis of slab-type bridges specified in LRFD Specifications is based on the *approximate strip model* as specified in Art. 4.6.2.3; its provisions are applicable to both cast-in-place solid slab- as well as voided slab-type bridges. Slabs in these types of bridges directly support the wheel loads. In the beam-line analysis used for slab-girder-type bridges, the live load effects are first computed on a typical interior and exterior beam. In analysis of slab-type bridges, the live load effects are first computed on a typical *interior strip* and a typical *exterior trip* (also called *edge strip*). The key to determining the live load force effects on a simply supported slab is the *equivalent strip width*; this is the width of the slab (spanning between the supports) that is assumed to carry the live load of one design lane.

The assumptions implicit in and limitations of the approximate strip model should be recognized. Although this method is referred to as *approximate strip method*, it should be recognized that in determining strip widths, the effects of flexure in the secondary direction and of torsion on the distribution of internal force effects are accounted for to obtain flexural force effects approximating those that would be provided by a more refined analysis. This method is based on rectangular layouts; however, currently about two-thirds of all bridges nationwide are skewed. While the effect of skew is to generally decrease force effects, it produces negative moments at corners, torsional moments in the end zones, substantial redistribution of reaction forces, and number of structural phenomena that should be considered in design.

www.EngineeringEBooksPdf.com

To determine the live load force effect (moment and shear) per unit width of the equivalent strip, the total load due to one design lane is divided by the width of this equivalent strip (Art. C4.6.2.1.3). This, in effect, means that the *inverse of the equivalent strip width is used as the distribution factor for designing 1 ft wide strip of the slab.* For example, if the equivalent strip width is computed to be 10 ft, the 1 ft wide strip would be designed for one-tenth of live load force effects (moment and shear). In other words, the live load distribution factor for both moment and shear in the 1 ft wide strip is 0.1. Furthermore, the equivalent strip width is the same for both live load moment and shear, which means that *the distribution factors for live load moment and shear are the same for slab bridges*. This is in contrast to the live load distribution factors for beams of multigirder bridges, which are different for moment and shear. Based on past practice and experience, slab bridges designed for moment are considered safe in shear (Art. 5.14.4.1).

Art. 4.6.2.3 specifies the following provisions pertaining to the determination of the equivalent strip widths.

Equivalent strip widths are computed separately for a typical interior strip and a typical exterior (or edge) strip. This, in effect, means live load distribution factors are different for the interior and the exterior strips.

1. Equivalent strip width for a typical interior strip is determined separately for two load cases (as in the case of multigirder bridges):
   a. One design lane loaded
   b. More than one design lane loaded (i.e., two or more design lanes loaded)
2. The equivalent strip width for the exterior strip is computed for only one wheel line (i.e., only one-half of the design lane) regardless of the design lanes that can occupy the bridge.
3. As in multibeam bridges, the number of design lanes (N_L) is obtained as the integer part of the clear roadway width divided by 12 (Art. 3.6.1.1.1).

The permanent load effects (*DC* and *DW*) are also computed for one-ft wide strip of the slab. This one-ft wide strip forms the design basis for the slab, which is designed for the combined effects of permanent loads and the applicable live loads. Once all the force effects are determined on the one-ft wide longitudinal strip, it is analyzed by classical beam theory (Art. 4.6.2.1.5), and the entire slab designed in the same manner as any other concrete simply supported floor slab.

Of necessity, the exterior strip consists of a traffic barrier (one on each side of the bridge). Because the traffic barriers would be cast *after* the slab hardens, some designers distribute the dead weight of the traffic barriers over the entire width of the slab; this approach has been used in all the examples of multigirder bridges presented in this book. Others, because of the uncertainty associated with the distribution of dead weight of the traffic barriers, follow a conservative approach and distribute the dead load of the traffic barriers on only the exterior strips (dead load of one traffic barrier on each exterior strip); this latter approach has been used in the design of the slab bridge and the decks presented in Examples 5.1 through 5.3.

LRFD provisions for limit states, load factors and load combinations (Art. 3.4, LRFD Table 3.4.1-1), dynamic load allowance (Art. 3.6.2), and multiple presence factors (Art. 3.6.1.1.2) are all applicable to slab-type highway bridges just like they are applicable to slab-beam types of highway bridges.

4.18.2.2.2 Equivalent Strip Width for the Interior Strip

4.18.2.2.2.1 One Design Lane Loaded The equivalent width of the longitudinal strips per design lane for both shear and moment with one lane loaded, that is, both wheels loaded, is given by Equation 4.46:

$$E = 10.0 + 5.0\sqrt{L_1 W_1} \qquad (4.46)\ [\text{A}4.6.2.3\text{-}1]$$

In Equation 4.46, the strip width has been divided by 1.2 to account for the multiple presence factor.

www.EngineeringEBooksPdf.com

4.18.2.2.2.2 More than One Design Lane Loaded The equivalent width of the longitudinal strips per design lane for both shear and moment with more than one design lane loaded is given by Equation 4.47:

$$E = 84.0 + 1.44\sqrt{L_1 W_1} \leq \frac{12.0W}{N_L} \qquad (4.47)\ [A4.6.2.3\text{-}2]$$

where

E = equivalent width (ft)
L_1 = modified span length taken equal to the lesser of the actual span or 60 ft
W_1 = modified edge-to-edge width of bridge taken to be equal to the lesser of the actual width or 60 for multiple lane loading, or 30 for single-lane loading (ft)
W = physical edge-to-edge width of bridge (ft)
N_L = number of design lanes as specified in Art. 3.6.1.1.1

For skewed bridges, the longitudinal force effects may be reduced by the factor r defined by Equation 4.48:

$$r = 1.05 - 0.25 \tan\theta \leq 1.00 \qquad (4.48)\ [A4.6.2.3\text{-}3]$$

4.18.2.2.3 Equivalent Strip Width for the Exterior Strip

Exterior strip (or the edge strip) refers to a portion of the slab located at its edges. The strip may be located at the longitudinal edges (Art. 4.6.2.1.4b) or at the transverse edges (Art. 4.6.2.1.4c).

The longitudinal edge strip of the slab is treated as a notional edge beam. This is the strip on which the traffic barriers are located and on which the exterior wheel of the design truck can be positioned. The dead weight of the traffic barriers, at the discretion of the designer, may be distributed on the equivalent width of the exterior strip.

Art. 4.6.2.1.4b implies that the exterior edge of the slab should have an *edge beam*, and requires that it *be assumed to support one line of wheels and, where appropriate, a tributary portion of the design lane load*. Accordingly, it is common practice to design the exterior strip as the edge beam, but on a unit-width basis. In other words, the exterior strip must be designed to carry one line of wheels *and* the tributary portion of the lane load.

The effective width of the exterior strip, with or without an edge beam, is taken as the sum of the following three distances:

1. Distance between the edge of the deck and inside face of the curb.
2. 12 in. (Art. 3.6.1.3: The center of a wheel cannot be closer than 12 in. from the inside face of the curb).
3. One-quarter of the strip width specified in either Art. 4.6.2.1.3 (refers to the width of equivalent interior strips), Art. 4.6.2.3 (Equation 4.44 or 4.45, as appropriate, is applicable here), or Art. 4.6.2.10 (refers to equivalent strip widths for box culverts), as appropriate, but not exceeding either one-half the full strip width or 72 in.

Figure 4.39 shows the schematics of the exterior strip as defined earlier.

The transverse edge beam is assumed to support one axle of design truck in one or more design lanes, positioned to produce maximum load effects. Multiple presence factors and dynamic load allowance apply to the load effects.

The effective width of a transverse strip, with or without an edge beam, is taken as the sum of the distance between transverse edge of the deck and the centerline of the first line of support for the deck, usually taken as the girder web, plus half the width of a strip specified in Table 4.A.11. The effective width so determined shall not exceed the strip width specified in Art. 4.6.2.1.3 and listed in Table 4.A.11.

www.EngineeringEBooksPdf.com

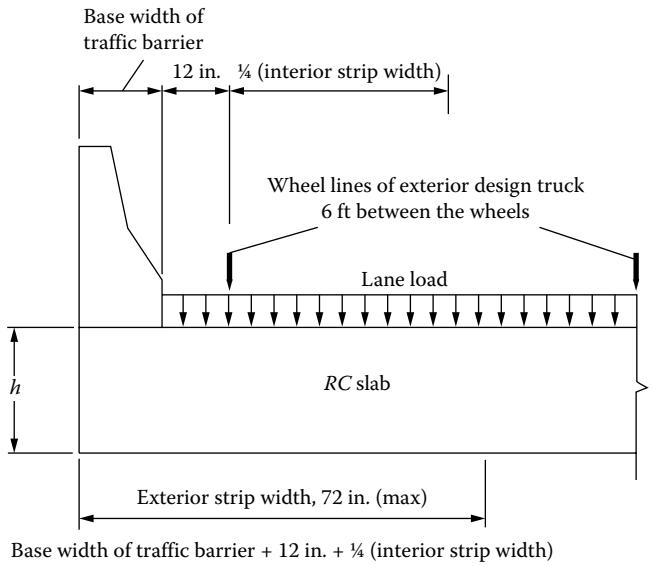

FIGURE 4.39 Width of the exterior strip of a slab-type bridge.

4.18.3 Analysis of Deck Systems

4.18.3.1 General

The strip method of analysis for deck systems is specified in Art. 4.6.2.1. The width of the equivalent strip of a deck may be taken as specified in Table 4.A.11 (LRFD Table 4.6.2.1.3-1). When this table is used, the following stipulations apply:

1. Where decks span primarily in the direction parallel to traffic, strip supporting an axle load shall not be greater than 40 in. for open grids and not greater than 144 in. for all other decks where multilane loading is being investigated.
2. For deck overhangs, where applicable, the loads may be distributed as specified in Art. 3.6.1.3.4 and discussed in Section 3.11.4.
3. The equivalent strips for decks that span primarily in the transverse direction are not subject to the width limits of Table 4.A.11.

4.18.3.2 Calculation of Force Effects

Provisions for calculating the force effects due to permanent and live loads on equivalent strips are specified in Art. 4.6.2.1.6. The strips should be analyzed by classical beam theory. The strips shall be treated as continuous beams or simply supported beams. Because of continuity, the slab is subjected to positive moment in the midspan and negative moment at the supports. A summary of these provisions follows.

Span lengths shall be taken as center-to-center distance between the supporting components.

1. For the purpose of determining the force effects in the strips, the supporting components (e.g., steel or concrete beams, or the webs of T-beams) shall be assumed infinitely rigid.
2. The wheel loads may be modeled as concentrated loads or as patch loads having lengths along the span equal to the length of the tire contact area (Art. 3.6.1.2.5) as discussed in Chapter 3, plus the depth of the deck.
3. In lieu of more precise calculations, the unfactored design live load moments can be found in LRFD Table 4.A.1 (discussed in Chapter 5 in the context of deck slab design).

www.EngineeringEBooksPdf.com

4. The design section for negative moments and shear forces where investigated (based on the past practice, it is not necessary to check shear in typical decks) may be taken as follows:
   a. For monolithic construction, closed boxes, closed concrete boxes, open concrete boxes without top flanges, and stemmed precast beams (i.e., cross sections (b) through (j) listed in LRFD Table 4.6.2.2.1-1), at the face of the supporting elements.
   b. For steel I-beams and steel tub girders (i.e., cross sections (a) and (c) listed in LRFD Table 4.6.2.2.1-1), one-quarter of the flange width from the centerline of the support.
   c. For precast I-shaped concrete beams and open concrete boxes with top flanges (i.e., cross sections (c) and (k) listed in LRFD Table 4.6.2.2.1-1), one-third the flange width, but not exceeding 15 in., from the centerline of the support.
   d. For wood beams (i.e., cross section (j) listed in LRFD Table 4.6.2.2.1-1), one-fourth the top beam width from the centerline.
   e. For open box beams, each web shall be considered as a separate supporting component for the deck. The distance from the centerline of each web and the adjacent sections for negative moment shall be determined based on the type of construction of the box and the shape of the top of the web using the requirements outlined earlier.

4.18.4 Deflection Analysis of Slab Bridges

4.18.4.1 General

LRFD provisions for limitations on live load deflections (Art. 2.5.2.6.2) discussed in Section 2.6 are applicable to slab bridges as well. Deflection due to the permanent load is calculated to provide for the required camber.

For the purposes of calculating deflections of slab bridges, formulas applicable to beams can be used. While the slab is designed based on the equivalent strip widths, they are *not* used to calculate its deflections. Rather, slab deflection is calculated by considering the entire slab as one beam spanning longitudinally between the supports (i.e., a beam having width b equal to the edge-to-edge or the overall width of the slab and depth equal to the thickness of the slab, h).

The total load on the slab consists of the permanent load and design live load (design truck or tandem, as applicable, and the lane load). The entire slab is considered as a beam loaded with all the design lanes present on it. Therefore, the number of design lanes influences the magnitude of live load deflection. This is in contrast with the deflection calculations for beams/girders of multi-girder bridges in which deflections are calculated based on the distribution factor for deflection. For example, consider the following cases:

1. If a slab bridge is designed as a single-lane bridge, it should be considered as fully loaded with one design lane—a design truck or tandem, as applicable, and lane load, both positioned to cause maximum deflections.
2. It the slab bridge is a two-lane bridge, it should be considered as fully loaded with two design lanes—each with a design truck or tandem, as applicable, and lane load, positioned to cause maximum deflections. In this case, the total deflection would be twice the total deflection caused by the presence of single lane live load on the bridge.
3. If the slab bridge is a three-lane bridge, it should be considered as fully loaded with three design lanes—each with a design truck or tandem, as applicable, and lane load, positioned to cause maximum deflections. In this case, the total deflection would be three times the total deflection caused by the presence of single lane live load on the bridge.

Multiple presence factors (Art. 3.6.1.1.2) should be used in all cases of live load deflection calculations.

www.EngineeringEBooksPdf.com

4.18.4.2 Influence of Cracking of Concrete Sections under Service Loads

It must be recognized that concrete sections crack under service loads. Therefore, for the purpose of calculating deflections, the *effective moment of inertia of the cracked section*, I_e, rather than the gross moment of inertia, I_g, must be used (Art. 5.7.3.6.2). The effective moment of inertia of the cracked section, I_e, is computed from Equation 4.49:

$$I_e = \left(\frac{M_{cr}}{M_a}\right)^3 I_g + \left[1 - \left(\frac{M_{cr}}{M_a}\right)^3\right] I_{cr} \le I_g \qquad (4.49)\ [A5.7.3.6.2\text{-}1]$$

in which

$$M_r = f_r\left(\frac{I_g}{y_t}\right) \qquad (4.50)\ [A5.7.3.6.2\text{-}2]$$

where

M_{cr} = cracking moment (kip-in.)
f_r = modulus of rupture of concrete specified in Art. 5.4.2.6 (ksi)
y_t = distance from the neutral axis to the extreme tension fiber (in.)
M_a = maximum moment in a component at the stage for which deformation is computed (kip-in.)

With respect to the cross-sectional shapes, the following guidelines should be followed:

1. For prismatic members, the effective moment of inertia may be taken as the value obtained from Equation 4.49 at midspan for simple and continuous members, and at support for cantilevers.
2. For continuous nonprismatic members, the effective moment of inertia may be taken as the average of the values obtained from Equation 4.49 for the critical positive and negative sections.

4.18.4.3 Long-Term Deflections

The long-term deflections may be taken as the instantaneous deflection multiplied by the following factors:

1. If the instantaneous deflection is based on the gross moment inertia, I_g: 4.0.
2. If the instantaneous deflection is based on the gross moment inertia, I_e: $3 - 1.2\left(\frac{A_s'}{A_s}\right) \ge 1.6$

where

A_s' = area of compression reinforcement (in.^{2})
A_s = area of nonprestressed tension reinforcement (in.^{2})

www.EngineeringEBooksPdf.com

4.A APPENDIX

TABLE 4.A.1
Common Deck Superstructure Types Covered in AASHTO LRFD 2012 Art. 4.6.2.2.2 and 4.6.2.2.3

Supporting Components	Type of Deck	Typical Cross Section
Steel beam	Cast-in-place concrete slab, precast concrete slab, steel grid, glued/spiked panels, stressed wood	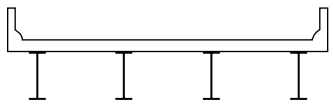 (a)
Closed steel or precast concrete boxes	Cast-in-place concrete slab	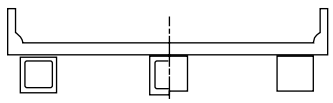 (b)
Open steel or precast concrete boxes	Cast-in-place concrete slab, precast concrete deck slab	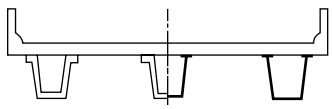 (c)
Cast-in-place concrete multicell box	Monolithic concrete	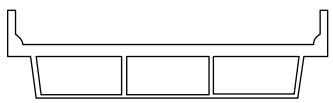 (d)
Cast-in-place concrete T-beam	Monolithic concrete	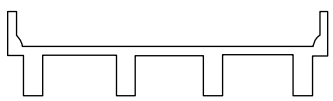 (e)
Precast solid, voided or cellular concrete boxes with shear keys	Cast-in-place concrete overlay	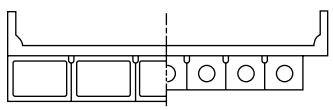 (f)
Precast solid, voided, or cellular concrete boxes with shear keys and with or without transverse posttensioning	Integral concrete	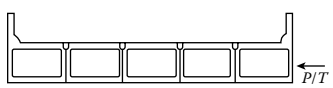 (g)
Precast concrete channel sections with shear keys	Cast-in-place concrete overlay	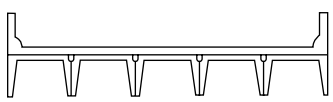 (h)

(*Continued*)

www.EngineeringEBooksPdf.com

TABLE 4.A.1 (*Continued*)
Common Deck Superstructure Types Covered in AASHTO LRFD 2012 Art. 4.6.2.2.2 and 4.6.2.2.3

Supporting Components	Type of Deck	Typical Cross Section
Precast concrete double-T section with shear keys and with or without transverse posttensioning	Integral concrete	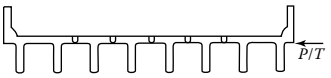 (i)
Precast concrete T-section with shear keys and with or without transverse posttensioning	Integral concrete	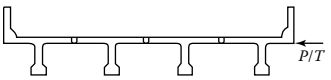 (j)
Precast concrete I or bulb-T sections	Cast-in-place concrete, precast concrete	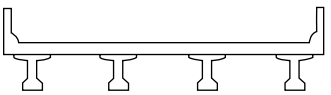 (k)
Wood beams	Cast-in-place concrete or plank, glued/spiked panels or stressed wood	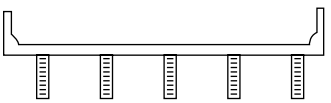 (l)

Source: From *AASHTO LRFD Bridge Design Specifications*, Copyright © 2012 by American Association of State Highway and Transportation Officials, Washington, DC. Used by permission.

TABLE 4.A.2
Distribution of Live Load per Lane for Bending Moment and Shear in Interior Beams with Wood Decks

Type of Deck	Applicable Cross Section from Table 4.6.2.2.1-1	One Design Lane Loaded	Two or More Design Lanes Loaded	Range of Applicability
Plank	(a), (1)	$S/6.7$	$S/7.5$	$S \leq 5.0$
Stressed laminated	(a), (1)	$S/9.2$	$S/9.0$	$S \leq 6.0$
Spike laminated	(a), (1)	$S/8.3$	$S/8.5$	$S \leq 6.0$
Glued laminated panels on glue laminated stringers	(a), (1)	$S/10.0$	$S/10.0$	$S \leq 6.0$
Glue laminated panels on steel stringers	(a), (1)	$S/8.8$	$S/9.0$	$S \leq 6.0$

Source: From *AASHTO LRFD Bridge Design Specifications*, Copyright © 2012 by American Association of State Highway and Transportation Officials, Washington, DC. Used by permission.

www.EngineeringEBooksPdf.com

TABLE 4.A.3
Distribution of Live Load per Lane for Bending Moment in Interior Beams

Type of Deck	Applicable Cross Section from Table 4.6.2.2.1-1	Two or More Design Lanes Loaded	Range of Applicability
Wood deck on wood or steel beams	(a), (1)	See Table 4.6.2.2.2a-1	
Concrete deck on wood beams	(1)	One design lane loaded: $S/12.0$ Two or more design lanes loaded: $S/10.0$	$S \le 6.0$
Concrete deck, filled gird, partially filled grid, or unfilled grid deck composite with reinforced concrete slab on steel or concrete beams; concrete T-beams, T- and double T-sections	(a), (e), (k), and also (i), (j) if sufficiently connected to act as a unit	One design lane loaded: $0.06+\left(\frac{S}{14}\right)^{0.4}\left(\frac{S}{L}\right)^{0.3}\left(\frac{K_g}{12.0Lt_s^3}\right)^{0.1}$ Two or more design lanes loaded: $0.075+\left(\frac{S}{14}\right)^{0.6}\left(\frac{S}{L}\right)^{0.2}\left(\frac{K_g}{12.0Lt_s^3}\right)^{0.1}$	$3.5 \le S \le 16.0$ $4.5 \le t_s \le 12.0$ $20 \le L \le 240$ $N_b \ge 4$ $10{,}000 \le K_g \le 7{,}000{,}000$
		Use lesser of the values obtained from the aforementioned equation with $N_b = 3$ or the lever rule	$N_b = 3$
Cast-in-place concrete multicell box	(d)	One design lane loaded: $\left(1.75+\frac{S}{3.6}\right)\left(\frac{1}{L}\right)^{0.35}\left(\frac{1}{N_c}\right)^{0.45}$ Two or more design lanes loaded: $\left(\frac{13}{N_c}\right)^{0.3}\left(\frac{S}{5.8}\right)\left(\frac{1}{L}\right)^{0.25}$	$7.0 \le S \le 13.0$ $60 \le L \le 240$ $N_c \ge 3$ If $N_c > 8$ use $N_c = 8$
Concrete deck on concrete spread box beams	(b), (c)	One design lane loaded: $\left(\frac{S}{3.0}\right)^{0.35}\left(\frac{Sd}{12.0L^2}\right)^{0.25}$ Two or more design lanes loaded: $\left(\frac{S}{6.3}\right)^{0.6}\left(\frac{Sd}{12.0L^2}\right)^{0.125}$	$6.0 \le S \le 18.0$ $20 \le L \le 140$ $18 \le d \le 65$ $N_b \ge 3$
		Use lever rule	$S > 18.0$
Concrete beams used in multibeam deck	(f) (g) if sufficiently connected to act as a unit	One design lane loaded: $k\left(\frac{b}{33.3L}\right)^{0.5}\left(\frac{I}{J}\right)^{0.25}$ where $k = 2.5(N_b)^{-0.2} \ge 1.5$ Two or more design lanes loaded: $k\left(\frac{b}{305}\right)^{0.6}\left(\frac{b}{12.0L}\right)^{0.2}\left(\frac{I}{J}\right)^{0.06}$	$35 \le b \le 60$ $20 \le L \le 120$ $5 \le N_b \le 20$

(*Continued*)

www.EngineeringEBooksPdf.com

TABLE 4.A.3 (*Continued*)
Distribution of Live Load per Lane for Bending Moment in Interior Beams

Type of Superstructure	Applicable Cross Section from Table 4.6.2.2.1-1	Distribution Factors	Range of Applicability
	(h)	Regardless of the number of loaded lanes:	Skew $\leq 45°$
	(g), (i), (j) if connected only enough to prevent relative vertical displacement at the interface	S/D where $C = K(W/L) \leq K$ $D = 11.5 - N_L + 1.4N_L(1 - 0.2C)^2$ when $C \leq 5$ $D = 11.5 - N_L$ when $C > 5$ $K = \sqrt{\frac{(1+\mu)I}{J}}$ For preliminary design, the following values of K may be used: Beam Type K Nonvoided rectangular beams 0.7 Rectangular beams with circular voids 0.8 Box section beams 1.0 channel beams 2.2 T-beam 2.0 Double T-beam 2.0	$N_L \leq 6$
Open steel grid deck on steel beams	(a)	One design lane loaded: $S/7.5$ If $t_g < 4.0$ $S/10.5$ If $t_g \geq 4.0$	$S \leq 6.0$
		Two or more design lanes loaded: $S/8.0$ if $t_g < 4.0$ $S/10.0$ if $t_g \geq 4.0$	$S \leq 10.5$
Concrete deck on multiple steel box girders	(b), (c)	Regardless of the number of loaded lanes: $0.05 + 0.85\left(\frac{N_L}{N_b}\right) + \left(\frac{0.425}{N_L}\right)$	$0.5 \leq 0.85\left(\frac{N_L}{N_b}\right) \leq 1.5$

Source: From *AASHTO LRFD Bridge Design Specifications*, Copyright © 2012 by American Association of State Highway and Transportation Officials, Washington, DC. Used by permission.

TABLE 4.A.4
Distribution of Live Load per Lane for Bending Moment in Interior Beams with Corrugated Steel Planks

One Design Lane Loaded	Two or More Design Lanes Loaded	Range of Applicability
$S/9.2$	$S/9.0$	$S \leq 5.5$ $t_g \geq 2.0$

Source: From *AASHTO LRFD Bridge Design Specifications*, Copyright © 2012 by American Association of State Highway and Transportation Officials, Washington, DC. Used by permission.

www.EngineeringEBooksPdf.com

TABLE 4.A.5
Distribution of Live Load per Lane for Bending Moment in Exterior Longitudinal Beams

Type of Superstructure	Applicable Cross Section from Table 4.6.2.2.1-1	One Design Lane Loaded	Two or More Design Lanes Loaded	Range of Applicability
Wood deck on wood or steel beams	(a), (l)	Lever rule	Lever rule	N/A
Concrete deck on wood beams	(l)	Lever rule	Lever rule	N/A
Concrete deck, filled grid, partially filled grid, or unfilled grid deck composite with reinforced concrete slab on steel or concrete beams; concrete T-beams, T- and double T-sections	(a), (e), (k) and also (i), (j) if sufficiently connected to act as a unit	Lever rule	$g = eg_{interior}$ $e = 0.77 + \frac{d_e}{9.1}$ Use lesser of the values obtained from the aforementioned equation with $N_b = 3$ or the lever rule	$-1.0 \le d_e \le 5.5$ $N_b = 3$
Cast-in-place concrete multicell box	(d)	$g = \frac{W_e}{14}$	$g = \frac{W_e}{14}$	$W_e \le S$
		Or the provisions for a whole-width design specified in Art. 4.6.2.2.1		
Concrete deck on concrete spread box beams	(b), (c)	Lever rule	$g = eg_{interior}$ $e = 0.97 + \frac{d_e}{28.5}$ Use lever rule	$0 \le d_e \le 4.5$ $6.0 < S \le 18.0$ $S > 18.0$
Concrete box beams used in multibeam decks	(f), (g)	$g = eg_{interior}$ $e = 1.125 + \frac{d_e}{30} \ge 1.0$	$g = eg_{interior}$ $e = 1.04 + \frac{d_e}{25} \ge 1.0$	$d_e \le 2.0$
Concrete beams other than box beams used in multibeam decks	(h) (i), (j) if connected only enough to prevent relative vertical displacement at the interface	Lever rule	Lever rule	N/A
Open steel grid deck on steel beams	(a)	Lever rule	Lever rule	N/A
Concrete deck on multiple steel box girders	(b), (c)	As specified in Table 4.6.2.2.2b-1		

Source: From *AASHTO LRFD Bridge Design Specifications*, Copyright © 2012 by American Association of State Highway and Transportation Officials, Washington, DC. Used by permission.

www.EngineeringEBooksPdf.com

TABLE 4.A.6
Reduction of Load Distribution Factors for Bending Moment in Longitudinal Beams on Skewed Supports

Type of Superstructure	Applicable Cross Section from Table 4.6.2.2.1-1	Any Number of Design Lanes Loaded	Range of Applicability
Concrete deck, filled grid, partially filled grid, or unfilled grid deck composite with reinforced concrete slab on steel or concrete beams; concrete T-beams, T- and double-T-sections	(a), (c), (k) and also (i), (j) if sufficiently connected to act as a unit	$1 - c_1 (\tan\theta)^{1.5}$ $c_1 = 0.25\left(\frac{K_g}{12Lt_s^3}\right)\left(\frac{S}{L}\right)^{0.5}$ If $\theta < 30°$ then $c_1 = 0.0$ If $\theta > 60°$ use $\theta = 60.0$	$30° \le \theta \le 60°$ $3.5 \le S \le 16.0$ $20 \le L \le 240$ $N_b \ge 4$
Concrete deck on concrete spread box beams, cast-in-place multicell box concrete box beam and double T-sections used in multibeam decks	(b), (c), (d), (f), (g)	$1.05 - 0.25 \tan\theta \le 1.0$ If $\theta > 60°$ use $\theta = 60°$	$0° \le \theta \le 60°$

Source: From *AASHTO LRFD Bridge Design Specifications*, Copyright © 2012 by American Association of State Highway and Transportation Officials, Washington, DC. Used by permission.

TABLE 4.A.7
Distribution of Live Load per Lane for Transverse Beams for Bending Moments and Shear

Type of Deck	Fraction of Wheel Load to Each Floor Beam	Range of Applicability
Plank	$\frac{S}{4}$	N/A
Laminated wood deck	$\frac{S}{5}$	$S \le 5.0$
Concrete	$\frac{S}{6}$	$S \le 6.0$
Steel grid and unfilled grid deck composite with reinforced concrete slab	$\frac{S}{4.5}$	$t_g \le 4.0$ $S \le 5.0$
Steel grid and unfilled grid deck composite with reinforced concrete slab	$\frac{S}{6}$	$t_g > 4.0$ $S \le 6.0$
Steel bridge corrugated plank	$\frac{S}{5.5}$	$t_g \ge 2.0$

Source: From *AASHTO LRFD Bridge Design Specifications*, Copyright © 2012 by American Association of State Highway and Transportation Officials, Washington, DC. Used by permission.

Note: S, spacing of floor beams (ft); t_g, depth of steel grid or corrugated steel plank including integral concrete overlay or structural concrete component, less a provision for grinding, grooving, or wear (in.).

www.EngineeringEBooksPdf.com

TABLE 4.A.8
Distribution of Live Load per Lane for Shear in Interior Beams

Type of Superstructure	Applicable Cross Section from Table 4.6.2.2.1-1	One Design Lane Loaded	Two or More Design Lanes Loaded	Range of Applicability
Wood deck on wood or steel beams	(a), (1)	See Table 4.6.2.2.2a-1		
Concrete deck on wood beams	(1)	Lever rule	Lever rule	N/A
Concrete deck, filled grid, partially filled grid, or unfilled grid deck composite with reinforced concrete slab on steel or concrete beams; concrete T-beams, T- and double-T-sections	(a), (c), (k) and also (i), (j) if sufficiently connected to act as a unit	$0.36+\frac{S}{25.0}$	$0.2+\frac{S}{12}-\left(\frac{S}{35}\right)^{2.0}$	$3.5 \le S \le 16.0$ $20 \le L \le 240$ $4.5 \le t_s \le 12.4$ $N_b \ge 4$
		Lever rule	Lever rule	$N_b = 3$
Cast-in-place concrete multicell box	(d)	$\left(\frac{S}{9.5}\right)^{0.6}\left(\frac{d}{12.0L}\right)^{0.1}$	$\left(\frac{S}{7.3}\right)^{0.9}\left(\frac{d}{12.0L}\right)^{0.1}$	$6.0 \le S \le 13.0$ $20 \le L \le 240$ $35 \le d \le 110$ $N_c \ge 3$
Concrete deck on concrete spread box beams	(b), (c)	$\left(\frac{S}{10}\right)^{0.6}\left(\frac{d}{12.0L}\right)^{0.1}$	$\left(\frac{S}{7.4}\right)^{0.8}\left(\frac{d}{12.0L}\right)^{0.1}$	$6.0 \le S \le 18.0$ $20 \le L \le 140$ $18 \le d \le 65$ $N_b \ge 3$
Concrete box beams used in multibeam decks	(f), (g)	Lever rule $\left(\frac{b}{130L}\right)^{0.15}\left(\frac{I}{J}\right)^{0.05}$	Lever rule $\left(\frac{b}{156}\right)^{0.4}\left(\frac{b}{12.0L}\right)^{0.1}\left(\frac{I}{J}\right)^{0.05}\left(\frac{b}{48}\right)$	$S > 18.0$ $35 \le b \le 60$ $20 \le L \le 120$ $5 \le N_b \le 20$ $25{,}000 \le J \le 610{,}000$ $40{,}000 \le I \le 610{,}000$
Concrete beams other than box beams used in multibeam decks	(h) (i), (j), if connected only enough to prevent relative vertical displacement at the interface	Lever rule	Lever rule	N/A
Open steel grid deck on steel beams	(a)	Lever rule	Lever rule	N/A
Concrete deck on multiple steel box beams	(b), (c)	As specified in Table 4.6.2.2.2b-1		

Source: From *AASHTO LRFD Bridge Design Specifications*, Copyright © 2012 by American Association of State Highway and Transportation Officials, Washington, DC. Used by permission.

www.EngineeringEBooksPdf.com

TABLE 4.A.9
Distribution of Live Load per Lane for Shear in Exterior Beams

Type of Superstructure	Applicable Cross Section from Table 4.6.2.2.1-1	One Design Lane Loaded	Two or More Design Lanes Loaded	Range of Applicability
Wood deck on wood or steel beams	(a), (l)	Lever rule	Lever rule	N/A
Concrete deck on wood beams	(l)	Lever rule	Lever rule	N/A
Concrete deck, filled grid, partially filled grid, or unfilled grid deck composite with reinforced concrete slab on steel or concrete beams; concrete T-beams, T- and double-T-beams	(a), (e), (k) and also (i), (j) if sufficiently connected to act as a unit	Lever rule	$g = eg_{interior}$ $e = 0.6 + \frac{d_e}{10}$ Lever rule	$-1.0 \le d_e \le 5.5$ $N_b = 3$
Cast-in-place concrete multicell box	(d)	Lever rule	$g = eg_{interior}$ $e = 0.64 + \frac{d_e}{12.5}$	$-2.0 \le d_e \le 5.0$
		Or the provisions for a whole-width design specified in Art. 4.6.2.2.1		
Concrete deck on concrete spread box beams	(b), (c)	Lever rule	$g = eg_{interior}$ $e = 0.8 + \frac{d_e}{10}$ Lever rule	$0 \le d_e \le 4.5$ $S > 18.0$
Concrete box beams used in multibeam decks	(f), (g)	$g = eg_{interior}$ $e = 1.25 + \frac{d_e}{20} \ge 1.0$	$g = eg_{interior}\left(\frac{48}{b}\right)$ $\frac{48}{b} \le 1.0$ $e = 1 + \left(\frac{d_e + \frac{b}{12} - 2.0}{40}\right)^{0.5} \ge 1.0$	$d_e \le 2.0$ $35 \le b \le 60$
Concrete beams other than box beams used in multibeam decks	(h) (i), (j) if connected only enough to prevent relative vertical displacement at the interface	Lever rule	Lever rule	N/A
Open steel grid deck on steel beams	(a)	Lever rule	Lever rule	N/A
Concrete deck on multiple steel box beams	(b), (c)		As specified in Table 4.6.2.2.2b-1	

Source: From *AASHTO LRFD Bridge Design Specifications*, Copyright © 2012 by American Association of State Highway and Transportation Officials, Washington, DC. Used by permission.

www.EngineeringEBooksPdf.com

TABLE 4.A.10
Correction Factors for Load Distribution Factors for Support Shear of the Obtuse Corner

Type of Superstructure	Applicable Cross Section from Table 4.6.2.2.1-1	Correction Factor	Range of Applicability
Concrete deck, filled grid, partially filled grid, or unfilled grid deck composite with reinforced concrete slab on steel or concrete beams; concrete T-beams, T- and double-T-section	(a), (e), (k), and also (i), (j) if sufficiently connected to act as a unit	$1.0 + 0.20\left(\frac{12.0Lt_s^3}{K_g}\right)^{0.3} \tan\theta$	$0° \le \theta \le 60°$ $3.5 \le S \le 16.0$ $20 \le L \le 240$ $N_b \ge 4$
Cast-in-place concrete multicell box	(d)	$1.0 + \left(0.25 + \frac{12.0L}{70d}\right)\tan\theta$	$0° < \theta \le 60°$ $6.0 < S \le 13.0$ $20 \le L \le 240$ $35 \le d \le 110$ $N_c \ge 3$
Concrete deck on spread concrete box beams	(b), (c)	$1.0 + \frac{\sqrt{\frac{Ld}{12.0}}}{6S}\tan\theta$	$0° < \theta \le 60°$ $6.0 \le S \le 11.5$ $20 \le L \le 140$ $18 \le d \le 65$ $N_b \ge 3$
Concrete box beams used in multibeam decks	(f), (g)	$1.0 + \frac{12.0L}{90d}\sqrt{\tan\theta}$	$0° < \theta \le 60°$ $20 \le L \le 120$ $17 \le d \le 60$ $35 \le b \le 60$ $5 \le N_b \le 20$

Source: From *AASHTO LRFD Bridge Design Specifications*, Copyright © 2012 by American Association of State Highway and Transportation Officials, Washington, DC. Used by permission.

www.EngineeringEBooksPdf.com

TABLE 4.A.11
Equivalent Strips

Type of Deck	Direction of Primary Strip Relative to Traffic	Width of Primary Strip (in.)
Concrete		
Cast-in-place	Overhang	$45.5 + 10.0X$
	Either parallel or perpendicular	$+M$: $26.0 + 6.6S$
		$-M$: $48.0 + 3.0S$
Cast-in-place with stay-in-place concrete formwork	Either parallel or perpendicular	$+M$: $26.0 + 6.6S$
		$-M$: $48.0 + 3.0S$
Precast, posttensioned	Either parallel or perpendicular	$-M$: $26.0 + 6.6S$
		$-M$: $48.0 + 3.0S$
Steel		
Open grid	Main bars	$1.25P + 4.0S_b$
Filled or partially filled grid	Main bars	Art. 4.6.2.1.8 applies
Unfilled, composite grids	Main bars	Art. 4.6.2.1.8 applies
Wood		
Prefabricated glulam		
Noninterconnected	Parallel	$2.0h + 30.0$
	Perpendicular	$2.0h + 40.0$
Interconnected	Parallel	$90.0 - 0.84L$
	Perpendicular	$4.0h + 30.0$
Stress laminated	Parallel	$0.8S + 108.0$
	Perpendicular	$10.0S + 24.0$
Strike laminated		
Continuous decks or interconnected panels	Parallel	$2.0h + 30.0$
	Perpendicular	$4.0h + 40.0$
Noninterconnected panels	Parallel	$2.0h + 30.0$
	Perpendicular	$2.0h + 40.0$

Source: From *AASHTO LRFD Bridge Design Specifications*, Copyright © 2012 by American Association of State Highway and Transportation Officials, Washington, DC. Used by permission.

Note: S, spacing of supporting components; h, depth of deck; L, span lengthy of deck (ft); P, axle load (kip); S_b, spacing of grids bars (in.); $+M$, positive moment; $-M$, negative moment; X, distance from load to point of support (ft).

www.EngineeringEBooksPdf.com

REFERENCES

AASHTO. 1996. *AASHTO Standard Specifications for Highway Bridges*.16th edition, American Association of State Highways and Transportation Officials, Washington, DC.

AASHTO. 2002. *AASHTO Standard Specifications for Highway Bridges*.17th edition, American Association of State Highways and Transportation Officials, Washington, DC.

AASHTO. 2012. *AASHTO LRFD Bridge Design Specifications for Highway Bridges*, American Association of State Highway Transportation Officials, Washington, DC.

American Iron and Steel Institute. 1997. *Four Design Examples of Steel Highway Bridges*, New York.

Bakth, B. and Jaeger, L.G. 1985. *Bridge Analysis Simplified*, McGraw-Hill Co., Inc., New York.

Bakth, B. and Jaeger, L.G. 1992. "Simplified methods of bridge analysis for the third edition of OHBDC", *Canadian Journal of Civil Engineering*, 19 (4), 551–559.

Balas, J. and Hanuska, A. 1964. *Influences Surfaces for Skew Plates*, Vydaratelstvo Slovenskej Akademic Vied, Bratislava.

Bares, R. and Massonet, C. 1968. *Analysis of Beam Grids and Orthotropic Plates by the Guyon-Massonet-Bares Method*, Frederic Unger Publishing Co., New York.

Barker, R.M. and Puckett, J.A. 2013. *Design of Highway Bridges: An LRFD Approach*, 3rd ed., John Wiley & Sons, Hoboken, NJ.

Chaudhary, V.K. 1978. Analysis of plates with various shapes and boundaries, PhD dissertation, West Virginia University, Morgantown, WV.

Coull, A. and Rao, K.S. 1969. "The analysis of bridge reinforced concrete bridge decks by the line-solution technique," *Concrete Bridge Design, ACI Publication SP-23, American Concrete Institute*, Detroit, MI, pp. 19–38.

Cusens, A.R. and Pama, R.P. 1965. "Design of concrete multibeam bridge decks," *Proceedings of the ASCE Journal of the Structural Division*, 91(ST5), pt. 1, Paper 4518, 255–278.

Elbeido, T. and Kennedy, J.B. 1996. "Shear and reaction distributions in continuous skew composite bridges", *Journal of Bridge Engineering, ASCE*, 1 (4), 155–165.

Hambly, E.C. 1991. *Bridge Deck Behavior*, 2nd ed., E & FN Spon, London, U.K. (Von Nostrand Reinhold, New York).

Hendry, A.W. and Jaeger, L.G. 1956. "The analysis of interconnected bridge girders by the distribution of harmonics," *The Structural Engineer* (England), 34(7), 79–109.

Huo, X.S., Connor, S.O., and Iqbal, R.A. 2003. Re-examination of the simplified method (Henry's method) for distribution factors for the live load bending moment and shear, Final Report, Project No. TNSPR-RES-1218, Tennessee Department of Transportation, Nashville, TN.

Huo, X.S., Wasserman, E.P., and Iqbal, R.A. 2005. "Simplified method for calculating lateral distribution factors for live load shear", *Journal of Bridge Engineering, ASCE*, 10 (5), 544–554.

Huo, X.S., Wasserman, E.P., and Zhu, P. 2004. "Simplified method for lateral distribution of live load bending moment", *Journal of Bridge Engineering, ASCE*, 9 (4), 382–390.

Jaeger, L.G. and Bakth, B. 1982. "The grillage analogy in bridge analysis", *Canadian Journal of Civil Engineering*, 9 (2), 224–235.

Jaeger, L.G. and Bakth, B. 1989. *Bridge Analysis by Microcomputer*, McGraw-Hill Co., Inc., New York.

Kerfoot, R.P. and Ostapenko, A. 1967. Grillages under axial and normal loads—Present status, Fritz Engineering Laboratory Report 323.1, Lehigh University, Bethlehem, PA.

Kocsis, P. 2005. Discussion of 'simplified method of lateral distribution of live load bending moment' by Xiaoming Sharon, Edward P. Wasserman, and Pingsheng Zhu, *Journal of Bridge Engineering, ASCE*, 9 (5), 630–631.

Kollbrunner, C.F. and Basler, K. 1969. *Torsion in Structures, An Engineering Approach*, Springer-Verlag, New York.

Mabsout, M.E., Tarhini, K.M., Frederick, G.R., and Taylor, C. 1997. "Finite element analysis of steel girder highway bridges", *Journal of Bridge Engineering, ASCE*, 2 (3), 83–87.

Morice, P.B. and Little, G. 1954. "Load distribution in prestressed concrete bridge systems". *The Structural Engineer*, 32 (3), Nr. 1, 83–111.

Morice, P.B. and Little, G. 1955. "Discussion of 'load distribution in prestressed concrete bridge systems", *The Structural Engineer*, 33, Nr. 1, 21.

Morice, P.B. and Little, G. 1956. *The Analysis of Bridge Decks Subjected to Abnormal Loading*, Cement and Concrete Association, London, U.K.

Nasser, K.W. 1965. "Design procedure for lateral load distribution in multibeam bridges", *Journal of Prestressed Concrete Institute*, 10 (4), 54–68.

www.EngineeringEBooksPdf.com

Newmark, N.M. 1938. *A Distribution Procedure for Analysis of Slabs Continuous over Flexible Beams*, University of Illinois Engineering Experiment Station Bulletin no. 304, University of Illinois, Urbana–Champaign, Urbana, IL.

Nutt, R.V., Schamber, R.A., and Zookaie, T. 1988. *Distribution of Wheel Loads on Highway Bridges*, NCHRP Project Report 12-26, April, Transportation Research, National Research Council, Washington, DC.

Patrick, M.D., Sharon Huo, X.S., Puckett, J.A., Jablin, M.C., and Mertz, D. 2006. "Sensitivity of live load distribution factors to vehicle spacing, technical note", *Journal of Bridge Engineering, ASCE*, 11 (1), 131.

Pool, R.B., Arya, A.S., Robinson, A.R., and Kachaturian, N. 1965. *Analysis of Multibeam Bridges with Beam Elements of Slab and Box Section*, University of Illinois Engineering Experiment Station Bulletin no. 483, University of Illinois, Urbana–Champaign, Urbana, IL.

Prestressed Concrete Institute, 2003. *Precast Prestressed Concrete Bridge Design Manual*, Chicago, IL.

Pucher, A. 1964. *Influence Surfaces of Elastic Plates*, Springer Verlag, Vienna.

Rowe, R.E. 1962. *Concrete Bridge Design*, C. R. Books, London.

Rusch, H. and Hergenroder, A. 1961. *Influence Surfaces for Moments in Skew Slabs*, Technological University, Munich, Germany (translated from German by C. R. Amerongen, Linden, Cement and Concrete Association).

Sanders, W.W. and Elleby, H.A. 1970. Distribution of wheel loads on highway bridges, NCHRP Report 83, Transportation Research Board, National Research Council, Washington, DC.

Taly, N. 1998. *Design of Modern Highway Bridges*, McGraw-Hill Co., Inc., New York.

Taly, N. 2003. *Loads and Load Paths in Buildings—Principles of Structural Design*, International Code Council (ICC), Country Club Hills, IL.

TDOT. 1996. Lateral distribution of structural loads, Tennessee Structures Memorandum 043, Tennessee Department of Transportation, Nashville, TN.

Timoshenko, S. 1953. *History of Strength of Materials*, McGraw-Hill Co., Inc., New York.

Timoshenko, S. and Woinowsky-Krieger, S. 1959. *Theory of Plates and Shells*, 2nd ed., McGraw-Hill Co., Inc., New York.

Zokaie, T., Imbsen, R.A., and Osterkamp, T.A. 1991a. "Distribution of wheel loads on highway bridges," Presented at the http://trid.trb.org/view/1178912 *Third Bridge Engineering Conference*, March 10–13, 1991, Denver, CO, *Transportation Research Record Report 1290*, Transportation Research Board, National Academy of Sciences, Washington, DC, pp. 119–126.

Zokaie, T., Osterkamp, T.A., and Imbsen, R.A. 1991b. Distribution of wheel loads on highway bridges, NCHRP Report 12-2611, Transportation Research Board, National Research Council, Washington, DC.

www.EngineeringEBooksPdf.com

5 Concrete Bridges

5.1 INTRODUCTION

Concrete bridges include reinforced concrete bridges, prestressed concrete bridges, and segmental bridges. This chapter presents a discussion on the design of reinforced concrete slab bridges, reinforced concrete decks, T-beam bridges, and precast, prestressed concrete bridges. Segmental (or segmentally constructed) bridges are not discussed herein. A multitude of precast, prestressed concrete girder shapes are available in the marketplace. Discussion in this chapter is limited to design of precast, prestressed concrete AASHTO-PCI girder bridges.

The first reinforced concrete bridge in America is reported to have been built in 1889. Designed and built by Earnest L. Ransome, the bridge is a 64 ft wide and 20 ft long arch bridge called the Alvord Lake Bridge in Golden Gate Park, San Francisco (Figure 5.1). Declared as a civil engineering landmark in the 1970s and still in service, the bridge survived the 1906 San Francisco earthquake and several subsequent earthquakes. In 1884, Ransome also patented the use of *twisted* steel bars for reinforcing concrete (which he probably used in building the Alvord Lake Bridge)—the first use of what later became known as reinforcing bar (Abrahamson 1989). Ironically, Ransome left San Francisco a few years after building the bridge, frustrated and bitter at the building community's indifference to concrete construction. Ironically, the city's few reinforced concrete structures then in existence, including the Alvord Lake Bridge, survived the 1906 earthquake and fire remarkably well, vindicating Ransome's faith in reinforced construction.

5.2 CONCRETE BRIDGES AND AESTHETICS

A bridge is undoubtedly an indispensible, functional link of a transportation system (highways) but also an emotional link to the society and the surrounding communities. The second aspect suggests that a bridge ought to be built having the appearance of a graceful structure; it is here that the potential of concrete as a building material can be harnessed. Concrete is a virtuous material as it can be shaped and formed at designer's discretion. This gives concrete bridges several advantages over the other types, the major one being the adaptability of concrete to a wide variety of structural shapes and forms. With reinforced concrete, a team of designers and architects can work together to create structurally functional shapes and forms and use them to build aesthetically pleasant bridges, limited by only their imagination. Expressiveness and beauty of concrete bridges have been well established by the grandeur of many world famous concrete bridges. Bridges designed by Robert Maillart (Figure 5.2) and Christian Menn (Figures 5.3 and 5.4), which stand as symbols of ultimate in bridge aesthetics and structural philosophy, *form follows function*, are but a few examples of potential of concrete as a bridge building material. These graceful structures illustrate vividly the potential of concrete as a building material for both superstructures and substructures.

www.EngineeringEBooksPdf.com

FIGURE 5.1 Lake Alvord Bridge, San Francisco Park, California, the oldest concrete bridge built in the United States in 1889 by Earnest L. Ransome, an innovator in reinforced concrete design, mixing equipment, and construction systems. The bridge, which arches over a pedestrian entrance to San Francisco's Golden Gate Park, was constructed as a single arch 64 ft (20 m) wide with a 20 ft (6.1 m) span. Ransome is believed to have used his patented cold-twisted square steel bar for reinforcement, placed longitudinally in the arch and curved in the same arc. The face of the bridge was scored and hammered to resemble sandstone; the interior features concrete *stalactites* (some of which have subsequently grown due to redeposition of limestone from the concrete). This bridge was designated a civil engineering landmark by the American Society of Civil Engineers in the 1970s. (From Library of Congress—Alvord Lake Bridge: General View Looking East.)

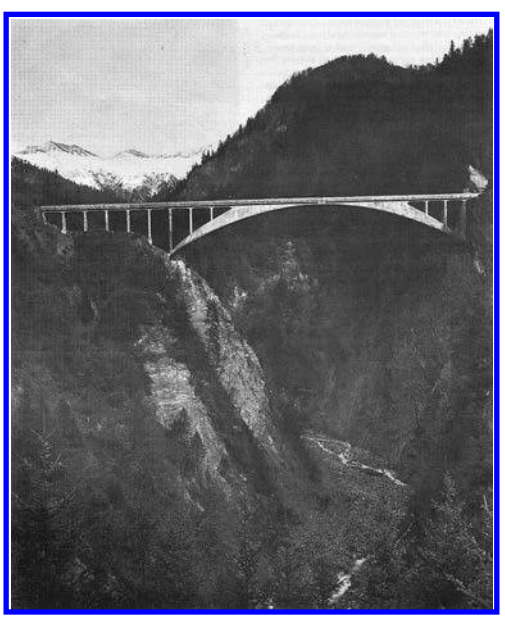

FIGURE 5.2 Maillart's Salginatobel Bridge near Scgiers, Switzerland, a reinforced concrete arch bridge spanning 90 m (295.3 ft) built in 1930, most famous for its aesthetic expressiveness. Maillart won the contract for this bridge by submitting the lowest bid out of 18 designs. (Reproduced with permission from *Bridge Aesthetics Around the World*, Committee on General Structures, Subcommittee on Bridge Aesthetics, Transportation Research Board, Washington, DC. Copyright 1991 by Transportation Research Board.)

www.EngineeringEBooksPdf.com

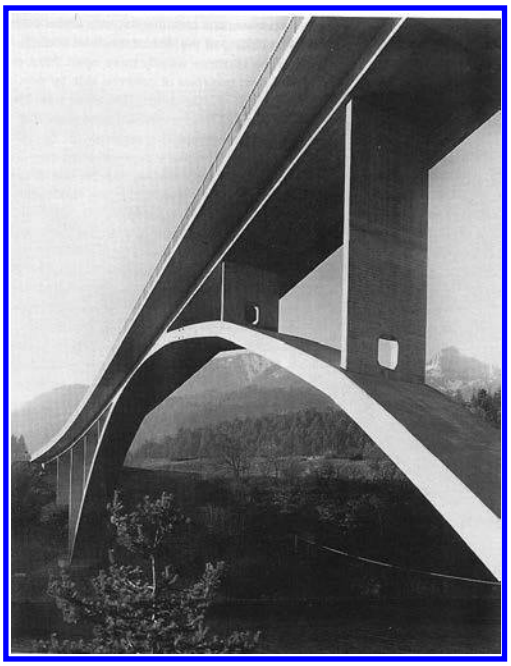

FIGURE 5.3 The Reichenau Bridge spanning 100 m (328.1 ft) and built in 1964 by Christian Menn. This bridge is known for its aesthetic qualities of expressiveness of the funicular line, the delicacy of members, and the transparency (openness through substructure). (Reproduced with permission from *Bridge Aesthetics Around the World*, Committee on General Structures, Subcommittee on Bridge Aesthetics, Transportation Research Board, Washington, DC. Copyright 1991 by Transportation Research Board.)

FIGURE 5.4 The Gantor Bridge on the Simplon Road above Brig, Switzerland, designed by Christian Menn in 1980. Note the expressiveness of the new form in which prestressed cables are embedded in the triangular wall above the roadway. The bridge has a main span 174 m (570.9 ft) and maximum column height of 150 m (492.1 ft). (Reproduced with permission from *Bridge Aesthetics Around the World*, Committee on General Structures, Subcommittee on Bridge Aesthetics, Transportation Research Board, Washington, DC. Copyright 1991 by Transportation Research Board.)

www.EngineeringEBooksPdf.com

5.3 CORROSION OF CONCRETE BRIDGES

5.3.1 Reinforcing Bar Corrosion Problem

While concrete can be used to build aesthetically pleasant bridges, reinforcing bars that must be used to enhance tensile-resisting strength of a concrete member tend to corrode and adversely affect the durability of concrete bridges. Reinforcing bars used for concrete bridges may be epoxy coated or uncoated. Those constructed with uncoated reinforcement and exposed to chloride salt solutions can, and often do, suffer accelerated deterioration due to corrosion of the reinforcing bars.

Corrosion of reinforcing bars can be attributed to four main causes: carbonation or sulfation, chloride attack, inadequate cover, and cracks. The corrosion process initiates by the use of deicing chemicals during the winter, which infiltrate concrete due to concrete's permeability and come into direct contact with the reinforcing steel. It is an electrochemical phenomenon that initiates in the presence of chlorides, carbonates, sulfides, oxygen, and water that is generally furnished by the water present in the pores of concrete. When reinforcing bars are embedded in fresh concrete, they are surrounded by cement mortar, and a thin coating of ferrous hydroxide forms on their surfaces. This acts as protective layer, thus passivating the steel surface (Mehta 1986, Gerwick 1993); chloride ions are the most common materials that break down this passive protective layer. In addition to their presence in the water of concrete mix, chlorides come from marine environments and from salt spread on bridge decks to prevent icing. Sodium chloride from washed deicing salts can be splashed (e.g., by tires) sideways over the traffic barriers, bridge piers, and columns, with subsequent absorption up to 8 in. deep into the concrete (Bennison 1987). The result is corrosion that often results in delaminations and spalling of concrete, ill effects that have been long known and well documented in the literature (Loren et al. 1969, Cady and Weyers 1983, FHWA 1992, Gaal et al. 2001). Left unchecked, corrosion can be so severe that replacement of the bridge becomes necessary, a costly alternative. Figures 5.5 through 5.8 show a few examples of concrete bridges with severe corrosion problems.

FIGURE 5.5 Corrosion of reinforcing bars in the bottom of a reinforced concrete bridge.

www.EngineeringEBooksPdf.com

FIGURE 5.6 Corrosion of reinforcing bars in the abutment of a reinforced concrete bridge.

FIGURE 5.7 Corrosion of reinforcing bars in the pier of a reinforced concrete bridge.

5.3.2 Mitigation of Corrosion Problem

5.3.2.1 Treated Reinforcing Steel

Concrete bridge decks can be constructed with uncoated or coated reinforcing bars. In an effort to minimize the corrosion problem and provide protection against chloride-induced corrosion, two basic approaches are used. One is the use of epoxy-coated or galvanized reinforcing bars, which are often used as top- and bottom-reinforcing bar mats in bridge decks, and the use of epoxy-coated prestressing strands. A discussion of the performance of coated reinforcing bars can be found in the literature (Smith and Virmani 1996, Sohanhgpurwala et al. 1997, Fanous 2005).

5.3.2.2 Concrete Cover for Reinforcing Steel

The other approach is to provide minimum concrete cover of all reinforcing bars as specified in Article 5.12.3 (Art.) and listed in Table 5.1. This specified cover requirement applies

www.EngineeringEBooksPdf.com

FIGURE 5.8 Corrosion of reinforcing bars in the bents of a reinforced concrete bridge.

also to pretensioned prestressing strands, anchorage hardware, and mechanical connections for reinforcing bars or posttensioned prestressing strands. Cover for unprotected prestressing and reinforcing steel in bridge decks and other concrete members is mandatory. Minimum cover is necessary for durability and prevention of splitting due to bond stresses and to provide for placing tolerance.

Cover for reinforcing steel specified in Art. 5.12.3 is the minimum cover requirement, which shall be modified for the water–cement (*W/C*) ratio as follows. These factors are to be used as modifiers to the minimum cover requirements listed in Table 5.1. The lower modification factor (0.8) recognizes decreased permeability of lower *W/C* ratio ($\leq$0.40) concrete.

1. For $W/C \leq 0.40$ 0.8
2. For $W/C \geq 0.50$ 1.2

From the standpoint of durability and corrosion protection, providing minimum cover to reinforcing steel is one of the most important construction aspects for not only concrete bridges but all concrete structures. The importance of proving concrete cover for reinforcing steel can be hardly overemphasized; it should be considered like an insurance against potential for corrosion. To this end, load and resistance factor design (LRFD) specifications mandate that minimum cover to main bars, including bars protected by epoxy coating, shall not be less than 1.0 in. Cover to ties and stirrups may be less than 0.5 in. less than the values shown in Table 5.1 for main bars but shall not be less than 1.0 in.

5.3.3 General Protective Requirements

Decks of bridges in the snow areas are exposed to tire studs or chain wear. For such decks, additional cover must be provided to compensate for the expected loss in depth due to abrasion as specified in Art. 2.5.2.4. Where concrete decks without an initial overlay are used, consideration should be given for an additional 1/2 in. cover to permit correction of the deck profile by grinding and to compensate for the loss of thickness due to abrasion.

www.EngineeringEBooksPdf.com

TABLE 5.1
Cover[a] for Unprotected Main Reinforcing Steel (in.)

Situation	Cover (in.)
Direct exposure to saltwater	4.0
Cast against earth	3.0
Coastal	3.0
Exposure to deicing salts	2.5
Deck surfaces subject to tire stud or chain wear	2.5
Exterior other than aforementioned situations	2.0
Interior other than aforementioned situations	
Up to No. 11 bar	1.5
No. 14 and No. 18 bars	2.0
Bottom of cast-in-place slabs	
Up to No. 11 bar	1.0
No. 14 and No. 18 bars	2.0
Precast soffit form panels	0.8
Precast reinforced piles	
Noncorrosive environments	2.0
Corrosive environments	3.0
Precast prestressed piles	2.0
Cast-in-place piles	
Noncorrosive environments	2.0
Corrosive environments	
• General	3.0
• Protected	3.0
Shells	2.0
Auger-cast, tremie concrete, or slurry construction	3.0

Source: LRFD Table 5.12.3-1: Cover for Unprotected Main Reinforcing Steel (in.), reprinted with permission from the American Association of Highway and Transportation Officials, Washington, DC.

[a] The following modification factors shall be used in conjunction with the minimum cover requirements specified in Table 5.1 (LRFD Art. 5.12.3):
1. For $W/C \leq 0.40$ 0.8
2. For $W/C \geq 0.50$ 1.2

Protection requirements for prestressing steel are specified in Art. 5.12.5. Ducts for internal post-tensioned tendons designed to provide bonded resistance are required to be grouted after stressing. Other tendons are required to be permanently protected against corrosion, and details of protection indicated on contract drawings.

5.4 MATERIAL PROPERTIES

5.4.1 Concrete for Bridge Construction

5.4.1.1 General

All materials of construction to be used for bridge construction should conform to the standards for the grades of construction materials as specified in *AASHTO LRFD Bridge Construction*

www.EngineeringEBooksPdf.com

Specifications (AASHTO 2010). Occasionally, it may be both necessary and appropriate to use materials other than those specified in *AASHTO LRFD Bridge Construction Specifications*; in such cases, their properties, including statistical variability, are required to be established prior to design; the minimum acceptable properties and test procedures for such materials must be specified in contract documents.

5.4.1.2 Normal-Weight and Structural Lightweight Concrete

5.4.1.2.1 Compressive Strength: LRFD Art. 5.4.2.1

The compressive strength of concrete, technically referred to as 28-day compressive strength, f'_c, is the most important and significant design parameter for designing all concrete structures. For bridge construction, LRFD specifications require that for each component, the specified compressive strength, f'_c, or the class of concrete be shown in the contract documents.

Concrete strengths above 10.0 ksi for normal-weight concrete are permitted only when allowed by specific LRFD articles or when physical tests are made to establish the relationship between the concrete strength and other properties.

Lightweight concrete is generally used only under conditions where the mass (or weight) is critical, for example, in seismic regions because greater mass (and hence greater weight) contributes to larger seismic forces.

5.4.1.2.2 Mandatory Minimum Compressive Strength and Other Requirements

1. Specified concrete with strengths below 2.4 ksi should not be used in the structural applications.
2. The specified compressive strength for prestressed concrete and decks shall not be less than 4.0 ksi.
3. For lightweight structural concrete, air-dried unit weight strength and any other properties required for application shall be specified in the contract documents.
4. For concrete Class A, A(AE), and P used in or over saltwater, the *W/C* ratio shall be specified not to exceed 0.45.
5. The sum of Portland cement and other cementitious materials shall be specified not to exceed 800 pounds per cubic yard (pcy), except for Class P (high-performance concrete [HPC]) concrete where the sum of Portland cement and other cementitious materials shall be specified not to exceed 1000 pounds pcy.
6. Air-entrained concrete, designated as *AE* in Table 5.2 (LRFD Table 5.4.2.1-1), shall be specified where the concrete will be subject to alternate freezing and thawing and exposure to deicing salts, saltwater, or other potentially damaging environments.

Table 5.2 lists concrete mix characteristics by class.

The evaluation of the strength of the concrete used in the work should be based on test cylinders produced, tested, and evaluated in accordance with Section 8 of the *AASHTO LRFD Bridge Construction Specification* (AASHTO 2010).

Research on high-strength concrete continues. LRFD Section 5.4.2.1 was originally developed based on an upper limit of 10.0 ksi for the design of concrete compressive strength. As research information for concrete compressive strengths greater than 10.0 ksi becomes available, individual articles are being revised to be extended to allow their use with higher-strength concretes. LRFD Appendix C5 contains a list of the articles affected by concrete compressive strength and their current upper limit.

It is common practice that the specified strength be attained 28 days after placement. Other maturity ages may be assumed for design and specified for components that will receive loads at times appreciably different than 28 days after placement.

www.EngineeringEBooksPdf.com

TABLE 5.2
Concrete Mix Characteristics by Class (LRFD Table C5.4.2.1-1)

Class of Concrete	Minimum Cement Content (pcy)[a]	Maximum *W/C* Ratio (lb/lb)	Air Content Range (percent)	Coarse Aggregate per AASHTO M 43 (ASTM D448) Square Size of Openings (in.)	28-Day Compressive Strength (ksi)
A	611	0.49	—	1.0 to No. 4	4.0
A(AE)	611	0.45	6.0 ± 1.5	1.0 to No. 4	4.0
B	517	0.58	—	2.0 to No. 3 and No. 3 to No. 4	2.4
B(AE)	517	0.55	5.0 ± 1.5	2.0 to No. 3 and No. 3 to No. 4	2.4
C	658	0.49	—	0.5 to No. 4	4.0
C(AE)	658	0.45	7.0 ± 1.5	0.5 to No. 4	4.0
P	564	0.49	As specified elsewhere	1.0 to No. 4 or 0.75 to No. 4	As specified elsewhere
P(HPC)					
S	658	0.58		1.0 to No. 4	—
Lightweight	564		As specified in contract documents		

Source: LRFD Table C5.4.2.1-1. Reprinted with permission from the American Association of Highway and Transportation Officials, Washington, DC.

[a] Limits may be raised in the future.

It is recommended that the classes of concrete shown in LRFD Table C5.4.2.1-1 and their corresponding specified strengths be used whenever appropriate. The classes of concrete indicated in Table 5.2 (Table C5.4.2.1-1) have been developed for general use and are included in *AASHTO LRFD Bridge Construction Specifications*, Section 8, "Concrete Structures," from which LRFD Table C5.1.2.1-1 was taken. However, the minimum concrete content limits listed in Table 5.2 may be raised in the future.

Table 5.3 presents a list of intended uses of concrete by class listed in Table 5.2.

Corrosion of reinforcing steel was discussed earlier in Section 5.3. There is considerable evidence that the durability of reinforced concrete exposed to saltwater, deicing salts, or sulfates is appreciably improved if the cover over the reinforcing steel is increased or the *W/C* ratio is limited

TABLE 5.3
Intended Uses of Various Classes of Concrete

Class of Concrete	Intended Uses
A	Class A concrete is generally used for all elements of structures, except when another class is more appropriate, and specifically for concrete exposed to saltwater.
B	Class B concrete is used in footings, pedestals, massive pier shafts, and gravity walls.
C	Class C concrete is used in thin sections, such as reinforced railings less than 4.0 in. thick, for filler in steel grid floors.
P	Class P concrete is used when strengths in excess of 4.0 ksi are required. For prestressed concrete, consideration should be given to limiting the nominal aggregate size to 0.75 in.
S	Class S concrete is used to concrete deposited underwater in cofferdams to seal out water.

Note: Strengths above 5.0 ksi should be used only when the availability of materials for such concrete in the locale is verified.

www.EngineeringEBooksPdf.com

to 0.40. If materials, with reasonable use of admixtures, will produce a workable concrete to *W/C* ratio lower than those listed in Table 5.2, the contract documents should alter the recommendations in Table 5.2 appropriately.

The specified strengths shown in LRFD Table C5.4.2.1-1 are generally consistent with *W/C* ratio shown. However, it is possible to satisfy one without the other. Both are specified because *W/C* ratio is a dominant factor contributing to both durability and strength; simply obtaining the strength needed to satisfy the design assumptions may not ensure adequate durability.

5.4.1.3 Coefficient or Thermal Expansion

The coefficient of thermal expansion is determined by the laboratory tests on the specific mix to be used. In the absence of more precise data, the thermal coefficient of expansion may be taken as follows (Art. 5.4.2.2):

1. For normal-weight concrete, $6.0 \times 10^{-6}/°F$
2. For lightweight concrete, $5.0 \times 10^{-6}/°F$

Interestingly, the coefficient of expansion for steel is $6.5 \times 10^{-6}/°F$, which is very close to that of normal-weight concrete. These are advantageous properties and sometimes characterized as thermal compatibility of the two materials—concrete and steel.

5.4.1.4 Shrinkage and Creep

5.4.1.4.1 General

Creep is defined as time-dependent deformation under permanent load. *Shrinkage* is defined as time-dependent deformation due to loss of moisture. Concrete members, both reinforced and prestressed, are subjected to deformation due to shrinkage and creep; both must be considered for their effects on deflections.

Specifications for shrinkage and creep are covered in Art. 5.4.2.3. Methods of estimating time-dependent prestress losses are covered in Arts. 5.9.5.3 and 5.9.5.4. These provisions are applicable for specified concrete strengths up to 15.0 ksi. In the absence of more accurate data, the shrinkage coefficients may be assumed to be 0.0002 after 28 days and 0.0005 after 1 year of drying. Art. 5.4.2.3.1 specifies substitute provisions for estimating shrinkage and creep when mix-specific data are not available.

5.4.1.4.2 Creep

The creep coefficient may be taken as follows:

$$\Psi(t, t_i) = 1.9 k_s k_{hc} k_f k_{td} t_i^{-0.118} \qquad (5.1)\ [A5.4.2.3.2\text{-}1]$$

in which

$$k_s = 1.45 - 0.13(V/S) \geq 1.0 \qquad (5.2)\ [A5.4.2.3.2\text{-}2]$$

$$k_{hc} = 1.56 - 0.008H \qquad (5.3)\ [A5.4.2.3.2\text{-}3]$$

$$k_f = \frac{5}{1 + f'_{ci}} \qquad (5.4)\ [A5.4.2.3.2\text{-}4]$$

www.EngineeringEBooksPdf.com

$$k_{td} = \frac{t}{61 - 4f'_{ci} + t} \quad (5.5)\ [A5.4.2.3.2\text{-}5]$$

where

H = relative humidity (percent) (In the absence of better information, H may be taken from Figure 5.14.) (LRFD Figure 5.4.2.3.3-1)
k_s = factor for the effect of the volume-to-surface area ratio of the component
k_f = factor for the effect of concrete strength
k_{hc} = humidity factor for creep
k_{td} = time development factor
t = maturity of concrete (day), defined as age of concrete between time of loading for creep calculations, or end of curing for shrinkage calculations, and time being considered for the analysis of creep or shrinkage effects
t_i = age of concrete at the time of load application (day)
V/S = volume-to-surface area ratio (in.)
f'_{ci} = specified compressive strength of concrete at the time of prestressing for pretensioned members and at the time of initial loading for nonprestressed members. If concrete age at time of initial loading is unknown at design time, f'_{ci} may be taken a 0.80 f'_c (ksi)

5.4.1.4.3 Shrinkage

Shrinkage is affected by many factors, mainly the following:

1. Aggregate characteristics and proportions
2. Average humidity at the bridge site (Figure 5.9)
3. W/C ratio (water/cement ratio)
4. Type of cure
5. Volume-to-surface area ratio of member
6. Duration of drying period

For concretes devoid of shrinkage-prone aggregates, the strain due to shrinkage, ε_{sh}, at time, t, may be taken as follows:

$$\varepsilon_{sh} = k_s k_{sh} k_f k_{td}\, 0.48 \times 10^{-3} \quad (5.6)\ [A5.4.2.3.3\text{-}1]$$

in which

$$k_{sh} = (2.00 - 0.014H) \quad (5.7)\ [A5.4.2.3.3\text{-}2]$$

where k_{sh} = humidity factor for shrinkage.

If the concrete is exposed to drying before 5 days of curing has elapsed, the shrinkage as determined in Equation 5.6 should be increased by 20 percent.

Large concrete members may undergo substantially less shrinkage than that measured by laboratory testing of small specimens of the same concrete. The constraining effects of reinforcement and composite actions with other elements of the bridge tend to reduce the dimensional changes in some components.

5.4.1.5 Modulus of Elasticity of Concrete

Modulus of elasticity of concrete, E_c, is a function of its unit weight and the square root of its 28-day compressive strength. In the absence of measured data, the modulus of elasticity for

www.EngineeringEBooksPdf.com

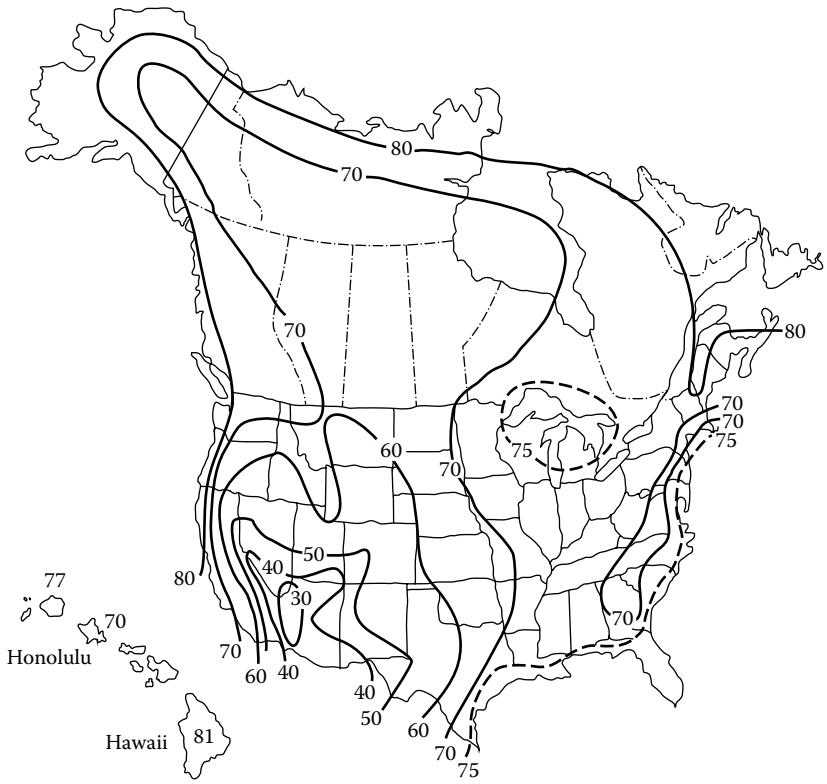

FIGURE 5.9 Annual average ambient relative humidity (percent). (From *AASHTO LRFD Bridge Design Specifications*, Copyright © 2012 by American Association of State Highway and Transportation Officials, Washington, DC. Used by permission.)

concretes with unit weights between 0.090 and 0.155 kcf and specified compressive strengths up to 15.0 ksi may be taken as follows:

$$E_c = 33{,}000\, K_1 w_c^{1.5} \sqrt{f_c'} \qquad (5.8)\ [A5.4.2.4\text{-}1]$$

where

K_1 = correction factor for source of aggregate, to be taken as 1.0 unless determined by physical test and as approved by the authority of jurisdiction

w_c = unit weight of concrete (kcf) as listed in LRFD Table 3.5.1-1 or Article C5.4.2.4

f_c' = specified compressive strength of concrete (ksi)

For normal-weight concrete with w_c = 0.145 kcf, E_c may be taken as follows:

$$E_c = 1820\sqrt{f_c'} \qquad (5.9)\ [A5.4.2.4\text{-}1]$$

It is noted that w_c = 0.145 kcf for normal weight concrete applies when $f_c' \leq 5.0$ ksi. For normal weight concrete with $5.0 < f_c' \leq 15.0$ ksi, the value of w_c may be taken as 0.140 + 0.001 f_c'. For example, for f_c' = 6.00 ksi or higher (typical for prestressed concrete), the value of w_c may be taken as 0.146 kcf and so on. For higher-strength concrete, w_c may be taken as high as 0.150 kcf; this is justified because of relatively low W/C ratio for such concretes.

www.EngineeringEBooksPdf.com

Tests have shown that the modulus of elasticity of concrete is influenced by the stiffness of the aggregate. The factor K_1 is included to allow the calculated modulus of elasticity to be adjusted for different types of aggregate and local materials. Unless a value has been determined by physical tests, K_1 should be taken as 1.0. The use of a measured K_1 factor permits a more accurate prediction of modulus of elasticity and other values that utilize it.

5.4.1.6 Modulus of Rupture

Modulus of rupture refers to the tensile strength of plain concrete as measured by flexure tests, usually on 4 in. × 4 in. × 16 in. long plain concrete beams, loaded centrally or at third points. The stress in the bottom of the beam is calculated by conventional flexure formula ($f = Mc/I$) assuming elastic behavior. Laboratory tests indicate wide scatter in data as shown in Figure 5.10. ACI 318 specifies the value of modulus of rupture for normal-weight concrete as follows:

$$f_r = 7.5\sqrt{f_c'}\ \text{lb/in.}^2 \tag{5.10}$$

where

f_r = modulus of rupture (lb/in.^{2})
f_c' = specified compressive strength of concrete (lb/in.^{2})

If f_c' is expressed in kip/in.^{2} units, Equation 5.10 can be expressed as follows:

$$f_r = 237.2\sqrt{f_c'}\ \text{lb/in.}^2 \tag{5.11}$$

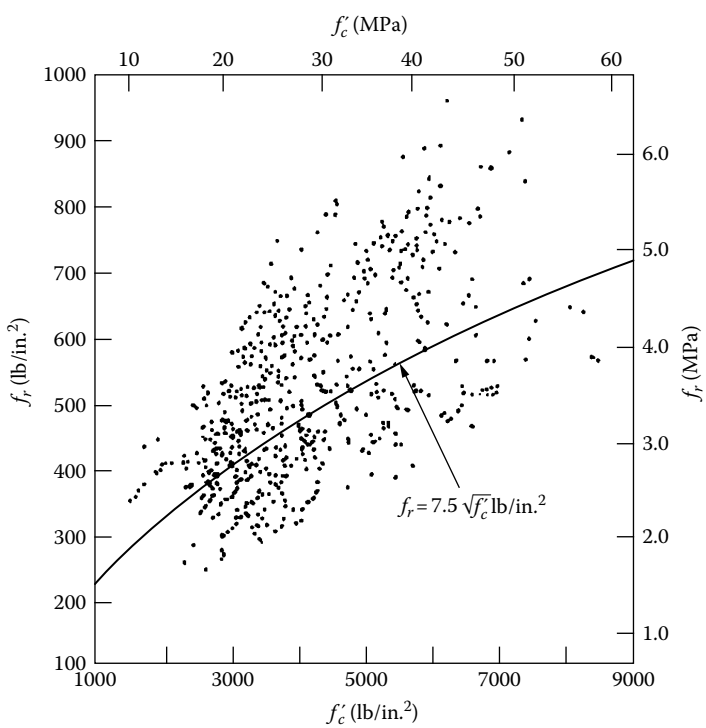

FIGURE 5.10 Variation in modulus of rupture of concrete with compressive strength of concrete. (Adapted from Mirza, A.S. et al., Statistical description of strength of concrete, *Proc. ASCE*, 105, ST6, 1021, June 1979.)

www.EngineeringEBooksPdf.com

Expressed in kip/in.^{2} units and rounding off the numbers, Equation 5.11 can be expressed as in Equation 5.12:

$$f_r = 0.24\sqrt{f'_c} \tag{5.12}$$

For lightweight concrete, the suggested value of modulus of rupture is given by Equation 5.13:

$$f_r = 0.17\sqrt{f'_c} \tag{5.13}$$

Unless determined by physical tests, the modulus of rupture of concrete, f_r, for specified concrete strengths up to 15.0 ksi may be taken as given by Equations 5.12 and 5.13 as applicable. Direct tensile strength of concrete may be determined by either using ASTM C900 or the split tensile strength method in accordance with ASTM C496.

5.4.2 High-Strength Concrete and Bridge Span Capabilities

General concrete compressive strengths used in bridge construction range between 4000 and 6000 psi. Occasionally, it might be necessary and even desirable and economical to use higher-strength concrete, often referred to as HPC, as demonstrated by several studies for prestressed concrete girders conducted in the 1980s. A study by Construction Technology Laboratories (CTLR) showed that increasing concrete strength from 5000 to 7000 psi could result in an increase of about 15 percent in span capability (Rabbat et al. 1982). A similar study (Jobse 1987, Roller et al. 1993, 1995) of various prestressed concrete beams of I and bulb-T shapes using 10,000 psi concrete also showed increased span capabilities (Figures 5.11 through 5.13). A study by Castrodale et al. (1988) of 12 different girder cross sections, fabricated from concretes of strength in the 6,000–15,000 psi range reported an increase of 10–40 percent in span for a given girder cross section. Based on a study by Durning and Rear (1993), Figure 5.14 shows influence of concrete strength on simple-span prestressed concrete girder bridges; Figure 5.15 shows a design comparison of AASHTO-PCI Type IV girder using 6,000 and 10,000 psi concretes. A brief summary on the potential of high strength for bridge construction can be found in the literature (Taly 1998).

5.4.3 Reinforcing Steel (Art. 5.4.3)

5.4.3.1 General

Reinforced concrete construction uses a variety of reinforcing materials that include reinforcing bars, deformed wire, cold-drawn wire, welded plain wire fabric, and welded deformed wire fabric. Art. 5.4.2 requires that these materials conform to the material standards as specified in Art. 9.2 of the *AASHTO LRFD Bridge Construction Specifications* (AASHTO 2010).

Reinforcement shall be deformed, except that plain bars or plain wire may be used for spirals, hoops, and wire fabric.

To distinguish ordinary reinforcing bars from prestressing strands, these two materials would be referred to as *nonprestressed steel* and *prestressed steel*, respectively, in this chapter.

Yield strength of steel, f_y, is one of the two key design parameters used in design (the other is the specified compressive strength of concrete, f'_c). The nominal yield strength shall be the minimum as specified for the grade of steel selected, except that yield strengths in excess of 75.0 ksi shall not be used for design purposes. The yield strength or grade of the bars or wires shall be shown in the contract documents. Bars with yield strengths less than 60.0 ksi are permitted to be used only with the approval of the owner.

www.EngineeringEBooksPdf.com

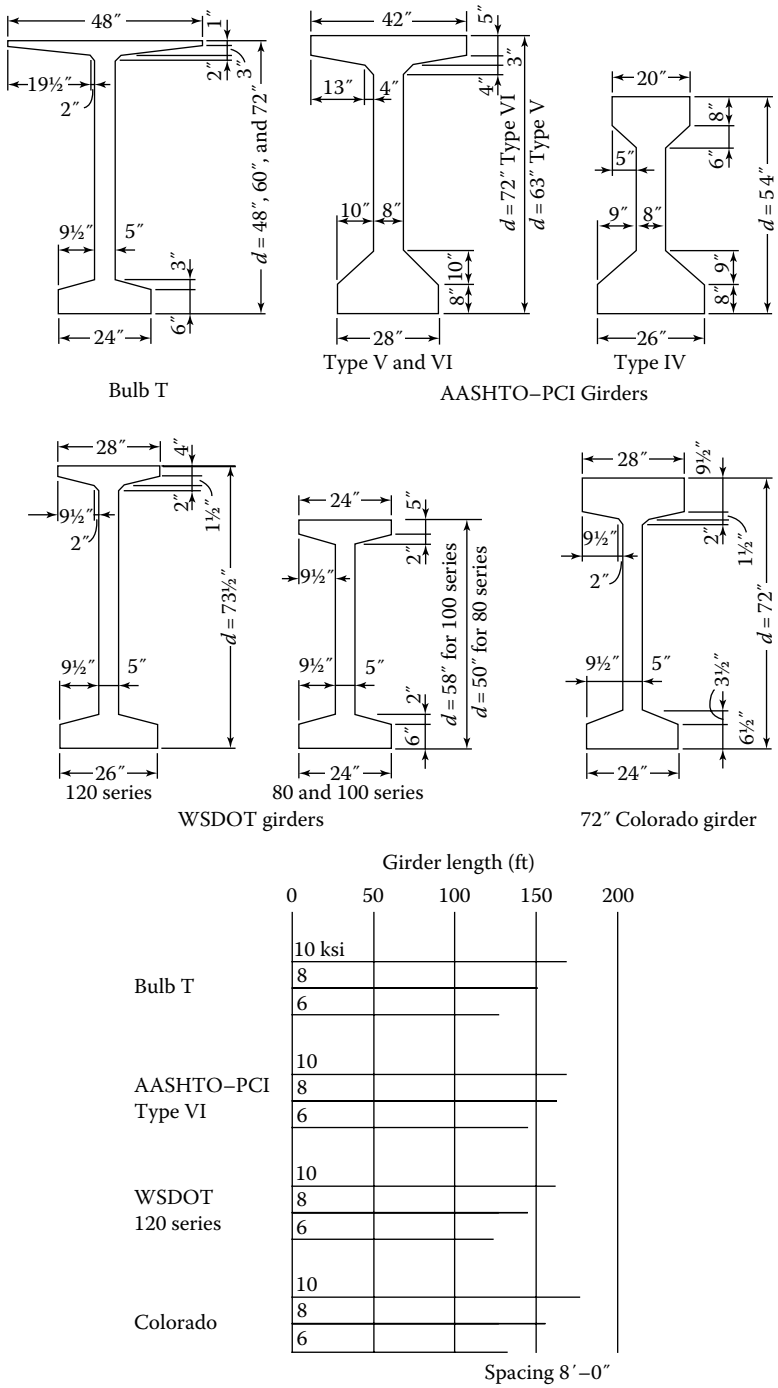

FIGURE 5.11 Span capabilities for basic 72 in. deep girders with cast-in-place decks. (From Jobse, H.J., Application of high-strength concrete for highway bridges. Adapted from Executive summary, Publication No. FHWA/RD-87/079, Federal Highway Administration, Washington, DC, October 1987.)

www.EngineeringEBooksPdf.com

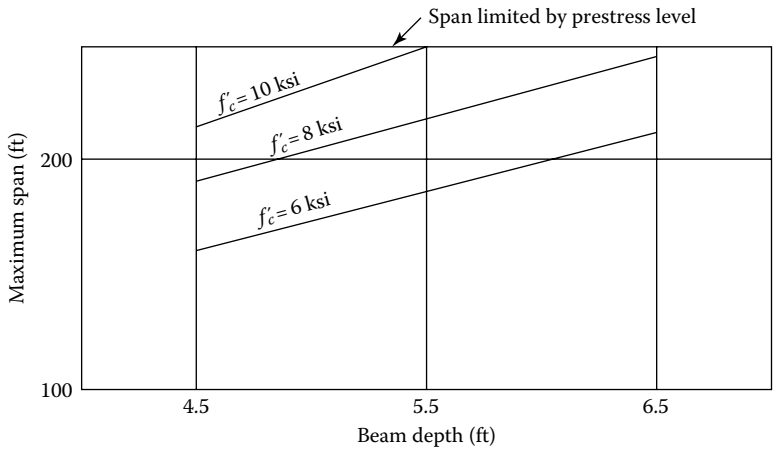

FIGURE 5.12 Span capabilities for two-span continuous box girder bridge. (From Jobse, H.J., Application of high-strength concrete for highway bridges. Adapted from Executive summary, Publication No. FHWA/RD-87/079, Federal Highway Administration, Washington, DC, October 1987.)

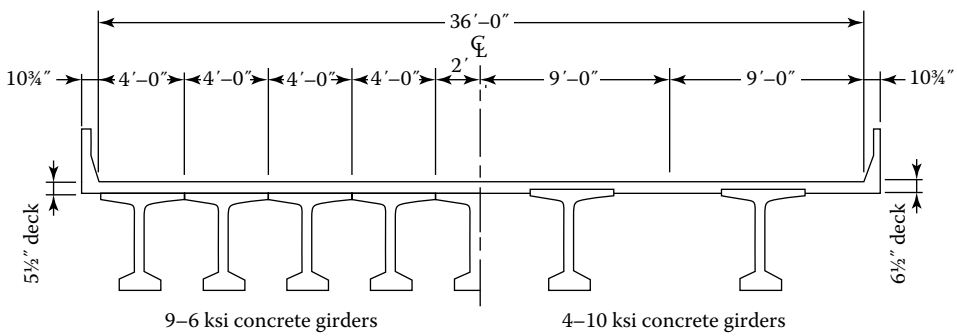

FIGURE 5.13 Two 150 ft simple-span bridge designs with different concrete strengths. (From Jobse, H.J., Application of high-strength concrete for highway bridges. Adapted from Executive summary, Publication No. FHWA/RD-87/079, Federal Highway Administration, Washington, DC, October 1987.)

Where ductility is to be assured or where welding is required, steel conforming to the requirements of ASTM A706, *Low-Alloy Steel Deformed Bars for Concrete Reinforcement*, should be specified. This specification covers bar sizes No. 3 through No. 18.

The modulus of elasticity, E_s, of steel reinforcing shall be assumed as 29,000 ksi.

Reinforcement to be welded shall be indicated in the contract documents, and the welding procedure to be used shall be specified.

Reinforcement conforming to ASTM A1035/A1035M may only be used as top and bottom flexural reinforcement in the longitudinal and transverse directions of bridge decks in seismic zones 1 and 2.

5.4.3.2 Reinforcing Bars

For reinforced construction, deformed reinforcing bars (i.e., bars produced with deformations or surface protrusions to provide a locking anchorage with the surrounding concrete) are the most used type of reinforcing material. General information about reinforcing bars can be found in publications by Concrete Reinforcing Steel Institute (CRSI), for example, (CRSI 2009). The profiles of surface

www.EngineeringEBooksPdf.com

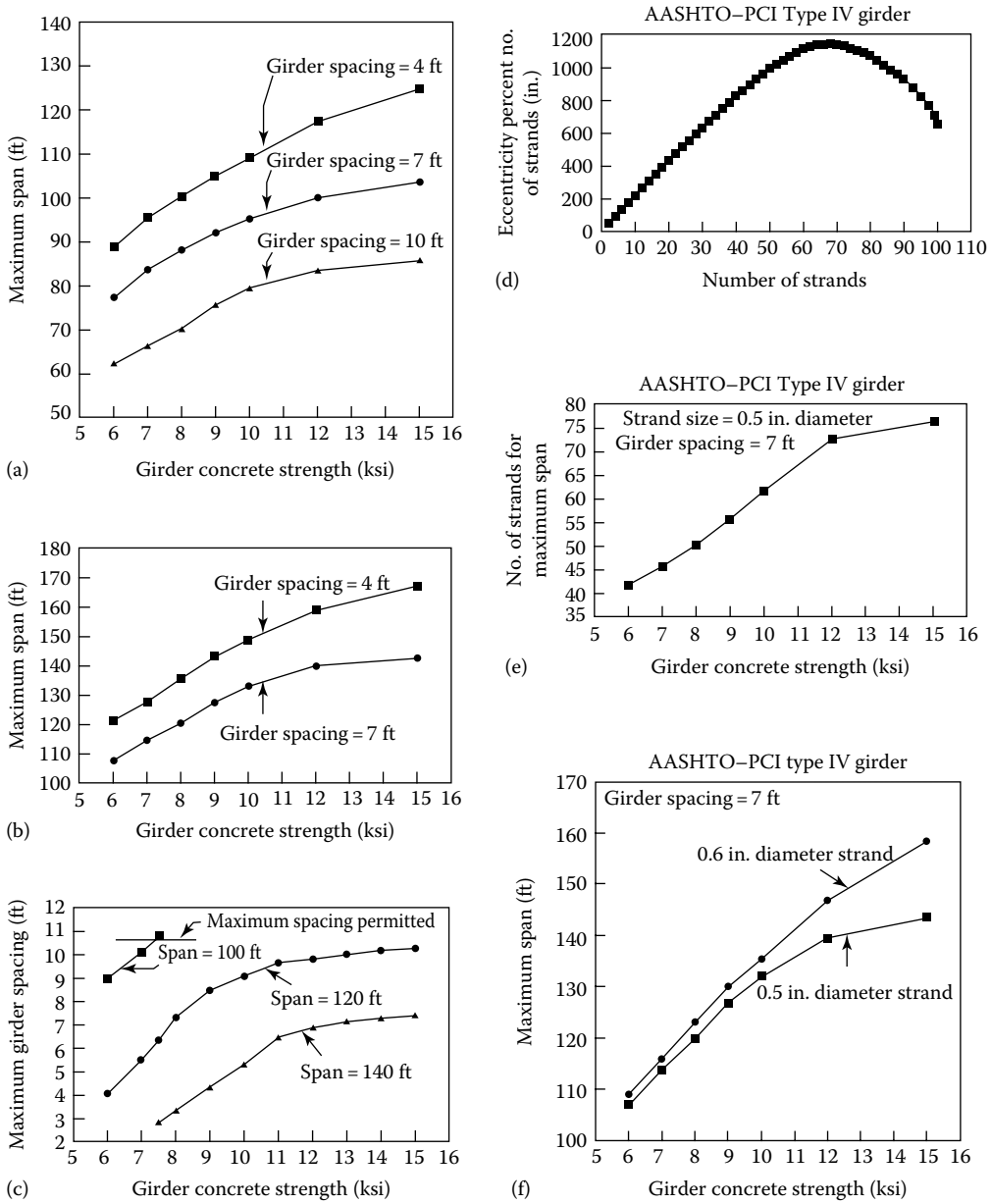

FIGURE 5.14 Influence of concrete strength on simple-span prestressed concrete girder bridges. (a) Texas Type (C) girder, (b) AASHTO–PCI Type IV girder, (c) AASHTO–PCI Type IV girder, (d) product of eccentricity and number of strands versus number of strands, (e) number of strands for maximum span versus concrete strength, and (f) maximum span versus concrete strength with 0.5 and 0.6 in. (13 and 15 mm) diameter strand. (Adapted from Durning, T.A. and Rear, K.B., *PCI J.*, 38 (3), 46, 1993.)

protrusions on the bars vary with the producing mill and the size of bars. Figure 5.16 shows samples of reinforcing bars with different protrusion profiles. Both ASTM and AASHTO specifications require that all reinforcing bars be identified by permanent, mill-printed markings. Figure 5.17 shows these bar markings indicating information about the producing mill, the bar size, and the type of steel used in producing the bars.

www.EngineeringEBooksPdf.com

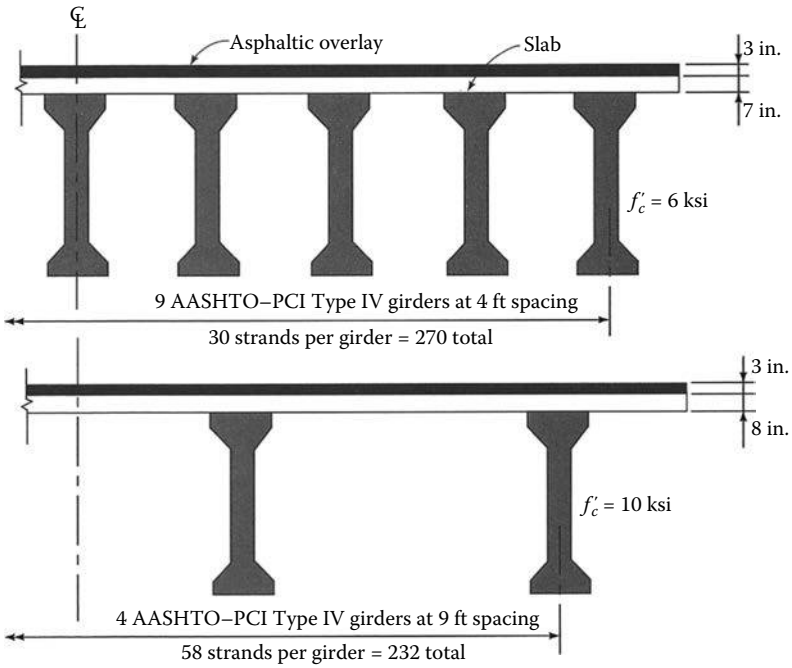

FIGURE 5.15 Bridge design comparison: 10 ksi versus 6 ksi concrete. (From Durning, T.A. and Rear, K.B., *PCI J.*, 38 (3), 46, 1993. Reproduced with permission from Prestressed Concrete Institute, Chicago, IL.)

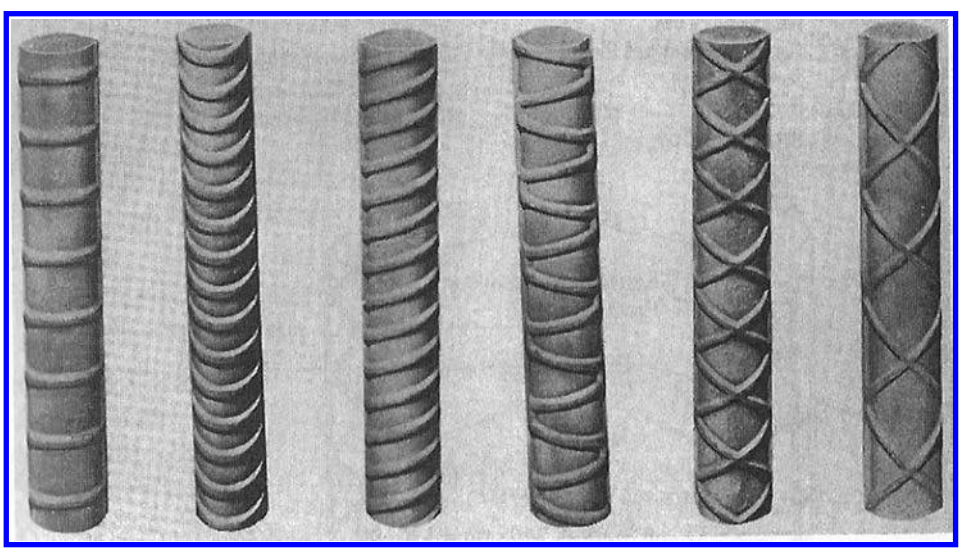

FIGURE 5.16 Samples of deformed reinforcing bars. (From CRSI, *Manual of Standard Practice 2009*, 28th ed., Concrete Reinforcing Steel Institute, Schaumburg, IL, 2009.)

Section properties of reinforcing bars commonly used for the design of bridge decks, beams, and columns are given in the appendix of this chapter in the form of the following tables:

1. Table 5.A.1 Cross-Sectional Areas of Reinforcing Bars
2. Table 5.A.2 Area of Groups of Standard Reinforcing Bars
3. Table 5.A.3 Spacing of Bars for Slab Reinforcement (in.^{2}/ft)

www.EngineeringEBooksPdf.com

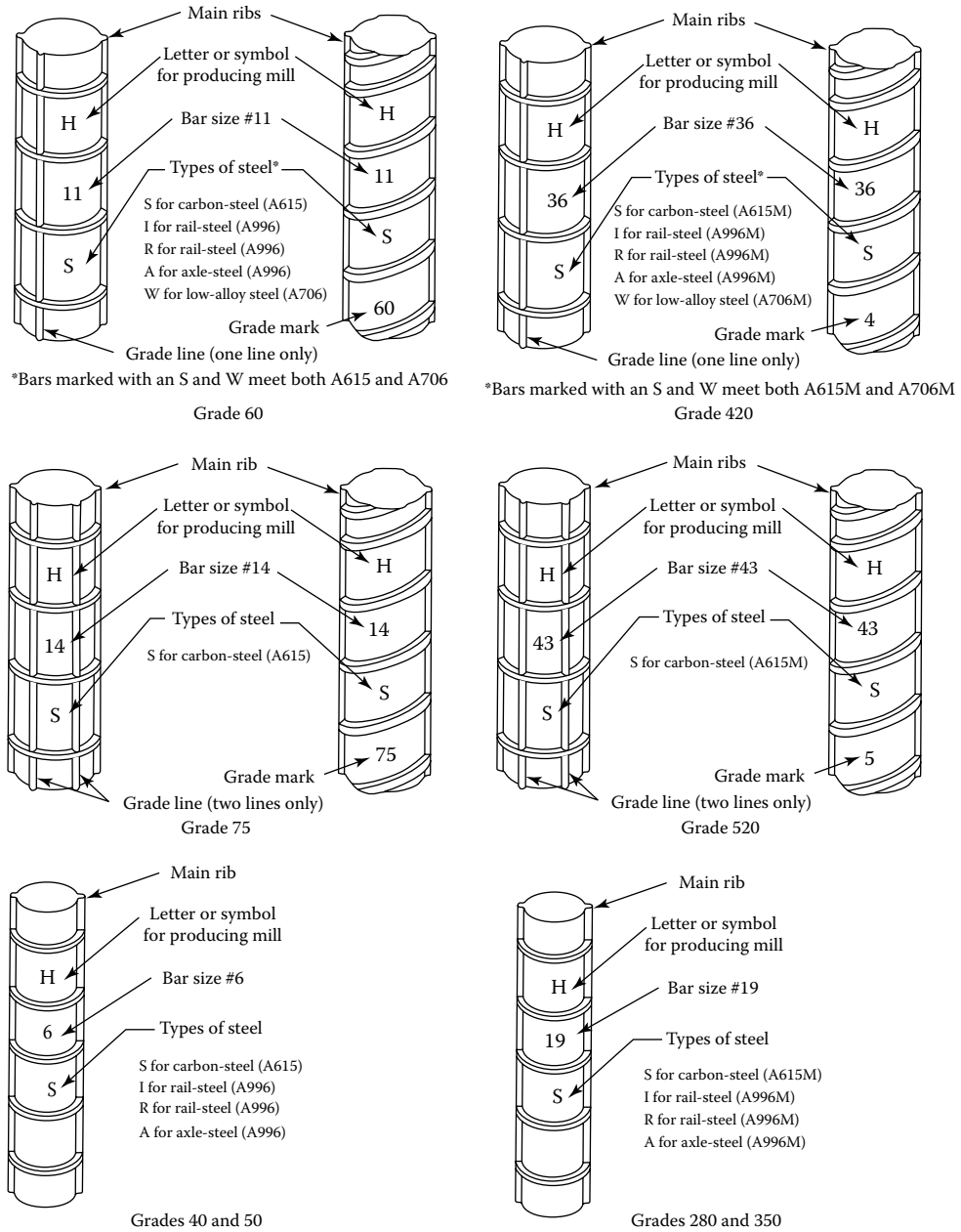

FIGURE 5.17 Identification marks rolled on the surface of reinforcing bars. The right-hand side in the figures shows marking in SI system. (From CRSI, *Manual of Standard Practice 2009*, 28th ed., Concrete Reinforcing Steel Institute, Schaumburg, IL, 2009.)

5.4.4 Prestressing Steel: Art. 5.4.4

5.4.4.1 General

In bridge construction, prestressing strands are most generally used in bridge decks, girders, and segmental construction. It is manufactured in three forms: *wires*, *strands*, and *bars*. LRFD Art. 5.4.4 requires uncoated, stress-relieved or low-relaxation, seven-wire strand, or uncoated plain or

www.EngineeringEBooksPdf.com

TABLE 5.4
Properties of Prestressing Strand and Bar (LRFD Table 5.4.4.1-1)

Material	Grade or Type	Diameter (in.)	Tensile Strength, f_{pu} (ksi)	Yield Strength, f_{py} (ksi)
Strand	250 ksi	1/4 to 0.6	250	85 percent of f_{pu}, except 90 percent of f_{pu} for low-relaxation strand
	270 ksi	3/8 to 0.6	270	
Bar	Type 1, plain	3/4 to 1-3/8	150	85 percent of f_{pu}
	Type 2, deformed	5/8 to 1-3/8	150	85 percent of f_{pu}

Source: Adapted from *AASHTO LRFD Bridge Design Specifications*, Copyright © 2012 by American Association of State Highway and Transportation Officials, Washington, DC. Used by permission.

deformed, high-strength bars to conform to the following material standards, as specified for use in *AASHTOMLRFD Bridge Construction Specifications* (AASHTO 2010):

1. AASHTO M 203/M 203M (ASTM A416/A416M)
2. AASHTO M 275/M 275M (ASTM A722/A722M)

Tensile and yield strengths for these steels may be taken as specified in Table 5.4 (LRFD Table 5.1).

Prestressing wire, ranging in diameters from 0.192 to 0.276 in., is made by cold-drawn high-carbon steel, followed by heat treatment for stress relieving to develop prescribed mechanical properties. To produce *prestressing tendons* of required strength, wires are bundled in groups of 50 individual wires. Strands (or stranded cables), ranging in diameters from 0.250 to 0.600 in., are fabricated by twisting six wires of equal diameters over a seventh wire, which is straight and of slightly larger diameter called the *control wire*, and the product is a *standard strand* (Figure 5.18a); stress relieving is achieved after the wires are twisted into the strand. To maximize the steel area within a given nominal diameter, the strand can be *compacted* by drawing it through a die, forming what is called a *compacted strand* (Figure 5.18b).

Alloy steel bars for prestressing, both in the form of plain round (Type 1) and deformed bars (Type 2), are manufactured in diameters from 0.635 to 1.375 in. Cold drawn in order to raise their yield strength, these bars are stress relieved as well to increase ductility.

Tables 5.5 and 5.6 present the properties of stress-relieved seven-wire standard strands and stress-relieved seven-wire compacted strands.

Two types of strands, *low relaxation* and *stress relieved* (normal relaxation), are in general use for prestressing and posttensioning purposes. These are available in two grades—Grade 250 and Grade 270—having minimum ultimate tensile strengths of 250 and 270 ksi, respectively, based on their nominal cross-sectional areas. For the alloy steel bars, two grades are used, Grade 145 and Grade 160, the former being common. Round wires are available in three grades, Grade 145,

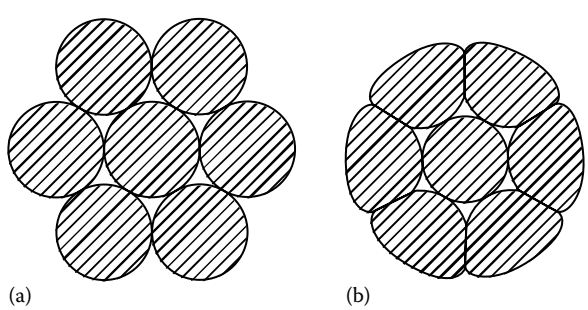

FIGURE 5.18 Cross section of typical prestressing strands: (a) standard strand and (b) compacted strand.

www.EngineeringEBooksPdf.com

TABLE 5.5
Properties of Stress-Relieved Seven-Wire Standard Strands

Nominal Diameter of Strand (in.)	Minimum Breaking Strength of Strand (lb)	Nominal Steel Area of Strand, (in.^{2})	Nominal Weight of Strand (lb/1000 ft)	Minimum Load at 1 percent Extension (lb)
		Grade 250		
1/4 (0.250)	9,000	0.036	122	7,650
5/16 (0.313)	14,400	0.058	197	12,300
3/8 (0.375)	20,000	0.080	272	17,000
7/16 (0.438)	27,000	0.108	367	23,000
1/2 (0.500)	36,000	0.144	490	30,600
3/4 (0.600)	54,000	0.216	737	45,900
		Grade 270		
3/8 (0.375)	23,000	0.085	290	19,500
7/16 (0.438)	31,000	0.115	390	26,350
1/2 (0.500)	41,300	0.153	520	35,100
4/4 (0.600)	58,600	0.217	740	49,800

TABLE 5.6
Properties of Seven-Wire Compacted Strand

Nominal Diameter (in.)	Minimum Breaking Strength (lb)	Nominal Steel Area (in.^{2})	Nominal Weight (lb/1000 ft)
1/2	23,000	0.174	600
0.6	67,440	0.256	873
0.7	85,340	0.346	1173

Grade 245, and Grade 250, depending on the diameter. All grade designations correspond to the minimum specified ultimate tensile strength (kip/in.^{2}).

Figure 5.19 shows typical stress–strain curves for high-strength steel used for the manufacture of prestressing wire, strands, and bars (Nawi 1989). Because the curves for these steels do not exhibit a well-defined yield point (there is no sharp break in the stress–strain curves to indicate a distinct elastic limit or yield point as in the case of ASTM A36 steel), the yield strength is measured at 1 percent extension under load for wire and strand and at 0.7 percent for alloy steel bars. Note that the spread between the yield strength and then tensile strength is smaller for prestressing steel than for the reinforcing steels; consequently, the prestressing steel has less ductility.

5.4.4.2 Modulus of Elasticity of Prestressing Steels: Art. 5.4.4.2

The modulus of elasticity of prestressing steels is a little lesser than that for ordinary reinforcing steels (29,000 ksi) and should be based on the data supplied by the manufacturers. If more precise data are not available, the modulus of elasticity for prestressing steel, E_p, based on nominal cross-sectional area may be taken as follows:

For strand, $E_p = 28{,}500$ ksi
For bar, $E_p = 28{,}500$ ksi

The suggested modulus of elasticity of 28,500 ksi for strands is based on recent statistical data. This value is higher than that previously assumed because of the slightly different characteristics and the near universal use of low-relaxation strands.

www.EngineeringEBooksPdf.com

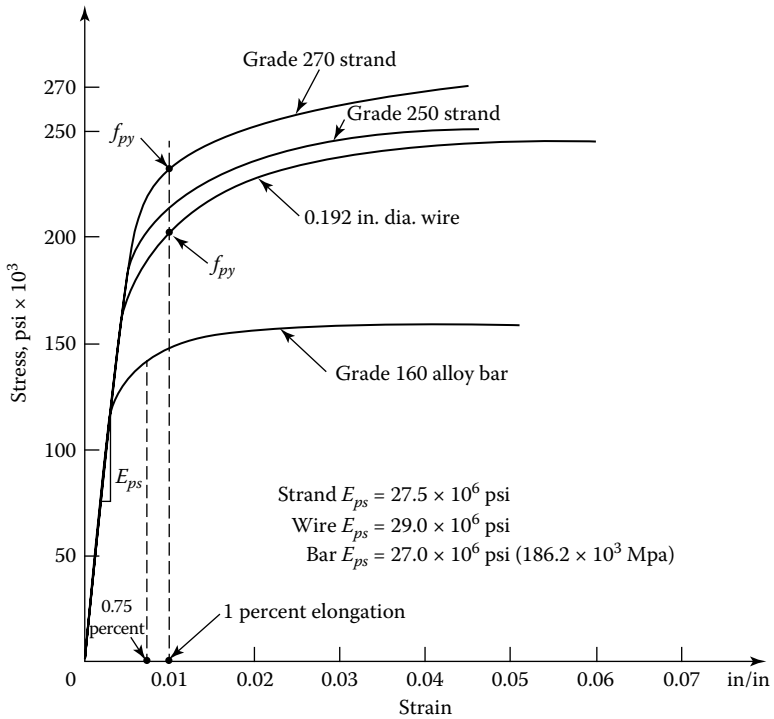

FIGURE 5.19 Typical stress–strain curves for prestressing steels. (From Nawy, E.G., *Prestressed Concrete—A Fundamental Approach*, 5th ed., Prentice-Hall, Englewood Cliffs, NJ, 2010. Reproduced with permission from Pearson Higher Education.)

5.4.4.3 Relaxation of Steel

Customarily, fabrication of prestressed concrete beams involves prestressing steel strands to very-high-stress levels—as much as 80–90 percent of their yield strengths. Under these conditions, unlike ordinary reinforcing steel bars, steel prestressing strands exhibit a unique phenomenon called *relaxation*, which is defined as *loss of stress* in stressed material (strands) held at constant length (between the ends of prestressed beam). In essence, it is analogous to *creep* in concrete (discussed earlier), which refers to change in strain under constant stress (e.g., stress due to permanent load). The magnitude of prestress losses can be as high as 35,000–60,000 psi. It is this property that requires prestressing steels to be *high-strength quality* so that even after the prestress losses, usable prestress will be left in the strands. Obviously, ordinary Grade 60 reinforcing bars would be left with hardly any prestress following the occurrence of prestress losses. Figure 5.20 shows typical relaxation behavior of prestressed steels.

Relaxation losses can be reduced by a process called *stabilization*; the resulting product is called *low-relaxation steel*, having relaxation stress loss of approximately 25 percent of the normal stress-relieved steel; consequently, it is the preferred type of prestressing steel. It is for this reason that Art. C5.4.4.1 specifies that low-relaxation strand shall be regarded as the standard type. Stress-relieved strand is not to be furnished for use unless specifically ordered, or by arrangement between purchaser and supplier.

It should be noted that the use of low-relaxation strands results in a reduced area of prestressed steel required and thus results in a reduced moment capacity as compared to that provided by the normal-relaxation strand. In such cases, nonprestressed steel (ordinary reinforcing bars) is often used in combination with prestressing steel in order to develop the required flexural strength of the beam.

www.EngineeringEBooksPdf.com

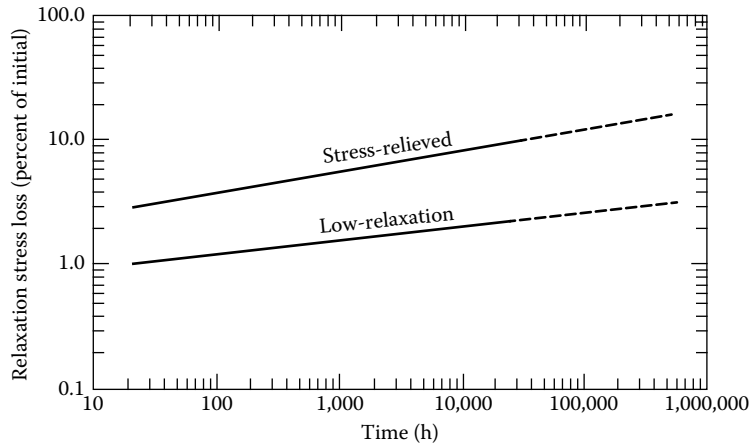

FIGURE 5.20 Loss of prestress as a result of relaxation over time in stress-relieved and low-relaxation prestressing steels. (Courtesy of Posttensioning Institute).

5.4.5 Strength Limit State

5.4.5.1 General

Limit state design philosophy was discussed in Chapter 1. All discussion pertaining to design of concrete structures is limited to LRFD. The strength limit state issues to be considered are related to strength and stability of a bridge.

Factored resistance is the product of nominal resistance as determined in accordance with the applicable provisions of Arts. 5.6, 5.7, 5.8, 5.9, 5.10, 5.13, and 5.14, unless another limit state is specifically identified, and the resistance factor is as specified in Art. 5.5.4.2.

5.4.5.2 Resistance Factors (ϕ-factors)

Art. 5.5.4.2 specifies resistance factors, commonly referred to as ϕ-factors, separately for conventional construction and segmental bridge construction; the latter is not discussed in this book.

5.4.5.3 ϕ-Factors for Conventional Construction

Resistance factors, ϕ, corresponding to various strength considerations specified in Art. 5.5.4.2.1 are listed in Table 5.7.

From a design perspective, concrete sections are classified as *tension controlled*, *transition*, or compression controlled, depending on the strain at the centroid of the tensile reinforcement closest to the extreme tension fibers, ε_t, as follows:

1. If the strain $\varepsilon_t \geq 0.005$, the section is defined as tension controlled.
2. If $0.005 > \varepsilon_t > 0.002$, the section is defined as transition.
3. If $0.002 > \varepsilon_t$, the section is defined as compression controlled.

Note that the steel strain of 0.002 corresponds to the yield strength of 60 ksi (stress/E = 60 ksi/29,000 ksi = 0.00205 ≈ 0.002) and the strain of 0.005 corresponds to the yield strength of 150 ksi (stress/E = 150 ksi/29,000 ksi = 0.00517 ≈ 0.005); the latter value of strain is set to include steel having a yield strength up to 150 ksi.

For sections in which the net tensile strain in the extreme tension steel at nominal resistance is between the limits for compression-controlled sections ($\varepsilon_t \leq 0.002$) and tension-controlled sections ($\varepsilon_t \geq 0.005$), the resistance factor, ϕ, may be linearly increased from 0.75 to that for tension-controlled

www.EngineeringEBooksPdf.com

TABLE 5.7
Resistance Factors for Strength Limit State for Conventional Construction (LRFD Art. 5.5.4.2-1)

Strength Consideration	Resistance Factor (ϕ-Factor)
Shear and torsion	
Normal-weight concrete	0.90
Lightweight concrete	0.80
For tension-controlled concrete section as defined in Art. 5.7.2.1	0.90
For tension-controlled prestressed concrete section as defined in Art. 5.7.2.1	1.00
For shear and torsion	
Normal-weight concrete	0.90
Lightweight concrete	0.70
For compression-controlled sections with spirals or ties, as defined in Art. 5.7.2.1, except as specified in Arts. 5.10.11.3 and 5.10.11, 11.4.1 lb for seismic zones 2 and 3 and at extreme-event limit state	0.75
For bearing on concrete	0.70
For compression in strut-and-tie models	0.70
For compression in anchorage zones	
Normal-weight concrete	0.80
Lightweight concrete	0.65
For tension in steel in anchorage zones	1.00
For resistance during pile driving	1.00

Source: Adapted from *AASHTO LRFD Bridge Design Specifications*, Copyright © 2012 by American Association of State Highway and Transportation Officials, Washington, DC. Used by permission; Art. 5.5.4.2-1.

sections as the net tensile strain in the extreme tension steel increases from the compression strain limit to 0.005. This variation in ϕ may be computed as follows:

1. For members with ordinary (or nonprestressed) reinforcement,

$$0.75 \le \phi = 0.65 + 0.15\left(\frac{d_t}{c} - 1\right) \le 0.9 \qquad (5.14)\ [A5.5.4.2.1\text{-}2]$$

2. For members with prestressed reinforcement,

$$0.75 \le \phi = 0.583 + 0.25\left(\frac{d_t}{c} - 1\right) \le 1.0 \qquad (5.15)\ [A5.5.4.2.1\text{-}1]$$

where

ε_t = net tensile strain in extreme tension steel at nominal resistance (Figure 5.21)
d_t = distance from the extreme compression fibers to the centroid to the tension reinforcement closest to the tension face of the member (Figure 5.21)
c = distance from the extreme compression fibers to the neutral axis (Figure 5.21)

In applying the resistance factors for tension-controlled and compression-controlled sections, the axial tension and compression to be considered are those caused by external forces. Effects of primary prestressing forces are not included. Figure 5.22 shows the variation in the value of resistance factor, ϕ, as represented by Equations 5.14 and 5.15. Figure 5.22 shows that a lower ϕ-factor is used for compression-controlled sections than that for tension-controlled sections mainly because the former possess less ductility, are more sensitive to variations in concrete strength, and generally occur in members that support larger loaded areas than members with tension-controlled sections.

www.EngineeringEBooksPdf.com

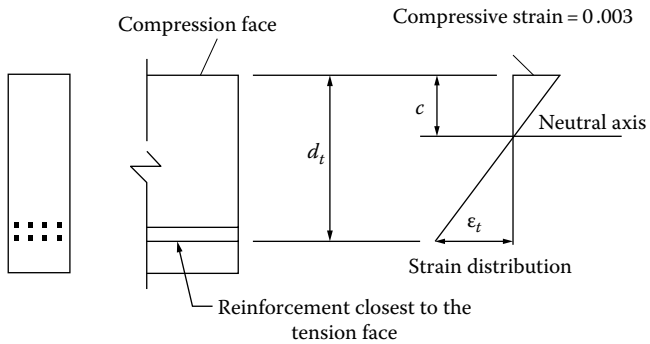

FIGURE 5.21 Strain distribution and net tensile strain at nominal resistance of a concrete section. (Adapted from *AASHTO LRFD Bridge Design Specifications*, Copyright © 2012 by American Association of State Highway and Transportation Officials, Washington, DC. Used by permission.)

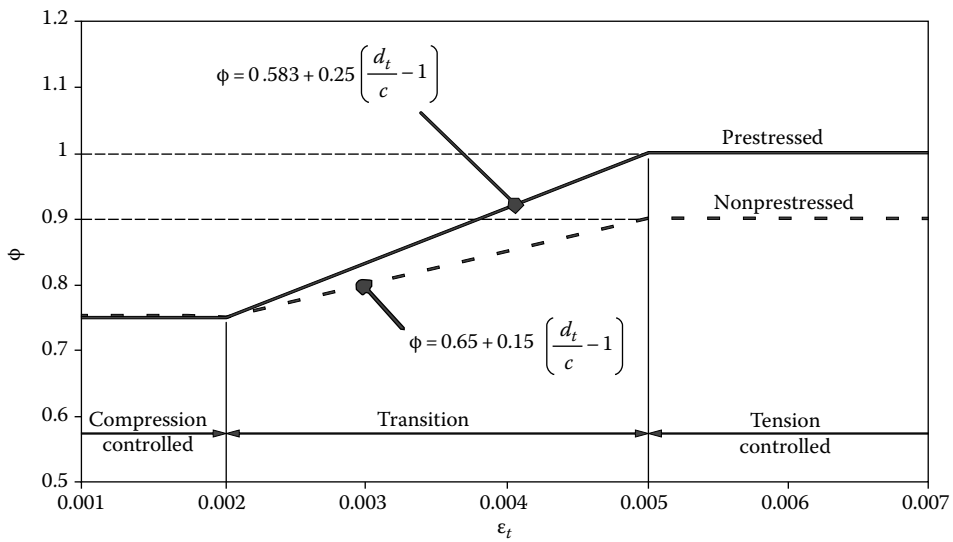

FIGURE 5.22 Variation of ϕ with net tensile strain ε_t and d_t/c for Grade 60 reinforcement and prestressing steel. (From *AASHTO LRFD Bridge Design Specifications*, Copyright © 2012 by American Association of State Highway and Transportation Officials, Washington, DC. Used by permission.)

5.5 DESIGN PROCEDURES FOR FLEXURE IN SECTION 5 OF LRFD SPECIFICATIONS

Section 5 of LRFD specifications (AASHTO 2012) is dedicated to design issues pertaining to both reinforced and prestressed concrete bridges. It has adopted a unified approach in that provisions for design of both reinforced and prestressed concrete bridges and related members are contained in a single chapter. This approach has been used because the same LRFD philosophy is used for both reinforced and prestressed concrete bridges.

For design purposes, pertinent information has to be obtained from many different LRFD articles that are contained in many different sections of LRFD specifications; Table 5.8 presents a summary of these articles.

www.EngineeringEBooksPdf.com

TABLE 5.8
LRFD Provisions for Design of Concrete Highway Bridges

Design Topic	LRFD Articles
A. Design philosophy	1.3.1
B. Limit states	1.3.2
C. Design objectives and location features	2.3, 2.5
Beam and Girder Superstructure Design	
A. Develop general section	
1. Roadway width	Highway-specified
2. Span arrangements	2.3.2, 2.5.4, 2.5.5, 2.6
3. Select bridge type	
B. Develop typical section	
1. Precast P/S beams	
a. Top flange	5.14.1.2.2
b. Bottom flange	5.14.1.2.2
c. Webs	5.14.1.2.2
a. Structure depth	2.5.2.6
b. Minimum reinforcement	5.7.3.3.2, 5.7.3.4
c. Lifting devices	5.14.1.2.3
d. Joints	5.14.1.3.2
2. CIP T-beams and multiweb box girders	5.14.1.5
a. Top flange	5.14.1.5.la
b. Bottom flange	5.14.1.5.1b
c. Webs	5.14.1.5.1c
d. Structure depth	2.5.2.6.3
e. Reinforcement	5.14.1.5.2
(1) Minimum reinforcement	5.7.3.3.2, 5.7.3.4
(2) Temperature and shrinkage reinforcement	5.10.8
f. Effective flange widths	4.6.2.6
g. Strut-and-tie areas, if any	5.6.3
C. Design conventionally reinforced concrete deck	
1. Deck slab	4.6.2.1
2. Minimum depth	9.7.1.1
3. Empirical design	9.7.2
4. Traditional design	9.7.3
5. Strip method	4.6.2.1
6. Live load application	3.6.1.3.3, 4.6.2.1.5
7. Distribution reinforcement	9.7.3.2
8. Overhang design	A13.4, 3.6.1.3.4
D. Select resistance factors	
Strength limit state (conventional)	5.5.4.2.1
E. Select load modifiers	
1. Ductility	1.3.3
2. Redundancy	1.3.4
3. Operational importance	1.3.5
F. Select applicable load combinations and load factors	3.4.1, Table 3.1.4-1
G. Calculate live load force effects	
1. Live loads and number of lanes	3.6.1, 3.6.1.1.1
2. Multiple presence	3.6.1.1.2
3. Dynamic load allowance	3.6.2

(*Continued*)

www.EngineeringEBooksPdf.com

TABLE 5.8 (*Continued*)
LRFD Provisions for Design of Concrete Highway Bridges

Design Topic	LRFD Articles
4. Distribution factor for moment	4.6.2.2.2
a. Interior beams with concrete decks	4.6.2.2.2b
b. Exterior beams	4.6.2.2.2d
c. Skewed bridges	4.6.2.2.2e
5. Distribution factor for shear	4.6.2.2.3
a. Interior beams	4.6.2.2.3a
b. Exterior beams	4.6.2.2.3b
c. Skewed bridges	4.6.2.2.3c2, Table 4.6.2.2.3c-1
6. Reactions to substructure	3.6
H. Calculate force effects from other loads as required	
I. Investigate service limit state	
1. P/S losses	5.9.5
2. Stress limitations for P/S tendons	5.9.3
3. Stress limitations for P/S concrete	5.9.4
a. Before losses	5.9.4.1
b. After losses	5.9.4.2
4. Durability	5.12
5. Crack control	5.7.3.4
6. Fatigue, if applicable	5.5.3
7. Deflection and camber	2.5.2.6.2, 3.6.1.3.2, 5.7.3.6.2
J. Investigate strength limit state	
1. Flexure	
a. Stress in P/S steel	
Bonded tendons	5.7.3.1.1
b. Stress in P/S steel	
Unbonded tendons	5.7.3.1.2
c. Flexural resistance	5.7.3.2
d. Limits for reinforcement	5.7.3.3
2. Shear (assuming no torsional moment)	
a. General requirements	5.8.2
b. Sectional design model	5.8.3
1. Nominal shear resistance	5.8.3.3
2. Determination of β and θ	5.8.3.4
3. Longitudinal reinforcement	5.8.3.5
4. Transverse reinforcement	5.8.2.4, 5.8.2.5, 5.8.2.6, 5.8.2.7
5. Horizontal shear	5.8.4
K. Check details	
1. Cover requirements	5.12.3
2. Development length—reinforcing steel	5.11.1, 5.11.2
3. Development length—prestressing steel	5.11.4
4. Splices	5.11.5, 5.11.6
5. Anchorage zone	
a. Posttensioned	5.10.9
b. Pretensioned	5.10.10
6. Ducts	5.4.6

(*Continued*)

www.EngineeringEBooksPdf.com

TABLE 5.8 (*Continued*)
LRFD Provisions for Design of Concrete Highway Bridges

Design Topic	LRFD Articles
7. Tendon profile limitation	
a. Tendon confinement	5.10.4
b. Curved tendons	5.10.4
c. Spacing limits	5.10.3.3
8. Reinforcement spacing limits	5.10.3
9. Transverse reinforcement	5.8.2.6, 5.8.2.7, 5.8.2.8
10. Beam ledges	5.13.2.5
Slab Bridges	
A. Check minimum recommended depth	2.5.2.6.3
B. Determine live load strip width	2.5.2.6.3
C. Determine applicability of live load for decks and deck systems	3.6.1.3.3
D. Design edge beam	9.7.1.4
E. Investigate shear	5.14.4.1
F. Investigate distribution reinforcement	5.14.4.1
G. If not solid	
1. Check if voided slab or cellular construction	5.14.4.2.1
2. Check minimum and maximum dimension	5.14.4.2.1
3. Design diaphragms	5.14.4.2.3
4. Check design requirements	5.14.4.2.4

Source: From *AASHTO LRFD Bridge Design Specifications*, Copyright © 2012 by American Association of State Highway and Transportation Officials, Washington, DC. Used by permission.

5.5.1 Assumption for Service and Fatigue Limit States: Art. 5.7.1

The following assumptions may be used in the design of reinforced, prestressed, and partially prestressed concrete components for the compressive strength levels:

1. Prestressed concrete resists tensions at sections that are uncracked, except as specified in Art. 5.7.6.
2. The strains in the concrete vary linearly, except in components or regions of components for which conventional strength of materials is inappropriate.
3. The modular ratio, n, is rounded to the nearest integer number.
4. The modular ratio is calculated as follows:

$$E_s/E_c \text{ for reinforcing bars}$$

$$E_p/E_c \text{ for prestressing tendons}$$

5. An effective modular ratio of $2n$ is applicable to permanent loads and prestress.

5.5.2 Assumptions for Strength and Extreme-Event Limit States

5.5.2.1 General

The design of reinforced and prestressed concrete bridge members is based on the general principles of strength design embodied in the ACI code, with minor variations. In AASHTO LRFD Specifications, factored resistance of concrete components is based on the conditions of equilibrium and strain compatibility, and the resistance factors as specified in Art. 5.5.4.2. LRFD assumptions

www.EngineeringEBooksPdf.com

that form the basis of flexural design of concrete bridge members are stated in Art. 5.7.2; these are a set of unified assumptions in that they apply to both reinforced and prestressed concrete members. A summary of these assumptions follows:

1. If the concrete is unconfined, the maximum usable strain, ε_c, at the extreme concrete compression fiber is not greater than 0.003. If the concrete is confined, a maximum usable strain exceeding 0.003 in. the confined core may be utilized if verified. Calculation of the factored resistance shall consider that the concrete cover may be lost at strains compatible with those in the confined concrete core.
2. Balanced strain conditions exist at a cross section when tension reinforcement reaches the strain corresponding to its specified yield strength f_y just as the concrete in compression reaches its assumed ultimate strain of 0.003.
3. The tensile strength of the concrete is neglected.
4. The concrete compressive stress–strain distribution is assumed to be rectangular, parabolic, or any other shape that results in a prediction of strength in substantial agreement with the test results.

There are few other underlying assumptions related to the bond between the reinforcing steel (both nonprestressed and prestressed) and the surrounding concrete, which must be valid when designing concrete members. These are summarized as follows:

1. In components with fully bonded reinforcement or prestressing steel, or in the bonded length of locally debonded or shielded strands, strain is directly proportional to the distance from the neutral axis, except for deep members that shall satisfy the requirements of Art. 5.13.2 and for other disturbed regions.
2. In components with fully unbonded or partially unbonded prestressing tendons, that is, not locally debonded or shielded strands, the difference in strain between the tendons and the concrete section and the effect of deflections on tendon geometry are included in the determination of the stress in the tendons.
3. Except for the strut-and-tie model, the stress in the reinforcement is based on a stress–strain curve representative of the steel or on an approved mathematical representation, including the development of reinforcing and prestressing elements and transfer of pretensioning.
4. The development of reinforcing and prestressing elements and transfer of pretensioning are considered.

Resistance factor, ϕ, to be used when calculating flexural resistance of beam depends on the strain in tension steel. From this perspective, sections are classified as follows (known as compression-/balanced/tension-controlled sections):

1. Sections are called tension-controlled when the net tensile strain in the extreme tension steel is equal to or greater than 0.005 just as the concrete in compression reaches its assumed strain limit of 0.003.
2. Sections with net tensile strain in the extreme tension steel between the compression-controlled strain limit 0.005 constitute a transition region between compression-controlled and tension-controlled sections.
3. Sections are called compression-controlled when the net tensile strain in the extreme tension steel is equal to or less than the compression-controlled strain limit at the time the concrete in compression reaches its assumed strain limit of 0.003. The compression-controlled strain limit is the tensile strain in the reinforcement at balanced strain conditions. For Grade 60 reinforcement, and for all prestressed reinforcement, the compression-controlled strain limit may be set equal to 0.002.

www.EngineeringEBooksPdf.com

The use of compression reinforcement in conjunction with additional tension reinforcement is permitted to increase the strength of flexural members.

Flexural members are usually tension-controlled. At the onset of failure, these sections are characterized by ample warning with excessive deflection; cracking may be expected.

5.5.2.2 Rectangular Stress Distribution: Art. 5.7.2.2

The nominal flexural resistance of a beam is calculated based on the assumption of equivalent rectangular stress distribution as shown in Figure 5.23. It is assumed that the natural relationship between concrete stress and strain may be considered satisfied by an equivalent rectangular concrete compressive stress block of 0.85 f'_c over a zone bounded parallel to the neutral axis at the distance $a = \beta_1 c$ from the extreme compression fiber. This is an important relationship frequently used in flexural calculations to determine distance c and can be expressed as follows:

$$a = \beta_1 c \tag{5.16}$$

$$c = \frac{a}{\beta_1} \tag{5.17}$$

The distance c shall be measured perpendicular to the neutral axis.

The factor β_1 shall be taken as 0.85 for concrete strengths not exceeding 4.0 ksi. For concrete strengths exceeding 4.0 ksi, β_1 shall be reduced at a rate of 0.05 for each 1.0 ksi of strength in excess of 4.0 ksi, except that β_1 shall not be taken to be less than 0.65. This assumption can be expressed by Equation 5.18:

$$\beta_1 = 0.85 - \frac{f'_c - 4000}{1000}(0.05) \tag{5.18}$$

Equation 5.18 is subject to the following limitations:

1. For $f'_c \leq 4$ ksi, $\beta_1 = 0.85$
2. $(\beta_1)_{min} = 0.65$

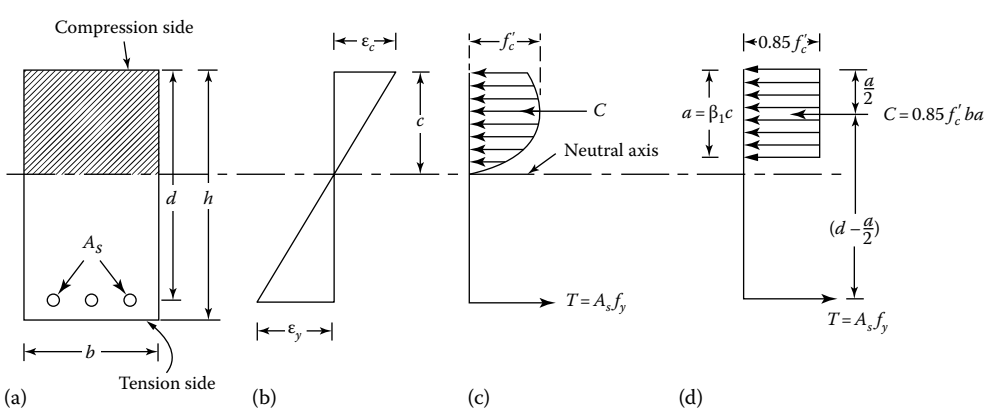

FIGURE 5.23 Rectangular stress distribution—strength design concept. (a) beam cross section, (b) strain distribution, (c) parabolic stress distribution in concrete, and (d) Whitney's equivalent rectangular stress distribution (used for design calculations).

www.EngineeringEBooksPdf.com

Art. 5.7.4.7 imposes limitations of the use of rectangular stress distribution for hollow rectangular concrete compression members having a wall slenderness ratio of ≥15, except as specified in Art. 5.7.4.7.2c. For hollow sections where wall slenderness ratio is less than 15, the rectangular stress block method may be used based on a compressive strain of 0.003. This provision is not applicable to flexural members and not discussed further.

5.5.3 Flexural Members

5.5.3.1 General

A concrete member subjected to flexure must be provided with tension reinforcement because of its inherent weakness in tension. Tension reinforcement is provided as close as possible to the bottom of a flexural member in positive flexure. Reinforcing materials can be used in several forms at designer's discretion:

1. Ordinary reinforcing bars (steel or composite) in reinforced concrete members
2. Reinforcing bars near both tension and compression faces of a member
3. Prestressing steel in prestressed concrete members
4. A combination of prestressing steel and reinforcing bars in prestressed concrete members

Flexural resistance of reinforced concrete members provided by reinforcement is determined from the principles of equilibrium of forces in concrete and steel and compatibility of strains in concrete and steel based on Whitney's equivalent rectangular stress distribution shown in Figure 5.23d and the assumptions discussed in Section 5.5.2.1.

5.5.3.2 Nominal Flexural Resistance of Concrete Members with Nonprestressed Reinforcement

The basis of the strength design approach is the assumed equivalent rectangular stress distribution in the cross section of a beam at nominal strength, originally proposed for reinforced concrete in the 1930s by Charles Whitney, which has been found to be simple and convenient for design calculations. According to this assumed stress distribution in concrete, the average stress in the compression zone of the beam is assumed to have a constant value of $0.85 f_c'$ over its entire depth a measured from the extreme compression fibers. This stress block is referred to as the *equivalent* rectangular stress block, the qualifier *equivalent* being used to imply that the value of the magnitude of the compression stress resultant C remains the same as that in the parabolic stress block (Figure 5.23c) and that the neutral axis is located at the same distance c from the extreme compression fibers. The relationship between the depth of the equivalent compression block, a, and the depth of neutral axis, c, both measured from the extreme compression fibers, is defined by Equation 5.16.

Because the compression stress block is *rectangular*, its centroid is located at $a/2$ from extreme compression fibers of the beam, which is where the compression stress resultant C acts. The nominal strength (moment capacity) of the beam, M_n, can be obtained from the principles of static equilibrium. The value of the compression stress resultant C can be expressed as

$$C = (\text{stress in concrete at nominal strength}) \times (\text{area of concrete in the compression zone})$$

$$C = 0.85 f_c' ab \tag{5.19}$$

where b = width of rectangular cross section.

www.EngineeringEBooksPdf.com

Assuming that reinforcement yields when the strain in concrete reaches a value of 0.003, so that stress in steel reinforcement equals the yield stress (i.e., $f_s = f_y$), the value of the tensile stress resultant, T, can be expressed as

$$T = A_s f_y \tag{5.20}$$

The line of action of the tensile stress resultant is assumed to be located at the centroid of the steel reinforcing bars. When all reinforcing bars are placed in one row, their centroid is obviously located at the same level as the centroid of bars and in the vertical plane of symmetry of the beam cross section. However, when the bars are placed in more than one row, the centroid of the bar group must be located from the principles of statics.

Equating $C = T$ from Equations 5.19 and 5.20, respectively, yields

$$0.85 f_c' ab = A_s f_y \tag{5.21}$$

The depth a of the equivalent compression block of concrete is obtained from Equation 5.21, which can be expressed as follows:

$$a = \frac{A_s f_y}{0.85 f_c' b} \tag{5.22}$$

Equation 5.22 represents one of the most frequently used relationships between various design parameters for flexural calculations.

The nominal strength of the beam, M_n, equals the moment provided by the C–T couple. Its magnitude can be determined by taking moments about the line of action of the compressive stress resultant C about the line of action of T. Thus,

$$M_n = C\left(d - \frac{a}{2}\right) \tag{5.23}$$

Substitution for C from Equation 5.19 in the aforementioned equation yields

$$M_n = 0.85 f_c' ab\left(d - \frac{a}{2}\right) \tag{5.24}$$

Alternatively, taking moment of T about the line of action of C and substituting $T = A_s f_y$ from Equation 5.20, the nominal strength can be expressed as Equations 5.25 and 5.26:

$$M_n = T\left(d - \frac{a}{2}\right) \tag{5.25}$$

$$M_n = A_s f_y\left(d - \frac{a}{2}\right) \tag{5.26}$$

www.EngineeringEBooksPdf.com

Multiplying both sides of Equation 4.12 by the strength reduction factor, ϕ, one obtains Equation 5.27:

$$\phi M_n = \phi A_s f_y \left(d - \frac{a}{2} \right) \tag{5.27}$$

Equations 5.24 and 5.26 are based on the principles of statics and are used to determine the nominal strength of reinforced concrete beams of rectangular cross sections. In practical beams, the amount of reinforcing steel is so limited (intentionally) that it yields before the onset of concrete strain of 0.003. Therefore, Equation 5.26, along with Equation 5.22, is used as the basic equation for determining the flexural strength of rectangular beams.

Equation 5.27 is based on the premise that the steel reinforcement has yielded, the validity of which must be checked. The value of strain in steel is also used as the basis for determining the value of resistance factor, ϕ, in order to determine if the section is tension-controlled, compression-controlled, or transition as discussed earlier. This is done by considering the compatibility of strains from the strain distribution diagram at the nominal resistance (Figure 5.23b). For a member of effective depth d, and having neutral axis located at a distance c from the extreme compression fibers, we have (from similar triangles)

$$\frac{\varepsilon_s}{\varepsilon_c} = \frac{d-c}{c} \tag{5.28}$$

The strain in reinforcement, ε_s, is obtained from Equation 5.28 and expressed Equation 5.29:

$$\varepsilon_s = \left(\frac{d-c}{c} \right) \varepsilon_c \tag{5.29}$$

where

ε_c = maximum usable compressive strain in concrete = 0.003
ε_s = strain in steel reinforcement corresponding to ε_c
c = distance of neutral axis from the extreme compression fibers as determined from Equation 5.17

5.5.3.3 Nominal Flexural Resistance of Prestressed Concrete Members

5.5.3.3.1 Stress in Prestressing Steel at Nominal Flexural Resistance

Prestressing steel in beams is provided in the form of tendons. In a beam, the tendons can be bonded, unbonded, or both.

5.5.3.3.1.1 Components with Bonded Tendons For rectangular or flanged sections subjected to flexure about one axis where the approximate stress distribution specified in Art. 5.7.2.2 is used and for which the effective prestressing stress, f_{pe}, is not less than $0.5f_{pu}$, the average stress in prestressing steel, f_{ps}, may be taken as given by Equation 5.30:

$$f_{ps} = f_{pu} \left(1 - k \frac{c}{d_p} \right) \tag{5.30} \text{ [A5.7.3.1.1-1]}$$

www.EngineeringEBooksPdf.com

in which the value of coefficient, k, is given by Equation 5.31:

$$k = 2\left(1.04 - \frac{f_{py}}{f_{pu}}\right) \tag{5.31} \text{ [A5.7.3.1.1-2]}$$

The nominal flexural resistance of a prestressed beam can be determined in the same manner as for the concrete sections with nonprestressed reinforcement.

For T-section behavior, the depth of neutral axis at a distance c from the extreme compression fibers can be determined from Equation 5.32:

$$c = \frac{A_{ps} f_{pu} + A_s f_s - A_s' f_s' - 0.85 f_c'(b - b_w) h_f}{0.85 f_c' \beta_1 b_w + k A_{ps} \dfrac{f_{pu}}{d_p}} \tag{5.32} \text{ [A5.7.3.1.1-3]}$$

Similarly, for rectangular section behavior, c can be determined from Equation 5.32 by simply substituting $b = b_w$, resulting in Equation 5.33

$$c = \frac{A_{ps} f_{pu} + A_s f_s - A_s' f_s'}{0.85 f_c' \beta_1 b + k A_{ps} \dfrac{f_{pu}}{d_p}} \tag{5.33} \text{ [A5.7.3.1.1-4]}$$

where

A_{ps} = area of prestressing steel (in.^{2})
f_{pu} = specified tensile strength of prestressing steel (ksi)
f_{ps} = average stress in prestressing steel at the time for which the nominal resistance is required (ksi)
f_{py} = yield strength of prestressing steel (ksi)
A_s = area of mild steel tension reinforcement (in.^{2})
A_s' = area of compression reinforcement (in.^{2})
f_s = stress in the mild steel tension reinforcement at nominal flexural resistance (ksi), as specified in Art. 5.7.2.1
f_s' = stress in the mild steel compression reinforcement at nominal flexural resistance (ksi), as specified in Art. 5.7.2.1
b = width of the compression face of the member; for a flange section in compression, the effective width of the flange as specified in Art. 4.6.2.6 (in.)
b_w = width of web (in.)
h_f = depth of compression flange (in.)
d_p = distance from the extreme compression fiber to the centroid of the prestressing tendons (in.)
c = distance between the neutral axis and the compressive face (in.)
β_1 = stress block factor specified in Art. 5.7.2.2

Equations 5.32 and 5.33 and those for flexural resistance in subsequent section (using these equations) are based on the assumption that the distribution of steel is such that it is reasonable to consider all of the tensile reinforcement to be lumped at the location defined by a distance d_p. In cases where a significant number of prestressing elements (e.g., strands) are placed on the compression side of the neutral axis, analysis method based on the conditions of equilibrium and strain compatibility discussed in Section 5.5.2.1 should be used.

www.EngineeringEBooksPdf.com

TABLE 5.9
Values of *k* in Equation 5.32

Type of Tendon	f_{py}/f_{pu}	Value of *k*
Low-relaxation strand	0.90	0.28
Stress-relieved strand and Type 1 high-strength bar	0.85	0.38
Type 2 high-strength bar	0.80	0.48

Source: From *AASHTO LRFD Bridge Design Specifications*, Copyright © 2012 by American Association of State Highway and Transportation Officials, Washington, DC. Used by permission; Table C5.7.3.3.3-1.

Values of f_{py}/f_{pu} appearing in Equation 5.31 are defined in Table 5.9. Therefore, the value of coefficient, k, in Equation 5.31 depends only on the type of tendon and its f_{py}/f_{pu} ratio shown in Table 5.9.

In the approximate flexural resistance equations of Arts. 5.7.3.1 and 5.7.3.2, f_y and f'_y may replace f_s and f'_s, respectively, subject to the following conditions:

1. f_y may replace f_s when, using f_y in the calculation as long as the resulting c/d ratio does not exceed 0.6. If c/d_s exceeds 0.6, strain compatibility shall be used to determine the stress in the mild steel tension reinforcement.
2. f'_y may replace f'_s when, using f'_y in the calculation, $c \geq 3d'_s$. If $c < 3d'_s$, strain compatibility shall be used to determine the stress in the mild steel compression reinforcement. The compression reinforcement shall be conservatively ignored, that is, $A'_s = 0$.

Additional limitations on the maximum usable extreme compressive strain in hollow rectangular concrete compressive strain in hollow rectangular compression members shall be investigated as specified in Art. 5.7.4.7.

5.5.3.3.1.2 Components with Unbonded Tendons For rectangular or flanged sections subjected to flexure about one axis and for biaxial flexure with axial load as specified in Art. 5.7.4.5, where the approximate stress distribution specified in Art. 5.7.2.2 is used, the average stress in unbonded prestressing steel, f_{ps}, may be taken as given by Equation 5.34:

$$f_{ps} = f_{pe} + 900\left(\frac{d_p - c}{\sim_e}\right) \leq f_{py} \qquad (5.34)\ [A5.7.3.1.2\text{-}1]$$

in which

$$\sim_e = \frac{2\sim_i}{2 + N_s} \qquad (5.35)\ [A5.7.3.1.2\text{-}2]$$

Since the value of c in Equation 5.34 is yet unknown, the first estimate of f_{ps} may be obtained from Equation 5.36:

$$f_{ps} = f_{pe} + 15\ \text{(ksi)} \qquad (5.36)\ [AC5.7.3.1.2\text{-}1]$$

The value of distance c in Equation 5.34 (LRFD Equation A5.7.3.1.2-1) is determined as follows.

For T-section behavior,

$$c = \frac{A_{ps} f_{ps} + A_s f_s - A'_s f'_s - 0.85 f'_c (b - b_w) h_f}{0.85 f'_c \beta_1 b_w} \qquad (5.37)\ [A5.7.3.1.2\text{-}3]$$

www.EngineeringEBooksPdf.com

For rectangular section behavior,

$$c = \frac{A_{ps} f_{ps} + A_s f_s - A'_s f'_s}{0.85 f'_c \beta_1 b} \quad \text{(5.38a) [A5.7.3.1.2-4]}$$

For prestressed concrete members without nonprestressed tension and compression reinforcement, quantities A_s and A'_s are both equal to zero, so that Equation 5.38a takes the following form:

$$c = \frac{A_{ps} f_{ps}}{0.85 f'_c \beta_1 b} \quad \text{(5.38b)}$$

In the aforementioned equations,

c = distance from the extreme compression fiber to the neutral axis assuming the tendon prestressing steel has yielded, given by Equations 5.37 and 5.38a for T-section behavior and rectangular section behavior, respectively (in.)

$\tilde{}_e$ = effective tendon length (in.)

$\tilde{}_i$ = length of tendon between anchorages (in.)

N_s = number of support hinges crossed by the tendon between anchorages or discretely bonded points

f_{py} = yield strength of prestressing steel (ksi)

f_{pe} = effective stress in prestressing steel at section under consideration after all losses (ksi)

5.5.3.4 Flexural Resistance: Art. 5.7.3.2

5.5.3.4.1 Factored Flexural Resistance

The factored resistance, M_r, is given as follows:

$$M_r = \phi M_n \quad \text{(5.39) [A5.7.3.2.1-1]}$$

where

M_n = nominal resistance (kip-in.)

ϕ = resistance factor as specified in Table 5.7 (Art. 5.5.4.2.5)

5.5.3.4.2 Flanged Sections

For flanged sections subjected to flexure about one axis and for biaxial flexure with axial load as specified in Art. 5.7.4.5, where the approximate stress distribution specified in Art. 5.7.2.2 is used and where compression flange depth is less than $a = \beta_1 c$, as determined in accordance with Equations 5.32, 5.33, 5.37, and 5.38a (LRFD Equation 5.7.3.1.1-3, 5.7.3.1.1-4, 5.7.3.1.2.3, and 5.7.3.1.2-4, respectively), the nominal flexural resistance may be determined from Equation 5.40:

$$M_n = A_{ps} f_{ps}\left(d_p - \frac{a}{2}\right) + A_s f_s\left(d_s - \frac{a}{2}\right) - A'_s f'_s\left(d'_s - \frac{a}{2}\right)$$
$$+ 0.85 f'_c (b - b_w) h_f \left(\frac{a}{2} - \frac{h_f}{2}\right) \quad \text{(5.40a) [A5.7.3.2.2-1]}$$

www.EngineeringEBooksPdf.com

For rectangular prestressed concrete flexural members without precompressed tensile and compression reinforcement, Equation 5.40a becomes

$$M_n = A_{ps} f_{ps} \left(d_p - \frac{a}{2} \right) \tag{5.40b}$$

where

A_{ps} = area of prestressing steel (in.^{2})
f_{ps} = average stress in prestressing steel at nominal bending resistance specified in Equation 5.7.3.1.1-1 (ksi)
d_p = distance from the extreme compression fiber to the centroid of prestressing tendons (in.)
A_s = area of nonprestressed tension reinforcement (in.^{2})
f_s = stress in the mild steel tension reinforcement at nominal flexural resistance (ksi), as specified in Art. 5.7.2.1
d_s = distance from the extreme compression fiber to the centroid of nonprestressed tensile reinforcement (in.)
A'_s = area of compression reinforcement (in.^{2})
f'_s = stress in the mild steel compression reinforcement at nominal flexural resistance (ksi), as specified in Art. 5.7.2.1
d'_s = distance from the extreme compression fiber to the centroid of compression reinforcement (in.)
f'_c = specified compressive strength of concrete at 28 days, unless another age is specified (ksi)
b = width of the compression face of the member; for a flange section in compression, the effective width of the flange as specified in Art. 4.6.2.6 (in.)
b_w = web width of diameter of a circular section (in.)
β_1 = stress block factor specified in Art. 5.7.2.2
h_f = compression flange depth of an I- or T-shaped member (in.)
$a = c\beta_1$, depth of the equivalent stress block (in.)

5.6 LIMITS OF REINFORCEMENT: ART. 5.7.3.3

5.6.1 Provisions for Maximum Reinforcement

The current LRFD specifications (AASHTO 2012) do not specify any provisions for maximum reinforcement in a section; those from 2005 and previous editions of the specifications have been eliminated.

The current edition (AASHTO 2012) gives unified provisions for the design of both nonprestressed and prestressed tension- and compression-controlled concrete members. The higher the percentage of reinforcing steel in a member, the lesser would be the strain in it (and consequently less ductile). As discussed earlier, below a steel strain of 0.005 (smallest value to qualify as a tension-controlled member and have the largest value of resistance factor), the value of resistance factor decreases linearly from 1.0 for members with prestressed steel and 0.9 for members with nonprestressed steel to 0.75 (for both) when the strain reaches 0.002; at this point, the section becomes compression-controlled. The decreasing values of resistance factor compensate for reduced ductility. A lower value of reduced resistance factor results in lower flexural resistance. Only the addition of compression reinforcement in conjunction with additional tension reinforcement can result in increased factored flexural resistance of the section.

www.EngineeringEBooksPdf.com

5.6.2 Provisions for Minimum Reinforcement: Art. 5.7.3.3.2

Provisions for minimum reinforcement are intended to reduce the probability of brittle failure by providing flexural strength greater than the cracking moment. These provisions require that the amount of prestressed and nonprestressed tensile reinforcement shall be adequate to develop a factored flexural resistance, M_r, equal to the lesser of the following two values:

1. 1.33 times the factored moment required by the applicable strength load combination specified in LRFD Table 3.4.1-1 (discussed in Chapter 3)
2. The cracking moment, M_r, given by Equation 5.41

$$M_{cr} = \gamma_3 \left[\left(\gamma_1 f_r + \gamma_2 f_{cpe} \right) S_c - M_{dnc} \left(\frac{S_c}{S_{nc}} - 1 \right) \right] \quad (5.41)\ [A5.7.3.3.2\text{-}1]$$

where

f_r = modulus of rupture specified in Art. 5.4.2.6

f_{cpe} = compressive stress in concrete due to effective prestress forces only (allowance for all prestress losses) at the extreme fiber of the section where tensile stress is caused by externally applied loads (ksi)

= 0 for sections with nonprestressed reinforcement only

M_{dnc} = total unfactored dead load moment acting on the monolithic or noncomposite section where tensile stress is caused by externally applied loads (ksi)

S_c = section modulus for the extreme fiber of the composite section where tensile stress is caused by externally applied loads (in.^{3})

= S_{nc} where beams are designed for the monolithic or noncomposite section to resist all loads

S_{nc} = section modulus for the extreme fiber of the monolithic or noncomposite section where tensile tress is caused by externally applied loads (in.^{3})

γ_1 = flexural cracking variability factor

$\gamma 2$ = prestress variability factor

γ_3 = ratio of specified minimum yield strength to ultimate tensile strength of the reinforcement

The values of γ-factors in Equation 5.41 are shown in Table 5.10.

Where the beams are designed for the monolithic (e.g., a T-beam) or noncomposite section to resist all loads, S_{nc} shall be substituted for S_c in Equation 5.41 to calculate M_{cr}. For this case, Equation 5.41 reduces to

$$M_{cr} = \gamma_3 \left[\left(\gamma_1 f_r + \gamma_2 f_{cpe} \right) S_c \right] \quad (5.42)$$

TABLE 5.10
Modification Factors for Cracking Moment, M_{cr} (Equations 5.41 and 5.42)

Modification Factors, γ	Applicable Structure or Component	Value of Modification Factor
Flexural cracking variability factor, γ_1	Precast segmental structures	1.2
	For all other structures	1.6
Prestress variability factor, γ_2	Bonded tendons	1.1
	Unbonded tendons	1.0
γ_3	A615, Grade 60 reinforcement	0.67
	A706, Grade 60 reinforcement	0.75
	Prestressed concrete structures	1.0

Source: Adapted from *AASHTO LRFD Bridge Design Specifications*, Copyright © 2012 by American Association of State Highway and Transportation Officials, Washington, DC. Used by permission.

www.EngineeringEBooksPdf.com

For beams with nonprestressed reinforcement, $f_{cpe} = 0$, so Equation 5.42 reduced to

$$M_{cr} = \gamma_3 \gamma_1 f_r S_c \tag{5.43}$$

Values of the modulus of rupture, f_r, are specified in LRFD Art. 5.4.2.6 (as discussed earlier).

For nonprestressed structures, $\gamma_1 = 1.6$ and $\gamma_3 = 0.75$ for A706 Grade 60 reinforcement. Substitution of these values in Equation 5.43 results in Equation 5.44:

$$M_{cr} = 1.2 f_r S_s \tag{5.44}$$

5.7 CONTROL OF CRACKING BY DISTRIBUTION OF REINFORCEMENT: ART. 5.7.3.4

Cracking is inherent material property of concrete. All concrete members exhibit cracking, under any load conditions, including temperature effects and restraint of deformations, which produce tension in the gross section in excess of the tensile strength of concrete. From appearance standpoint, finer cracks are preferable to wider ones. Experience has shown improved crack control when the steel reinforcement is well distributed over the zone of maximum tension, for example, bottom of simply supported beams and at supports of continuous beams. When selecting reinforcement for tension in a concrete beam, a designer has the option of selecting a smaller number of larger diameter bars or a larger number of smaller diameter bars. Several bars of smaller diameter have been found to be more effective than a few bars of larger diameter for control of cracking. Consider, for example, two No. 11 bars (A_s = 3.12 in.^{2}) versus four No. 8 bars (A_s = 3.14 in.^{2}), the latter is preferable for control of cracking as long as the mandatory spacing requirements of Art. 5.10.3.1 (minimum spacing of reinforcing bars) and 5.10.3.2 (maximum spacing of reinforcing bars) are complied with. Steps should be taken in detailing the reinforcement to control cracking.

The provisions specified in Art. 5.7.3.4 apply to reinforcement of all concrete beams, with the exception of deck slabs designed conforming to Art. 9.7.2 (using empirical method) in which the tension in the cross section exceeds 80 percent of the modulus of rupture at applicable service limit load combination.

For control of cracking, the spacing of reinforcement closest to the tension face shall satisfy Equation 5.45:

$$s \le \frac{700\gamma_e}{\beta_s f_{ss}} - 2d_c \tag{5.45} \text{ [A5.7.3.4-1]}$$

where

$$\beta_s = 1 + \frac{d_c}{0.7(h - d_c)} \tag{5.46}$$

γ_e = exposure factor
= 1.00 for Class 1 exposure
= 0.75 for Class 2 exposure
d_c = thickness of concrete cover measured from the extreme fiber to the center of the flexural reinforcement located closest thereto
f_{ss} = tensile stress in steel reinforcement at the service limit state (ksi)
h = overall thickness or depth of the component (in.)

www.EngineeringEBooksPdf.com

There are specific provisions for flanges of reinforced concrete T-girders and box girders when they are in tension at the service limit state. In such cases, flexural reinforcement is required to be distributed over the lesser of the following:

1. The effective flange width
2. A width equal to 1/10 of the average of adjacent span between bearings

In some cases, the effective flange width may exceed 1/10 of the span. In such cases, additional longitudinal reinforcement, with area not less than 0.4 percent of the excess slab area, shall be provided in the outer portions of the flange.

Skin reinforcement is required for members that are deep. If the distance between the extreme compression fiber and the centroid of extreme tension steel element, d_ℓ, of nonprestressed or partially prestressed concrete members exceeds 3 ft, longitudinal *skin reinforcement* is required to be uniformly distributed along both faces of the component for a distance of $d_\ell/2$ nearest the flexural tension reinforcement. The area of skin reinforcement, A_{sk}, in in.^{2}/ft of height on each side of the face shall satisfy Equation 5.47:

$$A_{sk} \geq 0.012\ (d_\sim - 30) \leq \frac{A_s + A_{ps}}{4} \qquad (5.47)\ [A5.7.3.4\text{-}2]$$

where

A_s = area of tensile reinforcement (in.^{2})
A_{ps} = area of prestressing steel (in.^{2})

Equation 5.47 suggests that the total area of longitudinal skin reinforcement (per face) need not exceed one-fourth of the required flexural tensile reinforcement, $A_s + A_{ps}$.

The maximum spacing of skin reinforcement is limited to the lesser of $d_e/6$ or 12 in.

5.8 SERVICE LIMIT STATE

5.8.1 Service Load Analysis of Reinforced Concrete Sections

Concrete sections crack at service loads. Therefore, *cracked section analysis* is required to determine the location of neutral axis and moment of inertia of the cracked section.

The neutral axis of a cracked concrete section is determined using the concept of transformed section in which the area of concrete below the neutral axis (which is assumed cracked) is ignored and the area of tension reinforcement is substituted by the equivalent area of concrete, nA_s, (= modular ratio times the area of tension reinforcement) as shown in Figure 5.24. The stress distribution in compression area of concrete is assumed linear.

Taking moments about the neutral axis of the concrete area located above the neutral axis and the transformed area of tension steel located below the neutral axis, the resulting expressions is Equation 5.48:

$$\frac{1}{2}(b)(kd)^2 = nA_s(d - kd) \qquad (5.48)$$

In Equation 5.48, substitute $\rho = A_s/bd$ so that $A_s = \rho bd$, where ρ is the percentage of steel expressed as the ratio of tension reinforcement to cross-sectional area, bd. With these substitutions, Equation 5.48 can be simplified and expressed as a quadratic in k given by Equation 5.49:

$$k^2 = 2kn\rho d^2 - 2n\rho d^2 = 0 \qquad (5.49)$$

www.EngineeringEBooksPdf.com

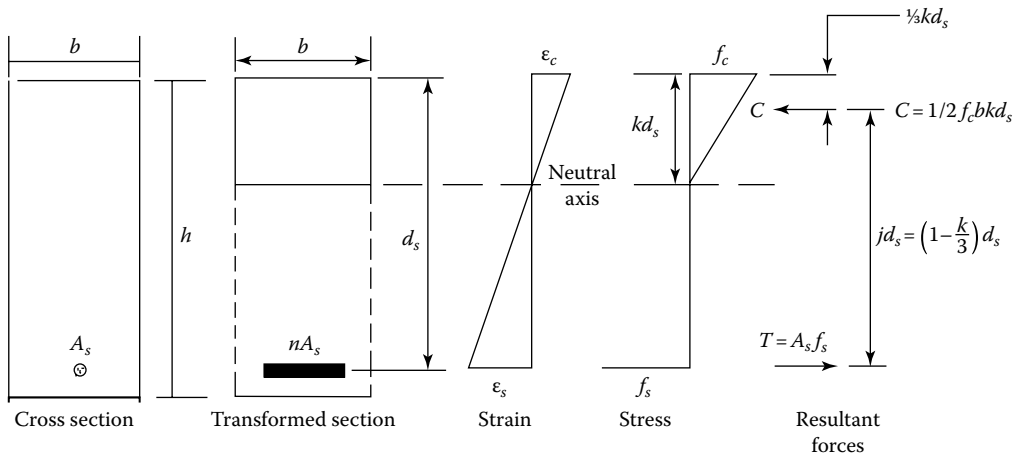

FIGURE 5.24 Service load analysis of a cracked reinforced concrete section.

The solution of Equation 5.49 is given by Equation 5.50:

$$k = \sqrt{(n\rho)^2 + 2n\rho} - n\rho \tag{5.50}$$

Once k (sometimes called the neutral axis factor) is determined, the neutral axis is located at a distance of kd from the extreme compression fibers. The flexural resistance of the section at service load can be determined from the C–T couple as shown in Figure 5.24.

$$\text{Compression resultant, } C = 1/2 f_c bkd$$

$$\text{Tension force resultant, } T = A_s f_s$$

where
f_c = stress in concrete at service load
f_s = stress in steel at service load

Denoting the perpendicular distance between the C and T resultants $= d - kd/3 = d(1 - k/3) = jd$, the flexural resistance of the section at service loads can be expressed by moment due to C–T couple:

$$M = Cjd = 1/2 f_c bkjd^2 \tag{5.51}$$

Alternatively,

$$M = Tjd = A_s f_s jd \tag{5.52}$$

The stress in concrete, f_c, and steel, f_s, at service load can be computed from Equations 5.51 and 5.52 by rewriting them in the following forms, respectively:

$$f_c = \frac{2M_s}{bkjd^2} \tag{5.53}$$

$$f_s = \frac{M_s}{A_s jd} \tag{5.54}$$

www.EngineeringEBooksPdf.com

Analysis of a reinforced concrete section is facilitated by using tables. For a set of given section properties (i.e., b, d, A_s, and the modular ratio, n), Equation 5.50 is easily solved from Table 5.A.4. Tables 5.A.1 through 5.A.3 provide other required information for nonprestressed steel reinforcement. The use of these tables is demonstrated later in several examples.

5.8.2 Deformations: Art. 5.7.3.6

5.8.2.1 General Requirements

General provision governing permitted deformations (deflections) specified in Art. 2.5.2.6 is discussed in Chapter 2. Deck joints and bearings should be designed to accommodate the dimensional changes caused by loads, creep, shrinkage, thermal changes, settlements, and prestressing.

5.8.3 Deflection and Camber

Deflections of slabs and beams/girders can be calculated using conventional deflection formulas given in texts on mechanics of materials, structural analysis, or in handbooks such as *Steel Construction Manual* (AISC 2011). However, because the concrete flexural members are assumed cracked at service loads, the moment of inertia to be used for computing instantaneous deflection should be either the effective moment of inertia, I_e, or the gross moment of inertia, I_g, as determined from Equation 5.55:

$$I_e = \left(\frac{M_{cr}}{M_a}\right)^3 I_g + \left[1 - \left(\frac{M_{cr}}{M_a}\right)^3\right] I_{cr} \le I_g \qquad (5.55)\ [A5.7.3.6.2\text{-}1]$$

in which

$$M_{cr} = f_r\left(\frac{I_g}{y_t}\right) \qquad (5.56a)\ [A5.7.3.6.2\text{-}2]$$

where y_t = distance from the extreme tension fiber to the neutral axis

Creep of concrete was described earlier in Section 5.4.1.4. Long-term deflections of concrete members are influenced by creep (deflection under dead load increases over time). This must be properly accounted for in design by estimating deflection due to creep and make required provisions for camber. Unless a more exact determination is made, Art. 5.7.3.6.2 permits determination of long-term deflection equal to the instantaneous deflection as discussed in Section 4.18.5.3 (Chapter 4). Art. 5.7.3.6.2 specifies that long-term deflections can be calculated by multiplying the instantaneous deflections by the following factors as appropriate:

1. If the instantaneous deflection is based on the gross moment inertia, I_g, use a multiplier of 4.0.
2. If the instantaneous deflection is based on the effective moment of inertia I_e (Equation 5.55), use a multiplier of $3.0 - 1.2\left(A_s'/A_s\right) \ge 1.6$.

where

A_s' = area of compression reinforcement

A_s = area of nonprestressed tension reinforcement

www.EngineeringEBooksPdf.com

Camber needs to be calculated for concrete girders, both with nonprestressed and with prestressed reinforcement. Both instantaneous and long-term deflections need to be calculated for these girders as discussed earlier.

In girders with nonprestressed steel, it is common practice to provide intentional camber equal to the long-term deflection so as to avoid the appearance of sagging structure, which might create a perception of impending failure, and for improved aesthetics.

Calculation of long-term deflections of prestressed concrete girder is rather cumbersome. Methods of and examples on calculating long-term, time-dependent deflections can be found in the literature (Martin 1997, PCI 2003, Nawy 2010). Calculations for deflection of reinforced concrete flexural members are presented in Examples 5.1 and 5.2. Calculations for camber and deflection of precast, prestressed concrete girders are illustrated in Example 5.5.

Live load deflections can be calculated using conventional formulas found in texts on structural mechanics. Computed live load deflections should conform to the live load deflection limits specified in Art. 2.5.2.6 (see discussion on methods of calculating live deflections in Section 2.6.6).

5.9 FATIGUE LIMIT STATE

5.9.1 General

The phenomenon fatigue was introduced in Chapter 1; fatigue loading was discussed in Chapter 3. Provisions related to limit state design of reinforced and prestressed concrete members are specified in Art. 5.5. These provisions address fatigue concerns for design of concrete flexural members as follows:

1. *Concrete deck slabs in multigirder bridges and box culverts*: Fatigue need not be investigated in these members/structures. This exemption is based on the fact that measured stresses in in-service deck slabs of bridges have been found to be far below infinite fatigue life.
2. *Regions of compressive stress due to permanent loads and prestress in reinforced concrete members*: Fatigue needs to be considered only if this compressive stress is less than the maximum tensile live load stress resulting from the Fatigue I Load Combination (refer to LRFD Table 3.4.1-1 for details of this load combination, discussed in Chapter 3). In simply supported nonprestressed concrete slab bridges, there are no compressive stresses in the bottom of slab under typical permanent load conditions; therefore, fatigue must always be considered in such bridges (see Example 6.1 for details of these calculations).

   The live load to be considered for fatigue consists of a single truck (called fatigue truck) as discussed in Chapter 3. It consists of an HL-93 design truck with the two 32-kip axles spaced at a fixed distance of 30 ft (instead of variable spacing of 14–30 ft considered for structural design); design lane load is not to be considered for fatigue loading. LRFD Table 3.4.1-1 specifies a load factor of 1.5 on the live load force effect resulting from the fatigue truck for Fatigue I Load Combination because this factored force effect represents the greatest stress that the bridge will experience during its life (Art. C5.5.3.1).
3. *Fully prestressed concrete members*: Fatigue of reinforcement need not be checked for these components when designed to have extreme fiber tensile stress due to Service III Limit State within the tensile stress limit specified in LRFD Table 5.9.4.2.2-1.

www.EngineeringEBooksPdf.com

5.9.2 Stress Limits for Stresses due to Fatigue

If the aforementioned conditions are not met, fatigue must be considered, in which case the force effect due to live load force effect (stress range due to the passage of the fatigue truck) must be limited as given by Equation 5.56a:

$$\gamma(\Delta f) \leq (\Delta F)_{TH} \qquad (5.56b)\ [A5.5.3.1\text{-}1]$$

where

γ = load factor as specified in LRFD Table 3.4.1-1 for Fatigue I Load Combination
Δf = force effect, live load stress due to fatigue truck
$(\Delta F)_{TH}$ = constant-amplitude fatigue threshold as specified in Arts. 5.5.3.2, 5.5.3.3, and 5.5.3.4

Arts. 5.5.3.2, 5.5.3.3, and 5.5.3.4 specify the limiting values of the constant-amplitude fatigue threshold for different concrete components as follows.

5.9.2.1 Reinforcing Bars

For straight reinforcement and welded wire reinforcement without a cross weld in the high-stress regions, the limiting value of the constant-amplitude fatigue threshold, $(\Delta F)_{TH}$, is given by Equation 5.56c:

$$(\Delta F)_{TH} = 24 - 0.33 f_{min} \qquad (5.56c)\ [A5.5.3.2\text{-}1]$$

For straight, welded wire reinforcement with a cross weld in the high-stress region, the limiting value of the constant-amplitude fatigue threshold, $(\Delta F)_{TH}$, is given by Equation 5.56d:

$$(\Delta F)_{TH} = 16 - 0.33 f_{min} \qquad (5.56d)\ [A5.5.3.2\text{-}2]$$

where f_{min} = minimum live load stress resulting from the Fatigue I Load Combination, combined with the more severe stress resulting from either the permanent loads or the permanent loads, shrinkage, and creep-induced external loads (positive if tension, negative if compression).

The high-stress regions referred to earlier are to be taken as one-third of the span on each side of the section of maximum moment.

5.9.2.2 Prestressing Tendons

The limiting value of the constant-amplitude fatigue threshold for prestressing tendons, $(\Delta F)_{TH}$, depends on their radii of curvature at harping points and in ducts of posttensioned members. The specified threshold values are as follows:

1. Radii of curvature 12 ft or less: $(\Delta F)_{TH}$ = 10.0 ksi.
2. Radii of curvature >30 ft: $(\Delta F)_{TH}$ = 18.0 ksi.
3. Linear interpolation may be used for radii between 12 and 30 ft.

5.9.2.3 Welded or Mechanical Splices

The limiting value of the constant-amplitude fatigue threshold for welded or mechanical splices, $(\Delta F)_{TH}$, depends on the number of stress range cycles they are expected to undergo during their service life. The value of $(\Delta F)_{TH}$ for greater than one million cycles is listed in LRFD Table 5.5.3.4-1.

www.EngineeringEBooksPdf.com

For smaller number of stress range cycles, the tabulated values of $(\Delta F)_{TH}$ may be increased by the quantity 24 (6 – log N), where N is the total number of cycles of loading. Readers are urged to refer to Art. C5.5.3.4 for more details on this topic.

5.10 SHEAR

5.10.1 General

Behavior of flexural members under shear is one of the least understood phenomena. Design procedures for shear have evolved over time and still continue to evolve as new research information becomes available.

Design procedures for computing the shear strength of concrete flexural members and designing them for the required shear resistance (or the shear demand) are specified in Art. 5.8.1. It recognizes two analytical models for shear design of flexural members for shear:

1. Section design model
2. Strut-and-tie model

Art. C5.8.1.1 clarifies the appropriateness of using the sectional model stating its suitability for design of typical bridge girders, slabs, and other regions of components where the assumptions of traditional engineering beam theory are valid. The details of this model are specified in Art. 5.8.3.

The sectional model is appropriate for the design of typical bridge girders, slabs, and other regions of components where traditional engineering beam theory is valid. Such analysis is based on well-established principles found in texts of mechanics of materials. This theory is based on the assumption that the response at a section under consideration depends only on the calculated values of the sectional force effects rather than *how* the specific force effects were introduced in the member. The sectional model is appropriate for typical straight or nearly straight, prismatic flexural members that do not have any discontinuities in the member cross section. Strut-and-tie model, on the other hand, is more appropriate for structural members that have regions of discontinuities (e.g., reentrant corners) where *actual flow* of forces should be considered in more detail. This is because the response of regions adjacent to abrupt changes in cross section, draped ends, deep beams, and corbels is affected significantly by the details of how the loads are introduced in the region and how the region is supported. The strut-and-tie model, although known since the early 1900s (Ritter 1899, Morsch 1909), its application in concrete design and incorporation in design codes is rather recent (CSA 1984, Collins and Mitchell 1986, Schlaich et al. 1987). Examples on AASHTO LRFD strut-and-tie model can be found in the literature (Mitchell et al. 2004).

The design for shear by sectional model is an iterative process that begins by assuming the value of angle θ, the angle of inclination of diagonal compressive stresses (strut angle). This procedure also needs determination of β, a factor indicating the ability of diagonally cracked concrete to transmit shear and tension. The iterative procedure used to determine θ and β is overly time consuming. The factor β is a function of the strut angle θ. The equations for θ and β are so complex that the values for a set θ and β had to be given in tables for practical use. The details of this procedure are described in Appendix B5 of LRFD Section 5. This procedure can be used as an alternative to the *General Procedure* specified in Art. 5.8.3.4.2.

The trial-and-error procedure of the sectional model can be avoided by assuming the value of the term "0.5 cot θ" equal to 2.0 (Art. C5.8.3.4.2) as explained in the *General Procedure* specified in Art. 5.8.3.4.2. Alternatively, the value of compression field angle θ is computed according to LRFD Eq. 5.8.3.4.2-1 (Art. 5.8.3.4.2). Readers are encouraged to refer to Art. C5.8.3.4.2 (AASHTO 2012) for details and research background of this procedure.

www.EngineeringEBooksPdf.com

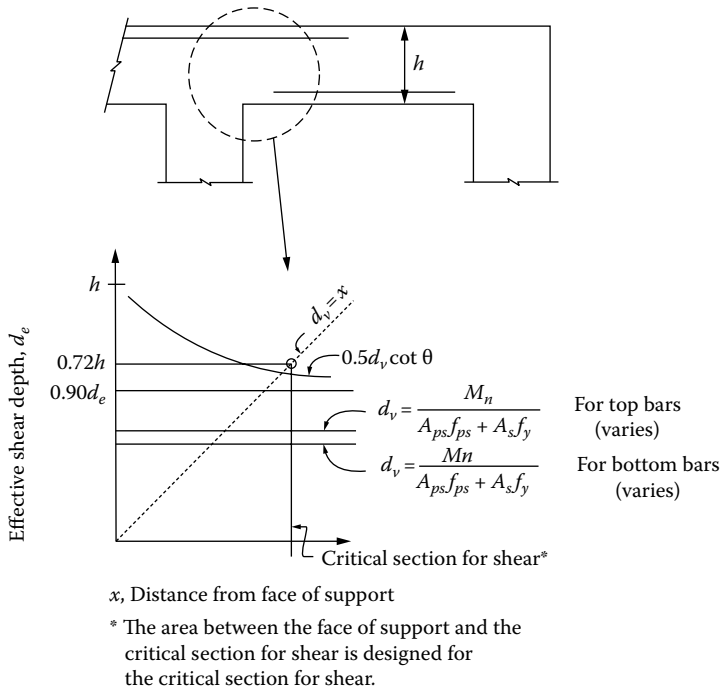

FIGURE 5.25 Critical section for shear. (From *AASHTO LRFD Bridge Design Specifications*, Copyright © 2012 by American Association of State Highway and Transportation Officials, Washington, DC. Used by permission.)

5.10.2 Check for Shear near Supports

In concrete beam design, it is common practice to make checks for shear at the 10th points of a span and at locations near the supports. Art. 5.8.3.2 specifies two provisions for checking shear near the supports:

1. It is assumed that loads close to the support are transferred directly to the support by arching action without causing additional stresses in the stirrups provided to resist shear in that region.
2. In regions near the support, where the reaction force in the direction of the applied shear introduces compression into the end region of a member, the location of the critical section for shear is to be taken at a distance d_v from the internal face of the support as shown in Figure 5.25.

5.10.3 Nominal Shear Resistance of a Concrete Section

5.10.3.1 General

The nominal shear resistance of concrete flexural member can be discussed in general for a concrete member that is reinforced with both nonprestressed and prestressed steel. For such a reinforced member, the shear resistance may be thought of as the sum of three separate resistances:

1. Shear resistance, V_c, that relies on the tensile stress in concrete
2. Shear resistance, V_s, that relies on the tensile stresses in transverse (or shear) reinforcement
3. Vertical component of the prestressing force, V_p

www.EngineeringEBooksPdf.com

Art. 5.8.3.3 specifies that the nominal shear resistance, V_n, be taken as the lesser of the following values:

$$V_n = V_c + V_s + V_p \quad (5.57)\ [A5.8.3.3\text{-}1]$$

$$V_n = 0.25 f_c' b_v d_v + V_p \quad (5.58)\ [A5.8.3.3\text{-}2]$$

where

V_n = nominal shear resistance of the section considered (kip)
V_c = nominal shear resistance by tensile stresses in concrete (kip)
V_p = component in the direction of the applied shear of the effective prestressing force, positive if resisting the applied force
V_s = factored shear resistance at the section (or factored shear demand)
b_v = width of web adjusted for the presence of ducts
d_v = effective shear depth, taken as the distance measured perpendicular to the neutral axis, between the resultants of compressive and tensile forces due to flexure; it need not be taken to be less than $0.9d_e$ or $0.72h$

Note that Equation 5.58 does not contain the contribution of the transverse reinforcement, V_s, to nominal shear resistance, V_n. Equation 5.58 serves as the upper limit of V_n; it is intended to ensure that the concrete in the web does not crush prior to yielding of the transverse reinforcement.

5.10.3.2 LRFD Procedures for Designing for Shear

Procedures for determining the shear resistance are specified in Art. 5.8.3.4 as follows:

1. *Simplified Procedure for Nonprestressed Sections* (Art. 5.8.3.4.1)
2. *General Procedure* (Art. 5.8.3.4.2)
3. *Simplified Procedure for Prestressed and Nonprestressed Sections* (Art. 5.8.3.4.3)

Procedure specified in Art. 5.8.3.4.2 is applicable for all prestressed and nonprestressed members, with and without axial load. Application of this method is presented in Example 5.2. Readers are cautioned to note that the simplified procedure (Art. 5.8.3.4.1) is not applicable to prestressed concrete members; it applies to nonprestressed members only. Application of the *General Procedure* (Art. 5.8.3.4.2) is illustrated in Example 5.5.

Readers should refer to Art. 5.8.1 for the details of these procedures. The value of V_c appearing in Equation 5.57 depends on appropriate application of the aforementioned three procedures. Art. 5.8.3.3 specifies the following provisions in this regard:

1. If the *Simplified Procedure for Nonprestressed Sections* specified in Art. 5.8.3.4.1 or the *General Procedure* specified in Art. 5.8.3.4.2 is followed, V_c is to be calculated from Equation 5.59:

$$V_c = 0.0316\beta\sqrt{f_c'}\, b_v d_v \quad (5.59)\ [A5.8.3.3\text{-}3]$$

   where β = factor indicating ability of diagonally cracked concrete to transmit tension and shear as specified in Art. 5.8.3.4.
2. V_c is to be taken as the lesser of V_{ci} and V_{cw} if the *Simplified Procedure for Prestressed and Nonprestressed Sections* of Art. 5.8.3.4.3 is followed.

Equation 5.57 is the fundamental equation to use for determining the magnitude of the shear resistance that must be provided by transverse reinforcement. For design purposes, Equation 5.57

www.EngineeringEBooksPdf.com

can be written slightly differently by multiplying both sides of the equation by the resistance factor, ϕ:

$$\phi V_n = \phi(V_c + V_s + V_p) \tag{5.60}$$

Equating ϕV_n to the shear demand (factored force effects), V_u, Equation 5.60 can be rewritten as Equation 5.61:

$$V_u = \phi(V_c + V_s + V_p) \tag{5.61}$$

Equation 5.61 can be rewritten as Equation 5.62 to determine the shear resistance to be provided by the transverse reinforcement, V_s:

$$V_s = \frac{V_u}{\phi} - V_c - V_p \tag{5.62}$$

Both Equations 5.57 and 5.58 contain the term V_p (= component in the direction of applied shear of the effective prestressing force) as these equations apply to concrete flexural members that may contain prestressed as well as nonprestressed reinforcement. For beams with only nonprestressed reinforcement (e.g., a reinforced concrete T-beam), $V_p = 0$, and Equation 5.57 can be expressed as Equation 5.63:

$$V_n = V_c + V_s \tag{5.63}$$

Similarly, for beams with only nonprestressed reinforcement, Equation 5.58 can be expressed as Equation 5.64:

$$V_n = 0.25 f_c' b_v d_v \tag{5.64}$$

For beams with only nonprestressed reinforcement, Equation 5.62 can be expressed as Equation 5.65:

$$V_s = \frac{V_u}{\phi} - V_c \tag{5.65}$$

For nonprestressed concrete sections not subjected to axial tension and containing at least the minimum amount of transverse reinforcement specified in Art. 5.8.2.5, or having an overall depth of less than 16 in., the following values can be used (Art. 5.8.3.4.1):

$$\beta = 2.0$$

$$\theta = 45°$$

When transverse reinforcement to resist shear in a concrete member is provided (as in Equation 5.57), the value of its contribution, V_s, is determined as Equation 5.66:

$$V_s = \frac{A_v f_{yd_v} (\cot\theta + \cot\alpha)\sin\alpha}{s} \tag{5.66} \text{ [A5.8.3.3-4]}$$

www.EngineeringEBooksPdf.com

For the value of $\alpha = 90°$, $\sin\alpha = 1.0$, and $\cot\alpha = 0$, therefore, Equation 5.66 can be expressed as Equation 5.67:

$$V_s = \frac{A_v f_{yd_v} \cot\theta}{s} \qquad (5.67)\ [AC5.8.3.3\text{-}1]$$

where

b_v = effective web width taken as the minimum web width within the depth d_v (see Art. 5.8.2.9) (in.)
d_v = defined earlier (Art. 5.8.2.9)
s = spacing of transverse reinforcement measured in a direction parallel to the longitudinal reinforcement (in.)
β = factor indicating ability of diagonally cracked concrete to transmit tension and shear as specified in Art. 5.8.3.4 (procedures for determining shear resistance)
θ = angle of inclination of diagonal compressive stresses as determined in Art. 5.8.3.4 (degrees); if procedures of Art. 5.8.3.4.3 are used, $\cot\theta$ is defined therein
α = angle of inclination of transverse reinforcement to longitudinal axis (degrees)
A_v = area of shear reinforcement within a distance, s
V_p = component in the direction of applied shear of the effective prestressing force; positive if resisting the applied shear; $V_p = 0$ when Art. 5.8.3.4.3 is applied (kip)

As specified in Art. 5.8.3.4.1, if simplified procedure is followed for designing shear reinforcement for nonprestressed sections (e.g., reinforced concrete T-beams), $\theta = 45°$. In common design practice, the size of the transverse reinforcement (the stirrups), A_v, is selected first, so it is known *a priori*. In such cases, the spacing of the stirrups, s, can be determined by rewriting Equation 5.67 in a slightly different format as Equation 5.68:

$$s = \frac{A_v f_{yd_v} \cot\theta}{V_s} \qquad (5.68)\ [AC5.8.3.3\text{-}1]$$

Where transverse reinforcement consists of a single longitudinal bar or a single group of parallel longitudinal bars bent up at the same distance from the support, the shear resistance, V_s, provided by such bars is determined as Equation 5.69:

$$V_s = A_v f_y \sin\alpha \le 0.095\sqrt{f_c'}\, b_v d_v \qquad (5.69)\ [A5.8.3.3\text{-}5]$$

5.10.4 Reinforcement for Shear Resistance: Regions Requiring Transverse Reinforcement

Transverse reinforcement is required in all concrete members where there is significant chance of diagonal cracking. Art. 5.8.2.4 specifies that the transverse reinforcement for resisting shear shall be provided to resist shear in all concrete structural members except slabs, footings, and culverts. Except for slabs, footings, and culverts, transverse reinforcement must be provided where the factored shear force (or the shear demand), V_u, is greater than that expressed by Equation 5.70:

$$V_u > 0.5\phi\,(V_c + V_p) \qquad (5.70)\ [A5.8.2.4\text{-}1]$$

www.EngineeringEBooksPdf.com

For beams with only nonprestressed tensile reinforcement (e.g., a reinforced concrete T-beam), $V_p = 0$, so Equation 5.70 can be expressed as Equation 5.71:

$$V_u > 0.5\phi V_c \tag{5.71}$$

where
V_p was defined earlier
V_u = factored shear force
V_c = nominal shear resistance of concrete (kip)
ϕ = resistance factor specified in Art. 5.5.4.2 (LRFD Table 5.5.4.2.2-1)

5.10.5 Minimum Transverse Reinforcement

The purpose of providing minimum reinforcement for resisting shear is to restrain the growth of diagonal cracking and increase the ductility of the sections. Except for segmental posttensioned concrete box girder bridges, where transverse reinforcement is required to satisfy provisions of Art. 5.8.2.4, the amount of minimum transverse reinforcement to be provided, A_v, shall satisfy Equation 5.5.72:

$$A_v \geq 0.0316\sqrt{f'_c}\left(\frac{b_v s}{f_y}\right) \tag{5.72} \text{ [A5.8.2.5-1]}$$

where
A_v = area of transverse reinforcement within a distance s (in.^{2})
b_v = width adjusted for the presence of ducts as specified in Art. 5.8.2.9 (in.)
s = spacing of transverse reinforcement
f_y = specified yield strength of transverse reinforcement (ksi)

It is interesting to note that the term $0.0316\sqrt{f'_c}$ in Equation 5.72 is equivalent to the familiar expression $1.0\sqrt{f'_c}$ psi.

Equation 5.72 shows that the amount of transverse reinforcement required increases with the increase in the strength of concrete. In design, it is common practice to first select the size of the transverse reinforcement, so A_v (= two cross-sectional areas for two-legged stirrups) is known *a priori*, and then calculate the required spacing from Equation 5.73 (rewritten Equation 5.72):

$$s = \frac{A_v f_y}{0.0316\sqrt{f'_c}b_v} \tag{5.73}$$

Art. 5.8.2.6 provides specifications for types of transverse reinforcement that can be provided to resist shear. Transverse reinforcement in beams is commonly provided in the form of transverse reinforcement. This type of reinforcement usually consists of two-legged shear stirrups placed perpendicular to the longitudinal bars provided for flexural resistance. In such cases, A_v = two times the cross-sectional area of the bar because a potential diagonal crack must intersect two legs of a stirrup. Inclined stirrups making an angle of 45° with the longitudinal reinforcement are permissible; however, stirrups inclined at less than 45° to the longitudinal reinforcement are not permitted because they are difficult to anchor against slip. To increase the shear capacity of a member, transverse reinforcement should be capable of undergoing substantial strain prior to failure.

The significance of Equations 5.70 (Equation 5.71 for beams with nonprestressed steel reinforcement) and Equation 5.73 is this: In all members where the factored shear demand, V_u, exceeds that

www.EngineeringEBooksPdf.com

given by Equation 5.70 or 5.71 as applicable, transverse reinforcement must be provided; the maximum spacing of transverse reinforcement (e.g., stirrups) so provided is limited by Equation 5.73.

For segmental posttensioned concrete box girder bridges, where transverse reinforcement is required, transverse reinforcement as expressed by Equation 5.74 must be provided:

$$A_v \geq 0.05\left(\frac{b_w s}{f_y}\right) \qquad (5.74)\ [A5.8.2.5.2]$$

where b_w = width of web (in.).

5.10.6 Maximum Spacing of Transverse Reinforcement

The maximum spacing of transverse reinforcement is governed by the concept that each 45° crack must be crossed by at least one stirrup. Sections that are highly stressed in shear (e.g., sections close to supports) require closely spaced transverse reinforcement to control shear cracking.

Art. 5.8.2.7 specifies provisions for maximum spacing of transverse reinforcement based on the shear stress due to the factored shear V_u at a section under consideration (to be calculated as specified in Art. 5.8.2.9, discussed in the next section). Two conditions limiting the maximum spacing of transverse reinforcement are stipulated as follows:

1. If $v_u < 0.125\sqrt{f'_c}$, then

$$s_{max} = 0.8d_v \leq 24 \text{ in.} \qquad (5.75)\ [A5.8.2.7\text{-}1]$$

2. If $v_u \geq 0.125\sqrt{f'_c}$, then

$$s_{max} = 0.4d_v \leq 12 \text{ in.} \qquad (5.76)\ [A5.8.2.7\text{-}2]$$

5.10.7 Shear Stress on Concrete

The shear stress on the concrete shall be determined from Equation 5.77, and the critical section for shear is taken at a distance d_v from the interior face of support:

$$v_u = \frac{|V_u - \phi V_p|}{\phi b_v d_v} \qquad (5.77)\ [A5.8.2.9\text{-}1]$$

For beams with only nonprestressed reinforcement, $V_p = 0$ in Equation 5.77, so that Equation 5.77 reduces to Equation 5.78:

$$v_u = \frac{V_u}{\phi b_v d_v} \qquad (5.78)$$

where

d_v = effective shear depth, measured as the distance perpendicular to the neutral axis, between the resultants of the tensile and compressive forces due to flexure; it need not be taken to be less than the greater of $0.9d_e$ or $0.72h$ (in.)

b_v = effective width taken as minimum web width, measured parallel to the neutral axis, between the resultants of the tensile and compressive forces due to flexure, or for circular sections, the diameter of the section, modified for the presence of ducts where applicable (in.)

www.EngineeringEBooksPdf.com

d_e = effective depth from the extreme compressive fiber to the centroid of the tensile force in the tensile reinforcement (in.); its value is expressed by Equation 5.79:

$$d_e = \frac{A_{ps} f_{ps} d_p + A_s f_y d_s}{A_{ps} f_{ps} + A_s f_y} \quad (5.79)\ [A5.8.2.9.2]$$

For beams with only nonprestressed reinforcement, A_{ps} = 0, so that Equation 5.79 reduces to Equation 5.80a

$$d_e = d_s \quad (5.80a)$$

For beams with prestressed reinforcement only, A_s = 0, so Equation 5.79 reduces to Equation 5.80b:

$$d_e = d_p \quad (5.80b)$$

5.10.8 Tensile Capacity of Longitudinal Reinforcement: Art. 5.8.3.5

The tensile capacity of longitudinal reinforcement at each section of the beam shall be proportioned to satisfy the following:

$$A_{ps} f_{ps} + A_s f_y \geq \frac{|M_u|}{d_v \phi_f} + 0.5\left(\frac{N_u}{\phi_c}\right) + \left(\left|\frac{V_u}{\phi_v} - V_p\right| - 0.5V_s\right)\cot\theta \quad (5.81)\ [A5.8.3.5\text{-}1]$$

where

A_s = area of prestressing steel (in.^{2})
f_{ps} = average stress in prestressing steel at the time at which the nominal resistance of the member is required
N_u = applied factored axial force taken as positive if tensile (kip)
V_p = component in the direction of the applied shear of the effective prestressing force, positive if resisting the applied shear (kip)
V_s = shear resistance provided by the transverse reinforcement at the section under investigation as given by LRFD Eq. 5.8.3.3-4, except that V_s need not be taken as greater than V_u/ϕ (kip)

Equation 5.81 is general and applicable to section with both nonprestressed steel and prestressed steel. The area of longitudinal reinforcement on the flexural tension side of the member need not exceed the area required to resist the maximum moment acting alone. This provision applies where the reaction force or the load introduces direct compression into the flexural compression side of the member, for example, at supports of a simple span.

For sections with nonprestressed steel, for example, a reinforced concrete T-beam, the quantities pertaining to prestressed steel (A_{ps}, N_u, V_p) are each set to zero. With θ = 45°, cot θ = 1.0, Equation 5.81 reduces to Equation 5.82:

$$A_s f_y \geq \frac{|M_u|}{d_v \phi_f} + \left(\left|\frac{V_u}{\phi_v}\right| - 0.5V_s\right) \quad (5.82)$$

5.11 ESTIMATING THE AREA OF REQUIRED NONPRESTRESSED TENSILE REINFORCEMENT IN CONCRETE SECTIONS

Preliminary design of concrete beams usually begins with an assumed trial size for which the area of reinforcement, which is not known *a priori*, must be guessed or estimated. Equation 5.26, with some simplified assumptions, can be used to estimate the area of required

www.EngineeringEBooksPdf.com

reinforcement. Equation 5.26 for calculation of nominal flexural strength of rectangular sections with nonprestressed steel was derived earlier:

$$M_u = \phi M_n = \phi A_s f_y \left(d_s - \frac{a}{2} \right) \tag{5.26}$$

For shallow rectangular sections, the depth of compression block, a, is small, so one can assume that

$$d_s - \frac{a}{2} \approx 0.9 d_s \tag{5.83}$$

Substituting for the parenthetical quantity in Equation 5.26 from Equation 5.83 yields

$$M_u = \phi A_s f_y (0.9 d_s) \tag{5.84}$$

The area of required nonprestressed reinforcing steel can be estimated by rewriting Equation 5.84 in the following form:

$$A_s = \frac{M_u}{0.9 f_y (0.9 d_s)} \tag{5.85}$$

Expressing M_u in kip-ft units, and substituting $f_y = 60$ ksi for Grade 60 reinforcement, Equation 5.85 can be expressed Equation 5.86:

$$A_s = \frac{12 M_u}{48.6 d_s} \approx \frac{M_u}{4 d_s} \tag{5.86}$$

Since M_u and d_s are known values, the area of required nonprestressed reinforcement can be easily estimated. Application of Equation 5.86 is illustrated in several examples in this chapter. It must be noted that Equation 5.86 is applicable for only Grade 60 reinforcement and M_u is in kip-ft units.

5.12 SLAB-TYPE CONCRETE BRIDGES AND CONCRETE DECKS

Reinforced concrete slabs and decks are structural components omnipresent in almost all highway bridges. They constitute integral structural components of highway bridges.

A deck is a structural component that directly supports traffic on a highway bridge. Most highway bridge decks, with the exception of orthotropic decks and open and filled steel grid decks, are built from reinforced concrete. Figure 5.26 shows examples of a few deck systems commonly used for highway bridges.

Most common type of highway concrete superstructures can be classified as slab-type bridges and slab–beam-type bridges; the former are used for very short spans and the latter for short spans and medium spans. For longer spans, other systems, such as segmentally constructed bridges, arch bridges, and cable-stayed bridges, are used (not discussed in this book).

Slab bridges are structurally different from typical slab–beam bridges (e.g., reinforced concrete T-beam bridges and prestressed concrete bridges discussed in this chapter and slab–steel beam bridges discussed in Chapter 6). A slab in a slab bridge itself acts as a primary load-carrying component. By contrast, the slab–beam-type bridges are characterized by decks that span transverse to several usually parallel supporting elements (beams) that act as primary load-carrying components.

www.EngineeringEBooksPdf.com

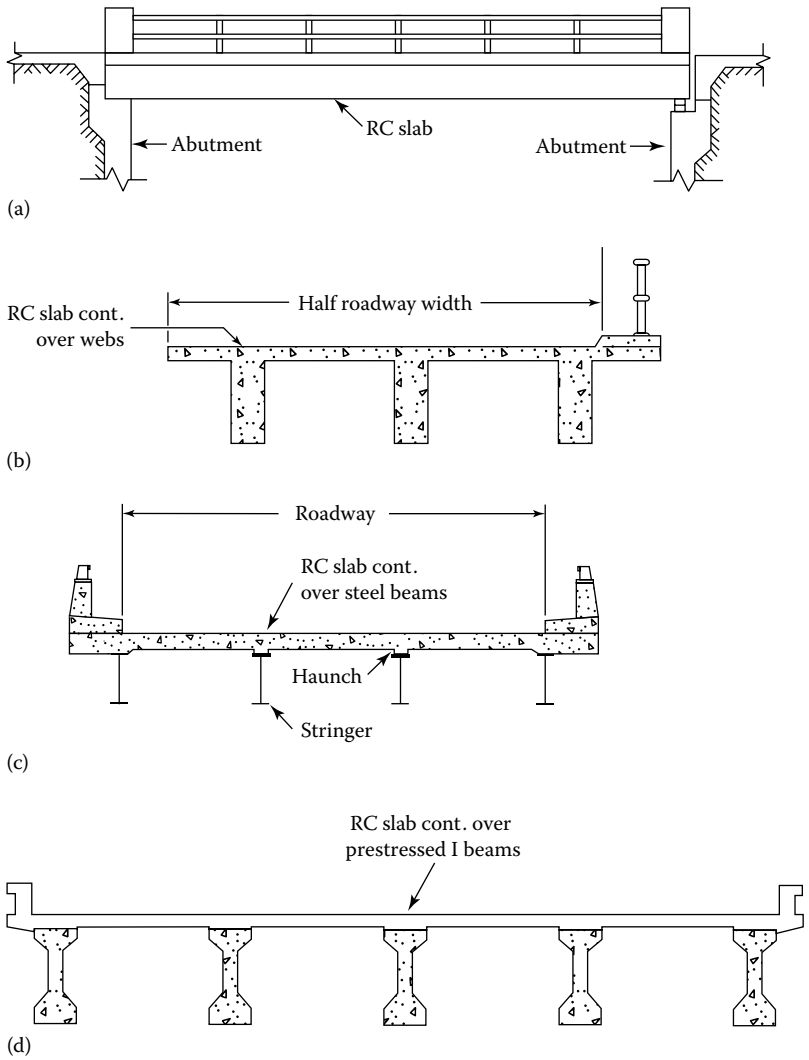

FIGURE 5.26 Concrete slabs and deck systems for highway bridges: (a) a slab bridge is supported directly over the abutments and/or intermediate piers, (b) deck of a T-beam bridge is cast monolithically with the webs, (c) deck supported over steel beams, and (d) deck supported over prestressed concrete girders. In figure (a), the primary reinforcement is oriented parallel to the traffic; in figures (b), (c), and (d), the primary reinforcement is oriented perpendicular to the traffic.

As discussed in Chapter 4, a slab-type bridge (or a slab bridge) is a beamless structure that carries highway traffic. Slab-type bridges are typically used for very short spans, usually in the 20–50 ft range. The primary reason for this limitation is a practical one. As span increases, the slab-type bridges require thicker slabs to satisfy flexural requirements, resulting in increased dead load and increased deflection. In short, they become relatively uneconomical. To overcome this problem, slab–beam-type bridges are preferred, which are comparatively lighter than slab-type bridges. In slab–beam-type bridges, the concrete desk is supported by a number of closely spaced, usually parallel longitudinal elements (beams). The closer spacing of these elements makes it possible to use relatively thinner slabs (decks), resulting in lighter and economical structures.

There are fundamental differences between the structural behaviors of decks of slab-type and slab–beam-type bridges. In a slab-type bridge, the slab spans longitudinally between the supports

www.EngineeringEBooksPdf.com

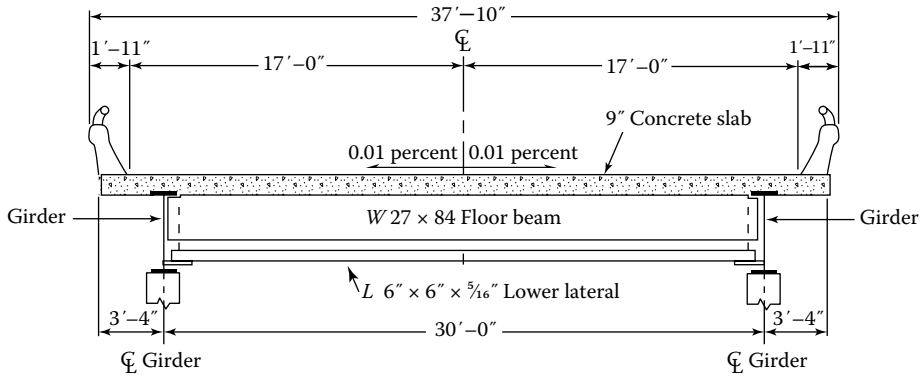

FIGURE 5.27 Example of a concrete slab spanning *longitudinally* over the transverse floor beams that are framed into two longitudinally spanning plate girders. The primary reinforcement in the slab is oriented *parallel* to traffic. (The dimensions shown are project specific, shown here for illustrative purposes only.)

and acts as the primary load-carrying structural component, acting essentially as a beam element with tension in the bottom. Therefore, the primary reinforcement in the slab of a slab-type bridge is placed *parallel to the direction of traffic*. The live load distribution factors computed to determine live load force effects in beams (see examples in Chapter 4) are not applicable to design of slab bridges. Instead, the slab is analyzed and designed using the equivalent strip method of Art. 4.6.2.3.

By contrast, in slab–beam-type bridges, the deck spans transversely, supported by the longitudinally spanning beams; the primary reinforcement in the deck is placed *perpendicular to the direction of traffic*. For this reason, different design methods are used to design these two different types of superstructures.

As primary load-carrying elements, slabs can be supported in other ways than just by the abutments and/or piers. Figure 5.27 shows a steel bridge in which the concrete slab spans longitudinally, that is, in the same direction as the main girders. In the bridge shown in Figure 5.28, the deck spans perpendicular to the supporting steel beams. Both are atypical slab–steel girder bridges.

5.13 CONCRETE DECKS

5.13.1 General

Figure 5.29 shows several cross sections having concrete decks. Concrete decks are designed and built as continuous slabs supported over a number (at least four) of parallel beams; in this respect, they span perpendicular to the supporting beams, and so is the direction of primary reinforcement in them; the direction of secondary reinforcement is parallel to the traffic. Because of continuity, deck slabs are subjected to positive moment in their midspan regions (between the supporting beams) and negative moment at the supports (over the beams).

5.13.2 Minimum Depth and Cover Requirements

Deck slabs must satisfy the minimum thickness requirements specified in Art. 2.5.2.6 (discussed in Chapter 2). Typical deck thickness is a minimum of 8 in. or more depending on the distance between the supporting girders. Unless approved by the owner, the depth of a concrete deck, excluding any provision for grinding, grooving, and sacrificial surface, shall not be less than 7.0 in. For slabs of depth less than 1/20 of the design span, consideration should be given to prestressing in the direction of that span in order to control cracking. Construction tolerances become a concern for thin decks.

www.EngineeringEBooksPdf.com

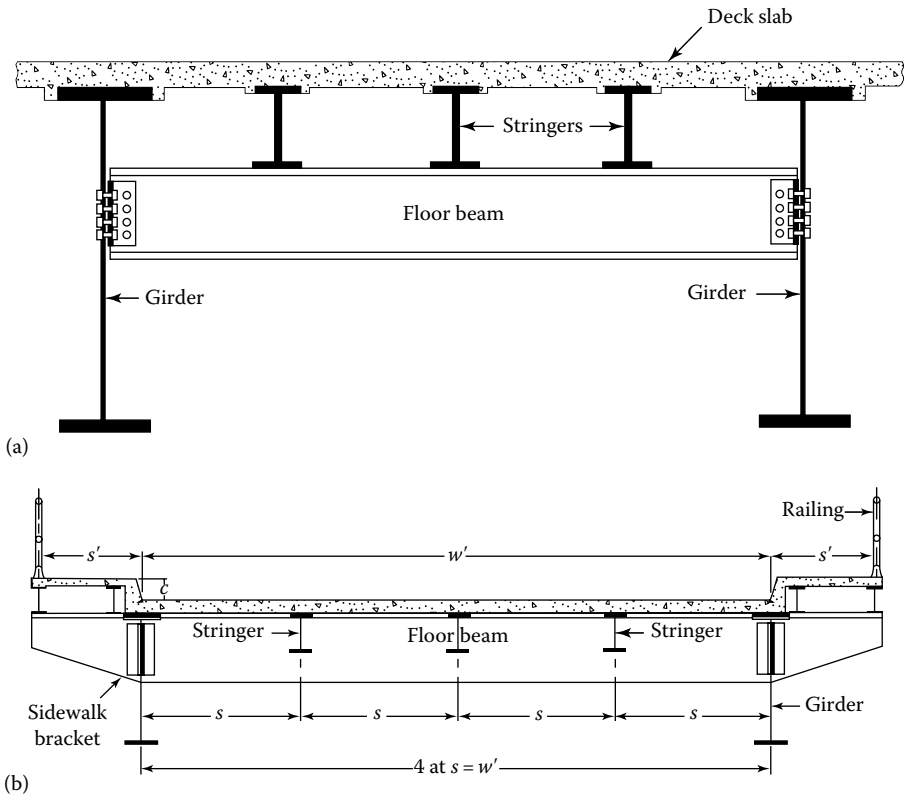

FIGURE 5.28 Examples of position of concrete deck in long-span slab–steel plate girder bridges. The deck is supported over the steel stringers—(a) the stringers are supported on the top of a transverse steel floor beam that is framed into longitudinal plate girders, and (b) stringers are framed into the transverse floor beams. In both cases, the primary reinforcement in the deck is *perpendicular* to traffic.

Concrete cover plays an important role in preserving the integrity of the deck and in protecting the reinforcement within from corrosion. Minimum cover is necessary for durability and prevention of splitting due to bond stresses and to provide for placing tolerance. Therefore, there are mandatory cover requirements as specified in Art. 5.12.3 (shown in Table 5.1/LRFD Table 5.12.3-1).

Minimum cover to main bars, including bars protected by epoxy coating, shall be 1.0 in. Cover to ties and stirrups may be 0.5 in. less than the values specified in Table 5.1 (LRDF Table 5.12.3-1) for main bars but shall not be less than 1.0 in. Increased cover may be required for decks by the owners of bridges in snow regions and in the marine environment to mitigate the corrosive effects of deicing salt and chemicals.

Minimum cover requirements are based on traditional concrete mixes and on the absence of protective coating on either the concrete or the steel inside. A combination of special mix design, protective coatings, dry or moderate climate, and the absence of corrosion chemicals may justify a reduction of these requirements subject to the owner's approval (Art. C9.7.1.1).

Decks are constantly subjected to wear and abrasion from chained tires and tire studs in the snow areas. Integrity of design (structural) thickness of the deck slab must be preserved under all conditions. Measures must be taken to minimize reduction in deck thickness due to wearing of the deck. Art. 5.12.3 specifies additional cover to be provided for decks exposed to tire studs or chain wear to compensate for the expected loss in depth due to abrasion. Where concrete decks without an initial overlay are used, consideration should be given to providing an additional 1/2 in. thickness to permit correction of the deck profile by grinding and to compensate for thickness loss due to tire abrasion (Art. 2.5.2.4).

www.EngineeringEBooksPdf.com

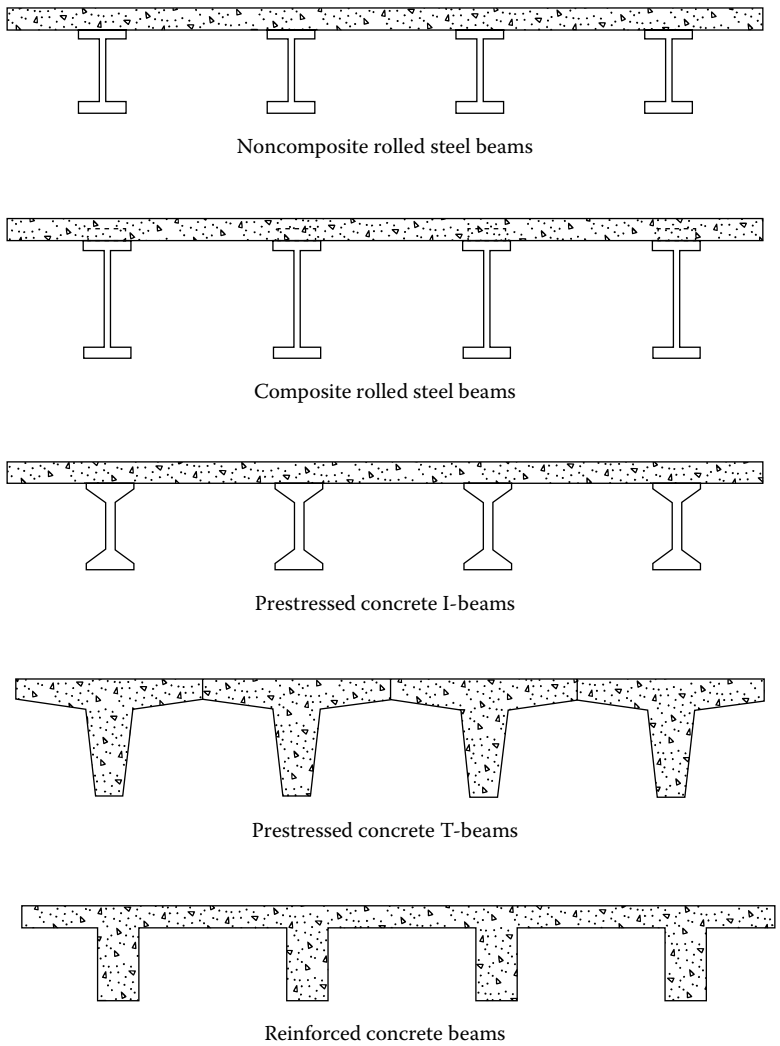

FIGURE 5.29 Examples of concrete deck systems. Except for prestressed concrete T-beams, the concrete deck spans transversely over the beams (steel or concrete). The primary reinforcement in the deck is placed *perpendicular* to traffic, and the same method is used for their analysis and design irrespective of the type of supporting beams.

The *W/C* ratio has an influence on the permeability of concrete. Lower *W/C* ratios decrease the permeability of concrete. In recognition of this property of concrete, Art. 5.12.3 permits modification of concrete cover based on the *W/C* ratios as follows:

For $W/C \leq 0.40$	0.8
For $W/C \geq 0.50$	1.2

5.13.3 Composite Action between Decks and Supporting Beams

With a few exceptions, decks are built to act compositely with the supporting girders. One exception is the deck in noncomposite slab–steel girder bridges in which the deck slab is sometimes built as noncomposite (discussed in Example 6.2).

www.EngineeringEBooksPdf.com

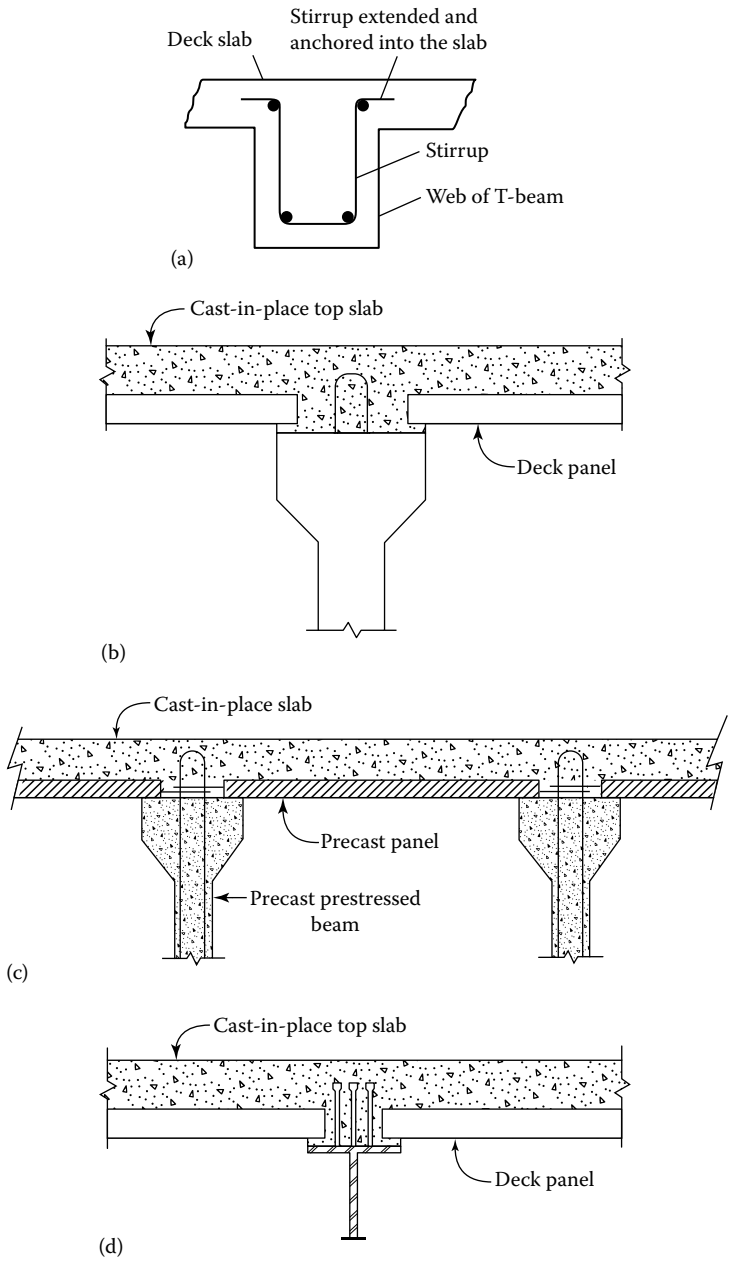

FIGURE 5.30 Methods of creating composite action between decks and supporting beams. (a) T-beam stirrups extending from the web and anchored in the deck, (b and c) hooks protruding from the top of precast, prestressed concrete girders and embedded in the deck, (d) shear studs welded to the top flange of steel girder and embedded into the deck.

A variety of schemes, depending on the material of supporting girders, are used to develop composite action in slab–beam deck systems shown in Figure 5.26, the following methods being the most common (Figure 5.30):

1. In reinforced concrete T-beam bridges, the deck is built monolithic with the girders; the stirrups from the webs are extended into the compression zone of the deck slab to develop composite action.

www.EngineeringEBooksPdf.com

2. In precast, prestressed concrete bridges, the girders are fabricated with steel hooks protruding from their top face, which are embedded in the cast-in-place decks to provide composite action.
3. In slab–steel girder bridges, composite action is developed by steel shear connectors welded to the top of girders, which get embedded in the cast-in-place decks and provide composite action. Shear connectors are designed to conform to the provisions of LRFD Section 5 for concrete beams and LRFD Sections 6 and 7 for metal beams.

5.13.4 Skewed Decks

In ideal situations, the deck would be oriented perpendicular to the center line of the bridge, but that is not always possible, and the decks might be skewed. If the skew angle of the deck does not exceed 25°, the primary reinforcement may be placed in the direction of the skew; otherwise, it shall be placed perpendicular to the main supporting components as shown in Figure 5.31. The objective of this provision is to prevent extensive cracking of the deck, which may result from the absence of appreciable reinforcement acting in the direction of principal flexural stresses due to heavily slewed reinforcement as shown in Figure 5.31.

The 25° limit stated earlier is arbitrary, and it could affect the area of steel by as much as 10 percent (Art. C9.7.1.3). This factor was not taken into account in the development of this specification because the analysis procedure and the use of bending moment as a basis of design were not believed to be sufficiently accurate to warrant such an adjustment. Owners interested in making this refinement should also consider one of the refined methods of analysis identified in Art. 4.6.3.2.

5.13.5 Edge Support Requirements

Unless otherwise specified, at lines of discontinuity, the edge of the deck shall either be strengthened or be supported by a beam or other line component. The beam or component shall be integrated in or make composite with the deck. The edge beams may be designed as beams whose width may be taken as the effective width of the deck specified in Art. 4.6.2.1.4. However, the additional edge beam need to be provided if the following two conditions are satisfied:

1. The primary direction of the deck is transverse.
2. The deck is composite with a structurally continuous concrete barrier.

5.13.6 Design of Cantilever Slabs

Decks almost always overhang past the exterior beams. The overhang portions of the decks carry traffic barriers and railing systems. The overhanging portion of the deck is required to be designed for

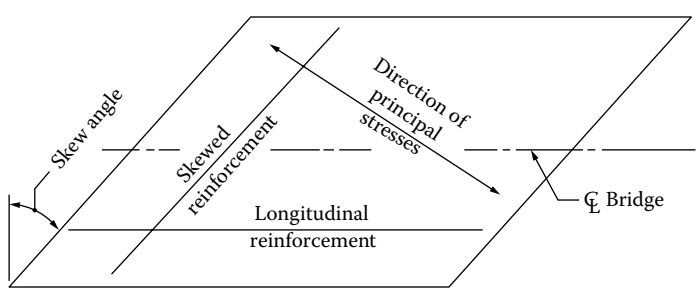

FIGURE 5.31 Reinforcement layout for skewed decks. (From *AASHTO LRFD Bridge Design Specifications*, Copyright © 2012 by American Association of State Highway and Transportation Officials, Washington, DC. Used by permission.)

www.EngineeringEBooksPdf.com

railing impact loads and in accordance with the provisions of Art. 3.6.1.3.4. Punching shear effects at the outside toe of the railing post or barrier due to vehicle collision loads must be investigated.

An acceptable method of analyzing deck overhangs for railing impact loads is presented in the appendix to LRFD Section 13. Any combination of increasing the depth of the slab, employing special reinforcement extending the slab width beyond the railing, and enlarging base plates under railing posts may be utilized to prevent failure due to punching shear.

5.13.7 Design Procedures for Deck Slabs

LRFD specifications specify two design methods for the design of reinforced concrete bridge decks:

1. Empirical Design Method (Art. 9.7.1, 9.7.2)
2. Traditional Design Method (Art. 9.7.3)

Both methods are discussed as follows.

5.13.7.1 Empirical Design Method

5.13.7.1.1 General

The provisions for using *empirical method* for the design of decks are specified in Art. 9.7.2; they are intended to be applied exclusively for the empirical design procedure for concrete deck slabs supported by longitudinal components.

The use of empirical method for the design of decks is in stark deviation from the past design practices specified in Standard Specifications, which was based on flexure. The empirical design method is based on extensive research into the behavior of concrete deck slabs, conducted mainly in Canada. It discovered that the primary structural action by which these slabs resist concentrated wheel loads is not flexure, as traditionally believed, but a complex internal membrane stress state referred to as internal arching. This action is made possible by the cracking of the concrete in the positive moment region of the slab and the resulting upward shift of the neutral axis in that portion of the slab. The action is sustained by in-plane membrane forces that develop as a result of lateral confinement provided by the surrounding concrete slab, rigid appurtenances, and supporting components acting compositely with the slab.

As described in Art. C9.7.2.1, the arching in the slab creates what can best be described as an internal compressive dome, the failure of which usually occurs as a result of overstraining around the perimeter of the applied concentrated load (the wheel footprint). The resulting failure mode is that of punching shear, although the inclination of the fracture surface is much less than 45° due to the presence of large in-plane compressive force associated with arching.

The design of reinforced concrete decks using the concept of internal arching action with the limits specified herein has been verified by extensive nonlinear finite element analysis (Batchelor et al. 1978, Fang et al. 1990). These analyses are accepted in lieu of project-specific design calculation as a preapproved basis of design. A discussion on the arching action in the deck slab can be found in the literature (Holowka et al. 1980, Fang, 1985, OHBDC 1991).

All available test data indicate that the factor of safety of a deck designed by the flexural method specified in the 16th edition of the AASHTO Standard Specifications (AASHTO 1998) working stress design is at least 10.0. Tests indicate a comparable factor of safety of about 8.0 for an empirical design. Therefore, the empirical design possesses extraordinary reserve strength.

5.13.7.1.2 Applicability Criteria: Art. 9.7.2.4

The empirical design may be used only if the following conditions are satisfied:

1. Cross frames or diaphragms are used throughout the cross section at lines of support.
2. For cross section involving torsionally stiff units, such as individual separated box beams, either intermediate diaphragms between the boxes are provided at a spacing not to exceed

www.EngineeringEBooksPdf.com

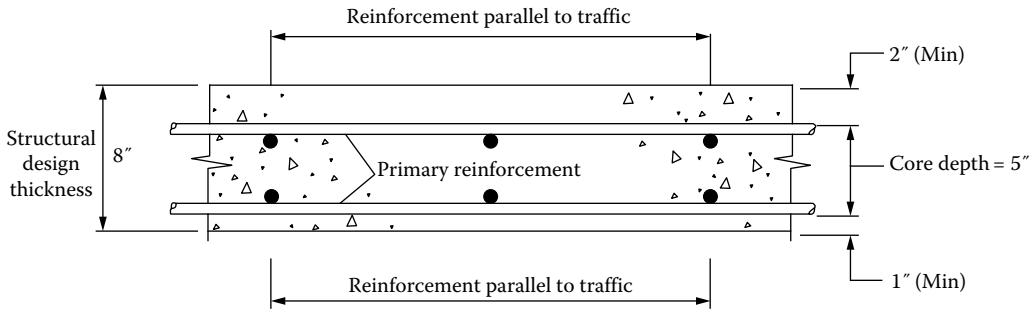

FIGURE 5.32 Core of a concrete slab (segment of transversely spanning deck shown). The core thickness is the distance between the outer surfaces of the reinforcing bars closest to the top and bottom surfaces of the slab.

25.0 ft or the need for supplemental reinforcement over the webs to accommodate transverse bending between the box units is investigated, and reinforcement is provided if necessary.

3. The supporting components are made of steel and/or concrete.
4. The deck is fully cast in place and water cured.
5. The deck is of uniform depth, except for haunches at girder flanges and other local thickening.
6. The ratio of effective length to design depth does not exceed 18.0 and is not less than 6.0.
7. Core depth of the slab is not less than 4.0 in. (Figure 5.32).
8. The effective length, as specified in Art. 9.7.2.3, does not exceed 13.5 ft.
9. The minimum depth of the slab is not less than 7.0 in., excluding a sacrificial wearing surface where applicable.
10. There is an overhang beyond the centerline of the outside girder of at least 5.0 times the depth of the slab; this condition is satisfied if the overhang is at least 3.0 times the depth of the slab and a structurally continuous concrete barrier is made composite with the overhang.
11. The specified 28-day strength of the deck concrete is not less than 4.0 ksi.
12. The deck is made composite with supporting structural elements.
13. For the purpose of this article, a minimum of two shear connectors at 24.0 in. centers shall be provided in the negative moment region of continuous steel superstructures. The provisions of Art. 6.10.1.1 shall also be satisfied. For concrete girders, the use of stirrups satisfies this requirement.

The 4.0 ksi limit specified earlier is based on the fact that none of the tests included concrete with less than 4.0 ksi strength at 28 days. Many jurisdictions specify 7.5 ksi concrete for ensuring reduced permeability of the deck. On the other hand, tests indicate that resistance is not sensitive to the compressive strength, and even 3.5 ksi strength concrete may be accepted with the approval of the owner.

5.13.7.1.3 Effective Length: Art. 9.7.2.3

Deck slabs may be supported over concrete T-beams; precast, prestressed concrete beams; or steel beams. When using the empirical design method, the effective length of slab for these two types of deck systems shall be taken as follows:

1. For slabs monolithic with walls or beams (e.g., T-beams), the face-to-face distance (Figure 5.33)
2. For slabs supported on steel or concrete girders (e.g., prestressed concrete girders), the distance between flange tips, plus the flange overhang, taken as the distance from the extreme flange tip to the face of the web, disregarding any fillets (Figure 5.34)

www.EngineeringEBooksPdf.com

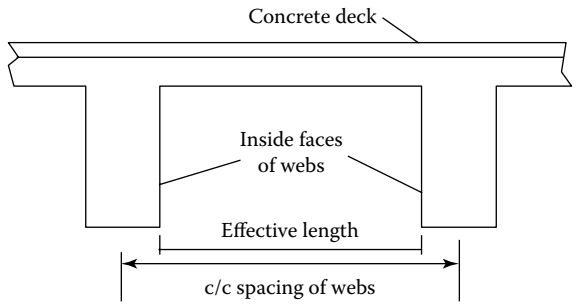

FIGURE 5.33 Effective length for slabs monolithic with beams or walls.

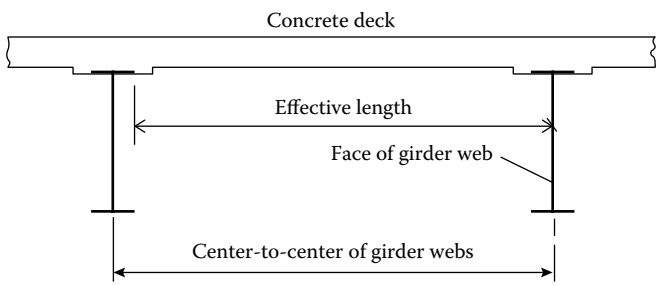

FIGURE 5.34 Effective length for deck slab supported on steel beams. The effective length is measured as the distance between the flange tips plus the flange overhang taken as the distance from the extreme flange tip to the face of the web disregarding any fillets.

In a majority of cases, the deck supporting elements (steel beams or the webs of T-beams) are parallel to each other. In exceptional cases where these supporting elements are nonuniformly spaced, the effective length, $S_{effective}$, is to be taken as the larger of the deck lengths at two locations as shown in Figure 5.35.

5.13.7.1.4 Reinforcement Requirements for Empirically Designed Decks

The reinforcement requirements for deck slabs when designed using the empirical method must conform to the following reinforcement layout (Art. 9.7.2.5):

1. Four layers of isotropic reinforcement are required to be provided in empirically designed slabs.
2. Reinforcement shall be located as close to the outside surfaces as permitted by cover requirements.
3. Reinforcement shall be provided in each face of the slab with the outmost layers placed in the direction of the effective length.
4. The minimum amount of reinforcement shall be 0.27 in.^{2}/ft of steel for each top layer. Spacing of steel shall not exceed 18.0 in.
5. Reinforcing steel shall be Grade 60 or better. All reinforcement shall be straight bars, except that hooks may be provided where required.
6. If the skew exceeds 25°, the specified reinforcement in both directions shall be doubled in the end zones of the deck. Each end zone shall be taken as a longitudinal distance equal to the effective length of the slab specified in Art. 9.7.2.3.

As stated in Art. C9.7.2.5, the validity of previously stated reinforcement requirements has been verified by tests. Prototype tests indicated that 0.2 percent reinforcement in each of four layers

www.EngineeringEBooksPdf.com

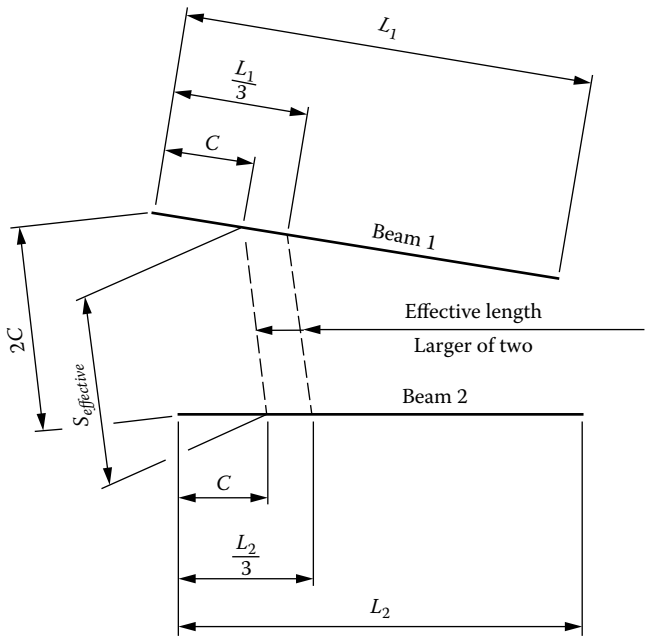

FIGURE 5.35 Effective length for nonuniform spacing of elements supporting the deck. (From *AASHTO LRFD Bridge Design Specifications*, Copyright © 2012 by American Association of State Highway and Transportation Officials, Washington, DC. Used by permission.)

based on the effective reinforcement in each of four layers based on the effective depth d satisfies strength requirements. However, the conservative value of 0.3 percent of the gross area, which corresponds to about 0.27 in.^{2}/ft in a 7.5 in. thick slab, is specified for better crack control in the positive moment area. Field measurements show very low stresses in negative moment reinforcement; this is reflected by the 0.18 in.^{2}/ft reinforcement requirement, which is about 0.2 percent reinforcement steel. The objective of this low amount of steel is to prevent spalling of the deck due to corrosion of the bars or wires.

Depending on the width of the deck, splicing of reinforcing bars may be required. Welded splices are not permitted due to fatigue considerations. The intent of this provision is crack control. Beam–slab bridges with a skew exceeding 25° have shown a tendency to develop torsional cracks due to differential deflections in the end zone (OHBDC 1991). The extent of cracking is usually limited to a width that approximates the effective length.

5.13.7.1.5 Exclusions to Application of the Empirical Method: Design of Overhang

The empirical method for designing reinforced concrete bridge deck slabs is to be used only when all of the aforementioned design conditions are met. Art. 9.7.2.2 specifies that the empirical method is not applicable to the design of overhangs (even though the remainder of the deck slab can be designed using this method). Instead, the overhang should be designed for the following conditions:

1. Wheel loads for decks with discontinuous railings and barriers using the equivalent strip method
2. Equivalent line load for decks with continuous barriers specified in Art. 3.1.1.3.4 as discussed in Chapter 3
3. Collision loads using a failure mechanism as specified in Art. A13.2

www.EngineeringEBooksPdf.com

5.13.7.1.6 Decks with Stay-in-Place Formwork (Art. 9.7.2.6)

For decks made with corrugated metal formwork, the design depth of the slab shall be assumed to be the minimum concrete depth.

Stay-in-place concrete formwork shall not be permitted if empirical design method is used for design of decks.

5.13.7.1.7 Calculation of Force Effects in Deck Slabs: Art. 4.6.2.1

5.13.7.1.7.1 Bending Moments Decks may be analyzed using the approximate method specified in Art. 4.6.2.1, which uses equivalent strips. The following procedure shall be used to calculate the force effects in the equivalent strips (Art. 4.6.2.1.6):

1. The equivalent strips shall be analyzed by classical beam theory.
2. The strips shall be analyzed either as simply supported or continuous beams, as appropriate.
3. The span length shall be taken as center-to-center distance between the supporting components.
4. For the purposes of calculating force effects in the strips, the supporting components shall be assumed as infinitely rigid.
5. The wheel loads may be modeled as concentrated loads or as patch loads whose length along the span shall be the tire contact area as specified in Art. 3.6.1.2.5, plus the depth of the deck.
6. The critical section for calculating negative moments and shear may be taken as follows:
   a. For monolithic construction, closed steel boxes, closed concrete boxes, open concrete boxes without top flanges, and stemmed precast beams, at the face of supporting components. This applies to cross sections (b), (c), (d), (e), (f), (g), (h), (i), and (j) in LRFD Table 4.6.2.2.1-1.
   b. For steel I-beams and steel tub girders, one-quarter of the flange width from the centerline of the support. This applies to cross sections (a) and (c) in LRFD Table 4.6.2.2.1-1.

In lieu of more precise calculations, Art. C4.6.2.1.6 permits using unfactored design live load moments tabulated in LRFD Table 4.1 (discussed in Chapter 4 and provided in the appendix of this chapter). This table is accompanied by several design notes; use of this table requires conformance to these notes, notably the following:

1. The moments are calculated using the equivalent strip method as applied to concrete slabs supported on parallel girders (the most common case).
2. Multiple presence factor and dynamic load allowance are included in the tabulated values.
3. The moments are applicable to decks supported on at least three girders and having a width of not less than 14 ft between the centerline of girders.
4. The moments that represent the upper bound for the moments in the interior regions of the slab, and for any specific girder spacing, were taken as the maximum value calculated, assuming different number of girders in the bridge cross section. For each combination of girder spacing and number of girders, the following cases of overhanging width were considered:
   a. Minimum total overhang width of 21 in. measured from the center of the exterior girder.
   b. Maximum total overhang width equal to the smaller of 0.625 times the girder spacing and 6.0 ft.
      A railing system width of 21 in. was used to determine the clear overhang width. For other widths of railing systems, the difference in the moments in the interior regions of the deck is expected to be within the acceptable limits of practical design.

www.EngineeringEBooksPdf.com

5. The moments do not apply to the deck overhangs and the adjacent regions of the deck that need to be designed taking into account the provisions of Art. A13.4.1.

For more information, refer to LRFD Appendix A4 (AASHTO 2012).

5.13.7.1.7.2 Shear: Art. C4.6.2.1.6, 5.14.4.1 Based on past design practices, slab bridges and concrete decks designed for moment are considered safe in shear. Except for unusual situations, it is not required to make checks for shear in slab-type bridges and concrete decks.

5.13.7.1.7.3 Fatigue: Art. 5.5.3, 9.5.3 Fatigue need not be investigated for decks.

5.13.7.2 Traditional Design Method

5.13.7.2.1 General

The *traditional design method* is based on flexure. This method involves designing strips of the deck slab oriented perpendicular to the longitudinal support elements (beams) as discussed in Section 4.18. Equivalent strips that span primarily in the transverse direction have no limit on their widths (Art. 4.6.2.1.3). As specified in Art. C4.6.2.1.6, in lieu of more precise calculations, the unfactored design live load moments can be taken from LRFD Table A4-1 (see appendix at the end of this chapter).

5.13.7.2.2 Applicability Criteria: Art. 9.7.3

1. The deck has four layers of reinforcement, two in each direction.
2. The deck complies with minimum depth (not less than 7.0 in.) and cover criteria (Art. 5.12.3) specified in Art. 9.7.1.1.

5.13.7.2.3 Distribution Reinforcement

Reinforcement shall be placed in the secondary direction in the bottom of slabs as a percentage of the primary reinforcement for positive moment as follows:

For primary reinforcement parallel to traffic,

$$A_{s,dist} = \frac{100}{\sqrt{S}} \leq 50 \text{ percent} \tag{5.87}$$

For primary reinforcement perpendicular to traffic,

$$A_{s,dist} = \frac{200}{\sqrt{S}} \leq 67 \text{ percent} \tag{5.88}$$

where S = effective span length taken as equal to the effective length specified in Art. 9.7.2.3 (ft).

5.13.8 Empirical Design versus Traditional Design

As illustrated later by examples in this chapter, empirical and traditional methods differ markedly in computational effort required for designing decks. The empirical method requires hardly any computational effort. To apply this design method, a designer has to simply ensure that the provisions of Art. 9.7.4 are satisfied. Once this is checked, required reinforcement is provided as specified in Art. 9.7.2.5.

The traditional method, on the other hand, is based on principles of flexure, which requires computational effort. In this method, permanent load effects are calculated in traditional manner.

www.EngineeringEBooksPdf.com

Calculation of live load bending moments is cumbersome. However, in lieu of more precise calculations, Art. C4.6.2.1.6 permits using unfactored design live load moments tabulated in LRFD Table 4.1, which is fairly simple to use. Also, based on past practices, as in the case of empirical method, shear and fatigue checks are not required for decks when using the traditional method.

5.14 DESIGN EXAMPLES

Several examples are presented herein to demonstrate the applications of LRFD provisions for the design of concrete bridges. Examples are presented for the design of a reinforced concrete slab bridge, reinforced concrete decks, a reinforced T-beam bridge, and a slab-prestressed concrete beam bridge. For each of these designs, step-by-step calculations, with references to pertinent LRFD articles and equations, have been presented.

For all bridges, loads (and their effects, *viz.*, moments and shears) are calculated separately into two categories: permanent loads (dead loads) and live loads. Permanent loads are further divided into two categories: (1) dead load of structural components (e.g., deck and girders, traffic barriers) denoted as w_{DC} and (2) dead load due to the future wearing surface (FWS) denoted as w_{WD}; this is necessary because different load factors apply to them (1.25 and 1.5, respectively, for w_{DC} and w_{DW} for the Strength I Limit State).

For computing the force effects from vehicular live loads on bridges, approximate methods specified in Section 4 of LRFD specifications (live load distribution factors for bending moment and shear specified in Arts. 4.6.2.2.2 and 4.6.2.2.3) and discussed in Chapter 4 would be used. As specified in Art. 4.6.2.2.1, the distribution of live load specified in Arts. 4.6.2.2.2 and 4.6.2.2.3 can be used if the following six conditions are satisfied:

1. Width of deck is constant.
2. Unless otherwise stated, the number of beams is not less than 4.
3. Beams are parallel and have approximately the same stiffness.
4. Unless stated otherwise, the roadway part of the overhang, d_e, does not exceed 3 ft.
5. Curvature in plan is less than the limit specified in Art. 4.6.1.2.4 (this article limits the arc span divided by the girder radius to 0.06 rad or 3.44°).
6. Cross section is constant with one of the cross sections shown in LRFD Table 4.6.2.2-1 (see this table in Chapter 4 appendix).

The earlier noted requirements are satisfied in all slab–beam examples presented in this chapter.

Example 5.1: Design of a Slab Bridge

Design a two-lane reinforced concrete slab bridge for a simple span of 48 ft between centers of bearings for which the cross section and elevation are shown in Figures 5.36 and 5.37, respectively. The clear roadway width is 28 ft between the curbs. The slab is to be provided with a 2 in.-thick nonstructural overlay, and should also have a provision of 25 lb/ft^2 for FWS. The traffic barriers are 1′–9″ wide at the base and weigh 505 lb/ft each. The bridge does not carry any utilities. The material properties are as follows:

Specified 28-day compressive strength of concrete = 4 ksi
Grade 60 reinforcement

Prepare a preliminary design for this bridge.

Solution

Art. 4.6.2.1.2 provides that slab bridges and concrete slabs spanning more than 15 ft and that span primarily in the direction parallel to traffic be designed according to the provisions of Art. 4.6.2.3.

www.EngineeringEBooksPdf.com

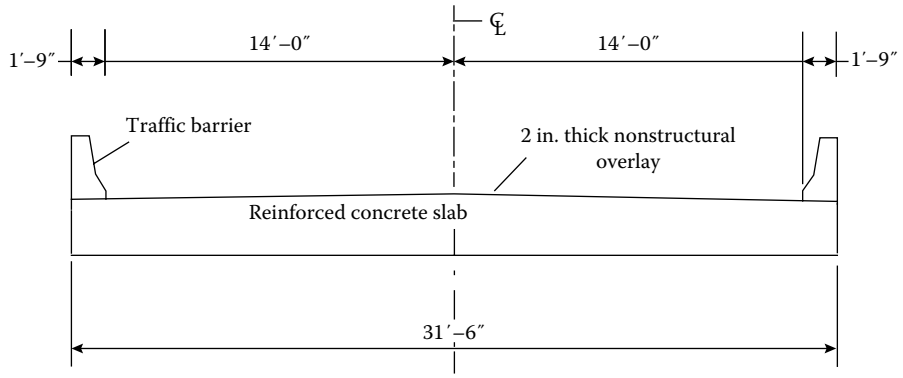

FIGURE 5.36 Cross section of the slab bridge.

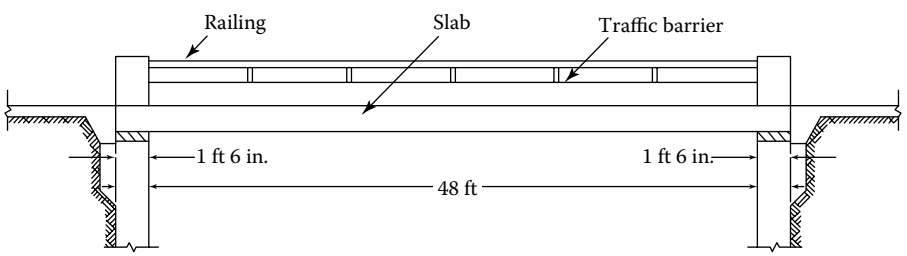

FIGURE 5.37 Elevation of the slab bridge.

Minimum Thickness of the Slab

The dead load due to the slab depends upon its thickness. The minimum thickness of the slab is governed by the optional criteria for span-to-thickness ratios as specified in Art. 2.5.2.6.3. The traditional minimum thickness for a slab with main reinforcement parallel to traffic is given as follows:

$$h_{min} = \frac{1.2S + 10}{30} \tag{5.89}$$

where S = span (ft). For 48 ft span,

$$h_{min} = \frac{1.2(48) + 10}{30}$$

$$= 2.25 \text{ ft or } 27 \text{ in.}$$

Minimum depth required = 27 in.

The design of the slab would be based on 1 ft wide strip with cross-sectional properties as follows:

Width of the strip, b = 12 in.
Overall depth of the slab, h = 27 in.
Cross-sectional area, A = 12(27) = 324 in.^{2}

Calculation of Loads

Permanent Loads (per Foot Width of Slab)

Dead load due to the slab,

$$w_{DC} = \left(\frac{27}{12}\right)(1.0)(0.15) = 0.338 \text{ kip/ft}$$

The dead weight of traffic barriers is assumed to be carried by the edge beams and would be considered in the design of edge beams.

www.EngineeringEBooksPdf.com

Dead load due to the 2 in. thick wearing surface,

$$w_{DW1} = \frac{2}{12}(1.0)(0.15)$$
$$= 0.025 \text{ kip/ft}$$

Dead load due to the FWS, w_{DW2} = 0.025(1.0) = 0.025 kip/ft

$$\text{Total } w_{DW} = 0.025 + 0.025 = 0.050 \text{ kip/ft}$$

Unfactored bending moments and shear (per unit width of the strip) are as follows:

Bending moment

$$M_{DC} = \frac{w_{DC}L^2}{8} = \frac{0.338(48)^2}{8} = 97.34 \text{ kip-ft}$$

$$M_{DW} = \frac{w_{DW}L^2}{8} = \frac{0.05(48)^2}{8} = 14.4 \text{ kip-ft}$$

Shear

$$V_{DC} = \frac{w_{DC}L}{2} = \frac{0.338(48)}{2} = 8.11 \text{kip}$$

$$V_{DW} = \frac{w_{DC}L}{2} = \frac{0.05(48)}{2} = 1.12 \text{ kip}$$

Live Load

Span = 48 ft > 40.27 ft; HL-93 design truck governs over the tandem. The maximum moment due to the design truck can be obtained from Equation 3.20:

$$M_{max,track} = 18L - 280 + \frac{392}{L}$$
$$= 18(48) - 280 + \frac{392}{48}$$
$$= 592.2 \text{ kip-ft}$$

Apply dynamic load allowance (33 percent) to the moment due to the design truck:

$$M_{LL+IM} = 592.2(1.33) = 787.6 \text{ kip-ft}$$

Moment due to design lane load, with w_{lane} = 0.64 kip/ft,

$$M_{max,lane} = \frac{wL^2}{8}$$
$$= \frac{0.64(48)^2}{8}$$
$$= 184.3 \text{ kip-ft}$$

Dynamic load allowance is not applicable to the lane load.

www.EngineeringEBooksPdf.com

Total unfactored moment due to the live load,

$$M_{total} = M_{truck} + M_{lane}$$

$$= 787.6 + 184.3$$

$$= 971.9 \text{ kip-ft} \approx 972.0 \text{ kip-ft}$$

Shear due to live load:

For $L > 41.6$ ft, design truck governs. From Table 3.13, for $x/L = 0–0.5$,

$$V_x = \frac{72}{L}(L - x - 9.33)$$

The maximum shear due to the design truck occurs near the support with the real 32-axle load over the left support:

$$V_{max} = \frac{72}{48}(L - 0 - 9.33)$$

$$= 58.0 \text{ kip}$$

Apply dynamic load allowance (33 percent) to the shear due to the design truck:

$$V_{LL+IM} = 58.0(1.33) = 77.14 \text{ kip}$$

Shear due to the lane load,

$$V_{lane} = \frac{w_{lane}L}{2}$$

$$= \frac{0.64(48)}{2}$$

$$= 15.36 \text{ kip}$$

Total unfactored shear due to live load = 77.14 + 15.36 = 92.5 kip.

The design of the slab bridge will be presented in two parts:

Part I: Design of the interior strip
Part II: Design of the edge beams

Part I: Design of the Interior Strip

1. Determine the equivalent strip width: Art. 4.6.2.3

For slab-type bridges, the width of equivalent strip depends on the number of design lanes on the bridge (see discussion in Chapter 4 for the details of the width of equivalent strip given by Equations 4.44 and 4.45).

Number of design lanes
Number of design lanes (Art. 3.6.1.1.1),

$$N_L = \frac{Clear\,roadway\ width}{12} = \frac{28}{12} = 2.33$$

Use the integer part of 2.33, $N_L = 2$

www.EngineeringEBooksPdf.com

Case 1: One design lane loaded

$$E_{1design\,lane} = 10.0 + 5\sqrt{L_1 W_1} \qquad (4.44)\ [A4.6.2.3\text{-}1]$$

Case 2: For more than one design lane loaded

$$E_{1+design\,lanes} = 84.0 + 1.44\sqrt{L_1 W_1} \le \frac{12.0W}{N_L} \qquad (4.45)\ [A4.6.2.3\text{-}2]$$

where

L_1 = modified span length taken equal to the lesser of the actual span or 60 ft (ft)
W_1 = modified edge-to-edge width of the bridge taken equal to the lesser of the actual width of the bridge or 60 ft for multilane loading or 30 ft for single lane loading (ft)
W = physical edge-to-edge width of the bridge (ft)
N_L = number of design lanes as specified in Art. 3.6.1.1.1 (use integer value)

The smaller of the two widths of the equivalent strips given by Equations 4.44 and 4.45 will be used (because it would result in higher design live load forces). For the present case,

$$L_1 = 48 \text{ ft}, \quad W_1 = W = 28 + 2(\text{base width of the traffic barrier})$$

$$= 28.0 + 2(1.75) = 31.5 \text{ ft}$$

For one design lane loaded:

$$E_{1design\,lane} = 10.0 + 5\sqrt{L_1 W_1}$$

$$= 10.0 + 5.0\sqrt{48(31.5)}$$

$$= 204.4 \text{ in.} = 17.04 \text{ ft} \approx 17 \text{ ft}$$

For more than one design lane loaded:

$$E_{1+design\,lanes} = 84.0 + 1.44\sqrt{L_1 W_1} \le \frac{12.0W}{N_L}$$

$$= 84.0 + 1.44\sqrt{(48)(31.5)} \le \frac{12.0(31.5)}{2}$$

$$= 140.0 \le 189 \text{ in.}$$

$$E = 140 \text{ in.} < 204.4 \text{ in.}$$

$$\text{Use } E = 140 \text{ in.} = 11.67 \text{ ft}$$

The widths of the equivalent strips would be used as follows to calculate the force effects:

1. Force effects due to both permanent loads and the live loads would be divided by E = 11.67 ft (two design lanes loaded case) to obtain force effects per foot width of the strip, which would be designed as a beam of unit width spanning 48 ft.
2. Force effects due to fatigue truck would be divided by E = 17.0 ft (one design lane loaded case) to obtain force effects per foot width of the strip.

Unfactored live load force effects per unit width of the equivalent strip are as follows:

$$M_{LL+IM} = \frac{972.0}{11.67} = 83.3 \text{ kip-ft}$$

$$V_{LL+IM} = \frac{92.5}{11.67} = 7.93 \text{ kip}$$

www.EngineeringEBooksPdf.com

Strength I Limit State: Factored Moments and Shear

$$Q_u = \Sigma\eta_i\gamma_i Q_i \tag{A3.4.11}$$

where

η_i = load modifier (= products of modifiers due to ductility η_D, redundancy η_R, and operational importance η_i as specified in Art. 3.4.1-1)

γ_i = load factor

Q_i = force effects from loads

For this example, $\eta_i = \eta_D\eta_R\eta_i = 1.0$.

$$\begin{aligned} M_u &= 1.0[1.25M_{DC} + 1.5M_{DW} + 1.75M_{LL+IM}] \\ &= 1.0[1.25(97.34 + 1.5(14.4) + 1.75(83.3)] \\ &= 289 \text{ kip-ft} \end{aligned}$$

$$\begin{aligned} V_u &= 1.0[1.25M_{DC} + 1.5M_{DW} + 1.75M_{LL+IM}] \\ &= 1.0[1.25(8.11 + 1.5(1.2) + 1.75(7.93)] \\ &= 25.82 \text{ kip} \end{aligned}$$

Strength of the Trial Section for the Strength Limit State

Check the strength of the trial section of the equivalent strip (12 in. × 27 in.). Assume trial reinforcement of No. 9 Grade 60 bars at 6 in. on center (o.c.) for longitudinal reinforcement; A_s = 2.0 in.^{2} (Figure 5.38).

Bottom cover for reinforcement in cast-in-place slabs = 1.0 in. (LRFD Table A5.12.3-1).

$$\begin{aligned} d_s &= h - \text{clear cover} - 0.5(\text{bar diameter}) \\ &= 27 - 1.0 - 0.5(1.128) \\ &= 25.44 \text{ in.} \end{aligned}$$

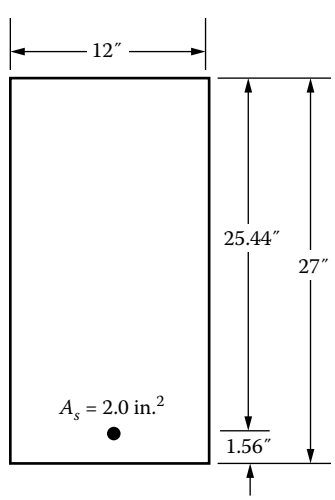

FIGURE 5.38 Trial section of the equivalent strip.

www.EngineeringEBooksPdf.com

For rectangular section behavior, the neutral axis can be located from Equation A5.7.3.1.1-4:

$$c = \frac{A_{ps}f_{pu} + A_s f_s - A'_s f'_s}{0.85 f'_c \beta_1 b + k A_{ps} \dfrac{f_{pu}}{d_p}}$$

For the present case of section with only nonprestressed reinforcement, $A_{ps} = 0$, and for singly reinforced section, $A'_s f'_s = 0$. Therefore,

$$c = \frac{A_s f_s}{0.85 f'_c \beta_1 b}$$

For the present case, $A_s = 2.0$ in.^{2}, $f_s = f_y = 60$ ksi, $f'_c = 4.0$ ksi, $b = 12$ in., and $\beta_1 = 0.85$ for 4 ksi concrete. Therefore,

$$c = \frac{2.0(60)}{0.85(4.0)(0.85)(12)} = 3.46 \text{ in.}$$

Depth of compression block, a, is determined to be

$$a = 0.85c = 0.86(3.46) = 2.94 \text{ in.}$$

$$\begin{aligned} M_n &= A_s f_y \left(d_s - \frac{a}{2} \right) \\ &= 20(60)\left(25.44 - \frac{2.94}{2} \right) \\ &= 2876.4 \text{ kip-in.} = 240 \text{ kip-ft} \end{aligned}$$

Calculate the resistance factor for flexure, ϕ: Art. 5.7.2.1.

Determine the strain in the longitudinal reinforcement from strain distribution (Figure 5.39):

$$\begin{aligned} \varepsilon_s &= \left(\frac{d_s - c}{c} \right)(\varepsilon_c) \\ &= \left(\frac{25.44 - 3.46}{3.46} \right)(0.003) \\ &= 0.19 > 0.005 \end{aligned}$$

Therefore, the section is tension-controlled and $\phi = 0.9$.

$$\phi M_n = 0.9(240) = 216 \text{ kip-ft} < M_u = 289 \text{ kip-ft, n.g.}$$

The section must be revised to increase flexural resistance.

www.EngineeringEBooksPdf.com

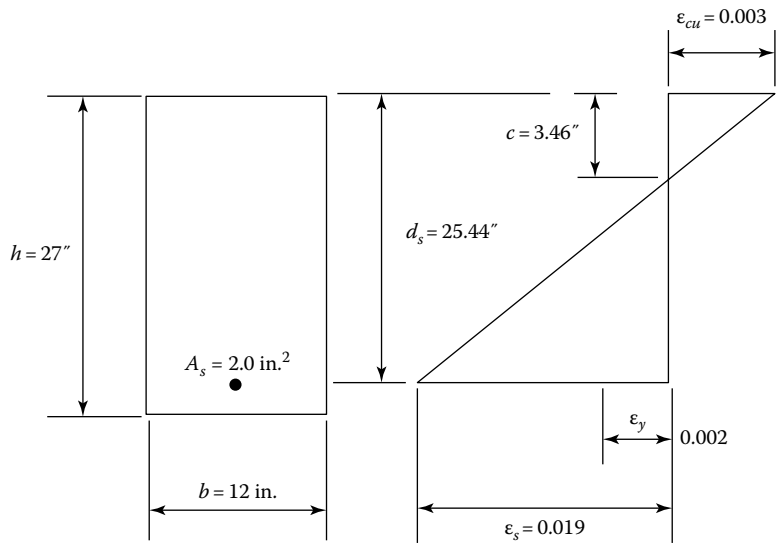

FIGURE 5.39 Strain distribution in the equivalent strip.

Alternatively, the amount of required longitudinal reinforcement can be estimated from Equation 5.86:

$$A_{s,est.} = \frac{M}{4d}$$

where
A_s = area of longitudinal (tensile) reinforcement (in.^{2})
M = design moment (kip-ft)
d = depth from the extreme compression fibers to the centroid of tensile reinforcement (in.)

For the present case, $M = 289$ kip-ft and $d = 25.44$ in.

$$A_{s,est.} = \frac{289}{4(25.44)} = 2.84 \text{ in.}^2$$

Try No. 11 bars at 6 in. o.c., $A_s = 3.12$ in.^{2}, diameter of bar = 1.41 in.

$$d_s = 27 - 1.0 - 0.5(1.41) = 25.3 \text{ in. (Figure 5.40)}$$

Calculate the location of neutral axis from Equations 5.17 and 5.22:

$$c = \frac{3.12(60)}{0.85(0.85)(4.0)(12)} = 5.4 \text{ in.}$$

Depth of compression block,

$$a = 0.85c = 0.85(5.4) = 4.59 \text{ in.}$$

www.EngineeringEBooksPdf.com

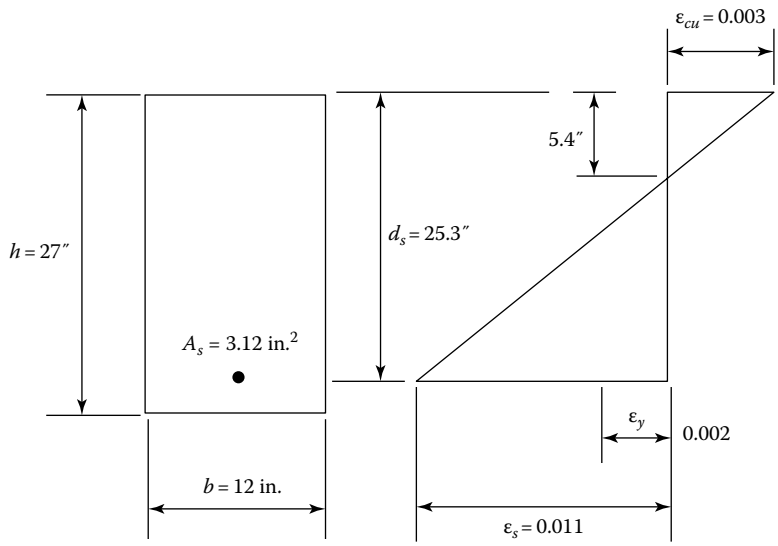

FIGURE 5.40 Cross section of unit equivalent strip.

$$a = 0.85c = 0.86(5.4) = 4.59 \text{ in.}$$

$$M_n = A_s f_y \left(d_s - \frac{a}{2} \right)$$

$$= 3.12(60)\left(25.3 - \frac{4.59}{2} \right)$$

$$= 4306.5 \text{ kip-in.} = 359 \text{ kip-ft}$$

Calculate the resistance factor for flexure, ϕ: Art. 5.7.2.1.

Determine the strain in the longitudinal reinforcement from strain distribution (Figure 5.40):

$$\varepsilon_s = \left(\frac{d_s - c}{c} \right)(\varepsilon_c)$$

$$= \left(\frac{25.3 - 5.4}{5.4} \right)(0.003)$$

$$= 0.011 > 0.005$$

Therefore, the section is tension controlled and $\phi = 0.9$.

$$\phi M_n = 0.9(359) = 323 \text{ kip-ft} > M_u = 289 \text{ kip-ft, OK}$$

Check for Minimum Reinforcement: Art. 5.7.3.3.2

Minimum reinforcement shall be adequate to develop a factored flexural resistance, M_r, at least equal to the lesser of the following:

1. 1.33 times the factored moment required by the applicable strength load combination specified in Art. 3.4.1-1.

www.EngineeringEBooksPdf.com

2. The cracking moment of the section, M_{cr}, as determined from Equation 5.41:

$$M_{cr} = \gamma_3 \left[(\gamma_1 f_r + \gamma_2 f_{cpe}) S_c - M_{dnc} \left(\frac{S_c}{S_{nc}} - 1 \right) \right] \qquad (5.41)\ [A5.7.3.3.2\text{-}1]$$

where
γ_1 = 1.6 for all other structures
γ_2 = prestress variability = 0 for nonprestressed members
γ_3 = 0.75 for A706, Grade 60 reinforcement

For the interior strip in this example, $f_{cpe} = 0$ (nonprestressed section) and $S_c = S_{nc}$ (noncomposite section). Therefore,

$$M_{cr} = \gamma_3 \gamma_1 f_r S_{nc}$$

With γ_1 = 1.6 (for all other structures), γ_3 = 0.75 for A706, Grade 60 reinforcement,

$$M_{cr} = 0.75(1.6)\, f_r S_{nc} = 1.2 f_r S_{nc} \qquad (5.44)$$

where S_{nc} = section modulus of the noncomposite section.

For a rectangular section,

$$S_{nc} = \frac{bh^2}{6} = \frac{12(27)^2}{6} = 1458 \text{ in.}^3$$

$$f_r = 0.24\sqrt{f'_c} = 0.24\sqrt{4} = 0.48 \text{ ksi} \qquad (\text{Art. } 5.4.2.6)$$

$$M_{cr} = 1.2 f_r S_c = 1.2(0.48)(1458) = 840 \text{ kip-in.} = 70 \text{ kip-ft}$$

$$1.33 M_u = 1.33(289) = 384 \text{ kip-ft} > M_{cr} = 70 \text{ kip-ft (governs)}$$

$$M_r = \phi M_n = 323 \text{ kip-ft} > 70 \text{ kip-ft, OK}$$

Control of Cracking: Art. 5.7.3.4

The spacing of reinforcement closest to the tension face shall satisfy the following:

$$s = \frac{700\gamma_e}{\beta_s f_{ss}} - 2d_c \qquad (5.45)\ [A5.7.3.4\text{-}1]$$

where

$$\beta_s = 1 + \frac{d_c}{0.7(h - d_e)} \qquad (5.46)$$

γ_e = exposure factor
= 1.00 for Class 1 exposure
= 0.75 for Class 2 exposure
d_c = thickness of concrete cover measured from the extreme fiber to center of the flexural reinforcement located closest thereto
f_{ss} = tensile stress in steel reinforcement at the service limit state (ksi)
h = overall thickness or depth of the component (in.)

www.EngineeringEBooksPdf.com

In this example,

$$d_c = 1.0 + 0.5(1.41) = 1.71 \text{ in.}$$

$$\beta_s = 1 + \frac{d_c}{0.7(h - d_c)} = 1 + \frac{1.71}{0.7(27 - 1.71)} = 1.10$$

Calculate the tensile stress, f_{ss}, in the longitudinal reinforcement at the service limit state. The moment at the service limit state is

$$\begin{aligned} M_s &= 1.0[1.0M_{DC} + 1.0M_{DW} + 1.0M_{LL+IM}] \\ &= 1.0[1.0(97.34) + 1.0(14.4) + 1.0(83.3)] \\ &= 195 \text{ kip-ft} \end{aligned}$$

Compressive stress in concrete, f_c (based on uncracked section),

$$f_c = \frac{M}{S} = \frac{6M}{bh^2} = \frac{6(195)(12)}{12(27)^2} = 1.6 \text{ ksi}$$

$$0.8f_r = 0.8(0.24)\sqrt{f_c'} = 0.8(0.24)\sqrt{4} = 0.384 \text{ ksi}$$

Since $f_c > 0.8f_r = 0.384$ ksi, the section must be cracked. Perform the cracked section analysis of the section.

Locate the neutral axis using the transformed section of the equivalent strip (Figure 5.41). Take moments about the neutral axis,

$$\frac{1}{2}(b)(kd)^2 = nA_s(d - kd) \tag{5.48}$$

Substitute $\rho = A_s/bd$ so that $A_s = \rho bd$, where ρ = percentage of steel expressed as the ratio of tension reinforcement to cross-sectional area, bd. With these substitutions, Equation 5.48 can be simplified and expressed as a quadratic in k:

$$k^2 = 2kn\rho d^2 - 2n\rho d^2 = 0 \tag{5.49}$$

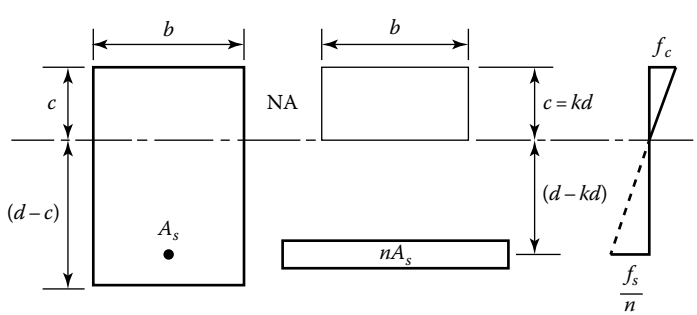

FIGURE 5.41 Transformed section of the equivalent strip.

www.EngineeringEBooksPdf.com

The solution of Equation 5.49 is given as follows:

$$k = \sqrt{(n\rho)^2 + 2n\rho} - n\rho \tag{5.50}$$

For the given section, $b = 12$ in., $d_s = 25.3$ in., $n = 8$, $\rho = A_s/bd = 3.12/12(25.3) = 0.01028$, and $n\rho = 0.08224$.

Substitution of these values in Equation 5.50 yields

$$k = \sqrt{(0.08224)^2 + 2(0.08224)} - 0.08224 = 0.3316$$

$$c = kd = 0.3316(25.3) = 8.39 \text{ in.}$$

Alternatively, the values of k can be determined from Table 5.A.4. By interpolation for $n\rho = 0.08224$, one obtains $k = 0.3315$, $kd = 0.3315(25.3) = 8.39$ in. The moment of inertia of the cracked section (Figure 5.41), I_{cr}, is given as follows:

$$I_{cr} = \frac{1}{3}bc^3 + nA_s(d-c)^2 \tag{5.90}$$

$$I_{cr} = \frac{1}{3}(12)(8.39)^3 + 8(3.12)(25.3 - 8.39)^2$$

$$= 9500 \text{ in.}^4$$

Stress in steel at service limit state can be found from conventional formula:

$$\frac{f_s}{n} = \frac{M(d_s - c)}{I_{cr}} = \frac{195(12)(25.3 - 8.39)}{9500} = 4.17 \text{ ksi}$$

$$f_s = n(4.17) = 8(4.17) = 33.36 \text{ ksi}$$

$$0.6f_y = 0.6(60) = 36 \text{ ksi}$$

$$f_s = 33.36 \text{ ksi} < 0.6f_y = 36 \text{ ksi, OK}$$

$$s \le \frac{700\gamma_e}{\beta_s f_{ss}} - 2d_c = \frac{700(0.75)}{1.10(33.36)} - 2(1.71) = 10.9 \text{ in.}$$

Spacing provided = 6 in. o.c. < 10.9 in., OK

Distribution Reinforcement: Art. 5.14.4.1

Amount of bottom reinforcement,

$$A_{s,dist} = \frac{100}{\sqrt{S}} \le 50 \text{ percent}$$

$$= \frac{100}{\sqrt{48}} = 14.43 \text{ percent} \le 50 \text{ percent} \tag{5.87}$$

Positive tensile reinforcement, $A_s = 3.12$ in.^{2}

$$A_{s,\,dist} = 0.1443(3.12) = 0.45 \text{ in.}^2$$

Provide No. 5 at 8 in. o.c., $A_s = 0.46$ in.^{2}

www.EngineeringEBooksPdf.com

Shrinkage and Temperature Reinforcement: Art. 5.10.8
The area of bars or welded wire fabric reinforcement per foot on each side and each direction shall satisfy the following:

$$A_s \geq \frac{1.30bh}{2(b+h)f_y} \qquad (5.91)\ [A5.10.8.1]$$

$$0.11 \leq A_s \leq 0.60 \text{ in.}^2 \qquad (5.92)\ [A5.10.8.2]$$

$$A_s \geq \frac{1.30bh}{2(b+h)f_y} = \frac{1.30(12)(27)}{2(12+27)(60)} = 0.09 \text{ in.}^2$$

$$0.09 < 0.11 \text{ in.};\ A_s = 0.11 \text{ in.}^2 \text{ (governs)}$$

$$s_{max} = 3h = 3(27) = 81 \text{ in. or } 18 \text{ in.}$$

Provide No. 4 at 18 in. o.c., $A_s = 0.13$ in.^{2}

Note that No. 3 at 12 in. o.c. ($A_s = 0.12$ in.^{2}) would also satisfy the reinforcement requirement. But No. 4 bars are preferred over No. 3 bars as the larger bars would provide sturdiness to the reinforcement mat so necessary for the walking construction crew and concrete pouring operations.

Fatigue: Art. 5.5.3
Maximum Fatigue Moment
Only one design truck with a fixed distance of 30 ft between the 32 kip axles will be placed on the bridge to calculate moment for fatigue investigation. Because of the span limitation, the fatigue design truck will be placed on the bridge as shown in Figure 5.42 for maximum moment (the center line of the girder bisects the distance between the resultant of the front and the middle axle and the 32-axle load, R). The influence line ordinations are computed as follows:

$$y_1 = \frac{ab}{L} = \frac{25.4(22.6)}{48} = 11.96 \text{ ft}$$

$$y_2 = \left(\frac{11.4}{25.4}\right)(11.96) = 5.37 \text{ ft}$$

$$M_{max,fat} = 32(11.96) + 8(5.37) = 425.68 \text{ kip-ft}$$

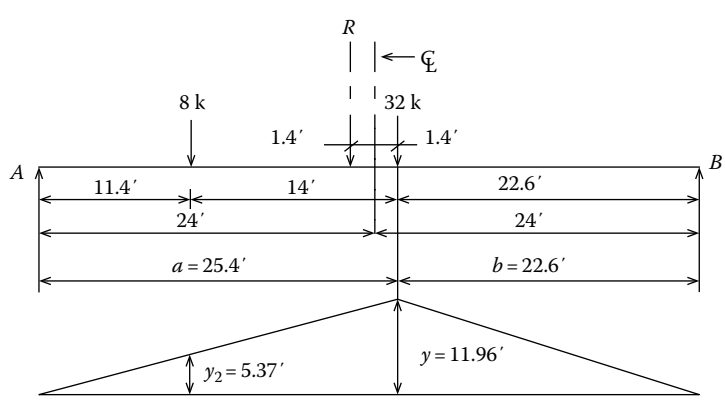

FIGURE 5.42 Influence line for maximum moment under the 32-kip axle of the fatigue truck.

www.EngineeringEBooksPdf.com

Width of the equivalent strip for one design lane loaded case, $E_{1,lane}$ = 17 ft (computed earlier)
Moment per foot width of the equivalent strip,

$$M_{fat} = \frac{425.68}{17} = 25.04 \text{ kip-ft}$$

Dynamic load allowance for fatigue = 15 percent

$$M_{fat,\ LL+IM} = 1.15(28.9) = 43.35 \text{ kip-ft}$$

Art. 5.5.3.1 specifies the following for fatigue investigation:

1. In regions of compressive stress due to permanent loads and prestress in reinforced concrete components, fatigue shall be considered only if this compressive stress is less than the maximum tensile stress resulting from Fatigue I Load Combination as specified in LRFD Table 3.4.1-1 in combinations with the provisions of Art. 3.6.1.4.
2. The section properties for fatigue investigation shall be based on cracked sections where the sum of the stresses due to unfactored permanent loads and prestress and the Fatigue I Load Combination is tensile and exceeds 0.095 $\sqrt{f'_c}$.

From previous calculations for service load analysis, calculate the stresses due to Fatigue I Load Combination:

$$M_{fat\ 1\ load\ comb} = 1.0M_{DC} + 1.0M_{DW} + 1.5M_{fat}$$

$$= 1.0(97.34 + 1.0(14.4) + 1.5(28.8)$$

$$= 155 \text{ kip-ft}$$

For the uncracked section, the section modulus (of the gross section) is

$$S = \frac{bh^2}{6} = \frac{12(27)^2}{6} = 1458 \text{ in.}^3$$

Tensile stress (in the bottom fibers) due to Fatigue I Load Combination,

$$f_{fat} = \frac{M_{fat}}{S} = \frac{155(12)}{1458} = 1.28 \text{ ksi}$$

$$0.095\sqrt{f'_c} = 0.095\sqrt{4.0} = 0.19 \text{ ksi} < f_{fat} = 1.28 \text{ ksi}$$

Therefore, cracked section analysis will be used for fatigue load investigation.

From previous calculations for the cracked analysis, k = 0.3316, kd = 8.39 in.

$$j = 1 - \frac{k}{3} = 1 - \frac{0.3316}{3} = 0.8895$$

The tensile stress in bottom reinforcement is calculated for the infinite fatigue life (Fatigue 1) for which the load factor is 1.5 (LRFD Table 3.4.1-1).

$$f_{s,fat} = \frac{M}{A_s jd} = \frac{1.5(28.8)(12)}{3.12(0.8895)(25.3)} = 7.38 \text{ ksi}$$

www.EngineeringEBooksPdf.com

Stresses in the Reinforcing Bars due to Fatigue: Art. 5.5.3.2

Art. 5.5.3.2 specifies that the constant-amplitude fatigue threshold, $(\Delta F)_{TH}$, for straight reinforcing bars and welded wire reinforcement without a cross weld in the high-stress region shall be taken as follows:

$$(\Delta F)_{TH} = 24 - 0.33 f_{min} \qquad (5.93)\ [A5.5.3.2\text{-}1]$$

where f_{min} = minimum live load stress resulting from the Fatigue I Load Combination, combined with the more severe stress from either the permanent loads or the permanent loads, shrinkage, and creep-induced external loads; positive if tension, negative if compression (ksi).

Calculate stress due to permanent loads:

$$M_{perm} = M_{DC} + M_{DW} = 97.34 + 14.4 = 111.74 \text{ kip-ft}$$

$$f_{s,perm} = \frac{M}{A_s jd} = \frac{(111.74)(12)}{3.12(0.8895)(25.3)} = 19.1 \text{ ksi}$$

$$f_{min} = +19.1 \text{ ksi (tension)}$$

$$(\Delta F)_{TH} = 24 - 0.33 f_{min}$$
$$= 24 - 0.33(+19.1)$$
$$= 17.7 \text{ ksi}$$

$$f_{s,fat} = 7.38 \text{ ksi} < (\Delta F)_{TH} = 17.7 \text{ ksi, OK}$$

The stress in tension reinforcement due to fatigue is less than the constant-amplitude threshold, $(\Delta F)_{TH}$.

Deformations: Art. 5.7.3.6

Deformation and Camber: Art. 5.7.3.6.2

Permanent deformation and camber would be determined based on the entire slab considered as on beam. Permanent loads are recomputed for the entire slab width as follows:

$$w_{DC} = 0.338 \text{ kip/ft (computed earlier)}$$

Dead load due to the traffic barriers = 0.505 kip/ft each

Overall width of the slab = clear roadway + 2(base width of traffic barriers)

= 28 + 2(1.75) = 31.5 ft

Total permanent load = 0.338(31.5) + 2(0.505) = 11.68 kip/ft

$$w_{DW} = 0.05 \text{ kip/ft}$$

Width of the roadway = 28 ft

Total load, w_{DW} = 0.05(28) = 1.4 kip/ft

Total dead load, w_{DL} = 11.68 + 1.4 = 13.08 kip/ft

$$M_{DC} = \frac{w_{DW} L^2}{8} = \frac{13.08(48)^2}{8} = 3767 \text{ kip-ft}$$

www.EngineeringEBooksPdf.com

The maximum deflection due to the dead load can be calculated in the following (Case 1, AISC 2011), by substituting E_cI_e for EI:

$$\Delta_{DL} = \frac{5w_{DL}L^4}{384E_cI_e} \tag{5.94}$$

The effective moment of inertia, I_e, in Equation 5.94 is calculated as follows:

$$I_e = \left(\frac{M_{cr}}{M_a}\right)^3 I_g + \left[1 - \left(\frac{M_{cr}}{M_a}\right)^3\right] I_{cr} \le I_g \qquad \text{(5.55) [A5.7.3.6.2-1]}$$

where

M_{cr} = moment of inertia of cracked section
M_a = applied moment at the stage for which deformation is being determined
I_g = moment of inertia of gross section

$$M_{cr} = f_r\left(\frac{I_g}{y_t}\right) \qquad \text{(5.56) [A5.7.3.6.2-2]}$$

Consider the entire width of the bridge equal to b for computing the gross moment of inertia, I_g:

$$I_g = \frac{bh^3}{12} = \frac{31.5(12)(27)^3}{12} = 620{,}015 \text{ in.}^4$$

$$f_r = 0.24\sqrt{f'_c} = 0.24\sqrt{4} = 0.48 \text{ ksi}$$

$$y_t = \frac{27}{2} = 13.5 \text{ in.}$$

$$M_{cr} = 0.48\left(\frac{620{,}015}{13.5}\right)\left(\frac{1}{12}\right) = 1837 \text{ kip-ft}$$

$$M_a = M_{DL} = 3767 \text{ kip-ft (computed earlier)}$$

For unit width of equivalent strip, the moment of inertia of the cracked section = 9500 in.^{4} (computed earlier). For the entire width of the slab, b = 31.5 ft, so the moment of inertia of the cracked section is computed to be

$$I_{cr} = (9500)(31.5) = 299{,}250 \text{ in.}^4$$

$$I_e = \left(\frac{1837}{3767}\right)^3 (620{,}015) + \left[1 - \left(\frac{1837}{3767}\right)^3\right](299{,}250) \le 620{,}015 \text{ in.}^4$$

$$I_e = 336{,}448 \text{ in.}^4 < 620.015 \text{ in.}^4\text{, OK}$$

www.EngineeringEBooksPdf.com

$$E_c = 33{,}000 K_1 w_c^{1.5} \sqrt{f'_c} \qquad (5.8)\ [A5.4.2.4.1]$$

$$E_c = 33{,}000(1.0)(0.145)^{1.5}\sqrt{4.0} = 3644 \text{ ksi}$$

$$\Delta_{DL} = \frac{5(13.08)(48)^4}{384(3{,}644)(336{,}448)}(12)^3 = 1.27 \text{ in.}$$

Instantaneous deflection = 1.27 in.

Compute dead load deflection based on the gross moment of inertia, I_g = 620,015 in.^{4},

$$\Delta_{DL} = 1.27\left(\frac{336{,}448}{620{,}015}\right) = 0.69 \text{ in.}$$

Provisions for long-term deflections (to account for the effects of creep), as specified in Art. 5.7.6.3.2, were discussed in Section 4.18.4.3. The long-term deflection is computed by multiplying instantaneous deflection by the long-term deflection multipliers as follows:

For deflection based on gross moment of inertia, long-term deflection factor = 4.0.
Long-term deflection based on gross moment inertia, Δ_{LT} = 4(0.69) = 2.76 in.

When the instantaneous deflection is computed based on the effective moment of inertia, the long-term deflection factor is computed as follows:

$$\text{Long-term deflection factor} = 3 - 1.2\left(\frac{A'_s}{A_s}\right) \geq 1.6 \qquad (5.95)$$

where
A'_s = area of compression reinforcement
A_s = area of tension reinforcement

For this example, there is no compression reinforcement, $A'_s = 0$; therefore,

Long-term deflection factor = 3 − 1.2(0) = 3.0 ≥ 1.6, OK

Required camber = $3(\Delta_{DL})$ = 3(1.27) = 3.81 in. ≈ 3⅞ in.

The estimated long-term deflection based on the effective moment of inertia is larger (3.81 in.) than that based on the gross moment of inertia (2.76 in.). In view of the approximations involved in estimating long-term deflection, provide a camber of 3⅞ in.

Live Load Deflection: Optional Criteria: Art. 2.5.2.6.2

1. Optional Live Load-Deflection Control
   Since no deflection criteria are specified, optional deflection criteria (Art. 2.6.2.6.2) will be used in this example.

$$\text{Allowable deflection due to vehicular load, } \Delta_{LL} = \frac{span}{800} = \frac{48(12)}{800} = 0.72 \text{ in.}$$

www.EngineeringEBooksPdf.com

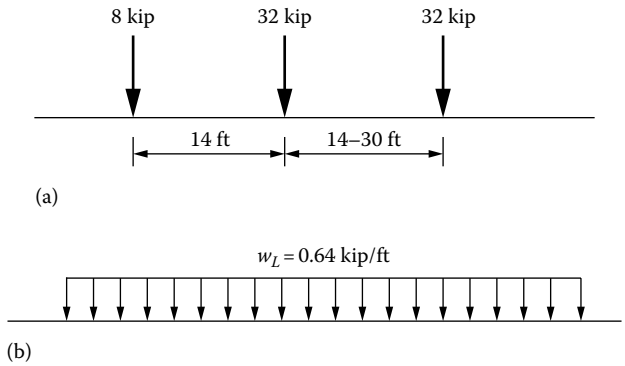

FIGURE 5.43 HL-93 live loads: (a) design truck and (b) lane load.

Art. 3.6.1.3.2: Calculated deflection will be taken as the larger of the following as discussed in Section 2.6.3:

1. Deflection due to design truck alone. Dynamic load allowance will be applied to this deflection.
2. Deflection due to 25 percent of the deflection due to the design truck *plus* deflection due to lane load. Dynamic load allowance is not applied to the deflection due to the lane load.

Calculate deflection due to vehicular live load.
Live load-deflections would be computed for the governing loading conditions—separately for the design truck and lane (Figure 5.43)—by the usual methods of computing deflections. Tandem load does not govern for a span of 48 ft. Formulas for relevant load cases given in AISC *Steel Construction Manual* (AISC 2011) would be used (see discussion in Section 2.6.6). Referenced formulas used in calculations are taken from Chapter 2.

Deflection Due to Design Truck
Calculate the effective moment of inertia:
The effective moment of inertia, I_e, depends on the applied moment, M_a. Calculate the effective moment of inertia of the slab, I_e, for the position of the design truck selected to determine the maximum deflection as shown in Figure 3.48 (Chapter 3, the middle 32-axle load is placed at 2.33 ft right of the centerline of the bridge).

M_{DC} = 3767 kip-ft (computed earlier)
Due to one design truck, M_{LL+IM} = 787.6 kip-ft (computed earlier)
Multiple presence factor, m = 1.0 (LRFD Table 3.6.1.1.2-1)

Due to two design trucks on the bridge,

$$M_{LL+IM} = 2(1.0)(787.6) = 1575.2 \text{ kip-ft} \approx 1575 \text{ kip-ft}$$

$$M_a = M_{DC} + M_{LL+IM} = 3767 + 1575 = 5342 \text{ kip-ft}$$

$$I_e = \left(\frac{M_{cr}}{M_a}\right)^3 I_g + \left[1 - \left(\frac{M_{cr}}{M_a}\right)^3\right] I_{cr} \le I_g \qquad (5.55)\ [A5.7.3.6.2\text{-}1]$$

$$I_e = \left(\frac{1{,}837}{5{,}342}\right)^3 (620{,}015) + \left[1 - \left(\frac{1{,}837}{5{,}342}\right)^3\right](299{,}250) \le 620{,}015 \text{ in.}^4$$

$$I_e = 312{,}293 \text{ in.}^4 < 620{,}015 \text{ in.}^4, \text{ OK}$$

Modulus of elasticity of concrete, E_c = 3644 ksi (calculated earlier).

www.EngineeringEBooksPdf.com

As discussed in Section 2.6.6, in the case of the design truck loading, it is difficult, although theoretically possible, to determine the exact positions of the three moving loads that will result in maximum deflection in the beam. As a practical matter, however, the maximum deflection in the slab can be computed by placing the middle 32-kip load at the center of the span and the other two loads (8-kip and 32-kip loads) placed at 14 ft from the midspan, one on the left and the other on the right side of the centerline of the span (Figure 5.44a). This load case can be split into two separate cases (AISC 2011) as shown in Figure 5.44:

a. Load Case 7 for the centrally placed point load
b. Load Case 8 for point loads placed at any point on the span

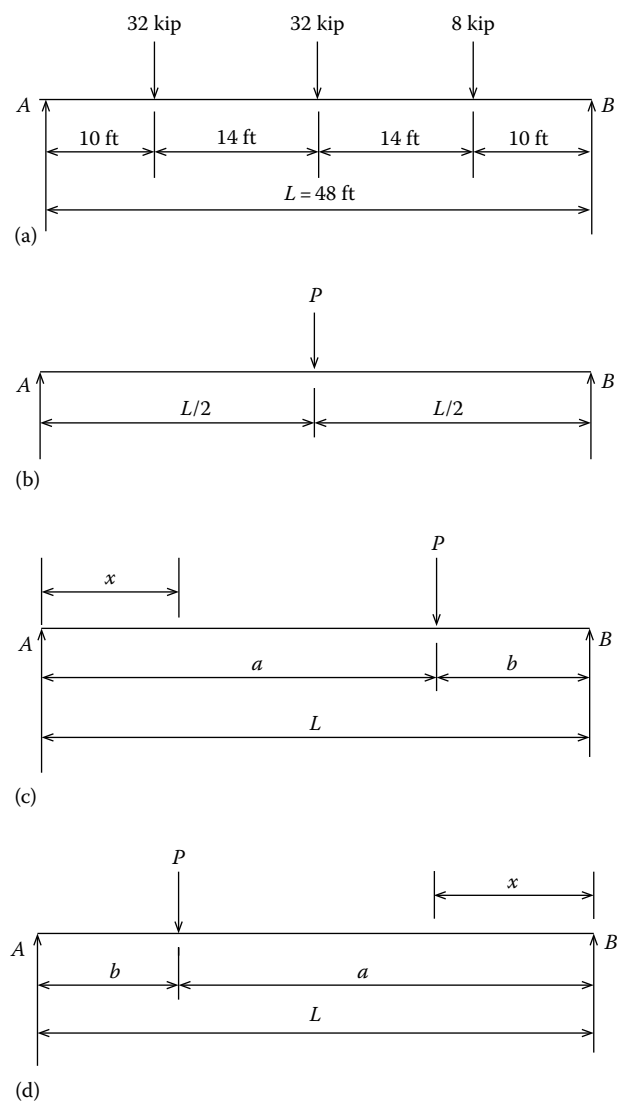

FIGURE 5.44 (a) Assumed position of the design truck for maximum deflection at midspan; (b) point load at center, $x = L/2$; (c) point load right of midspan, distance x measured from A, $x < a$; (d) point load left of midspan, distance x measured from B, $x < a$.

www.EngineeringEBooksPdf.com

Deflection Due to the Design Truck

Deflection due to the three axle loads would be computed separately. The middle 32-kip axle load is placed at the midspan (Load Case 7, Figure 5.22b). The maximum deflection for this case can be calculated in the following (by substituting E_cI_e for EI in Equation 2.2):

$$\Delta_c = \frac{PL^3}{48E_cI_e} \tag{5.96}$$

where

Δ_c = deflection at midspan due to point load
L = span = 48 ft
E_c = modulus of elasticity of concrete = 3644 ksi
I_e = effective moment of inertia = 312,293 in.^{4}

$$\Delta_c = \frac{PL^3}{48E_cI_e} = \frac{32(48)^3}{48(3,644)(312,293)}(12)^3 = 0.11\,\text{in.}$$

For the remaining 32-kip and 8-kip loads, use AISC (2011) Load Case 8. The deflection at a distance x (when $x < a$) from the left support can be calculated as follows:

$$\Delta_x = \frac{Pbx\left(L^2 - b^2 - x^2\right)}{6EIL} \tag{2.3}$$

1. For the 8-kip load, choose origin at A, so that

$$P = 8\text{ kip},\quad a = 38\text{ ft},\quad b = 10\text{ ft},\quad x = L/2 = 24\text{ ft} < a = 38\text{ ft}.$$

$$\Delta_{x=24\text{ ft}} = \frac{8.0(10)(24)\left[(48)^2 - (10)^2 - (24)^2\right]}{6(3,644)(312,293)(48)}(12)^3 = 0.016\text{ in.}$$

2. For the rear 32-kip load, choose origin at B, so that

$$P = 32\text{ kip},\quad a = 38\text{ ft},\quad b = 10\text{ ft},\quad x = 24\text{ ft} < a = 38\text{ ft}$$

$$\Delta_{x=24\text{ ft}} = \frac{32(10)(24)\left[(48)^2 - (10)^2 - (24)^2\right]}{6(3,644)(312,293)(48)}(12)^3 = 0.066\text{ in.}$$

Interestingly, note that the front 8-kip load and the rear 32-kip load, although unequal, are placed symmetrically about the centerline of the beam. Therefore, the deflection due to the rear 32-kip axle load could have been easily calculated from the deflection due to the 8-kip load using Maxwell's Reciprocal Theorem and the law of proportionality. Thus,

$$\Delta_{32\text{ kip},x=10\text{ ft from A}} = (32/8)\ \Delta_{8\text{ kip},x=10\text{ ft from B}}$$
$$= 4(0.016) = 0.064\text{ in.} \approx 0.066\text{ in.}$$

The minor difference is due to rounding off numbers:

$$\Delta_{total,1\ design\ truck} = 0.11 + 0.016 + 0.066 = 0.192\text{ in.} \approx 0.20\text{ in.}$$

www.EngineeringEBooksPdf.com

Apply dynamic allowance (33 percent):

$$\Delta_{total,1\ truck+IM} = 1.33(1.0)(0.20) = 0.266 \text{ in.}$$

Deflection due to two design lanes, multiple-presence factor, $m = 1.0$.

$$\Delta_{total,2\ design\ trucks+IM} = 1.00(2)(0.266) = 0.53 \text{ in.}$$

Deflection Due to the Lane Load
Deflection due to lane load can be calculated from Equation 5.94 (Equation 2.9 modified for reinforced concrete beams):

$$\Delta_{lane} = \frac{5wL^4}{384E_cI_e} \tag{2.9}$$

where
$w = 0.64$ kip/ft
L = span = 48 ft

Substituting these values along with $E_c = 3644$ ksi and $I_e = 312{,}293$ in.^{4} in Equation 5.94, the maximum deflection due to lane load is

$$\Delta_{lane.max} = \frac{5(0.64)(48)^4(12)^3}{384(3{,}644)(312{,}293)} = 0.07 \text{ in.}$$

Dynamic load allowance is not applicable to lane load.

Deflections due to two design lanes loaded,

$$\Delta_{2\ lanes} = 2(0.07) = 0.14 \text{ in.}$$

$$0.25\Delta_{truck} + \Delta_{lane} = 0.25(0.53) + 0.14 = 0.27 \text{ in.}$$

$$\Delta_{truck} = 0.53 \text{ in.} > (0.25\Delta_{truck} + \Delta_{lane}) = 0.27 \text{ in.}$$

Therefore, $\Delta_{truck} = 0.53$ in. (governs),
Allowable live load deflection,

$$\Delta_{allowable} = \frac{L}{800} = \frac{48 \times 12}{800} = 0.72 \text{ in.} > 0.53 \text{ in.}$$

Deflection criteria are satisfied.

Optional Criteria for Span-to-Depth Ratio (Art. 2.5.2.6.3)
Owner may choose to invoke span-to-depth ratios as specified in LRFD Table 2.5.2.6.3-1. These ratios specify minimum depths of the primary load-carrying components of the bridge (slab in this example). The 27 in. trial thickness of the slab selected for this example (see calculations at the beginning of this example) and adopted as the final slab thickness, was based on the specified minimum depth listed in LRFD Table 2.5.2.6.3-1. Therefore, optional depth-to-span ratio is satisfied for this example.

Check for Shear: Art. 5.14.4.1
Slab and slab bridges designed for moment in conformance with Art. 4.6.2.3 are considered safe in shear. Therefore, calculations are not required/provided for shear.
Part 2: Design of the Edge Beam
LRFD Art. 9.7.1.4 provides that at the lines of discontinuity, the deck either be strengthened or be supported by a beam or other line component. Furthermore, the beam or component shall

www.EngineeringEBooksPdf.com

be integrated in or make composite with the deck. The edge beams may be designed as beams whose widths may be taken as the effective width of the deck specified in Art. 4.6.2.1.4.

For spans oriented primarily in the direction of traffic, the effective width of edge strip, with or without an edge beam, is obtained as follows (Art. 4.6.2.1.4):

Edge beam width = sum of the following three lengths:

1. The distance between the edge of the deck and the inside face of the barrier = 21 in.
2. 12 in.
3. One-quarter of the strip width used in slab design

$$b_{edge} = 21 + 12 + \frac{140}{4} = 68 \text{ in. or } 5.67 \text{ ft}$$

$$b_{edge} \text{ not greater than 1/2 (full strip width) = 1/2 (140) = 70 in. > 68 in.}$$

In Art. 4.6.2.1.3 (Table 4.6.2.1.3-1),

$$b_{edge} = 26 + 6.6(S) = 26 + 6.6\ (48) = 342.8 \text{ in.} > 68 \text{ in. } (S = \text{span of the slab in feet})$$

Therefore, b_{edge} = 68 in. ≈ 5.67 ft governs (Figure 5.45).

To calculate loads per foot width of the exterior strip (i.e., the edge beam), design loads would be divided by 68 in. or 5.67 ft.

Permanent Loads: Per Foot Width of the Edge Strip

w_{DC1} = 0.338 kip/ft (computed earlier)

The dead load due to the traffic barriers (0.505 kip/ft each) can be distributed over the entire slab width or conservatively over the width of the edge beam; the latter option is used in this design.

Dead load due to the traffic barrier,

$$w_{DC2} = \frac{0.505}{5.67} = 0.089 \text{ kip/ft}$$

$$w_{DC} = w_{DC1} + w_{DC2} = 0.338 + 0.089 = 0.427 \text{ kip/ft} \approx 0.43 \text{ kip/ft}$$

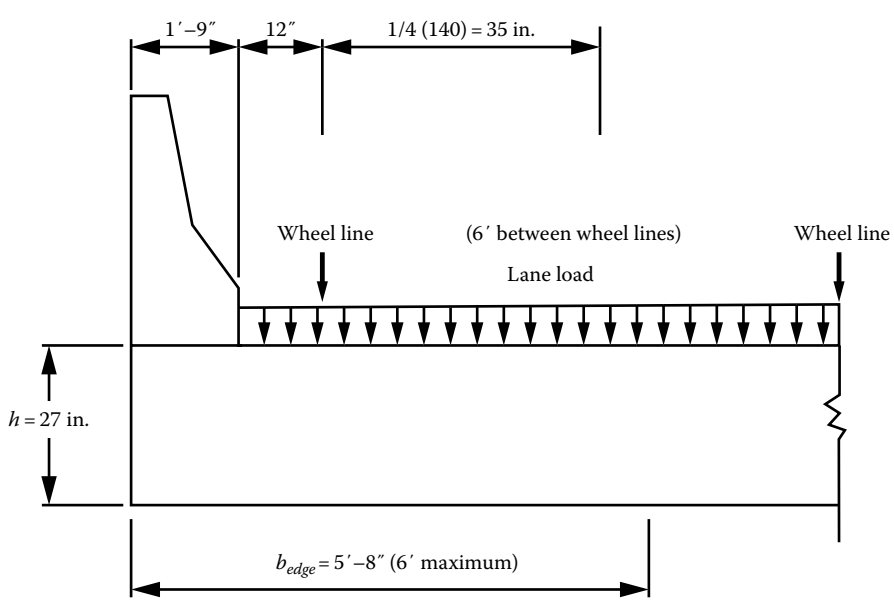

FIGURE 5.45 Calculation of the edge beam width.

www.EngineeringEBooksPdf.com

The 2 in. concrete overlay (0.025 kip/ft) and the FWS (0.025 kip/ft) occupy only 68 – 21 (base width of the traffic barrier) = 47 in. or approximately 4 ft of the edge beam width, but this load is distributed over b_{edge} = 5.67 ft.

$$w_{DW} = \frac{(0.025+0.024)(4)}{5.67} = 0.035 \text{ kip/ft}$$

$$M_{DC} = \frac{w_{DC}L^2}{8} = \frac{0.43(48)^2}{8} = 123.84 \text{ kip-ft}$$

$$V_{DC} = \frac{w_{DC}L}{2} = \frac{0.43(48)}{2} = 10.32 \text{ kip}$$

$$M_{DW} = \frac{w_{DW}L^2}{8} = \frac{0.035(48)^2}{8} = 10.08 \text{ kip-ft}$$

$$V_{DW} = \frac{w_{DW}L}{2} = 0.035(48) = 0.84 \text{ kip}$$

Live Load Force Effects

Bending Moment

As shown in Figure 5.45, the width of the edge beam is 5.67 ft. Within this width, only one wheel of the design truck can be placed (5.67 ft < 10 ft lane width). Therefore, moment and shear due to the design truck are determined by dividing the moment due to the full design truck by 2; the value of the moment so obtained would be divided by 5.67 ft (width of the edge strip) to obtain live load moment per unit width of the edge beam. Thus,

Moment due to the full design truck = 584 kip/ft (computed earlier for the design of the interior strip)

For the edge beam, moment per unit width,

$$M_{LL} = \frac{0.5(584)}{5.67} = 51.5 \text{ kip-ft}$$

Apply dynamic load allowance to the moment due to the design truck = 0.33:

$$M_{LL=IM} = 1.33(51.5) = 68.5 \text{ kip-ft}$$

Moment due to lane load (0.64 kip/ft) is computed on the tributary portion (68 – 21 = 47 in.) of the 10 ft lane width, to be divided by b = 5.67 ft to obtain moment per unit width:

M_{lane} = 184.3 kip-ft (computed earlier for the design of the interior strip)

$$M_{Lane} = \frac{184.3}{5.67}\left(\frac{47}{10(12)}\right) = 12.73 \text{ kip-ft}$$

Dynamic load allowance is not applicable to lane load:

$$M_{LL+IM,total} = 68.5 + 12.73 = 81.23 \text{ kip-ft}$$

Shear

Shear due to the design truck and the lane load is computed in the same manner as moments.

www.EngineeringEBooksPdf.com

Due to the design truck,

$$V_{LL+IM} = 77.14 \text{ kip (calculated earlier).}$$

For the edge beam,

$$V_{LL,tr} = \frac{0.5(77.14)}{5.67} = 6.80 \text{ kip}$$

Due to the design lane load,

$$V_{lane} = 15.36 \text{ kip (calculated earlier).}$$

For the edge beam, the shear due to the lane load is calculated in proportion to the length available to the lane load (12 + 35 = 47 in.), the full length width being 10 ft:

$$V_{lane} = \frac{15.36(47)}{5.7(10)(12)} = 1.06 \text{ kip/ft}$$

$$V_{LL+IM,total} = 6.8 + 1.06 = 7.86 \text{ kip/ft}$$

Strength I Limit State

$$M_u = \Sigma \eta_i \gamma_i Q_i$$

$$\begin{aligned} M_u &= 1.0\left(1.25M_{DC} + 1.5M_{DW} + 1.75M_{LL+IM}\right) \\ &= 1.0\left[1.25(123.84) + 1.5(10.08) + 1.75(81.23)\right] \\ &= 312.1 \text{ kip-ft} \end{aligned}$$

For the interior strip, $\phi M_n = 335$ kip-ft > $M_{u,ext} = 312.1$ kip-ft.
Therefore, provide the same reinforcement as for the interior strip.

Check for Maximum and Minimum Reinforcement

1. Maximum reinforcement: No provisions for maximum reinforcement
2. Minimum reinforcement

The section of the edge beam is the same with same longitudinal reinforcement.

$$M_{cr} = 70 \text{ kip-ft (computed earlier for the interior strip)}$$

$$1.3M_u = 1.3(312.1) = 405.7 \text{ kip-ft} > M_{cr} = 70 \text{ kip-ft (governs)}$$

$$\phi M_n = 335 \text{ kip-ft} \geq M_{cr} = 70 \text{ kip-ft, OK}$$

Minimum reinforcement requirement is satisfied.

Control of Cracking: Art. 5.7.3.1
Refer to calculations for the interior strip. The cross section of the edge beam is the same as that of the interior strip; therefore, $\beta_s = 1.07$.

www.EngineeringEBooksPdf.com

Moment at service load,

$$\begin{aligned} M_u &= \Sigma\eta_i\gamma_i Q_i \\ &= 1.0(1.0M_{DC} + 1.0M_{DW} + 1.0M_{LL+IM}) \\ &= 1.0\ (123.84 + 10.08 + 81.23) \\ &= 215.15 \text{ kip-ft} \end{aligned}$$

$$f_c = \frac{6M}{bh^2} = \frac{6(215.15)(12)}{12(27)^2} = 1.771 \text{ ksi}$$

$$0.8f_r = 0.8(0.24\sqrt{f'_c}) = 0.8\ (0.24\sqrt{4}) = 0.384 \text{ ksi} < 1.771 \text{ ksi}$$

Since $f_c > 0.8f_r$, the section must be assumed cracked.

For cracked section, c = 8.39 ksi (computed earlier)

$$\begin{aligned} \frac{f_s}{n} &= \frac{M(d-c)}{I_{cr}} \\ &= \frac{215.15(12)(25.3-8.39)}{9500} \\ &= 4.6 \text{ ksi} \end{aligned}$$

$$f_s = n(4.6) = 8(4.6) = 36.8 \text{ ksi}$$

$$0.6f_y = 0.6(60) = 36 \text{ ksi} \approx 36.8 \text{ ksi, OK (close enough)}$$

$$\begin{aligned} S_s &= \frac{700\gamma_e}{\beta_s f_s} - 2d_c \\ &= \frac{700(0.75)}{1.07(36.0)} - 2(1.71) \\ &= 10.21 \text{ in.} > s = 6 \text{ in., OK} \end{aligned}$$

The details of reinforcement are shown in Figure 5.46.

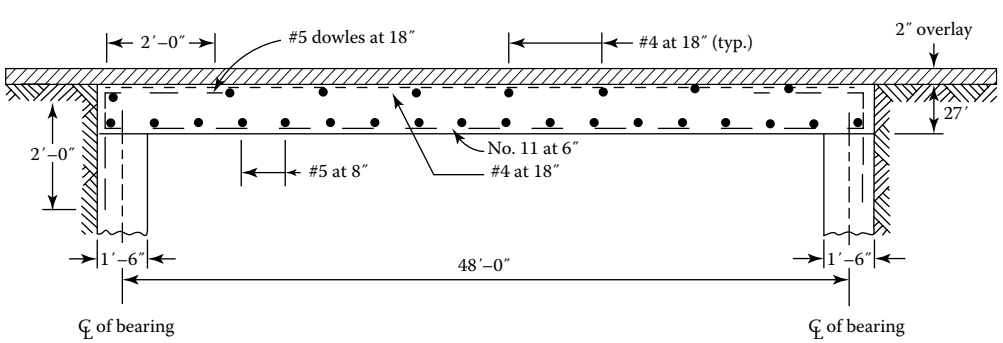

FIGURE 5.46 Details of reinforcement for the slab bridge of Example 5.1.

www.EngineeringEBooksPdf.com

5.15 DESIGN OF REINFORCED CONCRETE T-BEAM SUPERSTRUCTURES

A T-beam superstructure is an all-concrete structure that consists of a reinforced concrete deck cast monolithic with rectangular reinforced concrete beams (commonly referred to as webs or stems). The monolithic cast feature of a T-beam bridge sets it apart from typical slab–beam bridges in which the concrete deck is supported by prestressed concrete or steel beams and is cast to act compositely with them.

A T-beam superstructure differs from prestressed concrete superstructures in yet another respect. The concrete strength of the deck and the webs of a T-beam superstructure is the same, usually 4 ksi. In prestressed concrete superstructures, the deck is cast from a usually 4 ksi concrete; the strength of the supporting prestressed concrete girders is usually 5.5 ksi or higher.

For all slab–beam superstructures, including the T-beam, the supporting beams are usually designed first; the design of the deck follows, mainly for computational convenience. This is so because the effective length (span) of the deck depends on the spacing of the webs in a T-beam superstructure and of the beams/girders in slab–beam superstructures. It is convenient to select a trial size and spacing of beams/girders first and then complete their design. Once the design of beams/girders is finalized, the design of the deck follows based on the final spacing of the beams/girders. The design of beams/girders requires knowledge of the dead weight of the deck, which is not known *a priori*. Therefore, the deck thickness is assumed (or guessed!), and its dead weight estimated. The minimum permitted deck thickness is 7.0 in. (Art. 9.7.1.1) if the empirical design method (Art. 9.7.2, 9.7.2.4.4) is used (discussed in Section 5.13) and for many other reasons (e.g., thicker decks possess greater stiffness). A common design practice is to assume initially a deck thickness of 8.0 in. and check if it satisfies LRFD design provisions; the thickness may be increased if necessary (e.g., for increased concrete cover), preferably in 1/2 in. increments. A deck thickness of 8.0 in. is usually satisfactory for beam/girder spacing in the 7–8 ft range; greater deck thickness is required for wider spacing of the supporting beams/girders.

Example 5.2: Design of a Reinforced Concrete T-Beam Bridge Superstructure

Design a reinforced concrete T-beam bridge for a simple span of 50 ft between the centers of bearings. The bridge is required to carry two traffic lanes and have traffic barriers on each side weighing 505 lb/ft each. The design should make a provision for a dead load of 25 lb/ft^2 for FWS. The bridge does not carry any utilities. Use 28-day concrete compressive strength $f, f_c' = 4$ ksi and Grade 60 reinforcement.

Show all necessary design details.

Solution

The design of this T-beam superstructure is presented in two parts: (1) design of the webs and (2) design of the deck, in that order, for reasons stated earlier. The design of the webs (referred to as beams in this example) is presented also in two parts: (1) design of the interior beams/girders and (2) design of the exterior beams/girders.

Selection and Description of the Trial Cross Section of T-Beam Superstructure

The T-beam bridge will be designed in a simple span of 50 ft between centers of bearings. This type of superstructure is classified as Type (e) in LRFD Table 4.6.2.2.1-1. Approximate live load analysis method of Art. 4.6.2.2 will be used in this example, which requires that the following conditions be met; the proposed trial cross section meets these requirements:

1. Spacing between beams: $3.5 \le S \le 16.0$ ft	Proposed $S = 7.5$ ft
2. Thickness of slab: $4.5 \le t_s \le 12.0$ in.	Proposed $t_s = 8$ in.
3. Span: $20 \le L \le 240$ ft	Proposed $L = 50$ ft
4. Number of beams: $N_b \ge 4$	Proposed $N_b = 4$

www.EngineeringEBooksPdf.com

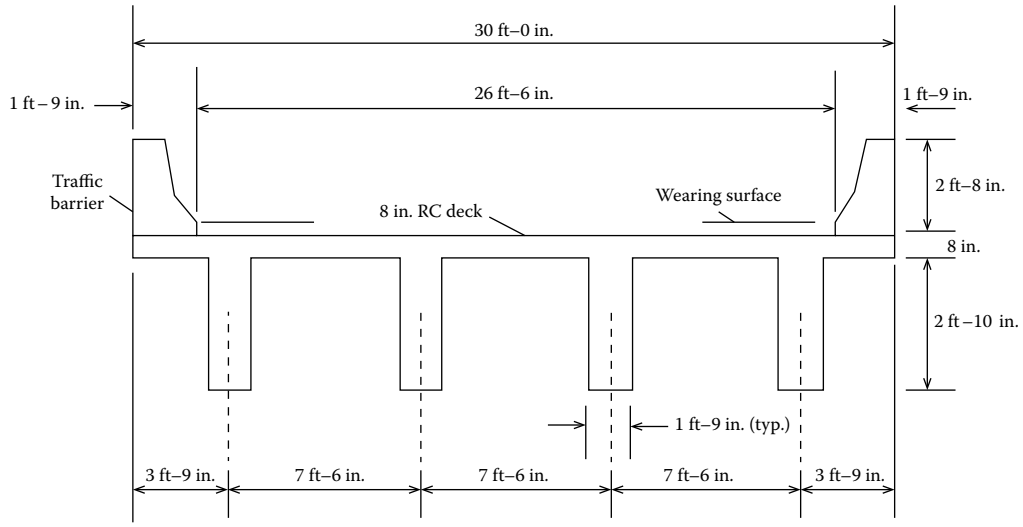

FIGURE 5.47 Cross section of T-beam bridge of Example 5.2.

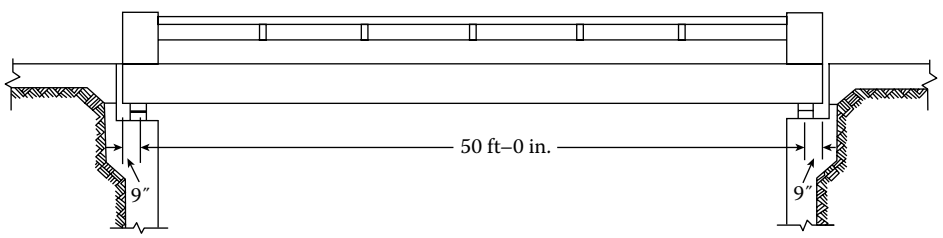

FIGURE 5.48 Elevation of T-beam bridge of Example 5.2.

Figures 5.47 and 5.48 show, respectively, the preliminary cross section of the T-beam superstructure and elevation of the bridge to be used for design calculations. The stems (webs) of the T-beams are spaced at 7 ft 6 in. o.c. A deck thickness of 8 in., greater than the minimum required 7 in. (Arts. 9.7.1.1 and 9.7.2.4), is selected to satisfy the requirements of empirical design method for the deck. In order to use design moments from LRFD TableA4-1 for the design of decks, it is required that the maximum deck overhanging widths be smaller of 0.625 times the girder spacing and 6.0 ft. For the selected trial cross section, 0.625(7.5) = 4.6875 ft < 6.0 ft; the width of the proposed overhang is 3.75 ft, which is smaller than the permitted width of 4.6875 ft.

The overall depth (from top of deck to bottom of T-beam, h_{min}) has been selected to satisfy optional criteria for span-to-depth ratio (Art. 2.5.2.6.3).

For simple-span T-beams, $h_{min} = 0.070L$. For the example bridge,

$$0.07L = 0.07(50) = 3.5 \text{ ft or } 42 \text{ in.}$$

$$\text{Overall depth selected, } h = 42 \text{ in.}$$

A trial width of $b_w = 21$ in. has been selected based on experience. It would be revised if necessary.

The overall width of this two-lane bridge is kept as 30 ft. The bridge is provided on each side with New Jersey–type traffic barriers having a base width of 21 in. and weighing 505 lb/ft, resulting in a clear roadway width of 26 ft 6 in.

Thus, the trial cross section satisfies the design stipulations.

www.EngineeringEBooksPdf.com

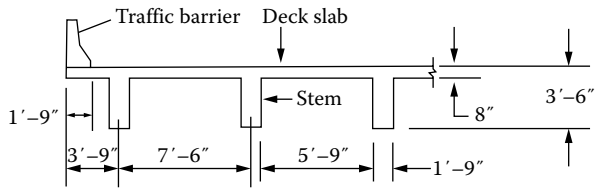

FIGURE 5.49 Cross section of T-beam.

Design Calculations
Part I: Design of T-Beam
The design of T-beams will be presented in two parts:

1. Design of the interior T-beam
2. Design of the exterior T-beam

Permanent Loads
Effective Flange Width of a T-Beam: Art. 4.6.2.6
The effective width of a concrete deck slab in composite or monolithic construction, b_e, is taken as the tributary width perpendicular to the axis of the member for determining the cross-sectional stiffness for analysis and for determining flexural resistances (Art. 4.6.2.6).

$$b_e = \text{tributary width of the web} = 7.5 \text{ ft} = 90 \text{ in. (Figure 5.49)}$$

$$\text{Area of cross section} = 90(8) + 21(34) = 1434 \text{ in.}^2 = 9.96 \text{ ft}^2$$

Dead weight of T-beam,

$$w_{DC1} = 9.96(1)(0.15) = 1.5 \text{ kip/ft}$$

The traffic barrier would be poured after the deck hardens. Therefore, the dead weight of the two traffic barriers (505 lb/ft each) would be distributed equally to four girders.

Dead weight of traffic barriers,

$$w_{DC2} = \frac{2(0.505)}{4} = 0.25 \text{ kip/ft}$$

Dead load due to the FWS at 25/ft^2,

$$w_{DW} = 0.025(7.5) = 0.19 \text{ kip/ft}$$

Force Effects from Permanent Loads
Bending Moments

$$M_{DC1} = \frac{w_{DC1}L^2}{8} = \frac{1.5(50)^2}{8} = 469 \text{ kip-ft}$$

$$M_{DC2} = \frac{w_{DC2}L^2}{8} = \frac{0.25(50)^2}{8} = 78 \text{ kip-ft}$$

$$M_{DW} = \frac{w_{DW}L^2}{8} = \frac{0.19(50)^2}{8} = 59 \text{ kip-ft}$$

www.EngineeringEBooksPdf.com

Shear

$$V_{DC1} = \frac{w_{DC1}L}{2} = \frac{1.5(50)}{2} = 37.5 \text{ kip}$$

$$V_{DC2} = \frac{w_{DC2}L}{2} = \frac{0.25(50)}{2} = 6.25 \text{ kip}$$

$$V_{DW} = \frac{w_{DL}L}{2} = 0.19(50) = 4.75 \text{ kip}$$

Force Effects from Live Load

Bending Moment

a. Maximum moments due to live load

For L = 50 ft (>40.27 ft), HL-93 truck governs over tandem (see Example 3.9).

Due to the design truck,

$$M_{truck} = 18L - 280 + \frac{392}{L} = 18(50) - 280 - \frac{392}{50} = 628 \text{ kip-ft}$$

Dynamic load allowance = 0.33 (design truck load only)

$$M_{truck}(1 + IM) = 628(1 + 0.33) = 835 \text{ kip-ft}$$

1. Moment due to the lane load

Referring to Figure 5.50, the influence line ordinate is

$$\frac{ab}{L} = \frac{(25 - 2.335)(25 + 2.335)}{50} = 12.391 \text{ ft}$$

$$M_{lane} = (0.64)\left(\frac{1}{2}\right)(L)\left(\frac{ab}{L}\right)$$

$$= (0.64)(0.5)(50)(12.391) = 198.3 \text{ kip-ft}$$

Total moment due to live load = 835 + 198.3 = 1033.3 kip-ft

Live load distribution factor would be applied to M_{LL+IM} = 1033.3 kip-ft

b. Maximum shear due to live load

1. Shear due to the design truck

The reaction at the left support is obtained from Equation 3.25 for x = 0:

$$V_x = \frac{72}{L}(L - x - 9.33)$$

www.EngineeringEBooksPdf.com

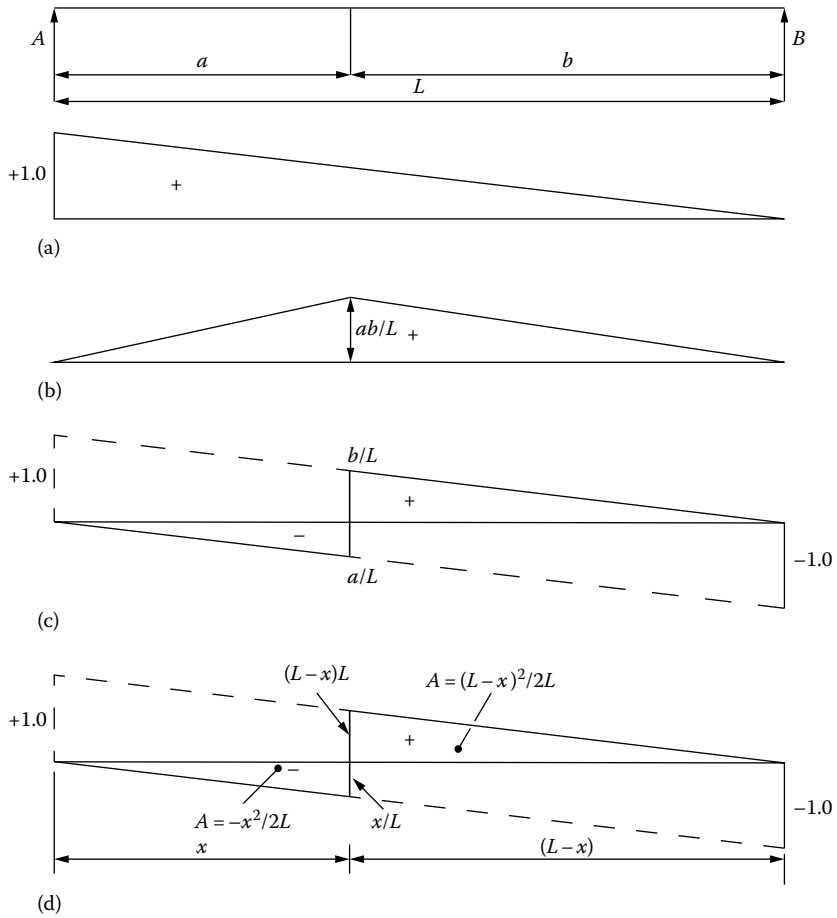

FIGURE 5.50 Influence line diagram for maximum reaction, moment, and shear due to uniform load (lane load). (a) Maximum reaction at the left support, (b) moment at a section located at a from the left support, (c) shear at a distance from a from the left support, and (d) general expression for calculating shear at a distance a from the left support.

For L = 50 ft > 28 ft, design truck governs over the tandem (see Example 3.12).

$$R_L = \frac{72}{50}(50 - 0 - 9.33) = 58.6 \text{ kip}$$

Dynamic load allowance = 0.33

$$V_{Truck} = 58.6\ (1 + 0.33) = 77.94 \text{ kip}$$

2. Shear due to the lane load

$$\text{Max shear due to lane load} = w_L\left(\frac{L}{2}\right)$$

$$= 0.64\frac{(50)}{2} = 16 \text{ kip}$$

www.EngineeringEBooksPdf.com

Total maximum shear due to live load,

$$L_{L+I} = V_{Truck} + V_{Lane} = 77.94 + 16 = 93.94 \text{ kip}$$

Live load distribution factor for shear would be applied to $V_L = 93.94$ kip.

Live Load Distribution Factors

The T-beam deck superstructure is classified as Type (e) cross section as listed in LRFD Table 4.6.2.2.1-1 (cast-in-place concrete T-beam with monolithic concrete deck). Approximate method of analysis specified in Art. 4.6.2.2.2 is applicable to this type of superstructure. Distribution factors for live load bending moment and live load shear will be determined from LRFD tables in Section 4 of LRFD specifications.

Check the applicability criteria:

$3.5 \le S \le 16.0$	$S = 7.5$ ft, OK
$4.5 \le t_s \le 12.0$	$t_s = 8.0$ in., OK
$20 \le L \le 240$	$L = 50$ ft, OK
$N_b \le 4$	$N_b = 4$, OK
$10{,}000 \le K_g \le 7{,}000{,}000$	
$K_g = n(I + Ae_g^2)$	

where

n = modular ratio = 1 for $f'_c = 4$ ksi for both the deck and the web
I = moment of inertia of girder (in.^{4})
e_g = eccentricity of girder from the midsurface of the slab (in.)
K_g = longitudinal stiffness parameter
$= n(1 + Ae_g^2)$
$10{,}000 \le (K_g = 47{,}200) \le 7{,}000{,}000$; $K_g = = 701{,}176$ in.^{4}, OK (calculations to follow)

Range of applicability is satisfied.

Number of design lanes, N_L

Clear roadway width for design lanes, w

$$\begin{aligned} w &= \text{overall bridge width} - 2(\text{width of the traffic barrier}) \\ &= 30.0 - 2(1.75) \\ &= 26.5 \text{ ft} \end{aligned}$$

$$N_L = \left(\frac{w}{12}\right)_{INT} = \left(\frac{26.5}{12}\right)_{INT} = 2.21$$

Use $N_L = 2$ design lanes

Moment of inertia of the T-section, I_g

Area of gross cross section, $A_g = 1434$ in.^{2} (computed earlier)

With reference to Figure 5.51,

$$\bar{y} = \frac{90(8)(34+4) + 21(34)(17)}{1434} = 27.54 \text{ in.}$$

www.EngineeringEBooksPdf.com

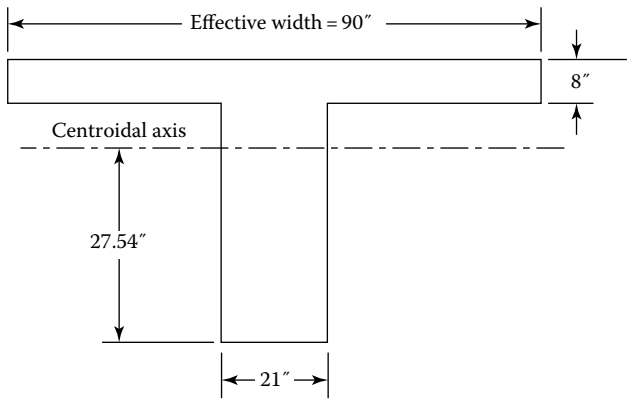

FIGURE 5.51 Cross section of T-section.

Moment of inertia of the basic beam (i.e., the web),

$$I_g = \frac{bh^3}{12} = \frac{21(34)^3}{12} = 68{,}782 \text{ in.}^4$$

e_g = eccentricity of girder from the midsurface of the slab = 0.5(34) + 4 = 21 in.

Modular ratio, n
E_c = same for both the deck concrete and the web concrete: $n = 1$

$$K_g = 1\left[68{,}782 + (1{,}434)(21)^2\right] = 701{,}176 \text{ in.}^4$$

Live Load Distribution Factor for Moment
Case 1. One Design Lane Loaded

$$g_{mi1} = 0.06\left(\frac{S}{14}\right)^{0.4}\left(\frac{S}{L}\right)^{0.3}\left(\frac{K_g}{12.0Lt_s^3}\right)^{0.1}$$

$$= 0.06 + \left(\frac{7.5}{14}\right)^{0.4}\left(\frac{7.5}{50}\right)^{0.3}\left(\frac{701{,}176}{(12.0)(50)(8)^3}\right)^{0.1}$$

$$= 0.06 + (0.779)(0.566)(1.086)$$

$$= 0.539$$

Case 2. Two Design Lanes Loaded

$$g_{mi2} = 0.075 + \left(\frac{S}{9.5}\right)^{0.6}\left(\frac{S}{L}\right)^{0.2}\left(\frac{K_g}{12.0Lt_s^3}\right)^{0.1}$$

$$= 0.075 + \left(\frac{7.5}{9.5}\right)^{0.6}\left(\frac{7.5}{50}\right)^{0.2}\left(\frac{701{,}176}{(12.0)(50)(8)^3}\right)^{0.1}$$

$$= 0.075 + (0.868)(0.684)(1.086)$$

$$= 0.72 > g_{mi1} = 0.539$$

Therefore, $g_{mi2} = 0.72$ governs.

www.EngineeringEBooksPdf.com

Live Load Distribution Factor for Shear
Check the range of applicability criteria.

The range of applicability criteria for shear for type (e) superstructure is the same as those for the moment checked earlier (except for the term K_g, which is not required). Therefore, the applicability criteria are satisfied.

Case 1. One Design Lane Loaded

$$g_{vi1} = 0.36 + \frac{S}{25.0} = 0.36 + \frac{7.5}{25} = 0.66$$

Case 2. Two or More Design Lanes Loaded

$$g_{vi2} = 0.2 + \frac{S}{12} - \left(\frac{S}{35}\right)^2$$

$$= 0.2 + \left(\frac{7.5}{12}\right) - \left(\frac{7.5}{35}\right)^2$$

$$= 0.779 > g_{vi1} = 0.66$$

$$g_{vi2} = 0.779 \text{ governs.}$$

1. Live load distribution factor for fatigue
   As discussed in Section 3.9.2, for fatigue limit state, only the design truck is placed in one lane with the distance between the two 32-kip axle loads equal to a fixed 30 ft (instead of 14 ft); lane load is ignored for fatigue limit state considerations. Multiple-presence factor is not applied when checking for fatigue. Therefore, live load distribution factor for fatigue is obtained by dividing the live load factors for moment and shear for the one lane loaded case by the multiple-presence factor, $m = 1.2$.

   For moment due to one lane loaded case, the distribution factor was determined as 0.539. Therefore,

$$g_{mi1,fat} = \frac{g_{mi1}}{m} = \frac{0.539}{1.2} = 0.449$$

   For shear due to one lane loaded case, the distribution factor was determined as 0.66. Therefore,

$$g_{vi1,fat} = \frac{g_{vi1}}{m} = \frac{0.66}{1.2} = 0.55$$

2. Live load distribution factor for deflection
   Live load distribution factor for deflection is the same for interior and exterior girders because it is assumed that all lanes are loaded and all girders deflect equally. For the two lanes loaded case, the multipresence factor, $m = 1.0$. Therefore,

$$g_{\Delta} = m\left(\frac{\textit{Number of lanes}}{\textit{Number of girders}}\right) = 1.0\left(\frac{2}{4}\right) = 0.5$$

www.EngineeringEBooksPdf.com

Strength I Limit State
Design Loads: Factored Loads
The following unfactored loads were calculated earlier:

Permanent loads

$$M_{DC} = 469 + 78 = 547 \text{ kip-ft},$$

$$V_{DC} = 37.5 + 6.25 = 43.75 \text{ kip}$$

$$M_{DW} = 59 \text{ kip-ft}$$

$$V_{DW} = 4.75 \text{ kip}$$

Live load force effects

$$M_{(L+I)} = 1033.3 \text{ kip-ft}$$

$$V_{L+I} = 93.94 \text{ kip}$$

Apply live load distribution factors to live load moment and shear.
For bending moment,

$$g_{mi} = 0.72$$

Maximum live load plus impact moment in the interior girder = (0.72)(1033.3) = 744 kip-ft

Factored Loads: Bending Moments

$$M_u = \Sigma\eta_i\gamma_i M_i$$

$$\eta_i = \eta_D\eta_R\eta_I \text{ (Art. 1.3.2.1)}$$

Select Load Modifiers
Ductility, $\eta_D = 1.0$ (Art. 1.3.3).
Redundancy, $\eta_R = 1.0$ (Art. 1.3.4)
Importance, $\eta_I = 1.0$ (Art. 1.3.5)

Therefore,

$$M_u = \eta\Sigma\gamma_i M_i$$

$$M_u = 1.0\ [1.25M_{DC} + 1.5M_{DW} + 1.75(M_{LL+IM})]$$

$$= 1.0\ [1.25(547) + 1.5(59) + 1.75(744)]$$

$$= 2074 \text{ kip-ft}$$

Estimation of Reinforcement Requirements
Estimate the required amount of reinforcement from Equation 5.86. For simplicity, assume that the neutral axis lies in the flange (to be verified later), so the section can be analyzed as a rectangular section:

$$A_{s,reqd} = \frac{M_u}{4d_s} \tag{5.86}$$

where d_s = depth of the centroid of nonprestressed tension reinforcement from the extreme compression fibers.

To use the aforementioned equation, d must be known *a priori*.

www.EngineeringEBooksPdf.com

Trial 1
Assume 1.5 in. clear cover, No. 4 stirrups, and No. 9 bars in one layer.

$$\text{Distance of the centroid of tensile reinforcement from the bottom} = 1.5 + 0.5 + 0.5(1.13)$$
$$= 2.57 \text{ in.}$$

$$d = 42 - 2.57 = 39.43 \text{ in.}$$

$$A_{s,reqd} = \frac{2074}{4(39.43)} = 13.15 \text{ in.}^2$$

From Table 5.A.2, try 15 No. 9 bars, $A_s = 15.0$ in.^{2} > 13.15 in.^{2}, OK.
Width of web, $b_w = 21$ in., so 15 No. 9 bars cannot be accommodated in one layer. Therefore, arrange 15 No. 9 bars in three layers, 5 bars in each layer. Minimum clearance between parallel bars to be the largest of the following (Art. 5.10.3.1.1):

1. 1.5 times the nominal diameter of the bar = 1.5(1.13) = 1.7 in. (governs)
2. 1.5 times the minimum size of the coarse aggregate = 1.5(3/4) = 1.125 in.
3. 1.5 in.

For five No. 5 bars in one layer, minimum web width required is calculated to be

$$b_{w,min.} = 5(\text{diameter of bars}) + 4(\text{spacing between the bars}) + 2(\text{diameter of stirrups}) + 2(\text{clear cover})$$
$$= 5(1.13) + 4(1.7) + 2(0.5) + 2(1.5) = 16.45 \text{ in.} < b_w = 21 \text{ in., OK}$$

So five No. 5 bars can be arranged in one row. Arrange 15 bars in three rows as shown in Figure 5.52. The distance of the centroid of the group of 15 bars from the bottom of the T-beam (tension face) is

$$y_{cg} = 1.5 + 0.5 + 1.13 + 1.13 + 0.5(1.13) = 4.825 \text{ in.}$$

$$d_s = 42.0 - 4.825 = 37.18 \text{ in.}$$

Calculate the nominal resistance, M_n, with $A_s = 15.0$ in.^{2} and $d_s = 37.18$ in.

$$0.85f'_c ba = A_s f_y$$

$$0.85(4)(90)a = 15.0(60)$$

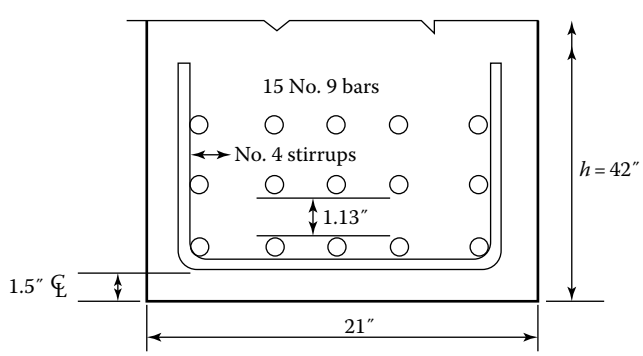

FIGURE 5.52 Arrangement of 15 No. 9 bars in 3 rows in the web of the T-beam.

www.EngineeringEBooksPdf.com

whence a = 2.94 in. < t_s = 8 in. Therefore, the assumption that neutral axis lies in the flange is valid, and the section can be analyzed as a rectangular section.

$$M_n = A_s f_y \left(d - \frac{a}{2}\right)$$

$$= 15.0(60)\left(37.18 - \frac{2.94}{2}\right) = 32{,}139 \text{ kip-in.}$$

$$= 2678 \text{ kip-ft}$$

Determine the strength factor, ϕ, from strain in steel reinforcement (Figure 5.53).

$$\varepsilon_s = \left(\frac{d_t - c}{c}\right)\varepsilon_c$$

where d_t = distance from the extreme compression fiber to the centroid of extreme tension reinforcement.

$d_t = h$ – clear cover – diameter of stirrup – half diameter of tension reinforcing bar

= 42 – 1.5 – 0.5 – 0.5(1.13)

= 39.44 in.

$$c = \frac{a}{\beta_1} = \frac{2.94}{0.85} = 3.46 \text{ in.}$$

$$\varepsilon_s = \left(\frac{39.44 - 3.46}{3.46}\right)(0.003) = 0.031 > 0.005$$

Therefore, ϕ = 0.9.

$$\phi M_n = 0.9(2678) = 2410 \text{ kip-ft} > M_u = 2074 \text{ kip-ft, OK}$$

Alternatively, one may use 10 No. 11 bars in two rows, 5 in each row as shown in Figure 5.54.

$$A_s = 15.62 \text{ in.}^2 > A_{s,reqd} = 13.15 \text{ in.}^2\text{, OK}$$

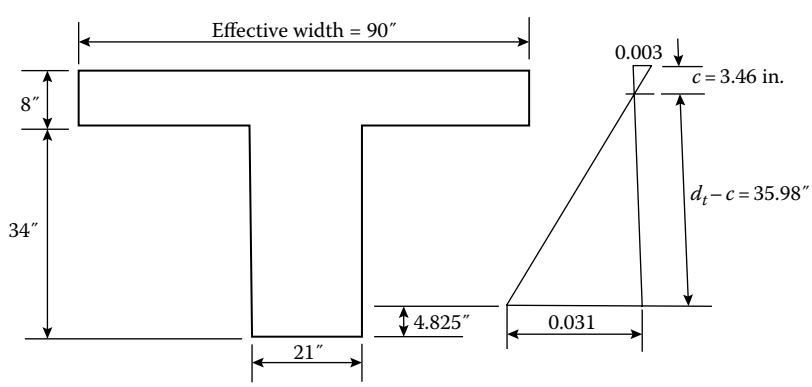

FIGURE 5.53 Strain diagram.

www.EngineeringEBooksPdf.com

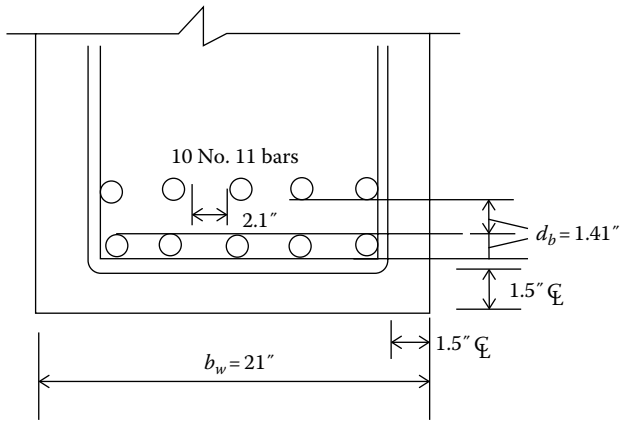

FIGURE 5.54 Arrangement of 10 No. 11 bars in 2 rows.

Minimum clearance between parallel bars to be the largest of the following (Art. 5.10.3.1.1):

1. 1.5 times the nominal diameter of the bar = 1.5(1.41) = 2.1 in. (governs)
2. 1.5 times the minimum size of the coarse aggregate = 1.5(3/4) = 1.125 in.
3. 1.5 in.

For five No. 5 bars in one layer, minimum web width required is calculated to be

$$b_{w,min.} = 5(\text{diameter of bars}) + 4(\text{spacing between the bars}) + 2(\text{diameter of stirrups}) + 2(\text{clear cover})$$

$$= 5(1.41) + 4(2.1) + 2(0.5) + 2(1.5) = 19.45 \text{ in.} < b_w = 21 \text{ in., OK}$$

$$y_{cg} = 1.5 + 0.5 + 1.41 + 0.5(1.41) = 4.12 \text{ in.}$$

$$d_s = 42 - 4.12 = 37.88 \text{ in.}$$

Calculate M_n with $A_s = 15.62$ in.^{2} and $d_s = 37.88$ in.

$$0.85f'_c ba = A_s f_y$$

$$0.85(4)(90)a = 15.62(60)$$

whence $a = 3.06$ in. $< t_s = 8$ in. Therefore, the assumption that neutral axis lies in the flange is valid, and the section can be analyzed as a rectangular section.

$$M_n = A_s f_y \left(d - \frac{a}{2} \right)$$

$$= 15.62(60)\left(37.88 - \frac{3.06}{2}\right) = 34{,}067 \text{ kip-in.}$$

$$= 2839 \text{ kip-ft}$$

Determine the strength factor, ϕ, from strain in steel reinforcement (Figure 5.55).

www.EngineeringEBooksPdf.com

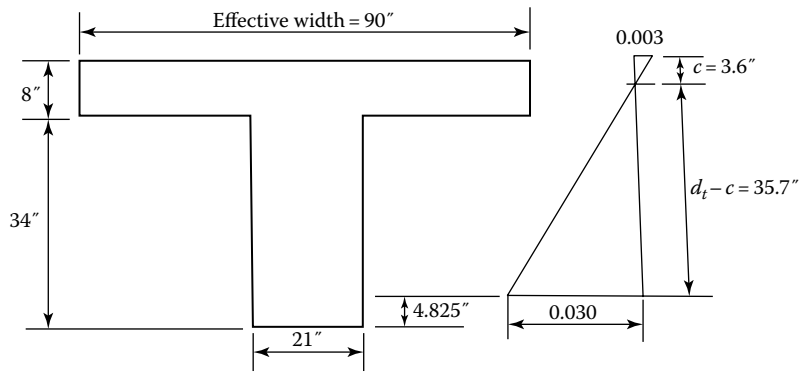

FIGURE 5.55 Strain diagram.

$$\varepsilon_s = \left(\frac{d_t - c}{c}\right)\varepsilon_c$$

where d_t = distance from the extreme compression fiber to the centroid of extreme tension reinforcement.

$d_t = h$ – clear cover – diameter of stirrup – half diameter of tension reinforcing bar

$= 42 - 1.5 - 0.5 - 0.5(1.41)$

$= 39.3$ in.

$$c = \frac{a}{\beta_1} = \frac{3.06}{0.085} = 3.6 \text{ in.}$$

$$\varepsilon_s = \left(\frac{39.3 - 3.6}{3.6}\right)(0.003) = 0.03 > 0.005$$

Therefore, $\phi = 0.9$.

$$\phi M_n = 0.9(2839) = 2555 \text{ kip-ft} > M_u = 2074 \text{ kip-ft, OK}$$

In the second trial, 10 No. 11 bars in 2 rows, 5 in each row, would be used (preferred because of lesser number of bars, hence saving in labor costs).

Reinforcement Requirements: Art. 5.7.3.3

1. Maximum reinforcement (Art. 5.7.3.3.1)
   No provisions in LRFD specifications for maximum reinforcement
2. Minimum reinforcement (Art. 5.7.3.3.2)

Minimum reinforcement shall be adequate to develop a factored flexural resistance, M_r, at least equal to the lesser of the following two values:

1. 1.33 times the factored moment required by the applicable strength load combination specified in Art. 3.4.1-1

www.EngineeringEBooksPdf.com

2. The cracking moment of the section, M_{cr}, as determined from Equation 5.41:

$$M_{cr} = \gamma_3 \left[(\gamma_1 f_r + \gamma_2 f_{cpe}) S_c - M_{dnc} \left(\frac{S_c}{S_{nc}} - 1 \right) \right] \qquad (5.41)\ [A5.7.3.3.2\text{-}1]$$

where
γ_1 = 1.6 for all other structures
γ_2 = prestress variability = 0 for nonprestressed members
γ_3 = 0.75 for A706, Grade 60 reinforcement

For the T-beam with nonprestressed steel in this example, f_{cpe} = 0 and $S_c = S_{nc}$ (noncomposite section). Therefore, Equation 5.55 reduces to the following expression:

$$M_{cr} = \gamma_3 \gamma_1 f_r S_{nc}$$

With γ_1 = 1.6 (for all other structures) and γ_3 = 0.75 for A706, Grade 60 reinforcement,

$$M_{cr} = 0.75(1.6) f_r S_{nc} = 1.2 f_r S_{nc}$$

where S_{nc} = section modulus of the noncomposite section (T-section).

$$S_{nc} = \frac{I_g}{y_t}$$

where y_t = distance of neutral axis from the top fibers. Therefore,

$$M_{cr} = 1.2 f_r \left(\frac{I_g}{y_t} \right)$$

Determination of y_t and I_g.

Assume that the neutral axis lies in the web. With reference to Figure 5.56, take moments about the neutral axis:

$$90(8)(4 + 34 - y_b) + \frac{21(34 - y_b)^2}{2} = 21 y_b \left(\frac{y_b}{2} \right)$$

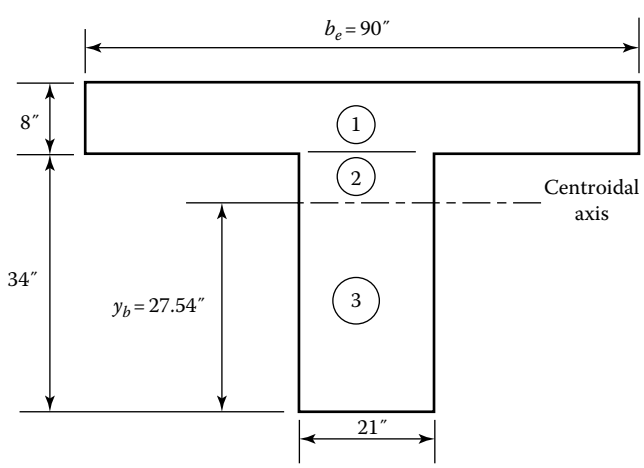

FIGURE 5.56 Determination of y_t and I_g of the T-section.

www.EngineeringEBooksPdf.com

The solution of the aforementioned quadric equation is y_b = 27.54 in. < 34 in. (depth of the web). So the assumption that the neutral axis lies in the web is valid.

$$I_g = \left[\frac{90(8)^3}{3} + 90(8)(4+34-27.54)^2\right] + \frac{21(27.54)^3}{3}$$

$$= 15{,}360 + 78{,}776 + 146{,}214$$

$$= 240{,}350 \text{ in.}^4$$

$$f_r = 0.24\sqrt{f'_c} = 0.24\sqrt{4} = 0.24 \text{ ksi} \qquad \text{(Art. 5.4.2.6)}$$

$$M_{cr} = 1.2 f_r \left(\frac{I_g}{y_t}\right) = 1.2(0.48)\left(\frac{240{,}350}{27.54}\right)$$

$$= 5{,}027 \text{ kip-in.} = 419 \text{ kip-ft}$$

$$1.33M_u = 1.33(2074) = 2758 \text{ kip-ft} > M_{cr}\ 419 \text{ kip-ft}$$

Flexural resistance,

$$M_r = \phi M_n = 2074 \text{ kip-ft ft} > M_{cr} = 419 \text{ kip-ft, OK}$$

The minimum reinforcement requirements are satisfied.

Deformations: Art. 5.7.3.6

Deformation and Camber: Art. 5.7.3.6.2

Deflections will be calculated based on the moment of inertia of the cracked section.

The maximum deflection due to the dead loads can be calculated as follows (Case 1, AISC 2010), by substituting E_cI_e for EI:

$$\Delta_{DL} = \frac{5w_dL^4}{384E_cI_e} = \frac{5M_aL^2}{48E_cI_e} \qquad (5.94)$$

The effective moment of inertia, I_e, in Equation 5.94 is calculated from Equation 5.55:

$$I_e = \left(\frac{M_{cr}}{M_a}\right)^3 I_g + \left[1 - \left(\frac{M_{cr}}{M_a}\right)^3\right] I_{cr} \le I_g \qquad \text{(5.55) [A5.7.3.6.2-1]}$$

The following quantities were computed earlier:

M_{cr} = 419 kip-ft
I_g = 240,350 in.^{4}
M_a = moment in the component at the stage for which deformation is computed
= $M_{DC1} + M_{DC2} + M_{DW}$
= 469 + 78 + 59 = 606 kip-ft

Calculate the moment of inertia of cracked section, I_{cr}. First, compute the center of gravity (c.g.) of the cracked section (Figure 5.57).

www.EngineeringEBooksPdf.com

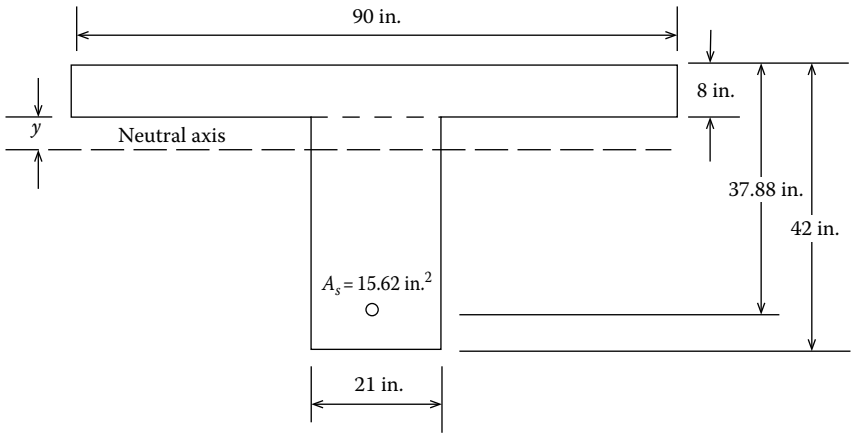

FIGURE 5.57 Calculation of the moment of inertia of cracked section of T-beam.

The position of the neutral axis is determined from trial and error. For the first trial, the neutral axis was assumed to lie in the flange ($\bar{y} < t_s = 8$ in.); calculations showed that $\bar{y} = 8.96$ in. $> t_s = 8$ in., which indicated that the assumption was not valid. Calculations are shown for the second trial based on the assumption that the neutral axis lies in the web.

Take moments about the neutral axis as shown in Figure 5.57:

$$90(8.0)(4+y)+\frac{21y^2}{2}=nA_s(37.88-y-8)$$

$$n = 8 \quad \text{for } f'_c = 4 \text{ ksi} \quad \text{and} \quad A_s = 15.62 \text{ in.}^2$$

Substituting the aforementioned values in the aforementioned equation, we obtain the following expression:

$$90(8.0)(4+y)+\frac{21y^2}{2}=8(15.62)(37.88-y-8)$$

The aforementioned expression is simplified to the following quadratic equation:

$$10.5y^2 + 849y - 853.8 = 0$$

The solution to the aforementioned quadratic is $y = 0.99$ in.

So the neutral axis lies 0.99 in. inside the web (or 8.99 in. below the top of the T-section).

Calculate I_{cr} from the parallel axis theorem as follows:

$$I_{cr}=\left[\frac{90(8)^3}{12}+90(8.0)(4+0.99)^2+\frac{21(0.99)^3}{3}8(15.62)(37.88-0.99-8.0)^2\right]$$

$$=126{,}064 \text{ in.}^4$$

$$I_e=\left(\frac{419}{606}\right)^3(240{,}350)+\left[1-\left(\frac{419}{606}\right)^3\right](126{,}064)\le 240{,}350 \text{ in.}^4$$

www.EngineeringEBooksPdf.com

$$I_e = 163{,}840 \text{ in.}^4 < 240{,}450 \text{ in.}^4, \text{ OK}$$

$$E_c = 33{,}000K_1(w_c)^{1.5}\sqrt{f'_c} \qquad (5.8)\ [A5.4.2.4.1]$$

$$E_c = 33{,}000(1.0)(0.145)^{1.5}\sqrt{4.0} = 3{,}644 \text{ ksi}$$

$$\Delta_{DL} = \frac{5(606)(50)^2}{48(3{,}644)(163{,}840)}(12)^3 = 0.46 \text{ in.}$$

Instantaneous deflection = 0.46 in.

Compute dead load deflection based on the gross moment of inertia, I_g = 240,350 in.^{4}, as follows:

$$\Delta_{DL} = 0.46\left(\frac{163{,}840}{240{,}350}\right) = 0.31 \text{ in.}$$

Provisions for long-term deflections (to account for the effects of creep), as specified in Art. 5.7.6.3.2, were discussed in Section 4.18.4.3. The long-term deflection is computed by multiplying instantaneous deflection by the long-term deflection multipliers as follows:

For deflection based on gross moment of inertia, long-term deflection factor = 4.0.
Long-term deflection based on gross moment inertia, Δ_{LT} = 4(0.31) = 1.24 in.

When the instantaneous deflection is computed based on the effective moment of inertia, the long-term deflection factor is computed as follows:

$$\text{Long-term deflection factor} = 3 - 1.2\left(\frac{A'_s}{A_s}\right) \geq 1.6 \qquad (5.95)$$

where
A'_s = area of compression reinforcement
A_s = area of tension reinforcement

For this example, there is no compression reinforcement, A'_s = 0; therefore,

Long-term deflection factor = 3 − 1.2(0) = 3.0 ≥ 1.6, OK

Use a long-term deflection factor = 3.0

Required camber = 3(Δ_{DL}) = 3(0.46) = 1.38 in.

The estimated long-term deflection based on effective moment of inertia is larger (1.38 in.) but very close to that based on the gross moment of inertia (1.24 in.). In view of the approximations involved in estimating long-term deflection, provide a camber of 1.38 in., say 1⅜ in.

www.EngineeringEBooksPdf.com

Live Load Deflection: Optional Criteria (Art. 2.5.2.6.2)

1. Optional Live Load-Deflection Control
   Since no deflection criteria are specified, optional deflection criteria (Art. 2.6.2.6.2) will be used in this example.

$$\text{Allowable deflection due to vehicular load, } \Delta_{LL} = \frac{span}{800} = \frac{50(12)}{800} = 0.75 \text{ in.}$$

Art. 3.6.1.3.2: Calculated deflection will be taken as the larger of the following as discussed in Section 2.6.3:

1. Deflection due to design truck alone. Dynamic load allowance will be applied to this deflection.
2. Deflection due to 25 percent of the deflection due to the design truck *plus* deflection due to lane load. Dynamic load allowance is not applied to the deflection due to the lane load.

Calculate Deflection Due to Vehicular Live Load
Live load deflections would be computed for the governing loading conditions—separately for the design truck and lane (Figure 5.58)—by the usual methods of computing deflections. Tandem load does not govern for a span of 50 ft. Formulas for relevant load cases given in AISC *Steel Construction Manual* (AISC 2011) would be used (see discussion in Section 2.6.6). Referenced formulas used in calculations are taken from Chapter 2.

Deflection Due to Design Truck
Calculate the effective moment of inertia:

The effective moment of inertia, I_e, depends on the applied moment, M_a. The value of M_a to be used in Equation 5.55 for calculating the effective moment of inertia is different from that used for calculating I_e used for computing dead load deflection. This is because of the additional moment caused by the live load.

$$M_{LL+IM} = 1033.3 \text{ kip-ft (computed earlier)}$$

$$M_a = M_D + M_{LL+IM} = 606 + 1033.3 = 1639.3 \text{ kip-ft}$$

$$M_{cr} = 419 \text{ kip-ft (computed earlier)}$$

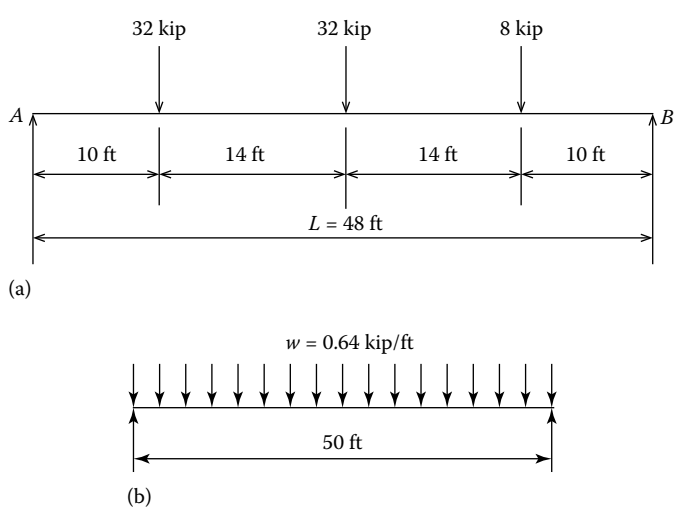

FIGURE 5.58 HL-93 live loads: (a) design truck and (b) lane load.

www.EngineeringEBooksPdf.com

$$I_e = \left(\frac{419}{1{,}639.3}\right)^3 (240{,}350) + \left[1 - \left(\frac{419}{1{,}639.3}\right)^3\right](126{,}064) \le 240{,}350 \text{ in.}^4$$

$$= 127{,}972 \text{ in.}^4 \le 240{,}350 \text{ in.},^4 \text{ OK}$$

As discussed in Example 5.1, deflection due to the design truck can be computed by placing the middle 32-kip load at the midspan, and the other two loads (8-kip and 32-kip loads) placed at 14 ft from the midspan, one on the left and the other on the right side of the midspan (Figure 5.59a). This load case can be split into two separate cases as shown in AISC (2011):

a. Load Case 7 for the centrally placed point load
b. Load Case 8 for point loads placed at any point on the span

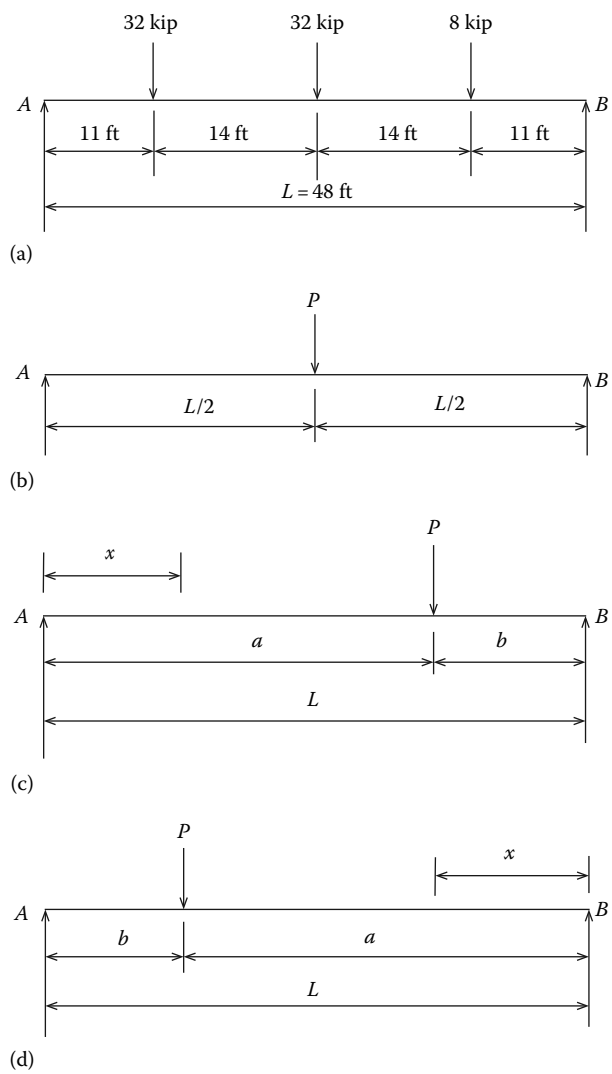

FIGURE 5.59 (a) Assumed position of the design truck for maximum deflection at midspan; (b) point load at center, $x = L/2$; (c) point load right of midspan, distance x measured from A, $x < a$; (d) point load left of midspan, distance x measured from B, $x < a$.

www.EngineeringEBooksPdf.com

Deflection due to the Design Truck

Deflection due to the three axle loads would be computed separately. The middle 32-kip axle load is placed at the center of the beam (Load Case 7, Figure 5.59b). The maximum deflection for this case can be calculated as follows (by substituting $E_c I_e$ for EI in Equation 2.2):

$$\Delta_c = \frac{PL^3}{48E_c I_e} \tag{5.96}$$

where

Δ_c = deflection at midspan due to point load
L = span = 50 ft
E_c = modulus of elasticity of concrete = 3644 ksi
I_e = effective moment of inertia = 127,976 in.^{4}

$$\Delta_c = \frac{PL^3}{48E_c I_e} = \frac{32(50)^3}{48(3{,}644)(127{,}972)}(12)^3 = 0.31\,\text{in.}$$

For the remaining 32-kip and 8-kip loads, use AISC (2011) Load Case 8. The deflection at a distance x (when $x < a$) from the left support can be calculated as follows:

$$\Delta_x = \frac{Pbx\left(L^2 - b^2 - x^2\right)}{6EIL} \tag{2.3R}$$

1. The rear 32-kip axle and the front 8-kip axle are 11 ft from support at A and B, respectively. For the 8-kip load, choose origin at A, so that

$$P = 8\text{ kip},\quad a = 39\text{ ft},\quad b = 11\text{ ft},\quad x = L/2 = 25\text{ ft} < a = 39\text{ ft}$$

$$\Delta_{x=25\text{ ft}} = \frac{8.0(11)(25)\left[(50)^2 - (11)^2 - (25)^2\right]}{6(3{,}644)(127{,}972)(50)}(12)^3 = 0.05\text{ in.}$$

2. For the rear 32-kip load, choose origin at B, so that

$$P = 32\text{ kip},\quad a = 39\text{ ft},\quad b = 11\text{f t},\quad x = 25\text{ ft} < a = 39\text{ ft}$$

$$\Delta_{x=25\text{ ft}} = \frac{32(11)(25)\left[(50)^2 - (11)^2 - (25)^2\right]}{6(3{,}644)(127{,}972)(50)}(12)^3 = 0.19\text{ in.}$$

Interestingly, note that the front 8-kip load and the rear 32-kip load, although unequal, are placed symmetrically about the centerline of the beam. Therefore, the deflection due to the rear 32-kip axle load could have been easily calculated from the deflection due to the 8-kip load using Maxwell's Reciprocal Theorem and the law of proportionality. Thus,

$$\Delta_{32\text{ kip},\, x = 11\text{ ft from A}} = (32/8)\ \Delta_{8\text{ kip},\, x = 11\text{ ft from B}}$$
$$= 4(0.05) = 0.20\text{ in.} \approx 0.19\text{ in.}$$

The minor difference is due to rounding off numbers.

$$\Delta_{total,1\ design\ truck} = 0.31 + 0.05 + 0.19 = 0.55\text{ in.}$$

www.EngineeringEBooksPdf.com

Apply dynamic allowance (33 percent) and live load distribution factor for deflection to the deflection due to the design truck.

$$\text{Live load distribution factor for deflection} = \frac{N_L}{N_B} = \frac{2}{4} = 0.5$$

$$\Delta_{total,1\ truck+IM} = 1.33(0.5)(0.55) = 0.37 \text{ in.}$$

Deflection Due to the Lane Load
Deflection due to the lane load can be calculated as follows:

$$\Delta_{lane} = \frac{5wL^4}{384E_cI_e} \tag{5.94}$$

where
w = 0.64 kip/ft
L = span = 50 ft

$$\Delta_{lane.max} = \frac{5(0.64)(50)^4(12)^3}{384(3,644)(127,972)} = 0.19 \text{ in.}$$

Dynamic load allowance is not applicable to lane load. Apply live load distribution factor for deflection.

Deflections Due to Design Lane

$$\Delta_{lane} = 0.5(0.19) = 0.10 \text{ in.}$$

$$0.25\Delta_{truck} + \Delta_{lane} = 0.25(0.55) + 0.10 = 0.24 \text{ in.}$$

$$\Delta_{truck} = 0.55 \text{ in.} > (0.25\Delta_{truck} + \Delta_{lane}) = 0.24 \text{ in.}$$

Therefore,

$$\Delta_{truck} = 0.55 \text{ in. governs.}$$

Allowable live load deflection,

$$\Delta_{allowable} = 0.75 \text{ in.} > 0.55 \text{ in., OK}$$

Deflection criteria are satisfied.

Optional Criteria for Span-to-Depth Ratio (Art. 2.5.2.6.3)
Owner may choose to invoke span-to-depth ratios as specified in LRFD Table 2.5.2.6.3-1. These ratios specify minimum depths of the primary load-carrying components of the bridge (T-beam in this example). The 42 in. trial depth of the T-beam in this example was selected based on the specified minimum depth listed in LRFD Table 2.5.2.6.3-1. Therefore, optional depth-to-span ratio is satisfied for the T-beam superstructure in this example.

Design for Shear
Strength Limit State

1. Location of the critical section: Arts. 5.8.3.2, 5.8.2.9

The critical section is located at a distance d_v from the internal face of support,

www.EngineeringEBooksPdf.com

where d_v = effective shear depth taken as the distance, measured perpendicular to the neutral axis, between the resultants of the tensile and compressive forces due to flexure; it need not be taken to be less than the greater of $0.9d_e$ or $0.72h$ (in.)

$$d_v = d_s - \frac{a}{2} = 37.88 - \frac{3.06}{2} = 36.35 \text{ in.}$$

Compare d_v with $0.9d_e$ and $0.72h$.

$$d_e = \frac{A_{ps}f_{ps}d_p + A_s f_y d_s}{A_{ps}f_{ps} + A_s f_y} \qquad (5.79)\ [A5.8.2.9\text{-}2]$$

For sections with nonprestressed steel, $A_{ps} = 0$; therefore,

$$d_e = d_s = 37.88 \text{ in.}$$

$$0.9d_e = 0.9(37.88) = 34.10 \text{ in.}$$

$$0.72h = 0.72(42) = 30.2 \text{ in.} < 34.00 \text{ in.} < d_v = 36.35 \text{ in.}$$

Therefore, d_v = 36.35 in. governs.

The segment of the T-beam over the bearings is under vertical compression from the reaction, so the critical section is taken at a distance of d_v from the face of the bearing, that is, at a distance of one-half of the bearing width plus d_v from the center line of the bearings or supports. For preliminary design, assume the width of bearing as 12 in. (it would likely be wider). Therefore, the critical section is located at a distance of x from the center line of the bearing:

$$x = d_v + 1/2(\text{bearing width}) = 36.35 + 1/2(12) = 42.35 \text{ in. or } 3.53 \text{ ft}$$

Calculate unfactored shear due to the permanent loads and the live load at a distance of 3.53 ft from the center of bearings. This is easily calculated from the influence line for shear as shown in Figure 5.60a.

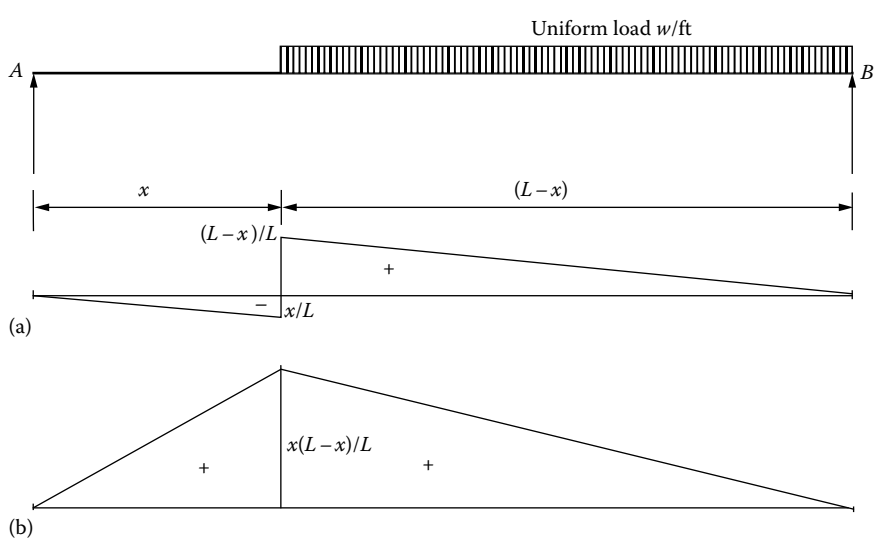

FIGURE 5.60 Influence line for (a) shear and (b) moment at a section x from the left support.

www.EngineeringEBooksPdf.com

Shear due to permanent loads,

$$V_x = \text{(intensity of uniform load)(area under the influence line diagram for shear)}$$

$$= \frac{w(L-x)^2}{2L}$$

$$w_{DC} = w_{DC1} + w_{DC2} = 1.5 + 0.25 = 1.75 \text{ kip/ft (computed earlier)}$$

$$w_{DW} = 0.19 \text{ kip/ft (computed earlier)}$$

$$V_{DC} = \frac{1.75}{2(50)}(50-3.53)^2 = 37.79 \text{ kip}$$

$$V_{DW} = \frac{0.19}{2(50)}(50-3.53)^2 = 4.10 \text{ kip}$$

a. Moment due to permanent loads
Referring to Figure 5.60b,

$$M = \text{load intensity (area under the influence line diagram for moment)}$$

$$= w\left[\frac{1}{2}(L)\left(\frac{x}{L}\right)(L-x) = \frac{wx(L-x)}{2}\right]$$

Moment due to $w_{DC} = 1.75$ kip/ft,

$$M_{DC} = \frac{1.75(3.53)(50-3.53)}{2} = 143.5 \text{ kip-ft}$$

Moment due to $w_{DW} = 0.19$ kip/ft,

$$M_{DW} = \frac{0.19(3.53)(50-3.53)}{2} = 15.6 \text{ kip-ft}$$

b. Bending moment due to live load
With reference to the influence line diagrams,
i. Design truck
Influence line ordinates from Figure 5.61b are as follows:

$$y_1 = \frac{x(L-x)}{L} = \frac{3.53(50-3.53)}{50} = 3.281 \text{ ft}$$

$$y_2 = 3.281\left(\frac{46.47-14}{46.47}\right) = 2.292 \text{ ft}$$

www.EngineeringEBooksPdf.com

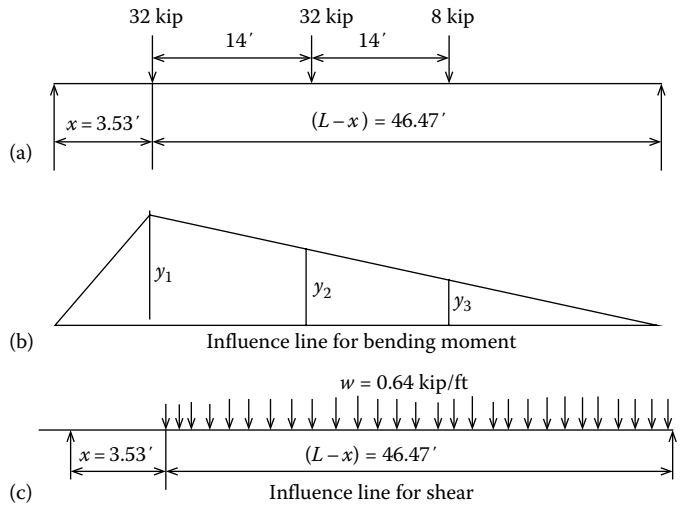

FIGURE 5.61 Influence line diagram for maximum moment at critical section (at $x = 3.53$ ft from the left support): (a) position of the design truck, (b) influence line diagram for moment, and (c) position of the lane load.

$$y_3 = 3.281\left(\frac{46.47-28}{46.47}\right) = 1.304 \text{ ft}$$

$$M_{truck} = 32(3.281 + 2.292) + 8(1.304) = 188.8 \text{ kip-ft}$$

Alternatively, from Equation 3.24, moment due to the design truck is calculated for $x/L = 3.53/50 = 0.0706 \leq 0.33$:

$$M_x = \frac{72x\left[(L-x)-9.33\right]}{L}$$

For $x = 3.53$ ft,

$$M_{x=3.53'} = \frac{72(3.53)[(50-3.53)-9.33]}{50} = 188.8 \text{ kip-ft}$$

ii. Design lane: From influence line (Figure 5.61b)

$$M_{lane} = w\left(\frac{1}{2}\right)(L)(y_1) = 0.64(0.5)(50)(3.281) = 52.5 \text{ kip-ft}$$

c. Shear due to live load, from Equation 3.25,

$$V_{truck} = \frac{72\left[(L-x)-9.33\right]}{L} = \frac{72(50-3.53-9.33)}{50} = 53.5 \text{ kip}$$

$$V_{lane} = \frac{w}{2L}(L-x)^2 = \frac{0.64}{2(50)}(50-3.53)^2 = 13.8 \text{ kip}$$

www.EngineeringEBooksPdf.com

Apply dynamic load allowance to shear and moment due to live load.

$$M_{(LL+IM),\ truck} = 1.33(188.8) = 251.1 \text{ kip-ft}$$

Dynamic load allowance is not applicable to moment due to the lane load.

$$M_{total} = M_{(LL+IM),\ truck} + M_{lane} = 251.1 + 52.5 = 303.6 \text{ kip-ft}$$

$$V_{(LL+IM),\ truck} = 1.33(53.5) = 71.2 \text{ kip}$$

Dynamic load allowance is not applicable to shear due to the lane load.

$$V_{total} = V_{(LL+IM),\ truck} + V_{lane} = 71.2 + 13.8 = 85 \text{ kip}$$

Apply distribution factors to shear and moments due to live load.

$$g_{mi2} = 0.72$$

$$M_{(LL+IM)} = (0.72)(303.6) = 218.6 \text{ kip-ft}$$

$$g_{vi2} = 0.779$$

$$V_{(LL+IM)} = 0.779(85) = 66.2 \text{ kip}$$

Factored loads at the critical section

Bending moment

$$\begin{aligned} M_u &= 1.0[1.25M_{DC} + 1.5M_{DW} + 1.75M_{(LL+IM)}] \\ &= 1.0[1.25(143.2) + 1.5(15.6) + 1.75(218.6)] \\ &= 585 \text{ kip-ft} \end{aligned}$$

Shear

$$\begin{aligned} V_u &= 1.0[1.25V_{DC} + 1.5V_{DW} + 1.75V_{(LL+IM)}] \\ &= 1.0[1.25(37.81) + 1.5(4.1) + 1.75(66.2)] \\ &= 169 \text{ kip} \end{aligned}$$

Shear resistance of the T-beam section at the critical section: Art. 5.8.3.3

V_n is lesser of

$$V_n = V_c + V_s + V_p \qquad (5.57)\ [A5.8.3.3\text{-}1]$$

For a nonprestressed section, $V_p = 0$. Therefore, for the present example,

$$V_n = V_c + V_s$$

www.EngineeringEBooksPdf.com

The maximum value of nominal shear resistance, V_n, is determined as follows:

$$\begin{aligned} V_n &= 0.25 f_c' b_v d_v \\ &= 0.25(4)(21)(36.35) \\ &= 763.4 \text{ kip} \end{aligned} \qquad (5.64)\ [A5.8.3.3\text{-}2]$$

Compare the nominal shear resistance with the factored shear demand.

$$\phi V_n = 0.9(763.4) = 687 \text{ kip} > V_u = 169 \text{ kip}$$

Therefore, the section is adequate to resist shear.

Transverse reinforcement required to resist shear will be determined based on the Simplified Procedure for Nonprestressed Sections (Art. 5.8.3.4-1) and the General Procedure (Art. 5.8.3.4-2). Calculate the maximum shear that can be permitted by concrete to resist at the critical section.

$$V_c = 0.0316\beta\sqrt{f_c'}\, b_v d_v \qquad (5.59)\ [A5.8.3.3\text{-}3]$$

where b_v = effective web width, taken as the minimum web width, measured parallel to the neutral axis, between the resultant of compressive and tensile forces due to flexure, or for circular section, modified for the presence of ducts as specified in Art. 5.8.2.9 (in.).

For the present example, b_v = 21 in. and d_v = 36.35 in.; therefore,

$$V_c = 0.0316(2.0)(V_c = 0.0316(2.0)(\sqrt{4})(21)(36.35) = 96.5 \text{ kip}$$

So, of the total shear demand at the critical section of 196 kip, concrete can be permitted to resist a shear of 96.5 kip. The remainder of the shear must be resisted by transverse reinforcement, which is calculated as follows:

$$V_s = \frac{V_u}{\phi} - V_c \qquad (5.65)$$

$$\begin{aligned} V_{s,reqd} &= \frac{V_u}{\phi} - V_c \\ &= \frac{169}{0.9} - 96 \\ &= 92 \text{ kip} \end{aligned}$$

The T-section is not subjected to axial tension. Provide minimum amount of transverse reinforcement as specified in Art. 5.8.2.5 for conformance to Art. 5.8.3.4.1.

Minimum Amount of Transverse Reinforcement: Arts. 5.8.2.4. 5.8.2.5, and 5.8.2.6
Transverse reinforcement is required where

$$V_u > 0.5\phi(V_c + V_p) \qquad (5.70)\ [A5.8.2.4\text{-}1]$$

where

V_p = component of prestressing force in the direction of the shear force
= 0 for sections with nonprestressed steel

For the present case of T-beam with nonprestressed steel section, transverse will be provided where

$$V_u > 0.5\phi V_c$$

www.EngineeringEBooksPdf.com

For this example,

$$V_u = 169 \text{ kip} > 0.5\phi V_c = 0.5(0.9)(96) = 43.2 \text{ kip}$$

Therefore, minimum transverse must be provided as specified in Art. 5.8.2.5:

$$A_v \geq 0.0316\sqrt{f_c'}\left(\frac{b_v s}{f_y}\right) \qquad (5.72)\ [A5.8.2.5\text{-}1]$$

where
A_v = area of transverse reinforcement within distance s (in.^{2})
b_v = width of web adjusted for the presence of ducts as specified in Art. 5.8.2.9 (in.)
s = spacing of reinforcement
f_y = specified yield strength of reinforcement

Art. 5.8.2.6 permits transverse reinforcement in the form of stirrups perpendicular to the longitudinal axis of the member. Try two-legged No. 4 stirrups, $A_v = 0.39$ in.^{2} Calculate the required spacing from Equation 5.73:

$$s_{max} = \frac{A_v f_y}{0.0316\sqrt{f_c'}b_v}$$

$$= \frac{0.39(60)}{0.0316\sqrt{4}(21)} = 17.63 \text{ in., say 16 in.}$$

The spacing of stirrups would be limited to 16 in.

Maximum Permissible Spacing of Transverse Reinforcement
Maximum permitted spacing of stirrups, s_{max}, is governed by two conditions (Art. 5.8.2.7):

1. If $v_u < 0.125f_c'$, then

$$s_{max} = 0.8d_v \leq 24 \text{ in.} \qquad (5.75)\ [A5.8.2.7\text{-}1]$$

2. If $v_u > 0.125f_c'$, then

$$s_{max} = 0.4d_v \leq 12 \text{ in.} \qquad (5.76)\ [A5.8.2.7\text{-}2]$$

where v_u = shear stress calculated as specified in Art. 5.8.2.9 (ksi).

To check applicability of Equation 5.75 or Equation 5.76, calculate shear stress on concrete section at the critical section and at the midspan as follows:

$$v_u = \frac{|V_u - \phi V_p|}{\phi b_v d_v} \qquad (5.77)\ [A5.8.2.9\text{-}1]$$

For the present case of nonprestressed steel, $V_p = 0$.

Shear at the critical section,

$$v_u = \frac{169}{0.9(21)(36.35)} = 0.25 \text{ ksi}$$

$$0.125f_c' = 0.125(4) = 0.50 \text{ ksi}$$

$$v_u = 0.25 \text{ ksi} < 0.50 \text{ ksi}$$

www.EngineeringEBooksPdf.com

Therefore, $s_{max} = 0.8(d_v = 36.35) = 29.0$ in. > 16 in. (governs). Use $s_{max} = 16$ in. (calculated earlier).

Shear at midspan

1. Due to permanent loads, the shear at midspan = 0
2. Shear due to live load

Shear due to design truck: At $x = L/2 = 25$ ft,

$$V_{truck} = \frac{72[(L-x)-9.33]}{L} = \frac{72(50-25-9.33)}{50} = 22.56 \text{ kip}$$

$$V_{lane} = \frac{w}{2L}(L-x)^2 = \frac{0.64)}{2(50)}(50-25)^2 = 4.0 \text{ kip}$$

Apply dynamic load allowance to shear due to design truck. Dynamic load allowance is not applicable to the lane load.

$$V_{(LL+IM),\ truck} = 1.33(22.56) = 30.00 \text{ kip}$$

Shear due to live load, $V_{LL} = V_{(LL+IM),\ \text{truck}} + V_{lane} = 30 + 4.0 = 34.0$ kip

Apply distribution factor for shear, $g_{vi2} = 0.779$

Live load shear in the T-beam at the midspan,

$$V_{LL,\ midspan} = 0.779(34.0) = 26.5 \text{ kip}$$

$$v_u = \frac{26.5}{0.9(21)(36.35)} = 0.039 \text{ ksi}$$

$$0.125f'_c = 0.125(4) = 0.50 \text{ ksi}$$

$$v_u = 0.039 \text{ ksi} < 0.50 \text{ ksi}$$

Therefore, $s_{max} = 0.8(36.35) = 29.0$ in. > 16 in. (governs). Use $s_{max} = 16$ in.

So No. 4 shear stirrups at $s_{max} = 16$ in. can be used for the entire beam.

Spacing of Stirrups along the Span

1. At the critical section

$$V_{s,\ reqd} = 92 \text{ kip (calculated earlier).}$$

The required spacing of stirrups along the span is determined as follows:

$$V_s = \frac{A_v f_y d_v\ (\cot\theta + \cot\alpha)\ \sin\alpha}{s} \qquad (5.66)\ [A5.8.3.3\text{-}1]$$

where

θ = angle of inclination of diagonal compressive stresses as determined in Art. 5.8.3.4 (degrees)

α = angle of inclination of transverse reinforcement to longitudinal reinforcement (degrees)

www.EngineeringEBooksPdf.com

For vertical stirrups, $\alpha = 90°$, Equation A5.8.3.3-1 reduces to

$$V_s = \frac{A_v f_y d_v \cot\theta}{s} \qquad (5.67)\ [AC5.8.3.3\text{-}1]$$

Art. 5.8.2.6 permits stirrups making an angle not less than 45° with the longitudinal tension reinforcement. The reason for this limitation is the fact that stirrups inclined at less than 45° to the longitudinal reinforcement are difficult to anchor effectively against slip. In this example, vertical stirrups will be used.

When using Art. 5.8.3.4.1, $\theta = 45°$, so $\cot\theta = 1.0$, so Equation 5.67 reduces to the following equation:

$$V_s = \frac{A_v f_y d_v}{s}$$

For No. 4 two-legged stirrups, $A_v = 0.39$ in.^{2} for which the aforementioned equation can be expressed in terms of the required spacing, s_{reqd}:

$$s_{reqd} = \frac{A_v f_y d_v}{V_s} = \frac{0.39(60)(36.35)}{92} = 9.25 \text{ in.}$$

Provide No. 4 stirrups at 9 in. o.c. near the support.

2. In the beam between the critical section and the midspan
In the remainder of the beam, the stirrups can be spaced at arbitrary intervals of 9, 10, 12, and 16 in. ($s_{max} = 16$ in.); whole numbers are selected for practical convenience. The shear that can be resisted by No. 4 stirrups at these spacings can be determined from Equation 5.67:

$$V_s = \frac{0.39(60)(36.35)(1.0)}{s} = \frac{850.6}{s}$$

$$s = 9 \text{ in. } V_s = \frac{850.6}{9} = 94.5 \text{ kip}$$

$$s = 10 \text{ in. } V_s = \frac{850.6}{10} = 85.1 \text{ kip}$$

$$s = 12 \text{ in. } V_s = \frac{850.6}{12} = 70.9 \text{ kip}$$

$$s = 16 \text{ in. } V_s = \frac{850.6}{16} = 53.2 \text{ kip}$$

Minimum shear reinforcement must be provided where $V_u > 0.5\phi\,(V_c + V_p)$ (Art. 5.8.2.4).

$$0.5\phi V_c = 0.5(0.9)(96 + 0) = 43.2 \text{ kip}$$

It is not required to provide stirrups in the midspan region where $V_u < 0.5\phi V_c = 43.2$ kip.

To determine spacing of stirrups along the span, shear would be calculated (typically) at $0.1L$ intervals or at every 5 ft.

Shear due to permanent loads and the design lane load will be calculated from the influence lines for shear. Shear due to live load will be calculated from Equation 3.25, which is more convenient to use than influence lines.

www.EngineeringEBooksPdf.com

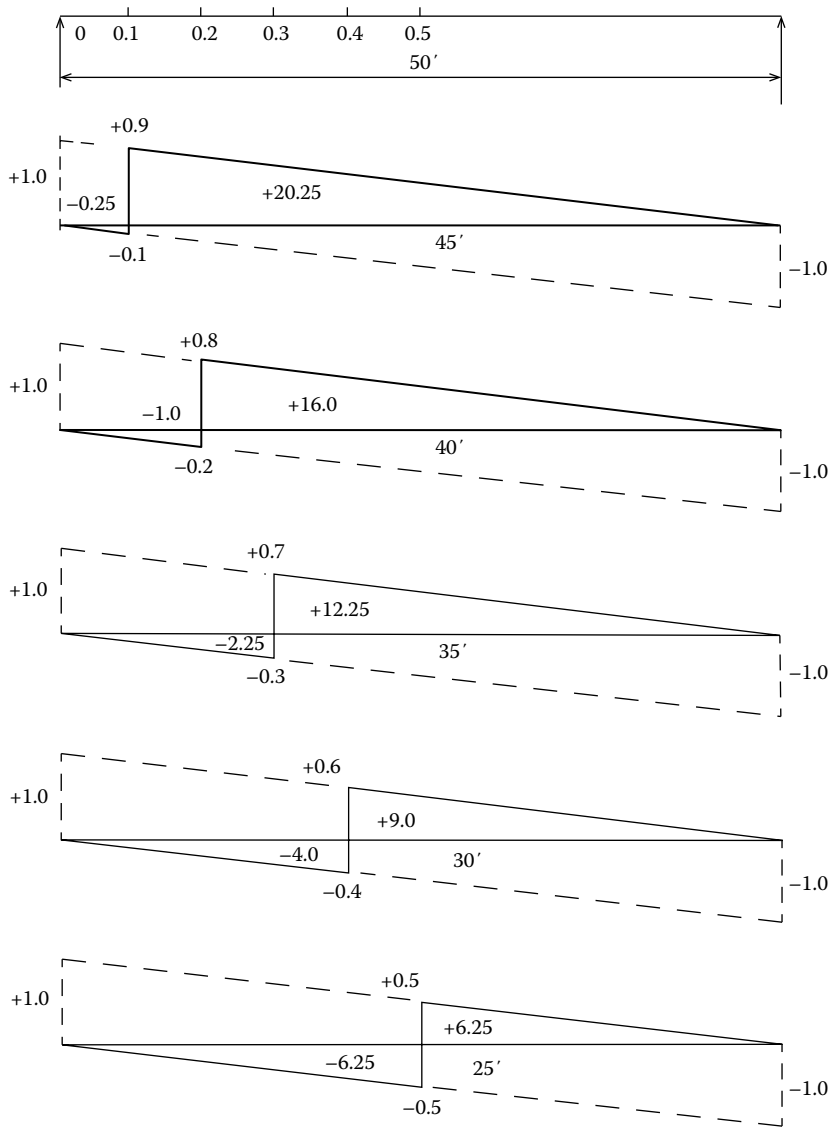

FIGURE 5.62 Influence line diagram for shear at 0.1L intervals along the span. Numbers inside the triangle represent the areas of the respective triangles.

Figure 5.62 shows influence lines for shear at 0.1L intervals along the span. The shears at various intervals are determined as follows:

1. $V_{DC} = w_{DC}$ (area under the influence line diagram)
2. $V_{DW} = w_{DW}$ (area under the influence line diagram)
3. $V_{lane} = 0.64$ (area under the influence line diagram) (distribution factor for shear = 0.779)

Values of shear for the aforementioned three items are noted in Table 5.11.
Shear due to Design Truck

For $x \leq 0.5L$, the shear due to design truck is given by Equation 3.25 as follows:

$$V_x = \frac{72\left[\left(L - x\right) - 9.33\right]}{L}$$

www.EngineeringEBooksPdf.com

TABLE 5.11
Shear Demand and Spacing of No. 4 Stirrups along the Span

	Distance along the Span, x/L					
Type of Shear	**0.0704**	**0.1**	**0.2**	**0.3**	**0.4**	**0.5**
w_{DC} = 1.75 kip/ft	37.81	35.00	26.25	17.50	8.75	0.00
w_{DW} = 0.19 kip/ft	4.10	3.80	2.85	1.90	0.95	0.00
Design truck	55.43	53.21	45.75	38.29	30.83	23.37
Design lane, kip	10.76	10.10	8.00	6.11	4.49	3.12
V_{LL+IM}, kip	66.21	65.38	53.75	44.40	35.32	26.5
V_u,[a] kip	169.3	163.9	131.2	102.4	75.6	46.4
V_u/ϕ, kip	188.1	182.1	145.8	113.8	84.0	46.4
V_c	96.0	96.0	96.0	96.0	96.0	96.0
$V_s = V_u/\phi - V_c$, kip	92.1	86.1	49.8	17.8	—	—
$s_{calculated}$, in.	9.21	9.85	17.03	47.65	—	—
$s_{provided}$, in.	9	9	16	16	16	16

[a] $V_u = 1.0\,[1.25V_{DC} + 1.5V_{DW} + 1.75(V_{LL+IM})]$.

At the critical section, x = 3.53 ft = 0.0706L,

$$V_{0.0706L} = \frac{72\left[(50-3.53)-9.33\right]}{50} = 53.5 \text{ kip}$$

$$V_{0.1L} = \frac{72\left[(50-5)-9.33\right]}{50} = 51.36 \text{ kip}$$

$$V_{0.2L} = \frac{72\left[(50-10)-9.33\right]}{50} = 44.16 \text{ kip}$$

$$V_{0.3L} = \frac{72\left[(50-15)-9.33\right]}{50} = 36.96 \text{ kip}$$

$$V_{0.4L} = \frac{72\left[(50-20)-9.33\right]}{50} = 29.76 \text{ kip}$$

$$V_{0.5L} = \frac{72\left[(50-25)-9.33\right]}{50} = 22.56 \text{ kip}$$

Apply dynamic load allowance and live load distribution factor (=0.779) to the aforementioned shear values:

$$V_{0.0706L} = 1.33(0.779)(53.5) = 55.43 \text{ kip}$$

$$V_{0.1L} = 1.33(0.779)(51.36) = 53.21 \text{ kip}$$

$$V_{0.2L} = 1.33(0.779)(44.16) = 45.75 \text{ kip}$$

www.EngineeringEBooksPdf.com

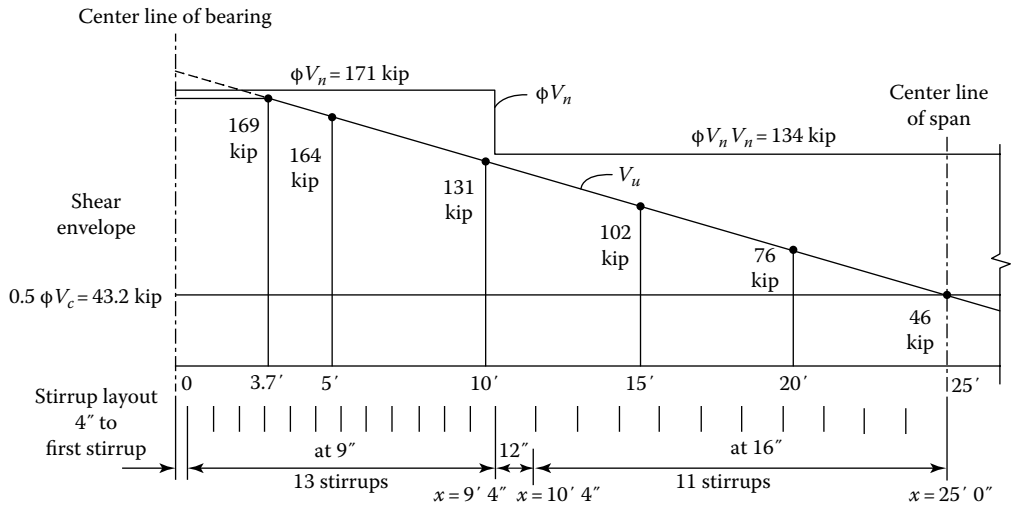

FIGURE 5.63 Layout of No. 4 stirrups along the left half span from then center of bearing to the midspan. The layout for the right half span is symmetrical about the center line of span.

$$V_{0.3L} = 1.33(0.779)(36.96) = 38.29 \text{ kip}$$

$$V_{0.4L} = 1.33(0.779)(29.76) = 30.83 \text{ kip}$$

$$V_{0.5L} = 1.33(0.779)(22.56) = 23.37 \text{ kip}$$

Table 5.11 presents shear values at the critical section and 0.1L intervals along the span as well as calculated spacing of stirrups and the actual spacing of stirrups along the span. Figure 5.63 presents the layout of stirrups along the span from the center of bearing to the midspan.

Tensile Capacity of Longitudinal Reinforcement: Art. 5.8.3.5
The tensile capacity of longitudinal reinforcement at each section of the beam shall be proportioned to satisfy Equation A5.8.3.5-1:

$$A_{ps}f_{ps} + A_s f_y \geq \frac{|M_u|}{d_v \phi_f} + 0.5\left(\frac{N_u}{\phi_c}\right) + \left(\left|\frac{V_u}{\phi_v} - V_p\right| - 0.5V_s\right)\cot\theta \qquad (5.81)\ [\text{A}5.8.3.5\text{-}1]$$

where
A_s = area of prestressing steel (in.^{2})
f_{ps} = average stress in prestressing steel at the time at which the nominal resistance of the member is required
N_u = applied factored axial force, taken as positive if tensile (kip)
V_p = component in the direction of the applied shear of the effective prestressing force, positive if resisting the applied shear (kip)

The aforementioned equation is general and applicable to section with both nonprestressed and prestressed steel. For the present case of T-beam section with nonprestressed steel, the quantities pertaining to prestressed steel (A_{ps}, N_u, V_p) are set to zero, with $\theta = 45°$ and $\cot\theta = 1.0$. With these substitutions, the aforementioned equation reduces

$$A_s f_y \geq \frac{|M_u|}{d_v \phi_f} + \left(\left|\frac{V_u}{\phi_v}\right| - 0.5V_s\right) \qquad (5.82)$$

www.EngineeringEBooksPdf.com

1. Capacity of flexural reinforcement at the critical section
From previous calculations, M_u = 585 kip-ft, V_u = 169 kip, and with No. 4 stirrups at 9 in. o.c., V_s = 94.25 kip. Substitution of these values in the aforementioned equation yields

$$A_s f_y \geq \frac{|585(12)|}{36.35(0.9)} + \left(\left|\frac{169}{0.9}\right| - 0.5(94.25)\right) = 355.2 \text{ kip}$$

A check must be made to ensure that $A_s f_y \geq 354.7$ kip is available at the support, which depends on the available development length, ℓ_d.

For No. 11 and smaller diameter bars, the basic development length, ℓ_d, of bar is the larger of the following three lengths (Art. 5.11.2.1.2):

1. $\dfrac{1.25 A_b f_y}{\sqrt{f'_c}} = \dfrac{1.25(1.56)(60)}{\sqrt{4.0}} = 58.5$ in.
2. $0.4 d_b f_y = 0.4(1.41)(60) = 33.8$ in. < 58.5 in. (governs)
3. $\ell_{d,\,min.} = 12$ in.

where
A_b = area of the cross section of the bar
d_b = diameter of the bars

Art. 5.11.2.1.2 requires use of a modification factor to increase the development length. A minimum modification factor of 1.2 is applied for epoxy-coated bars. For epoxy-coated bars with cover less than $3d_b$ or with clear spacing between bars less than $6d_b$, a modification factor of 1.5 applies.

$$\text{Concrete cover} = 1.5 \text{ in.} < 3(d_b = 1.14) = 3.42 \text{ in.}$$

Therefore, use a modification factor of 1.5.

$$\ell_{d,mod} = 58.5(1.5) = 88.75 \text{ in.} \approx 88 \text{ in.}$$

Available development length, assuming 3 in. clearance from the end (Figure 5.64),

$$\ell_{d,avail} = d_v + 12 \text{ in.}$$

$$= 36.35 + 12 = 48.35 \text{ in.}$$

The available development length (48.35 in.) is smaller than the required development length (88 in.). Therefore, the tensile stress in the longitudinal reinforcement must be reduced linearly.

$$f_s = \left(\frac{48.35}{88}\right)(60) = 33.0 \text{ ksi}$$

The tensile capacity of 10 No. 11 bars, A_s = 15.62 in.^{2}, is determined as

$$A_s f_s = 15.62(33.0) = 517 \text{ kip} > A_s f_{y,\,reqd} = 355.2 \text{ kip, OK}$$

2. Capacity of flexural reinforcement at midspan
At midspan, V_u = 46.4 kip, M_u = 2074 kip-ft, and for No. 4 stirrups at 16 in. o.c., V_s = 53.2 kip.

$$A_s f_y \geq \frac{|2074(12)|}{36.35(0.9)} + \left(\left|\frac{46.4}{0.9}\right| - 0.5(53.2)\right) = 785.7 \text{ kip}$$

www.EngineeringEBooksPdf.com

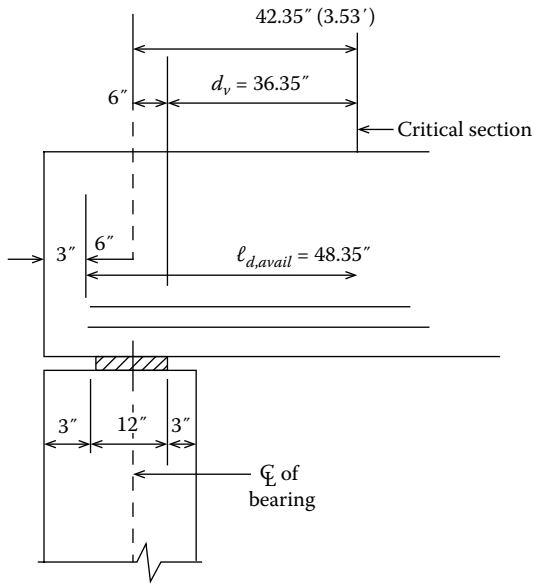

FIGURE 5.64 Development length of tension reinforcement at critical section.

Compare with the capacity of tensile reinforcement provided.

$$A_s f_y = 15.62(60) = 937.2 \text{ kip} > 785.7 \text{ kip, OK}$$

3. At the face of bearing
   At the face of bearing, $M_u = 0$, $V_u = 169$ kip, and for No. 4 stirrups at 9 in. o.c., $V_s = 94.25$ kip.

$$A_s f_y \geq 0 + \left(\left|\frac{169}{0.9}\right| - 0.5(94.25)\right) = 140.7 \text{ kip}$$

The required development length at the support was calculated to be 88 in. But the available length is only 1 ft 3 in. or 15 in. (Figure 5.65). Therefore, the tensile stress in the longitudinal reinforcement must be reduced linearly.

$$f_s = \left(\frac{15}{88}\right)(60) = 10.23 \text{ ksi}$$

The tensile capacity of 10 No. 11 bars, $A_s = 15.62$ in.^{2} is determined as

$$A_s f_s = 15.62(10.23) = 159.8 \text{ kip} > A_s f_{y,reqd} = 140.7 \text{ kip, OK}$$

Fatigue Limit State: Arts. 3.6.1.4, 3.6.1.4.3, 5.5.3
For fatigue considerations, concrete members shall satisfy the following:

$$\gamma(\Delta f) \leq (\Delta F)_{TH} \qquad \text{(A5.5.3.1-1)}$$

where
γ = load factor specified in LRFD Table 3.4.1.1 for Fatigue I Load Combination
Δf = force effect, live load stress range due to the passage of the fatigue load as specified in Art. 3.6.4.1 (ksi)
$(\Delta F)_{TH}$ = constant-amplitude fatigue threshold

www.EngineeringEBooksPdf.com

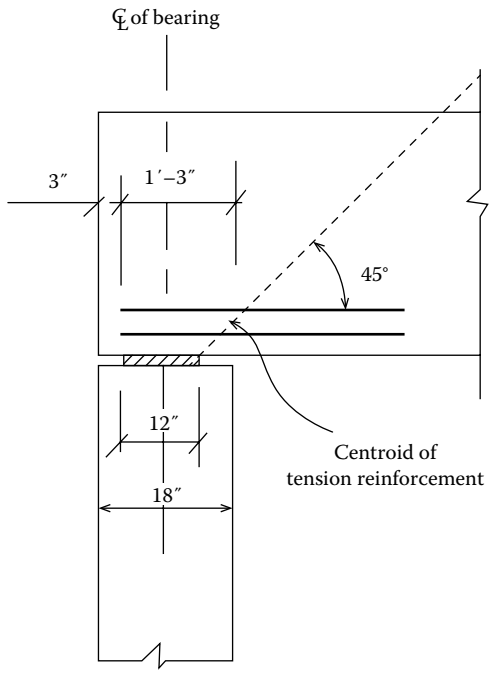

FIGURE 5.65 Development length of tension reinforcement at the support (face of bearing).

Bending moment due to fatigue is determined from Fatigue I Load Combination (Art. 5.5.3.1):

$$M_{fat} = \eta_i[1.0(M_{DC}) + 1.0(M_{DW}) + 1.5(M_{LL+IM})]$$

where

η_i = product of load modification factors = η_D, η_R, η_I
η_D = modification factor for ductility = 1.0
η_R = modification factor for redundancy = 1.0
η_I = modification factor for operational importance = 1.0

Therefore,

$$M_{fat} = 1.0[1.0(M_{DC}) + 1.0(M_{DW}) + 1.5(M_{LL+IM,fat})]$$

$$M_{fat} = (1.0)(M_{DC} + M_{DW} + 1.5M_{LL+IM,fat})$$

$$M_{DC} = 469 + 78 = 547 \text{ kip-ft (calculated earlier)}$$

$$M_{DW} = 59 \text{ kip-ft (calculated earlier)}$$

Fatigue due to Live Load

The fatigue truck consists of the design truck but with a fixed distance of 30 ft between the two 32-kip axles; only one design truck is to be placed on the span. Lane load is not considered in fatigue load.

For the 50 ft span bridge under consideration, it is not possible to place the fatigue truck with all the three truck axles on the bridge. The position of the two axles (the 8-kip and 32-kip axles) is shown in Figure 5.66. The maximum moment occurs under the 32-kip axle load, which is so

www.EngineeringEBooksPdf.com

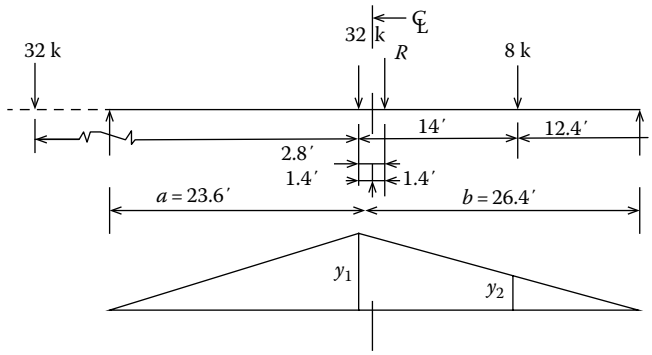

FIGURE 5.66 Position of fatigue truck for maximum moment in beam.

positioned on the bridge that the center line of the bridge bisects the distance between the resultant of the two loads and the 32-kip load. The influence line for the moment under the 32-kip load is shown in Figure 5.66.

The c.g. of loads (take moments of loads about the 32-kip load) is located at a distance x to the left of 32-kip load:

$$x = \frac{8(14)}{8+32} = 2.8 \text{ ft}$$

The influence line ordinate under the 32-kip load, y_1, is

$$y_1 = \frac{ab}{L} = \frac{23.6(26.4)}{50} = 12.4608 \text{ ft}$$

$$y_2 = y_1\left(\frac{12.4}{26.4}\right) = 12.4608\left(\frac{12.4}{26.4}\right) = 5.8528 \text{ ft}$$

$$M_{fat} = 32y_1 + 8y_2 = 32(12.4608) + 8(5.8528) = 445.6 \text{ kip-ft}$$

Apply distribution factor for bending moment. The distribution factor for bending moment for the one lane loaded case was calculated to be 0.539. The multiple-presence factor, $m = 1.2$. So the distribution factor for bending moment for fatigue is

$$g_{fat} = \frac{g_{mi1}}{1.2} = \frac{0.539}{1.2} = 0.45$$

Dynamic load allowance for fatigue, $DLA_{fat} = 1.15$

$$M_{LL+IM,\ fat} = 0.45(1.15)(445.6) = 230.6 \text{ kip-ft}$$

$$M_{fat} = 1.0[1.0(547) + 1.0(59) + 1.5(230.6)] = 951.9 \text{ kip-ft}$$

Stress in the bottom of the beam based on elastic principles,

$$f_b = \frac{My_b}{I_g} = \frac{951.9(12)(27.54)}{240{,}350} = 1.31 \text{ ksi}$$

www.EngineeringEBooksPdf.com

Cracked section analysis must be used when the sum of stresses in the section due to the unfactored permanent loads and prestress (=0 in this example) and the Fatigue I Load Combination is tensile and exceeds $0.095\sqrt{f'_c}$.

$$0.095\sqrt{f'_c} = 0.095\sqrt{4} = 0.19 \text{ ksi}$$

$$f_b = 1.31 \text{ksi} > 0.095\sqrt{f'_c} = 0.19 \text{ ksi}$$

Therefore, cracked section analysis must be used to investigate fatigue.

Art. 5.5.3.2 requires that the constant-amplitude fatigue threshold, $(\Delta F)_{TH}$, for straight reinforcement and welded wire reinforcement without a weld in high-stress region shall be taken as given by Equation A5.5.3.2-1:

$$(\Delta F)_{TH} = 24 - 0.33 f_{min} \qquad \text{(A5.5.3.2-1)}$$

where f_{min} = minimum live-load stress resulting from the Fatigue I Load Combination with the more severe stress from either the permanent loads or permanent loads, shrinkage, and creep-induced loads; positive if tension, negative if compression (ksi).

Live load stress from Fatigue I Load Combination: $M_{LL+IM,fat}$ = 230.6 kip-ft

Calculate stress in the tensile reinforcement from elastic principles.

$$A_s = 15.62 \text{ in.}^2,\ d_s = 37.88 \text{ in. (calculated earlier)}$$

$$\rho = \frac{A_s}{bd} = \frac{15.62}{90(37.88)} = 0.00458$$

$$n\rho = 8(0.00458) = 0.0366$$

$$k = \sqrt{(n\rho)^2 + 2n\rho} - n\rho$$

$$= \sqrt{(0.0366)^2 + 2(0.0366)} - 0.0366$$

$$= 0.236$$

$$j = 1 - \frac{k}{3} = 1 - \frac{0.236}{3} = 0.921$$

$$\Delta_f = \frac{M_{LL,fat}}{A_s jd} = \frac{230.6(12)}{15.62(0.921)(37.88)} = 5.08 \text{ ksi}$$

For Fatigue I live load combination, γ = 1.5 (LRFD Table 3.4.1-1)

$$\gamma(\Delta f) = 1.5(5.08) = 7.62 \text{ ksi}$$

Stress from permanent load

$$M_{DC} = 547 \text{ kip-ft}$$

$$M_{DW} = 59 \text{ kip-ft}$$

$$M_{perm\ loads} = 547 + 59 = 606 \text{ kip-ft}$$

www.EngineeringEBooksPdf.com

$$f_{perm\ loads} = \frac{M_{perm\ loads}}{A_s jd}$$

$$= \frac{606(12)}{15.62(0.921)(37.88)}$$

$$= 13.34 \text{ ksi}$$

$$f_{min} = 7.64 + 13.34 = 21.00 \text{ ksi}$$

$$(\Delta F)_{TH} = 24 - 0.33 f_{min}$$

$$= 24 - 0.33(21.00)$$

$$= 17.07 \text{ ksi}$$

$$\gamma(\Delta f) = 7.62 \text{ ksi} < (\Delta F)_{TH} = 17.07 \text{ ksi, OK}$$

Service I Limit State

Control of Cracking by Distribution of Reinforcement: Art. 5.7.3.4

Concrete members are known for cracking under any load condition, including thermal effects and restraint of deformations. These effects produce tension in the gross section in excess of the cracking strength of concrete. Improved crack control is achieved when the tension reinforcement is well distributed over the zone of maximum tension in concrete (e.g., in the bottom of simply supported beams). It has been established that several bars at moderate spacing are more effective in controlling cracking than one or two larger bars of equivalent area.

To control cracking, the spacing of mild reinforcement in the layer closest to the tension face, s, shall satisfy Equation 5.45:

$$s \le \frac{700\gamma_e}{\beta_s f_{ss}} - 2d_c \qquad (5.45)\ [A5.7.3.4\text{-}1]$$

in which

$$\beta_s = 1 + \frac{d_c}{0.7(h - d_c)} \qquad (5.46)$$

where

γ_e = exposure factor

d_c = thickness of concrete cover measured from the extreme tension fiber to center of the flexural reinforcement closest thereto (in.)

f_{ss} = tensile stress in steel reinforcement at the service limit state (ksi)

h = overall thickness or depth of the component (in.)

Moment at Service I Limit State,

$$M_{ser} = \eta_i(1.0M_{DC} + 1.0M_{DW} + 1.0M_{LL+IM})$$

$$= 1.0[1.0(547) + 1.0(59) + 1.0(744)]$$

$$= 1350 \text{ kip-ft}$$

www.EngineeringEBooksPdf.com

Modulus of rupture (Art: 5.4.2.6),

$$f_r = 0.24\sqrt{f'_c} = 0.24\sqrt{4} = 0.48 \text{ ksi}$$

$$0.8f_r = 0.8(0.48) = 0.348 \text{ ksi}$$

Tensile in the bottom fibers,

$$f_b = \frac{My_b}{I_g}$$

$$= \frac{1{,}350(12)(27.54)}{240{,}350}$$

$$= 1.856 \text{ ksi} > 0.8f_r = 0.348 \text{ ksi}$$

Therefore, the maximum spacing is limited by Equation 5.45.

γ_e = exposure factor = 0.75 for Class 2 exposure

d_c = clear cover diameter of No. 4 stirrup + half tension bar diameter

= 1.5 + 0.5 + 1/2(1.41)

= 2.71 in.

f_s = tensile stress in the steel reinforcement at the service limit state

$$f_s = \frac{M}{A_s jd} = \frac{1350(12)}{15.62(0.921)(37.88)} = 29.73 \text{ ksi}$$

$$\beta_s = 1 + \frac{d_c}{0.7(h - d_c)}$$

$$= 1 + \frac{2.71}{0.7(42 - 2.71)} = 1.10$$

$$s \le \frac{700\gamma_c}{\beta_s f_{ss}} - 2d_c = \frac{700(0.75)}{1.10(29.73)} - 2(2.71) = 10.6 \text{ in.}$$

Five No. 10 bars are provided in the layer closest to the tension face. The spacing of bars provided is

$$s_{provided} = \frac{1}{4}\left[b_w - 2(\text{side cover}) - 2(\text{diameter of No.4 stirrups}\right]$$

$$= \frac{1}{4}\left[21 - 2(1.5) - 2(0.5)\right]$$

$$= 4.25 \text{ in.} < 10.6 \text{ in., OK}$$

www.EngineeringEBooksPdf.com

Part II: Design of the Exterior Girder
Live Load Distribution Factors for the Exterior Girder
Resistance of the exterior girder may not be less than that of the interior girder. This requirement is mandated because in the likely case of widening the bridge, the exterior girder would become an interior girder. Calculate the live load distribution factors for bending moment and shear in the exterior girder and compare them with those for the interior girder; use the larger values for design.

The following values for the interior girder were computed earlier:

Bending moment

$$g_{mi1} = 0.539$$

$$g_{mi2} = 0.72$$

Shear

$$g_{vi1} = 0.66$$

$$g_{vi2} = 0.779$$

Exterior Girder
Bending Moment: LRFD Table 4.6.2.2.2d-1

1. One design lane loaded: Use lever rule.
   With reference to Figure 5.67,

$$R_e = \frac{4.5}{7.5}R = 0.6R$$

$$\text{Multiple-presence factor} = 1.2$$

$$g_{me1} = 1.2(0.6) = 0.72$$

2. Two or more lanes loaded: Modify interior-girder factors by e

$$e = 0.77 + \frac{d_e}{9.1}$$

$$= 0.77 + \frac{2.0}{9.1} = 0.99$$

$$g_{me2} = 0.99(0.72) = 0.713 < g_{me1} = 0.72 \text{ (governs)}$$

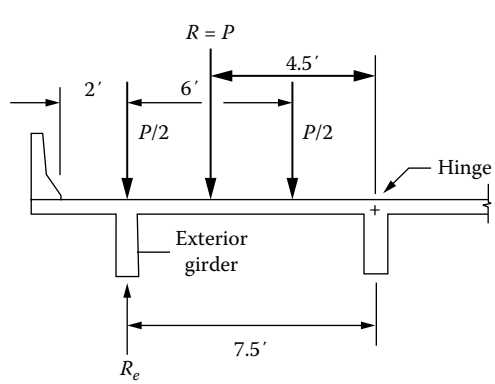

FIGURE 5.67 Lever rule for the exterior girder.

www.EngineeringEBooksPdf.com

TABLE 5.12
Comparison of Live Load Distribution Factors for Interior and Exterior Girders

Bending Moment		
Interior girder	0.539	0.72
Exterior girder	0.72	0.713
Shear		
Interior girder	0.66	0.779
Exterior girder	0.72	0.623

Shear: LRFD Table 4.6.2.2.3b-1

1. One design loaded: Use lever rule.

$$g_{ve1} = 0.72 \text{ (see previous calculations)}$$

2. Two or more lanes loaded: Modify interior-girder factor by e

$$e = 0.6 + \frac{d_e}{10}$$

$$= 0.6 + \frac{2.0}{10} = 0.80$$

$$g_{ve2} = 0.80(0.779) = 0.623 < g_{ve1} = 0.72 \text{ (governs)}$$

Table 5.12 shows a comparison of live load distribution factors for interior and exterior beams. Distribution factors for both bending moment and shear for the interior girder are greater than the corresponding values for the exterior girder. Therefore, both live load moment and shear for the interior girder are greater than the corresponding values for the exterior girder. Force effects due to permanent loads are slightly larger for the interior girder than for the exterior girder (less dead load from the wearing surface). The overall result is greater force effects for the interior girder than for the exterior girder. However, it is required that the resistance of the exterior girder shall not be lesser than that of the interior girder. Therefore, provide the design for the exterior girder identical to that for the interior girder.

Part II: Design of the Deck Slab

The deck slab will be designed using both the empirical design method (Art. 9.7.2) and the traditional design method (Art. 9.7.3) for illustrative purposes. Both methods were discussed in Section 5.13. Either design is acceptable as the final design.

Solution

a. Design by the empirical method: Art. 9.7.2

Art. 9.7.2 permits designing a deck slab if the following conditions are satisfied:

1. Cross frames or diaphragms are used throughout the cross section at lines of support. Assume that diaphragms are provided at the supports.
2. For cross section involving torsionally stiff units, such as individual separated box beams, either intermediate diaphragms between the boxes are provided at a spacing not to exceed 25.0 ft or the need for supplemental reinforcement over the webs to accommodate transverse bending between the box units is investigated and reinforcement is provided if necessary.
   This provision does not apply to the T-beam bridge.

www.EngineeringEBooksPdf.com

3. The supporting components are made of steel and/or concrete.
   The supporting components are stems of the T-beams made from concrete.
4. The deck is fully cast in place and water cured.
   The deck will be cast in place and water cured.
5. The deck is of uniform depth, except for haunches at girder flanges and other local thickening.
   The deck is a part of the T-beam bridge of uniform depth, except for local thickening and local thickening for drainage.
6. The ratio of effective length to design depth does not exceed 18.0 and is not less than 6.0.
   For this T-beam bridge, effective length, L_{eff}, of the deck (between the inside faces of adjacent webs),

$$L_{eff} = 7.5(12) - 21 = 69 \text{ in.} = 5.75 \text{ ft}$$

   Structural thickness of the slab, $t_s = 8.0$ in.

$$\frac{L_{eff}}{t_s} = \frac{69}{8.0} = 8.63$$

$$18.0 > 8.63 > 6.0, \text{ OK}$$

7. Core depth of the slab is not less than 4.0 in.
   Assume that the concrete cover at the top = 2.5 in. and 1.5 in. clear cover at the bottom, then the core depth of the slab = 8.0 − 2.5 − 1.5 = 4.0 in., OK.
8. The effective length, as specified in Art. 9.7.2.3, does not exceed 13.5 ft.

$$L_e = 5.75 \text{ ft} < 13.5 \text{ ft, OK}$$

9. The minimum depth of the slab is not less than 7.0 in., excluding a sacrificial wearing surface where applicable.
   Thickness of slab, $t_s = 8.0$ in. > 7.0 in., OK
10. There is an overhang beyond the centerline of the outside girder of at least 5.0 times the depth of the slab; this condition is satisfied if the overhang is at least 3.0 times the depth of the slab and a structurally continuous concrete barrier is made composite with the overhang.
    Length of overhang from the centerline of the outside stem = 3.75 ft = 45 in.

$$5t_s = 5(8.0) = 40 \text{ in.}$$

$$45 \text{ in.} > 5t_s = 40 \text{ in., OK}$$

    The traffic barrier will be made composite with the deck overhang.
11. The specified 28-day strength of the deck concrete is not less than 4.0 ksi.
    Specified 28-day compressive strength, $f'_c = 4.0$ ksi, OK
12. The deck is made composite with the supporting structural components. For this purpose, a minimum of two shear connectors at 24.0 in. o.c. shall be provided in the negative moment region of continuous steel superstructures. The provisions of Art. 6.10.1.1 shall also be satisfied. For concrete girders, the use of stirrups satisfies this requirement.
    The deck will be cast monolithic with the beams, so the deck and the beams will act compositely.
    The stirrups from the supporting webs of T-beams will be extended in the deck slab, which will satisfy this requirement.

Thus, all requirements of the empirical method are satisfied. The deck can be designed by the empirical method.

www.EngineeringEBooksPdf.com

Reinforcement Requirements: Art. 9.7.2.5

Reinforcement requirements for the empirically designed slabs were discussed in Section 5.13. Four isotropic layers of reinforcement are required as follows:

1. Minimum 0.18 in.^{2}/ft of steel for each top layer with a maximum allowable spacing of 18 in.
   Provide No. 5 Grade 60 bars at 12 in. o.c., top reinforcement, $A_{s,provided} = 0.31$ in.^{2}
   Note that No. 5 at 18 in. o.c. would have provided $A_s = 0.21$ in.$^2 > A_s = 0.18$ in.^{2} required.
   Instead, the 12 in. spacing is provided to be consistent (and ease of construction) with the bottom layer of reinforcement as determined in the following.
2. Minimum of 0.27 in.^{2}/ft in each bottom layer
   Select No. 5 bar ($A_s = 0.31$ in.^{2}) as provided in the top layer of reinforcement. The required spacing is

$$spacing = \frac{0.31(12)}{0.27} \approx 13.8 \text{ in.}$$

   Provide No. 5 Grade 60 bars at 12 in. o.c., bottom reinforcement, $A_{s,provided} = 0.31$ in.^{2}
   The reinforcement details are shown in Figure 5.68.

b. Design by the traditional method: Art. 4.6.2.1

This method is based on designing strips of the deck slab oriented perpendicular to the supports as discussed in Section 4.18. Equivalent strips that span primarily in the transverse direction have no limit on their widths (Art. 4.6.2.1.3). As specified in Art. C4.6.2.1.6, in lieu of more precise calculations, the unfactored design live load moments can be taken from LRFD Table A4-1 (see appendix of this chapter).

Applicability Criteria: Art. 9.7.3

1. The deck has four layers of reinforcement, two in each direction, OK.
2. The deck complies with Art. 9.7.1.1:
   a. The deck is 8 in. thick, OK.
   b. The deck meets the minimum cover requirements of Art. 9.7.1.1:
      i. 2.5 in. clear cover for top bars, OK.
      ii. 1 in. clear cover for the bottom bars, OK.

The deck meets the aforementioned requirements; the deck can be designed using the traditional method.

Loads

Permanent Loads

Dead load of the 8 in. thick deck,

$$w_{DC} = \frac{8}{12}(1.0)(1.0)(0.15) = 0.1 \text{ kip/ft}$$

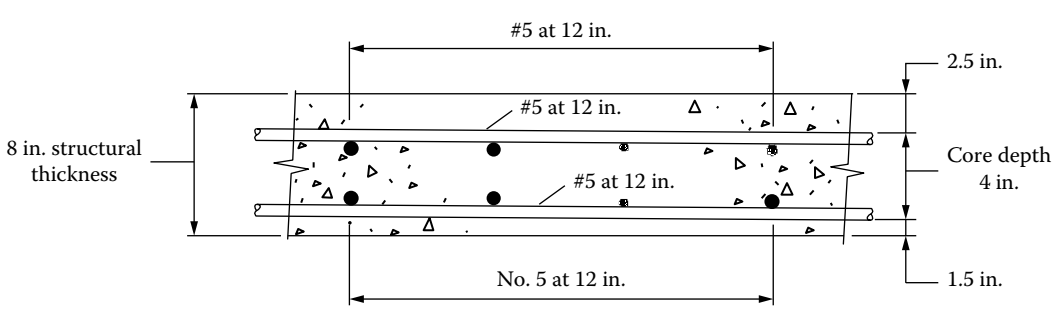

FIGURE 5.68 Deck reinforcement for Example 5.2 (empirical method).

www.EngineeringEBooksPdf.com

Dead load due to the 25 lb/ft² FWS,

$$w_{DW} = 0.025 \text{ kip/ft}$$

Moments due to permanent loads are obtained assuming the deck as fixed-ended beam having length equal to the distance between the center lines of supports:

$$L = 7.5 \text{ ft}$$

Maximum positive moment occurs at the midspan:

$$+M_{DC} = \frac{wL^2}{24} = \frac{0.1(7.5)^2}{24} = 0.23 \text{ kip-ft}$$

$$+M_{DW} = \frac{wL^2}{24} = \frac{0.025(7.5)^2}{24} = 0.06 \text{ kip-ft}$$

Maximum negative moment occurs at the supports:

$$-M_{DC} = \frac{wL^2}{12} = \frac{0.1(7.5)^2}{12} = 0.47 \text{ kip-ft}$$

$$-M_{DW} = \frac{wL^2}{12} = \frac{0.025(7.5)^2}{12} = 0.12 \text{ kip-ft}$$

(*Note*: In view of the small moments due to the permanent loads, the assumption of fixed-ended support conditions is considered applicable.)

Shear is not calculated because the shear check is not required for decks (Art. C4.6.2.1.6).

Live Load Force Effects

The deck is continuous over the supports (webs of T-beams). Because of continuity, the deck is subjected to positive moment at the midspan between the supports and negative moment at the supports. In lieu of more precise calculations, unfactored live load moments are obtained from LRFD Table A4-1 (see appendix of this chapter). Multiple-presence factors and dynamic allowance are included in the tabulated values of the moments.

S = distance between the center lines of supports = 7.5 ft

$+M_{pos}$ = 5.44 kip-ft

For negative moment, the critical section is taken at the face of the web. Negative moment is computed at the face of the web from interpolation of the tabulated values.

For the 21 in. wide stem, the distance from the face of the web to the centerline of the web = 21/2 = 10.5 in. The negative moment at this location is obtained from interpolation of values of negative moment at 9 in. from the centerline of the support (–3.78 kip-ft) and at 12 in. from the centerline of the support (–3.15 kip-ft). At 10.5 in. from the centerline of the support,

$$-M = \frac{3.78 + 3.15}{2} = 3.47 \text{ kip-ft}$$

The live load shear is not computed because shear check is not required for decks (Art. C4.6.2.1.6).

Strength I Limit State

$$M_u = \eta_i \Sigma \gamma_i Q_i$$

$$M_u = 1.0[1.25M_{DC} + 1.50M_{DW} + 1.75M_{LL+IM}]$$

www.EngineeringEBooksPdf.com

$$+M_u = 1.0[1.25(0.23) + 1.5(0.06) + 1.75(5.44)]$$
$$= 9.90 \text{ kip-ft}$$

$$-M_u = 1.0[1.25(0.47) + 1.5(0.12) + 1.75(3.47)]$$
$$= 6.84 \text{ kip-ft}$$

Since M_u and d_s are known values, the value of A_s can be calculated as follows:

$$A_s \approx \frac{M_u}{4d_s} \tag{5.86}$$

where M_u is expressed in kip-ft units. Assume No. 5 bar for the bottom reinforcement and 1.5 in. clear cover at the bottom. Then

$$d_s = 8 - 1.5 - 1/2(0.625) = 6.19 \text{ in.}$$

For positive moment, $M_u = 9.9$ kip-ft.

$$A_{s,est} = \frac{9.9}{4(6.19)} = 0.40 \text{ in.}^2/\text{ft}$$

Try No. 5 bar at 9 in. o.c. and $A_s = 0.40$ in.^{2}/ft. Calculate M_n for 1 ft wide strip perpendicular to supports (stems). The cross section measures 12 in. wide × h = 8 in. deep, with $d_s = 6.19$ in. (Figure 5.69).

Calculate the nominal flexural resistance of 1 ft wide strip from Equations 5.21 through 5.23:

$$0.85 f'_c\, ab = A_s f_y \tag{5.21}$$

$$a = \frac{A_s f_y}{0.85 f'_c b}$$
$$= \frac{0.40(60)}{0.85(4.0)(12)}$$
$$= 0.59 \text{ in.} \tag{5.22}$$

$$M_n = A_s f_y \left(d_s - \frac{a}{2}\right)$$
$$= 0.40(60)\left(6.19 - \frac{0.59}{2}\right)$$
$$= 141.5 \text{ kip-in.} = 11.79 \text{ kip-ft} \tag{5.26}$$

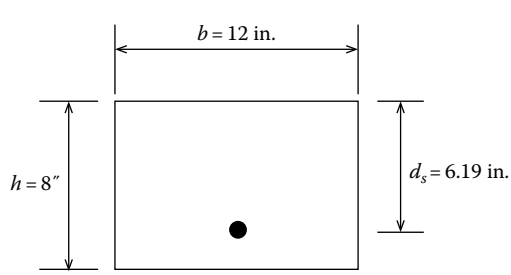

FIGURE 5.69 Cross section of 1 ft wide strip for positive moment.

www.EngineeringEBooksPdf.com

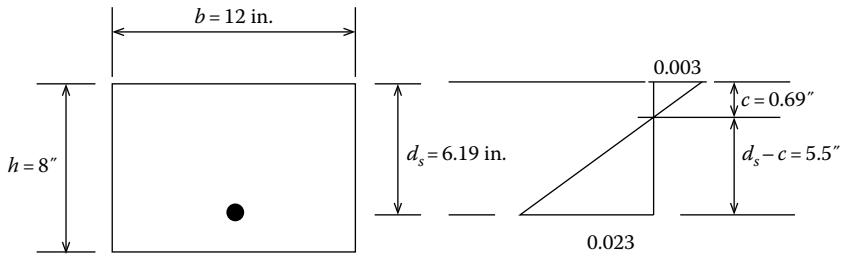

FIGURE 5.70 Strain distribution in the slab.

Strength Reduction Factor, ϕ

The value of strength reduction factor, ϕ, depends on the strain in the reinforcement. From the aforementioned calculations, the neutral axis is located at c from the top of the slab given as follows:

$$c = \frac{a}{\beta_1} \tag{5.17}$$

$$c = \frac{a}{\beta_1} = \frac{0.59}{0.85} = 0.69 \text{ in.}$$

From the strain distribution diagram (Figure 5.70), the strain in the reinforcement is obtained from Equation 5.29 by substituting $d = d_s$:

$$\begin{aligned} \varepsilon_s &= \frac{d_s - c}{c}(\varepsilon_c) \\ &= \left(\frac{6.19 - 0.69}{0.69}\right)(0.003) \\ &= 0.024 > 0.005 \end{aligned} \tag{5.29}$$

Therefore, the section is tension-controlled and ϕ = 0.9.

$$\phi M_n = 0.9(11.79)$$

$$= 10.61 \text{ kip-ft} > M_u = 9.90 \text{ kip-ft, OK}$$

Provide No. 5 at 9 in. o.c. transverse reinforcement at the bottom.

Reinforcement Requirements: Art. 5.7.3.3:

1. Maximum reinforcement: Art. 5.7.3.3.1 (No requirements specified)
2. Minimum reinforcement: Art. 5.7.3.3.2
   The amount of prestressed and nonprestressed tensile reinforcement shall be adequate to develop a factored flexural resistance, M_r, equal to the lesser of the following two values:
   a. 1.33 times the factored moment required by the applicable strength load combination specified in LRFD Table 3.4.1-1.

www.EngineeringEBooksPdf.com

b. The cracking moment is given as follows:

$$M_{cr} = \gamma_3 \left[\left(\gamma_1 f_r + \gamma_2 f_{cpe} \right) S_c - M_{dnc} \left(\frac{S_c}{S_{nc}} - 1 \right) \right] \tag{5.41}$$

where

f_r = modulus of rupture specified in Art. 5.4.2.6

f_{cpe} = compressive stress in concrete due to effective prestress forces only (allowance for all prestress losses) at the extreme fiber of the section where tensile stress is caused by externally applied loads (ksi)

= 0 for sections with nonprestressed reinforcement only

M_{dnc} = total unfactored dead load moment acting on the monolithic or noncomposite section where tensile stress is caused by externally applied loads (ksi)

S_c = section modulus for the extreme fiber of the composite section where tensile stress is caused by externally applied loads (in.^{3})

= S_{nc} where beams are designed for the monolithic or noncomposite section to resist all loads

S_{nc} = section modulus for the extreme fiber of the monolithic or noncomposite section where tensile stress is caused by externally applied loads (in.^{3})

In the present case of the section with nonprestressed reinforcement, $f_{cpe} = 0$, $S_{nc} = S_c$, $\gamma_1 = 1.6$ (for all other structures), and $\gamma_3 = 0.75$ (for A 706, Grade 60 reinforcement). Substitution of these values in Equation 5.41 yields

$$M_{cr} = 0.75(1.6) f_r S_c$$

$$= 1.2 f_r S_c \tag{5.44}$$

For normal-weight concrete (Art. 5.4.2.6),

$$f_r = 0.24 \sqrt{f'_c \text{ ksi}} \tag{5.12}$$

For a 4 ksi concrete,

$$f_r = 0.24 \sqrt{4 \text{ ksi}} = 0.48 \text{ ksi}$$

For a rectangular section,

$$S_c = \frac{bh^2}{6} = \frac{12(8)^2}{6} = 128 \text{ in.}^3$$

Substituting in Equation 5.44, we obtain

$$M_{cr} = 1.2(0.48)(128) = 73.73 \text{ kip-in.} = 6.14 \text{ kip-ft}$$

$$1.33 M_u = 1.33(9.90) = 13.17 \text{ kip-ft} > M_{cr} = 6.14 \text{ kip-ft (smaller value governs)}$$

Flexural resistance, $M_r = \phi M_n = 10.61$ kip-ft > $M_{cr} = 6.14$ kip-ft, OK

Shrinkage and Temperature Reinforcement: Art. 5.10.8.2

For bars and welded wire fabric, the area of reinforcement per foot on each face and in each direction shall satisfy the following:

$$A_s \geq \frac{1.3bh}{2(b+h) f_y} \tag{5.91} \text{ [A5.10.8-1]}$$

www.EngineeringEBooksPdf.com

$$0.11 \le A_s \le 0.6 \text{ in.}^2 \qquad (5.92)\ [A5.10.8\text{-}2]$$

where
A_s = area of reinforcement in each direction and on each face (in.^{2}/ft)
b = least width of component section (in.)
h = least thickness of the component
f_y = specified yield strength of reinforcing bars
$\le$ 75 ksi

For the present case, b = 12 in., d = 8 in., and f_y = 60 ksi. Substitution of these values in Equation 5.10 gives

$$A_s \ge \frac{1.3(12)(8)}{2(12+8)(60)} = 0.052 \text{ in.}^2/\text{ft} < 0.11 \text{ in.}^2 \text{ (governs)}$$

Provide minimum reinforcement, A_s = 0.11 in.^{2}/ft.

Spacing not to exceed three times the depth of component or 18 in.

$$3h = 3(8) = 24 \text{ in.} > 18 \text{ in. (governs).}$$

Provide No. 4 at 18 in. o.c., A_s = 0.13 in.^{2}/ft, OK.

Note that No. 3 at 12 in. o.c. also would provide the required amount of reinforcement. But No. 4 bars are preferred for greater stiffness (overall sturdiness) to facilitate construction (pouring concrete, walking crew with equipment, etc.).

Distribution Steel: Art. 9.7.3.2
For primary reinforcement perpendicular to traffic, the distribution steel is given as follows:

$$A_{s,dist} = \frac{200}{\sqrt{S}} \le 67 \text{ percent} \qquad (5.88)$$

where S = effective span length taken as equal to the effective length specified in Art. 9.7.2.3 (ft).
S = distance between the inside faces of stems = 7.5 – 1.75 = 5.75 ft

$$A_{s,dist} = \frac{200}{\sqrt{5.75}} = 83.41 \text{ percent} > 67 \text{ percent}$$

Therefore, $A_{s,dist}$ = 67 percent governs.

Area of bottom reinforcement, A_s = 0.41 in.^{2}/ft

$$A_{s,dist} = 0.67(0.41) = 0.27 \text{ in.}^2/\text{ft}$$

Provide No. 5 at 14 in. o.c., A_s = 0.27 in.^{2}

Reinforcement in the Top of Deck
Top reinforcement is provided to resist the negative moment in the support region of the deck.

$$-M_u = 6.84 \text{ kip-ft}$$

www.EngineeringEBooksPdf.com

Estimate the required area of reinforcement from the following:

$$A_s \approx \frac{M_u}{4d_s} \tag{5.86}$$

where M_u is in kip-ft units. Assume No. 5 bar for the top reinforcement and 2.5 in. clear cover at the top. Then

$$d_s = 8 - 2.5 - 1/2(0.625) = 5.19 \text{ in.}$$

$$A_{s,est} = \frac{6.84}{4(5.19)} = 0.33 \text{ in.}^2/\text{ft}$$

Try No. 5 bar at 10 in. o.c., $A_s = 0.37$ in.^{2}/ft. Calculate M_n for 1 ft wide strip (Figure 5.71) perpendicular to supports (webs). The cross section measures 12 in. wide × 8 in. deep, with $d_s = 5.19$ in.

$$0.85 f_c' \, ba = A_s f_y$$

$$a = \frac{A_s f_y}{0.85 f_c' \, b}$$

$$= \frac{0.37(60)}{0.85(4.0)(12)}$$

$$= 0.54 \text{ in.}$$

$$M_n = A_s f_y \left(d_s - \frac{a}{2} \right)$$

$$= 0.37(60)\left(5.19 - \frac{0.54}{2} \right)$$

$$= 109.24 \text{ kip-in.} = \mathbf{9.1} \text{ kip-ft}$$

Calculate the Strength Reduction Factor, ϕ

The value of strength reduction factor, ϕ, depends on the strain on the reinforcement. From the aforementioned calculations, the neutral axis is located at c from the top of the slab given by Equation 5.17:

$$c = \frac{a}{\beta_1} = \frac{0.54}{0.85} = 0.64 \text{ in.}$$

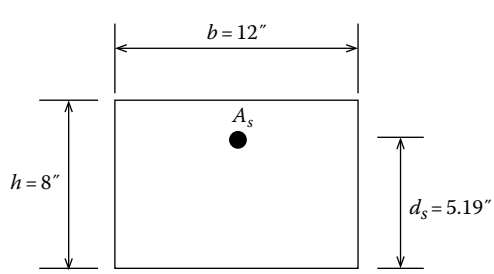

FIGURE 5.71 Cross section of 1 ft wide strip for negative moment.

www.EngineeringEBooksPdf.com

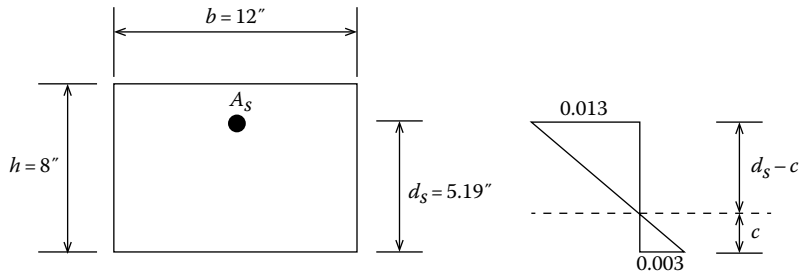

FIGURE 5.72 Strain distribution in the slab.

Strain in reinforcement is determined from Equation 5.29 (by substituting $d = d_s$). From the strain distribution diagram, the strain in the reinforcement is obtained as (Figure 5.72)

$$\begin{aligned}\varepsilon_s &= \frac{d_s - c}{c}(\varepsilon_c)\\ &= \left(\frac{5.19 - 0.64}{0.64}\right)(0.003)\\ &= 0.021 > 0.005\end{aligned} \tag{5.29}$$

Therefore, the section is tension-controlled and $\phi = 0.9$.

$$\phi M_n = 0.9(9.1)$$

$$= 8.19 \text{ kip-ft} > M_u = 6.84 \text{ kip-ft, OK}$$

Provide No. 5 at 10 in. o.c. transverse reinforcement at top.

Shrinkage and Temperature Reinforcement

$$A_s = 0.11 \text{ in.}^2 \text{ (computed earlier)}$$

Provide minimum reinforcement, $A_s = 0.11$ in.^{2}/ft. Spacing not to exceed three times the component or 18 in.

$$3h = 3(8) = 24 \text{ in.} > 18 \text{ in. (governs)}$$

$$\text{Provide No. 4 at 18 in. o.c., } A_s = 0.13 \text{ in.}^2\text{/ft, OK}$$

Note that No. 3 at 12 in. o.c. also would provide the required amount of reinforcement. But No. 4 bars are preferred for greater stiffness (overall sturdiness) to facilitate construction (pouring concrete, walking crew with equipment, etc.).

Summary of Deck Reinforcement by the Empirical and Traditional Methods

Reinforcement Provided		Empirical Method	Traditional Method
Longitudinal direction	Top	No. 5 at 12 in.	No. 4 at 18 in.
	Bottom	No. 5 at 12 in.	No. 5 at 14 in.
Transverse direction	Top	No. 5 at 12 in.	No. 5 at 10 in.
	Bottom	No. 5 at 12 in.	No. 5 at 9 in.

www.EngineeringEBooksPdf.com

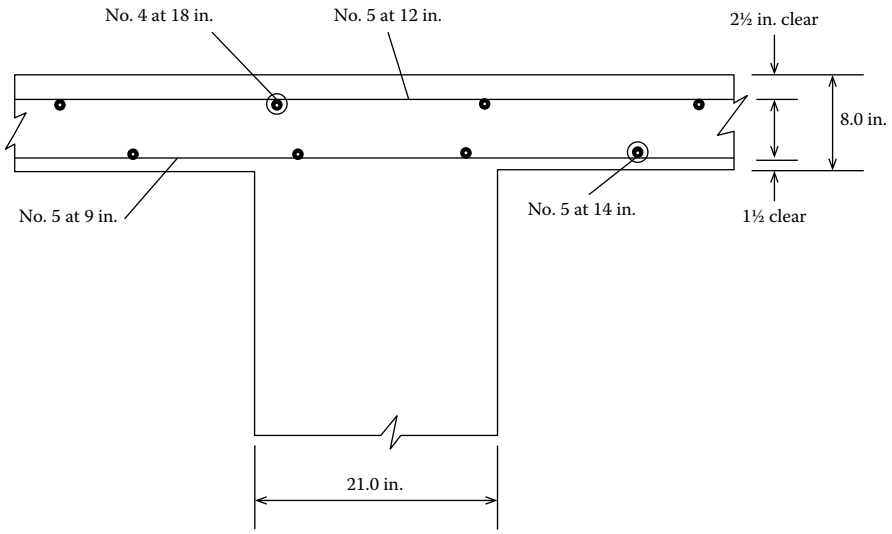

FIGURE 5.73 Deck reinforcement details (traditional method).

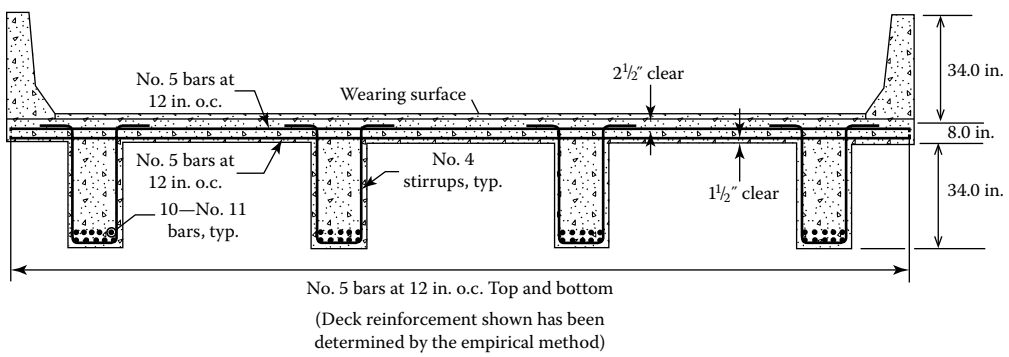

FIGURE 5.74 T-beam bridge cross section showing final layout of reinforcement. (Adapted from Achneider, E.F. and Bhide, S., *LRFD of Cast-in-Place Concrete Bridges*, Portland Cement Association, Chicago, IL, 2004.)

Fatigue and Fracture Limit State: Art. 9.5.3
Check for fatigue is not required for concrete decks.

Reinforcing details for the deck are shown in Figure 5.73. Final layout of reinforcement for the T-beam superstructure is shown in Figure 5.74.

Example 5.3: Design of Concrete Deck over Steel Girders

Figure 5.75 shows the cross section of the composite slab–steel girder bridge of Example 6.10.

The superstructure consists of five W30 × 90 steel girders spaced at 7 ft 6 in. center to center. The concrete deck would be cast in place to act compositely with the girders. Design a concrete deck for this bridge. The specified compressive strength of concrete is, f'_c = 4.0 ksi. Use Grade 60 reinforcement. Show details of reinforcement.

The deck for the bridge can be designed either by the empirical method (Art. 9.7.2) or by the traditional method (Art. 9.7.3) as demonstrated for the T-beam bridge of Example 5.2. Because of its simplicity, design of the deck by empirical method would be demonstrated for this

www.EngineeringEBooksPdf.com

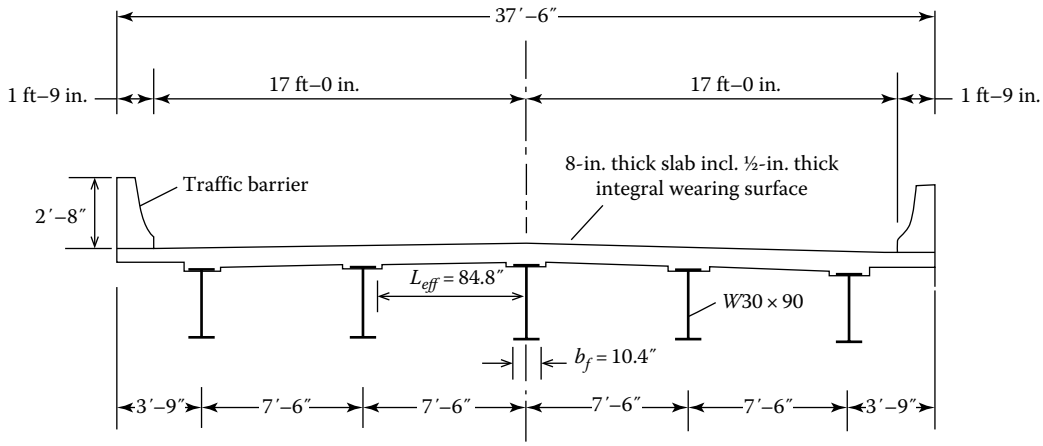

FIGURE 5.75 Cross section of composite slab–steel girder bridge cross section for Example 6.10.

example. Design calculations using the traditional method would be similar to those presented in Example 5.2.

It would be noted that the only difference between the design of deck for this example and that of Example 5.2 is the deck thickness and the calculation of the effective length. For this example, a deck thickness of 7.5 in. is selected. To preserve completeness, all requirements of the empirical method are checked as follows:

Design of Deck by Empirical Method

Art. 9.7.2 permits designing a deck slab if the following conditions are satisfied:

1. Cross frames or diaphragms are used throughout the cross section at lines of support. Assume that diaphragms are provided at the supports.
2. For cross section involving torsionally stiff units, such as individual separated box beams, either intermediate diaphragms between the boxes are provided at a spacing not to exceed 25.0 ft or the need for supplemental reinforcement over the webs to accommodate transverse bending between the box units is investigated and reinforcement is provided if necessary.

   This provision does not apply to the slab–steel bridge superstructure of this example.
3. The supporting components are made of steel and/or concrete.

   The supporting components are W30 × 90 steel girders, OK.
4. The deck is fully cast in place and water cured.
5. The deck is of uniform depth, except for haunches at girder flanges and other local thickening.

   The deck would be of uniform depth, except for local thickening and local thickening for drainage.
6. The ratio of effective length to design depth does not exceed 18.0 and is not less than 6.0. For the slab–steel girder superstructure, the effective length, L_{eff}, of the deck is taken as the distance between the tip of the flange of one girder and the inside face of the web of the adjacent girder.

$$L_{eff} = \text{center-to-center spacing between the girders} - 1/2\ (\text{flange width})$$

$$= 7.5(12) - 1/2(10.4) = 84.8 \text{ in.} = 7.07 \text{ ft}$$

Structural thickness of the slab, t_s = 7.5 in.

www.EngineeringEBooksPdf.com

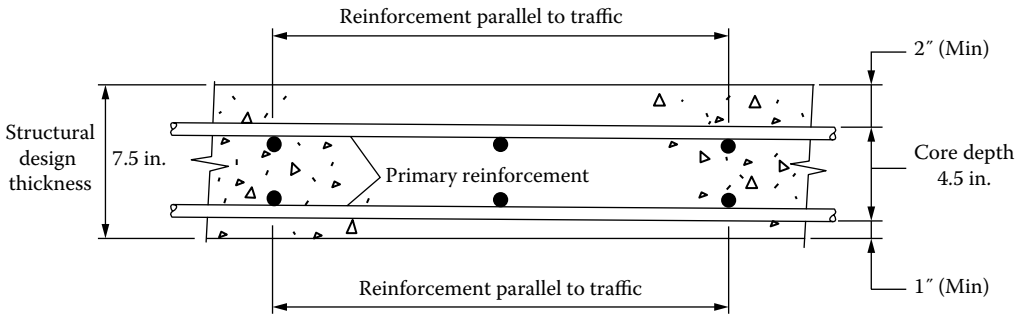

FIGURE 5.76 Core depth of the slab.

$$\frac{L_{eff}}{t_s} = \frac{84.8}{7.5} = 11.31$$

$$18.0 > 11.31 > 6.0, \text{ OK}$$

7. Core depth of the slab is not less than 4.0 in.
   Assuming concrete cover at the top = 2.0 in. and 1.0 in. clear cover at the bottom,
   Core depth of the slab = 7.5 − 2.0 − 1.0 = 4.5 in., OK (Figure 5.76)
8. The effective length, as specified in Art. 9.7.2.3, does not exceed 13.5 ft.

$$L_e = 7.07 \text{ ft} < 13.5 \text{ ft, OK}$$

9. The minimum depth of the slab is not less than 7.0 in., excluding a sacrificial wearing surface where applicable.

$$\text{Thickness of slab, } t_s = 7.5 \text{ in.} > 7.0 \text{ in., OK}$$

10. There is an overhang beyond the centerline of the outside girder of at least 5.0 times the depth of the slab; this condition is satisfied if the overhang is at least 3.0 times the depth of the slab and a structurally continuous concrete barrier is made composite with the overhang.
    Length of overhang from the centerline of the outside stem = 3.75 ft = 45 in.

$$5t_s = 5(7.5) = 37.5 \text{ in.}$$

$$45 \text{ in.} > 5t_s = 37.5 \text{ in. OK}$$

    There is no need to make the traffic barrier composite with the deck overhang.
11. The specified 28-day strength of the deck concrete is not less than 4.0 ksi.

$$\text{Specified 28-day compressive strength, } f'_c = 4.0 \text{ ksi, OK}$$

12. The deck is made composite with the supporting structural components. For this purpose, a minimum of two shear connectors at 24.0 in. o.c. shall be provided in the negative moment region of continuous steel superstructures. The provisions of Art. 6.10.1.1 shall also be satisfied. For concrete girders, the use of stirrups satisfies this requirement.
    The deck will be made composite with the steel girders by providing sufficient shear connectors welded to the girders and embedded in the deck.

Thus, all requirements of the empirical method are satisfied. The deck can be designed by the empirical method.

www.EngineeringEBooksPdf.com

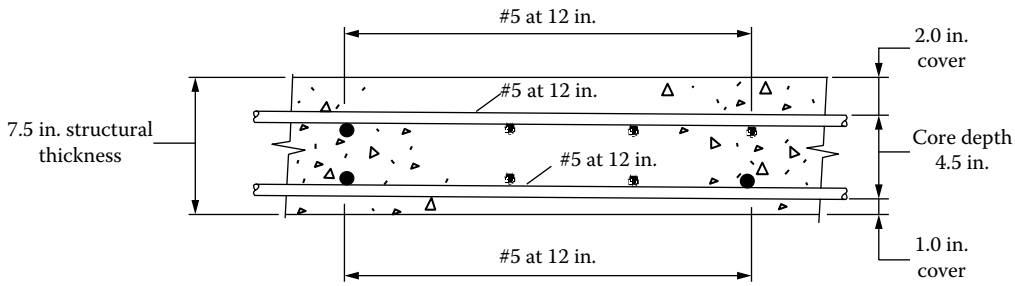

FIGURE 5.77 Deck reinforcement details.

Reinforcement Requirements: Art. 9.7.2.5
Reinforcement requirements for the empirically designed slabs were discussed in Section 5.13:

1. Minimum of 0.18 in.^{2}/ft of steel for each top layer with a maximum allowable spacing of 18 in.
   Provide No. 5 Grade 60 bars at 18 in. o.c. top reinforcement, $A_{s,provided}$ = 0.31 in.^{2}
2. Minimum of 0.27 in.^{2}/ft in each bottom layer.
   Provide No. 5 Grade 60 bars at 18 in. o.c., bottom reinforcement, $A_{s,provided}$ = 0.21 in.^{2}
   The reinforcement details are shown in Figure 5.77.

5.16 DESIGN OF DECK OVERHANG AND BARRIER WALLS

5.16.1 General

Deck overhangs with some type of mounted metal railings are structural components common to all types of highway bridges. Overhang portions of the decks carry traffic barriers on each side of the bridge. For design purposes, all *bridge traffic barrier systems* are referred to as *railings* (Art. 13.1). Metal railings are often mounted on concrete *barrier walls* or *parapets* that essentially are railing systems of reinforced concrete, usually considered as adequately reinforced concrete walls. The barrier is cast separately from the deck, after the deck has hardened. This makes it necessary to have dowel bars extending from the deck into the bottom portion of the barrier.

Railing systems serve several functions, but their primary function is to contain and redirect colliding vehicles using the bridge. For this reason, all vehicle traffic barriers should have test record of being structurally and geometrically crashworthy.

While selecting a railing system, consideration should be given to many factors such as protection of the occupants of a vehicle in collision with the railing, protection of other vehicles near the collision, and protection of persons and property on roadways and other areas underneath the structure. Profiles of railings should be aesthetically pleasing and allow freedom of view from passing vehicles. Other factors that influence traffic railing performance requirements are variations in traffic volume, speed, vehicle mix, roadway alignment, activities and conditions beneath the structure, and owner's project-specific performance requirement.

5.16.2 Traffic Railing Design Forces and Design Criteria

Irrespective of the type of traffic barriers used on a bridge, they must be designed to resist impact loads from colliding vehicles. For design purposes, the corresponding limit state of forces is referred to as extreme-event limit state (Art. 1.3.2.5) as discussed in Chapter 1. A bridge is required to be designed for the extreme-event limit state to ensure its structural survival during a major earthquake, or flood, when collided by a vehicle, vessel, or ice flow. These events are called extreme events because their return period may be significantly greater than the design life of the bridge.

www.EngineeringEBooksPdf.com

TABLE 5.13
Design Forces for Traffic Railings

Design Forces and Designations	Railing Test Levels					
	TL-1	TL-2	TL-3	TL-4	TL-5	TL-6
F_t transverse (kip)	13.5	27.0	54.0	54.0	124.0	175.0
F_L longitudinal (kip)	4.5	9.0	18.0	18.0	41.0	58.0
F_V vertical (kip)	4.5	4.5	4.5	18.0	80.0	80.0
L_t and L_L (ft)	4.0	4.0	4.0	3.5	8.0	8.0
L_v (ft)	18.0	18.0	18.0	18.0	40.0	40.0
H_e (ft)	18.0	20.0	24.0	32.0	42.0	56.0
Minimum H height of rail (in.)	27.0	27.0	27.0	32.0	42.0	90.0

Source: From *AASHTO LRFD Bridge Design Specifications*, Copyright © 2012 by American Association of State Highway and Transportation Officials, Washington, DC. Used by permission.

Design of decks was discussed in Section 5.14 in which it was pointed out that design of deck overhang shall not be permitted by using empirical design method (Art. 9.7.2.2). Instead, the overhang is to be designed based on the failure mechanism specified in Art. A13.2.

Design of deck overhang consists of three parts:

1. Design and selection of *crashworthy* railing systems
2. Design of the concrete barrier parapet to which the metal railings are attached or on which they are mounted
3. Design of the overhang portion of the deck to resist permanent and live load from the deck and the forces transferred to it from the barrier wall

In any case, the impact loads from the colliding vehicles are transmitted from the railing to the supports (e.g., barrier walls) on which they are mounted, which, in turn, transmit those loads to the deck overhang in the form of overturning moment and a tensile force.

Design provisions for calculating forces on railing systems are specified in Art. A13.2, which are based on collision forces determined from crash test data for various railing test levels. Design forces corresponding to specific railing test levels are given in Table 5.13 with reference to Figure 5.78.

Railing design forces should be taken as shown in Table 5.13. The transverse and longitudinal forces shown in Table 5.13 need not be applied in conjunction with the vertical loads. The significance of the data shown in Table 5.13 is explained in Art. CA13.2.

A schematic of design forces shown in Table 5.13 is shown in Figure 5.78. Various design forces are defined as follows.

The effective height of the vehicle rollover force, H_e, is given as follows:

$$H_e = G - \frac{12WB}{2F_t} \qquad (5.97)\ [AA13.2\text{-}1]$$

where

G = height of vehicle c.g. above bridge desk as specified in LRFD Table 13.7.2-1 (in.)
W = weight of vehicle corresponding to the required test level, as specified in LRFD Table 13.7.2-1 (kip)
B = out-to-out wheel spacing on an axle as specified in LRFD Table 13.7.2-1 (ft)
F_t = transverse force corresponding to the required test level as specified in Table 5.13 (kip)

www.EngineeringEBooksPdf.com

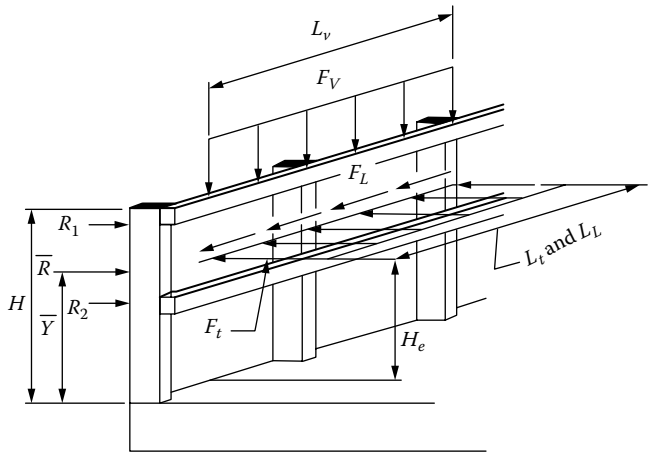

FIGURE 5.78 Metal bridge railing design forces, vertical location, and horizontal distribution length. (From *AASHTO LRFD Bridge Design Specifications*, Copyright © 2012 by American Association of State Highway and Transportation Officials, Washington, DC. Used by permission.)

Equation 5.97 has been found to give reasonable predictions of effective railing height requirements to prevent rollover. For concrete railings, Equation 5.97 results in a theoretically required height of 34.0 in. for Test Level 4 (TL-4). However, a height of 32 in. shown in Table 5.13 has been found to be acceptable based on past experience with the satisfactory performance of railings of that height. (This is the basis for the 32 in. height of barrier wall used in examples in this chapter and in Chapter 6.)

Railing should be designed to satisfy the following requirements (see Figure 5.79 for nomenclature):

$$\overline{R} \geq F_t \qquad (5.98)\ [AA13.2\text{-}2]$$

$$\overline{Y} \geq \frac{H_e}{12} \qquad (5.99)\ [AA13.2\text{-}3]$$

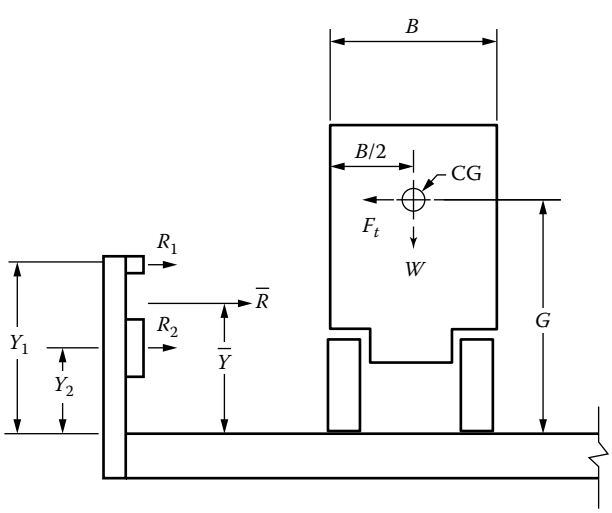

FIGURE 5.79 Traffic railing forces nomenclature. (From *AASHTO LRFD Bridge Design Specifications*, Copyright © 2012 by American Association of State Highway and Transportation Officials, Washington, DC. Used by permission.)

www.EngineeringEBooksPdf.com

The force $\bar{R}$ in Equation 5.98 is the resultant of forces R_1 and R_2 shown in Figure 5.79, which can be expressed by Equation 5.100:

$$\bar{R} = \Sigma R_i \qquad (5.100)\ [AA13.2\text{-}4]$$

The centroid of railing forces, R_1 and R_2 (Figure 5.79), can be obtained from statics by taking moments of these forces about either of them; the resulting expression is given by Equation 5.101:

$$\bar{Y} = \frac{\Sigma R_i Y_i}{\bar{R}} \qquad (5.101)\ [AA13.2\text{-}5]$$

where

R_i = resistance of the rail (kip)

Y_i = vertical distance of the point of application of force R_i measured from the base

5.16.3 Yield Line Analysis for Concrete Traffic Barriers or Parapets

When a barrier wall is subjected by an impact load, it causes the wall to bend about both its horizontal axis and vertical axis. Therefore, to provide flexural resistance about both axes, the wall is reinforced both horizontally and vertically. The horizontal reinforcement provides resistance to flexure about the vertical axis (denoted by M_w); the vertical reinforcement provided resistance to flexure about the horizontal axis (M_c). The net result of these forces is to separate the wall from the overhang (shear) and cause an overturning moment about the interface between the two. To provide resistance against these forces, reinforcement from the wall must be adequately anchored inside the overhang. Barrier walls are typically cast after the deck has hardened; therefore, required reinforcement must project from the hardened deck to be anchored into the walls during casting.

Art. A13.3.1 provides that yield line analysis may be used for analysis and strength design of reinforced concrete and prestressed concrete barriers or parapets. A discussion on yield analysis can be found in the literature (Hirsch 1978, Barker and Puckett 2013). Design forces acting on the traffic barrier system and their locations are shown in Figure 5.79; schematic of analytical model is shown in Figure 5.78. The following assumptions are implicit in the yield line analysis specified in Art. 13.3.1:

1. The analysis includes only the ultimate flexural capacity of the concrete component. Necessary stirrups or ties should be provided to resist the shear and/or diagonal tension forces.
2. The ultimate flexural resistance of the bridge deck or the slab, M_s, should be determined in recognition that the deck is also resisting a tensile force, caused by the component of the impact forces, F_t.
3. It is assumed that the yield line failure pattern occurs within the parapet (Figure 5.80) and does not extend into the deck. It implies that the deck must have sufficient resistance to force the yield line failure to remain within the parapet. If the failure extends into the deck, the equations for the resistance of the parapet are not valid.
4. Sufficient longitudinal length of the parapet exists to result in the yield line failure pattern shown in Figure 5.80. For short lengths of parapet, a single yield line may form along the juncture of the parapet and the deck (Figure 5.81).
5. The analysis is based on the assumption that the negative and positive wall resisting moments are equal and that the negative and positive beam resisting moments are equal.

www.EngineeringEBooksPdf.com

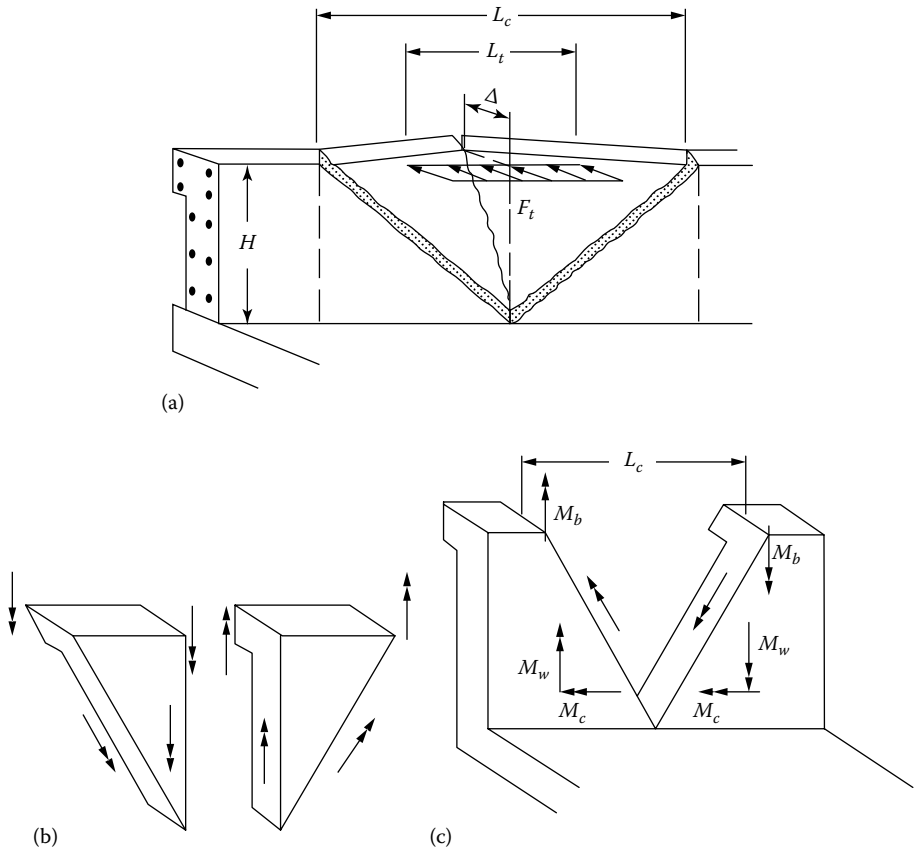

FIGURE 5.80 Yield line analysis of concrete parapet walls for impact loads within wall segment: (a) formation of yield lines in the barrier wall due to applied force F_t, (b) free body diagram showing forces acting on the of the failed segment of the barrier wall, and (c) free body diagram showing equilibrating forces acting along the yield lines in the failed barrier wall. (From *AASHTO LRFD Bridge Design Specifications*, Copyright © 2012 by American Association of State Highway and Transportation Officials, Washington, DC. Used by permission.)

The nominal railing resistance to transverse load, R_w, depends on the location of the formation of the yield line mechanism. Two cases are considered as follows:

1. When impact occurs within a given wall (Figure 5.76), R_w may be calculated from Equation 5.102:

$$R_{w1} = \left(\frac{2}{2L_c - L_t}\right)\left(8M_b + 8M_w + \frac{M_c L_c^2}{H}\right) \qquad (5.102)\ [\text{AA13.3.1-1}]$$

The critical wall length, L_c, over which the yield mechanism occurs, is given by Equation 5.103:

$$L_c = \left(\frac{L_t}{2}\right) + \sqrt{\left(\frac{L_t}{2}\right)^2 + \frac{8H(M_b + M_w)}{M_c}} \qquad (5.103)\ [\text{AA13.3.1-2}]$$

www.EngineeringEBooksPdf.com

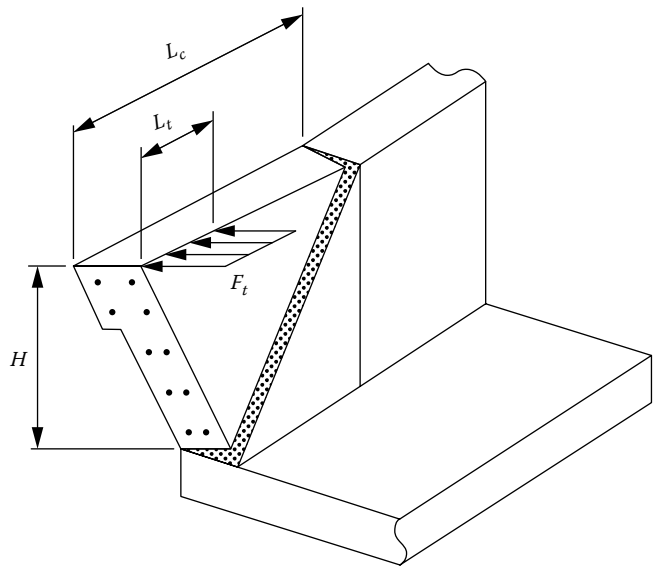

FIGURE 5.81 Yield line analysis for concrete parapet walls for impact near end of wall segment. (From *AASHTO LRFD Bridge Design Specifications*, Copyright © 2012 by American Association of State Highway and Transportation Officials, Washington, DC. Used by permission.)

2. When impact occurs at the end of the wall (Figure 5.77), R_w may be calculated from Equation 5.104:

$$R_{w2} = \left(\frac{2}{2L_c - L_t}\right)\left(M_b + M_w + \frac{M_c L_c^2}{H}\right) \qquad (5.104)\ [AA13.3.1\text{-}3]$$

The critical wall length, L_c, over which the yield mechanism occurs, is given as follows:

$$L_c = \left(\frac{L_t}{2}\right) + \sqrt{\left(\frac{L_t}{2}\right)^2 + \frac{H(M_b + M_w)}{M_c}} \qquad (5.105)\ [AA13.3.1\text{-}2]$$

where

F_t = transverse force specified in Table 5.13, assumed to be acting at the top of a concrete wall (kip)
H = height of wall (ft)
L_c = critical length of yield line failure pattern (ft)
L_t = longitudinal length of distribution of impact force F_1 (ft)
M_b = additional flexural resistance of beam in addition to M_w, if any, at top of wall (kip-ft)
M_c = flexural resistance of cantilevered walls about an axis parallel to the longitudinal axis of the bridge (kip-ft/ft)
M_w = flexural resistance of the wall about its vertical axis

For use in the aforementioned equations, M_c and M_w should not vary significantly over the height of the wall. For other cases, a rigorous yield line analysis should be used. Where the width of the concrete railing varies along the height (as in examples in Chapters 5 and 6), the value of M_c appearing in Equations 5.102 through 5.104 should be taken as the average of its value along the height of the barrier wall.

Example 5.4 presents typical calculations for the design of a barrier wall.

www.EngineeringEBooksPdf.com

Example 5.4: Design of a Railing System (Traffic Barrier)

Determine the flexural resistance of the traffic barrier shown in Figure 5.82. The reinforcement details of the traffic barrier are shown in Figure 5.83.

The profile of standard Illinois Department of Transportation (IDOT) *F-shape* concrete barrier with modified reinforcement configuration is used for this example. The first step is to calculate M_c and M_w, which are the barrier's factored flexural resistances about the horizontal and vertical axes, respectively. Figures 5.82 and 5.83 show the barrier geometry and reinforcement. As commonly practiced, the barrier is cast separately from the deck, after the deck has hardened. It is, therefore, necessary to have dowel bars extending from the deck into the lower portion of the barrier.

The nominal railing resistance to transverse load, R_w, depends on the flexural resistance of the wall about its vertical axis, M_w, and the flexural resistance of cantilevered walls about an axis parallel to the longitudinal axis of the bridge, M_c. These two moment values need to be calculated first.

Calculation of Flexural Resistance of the Wall about Its Vertical Axis, M_w

The barrier wall has a variable cross section. The flexural resistance of the entire wall, M_w, can be calculated as the sum of the flexural resistances of the upper and lower segments of the wall calculated separately. Alternatively, the M_w for the entire wall can be calculated by considering an equivalent rectangular cross section instead of the variable cross section. Both methods will be demonstrated.

1. Wall segments considered separately
   a. Upper wall segment

      The reinforcement consists of 3 No. 5 bars, $A_s = 0.91$ in.^{2}

      Average width of the wall, $b' = 0.5(9.5 + 14.0) = 11.75$ in.

      d' = equivalent depth of reinforcement for moment capacity calculation

      $= b' - \text{cover} - 0.5(\text{diameter of the bar})$

      $= 11.75 - 1.5 - 0.5(0.625) = 9.94$ in.

      b' = equivalent width for moment capacity calculation

      = height of the upper wall segment = 24 in.

      The nominal flexural strength of the equivalent upper segment of the wall section, M_w, can be determined from Equation 5.26:

$$M_n = A_s f_y \left(d - \frac{a}{2} \right) \tag{5.26}$$

      Substitution for a from Equation 5.22 into Equation 5.26 gives Equation 5.106:

$$M_n = A_s f_y \left(d - \frac{A_s f_y}{1.7 f_c' b} \right) \tag{5.106}$$

      In Equation 5.106, substitute $d = d' = 9.94$ in., $A_s = 0.91$ in.^{2}, $f_y = 60$ ksi, $f_c' = 4$ ksi, and $b' = H = 44$ in. (height of the barrier wall at the outside face):

$$\phi M_{w1} = \phi \left(\frac{A_s f_y}{12} \right) \left(d' - \frac{A_s f_y}{1.7 f_c' H} \right)$$

$$= (1.0) \left(\frac{(0.91)(60)}{12} \right) \left(10.0 - \frac{(0.91)(60)}{1.7(4)(24)} \right)$$

$$= 43.70 \text{ kip-ft/ft}$$

www.EngineeringEBooksPdf.com

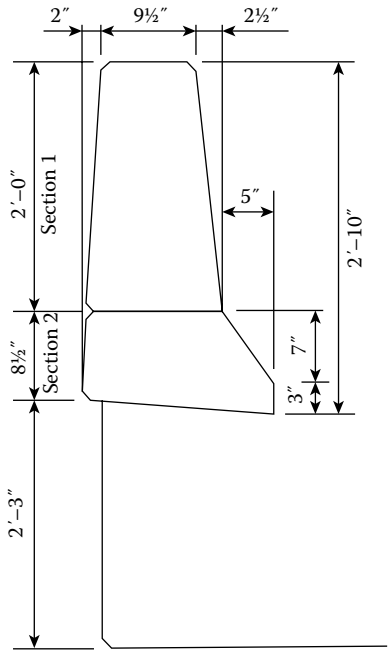

FIGURE 5.82 Barrier geometry. (From Achneider, E.F. and Bhide, S., *LRFD of Cast-in-Place Concrete Bridges*, Portland Cement Association, Chicago, IL, 2004. Reproduced with permission from Portland Cement Association, Chicago, IL.)

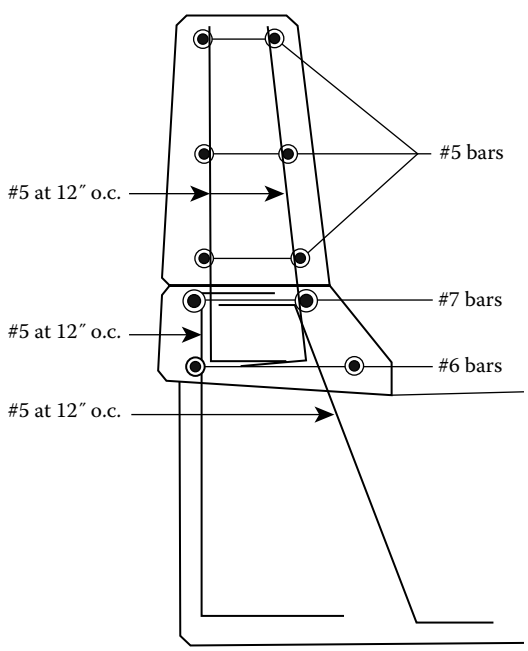

FIGURE 5.83 Barrier reinforcement. (Adapted from Achneider, E.F. and Bhide, S., *LRFD of Cast-in-Place Concrete Bridges*, Portland Cement Association, Chicago, IL, 2004.)

www.EngineeringEBooksPdf.com

b. Lower wall segment
The reinforcement consists of 1 No. 7 bar and 1 No. 6 bar, $A_s = 0.60 + 0.44 = 1.04$ in.^{2}
Average diameter of the bars = 0.5(0.875 + 0.75) = 0.813 in.
Average width of the wall, $b' = 0.5(14.0 + 19.0) = 16.5$ in.
d' = equivalent depth of reinforcement for moment capacity calculation
= b' – cover – 0.5(average diameter of the bar)
= 16.5 – 1.5 – 0.5(0.813) = 14.6 in.

$$\text{Equivalent height of the wall segment} = \frac{A_w}{b_{avg}}$$

$$H_{avg} = \frac{0.5(14+19)(8.5)+0.5(19)(3)}{(14+19)/2} = 10.23 \text{ in.}$$

b' = equivalent width for moment capacity calculation
= average height of the lower wall segment = 10.23 in.

$$\phi M_{w2} = \phi\left(\frac{A_s f_y}{12}\right)\left(d' - \frac{A_s f_y}{1.7 f_c' H}\right)$$

$$= (1.0)\left(\frac{(1.04)(60)}{12}\right)\left(14.6 - \frac{(1.04)(60)}{1.7(4)(10.23)}\right)$$

$$= 71.26 \text{ kip-ft/ft}$$

$$\text{Total } \phi M_w = \phi M_{w1} + \phi M_{w2} = 43.7 + 71.26 = 115.0 \text{ kip-ft/ft}$$

2. Entire wall considered as single equivalent rectangular cross section
For calculating the flexural resistance of the wall about its vertical axis, M_w, consider, for simplicity, the variable depth barrier as consisting of the constant depth, rectangular cross section.
The reinforcement consists of the following reinforcing bars:

3 No. 5 bars ($A_s = 0.91$ in.^{2})
1 No. 7 bar ($A_s = 0.60$ in.^{2})
1 No. 6 bar ($A_s = 0.44$ in.^{2})

The total area of reinforcing bars is calculated to be

A_s = area of longitudinal bars = 0.91 + 0.60 + 0.44 = 1.95 in.^{2}
b' = equivalent width of traffic barrier = A_w/H
A_w = cross-sectional area of barrier wall
H = height of barrier wall = 24 + 8.5 + 0.5(3) = 34.0 in. = 2.83 ft

$$b' = \frac{A_w}{H} = \frac{\left(\frac{9.5+14}{2}\right)(24)+\left(\frac{8.5+10}{2}\right)(12)+\left(\frac{3+10}{2}\right)(5)}{0.5(32.5 + 34.0)} = 12.80 \text{ in.}$$

Calculate d', equivalent depth of reinforcement for moment capacity calculation

c = clear cover to horizontal bars = 1.5 in.
d_r = average diameter of longitudinal bars = $\left[(3)(0.625)+0.875 + 0.75\right]/5 = 0.70$ in.
d' = equivalent depth of reinforcement for capacity calculation

$$d' = b' - c - \frac{d_r}{2} = 12.8 - 1.5 - \frac{0.70}{2} = 10.95 \text{ in.}$$

www.EngineeringEBooksPdf.com

The nominal flexural strength of the equivalent barrier wall section, M_w, can be determined from Equation 5.106 as before.

In Equation 5.106, substitute $d = d' = 10.5$ in., $A_s = 1.7$ in.^{2}, $f_y = 60$ ksi, $f_c' = 4$ ksi, and $b = H = 34$ in. (height of the barrier wall at the inside face):

$$\phi M_w = \phi\left(\frac{A_s f_y}{12}\right)\left(d' - \frac{A_s f_y}{1.7 f_c' H}\right)$$

$$= (1.0)\left(\frac{(1.95)(60)}{12}\right)\left(10.95 - \frac{(1.955)(60)}{1.7(4)(34)}\right)$$

$$= 101.83 \text{ kip-ft/ft}$$

The calculated value of $\phi M_w = 101.83$ kip-ft/ft compares well with the value of 115.0 kip-ft/ft calculated earlier. However, the lower value of $\phi M_w = 103.85$ kip-ft/ft would be used for further calculations.

Distributed over the height H of the wall, the flexural resistance of the barrier wall is calculated as (Figure 5.84)

$$\frac{\phi M_w}{H} = \frac{(101.83)(12)}{34} = 35.94 \text{ kip-in./in.}$$

Calculation of Flexural Resistance of Cantilevered Walls about an Axis Parallel to the Longitudinal Axis of the Bridge, M_c

The width of the barrier wall varies along its height. Where the width of the barrier varies along the height, the barrier resistance, M_c, can be taken as the average of its value along the height (Art. CA13.3.1).

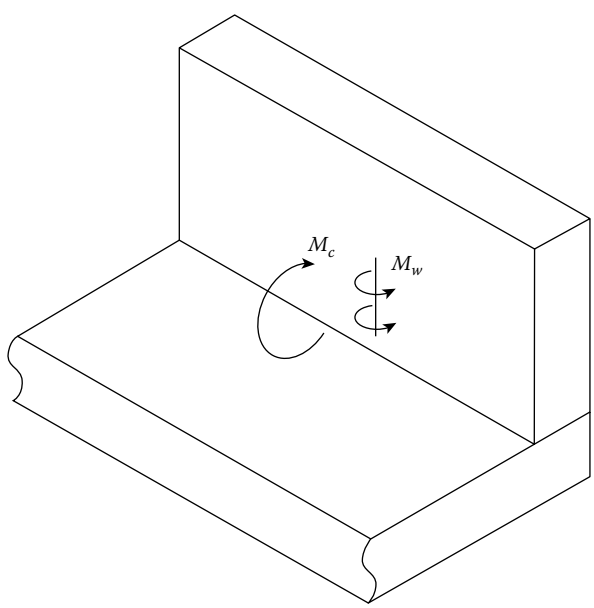

FIGURE 5.84 Longitudinal and transverse flexural strength of concrete barrier wall. (From Achneider, E.F. and Bhide, S., *LRFD of Cast-in-Place Concrete Bridges*, Portland Cement Association, Chicago, IL, 2004. Reproduced with permission from Portland Cement Association, Chicago, IL.)

www.EngineeringEBooksPdf.com

a. For portion above dowel bars, Section 1
A_{sv1} = area of vertical bars in Section 1 (No. 5 (at 12 in. o.c.) = 0.31/12 = 0.026 in.^{2}/in.
w_1 = equivalent width of barrier in Section 1

$$w_1 = \frac{b_1 + b_2}{2} = \frac{9.5 + 14}{2} = 11.8 \text{ in.}$$

d_1' = equivalent depth of reinforcement for moment capacity calculation of Section 1.

$$d_1' = w_1 - C - \frac{0.625}{2} = 11.8 - 1.5 - 0.625 - \frac{0.625}{2} = 9.36 \text{ in.}$$

where C = cover = 1.5 in.
From Equation 5.106,

$$\phi M_{c1} = \phi A_{sv1} f_y \left(d' - \frac{A_{sv} f_y}{1.7 f_c'} \right)$$

$$= (1.0)(0.026)(60)\left(9.36 - \frac{(0.026)(60)}{1.7(4)} \right)$$

$$= 14.2 \text{ kip-in./in. (kip-ft/ft)}$$

b. For portion including dowel bars, Section 2
Check if sufficient distance is available to develop No. 5 bar (in tension) inside the slab. The minimum required development length of No. 5 bar is determined from Art. 5.11.2.1.
For No. 11 bars and smaller,

$$\sim_{d,min} = \frac{1.25 A_b f_y}{\sqrt{f_c'}}$$

For No. 5 bar,

$$\sim_{d,min} = \frac{1.25(0.31)(60)}{\sqrt{4}} = 11.625 \text{ in.}$$

But not less than $0.4 d_b f_y$ = 0.4(0.625)(60) = 15 in. (governs)

Use a multiplier of 1.2 for using an epoxy-coated bar:

$$\ell_{d,min.} = 15(1.2) = 18 \text{ in.}$$

The development length for No. 5 bars is 18 in. In a 27 in. thick slab (of Example 5.1), No. 5 bars can be fully developed. If the deck is thinner, for example, 8–9 in. thick in typical deck overhangs, the area of steel used for the moment calculations is reduced accordingly.

A_{sv2} = area of vertical bars in Section 2 (No. 5 at 12 in. o.c.) = 0.31/12 = 0.026 in.^{2}/in.
w_2 = equivalent width of wall in Section 2

$$w_2 = \frac{b_2 + b_3}{2} = \frac{14 + 19}{2} = 16.5 \text{ in.}$$

www.EngineeringEBooksPdf.com

Average diameter of longitudinal bar in Section 2 (average of No. 8 and No. 5 bars)

$$= \frac{(0.875 + 0.75)}{2} = 0.81\,\text{in.}$$

d_2' = equivalent depth of reinforcement for moment capacity calculation for Section 2

$$d_2' = w_2 - C - 0.81 - \frac{0.685}{2} = 16.5 - 1.5 - 0.81 - \frac{0.625}{2} = 13.88\text{ in.}$$

$$\begin{aligned}
\phi M_{c2} &= \phi A_{sv2} f_y \left(d_2' - \frac{a}{2} \right) \\
&= \phi A_{sv2} f_y \left(d_2' - \frac{A_{sv2} f_y}{1.7 f_c'} \right) \\
&= (1.0)(0.026)(60)\left(13.88 - \frac{(0.026)(60)}{1.7(4)} \right) \\
&= 21.3\text{ kip-in./in. (kip-ft/ft)}
\end{aligned}$$

Calculate the weighted moment capacity of the entire wall:

$$\begin{aligned}
M_c &= \frac{M_{c1} h_1 + M_{c2} h_2}{H} \\
&= \frac{14.2(24) + 21.3(10)}{34} = 16.3\text{ kip-in./in. (kip-ft/ft)}
\end{aligned} \tag{5.107}$$

Yield Line Analysis: Capacity of Barrier versus R_w

Now that M_c and M_w have been calculated, the remaining parameters required to check the barrier capacity can be determined. The following equations for the nominal barrier resistance (capacity) to transverse load, R_w, and the critical length of yield line failure pattern, L_c, are derived by applying the virtual work equation to the yield line mechanisms shown in Figures 5.80 and 5.81.

The nominal resistance of the barrier wall, R_w, would be calculated for two load cases: (1) R_{w1}, when the impact force F_t occurs within the wall, using Equations 5.102 and 5.103, and (2) R_{w2}, when the impact load F_t occurs at the end of the wall, using Equations 5.104 and 5.105.

1. For impacts within a wall segment, use Equations 5.102 and 5.103:
   L_c = critical length of yield line failure pattern (in.)

$$L_c = \left(\frac{L_t}{2} \right) + \sqrt{\left(\frac{L_t}{2} \right)^2 + \frac{8H(M_b + M_w)}{M_c}} \tag{5.103}$$

L_t = longitudinal length of distribution of impact force F_1
= 3.5 ft for TL-4
M_b = additional flexural resistance of beam in addition to M_w, if any, at top of wall
= 0.0 kip-in./in. (kip-ft/ft)
M_c = flexural resistance of cantilevered walls about an axis parallel to the longitudinal axis of the bridge
= 16.3 kip-in./in. (kip-ft/ft) (calculated earlier)

www.EngineeringEBooksPdf.com

M_w = flexural resistance of the wall about its vertical axis
= 101.83 kip-in./in. (kip-ft/ft) (calculated earlier)

$$L_c = \left(\frac{3.5}{2} + \sqrt{\left(\frac{3.5}{2}\right)^2 + \frac{8(2.83)(0+101.83)}{16.3}}\right) = 13.8 \text{ ft}$$

The nominal resistance to transverse load, R_{w1}, can now be calculated as follows:

$$R_{w1} = \left(\frac{2}{2L_c - L_t}\right)\left(8M_b + 8M_w + \frac{M_c L_c^2}{H}\right) \tag{5.102}$$

$$R_{w1} = \left(\frac{2}{2(13.8) - 3.5}\right)\left[8(0.0) + 8(101.83) + \frac{(16.3)(13.8)^2}{2.83}\right] = 158.6 \text{ kip}$$

2. For impacts at end of wall or at a joint, use Equations 5.104 and 5.105:

$$L_c = \left(\frac{L_t}{2}\right) + \sqrt{\left(\frac{L_t}{2}\right)^2 + \frac{H(M_b + M_w)}{M_c}}$$

$$= \left(\frac{3.5}{2}\right) + \sqrt{\left(\frac{3.5}{2}\right)^2 + \frac{2.83(0+103.83)}{16.3}} = 6.3 \text{ ft} \tag{5.105}$$

$$R_{w2} = \left(\frac{2}{2L_c - L_t}\right)\left(M_b + M_w + \frac{M_c L_c^2}{H}\right)$$

$$= \left(\frac{2}{2(6.3) - 3.5}\right)\left(0.0 + 101.83 + \frac{16.3(6.3)^2}{2.83}\right) = 72.6 \text{ kip}$$

R_{w1} = 158.6 kip > R_{w2} = 72.6 kip (governs).

Transverse force to be resisted for TL-4 railing (Table 5.13) = 54 kip
Check if $R_w > F_t$; 72.6 kip > 54 kip, OK.

Deck Overhang Design

Deck overhangs are required to be designed for the following three separate load cases (Art. A13.4.1):

Design Case 1: The transverse and longitudinal forces specified in Art. A13.2
Extreme-Event Load Combination II limit state

Design Case 2: The vertical forces specified in Art. A13.2
Extreme-Event Load Combination II limit state

Design Case 3: The loads that occupy the overhang, specified in Art. 3.6.1
Load Combination Strength I Limit State

As discussed in Section 3.11.4, the load for Design Case 3 consists of a design truck axle with the wheel closest to the barrier placed at a distance of 1.0 ft from the face of the barrier. The multiple-presence factor, m, of 1.2 applies. The equation for Strength I Limit State load combination is expressed as Equation 3.4:

$$Q = \Sigma \eta_i \gamma_i Q_i \tag{3.4} \text{ [AA13.4.1-1]}$$

where
η_i = load modifier (Art. 1.3.2)
γ_i = load factors specified in LRFD Tables 3.4.1-1 and 3.4.1-2
Q_i = force effects from loads specified herein

www.EngineeringEBooksPdf.com

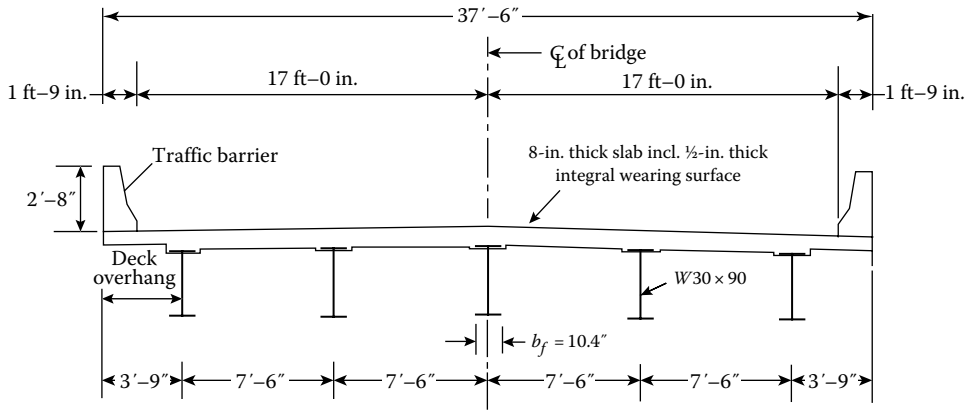

FIGURE 5.85 Cross section of slab–steel girder superstructure of Example 6.10.

In terms of bending moments, Equation 3.4 is expressed as follows:

$$M_u = 1.25M_{DC} + 1.5M_{DW} + 1.75M_{LL+IM}$$

For slab-type bridges in which the primary reinforcement is parallel to traffic (as in Example 5.1), Design Case 3 need not be considered.

Example 5.5: Design of Deck Overhang

Figure 5.85 shows the cross section for the composite slab–steel girder bridge of Example 6.10. The steel girders are typically W30 × 90 spaced at 7 ft 6 in. o.c. The slab is 7.5 in. thick with 1/2 in. thick integral wearing surface. Provision is made for 25 lb/ft^2 of future wearing surface. The specified 28-day compressive strength of concrete is 4 ksi; reinforcing steel is Grade 60. Design the overhang of the deck.

Solution

Design Method

As discussed in Section 5.13.7.1.7, deck overhang cannot be designed by the empirical design method (Art. 9.7.2.2). Instead, the deck overhang is to be designed by the traditional design method specified in Art. 9.7.3. The barrier wall has to be designed for Extreme Event Limit State using the yield line failure mechanism specified in Art. A13.2. This example presents the design of the overhang for permanent load and live load. Design of the barrier wall is presented in Example 5.4.

Design Procedure

As specified in Art. 4.6.2.1.6, bending moments for the design of the overhang are taken at section *f–f* located at a distance, L_c, measured from the outside face of the barrier wall to one-quarter of the flange width from the center of line of support (center line of the exterior girder) as shown in Figure 5.86.

$$L_c = 45 - 0.25b_f = 45 - 0.25(10.4) = 42.4 \text{ in.}$$

Force Effects

Permanent Loads

Determine the centroid of the barrier wall. The cross-sectional area of the wall is calculated to be (see Figure 5.87)

$$A_w = 12(19) + 1/2\ (2)(19) + 14(10) + 1/2\ (7)(10) + 21(3)$$

$$= 228 + 19 + 140 + 35 + 63$$

$$= 485 \text{ in.}^2$$

www.EngineeringEBooksPdf.com

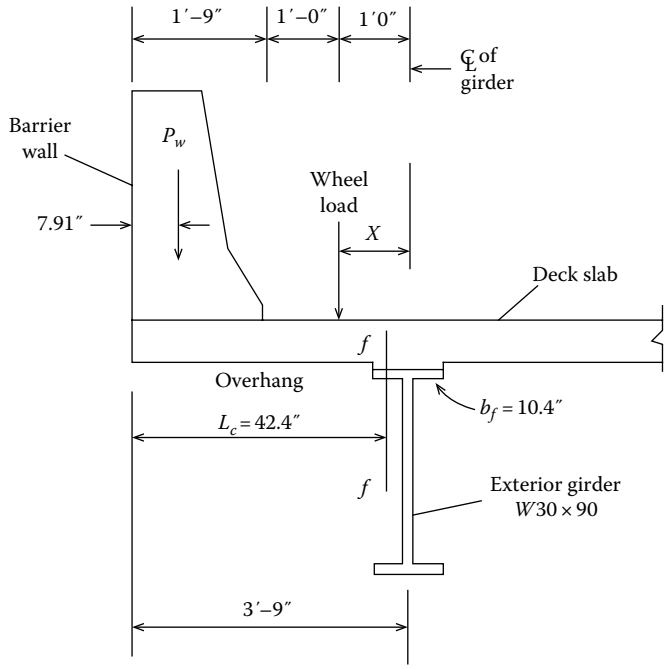

FIGURE 5.86 Critical section for bending moment in the overhang.

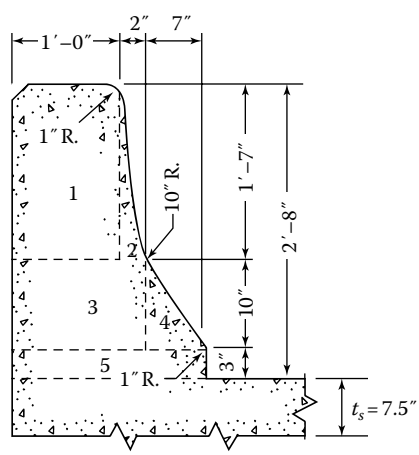

FIGURE 5.87 Cross section and geometry of barrier wall.

Location of the centroid of the wall from its outside face is calculated to be

$$\bar{x} = \frac{228(6) + 19\left[\left(12 + \frac{2}{3}(2)\right)\right] + 140(7) + 35\left[\left(14 + \frac{1}{3}(7)\right)\right] + 63(10.5)}{485} = 7.91\,\text{in.}$$

Dead load of the barrier wall,

$$P_w = \frac{485}{144}(150) = 505\ \text{lb/ft}$$

www.EngineeringEBooksPdf.com

Length of the overhang,

$$a = 42.4 \text{ in. (computed earlier)}$$

$$w_{DC} = \text{slab including integral wearing surface}$$
$$= (8.0)(42.4)(0.15(1/144) = 0.353 \text{ kip/ft}$$

$$w_{barrier\ wall} = 0.505 \text{ kip/ft (calculated earlier)}$$

$$w_{DW} = \text{dead load of FWS}$$
$$= 0.025(2.) = 0.050 \text{ kip/ft}$$

Live Load
Wheel load (16 kip) is placed at a distance of 1.0 ft from the face of the curb (Art. 3.6.1.3.1). Dynamic load allowance of 0.33 and the multiple-presence factor, m, of 1.2 apply to the wheel load.

Equivalent width of the overhang of the cast-in-place deck is obtained from LRFD Table 4.6.2.1.3-1.

$$\text{Width of the overhang} = 45 + 10.0X \tag{5.108}$$

where X = distance from the wheel load to the point of support (ft) (Figure 5.86)

$$= 42.4 - 21 - 12 = 9.4 \text{ in.} = 0.78 \text{ ft}$$

$$\text{Width of the overhang} = 45 + 10.0X = 45 + 10.0(9.4/12) = 52.8 \text{ in. or } 4.4 \text{ ft}$$

Moment due to 16-kip wheel load will be divided by 4.3775 ft to obtain live load moment per unit width of the overhang:

$$M_{DC} = (0.353)\left(\frac{42.4}{2}\right)\left(\frac{1}{12}\right) = 0.624 \text{ kip-ft/ft}$$

$$M_{barrier} = (0.505)(45.0 - 7.91)\left(\frac{1}{12}\right) = 1.561 \text{ kip-ft/ft}$$

$$M_{DW} = (0.05)\left(\frac{42.4 - 21}{2}\right)\left(\frac{1}{12}\right) = 0.045 \text{ kip-ft/ft}$$

$$M_{LL+IM} = 16\left(\frac{9.4}{12}\right)(1.33)(1.2)\left(\frac{1}{4.4}\right) = 4.55 \text{ kip-ft/ft}$$

A load modifier of $\eta = 0.95$ is used for the extreme-event limit state.

$$M_u = [1.25M_{DC} + 1.5M_{DW} + 1.75M_{LL+IM}]$$
$$= [1.25(0.624 + 1.561) + 1.5(0.045) + 1.75(4.55)]$$
$$= 10.76 \text{ kip-ft/ft}$$

Factored flexural resistance of the overhang, M_r

www.EngineeringEBooksPdf.com

Estimate the required area of flexural reinforcement in the overhang from the following:

$$A_s \approx \frac{M_u}{4d_s} \tag{5.86}$$

where
M_u = bending moment (kip-ft)
d_s = design depth of the slab overhang (in.)

Assume No. 6 bar at 12 in. o.c., A_s = 0.44 in.^{2}/ft. For the 7.5 in. thick slab,

$$d_s = \text{slab thickness} - \text{cover} - 1/2(\text{diameter of bar})$$
$$= 7.5 - 2.0 - 1/2(0.75) = 5.13 \text{ in.}$$

$$A_s \approx \frac{M_u}{4d_s} = \frac{10.76}{4(5.13)} = 0.52 \text{ in.}^2 > 0.44 \text{ in.}^2, \text{ n.g.}$$

Try No. 7 bar at 12 in. o.c., A_s = 0.60 in.^{2}/ft. Calculate the depth of compression block, a:

$$a = \frac{A_s f_y}{0.85 f_c' b} = \frac{0.60(60)}{0.85(4.0)(12)} = 0.88 \text{ in.}$$

$$d_s = \text{slab thickness} - \text{cover} - 1/2(\text{diameter of bar})$$
$$= 7.5 - 2.0 - 1/2(0.875) = 5.06 \text{ in.}$$

$$M_n = A_s f_y \left(d - \frac{a}{2}\right)$$
$$= 0.60(60)\left(5.06 - \frac{0.88}{2}\right)\left(\frac{1}{12}\right) = 13.86 \text{ kip-ft/ft}$$

$$M_r = \phi M_n = 0.9(13.86) = 12.47 \text{ kip-ft/ft} > M_u = 10.76 \text{ kip-ft/ft, OK.}$$

Provide No. 7 bars at 12 in. o.c. These bars must be extended into the deck slab past the critical section *f–f* (Figure 5.86) to provide the required development length.

Development length for No. 7 bar (Art. 5.11.2.1.2),

$$\sim_d = \frac{1.25 A_b f_y}{\sqrt{f_c'}} = \frac{1.25(0.60)(60)}{\sqrt{4}} = 22.5 \text{ in.}$$

$$\ell_{d,min.} = 0.4 d_b f_y = 0.4(0.875)(60) = 21.0 \text{ in.} < 22.5 \text{ in. (governs)}$$

Use a modifier of 1.2 for epoxy-coated bar (Art. 5.11.2.1.2):

$$\ell_{d,reqd} = 1.2(22.5) = 27 \text{ in.}$$

No. 7 bars at 12 in. o.c. should be extended by 2 ft 3 in. into the deck slab past the critical section *f–f* to develop fully. These bars should be tied with the bars in the main deck that also have a spacing of 12 in. o.c.

www.EngineeringEBooksPdf.com

Reinforcement Requirements: Art. 5.7.3.3

1. Maximum reinforcement: Art. 5.7.3.3.1 (No requirements specified)
2. Minimum reinforcement: Art. 5.7.3.3.2
   The amount of prestressed and nonprestressed tensile reinforcement shall be adequate to develop a factored flexural resistance, M_r, equal to the lesser of the following two values:
   a. 1.33 times the factored moment required by the applicable strength load combination specified in LRFD Table 3.4.1-1
   b. The cracking moment given as

$$M_{cr} = \gamma_3 \left[\left(\gamma_1 f_r + \gamma_2 f_{cpe} \right) S_c - M_{dnc} \left(\frac{S_c}{S_{nc}} - 1 \right) \right] \tag{5.41}$$

where
f_r = modulus of rupture specified in Art. 5.4.2.6
f_{cpe} = compressive stress in concrete due to effective prestress forces only (allowance for all prestress losses) at the extreme fiber of the section where tensile stress is caused by externally applied loads (ksi)
= 0 for sections with nonprestressed reinforcement only
M_{dnc} = total unfactored dead load moment acting on the monolithic or noncomposite section where tensile stress is caused by externally applied loads (ksi)
S_c = section modulus for the extreme fiber of the composite section where tensile stress is caused by externally applied loads (in.^{3})
= S_{nc} where beams are designed for the monolithic or noncomposite section to resist all loads
S_{nc} = section modulus for the extreme fiber of the monolithic or noncomposite section where tensile tress is caused by externally applied loads (in.^{3})

In the present case of a section with nonprestressed reinforcement, $f_{cpe} = 0$, $S_{nc} = S_c$, $\gamma_1 = 1.6$ (for all other structures), and $\gamma_3 = 0.75$ (for A 706, Grade 60 reinforcement). Substitution of these values in Equation 5.41 yields

$$\begin{aligned} M_{cr} &= 0.75(1.6) f_r S_c \\ &= 1.2 f_r S_c \end{aligned} \tag{5.44}$$

For normal-weight concrete (Art. 5.4.2.6),

$$f_r = 0.24 \sqrt{f_c' \text{ ksi}} \tag{5.12}$$

For a 4 ksi concrete,

$$f_r = 0.24 \sqrt{4 \text{ ksi}} = 0.48 \text{ ksi}$$

For a rectangular section,

$$S_c = \frac{bh^2}{6} = \frac{12(8)^2}{6} = 128 \text{ in.}^3$$

Substituting in Equation 5.44, we obtain

$$M_{cr} = 1.2(0.48)(128) = 73.73 \text{ kip-in.} = 6.14 \text{ kip-ft}$$

$$1.33 M_u = 1.33(10.76) = 14.31 \text{ kip-ft} > M_{cr} = 6.14 \text{ kip-ft (smaller value governs)}$$

www.EngineeringEBooksPdf.com

Flexural resistance,

$$M_r = \phi M_n = 12.47 \text{ kip-ft} > M_{cr} = 6.14 \text{ kip-ft, OK.}$$

Shrinkage and Temperature Reinforcement: Art. 5.10.8.2
For bars and welded wire fabric, the area of reinforcement per foot on each face and in each direction shall satisfy the following:

$$A_s \geq \frac{1.3bh}{2(b+h)f_y} \qquad (5.91)\ [A5.10.8\text{-}1]$$

$$0.11 \leq A_s \leq 0.6 \text{ in.}^2 \qquad (5.92)\ [A5.10.8\text{-}2]$$

where
A_s = area of reinforcement in each direction and on each face (in.^{2}/ft)
b = least width of component section (in.)
h = least thickness of the component
f_y = specified yield strength of reinforcing bars
$\leq$ 75 ksi

For the present case, b = 12 in., h = 7.5 in., and f_y = 60 ksi. Substitution of these values in Equation 5.10 gives

$$A_s \geq \frac{1.3(12)(7.5)}{2(12+7.5)(60)} = 0.05 \text{ in.}^2/\text{ft} < 0.11 \text{ in.}^2 \text{ (governs)}$$

Provide minimum reinforcement, $A_s \geq 0.11$ in.^{2}/ft

Spacing not to exceed three times the depth of component or 18 in.

$$3h = 3(7.5) = 22.5 \text{ in.} > 18 \text{ in. (governs).}$$

Try No. 4 bars at 18 in. o.c., A_s = 0.13 in.^{2}/ft > 0.11 in.^{2}

Note that No. 3 at 12 in. o.c. also would provide the required amount of reinforcement. But No. 4 bars are preferred for greater stiffness (overall sturdiness) to facilitate construction (pouring concrete, walking crew with equipment, etc.).

So No. 4 bars at 18 in. o.c. would be satisfactory. Instead, for construction convenience, provide No. 5 at 12 in. o.c., the same as the longitudinal reinforcement in the top of the main deck. A_s = 0.31 in.^{2}

Distribution Steel: Art. 9.7.3.2
Slabs designed by the traditional design method shall comply with the distribution reinforcement requirements specified in Art. 9.7.3.2.

For primary reinforcement perpendicular to traffic, the distribution steel is given as follows:

$$A_{s,dist} = \frac{200}{\sqrt{S}} \leq 67 \text{ percent} \qquad (5.88)$$

where S = effective span length (ft) taken as equal to the effective length specified in Art. 9.7.2.3.

$$S = \text{distance between the inside faces of stems} = 7.5 - 1.75 = 5.75 \text{ ft}$$

$$A_{s,dist} = \frac{200}{\sqrt{5.75}} = 83.4 \text{ percent} > 67 \text{ percent}$$

www.EngineeringEBooksPdf.com

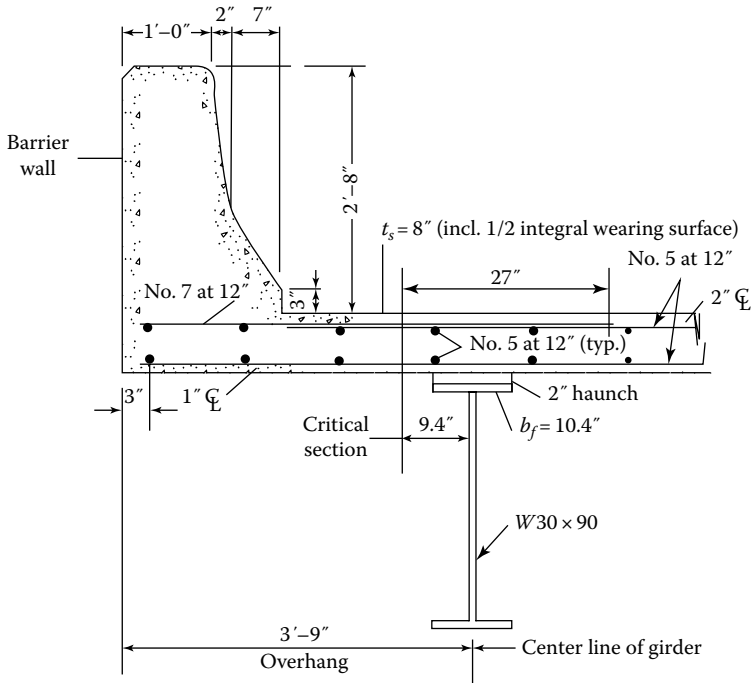

FIGURE 5.88 Reinforcement details for the deck overhang. (Reinforcement from the barrier wall will also be anchored inside the overhang; those reinforcement details are not shown here.)

Therefore, $A_{s,dist}$ = 67 percent (smaller percentage governs).
Area of bottom reinforcement, No. 5 bars at 12 in. o.c., A_s = 0.31 in.^{2}/ft

$$A_{s,dist} = 0.67(0.31) = 0.21 \text{ in.}^2/\text{ft}$$

Provide No. 5 at 12 in. o.c., A_s = 0.31 in.^{2}, OK.

For convenience in construction, provide the same reinforcement at the bottom of the overhang as in the bottom of the main deck (see Example 5.3). Provide No. 5 at 12 in. o.c. in both directions.

Reinforcement details for the overhang are shown in Figure 5.88.

5.17 SLAB-PRECAST, PRESTRESSED CONCRETE BRIDGES

5.17.1 Introduction

The credit of discovering the concept of prestressing goes to San Francisco, California, engineer P. H. Jackson, who patented the concept in 1886 and used for tightening concrete blocks and concrete arches to serve as floor slabs. About 1888, German engineer C. E. W. Doehring independently obtained a patent for prestressing concrete slabs with metal wires. However, these early attempts were unsuccessful because the prestressing was lost through shrinkage and creep of concrete. The credit of successfully developing the modern concept of prestressed concrete goes to French engineer E. Fressynet (1879–1962), who, about 1927, demonstrated the usefulness of prestressing using high-strength steel to control prestress losses (Steinman and Watson 1957, Lin 1963). Starting in 1941 with a 180 ft, segmentally constructed, two-hinged, portal-framed bridge of arch form over river Marne at Lucany, France, and followed by five other nearly identical bridges, Fressynet convincingly demonstrated and popularized the virtues of prestressed concrete as a new building material. His methods also provided model for the modern segmental construction methods (Nilson 1978, Podolny and Muller 1982).

www.EngineeringEBooksPdf.com

In the United States, the practice of prestressing was introduced by R. E. Dill for producing concrete planks and fence posts in 1925 (Naaman 1982). Prestressed concrete bridge construction evolved with a small two-span (20–30 ft) bridge built in 1950 in Madison County, Tennessee (Steinman and Watson 1957, PTI 1985), in 2 weeks' time, at a savings of nearly 40 percent over conventional reinforced concrete. The first major prestressed concrete highway bridge, the three-span (74 – 160 – 74 ft), cast-in-place, posttensioned Walnut Lane Bridge in Philadelphia, Pennsylvania, was built in 1951. Following its construction, the Bureau of Public Roads, now the Federal Highway Administration (FHWA), published *Criteria for Prestressed Concrete Bridges*, which was revised in 1954 (PCI 1981). Since then, prestressed concrete bridges have continued to replace reinforced concrete and steel girder bridges as bridges of choice in small- and medium-span-range categories. A new type in 1950, prestressed concrete bridges today have become the most commonly type of highway bridges being built throughout the world.

5.17.2 Characteristics of Prestressed Concrete Bridges

5.17.2.1 Use of High-Strength Concrete

The most common types of prestressed concrete bridges in short- and medium-span bridges can be classified as slab–girder bridges in which a reinforced concrete deck is supported by a number of parallel, precast, prestressed concrete girders (or beams). Precast girders are produced in a fabrication plant in a controlled environment, as such they possess qualities of consistency in both the quality of concrete and dimensional tolerances. Production in a controlled environment of a fabrication plant also producers the ability to use high-strength concrete, often as high as 19,000 psi. The 28-day compressive strength of concrete, f'_c, for the plant-produced prestressed concrete girders ranges usually between 6000 and 8000 psi range, sometimes even higher. Equally important is the freedom that designers and fabricators enjoy for producing girders of innovative and desirable forms (shapes) and strength properties.

5.17.2.2 Shapes, Sizes, and Uses of Precast, Prestressed Concrete Girders

Precast, prestressed concrete girders, as bridge deck supporting structural components, are like W-shape steel beams that are manufactured by the steel industry but with many advantages specific to concrete. Rolled steel shapes are available only in specific sizes and in few steel grades listed in the producers' catalogs or handbooks such as AISC's *Steel Construction Manual* (AISC 2011). Precast, prestressed concrete girders can be produced with different shapes, sizes, lengths, and concrete strengths to suit the needs of designers/architects. These concrete-specific properties have made precast, prestressed concrete girders as choice products for highway bridges all over the world.

Many different shapes and sizes of precast, prestressed concrete sections have evolved over time, in different parts of the United States and elsewhere in the world, primarily because of lack of standardization. Because of their worldwide popularity with highway bridge designers, innovative shapes have been developed specific to the user needs, notably the span ranges varying from 40 ft to over 160 ft. Interestingly, the commercially available lengths of precast, prestressed concrete girders are limited not by the production plant limitations but by limitations of transportable lengths. A comprehensive summary of the many different available shapes and sizes and their applications for highway bridge construction has been provided by Taly (1998).

Examples of different cross-sectional shapes of precast, prestressed concrete girders produced and used for highway bridges in various parts of the United States are presented in the following discussion, but the list continues to grow:

1. AASHTO-PCI solid and voided slabs (Figure 5.89)
2. AASHTO-PCI standard precast sections (Figure 5.90)

www.EngineeringEBooksPdf.com

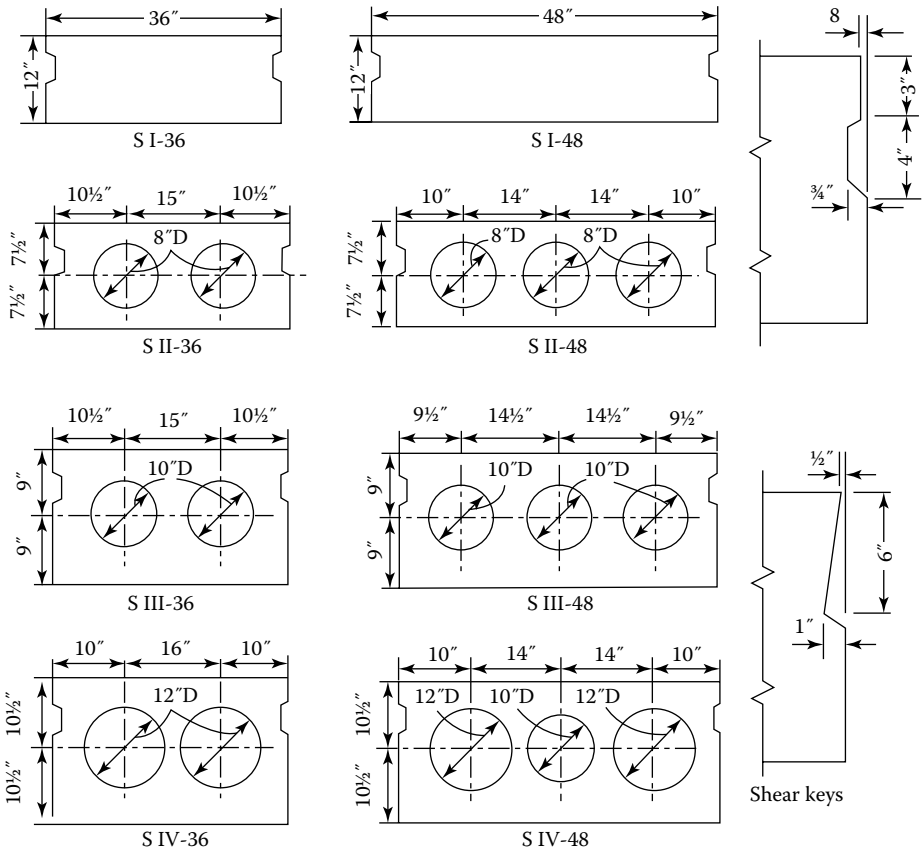

(a)

Section	Area (in.^{2})	Moment of Inertia (in.^{4})	Section Modulus (in.^{3})
SI-36	432	5,180	864
SII-36	439	9,720	1296
SIII-36	491	16,510	1835
SIV-36	530	25,750	2452
SI-48	576	6910	1152
SII-48	569	12,900	1720
SII-48	628	21,850	2428
SIV-48	703	34,520	3287

(b)

FIGURE 5.89 AASHTO–PCI solid and voided slabs. (a) Cross sections and (b) section properties.

3. Standard I-beams used by the Pennsylvania Department of Transportation (PennDOT) (Figure 5.91)
4. Washington state standard I-shaped girders (Figure 5.92)
5. Florida Department of Transportation standard beams (Figure 5.93)
6. I-girder series developed by Nebraska University for the Nebraska Department of Transportation (Figure 5.94)

www.EngineeringEBooksPdf.com

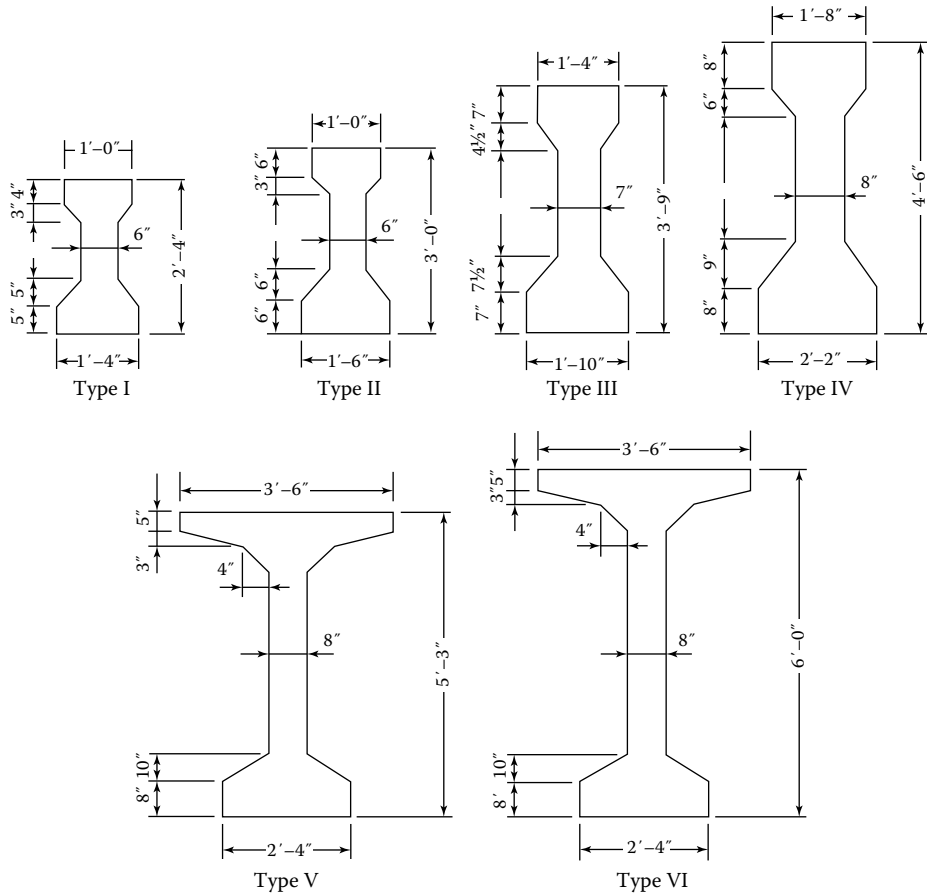

(a)

AASHTO Beam Type	Area (in.^{2})	I (in.^{4})	y_b*(in.)
I	276	22,750	12.59
II	369	50,980	15.83
III	560	125,390	20.27
IV	789	260,730	24.73
V	1013	521,180	31.96
VI	1085	733,320	36.38

*From center of gravity to bottom fibers.

(b)

FIGURE 5.90 AASHTO–PCI standard precast sections: (a) cross-sectional shapes and (b) section properties.

A typical slab-precast, prestressed concrete superstructure consists of a reinforced concrete deck supported by precast, prestressed concrete girders, which can be any of the aforementioned types. Figure 5.95 shows a typical bridge superstructure using AASHTO-PCI I-shaped, precast, prestressed concrete girders that support reinforced concrete deck.

A number of precast, prestressed concrete girders having T-shapes have been developed whose top flanges provide a ready-made deck. These girders are placed with their flanged touching those

www.EngineeringEBooksPdf.com

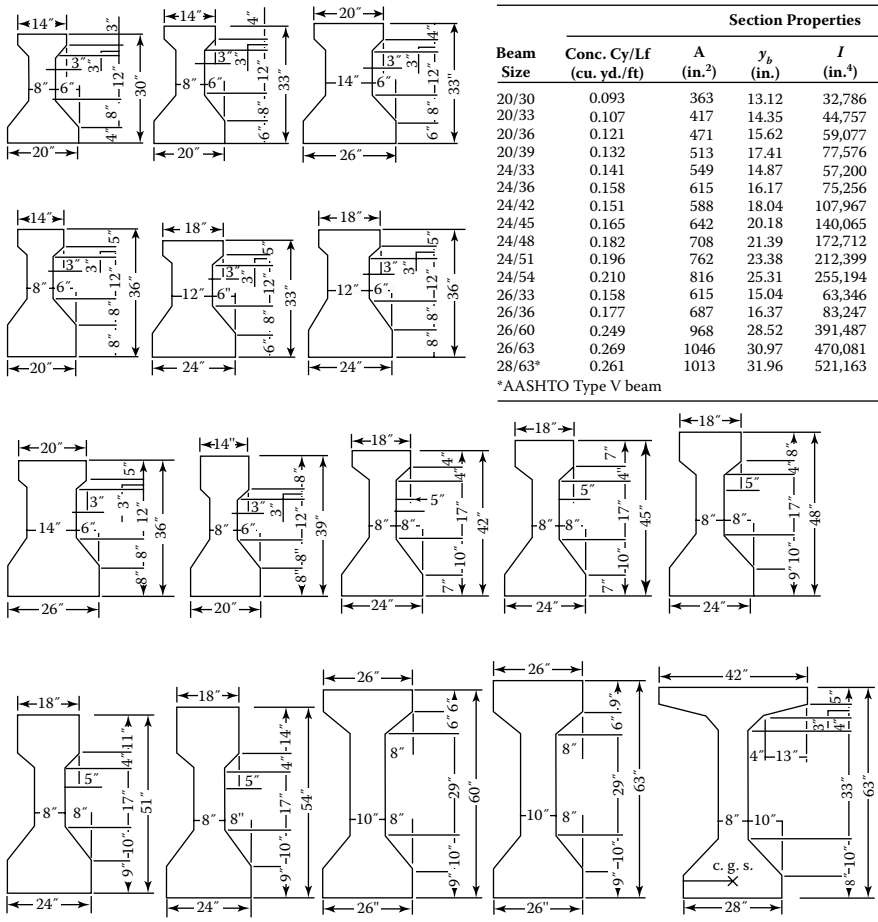

Beam Size	Conc. Cy/Lf (cu. yd./ft)	Section Properties A (in.^{2})	y_b (in.)	I (in.^{4})	Z_t (in.^{3})	Z_b (in.^{3})
20/30	0.093	363	13.12	32,786	1942	2499
20/33	0.107	417	14.35	44,757	2400	3119
20/36	0.121	471	15.62	59,077	2898	3783
20/39	0.132	513	17.41	77,576	3593	4457
24/33	0.141	549	14.87	57,200	3154	3847
24/36	0.158	615	16.17	75,256	3796	4653
24/42	0.151	588	18.04	107,967	4504	5985
24/45	0.165	642	20.18	140,065	5644	6940
24/48	0.182	708	21.39	172,712	6490	8075
24/51	0.196	762	23.38	212,399	7691	9084
24/54	0.210	816	25.31	255,194	8895	10,083
26/33	0.158	615	15.04	63,346	3528	4211
26/36	0.177	687	16.37	83,247	4240	5087
26/60	0.249	968	28.52	391,487	12,434	13,729
26/63	0.269	1046	30.97	470,081	14,678	15,176
28/63*	0.261	1013	31.96	521,163	16,788	16,308

*AASHTO Type V beam

FIGURE 5.91 Standard I-beams used by the Pennsylvania Department of Transportation.

of adjacent girders, and the joints between the adjacent flanges are grouted with a shear key. Several examples of T-shaped girders are shown in Figure 5.96.

Typically, depending on the span lengths, slab-precast, prestressed concrete girder superstructures can be built from a wide variety of girders as follows (in order of increasing, albeit overlapping, span lengths):

1. Solid and voided slabs (Figure 5.89)
2. Channel, inverted channel, and U-beam
3. T-beam, single, double, multiple, and bulb-T (Figures 5.90 and 5.96)
4. I-beams (Figures 5.91 through 5.94)
5. Spread box beams and adjacent box beams (Figures 5.97 through 5.101)
6. Multicell box girders (Figure 5.102)
7. Segmental box beams (Figures 5.103 and 5.104)

Because of their high torsional rigidity, box girders are superior to other types of cross-sectional configurations. This inherent property of box beams is advantageously used in building precast, prestressed concrete box beam superstructures (Figures 5.97 and 5.98). Box beams are available typically in 3 and 4-ft wide modules and in various standard depths as shown in the table

www.EngineeringEBooksPdf.com

Beam Properties			
Type	Area (in.^{2})	y_b (in.)	Moment of Inertia (in.^{4})
40	253	15.16	31,000
60	332	18.63	70,100
80	476	22.53	154,900
100	546	27.90	249,000
120	626	35.60	456,000

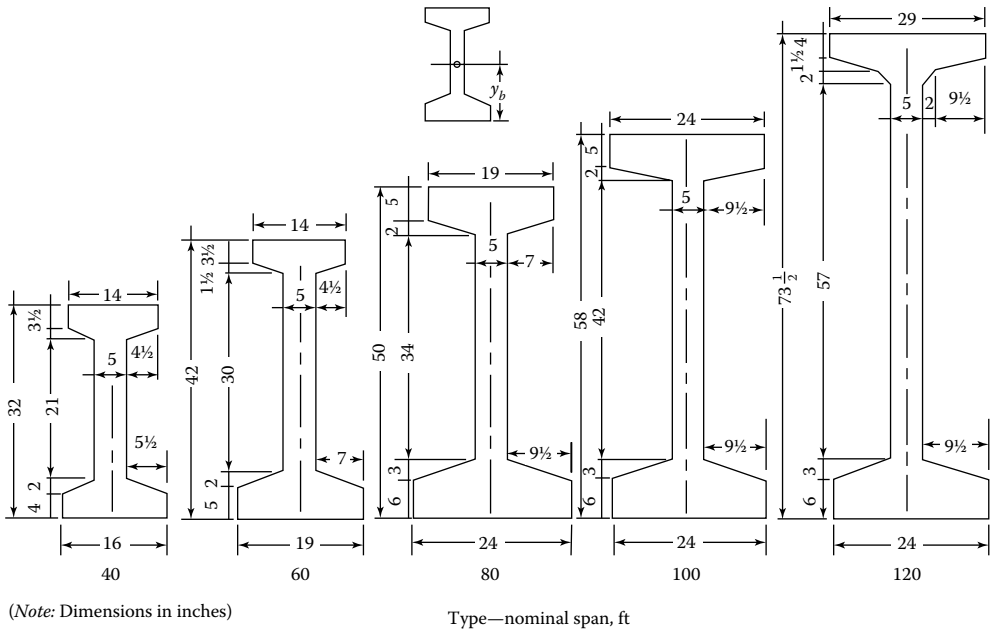

FIGURE 5.92 Washington state standard I-shaped girders.

of section properties in Figure 5.97, which also shows the cross section of a precast, prestressed spread box beam superstructure. Figure 5.98 shows a spread box beam (also called multibeam) superstructure. It consists of box beams shown in Figure 5.97. The top flanges of contiguously placed box beams provide a ready deck, which is covered with a wearing surface. This type of structure provides two distinct advantages over the other superstructure systems: (1) their shallow depths provide easy solutions where site conditions allow only limited superstructure depths, and (2) 3 and 4 ft wide modules can be combined to produce arbitrary bridge widths. Shear keys are provided in between the box beams, which are grouted with nonshrink grout after the beams are installed.

Figure 5.99 shows details of adjacent, flanged, trapezoidal T-box beam girder proposed by the author in 1976 (Taly 1976) for short-span bridge applications. The proposed girders have standard modular widths of 6 and 8 ft and standard depths of 30, 36, and 42 in., which can be used for many short-span-range applications. Figure 5.100 shows the application of T-box girders for the elevated, 71 ft 3 in. wide, three-span (40.5, 71.5, 40.5 ft) T-box girder bridge in Queretaro City, Mexico, completed in 1973 (ASCENT 1994). T-box girders can also be fabricated with wider top flanges suitable for narrow-width bridges, for example, a single-lane bridge. Figure 5.101 shows the cross section of a precast, prestressed T-box used for the Bay Area Rapid Transit System (BART), San Francisco, CA (Grafton 1994); the top flange width of this girder is 11 ft 8 in.

www.EngineeringEBooksPdf.com

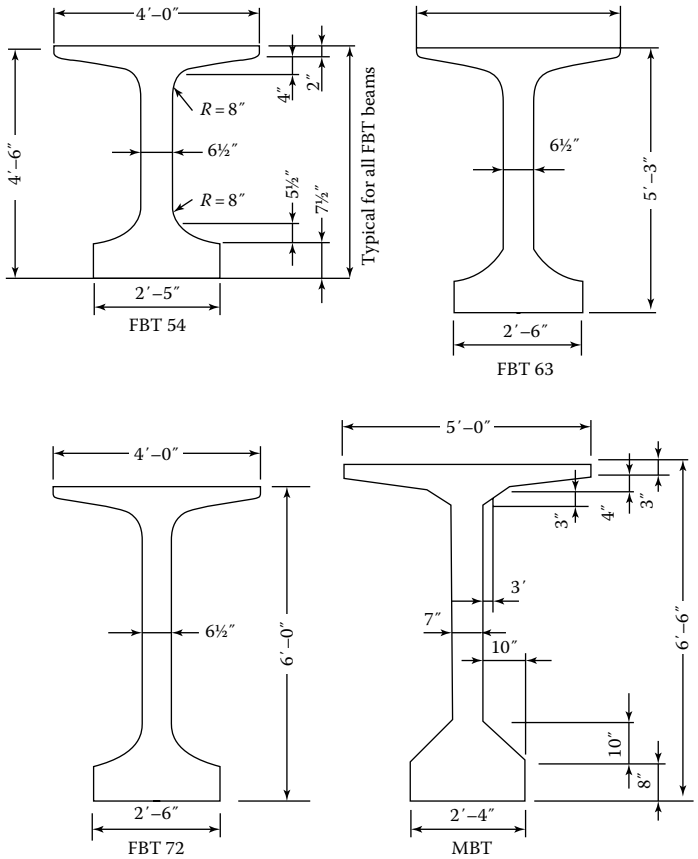

FIGURE 5.93 Florida Department of Transportation standard beams.

Figure 5.102 shows few typical cross sections of multicell box girders; these are usually cast in place and posttensioned. (The girders described earlier are precast and prestressed.) These types of superstructures are suitable for medium-span bridges, usually over 150 ft. Because of their high torsional rigidity and aesthetics, these types of bridges became very popular starting in the 1970s, mainly in California where hundreds of these bridges were built.

Figure 5.103 shows cross sections for segmental bridge construction, which are often used for medium-span bridges. The type of these box girders to be used depends on the width requirements of a bridge. Often a single-cell box shape can be used for deck widths of about 35 ft. For wider deck widths, two-cell (Figure 5.103) or multiple-cell box sections (Figure 5.104) are used. Alternatively, two single-cell box girders can be used side by side (Figure 5.103).

Box girder and segmentally constructed bridges are not discussed further in this book.

5.17.3 Concepts of Prestressing

Prestressed concrete may be defined as structural concrete in which internal stresses are introduced to reduce tensile stresses resulting from loads. In beams with nonprestressed steel, the flexural capacity is limited by two material properties: (1) compressive strength of concrete, usually 4 ksi, and (2) the yield strength of nonprestressed reinforcing steel (f_y = 60 ksi). Such a beam cannot be permitted to carry loads that would cause the reinforcing steel to go past its yield strength.

www.EngineeringEBooksPdf.com

I-Sections with Curved Surfaces

Agency	Type	D1	D2	D3	D4	D5	B1	B2	B3	R1	R2	R3	R4	A	I	y_b
Florida Kentucky[a]	BT-72	72	2	4	5.5	7.5	48.4	30.4	6.9	8	8	0	0	930	651,190	34.4
	BT-1800	70.9	3	3.9	6.9	8.9	58.9	27.6	6.9	7.5	7.5	0	7.5	996	696,975	36.5
	NU750	29.5	2.6	1.8	5.5	5.3	49.2	39.4	6.9	7.9	7.9	2.0	2.0	643	71,554	13.6
	NU900	35.4	2.6	1.8	5.5	5.3	49.2	39.4	6.9	7.9	7.9	2.0	2.0	684	114,178	16.2
	NU1100	43.3	2.6	1.8	5.5	5.3	49.2	39.4	6.9	7.9	7.9	2.0	2.0	738	189,390	19.7
Nebraska University	NU1350	53.1	2.6	1.8	5.5	5.3	49.2	39.4	6.9	7.9	7.9	2.0	2.0	806	315,398	24.1
	NU1600	63.0	2.6	1.8	5.5	5.3	49.2	39.4	6.9	7.9	7.9	2.0	2.0	874	480,111	28.6
	NU1800	70.9	2.6	1.8	5.5	5.3	49.2	39.4	6.9	7.9	7.9	2.0	2.0	928	642,003	32.3
	NU2000	78.7	2.6	1.8	5.5	5.3	49.2	39.4	6.9	7.9	7.9	2.0	2.0	982	832,521	36.0
	NU2400	94.5	2.6	1.8	5.5	5.3	49.2	39.4	6.9	7.9	7.9	2.0	2.0	1091	1,306,244	43.4

[a] Kentucky girder section properties were computed from a straight-line approximation of curved surface.
Note: Units are in inches and 1 in. = 25.4 mm.

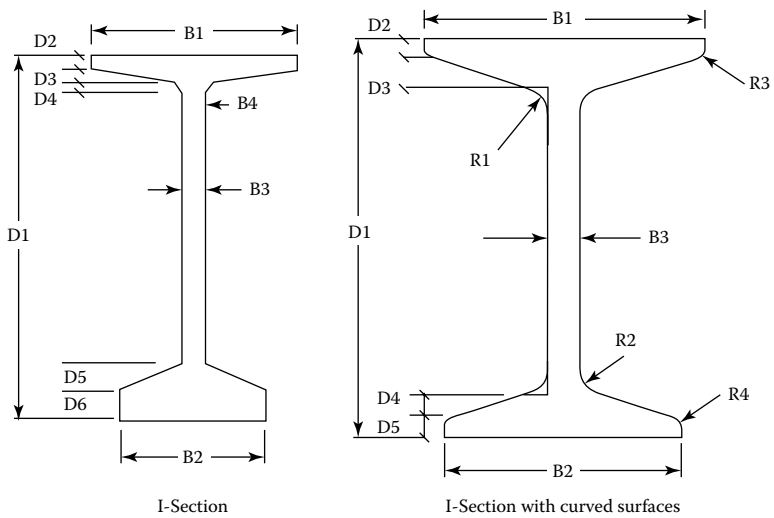

FIGURE 5.94 I-girder series developed by Nebraska University for the Nebraska Department of Transportation.

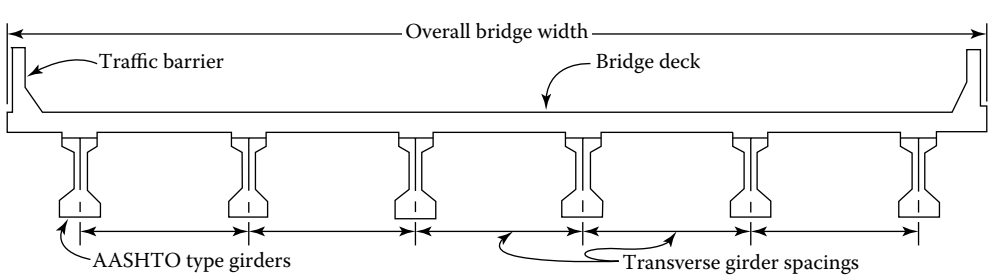

FIGURE 5.95 Typical cross section of slab-precast, prestressed concrete superstructure.

One solution of increasing the flexural strength of the beam is to precompress the beam longitudinally, so the entire beam is in compression before it is loaded. The compressive stresses so introduced will counter the tensile stress to be caused by the loads. The beam can be precompressed by using high-strength steel tendons. Such a precompressing scheme is illustrated in Figure 5.105. The simply supported beam in Figure 5.105a is compressed concentrically by a force P applied at

www.EngineeringEBooksPdf.com

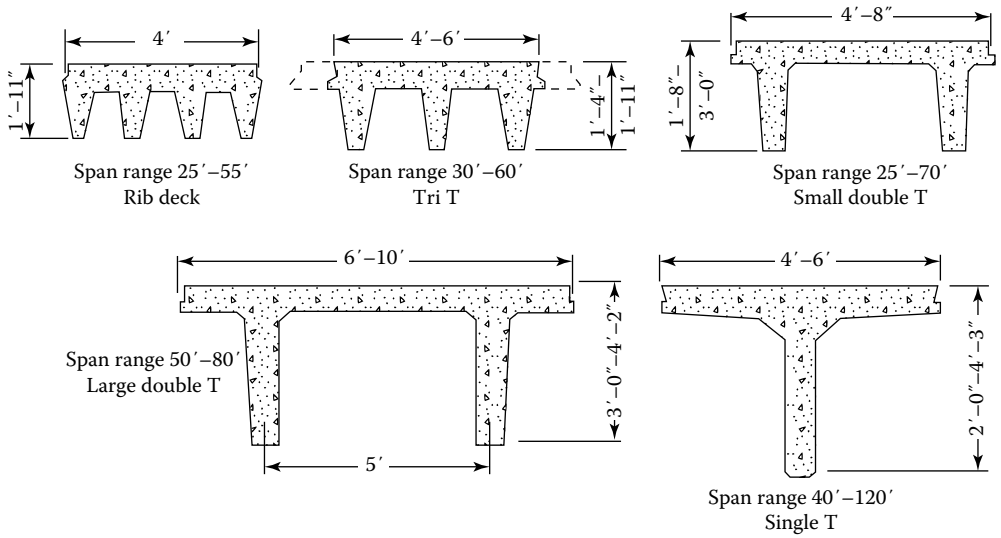

FIGURE 5.96 Forms of T-girders used for short-span highway bridges. (Adapted from Tokerud, R., *Prestressed Concrete Institute Journal*, 24, 42, 1979.)

the c.g. of the beam cross section, so the c.g. of steel (cgs) is the same as the c.g. of concrete (cgc). Under this loading condition, the beam is in the state of compressive axial stress, which can be calculated as follows:

$$f = -\frac{P}{A} \tag{5.109}$$

where

f = compressive force
P = axial compressive force
A = area of cross section of the beam = bh

As a matter of sign convention, a *minus* sign is assigned to compressive stress, and a *plus* sign to tensile stress throughout the following discussion.

Consider now that external transverse loads are applied to the prestressed compressed beam. If the moment caused by these loads is M, the resulting stresses can be determined by the conventional flexural formula:

$$f = \mp\frac{Mc}{I_g} \tag{5.110}$$

in which the minus sign represents the compressive stress in the top fibers and the positive sign represents tensile stress in the bottom fibers. The use of conventional flexural formula and the moment of inertia of the gross section, I_g, in Equation 5.110 is appropriate because the beam under precompression is assumed to remain uncracked. The combined stresses in the beam can be expressed by Equation 5.111:

$$f_t = -\frac{P}{A} - \frac{Mc}{I_g} \tag{5.111}$$

www.EngineeringEBooksPdf.com

Section	Area (in.^{2})	Moment of Inertia (in.^{4})	c_b, (in.)[a]	Span Limit (ft) Draped Strand	Span Limit (ft) Straight Strand
BI-36	560	50,330	13.35	74	62
BI-48	692	65,940	13.37	73	63
BII-36	620	85,150	16.29	86	73
BII-48	752	110,500	16.33	86	74
BIII-36	680	131,140	19.25	97	83
BIII-48	812	168,370	19.29	96	83
BIV-36	710	158,640	20.73	103	87
BIV-48	842	203,090	20.78	103	88

[a] From center of gravity to bottom surface.

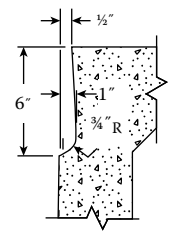

Alternate shear key

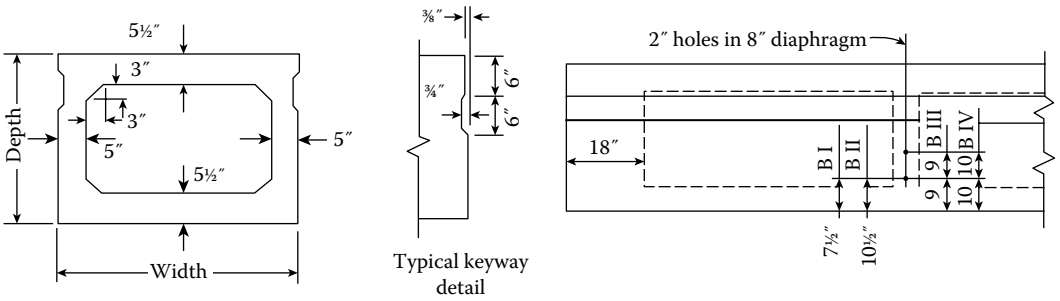

Section properties of standard AASHTO–PCI box sections [Elliot, 1990].

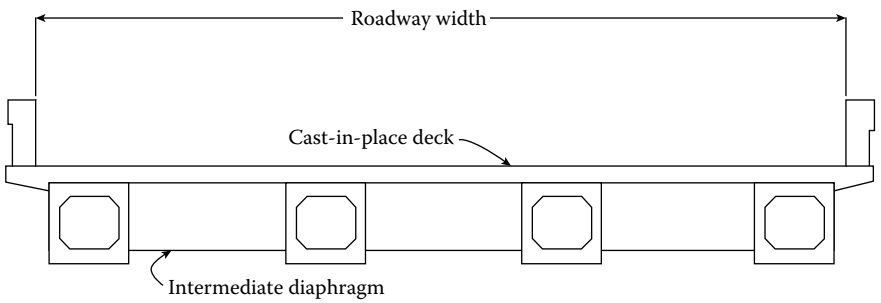

FIGURE 5.97 Cross section of a precast, prestressed spread box beam superstructure.

$$f_b = -\frac{P}{A} + \frac{Mc}{I_g} \tag{5.112}$$

where

f_t = stress in the top fibers
f_b = stress in the bottom fibers
P = prestressing force
M = moment due to external transverse loads
$c = h/2$ for the rectangular section
I_g = moment of inertia of the gross concrete cross section

www.EngineeringEBooksPdf.com

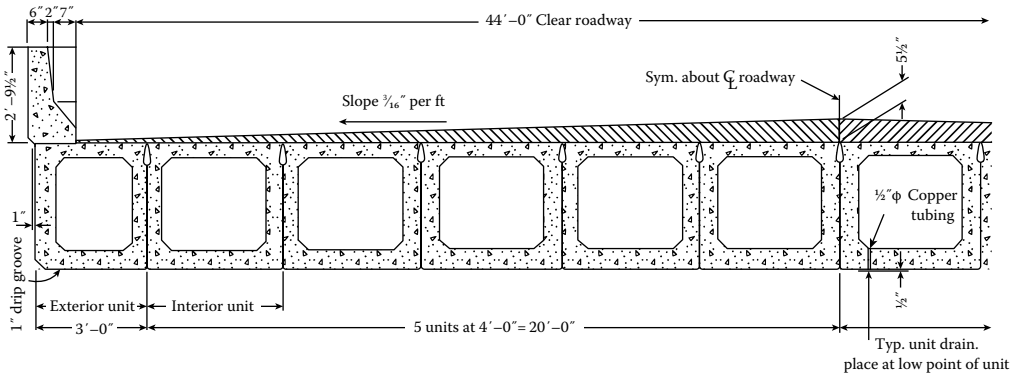

FIGURE 5.98 Cross section of a precast, prestressed spread box beam superstructure. In this cross section, 3 ft wide box beams are used as exterior girders with 4 ft wide box beams as interior girders.

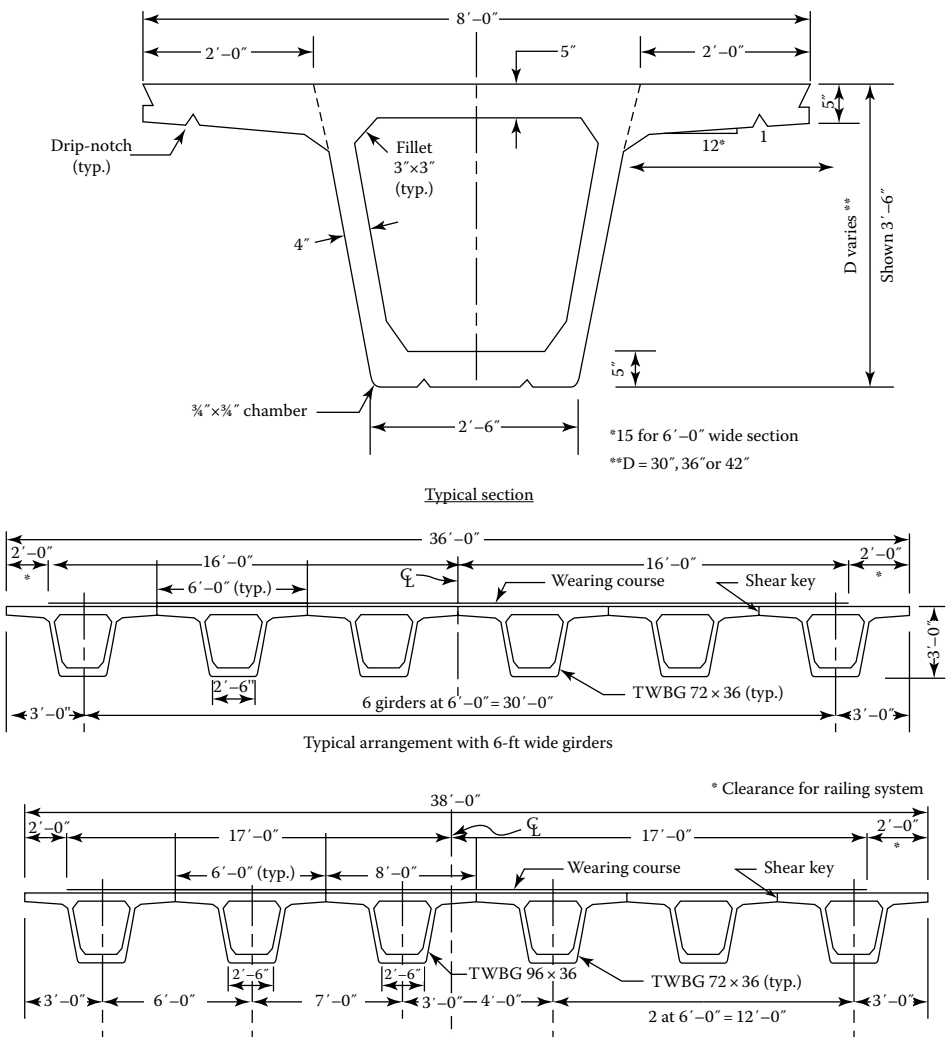

FIGURE 5.99 Precast, prestressed trapezoidal T-box girder system. (From Taly, N., *Development and Design of Standardized Short Span Superstructural Bridge Systems*, Ph.D. Dissertation, Civil Engineering Department, West Virginia University, Morgantown, WV, 1976..)

www.EngineeringEBooksPdf.com

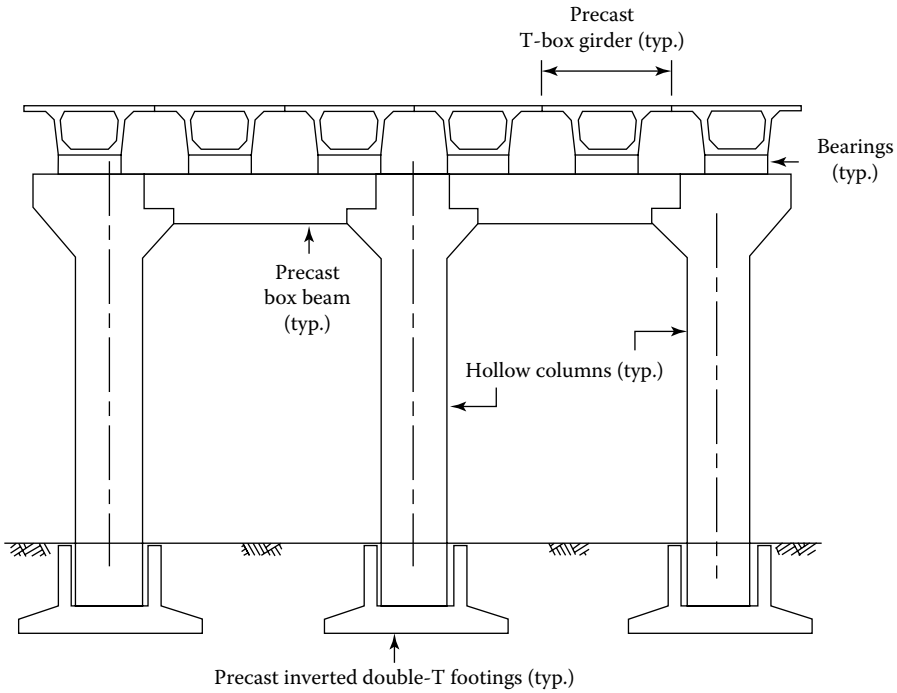

FIGURE 5.100 Transverse section of the T-box girder bridge, Queretaro City, Mexico, Mexico.

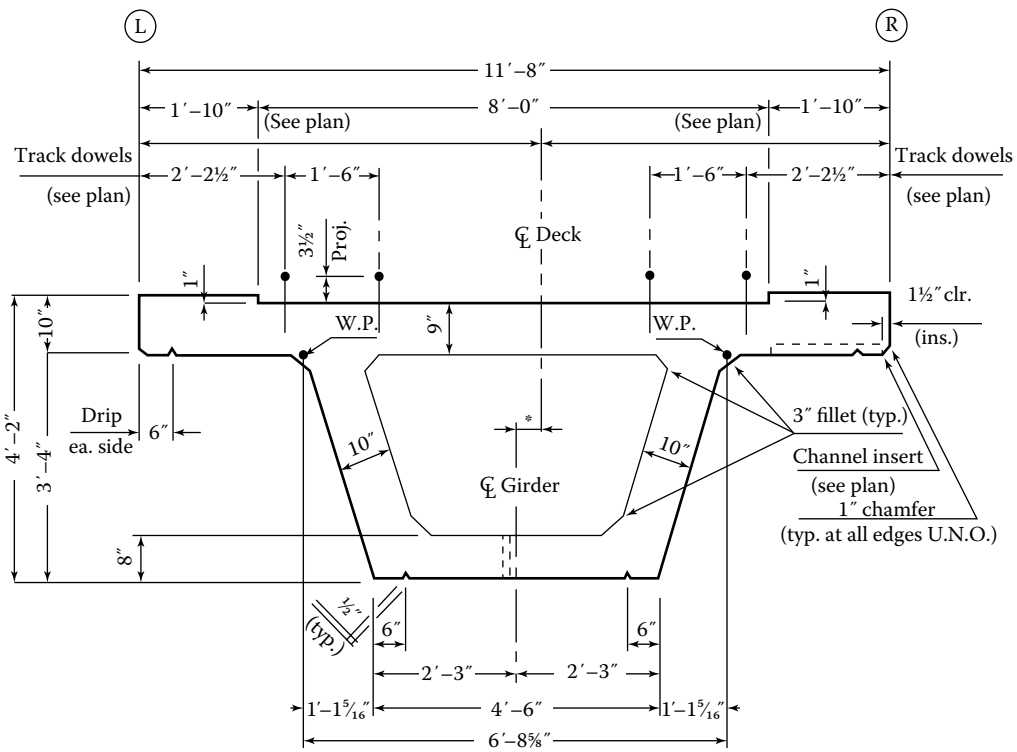

FIGURE 5.101 Precast, prestressed T-box girder for the BART, San Francisco, CA. (From Grafton, J., Pomeroy Corp., Petaluma, CA, *Personal Correspondence*, 1994.)

www.EngineeringEBooksPdf.com

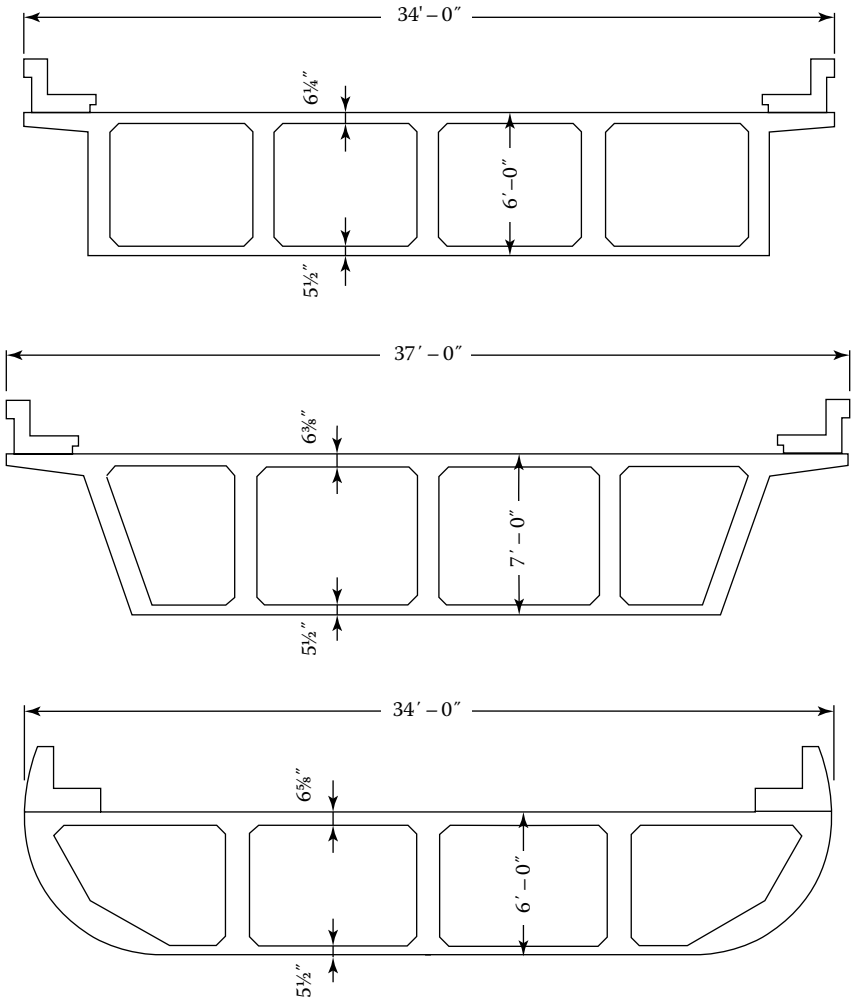

FIGURE 5.102 Cast-in-place, posttensioned box girders. (Adapted from Libby, J.R. and Perkins, N.D., *Modern Prestressed Concrete: Design Principles and Construction Methods*, Van Nostrand Reinhold, New York, 1976.)

Advantage of prestressing the beam should now be obvious from Equation 5.112 that indicates that the influence of axial stress due to prestressing (=$-P/A$) is to reduce the possibly unacceptable tensile stress caused by the imposed transverse loads. But there also is an undesirable consequence; the compressive stress in the top fibers due to the imposed transverse loads is additive to compressive stress due to prestressing. This increased compressive stress in the top fibers may be greater than the acceptable compressive stress and thus reduce the ability of the beam to carry the transverse loads. Fortunately, this adverse situation can be improved by placing the prestressing tendon below the neutral axis at the midspan (location of maximum moment) as shown in Figure 5.105b. This eccentrically applied prestressing force causes axial compressive stress (=$-P/A$) and a moment equal to $-Pe$ throughout the entire beam, which causes tension in the top fibers and compression in the bottom fibers of the beam. The resulting net stresses can be expressed by Equations 5.113 and 5.114:

$$f_t = -\frac{P}{A} + \frac{Pec}{I_g} - \frac{Mc}{I_g} \tag{5.113}$$

www.EngineeringEBooksPdf.com

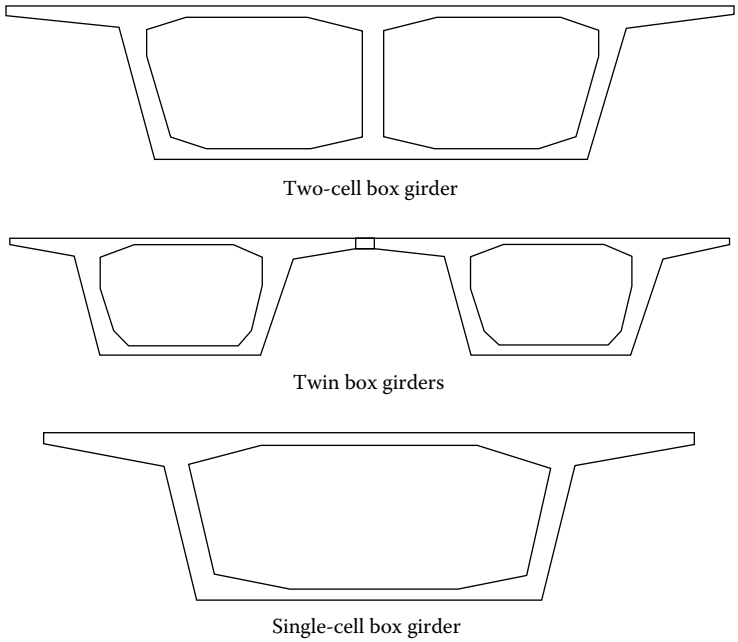

FIGURE 5.103 Typical cross sections for segmental bridges. (Adapted from Libby, J.R. and Perkins, N.D., *Modern Prestressed Concrete: Design Principles and Construction Methods*, Van Nostrand Reinhold, New York, 1976.)

$$f_b = -\frac{P}{A} - \frac{Pec}{I_g} + \frac{Mc}{I_g} \tag{5.114}$$

where e = eccentricity of the prestressing force. Equations 5.113 and 5.114 can be expressed in a compact form by substituting $I_g = Ar^2$. Thus,

$$f_t = -\frac{P}{A}\left(1 - \frac{ec}{r^2}\right) - \frac{Mc}{Ar^2} \tag{5.115}$$

$$f_b = -\frac{P}{A}\left(1 + \frac{ec}{r^2}\right) + \frac{Mc}{Ar^2} \tag{5.116}$$

In a bridge superstructure, the beams are subjected to bending moments due to the permanent loads (including the dead load due to their self-weight) and the live load; the total moment, M_T, can be expressed as follows:

$$M_T = M_s + M_D + M_{LL+IM} \tag{5.117}$$

where

M_T = total bending moment
M_D = bending moment due to permanent loads
M_{LL+IM} = moment due to live load plus impact

Note that the first terms on the right-hand side of Equations 5.115 and 5.116 represent the stresses due to the prestressing force only. In a simply supported beam, the moment due to external loads is

www.EngineeringEBooksPdf.com

Bridge	Cross Section	Type of Construction	Span (ft)
Rio Niteroi, Brazil	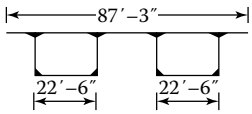	Precast	262
Pine Valley, USA	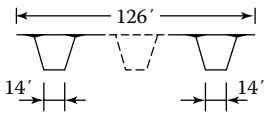	Cast-in-place	450
Kipapa, USA	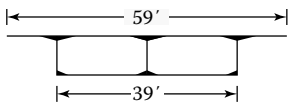	Cast-in-place	250
Kishwaukee, USA	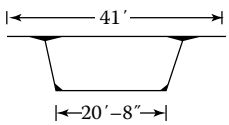	Precast	250
Long Key, USA	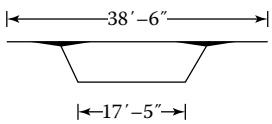	Precast	118
Seven Mile, USA	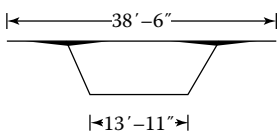	Precast	135
Columbia River, USA	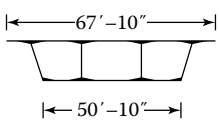	Cast-in-place and precast	600
Zilwaukee, U.S.A	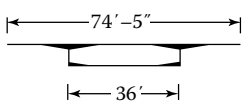	Precast	375
Houston Ship Channel, USA	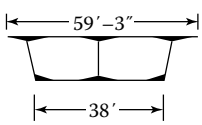	Cast-in-place	750

FIGURE 5.104 Typical cross sections for some segmental bridges in the Americas. (Adapted from Podolny, W. Jr. and Muller, J., *Construction and Design of Prestressed Concrete Segmental Bridges*, John Wiley & Sons, New York, 1982.)

maximum at midspan and zero at the supports. Therefore, stresses at the ends of the beam are due only to the eccentrically applied prestressing force, P, which can be expressed as follows:

$$f_t = -\frac{P}{A}\left(1 - \frac{ec}{r^2}\right) \tag{5.118}$$

$$f_b = -\frac{P}{A}\left(1 + \frac{ec}{r^2}\right) \tag{5.119}$$

www.EngineeringEBooksPdf.com

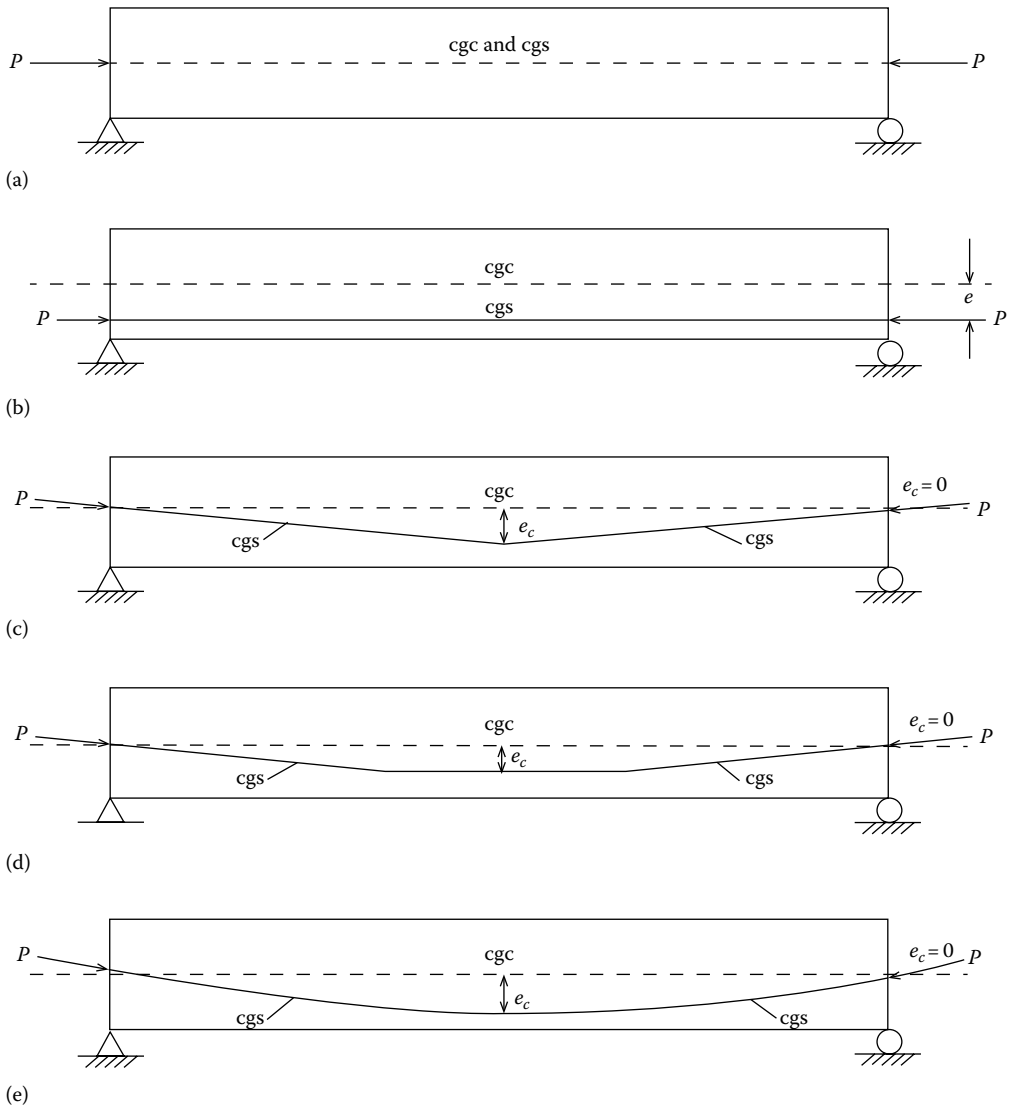

FIGURE 5.105 Concepts of prestressing: (a) concentric prestressing, (b) constant eccentricity, (c) single-point harped tendon, (d) two-point harped tendon, and (e) draped tendon.

In some situations, the tensile stress in the top fibers at the ends of the beam given by Equation 5.118 may not be acceptable. In such cases, the eccentricity of the prestressing force at the ends of the beam can be made zero by elevating the c.g. of the prestressing forces at the ends to the c.g. of concrete section as shown in Figure 5.105c. In such a case, the eccentricity of the prestressing force varies linearly from a maximum of e at midspan to zero at the support. If necessary, the c.g. of the prestressing force can be located even a little *above* the c.g. of the section at the ends.

This situation can be ideal in some but not in all cases. For example, if a simple beam is subjected to a concentrated load at midspan, the maximum moment occurs at the midspan and reduces linearly to zero at the supports. For such a case, the layout of the centrally harped tendon (Figure 5.105c) may be satisfactory. In a majority of cases, however, the beams are subjected to uniform loads, including their self-weight. In such beams, the moment is maximum at midspan ($= 0.125wL^2$) and reduces to zero at the supports, but the variation in moment is parabolic, not linear. For example,

www.EngineeringEBooksPdf.com

at 0.45L from the support, the moment is still $0.12375wL^2$, not much of a change. In such cases, a centrally harped tendon layout is not very helpful in managing stresses to acceptable levels. Instead, a two-harped tendon layout as shown in Figure 5.105d may be desirable. For example, the two harping points can be selected to be at 0.45L from each support. This tendon layout would be used in Example 6.6.

There may yet be a situation where even the two-point harped tendon layout may not be satisfactory to manage stresses to desirable/acceptable levels. In such cases, the tendons can be draped (i.e., layout along a predefined curved profile) as shown in Figure 5.105e.

The preceding discussion focused on simply supported beams in which the moments are zero at the support. In a continuous beam, the moments would be zero at the end supports, but there would be negative moment at the interior support. In such cases, the layout of tendons would need to be reversed in the regions of the negative moments. An example of curvilinear tendon profile in a two-span, continuous, two-lane posttensioned box girder is shown in Figure 5.106 (see Example 7.1 in Taly 1998, pp. 550–556).

From the aforementioned discussion, it should be clear that stress levels in a loaded beam can be kept at acceptable or desirable levels by simply selecting proper eccentricity. In fact, the freedom to layout the prestressing tendon at designer's discretion is the single most important advantage that has made prestressed concrete as the preferred material of choice worldwide.

5.17.4 Pretensioned and Posttensioned Girders

The term *prestressed* implies that a member has been subjected to a compressive force *before* external loads are applied on it. Typically, there are two methods of prestressing in common use: (1) *pretensioning* and (2) *posttensioning*. Precast, prestressed girders discussed in Section 5.17.2.2 are essentially *pretensioned* girders. These girders are typically precast in molds affixed to prestressing beds in manufacturing plants. The prestressing strands are stretched (or tensioned) to predetermined force levels in these beds and held in position by the bulkheads, *before* the concrete has been poured. Concrete is poured in the molds, which surrounds the pretensioned strands. After the concrete has attained sufficient compressive strength, the stretched strands are released by cutting them. As the strands try to shorten upon release, the surrounding concrete gets compressed, a phenomenon called pretensioning. Posttensioning, on the other hand, is a method of prestressing in which the tendons are tensioned *after* the concrete has reached a predetermined strength.

5.17.5 Layout and Location of the Center of Gravity of Multiple Strands in a Prestressed Girder

Prestressing steel was discussed earlier in Art. 5.4.4. In Figures 5.105 and 5.106, the prestressing force is applied at the c.g. of prestressing steel (cgs). Prestressing tendons consist of strands as discussed in Section 5.4.4. Typically, 1/2 in. diameter, seven-wire strands are commonly used; several of these strands are required in a girder depending on the magnitude of the required prestressing force. Properties of prestressing strands and bars are given in Table 5.4.

Prestressed girders typically do not have rectangular shapes; most have I, T, or bulb-T shapes as discussed earlier. Depending on the cross-sectional shape of a girder, the prestressing strands should be arranged in a given cross section in such a manner that requirements for cover (Table 5.1) and clear distance between adjacent strands are satisfied (Art. 5.12.3).

Figure 5.107 shows examples of typical spacing patterns for several I and bulb-T sections and a box section. Note that the strands are placed in 2 in. grid both vertically and horizontally. The number of grid columns varies depending on the width of the web and the cross-sectional shape of the bottom flange of the girders. The examples shown in Figure 5.107 are strand patterns used for the standard prestressed concrete girder shapes of the Pennsylvania Department of Transportation (PennDOT); however, they represent typical industry practice.

www.EngineeringEBooksPdf.com

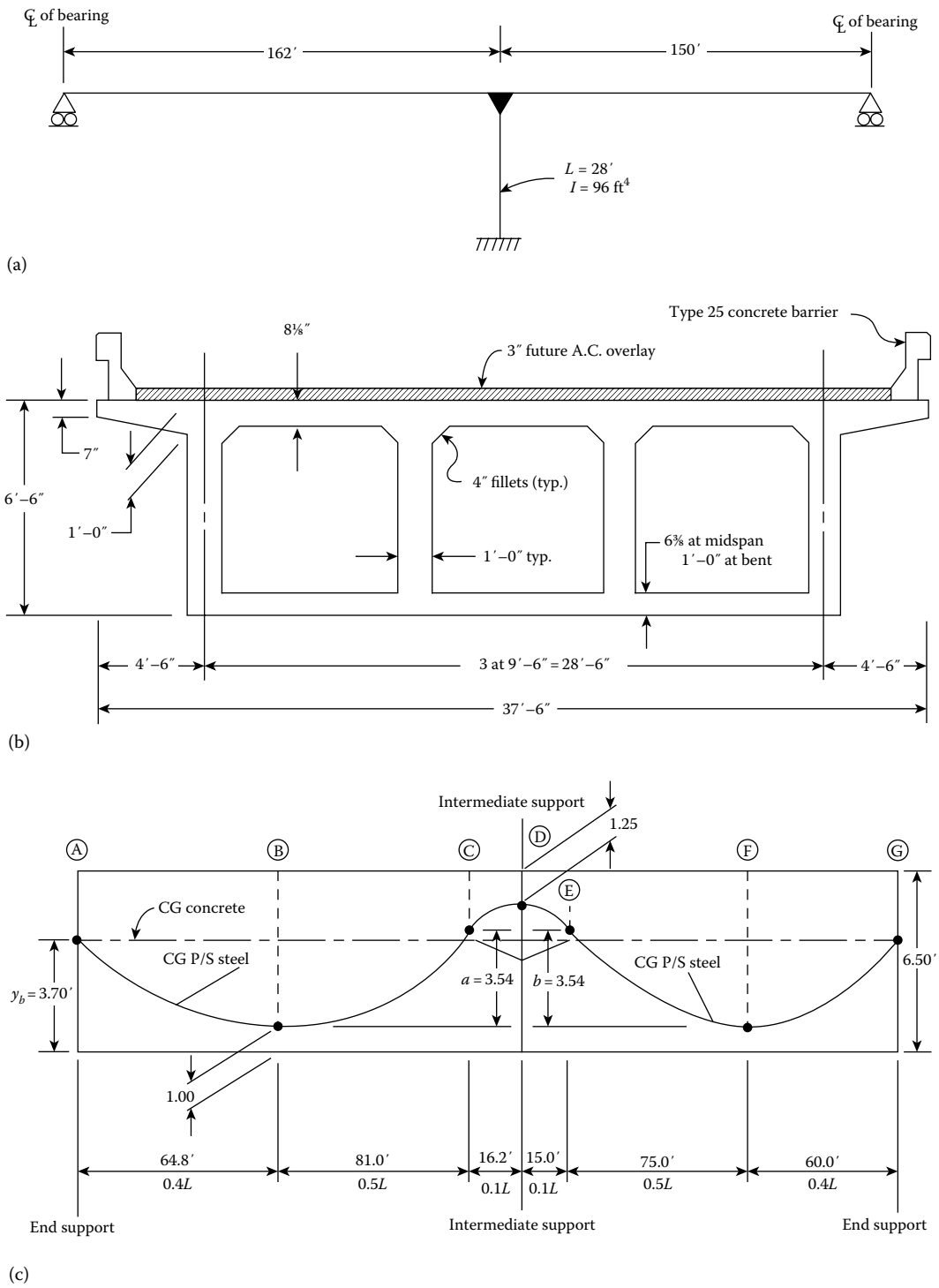

FIGURE 5.106 Curved tendon profile in a two-span, continuous, two-lane posttensioned box girder bridge. (a) Bridge elevation, (b) cross section of box girder, and (c) layout details of prestressing tendon.

www.EngineeringEBooksPdf.com

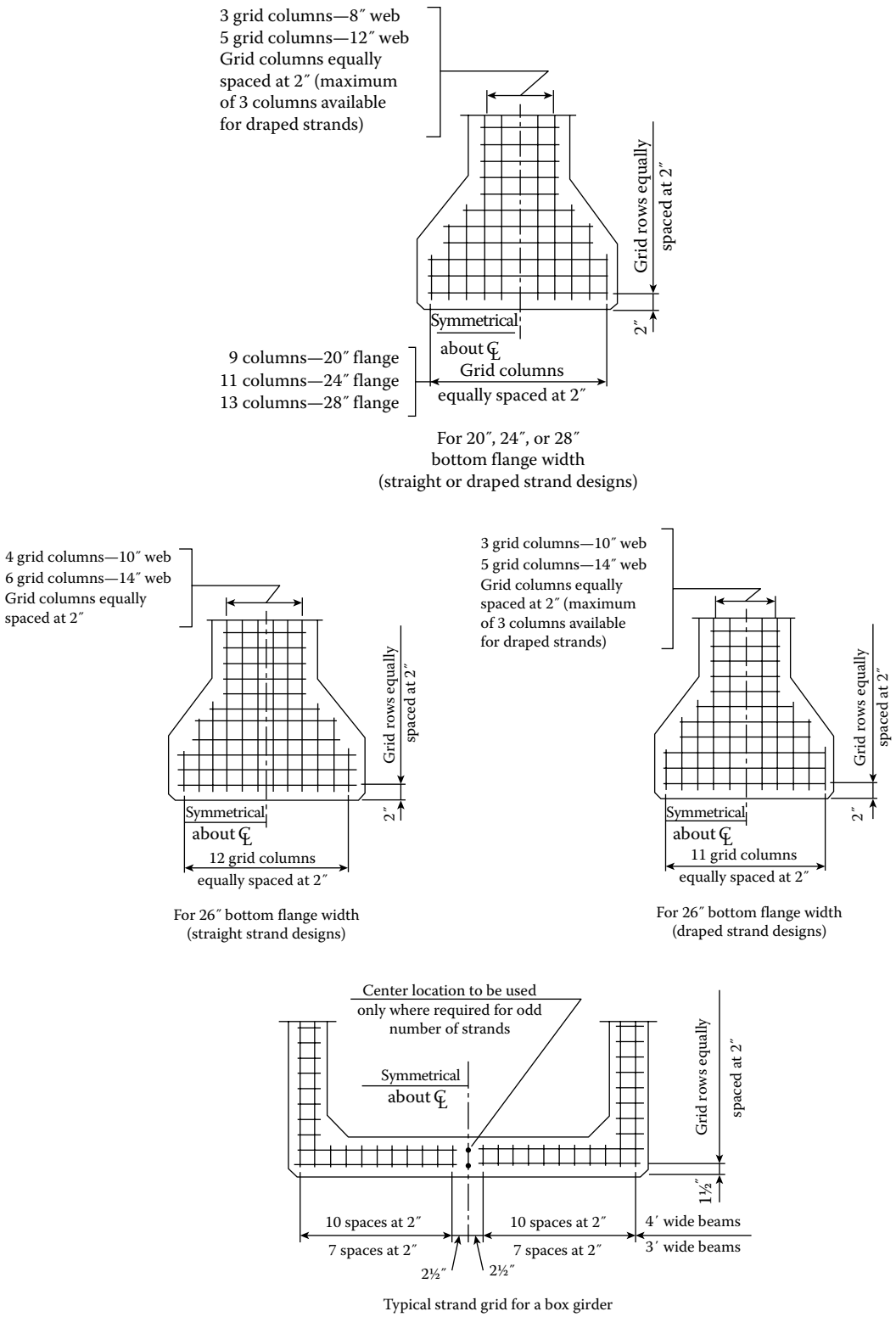

FIGURE 5.107 Strand patterns in prestressed concrete girders. (Courtesy of Pennsylvania Department of Transportation, Harrisburg, PA.)

www.EngineeringEBooksPdf.com

5.17.6 Design of a Prestressed Concrete Girder for a Highway Bridge

Example 5.6 presents design of the interior girder of simple-span, three-lane highway bridge superstructure that uses precast, prestressed concrete girders to support a reinforced concrete deck. The design calculations are performed conforming to the LRFD specifications. The design uses 1/2 in. diameter, low-relaxation seven-wire strands. Stress limits for prestressing strands are given in Table 5.A.5. Tensile stress limits in prestressed concrete at service limit state after losses in fully prestressed components are given in Table 5.A.6.

Example 5.6: Design of Slab Precast, Prestressed Concrete Girder Bridge

Design a highway bridge for a simple span of 110 ft between centers of bearings and a clear roadway width of 48 ft. The deck is to be 8 in. thick (structural) cast-in-place slab supported by PCI BT-72 (72 in. bulb-T) precast, prestressed concrete girders spaced at 9 ft o.c. The cross section of the proposed bridge and BT-72 girder is shown in Figure 5.108. The deck is to be provided with 1/2 in. thick integral concrete wearing surface (nonstructural). The traffic barriers weigh 505 lb/ft. It is required that a provision be made in design for 25 lb/ft^2 of dead load for FWS. The following material properties are specified:

Girder Concrete

28-day compressive strength, f'_c = 6.0 ksi
Initial compressive strength (strength at transfer), f'_{ci} = 5.5 ksi
w_c = 150 lb/ft^3

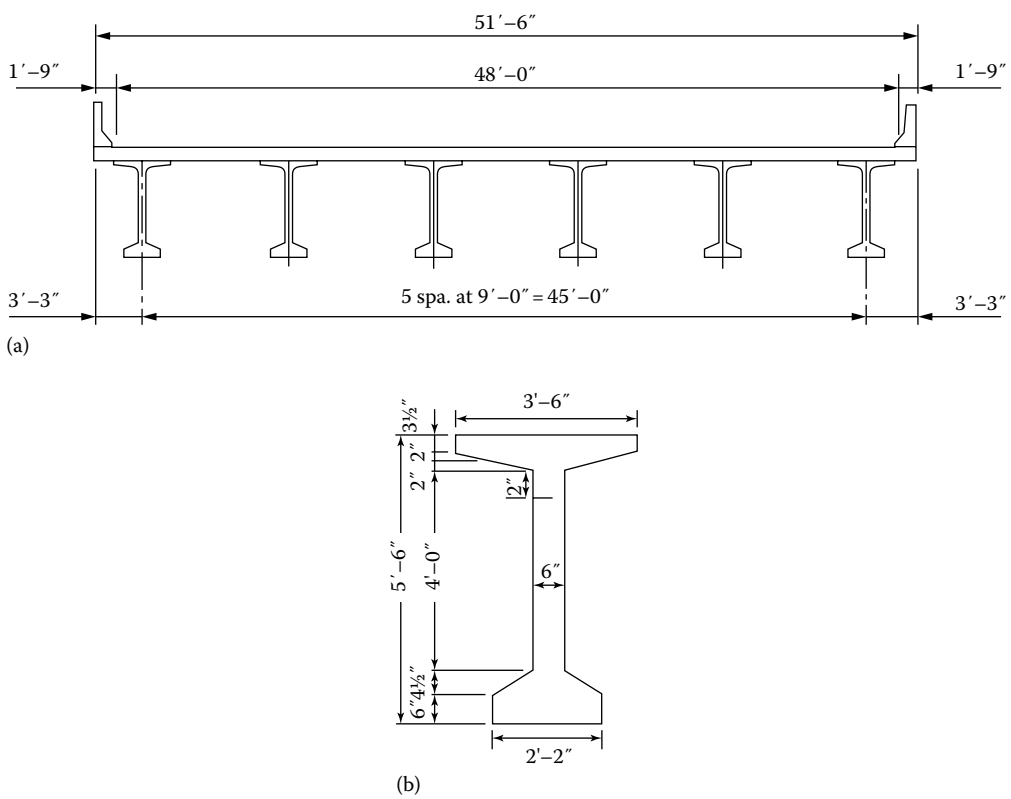

FIGURE 5.108 Cross section of proposed slab–prestressed concrete girder bridge. (a) Bridge cross section and (b) cross section of BT-72 precast prestressed concrete girder.

www.EngineeringEBooksPdf.com

Deck Concrete

f'_c = 4.0 ksi
w_c = 150 lb/ft^3

(Art. C5.4.2.4 suggests that the unit weight of normal-weight concrete is 0.145 kcf. The precast concrete mixes typically have a relative low *W/C* ratio. Therefore, a unit weight of 0.15 kcf is assumed for both the deck and the girder concrete.)

Prestressing Steel

0.5 in. diameter, 270 ksi, low-relaxation, seven-wire strands
Cross-sectional area of one strand = 0.153 in.^{2}
Ultimate strength, f_{pu} = 270 ksi
Yield strength = $0.9f_{pu}$ = 0.9(270.0) = 243.0 ksi
Modulus of elasticity of prestressing strands, E_{ps} = 28,500 ksi (Art. 5.4.4.2)
Stress limits for prestressing strands (LRFD Table 5.9.3-1)
Pull = 75 percent
Before transfer, $f_{pi} \leq 0.75f_{pu}$ = 202.5 ksi
Release time = 24 h
Strand profile = two-point depressed
Depression point = 0.45*L*
Relative humidity, *H* = 75 percent

Reinforcing Steel

f_y = 60 ksi
Modulus of elasticity, E_s = 29,000 ksi (Art. 5.4.3.2)
New Jersey–type barrier: Unit weight = 0.505 kip/ft
The bridge has no skew.
The overall length of the girder is 111 ft.

General Description and Initial Assumptions

The design of this bridge entails design of the deck and the design of interior and exterior girders. The thickness of the deck is kept as 8 in. (structural) plus additional 1/2 in. thick integral wearing surface. A provision of 25 psf for FWS would be made in the design.

This superstructure will be designed as a composite slab, prestressed girder system.

The design of 8 in. thick reinforced concrete deck is not presented in this example. Examples 5.2 and 5.3 present the design of identical decks by the empirical design method (Art. 9.7.2) as well as by the traditional design method (Art. 9.7.3). This example presents the design of a typical interior girder for this bridge.

The data/assumptions listed earlier would be used for the design of the superstructure of this bridge.

This design presents sample calculations for a typical interior girder of the previously defined superstructure. Like typical structural design problems, the calculations presented here are the result of a few iterations; only final calculations are presented (to save the space in this book).

Several design parameters have been selected arbitrarily but based on practical experience and industry practice. These include the deck thickness, type, size and spacing of girders, and the 28-day compressive strengths of concrete for precast slab (typically 4 ksi as used in this design example) and of precast, prestressed concrete bulb-T girder. The initial (or at-release) and in-service (or final) compressive strengths of concrete for the girder, 5.5 and 6.0 ksi, respectively, were selected after a few iterations so as to satisfy the required stress limits.

The number of prestressing strands used in the girder was also selected after a few iterations. The strands are arranged in the girder cross section in a 2 in.-grid pattern as discussed earlier (see Figure 5.107). A two-point harping of strands (at 0.45*L*, typical for this type of girder and design) was found suitable for this design and has been used. A typical New Jersey–type traffic barrier has been used for the deck.

As specified in LRFD Art. 4.6.2.2.1 and discussed in Section 4.3, the dead load of concrete traffic barriers, which will be cast after the deck hardens, would be distributed equally to all girders

www.EngineeringEBooksPdf.com

(exterior and interior). This assumption is used in this example. However, designers, at their discretion, may choose to distribute the dead load of traffic barriers to only the exterior girders and none of it to the interior girders; this option is not followed in this book.

Solution

Trial Girder Section

Precast, prestressed concrete bulb-T girders are selected as the trial size for both interior and exterior girders for this bridge. This selection is based on the knowledge that AASHTO-PCI BT-72 is suitable for this span range.

The section properties of the basic PCI BT-72 are as follows:

Area of cross section, A = 767.0 in.^{2}
Moment of inertia, I = 545,894 in.^{4}
Height of girder, H = 72.00 in.
Centroid of girder from bottom, y_b = 36.6 in.
Centroid of girder from top, y_t = 35.4 in.
Section modulus for the bottom fibers, S_b = 545,894/36.60 = 14,915 in.^{3}
Section modulus for the top fibers, S_b = 545,894/35.40 = 15,421 in.^{3}

Section Properties of Composite Section (see Figure 5.109)

Art. 5.9.1.4 provides that for both pretensioned and posttensioned members after bonding, section properties may be based on either gross area or transformed section. In this example, section properties are based on transformed areas of deck and the girder, but for simplicity, the contribution of the strands to the section properties of composite section is neglected. A 2 in. thick haunch is provided between the deck and the girders, but it is not included in the determination of section properties.

The deck thickness is 8.5 in. including a 1/2 in. thick integral wearing surface. The structural thickness is 8.0 in. for the purposes of calculating section properties.

The tributary width of the girder, TW = center-to-center distance between adjacent girders
= 9.0 ft = 108 in.

Effective width, b_e = tributary width = 108 in. (Art. 4.6.2.6.1)

Modulus of elasticity of concrete, E_c

$$E_c = 33{,}000\left(w_c\right)^{1.5}\sqrt{f'_c}\ \text{ksi}$$

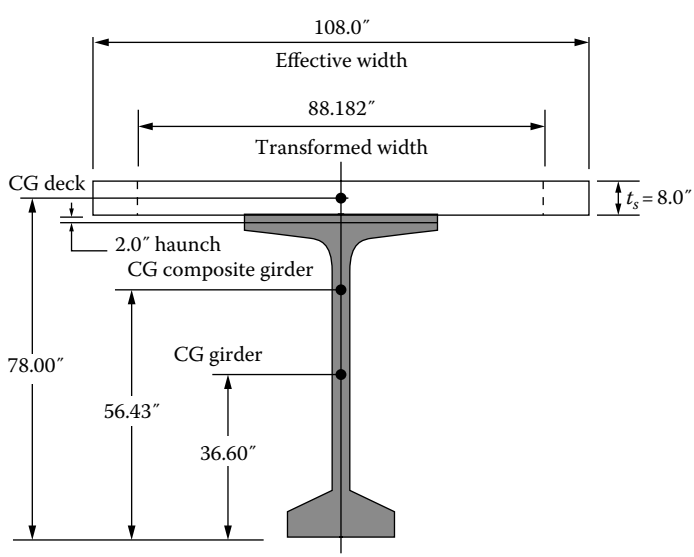

FIGURE 5.109 Computation of section properties of composite section.

www.EngineeringEBooksPdf.com

For the cast-in-place deck,

$$E_c = 33{,}000(0.15)^{1.5}\sqrt{4.0} = 3{,}834 \text{ ksi}$$

For the precast beam at transfer,

$$E_{ci} = 33{,}000(0.15)^{1.5}\sqrt{5.5} = 4{,}496 \text{ ksi}$$

For the precast beam at service loads,

$$E_c = 33{,}000(0.15)^{1.5}\sqrt{6.0} = 4{,}696 \text{ ksi}$$

Modular ratio to determine transformed width,

$$n = \frac{E_{c,deck}}{E_{c,girder}} = \sqrt{\frac{f'_{c,deck}}{f'_{c,girder}}} = \sqrt{\frac{4.0 \text{ ksi}}{6.0 \text{ ksi}}} = 0.8165$$

Transformed width of the deck = $n(b_e)$ = 0.8165(108) = 88.182 in.
Thickness of deck, $t_s = h_f$ = 8 in.
Contributory deck area = TW(t_s) = (9.0)(12)(8.0) = 864 in.^{2}
Transformed area of deck = n (deck cross-sectional area)
= (0.8165)0(864) = 705.45 in.^{2}
Moment of inertia of the transformed deck,

$$I_0 = \frac{b_{e,tr}h^3}{12} = \frac{88.182(8)^3}{12} = 3762 \text{ in.}^4$$

Calculation of section properties of the composite section are shown in Table 5.14.

All distances are measured from the bottom of the girder as shown in Figure 5.109.

A = total area of composite section = 1472.45 in.^{2}
h_c = overall depth of composite section (including haunch) = 72.0 + 2.0 + 8.0 = 82 in.
y_{bcg} = distance from the bottom of the girder to the centroid of composite section to the extreme fiber of the precast girder = $(Ay_b)/A$ = 83,097 in.^{3}/1472.45 in. = 56.43 in.
y_{tcg} = distance from the centroid of composite section to the extreme top fiber of the precast girder = $H - y_{bcg}$ = 72.00 in. −56.43 in. = 15.57 in.
y_{tcd} = distance from the centroid of composite section to the extreme top fiber of the composite deck = $h_c - y_{bc}$ = 76 + 2 + 8 − 56.43 in. = 25.57 in.
S_{bcg} = composite section modulus for the extreme bottom fibers of the precast girder
= I_c/y_{bcg} = 1,179,484 in.^{4}/56.43 in. = 20,902 in.^{3}
S_{tcg} = composite section modulus for the extreme top fibers of the precast girder
= I_c/y_{tcg} = 1,179,484 in.^{4}/15.57 in. = 75,754 in.^{3}
S_{tcd} = composite section modulus for the extreme top fibers of the deck slab
= $(I_c/y_{tcd})/n$ = [(1,179,484 in.^{4}/25.57 in)]/(0.8165) = 56,494 in.^{3}

TABLE 5.14
Computation of Section Properties of Composite Section

Component	Area (in.^{2})	y_b (in.)	Ay_b (in.^{3})	$A(y_b - y_{bc})^2$ (in.^{4})	I_o (in.^{4})	I_c (in.^{4})
Girder	767.00	36.60	28,072	301,607	545,894	847,501
Effective deck	705.45	78.00	55,025	328,221	3,762	331,993
Total	1,472.50		83,097			1,179,484

www.EngineeringEBooksPdf.com

LRFD Parameters

For structural design based on the LRFD philosophy, the following parameters as specified in LRFD specifications will be used.

Load Modifiers

$$\eta = \eta_D \eta_R \eta_I \qquad (1.69)\ [A1.3.2.1\text{-}1]$$

For this example, the bridge is assumed to be a typical, conventional bridge. Therefore, the following values of load modifiers will be used:

η_D = a factor related to ductility = 1.0
η_R = a factor related to redundancy = 1.0
η_I = a factor related to operational classification = 1.0

Therefore, $\eta = (1.0)(1.0)(1.0) = 1.0$.

Limit States Considered

The structural design of the superstructure presented herein would be checked for Strength I Limit State. No permit vehicle is specified in this example, so Strength II Limit State is not checked. The Strength IV Limit State relates to very high dead-to-live load force effect ratios, which is not the case in this example and, therefore, not checked.

Wind load checks are not presented in this example; therefore, load combinations Strength III Limit State and Strength V Limit State are also not checked.
Extreme-event checks are not performed in this example.
Service I and Service III Limit States are related to prestressed concrete girders; these limit states would be checked in this example.
Live load deflection check would be performed as specified in Art. 2.5.2.6.2.

Load Combinations and Load Factors

The following load combination specified in AASHTO LRFD Art. 3.4.1 would be used in this example. Only the maximum permanent load factors γ_p (from AASHTO Table 3.4.1-2) would be used here because uplift is not a concern in this bridge geometry. In case potential for uplift at the end abutments exists, the minimum permanent load factors specified in the table should be used in the strength load combinations when checking for uplift.

The following load combinations are obtained directly from LRFD Table 3.4.1-10; the applicable load factors are obtained from LRFD Table 3.4.1-2:

Strength I Limit State

$$U = \eta[1.25DC + 1.5DW + 1.75(LL + IM) + 1.0WA + 1.0FR + (0.5 \text{ or } 1.2)TU + \gamma_{TG}TG + \gamma_{SE}SE]$$

The forces *WA* (water load and stream pressure), *FR* (friction load), *TU* (force effects due to uniform temperature), *TG* (force effects due to temperature gradient), and *SE* (force effect due to settlement) in the aforementioned load combination equation are not relevant to this design example and therefore dropped from the aforementioned equation (also dropped from load combinations equations for other limit states) resulting in the following load combination equation that would be used in this example:

$$U = \eta[1.25DC + 1.5DW + 1.75(LL + IM)]$$

Service II Limit State

$$U = \eta[1.00DC + 1.00DW + 1.30\ (LL + IM)]$$

Fatigue Limit States

Fatigue I, $1.5(LL + IM)$
Fatigue II, $0.75(LL + IM)$

where *LL* is the HL-93 vehicular live load as specified in Art. 3.6.1.4.1.

www.EngineeringEBooksPdf.com

Dynamic load allowance (see Section 3.8.3, Table 3.18/Art. 3.6.2.1)
Fatigue and fracture limit state $IM = 0.15$
All other limit states $IM = 0.33$

Structural Design of the Bridge Superstructure
The structural design of this bridge superstructure consists of three parts:

Design of deck slab
Design of a typical interior girder
Design of a typical exterior girder

Part 1. Design of Deck Slab
Sample calculations for the design of the deck slab are presented in Examples 5.2 and 5.3. Similar calculations would be used for the design of the deck slab for this bridge.

Part 2: Design of a Typical Interior Girder
Calculations for the design of a typical interior girder are presented as follows. All calculations are presented in a step-by-step format.

Unfactored Loads on a Typical Interior Girder
Permanent loads: DC1 due to permanent loads

$$\text{Deck slab 8 in. thick (structural)} = \left(\frac{8}{12}\right)(1)(0.15) = 0.10\,\frac{\text{k}}{\text{ft}^2}$$

Tributary width of deck slab contributory to each girder
= center-to-center distance between girders = 9.0 ft

$$\text{Dead load due to the deck slab} = (0.10)(9.0) = 0.90 \text{ kip/ft} \tag{1}$$

1/2 in. thick integral wearing surface,

$$w = \left(\frac{0.5}{12}\right)(1.0)(9.0)(0.15) = 0.0563 \text{ kip/ft} \tag{2}$$

Self-weight of girder PCI bulb-T, with $A_g = 767$ in.^{2},

$$w_{gdl} = \frac{767}{144}(0.15)(1.0) = 0.799 \approx 0.8 \text{ kip/ft} \tag{3}$$

Top flange width of BT-72 girder = 3.5 ft = 42 in.

Depth of haunch = 2 in. (assumed)

$$\text{Weight of concrete haunch} = \left(\frac{2.0}{12}\right)\left(\frac{42}{12}\right)(0.15)(1.0) = 0.088 \text{ kip/ft} \tag{4}$$

Weight of intermediate diaphragms: Assume 12 in. thick, 36 in. deep at 1/3 points:

Width of the diaphragms = spacing of girders − web thickness
− 2 in. clearance on each side of the diaphragms

= 9 − 0.50 − 0.17 = 8.33 ft

$$\text{Dead load due to diaphragms} = \frac{12(36)}{144}(0.15)(8.33) = 3.75 \text{ kip each}$$

www.EngineeringEBooksPdf.com

For simplicity in calculations, distribute the weight of intermediate diaphragms over the entire girder length:

$$\text{Additional dead load} = \frac{2(3.75)}{110} = 0.068 \text{ kip/ft} \tag{5}$$

Dead weight of the traffic barriers = 0.505 kip/ft (see Example 5.1)

Dead load of the two traffic barriers on the deck is distributed equally to all six girders.

Dead load due to two traffic barriers = 2(0.505)/6 = 0.168 kip/ft (6)

Dead load due to the FWS at 25 lb/ft^2, w_{DW} = (0.025)(1)(9.0)

= 0.225 kip/ft (7)

Dead load *DC* is separated into two parts: *DC*1, which acts on the noncomposite section, and *DC*2, which acts on the composite section. The load factors for both are 1.25.

w_{DC1} = Sum of Items 1 through 5 = 0.90 + 0.0563 + 0.80 + 0.088 + 0.068 = 1.912 kip/ft

Permanent load on the girder, Item 6, w_{DC2} = 0.168 kip/ft
Permanent load on the girder, Item 7, w_{DW} = 0.225 kip/ft

Total dead load on a typical interior girder,

$$w_{DC} = w_{DC1} + w_{DC2} = 1.912 + 0.168 = 2.08 \text{ kip/ft}$$

$$w_{DW} = 0.225 \text{ kip/ft}$$

The aforementioned dead load values would be used to calculate midspan deflection of the interior girder, which would be used to determine the required camber.

Calculate maximum moments and shear in the span (unfactored loads):

Maximum moment due to w_{DC1},

$$M_{DC1} = \frac{w_{DC1}L^2}{8} = \frac{(1.912)(110)^2}{8} = 2891.9 \text{ kip-ft}$$

Maximum moment due to w_{DC2},

$$M_{DC2} = \frac{w_{DC2}L^2}{8} = \frac{(0.168)(110)^2}{8} = 254.1 \text{ kip-ft}$$

Total moment due to dead load = 2891.9 + 254.1 = 3146 kip-ft
Maximum moment due to w_{DW},

$$M_{DW} = \frac{w_{DW}L^2}{8} = \frac{(0.225)(110)^2}{8} = 340.3 \text{ kip-ft}$$

Maximum shear due to dead load w_{DC1},

$$V_{DC1} = \frac{w_{DC1}L}{2} = \frac{1.912(110)}{2} = 105.16 \text{ kip}$$

www.EngineeringEBooksPdf.com

Maximum shear due to dead load w_{DC2},

$$V_{DC2} = \frac{w_{DC2}L}{2} = \frac{0.168(110)}{2} = 9.24 \text{ kip}$$

Maximum shear due to dead load = 105.16 + 9.24 = 114.40 kip
Maximum shear due to w_{DW},

$$V_{DW} = \frac{w_{DW}L}{2} = \frac{0.225 \times (110)}{2} = 12.38 \text{ kip}$$

Maximum Moments Due to Live Load
Moment due to design truck (see Example 3.5, Equation 3.20)
For L = 50 ft (>40.27 ft), the truck load governs over tandem (see Example 3.9).
Due to the design truck,

$$\begin{aligned} M_{truck} &= 18L - 280 + \frac{392}{L} \\ &= 18(110) - 280 + \frac{392}{110} \\ &= 1703.56 \text{ kip-ft} \end{aligned}$$

Dynamic load allowance = 0.33 (design truck load only)

$$M_{truck}(1 + IM) = 1703.56(1 + 0.33) = 2265.7 \text{ kip-ft}$$

Moment due to lane load (see Example 3.6, Chapter 3)

The influence line ordinate is

$$\frac{ab}{L} = \frac{(55 - 2.335)(55 + 2.335)}{110} = 27.45 \text{ ft}$$

$$\begin{aligned} M_{lane} &= (0.64)\left(\frac{1}{2}\right)(L)\left(\frac{ab}{L}\right) \\ &= (0.64)(0.5)(110)(27.45) = 966.2 \text{ kip-ft} \end{aligned}$$

Total moment due to live load,

$$M_{LL+IM} = 2265.7 + 966.2 = 3219.9 \text{ kip-ft}$$

Live load distribution factor would be applied to M_{LL} = 3231.9 kip-ft

Maximum Shear Due to Live Load
Shear due to design truck

The reaction at the left support is obtained from Equation 3.25 for x = 0:

$$V_x = \frac{72}{L}(L - x - 9.33)$$

www.EngineeringEBooksPdf.com

For L = 50 ft (>26 ft), truck load governs over the tandem (see Example 3.12).

Reaction at the left support,

$$R_L = \frac{72}{110}(110 - 0 - 9.33) = 65.89 \text{ kip}$$

Dynamic load allowance = 0.33

$$V_{Truck+IM} = 65.89\ (1 + 0.33) = 87.63 \text{ kip}$$

$$\text{Maximum shear due to lane load} = w_L\left(\frac{L}{2}\right)$$

$$= 0.64\left(\frac{110}{2}\right)$$

$$= 35.20 \text{ kip}$$

Total maximum shear due to live load,

$$V_L = V_{Truck} + V_{Lane} = 87.63 + 35.20 = 122.83 \text{ kip}$$

Live load distribution factor for shear would be applied to V_L = 122.83 kip

Live Load Distribution Factors for the Interior Girder

The superstructure of the bridge conforms to type (k) in LRFD Table 4.6.2.2.1.1 (cast-in-place deck over steel girders). Check the applicability criteria:

$3.5 \le S \le 16.0$	$S = 9.0$ ft, OK
$4.5 \le t_s \le 12.0$	$t_s = 8.0$ in., OK
$20 \le L \le 240$	$L = 110$ ft, OK
$N_b \le 4$	$N_b = 6$, OK
$10{,}000 \le K_g \le 7{,}000{,}000$	
$K_g = n(I + Ae_g^2)$	

where

n = modular ratio

I = moment of inertia of the PCI bulb-T girder

$$n = \frac{E_{c,girder}}{E_{c,deck}} = \sqrt{\frac{f'_{c,girder}}{f'_{c,deck}}} = \sqrt{\frac{6.0 \text{ ksi}}{4.0 \text{ ksi}}} = 1.2247$$

I_g = 545,894 in.^{4}

e_g = girder eccentricity = $y_t + t_h + 0.5t_s$

= 35.4 + 2.0 + 0.5(8.0) = 41.4 in.

K_g = 1.2247 [545,894 + 767(41.4)^2] = 2,278,556 in.^{4}

10,000 ≤ (K_g = 2,278,556) ≤ 7,000,000, OK

Range of applicability is satisfied.

Number of design lanes, N_L

Clear roadway width for design lanes, w

w = Overall bridge width − 2(width of the traffic barrier) − 2(distance between the inside face of curb and the centerline of the exterior wheel of the design truck)

= 51.5 − 2(1.75) − 2(2.0)

= 44.0 ft

www.EngineeringEBooksPdf.com

$$N_L = \frac{w}{12} = \frac{44.0}{12} = 3.67 < 4$$

Use the integer part of 3.67, use $N_L = 3$ design lanes.

Based on clear roadway width of 48 ft, $N_L = 48.0/12 = 4$ lanes. In this example, three design lanes have been chosen for design; the bridge would be restricted to three design lanes.

Live Load Distribution Factor for Bending Moment

Case 1. One Design Lane Loaded

$$g_{mi1} = 0.06 + \left(\frac{S}{14}\right)^{0.4}\left(\frac{S}{L}\right)^{0.3}\left(\frac{K_g}{12.0Lt_s^3}\right)^{0.1}$$

$$= 0.06 + \left(\frac{9.0}{14}\right)^{0.4}\left(\frac{9.0}{110}\right)^{0.3}\left(\frac{2,278,556}{(12.0)(110)(8.0)^3}\right)^{0.1}$$

$$= 0.06 + (0.838)(0.472)(1.129)$$

$$= 0.507$$

Case 2. Two or More Design Lanes Loaded

$$g_{ml2} = 0.075 + \left(\frac{S}{9.5}\right)^{0.6}\left(\frac{S}{L}\right)^{0.2}\left(\frac{K_g}{12.0Lt_s^3}\right)^{0.1}$$

$$= 0.075 + \left(\frac{9.0}{9.5}\right)^{0.6}\left(\frac{9.0}{110}\right)^{0.2}\left(\frac{2,278,556}{(12.0)(110)(8.0)^3}\right)^{0.1}$$

$$= 0.075 + (0.968)(0.606)(1.129)$$

$$= 0.737 > 0.507$$

Therefore, $g_{mi} = 0.737$ governs.

Live Load Distribution Factor for Shear

Check the range of applicability criteria.

The range of applicability criteria for shear for type (k) superstructure is the same as those for the moment checked earlier (except for the term K_g, which is not required). Therefore, the applicability criteria are satisfied.

Case 1. One Design Lane Loaded

$$g_{vi1} = 0.36 + \frac{S}{25.0} = 0.36 + \frac{9.0}{25} = 0.72$$

Case 2. Two or More Design Lanes Loaded

$$g_{vi2} = 0.2 + \frac{S}{12} - \left(\frac{S}{35}\right)^2$$

$$= 0.2 + \left(\frac{9.0}{12}\right) - \left(\frac{9.0}{35}\right)^2$$

$$= 0.884 > 0.72$$

$g_{vi2} = 0.884$ governs

www.EngineeringEBooksPdf.com

Live Load Distribution Factor for Fatigue
Live load distribution factor for bending moment for one design loaded case, $g_{mi1} = 0.507$
Multiple-presence factor = 1.2
Live load distribution factor for fatigue,

$$g_{m,fat} = \frac{g_{mi1}}{m} = \frac{0.507}{1.2} = 0.4225$$

Check for fatigue is not required for prestressed concrete girders except as specified in Art. 5.5.3.1.

Live Load Distribution Factor for Deflection
Live load distribution factor for deflection is the same for interior and exterior girders because it is assumed that all lanes are loaded and all girders deflect equally. For two lanes loaded, the multi-presence factor, $m = 1.0$. Conservatively, three lanes are assumed to occupy the bridge. Therefore, the distribution factor for live load deflection is

$$g_{\Delta} = m\left(\frac{Number\ of\ lanes}{Number\ of\ girders}\right) = 1.0\left(\frac{3}{6}\right) = 0.5$$

Design Loads (Factored Loads)
The following unfactored loads were calculated earlier:

Bending moments

$$M_{DC1} = 2891.9 \text{ kip-ft,}$$

$$M_{DC2} = 254.1 \text{ kip-ft, s}$$

$$M_{DC} = M_{DC1} + M_{DC2} = 2891.9 + 254.1 = 3146 \text{ kip ft}$$

$$M_{DW} = 340.3 \text{ kip-ft}$$

$$M_{(L+IM)} = 3231.9 \text{ kip-ft}$$

Shears

$$V_{DC1} = 105.16 \text{ kip}$$

$$V_{DC2} = 9.24 \text{ kip}$$

$$V_{DC} = V_{DC1} + V_{DC2} = 105.16 + 9.24 = 114.4 \text{ kip}$$

$$V_{DW} = 12.38 \text{ kip}$$

$$V_{L+I} = 122.83 \text{ kip}$$

Apply load factors to unfactored loads to calculate factored loads and live load distribution factors to live load moment and shear.

For bending moment, $g_{mi2} = 0.737$

$$\begin{aligned}\text{Design live load plus impact moment} &= g_{mi}\,(M_{LL+IM})\\ &= (0.737)(3233.7)\\ &= 2383.0 \text{ kip-ft}\end{aligned}$$

For shear, $g_{vi2} = 0.884$

$$\begin{aligned}\text{Design live load plus impact shear} &= g_{vi2}\,(V_{LL+IM})\\ &= (0.884)(122.83)\\ &\approx 109.0 \text{ kip}\end{aligned}$$

www.EngineeringEBooksPdf.com

Load Combinations and Limit States
Loads for Strength I Limit State
Factored Loads: Moments

$$M_u = \Sigma\eta_i\gamma_i M_i$$

$$\eta_i = \eta_D\eta_R\eta_I \text{ (Art. 1.3.2.1)}$$

Select Load Modifiers

Ductility, $\eta_D = 1.0$ (Art. 1.3.3).
Redundancy, $\eta_R = 1.0$ (Art. 1.3.4)
Importance, $\eta_I = 1.0$ (art. 1.3.5)
Therefore, $M_u = \eta\Sigma\gamma_i M_i$

$$M_u = 1.0\ [1.25M_{DC} + 1.5M_{DW} + 1.75(M_{LL+IM})]$$
$$= 1.0\ [1.25(3146.0) + 1.5(340.3) + 1.75(2383.0)]$$
$$= 8613 \text{ kip-ft}$$

Factored Loads: Shear

$$V_u = 1.0\ [1.25V_{DC} + 1.5V_{DW} + 1.75(V_{LL+IM})]$$
$$= 1.0\ [1.25(114.4) + 1.5(12.38) + 1.75(122.83)]$$
$$= 376.5 \text{ kip} \approx 377 \text{ kip}$$

Loads for Service I Limit State

Load factors for this load combination are all equal to 1.0 (LRFD Table 3.4.1-1).
Moments at midspan acting on the noncomposite section = M_{DC1} = 2891.9 ≈ 2892 kip-ft
Moments at midspan acting on the composite section = $M_{DC2} + M_{DW} + M_{LL+IM}$
= 254.1 + 340.3 + 2383.0 = 2977.4 kip-ft

Loads for Service III Limit State
As specified in Art. 3.4.1, this load combination is a special load combination for service limit stress checks that applies "to tension in prestressed concrete superstructures with the objective of crack control and to principal tension in the webs of segmental concrete girders"; the latter provision part does not apply here. The load factors for this load combination are the same as for service I load combination except the load factor is 0.8 for moment due to live load plus impact (LRFD Table 3.4.1-1).

Moments at midspan acting on the noncomposite section = M_{DC1} = 2892 kip-ft
Moments at midspan acting on the composite section = $M_{DC2} + M_{DW} + 0.8M_{LL+IM}$
= 254.1 + 340.3 + 0.8(2383.0)
= 2501 kip-ft

Fatigue Limit States
Art. 5.5.3 specifies that fatigue need not be investigated for concrete deck slabs in multigirder applications. In regions of compressive stress due to permanent loads and prestress in reinforced concrete components, fatigue is to be considered only if this compressive stress is less than the maximum tensile live load stress resulting from the Fatigue I Load Combination as specified in LRFD Table 3.4.1-1. Fatigue of reinforcement need not be checked for fully prestressed components designed to have extreme fiber tensile stress due to Service III Limit State within the tensile stress limit specified in Table 5.A.7 (LRFD Table 5.9.4.2.2-1).

www.EngineeringEBooksPdf.com

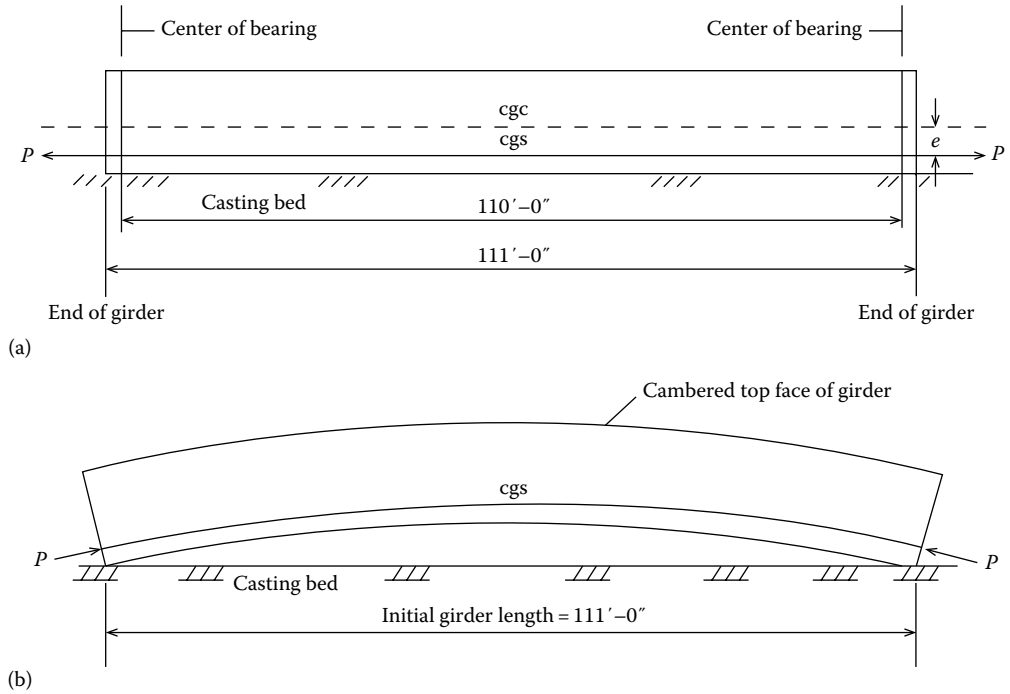

FIGURE 5.110 Prestressing a concrete girder: (a) girder in the casting bed with tendons pulled with a force P at eccentricity e, (b) cambered girder after the prestressing force is released and the beam is compressed.

Moments and Shear due to Dead Loads at Release

This is a special condition that applies to design of prestressed concrete girders. Therefore, moments are computed separately from other moments because the full length of girder of 111.0 ft, rather than the center-to-center distance of 110 ft, is used for moment computations. The reason for using the full girder length (111.0 ft) is that when the girder cambers (deflects upward) during release of prestressing force, its only points of contact (and therefore its support locations) with the prestressing bed would be the ends of the full girder length (111.0 ft). This condition of the girder is shown schematically in Figure 5.110.

Locations of Interest at Release Condition

Transfer point: Art. 5.11.4.1 specifies that the transfer length of a prestressing strand shall be taken as 60 strand diameters and the development length shall be taken as specified in Art. 5.11.4.2.

$$\ell_t = 60d_b = 60(0.5) = 30.0 \text{ in.} = 2.5 \text{ ft}$$

Strand depression point: Strands will be harped or depressed at $0.45L$ (Figure 5.105d).

$$x = 0.45L = 0.45(111.0) = 49.95 \text{ ft}$$

Midspan,

$$x = 0.5L = 0.5(111.0) = 55.5 \text{ ft}$$

Dead weight of the girder = 0.80 kip/ft (computed earlier)

Moments at distance x from the left support of a simply supported beam can be calculated from the following general expression:

$$M_x = \frac{wx}{2}(L - x)$$

www.EngineeringEBooksPdf.com

Due to camber of the beam at release, the dead weight of the girder acts on its overall length of 111.0 ft as it cambers as illustrated in Figure 5.107. Therefore, the midspan moments that were calculated earlier for a span of 110 ft cannot be used for certain calculations.

The initial moment due to the dead load of girder when the girder cambers upon release, L = 111.0 ft,

$$M_x = \frac{0.80x}{2}(111.0 - x) = 44.4x - 0.40x^2$$

Moments at Release at Different Points along the Span

At transfer point, x = 2.5 ft,

$$M_{x=2.5\text{ ft}} = 44.4(2.5) - 0.40(2.5)^2 = 108.5\text{ kip-ft}$$

At depression point, $x = 0.45L$ = 49.95 ft,

$$M_{x=49.95\text{ ft}} = 44.4(49.95) - 0.40(49.95)^2 = 1219.8\text{ kip-ft}$$

At midspan, $x = 0.5L$ = 55.5 ft,

$$M_{x=49.95\text{ ft}} = 44.4(55.5) - 0.40(55.5)^2 = 1232.1\text{ kip-ft}$$

Moments and Shears Acting on the Noncomposite Girder

At midspan

In the final condition, the girder length between centers of bearings = 110.0 ft. In this condition,

$$M_x = \frac{wx}{2}(110.0 - x)$$

$$V_x = w\left(\frac{L}{2} - x\right)$$

Moment due to the self-weight of the girder of w_{gdl} = 0.8 kip/ft (calculated earlier) moment at x = 55.0 ft,

$$M_{x=55\text{ ft}} = \frac{0.80(55.0)}{2}(110.0 - 55.0) = 1210\text{ kip-ft}$$

Moment due to the deck (structural; w = 0.9 kip/ft [calculated earlier]),

$$M_{x=55\text{ ft}} = \frac{0.9(55.0)}{2}(110.0 - 55.0) \approx 1361\text{ kip-ft}$$

Moment due to additional dead load (1/2 in. thick integral wearing surface and haunch) of

$$w = 0.0563 + 0.088 = 0.1443\text{ kip/ft},$$

$$M_{x=55\text{ ft}} = \frac{0.1443(55.0)}{2}(110.0 - 55.0) = 218.3\text{ kip-ft}$$

www.EngineeringEBooksPdf.com

Flexural Design of Girder

Estimation of Required Prestressing Force

The required number of prestressing strands is usually governed by concrete tensile stress at the bottom fibers of the girder due to load combination Service III loads. The tensile stress in the bottom fibers of the girder due to the applied loads using Service III load combination can be calculated as follows (PCI 2003):

$$f_b = \frac{M_g + M_s}{S_b} + \frac{M_b + M_{ws} + 0.80(M_{LL+IM})}{S_{bcg}} \tag{5.120}$$

where

f_b = bottom tensile stress (ksi)
M_g = unfactored bending moment due to the self-weight of the girder
M_s = unfactored bending moment due to the deck slab and haunch weights
M_b = unfactored bending moment due to the barrier weights
$M_{ws} = M_{DW}$ = unfactored bending moment due to the FWS
M_{LL+IM} = unfactored bending moment due to the live load plus impact
S_b = section modulus for the bottom fibers of noncomposite girder
S_{bcg} = section modulus for the bottom fibers of composite girder

All of the aforementioned moment values are given in Table 5.15. The section properties of the girder were mentioned earlier. Therefore,

$$f_b = \frac{(1{,}210 + 1361 + 281.3)(12)}{14{,}915} + \frac{[254.1 + 340.3 + 0.80(2{,}383)](12)}{20{,}902}$$

$$= 2.244 + 1.436 = 3.68 \text{ ksi}$$

TABLE 5.15
Summary of Dead and Live Load Effects

	Moments at Release (kip-ft) L = 111.0 ft		
Component	Transfer pt. (2.5 ft)	0.45L (49.95 ft)	Midspan (55.5 ft)
Girder	108.5	1219.8	1232.1

	Moments and Shears, L = 110.0 ft		
	At the critical section for shear (5.7 ft from the center of support)		Midspan (55.0 ft)
Component	***V* (kip)**[a]	***M* (kip-ft)**[a]	***M* (kip-ft)**
Acting on Noncomposite Girder			
Girder	39.4	237.8	1210.0
Deck (structural)	44.3	267.5	1361.0
Additional			
Noncomposite (incl. haunch)	7.1	42.9	218.3
Subtotal	90.8	548.2	2789.3
Acting on Composite Girder			
Barriers	8.3	49.9	254.1
FWS	11.1	66.9	340.3
Live load + impact	101.0	487.5	2383.0
Subtotal—Service I	120.4	604.3	2977.4
Subtotal —Service III	—	—	2501
Total—Strength I	317.3	1701.1	8613

[a] Detailed calculations for these values are provided later in the chapter; see *Design for Shear*.

www.EngineeringEBooksPdf.com

Stress limits for tensile loads at service loads (LRFD Table 5.9.4.1.2-1)

$$f_t = 0.24\sqrt{f'_{ci}} = 0.24\sqrt{5.5} = -0.563 \text{ ksi}$$

The required precompressive stress, f_{pb}, at the bottom fibers of the girder is the difference between the bottom tensile stress due to the applied loads and the allowable tensile stress:

$$f_{pb} = 3.68 - 0.563 = 3.117 \text{ ksi}$$

Location of the c.g. of prestressing force is assumed to be approximately 5–15 percent of the girder depth, measured from the bottom of the beam. A value of 5 percent is appropriate for newer efficient girder sections (such as the bulb-T girder used in this example) (PCI 2003).

$$0.05h = 0.05(72.0) = 3.6 \text{ in.}$$

$$\text{Eccentricity at midspan, } e_c = y_b - y_{bs} = 36.6 - 3.6 = 33.0 \text{ in.}$$

The stress at the bottom of the girder due to the effective prestressing force, P_{pe}, can be calculated as follows:

$$f_{pb} = \frac{P_{pe}}{A} + \frac{P_{pe}e_c}{S_b} \tag{5.121}$$

$$3.117 = \frac{P_{pe}}{767} + \frac{P_{pe}(33.0)}{14{,}915}$$

The solution of the aforementioned equation is P_{pe} = 886.4 kip

$$\text{Final prestress force per strand} = (\text{area of strand})(f_{pi})(1 - \text{losses, percent})$$

where f_{pi} = initial prestressing stress = $0.75f_{pu}$ = 0.75(270) = 202.5 ksi.

Assuming a final prestress loss of 25 percent,

$$\text{Final prestress force per strand} = (0.153)(202.5)(1 - 0.25) = 23.2 \text{ ksi}$$

$$\text{No. of strands required} = \frac{P_{pe}}{23.2} = \frac{886.4}{23.2} = 38.2 \text{ strands, say 39 strands}$$

Add 5 percent extra number of strands due to uncertainties in the location of the centroid of the prestressing force and the loss of prestress.

$$\text{Number of strands} = 39(1.05) = 41 \text{ strands}$$

The number of strands needs to be even for the specific cross section of bulb-T girder and the strand pattern to be used. Use 42 strands.

$$A_{ps} = 42(0.153) = 6.426 \text{ in.}^2$$

Strand Pattern

Now that 42 strands have been selected, they need to be arranged in the girder cross section. All 42 strands are arranged in the bottom flange of the bulb-T girder in the midspan section.

The strands will be arranged in a grid pattern of 2 in. both horizontally and vertically in the girder cross section as shown in Figure 5.111. The strands in each row have been arranged in such

www.EngineeringEBooksPdf.com

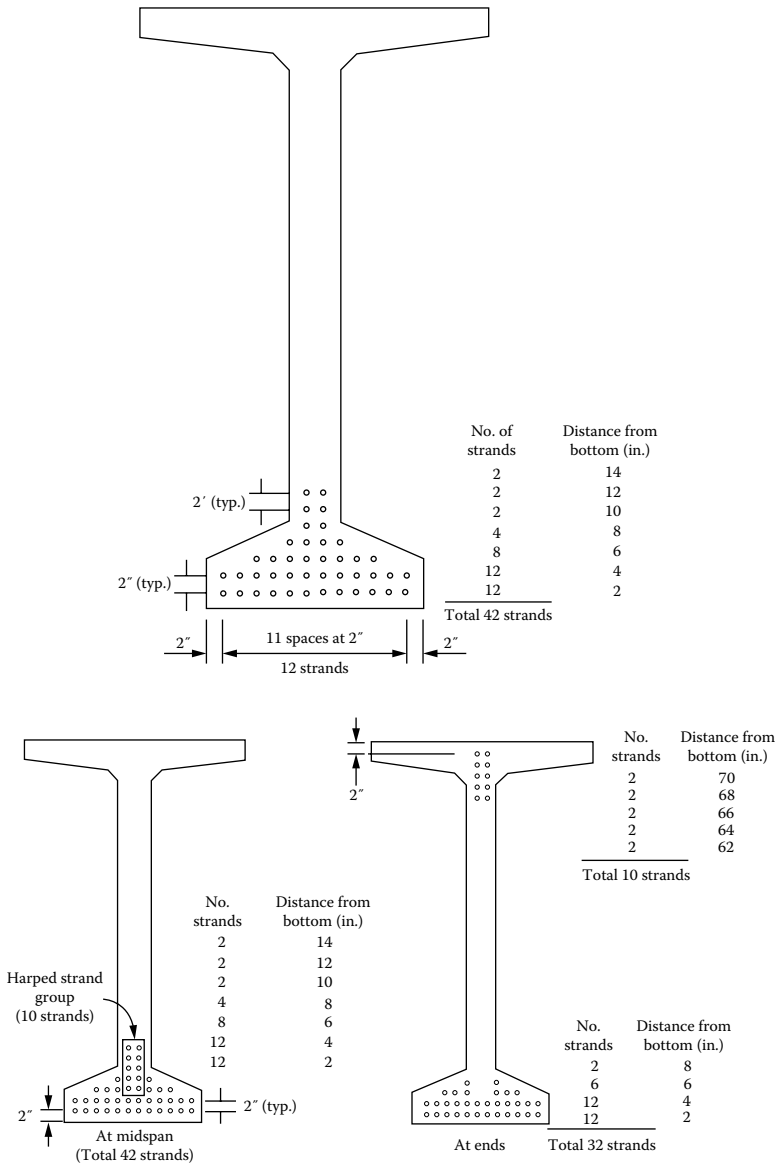

FIGURE 5.111 Strand pattern and profile in the girder. (Adapted from PCI, *Precast Prestressed Concrete Bridge Design Manual*, 1st ed., Precast/Prestressed Concrete Institute, Chicago, IL, 2003.)

a manner that adequate cover is provided to all strands in every row. The web of the girder is only 6 in. wide, which permits only two vertical columns of strands.

The strand pattern is different at the midspan and at the ends. At the midspan, all 42 strands are placed in the bottom flange of the girder so as to provide maximum eccentricity of the prestressing force at the midspan. Of the 42 strands, the top 10 strands are depressed (harped) at $0.45L$ (L = 111.0 ft) from each end of the girder so as to reduce the eccentricity of the prestressing force at the ends. The strand pattern and the profile of harped strands along the span are shown in Figure 5.111.

The c.g. of the bottommost row of strands will be placed at 2 in. above the bottom of the beam. With No. 4 stirrups, the clear cover at the bottom will be

$$\text{Cover} = 2 - \text{diameter of No. 4 stirrup} - 1/2(\text{diameter of strand}) = 2 - 0.5 - 0.5(0.5) = 1.25 \text{ in.}$$

www.EngineeringEBooksPdf.com

Compute the c.g. of prestressing strands. For the following computations, all c.g. dimensions are measured from the bottom of the girder.

At Midspan (and between Depression Points)
Depression point location,

$$0.45L = 0.45(110 \text{ ft}) = 49.5 \text{ ft from the center line of bearing} = 55.5 \text{ ft from end of girder}$$

c.g. at midspan,

$$\bar{y}_m = \frac{1}{42}[(12)(2 \text{ in.}) + (12)(4 \text{ in.}) + (8)(6 \text{ in.}) + (4)(8 \text{ in.}) + (2)(10 \text{ in.}) + (2)(12 \text{ in.}) + (2)(14 \text{ in.})]$$

$$= 5.33 \text{ in.}$$

$$\text{Eccentricity at midspan, } e_m = \text{cgc} - \bar{y}_m = 36.60 - 5.33 = 31.27 \text{ in.}$$

At End of Girder
At the end section of the beam, the group of prestressing strands consists of two subgroups: (1) 32 straight strands and (2) 10 harped strands. Calculate the c.g. of strands at the end.

c.g.s. at the end,

$$\bar{y}_{end} = \frac{1}{42}[(12)(2 \text{ in.}) + (12)(4 \text{ in.}) + (6)(6 \text{ in.}) + (2)(8 \text{ in.}) + (2)(62 \text{ in.}) + (2)(64 \text{ in.})$$
$$+ (2)(66 \text{ in.}) + (2)(68 \text{ in.}) + (2)(70 \text{ in.}) = 18.67 \text{ in.}$$

Alternatively, the cgs of strands at the ends can be computed by calculating separately the cgs of the bottom 32 straight strands and the 10 harped strands at the top, and then calculate the cgs of the two groups.

cgs of the bottom 32 straight strands (distances are measured from the bottom of girder),

$$cgs_{32\,bot\,str} = \frac{1}{32}\left[12(2.0) + 12(4.0) + 6(6.0) + 2(8.0)\right]$$
$$= 3.875 \text{ in.}$$

cgs of the top 10 straight strands (distances are measured from the top of girder),

$$cgs_{10\,top\,str} = \frac{1}{10}\left[2(2.0) + 2(4.0) + 2(6.0) + 2(8.0) + 2(10.0)\right]$$
$$= 6.0 \text{ in.}$$

The cgs of the 42 strands (32 straight plus 10 harped) at the end as measured from the bottom of the girder is computed to be

$$cgs_{end} = \frac{1}{42}\left[32(3.875) + 10(72 - 6)\right] = 18.67 \text{ in. (same as before)}$$

The aforementioned distances are shown in Figure 5.112.

Eccentricity at the end,

$$e_{end} = \text{cgc} - \bar{y}_{end} = 36.60 - 18.67 = 17.93 \text{ in.}$$

www.EngineeringEBooksPdf.com

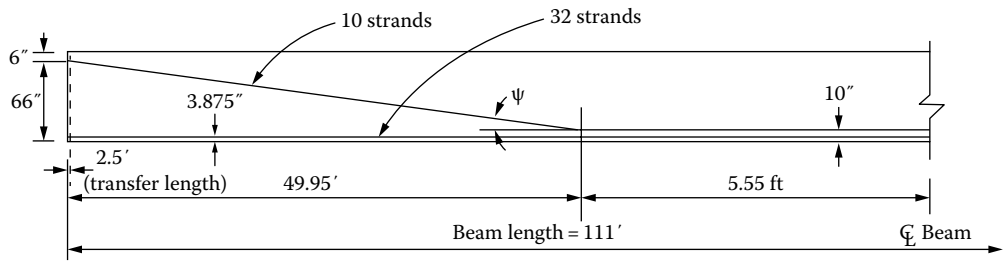

FIGURE 5.112 Location of c.g. of strands at midspan and at ends. (Adapted from PCI, *Precast Prestressed Concrete Bridge Design Manual*, 1st ed., Precast/Prestressed Concrete Institute, Chicago, IL, 2003.)

cgs at transfer length, ℓ_t, from end of member,

$$\ell_t = 60d_b = 60\ (0.5\ \text{in.}) = 30\ \text{in.} = 2.5\ \text{ft (Arts. 5.8.2.3, 5.11.4.1)}$$

Calculate the cgs of strands at transfer point:

cgs of 10 harped strands at depression point (distances are measured from the bottom),

$$cgs_{10\,harped\,str} = \frac{1}{10}\left[2(6.0)+2(8.0)+2(10.0)+2(12.0)+2(14.0)\right] = 10.0\ \text{in.}$$

c.g. of strand pattern at end = 18.67 in.

c.g. of 10 harped strands at harp point = 10.00 in.

Calculate the c.g. of strands at the transfer point by interpolation (Figure 5.113).

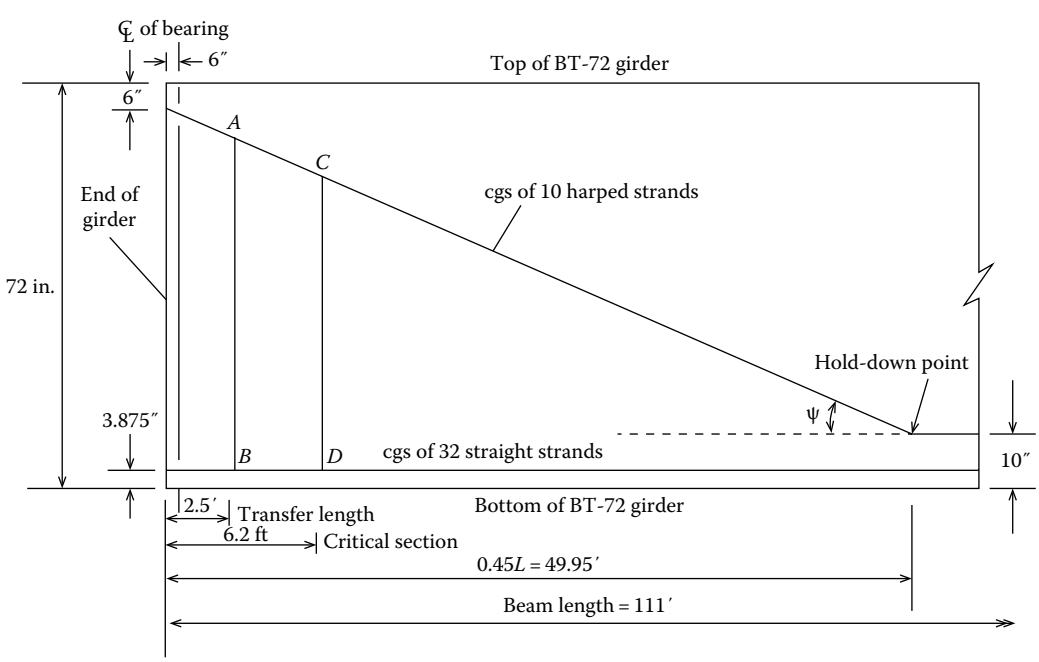

FIGURE 5.113 Calculation of the c.g. of strands at the transfer point and at the critical section.

www.EngineeringEBooksPdf.com

From similar triangles,

$$\frac{AB}{49.95-2.5}=\frac{18.67-10}{49.95}$$

$$AB = 8.236 \text{ in.} \approx 8.24 \text{ in}$$

cgs of strands at transfer point = 8.24 + 10.0 = 18.24 in. from the bottom of the girder
cgs at the critical section: 6.2 ft from the end. (Calculation for location of critical section shown later in the chapter under *Design for Shear*.)

From similar triangles (Figure 5.113),

$$\frac{CD}{49.95-6.2}=\frac{18.67-10}{49.95}$$

$$CD = 7.59 \text{ in.}$$

cgs at the critical section = 7.59 + 10.0 = 17.59 in.

The angle of inclination of the cgs of the 10 draped strands with horizontal, ψ, is computed to be

$$\psi=\tan^{-1}\left(\frac{72-10-6}{49.95(12)}\right)=5.34°$$

Calculation of Prestress Losses (Art. 5.9.5.1)
In lieu of more detailed analysis, prestress losses in members constructed and prestressed in a single stage, relative to the stress immediately before transfer, may be determined for pretensioned members as follows:

$$\Delta f_{pT} = \Delta f_{pES} + \Delta f_{pLT} \qquad (5.122)\ [A5.9.5.1\text{-}1]$$

where
Δf_{pT} = total loss (ksi)
Δf_{pES} = sum of all losses or gain due to elastic shortening or extension at the time of application of prestress and/or external loads (ksi)
Δf_{pLT} = losses due to long-term shrinkage and creep of concrete and relaxation of the steel (ksi)

Elastic Shortening (Art. 5.9.5.2.3)
The loss of prestress due to elastic shortening, Δf_{pES}, shall be determined as follows:

$$\Delta f_{pEs} = \frac{E_p}{E_{ct}} f_{cgp} \qquad (5.123)\ [A5.9.5.2.3a\text{-}1]$$

where
f_{cgp} = the concrete stress at the c.g. of prestressing tendons due to prestressing force immediately after transfer and the self-weight of the member at the section of maximum moment (ksi)
E_p = modulus of elasticity of prestressing steel (ksi)
E_{ct} = modulus of elasticity of concrete at transfer or at the time of load application (ksi)

The total elastic loss or gain may be taken as the sum of the effects of prestress and applied loads.

www.EngineeringEBooksPdf.com

Alternatively, as specified in Art. C5.9.5.3a, the loss of prestress due to elastic shortening, Δf_{pES}, may be determined as follows:

$$\Delta f_{pES} = \frac{A_{ps} f_{pbt}(I_g + e_m^2 A_g) - e_m M_g A_g}{A_{ps}(I_g + e_m^2 A_g) + \dfrac{A_g I_g E_{ci}}{E_{ps}}} \qquad (5.124)\ [\text{AC5.9.5.2.3a-1}]$$

where

E_{ci} = modulus of elasticity of concrete at transfer = $33{,}000 w_c^{1.5}\sqrt{f'_{ci}} = 33{,}000(0.150\,\text{kcf})^{1.5}\sqrt{5.5\,\text{ksi}}$ = 4,496 ksi (A 5.4.2.4-1)
E_{ps} = modulus of elasticity of prestressing steel = 28,500 ksi (Art. 5.4.4.2)
A_{ps} = area of prestressing steel = 6.426 in.^{2}
f_{pbt} = stress in prestressing immediately before transfer = $0.75 f_{pu}$ = 0.75(270) = 202.5 ksi (LRFD Table 5.9.3-1)
e_m = average prestressing steel eccentricity at midspan (in.) = 31.27 in.
M_g = midspan moment due to member self-weight = 1210 (12) = 14,520 kip-in. (Table 5.15)

Therefore,

$$\Delta f_{pes} = \frac{6.426(202.5)\left[545{,}894 + (31.27)^2(767) - 31.27(14{,}520)(767)\right]}{6.426\left[545{,}894 + (31.27)^2(767) + \dfrac{(767)(545{,}894)(4496)}{28{,}500}\right]} = 17.99\ \text{ksi}$$

(**Note:** Δf_{pes} = 17.99/(0.75 × 270) = 8.9 percent of initial prestressing force.)

Approximate Estimate of Time-Dependent Losses (Art. 5.9.5.3)

For precast, pretensioned members, the long-term loss of prestress due to creep, shrinkage of concrete, and relaxation of steel, Δf_{pT}, may be estimated from Equation 5.125 provided the following conditions are satisfied:

1. Members are made from normal-weight concrete.
2. The concrete is either steam or moist cured.
3. Pretensioning is by the bars or strands with normal and low-relaxation properties.
4. Average exposure conditions and temperatures characterize the site.

$$\Delta f_{pLT} = 10.0(f_{pi} A_{ps}/A_g)\gamma_h \gamma_{st} + 12.0\gamma_h \gamma_{st} + \Delta f_{pR} \qquad (5.125)\ [\text{A5.9.5.3-1}]$$

where

γ_h = correction factor for relative humidity of the ambient air = $1.7 - 0.01H$ = 1.7 − 0.01(75) = 0.95 (H = average annual ambient relative humidity, percent)
γ_{st} = correction factor for specified concrete strength at time of prestress transfer to concrete member = $5/(1 + f'_{ci})$ = 5/(1 + 5.5) = 0.77
f_{pi} = prestressing steel stress immediately prior to transfer = 202.5 ksi
Δf_{pR} = estimate of relaxation loss = 2.4 ksi for low-relaxation strands

Therefore,

$$\Delta f_{pLT} = \frac{10.0(202.5)(6.426)}{767}\left[(0.95)(0.77)\right] + 12(0.95)(0.77) + 2.4$$
$$= 23.59\ \text{ksi}$$

(**Note**: Δf_{pLT} = 23.59/(0.75 × 270) = 11.70 percent of initial prestressing force.)

www.EngineeringEBooksPdf.com

Refined Estimates of Time-Dependent Losses (Art. 5.9.5.4)

Art. 5.9.5.4 provides elaborate equations (refined estimates) for estimating various components of time-dependent prestress losses such as those due to shrinkage of girder and deck concrete, due to creep of prestress force and external loads applied at different times. Equation 5.126 can be used to calculate the long-term loss of prestress, Δf_{pLT}, due to various causes:

$$\Delta f_{pLT} = \left(\Delta f_{pSR} + \Delta f_{pCR} + \Delta f_{pPR1}\right)_{id} + \left(\Delta f_{pSD} + \Delta f_{pCD} + \Delta f_{pPR2} - \Delta f_{pSS}\right)_{df} \qquad (5.126)\ [A5.9.5.4.1]$$

Refer to Art. 5.9.5.4.1 for definitions of various terms in Equation 5.126.

Equation 5.126 has not been used in this example. It has been found that the total long-term loss calculated by the approximate method is quite close to the one calculated using the refined method (Equation 5.126). In view of its simplicity, the approximate loss of prestress will be used in the remainder of this example. Readers are encouraged to refer to Art. 5.9.5.4 and Art. C5.9.5.4 for the details of the refined method.

Prestress Loss and Effective Prestress at Release

Compute initial prestress loss:

$$\Delta f_{pi} = \Delta f_{pES}$$

$$\Delta f_{pi} = 17.99 \text{ ksi (calculated earlier)}$$

Compute effective stress and force after losses:

$$f_{pi} = 202.5 - 17.99 = 184.51 \text{ ksi}$$

$$P_i = (A_{ps})\,(f_{pi}) = (6.426 \text{ in.}^2)\,(184.51 \text{ ksi}) = 1186 \text{ kip}$$

Prestress Loss and Effective Prestress After All Losses (Final)

Calculate the final prestress loss:

$$\Delta f_{pT} = \Delta f_{pES} + \Delta f_{pLT} \qquad (5.127)\ [A5.9.5.1\text{-}1]$$

$$\Delta f_{pT} = 17.99 + 23.69 = 41.68 \text{ ksi}$$

$$\left(\Delta f_{pT} \text{ as percentage of } f_{pj} = \frac{41.58}{0.75(270)} = 0.2053 \text{ or } 20.53 \text{ percent}\right)$$

Compute effective stress and force after losses:

$$f_{pe} = 202.5 - 41.58 = 160.92 \text{ ksi}$$

$$P_e = (A_{ps})\,(f_{pe}) = (6.426 \text{ in.}^2)\,(160.92 \text{ ksi}) = 1034 \text{ kip}$$

Check Effective Stress: Art. 5.9.3

The tendon stress due to prestressed or at service load shall not exceed the values given in LRFD Table 5.9.3-1.

Calculate gain in prestressing steel due to deck weight (g_{dw}), superimposed dead load (g_{sdl}), and 0.8 times the live load with impact ($g_{0.8LL+IM}$).

For $f'_c = 6.0$ ksi, $E_c = 4696$ ksi (calculated earlier).

$$n_{ps\ girder\ concrete} = \frac{E_p}{E_c} = \frac{28{,}500}{4{,}696} = 6.07$$

$$S_{cgPS} = \frac{545{,}894}{31.27} = 17{,}457 \text{ in.}^3$$

www.EngineeringEBooksPdf.com

$$S_{comp\,cgPS} = \frac{1{,}179{,}484}{(56.43 - 5.33 = 51.1)} = 23{,}082 \text{ in.}^3$$

$$g_{dw} = \frac{M_{deck\,weight}}{S_{cg\,PS}}\left(n_{ps\,girder\,concrete}\right)$$

$$= \frac{(1{,}361 + 218.3)(12)}{17{,}457}(6.07) = 6.59 \text{ ksi}$$

$$g_{sdl} = \frac{(254.1 + 340.3)(12)}{23{,}082}(6.07) = 1.88 \text{ ksi}$$

$$g_{0.8(LL+IM)} = \frac{0.8(2{,}383)(12)}{23{,}082}(6.07) = 6.02 \text{ ksi}$$

Total gain in prestress = 6.59 + 1.88 + 6.02 = 14.49 ksi

Stress in prestressing steel due to prestress after all losses should be limited to $0.8f_{py}$ (LRFD Table 5.9.3-1).

$$f_{pe} = 160.92 + 14.49 = 175.41 \text{ ksi}$$

$$0.8f_{py} = (0.8)\,(0.9)(270) = 194.4 \text{ ksi}$$

$$174.41 \text{ ksi} < 0.8f_{py} = 194.4 \text{ ksi, OK}$$

At midspan
Concrete Stresses due to Loads
All moment values are taken from Table 5.15.
Sign convention for stresses: (+) = compression
(–) = tension

Girder Dead Load—At Release with L = 111.0 ft
Use section properties of noncomposite girder.

$$f_t = \frac{M_{sw}}{S_t} = \frac{1{,}232.1(12)}{15{,}421} = 0.959 \text{ ksi}$$

$$f_b = \frac{1{,}232.1(12)}{14{,}915} = -0.991 \text{ ksi}$$

Girder Dead Load—Final with L = 110 ft

$$f_t = \frac{M_{sw}}{S_t} = \frac{1{,}210(12)}{15{,}421} = 0.942 \text{ ksi}$$

$$f_b = \frac{M_{sw}}{S_b} = \frac{1{,}210(12)}{14{,}915} = -0.974 \text{ ksi}$$

Deck (Structural) Dead Load

$$f_t = \frac{M_{sw}}{S_t} = \frac{1{,}361(12)}{15{,}421} = 1.059 \text{ ksi}$$

$$f_b = \frac{M_{sw}}{S_t} = \frac{1{,}361(12)}{14{,}915} = -1.095 \text{ ksi}$$

www.EngineeringEBooksPdf.com

Additional Noncomposite Dead Load (Nonstructural Deck)

$$f_t = \frac{218.3(12)}{15,421} = 0.170 \text{ ksi}$$

$$f_b = \frac{218.3(12)}{14,915} = -0.176 \text{ ksi}$$

Composite Dead Load: Barriers + FWS

Use section properties of composite girder.

$$f_t = \frac{(254.1+340.3)(12)}{75,754} = 0.094 \text{ ksi}$$

$$f_b = \frac{(254.1+340.3)(12)}{20,902} = -0.341 \text{ ksi}$$

Stress at the top of deck,

$$f_{td} = \frac{(254.1+340.3)(12)}{56,494} = 0.126 \text{ ksi}$$

Stresses due to Live Load I: M_{LL+IM}

Stress at the top of the girder,

$$f_t = \frac{2,383(12)}{75,754} = 0.377 \text{ ksi}$$

Stress at the top of deck,

$$f_{td} = \frac{2,383(12)}{56,494} = 0.506 \text{ ksi}$$

Stresses due to Live Load III: $0.8M_{LL+IM}$

Stress at the bottom of the girder,

$$f_{bg} = \frac{0.8(2,383)(12)}{20,902} = -1.094 \text{ ksi}$$

Concrete Stresses Due to Prestress

At release, use section properties of noncomposite girder.

At bottom,

$$f_b = P_i\left[\frac{1}{A} + \frac{e_{CL}}{S_b}\right] = 1,186\left[\frac{1}{767} + \frac{31.27}{14,915}\right] = 4.03 \text{ ksi}$$

At top,

$$f_t = P_i\left[\frac{1}{A} - \frac{e_{CL}}{S_t}\right] = 1,186\left[\frac{1}{767} - \frac{31.27}{15,421}\right] = -0.859 \text{ ksi}$$

www.EngineeringEBooksPdf.com

Stresses after All Losses (Final)
At bottom,

$$f_b = P_e\left[\frac{1}{A} + \frac{e_{CL}}{S_b}\right] = 1{,}034\left[\frac{1}{767} + \frac{31.27}{14{,}915}\right] = 3.516 \text{ ksi}$$

At top,

$$f_t = P_e\left[\frac{1}{A} - \frac{e_{CL}}{S_t}\right] = 1{,}034\left[\frac{1}{767} - \frac{31.27}{15{,}421}\right] = -0.749 \text{ ksi}$$

Concrete Stresses at Service Limit State—Before Losses (at Release)
Note: Stresses at depression point will be more critical at release.
Service I
Bottom of Girder (Compressive Stress)

$$f_b = 4.03 - 0.991 = 3.039 \text{ ksi}$$

Check limiting compressive stress: Art. 5.9.4.1.1

$$\text{Limiting compressive stress} = 0.6\, f'_{ci} = 0.6(5.5) = 3.30 \text{ ksi}$$

$$3.039 \text{ ksi} < 0.6\, f'_{ci} = 3.30 \text{ ksi, OK}$$

Top of Girder (Tensile Stress)

$$f_t = -0.859 + 0.959 = 0.100 \text{ ksi}$$

Check limiting stress, without bonded auxiliary reinforcement: Art. 5.9.4.2.1, LRFD Table 5.9.4.1.2-1.

In areas other than prestressed tensile zone and without bonded reinforcement, the stress limit is

$$0.0948\sqrt{f'_{ci}} \le 0.2 \text{ ksi}$$

$$0.0948\sqrt{f'_{ci}} = 0.0948\sqrt{5.5} = 0.222 \text{ ksi} > 0.2 \text{ ksi}$$

Therefore, limiting stress = 0.2 ksi governs.

$$f_t = 0.100 \text{ ksi} < 0.20 \text{ ksi, OK}$$

Concrete Stresses at Service Limit States—After All Losses (Final)

1. Service III (tensile stress in bottom of girder)

$$f_b = 3.516 - 0.974 - 1.095 - 0.176 - 0.341 - 1.094 = -0.164 \text{ ksi}$$

PS Girder Deck Addnl. Deck Barrier + FWS LL + I

www.EngineeringEBooksPdf.com

Check limiting stress tensile stress: $-0.190\sqrt{f'_c} = -0.190\sqrt{6.0} = -0.465$ ksi

$$-0.164 \text{ ksi} < -0.465 \text{ ksi, OK}$$

2. Service I (compressive stress in top of girder; Art. 5.9.4.2.1)
   a. Compressive stress due to the sum of effective prestress and permanent loads,

$$f_t = -0.749 + 0.942 + 1.059 + 0.170 + 0.094 = 1.516 \text{ ksi}$$

PS Girder Deck Addnl. Deck Barrier + FWS

Check limiting stress: LRFD Table 5.9.4.2.1-1

$$1.516 \text{ ksi} < 0.45\sqrt{f'_c} = 0.45\sqrt{6.0} = 2.7 \text{ ksi, OK}$$

   b. Compressive stress due to the sum of effective prestress, permanent loads, and transient loads (full service load),

$$f_t = -0.748 + 0.942 + 1.059 + 0.066 + 0.094 + 0.377 = 1.893 \text{ ksi}$$

PS Girder Deck Addnl. Deck Barrier + FWS LL + IM

Check limiting stress: LRFD Table 5.9.4.2.1-1

$$1.893 \text{ ksi} < 0.60\phi_w f'_c = 0.60(1.0)(6.00) = 3.60 \text{ ksi, OK}$$

In the aforementioned calculation, the value of the reduction factor, ϕ_w, has taken equal to 1.0 for the top flange of girder with composite deck, as permitted for span/thickness ratio of flange less than 15 (Arts. 5.9.4.2.1, 5.7.4.7.2). For the selected cross section of the superstructure, the span-to-thickness ratio for the deck between the tips of the top flanges of the girder is

$$\frac{span}{thickness} = \frac{(9.0 - 3.5)(12)}{8} = 8.25 < 15$$

Service I (Compressive Stress in Top of Deck): Art. 5.9.4.2.1

a. Compressive stress due to the sum of effective prestress and permanent loads,

$$f_t = 0.126 \text{ ksi}$$

Check limiting stress:

$$0.126 \text{ ksi} < 0.45 f'_{cd} = 0.45(4.0) = 1.80 \text{ ksi, OK}$$

b. Compressive stress due to the sum of effective prestress, permanent loads, and transient loads (full service load),

$$f_t = 0.126 + 0.506 = 0.632 \text{ ksi}$$

Check limiting stress:

$$0.632 \text{ ksi} < 0.60\phi_w f'_{cd} = 0.60(1.0)(4.0) = 2.40 \text{ ksi, OK}$$

where $\phi_w = 1.0$ for deck between tips of girder flanges as discussed earlier.

www.EngineeringEBooksPdf.com

Strength Limit State (Strength I)

Calculate the nominal moment capacity, M_n:

First, verify if the section behaves as a rectangular beam or a T-beam. The depth of neutral axis, c, is given by Equation 5.33:

For rectangular section behavior,

$$c = \frac{A_{ps}f_{pu} + A_s f_s - A'_s f'_s}{0.85 f'_c \beta_1 b + k A_{ps} \dfrac{f_{pu}}{d_p}} \qquad (5.33)\ [A5.7.3.1.1\text{-}4]$$

Since the girder does not have any nonprestressed steel and compression steel, Equation 5.33 simplifies to the following equation:

$$c = \frac{A_{ps}f_{pu}}{0.85 f'_c \beta_1 b + k A_{ps}\left(f_{pu}/d_p\right)}$$

where the value of k is given as follows:

$$k = 2\left(1.04 - \frac{f_{py}}{f_{pu}}\right)$$

$$= 2\left(1.04 - \frac{243}{270}\right) = 0.28 \qquad (5.31)$$

Alternatively, the value of k can be obtained from Table 5.9.

$$d_p = h_c + h_h + h_f - \text{cgs at midspan}$$

$$= 72.0 + 2.0 + 8.0 - 5.33 = 76.67 \text{ in.}$$

$$c = \frac{6.426(270.0)}{0.85(4.0)(0.85)(108) + 0.28(6.426)\dfrac{270}{76.67}} = 5.45 \text{ in.}$$

Compute depth of compression block, a:

$$a = \beta_1 c$$

where $\beta_1 = 0.85$ for $\sqrt{f'_c} \leq 4.0$ ksi

$a = \beta_1 c = 0.85(5.45) = 4.63$ in.

Because $a = 4.63$ in. < thickness of the flange, 8 in., the compression block lies in the flange; hence, the rectangular behavior of the girder is confirmed.

Compute the average stress in prestressing strand at strength limit state:

$$f_{ps} = f_{pu}\left(1 - k\frac{c}{d_p}\right) = 270\left(1 - 0.28\left(\frac{5.45}{76.67}\right)\right) = 264.63 \text{ ksi}$$

($k = 0.28$ was calculated earlier)

Compute nominal moment capacity, M_n:

$$M_n = A_{ps}f_{ps}\left(d_p - \frac{a}{2}\right) \qquad (5.128)\ [A5.7.3.2.2\text{-}1]$$

$$M_n = 6.426(264.63)\left(76.67 - \frac{4.63}{2}\right) = 126{,}442 \text{ kip-in.} = 10{,}537 \text{ kip-ft}$$

www.EngineeringEBooksPdf.com

Calculate the factored flexural resistance of the section, M_r. Verify if the section is tension controlled. The tensile strain, ε_t, in the bottom row of prestressing strands is given as follows (see Figure 5.39):

$$\varepsilon_t = \left(\frac{d_t - c}{c}\right)\varepsilon_c \tag{5.129}$$

$dt = h_c + h_h + h_f$ – distance of the c.g. of bottom row of strands

$= 72 + 2 + 8 - 2 = 80$ in.

$$\varepsilon_t = \left(\frac{80 - 5.45}{5.45}\right)(0.003) = 0.041 \geq 0.005$$

Hence, the section is tension controlled, and $\phi = 1.0$ for flexure (Art. 5.5.4.2).

$M_r = \phi M_n = (1.0)(10{,}537) = 10{,}537$ kip-ft $> M_u = 8{,}613$ kip-ft (Table 5.15), OK

Reinforcement Limits: Art. 5.7.3.3

1. Maximum reinforcement: No limits specified (Art. 5.7.3.3-1).
2. Minimum reinforcement limits (Art. 5.7.3.3-2)

It is required that

$$M_r = lesser\,of \begin{cases} M_r \\ 1.33M_u \end{cases}$$

Calculate M_{cr} as

$$M_{cr} = \gamma_3\left[\left(\gamma_1 f_r + \gamma_2 f_{cpe}\right)S_c - M_{dnc}\left(\frac{S_c}{S_{nc}} - 1\right)\right] \qquad (5.41)\ [A5.7.3.3.2\text{-}1]$$

where

f_r = modulus of rupture specified in Art. 5.4.2.6

f_{cpe} = compressive stress in concrete due to effective prestress forces only (allowance for all prestress losses) at the extreme fiber of the section where tensile stress is caused by externally applied loads (ksi)

= 0 for sections with nonprestressed reinforcement only

M_{dnc} = total unfactored dead load moment acting on the monolithic or noncomposite section where tensile stress is caused by externally applied loads (ksi)

S_c = section modulus for the extreme fiber of the composite section where tensile stress is caused by externally applied loads (in.^{3})

= S_{nc} where beams are designed for the monolithic or noncomposite section to resist all loads

S_{nc} = section modulus for the extreme fiber of the monolithic or noncomposite section where tensile tress is caused by externally applied loads (in.^{3})

γ_1 = flexural cracking variability factor

γ_2 = prestress variability factor

γ_3 = ratio of specified minimum yield strength to ultimate tensile of the reinforcement

www.EngineeringEBooksPdf.com

For the present case,

γ_1 = 1.6 for all other concrete structures
γ_2 = 1.1 for bonded tendons
γ_3 = 1.0 for prestressed concrete structures
$f_r = 0.24\sqrt{f'_c} = 0.24\sqrt{6.0} = 0.588$ ksi
f_{cpe} = compressive stress in concrete due to effective stress forces only (allowance for all prestress losses) at the extreme fiber of the section where tensile stress is caused by externally applied loads
= 3.516 ksi (computed earlier)
M_{dnc} = the noncomposite dead load moment
= 1210 + 1361 + 218.3 = 2789.3 kip-ft (from Table 5.15)
$S_c = S_{bcg}$ = composite section modulus for the tension face = 20,902 in.^{3}
S_{nc} = noncomposite for the tension face = 14,915 in.^{3}

$$M_{cr} = 1.0\left[(1.6\times 0.588 + 1.1\times 3.516)(20{,}902)\left(\frac{1}{12}\right) - 2{,}789.3\left(\frac{20{,}902}{14{,}915} - 1\right)\right]$$
$$= 7{,}256 \text{ kip-ft}$$

$$1.33M_u = 1.33\ (8{,}537) = 11{,}455 \text{ kip-ft} > M_{cr} = 7{,}256 \text{ kip-ft}$$

Therefore, M_{cr} = 7,256 kip-ft governs.

$$M_r = 10{,}537 \text{ kip-ft} > M_{cr} = 7{,}256 \text{ kip-ft, OK}$$

End and Transfer Point at Release

Stresses only need to be checked at release at this location because losses with time will reduce the concrete stresses, making them less critical.

Use noncomposite section properties of the girder section.

From Table 5.15, moment at transfer point due to the self-weight of the girder, M_{sw}, is 108.5 kip-ft.

$$f_t = \frac{M_{sw}}{s_t} = \frac{108.5(12)}{15{,}421} = 0.084 \text{ ksi}$$

$$f_b = \frac{M_{sw}}{s_t} = \frac{108.5(12)}{14{,}915} = 0.087 \text{ ksi}$$

Stresses due to prestress at transfer point:

Stress at bottom,

$$f_b = P_i\left[\frac{1}{A} + \frac{e_{tr}}{S_b}\right] = 1{,}186\left[\frac{1}{767} + \frac{18.0}{14{,}915}\right] = 2.978 \text{ ksi}$$

Stress at top,

$$f_t = P_i\left[\frac{1}{A} - \frac{e_{tr}}{S_t}\right] = 1{,}186\left[\frac{1}{767} - \frac{18.0}{15{,}421}\right] = 0.162 \text{ ksi}$$

www.EngineeringEBooksPdf.com

Check concrete stresses at Service I limit state before losses (at release):

1. Bottom of girder (compressive stress)

$$f_b = 2.978 - 0.087 = 2.891 \text{ ksi}$$

Check stress limit (Art. 5.9.4.1.1)
Compressive stress limit in pretensioned or posttensioned members = 0.60 f'_{ci} = 0.60(5.5) = 3.30 ksi

$$2.891 \text{ ksi} < 3.30 \text{ ksi, OK}$$

2. Top of girder (tensile stress)

$$f_t = -0.084 + 0.162 = 0.075 \text{ ksi (compressive)}$$

Check stress limit, without bonded reinforcement (Art. 5.9.4.1.2):

Stress limit = $-0.0948\sqrt{f'_{ci}} = -0.0948\sqrt{5.5} = -0.222$ ksi ≥ -0.200 ksi (governs)
Stress on top of girder is compressive, OK

3. Depression point (0.45L) at release
Stresses only need to be checked at this location because the midspan stresses will govern for final stress conditions.
   a. Calculate stresses due to loads (girder only). Use section properties of noncomposite girder.
   Moment at 0.45L at release = 1219.8 kip-ft (Table 5.14)

   Stress at top,

$$f_t = \frac{1,219.8(12)}{15,421} = 0.949 \text{ ksi}$$

   Stress at bottom,

$$f_b = \frac{1,219.8(12)}{14,915} = -0.981 \text{ ksi}$$

   b. Calculate stresses due to prestress

   Stress at bottom, f_b = 4.03 ksi (same as at midspan, calculated earlier)
   Stress at top, f_t = −0.859 ksi (same as at midspan, calculated earlier)

   c. Check concrete stresses at Service I limit state—before losses (at release)
   Stress at bottom of girder,

$$f_b = 4.03 - 0.981 = 3.049 \text{ ksi}$$

   Check stress limit.

$$\text{Stress limit} = 0.60\, f'_{ci} = 0.60(5.5) = 3.30 \text{ ksi}$$

$$f_b = 3.049 \text{ ksi} < 3.30 \text{ ksi, OK}$$

   Stress at top of girder (tensile stress),

$$f_t = -0.859 + 0.949 = 0.090 \text{ ksi (compressive)}$$

www.EngineeringEBooksPdf.com

Check stress limit.

$$\text{Stress limit} = -0.0948\sqrt{f'_{ci}} = -0.0948\sqrt{5.5} = -0.222 \text{ ksi} \geq -0.200 \text{ ksi (governs)}$$

$$0.900 \text{ ksi} > -0.200 \text{ ksi, OK}$$

All stress conditions are satisfied.

Fatigue I Limit State: Art. 5.5.3.1

Art. 5.5.3.1 specifies three cases that need to be considered for checking for fatigue:

1. In regions of compressive stress due to permanent loads and prestress in reinforced concrete members, fatigue shall be considered only if this compressive stress is less than the maximum tensile live load stress resulting from the Fatigue I Load Combinations as specified in LRFD Table 4.4.1-1 in combination with the provisions for Art. 3.6.1.4, which specifies the magnitude of fatigue live load (discussed in Chapter 3).
2. Fatigue of the reinforcement need not be checked for fully prestressed members designed to have extreme tensile stress due to Service III Limit State within the tensile stress limit specified in Table 5.9.4.2.2-1.
3. Structural components with a combination of prestressing strands and reinforcing bars that allow the tensile stress in the concrete to exceed the Service III limit specified in Table 5.9.4.2.2-1 are required to be checked for fatigue.

The first two cases would be checked for this example; the third case is not applicable to this example (no combination reinforcement).

Case 1

Check stress due to Fatigue I Load Combination. First, determine the bending moment due to fatigue loading. As specified in Art. 3.6.1.4, the fatigue live load consists of a HL-93 truck with a fixed distance of 30 ft between the two 32-kip axles. Bending moment due to fatigue live load can be determined from Equation 3.41, which is applicable for the range $0.241 \leq x/L \leq 0.50$:

$$M_{fat,x=0.5L} = \frac{72x}{L}(L - x - 11.78) - 112 \tag{3.41}$$

For $x/L = 0.5$, $x = 110/2 = 55$ ft. Substituting in Equation 3.41,

$$M_{fat,x=0.5L} = \frac{72(55)}{110}(110 - 55 - 11.78) - 112 = 1444 \text{ kip-ft}$$

Instead of using Equation 3.41 for calculating moment due to the fatigue truck, one can use influence lines for the bending moment due to the fatigue truck by placing the fatigue truck as shown in Figure 5.114. It is assumed that the maximum moment due to fatigue truck occurs when the middle 32-axle load is placed at midspan; the influence line in Figure 5.114 is drawn for moment at midspan.

The influence line ordinates for load positions shown in Figure 5.114 are calculated as follows:

$$y_1 = \frac{55(55)}{110} = 27.50 \text{ ft}$$

$$y_2 = y_1\left(\frac{25}{55}\right) = 27.50\left(\frac{25}{55}\right) = 12.50 \text{ ft}$$

www.EngineeringEBooksPdf.com

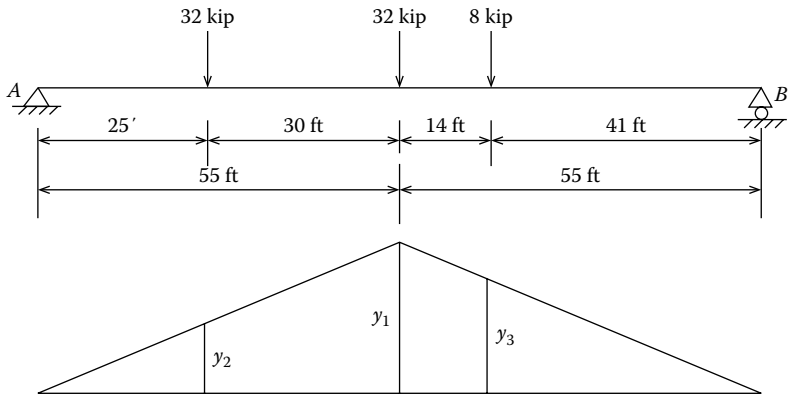

FIGURE 5.114 Position of fatigue truck for maximum moment in the span and influence lines for maximum moment at midspan.

$$y_3 = y_1\left(\frac{41}{55}\right) = 27.50\left(\frac{41}{55}\right) = 20.50 \text{ ft}$$

$$M_{x=0.5L} = 32.0(27.50 + 12.50) + 8(20.50) = 1444 \text{ kip-ft}$$

Alternatively, the maximum moment due to the fatigue truck load positioned for maximum moment in span (Figure 5.114) can be computed from statics by calculating reaction at A by taking moments about B:

$$R_A = \frac{1}{110}\left[32(55+85)+8(41) = 43.71\,\text{kip}\right]$$

$$M_{x=0.5L} = R_A(55) - 32(30)$$
$$= 43.71(55) - 32(30) = 1444 \text{ kip-ft}$$

Dynamic load allowance for fatigue = 0.15
Live load distribution for fatigue = 0.4225 (computed earlier)

$$M_{LL+IM,fat} = 1444(1.15)(0.4225) = 702 \text{ kip-ft}$$

A load factor of 1.5 will be applied to live load moment due to fatigue when calculating stresses due to Fatigue I Load Combination.

The stress in the extreme bottom fibers of the girder due to Fatigue I Load Combination is determined as follows:

$$f_b = -\frac{P_e}{A_G} - \frac{P_e e_m}{S_{bg}} + \frac{M_{DC1}}{S_{bg}} + \frac{M_{DC2} + M_{DW} + M_{fat1}}{S_{bc}} \tag{5.130}$$

where
P_e = effective prestress = 1034 kip (computed earlier)
A_G = gross cross-sectional area of girder
e_m = eccentricity of prestressing force at midspan = 31.27 in. (computed earlier)
S_{bg} = section modulus for the extreme bottom fibers of girder (noncomposite)
S_{bc} = section modulus for the extreme bottom fibers of girder (composite)
M_{DC1}, M_{DC2}, M_{DW}, and $M_{fat\,1}$ are bending moments as defined earlier.

www.EngineeringEBooksPdf.com

Values of M_{DC1}, M_{DC2}, and M_{DW} are given in Table 5.15. Thus,

$$f_b = \frac{1{,}034}{767} + \frac{1{,}034(31.27)}{14{,}915} - \frac{2{,}789.3(12)}{14{,}915} - \frac{\left[(254.1+340.3)+1.5(702)\right](12)}{20{,}902}$$

$$= 1.348 + 2.168 - 2.244 - 0.946$$

$$= +0.326 \text{ ksi}$$

Because the net stress is compressive, fatigue investigation is not required.

Case 2
Earlier, net stress due to Service III load combination was determined to be –0.06 ksi (tensile). The limiting stress as specified in Table 5.9.4.2.2-1 is

$$\text{Limiting stress} = -0.190\sqrt{f'_c} = -0.190\sqrt{6.0} = -0.465 \text{ ksi}$$

$$-0.164 \text{ ksi} < -0.465 \text{ ksi, OK}$$

Therefore, fatigue check is not required for Case 2 in this example.

Had the aforementioned condition not been satisfied, a check would be required for fatigue conforming to the provisions of Art. 5.5.3.1, which requires that the factored force effect (i.e., live load stress range due to the fatigue load, $\gamma\Delta f$) need not exceed the constant-amplitude fatigue threshold as specified in AASHTO Arts. 5.5.3.2, 5.5.3.3, and 5.5.3.4.

Design for Shear
LRFD procedures for shear design of concrete members are discussed in Section 5.10. Because of its simplicity, the General Procedure specified in Art. 5.8.3.4.2 will be used here.

First determine the location of the critical section for shear, as detailed in the following procedure.

As specified in Art. 5.8.3.2, the critical section for shear shall be taken at a distance d_v from the internal face of support, where

d_v = effective shear depth as determined in Art. 5.8.2.9 (in.)
= distance between resultants of tensile and compressive resultant forces due to flexure, $(d_e - (a/2))$; it need not be taken to be less than greater of $0.9d_e$ or $0.72h$ (in.)
d_e = corresponding effective depth from the extreme compressive fiber to the centroid of the tensile reinforcement as given by Equation 5.79 (defined in Art. 5.8.2.9). For beams with only prestressed reinforcement, $d_e = d_p$.
a = depth of compression block = 4.63 in. (computed earlier)

At midspan
Distance of c.g. of prestressing strands at the end = 18.67 in.
h = total height of the section = $h_g + h_h + h_f$ = 72 + 2 + 8 = 82.0 in.
$d_e = d_p = h$ – cgs from the bottom = 82.0 – 5.33 = 76.67 in.

$$d_v \geq \max\begin{cases} 0.9d_e = 0.9(76.67) = 69.00 \text{ in.} \\ 0.72h = 0.72(82) = 59.04 \text{ in.} \end{cases}$$

$$d_v = d_e - \frac{a}{2} = \left(76.67 - \frac{4.63}{2}\right) = 74.36 \text{ in.}$$

$$d_v = 74.36 \text{ in. (governs)}$$

At the end of the beam,

$$d_e = h - \bar{y}_{end} = 82.0 - 18.67 = 63.33 \text{ in.}$$

www.EngineeringEBooksPdf.com

$$d_v \geq max\begin{cases} 0.9d_e = 0.9(63.33) = 57.00 \text{ in.} \\ 0.72h = 0.72(82) = 59.04 \text{ in.} \end{cases}$$

$$d_e = 63.33 \text{ in. (governs)}$$

$$d_v = d_e - \frac{a}{2} = \left(63.33 - \frac{4.63}{2}\right) = 61.02 \text{ in. (governs)}$$

The location of the critical section is taken as the greater of d_v or $0.5d_v \cot\theta$ (θ = angle of compressive stresses at the section) from the internal face of support, as suggested in Art. C5.8.3.2. Value of θ depends on the magnitude of shear and moment at the section. It ranges from 20° to 30° in areas that have high shear forces and low bending moments, whereas for areas of low shear and high bending moments, it ranges to 45°. Assuming a value of θ = 26°,

$$0.5d_v \cot(26°) = 0.5(61.02)(2.05) = 62.55 \text{ in.} > d_v = 61.02 \text{ in.}$$

$$d_v = 62.55 \text{ in.} = 5.2 \text{ ft (governs)}$$

The critical section is located at 5.2 ft from the face of support. Since the support width is unknown, it would be assumed as 12 in. in this example. Therefore, the critical section is located at 5.2 + 0.5 = 5.7 ft from the centerline of the support and 5.7 + 0.5 = 6.2 ft from the end of the beam.

At critical location for shear (6.20 ft from the end of the member), determine the location of cgs by interpolation:

$$\text{cgs at the critical section} = 10 + \left(\frac{8.67}{49.95}\right)(49.95 - 6.2) = 17.59 \text{ in.}$$

Forces acting at the critical section: at 5.7 ft from the center line of bearings.
Moment due to the self-weight of the girder, w_{gdl} = 0.80 kip/ft,

$$M_{x=5.7\text{ ft}} = \frac{0.8(5.7)}{2}(110.0 - 5.7) = 237.8 \text{ kip-ft}$$

Shear due to the self-weight of the girder, w_{gdl} = 0.8 kip/ft,

$$V_{x=5.7\text{ ft}} = 0.80\left(\frac{110.0}{2} - 5.7\right) = 39.4 \text{ kip}$$

Moment due to the dead load of the deck, w = 0.9 kip/ft,

$$M_{x=5.7\text{ ft}} = \frac{0.9(5.7)}{2}(110.0 - 5.7) = 267.5 \text{ kip-ft}$$

Shear due to the dead weight of the deck slab, w_{deck} = 0.90 kip/ft,

$$V_{x=5.7\text{ ft}} = 0.90\left(\frac{110.0}{2} - 5.7\right) = 44.3 \text{ kip}$$

Moment due to additional dead load, w = 0.0563 kip/ft (due to ½ in. thick integral wearing surface),

$$M_{x=5.7\text{ ft}} = \frac{0.0563(5.7)}{2}(110.0 - 5.7) = 16.7 \text{ kip-ft}$$

www.EngineeringEBooksPdf.com

$$V_{x=5.7\text{ ft}} = 0.0563\left(\frac{110.0}{2} - 5.7\right) = 2.8\text{ kip}$$

Moment due to additional dead load due to the weight of haunch, w_{haunch} = 0.088 kip/ft,

$$M_{x=5.7\text{ ft}} = \frac{0.088(5.7)}{2}(110.0 - 5.7) = 26.2\text{ kip-ft}$$

$$V_{x=5.7\text{ ft}} = 0.088\left(\frac{110.0}{2} - 5.7\right) = 4.3\text{ kip}$$

Total moment due to additional dead load = 16.7 + 26.2 = 42.9 kip-ft
Total shear due to additional dead load = 2.8 + 4.3 = 7.1 kip
Moments and shears acting on the composite girder
At the critical section, x = 5.7 ft
Moment due to the dead weight of barriers, w = 0.168 kip/ft,

$$M_{x=5.7\text{ ft}} = \frac{0.168(5.7)}{2}(110.0 - 5.7) = 66.9\text{ kip-ft}$$

Shear due to the dead weight of barriers, w = 0.168 kip/ft,

$$V_{x=5.7\text{ ft}} = 0.168\left(\frac{110.0}{2} - 5.7\right) = 11.1\text{ kip}$$

Moment due to the FWS, w = 0.225 kip/ft,

$$M_{x=5.7\text{ ft}} = \frac{0.225(5.7)}{2}(110.0 - 5.7) = 49.9\text{ kip-ft}$$

Shear due to the FWS, w = 0.225 kip/ft,

$$V_{x=5.7\text{ ft}} = 0.225\left(\frac{110.0}{2} - 5.7\right) = 8.3\text{ kip}$$

Moment Due to Live Load Plus Impact

Moment due to the design truck is computed as follows:

$$M_x = \frac{72x}{L}(L - x - 9.33)$$

$$M_{x=5.7\text{ ft}} = \frac{72(5.7)}{110}(110 - 5.7 - 9.33) = 354.3\text{ kip-ft}$$

Apply live load distribution factor for moment (=0.737) and dynamic load allowance (=0.33) to live load moment due to the design truck.

$$M_{truck+IM} = 354.3(0.737)(1.33) = 347.3\text{ kip-ft}$$

www.EngineeringEBooksPdf.com

Moment due to the lane load, w = 0.64 kip/ft,

$$M_x = \frac{wx}{2}(110.0 - x) = \frac{0.64(5.7)}{2}(110.0 - 5.7) = 190.2 \text{ kip-ft}$$

Apply live load distribution factor for moment (=0.737) to live load moment due to the lane load. Dynamic load allowance is not applicable to lane load.

$$M_{lane} = 190.2(0.737) = 140.2 \text{ kip-ft}$$

Total live load moment,

$$M_{L,total} = 347.3 + 140.2 = 487.5 \text{ kip-ft}$$

Shear due to live load plus impact:

Shear due to the design truck is given by Equation 3.25:

$$V_x = \frac{72}{L}(L - x - 9.33)$$

$$V_{x=5.7\text{ ft}} = \frac{72}{110}(110 - 5.7 - 9.33) = 62.2 \text{ kip}$$

Apply live load distribution factor for shear (=0.884) and dynamic load allowance (=0.33) to live load shear due to the design truck.

$$V_{truck+IM} = 62.2(0.884)(1.33) = 73.1 \text{ kip}$$

Shear due to lane load, w = 0.64 kip/ft,

$$V_{x=5.7\text{ ft}} = 0.64\left(\frac{110.0}{2} - 5.7\right) = 31.55 \text{ kip}$$

Apply live load distribution factor for shear (=0.884). Dynamic load allowance does not apply to shear due to lane load.

$$V_{lane} = 31.55(0.884) = 27.9 \text{ kip}$$

Total shear due to live load = 73.1 + 27.9 = 101.0 kip

Strength I forces at the critical section,

$$Q_u = 1.25DC1 + 1.5DW + 1.75(LL + IM)$$

From aforementioned calculations,

$$M_u = 1.25(548.2 + 49.9) + 1.5(66.9) + 1.75(487.5) = 1701.1 \text{ kip-ft}$$

$$V_u = 1.25(90.8 + 8.3) + 1.5(11.1) + 1.75(101.0) = 317.3 \text{ kip}$$

www.EngineeringEBooksPdf.com

Service III loads acting at midspan,

$$Q = 1.0DC1 + 1.0\ DW + 0.8(LL + IM)$$
$$= 1.0(254.1) + 1.0(340.3) + 0.8(2383) = 2501 \text{ kip-ft}$$

A summary of the aforementioned calculated forces is presented in Table 5.15.

At critical location for shear, V_u = 317.3 kip (Table 5.15).

Calculate the component for shear resistance from the prestress, V_p.

V_p = effective prestressing force in the 10 inclined strands
Cross-sectional area of 10 strands = (0.153)(10) = 1.53 in.^{2}
Effective prestress, f_{pe} = 160.92 ksi (computed earlier)
Force in harped strands = 1.53(160.92) = 246.21 kip
Angle of inclination with horizontal, ψ = 5.34° (calculated earlier)

Component of prestressing force contributory to shear resistance,

$$V_p = 246.21 \sin \psi = 246.05 \sin (5.34°) = 22.9 \text{ kip}$$

Governing equation for shear

$$V_u \leq V_r = \phi V_n \qquad \text{(A5.8.2.1-2)}$$

For shear,

$$\phi = 0.9 \qquad \text{(Art. 5.5.4.2-1)}$$

$$V_n = V_c + V_s + V_p \qquad \text{(5.57) [A5.8.3.3-1]}$$

Calculate the maximum shear capacity of the section:

$$V_n = 0.25 f_c' b_v d_v + V_p \qquad \text{(5.58) [A5.8.3.3-2]}$$

d_v = 62.55 in. from the face of support (computed earlier)

$$V_{n,max} = 0.25(6.0)(6.0)(62.55) + 22.9 = 586 \text{ kip}$$

Contribution of Concrete to Shear Resistance

The contribution of concrete to shear resistance is specified in Art. 5.8.3.3:

$$V_c = 0.0316\beta\sqrt{f_c'}\, b_v d_v \qquad \text{(5.59) [A5.8.3.3-3]}$$

In the aforementioned equation, the factor β, which indicates the ability of diagonally cracked concrete to transmit tension and shear as specified in Art. 5.8.3.4, needs to be determined:

$$\beta = \frac{4.8}{1 + 750\varepsilon_s} \qquad \text{(5.131) [A5.8.3.4.2-1]}$$

where ε_s = net longitudinal tensile strain in the section at the centroid of tension reinforcement as given in the following :

$$\varepsilon_s = \frac{\left(\dfrac{|M_u|}{d_v} + 0.5N_u + |V_u - V_p|\right) - A_{ps} f_{po}}{E_s A_s + E_p A_{ps}} \qquad \text{(5.132) [A5.8.3.4-4]}$$

$$M_u = 1701.1 \text{ kip-ft} = 24{,}413 \text{ kip-in. (Table 5.15)}$$

www.EngineeringEBooksPdf.com

M_u to be not less than

$$(V_u - V_p)d_v = (317.3 - 22.9)(62.55) = 18{,}415 \text{ kip-in.} < 24{,}413 \text{ kip-in. (governs)}$$

$N_u = 0$ (no axial load on the member)
$F_{po} = 0.7f_{pu} = 0.7(270.0) = 189.0$ ksi
A_{ps} = area of prestressing straight strands on tension side of the member (i.e., 32 straight strands)
$A_{ps} = 0.153(32) = 4.896$ in.^{2}
$A_s = 0$ (no nonprestressed reinforcement)
$E_p = 28{,}500$ ksi

Substituting in the aforementioned equation,

$$\varepsilon_s = \frac{\left(\frac{|20{,}413|}{62.55} + 0.5(0) + |317.3 - 22.9|\right) - 4.896(189.0)}{0 + 28{,}500(4.896)} = -0.00218$$

Since ε_s is negative, it will be assumed equal to zero (Art. 5.8.3.4.2). Therefore,

$$\beta = \frac{4.8}{1+0} = 4.8$$

$$V_c = 0.0316\beta\sqrt{f'_c}b_v d_v = 0.0316(4.8)\sqrt{6.0}(6.0)(62.55) = 139.4 \text{ kip}$$

Shear force for which shear reinforcement is required,

$$\begin{aligned} V_s &= \frac{V_u}{\phi} - V_c - V_p \\ &= \frac{317.3}{0.9} - 139.4 - 22.9 \\ &= 190.3 \text{ kip} \end{aligned} \tag{5.62}$$

Therefore, transverse reinforcement must be provided to resist $V_s = 189$ kip.

Calculate the area of shear (transverse) reinforcement.
Assuming vertical stirrups as shear reinforcement, the contribution of shear reinforcement is

$$V_s = \frac{A_v f_y d_v (\cot\theta + \cot\alpha)\sin\alpha}{s} \qquad (5.66)\ [A5.8.3.3\text{-}4]$$

For vertical stirrups, $\alpha = 90°$; therefore, $\cot\alpha = 0$ and $\sin\alpha = 1.0$. Therefore,

$$V_s = \frac{A_v f_y d_v \cot\theta}{s} \qquad (5.67)\ [AC5.8.3.3\text{-}1]$$

The value of angle θ is given by

$$\theta = 29 + 3500\varepsilon_s = 29° \qquad (A5.8.3.4.2\text{-}3)$$

www.EngineeringEBooksPdf.com

Earlier, the value of θ was assumed as 26° for the computation of d_v; this value is very close to the calculated value of 29°. Because of the uncertainty associated with the value of θ, recalculation of d_v is not considered necessary For consistency, θ = 26° would be used for subsequent calculations.

The area of the required shear reinforcement can be expressed as (modified Equation 5.67)

$$A_v = \frac{V_s s}{f_y d_v \cot\theta}$$

Assume a stirrup spacing of 12 in. Then the required area of transverse reinforcement is

$$A_v = \frac{190.3(12)}{(60)(62.55)\cot(26°)} = 0.30 \text{ in.}^2$$

Check requirement for minimum transverse reinforcement (Art. 5.8.2.5).
A minimum amount of transverse reinforcement is required to restrain the growth of diagonal cracking and to increase the ductility of the section. The amount of required minimum transverse reinforcement, A_v, is given as

$$A_v = 0.0316\sqrt{f'_c}\left(\frac{b_v s}{f_y}\right)$$

$$= 0.0316\sqrt{6.0}\left(\frac{6.0(12)}{60}\right)$$

$$= 0.093 \text{ in.}^2/\text{ft} < 0.30 \text{ in.}^2 \text{ (governs)} \qquad (5.72)\ [A5.8.2.5\text{-}1]$$

Provide A_v = 0.30 in.²/ft

Provide No. 4 two-legged stirrups at 12 in. o.c., A_v = 0.4 in.² > $A_{v,\,reqd}$ = 0.30 in.², OK.

Check maximum permitted spacing of transverse reinforcement (Art. 5.8.2.7).

$$V_u = 317.3 \text{ kip} > 0.125 f'_c b_v d_v = 0.125(6.0)(6.0)(62.55) = 281.5 \text{ kip}$$

Therefore, the maximum permitted spacing is

$$s_{max} = smaller\ of \begin{cases} 0.4d_v = 0.4(62.55) = 25 \text{ in.} \\ 12 \text{ in.} \end{cases}$$

$$s_{max} = 0.4d_v \leq 12 \text{ in.}$$

$$S_{max} = 12 \text{ in. (governs)}$$

Therefore, provide No. 4 stirrups at 12 in. o.c., with the first stirrup at 3.0 in. from the end.

Interface Shear Reinforcement: Art. 5.8.4
Art. 5.8.4 requires interface shear transfer to be considered across a given plane when the following conditions exist:

1. An existing or potential crack
2. An interface between dissimilar materials
3. An interface between two concretes cast at different times, such as the girder–slab interface where the cast-in-place slab is poured at different time than the girder
4. The interface between different elements of the cross section, such as the interface between the prestressed concrete girder and the deck slab in this example

www.EngineeringEBooksPdf.com

Therefore, the interface between the deck slab and the girder must be provided with interface shear reinforcement. The factored interface shear resistance, V_{ri}, is to be taken as

$$V_{ri} = \phi V_{ni} \quad (5.133)\ [A5.8.4.1\text{-}1]$$

For design purposes, it is required that

$$V_{ri} \geq V_{ui} \quad (5.134)\ [A5.8.4.1\text{-}2]$$

where

V_{ni} = nominal interface shear resistance (kip)
V_{ui} = factored interface shear force due to load based on the applicable strength and extreme load combinations in LRFD Table 3.4.1-1 (kip)
ϕ = resistance factor for shear specified in Art. 5.5.4.2.1

The nominal shear resistance of the interface plane is to be calculated as follows:

$$V_{ni} = cA_{cv} + \mu(A_{vf}f_y + P_c) \quad (5.135)\ [A5.8.4.1\text{-}3]$$

The shear resistance given by the aforementioned equation shall not be greater than the lesser of value given as follows:

$$V_{ni} \leq K_1 f'_c A_{cv} \quad (5.136)\ [A5.8.4.1\text{-}4]$$

or

$$V_{ni} \leq K_2 A_{cv} \quad (5.137)\ [A5.8.4.1\text{-}5]$$

in which

$$A_{cv} = b_{vi}L_{vi} \quad (5.138)\ [A5.8.4.1\text{-}6]$$

Various quantities in the aforementioned two equations are defined as follows:

A_{cv} = area of concrete considered to be engaged in interface shear transfer
A_{vf} = area of interface shear reinforcement crossing the shear plane within the area A_{cv} (in.^{2})
b_{vi} = interface width considered to be engaged in shear transfer (in.)
L_{vi} = interface length considered to be engaged in shear transfer
c = cohesion factor specified in Art. 5.8.4.3 (ksi)
μ = friction factor specified in Art. 5.8.4.3 (dimensionless)
f_y = yield stress of reinforcement but design value not to exceed 60 ksi
P_c = permanent net compressive force normal to the shear plane; if force is tensile, $P_c = 0$
f'_c = specified compressive strength of the weaker concrete on either side of the interface (ksi)
K_1 = fraction of concrete strength available to resist interface shear, as specified in Art. 5.8.4.3
K_2 = limiting interface shear resistance specified in Art. 5.8.4.3 (ksi)

Computation of Factored Interface Shear Force, V_{ui}, for Concrete Girder/Slab Bridges: Art. 5.8.4.2

$$v_{ui} = \frac{V_{u1}}{b_{vi}d_v} \quad (5.139)\ [A5.8.4.2\text{-}1]$$

where

V_{ui} = factored interface shear force (kip/ft)
V_{u1} = conservative envelope value of total shear
d_v = distance between the centroid of the tension steel and mid-thickness of the slab to compute a factored interface shear stress

www.EngineeringEBooksPdf.com

From previous calculations,

$$V_{u1} = 317.3 \text{ kip (Table 5.15)}$$

b_{vi} = width of the top flange of BT-72 girder = 42 in.
c.g.s at critical section = 17.59 in. (calculated earlier)

$$d_v = 72 + 2 + 4 - 17.59 = 60.41 \text{ in.}$$

The factored interface shear stress is computed to be

$$v_{ui} = \frac{317.3}{(42)(60.41)} = 0.126 \text{ ksi}$$

The interface shear force,

$$V_{ui} = v_{ui}b_{vi} = 0.126(42.0) = 5.3 \text{ kip/in.}$$

The cohesion and friction values are specified in Art. 5.8.4.3. For cast-in-place concrete slab on clean concrete girder surface, free of laitance with surface roughened to amplitude of 0.25 in., the following design values are to be used:

c = 0.28 ksi
μ = 1.0
K_1 = 0.3
K_2 = 1.8 ksi for normal-weight concrete

Calculate the nominal interface shear resistance, V_{ni} (Art. 5.8.4.1):

$$V_{ni} = cA_{cv} + \mu(A_{vf}f_y + P_c) \qquad (5.140)\ [A5.8.4.1\text{-}3]$$

A_{vf} = area of shear reinforcement crossing the shear plane within A_{cv} = 0.40 in.^{2}/12 in. spacing or 0.40 in.^{2}/12 in. = 0.033 in.^{2}/in.

$$A_{cv} = b_{vi}\,(1 \text{ in.})\ 42.0(1.0) = 42 \text{ in.}^2$$

$$f_y = 60 \text{ ksi (maximum)}$$

$$P_c = \text{permanent net compressive force normal to shear plane} = 0$$

$$V_{ni} = 0.28(42) + 1.0(0.033)(60) \approx 13.8 \text{ kip/in.}$$

Check limits on V_{ni}.

$$V_{ni} = \text{smaller of} \begin{cases} K_1 f'_c A_{cv} = 0.3(4)(42) = 50.4 \text{ kips/in.} & (5.141)\ [A5.8.4.1\text{-}4] \\ K_2 A_{cv} = 1.8(42) = 75.6 \text{ kips/in.} & (5.142)\ [A5.8.4.1\text{-}5] \end{cases}$$

The smaller value governs: V_{ni} = 50.4 kip/in.

$$V_{ni,calc.} = 13.8 \text{ kip/in.} < V_{ni} = 50.4 \text{ kip}$$

Therefore,

$$V_{ni} = 13.8 \text{ kip/in. (governs)}$$

$$\phi V_{ni} = 0.9(13.8) = 12.42 \text{ kip/in.} > V_{ui} = 5.30 \text{ kip/in., OK}$$

Check Minimum Area of Interface Shear Reinforcement (Art. 5.8.4.4)
The required minimum area of interface shear reinforcement is given by Equation 5.143:

$$A_{vf} \geq \frac{0.05A_{cv}}{f_y} \qquad (5.143)\ [5.8.4.4\text{-}1]$$

www.EngineeringEBooksPdf.com

However, Art. 5.8.4.4 exempts the aforementioned minimum interface shear reinforcement for girder/slab interfaces with surface roughened to an amplitude of 0.25 in. where factored interface shear stress, v_{ui}, computed from LRFD Equation 5.8.4.2-1 is less than 0.210 ksi and all vertical (transverse) shear reinforcement required by the provisions of Art. 5.8.11 is extended across the interface and adequately anchored into the slab.

All vertical reinforcement will be extended across the interface and adequately anchored in the slab.

$$\phi V_{ni} = 12.42 \text{ kip/in} > V_{ui} = 5.3 \text{ kip/in, OK}$$

Longitudinal Reinforcement Requirement (Art. 5.8.3.5)

Shear causes tension in the longitudinal reinforcement. It is required that at each section, the tensile capacity of the flexural reinforcement on the flexural tension side of the member shall be proportioned to satisfy the following:

$$A_{ps}f_{ps} + A_s f_y \geq \frac{|M_u|}{d_v \phi_f} + 0.5\frac{N_u}{\phi_c} + \left(\left|\frac{V_u}{\phi_v} - V_p\right| - 0.5V_s\right)\cot\theta \qquad (5.144)\ [A5.8.3.5\text{-}1]$$

where

V_s = shear resistance provided by transverse reinforcement at the section under investigation as given by Equation 5.8.3.3-4, except V_s shall not be taken greater than V_u/ϕ_v (kip)

θ = angle of inclination of diagonal compressive stress used in determining the nominal shear resistance of the section under investigation as determined by Art. 5.8.3.4 (degrees)

ϕ_f, ϕ_v, ϕ_c = resistance factors taken from Art. 5.5.4.2 as appropriate for moment, shear, and axial resistance

However, at the inside face of the bearing area of simple end supports to the section of critical shear, the longitudinal reinforcement on the flexural tension side of the member is required to satisfy the following:

$$A_{ps}f_{ps} + A_s f_y \geq +\left(\frac{V_u}{\phi_v} - 0.5V_s - V_p\right)\cot\theta \qquad (5.145)\ [A5.8.3.5\text{-}2]$$

The left-hand side terms in the aforementioned equations represent the required tensile capacity of the flexural reinforcement on the flexural tension side of the member, T_{reqd}. The values of V_u, V_s, V_p, and θ may be the same as those for the section at d_v from the face of the support (Art. C5.3.8.5).

V_s = shear resistance provided by transverse reinforcement, not to exceed V_u/ϕ

$$V_s = \frac{A_v f_y d_v \cot\theta}{s}$$

$$= \frac{0.40(60)(62.55)\cot 26°}{12.0} = 256.5 \text{ kip} \qquad (5.67)\ [AC5.8.3.3\text{-}1]$$

$$\frac{V_u}{\phi} = \frac{317.3}{0.9} = 353 \text{ kip} > V_s = 256.5 \text{ kip}$$

$$A_{ps}f_{ps} + A_s f_y \geq +\left(\frac{317.3}{0.9} - 0.5(256.5) - 22.9\right)\cot 26°$$

$$A_{ps}f_{ps} + A_s f_y \geq 413 \text{ kip}$$

$T_{reqd.}$ = tensile capacity of the flexural reinforcement on the flexural tension side of the member = 413 kip

www.EngineeringEBooksPdf.com

Calculate the available longitudinal force.

Art. 5.8.3.5 specifies that the area of longitudinal reinforcement on the flexural side of the member need not exceed the area of flexural reinforcement required to resist the maximum moment acting alone. This provision applies to the case where the reaction from the loads introduces direct compression into the flexural compression face of the member, a condition that is satisfied in this example.

In this example, the available tensile reinforcement consists of 32 straight strands (out of 42 straight strands used in the girder at midspan). The available force that can be provided by these strands at the critical section for shear must be calculated by considering the lack of full development due to the proximity to the end of the girder.

Area of 32 straight strands,

$$A_{ps} = (0.153)(32) = 4.896 \text{ in.}^2$$

The force, P_{es}, in these 32 straight strands is calculated to be

$$P_{es} = A_{ps}f_{pe} = 4.896(160.92) = 787.9 \text{ kip}$$

where the effective prestress, f_{pe} = 160.82 ksi, was calculated earlier.

The centroid of the 32 straight strands from the bottom of the girder is calculated as

$$\text{cgs from the bottom, } d_g = \frac{1}{32}\left[12(2.0)+12(4.0)+6(6.0)+2(8.0)\right] = 3.875 \text{ in.}$$

The location of the failure crack must be assumed, which is where the required longitudinal force, T_{reqd}, must be provided. In this example, it is assumed that the failure crack radiates from the inside face of support and propagates upward at angle crossing the centroid of strands. The angle θ (=26°) determined earlier will be used here to locate the intersection of the failure crack with the centroid of strands (Figure 5.115).

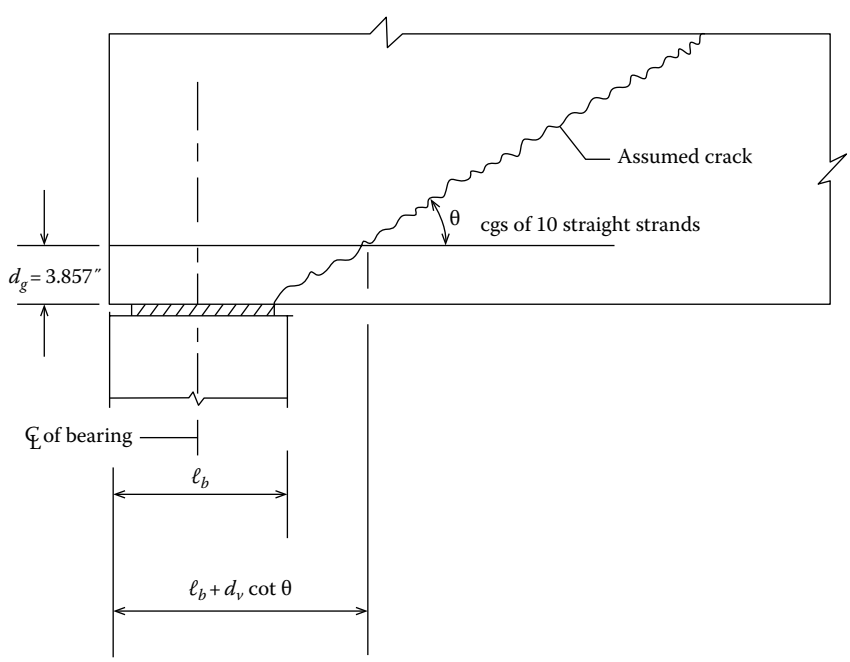

FIGURE 5.115 Location of the failure crack at the ends of the girder.

www.EngineeringEBooksPdf.com

The distance of the intersection of the crack with the centroid of strands, x, measured from the end of the girder, is calculated as

$$x = \ell_b + d_g \cot \theta$$

where ℓ_b = width of support = 12 in. (assumed in this example).

The actual width of support would be designed based on many considerations, primarily based on the temperature variations that must be accounted for in the design.

$$x = \ell_b + d_g \cot \theta = 12 + 3.875 \cot (26°) = 20.0 \text{ in.}$$

Transfer length,

$$\ell_t = 60d_b = 60(0.6) = 30 \text{ in. (Art. 5.11.4.1)}$$

Because the distance x is less than the transfer length (=30 in.), the available stress is less than the effective prestress for the straight strands. Therefore, the available force, T_{avail}, at distance x is computed assuming a linear variation from the end of the girder to transfer length (Art. C5.3.8.5). Therefore,

$$T_{avail} = P_{ex}\left(\frac{x}{\sim_t}\right) = 787.9\left(\frac{20.0}{30.0}\right) = 525 \text{ kip}$$

The available tensile force (+525 kip) is greater than T_{reqd} (=413 kip). Therefore, the 32 straight strands are adequate to resist the required longitudinal force at this location; consequently, no additional reinforcement is required.

Note that had the force in the strands not been adequate to resist the required tensile force, additional nonprestressed reinforcement would be required to make up for the deficiency. Another alternative would be to reduce the value of required tensile force, T_{reqd}. This can be done by increasing V_s by reducing spacing in Equation 5.67, which, in turn, would reduce T_{reqd}.

Anchorage Zone Requirement: Art. 5.10.10.1

The end of the girder is required to be designed to provide certain amount of splitting resistance in the vicinity of anchorage zones. Splitting resistance is of prime importance in relatively thin portions of pretensioned members that are tall or wide such as the webs of I-girders and the webs and flanges of box and tub girders (the bulb-T girder used in this example has a web that is mere 6 in. thick and the flange 36 in. wide).

Sufficient reinforcement must be provided in the anchorage zones. The amount of reinforcement provided to develop the required splitting resistance should satisfy the following:

$$P_r = f_s A_s \qquad (5.146)\ [A5.10.10.1\text{-}1]$$

where

f_s = stress in steel reinforcement, not to exceed 20 ksi

A_s = total area of reinforcement located within the distance $h/4$ from the end of the girder

h = overall dimension of the precast member in which splitting resistance is being evaluated

As specified in Art. 5.10.10.1, for pretensioned I-girders or bulb-Ts, A_s is to be taken as the total area of vertical reinforcement located within a distance of $h/4$ from the end of the member where h is the overall height of the member. This specification also provides that

1. The resistance shall not be less than four percent of the total prestressing force at transfer
2. The reinforcement shall be as close to the end of the member as practicable
3. Reinforcement used to satisfy this requirement can also be used to satisfy other design requirements

www.EngineeringEBooksPdf.com

Total area of prestressing strands provided,

$$A_s = 6.428 \text{ in.}^2$$

Four percent of total prestressing force at transfer is calculated to be

$$P_r = (0.04)P_o = (0.04)(0.75)(270)(6.428) = 52.07 \text{ kip}$$

With a value of f_s = 20 ksi, the amount of reinforcement required is

$$A_{s,reqd.} = \frac{P_r}{f_s} = \frac{52.07}{20.0} = 2.60 \text{ in.}^2$$

$$\frac{h}{4} = \frac{72.0}{4} = 18 \text{ in.}$$

Therefore, at least 2.60 in.^{2} of vertical reinforcement must be placed within a distance of 18 in. from the end of the girder. As permitted by the specification, the stirrups provided in the end zone of the girder can also be used to satisfy this requirement since this reinforcement is only required to resist forces at release.

Calculate the number of No. 4 stirrups required to provide a reinforcement area of 2.60 in.^{2} The area provided by one No. 4 stirrup = 0.4 in.^{2} Therefore, the number of No. 4 stirrups required is

$$\text{No. of stirrups required} = \frac{2.60}{0.4} = 6.5 \approx 7$$

So, a total of seven stirrups are required to resist splitting force in the anchorage zone of the girder; these seven stirrups must be placed within 18 in. from the end of the girder. Placing the first (or the end) stirrup at 3 in. from the end, the required seven stirrups can be placed at 2.5 in. o.c. in a distance of 18 in. from the end.

Total distance from the end = 3 + 6 spacings at 2.5 in. o.c. = 3 + 15 = 18 in.

(The number of stirrups can be reduced by selecting stirrups of larger diameter than that of No. 4 stirrups. For example, five No. 5 stirrups would furnish an area of 3.05 in.^{2} > 2.60 in.^{2} required. However, for simplicity in construction, No. 4 stirrups are provided throughout the girder.)

Confinement Reinforcement: Art. 5.10.10.2

Art. 5.10.10.2 specifies that confinement reinforcement be provided to confine prestressing steel in the bottom flange, for a distance of 1.5*d*. The amount of reinforcement required for this purpose shall not be less than No. 3 deformed bars, placed with spacing not exceeding 6 in. and shaped to enclose the strands.

1.5*d* = 1.5(72.0) = 108 in. = 9 ft from the end of the beam

Provide 19 No. 3 deformed bars at 6 in. o.c. (18 spacings at 6 in. o.c. = 9 ft), with the first bar at 3 in. from the end. These bars should be shaped to the contours of the bottom flange of BT-72 girder to enclose the strands. Details of the reinforcement in the end region of the girder are shown in Figure 5.116.

Hold-Down Forces

The angle of inclination of 10 harped strands with the horizontal was calculated to be ψ = 5.34°. Assuming that the stress in the strands at the time of prestressing, f_{pj}, before seating losses, is as follows:

$$\text{Stress in the strands, } f_{pj} = 0.8f_{pu} = 0.8(270) = 216 \text{ ksi}$$

$$\text{Force per strand} = (A_{ps} \text{ per strand})\,(f_{pj}) = 0.153(216) = 33 \text{ kip}$$

$$\text{Force in 10 strands} = 10(33) = 330 \text{ kip}$$

$$\text{Total hold-down force} = 1.05(330)\sin(5.34°) = 32.25 \text{ kip}$$

www.EngineeringEBooksPdf.com

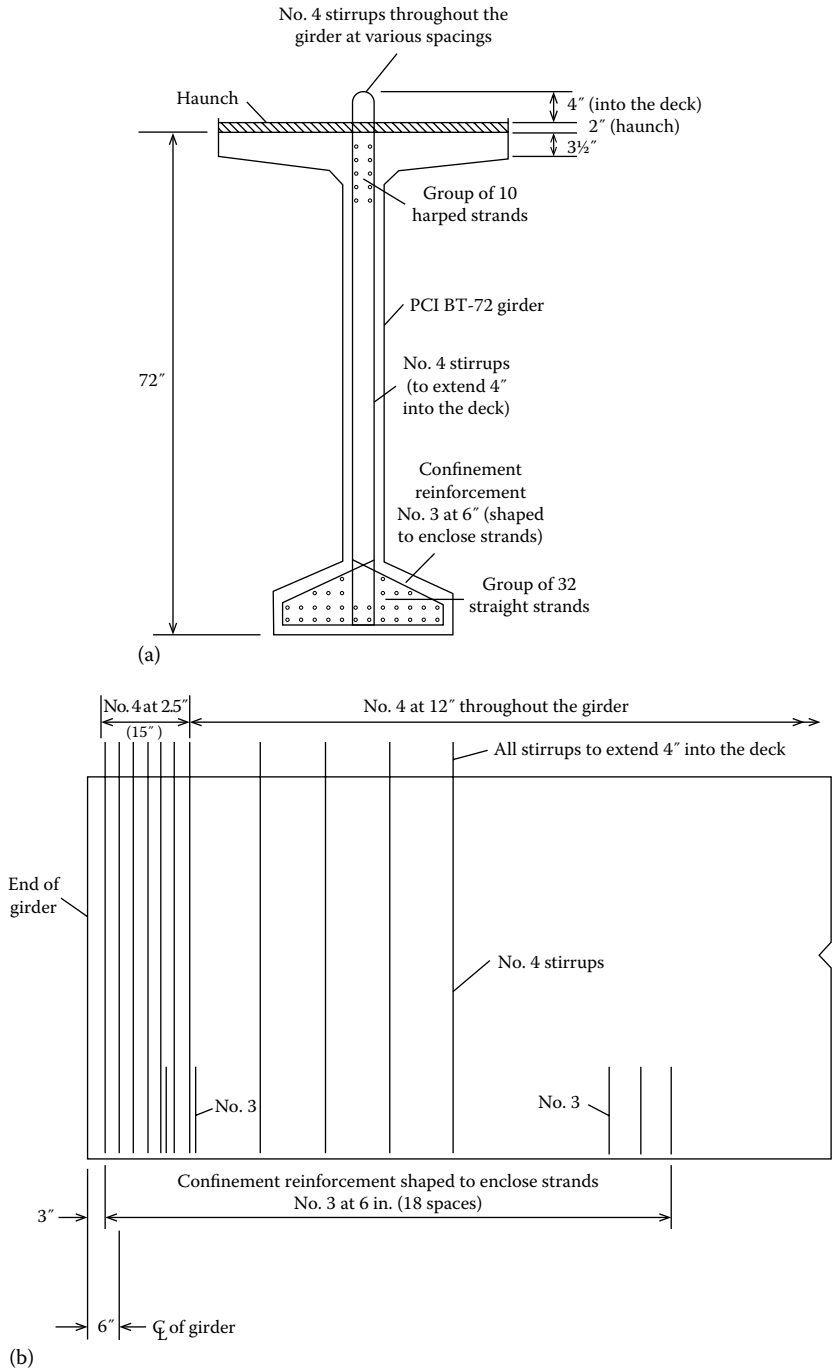

FIGURE 5.116 Details for reinforcement in the end region of the girder. (a) Girder cross section of BT-72 and (b) elevation of the girder.

www.EngineeringEBooksPdf.com

The multiplier (1.05) in the aforementioned calculation has been applied to account for friction (PCI 2003). The hold-down force at each harping point is 32.25 kip. The producer of the prestressing girder would be responsible to provide adequate hold-down devices.

Deflection and Camber

The phenomenon of camber was illustrated in Figure 5.107. Camber is a behavior specific to prestressed concrete girders; nonprestressed concrete beams and steel beams do not have camber as a result of the imposed loads (no prestressing force in these girders).

Camber of a prestressed concrete girder with two point-harping prestressing strands is determined based on the modulus of elasticity of concrete at release, f'_{ci}, and the moment of inertia of noncomposite section of the girder.

Camber of a prestressed concrete girder can be determined as follows (PCI 2003):

$$\Delta_P = \frac{P_i}{E_{ci} I_{nc}} \left(\frac{e_m L^2}{8} - \frac{e' a^2}{6} \right) \tag{5.147}$$

where

Δ_P = camber due to prestressing force
E_{ci} = modulus of elasticity of concrete at release = 4496 ksi
I_{nc} = moment of inertia of noncomposite girder = 545,895 in.^{2}
e_m = eccentricity of prestressing steel at midspan
e' = difference between eccentricity of prestressing steel at midspan and at end
= 31.27 − 18.67 = 12.67 in.
P_i = total prestressing force after transfer = 1186 kip
L = 111.0 ft (total length of member)
a = distance from the end of the beam at harp point = 49.95 + 0.5 = 50.45 ft

All of the aforementioned values were calculated earlier. Substituting the aforementioned values in Equation 5.147 yields

$$\Delta_P = \frac{1{,}186}{(4{,}496)(545{,}894)} \left[\frac{(31.27)(111 \times 12)^2}{8} - \frac{12.67(50.45 \times 12)^2}{6} \right]$$

$$= 2.98 \text{ in.} (\uparrow)$$

Instantaneous Deflection

Deflection due to the self-weight of the girder,

$$\Delta_g = \frac{5 w_g L^4}{384 E_{ci} I_{nc}}$$

$$\Delta_g = \frac{5(0.8/12)(111 \times 12)^4}{384(4{,}496)(545{,}894)} = 1.11 \text{ in.} (\downarrow)$$

Calculate deflections due to the superimposed dead loads: dead weight of concrete deck, haunch, and diaphragms. Use moment of inertia of noncomposite girder. These dead weights were computed earlier. From previous calculations,

$$w_s = w_{deck} + w_{haunch} + w_{diaphragms} = 0.9 + 0.088 + 0.068 = 1.056 \text{ kip/ft}$$

$$\Delta_s = \frac{5(1.056/12)(111 \times 12)^4}{384(4{,}496)(545{,}894)} = 1.47 \text{ in.} (\downarrow)$$

www.EngineeringEBooksPdf.com

Calculate deflections due to the dead loads from the dead weight of barriers and the FWS. Use moment of inertia of composite girder for this calculation. From previous calculations, I_C = 1,179,484 in.^{4} (Table 5.14)

$$w_{comp} = w_{DC2} + w_{DW} = 0.168 + 0.225 = 0.393 \text{ kip/ft}$$

$$\Delta_{comp} = \frac{5(0.393/12)(110 \times 12)^4}{384(4,496)(1,179,484)} = 0.24 \text{ in.}(\downarrow)$$

Summary of Camber and Deflections

$$\text{Deflection at transfer} = \Delta_P + \Delta_g = 2.98 - 1.11 \text{ in.} = 1.87 \text{ in. } (\uparrow)$$

To account for creep, multipliers have been developed (Martin 1977), which are to be applied to deflections due to prestress and self-weight of the girder. Details of these multipliers are summarized in (PCI 2003). These multipliers are (Table 5.16)

Deflection due to prestress 1.8
Deflection due to self-weight of the girder 1.85

Therefore, total deflection at erection is estimated to be

$$\Delta_{erection} = 1.8(2.98) - 1.85(1.11) = 3.31 \text{ in. } (\uparrow)$$

Long-Term Deflection
Long-term deflection was discussed in Section 4.18.5.3. Art. 5.7.3.6.2 specifies that the long-term deflection may be taken as four times the instantaneous deflection if the latter is computed based on the moment of inertia of gross cross section of the girder. As suggested in PCI (2003), a multiplier factor of four is not appropriate for this type of construction. Designers should follow the guidelines

TABLE 5.16
Guide for Deflection Multipliers for Camber and Long-Term Deflections for Typical Precast, Prestressed Concrete Members

	Without Composite Topping	With Composite Topping
At erection:		
1. The deflection (↓) component—apply to the elastic deflection due to the member weight at release of prestress	1.85	1.85
2. Camber (↑) component—apply to the elastic camber due to prestress at the time of release of prestress	1.80	1.80
Final:		
3. Deflection (↓) component—apply to the elastic deflection due to the member weight at release of prestress	2.70	2.40
4. Camber (↑) component—apply to the camber due to prestress at the time of release of prestress	2.45	2.20
5. Deflection (↓) component—apply to the elastic deflection due to superimposed dead load only	3.00	3.00
6. Deflection (↓) component—apply to the elastic deflection caused by the composite topping	—	2.30

Source: In PCI Table 8.7.1-1. Adapted from PCI, *Precast Prestressed Concrete Bridge Design Manual*, 1st ed., Precast/Prestressed Concrete Institute, Chicago, IL, 2003. Copyright © 2003 by the Precast/Prestressed Concrete Institute, Chicago, IL.

www.EngineeringEBooksPdf.com

of the owner agency having jurisdiction over the bridge. Alternatively, a more rigorous, time-dependent analysis may be performed. A comprehensive discussion and examples on long-term deflections of prestressed concrete girders can be found in the literature (PCI 2003, Nawy 2010).

Live Load Deflection
Optional Deflection Due to Vehicular Live Load
Optional Live Load Deflection Control
Since no deflection criteria are specified, optional deflection criteria (Art. 2.6.2.6.2) will be used in this example.

Allowable deflection due to vehicular load,

$$\Delta_{LL} = \frac{span}{800} = \frac{110(12)}{800} = 1.65 \text{ in.}$$

Art. 3.6.1.3.2 specifies that the calculated deflection will be taken as the larger of the following as discussed in Section 2.6.3:

1. Deflection due to design truck alone. Dynamic load allowance will be applied to this deflection.
2. Deflection due to 25 percent of the deflection due to the design truck *plus* deflection due to lane load. Dynamic load allowance is not applied to the deflection due to the lane load.

Calculate Deflection Due to Vehicular Live Load
Deflections will be calculated for the design truck and the design lane load (tandem load does not govern for a span of 110 ft).

Deflection Due to Design Truck
As a practical matter, the maximum deflection in the girder would be computed by placing the middle 32-kip load at the midspan and the other two loads (8-kip and 32-kip loads) placed at 14 ft from the midspan, one on the left and the other on the right side of the midspan (see Figure 5.117a). This load case can be split into two separate cases as shown in AISC (2011):

a. Load Case 7 for the centrally placed point load
b. Load Case 8 for point loads placed at any point on the span

For the centrally placed point load P (Load Case 7), the maximum deflection occurs at the center, which can be calculated as follows (by substituting E_cI_c for EI in Equation 2.2):

$$\Delta_c = \frac{PL^3}{48E_cI_c} \tag{5.96}$$

where
Δ_c = deflection at midspan due to point load
L = span = 110 ft
E_c = modulus of elasticity of concrete = 4496 ksi
I_c = moment of inertia of composite girder cross section = 1,179,848 in.^{4}

For the 32-kip and 8-kip loads closer to the supports, use AISC (2011) Load Case 8. For a point load P placed at a distance a from the left support, the deflection at a distance x (when $x < a$) from the left support can be calculated as follows:

$$\Delta_x = \frac{Pbx\left(L_2 - b^2 - x^2\right)}{6EIL} \tag{2.3}$$

1. For the 32-kip load at midspan (Figure 5.117b),

$$P = 32 \text{ kip}$$
$$L = 110 \text{ ft}$$

www.EngineeringEBooksPdf.com

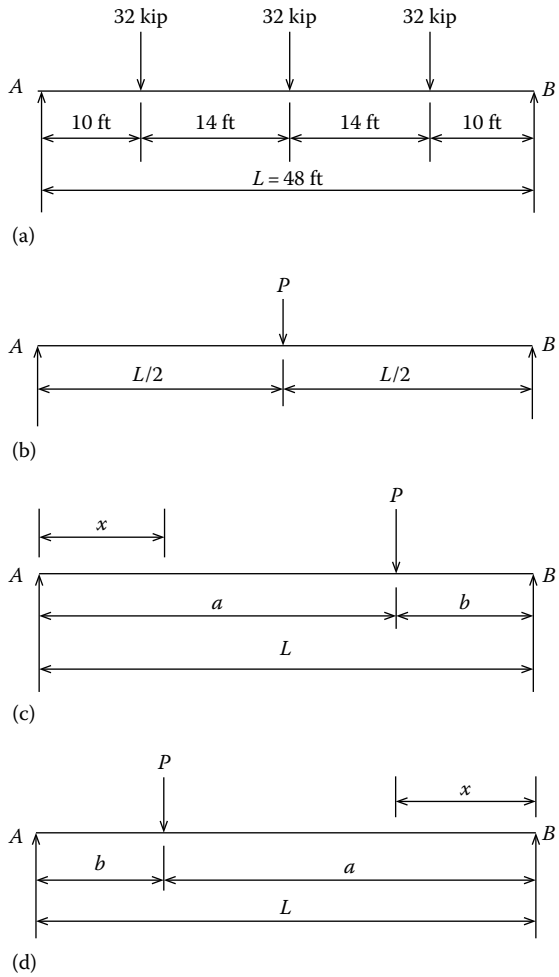

FIGURE 5.117 (a) Assumed position of the design truck for maximum deflection at midspan; (b) point load at center, $x = L/2$; (c) point load right of midspan, distance x measured from A, $x < a$; (d) point load left of midspan, distance x measured from B, $x < a$.

$$\Delta_c = \frac{PL^3}{48E_cI_c} = \frac{32(110)^3(12)^3}{48(4,496)(1,179,484)} = 0.289 \text{ in.}$$

2. For deflection due to the 8-kip load right of midspan (Figure 5.117c), distances are measured from the left support of the slab:

$$P = 8 \text{ kip}$$

$$L = 110 \text{ ft}$$

$$a = 55 + 14 = 69 \text{ ft}$$

$$b = 110 - 69 = 41 \text{ ft}$$

$$x = 55 \text{ ft} < a = 69 \text{ ft}$$

$$\Delta_{x=41\text{ ft}} = \frac{8.0(41)(55)\left[(110)^2 - (41)^2 - (55)^2\right]}{6(4,496)(1,179,484)(110)}(12)^3 = 0.066 \text{ in.}$$

www.EngineeringEBooksPdf.com

3. For 32-kip load closer to the left support (Figure 5.117d), distances are measured from the right support:

$$P = 32 \text{ kip}$$

$$a = 110 - 41 = 69 \text{ ft}$$

$$b = 110 - 69 = 41 \text{ ft}$$

$$x = 55 \text{ ft} < a = 69 \text{ ft}$$

$$\Delta_{x=41\,\text{ft}} = \frac{32.0(41)(55)\left[(110)^2 - (41)^2 - (55)^2\right]}{6(4,496)(1,179,484)(110)}(12)^3 = 0.263 \text{ in.}$$

Note that the rear 32-kip load and the front 8-kip loads are placed equidistant from the supports. Therefore, deflection under the rear 32-kip load could have been easily computed from Maxwell's Reciprocal Theorem and the law of proportionality. Thus,

$$\Delta_{32\ kip\ load} = \left(\frac{32}{8}\right)\Delta_{8\ kip\ load} = \left(\frac{32}{8}\right)(0.066) = 0.264 \text{ in.} \approx 2.63 \text{ in.}$$

$$\Delta_{total,1\ design\ truck} = 0.289 + 0.066 + 0.263 = 0.618 \text{ in.}$$

Apply dynamic allowance (33 percent).
Apply distribution factor for live load.

Calculated distribution factor for live load = 0.5
Multiple-presence factor for three design lanes = 0.85
Applicable distribution factor for live load = (0.85) (0.5) = 0.425

$$\Delta_{total,1\ truck+IM} = 1.33(0.425)(0.618) = 0.35 \text{ in.}$$

Deflection due to Design Lane Load
Deflection due to design lane load can be calculated as follows:

$$\Delta_{lane} = \frac{5wL^4}{384E_cI_c}$$

where
w = 0.64 kip/ft
L = span = 110 ft

Substituting these values along with E_c = 38,340 ksi and I_c = 1,127,484 in.^{4} in Equation 5.94, the maximum deflection due to design lane load is

$$\Delta_{lane.max} = \frac{5(0.64)(110)^4(12)^3}{384(4,496)(1,179,484)} = 0.40 \text{ in.}$$

www.EngineeringEBooksPdf.com

Dynamic load allowance is not applicable to lane load. Apply live load distribution factor for deflection.

$$\Delta_{lane} = 0.425(0.4) = 0.17 \text{ in.}$$

$$0.25\Delta_{truck} + \Delta_{lane} = 0.25(0.35) + 0.17 = 0.26 \text{ in.}$$

$$\Delta_{truck} = 0.35 \text{ in.} > (0.25\Delta_{truck} + \Delta_{lane}) = 0.26 \text{ in.}$$

Therefore, $\Delta_{truck} = 0.35$ in. governs
Allowable live load deflection, $\Delta_{allowable} = L/800 = (110 \times 12)/800 = 1.65$ in. > 0.35 in.

Deflection criteria are satisfied.

Optional Criteria for Span-to-Depth Ratio (Art. 2.5.2.6.3)
The owner may invoke the minimum girder depth equal to $0.033L$ as specified in Table 2.5 (LRFD Table 2.5.2.6.3-1). For this example,

$$0.033(110)(12) = 43.56 \text{ in.} < d = 82\ 0 \text{ in., OK.}$$

Span-to-depth ratio is satisfied.

Figure 5.118 shows a typical precast, prestressed concrete girder highway bridge superstructure under construction. It uses 11 AASHTO-PCI bulb-T girders, similar to the one used in this example.

FIGURE 5.118 A precast, prestressed concrete girder bridge over Jefferson Street, Albuquerque, NM, under construction (August 2014). This superstructure consists of 11 AASHTO-PCI bulb-T girders.

www.EngineeringEBooksPdf.com

5.A APPENDIX

5.A.1 LRFD Appendix A4: Deck Slab Design Table

Table A4-1 may be used in determining the design moments for different girder arrangements. The following assumptions and limitations were used in developing this table and should be considered when using the listed values for design:

- The moments are calculated using the equivalent strip method as applied to concrete slabs supported on parallel girders.
- Multiple-presence factors and the dynamic load allowance are included in the tabulated values.
- See Art. 4.6.2.1.6 for the distance between the center of the girders and the location of the design sections for negative moments in the deck. Interpolation between the listed values may be used for distances other than those listed in Table A4-1.
- The moments are applicable for decks supported on at least three girders and having a width of not less than 14.0 ft between the centerlines of the exterior girders.
- The moments represent the upper bound for the moments in the interior regions of the slab and, for any specific girder spacing, were taken as the maximum value calculated, assuming different number of girders in the bridge cross section. For each combination of girder spacing and number of girders, the following two cases of overhang width were considered:
  (a) Minimum total overhang width of 21.0 in. measured from the center of the exterior girder
  (b) Maximum total overhang width equal to the smaller of 0.625 times the girder spacing and 6.0 ft

  A railing system width of 21.0 in. was used to determine the clear overhang width. For other widths of railing systems, the difference in the moments in the interior regions of the deck is expected to be within the acceptable limits for practical design.
- The moments do not apply to the deck overhangs and the adjacent regions of the deck that need to be designed taking into account the provisions of Art. A13.4.1.
- It was found that the effect of two 25^k axles of the tandem, placed at 4.0 ft from each other, produced maximum effects under each of the tires approximately equal to the effect of the 32^k truck axle. The tandem produces a larger total moment, but this moment is spread over a larger width. It was concluded that repeating calculations with a different strip width for the tandem would not result in a significant difference.

www.EngineeringEBooksPdf.com

TABLE LRFD TABLE A4-1
Maximum Live Load Moments per Unit Width, kip-ft/ft

		Negative Moment						
		Distance from CL of Girder to Design Section for Negative Moment						
S	Positive Moment	0.0 in.	3 in.	6 in.	9 in.	12 in.	18 in.	24 in.
4′–0″	4.68	2.68	2.07	1.74	1.60	1.50	1.34	1.25
4′–3″	4.66	2.73	2.25	1.95	1.74	1.57	1.33	1.20
4′–6″	4.63	3.00	2.58	2.19	1.90	1.65	1.32	1.18
4′–9″	4.64	3.38	2.90	2.43	2.07	1.74	1.29	1.20
5′–0″	4.65	3.74	3.20	2.66	2.24	1.83	1.26	1.12
5′–3″	4.67	4.06	3.47	2.89	2.41	1.95	1.28	0.98
5′–6″	4.71	4.36	3.73	3.11	2.58	2.07	1.30	0.99
5′–9″	4.77	4.63	3.97	3.31	2.73	2.19	1.32	1.02
6′–0″	4.83	4.88	4.19	3.50	2.88	2.31	1.39	1.07
6′–3″	4.91	5.10	4.39	3.68	3.02	2.42	1.45	1.13
6′–6″	5.00	5.31	4.57	3.84	3.15	2.53	1.50	1.20
6″–9″	5.10	5.50	4.74	3.99	3.27	2.64	1.58	1.28
7′–0″	5.21	5.98	5.17	4.36	3.56	2.84	1.63	1.37
7′–3″	5.32	6.13	5.31	4.49	3.68	2.96	5.65	1.51
7′–6″	5.44	6.26	5.43	4.61	3.78	3.15	1.88	1.72
7′–9″	5.56	6.38	5.54	4.71	3.88	3.30	2.21	1.94
8′–0″	5.69	6.48	5.65	4.81	3.98	3.43	2.49	2.16
8′–3″	5.83	6.58	5.74	4.90	4.06	3.53	2.74	2.37
8′–6″	5.99	6.66	5.82	4.98	4.14	3.61	2.96	2.58
8′–9″	6.14	6.74	5.90	5.06	4.22	3.67	3.15	2.79
9″–0″	6.29	6.81	5.97	5.13	4.28	3.71	3.31	3.00
9′–3″	6.44	6.87	6.03	5.19	4.40	3.82	3.47	3.20
9′–6″	6.59	7.15	6.31	5.46	4.66	4.04	3.68	3.39
9′–9″	6.74	7.51	6.65	5.80	4.94	4.21	3.89	3.58
10′–0″	6.89	7.85	6.99	6.13	5.26	4.41	4.09	3.77
10′–3″	7.03	8.19	7.32	6.45	5.58	4.71	4.29	3.96
10′–6″	7.17	8.52	7.64	6.77	5.89	5.02	4.48	4.15
10′–9″	7.32	8.83	7.95	7.08	6.20	5.32	4.68	4.34
11′–0″	7.46	9.14	8.26	7.38	6.50	5.62	4.86	4.52
11′–3″	7.60	9.44	8.55	7.67	6.79	5.91	5.04	4.70
11′–6″	7.74	9.72	8.84	7.96	7.07	6.19	5.22	4.87
11′–9″	7.88	10.01	9.12	8.24	7.36	6.47	5.40	5.05
12′–0″	8.01	10.28	9.40	8.51	7.63	6.74	5.56	5.21
12′–3″	8.15	10.55	9.67	8.78	7.90	7.02	5.75	5.38
12′–6″	8.28	10.81	9.93	9.04	8.16	7.28	5.97	5.54
12′ 9″	8.41	11.06	10.18	9.30	8.42	7.54	6.18	5.70
13′–0″	8.54	11.31	10.43	9.55	8.67	7.79	6.38	5.86
13′–3″	8.66	11.55	10.67	9.80	8.92	8.04	6.59	6.01
13′–6″	8.78	11.79	10.91	10.03	9.16	8.28	6.79	6.16
13′–9″	8.90	12.02	11.14	10.27	9.40	8.52	6.99	6.30
14′–0″	9.02	12.24	11.37	10.50	9.63	8.76	7.18	6.45
14′–3″	9.14	12.46	11.59	10.72	9.85	8.99	7.38	6.58
14′–6″	9.25	12.67	11.81	10.94	10.08	9.21	7.57	6.72
14′–9″	9.36	12.88	12.02	11.16	10.30	9.44	7.76	6.86
15′–0″	9.47	13.09	12.23	11.37	10.51	9.65	7.94	7.02

www.EngineeringEBooksPdf.com

TABLE 5.A.1
Cross-Sectional Areas of Reinforcing Bars

Bar Size Designation			
Standard	**Metric Conversion**	**Nominal Diameter, in. (mm)**	**Area, in.^{2} (mm^2)**
No. 2	No. 6	0.250 (6.4)	0.05 (31.6)
No. 3	No. 10	0.375 (9.5)	0.11 (71)
No. 4	No. 13	0.500 (12.7)	0.20 (129)
No. 5	No. 16	0.625 (15.9)	0.31 (199)
No. 6	No. 19	0.75 (19.1)	0.44 (284)
No. 7	No. 22	0.875 (22.2)	0.60 (387)
No. 8	No. 25	1.000 (25.4)	0.79 (510)
No. 9	No. 29	1.128 (28.7)	1.00 (645)
No. 10	No. 32	1.270 (32.3)	1.27 (819)
No. 11	No. 36	1.410 (35.8)	1.56 (1006)
No. 14	No. 43	1.693 (43.0)	2.25 (1452)
No. 18	No. 57	2.257 (57.3)	4.00 (2581)

TABLE 5.A.2
Area of Groups of Standard Reinforcing Bars

	Number of Bars								
Bar No.	**2**	**3**	**4**	**5**	**6**	**7**	**8**	**9**	**10**
4	0.39	0.58	0.78	0.98	1.18	1.37	1.57	1.77	1.96
5	0.61	0.91	1.23	1.53	1.84	2.15	2.45	2.76	3.07
6	0.88	1.32	1.77	2.21	2.65	3.09	3.53	3.98	4.42
7	1.20	1.80	2.41	3.01	3.61	4.21	4.81	5.41	6.01
8	1.57	2.35	3.14	3.93	4.71	5.50	6.28	7.07	7.85
9	2.00	3.00	4.00	5.00	6.00	7.00	8.00	9.00	10.00
10	2.53	3.79	5.06	6.33	7.59	8.86	10.12	11.39	12.66
11	3.12	4.68	6.25	7.81	9.37	10.94	12.50	14.06	15.62
14	4.50	6.75	9.00	11.25	13.50	15.75	18.00	20.25	22.50
18	8.00	12.00	16.00	20.00	24.00	28.00	32.00	36.00	40.00

	Number of Bars									
Bar No.	**11**	**12**	**13**	**14**	**15**	**16**	**17**	**18**	**19**	**20**
4	2.16	2.36	2.55	2.75	2.95	3.14	3.34	3.53	3.73	3.93
5	3.37	3.68	3.99	4.30	4.60	4.91	5.22	5.52	5.83	6.14
6	4.86	5.30	5.74	6.19	6.63	7.07	7.51	7.95	8.39	8.84
7	6.61	7.22	7.82	8.42	9.02	9.62	10.22	10.82	11.43	12.03
8	8.64	9.43	10.21	11.00	11.78	12.57	13.35	14.14	14.92	15.71
9	11.00	12.00	13.00	14.00	15.00	16.00	17.00	18.00	19.00	20.00
10	13.92	15.19	16.45	17.72	18.98	20.25	21.52	22.78	24.05	25.31
11	17.19	18.75	20.31	21.87	23.44	25.00	26.56	28.13	29.69	31.25
14	24.75	27.00	29.25	31.50	33.75	36.00	38.25	40.50	42.75	45.00
18	44.00	48.00	52.00	56.00	60.00	64.00	68.00	72.00	76.00	80.00

www.EngineeringEBooksPdf.com

TABLE 5.A.3
Spacing of Bars for Slab Reinforcement (in.²/ft)

	Bar No.								
Spacing (in.)	**3**	**4**	**5**	**6**	**7**	**8**	**9**	**10**	**11**
3	0.44	0.78	1.23	1.77	2.40	3.14	4.00	5.06	6.25
3.5	0.38	0.67	1.05	1.51	2.06	2.69	3.43	4.34	5.36
4	0.33	0.59	0.92	1.32	1.80	2.36	3.00	3.80	4.68
4.5	0.29	0.52	0.82	1.18	1.60	2.09	2.67	3.37	4.17
5	0.26	0.47	0.74	1.06	1.44	1.88	2.40	3.04	3.75
5.5	0.24	0.43	0.67	0.96	1.31	1.71	2.18	2.76	3.41
6	0.22	0.39	0.61	0.88	1.20	1.57	2.00	2.53	3.12
6.5	0.20	0.36	0.57	0.82	1.11	1.45	1.85	2.34	2.89
7	0.19	0.34	0.53	0.76	1.03	1.35	1.71	2.17	2.68
7.5	0.18	0.31	0.49	0.71	0.96	1.26	1.60	2.02	2.50
8	0.17	0.29	0.46	0.66	0.90	1.18	1.50	1.89	2.34
9	0.15	0.26	0.41	0.59	0.80	1.05	1.33	1.69	2.08
10	0.13	0.24	0.37	0.53	0.72	0.94	1.20	1.52	1.87
11	0.12	0.22	0.34	0.48	0.65	0.86	1.09	1.39	1.70
12	0.11	0.20	0.31	0.44	0.60	0.78	1.00	1.27	1.56
13	0.10	0.18	0.29	0.41	0.55	0.73	0.92	1.17	1.44
14	0.09	0.17	0.27	0.38	0.51	0.68	0.86	1.09	1.34
15	0.09	0.16	0.25	0.35	0.48	0.63	0.80	1.02	1.25
16	0.08	0.15	0.23	0.33	0.45	0.59	0.75	0.95	1.17
17	0.08	0.14	0.22	0.31	0.42	0.56	0.71	0.90	1.10
18	0.07	0.13	0.21	0.29	0.40	0.53	0.67	0.85	1.04

www.EngineeringEBooksPdf.com

TABLE 5.A.4
Values of Coefficients for Elastic Analysis of Reinforced Concrete Sections

$$\rho = \frac{A_s}{bd}, \quad n = \frac{E_s}{E_c}, \quad k = \sqrt{(n\rho)^2 + 2n\rho} - n\rho, \quad j = 1 - \frac{k}{3}, \quad f_c = \frac{M}{bd^2}\frac{2}{kj}$$

$n\rho$	k	j	$2/kj$	$n\rho$	k	j	$2/kj$	$n\rho$	k	j	$2/kj$
0.001	0.0437	0.9854	46.41	0.046	0.2608	0.9131	8.40	0.091	0.3452	0.8849	6.55
0.002	0.0613	0.9796	33.32	0.047	0.2632	0.9123	8.33	0.092	0.3467	0.8844	6.52
0.003	0.0745	0.9752	27.52	0.048	0.2655	0.9115	8.26	0.093	0.3482	0.8839	6.50
0.004	0.0855	0.9715	24.07	0.049	0.2679	0.9107	8.20	0.094	0.3497	0.8834	6.47
0.005	0.0951	0.9683	21.71	0.050	0.2702	0.9099	8.14	0.095	0.3511	0.8830	6.45
0.006	0.1037	0.9654	19.98	0.051	0.2724	0.9092	8.07	0.096	0.3526	0.8825	6.43
0.007	0.1115	0.9628	18.63	0.052	0.2747	0.9084	8.02	0.097	0.3540	0.8820	6.41
0.008	0.1187	0.9604	17.54	0.053	0.2769	0.9077	7.96	0.098	0.3554	0.8815	6.38
0.009	0.1255	0.9582	16.64	0.054	0.2790	0.9070	7.90	0.099	0.3569	0.8810	6.36
0.010	0.1318	0.9561	15.87	0.055	0.2812	0.9063	7.85	0.100	0.3583	0.8806	6.34
0.011	0.1377	0.9541	15.22	0.056	0.2833	0.9056	7.80	0.101	0.3597	0.8801	6.32
0.012	0.1434	0.9522	14.65	0.057	0.2854	0.9049	7.74	0.102	0.3610	0.8797	6.30
0.013	0.1488	0.9504	14.15	0.058	0.2875	0.9042	7.69	0.103	0.3624	0.8792	6.28
0.014	0.1539	0.9487	13.70	0.059	0.2895	0.9035	7.65	0.104	0.3638	0.8787	6.26
0.015	0.1589	0.9470	13.29	0.060	0.2916	0.9028	7.60	0.105	0.3651	0.8783	6.24
0.016	0.1636	0.9455	12.93	0.061	0.2936	0.9021	7.55	0.106	0.3665	0.8778	6.22
0.017	0.1682	0.9439	12.60	0.062	0.2956	0.9015	7.51	0.107	0.3678	0.8774	6.20
0.018	0.1726	0.9425	12.30	0.063	0.2975	0.9008	7.46	0.108	0.3691	0.8770	6.18
0.019	0.1769	0.9410	12.02	0.064	0.2995	0.9002	7.42	0.109	0.3705	0.8765	6.16
0.020	0.1810	0.9397	11.76	0.065	0.3014	0.8995	7.38	0.110	0.3718	0.8761	6.14
0.021	0.1850	0.9383	11.52	0.066	0.3033	0.8989	7.34	0.111	0.3731	0.8756	6.12
0.022	0.1889	0.9370	11.30	0.067	0.3051	0.8983	7.30	0.112	0.3744	0.8752	6.10
0.023	0.1927	0.9358	11.09	0.068	0.3070	0.8977	7.26	0.113	0.3756	0.8748	6.09
0.024	0.1964	0.9345	10.90	0.069	0.3088	0.8971	7.22	0.114	0.3769	0.8744	6.07
0.025	0.2000	0.9333	10.71	0.070	0.3107	0.8964	7.18	0.115	0.3782	0.8739	6.05
0.026	0.2035	0.9322	10.54	0.071	0.3125	0.8958	7.15	0.116	0.3794	0.8735	6.03
0.027	0.2069	0.9310	10.38	0.072	0.3142	0.8953	7.11	0.117	0.3807	0.8731	6.02
0.028	0.2103	0.9299	10.23	0.073	0.316	0.8947	7.07	0.118	0.3819	0.8727	6.00
0.029	0.2136	0.9288	10.08	0.074	0.3178	0.8941	7.04	0.119	0.3832	0.8723	5.98
0.030	0.2168	0.9277	9.94	0.075	0.3195	0.8935	7.01	0.120	0.3844	0.8719	5.97
0.031	0.2199	0.9267	9.81	0.076	0.3212	0.8929	6.97	0.121	0.3856	0.8715	5.95
0.032	0.2230	0.9257	9.69	0.077	0.3229	0.8924	6.94	0.122	0.3868	0.8711	5.94
0.033	0.2260	0.9247	9.57	0.078	0.3246	0.8918	6.91	0.123	0.3880	0.8707	5.92
0.034	0.2290	0.9237	9.46	0.079	0.3263	0.8912	6.88	0.124	0.3892	0.8703	5.90
0.035	0.2319	0.9227	9.35	0.080	0.3279	0.8907	6.85	0.125	0.3904	0.8699	5.89
0.036	0.2347	0.9218	9.24	0.081	0.3296	0.8901	6.82	0.126	0.3916	0.8695	5.87
0.037	0.2375	0.9208	9.14	0.082	0.3312	0.8896	6.79	0.127	0.3927	0.8691	5.86
0.038	0.2403	0.9199	9.05	0.083	0.3328	0.8891	6.76	0.128	0.3939	0.8687	5.84
0.039	0.2430	0.9190	8.96	0.084	0.3344	0.8885	6.73	0.129	0.3951	0.8683	5.83
0.040	0.2457	0.9181	8.87	0.085	0.3360	0.8880	6.70	0.130	0.3962	0.8679	5.82
0.041	0.2483	0.9172	8.78	0.086	0.3376	0.8875	6.68	0.131	0.3974	0.8675	5.80
0.042	0.2509	0.9164	8.70	0.087	0.3391	0.8870	6.65	0.132	0.3985	0.8672	5.79
0.043	0.2534	0.9155	8.62	0.088	0.3407	0.8864	6.62	0.133	0.3996	0.8668	5.77
0.044	0.2559	0.9147	8.54	0.089	0.3422	0.8859	6.60	0.134	0.4007	0.8664	5.76
0.045	0.2584	0.9139	8.47	0.090	0.3437	0.8854	6.57	0.135	0.4019	0.8660	5.75

(*Continued*)

www.EngineeringEBooksPdf.com

TABLE 5.A.4 (*Continued*)
Values of Coefficients for Elastic Analysis of Reinforced Concrete Sections

$$\rho = \frac{A_s}{bd}, \quad n = \frac{E_s}{E_c}, \quad k = \sqrt{(n\rho)^2 + 2n\rho} - n\rho, \quad j = 1 - \frac{k}{3}, \quad f_c = \frac{M}{bd^2}\frac{2}{kj}$$

$n\rho$	k	j	$2/kj$	$n\rho$	k	j	$2/kj$	$n\rho$	k	j	$2/kj$
0.136	0.4030	0.8657	5.73	0.181	0.4473	0.8509	5.25	0.36	0.5617	0.8128	4.38
0.137	0.4041	0.8653	5.72	0.182	0.4482	0.8506	5.25	0.37	0.5664	0.8112	4.35
0.138	0.4052	0.8649	5.71	0.183	0.4491	0.8503	5.24	0.38	0.5710	0.8097	4.33
0.139	0.4063	0.8646	5.69	0.184	0.4499	0.8500	5.23	0.39	0.5755	0.8082	4.30
0.140	0.4074	0.8642	5.68	0.185	0.4508	0.8497	5.22	0.40	0.5798	0.8067	4.28
0.141	0.4084	0.8639	5.67	0.186	0.4516	0.8495	5.21	0.41	0.5840	0.8053	4.25
0.142	0.4095	0.8635	5.66	0.187	0.4525	0.8492	5.20	0.42	0.5882	0.8039	4.23
0.143	0.4106	0.8631	5.64	0.188	0.4534	0.8489	5.20	0.43	0.5922	0.8026	4.21
0.144	0.4116	0.8628	5.63	0.189	0.4542	0.8486	5.19	0.44	0.5961	0.8013	4.19
0.145	0.4127	0.8624	5.62	0.190	0.4551	0.8483	5.18	0.45	0.6000	0.8000	4.17
0.146	0.4137	0.8621	5.61	0.191	0.4559	0.8480	5.17	0.46	0.6038	0.7987	4.15
0.147	0.4148	0.8617	5.60	0.192	0.4567	0.8478	5.17	0.47	0.6075	0.7975	4.13
0.148	0.4158	0.8614	5.58	0.193	0.4576	0.8475	5.16	0.48	0.6111	0.7963	4.11
0.149	0.4169	0.8610	5.57	0.194	0.4584	0.8472	5.15	0.49	0.6146	0.7951	4.09
0.150	0.4179	0.8607	5.56	0.195	0.4592	0.8469	5.14	0.50	0.6180	0.7940	4.08
0.151	0.4189	0.8604	5.55	0.196	0.4601	0.8466	5.13	0.51	0.6214	0.7929	4.06
0.152	0.4199	0.8600	5.54	0.197	0.4609	0.8464	5.13	0.52	0.6247	0.7918	4.04
0.153	0.4209	0.8597	5.53	0.198	0.4617	0.8461	5.12	0.53	0.6280	0.7907	4.03
0.154	0.4219	0.8594	5.52	0.199	0.4625	0.8458	5.11	0.54	0.6312	0.7896	4.01
0.155	0.4229	0.8590	5.50	0.200	0.4633	0.8456	5.11	0.55	0.6343	0.7886	4.00
0.156	0.4239	0.8587	5.49	0.205	0.4673	0.8442	5.07	0.56	0.6373	0.7876	3.98
0.157	0.4249	0.8584	5.48	0.210	0.4712	0.8429	5.03	0.57	0.6403	0.7866	3.97
0.158	0.4259	0.8580	5.47	0.215	0.4751	0.8416	5.00	0.58	0.6433	0.7856	3.96
0.159	0.4269	0.8577	5.46	0.220	0.4789	0.8404	4.97	0.59	0.6462	0.7846	3.94
0.160	0.4279	0.8574	5.45	0.225	0.4825	0.8392	4.94	0.60	0.6490	0.7837	3.93
0.161	0.4288	0.8571	5.44	0.230	0.4862	0.8379	4.91	0.61	0.6518	0.7827	3.92
0.162	0.4298	0.8567	5.43	0.235	0.4897	0.8368	4.88	0.62	0.6545	0.7818	3.91
0.163	0.4308	0.8564	5.42	0.240	0.4932	0.8356	4.85	0.63	0.6572	0.7809	3.90
0.164	0.4317	0.8561	5.41	0.245	0.4966	0.8345	4.83	0.64	0.6598	0.7801	3.89
0.165	0.4327	0.8558	5.40	0.250	0.5000	0.8333	4.80	0.65	0.6624	0.7792	3.87
0.166	0.4336	0.8555	5.39	0.255	0.5033	0.8322	4.77	0.66	0.6650	0.7783	3.86
0.167	0.4346	0.8551	5.38	0.260	0.5066	0.8311	4.75	0.67	0.6675	0.7775	3.85
0.168	0.4355	0.8548	5.37	0.265	0.5097	0.8301	4.73	0.68	0.6700	0.7767	3.84
0.169	0.4364	0.8545	5.36	0.270	0.5129	0.8290	4.70	0.69	0.6724	0.7759	3.83
0.170	0.4374	0.8542	5.35	0.275	0.5160	0.8280	4.68	0.70	0.6748	0.7751	3.82
0.171	0.4383	0.8539	5.34	0.280	0.5190	0.8270	4.66	0.71	0.6771	0.7743	3.81
0.172	0.4392	0.8536	5.33	0.285	0.5220	0.8260	4.64	0.72	0.6794	0.7735	3.81
0.173	0.4401	0.8533	5.33	0.290	0.5249	0.8250	4.62	0.73	0.6817	0.7728	3.80
0.174	0.4410	0.8530	5.32	0.295	0.5278	0.8241	4.60	0.74	0.6839	0.7720	3.79
0.175	0.4419	0.8527	5.31	0.300	0.5307	0.8231	4.58	0.75	0.6861	0.7713	3.78
0.176	0.4429	0.8524	5.30	0.310	0.5362	0.8213	4.54	0.76	0.6883	0.7706	3.77
0.177	0.4437	0.8521	5.29	0.320	0.5416	0.8195	4.51	0.77	0.6904	0.7699	3.76
0.178	0.4446	0.8518	5.28	0.330	0.5469	0.8177	4.47	0.78	0.6925	0.7692	3.75
0.179	0.4455	0.8515	5.27	0.340	0.5520	0.8160	4.44	0.79	0.6946	0.7685	3.75
0.180	0.4464	0.8512	5.26	0.350	0.5569	0.8144	4.41	0.80	0.6967	0.7678	3.74

www.EngineeringEBooksPdf.com

TABLE 5.A.5
Stress Limits for Prestressing Tendons

	Tendon Type		
Condition	**Stress-Relieved Strand and Plain High-Strength Bars**	**Low-Relaxation Strand**	**Deformed High-Strength Bars**
Pretensioning			
Immediately prior to transfer (f_{pbt})	$0.70f_{pu}$	$0.75f_{pu}$	—
At service limit state after all losses (f_{pe})	$0.80f_{py}$	$0.80f_{py}$	$0.80f_{py}$
Posttensioning			
Prior to seating—short-term f_{pbt} may be allowed	$0.90f_{py}$	$0.90f_{py}$	$0.90f_{py}$
At anchorages and couplers immediately after anchor set	$0.70f_{pu}$	$0.70f_{pu}$	$0.70f_{pu}$
Elsewhere along length of member away from anchorages and couplers immediately after anchor set	$0.70f_{pu}$	$0.74f_{pu}$	$0.70f_{pu}$
At service limit state after losses (f_{pe})	$0.80f_{py}$	$0.80f_{py}$	$0.80f_{py}$

Source: From *AASHTO LRFD Bridge Design Specifications*, Copyright © 2012 by American Association of State Highway and Transportation Officials, Washington, DC. Used by permission.

www.EngineeringEBooksPdf.com

TABLE 5.A.6
Temporary Tensile Stress Limits in Prestressed Concrete before Losses, Fully Prestressed Components

Bridge Type	Location	Stress Limit
Other than segmentally constructed bridges	In precompressed tensile zone without bonded reinforcement	N/A
	In areas other than the precompressed tensile zone and without bonded reinforcement	$0.0948\sqrt{f'_{ci}} \leq 0.2$ (ksi)
	In areas with bonded reinforcement (reinforcing bars or prestressing steel) sufficient to resist the tensile force in the concrete computed assuming an uncracked section, where reinforcement is proportioned using a stress of $0.5f_y$, not to exceed 30 ksi	$0.24\sqrt{f'_{ci}}$ (ksi)
	For handling stresses in prestressed piles	$0.158\sqrt{f'_{ci}}$ (ksi)
Segmentally constructed bridges	Longitudinal stresses through joints in the precompressed tensile zone	
	Joint with minimum bonded auxiliary reinforcement through the joints, which is sufficient to carry the calculated tensile force at a stress of $0.5f_y$, with internal tendons or external tendons	$0.0948\sqrt{f'_{ci}}$ maximum tension (ksi)
	Joints without the minimum bonded auxiliary reinforcement through the joints	No tension
	Transverse stresses through joints	$0.0948\sqrt{f'_{ci}}$ (ksi)
	For any type of joint	
	Stresses in other areas	
	For areas without bonded nonprestressed reinforcement	No tension
	In areas with bonded reinforcement (reinforcing bars or prestressing steel) sufficient to resist the tensile force in the concrete computed assuming an uncracked section, where reinforcement is proportioned using a stress of $0.5f_y$, not to exceed 30 ksi	$0.19\sqrt{f'_{ci}}$ (ksi)
	Principal tensile stress at neutral axis in web	$0.110\sqrt{f'_{ci}}$ (ksi)
	All types of segmental concrete bridges with internal and/or external tendons, unless the Owner imposes other criteria for critical structures	

Source: From *AASHTO LRFD Bridge Design Specifications*, Copyright © 2012 by American Association of State Highway and Transportation Officials, Washington, DC. Used by permission.

www.EngineeringEBooksPdf.com

TABLE 5.A.7
Tensile Stress Limits in Prestressed Concrete at Service Limit State after Losses Fully Prestressed Components

Bridge Type	Location	Stress Limit
Other than segmentally constructed Bridges	Tension in the precompressed tensile zone bridges assuming uncracked sections	
	For components with bonded prestressing tendons or reinforcement that are subjected to not worse than moderate corrosion conditions	$0.19\sqrt{f'_{ci}}$ (ksi)
	For components with bonded prestressing tendons or reinforcement that are subject to serve corrosive conditions	
	For components with unbonded prestressing tendons	$0.0948\sqrt{f'_{ci}}$ (ksi)
		No tension
Segmentally constructed bridges	Longitudinal stresses through joints in the precompressed tensile zone	
	Joint with minimum bonded auxiliary reinforcement through the joints, sufficient to carry the calculated longitudinal tensile force at a stress of $0.5f_y$; internal tendons or external tendons	$0.0948\sqrt{f'_{ci}}$ (ksi)
	Joints without the minimum bonded auxiliary reinforcement through the joints	No tension
	Transverse stresses through joints	$0.0948\sqrt{f'_{ci}}$ (ksi)
	Tension in the transverse direction in precompressed tensile zone	
	Stresses in other areas	
	For areas without bonded nonprestressed reinforcement	No tension
	In areas with bonded reinforcement (reinforcing bars or prestressing steel) sufficient to resist the tensile force in the concrete computed assuming an uncracked section, where reinforcement is proportioned using a stress of $0.5f_y$, not to exceed 30 ksi.	$0.19\sqrt{f'_c}$ (ksi)
	Principal tensile stress at neutral axis in web	
	All types of segmental concrete bridges with internal and/or external tendons, unless the Owner imposes other criteria for critical structures	$0.110\sqrt{f'_c}$ (ksi)

Source: From *AASHTO LRFD Bridge Design Specifications*, Copyright © 2012 by American Association of State Highway and Transportation Officials, Washington, DC. Used by permission.

REFERENCES

AASHTO. 1998. *Standard Specifications for Highway Bridges*, American Association of State Highways and Transportation Officials, Washington, DC.

AASHTO. 2010. *AASHTO LRFD Bridge Construction Specifications, 2010*, American Association State Highway and Transportation Officials, Washington, DC. *Prestressed Concrete Institute Journal*, 24 (4), 42–56.

AASHTO. 2012. *AASHTO LRFD Specifications for Highway Bridges*, American Association of State Highways and Transportation Officials, Washington, DC.

Abrahamson, E. 1989. "The first reinforced concrete bridge built in America celebrate 100 years", *California Builders and Engineers* (CB&E), July 3, p. 37.

Achneider, E.F. and Bhide, S. 2004. *LRFD of Cast-in-Place Concrete Bridges*, Portland Cement Association, Chicago, IL.

AISC. 2011. *Steel Construction Manual*, American Institute of Steel Construction, Chicago, IL.

ASCE. 2010. *Minimum Design Loads for Buildings and Other Structures*, ASCE Standard ASCE/SEI 7-10, American Society of Civil Engineers/Structural Engineering Institute, New York.

ASCENT. 1994. "Best Bridge Spanning 65-135 ft, Bridge 'Peñelas,' Queretaro City, Queretaro State, Mexico," *ASCENT* Fall 1994, p. 32.

www.EngineeringEBooksPdf.com

Barker, R.M. and Puckett, J.A. 2013. *Design of Highway Bridges: An LRFD Approach*, John Wiley & Sons, New York.

Bennison, P. 1987. "Repair and protection of concrete bridges," *in Concrete Bridge Engineering: Performance and Advances*, R.J. Cope, ed., Elsevier Applied Science, New York, pp. 107–141.

Cady, P.D. and Weyers, R.E. 1983. "Chloride penetration and deterioration of concrete bridge decks", *Journal of Cement and Concrete, Aggregates*, 5 (2), 81–87.

Castrodale, R.W., Kreger, M.E., and Burns, N.H. 1988. A study of pretensioned high-strength concrete girders in composite highway bridges—Design considerations, Research Report 381-4F, Project 3-5-84-381, Center of Transportation Research, University of Texas at Austin, Austin, TX, January.

Collins, M.P. and Mitchell, D. 1986. "A rational approach to shear design—The 1984 Canadian code provisions", *ACI Journal*, 83 (6), 925–933.

CRSI. 2009. *Manual of Standard Practice 2009*, 28th ed., Concrete Reinforcing Steel Institute, Schaumburg, IL, 2009.

CSA Standard A23.3. 1984 *Design of Concrete Structures for Buildings*, Canadian Standards Association, Rexdale, Ontario, Canada, 281 pp.

Batchelor, D.B., Hewitt, B.E., and Csagoly, P.F. 1978. "Investigation of fatigue strength of deck slabs of composite steel/concrete bridges", *Transportation Research Record 664*, Transportation Research Board, National Research Council, Washington, DC.

Durning, T.A. and Rear, K.B. 1993. "Braker Lena bridge—High-strength concrete in prestressed concrete girders", *PCI Journal*, 38 (3), 46–51.

Fang K.I. 1985. "Behavior of Ontario-type bridge deck on steel girders", PhD dissertation, University of Texas, Austin, TX, December 1985.

Fang, K.I., Worley, J., Burns, N.H., and Klingner, R.E. 1990. "Behavior of isotropic reinforced concrete bridge decks on steel girders", *Journal of Structural Engineering*, 116 (3), 659–678.

Fanous, F. 2005. "Performance of coated reinforcing bars in cracked bridge decks", *Journal of Bridge Engineering*, 10 (3), 255–261.

FHWA. 1992. "Corrosion detection in concrete bridge structures", *Demonstration Project 84*, Federal Highway Administration, Washington, DC.

Gaal, G.G., van der Veen, C., and Djoati, M.H. 2001. "Deterioration of Concrete Bridges in the Netherlands", in *Proceedings of the Ninth International Conference on Structural Faults and Repairs*, London, U.K.

Gerwick, B.C. Jr. 1993. *Construction of Prestressed Concrete Structures*, 2nd ed. John Wiley & Sons, New York.

Grafton, J. 1994. Pomeroy Corp., Petaluma, CA. *Personal Correspondence*.

Hirsch, T.J. 1978. "Analytical evaluation of Texas bridge rails to contain buses and trucks," *Research Report 230-2*, August, Texas Transportation Institute, Texas A&M University, College Station, TX.

Holowka, M., Dorton, R.A., and Csagoly, P.F. 1980. *Punching Shear Strength of Restrained Circular Slab*, Ministry of Transportation and Communication, Downsview, Ontario, Canada.

Jobse, H.J. 1987. Application of high-strength concrete for highway bridges—Executive summary, Publication No. FHWA/RD-87/079, Federal Highway Administration, Washington, DC, October.

Libby, J.R. and Perkins, N.D. 1976. *Modern Prestressed Concrete: Design Principles and Construction Methods*, Van Nostrand Reinhold, New York.

Lin, T.Y. 1963. *Design of Prestressed Concrete Structures*, 2nd ed., John Wiley & Sons, New York.

Loren, T.D., Cady, P.D., and Theisen, J.C. 1969. Durability of bridge deck concrete, Report 7, Pennsylvania State University, University Park, PA, p. 173.

Martin, L.D. 1977. "A rational method of estimating camber and deflection of precast prestressed concrete members," *Prestressed Concrete Institute Journal*, 22 (1), 100–108.

Mehta, P.K. 1986. *Concrete: Structure, Properties, and Materials*, Prentice Hall, Englewood Cliffs, New Jersey.

Mirza, A.S., Harzinkolas, M., and MacGregor, J. 1979. "Statistical description of strength of concrete", *Proceedings of the ASCE*, 105, ST6, 1021.

Mitchell, D., Collins, M., Bhide, S.B., and Rabbat, B.G. 2004. *AASHTO LRFD Strut-And-Tie Model: Design Examples*, Bulletin EB231, Portland Cement Association, Skokie, IL.

Morsch, E. 1909. *Concrete-Steel Construction*, McGraw-Hill, New York (English translation by E. P. Goodrich), 368 pp.

Naaman, A.E. 1982. *Prestressed Concrete Analysis and Design: Fundamentals*, McGraw-Hill Cos., New York.

Nawy, E.G. 1989. *Prestressed Concrete: A Fundamental Approach*, Prentice Hall, Englewood Cliffs, New Jersey.

Nawy, E.G. 2010. *Prestressed Concrete—A Fundamental Approach*, 5th ed., Prentice-Hall, Englewood Cliffs, NJ.

www.EngineeringEBooksPdf.com

Nilson, A.H. 1978. *Design of Prestressed Concrete*, 2nd ed., John Wiley & Sons, New York.

OHBDC. 1991. Ontario Highway Bridges Design Code. Highway Engineering Division, Ministry of Transportation and Communications, Toronto, Ontario, Canada.

PCI. 1981. *Reflections on the Beginning of Prestressed Concrete in America*, Prestressed Concrete Institute, Chicago, IL.

PCI. 2003. *Precast Prestressed Concrete Bridge Design Manual*, Precast/Prestressed Concrete Institute, Chicago, IL.

Podolny, W. Jr. and Muller, J. 1982. *Construction and Design of Prestressed Concrete Segmental Bridges*, John Wiley & Sons, New York.

PTI. 1985. *Post-Tensioning Manual*, 4th ed., Post-Tensioning Institute, Phoenix, AZ.

Rabbat, B.G., Takayanagi, T., and Russell, H.G. 1982. Optimized sections for major prestressed concrete bridge girders, Publication No. FHWA/RD-82/005, Federal Highway Administration, Washington, DC, February.

Ritter, W. 1899. *Die bauweise hennebique*, *Schweizerische Bauzeitung*, 33 (7), 59–61.

Roller, J.J., Martin, B.T., Russell, H.G., and Bruce, R.N. 1993. "Performance of prestressed high-strength concrete bridge girders", *PCI Journal*, 38 (3), 34–45.

Roller, J.J., Russell, H.G., Bruce, R.N., and Martin, B.T. 1995. "Long-term performance of prestressed high-strength concrete bridge girders", *PCI Journal*, 40 (6), pp. 48–58.

Schlaich, J., Shafer, K., and Jennewein, M. 1987. "Towards a consistent design of reinforced concrete structures", *PCI Journal*, 32 (3), 74–150.

Smith, J.L. and Virmani, Y.P. 1996. Performance of epoxy-coated rebars in bridge decks, Report, FHWA-RD-96-092, Federal Highway Administration, Washington, DC.

Sohanhgpurwala, A.A., Scannel, W.T., and Viarengo, J. 1997. Verification of effectiveness of epoxy-coated rebar, Project No. 94-05, Pennsylvania Department of Transportation.

Steinman, D.B. and Watson, S.R. 1957. *Bridges and their Builders*, Dover Publications, New York.

Taly, N. 1976. *Development and Design of Standardized Short Span Superstructural Bridge Systems*, Ph.D. Dissertation, Civil Engineering Department, West Virginia University, Morgantown, WV.

Taly, N. 1998. *Design of Modern Highway Bridges*, McGraw-Hill, New York.

Tokerud, R. 1979. "Precast prestressed concrete bridges for low-volume roads," *Prestressed Concrete Institute Journal*, 24 (4), 42–56.

Transportation Research Board, *Bridge Aesthetics Around the World*, Committee on General Structures, Subcommittee on Bridge Aesthetics, Transportation Research Board, Washington, DC.

www.EngineeringEBooksPdf.com

6 Slab–Steel Girder Bridges

6.1 INTRODUCTION

History was made when Abraham Darby III (1750–1791) built during 1776–1779 the world's first iron bridge at Coalbrookdale, England. This nearly semicircular arch bridge (Figure 6.1) with approximately 100 ft main span is still in service, albeit limited to only pedestrian traffic. In the United States, the first cast-iron bridge was an 80-ft span structure made up of five tubular arch ribs; it was built in 1836 by Richard Delafield (1798–1873) of the US Engineers Corps (Steinman and Watson 1957). However, the modern era in bridge building began in the United States with the construction (1868–1874) of the famed double-deck Eads Bridge (Figure 2.4) over the Mississippi in St. Louis, Missouri, which marked the first extensive use of structural steel in bridges. Steel bridges then became the most common type of highway structures built in the United States, and steel continued to dominate bridge construction until the advent of reinforced concrete and, later, prestressed concrete. The first major prestressed concrete bridge—the three-span (74, 160, 74 ft), cast-in-place, posttensioned Walnut Lane Memorial Bridge, Philadelphia, Pennsylvania—was built in 1951.

During the nineteenth and twentieth centuries, steel remained a material of choice all over the world for building truss, arch, and suspension bridges; the latter still remains domain of steel.

6.2 STRUCTURAL FORMS AND CHARACTERISTICS OF STEEL BRIDGES

6.2.1 Common Forms of Slab–Steel Beam Bridges

Variously referred to as *slab–steel beam*, *slab-stringer*, *slab–steel girder*, *steel bridges* represent the most type of short- and medium-span highway structures. Structurally, they consist of rolled steel beams, usually equally spaced transversely (i.e., parallel to traffic) to span the bridge (Figure 6.2) and a reinforced concrete deck. For longer spans, *plate girders* are used (Figure 6.3). Plate girders are simply *built-up steel beams* fabricated from two flange plates and a web plate, the webs being deeper than those available with the deepest rolled beams. The beams are typically transversely spanned by a cast-in-place reinforced concrete slab that serves as a bridge deck and provides lateral stability to the supporting beams. Diaphragms (discussed in Chapter 2) are provided at intermediate points and at the ends of the beams to provide lateral stability to the whole superstructure.

Depending on whether they are simple span or continuous, plate girder bridges are economically suitable for spans in the 100–200 ft range, although plate girder bridges with spans exceeding 950 ft have been built because of exceptional circumstances (after World War II) as discussed in the next section. Because of their ability to span large distances, they minimize clearance problems in traffic interchanges and complex multilevel overpasses. Steel plate girder bridges are particularly suitable for bridges curved in plan (Figure 6.4).

6.2.2 Orthotropic Steel Bridges

Spurred by the shortages of steel in the post–World War II years, German bridge engineers developed lightweight bridge decks that were not only very economical but also possessed excellent structural characteristics. Called *orthotropic bridges* (or *orthotropic steel deck bridges*), they are characterized by stiffened steel plate decks supported on longitudinal girders. The final form of the superstructure may be either a stiffened steel plate deck supported on longitudinal I-beams or on box beams. These bridge types evolved in Europe, primarily Germany, with the purpose of

www.EngineeringEBooksPdf.com

FIGURE 6.1 The first iron bridge, at Coalbrookdale, England. (Reproduced with permission from *Bridge Aesthetics Around the World*, Committee on General Structures, Subcommittee on Bridge Aesthetics, Transportation Research Board, Washington, DC. Copyright 1991 by Transportation Research Board.)

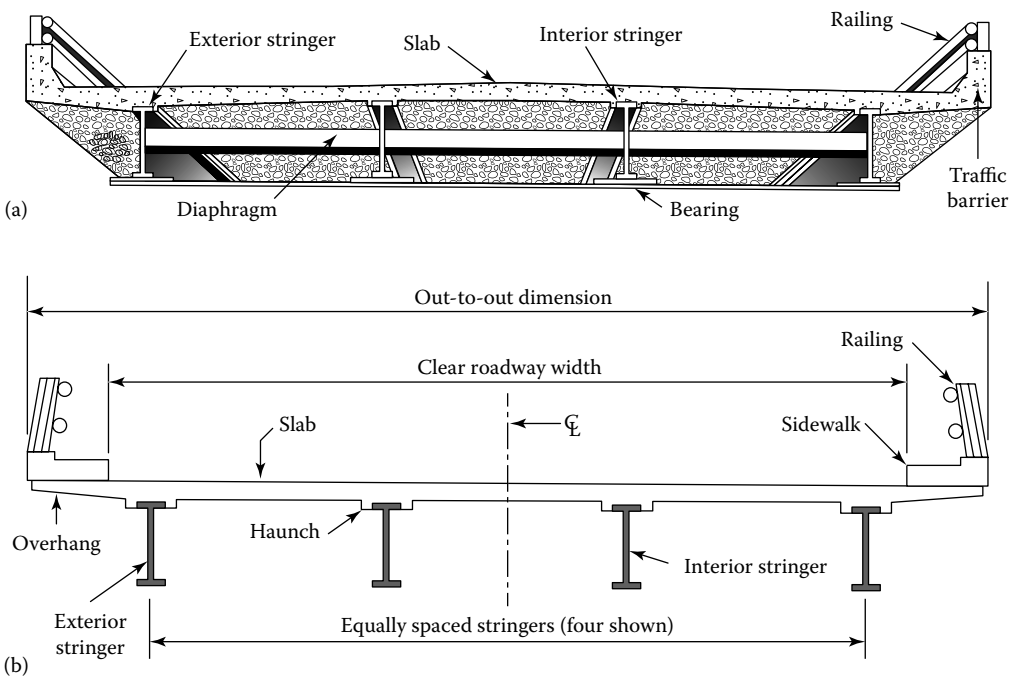

FIGURE 6.2 Typical slab–steel beam superstructure: (a) without a sidewalk and (b) with a sidewalk.

obtaining optimum structural performance from materials. With the exception of asphaltic wearing surface, orthotropic bridges can be regarded as true all-steel bridges (steel deck and the supporting structure). Figure 6.5 shows the cross section of a typical orthotropic deck (Wolchuk 1990).

Orthotropic bridges remain some of the most impressive spans built in the twentieth century, mostly in Europe. Some of the well-known orthotropic bridges are Wiesbaden–Schierstein Bridge (4206 ft, built 1959–1962), Germany; Dusseldorf–Neuss Bridge across Rhine, Germany (338-676-338 ft) built in 1951; Zoo Bridge, Koln, Germany (850 ft) built 1966; Charlotte Bridge, Luxemburg (768 ft) built in 1966; Auckland Harbor, New Zealand (800 ft) built in 1969; and Gazelle, Belgrade,

www.EngineeringEBooksPdf.com

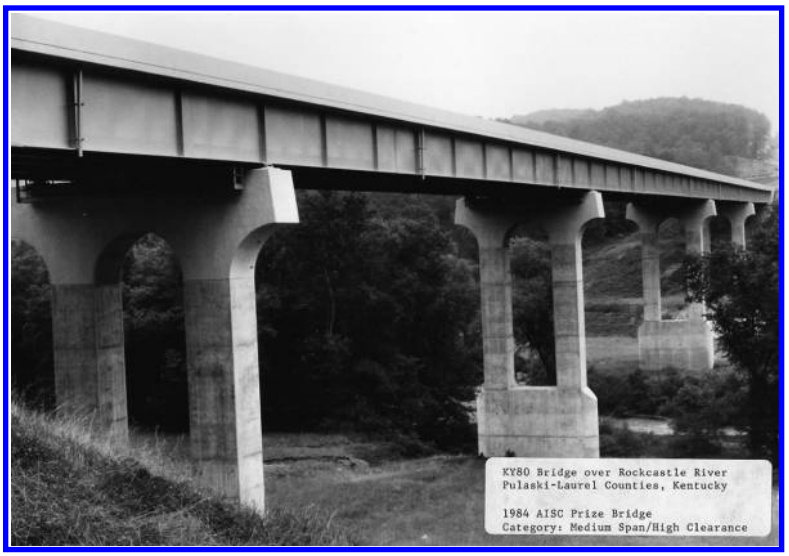

FIGURE 6.3 A typical plate girder bridge. (Courtesy of AISC, Chicago, IL.)

FIGURE 6.4 A curved steel plate girder railroad bridge (The Gulf Bridge, Lock, New York). (Courtesy of AISC, Chicago, IL.)

Yugoslavia (820 ft) built in 1970 (Trotsky 1967). The 7-mile long San Mateo–Hayward Bridge, across San Francisco Bay, California, has 5542 ft of orthotropic spans, making it the longest structure of this type ever built in the world. Built in 1967, a major section of this bridge comprises a 750 ft channel span with 575 ft side spans, flanked by six 292 ft spans on each end.

One of the most notable orthotropic steel bridges, also the world's largest plate girder structure, is the three-span (246, 856, and 246 ft) continuous highway bridge over the Save River (Sava I) in Belgrade, Yugoslavia, built in 1956. The depth of its haunched girders varies from 14 ft 9 in. at the midspan to 31 ft 6 in. at the piers (AISC 1963, Simpson 1970, O'Connor 1971). This bridge was built to replace a suspension bridge of equal spans built in 1930 which was destroyed in World War II. Interestingly, this plate girder bridge used 5200 tons as compared with 13,000 tons of steel (including weight of steel towers and cables) used for the suspension bridge which it replaced. The continuous Bonn-Beuel plate girder bridge (main span 643 ft) over the Rhine in Germany is another notable structure (AISC 1963).

Orthotropic bridges are outside the scope of this book and not discussed herein.

www.EngineeringEBooksPdf.com

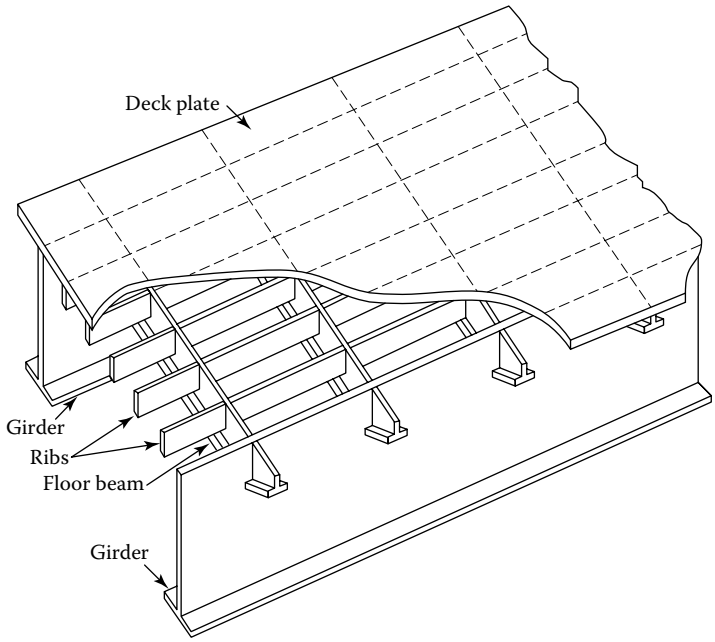

FIGURE 6.5 A typical steel orthotropic deck. (Adapted from Wolchuk 1990.)

Interestingly, in modern highway bridge construction practice for long, continuous spans, it is often advantageous to employ a combination of steel girder spans and prestressed concrete girder spans, particularly when bridges are curved. Figure 6.6 shows a curved, nine-span, continuous highway bridge under construction (September 2014) over Interstate 25, Albuquerque, New Mexico. The three approach spans at the west end, and the approach span at the south end of this bridge (the bridge curves from west to south), consist of simple, prestressed concrete girders (Figure 6.6), whereas the five intermediate spans consist of continuous steel plate girders (Figure 6.7).

6.2.3 Composite Steel Box Girder Bridges

Composite steel box girder bridges are suitable for single spans of 75 ft or longer or for continuous spans of 120 ft or longer. These are tubular bridge superstructures in which the bottom flange and the web are fabricated from steel plate and the deck is made from reinforced concrete (hence the term *composite*). As shown in Figure 6.8, a box girder may be a single-cell, twin-cell, or multiple-cell structure (also referred to as a structure with *multicellular deck*). Alternatively, a steel box girder may have two or more separate closed cross sections with reinforced concrete deck (also known as *multispine bridge*). The webs of box girders may be vertical or inclined; the latter gives the advantage of narrower bottom flange. The top flange widths are usually large—wide enough to provide the required bearing surface for the concrete deck supported on them as well as for placement of shear connectors necessary to develop composite action. Figure 6.9 shows a typical steel box girder highway bridge in service.

Box girder bridges offer several advantages. Because of their closed cross sections, they possess high torsional rigidity and strength compared with an equal number of open cross sections such as rolled beams or plate girders. Their high torsional strength makes them especially suitable for curved bridges that are inherently subjected to torsional moments. Consequently, they are preferred for grade separation structures in urban areas. The inclined webs of a box girder give the bridge an aesthetically pleasing appearance, often a reason for selecting a composite box girder bridge. Figure 6.10 shows the 806 ft, three-span (248, 310, 248 ft) Whitebird Canyon Bridge, which is a slant-leg, trapezoidal box girder bridge. Design of box girder bridges is outside the scope of this book.

www.EngineeringEBooksPdf.com

FIGURE 6.6 A nine-span, curved, prestressed concrete girder and steel plate girder combination highway bridge over Interstate-25 under construction in Albuquerque, New Mexico (September 2014). The photo shows six spans beginning at the west end of the bridge. The three west-end approach spans and the south-end approach span are simply supported by precast, prestressed concrete bulb-T girders. The intermediate five spans consist of continuous, curved steel plate girders. (See details in Figure 6.7a–c.)

(a)

(b)

(c)

FIGURE 6.7 (a) West-end approach spans of the continuous bridge shown in Figure 6.6. The end three spans (the first two shown in this photo) are precast, prestressed concrete bulb-T girder spans. (b) South end of the bridge showing the precast, prestressed concrete girder approach span. (c) An intermediate, five-span, continuous, curved steel plate girder bridge superstructure under construction.

www.EngineeringEBooksPdf.com

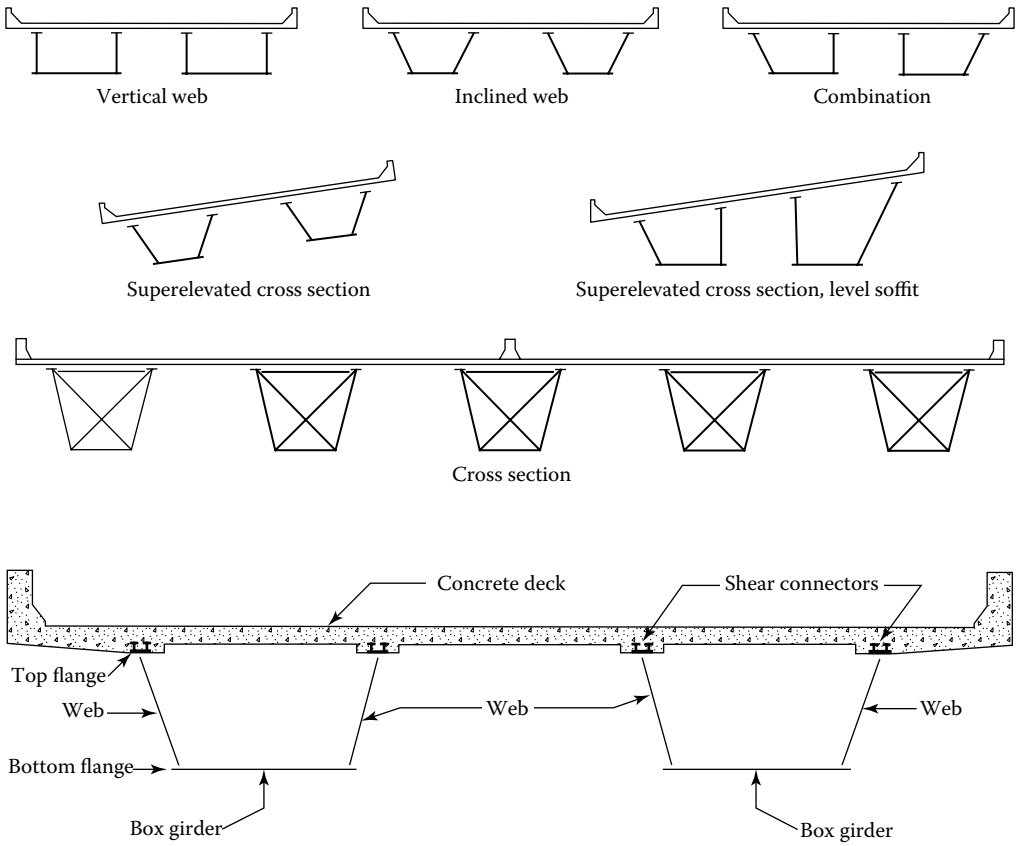

FIGURE 6.8 Configurations of steel box girder bridges.

FIGURE 6.9 A typical steel box girder highway bridge in service. (Courtesy of AISC, Chicago, IL.)

www.EngineeringEBooksPdf.com

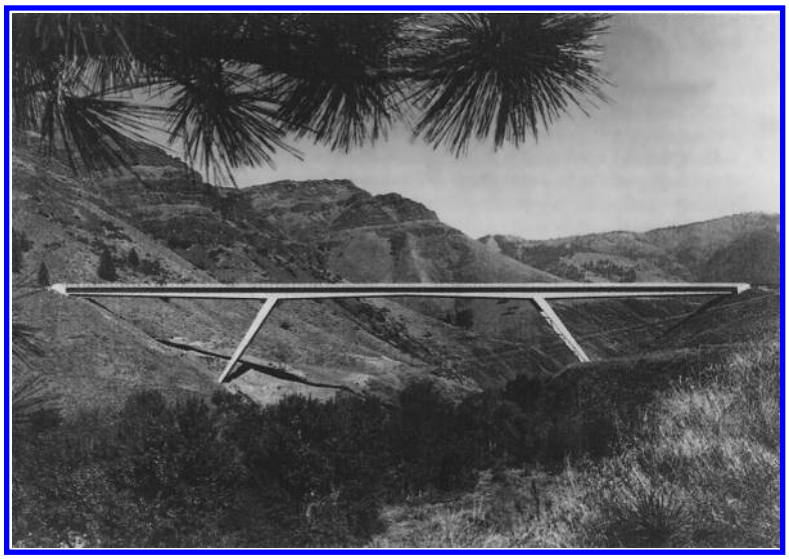

FIGURE 6.10 The three-span (248, 310, 248 ft), slant-leg Whitebird Canyon Bridge (built 1975) in the state of Idaho (USA). (Courtesy of Idaho Department of Transportation, Boise, ID.)

6.2.4 Delta Frame Steel Bridges

Delta frame bridges are essentially *rigid frame structures* that consist of superstructures supported on vertical or slanted monolithic legs (columns). They are considered economically suitable for moderate medium-span lengths. Figure 6.11a through c show details of delta frame bridges. For analytical purposes, delta frame bridges may be treated similar to two-hinged or fixed arches. The only difference is that instead of generally accepted form of continuous smooth curve of an arch axis, a rigid frame bridge with inclined legs has an arch axis that is trapezoidal in form, and one with vertical legs has a rectangular form. Delta frame bridges are not discussed in this book.

The remainder of this chapter is devoted to a detailed discussion of design of noncomposite and composite slab-beam bridges suitable for short spans.

6.3 CORROSION OF STEEL BRIDGES

Corrosion is a notorious problem associated with steel bridges. The problem is particularly acute with steel bridges that are not maintained properly. Corrosion-resistant steel may be used to mitigate the corrosion problem.

The accumulation of salt and water is considered the primary cause of corrosion of steel in highway bridges. The source of water and salt is either leakage from the deck or the accumulation of road spray and condensation. Kayser and Nowak (1987, 1989) have identified five main forms of corrosion that can affect steel:

1. General corrosion
2. Pitting corrosion
3. Galvanic corrosion
4. Crevice corrosion
5. Stress corrosion

The components of a bridge can be affected by more than one form of corrosion.

www.EngineeringEBooksPdf.com

(a)

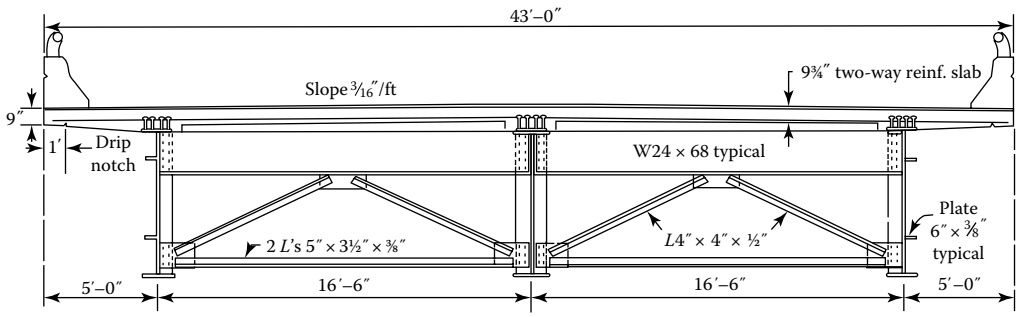

(b)

(c)

FIGURE 6.11 (a) A multi-span welded delta-frame bridge on I-64 near Lexington, VA. (Courtesy of Bethlehem Corporation, Easton, PA.) (b) Cross section of delta-frame bridge shown in Figure 6.11a. (c) Delta-section of a welded delta-frame bridge shown in Figure 6.11a.

www.EngineeringEBooksPdf.com

FIGURE 6.12 An extremely corroded steel stringer supporting an open steel deck of a steel through-truss bridge (inspected by the author). The corroded web of the stringer is clearly visible; a portion of the web has crumbled and disappeared resulting in loss of cross-sectional area and load-carrying capacity.

FIGURE 6.13 An extremely corroded floor beam in a steel through truss bridge of Figure 6.12 (inspected by the author). Note that a bottom portion of the corroded web has crumbled and disappeared resulting in loss of cross-sectional area and load-carrying capacity.

General corrosion, the most prevalent form of corrosion, refers to the general loss of surface material over time, leading to gradual thinning of members. This form of corrosion accounts for the largest percentage of corrosion. In some cases, over time, this type of corrosion can be extreme resulting in the loss of members' cross-sectional area and load-carrying capacity (Figures 6.12 and 6.13).

Pitting corrosion also causes loss of material, although it is localized and restricted to small areas. Pits can be characterized as rolled-in imperfections that can be dangerous, for they inconspicuously extend into the metal. Their presence in high-stress regions becomes a source of stress concentration.

Galvanic corrosion occurs when two dissimilar metals, for example, steels with different chemical compositions, are electrochemically coupled, for example, in welded or bolted connections,

www.EngineeringEBooksPdf.com

in which the bolt metal is different from the weld metal. Mill scale (surface scale or iron oxide that forms on structural steel after hot rolling) can galvanically encourage corrosion of the underlying base metal.

Crevice corrosion refers to corrosion that occurs in small confined areas, such as peeling paint, between faying surfaces, or at pit locations.

Stress corrosion refers to tensile loading of metal in a corrosive environment. An existing crack on a metal's surface spreads gradually under repetitive loading. However, formation of rust at the crack tip accelerates this spreading of the crack. For mild carbon steel in ordinary bridge environments, stress corrosion is usually not a problem. However, corrosion fatigue has been identified as a corrosion problem (Kayser and Nowak 1989). It is a phenomenon that is actually a combination of pitting corrosion, crevice corrosion, and stress corrosion. This phenomenon was believed to be the cause of the sudden collapse of the Point Pleasant Bridge in West Virginia on December 15, 1967 (NTSB 1968, Fisher 1984, Kayser 1988). This bridge had been built in 1927.

The effect of corrosion is the reduction in the fatigue life of a metal. Case studies of bridge collapses due to fatigue and fracture have been discussed by Fisher (1988). A brief summary of corrosion effects on steel bridge has been provided by Taly (1998).

6.4 CONSTRUCTION CONSIDERATIONS

Issues pertaining to constructibility of bridges are briefly addressed in AASHTO LRFD Article 2.5.3 (AASHTO 2012). These issues should include, but not limited to, the considerations of the following:

1. Deflection
2. Strength of steel and concrete
3. Stability during construction

Bridges should be designed in a manner such that fabrication and erection can be performed without undue difficulty or distress and that locked-in construction force effects are within acceptable limits.

By its very nature, bridge design focuses on completed structure in service. But bridges are in their most vulnerable state during construction, which designers might not be aware of. Stability of superstructure during construction is a major issue. Structures are particularly vulnerable to failure during erection because stiffening elements—for example, deck slabs (or floor slabs in buildings) and bracing—may not be in place. In addition, the structure's strength may be reduced when certain connections are partially bolted or not fully welded to permit precise alignment of members. It is incumbent on a designer to build a constructible bridge. A lack of understanding of the behavior of a bridge during construction can lead to disastrous consequences (Figure 6.14).

Art. 6.10.1.1 specifies load and resistance factor design (LRFD) provisions for investigating stability and strength, during construction, of I-section flexural members built using commonly used unshored construction. For this purpose, appropriate load combinations specified in Table 3.4 should be used. All checks are to be made for steel section only under the factored load $DC1$. For these checks, the value of η (combined load modifier) may be conservatively taken as 1.0. The changes to load, stiffness, and bracing during the stages of deck-casting sequence should be considered in these checks. However, in the examples presented in this chapter, it is assumed that the entire deck would be cast in one sequence; therefore, no separate analysis for deck casting is required.

As stated in LRFD Commentary C6.10.1, for a majority of straight, nonskew bridges, flange lateral bending effects tend to be most significant during construction and tend to be insignificant in the final constructed condition. By far, the most critical state of a steel superstructure occurs during construction when, prior to hardening of the deck, the girders are braced by only the diaphragms

www.EngineeringEBooksPdf.com

FIGURE 6.14 Collapse of the Brazos River Bridge, Brazos, Texas, during erection of the 973 ft, continuous steel plate girders that support the roadway. The failure was initiated by overstress of the connections between the web and flange during erection. (Courtesy of Simpson, Gumpertz, and Heger, Inc.)

or cross frames at discrete points along the span, which leaves compression flanges prone to lateral-torsional buckling (LTB). Significant lateral bending of the compression flange during construction may be caused by several factors including, but not limited to

1. Wind
2. From torsion
3. From eccentric concrete deck overhang loads acting on cantilever forming brackets placed along the exterior girders
4. Use of discontinuous cross frames (i.e., not forming a continuous line between multiple girders)

Constructibility criteria and related design provisions and required checks for I-section bridges are discussed and illustrated by examples later in this chapter.

6.5 MECHANICAL PROPERTIES OF STEEL FOR HIGHWAY BRIDGES

Mechanical properties of steel for highway bridges are specified in LRFD Art. 6.4. Structural steel is required to conform to Table 6.A.1. Design is to be based on the minimum properties indicated in that table, which specifies steel of various grades by AASHTO Material Specifications (AASHTO 2014) as well as equivalent ASTM Specifications (ASTM 2014). The term *yield strength* is used in these specifications as a generic term to denote either the minimum specified yield point or minimum specified yield strength. Detailed information about these specifications is provided in commentary to Art. 6.4.1 (see Art. C6.4.1). Minimum mechanical properties of pins, rollers, and rockers (by size and strength) are listed in Table 6.A.2.

www.EngineeringEBooksPdf.com

The following design properties shall be used for all grades of structural steel used in design:

Modulus of elasticity of steel: $E = 29{,}000$ ksi
Coefficient of thermal expansion = 6.5×10^{-6} in./in./°F

6.6 HYBRID STEEL GIRDERS

A *hybrid girder* is a girder fabricated from two different grades of steels, typically with a web of lower-grade steel and one or both flanges of higher-grade steel.

Specifications for design of hybrid girders are covered in LRFD Art. 6.10.1.3. Hybrid girders are required to meet the following minimum requirements:

1. The minimum yield strength of the web should not be less than the larger of 70 percent of specified minimum yield strength of the higher-strength flange and 36 ksi.
2. For members with higher-strength steel in one or both flanges, the yield strength of the web shall not be taken greater than 120 percent of the specified minimum yield strength of the lower strength flange in determining the flexural and shear resistance.
3. Composite girders in positive flexure with a higher-strength steel in the web than in the compression flange may use the full web strength in determining their flexural and shear resistance.

It is recommended that the difference in the specified minimum yield strengths of the web and higher-strength flange preferably be limited to one steel grade. Such girders are believed to possess greater design efficiency.

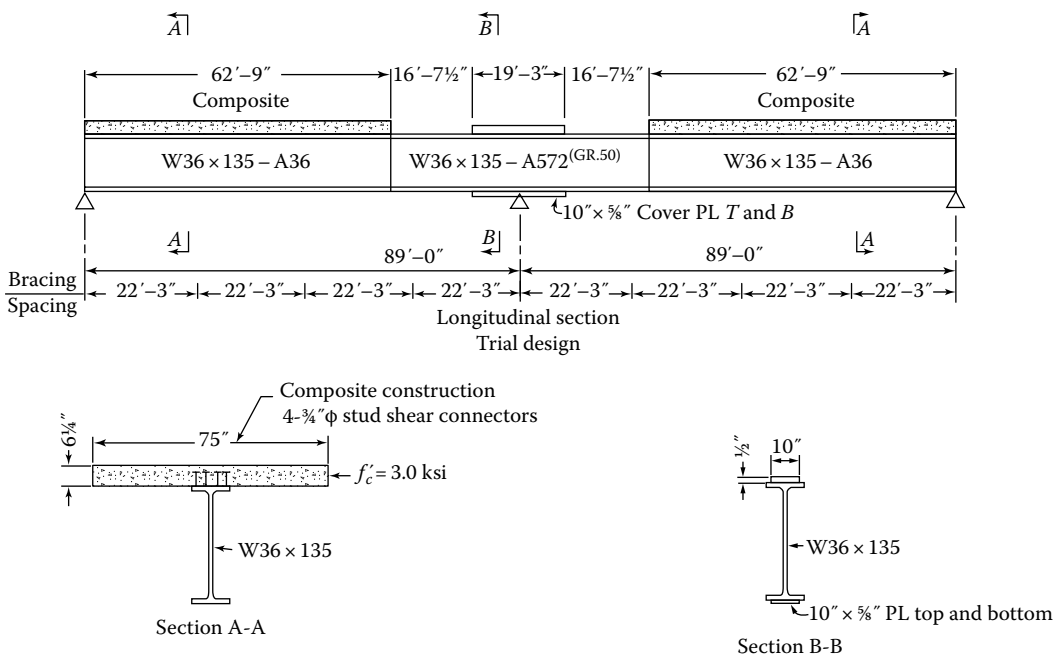

FIGURE 6.15 Use of rolled beams of different grade steels along a bridge span. (Courtesy of Breen, F.L., Load factor design of W-beams, in *Four Design Examples, Load Factor Design of Steel Highway Bridges*, T.J. Moon, Y.I. Gonulsen, and A.P. Bezzone, ed., AISI Pub. 123(PSB010), American Iron and Steel Institute, New York.)

www.EngineeringEBooksPdf.com

The concept of hybrid girders is advantageously used for built-up steel girders, where a designer has the freedom of designing individual elements (flanges and the web) from the same or different grades of steel. In some cases, it may be economically advantageous to design a continuous rolled beam by welding together two rolled shapes of the same size but of different grades. The basic idea behind this scheme is to use higher-grade steel in the area of higher moments while maintaining the same overall girder depth for the entire span instead of a haunched girder (characterized by larger depth at the intermediate support where the moment and shear are higher and smaller girder depth in span where these forces are smaller). Such a scheme for a continuous steel beam bridge is shown in Figure 6.15. Here, a W36 × 135 (ASTM A36, F_y = 36 ksi, F_u = 58 ksi) has been used for positive moment and the same section (W36 × 135) of higher-grade steel (A572, F_y = 50 ksi, F_u = 65 ksi) for negative moment at the support, which is greater than the maximum positive moment in the span (Breen 1972).

Another technique of fabricating hybrid girders consists of welding WTs of higher-grade steel to a web of lower-grade steel (because flanges are required to resist a greater portion of the applied moment than that by the web, elastic stresses are greater in the flange than in the web). Figure 6.16 shows a few details for the cantilevered superstructure of Whisky Creek Bridge, California (an old bridge designed according to AASHTO Standard using allowable stress design). Note that the girder web consists of three different grades of steel.

Design of hybrid girders is beyond the scope of this book. A comprehensive discussion of hybrid girder can be found in ASCE-AASHTO (1968).

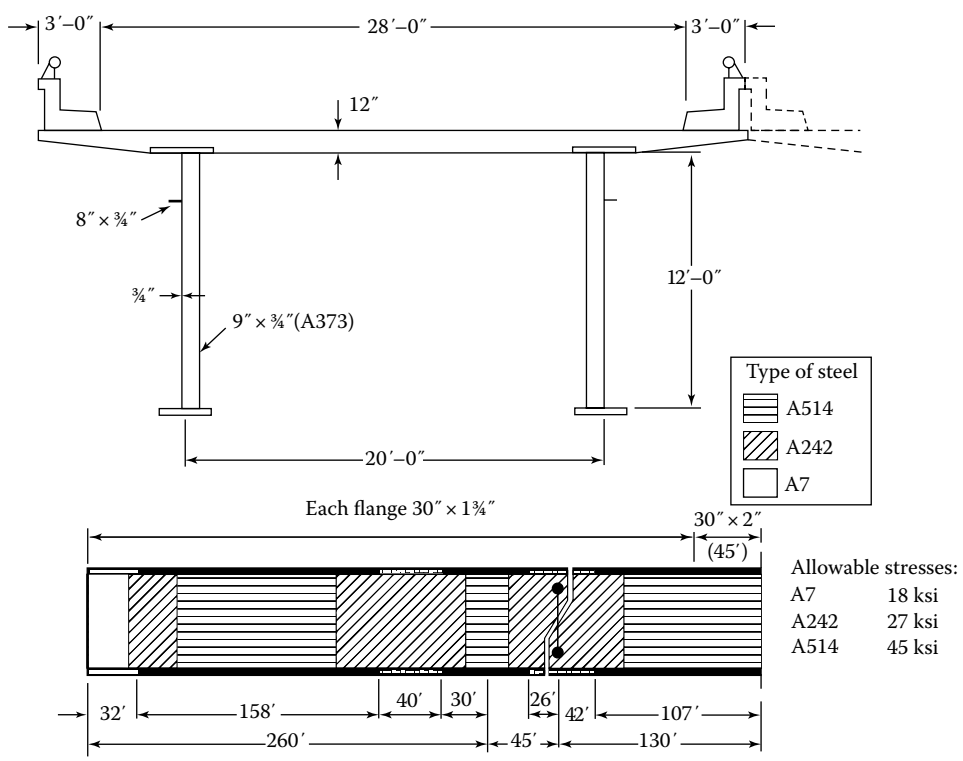

FIGURE 6.16 Details of the hybrid girder of the three-span, cantilevered Whisky Creek Bridge, California: (top) bridge elevation, (middle) cross section of superstructure, (bottom) details of the left half of the hybrid plate girder (note the three different grades used for the web).

www.EngineeringEBooksPdf.com

6.7 NONCOMPOSITE AND COMPOSITE SECTIONS

6.7.1 Noncomposite Sections

The basic layout for a slab–steel girder bridge consists of a concrete deck slab supported over steel beams. In one of the simplest types of this construction scheme, the deck is *not* physically connected to the girders by shear connectors, it merely sits on them and transfers loads by bearing on them. No mechanism exists in this scheme to transfer longitudinal shear from the primary load-bearing members (beams or girders) to the deck. Steel girders in this case are so designed that they alone carry the entire gravity load on the bridge. This is called *noncomposite construction* and the girder sections so designed are referred to as *noncomposite sections*.

Noncomposite sections are not recommended because they are relatively uneconomical as compared to composite sections, but they are permitted by LRFD Specifications. Example 4.2 presents design of a noncomposite highway superstructure.

6.7.2 Composite Sections

In another type of construction, top flanges of steel girders are provided with *shear connectors* that are welded to the top flanges of the girders and embedded in the bottom of the concrete deck during pouring. The dead load of the deck is resisted by the steel girders alone, by bearing. After the concrete hardens, subsequent loads (superimposed dead load and the live load) on the superstructure are resisted by the girders and the deck acting as a unit. This type of construction is called *composite construction*, and the girder section so designed is referred to as *composite section*. Additionally, the shear connectors provide lateral resistance to the supporting girders. Design of shear connectors is illustrated in Example 6.1.

6.7.3 Section Properties of Noncomposite and Composite Sections

Section properties of noncomposite sections (bare steel sections) are listed in American Institute of Steel Construction (AISC)'s Steel Construction Manual (AISC 2011) from which they can be readily obtained for computational purposes.

Section properties and flexural strength of composite sections are calculated based on the following parameters:

1. Compressive strength of concrete (f_c')
2. Effective width of concrete deck slab (b_e)
3. Grade (yield strength) and area of longitudinal reinforcement (oriented parallel to the longitudinal axis of the beam)
4. Girder size and grade of steel (usually F_y = 50 ksi, except for hybrid girders)

Many design calculations involving composite sections (e.g., stresses, deflections) are based on elastic behavior of the composite beams. This requires calculations of such section properties as location of (elastic) neutral axis, moment of inertia, and section modulus (top and bottom of the steel girder). Of necessity, the sections properties of composite sections must be calculated twice: one for the short-term composite action of the girder and the other for the long-term composite action of the girder; the latter is required to account for the effects of *creep*. These two sets of section properties are referred to, respectively, as the *short-term section properties* and the *long-term section properties*. For example, the long-term section properties are used to calculate deflections due to permanent loads to account for creep, whereas the short-term section properties are used to calculate deflection due to transient loads (live load).

The determination composite section properties are based on the principle of *transformed section*. This is necessary because a composite cross section is not made of homogeneous material (conventional flexure formula, $f = Mc/I$, can be used only for sections of homogeneous materials). When designing a

www.EngineeringEBooksPdf.com

composite steel section, all sectional areas other than steel (reinforced concrete in the context of present discussion) are transformed into equivalent area of steel. For example, in the case of concrete slab–steel girder composite section, the area of concrete section would be transformed into equivalent area of steel. This is done by dividing the *effective width of flan*ge (b_e, discussed in Section 6.13.3, Art. 4.6.2.6) by the modular ratio, n (Section 4.7.2.1.1, values shown in Table 4.4); the resulting width is called *transformed effective width of flange* ($b_{e,tr}$) and determined as follows:

1. To calculate the properties of the short-term composite section, the effective width is divided by the modular ratio, n.
2. To calculate the properties of the long-term composite section, the effective width is divided by three times the modular ratio, $3n$.

In both cases, the thickness of the effective flange remains the same as the thickness of the deck slab. Calculations for both short-term and long-term section properties are illustrated in Examples 6.8 and 6.10.

Just to reiterate the aforementioned concepts and avoid confusion, we have defined two terms related to *width* of a flange of a composite section (different from the width of the top flange of steel girder, b_c or b_f): (1) effective width of flange, b_e, which is used for computing the plastic moment strength of composite sections (Examples 4.3 through 4.7) and (2) transformed effective width of flange, $b_{e,tr}$, which is used to calculate the elastic section properties of a composite section.

6.8 SHORED AND UNSHORED CONSTRUCTION

6.8.1 Sequence of Loading during Construction

As stated earlier, the slab–steel beam type of superstructure consists of usually equally spaced steel beams that support a concrete deck. The sequence of loading during construction influences magnitude of elastic stresses in the beams. In the examples that follow, it is assumed that the deck is cast in one operation by continuous pouring of concrete, so stresses due to sequence of loading are not considered in design. That said, this underlying design assumption should be clearly documented on the construction drawings for the attention of the contractor.

The superstructure construction can be *shored* or *unshored*, described as follows.

6.8.2 Shored Construction

In the shored construction, the beams are installed between the end supports and supported at intermediate points by temporary shores placed at close intervals. The temporary shores supposedly keep the beams in almost undeformed (level, practically no deflection) condition. When the deck concrete is poured, the beams support dead load due to their own weight as well as the weight of the freshly poured deck concrete. Because the beams are supported at close intervals, it is assumed that they do not develop any stresses due either to their own dead weight or the fresh concrete. The temporary shores are removed after sufficient hardening of concrete occurs, following which the beam develops composite action, and all loads—permanent, superimposed loads, and the live load—are assumed to be resisted by the composite girder section. A concrete deck may be assumed to have sufficiently hardened after the concrete attains 75 percent of its specified 28-day compressive strength, f'_c.

While shored construction is permitted according to LRFD Specifications, its use is not recommended because unshored construction is supposedly more economical. Research on the effects of creep on composite beams under large loads is limited as there have been no known significant demonstration bridges built in the United States. Shored composite bridges that are known to have been built in Germany did not retain composite action (LRFD Commentary C6.10.1.1.1a). Also, there is an increased likelihood of significant tensile stresses occurring in the concrete deck at the permanent support points when shored construction is used, an undesirable condition.

www.EngineeringEBooksPdf.com

6.8.3 Unshored Construction

In the unshored construction, the beams are installed between the end supports, and concrete is poured. Until the concrete hardens, the loads due to dead weight of the beams and concrete are resisted by the steel section alone. Permanent loads and live load applied after hardening of concrete are assumed to be resisted by the composite section.

6.9 RESISTANCE FACTORS

One of the parameters associated with the LRFD is the so-called resistance factor, denoted as ϕ. The significance of resistance factor in the context of LRFD was discussed in Chapter 1. Its values depend on the type of force in the member or the connector. In contrast with the AISC-recommended resistance factors used in design of steel buildings, there are far too many resistance factors to be used in bridge design as specified in LRFD Art. 6.5.4.2:

- For flexure, $\phi_f = 1.00$
- For shear, $\phi_v = 1.00$
- For axial compression, steel only $\phi_c = 0.90$
- For axial compression, composite $\phi_c = 0.90$
- For tension, fracture in net section $\phi_u = 0.80$
- For tension, yielding in gross section $\phi_y = 0.95$
- For bearing on pins in reamed, drilled or bored holes and on milled surfaces $\phi_b = 1.00$
- For bolts bearing on material $\phi_{bb} = 0.80$
- For shear connectors $\phi_{sc} = 0.85$
- For A 325 and A 490 bolts in tension $\phi_t = 0.80$
- For A 307 bolts in tension $\phi_t = 0.80$
- For F 1554 bolts in tension $\phi_t = 0.80$
- For A 307 bolts in shear $\phi_s = 0.75$
- For F 1554 bolts in shear $\phi_s = 0.75$
- For A325 and A 490 bolts in shear $\phi_s = 0.80$
- For block shear $\phi_{bs} = 0.80$
- For shear, rupture in connection element $\phi_{vu} = 0.80$
- For web crippling $\phi_w = 0.80$
- For weld metal in complete penetration welds:
  - Shear on effective area $\phi_{e1} = 0.85$
  - Tension or compression normal to effective area same as base metal
  - Tension or compression parallel to axis of weld same as base metal
- For weld metal in partial penetration welds:
- Shear parallel to axis of weld $\phi_{e2} = 0.80$
  - Tension or compression parallel to axis of weld same as base metal
  - Compression normal to the effective area same as base metal
  - Tension normal to the effective area $\phi_{e1} = 0.80$
- For weld metal in fillet welds:
  - Tension or compression parallel to axis of weld same as base metal
  - Shear in throat of weld metal $\phi_{e2} = 0.80$
- For resistance during pile driving $\phi = 1.00$
- For axial resistance of piles in compression and subject to damage due to serve driving conditions where use of a pile tip is necessary:
  - H-piles $\phi_c = 0.50$
  - Pipe piles $\phi_c = 0.60$

www.EngineeringEBooksPdf.com

- For axial resistance of piles in compression under good driving conditions where use of a pile tip is not necessary:
  - H-piles $\phi_c = 0.60$
  - Pipe piles $\phi_c = 0.70$
- For combined axial and flexural resistance of undamaged piles:
  - Axial resistance for H-piles $\phi_c = 0.70$
  - Axial resistance for pipe piles $\phi_c = 0.80$
  - Flexural resistance $\phi_f = 1.00$
- For shear connectors in tension $\phi_{st} = 0.75$

6.10 DESIGN PROVISIONS FOR I-SECTION FLEXURAL MEMBERS

6.10.1 General

6.10.1.1 General Format for LRFD Specifications for Steel Superstructures

I-sections are the most commonly used flexural members used for building slab–steel beam highway bridges. General provisions for the design of I-section flexural members are specified in LRFD Art. 6.10. These provisions apply to flexure of both rolled and fabricated (i.e., built-up girders such as plate girders); straight, kinked (chorded), or continuous; or horizontally curved steel I-section members symmetrical about the vertical axis through the web. They also apply to the design of noncomposite and composite sections, hybrid and nonhybrid sections, and constant and variable depth members.

As a rule, all structural designs should conform to the minimum requirements specified by AISC, which are discussed in books on structural steel design. But bridges are different from buildings in many respects. For one, the loads on buildings are static (except crane loads in industrial buildings), whereas those on bridges are both static *and* dynamic (vehicular loads including impact). For this reason, steel bridges must conform to specific design requirements specified by LRFD Specifications that are discussed and illustrated by several examples in the remainder of this chapter.

LRFD Art. 6.10 provides detailed design requirements for the design of I-shaped flexural members, which are the most commonly used type of steel sections. General requirements for the design of I-section flexural members are stated in Art. 6.10.1, which specifies that all types of I-section flexural members must be designed to satisfy, as a minimum, the following requirements:

1. The cross-section proportion limits specified in Art. 6.10.2
2. The constructibility requirements specified in Art. 6.10.3 (Figure 6.17)
3. The service limit state requirements specified in Art. 6.10.4 (Figure 6.18)
4. The fatigue and fracture limit state requirements specified in Art. 6.10.5 (Figure 6.19)
5. The strength limit state requirements specified in Art. 6.10.6 (Figure 6.20)

The aforementioned five items of Art. 6.10.1 indicate the overarching organization of subsequent provisions for the design of straight-section flexural members specified in LRFD Specification in Section 6. Each sub-article of Art. 6.10 is written in a self-contained manner. For strength limit state, Art. 6.10 further directs a designer to Art. 6.10.7 through Art. 6.10.12 and, optionally for straight I-sections only, to Appendices A and B. The significance of these provisions lies in the fact that they must be complied with in all steel superstructure designs using I-sections as illustrated in several examples presented in this chapter. The specific provisions of these articles and their intent are discussed in the corresponding Articles of the Commentary to LRFD Specifications. Design flowcharts to follow for compliance with Items 2 through 5 are shown in Figures 6.17 through 6.20. A thorough reading of these articles would be helpful for understanding the discussion presented in this chapter.

www.EngineeringEBooksPdf.com

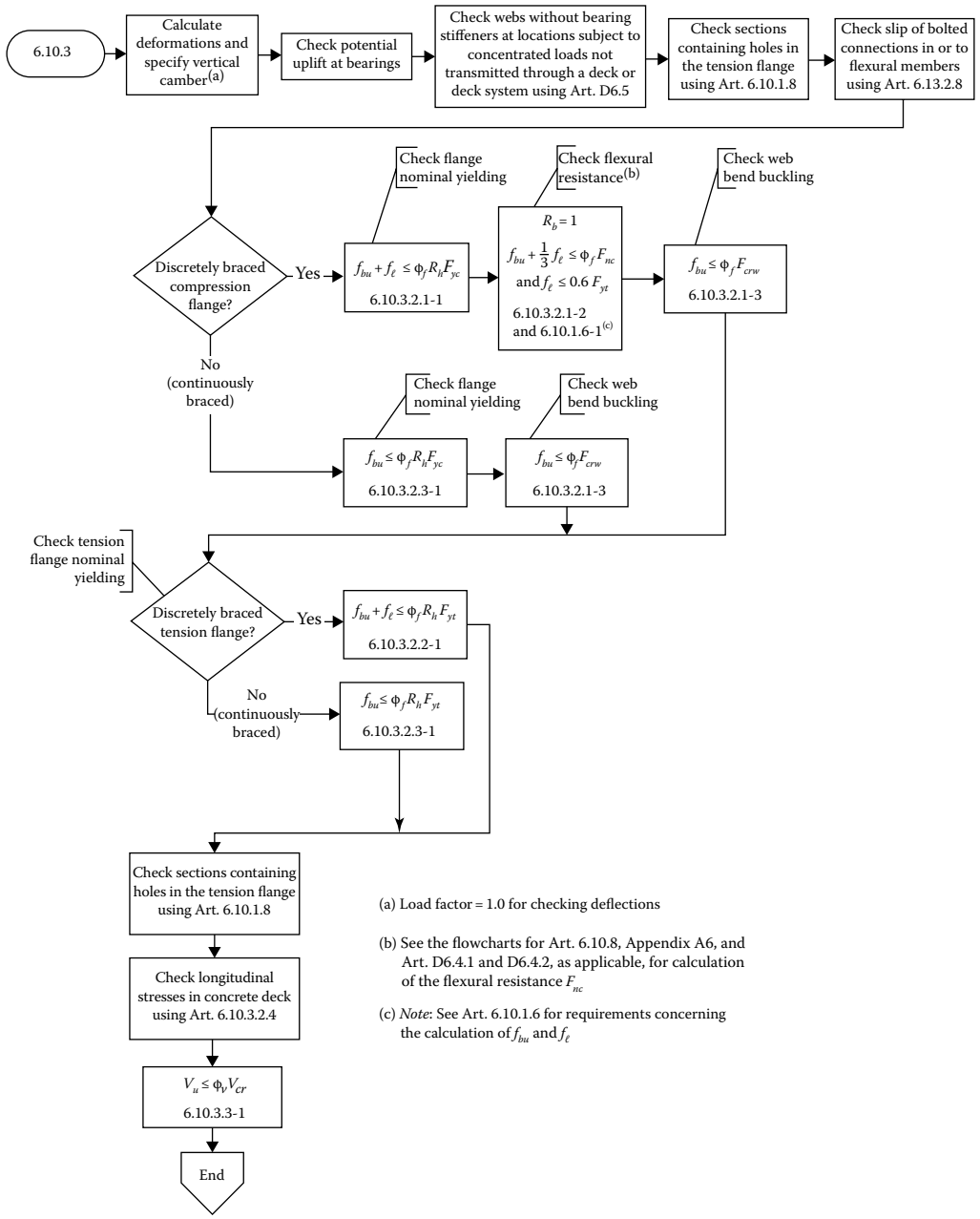

FIGURE 6.17 Flowchart for LRFD Art. 6.10.3—constructibility (LRFD Figure C6.4.1-1). (From *AASHTO LRFD Bridge Design Specifications*, Copyright © 2012 by American Association of State Highway and Transportation Officials, Washington, DC. Used by permission.)

Additionally, the steel superstructure should satisfy the following requirements:

6. Cross frames and diaphragms for I-sections shall satisfy the provisions of Art. 6.7.4.
7. Where required, lateral bracings for I-sections shall satisfy the provisions of Art. 6.7.5.

Various design requirements I-shaped flexural members are discussed in the following several sections.

www.EngineeringEBooksPdf.com

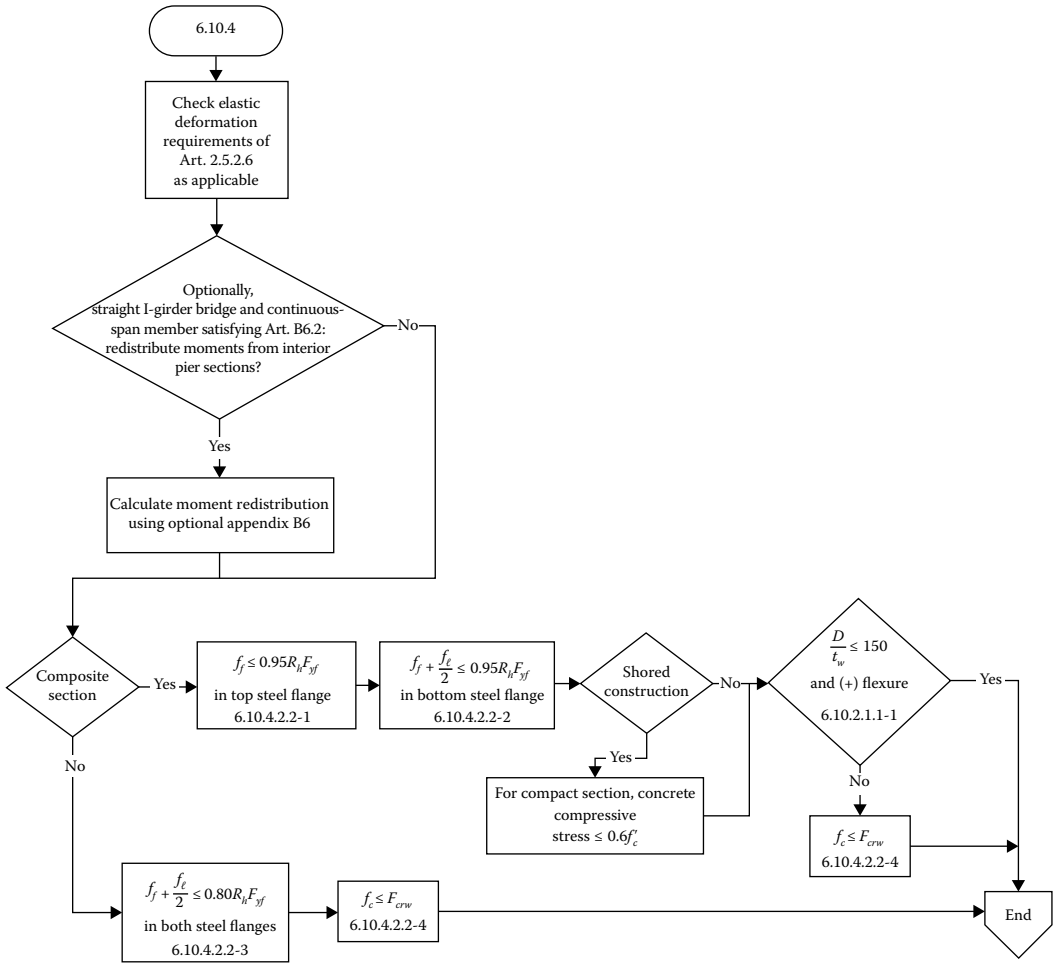

FIGURE 6.18 Flowchart for LRFD Art. 6.10.4—service limit state (LRFD Figure C6.4.2-1). (From *AASHTO LRFD Bridge Design Specifications*, Copyright © 2012 by American Association of State Highway and Transportation Officials, Washington, DC. Used by permission.)

It should be noted at the outset that various compliance equations specified in LRFD Specifications and discussed in the following sections are in terms of *stresses* rather than in terms of *moments*. As explained in LRFD Commentary C10.6.1, the intent of this approach is to emphasize the fact that the maximum resistance is always less than or equal to yield moment M_y in major-axis bending. This implicitly is due to the nature of the many different types of loadings that contribute to the member flexural stresses: noncomposite, short-term composite, and long-term composite. From a designer's perspective, the combined effects of loadings on these different states of member cross sections are better handled with flange stress rather than moments. Also, practically speaking, a bridge designer is typically more used to working with stresses rather than moments (apparently due to familiarity with the allowable stress design and working stress design). Therefore, although the provisions can be written equivalently in terms of bending moments, the provisions of various LRFD articles are written in terms of stresses whenever the maximum potential resistance in terms of f_{bu} (the largest value of the compressive stress throughout the unbraced length under consideration, calculated without consideration of lateral flange bending stress) is less than or equal to the yield stress, F_y. This is an important difference from AISC Specifications for steel structures in which design equations are specified in terms of moments.

www.EngineeringEBooksPdf.com

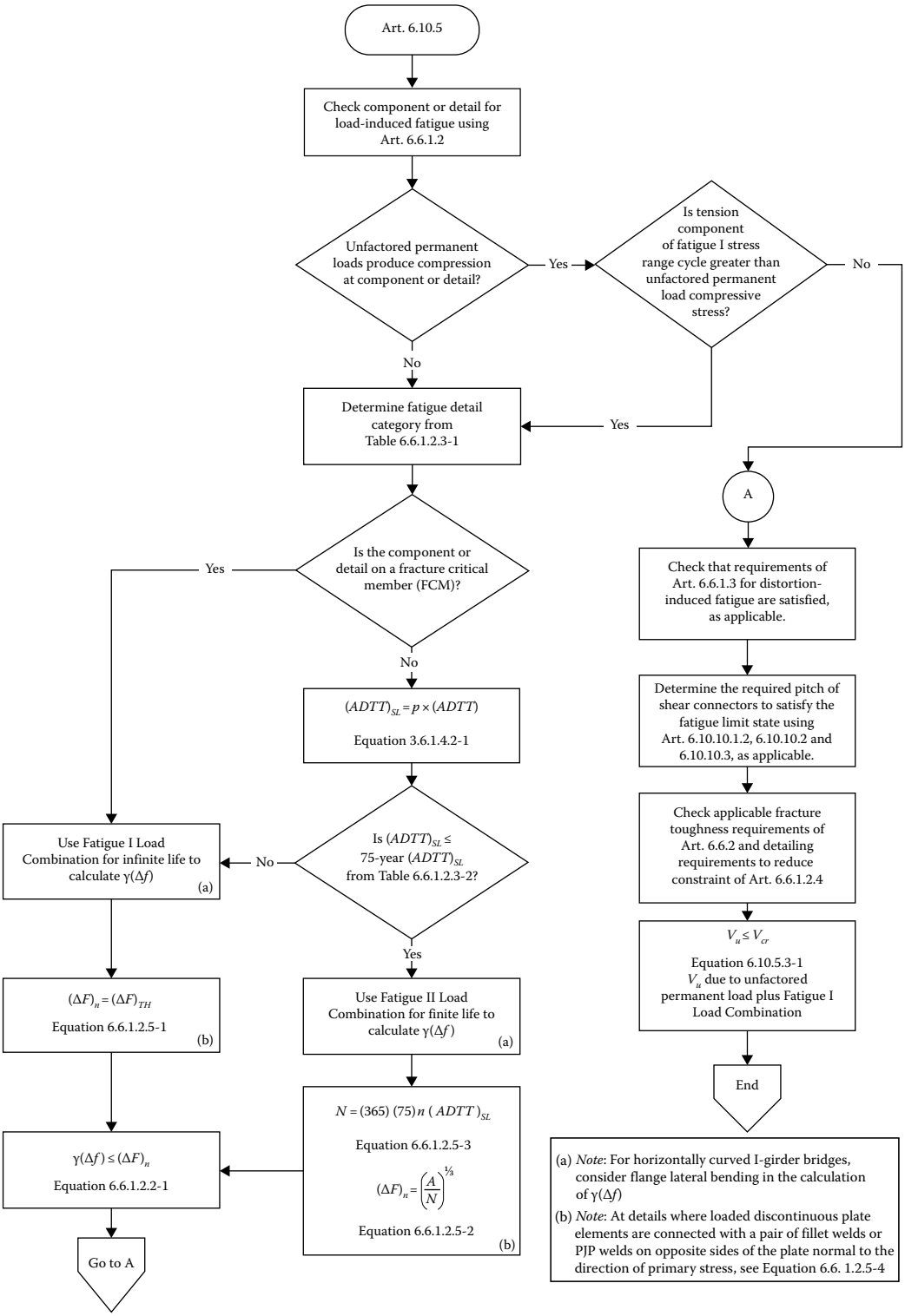

FIGURE 6.19 Flowchart for Art. 6.10.5—fatigue and fracture limit state (LRFD Figure C6.4.3-1). (From *AASHTO LRFD Bridge Design Specifications*, Copyright © 2012 by American Association of State Highway and Transportation Officials, Washington, DC. Used by permission.)

www.EngineeringEBooksPdf.com

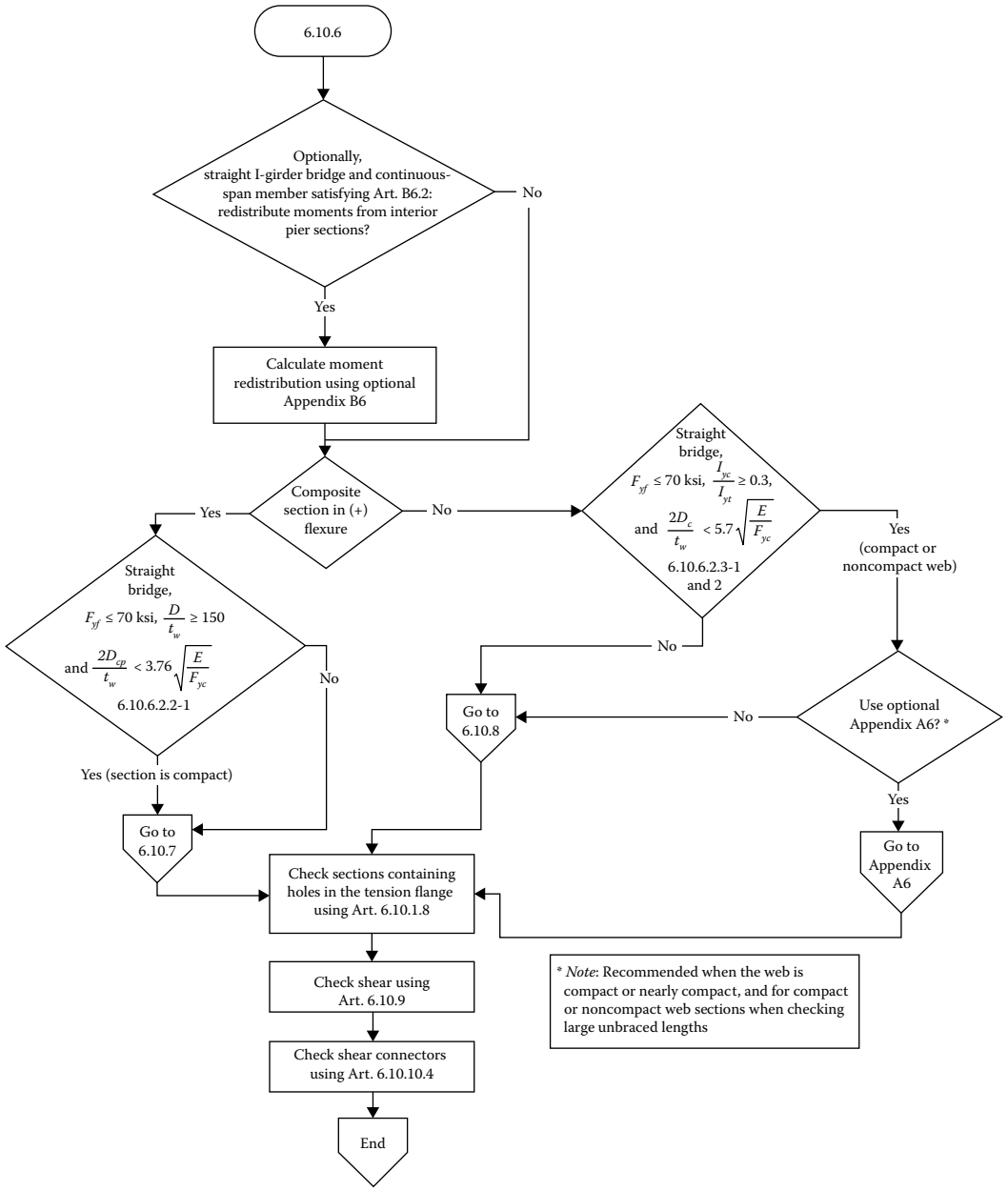

FIGURE 6.20 Flowchart for LRFD Art. 6.10.6—strength limit state (LRFD Figure C6.4.4-1). (From *AASHTO LRFD Bridge Design Specifications*, Copyright © 2012 by American Association of State Highway and Transportation Officials, Washington, DC. Used by permission.)

LRFD Commentary C6.10.1 presents an instructive reading regarding the numerous equations presented in Section 6 of LRFD Specifications. Many of these equations are different from those of the previous specifications, but that *does not imply that that existing bridges are unsafe or are deficient. It also does not mandate the need to rehabilitate or perform new load rating of existing structures to satisfy these provisions*. Rather, these new equations simply reflect the state-of-the-art as well as more desirable formats.

www.EngineeringEBooksPdf.com

6.10.1.2 Sequence of Loading and Elastic Stresses

The elastic stresses at any location on the composite section due to the applied loads should be taken as the sum of the stresses caused by the loads applied separately to

1. Steel section (stresses caused by permanent loads)
2. Short-term composite section (stresses caused by transient or live loads)
3. Long-term composite action (stresses due to permanent loads applied after hardening of concrete, to account for creep)

For transient loads assumed applied to the short-term composite action, the concrete deck area is transformed by using the *short-term modular ratio*, n. For permanent loads assumed applied to the long-term composite section, the concrete deck area is transformed by using the *long-term modular ratio*, $3n$ (to account for the effects of *creep*).

A discussion on the concept of modular ratio has been presented in Section 4.7.2.1.1. For steel structures, the modular ratio is defined by Equation 4.7R (the letter R following 4.7 stands for *repeated*, indicating that this is Equation 4.7 repeated from Chapter 4). Values of n corresponding to different values of compressive strength of concrete, f_c', are given in Table 4.4.

$$n = \frac{E_s}{E_c} \tag{4.7}$$

In the case of unshored construction, permanent load applied *before* concrete deck has hardened or is made composite is assumed to be carried by the steel section alone; permanent loads and live load applied after this stage are assumed to be resisted by the composite action. For shored construction, all permanent loads are assumed applied *after* the concrete has hardened and section has been made to act as composite. As a major advantage of composite construction, there are no compression flange slenderness or compression flange bracing requirements for composite section in positive flexure at the strength limit state because the compression flange is assumed to be adequately (continuously) braced against lateral-torsional buckling by the hardened concrete.

Many practical situations can arise during construction. In some cases of construction, the concrete deck may not be poured in one single operation. As a consequence, parts of the girders may become composite in sequential stages. If certain deck pouring sequences are followed, the temporary moments induced in girders during deck placement can be considerably higher than the final noncomposite dead load moments after the sequential placement of the deck concrete is complete. Such situations should be properly accounted for in design.

6.10.1.3 Flange-Strength Reduction Factors

Fundamentally speaking, in the context of steel beam design, unbraced length L_p is defined as the limiting unbraced length to achieve the nominal flexural resistance M_p (plastic moment) under uniform bending. In LRFD Specifications, L_p is defined as the limiting unbraced length to achieve the nominal flexural resistance $R_h R_b F_{yc}$, where R_h and R_b are *flange-strength reduction factors* (Art. 6.10.1.10) defined as follows and discussed in Section 6.10.1.3.1:

R_h = hybrid factor
R_b = web-shedding factor
F_{yc} = minimum yield strength of compression flange

Flange-strength reduction factors are used as modifiers to the nominal flexural strength of flanges of I-beams to account for their reduced strength owing to a variety of reasons as discussed herein. The two modifiers, R_h and R_b, are used as follows.

www.EngineeringEBooksPdf.com

6.10.1.3.1 Hybrid Factor, R_h (LRFD Art. 6.10.1.10-1)

The R_h factor accounts for the reduced contribution of the web to the normal flexural resistance at first yield in any flange element and due to earlier yielding of the lower strength steel in the web of a hybrid section. In this context, the term *flange element* is defined as a flange or cover plate or the longitudinal reinforcement. For most common types of I-girders (rolled shapes, built-up sections, and hybrid sections with a higher-strength steel in the web than in both flanges, Figure 6.14), R_h is to be taken as 1.0 (Art. 6.10.1.10).

As specified in Art. C6.10.3.2.1, for sections that are composite in the final condition but are noncomposite during construction, different values of hybrid factor, R_h, must be calculated for checks in which the member is noncomposite and in which the member is composite.

Art. 6.10.1.10.1 specifies a method for the determination of R_h, which is to be used in lieu of an alternative analysis. Art. C6.10.1.10.1 suggests that computed values of R_h by any approach are typically close to unity.

6.10.1.3.2 Web Load-Shedding Factor, R_b (LRFD Art. 6.10.1.10.2)

The R_b factor represents a post-buckling strength reduction factor that accounts for nonlinear variation of stresses subsequent to local bend buckling of slender webs. This factor accounts for the reduction in the section flexural resistance caused by shedding of compressive stresses from a slender web and corresponding increase in the flexural stress in the compression flange.

For any of the following conditions, the value of R_b factor shall be taken as 1.0:

1. When checking constructibility according to Art. 6.10.3.2.
2. When the section is composite and is in positive flexure and the web satisfies the requirements of Art. 6.10.2.1.1 or Art. 6.11.2.1.2, as applicable
3. When one or more horizontal stiffeners are provided and the web satisfies Equation 6.1

$$\frac{D}{t_w} \le 0.95\sqrt{\frac{Ek}{F_{yc}}} \qquad (6.1)\ [A6.10.1.10.2\text{-}1]$$

4. When the webs satisfy Equation 6.2, the value of R_b is taken as equal to 1.0:

$$\frac{2D}{t_w} \le \lambda_{rw} \qquad (6.2)\ [A6.10.1.10.2\text{-}2]$$

where λ_{rw} = limiting slenderness ratio for a noncompact web

$$= 5.7\sqrt{\frac{E}{F_{yc}}} \qquad (6.3)\ [A6.10.1.10.2\text{-}4]$$

For all other cases, R_b is to be taken as given by Equation 6.4:

$$R_b = 1 - \left(\frac{\alpha_{wc}}{1200 + 300\alpha_{wc}}\right)\left(\frac{2D_c}{t_w} - \lambda_{rw}\right) \le 1.0 \qquad (6.4)\ [A6.10.1.10.2\text{-}3]$$

www.EngineeringEBooksPdf.com

The value of coefficient α_{wc} in Equation 6.4 is determined as follows:

1. For composite longitudinally stiffened sections in positive sections, α_{wc} is determined from the following:

$$\alpha_{wc} = \frac{2D_c t_w}{b_{fc}t_{fc} + b_s t_s \left(1 - f_{DC1/F_{yc}}\right)/3n} \qquad (6.5)\ [A6.10.1.10.2\text{-}6]$$

2. For all other cases, α_{wc} is determined as the ratio of two times the web area in compression to the area of compression flange, expressed as given by Equation 6.6:

$$\alpha_{wc} = \frac{2D_c t_w}{b_{fc}t_{fc}} \qquad (6.6)\ [A6.10.1.10.2\text{-}5]$$

In the equations:
b_s = effective width of concrete deck (in.)
f_{DC1} = compressive flange stress at the section under consideration, calculated without consideration of flange lateral bending and caused by the factored permanent load before the concrete deck has hardened or is made composite (ksi), applied
k = bend-buckling coefficient for webs with longitudinal stiffeners determined as specified in Art. 6.10.1.9.2
t_s = thickness of concrete deck (in.)
D = clear distance between the flanges (in.)
D_c = depth of the web in compression in the elastic range (in.). For composite section, D_c is to be determined as specified in Art. D6.3.1
F_{yc} = specified minimum yield strength of compression flange
n = modular ratio

When calculating the nominal resistance of the compression flange for checking constructibility (Art. 6.10.3.2, see discussion in Section 6.10.3), R_b is to be taken as equal to 1.0. For composite sections in negative flexure and noncomposite sections that satisfy Equation 6.2 (A6.10.1.10.2-2), R_b is also taken equal to 1.0 since the web slenderness ratio, $2D_c/t_w$, is at or below the value at which the theoretical elastic bending stress is equal to F_{yc}.

Equation 6.2 also defines the slenderness limit for noncompact webs; webs exceeding this limit are termed *slender*.

Further discussion on R_b can be found in LRFD Commentary C6.10.1.10.2.

6.10.2 Cross-Section Proportion Limits

6.10.2.1 Minimum Metal Thickness (LRFD Art. 7.7.3)

As a rule, minimum thickness of all metal parts should conform to requirements of LRFD Art. 6.7.3, *Minimum Thickness of Metal*, which specifies the following requirements:

1. Structural steel, including bracing, cross frames, and all types of gusset plates, except for webs of rolled shapes, closed ribs in orthotropic decks, fillers, and in railings, shall not be less than 0.3125 in. (i.e., 5/16 in.) in thickness.
2. For orthotropic decks, the following minimum requirements apply:
   a. The web thickness of rolled beams or channels and of closed ribs in orthotropic decks shall not be less than 1/4 in.
   b. The deck plate thickness shall not be less than 5/8 in. or four percent of the larger spacing of the ribs.
   c. The thickness of closed ribs shall not be less than 3/16 in. (or 0.1875 in.).

www.EngineeringEBooksPdf.com

Additionally, where metal is expected to be exposed to severe corrosive environment, it shall be specially protected against corrosion, or sacrificial metal thickness shall be specified.

6.10.2.2 Web Proportion Limits (LRFD 6.10.2.1)

There are two requirements for initial proportioning of webs:

1. Webs without longitudinal stiffeners
2. Webs with longitudinal stiffeners

Longitudinal stiffeners are discussed in Section 6.11.

Webs *without* longitudinal stiffeners must satisfy Equation 6.7a:

$$\frac{D}{t_w} \leq 150 \qquad \text{(6.7a) [A6.10.2.1.1-1]}$$

Webs *with* longitudinal stiffeners must satisfy Equation 6.7b:

$$\frac{D}{t_w} \leq 300 \qquad \text{(6.7b) [A6.10.2.1.2-1]}$$

where

D = depth of the web, clear distance between flanges (in.)
t_w = thickness of the web (in.)

Equation 6.7a is a practical upper limit on the slenderness of webs without longitudinal stiffeners expressed in terms of the depth of the web, D. Likewise, Equation 6.7b is a practical upper limit on the slenderness of webs with longitudinal stiffeners expressed in terms of the depth of the web, D. Both equations allow for easier proportioning of webs (as applicable) for preliminary design. The limit in both equations is valid for sections with specified minimum yield strengths up to and including 100.0 ksi.

6.10.2.3 Flange Proportion (LRFD Art. 6.10.2.2)

Compression and tension flanges of the beam must be proportioned so as to satisfy Equations 6.8 through 6.11:

$$\frac{b_f}{2t_f} \leq 12 \qquad \text{(6.8) [A6.10.2.2-1]}$$

$$b_f \geq D/6 \qquad \text{(6.9) [A6.10.2.2-2]}$$

$$t_f \geq 1.1t_w \qquad \text{(6.10) [A6.10.2.2-3]}$$

$$0.1 \leq \frac{I_{yc}}{I_{yt}} \leq 10 \qquad \text{(6.11) [A6.10.2.2-4]}$$

where

b_f = width of flange
t_f = thickness of flange
I_{yc} = moment of inertia of the compression flange of the steel section about the vertical axis in the plane of the web
I_{yt} = moment of inertia of the tension flange of the steel section about the vertical axis in the plane of the web

www.EngineeringEBooksPdf.com

Equation 6.8 is a practical upper limit to ensure that the flange will not distort excessively when welded to the web. The aspect ratio D/b_f has been found to be a significant parameter affecting the strength and moment-rotation characteristics of I-sections; Equation 6.9 limits this ratio to a maximum value of 6. Equation 6.10 is intended to ensure that some restraint would be provided by flanges against web shear buckling and also that the boundary conditions assumed in the web bend-buckling and compression flange buckling formulations within LRFD specifications are sufficiently accurate. Equation 6.11 ensures more efficient proportions and prevents the use of sections that may be particularly difficult to handle during construction. Equation 6.11 also ensures the validity of the equations for $C_b > 1$ in cases involving moment gradients. Additionally, limits imposed by Equation 6.11 tend to prevent the use of extremely monosymmetric sections for which the larger of the yield moments, M_{yc} or M_{yt} may be greater than the plastic moment, M_p.

For composite construction, built-up girders are often used when suitable rolled sections cannot be found. For reasons of economics, the top (or compression) flanges of such girders usually are narrower than the bottom or tension flanges. As a result, more than half the web depth is typically in compression in the regions of positive flexure during construction. If the maximum moments produced during the deck placement sequence are not considered in design, these conditions, coupled with narrow top compression flanges, can lead to stability problems such as out-of-plane distortion of the girder compression flanges and the web. This situation can be avoided by selecting the top flange width to comply with Equation 6.12:

$$b_{fc} \geq \frac{L}{85} \qquad (6.12)\ [\text{A C6.10.3.4-1}]$$

where

b_{fc} = width of compression flange, in.
L = length of the girder shipping piece

It is noted that Equation 6.12 is merely a guideline, not an absolute requirement. It should be used in conjunction with Equation 6.9 ($b_f \geq D/6$) to establish a minimum required top width in positive moment regions of composite girders.

6.10.3 Constructibility Requirements (LRFD Art. 6.10.3)

6.10.3.1 General

Constructibility issues are of concern for all types of superstructures. These issues should include, but not limited to, considerations of deflection, strength of steel and concrete, and stability during critical stages of construction (Art. 2.5.3).

Regardless of whether the construction is noncomposite or composite, the girders should possess adequate strength to carry loads during construction, particularly during pouring of deck concrete. Girders are the main load-carrying members of a steel bridge superstructure. Art. 6.10.3.1 specifies that in addition to providing adequate strength, nominal yielding or reliance on post-buckling strength shall not be permitted for main load-carrying members during critical stages of construction, except for yielding of hybrid sections. To ensure that the girders possess the required strength, they must comply with the requirements of Arts. 6.10.3.2 and 6.10.3.3 at critical stages of construction. For sections in flexure that are composite in the final condition, but are noncomposite during construction, provisions of Art. 6.10.4 must be satisfied. Buckling of compression flange is a major concern during construction; therefore, it should be properly braced as discussed in Section 6.10.8.2.3.

For investigating constructibility of flexural members, all loads should be factored as specified in Art. 3.4.2. For the calculations of deflections, load factor shall be taken as 1.0.

www.EngineeringEBooksPdf.com

6.10.3.2 Dead Load Deflection and Camber

Dead and live deflections are calculated from the principles of structural mechanics using conventional formulas found in texts on mechanics of materials and structural analysis. Requirements for accounting for dead deflections are specified in Arts. 6.7.2 and 6.10.3.5, which must be satisfied when designing steel superstructures.

Steel superstructures, as other steel structures, should be cambered for dead load deflections and vertical alignment. The following dead deflection values/information should be provided in design documents:

1. Deflection due to steel weight and concrete weight should be reported separately.
2. Deflections due to future wearing surfaces (FWS) or other loads not considered at the time of construction should be reported separately.
3. Vertical camber shall be specified to account for the computed dead load deflection.
4. When staged construction is specified, the sequence of load application should be considered when determining the cambers. In this context, stage construction refers to the situation in which superstructures are built in separate longitudinal units with a longitudinal joint (it does not refer to the deck pouring sequence).

Requirements for cambering of straight skewed I-girder bridges and horizontally curved I-girder bridges are not discussed herein; readers should refer to LRFD Art. C6.7.2 for guidance on this topic.

6.10.3.3 Instability of I-Beams: The Lateral-Torsional-Buckling Phenomenon

Construction considerations were briefly discussed earlier in Section 6.4. It was pointed out that bridges are in their most vulnerable state during construction, stability of unbraced I-beams being a major issue. The compression flanges of the girders are not laterally supported until after the deck concrete has hardened, which renders them susceptible to LTB. This section presents a discussion of requirements for flexural members of I-shaped sections that must be satisfied during various stages of construction.

By design, rolled and built-up I-shaped beams possess much larger flexural rigidity in the plane of bending (i.e., bending *about* the strong- or x-axis) as compared to that about the weak axis (i.e., the y-axis). However, the compression flanges of these beams are prone to lateral buckling at a certain critical value of the load. As long as the load on the beam is below a critical value, the beam will be stable. As the load is increased, a condition is reached at which a slightly deflected (and twisted) form of configuration becomes possible. This tendency of I-shaped beams bent about the strong axis to buckle about the weak axis (i.e., to bend out of plane) is referred to as *lateral-torsional buckling* (LTB) or lateral buckling of the beam. The plane configuration of the beam is now unstable, and the lowest load at which this critical condition occurs is referred to as the *critical load* for the beam; the moment and stress corresponding to this condition are, referred to, respectively, as *critical moment*, M_{cr}, and *critical stress*, F_{cr}.

Figure 6.21 illustrates schematically the LTB phenomenon. In buildings, most beams are braced by other parts of the structure such that they can deform in only one direction—in the direction of the load (i.e., vertically downward under gravity loads). A crane girder is an example of a girder with entirely laterally unbraced compression flange between supporting columns. Figure 6.21a shows a steel I-beam under pure bending; at the supports, it is held firmly against tipping (Figure 6.21b). As a result of bending, the portion of the beam above the neutral axis is under compression and analogous to a column and tends to buckle in the weak direction, that is, downward, but this deformation is restrained by the portion of the beam below the neutral axis, which is in tension. If the force in the compression portion of the beam is large enough, it tends to buckle in the only direction in which it is free to deform, that is, buckle horizontally. The bottom flange of the beam, which is in

www.EngineeringEBooksPdf.com

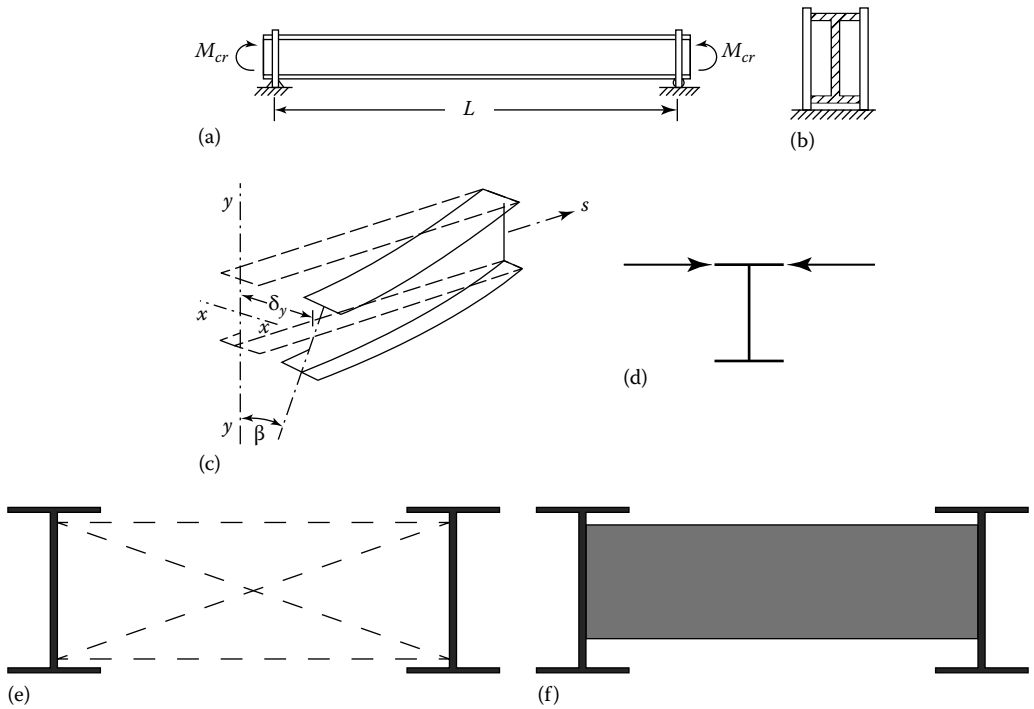

FIGURE 6.21 LTB of I-sections in flexure: (a, b, and c) LTB of compression flange, (d) schematic representation of lateral bracing of compression flange, (e) cross frames and (f) diaphragms as a means of preventing LTB of compression flange.

tension, remains straight. Thus, the top flange tends to buckle and moves horizontally farther than the bottom flange, which, being in tension, remains straight; as a consequence, the beam rotates (shown by solid lines in Figure 6.21c); the vertical axis of the beam has rotated clockwise through an angle β accompanied by a lateral displacement of δ_y (dotted lines show initial unbuckled position of the beam). Additionally, this lateral bending (about the weak axis of the beam) also induces flexural stress (referred to as f_ℓ in Section 6.10.3.5) in the beam.

In order to prevent lateral-torsional buckling of I-beams, the compression flanges must be adequately braced (to prevent translation in the horizontal plane). Generally speaking, the compression flange of a beam is hardly entirely free of lateral restraint. Even when it does not have a positive connection to the supported deck, there is still friction between it and the underside of the deck. However, due to uncertainties, this lateral frictional resistance is not quantifiable and cannot be relied upon. The only sure way to provide lateral support to the compression flanges of the beams is to provide positive lateral support.

Two commonly used schemes to prevent lateral-torsional buckling of I-beams are *lateral bracings* (Figure 6.21d) and *torsional bracings* (Figure 6.21e and f). The idea behind providing these bracing schemes is to simply prevent out-of-plane displacement and twisting (not bending) of the beam. To be effective, bracings should be provided at close intervals. The bracing interval, which is the distance between the points of bracings (called *unbraced length*) is an important parameter to be used in the determination of the moment strength of the beam.

Figure 6.21d shows a schematic representation of lateral bracings that directly brace the compression flange of an I-section. Their purpose is to prevent lateral translation, and, to be effective, they should be positioned as close to the compression flange as possible. Figure 6.21e (cross frames) and 6.21f (diaphragms) represent torsional bracings; they prevent twisting of the beam directly.

www.EngineeringEBooksPdf.com

Either can be placed in between the adjacent I-beams at selected intervals along the span to prevent lateral-torsional buckling. Both schemes are commonly used in steel beam bridges.

Whether the bracing schemes are used or not, stresses in the *compression flanges* of beams at all stages of construction must be checked as explained in the next subsection. It is for this reason that the following discussion emphasizes on the many required checks for stresses in the *compression flanges* of beams.

6.10.3.4 Lateral-Torsional Buckling and Bracing of Beams

It is convenient to classify flexural members based on the length, L_b, between braced points. Braced points are points at which resistance against lateral-torsional buckling is provided according to LRFD Specifications (similar to AISC Specifications for steel buildings). Three braced lengths, L_b, L_p, and L_r, used in conjunction with determining the nominal flexural resistance of a beam are defined as follows:

1. If $L_b \leq L_p$, flexural member is not subjected to LTB.
2. If $L_p < L_b \leq L_r$, flexural member is subject to inelastic LTB.
3. $L_b > L_r$, flexural member is subject to elastic LTB.

6.10.3.5 Flange Stresses and Member Bending Moments

For checking the lateral-torsional buckling resistance of a flexural member having I-shaped cross section, which may be entirely unbraced or discretely braced, a designer needs to check stresses f_{bu} and f_ℓ (due to the factored moment, M_u) defined as follows:

f_{bu} = largest value of compressive stress throughout the unbraced length in the flange under consideration without consideration of flange lateral bending, ksi (Art. 6.10.1.6)
f_ℓ = flange lateral bending stress due to Service II loads, ksi (Art. 6.10.1.6)
M_u = moment due to the factored loads; largest value of the major axis-bending moment throughout the unbraced length causing compression in the flange under consideration

The *flange lateral bending stress*, f_ℓ, referred previously can result from lateral loads applied directly to girders such as wind, earthquake, and construction loading. Flange lateral stress can also be caused as a result of lateral-torsional buckling of a beam. Determination of flange wind moments is addressed in LRFD Art. 4.6.6.7 (see discussion in Section 4.17) and explained in Example 6.2.

For calculating the aforementioned stress values, the following should be noted:

1. The values of M_u, f_{bu}, and f_ℓ are to be determined based on factored loads, and are to be taken as positive in all resistance equations.
2. Lateral bending stress in continuously braced flanges is to be taken as equal to zero.
3. Lateral bending stresses in discretely braced flanges are to be determined from conventional stress analysis.
4. All discretely braced flanges must comply with the following requirements:

$$f_\ell \leq 0.6F_{yf} \qquad (6.13)\ [A6.10.1.6\text{-}1]$$

The flange lateral bending stress, f_ℓ, is to be determined in the discretely braced compression flange of braced length L_b defined by Equation 6.14:

$$L_b = 1.2L_p\sqrt{\frac{C_bR_h}{f_{bu}/F_{yc}}} \qquad (6.14)\ [A6.10.1.6\text{-}2]$$

www.EngineeringEBooksPdf.com

Since the elastic stresses f_{bu} and F_{yc} are, respectively proportional to moments M_u and M_{yc}, Equation 6.14 can also be stated equivalently as Equation 6.15:

$$L_b = 1.2L_p\sqrt{\frac{C_b R_h}{M_u/M_{yc}}} \qquad (6.15)\ [A6.10.1.6\text{-}3]$$

where

C_b = moment gradient modifier specified in Art. 6.10.8.2.3 or Art. A6.3.3, as applicable (discussed in Section 6.10.3.6)
L_b = unbraced length, in.
L_p = limiting unbraced length, in., specified in Art. 6.10.8.2.3
M_{yc} = yield moment with respect to the compression flange determined as specified in Art. D6.2 (kip-in.)

If Equation 6.14 (or Equation 6.15) is not satisfied, the second-order elastic compression flange lateral bending stress should be determined, which may be approximated by simplifying the first-order stress value as given by Equation 6.16:

$$f_\ell = \left(\frac{0.85}{1-\dfrac{f_{bu}}{F_{cr}}}\right) f_{\ell 1} \geq f_{\ell 2} \qquad (6.16)\ [A6.10.1.6\text{-}4]$$

Alternatively, as stated previously (the principle of proportionality), Equation 6.16 can be stated as Equation 6.17:

$$f_\ell = \left(\frac{0.85}{1-\dfrac{M_u}{F_{cr}S_{xc}}}\right) f_{\ell 1} \geq f_{\ell 2} \qquad (6.17)\ [A6.10.1.6\text{-}5]$$

where

f_ℓ = largest value of the compressive stress throughout the unbraced length in the flange under consideration (ksi)
$f_{\ell 1}$ = first-order compression flange lateral bending stress at the section under consideration, or the maximum first-order lateral bending stress in the compression flange under consideration, as applicable (ksi)
F_{cr} = elastic LTB stress for the flange under consideration
S_{xc} = elastic section modulus about the major axis of the section of the compression flange taken as M_{yc}/F_{yc} (in.^{3})

Several parameters used in the aforementioned equations are explained in the following subsections.

6.10.3.6 Moment Gradient Modifier, C_b

The *moment gradient modifier*, C_b, is an important design parameter that is used in conjunction with equations used for calculating the flexural resistance of beams having I-shaped cross sections subjected to different load conditions. Mathematically, it is convenient to derive a general expression for critical moment, M_{cr}, when a beam is subjected to *uniform moment* (i.e., constant moment

www.EngineeringEBooksPdf.com

throughout the beam, no moment gradient, Figure 6.21a). M_{cr} is defined as the smallest value of the applied moment that will cause the beam to buckle *elastically*. For this specific condition, the expression for critical moment is given by Equation 6.18 (Timoshenko and Gere 1961):

$$M_{cr} = \frac{\pi}{L}\sqrt{EI_yGJ + \left(\frac{\pi E}{L}\right)^2 I_yC_w} \tag{6.18}$$

where

G = shear modulus of elasticity (or torsional rigidity) = $E/[2(1 + \mu)]$
C_w = torsional warping constant
L = laterally unsupported length of the beam = L_b

It is instructive to study the composition of the right-hand side of Equation 6.18 that can be expressed slightly differently as given by 6.19:

$$M_{cr} = \left(\frac{\pi^2 EI_yGJ}{L^2} + \frac{\pi^4 E^2 C_w I_y}{L^4}\right)^{0.5} \tag{6.19}$$

It is readily seen that the right-hand side of Equation 6.19 consists of square root of the sum of two terms. The first term ($\pi^2 EI_yGJ/L^2$) is the contribution of St. Venant torsional resistance, and the second term ($\pi^4 E^2 C_w I_y/L^4$) represents the contribution of warping torsion. Accordingly, the two terms of Equation 6.7 can be expressed individually as given by 6.20 and 6.21:

$$M_s = \frac{\pi^2 EI_yGJ}{L^2} \tag{6.20}$$

$$M_w = \frac{\pi^4 E^2 C_w I_y}{L^4} \tag{6.21}$$

The presence of the second term in Equation 6.19 can be explained by the fact that when a member having an I-section buckles torsionally, plane sections do not remain plane (they warp); only cross sections of members with circular cross section remain plane after twisting.

Equation 6.18, first derived by Timoshenko in 1910 (Bleich 1952), gives the elastic lateral-torsional buckling strength of an I-shaped section under constant moment in the plane of the web over the laterally unsupported length, L. To adjust for moment gradient (varying moment over the length of a beam), the right-hand side of Equation 6.18 is multiplied by a factor C_b, called *moment gradient modifier*, resulting in Equation 6.22:

$$M_{cr} = C_b\frac{\pi}{L}\sqrt{EI_yGJ + \left(\frac{\pi E}{L}\right)^2 I_yC_w} \tag{6.22}$$

The elastic lateral-torsional buckling stress, F_{cr}, can be expressed by Equation 6.23:

$$F_{cr} = \frac{M_{cr}}{S_x} = \frac{C_b\pi}{LS_x}\sqrt{EI_yGJ + \left(\frac{\pi E}{L}\right)^2 I_yC_w} \tag{6.23}$$

where S_x = section modulus of I-beam about the x-axis.

www.EngineeringEBooksPdf.com

Equations 6.22 and 6.23 are used in AISC Specifications for the design of steel structures (different forms of equations are used for steel bridge girders). A comprehensive discussion on lateral-torsional buckling of beams can be found in the literature (Bleich 1952, Timoshenko and Gere 1961); an expanded summary can be found in texts on steel design (McGuire 1968, Englekirk 1994, Salmon et al. 2009).

The value of moment gradient modifier, C_b, depends on the nature of the moment diagram; its numerical value depends on the ratio of stresses in the braced segment of the beam. It follows that the value of C_b depends on the applied loading. Art. 6.10.8.2.3 specifies the following values of C_b:

1. For unbraced cantilevers and for members where $f_{mid}/f_2 > 1$ or $f_2 = 0$.

$$C_b = 1.0 \qquad (6.24)\ [A6.10.8.2.3\text{-}6]$$

2. For all other cases, C_b is determined from Equation 6.25:

$$C_b = 1.75 - 1.05\left(\frac{f_1}{f_2}\right) + 0.3\left(\frac{f_1}{f_2}\right)^2 \le 2.3 \qquad (6.25)\ [A6.10.8.2.3\text{-}7]$$

Equation 6.25 is the general expression for calculating C_b for when used for designing steel flexural members for highway bridges. It should be noted that this equation is different from the one specified for C_b in AISC Specifications for design of flexural members of steel structures (C_b is expressed in terms of moments in different parts of the braced segment L_b) although the intent for applying the moment gradient modifier C_b is the same in both specifications.

The elastic lateral-torsional buckling stress, F_{cr}, is given by Equation 6.26:

$$F_{cr} = \frac{C_b R_b \pi^2 E}{\left(\dfrac{L_b}{r_t}\right)^2} \qquad (6.26)\ [A6.10.8.2.3\text{-}8]$$

where the term r_t in Equation 6.26 is the effective radius of gyration for LTB given by

$$r_t = \frac{b_{fc}}{\sqrt{12\left(1 + \dfrac{1}{3}\dfrac{D_c t_w}{b_{fc} t_{fc}}\right)}} \qquad (6.27)\ [A6.10.8.2.3\text{-}9]$$

D_c = depth of the web in compression in the elastic range (in.). For composite sections, D_c is to be determined as specified in Art. D6.3.1 (discussed in Section 6.13.7)

f_{mid} = stress without consideration of lateral bending at the middle of the unbraced length of the flange under consideration, calculated from the moment envelope value that produces the largest compression at the point, or the smallest tension if this point is never in compression (ksi). f_{mid} is to be calculated as that due to factored loads and shall be taken as positive in compression and negative in tension

f_1 = stress without consideration of lateral bending at brace point opposite to one corresponding to f_2, calculated at the intercept of the most critical assumed linear stress variation passing through f_2 and either f_{mid} or f_0, whichever produces the smaller value of C_b (ksi). f_1 may be determined as follows:

1. When the variation in the moment along the entire length between the brace points is concave in shape,

$$f_1 = f_0 \qquad (6.28)\ [A6.10.8.2.3\text{-}10]$$

www.EngineeringEBooksPdf.com

2. For all other cases,

$$f_1 = 2f_{mid} - f_2 \geq f_0 \qquad (6.29)\ [A6.10.8.2.3\text{-}11]$$

where

f_0 = stress without consideration of lateral brace point opposite to one corresponding to f_2, calculated from the moment envelope value that produces the largest compression at this point in the flange under consideration, or the smallest tension if this point is never in compression (ksi). f_0 shall be due to the factored loads and shall be taken a positive in compression and negative in tension.

f_2 = except as noted later, largest compressive stress without consideration of lateral bending at either end of the unbraced length of the flange under consideration, calculated from the critical moment envelope value (ksi). f_2 shall be due to the factored loads and shall be taken as positive.

Exception: If the stress is zero or tensile in the flange under consideration at both ends of unbraced length, f_2 shall be taken as zero.

Figure 6.22 illustrates several examples of calculating C_b for a variety of moment diagrams. An excellent discussion on the determination of C_b is provided by LRFD Commentary C6.10.8.2.1.

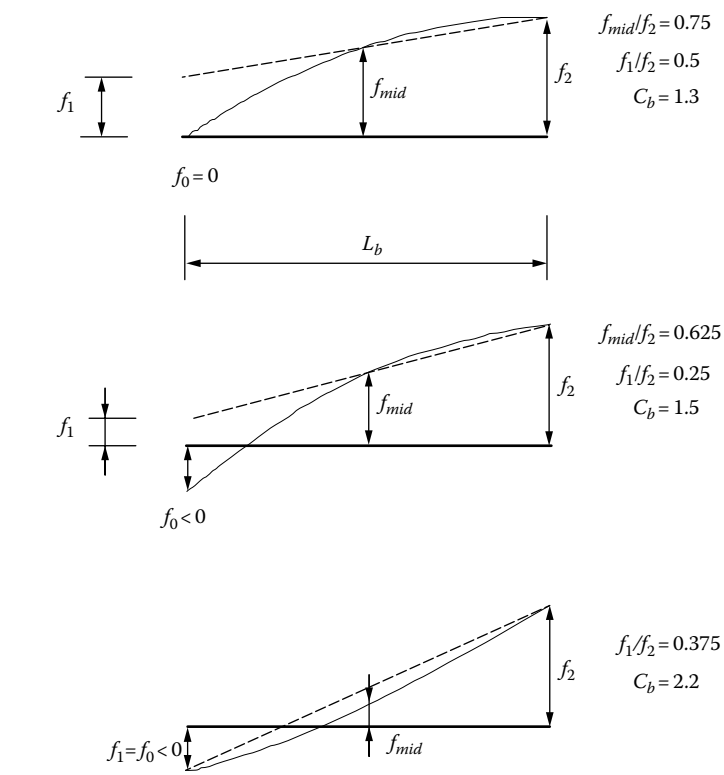

Note: The above examples assume that the member is prismatic within the unbraced length or the transition to a smaller section is within $0.2L_b$ from the braced point with the lower moment. Otherwise, use $C_b = 1$.

FIGURE 6.22 Sample cases for determination of the moment gradient modifier, C_b (LRFD Figure C6.4.10-1). (*Continued*)

www.EngineeringEBooksPdf.com

C6.4.10—Moment gradient modifier, C_b (sample cases)

Unbraced cantilevers and members where $f_{mid}/f_2 > 1$ or $f_2 = 0$: $C_b = 1$

Otherwise: $C_b = 1.75 - 1.05(f_1/f_2) + 0.3(f_1/f_2)^2 \leq 2.3$
If variation of moment is concave between brace points: $f_1 = f_0$
Otherwise: $f_1 = 2f_{mid} - f_2 \geq f_0$

Examples:

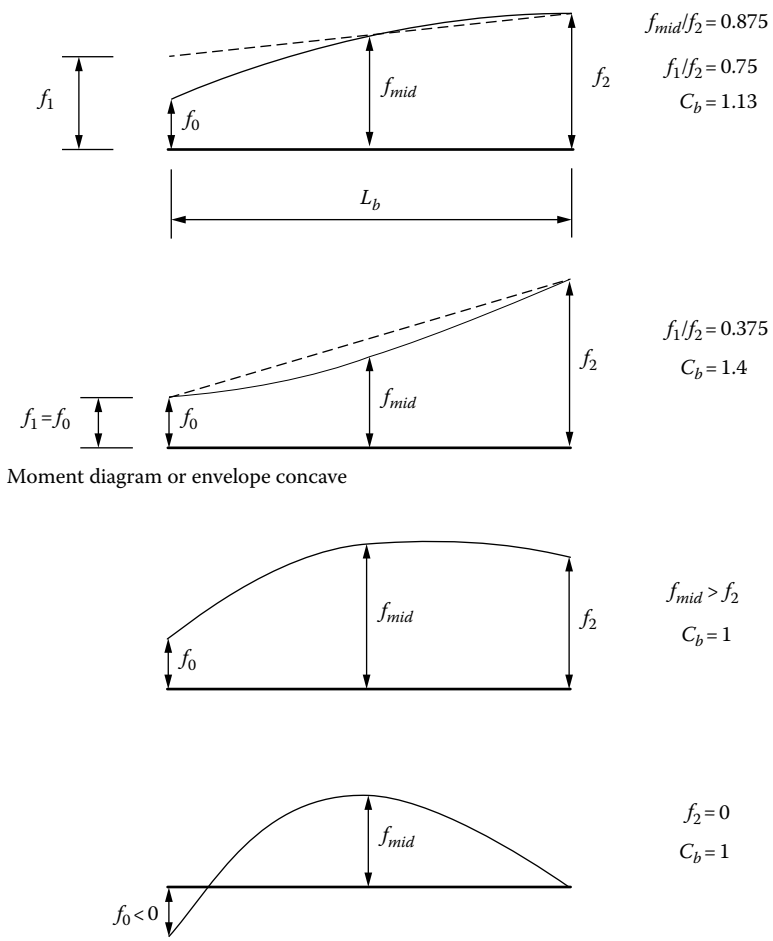

FIGURE 6.22 (*Continued*) Sample cases for determination of the moment gradient modifier, C_b (LRFD Figure C6.4.10-1). (From *AASHTO LRFD Bridge Design Specifications*, Copyright © 2012 by American Association of State Highway and Transportation Officials, Washington, DC. Used by permission.)

6.10.3.7 Flange Stresses and Member Bending Moments: Critical Stages of Construction

6.10.3.7.1 Discretely Braced Flanges in Compression: Art. 6.10.3.2.1

Problem of instability of I-shaped beams was discussed in preceding paragraphs. A clear distinction should be made between *discretely braced compression flanges* and continuously braced flanges (e.g., in composite sections) for the simple reason that for continuously braced compression flanges, flange lateral bending stress, f_ℓ, need not be considered.

www.EngineeringEBooksPdf.com

Art. 6.10.3.2.1 addresses constructibility requirements for discretely braced compression flanges. The required provisions are expressed in terms of the combined factored vertical and flange lateral bending stresses during construction. To prevent lateral-torsional buckling during construction (i.e., before the deck concrete hardens), flexural members must be adequately braced laterally at certain intervals along the span. The stress conditions in compression flanges of discretely braced beams must be satisfied as given by Equation 6.30 (Art. 6.10.3.2-1):

$$f_{bu} + f_{\ell} \leq \phi_f R_h F_{nc} \qquad (6.30)\ [A6.10.3.2.1\text{-}1]$$

The intent of Equation 6.30 is to ensure that the maximum combined stress in the compression flange would not exceed the specified minimum yield strength of the flange times the hybrid factor, R_h, that is, it is a check for the yield limit state of the compression flange. Stresses f_{bu} and f_{ℓ} are to be checked as specified in Art. 6.10.1.6.

For critical stages of construction, it should be ensured that the flexural member has sufficient strength with respect to lateral torsional and flange local buckling-based limit states, including the consideration of flange lateral bending where these effects are judged to be significant. This is accomplished by compliance with Equation 6.31:

$$f_{bu} + \frac{1}{3} f_{\ell} \leq \phi_f F_{nc} \qquad (6.31)\ [A6.10.3.2.1\text{-}2]$$

Equation 6.31 is effectively a beam–column interaction equation, expressed in terms of flange stresses computed from elastic analysis. The f_{bu} term is analogous to axial load, and the f_{ℓ} term is analogous to bending moment within the equivalent beam–column member. The 1/3 multiplier to f_{ℓ} gives an accurate linear approximation of the equivalent beam–column resistance within the limits specified in Art. 6.10.1.6 [White and Grubb 2005].

To ensure that theoretical web bend buckling would be prevented during construction, the following shall be satisfied:

$$f_{bu} \leq \phi_f F_{crw} \qquad (6.32)\ [A6.10.3.2.1\text{-}3]$$

where

f_{bu} = flange stress calculated without consideration of flange lateral bending stress as determined as specified in Art. 6.10.1.6
f_{ℓ} = flange lateral bending stress determined as specified in Art. 6.10.1.6
ϕ_f = resistance factor for flexure
R_h = hybrid factor (a flange-strength reduction factor, discussed in Section 6.10.1.3.1)
F_{crw} = nominal bend-buckling resistance for webs as specified in Art. 6.10.1.9
F_{nc} = nominal flexural resistance of the flange determined as follows:

1. F_{nc} shall be determined as specified in Art. 6.10.8.2.
2. For sections in straight I-girder bridges with compact or noncompact webs, the lateral-torsional buckling resistance may be taken as M_{nc} divided by S_{xc}.
3. In computing F_{nc}, for constructibility, the web load-shedding factor, R_b, shall be taken as 1.0.

For sections that are composite in the final condition but are noncomposite during construction (e.g., common slab–steel girder composite bridges), different values of hybrid factor,

www.EngineeringEBooksPdf.com

R_h (in Equation 6.30), must be calculated for checks in which the member is noncomposite and for checks for which the member is composite.

The procedure for determining the nominal web bend-buckling resistance, F_{crw}, is specified in Art. 6.10.1.9. Its value is given by Equation 6.33:

$$F_{crw} = \frac{0.9Ek}{\left(\frac{D}{t_w}\right)^2} \qquad (6.33)\ [A6.10.1.9.1\text{-}1]$$

The value of F_{crw} given by Equation 6.33 is limited to the smaller of R_hF_{yc} and $F_{yw}/0.7$.

In Equation 6.33, various terms are defined as follows:

k = bend-buckling coefficient

$$= \frac{9}{\left(\frac{D_c}{D}\right)^2} \qquad (6.34)\ [A6.10.1.9.1\text{-}2]$$

where

D_c = depth of the web in compression in the elastic range as discussed in Section 6.13.6.1

R_h = hybrid factor as specified in Art. 6.10.1.10.1

6.10.3.7.2 Discretely Braced Flanges in Tension

For critical stages of construction, the following requirements must be satisfied

$$f_{bu} + f_f = \phi_f R_h F_{yt} \qquad (6.35)\ [A6.10.3.3.2.2\text{-}1]$$

where F_{yt} = minimum specified yield strength of tension flange.

6.10.3.7.3 Continuously Braced Flanges in Tension or Compression

For critical stages of construction, the following requirements must be satisfied

$$f_{bu} = \phi_f R_h F_{yf} \qquad (6.36)\ [A6.10.3.3.2.3\text{-}1]$$

where F_{yf} = minimum specified yield strength of a flange.

Noncomposite sections with slender webs must also satisfy Equation 6.32.

6.10.3.7.4 Shear Strength Requirements

During critical stages of construction, the webs of I-sections must satisfy Equation 6.37:

$$V_u \le \phi_v V_{cr} \qquad (6.37)\ [A6.10.3.3\text{-}1]$$

where

ϕ_v = resistance factor for shear

V_u = shear in the web at the section under consideration due to the factored permanent loads and factored construction loads applied to the noncomposite section (kip)

V_{cr} = shear-buckling resistance determined from LRFD Equation 6.10.9.3.3-1 (discussed later)

www.EngineeringEBooksPdf.com

6.10.4 Considerations for Service Limit State

6.10.4.1 Permanent Deformations

All flexural members undergo elastic deformations under loads. Elastic deformations in superstructures should conform to LRFD Art. 2.5.2.6, which specifies acceptable elastic deformations (deflections). A detailed discussion on this topic is presented in Section 2.6. Deflection criteria for steel superstructures (also for aluminum and concrete superstructures) are listed in Table 2.4.

6.10.4.2 General

Serviceability should be checked for Service Limit State II (LRFD Art. 6.10.4.2-1). Flexural stresses caused in structural steel caused by Service II loads applied to the composite section are calculated using the short-term or long-term composite section properties as appropriate as discussed earlier in Section 6.10.2. For this purpose, the concrete deck may be assumed to be effective for both positive and negative flexure provided that maximum longitudinal tensile stress in the concrete deck under consideration caused by Service II loads are smaller than $2f_r$ where f_r is the modulus of rupture given by Equations 6.38 through 6.40:

For normal-weight concrete

$$f_r = 0.24\sqrt{f'_c} \tag{6.38}$$

For sand-lightweight concrete

$$f_r = 0.20\sqrt{f'_c} \tag{6.39}$$

For all-lightweight concrete

$$f_r = 0.17\sqrt{f'_c} \tag{6.40}$$

The section properties to be used for calculating stresses in structural steel caused by Service II loads should be determined as follows:

1. For sections that are composite for negative flexure with maximum longitudinal tensile stresses in the concrete deck greater than or equal to $2f_r$, the section consisting of the steel section and the longitudinal reinforcement within the effective width of the concrete deck should be used.
2. For sections that are noncomposite for negative flexure, the properties of the steel section alone should be used for calculation of the flexural stresses in the structural steel.

6.10.4.3 Flange Stresses

Flanges of composite sections should comply with the following requirements:

1. For the top flange of composite section,

$$f_f \le 0.95R_h f_{yf} \qquad (6.41)\ [\text{A}6.10.4.2.2\text{-}1]$$

2. For the bottom flange of composite sections,

$$f_f + \frac{f_\ell}{2} \le 0.95R_h f_{yf} \qquad (6.42)\ [\text{A}6.10.4.2.2\text{-}2]$$

www.EngineeringEBooksPdf.com

3. For both flanges of noncomposite sections,

$$f_f + \frac{f_\ell}{2} \leq 0.80 R_h f_{yf} \qquad (6.43)\ [A6.10.4.2.2\text{-}3]$$

where

f_f = flange stress at the section under consideration due to Service II loads calculated without consideration of flange lateral bending (ksi)

f_ℓ = flange lateral bending stress at the section under consideration due to Service II loads determined as specified in Art. 6.10.1.6 (ksi)

R_h = hybrid factor as discussed earlier in Section 6.10.4.1

Note that flange lateral bending stress, f_ℓ, is not included in Equation 6.41 because in a composite section the top flange is continuously braced by the deck slab (therefore, $f_\ell = 0$). The flange lateral bending stress, f_ℓ, may also be taken as equal to zero in Equation 6.43 for continuously braced top flanges of noncomposite section (Art. C6.10.4.2.2).

Lateral bending in the bottom flange is only a consideration at the service limit state for all horizontally curved I-girder bridges and for straight I-girder bridges with discontinuous cross-frame or diaphragm lines in conjunction with skews exceeding 20°. Wind load and deck overhang effects are not considered at the service limit state.

6.10.5 Special Fatigue Requirements for Webs

Fatigue requirements are to be checked for Fatigue I Limit State as specified in Table 3.7 (LRFD Table 3.4.1-1). The fatigue live load should be determined as discussed in Section 3.9. The shear buckling resistance of web, V_{cr}, should be checked for factored shear force in the interior panels, with transverse stiffeners, with or without longitudinal stiffeners, V_u, to satisfy Equation 6.44:

$$V_u \leq \phi_v V_{cr} \qquad (6.44)\ [A6.10.5.3\text{-}1]$$

where

V_u = shear in the web at the section under consideration due to the unfactored permanent load plus the factored fatigue load (kip)

V_{cr} = shear-buckling resistance determined from

$$V_n = V_{cr} = CV_p \qquad (6.45)\ [A6.10.9.3.3\text{-}1]$$

where V_p = plastic shear force to be determined from Equation 6.46:

$$V_p = 0.58 F_{yw} D t_w \qquad (6.46)\ [A6.10.9.3.3\text{-}2]$$

Equation 6.45 represents the shear resistance of a web end panel (A6.10.9.3.3). In Equation 6.45, C = ratio of shear-buckling resistance to the shear-yield strength determined as follows:

If $\frac{D}{t_w} \leq 1.12\sqrt{\frac{Ek}{F_{yw}}}$, then

$$C = 1.0 \qquad (6.47)\ [A6.10.9.3.2\text{-}4]$$

www.EngineeringEBooksPdf.com

If $1.12\sqrt{\frac{Ek}{F_{yw}}} < \frac{D}{t_w} \le 1.4\sqrt{\frac{Ek}{F_{yw}}}$, then

$$C = \frac{1.12}{\frac{D}{t_w}}\sqrt{\frac{Ek}{F_{yw}}} \qquad (6.48)\ [A6.10.9.3.2\text{-}5]$$

If $\frac{D}{t_w} > 1.4\sqrt{\frac{Ek}{F_{yw}}}$, then

$$C = \frac{1.57}{\left(\frac{D}{t_w}\right)^2}\left(\frac{Ek}{F_{yw}}\right) \qquad (6.49)\ [A6.10.9.3.2\text{-}6]$$

In the aforementioned equations, the value of shear-buckling coefficient, k, is to be taken equal to 5. For stiffened webs, the value of coefficient k depends on the aspect ratio of panels, do/D, and is given by Equation 5.50 (A6.10.9.3.2-7):

$$k = 5 + \frac{5}{\left(\frac{d_o}{D}\right)^2} \qquad (6.50)\ [A6.10.9.3.2\text{-}7]$$

6.10.6 Design Requirements for Strength Limit State

6.10.6.1 General

As discussed in Section 6.7, slab–steel superstructures can be composite or noncomposite. Also, composite sections in positive flexure would be noncomposite in negative flexure. Accordingly, the design requirements are presented separately for composite sections, and for composite section in negative flexure and noncomposite sections.

6.10.6.2 Composite Sections in Positive Flexure

Composite sections can be *compact* or *noncompact*. Composite sections in straight bridges that comply with the following requirements qualify as compact sections:

1. The specified minimum yield strengths of flanges do not exceed 70 ksi.
2. The web satisfies the requirements specified in Art. 6.10.1.1 (discussed in the next section).
3. The section satisfies the web slenderness limit given by Equation 6.51:

$$\frac{2D_{cp}}{t_w} \le 3.76\sqrt{\frac{E}{F_{yc}}} \qquad (6.51)\ [A6.10.2.2\text{-}1]$$

where D_{cp} = depth of the web in compression at the plastic moment determined as specified in LRFD Art. D6.3.2 (discussed in Section 6.13.7.2).

www.EngineeringEBooksPdf.com

Additionally, compact sections must satisfy design requirements discussed in Section 6.10.7; otherwise, the sections shall be considered noncompact. Both compact and noncompact sections must also satisfy the ductility requirements discussed in Section 6.10.7.3.

6.10.6.3 Composite Sections in Negative Flexure and Noncomposite Sections

The design requirements for composite sections in negative flexure and for noncomposite sections (Art. 6.10.6.2.3) are the same because the composite sections in negative flexure behave essentially as noncomposite.

The following design requirements are intended for cross sections of straight bridges meeting the following conditions:

1. Supports are normal or skewed not more than 20° from normal.
2. Intermediate diaphragms or cross frames are placed in contiguous lines parallel to supports.
3. The specified minimum yield strengths of flanges do not exceed 70 ksi.
4. The web satisfies the noncompact limit given by Equation 6.52.
5. The flanges satisfy Equation 6.53.

$$\frac{2D_c}{t_w} < 5.7\sqrt{\frac{E}{F_{yc}}} \qquad (6.52)\ [A6.10.6.2.3\text{-}1]$$

$$\frac{I_{yc}}{I_{yt}} \geq 0.3 \qquad (6.53)\ [A6.10.6.2.3\text{-}2]$$

where

D_c = depth of web in compression in the elastic range (in.).
Exception: For composite sections, D_c is to be determined as specified in Art. D6.3.1 (discussed in Section 6.13.6.1)

I_{yc} = moment of inertia of the compression flange of the steel section about the vertical axis in the plane of the web

I_{yt} = moment of inertia of the tension flange of the steel section about the vertical axis in the plane of the web

Equation 6.52 defines the slenderness limit for a *noncompact web*. A web with a greater slenderness is termed *slender*.

6.10.7 Flexural Resistance of Composite and Noncomposite Sections in Positive Flexure: Strength Limit State

6.10.7.1 Compact Sections in Positive Flexure

As in the previous section, this section discusses design specifications for composite and noncomposite sections for the strength limit state. Flexural resistance depends on whether the section is compact or noncompact. The following several conditions should be satisfied.

At the strength limit state, the section should satisfy Equation 6.54:

$$M_u + \frac{1}{3} f_\ell S_{xt} \leq \phi_f M_n \qquad (6.54)\ [A6.10.7.1.1\text{-}1]$$

www.EngineeringEBooksPdf.com

where

ϕ_f = resistance factor (see Section 6.9)

f_ℓ = flange lateral bending stress determined as specified in Art. 6.10.1.6 (ksi)

M_n = nominal flexural resistance of the section determined from Equations 6.56 to 6.55 as applicable

M_u = bending moment about the major axis of the cross section determined as specified in Art. 6.10.1.6 (kip-in.)

M_{yt} = yield moment with respect to the tension flange determined as specified in Art. D6.2 (kip-in.) (discussed in Section 6.13.6)

S_{xt} = elastic section modulus (in.^{3}) about the major axis of the section to the tension flange as given by Equation 6.55:

$$S_{xt} = \frac{M_{yt}}{f_{yt}} \tag{6.55}$$

The nominal flexural resistance in Equation 6.54 is determined as follows:

If $D_p \leq 0.1D_t$, then

$$M_n = M_p \qquad \text{(6.56) [A6.10.7.1.2-1]}$$

For other cases,

$$M_n = M_p\left(1.07 - 0.7\frac{D_p}{D_t}\right) \qquad \text{(6.57) [A6.7.10.1.2-2]}$$

where

D_p = distance from the top of the concrete deck to the neutral axis of the composite section at the plastic moment (in.)

D_t = total depth of the composite section (in.)

M_p = plastic moment of the composite section as determined from Art D6.1 (kip-in.) (discussed in Section 6.13.4)

In continuous spans, the nominal flexural resistance should be determined from Equation 6.58:

$$M_n \leq 1.3R_hM_y \qquad \text{(6.58) [A6.10.7.1.2-3]}$$

where

M_n = nominal flexural resistance determined from Equations 6.56 through 6.58 as applicable (kip-in.)

M_y = yield moment determined as specified in Art. D6.2 (discussed in Section 6.13.6)

R_h = hybrid factor

6.10.7.2 Noncompact Sections

Noncompact sections should meet the following requirements:

1. At the strength limit state, the compression flange shall satisfy Equation 6.59:

$$f_{bu} \leq \phi_f F_{nc} \qquad \text{(6.59) [A6.10.7.2.1-1]}$$

www.EngineeringEBooksPdf.com

where
ϕ_f = strength reduction factor
f_{bu} = flange stress calculated without consideration of flange lateral bending determined as specified in Art. 6.10.1.6 (ksi)
F_{nc} = nominal flexural resistance of the compression flange determined as specified in Art. 6.10.7.2.2

2. The tension flange should satisfy Equation 6.60:

$$f_{bu} + \frac{1}{3} f_\ell \leq \phi_f F_{nt} \qquad (6.60)\ [A6.10.7.2.1\text{-}2]$$

where
f_ℓ = flange lateral bending stress determined as specified in Art. 6.10.1.6 (ksi)
F_{nt} = nominal flexural resistance of the tension flange as determined from Art. 6.7.2.2 (ksi)

3. The maximum longitudinal compressive stress in the concrete deck at the strength limit state, determined as specified in Art. 6.10.1.1.d, shall not exceed $0.6f'_c$.
4. The nominal flexural resistance of the compression flange shall be taken as as given by Equation 6.61:

$$F_{nc} = R_b R_h F_{yc} \qquad (6.61)\ [A6.7.2.2\text{-}1]$$

5. The nominal flexural resistance of the tension flange shall be taken as given by Equation 6.62:

$$F_{nt} = R_h F_{yt} \qquad (6.62)\ [A6.10.7.3\text{-}1]$$

6.10.7.3 Ductility Requirements: Art. 6.10.7.3

Both compact and noncompact sections shall satisfy Equation 6.63:

$$D_p \leq 0.42 D_t \qquad (6.63)\ [A6.10.7.3\text{-}1]$$

where
D_p = distance from the top of the concrete deck to the neutral axis of the composite section at the plastic moment (in.)
D_t = total depth of the composite section (in.)

The intent of ductility requirement expressed by Equation 6.61 is to protect the concrete deck from premature crushing.

As a designer's guide, Figure 6.23 presents a convenient flowchart covering requirements of LRFD Art. 6.10.7.

6.10.8 Flexural Resistance: Compact Sections in Negative Flexure and Noncomposite Sections—Strength Limit State

6.10.8.1 General Requirements

Flexural resistance of I-beams depends on whether compression flanges are discretely braced as in the case of noncomposite sections or continuously braced as in the case of composite sections.

www.EngineeringEBooksPdf.com

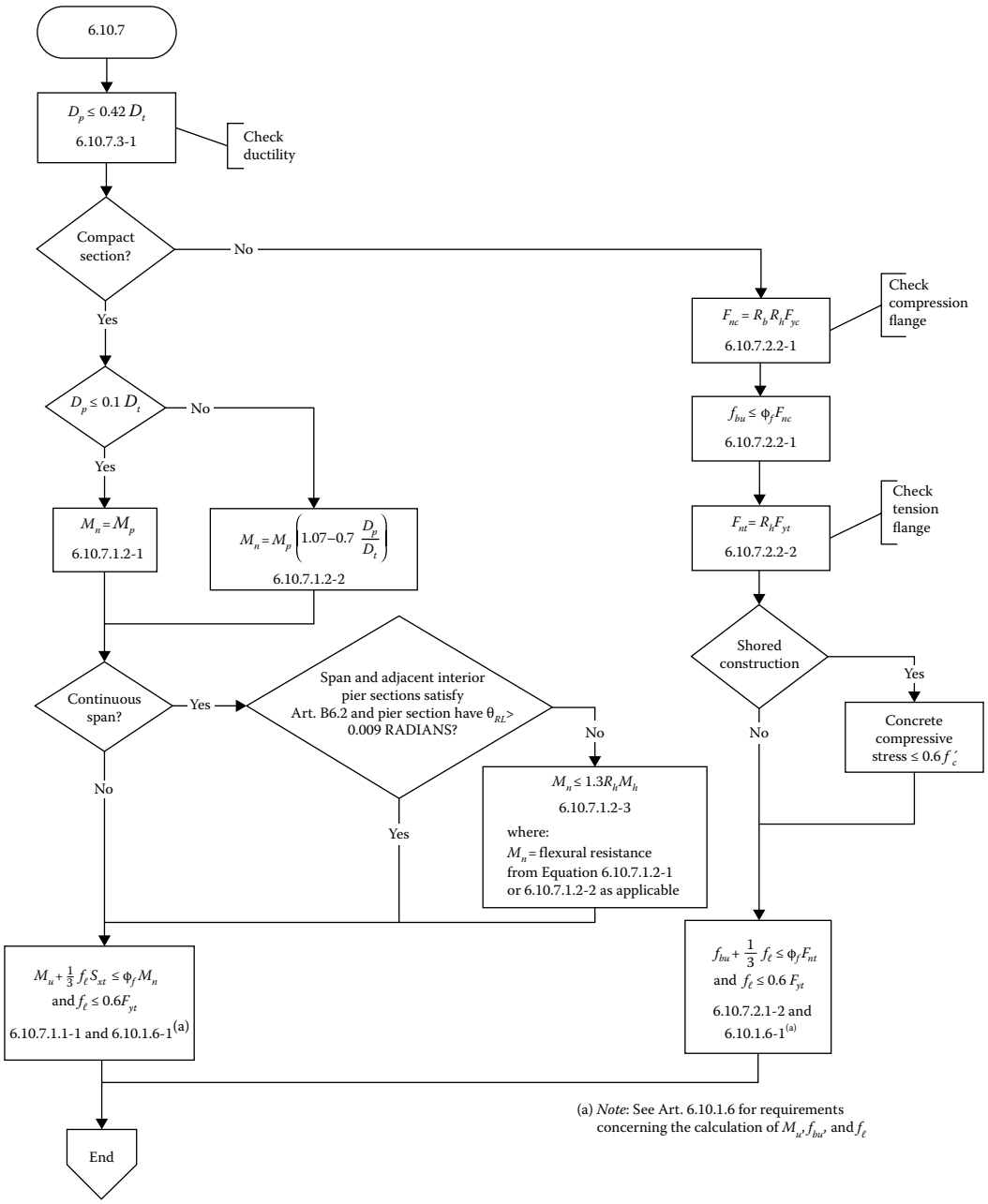

FIGURE 6.23 Flowchart for LRFD Art. 6.10.7—composite sections in positive flexure (LRFD Figure C6.4.5-1). (From *AASHTO LRFD Bridge Design Specifications*, Copyright © 2012 by American Association of State Highway and Transportation Officials, Washington, DC. Used by permission.)

www.EngineeringEBooksPdf.com

6.10.8.1.1 Discretely Braced Flanges in Compression: Art. 6.10.8.3

At the strength limit state, the following requirement should be satisfied:

$$f_{bu} + \frac{1}{3} f_{\ell} \leq \phi_f F_{nc} \qquad (6.64)\ [A6.10.8.1.1\text{-}1]$$

where

ϕ_f = strength reduction factor

f_{bu} = flange stress calculated without consideration of flange lateral bending determined as specified in Art. 6.10.1.6 (ksi)

f_{ℓ} = flange lateral bending stress determined as specified in Art. 6.10.1.6 (ksi)

F_{nc} = nominal flexural resistance of the compression flange determined as specified in Art. 6.10.8.2 (ksi) (discussed in Section 6.10.8.2.2)

6.10.8.1.2 Discretely Braced Flanges in Tension: Art. 6.10.8.1.2

At the strength limit state, the stress in the tension flange should satisfy the following requirement:

$$f_{bu} + \frac{1}{3} f_{\ell} \leq \phi_f F_{nt} \qquad (6.65)\ [A6.10.8.1.2\text{-}1]$$

where

F_{nt} = nominal flexural resistance of the tension flange determined as specified in Art. 6.10.8.3 = $R_h F_{yt}$ (ksi); R_h = hybrid factor (discussed in Section 6.10.1.3.1)

6.10.8.1.3 Discretely Braced Flanges in Tension or Compression: Art. 6.10.8.1.3

At the strength limit state, the following requirement should be satisfied:

$$f_{bu} \leq \phi_f R_h F_{yf} \qquad (6.66)\ [A6.10.8.1.3\text{-}1]$$

6.10.8.2 Compression Flange Flexural Resistance: Art. 6.10.8.2.1

6.10.8.2.1 General Requirements

The term F_{nc} was used in Section 6.10.8.1 (Equation 6.64). Value of F_{nc} depends on bracing intervals for the compression flange. This section presents a discussion on the determination of F_{nc}. The underlying principle is the same as followed in AISC Specifications for steel structures.

Figure 6.24 is presented to illustrate the AASHTO LRFD methodology for the determination of the nominal flexural resistance of the compression flange, F_{nc}. The curve in Figure 6.23 is essentially a function of two parameters: bracing intervals L_b, L_p, and L_r (discussed in Section 6.10.3.2) and the flange slenderness ratios (shown by the subscripted symbol λ). The concept of the moment gradient modifier, C_b (shown on the right-hand side of Figure 6.23), was discussed earlier in Section 6.10.3.4.

The lateral-torsional buckling of I-section beams was discussed earlier in Section 6.10.3.1. At the strength limit state, flexural resistance of the compression flange is determined separately in terms of *local buckling resistance* and *lateral-torsional buckling resistance*; both are discussed as follows.

6.10.8.2.2 Local Buckling Resistance: Art. 6.10.8.2.2

The phenomenon of instability of I-shaped flexural members was discussed in Section 6.10.3.3. Buckling is a compression phenomenon. Plates under compressive loads are prone to buckling. Buckling can be classified as *overall buckling* and *local buckling*; the former was discussed in Section 6.10.3.3. The strength corresponding to overall buckling, such as flexural buckling, however, cannot be developed if the elements of a cross section are so thin that local buckling develops before the onset of overall buckling. Elements of many commonly used structural sections

www.EngineeringEBooksPdf.com

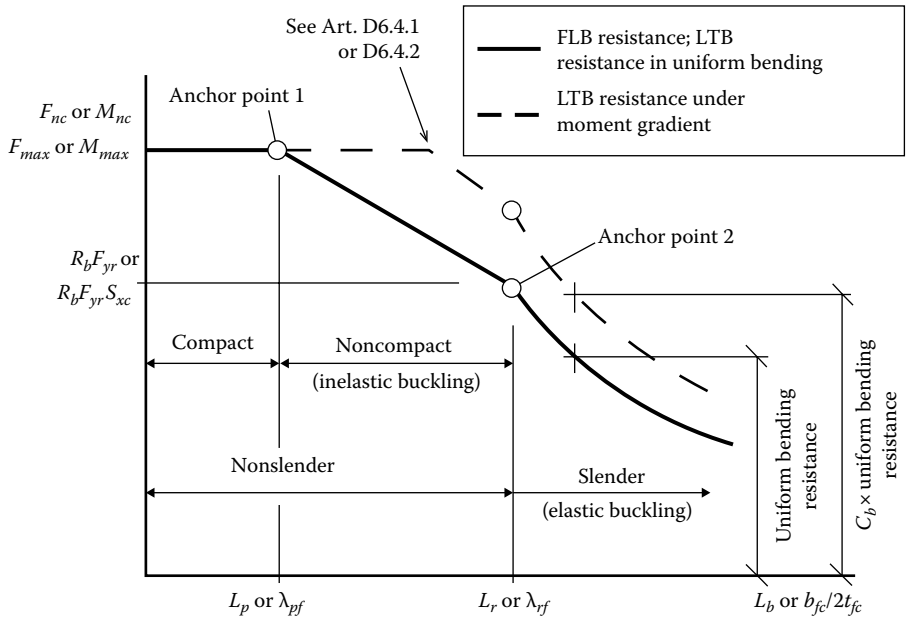

FIGURE 6.24 Basic form of all I-section compression flange flexural resistance equations (LRFD Figure C6.10.8.2.1-1). (Reprinted with permission from American Association of State Highway and Transportation Officials [AASHTO], Washington, DC.)

(e.g., I-shapes, tee sections, and channels) are thin (therefore, referred to as *thin-walled sections*). Local buckling is a type of instability characterized by wrinkling of an element at an isolated location along its length; if this occurs, the cross section ceases to be fully effective, and the member is considered to have failed. I-section cross sections with thin flanges and webs are prone to local buckling, and their use should be avoided whenever possible. In all cases, slenderness ratios of flange and the web of I-sections should be checked to ensure that local buckling would not occur under all possible loading conditions.

The local buckling resistance of the compression flange depends on the slenderness ratio of the compression flange. The two flange slenderness ratio conditions are as follows:

1. If $\lambda_f \leq \lambda_{pf}$, then

$$F_{nc} = R_b R_h F_{yc} \qquad (6.67)\ [A6.10.8.2.2\text{-}1]$$

2. If $\lambda_f > \lambda_{pf}$, then

$$F_{nc} = \left[1 - \left(1 - \frac{F_{yr}}{R_h F_{yc}}\right)\left(\frac{\lambda_f - \lambda_{pf}}{\lambda_{rf} - \lambda_{pf}}\right)\right] R_b R_h F_{yc} \qquad (6.68)\ [A6.10.8.2.2\text{-}2]$$

wherein R_b and R_h were defined earlier, and various flange slenderness ratios (the λ-terms) and other terms are defined as follows:

λ_f = flange slenderness ratio:

$$\lambda_f = \frac{b_{fc}}{t_{fc}} \qquad (6.69)\ [A6.10.8.2.2\text{-}3]$$

www.EngineeringEBooksPdf.com

$$\lambda_{pf} = 0.38\sqrt{\frac{E}{F_{yc}}} \quad (6.70)\ [A6.10.8.2.2\text{-}4]$$

$$\lambda_{rf} = 0.56\sqrt{\frac{E}{F_{yc}}} \quad (6.71)\ [A6.10.8.2.2\text{-}5]$$

F_{yr} = compression flange stress at the onset of nominal yielding within the cross section, including residual stress effects, but not including compression flange lateral bending, taken as the smaller of $0.7F_{yc}$ and F_{yw}, but not less than $0.5F_{yc}$.

6.10.8.2.3 Lateral-Torsional Buckling Resistance: Art. 6.10.8.2.3

In contrast to the local buckling resistance, the lateral-torsional buckling resistance of the compression flange depends on the length of unbraced segment, L_b, within a span as discussed earlier (Section 6.10.3.2). The three governing ratio conditions are as follows:

1. If $L_b \le L_p$, then

$$F_{nc} = R_b R_h F_{yc} \quad (6.72)\ [A6.10.8.2.3\text{-}1]$$

2. If $L_p < L_b \le L_r$, then

$$F_{nc} = C_b\left[1-\left(1-\frac{F_{yr}}{R_h F_{yc}}\right)\left(\frac{L_b - L_p}{L_r - L_p}\right)\right]R_b R_h F_{yc} \le R_b R_h F_{yc} \quad (6.73)\ [A6.10.8.2.3\text{-}2]$$

3. If $L_b > L_r$, then

$$F_{nc} = F_{cr} \le R_b R_h F_{yc} \quad (6.74)\ [AA6.10.8.2.3\text{-}3]$$

where the moment gradient modifier, C_b, was discussed earlier in Section 6.10.3.4 (its values are given by Equations 6.10 through 6.13). The other terms in the aforementioned equations are defined as follows:

L_b = length of unbraced segment (in.)

L_p = limiting unbraced length to achieve the nominal flexural resistance of $R_b R_h F_{yc}$ and defined by Equation 6.75:

$$L_p = 1.0 r_t\sqrt{\frac{E}{F_{yc}}} \quad (6.75)\ [A6.10.8.2.3\text{-}4]$$

L_r = limiting unbraced length to achieve the onset of nominal yielding in either flange under uniform bending with consideration of compression flange residual stress (ksi) and defined by Equation 6.76:

$$L_r = \pi r_t\sqrt{\frac{E}{F_{yr}}} \quad (6.76)\ [A6.10.8.2.2\text{-}5]$$

r_t = effective radius of gyration for LTB as defined by Equation 6.27 (A6.10.8.2.3-9).

Figure 6.25 presents a flowchart as a guide to design requirements specified in LRFD Art. 6.10.8.

www.EngineeringEBooksPdf.com

6.10.9 Shear Resistance

6.10.9.1 General: Shear Strength of Steel Girders

Provisions governing shear resistance of steel girders are specified in Art. 6.10.9.

Shear resistance of flexural members depends on the strength and stiffness of the web. Depending on the slenderness, a web may be (1) *unstiffened* (without any stiffeners), (2) *stiffened* with *transverse* (vertical) stiffeners, and (3) stiffened with a combination of transverse and longitudinal

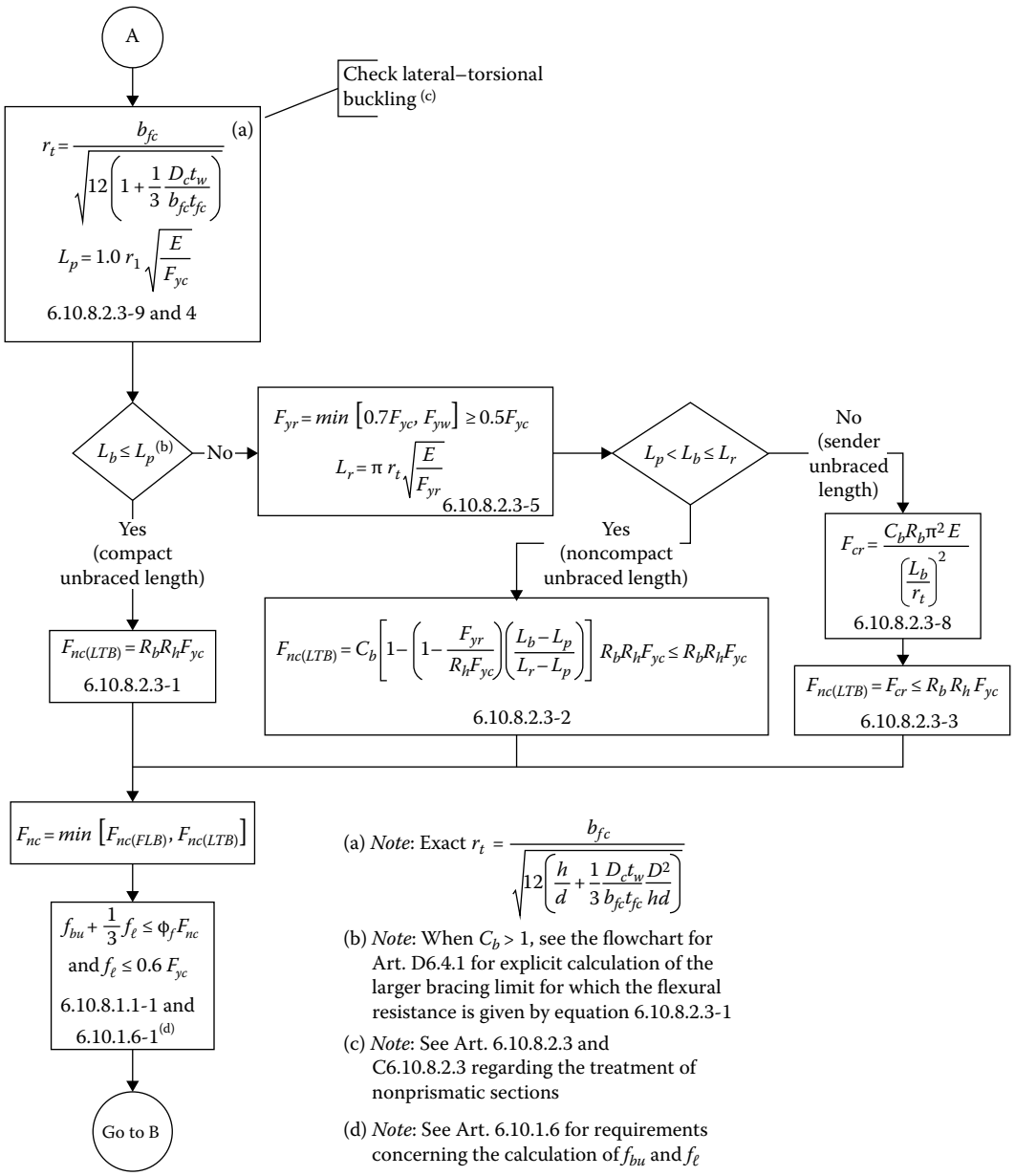

FIGURE 6.25 Flowchart for LRFD Art. 6.10.8—composite sections in negative flexure and noncomposite sections (LRFD Figure C6.4.6-1). (*Continued*)

www.EngineeringEBooksPdf.com

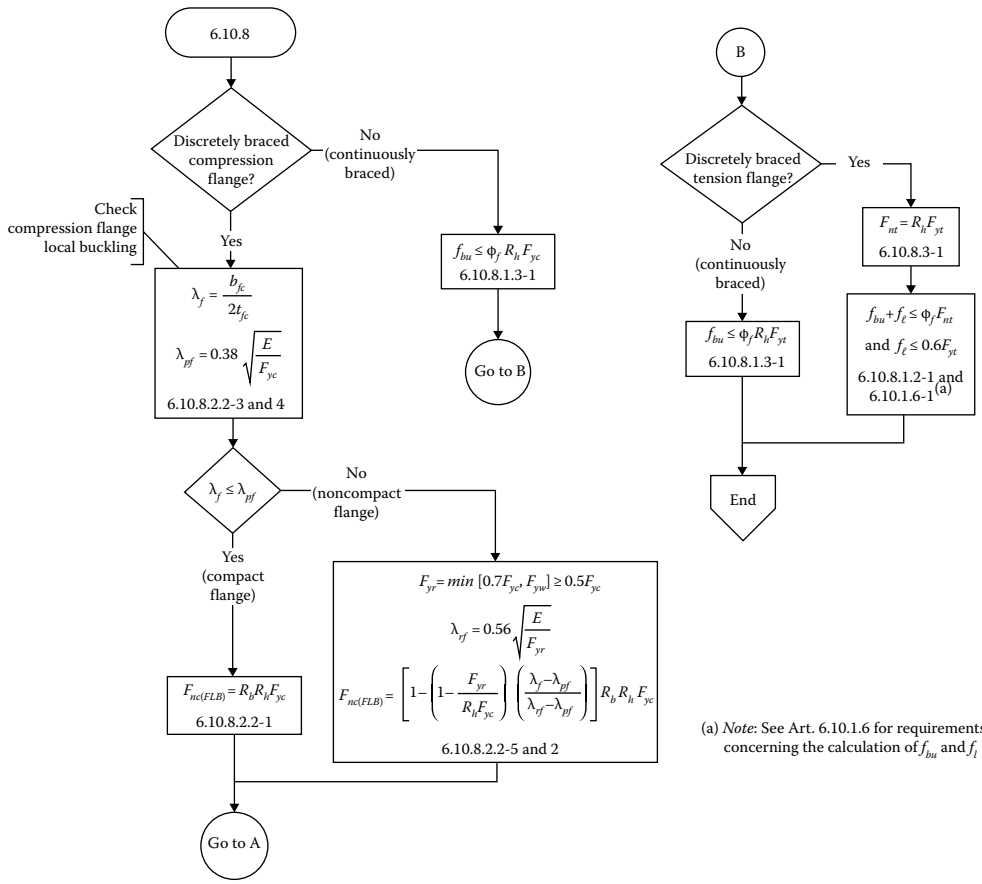

FIGURE 6.25 (*Continued*) Flowchart for LRFD Art. 6.10.8—composite sections in negative flexure and noncomposite sections (LRFD Figure C6.4.6-1). (From *AASHTO LRFD Bridge Design Specifications*, Copyright © 2012 by American Association of State Highway and Transportation Officials, Washington, DC. Used by permission.)

(usually horizontal) stiffeners. In each case, the shear resistance of the girder is to be determined separately because *tension field action* is present in stiffened webs but not in unstiffened webs and hence ignored when considering the shear strength of the latter. Comprehensive discussion on the stability and strength plates, which form the basis for LRFD equations presented in this section can be found in the literature (Bleich 1952, Timoshenko and Gere 1961); a summary has been provided by Taly (1998).

Stiffeners are discussed in Section 6.11.

At the strength limit state, the shear resistance of a straight or curved girder is determined from Equation 6.77:

$$V_u = \phi_v V_n \qquad (6.77)\ [A6.10.9.1\text{-}1]$$

where

ϕ_v = resistance factor for shear
V_n = nominal shear resistance of the girder
V_u = shear in the web at the section under consideration due to the factored loads

www.EngineeringEBooksPdf.com

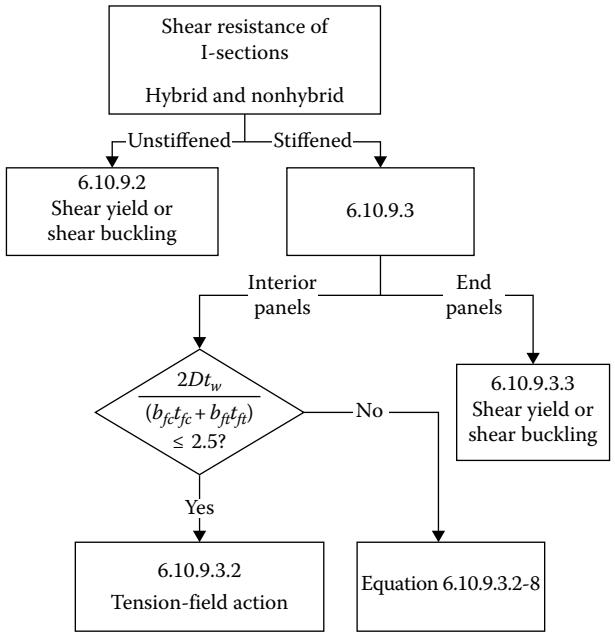

FIGURE 6.26 Flowchart for shear design of I-sections (LRFD Figure C6.10.9.1-1). (From *AASHTO LRFD Bridge Design Specifications*, Copyright © 2012 by American Association of State Highway and Transportation Officials, Washington, DC. Used by permission.)

Whether a web is to be considered stiffened or unstiffened depends on the spacing of transverse stiffeners. A web is considered stiffened if the following conditions are satisfied:

1. The web is without a longitudinal stiffener, and the spacing of the transverse stiffeners does not exceed $3D$.
2. The web has one or more longitudinal stiffeners and with a transverse stiffener spacing not exceeding $3D$.

If the aforementioned conditions are not satisfied, the web panel is considered unstiffened. A discussion on the different types of stiffeners is presented in Section 6.10.11. Figure 6.26 presents a flowchart for determining the shear resistance of flexural members having I-sections. Various LRFD provisions for determining the nominal shear resistance of unstiffened and stiffened webs are presented in the next two sections.

6.10.9.2 Nominal Resistance of Unstiffened Webs

The nominal shear resistance of an unstiffened web is determined from Equation 6.78 (Art. 6.10.9.2):

$$V_n = V_{cr} = CV_p \qquad (6.78)\ [A6.10.9.2\text{-}1]$$

The value of V_p in Equation 6.78 is determined as the product of the cross-sectional area of the web and its assumed shear strength of $F_{yw}/\sqrt{3}$ $(= 0.577F_{yw} \approx 0.58F_{yw})$, which is expressed as given by Equation 6.79:

$$V_p = 0.58F_{yw}Dt_w \qquad (6.79)\ [A6.10.9.2\text{-}2]$$

www.EngineeringEBooksPdf.com

where

C = ratio of shear-buckling resistance to the shear-yield strength determined from Equations 6.80 through 6.82 as applicable with the shear-buckling coefficient, k, taken equal to 5 for unstiffened panels, which is a conservative approximation of the exact value of 5.35 for an infinitely long strip with simply supported edges (Timoshenko and Gere 1961).
(*Note*: k is different for stiffened webs)

V_{cr} = shear-buckling resistance

V_p = plastic shear force

Equations 6.78 and 6.79 are the basic LRFD equations to be used to calculate the shear strength of steel girders. The plastic shear strength, V_p, is clearly a function of the yield strength of the web, F_{yw}, and web's cross-sectional area, Dt_w, where D = depth of the web (= distance between flanges; it is different from and smaller than the depth of the steel section, d). The coefficient, C, is a function of the slenderness of the web.

For unstiffened webs, C in Equation 6.78 is determined as follows based on the slenderness ratio of the web (Art. 6.10.9.3.2):

1. If $\frac{D}{t_w} \le 1.12\sqrt{\frac{Ek}{F_{yw}}}$, then

$$C = 1.0 \qquad (6.80)\ [A6.10.9.3.2\text{-}4]$$

2. If $1.12\sqrt{\frac{Ek}{F_{yw}}} \le \frac{D}{t_w} \le 1.40\sqrt{\frac{Ek}{F_{yw}}}$, then

$$C = \frac{1.12}{\frac{D}{t_w}}\sqrt{\frac{Ek}{F_{yw}}} \qquad (6.81)\ [A6.10.9.3.2\text{-}5]$$

3. If $\frac{D}{t_w} > 1.40\sqrt{\frac{Ek}{F_{yw}}}$, then

$$C = \frac{1.57}{\left(\frac{D}{t_w}\right)^2}\left(\frac{Ek}{F_{yw}}\right) \qquad (6.82)\ [A6.10.9.3.2\text{-}6]$$

In Equations 6.80 through 6.82, the value of the shear-buckling coefficient, k, shall be taken equal to 5.0 (value of k is different for stiffened webs).

If conditions stipulated by Equations 6.80 through 6.82 are not satisfied, then the nominal shear resistance shall be determined from Equation 6.83.

$$V_n = V_p\left[C + \frac{0.87(1-C)}{\sqrt{1+\left(\frac{d_o}{D}\right)^2} + \frac{d_o}{D}}\right] \qquad (6.83)\ [A6.10.9.3.2\text{-}8]$$

www.EngineeringEBooksPdf.com

6.10.9.3 Nominal Resistance of Stiffened Webs: Interior Panels

For a web to be considered stiffened, two conditions specified in Section 6.10.9.1 should be satisfied. At the strength limit state, a stiffened interior web panel must satisfy Equation 6.79. However, the value of the nominal shear resistance in Equation 6.78, V_n, is to be calculated as follows (Art. 6.10.9.3.2):

1. If Equation 6.84 is satisfied

$$\frac{2Dt_w}{b_{fc}t_{fc} + b_{ft}t_{ft}} \leq 2.5 \qquad (6.84)\ [A6.10.9.3.2\text{-}1]$$

then, V_n can be calculated from Equation 6.85:

$$V_n = V_p\left[C + \frac{0.87(1-C)}{\sqrt{1+\left(\frac{d_o}{D}\right)^2}}\right] \qquad (6.85)\ [A6.10.9.3.2\text{-}2]$$

where
d_o = transverse stiffener spacing
V_n = nominal shear resistance of the web panel (kip)
V_p = plastic shear force (kip)
C = ratio of shear-buckling resistance to the shear-yield strength, which is to be determined from Equations 6.80 through 6.82 as applicable

6.10.9.4 Shear Resistance of End Panels

Provisions governing the shear resistance of the end panels of girders are specified in Art. 6.10.9.3.3. The nominal shear resistance of a web end panel is to be determined from Equation 6.86a:

$$V_n = V_{cr} = CV_p \qquad (6.86a)\ [A6.10.9.3.3\text{-}1]$$

$$V_p = 0.58F_{yw}Dt_w \qquad (6.86b)\ [A6.9.10.9.3\text{-}2]$$

where
V_{cr} = shear-bucking resistance (kip)
V_p = plastic shear force (kip)
C = ratio of shear-buckling resistance to the shear-yield strength determined by Equations 6.81 (A6.10.9.3.2-4), 6.82 (A6.10.9.3.2-5), or 6.83 (A6.10.9.3.2-6) as applicable (same as for intermediate panels)

In these equations, the value of shear-buckling coefficient, k, is to be determined from Equation 6.87:

$$k = 5 + \frac{5}{\left(\frac{d_o}{D}\right)^2} \qquad (6.87)\ [A6.10.9.3.2\text{-}7]$$

In case Equations 6.80 through 6.82 are not satisfied, then the nominal shear resistance shall be determined from Equation 6.83.

Stiffeners are discussed in Section 6.11.

6.10.10 Shear Connectors

6.10.10.1 Role of Shear Connectors

The purpose of providing shear connectors is to develop horizontal resistance at the concrete slab–steel girder interface. *Shear connectors* are so called because they are subjected to horizontal shear

www.EngineeringEBooksPdf.com

at the slab–girder interface (hence, the term *shear* connectors). Shear connectors are welded to the top of the steel girder, which get embedded in the concrete when the deck is poured. Thus, the concrete deck grips the steel girders via shear connectors; the latter must deform when a slip develops between the concrete deck and the steel girders. The shear connectors provide resistance to horizontal movement at the slab–girder interface as well as resistance to any possible vertical separation between the deck slab and the girders (hence the use of *headed* connectors).

Shear connectors are required to be designed to satisfy both the fatigue limit state and the strength limit state. The design criteria for satisfying strength requirements for these two limit states are different.

Fatigue can be characterized as the initiation and/or propagation of cracks due to a repeated variation of normal stress with a tensile component. *Fatigue life* refers to number of repeated stress cycles that result in fatigue failure of a detail. *Fatigue design life* refers to number of years that a detail is expected to resist the assumed traffic loads without fatigue cracking; in the development of LRFD Specifications, it has been taken as 75 years. *Fatigue resistance* refers to the maximum stress range that can be sustained for a specified number of cycles without failure of a detail.

The fatigue limit state criteria take into account the shear stress range at the slab–girder interface and the number of cycles of shear stress *range* for which the (welded) connection between the shear connectors and the steel girders would not develop fracture (i.e., cracks would not develop in the welds between the connectors and the top flange of steel girders). The *shear stress range* is the difference between the maximum and minimum shear forces in the beam. The strength limit state takes into account the limiting shear strength that the shear connectors must possess to preclude the possibility of failing in shear. The LRFD methodology for designing shear connectors for these two limit states studs is discussed in the following two sections.

6.10.10.2 Types and Sizes of Shear Connectors

Shear connectors should be of a type that permits a thorough compaction of the deck concrete to ensure that their entire surfaces are in contact with the concrete. The connectors should be capable of resisting both horizontal and vertical movement between the deck slab and the top flange of the steel girder to which they are attached by welding. The resistance to horizontal slip at the slab–steel girder interface is provided by the shear resistance of the connectors, whereas the resistance to vertical slip (separation) is provided through friction between the connectors and the surrounding concrete. Therefore, shear connectors should be embedded sufficiently deep inside the concrete slab, and their heads should be of larger diameter to prevent vertical slip from the surrounding concrete.

While there are many types of shear connectors that are used in steel construction to develop composite action between the slab and the supporting steel girders (Figure 6.27), LRFD Specifications recognize two types of shear connectors:

1. Headed studs (Figure 6.28).
2. Channel shear connectors (Figure 6.29)

The most commonly used standard headed shear studs are 5/8-in., 3/4-in., and 7/8-in. diameter studs. These dimensions represent the diameter of the stud shaft; the diameter of the head is larger. Headed shear studs are required to meet the following requirements (Art. 6.10.10.1.1):

1. The ratio of the height to the diameter of a stud shear connector shall not be less than 4.0. This restriction is based on the fact that shear resistance of headed studs was determined from tests on this specific category of shear studs.
2. Channel shear connectors shall have fillet welds not smaller than 0.1875 in. placed along the heel and toe of the channel.

www.EngineeringEBooksPdf.com

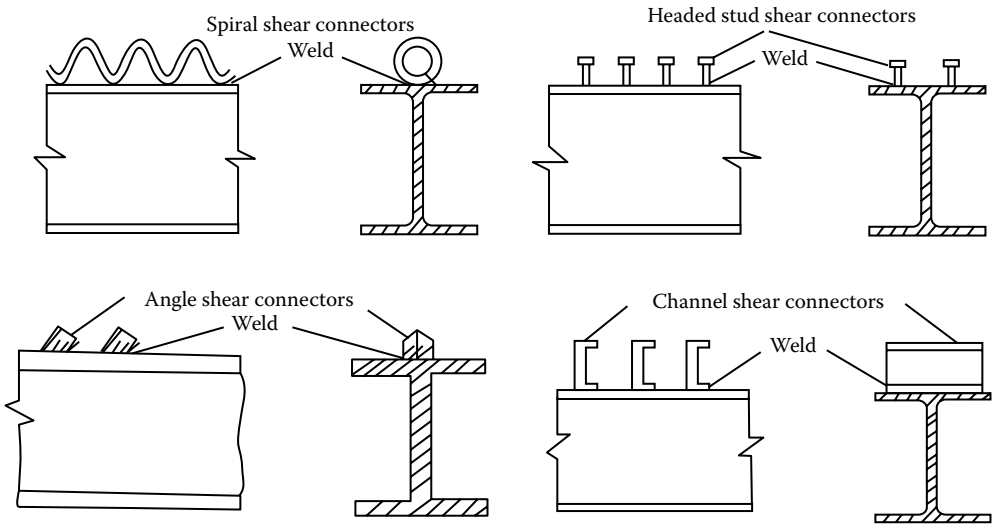

FIGURE 6.27 Types of shear connectors. Only headed stud and channel shear connectors are covered in AASHTO LRFD Bridge Design Specifications (Article 6.10.10.1.1).

FIGURE 6.28 Headed shear studs for composite construction. The distance (measured along the length of the flange) between the two adjacent shear studs is called *pitch*; the distance between two adjacent shear studs measured perpendicular to the flange is called *transverse spacing*.

The size and number of headed shear connectors for a given design of a composite steel girder would depend on the requirements dictated separately by the fatigue limit state and the strength limit state, both of which must be satisfied simultaneously. In any case, the strength of a headed shear connector is proportional to the square of its diameter. Therefore, larger diameter shear connectors have greater shear resisting strength and, therefore, would result in a smaller number to satisfy a given shear resistance requirement.

www.EngineeringEBooksPdf.com

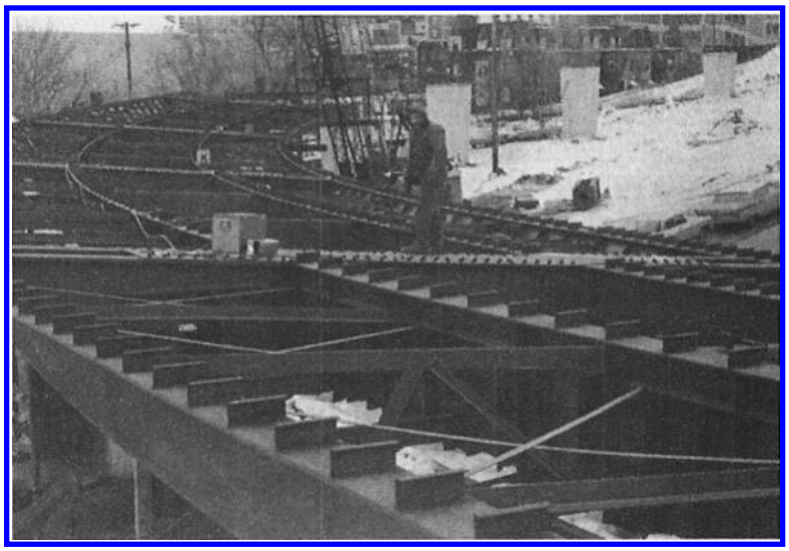

FIGURE 6.29 Channel shear connectors. (Courtesy of United States Steel, Pittsburgh, PA.)

6.10.10.3 Fatigue Limit State: Loads for Fatigue Limit State

Fatigue loads were discussed in Chapter 3. LRFD Specifications specify the magnitude and configuration of fatigue loading as follows:

1. The fatigue load consists of one design truck or axles thereof; tandem or the lane load is *not* to be considered.
2. The distance between the two 32 kip axles of the design truck (the two rear axles of the HL-93 truck) is to be kept at 30 ft constant (not as variable between 14 and 30 ft as considered for HL-93 truck loading).
3. The dynamic load allowance (1.15) is applicable to fatigue load.
4. Live load distribution factor (discussed in Chapter 4) is applicable to fatigue loading.
5. The multiple presence factor (discussed earlier) is *not* applicable to loads for fatigue limit state for which only one design truck is to be considered regardless of the number of design lanes (AASHTO LRFD Art. 3.6.1.1.2). The (approximate) equations for live load distribution factors (discussed in Chapter 4) include the multiple presence factor of 1.2 for one design lane loaded case. Therefore, the calculated live load distribution factor for one lane loaded case should be divided by 1.2 before applying it to the fatigue loading.
6. Load factors applicable to live load (LL), impact (IM), and vehicular centrifugal force (CE) in evaluating fatigue limit states are as follows (LRFD Table 3.4.1-1):

   Fatigue I Limit State 1.5
   Fatigue II Limit State 0.755

6.10.10.4 Fatigue Resistance of Shear Connectors: LRFD Art. 6.10.10.2

The frequency of fatigue load is determined from Equation 6.88:

$$ADTT_{SL} = p(ADTT) \qquad (6.88)\ [A3.6.1.4.2\text{-}1]$$

where

$ADTT$ = number of trucks per day in one direction averaged over the design life (Art. 3.6.1.4.2)
$ADTT_{SL}$ = number of trucks per day in a single lane averaged over the design life
p = fraction of truck traffic in a single lane (as specified in Table 3.6)

www.EngineeringEBooksPdf.com

The fatigue shear resistance offered by a shear connector depends on the frequency of the fatigue load.

1. Fatigue shear strength of a headed shear stud
   Two average daily truck traffic (ADTT) conditions are recognized for determining the fatigue shear resistance of a headed stud shear connector:
   a. Where the projected 75-year single-lane ADTT is greater than or equal to 960 trucks per day, Fatigue I Load Combination is to be used; the fatigue shear resistance for the infinite life is determined from Equation 6.89:

$$Z_r = 5.5d^2 \qquad (6.89)\ [A6.10.10.2\text{-}1]$$

   b. For the ADTT conditions other than in (a) above, Fatigue II Load Combination is to be used; in this case, the fatigue shear resistance for the finite life is determined from Equation 6.90:

$$Z_r = \alpha d^2 \qquad (6.90)\ [A6.10.10.2\text{-}2]$$

   where

$$\alpha = 34.5 - 4.28 \log N \qquad (6.91)\ [A6.10.10.2\text{-}3]$$

   Z_r = shear fatigue resistance of an individual shear connector
   d = diameter of the shear stud
   N = number of stress cycles (Art. 6.6.1.2.5)

2. Fatigue shear strength of a channel-type shear connector
   Two ADTT conditions are recognized for determining the fatigue shear resistance of a channel-type shear connector:
   a. Where the projected 75-year single-lane ADTT is greater than or equal to 1850 trucks per day, Fatigue I Load Combination is to be used; the fatigue shear resistance for the infinite life is determined from Equation 6.92:

$$Z_r = 2.1w \qquad (6.92)\ [A6.10.10.2\text{-}4]$$

   b. For the ADTT conditions other than in (a) the previous, Fatigue II Load Combination is to be used; in this case, the fatigue shear resistance for the finite life is determined from Equation 6.93:

$$Z_r = Bw \qquad (6.93)\ [A6.10.10.2\text{-}5]$$

   where

$$B = 9.37 - 1.08 \log N \qquad (6.94)\ [A6.10.10.2\text{-}6]$$

   w = length of the channel measures transverse to the direction of the flange (in.)

Note that in the aforementioned equations, a negative value of α is *not* admissible.

www.EngineeringEBooksPdf.com

The value of N in Equation 6.94, for a service life of 75 years, is given by Equation 6.95:

$$N = (365)(75)(n)(ADTT)_{SL} \quad (6.95)\ [A6.6.1.2.5\text{-}3]$$

The number 75 used in Equation 6.95 represents the years of assumed service life of a typical bridge, which has been used in overall development of LRFD Specifications. If a design life other than 75 years is sought, the number 75 in the aforementioned expression should be replaced by that other number. Parameter n represents the number of stress range cycles per truck passage as given in Table 3.22 (same as LRFD Table 6.6.1.2.5-2). For simple girder spans longer than 40 ft, $n = 1$.

6.10.10.5 Pitch of Shear Connectors (Art. 6.10.10.1.2)

At the fatigue limit state, shear connectors are designed for the range of live load shear between the deck and top flange of the girder. For a specific section in a composite beam, pitch, p (spacing between the adjacent shear studs along the length of the flange) of shear connectors shall satisfy Equation 6.96:

$$p \le \frac{nZ_r}{V_{sr}} \quad (6.96)\ [A6.10.10.1.2\text{-}1]$$

where

V_{sr} = horizontal shear force range (kip) per unit length at the section for the fatigue limit state
n = number of shear connectors in a cross section

In straight girders, the shear range normally is due to only major-axis bending if torsion is ignored. Curvature, skew, and other conditions may cause torsion, which introduces a radial component of the horizontal shear, F_{fat}. Accordingly, LRFD provisions for fatigue limit state provide for consideration of both components of the shear by adding them vectorially as expressed by Equation 6.97. In Equation 6.96, the value of V_{sr} is given by Equation 6.97:

$$V_{sr} = \sqrt{\left(V_{fat}\right)^2 + \left(F_{fat}\right)^2} \quad (6.97)\ [A6.10.10.1.2\text{-}2]$$

where

V_{fat} = longitudinal fatigue shear range per unit length (kip/in.)
F_{fat} = radial fatigue shear range per unit length (kip/in.)

The value of the V_{fat} in Equation 6.97 is determined from Equation 6.98:

$$V_{fat} = \frac{V_f Q}{I} \quad (6.98)\ [A6.10.10.1.2\text{-}3]$$

The parameters Q and I appearing in Equation 6.98 should be determined using the deck within the effective flange width. However, in negative flexure regions of straight girders only, the parameters I and Q may be determined using the longitudinal reinforcement within the effective flange width for negative moment, unless the concrete deck is considered to be effective in tension for negative moment in computing the range of the longitudinal stress, as permitted in Art. 6.6.1.2.1.

www.EngineeringEBooksPdf.com

In Equation 6.98, the value of F_{fat} (radial fatigue shear range per unit length, kip/in.) is taken as the *larger* of the values given by Equations 6.99 and 6.100:

$$F_{fat1} = \frac{A_{bot} Q_{flg} \ell}{wR} \qquad (6.99)\ [A6.10.10.1.2\text{-}4]$$

$$F_{fat2} = \frac{F_{yc}}{w} \qquad (6.100)\ [A6.10.10.1.2\text{-}5]$$

where

Q_{flg} = range of longitudinal fatigue stress in the bottom flange without consideration of flange lateral bending (ksi)
A_{bot} = area or the bottom flange (in.^{2})
F_{rc} = net range of cross-frame or diaphragm force at the top flange (kip)
F_{yc} = yield strength of compression flange
I = moment of inertia of the short-term composite section (in.^{4})
ℓ = distance between brace points (ft.)
n = number of shear connectors in a cross-section
p = pitch of shear connectors along the longitudinal axis (in.)
Q = first moment of the transformed short-term area of the concrete deck about the neutral axis of the short-term composite section (in.^{3})
R = minimum girder radius within the panel (ft.)
V_f = vertical shear force range under the fatigue load combination specified in LRFD Table 3.4.1-1, with the fatigue live load taken as specified in LRFD Art. 3.6.1.4 (kip)
w = effective length of deck (in.) taken as 48.0 in., except at end supports where w may be taken as 24.0 in.
Z_r = shear fatigue resistance of an individual shear connector determined as discussed in Section 6.10.12.4 (Art. 6.10.2.2)

For simplicity in design, the following may be assumed:

1. For straight spans or segments, the radial fatigue shear range (F_{fat}) in Equation 6.99 (A6.10.10.1.2-4) may be taken equal to zero.
2. For straight or horizontally curved bridges with skews not exceeding 20°, the radial fatigue shear range, F_{fat}, from Equation 6.100 (A6.10.10.1.2-5) may be taken equal to zero.

Under the aforementioned conditions, Equations 6.99 and 6.100 yield

$$V_{sr} = V_{fat} = \frac{V_f Q}{I} \qquad (6.101)$$

Substitution of value of V_{sr} from Equations 6.101 to 6.96 yields Equation 6.102:

$$p \le \frac{n Z_r I}{V_f Q} \qquad (6.102)$$

Equation 6.102 is to be used to determine the pitch p of shear connectors at a section in the beam where the shear force range equals V_f. This shear force range is calculated by finding the difference in the positive and negative shears at the section in the beam under consideration.

In order to determine requirements for shear connectors in a composite beam for the fatigue limit state, it is common practice to determine pitch p at sections of a beam at $0.1L$ intervals along the span. Because the shear force range V_f varies along the span, Equation 6.102 gives different pitches

www.EngineeringEBooksPdf.com

at different sections of the beam; a suitable spacing is selected from the plot of these pitches. The number of shear connectors, n, in Equation 6.102 should be selected such that pitch p is within the permissible limits ($6d \leq p \leq 24$ in., Art. 6.10.10.1.1).

The total number of shear connectors determined to satisfy the fatigue limit state should not be less than that required to satisfy the strength limit state. LRFD requirements governing the number of shear connectors required to satisfy the strength limit state are discussed in the next section.

The maximum longitudinal fatigue shear range, V_{fat}, is produced by placing the fatigue live load immediately to the left and to the right of the point under consideration. For the load in these positions, positive moments are produced over significant portions of the girder length. Thus, the use of the full composite section, including the concrete deck, is reasonable for determining the stiffness used to determine the shear range along the entire span. Also, the horizontal shear force in the deck is most often considered to be effective along the entire span in the analysis.

To satisfy this assumption, the shear force in the deck should be developed along the entire span. For straight girders, an option is permitted to ignore the concrete deck in computing the shear range in regions of negative flexure, unless the concrete is considered to be effective in tension in computing the range of the longitudinal stress, in which case the shear force in the deck must be developed. If the concrete is ignored in these regions, the maximum pitch given by Equation 6.102 must not be exceeded.

The radial fatigue shear range (F_{fas}) typically is determined for the fatigue live load positioned to produce the largest positive and negative major-axis bending moments in the span. Therefore, vectorial addition (Equation 6.97) of the longitudinal (V_{fat}) and radial (F_{fat}) components of the shear range is conservative because the longitudinal and radial shears are not produced by concurrent loads.

Equation 6.99 (A6.10.10.1.2-4) may be used to determine the radial fatigue shear range resulting from the effect of any curvature between brace points. The shear range is taken as the radial component of the maximum longitudinal range of force in the bottom flange between brace points, which is used as a measure of the major-axis bending moment. The radial shear range is distributed over an effective length of girder flange, w. At end supports, w is halved. Equation 6.99 gives the same units as V_{fat}.

Equation 6.100 would typically govern the radial fatigue shear range where torsion is caused by effects other than curvature, such as skew. This equation is most likely to control when discontinuous cross-frame or diaphragm lines are used in conjunction with skew angles exceeding 20° in either a straight or horizontally curved bridge. For all other cases, F_{rc} can be taken equal to zero. Equations 6.99 and 6.100 yield approximately the same value if the span or segment is curved, and there are no other sources of torsion in the region under consideration. Note that F_{rc} represents the resultant range of horizontal force from all cross frames or diaphragms at the point under consideration due to the factored fatigue load plus impact that is resisted by the shear connectors. In lieu of the refined analysis, F_{rc} may be taken as 25.0 kip for an exterior girder, which is typically the critical girder. F_{yc} should not be multiplied by the factor of 0.75 as discussed in Art. C6.6.1.2.1.

Equations 6.99 and 6.101 have been provided to ensure that a load path is provided through the shear connectors to satisfy equilibrium at a transverse section through the girders, deck, and cross frame or diaphragm.

6.10.10.6 Design of Shear Connectors for Strength Limit State (Art. 6.10.10.4)

6.10.10.6.1 Nominal Shear Strength and Shear Resistance of Shear Connectors

At the strength limit state, the number of shear connectors, n, to be provided over the region under consideration depends on the factored shear resistance of the shear connector, Q_r, and the total nominal shear force, P. Shear resistance of the shear connector, Q_r, is determined from Equation 6.103:

$$Q_r = \phi_{SC} Q_n \qquad (6.103)\ [A6.10.10.4.1\text{-}1]$$

where

Q_n = nominal shear resistance of a single shear connector, kip (Art. 6.10.10.4.3)

ϕ_{SC} = resistance factor for the shear connector ($\phi_{SC} = 0.85$ is assigned for the shear connectors (Art. 6.5.4.2))

www.EngineeringEBooksPdf.com

The number of headed shear connectors required over the region under consideration, n (rounded off to the next highest number), is determined by Equation 6.104:

$$n = \frac{P}{Q_r} \qquad (6.104)\ [A6.10.10.4.1\text{-}2]$$

where
P = total nominal shear force determined as explained in Section 6.10.10.6 (A6.10.10.4.2)
Q_r = factored shear resistance of one shear connector determined from Equation 6.103

6.10.10.6.2 Nominal Shear Force: Simple Spans and Continuous Spans in Negative Flexure

For simple spans and for continuous spans that are noncomposite in negative flexure in the final condition, the total nominal shear force, P (in Equation 6.104), between the point of maximum positive design live load plus impact moment and each adjacent point of zero moment, is determined from Equation 6.105 (Art. 6.10.10.4.4):

$$P = \sqrt{P_p^2 + F_p^2} \qquad (6.105)\ [A6.10.10.4.2\text{-}1]$$

where P_p = total longitudinal force in the concrete deck at the point of maximum live load plus impact moment (kip) taken as the smaller of either P_{1p} or P_{2p}, to be determined, respectively, from Equations 6.106 and 6.107.

The strength limit state philosophy for designing shear connectors is based on the premise that the maximum interfacial shear (i.e., horizontal shear between the bottom of the concrete slab and the top of steel girder) cannot exceed the *smaller* of the crushing strength of the deck slab, P_{1p}, and the axial tensile yield strength of the steel girder, P_{2p}.

The crushing strength of the deck slab is determined as the axial compressive strength of concrete slab, P_{1p}, given by Equation 6.106:

$$P_{1p} = 0.85 f_c' b_s t_s \qquad (6.106)\ [A6.10.10.4.2\text{-}2]$$

where
f_c' = compressive strength of concrete
b_s = effective width of the concrete deck
t_s = thickness of the concrete deck

The axial tensile strength of steel section, P_{2p}, is expressed as the sum of the axial strengths of all the elements of the girder (flanges and the web):

$$P_{2P} = F_{yw} D t_w + F_{yt} b_{ft} t_{ft} + F_{yc} b_{fc} t_{fc} \qquad (6.107)\ [A6.10.10.4.2\text{-}3]$$

where
b_{fc} = width of compression flange (in.)
t_{fc} = thickness of the compression flange (in.)
t_w = thickness of web (in.)
D = clear distance between the flanges (in.)
b_{ft} = width of the tension flange (in.)
t_{ft} = thickness of the tension flange (in.)
F_{yc} = yield strength of the compression flange (ksi)
F_{yw} = yield strength of web (ksi)
F_{yt} = yield strength of the tension flange (ksi)

www.EngineeringEBooksPdf.com

Equation 6.107 applies to hybrid girders in which the yield strength of flanges and web may be different. For nonhybrid girders, $F_{yw} = F_{yt} = F_{yc} = F_y$, so that Equation 6.107 can be expressed as given by Equation 6.108:

$$P_{2p} = A_s F_y \tag{6.108}$$

where A_s = cross-sectional area of steel girder.

F_p = total radial force in the concrete deck at the point of maximum positive live load plus impact moment (kip) as determined from Equation 6.109:

$$F_p = P_p \frac{L_p}{R} \qquad \text{(6.109) [A6.10.10.4.2-4]}$$

where

L_p = arc length between the point of maximum positive live load plus impact moment and the centerline of an adjacent interior support (ft)

R = minimum girder radius over the length, L_p (ft)

For straight spans or segments, F_p in Equation 6.105 may be taken equal to zero. With this substitution in Equation 6.105, the result is

$$P = P_p \tag{6.110}$$

where P_p = smaller of P_{1p} and P_{2p} discussed earlier.

6.10.10.6.3 Nominal Shear Force: Continuous Spans Composite for Negative Flexure

For continuous spans that are composite for negative flexure in the final condition, the total amount of shear force, P, between the point of maximum positive live load plus impact moment and an adjacent end of the member shall be determined form Equation 6.105 (A6.10.10.4.2-1).

The total nominal shear force, P, between points of maximum positive moment due to live load plus impact and the centerline of an adjacent interior support shall be determined from Equation 6.111:

$$P = \sqrt{P_T^2 + F_T^2} \qquad \text{(6.111) [A6.10.10.4.2-5]}$$

where P_T = total longitudinal force in the concrete deck at the point of maximum live load plus impact moment (kip) and the centerline of an adjacent interior support (kip), taken as

$$P_T = P_P + P_n \qquad \text{(6.112) [AA6.10.10.4.2-6]}$$

where P_n = total longitudinal force in the concrete deck over an interior support (kip) taken as the smaller of P_{1n} or P_{2n} to be determined, respectively, from Equations 6.113 and 6.114:

$$P_{1n} = F_{yw} D t_w + F_{yt} b_{ft} t_{ft} + F_{yc} b_{fc} t_{fc} \qquad \text{(6.113) [A6.10.10.4.2-7]}$$

$$P_{2n} = 0.85 f_c' b_s t_s \qquad \text{(6.114) [A6.10.10.4.2-8]}$$

www.EngineeringEBooksPdf.com

F_T = total radial force in the concrete deck between the point of maximum positive live load plus impact moment (kip) and the centerline of an adjacent interior support (kip) as determined from

$$F_T = P_T \frac{L_n}{R} \qquad (6.115)\ [A6.10.10.4.2\text{-}9]$$

where

L_n = arc length between the point of maximum positive live load plus impact moment and the centerline of an adjacent interior support (ft)

R = minimum girder radius over the length, L_p (ft)

Note again that Equation 6.113 represents the sum of the axial yield strengths of all of the elements of the girder and Equation 6.114 represents the compressive strength of the cross section of the concrete deck.

For straight spans or segments, F_T in Equation 6.111 may be taken equal to zero.

LRFD Commentary C10.10.4.2 provides an important insight about the longitudinal spacing (pitch) of shear connectors in composite beams—the variable spacing for satisfying the fatigue limit state (Equation 6.102) and the uniform spacing for satisfying the strength limit state (Equation 6.104). Composite beams in which the longitudinal spacing of shear connectors has been varied according to intensity of shear (i.e., using Equation 6.102) and duplicate beams where the connectors were essentially uniformly spaced (i.e., using Equation 6.104) have exhibited essentially the ultimate strength and the same amount of deflection at service loads. Only a slight deformation in concrete and more heavily stressed connectors are needed to redistribute horizontal shear to other less heavily stressed connectors. The important consideration is that the total number of connectors be sufficient to develop the nominal longitudinal force P_n. This is an important concept to be followed in design for shear connectors.

6.10.10.7 Strength of Shear Connectors

6.10.10.7.1 Headed Shear Connectors

Research has shown that the strength of a stud shear connector is a function of both the strength of concrete and the modulus of elasticity of concrete (Ollgaard et al. 1971). Accordingly, the nominal shear strength, Q_n, of a headed shear stud embedded in a concrete deck is determined from Equation 6.116:

$$Q_n = 0.5A_{sc}\sqrt{f'_c E_c} \le A_{sc}F_u \qquad (6.116)\ [A6.10.10.4.3\text{-}1]$$

where

A_{sc} = cross-sectional area of stud shear connector (in.^{2})

f'_c = compressive strength of concrete (ksi)

E_c = modulus of elasticity of concrete (ksi)

F_u = specified minimum tensile strength of a stud shear connector (ksi) (Art. 6.4.4)

Equation 6.116 is based on tests for headed shear connectors with a height-to-diameter ratio of 4 or larger. Therefore, the height-to-diameter ratio of headed shear connectors used must comply with this ratio (Art. 6.10.10.1.1). The last term in Equation 6.116 (stud cross-sectional area, A_{sc}, times the ultimate tensile strength, F_u) represents an upper bound on the stud shear strength.

The modulus of elasticity of concrete E_c in Equation 6.116 is calculated from Equation 6.117:

$$E_c = 33{,}000(w)^{1.5}\sqrt{f'_c}\ \text{ksi} \qquad (6.117)$$

where

w = 0.145 kip/ft^3 for normal weight concrete.

f_c' = 28-day compressive strength of concrete (ksi)

www.EngineeringEBooksPdf.com

For shear studs, the minimum values are specified as F_y = 50 ksi and F_u = 60 ksi (Art. 6.4.4). A strength reduction factor, ϕ_{SC} = 0.85, is assigned for the shear connectors (Art. 6.5.4.2).

It should be recognized from the preceding discussion that should the crushing strength of concrete (P_{1p}) control the strength design of shear connectors (i.e., when $P_{1p} < P_{2p}$), a greater slab thickness (than required for gravity loads) would result in a greater number of shear connectors. It should, therefore, be incumbent on a designer that only sufficient slab thickness be provided to satisfy the strength limit state. This would economize the design of both the slab and the girder.

6.10.10.7.2 Channel Shear Connectors

The nominal shear resistance Q_n of one channel shear embedded in a concrete deck shall be taken as given by Equation 6.118:

$$Q_n = 0.3\left(t_f + 0.5t_w\right)L_c\sqrt{f'_c E_c} \qquad (6.118)\ [A6.10.10.4.3\text{-}2]$$

where

t_f = flange thickness of channel shear connector (in.)
t_w = web thickness of channel shear connector (in.)
L_c = length of channel shear connector (in.)

6.10.10.7.3 Special Requirements for Points of Permanent Load Contraflexure: LRFD Art. 6.10.10.3

In continuous spans, composite flexural members in the region of negative moments (on both sides of interior supports) would be in negative flexure in the final condition. In such regions of the girder, it is necessary to provide additional shear connectors in the regions of points of permanent load contraflexure. The purpose of providing additional shear connectors is to develop the reinforcing bars used as part of the negative flexural composite section.

The number of additional shear connectors, n_{ac}, shall be computed from Equation 6.119:

$$n_{ac} = \frac{A_s f_{sp}}{Z_p} \qquad (6.119)$$

where

A_s = total area of longitudinal reinforcement over the support within the effective concrete deck width
f_{sp} = stress range in the longitudinal reinforcement over the interior support under the applicable fatigue load combination in LRFD Table 4.4.1-1 with the fatigue live load taken as specified in Art. 3.6.1.4 (kip)
Z_p = fatigue shear resistance of individual shear connector determined as specified in Art. 6.10.10.2 (kip)

The additional shear connectors shall be placed within a distance extending one-third of the effective flange width specified in Art. 4.6.2.6 from each side of the point of steel dead load contraflexure.

6.10.10.8 LRFD Provisions for Providing Shear Connectors

6.10.10.8.1 General

The purpose of providing shear connectors between the concrete deck and the supporting steel girder is to develop composite action between the deck slab and the supporting steel girder. Physically, the shear connectors resist horizontal shear at the interface between the concrete deck and the steel girder. In continuous beams, they also help control cracking in the regions of negative moment where the deck is subjected to tensile stress and has longitudinal reinforcement.

www.EngineeringEBooksPdf.com

The following are general LRFD provisions for providing shear connectors to develop composite action:

1. In simple-span bridges, composite girders are to be provided with shear connectors throughout their entire lengths.
2. Shear connectors should penetrate through the haunch between the bottom of the concrete deck and the top flange of the girder, when present, and into the deck. Otherwise, the haunch should be reinforced to contain the stud connectors and develop its load in the deck.
3. In straight continuous bridges, composite girders should normally be provided with shear connectors over their entire lengths. However, in the regions of negative moment, shear connectors are to be provided if the longitudinal reinforcement in the slab is considered to be a part of the composite section. If the contribution of the longitudinal reinforcement to nominal strength (M_n) of the girder is ignored, then shear connectors need not be provided in the region of negative flexure, provided that two mandatory conditions are satisfied: (a) additional shear connectors are provided in the region of points of permanent contraflexure as specified in Art. 6.10.10.3 (discussed earlier) and (b) the longitudinal reinforcement is extended into the positive flexure region as specified in Art. 6.10.1.7.
4. In curved continuous bridges, composite girders must be provided with shear connectors throughout their entire lengths.
5. Shear connectors are to be provided in regions of negative flexure in curved continuous composite girders because torsional shear exists and is developed in the full composite section along their entire lengths. For bridges containing one or more curved segments, the effects of curvature usually extend beyond the curved segment. Therefore, it is conservatively specified that shear connectors be provided along their entire lengths in this case as well.

6.10.10.8.2 Placement Requirements for Shear Connectors

6.10.10.8.2.1 Longitudinal Spacing (Pitch)

1. Art. 6.10.10.1.2 requires that the pitch (i.e., spacing along the length of the girder) of the shear connectors be determined to satisfy the fatigue limit state, as specified in Art. 6.10.10.2 and 6.10.10.3. The resulting number of shear connectors should not be less than the number required to satisfy the strength limit state as specified in Art. 6.10.10.4.
2. The center-to-center pitch of shear connectors shall (Art. 6.10.10.1.2).
   a. Not exceed 24.0 in.
   b. Not be less than six stud diameters (i.e., $6d \leq p \leq 24$ in., where d = diameter of the stud shear connector).

6.10.10.8.2.2 Transverse Spacing

1. Art. 6.10.10.1.3 specifies that shear connectors be placed transversely across the top flange of the steel section, either at regular intervals (i.e., spacing) or variable intervals (at the discretion of the designer).
2. It is required that stud shear connectors not be closer than 4.0 stud diameters center-to-center transverse to the longitudinal axis of the supporting member.
3. The clear distance between the edge of the top flange and the edge of the nearest connector shall not be less than 1.0 in.

6.10.10.8.2.3 Cover and Penetration (Art. 6.10.10.1.4)

1. The clear depth of concrete cover over the tops of the shear connectors should not be less than 2.0 in.
2. Shear connectors should penetrate at least 2.0 in. into the concrete deck.

www.EngineeringEBooksPdf.com

Example 6.1 presents application of LRFD provisions for design of shear connectors for a composite girder.

Example 6.1: Calculations for Headed Shear Studs for Composite Construction

Figures 6.30 and 6.31 show, respectively, the cross sections of a slab–steel girder bridge and the plate girder for a single-span highway bridge spanning 75 ft for an urban interstate highway in the Greater Los Angeles Area. The plate material for the girder is Grade 50 steel, which is to be designed to act compositely with the concrete deck (f'_c = 4500 psi). The average daily traffic (ADT) for this bridge is expected to be 25,000 for a 75-year design life. The site-specific study shows that 18 percent of the ADT would consist of trucks for which two traffic lanes would be available. For this bridge, determine the number of 4 in. high, 3/4 in. diameter headed studs (F_y = 50 ksi, F_u = 60 ksi) required to

a. Satisfy fatigue limit state
b. Develop composite action between the slab and an interior girder of the bridge for the strength limit state

Commentary: Examples 3.1 and 4.9 present detailed calculations for loads and distribution factors for this bridge. Information from those examples has been used in the following example.

Solution

The number of shear studs required will be calculated separately for (a) the fatigue limit state and (b) strength limit state.

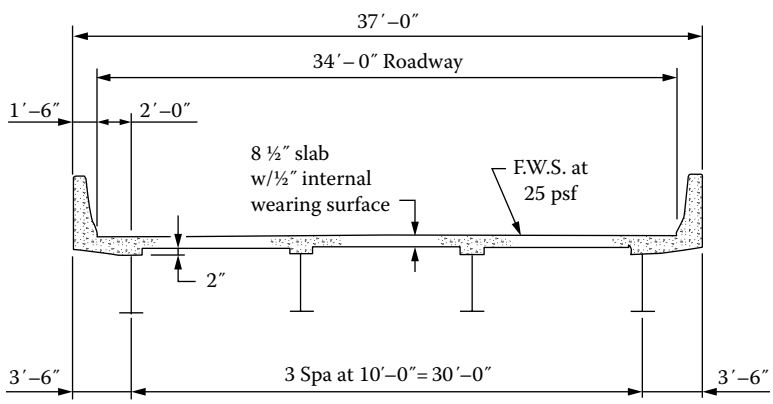

FIGURE 6.30 Cross section of the slab–steel girder bridge.

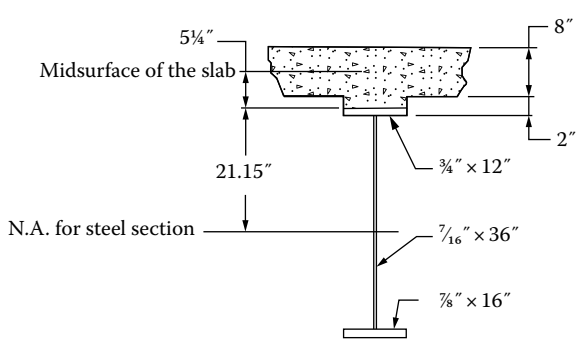

FIGURE 6.31 Composite bridge girder cross section.

www.EngineeringEBooksPdf.com

a. Fatigue limit state

Determine the frequency of the fatigue load.

ADT = 25,000 vehicles

18 percent of traffic consists of trucks: percentage of truck traffic, p_{TT} = 0.18

$ADTT = p_{TT}\,(ADT)$ = 0.18(25000) = 4500 trucks

For two traffic lanes for trucks, p = 0.85 (Table 3.21)

$ADTT_{SL} = p(ADTT)$ = 0.85(4500) = 3825 trucks/day

Calculate fatigue resistance of 4 in. high, 3/4 in. diameter headed shear studs. First, check the height-to-diameter ratio of the stud.

$$\frac{h}{d} = \frac{4}{0.75} = 5.33 > 4, \text{ OK}$$

Because the number of trucks (3835) is greater than 960, the fatigue resistance of the shear connector is controlled by the infinite life criterion as determined from Equation 6.89:

$$Z_r = 5.5d^2$$

$$= 5.5(0.75)^2$$

$$= 3.09 \text{ kip} \qquad (6.89)\ [A6.10.10.2\text{-}1]$$

Based on Z_r = 3.09 kip, pitch p of shear studs at 0.1L intervals along the span would be determined from Equation 6.102:

$$p \le \frac{nZ_rI}{V_fQ} \qquad (6.102)$$

Calculate the range of shear, V_r, at 0.1L intervals along the span due to fatigue truck. Design value of range of shear, V_f, would be calculated later from values of V_r. Note that for determining the force effects due to fatigue, the distance between the two rear 32 kip axles of HL-93 truck (herein after referred to as *fatigue* truck) is maintained at a constant distance of 30 ft (instead of 14 ft); lane load is not to be used for this purpose (Art. 3.6.1.4.1). Method of influence lines is used to determine maximum positive and maximum negative shear at 0.1L intervals; these values are determined for left half span only (the right half would be symmetrical).

Range of shear force at x = 0 ft from the left support.

Figure 6.32 shows the influence line for maximum shear at the support (same as the influence line for reaction at the left support).

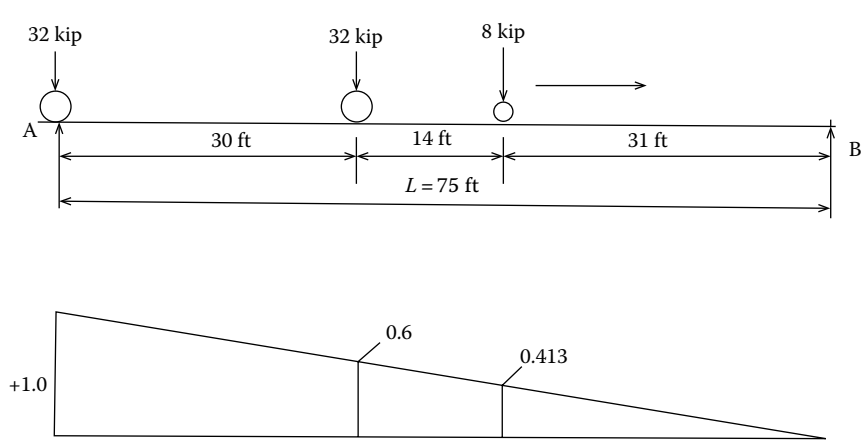

FIGURE 6.32 Influence line for maximum live load shear due to fatigue truck at the left support.

www.EngineeringEBooksPdf.com

From the influence line,

$$V_{max}^{+} = \text{Reaction at A}$$
$$= \sum P_i y_i$$
$$= 32(1+0.6)+8(0.413) = 54.5 \text{ kip}$$
$$V_{max}^{-} = 0$$

Range of shear, $V_r = V_{max}^{+} - V_{max}^{-} = 54.5 - 0 = 54.5$ kip

1. Range of shear force at $x = 0.1L = 0.1(75) = 7.5$ ft from the left support
   Figure 6.33 shows the influence line for shear at $x = 7.5$ ft from the left support.
   From the influence line,

$$V_{max}^{+} = \sum P_i y_i$$
$$= 32(0.9+0.5)+8(0.313) = 47.3 \text{ kip}$$
$$V_{max}^{-} = \sum P_i y_i = 32(-0.1) = -3.2 \text{ kip}$$

   Range of shear, $V_r = V_{max}^{+} - V_{max}^{-} = 47.3 - (-3.2) = 50.5$ kip
2. Range of shear force at $x = 0.2L = 0.2(75) = 15$ ft from the left support
   Figure 6.34 shows the influence line for shear at $x = 15$ ft from the left support.

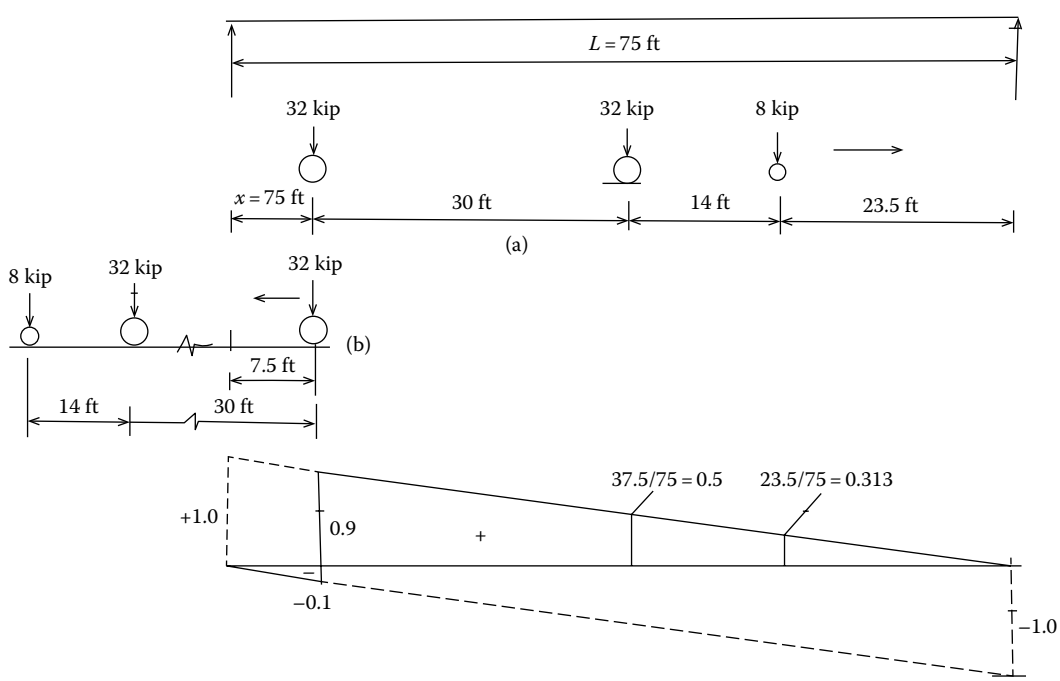

FIGURE 6.33 Influence line for shear at $x = 0.1L = 7.5$ ft from the left support. Position of the fatigue truck for (a) maximum positive shear and (b) maximum negative shear.

www.EngineeringEBooksPdf.com

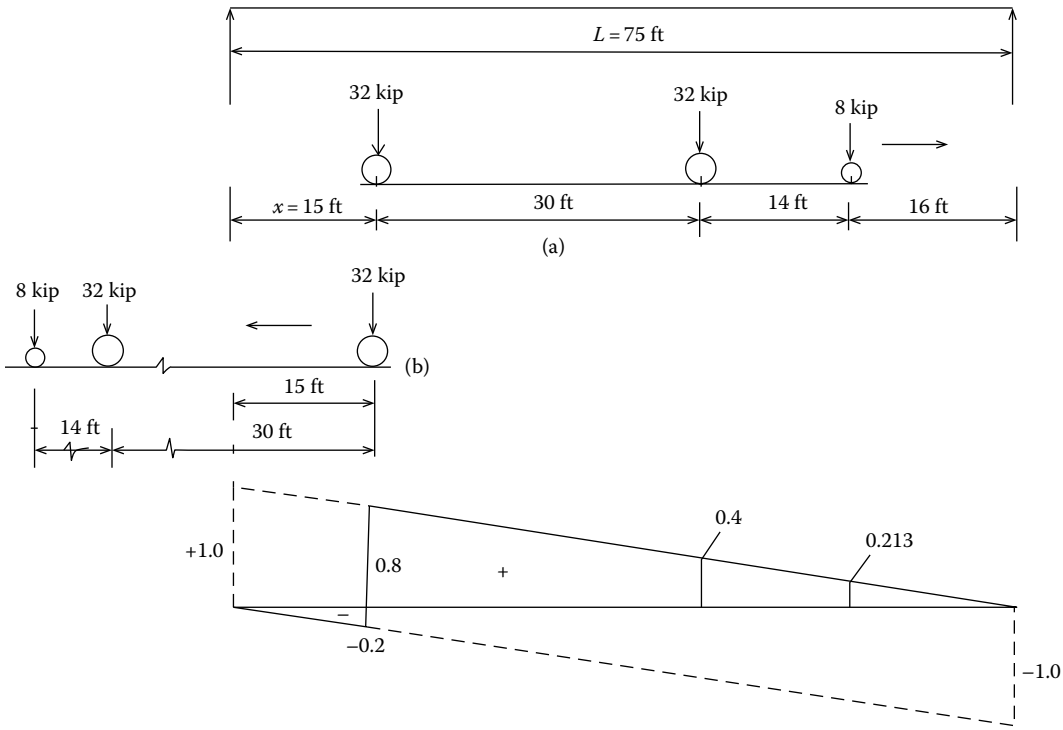

FIGURE 6.34 Influence line for shear at $x = 0.2L = 15$ ft from the left support. Position of the fatigue truck for (a) maximum positive shear and (b) maximum negative shear.

From the influence line,

$$V_{max}^{+} = \sum P_i y_i$$

$$= 32(0.8 + 0.4) + 8(0.213) = 40.10 \text{ kip}$$

$$V_{max}^{-} = \sum P_i y_i = 32(-0.1) = -3.2 \text{ kip}$$

Range of shear, $V_r = V_{max}^{+} - V_{max}^{-} = 40.10 - (-3.2) = 43.30$ kip

3. Range of shear force at $x = 0.3L = 0.3(75) = 22.5$ ft from the left support
   Figure 6.35 shows the influence line for shear at $x = 22.5$ ft from the left support.
   From the influence line,

$$V_{max}^{+} = \sum P_i y_i$$

$$= 32(0.7 + 0.3) + 8(0.113) = 32.9 \text{ kip}$$

$$V_{max}^{-} = \sum P_i y_i = 32(-0.3) = -9.6 \text{ kip}$$

Range of shear, $V_r = V_{max}^{+} - V_{max}^{-} = 32.9 - (-9.6) = 42.5$ kip

4. Range of shear force at $x = 0.4L = 0.4(75) = 30$ ft from the left support
   Figure 6.36 shows the influence line for shear at $x = 30$ ft from the left support.

www.EngineeringEBooksPdf.com

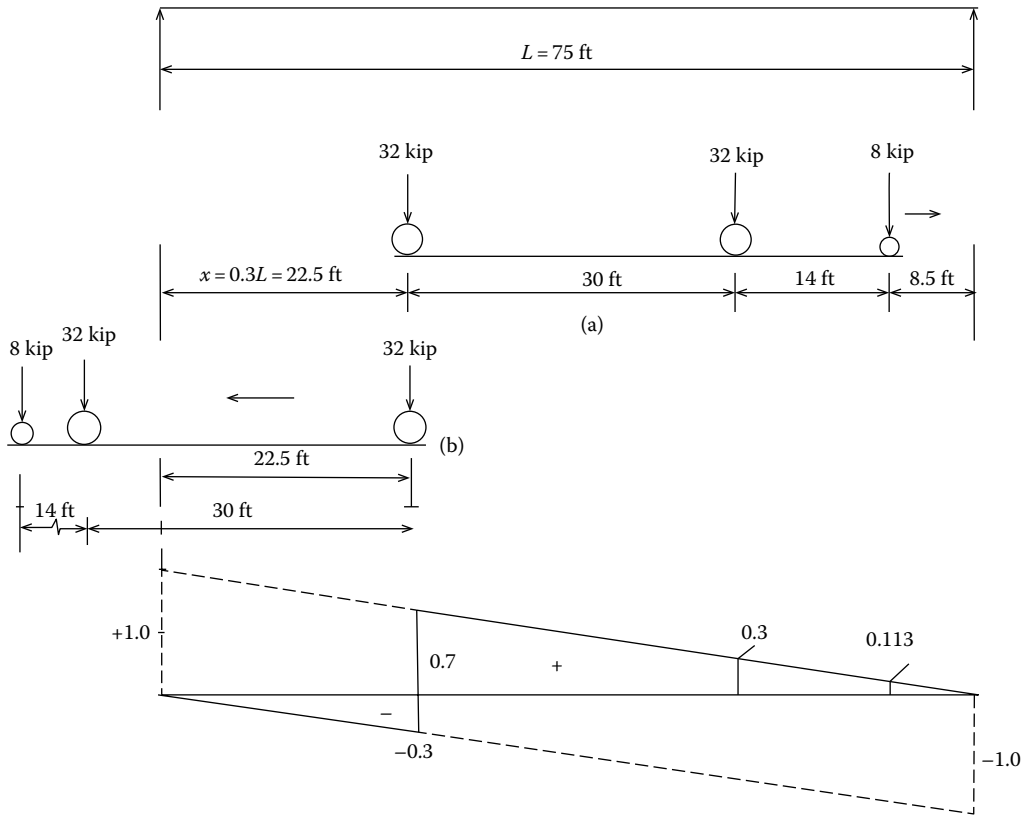

FIGURE 6.35 Influence line for shear at $x = 0.3L = 22.5$ ft from the left support. Position of the fatigue truck for (a) maximum positive shear and (b) maximum negative shear.

From the influence line,

$$V_{max}^{+} = \sum P_i y_i$$

$$= 32(0.6 + 0.2) + 8(0.013) = 25.7 \text{ kip}$$

$$V_{max}^{-} = \sum P_i y_i = 32(-0.4) = -12.8 \text{ kip}$$

Range of shear, $V_r = V_{max}^{+} - V_{max}^{-} = 25.7 - (-12.8) = 38.5$ kip

5. Range of shear force at $x = 0.5L = 0.5(75) = 37.5$ ft from the left support
   Figure 6.37 shows the influence line for shear at $x = 37.5$ ft from the left support.
   From the influence line,

$$V_{max}^{+} = \sum P_i y_i$$

$$= 32(0.5 + 0.1) = 19.2 \text{ kip}$$

$$V_{max}^{-} = \sum P_i y_i = 32(-0.5 - 0.1) = -19.2 \text{ kip}$$

Range of shear, $V_r = V_{max}^{+} - V_{max}^{-} = 19.2 - (-19.2) = 38.4$ kip

The aforementioned values of range of shears are unfactored shear values.

www.EngineeringEBooksPdf.com

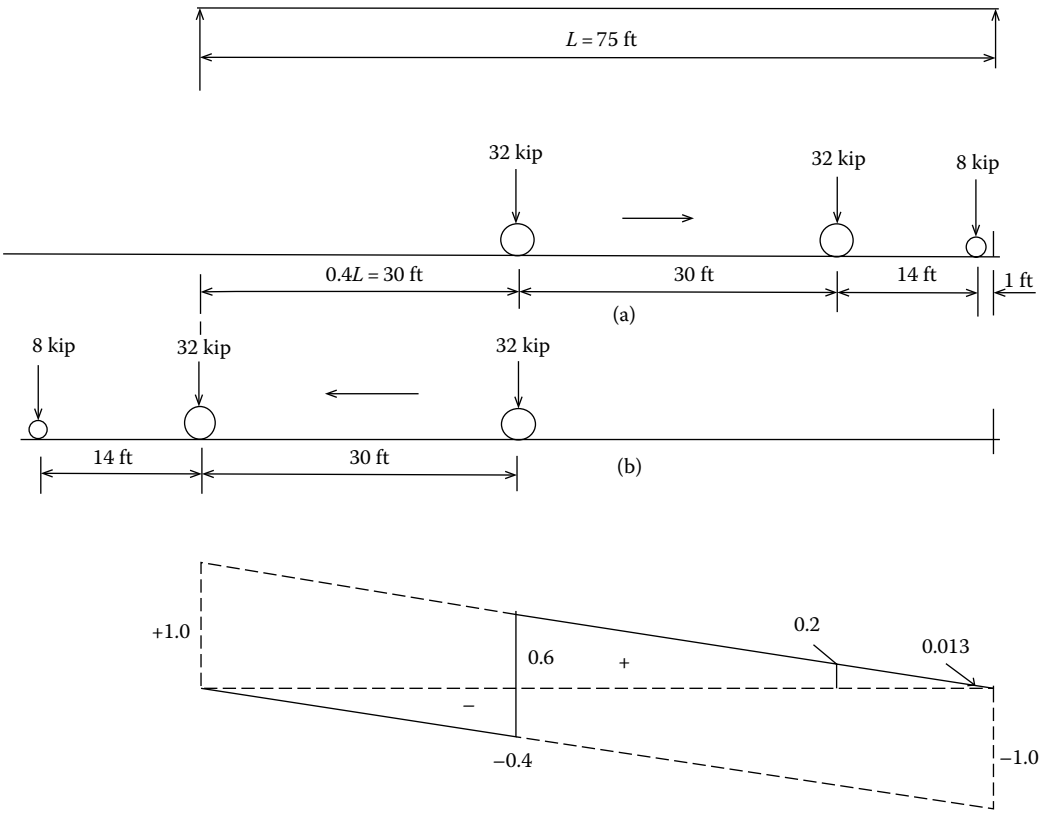

FIGURE 6.36 Influence line for shear at $x = 0.4L = 30$ ft from the left support. Position of the fatigue truck for (a) maximum positive shear and (b) maximum negative shear.

Calculate the live load distribution factors for shear in the interior girder for the case of one design lane loaded case. This was calculated in Example 4.9:

One design lane loaded: $g_{vi1} = 0.76$ lane

To obtain the distribution factor for fatigue, the aforementioned value should be divided by 1.2 (the multiple presence factor is embedded in the live load distribution factor). Therefore, the live load distribution factor for fatigue is

$$g_{i,fat} = \frac{DF\ for\ shear\ for\ one\ loaded\ lane}{1.2} = \frac{0.76}{1.2} = 0.633$$

The design value of the range of shear, V_f, is obtained by multiplying the unfactored value of the range of shear (V_r) by the following factors:

1. $1 + IM = 1.15$
2. Distribution factor for fatigue, $g_{i,fat} = 0.633$
3. Load factor for fatigue limit state = 0.75

$$V_f = (V_r)(1.15)(0.633)(0.75) = 0.546V_r$$

Calculate the moment of inertia, I, of the short-term composite section (Figure 6.38).

The location of neutral axis of the steel section was calculated in Example 4.9:

$y_t = 21.15$ in. (from the top of the girder)

$$A = 38.75 \text{ in.}^2, \quad I_{steel} = 9278 \text{ in.}^4$$

www.EngineeringEBooksPdf.com

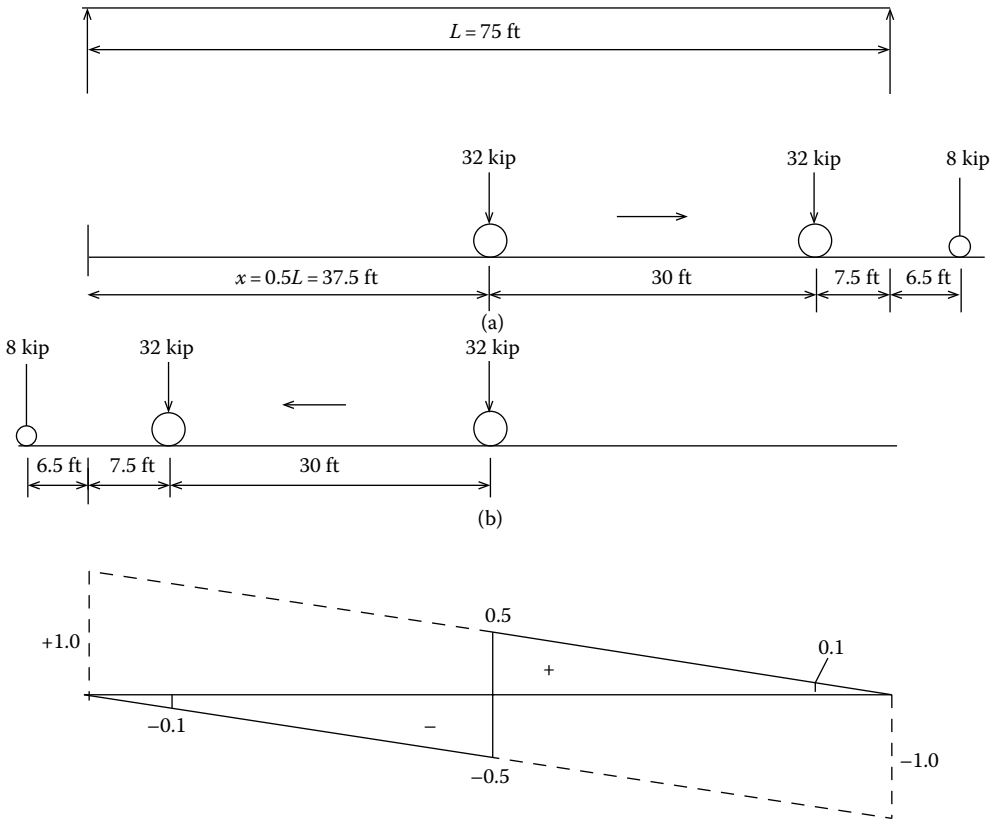

FIGURE 6.37 Influence line for shear at $x = 0.5L = 37.5$ ft from the left support. Position of the fatigue truck for (a) maximum positive shear and (b) maximum negative shear.

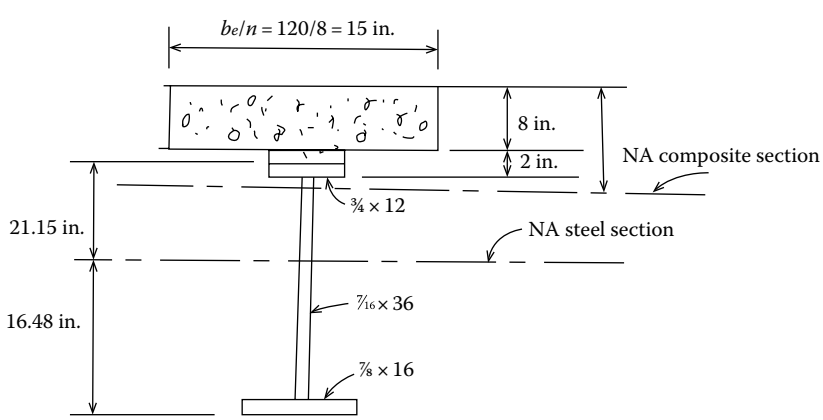

FIGURE 6.38 Cross section of composite steel girder.

www.EngineeringEBooksPdf.com

Calculate the transformed area of slab, A_{tr}. The effective width of slab,
b_e = tributary width of slab = 10 ft = 120 in.
For f'_c = 4500 psi, n = 8

$$A_{tr} = \frac{b_e t_s}{n} = \frac{(120)(8)}{8} = 120 \text{ in.}^2$$

Take moment of areas about the top of slab to determine the neutral axis of the short-term composite section.

$$y_t = \frac{(120)(4)+(38.75)(21.15+9.25)}{(120+38.75)} = 10.44 \text{ in.}$$

The distance between the neutral axis of steel section alone and that of the short-term composite section = 21.15 − 0.75 + 10 − 10.44 = 19.96 in.

$$\begin{aligned} I_{comp} &= I_o + A\bar{d}^2 \\ &= \left[\frac{120(8)^3}{(8)(12)} + 120(10.44-4.0)^2\right] + \left[9278 + (38.75)(19.96)^2\right] \\ &= 30{,}333 \text{ in.}^4 \end{aligned}$$

Q = first moment of the transformed area of slab (A_{tr}) taken about the neutral axis of the short-term composite section

$$= 120(10.44 - 4) = 772.8 \text{ in.}^3$$

Calculate pitch, p, for short-term composite section near the support from Equation 6.102.

$$V_f = 0.546V_r = 0.546(54.5) = 29.76 \text{ kip}$$

Try one shear connector per transverse section, n = 1. For a 3/4-in. diameter headed shear stud, Z_r = 3.09 kip.

$$p \le \frac{nZ_r I}{V_f Q} \tag{6.102}$$

$$p \le \frac{nZ_r I}{V_f Q} = \frac{(1)(3.09)(30{,}333)}{(29.76)(772.8)} = 4.08 \text{ in.}$$

$$p = 4.08 \text{ in.} < 6d_s = 6(0.75) = 4.5 \text{ in, ng.}$$

where d_s = diameter of the headed shear connector = 0.75 in.

The calculated spacing of p = 4.08 in., with one shear stud per transverse section, is smaller than the minimum pitch of 4.5 in. Try two shear studs per transverse section of the composite girder, n = 2:

$$p \le \frac{nZ_r I}{V_f Q} = \frac{(2)(3.09)(30{,}333)}{(29.76)(772.8)} = 8.15 \text{ in.}$$

Calculate pitch for other points along the span (at 0.1L intervals). Pitch p for various 0.1L intervals shown in Table 6.1 values are rounded off to one decimal place.

www.EngineeringEBooksPdf.com

TABLE 6.1
Range of Shear Due to Fatigue Truck at 0.1*L* Intervals for Half Span

x from Left Support, ft (at 0.1*L* Intervals)	Unfactored Shear Force Range, V_r, kip	Design Shear Range, $V_f = 0.546V_r$, kip	Pitch, $p \le \frac{nZ_rI}{V_fQ}+$, in.
0.0	54.5	29.76	8.0
7.5	50.5	27.57	8.6
15.0	43.6	23.81	10.0
22.5	42.5	23.21	10.2
30.0	38.5	21.02	11.3
37.5	38.4	20.97	11.3

Apparently, there is not too much of a difference between the pitches for various intervals along the span. Therefore, provide, p = 8 in. throughout the span, two shear studs per transverse section. Provide the first row of shear studs at 4 in. from the end of the girder.

The total number of spacings = $\frac{75\times12-2\times4}{8} = 112.5$ *or* 113

Total number of transverse row of shear studs = 113 + 1 = 114 for half span

Total number of shear studs required = 114 × 2 = 228

This total number of shear studs (228) should be compared with that required to satisfy Strength Limit State requirements (calculations follow), and the *larger* of the two numbers of shear studs so determined should be provided.

b. Strength limit state

Determine P_{1p}, the compressive strength of concrete slab:

The effective width of the slab, b_s, equals the tributary width, *TW*, for the girder.

b_s = *TW* = center-to-center adjacent beams = 10 ft = 120 in.

$$f'_c = 4500 \text{ psi}$$

Therefore, $P_{1p} = 0.85f'_cb_st_s = (0.85)(4.5)(120)(8) = 3672$ kip

Determine P_{2p}, the axial tensile yield strength of steel section.

$$P_{2P} = F_{yc}b_{fc}t_{fc} + F_{yw}d_wt_w + F_{yt}b_{ft}t_{ft}$$

In the present example, $F_{yw} = F_{yt} = F_{yc} = F_y = 50$ ksi. Therefore, $P_{2P} = A_sF_y$

Calculate the cross-sectional area of steel girder, A_s.

$$A_s = (0.75)(12) + (7/16)(36) + (7/8)(16) = 38.75 \text{ in.}^2$$

Therefore, $P_{2P} = F_yA_s = (50)(38.75) = 1937.5$ kip < $P_{1P} = 3672$ kip

Therefore, P_{2P} = 1937.5 kip (smaller value) governs. Determine the nominal shear strength, Q_n, of a 3/4 in. diameter headed shear connector:

$$Q_n = 0.5A_{sc}\sqrt{f'_cE_c} \le A_{sc}F_u \qquad (6.116)\ [A6.10.10.4.3\text{-}1]$$

The cross-sectional area of a 3/4 in. diameter shear connector is

$$A_{sc} = \frac{\pi d^2}{4} = \frac{\pi(0.75)^2}{4} = 0.442 \text{ in.}^2$$

www.EngineeringEBooksPdf.com

The modulus of elasticity of concrete is given by

$$E_c = 33{,}000(w)^{1.5}\sqrt{f'_c}\ \text{ksi} \tag{6.117}$$

$$E_c = 33{,}000(0.145)^{1.5}\sqrt{4.5}\ \text{ksi}$$
$$= 3{,}865\ \text{ksi}$$

Substitution for f'_c and E_c in Equation 6.116 yields

$$Q_n = 0.5A_{sc}\sqrt{f'_c E_c}$$
$$= 0.5(0.442)\sqrt{(4.5)(3865)}$$
$$= 29.14\ \text{kip}$$

For stud shear connectors, F_u = 60 ksi (Art. 6.4.4). Therefore,

$$A_{sc}F_u = (0.442)(60) = 26.52\ \text{kip} < 29.14\ \text{kip}$$

Use Q_n = 26.52 kip (the *smaller* value governs)

With a strength reduction factor, ϕ_{SC} = 0.85 for shear connectors, the factored shear resistance of the headed shear stud is (Art. 6.5.4.2)

$$Q_r = \phi_{SC}Q_n = 0.85(26.52) = 22.54\ \text{kip} \tag{A6.10.10.4.1-1}$$

The number of 3/4 in. diameter headed shear studs required for the half span is

$$n = \frac{P_{2p}}{Q_r} = \frac{1937.5}{22.54} = 86 \tag{A6.10.10.4.1-2}$$

Total number of shear studs for the entire span = 2(86) = 172 studs.

It is seen that the number of headed shear studs required to satisfy Strength I Limit State (172 studs) is smaller than the number of shear studs required to satisfy the fatigue limit state (228 studs) as calculated earlier. Therefore, provide a total of 228 studs, p = 8 in., two shear studs per transverse section of the girder, as shown in Figure 6.39. Placement requirements stated in Section 6.12.13.2 must be complied with.

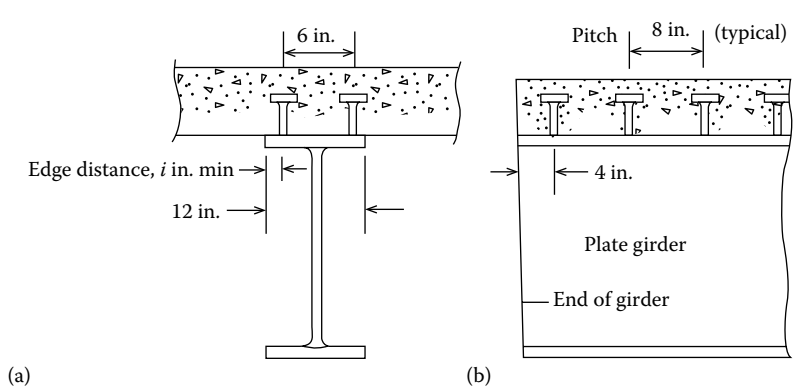

FIGURE 6.39 Layout of 3.4 in. × 4 in. long headed shear studs for Example 6.1. (a) Cross section of the composite girder and (b) longitudinal view of the girder with shear studs, p = 8 in. (not to scale).

www.EngineeringEBooksPdf.com

6.10.11 Stiffeners

6.10.11.1 Definitions and Description of Stiffeners

In built-up girders, thin webs are logical choice because of economics; however, thin webs are prone to buckling. The stability of the web can always be increased by increasing its thickness, but such a design will not be economical because the increased weight of the girder leads to higher material costs and moments. A more economical solution is obtained by keeping the web as thin as possible and increasing its stability by introducing reinforcing ribs called *stiffeners*.

As the term *stiffener* implies, a stiffener is simply a member that is used to stiffen thin webs of girders. It is usually an angle (used in older riveted or bolted plate girders) or more generally a rectangular bar (as used in modern-welded plate girders) attached to the web of a girder to transfer shear or to prevent web buckling (Figure 6.3). A comprehensive discussion on the theory of stiffeners has been provided by Timoshenko and Gere (1961) and Bleich (1952) and summarized by Taly (1998). A summary from these references is presented here.

It is often advantageous and economical to use narrow flanges and thin, deep webs (to have large moment of inertia); this results in noncompact, light, slender members (least-weight approach) with flanges and web ending up having large *width-to-thickness ratios*. But this high element slenderness causes a problem. Presence of large compressive forces in the plane of these elements makes them highly susceptible to buckling. The maximum strength of a built-up girder can be realized only if the component plates do not buckle locally because local buckling can lead to premature failure of the entire plate girder or at least compromise its load-carrying capacity. To prevent this buckling tendency, slender webs need to be stiffened. This stiffening is accomplished by providing either *transverse* (vertical) stiffeners (Figure 6.40) or a combination of transverse and *longitudinal* (usually horizontal) stiffeners (Figure 6.41).

Transverse stiffeners (Figure 6.3) are oriented in the direction of the applied load, whereas the longitudinal stiffeners are oriented parallel to flanges and the longitudinal axis of the girder. A web may be stiffened with transverse stiffeners only or with a combination of transverse and longitudinal stiffeners (single or multiple) depending on the proportion (slenderness) of the web and applicable specifications. Longitudinal stiffeners are generally used for long-span bridges.

Transverse stiffeners can be *intermediate* (or nonbearing) stiffeners, *bearing stiffeners*, or *end stiffeners* (Figure 6.40). Intermediate stiffeners are transverse stiffeners placed perpendicular to the compression flange at various intervals along the span (Figure 6.3). The spacing of transverse stiffener spacing may be the same throughout the span, or it may increase progressively away from the support (where the shear is maximum) toward the midspan (where the shear is minimum).

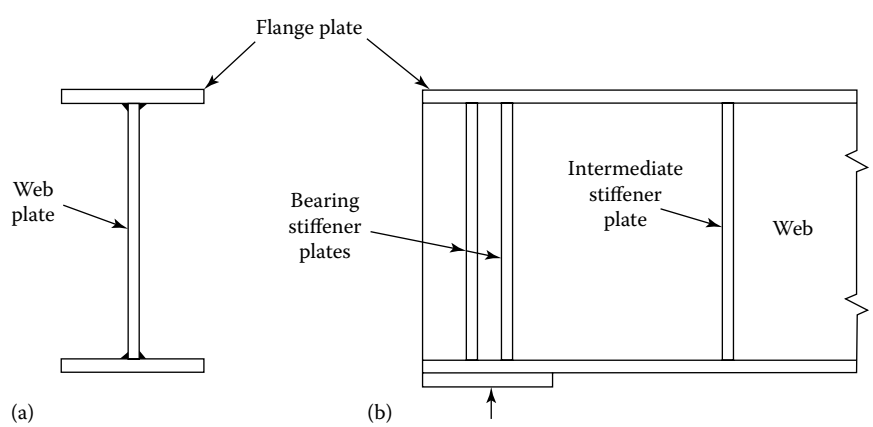

FIGURE 6.40 Transverse stiffeners in a plate girder. (a) Cross section and (b) elevation at end of span.

www.EngineeringEBooksPdf.com

The segment between the adjacent transverse stiffeners is called a *panel*; the one between the end stiffener and the adjacent stiffener is called the *end panel*. A web panel divided by one or more longitudinal stiffeners results in two or more subpanels (Figure 6.40). That is, a subpanel is a segment of the plate girder bounded by two adjacent transverse stiffeners, a longitudinal stiffener, and the flange (Figure 6.42). In the case of a web having multiple longitudinal stiffeners, a subpanel is a segment of the web bounded by two adjacent transverse stiffeners and two adjacent longitudinal stiffeners.

The end stiffeners are the bearing stiffeners that are placed at the ends of girders (Figure 6.40). They are called bearing stiffeners because their purpose is to distribute reactions from the superstructure to the full depth of the web without putting the entire load on the flange connections. The bearing stiffeners participate integrally with a portion of the web (extending on both sides of the stiffeners) and act as a column having a cross section resembling a "plus" sign (+) in transmitting the concentrated load (the reaction from the girder) to the supports (abutments and/or piers). An intermediate stiffener can also be a bearing stiffener when used to transmit a concentrated load on the girder. All plate girders, stiffened or unstiffened, are provided with bearing stiffeners and intermediate stiffeners; the latter are placed at diaphragms or cross-frame locations. Girder webs that are transversely stiffened at the diaphragm locations only are to be considered unstiffened for design purposes.

Longitudinal stiffeners are usually oriented horizontally, parallel to the compression flange in straight built-up girders. In some cases of long-span *haunched* built-up girders, longitudinal stiffeners may be oriented curved, parallel to the curved bottom flange over the supports, which is in compression (Figure 6.41) With the exceptions of the bearing stiffeners that must be provided in pairs, that is, on both sides of the web (Art. 6.10.11.2.1), a designer has the option of providing both transverse and longitudinal stiffeners on one side of the web only or transverse stiffeners on one side and the longitudinal stiffeners on the other side of the web; the latter scheme allows both types of

FIGURE 6.41 Union Pacific Railroad Overpass, Cheyenne, Wyoming. Longitudinal stiffeners are oriented horizontally, parallel to the compression flange (top flanges between the span and bottom flanges over the support). The longitudinal stiffeners are oriented parallel to the haunched curved bottom flange (in compression) over one of the supports on the left side of the bridge. (Courtesy of American Institute of Steel Construction, Chicago, IL.)

www.EngineeringEBooksPdf.com

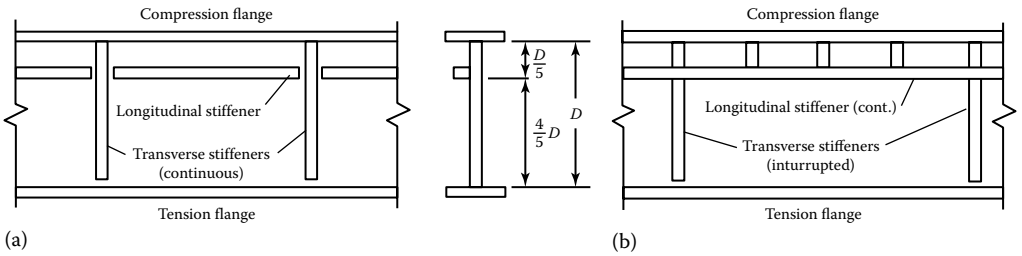

FIGURE 6.42 Schemes for stiffeners arrangements: (a) transverse stiffeners are continuous; the horizontal stiffeners are placed in between the adjacent transverse stiffeners; the vertical distance of the longitudinal stiffener can vary from $h/5$ (shown) to $2h/5$. (b) The longitudinal stiffener is continuous, whereas the transverse stiffeners are interrupted by the longitudinal stiffener.

stiffeners to run uninterruptedly, often a convenient and economical fabrication practice. For convenience of fabrication, transverse stiffeners are often placed on one side of the web only (Figure 6.3). When provided on only one side of the web, the stiffeners are provided generally on the inside face of the web of improved esthetics, in which case they are called *internal stiffeners*. When placed on the same side of the web, the transverse and longitudinal stiffeners intersect each other, and several schemes of stiffener arrangements can be used at the discretion of the designer. For example, transverse stiffeners can be placed on one side of the web, and the longitudinal stiffener can be placed on the other side, without any interruption by the transverse stiffeners, essentially a cost-effective fabrication scheme. Alternatively, the transverse stiffeners can be continuous for the full depth of the web, and the longitudinal stiffener, which need not be continuous, is cut to fit in between the adjacent transverse stiffeners (Figure 6.42a). Yet another scheme is to use short transverse stiffeners in the smaller subpanels (positioned between the compression flange and the continuous longitudinal stiffener) (Figure 6.42b).

6.10.11.2 Web Bend-Buckling Resistance

6.10.11.2.1 Webs without Longitudinal Stiffeners

The nominal bend-buckling resistance of a web without longitudinal stiffeners is determined from Eqiation 6.120:

$$F_{crw} = \frac{0.9EK}{\left(\dfrac{D}{t_w}\right)^2} \qquad (6.120)\ [A6.10.1.1.1\text{-}1]$$

but not to exceed the smaller of R_hF_{yc} and $F_{yw}/0.7$.

In Equation 6.120, k = bend-buckling coefficient; its value is determined from Equation 6.121:

$$k = \frac{9}{\left(\dfrac{D_c}{D}\right)^2} \qquad (6.121)\ [AA6.10.1.1.1\text{-}2]$$

where D_c = depth of the web in compression in the elastic range (in.). For composite sections, D_c is determined as specified in Art. D6.3.1.

www.EngineeringEBooksPdf.com

6.10.11.2.2 Webs with Longitudinal Stiffeners

Equation 6.118 may be used to determine the nominal bend-buckling resistance of a web with longitudinal stiffener but with k determined from Equations 6.122 and 6.123 as appropriate:

If $\frac{D_s}{D_c} \geq 0.4$, then

$$k = \frac{5.17}{\left(\frac{D_c}{D}\right)^2} \geq \frac{9}{\left(\frac{D_c}{D}\right)^2} \quad (6.122)\ [AA6.10.1.1.2\text{-}1]$$

If $\frac{D_s}{D_c} < 0.4$, then

$$k = \frac{11.64}{\left(\frac{D_c - D_s}{D}\right)^2} \quad (6.123)\ [AA6.10.1.1.2\text{-}2]$$

where D_s = distance from the centerline of the closest plate longitudinal stiffener or from the gage line of the closest angle longitudinal stiffener surface or leg of the compression flange element (in.).

When both edges of the web are in compression, $k = 7.2$.

6.10.11.3 Design of Transverse Stiffeners

6.10.11.3.1 General Requirements

As discussed in Section 6.10.11.1, the primary function of transverse stiffeners (Figure 6.3) is to stiffen the webs so as to prevent their buckling. Depending on the design requirements, stiffeners may be provided on one or both sides of the web. To this end, they are required to satisfy certain design requirements as follows:

1. Transverse stiffeners shall consist of plates or angles welded or bolted to one or both sides of the web.
2. Stiffeners in straight girders not used as connection plates shall be tight fit or attached to the compression flange, but need not be in bearing with the tension flange (Figure 6.42).
3. Single-sided stiffeners on horizontally curved girders should be attached to both flanges (Figure 6.43). Attachment of transverse stiffeners to both flanges is required to help retain the cross-sectional configuration of the curved girder when subjected to torsion and to avoid high localized bending within the web.
4. When transverse stiffeners are provided on both sides of curved girders, they shall be tightly fitted or attached to both flanges of the girders (for the same reason as in 3 previously).
5. Stiffeners used as connecting plates for diaphragms or cross frames shall be attached to both flanges.
6. The distance between the end of the web-to-stiffener weld and the near edge of the adjacent web-to-flange or longitudinal stiffener-to-web weld is subject to limitations as follows. The said distance
   a. Shall not be less than four times the web thickness ($4t_w$)
   b. Shall not exceed the lesser of six times the web thickness ($6t_w$) and 4 in.

www.EngineeringEBooksPdf.com

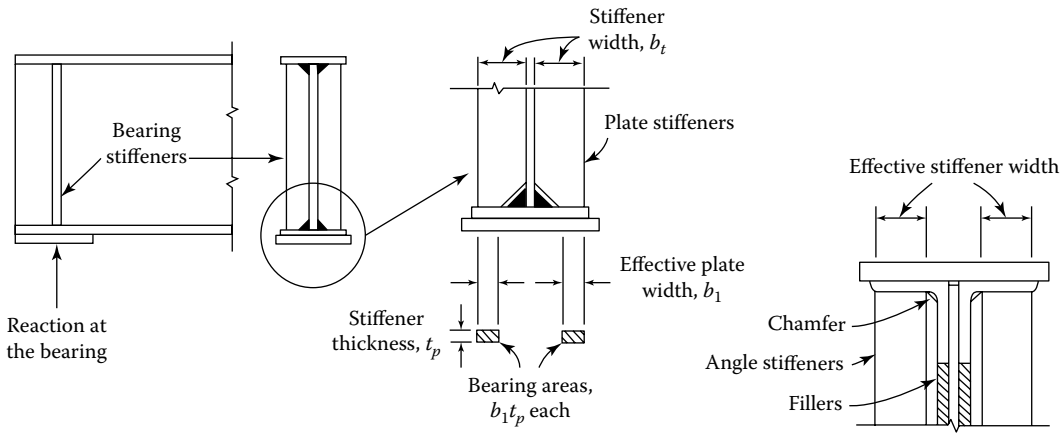

FIGURE 6.43 Single-sided stiffeners on horizontally curved girders should be attached to both flanges.

6.10.11.3.2 Section Properties of Transverse Stiffeners

There are two requirements pertaining to the section properties of transverse stiffeners:

1. Projecting width, b_t (Art. 6.10.11.1.2)
2. Moment of inertia (Art. 6.10.11.1.3)

1. Projecting width, b_t
   The width, b_t, of each projecting stiffener element shall satisfy Equations 6.124 and 6.125:

$$b_t \geq 2.0 + \frac{D}{30} \qquad (6.124)\ [A6.10.11.1.2\text{-}1]$$

$$16t_p \geq b_t \geq \frac{b_f}{4} \qquad (6.125)\ [A6.10.11.1.2\text{-}2]$$

where

b_f = for I-sections, full width of the widest compression flange within the field section under consideration; for tub sections, full width of the widest top flange within the field under consideration; and, for closed box sections, the limit of $b_f/4$ (in.) does not imply

t_p = thickness of projecting stiffener element

2. Moment of inertia
   The key quantity pertaining to the moment of inertia requirement is the factored shear-buckling resistance of the web panel under consideration, $\phi_v V_{cr}$. The moment of inertia requirement depends on whether $\phi_v V_{cr}$ is less than or greater than the smaller of the nominal shear-buckling resistances of the adjacent web panels.
   a. For transverse stiffeners adjacent to web panels in which neither panel supports a shear force V_u larger than $\phi_v V_{cr}$, the moment of inertia, I_t, of the transverse stiffener shall satisfy both Equations 6.126 and 6.127:

$$I_t \geq I_{t1} \qquad (6.126)\ [A6.10.11.1.3\text{-}1]$$

$$I_t \geq I_{t2} \qquad (6.127)\ [A6.10.11.1.3\text{-}2]$$

www.EngineeringEBooksPdf.com

in which

$$I_{t1} = bt_w^3 J \qquad (6.128)\ [A6.10.11.1.3\text{-}3]$$

$$I_{t2} = \frac{D^4 \rho_t^{1.3}}{40}\left(\frac{F_{yw}}{E}\right)^{1.5} \qquad (6.129)\ [A6.10.11.1.3\text{-}4]$$

$$J = \frac{2.5}{\left(d_o/D\right)^2} \qquad (6.130)\ [A6.10.11.1.3\text{-}5]$$

$$F_{cr} = \frac{0.31E}{\left(\frac{b_t}{t_p}\right)^2} \le F_{ys} \qquad (6.131)\ [A6.10.11.1.3\text{-}6]$$

$$V_{cr} = CV_p \qquad (6.132)\ [A6.10.11.1.3\text{-}7]$$

$$V_p = 058F_{yw}Dt_w \qquad (6.133)\ [A6.10.11.1.3\text{-}8]$$

where

ϕ_v = resistance factor for shear specified in Section 6.9 (Art. 6.5.4.2)
V_{cr} = smaller of the shear-buckling resistances of the adjacent panels (kip)
V_u = larger of the shears in adjacent web panels due to the factored loads (kip)
I_t = moment of inertia of transverse stiffener taken about the edge in contact with the web for single stiffeners and about the mid-thickness of the web for stiffeners in pairs
b = smaller of d_o and D (in.)
d_o = smaller of the adjacent web panel widths (in.)
J = stiffener bending rigidity parameter
ρ_t = larger of F_{yw}/F_{crs} and 1.0
F_{cr} = local buckling stress for the stiffener (ksi)
F_{ys} = specified minimum yield strength for the stiffener
C = ratio of the shear-buckling resistance to the shear-yield strength determined by Equations 6.80 through 6.83 (A6.10.9.3.2-4 through A6.10.9.3.2-6) as applicable
V_p = plastic shear force (kip)

The term ρ_t in Equation 6.129 accounts conservatively for the effect of early yielding in transverse stiffeners when the yield strength of the transverse stiffener, F_{ys}, is lesser than the yield strength of the web, F_{yw} (i.e., $F_{ys} < F_{yw}$), and for the effect of potential local buckling of stiffeners having a relatively large width-to-thickness ratio b_t/t_p.

b. For transverse stiffeners adjacent to web panels in which the shear force V_u is larger than the factored shear-buckling resistance, $\phi_v V_{cr}$, and thus web post-buckling or tension field resistance is required in one or both panels, the moment of inertia, I_t, of the transverse stiffener shall satisfy the following as applicable:

www.EngineeringEBooksPdf.com

If $I_{t2} > I_{t1}$, then

$$I_t \geq I_{t1} + \left(I_{t2} - I_{t1}\right)\left(\frac{V_u - \phi_v V_{cr}}{\phi_v V_n - \phi_v V_{cr}}\right) \qquad (6.134)\ [A6.10.11.1.3\text{-}9]$$

Otherwise

$$I_t \geq I_{t2} \qquad (6.135)\ [A6.10.11.1.3\text{-}10]$$

where V_n = smaller of nominal combined buckling and tension-field shear resistances of adjacent web panels, determined as specified in Art. 6.10.9.3.2 (kip)

When transverse stiffeners are used in web panels with longitudinal stiffeners, they shall also satisfy Equation 6.136:

$$I_t \geq \left(\frac{b_t}{b_\ell}\right)\left(\frac{D}{3.0d_o}\right)I_\ell \qquad (6.136)\ [A6.10.11.1.3\text{-}11]$$

where

b_t = projecting width of the transverse stiffener
b_ℓ = projecting width of the longitudinal stiffener
I_ℓ = moment of inertia of the longitudinal stiffener determined as specified in Art 6.10.11.3.3 (in.^{3})

6.10.11.4 Design for Bearing Stiffeners

6.10.11.4.1 General Requirements

As the term *bearing stiffeners* suggest, these are transverse stiffeners that must be provided at locations where loads are transferred to or from the girder by bearing. Webs of rolled shapes and built-up sections without bearing stiffeners at location concentrated loads must be investigated for the limit states of web local yielding and web crippling (Figure 6.44) according to the procedures specified

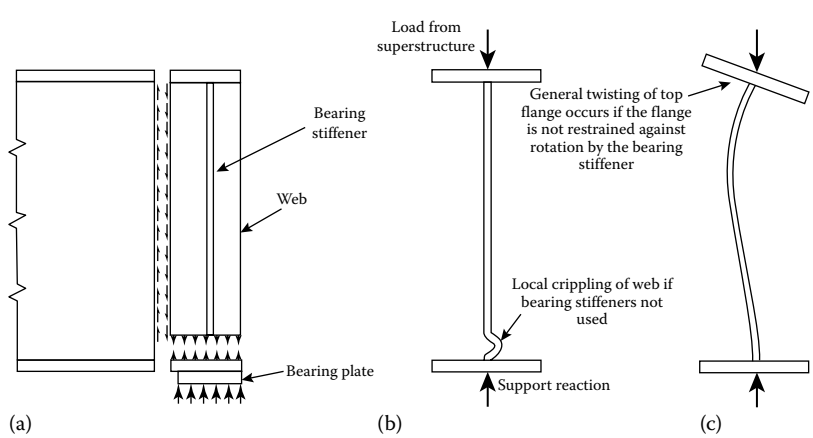

FIGURE 6.44 Support conditions and possible distortions at the ends of a steel wide flange girder. (a) Bearing stiffener, (b) local crippling of web due to support reaction (compressive force), and (c) general twisting of flange due to lack of restraint to prevent rotation of the top flange. (Adapted from Johnston, B.G. et al., *Basic Steel Design*, Prentice-Hall, Englewood Cliffs, NJ., 1986.)

www.EngineeringEBooksPdf.com

in Art. D6.5. Otherwise, bearing stiffeners must be provided as specified in Art. 6.10.11.2.1, which must satisfy the following general requirements:

1. At bearing locations on rolled shapes and other locations on built-up sections or rolled shapes subjected to concentrated loads, where the loads are not transmitted through the deck or deck system, either bearing stiffeners shall be provided or the web shall satisfy the provisions of Art. D6.5.
2. Bearing stiffeners shall be placed on the webs of built-up sections at all bearing locations.
3. Bearing stiffeners shall consist of one or more plates or angles welded to both sides of the web. The connections to the web shall be designed to transfer full bearing force due to the factored loads.
4. The stiffeners shall extend the full depth of the web and as closely as possible to the outer edges of the flanges.
5. Each stiffener shall be either milled to bear against the flange through which it receives the load or attached to that flange by a full penetration groove weld.
6. The width, b_t, of each projecting stiffener element shall satisfy Equation 6.137:

$$b_t \leq 0.48 t_p \sqrt{\frac{E}{F_{ys}}} \qquad (6.137)\ [A6.10.11.2.2\text{-}1]$$

where
F_{ys} = specified minimum yield strength of the stiffener (ksi)
t_p = thickness of the projecting stiffener element

For F_{ys} = 50 ksi, Equation 6.137 suggests that the width of a bearing stiffener should not exceed 11.56 times or approximately 12 times its thickness.

7. The factored bearing resistance for the fitted ends of bearing stiffeners shall be determined from Equation 6.138:

$$(R_{sb})_r = \phi_b (R_{sb})_n \qquad (6.138)\ [A6.10.11.2.3\text{-}1]$$

where
$(R_{sb})_r$ = factored bearing resistance for the fitted end of bearing stiffener (kip)
ϕ_b = resistance factor for bearing stiffener specified in Section 6.9 (Art 6.5.4.2)
$(R_{sb})_n$ = nominal bearing resistance for the fitted ends of bearing stiffeners (kip)

The value of $(R_{sb})_n$ in Equation 6.138 is to be determined from Equation 6.139:

$$(R_{sb})_n = 1.4 A_{pn} F_{ys} \qquad (6.139)\ [A6.10.11.2.3\text{-}2]$$

where
A_{pn} = area of the projecting elements of the stiffener outside of the web-to-flange fillet welds but not beyond the edge of the flange (in.^{2})
= $b_1 t_p$ in Figure 6.45

It must be recognized that to bring bearing stiffener plates tight against the flanges, part of the stiffener at both ends, as a matter of practical necessity, must be clipped to clear the web-to-flange fillet weld (Figure 6.43). This results in the reduced contact width b_1 ($<b_t$) of the stiffener and area of the

www.EngineeringEBooksPdf.com

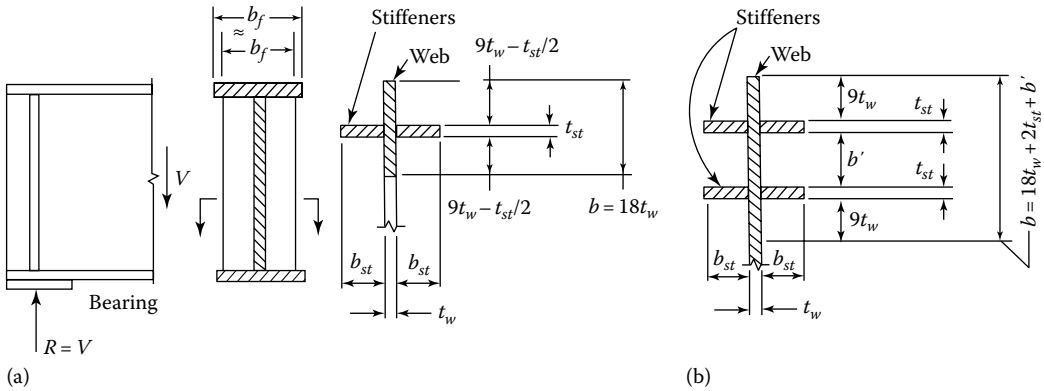

FIGURE 6.45 Bearing stiffeners for rolled shapes and built-up sections. (a) Two bearing stiffeners and (b) four bearing stiffeners.

bearing stiffener in direct bearing, A_{pn} ($=b_1t_p$ in Figure 6.45) to be less than the gross cross-sectional area of the bearing stiffener, b_tt_p (i.e., $A_{pn} < b_tt_p$). This is the basis of Equation 6.139. This reduced cross-sectional area of the bearing stiffener must be adequate to transmit the factored girder reaction to the support.

6.10.11.4.2 Axial Resistance of Bearing Stiffener

Bearing stiffeners are designed as concentrically loaded columns. The factored axial resistance, P_r, is determined from Equation 6.140 as specified in Art. 6.9.2.1 using the specified minimum yield strength of the stiffener, F_{ys}:

$$P_r = \phi_c P_n \qquad (6.140)\ [A6.9.2.1\text{-}1]$$

where

P_n = nominal compressive resistance as specified in Art. 6.9.4 or 6.9.5 as applicable
ϕ_c = resistance factor for compression as specified in Section 6.9 (Art 6.5.4.2)

The radius of gyration of this fictitious column shall be calculated about the mid-thickness of the web, and its effective length shall be taken as $0.75D$ where D is the depth of the web. This reduced column length is permitted because of the welded end restraints provided by tight fit against the flanges. The specified minimum yield strength of the stiffeners plates, F_{ys}, must be used to determine their axial resistance to account for early yielding of the lower strength stiffener plates.

A portion of the web extending longitudinally on both sides of the welded bearing stiffeners is considered participatory in carrying the factored girder reaction to the support. The effective cross-sectional area of this fictitious column is determined as follows (Art. 6.10.11.2.4a):

1. For stiffeners bolted to the web, the effective section shall consist of stiffener elements only.
2. For stiffeners consisting of two plates welded to the web, a portion of the web shall be included as part of the column section.
3. For stiffeners consisting of two plates welded to the web, the effective column shall consist of two stiffener elements plus a centrally located strip of web extending not more than $9t_w$ on each side of the stiffeners (Figure 6.45).
4. If more than one pair of stiffeners is used, the effective column section shall consist of all stiffener elements, plus a centrally located strip of web extending not more than $9t_w$ on each side of the outer projecting elements of the group.

www.EngineeringEBooksPdf.com

5. The strip of the web shall not be included in the effective section at the interior supports of continuous-span hybrid members for which the minimum yield strength of the web is less than 70 percent of the specified minimum yield strength of the higher-strength flange.
6. If the specified minimum yield strength of the web is less than that of the stiffener plates, the strip of the web included in the effective section shall be reduced by the ratio F_{yw}/F_{ys}.

6.10.11.5 Design for Longitudinal Stiffeners

6.10.11.5.1 General Requirements

Research has shown that transverse stiffeners alone contribute little to the buckling strength of a plate unless they are spaced much closer than the width of the plate. The critical stress of the plate will increase significantly only if spacing of the transverse stiffeners is much smaller than the width of the plate. Because of the web's inherent post-buckling strength, the web's initial buckling does not indicate failure of the girder. Investigations have demonstrated that the bend-buckling of webs can be considerably enhanced if longitudinal stiffeners are provided. A longitudinal stiffener essentially forces a web to buckle in a higher mode (number of modes, $n \geq 2$) by forming a nodal line in the buckled configuration (Figure 6.46), with waves much shorter than those of the unstiffened plate. In essence, "these stiffeners only carry a portion of the compressive load, but subdivide the plate into smaller panels thus increasing considerably the critical stress at which the plate will buckle" (Bleich 1952, Chapter 9). This is the most significant advantage of providing longitudinal stiffeners embedded in LRFD Art. 6.10.2.1: Web Proportions, which permits, for preliminary design, a web slenderness ratio of 300 for webs with longitudinal stiffeners, which is twice that for webs without the longitudinal stiffeners (150) (see Section 6.10.2.1, Equations 6.7a and 6.7b).

Schematics of longitudinal stiffeners are shown in Figure 6.41. The following are general requirements for providing longitudinal stiffeners.

1. Where required (Art, 6.10.1.9.2), longitudinal stiffeners should consist of either a plate welded to one side of the web or a bolted angle.
2. Whenever practical, longitudinal stiffeners shall extend uninterrupted over their specified length, unless otherwise permitted in contract documents. Therefore, it is preferred that longitudinal stiffeners be placed on the opposite side of the web from transverse stiffeners.
3. If transverse stiffeners are interrupted by a longitudinal stiffener (causing discontinuity), the transverse stiffeners must be fitted to both sides of the longitudinal stiffeners with connection sufficient to develop the flexural and axial resistance of the transverse stiffener. Similarly, if the longitudinal stiffener be interrupted, it should be similarly attached to

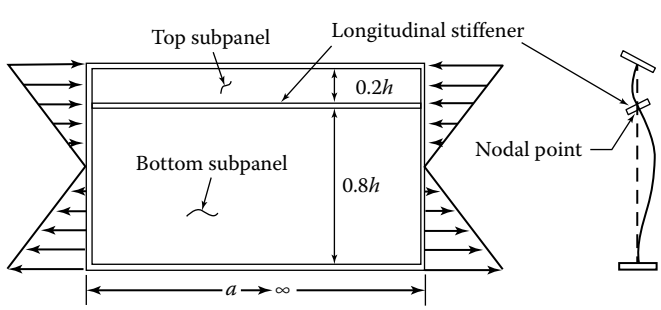

($h = D$ = clear depth of web between flanges, a = length of the plate or panel)

FIGURE 6.46 Bend-buckling of a plate reinforced with a longitudinal stiffener at $0.2D$ from the compression flange. *Note*: $h = D$ = clear depth of web between flanges; a, length of the plate or panel. (Adapted from Bleich, F., *Buckling of Metal Structures*, McGraw-Hill Book Company, New York, 1952.)

www.EngineeringEBooksPdf.com

all transverse stiffener web elements. All interruptions should be carefully designed with respect to fatigue, particularly if the longitudinal stiffener is not attached to the transverse web elements.

4. Longitudinal stiffeners shall be located at a vertical position on the web such that (a) flexural stress given by Equation 6.32 shall be satisfied when checking constructibility, (b) Equation 6.141 is satisfied at the service limit state and (c) all other design requirements at the strength limit state:

$$f_{bu} \leq F_{crw} \qquad (6.32)\ [A6.10.3.2.1\text{-}3]$$

$$f_c \leq F_{crw} \qquad (6.141)\ [A6.10.4.2.2\text{-}4]$$

5. The flexural stress in the longitudinal stiffener, f_s, due to the factored loads at the strength limit state, and when checking constructibility, shall satisfy Equation 6.142:

$$f_s = \phi_f R_h F_{ys} \qquad (6.142)\ [A6.10.11.3.1\text{-}1]$$

where

f_{bu} = flange stress calculated without consideration of flange lateral bending determined as specified in Art. 6.10.1.6 (ksi)

f_c = compression flange stress at the section under consideration due to the Service II loads calculated without consideration of flange lateral bending (ksi) stiffeners, as applicable, determined as specified in Art. 6.10.1.9

F_{ys} = specified minimum yield strength of the longitudinal stiffener

R_h = hybrid factor (discussed in Section 6.10.1.3.1)

6. In regions where the web undergoes stress reversal, it may be necessary, or desirable, to use two longitudinal stiffeners on the web.
7. Copes should be provided to avoid intersecting welds.

A longitudinal stiffener placed at the neutral axis of a web is relatively ineffective in improving the stability of web plates in pure bending. Such a longitudinal stiffener can increase the buckling strength to the order of 60 percent of that of the unstiffened plate in the elastic range; the increase is more modest in the inelastic range. However, the buckling strength increases substantially when the longitudinal stiffener is placed between the compression flange and the neutral axis (Bleich 1952).

Optimum location of longitudinal stiffener on the web is based on theoretical and experimental studies. It has been suggested that the optimum location for one longitudinal stiffener is $0.4D_c$ (D_c = depth of web in compression) for bending and $0.5D$ (D = clear depth of web between flanges) for shear. Tests have shown that longitudinal stiffeners located at these locations can effectively control lateral web deflections under flexure (Cooper 1967). The distance $0.4D_c$ is recommended because shear is always accompanied by moment and because a properly proportioned longitudinal stiffener also reduces the web lateral deflection caused by shear. Readers should refer to LRFD Commentary C6.10.11.3.1 for a comprehensive discussion on the location of the longitudinal stiffeners on the web. Detailed information on the design of longitudinally stiffened girders can be found in the literature (Vincent 1969, ASCE-AASHTO 1978).

6.10.11.5.2 Section Properties of Longitudinal Stiffeners

There are two requirements pertaining to the section properties of longitudinal stiffeners:

1. Projecting width, b_t (Art. 6.10.11.3.2)
2. Moment of inertia (Art. 6.10.11.3.3)

www.EngineeringEBooksPdf.com

1. Projecting width, b_t
   In order to prevent local buckling of the longitudinal stiffener, its width, b_t, shall satisfy Equation 6.143:

$$b_t \leq 0.48 t_s \sqrt{\frac{E}{F_{ys}}} \qquad (6.143)\ [A6.10.11.3.2\text{-}1]$$

   where
   F_{ys} = specified minimum yield strength of the stiffener (ksi)
   t_s = thickness of the longitudinal stiffener

   For F_{ys} = 50 ksi, Equation 6.143 suggests that the width of a longitudinal stiffener should not exceed 11.56 times or approximately 12 times its thickness (a requirement similar to that for bearing stiffeners, Equation 6.137).
2. Moment of inertia, I_t
   The requirement for moment of inertia, I_ℓ, for straight girders is based on the work of Moiseiff and Lienhard (1941) as expressed by Equation 6.144:

$$I_\ell \not< D t_w^3 \left[2.4 \left(\frac{d_0}{D} \right)^2 - 0.13 \right] \qquad (6.144)$$

   The LRFD expression for I_ℓ is a slightly modified version for Equation 6.144, which includes a modifier β to account for curvature of horizontally curved girders as given by Equation 6.145:

$$I_\ell = D t_w^3 \left[2.4 \left(\frac{d_0}{D} \right)^2 - 0.13 \right] \beta \qquad (6.145)\ [A6.10.11.3.3\text{-}1]$$

   The radius of gyration of a longitudinal stiffener shall satisfy Equation 6.146:

$$r \geq \frac{0.16 d_o \sqrt{\frac{F_{ys}}{E}}}{1 - 0.6 \left(\frac{F_{yc}}{R_h F_{ys}} \right)} \qquad (6.146)\ [A6.10.11.3.3\text{-}2]$$

   where β = curvature correction factor to be determined based on the curvature parameter, Z, as follows:

   1. For cases where the longitudinal stiffener is on the side of the web away from the center of curvature,

$$\beta = \frac{Z}{6} + 1 \qquad (6.147)\ [A6.10.11.3.3\text{-}3]$$

   2. For cases where the longitudinal stiffener is on the side of the web toward the center of curvature,

$$\beta = \frac{Z}{12} + 1 \qquad (6.148)\ [A6.10.11.3.3\text{-}4]$$

www.EngineeringEBooksPdf.com

3. $\beta = 1.0$ for longitudinal stiffeners on straight webs.
   The curvature parameter, Z, is determined from Equation 6.149:

$$Z = \frac{0.95 d_o^2}{R t_w} \leq 10 \qquad (6.149)\ [A6.10.11.3.3\text{-}5]$$

where
d_o = transverse stiffener spacing
D = clear distance between flanges
I_ℓ = moment of inertia of the longitudinal stiffener including an effective width of the web equal to $18t_w$ taken about the neutral axis of the combined section (in.^{4}) If F_{yw} is smaller than F_{ys}, than F_{ys}, the strip of the web included in the effective section shall be reduced by the ratio F_{yw}/F_{ys}
R = minimum girder radius in the panel (in.)
R = radius of gyration of the longitudinal stiffener including an effective width of the web equal to $18t_w$ taken about the neutral axis of the combined section

6.10.12 Cover Plates

Whenever necessary and permitted, using cover plates to augment the flexural strength of flanges of rolled and built-up sections is an economical way to design girders for flexural strength. This is so because, with the exception of continuous girders that have negative moments at the supports, the moments due to uniform loads in a girder are maximum near the midspan and zero at the free ends. Moments due to combined truck load and lane load are also maximum near the midspan and decrease gradually toward the free ends. As such, the flange area requirements are maximum near the midspan and smaller near the ends. It is common practice to use cover plates in the regions of larger moments in a girder.

The length of any cover plate, L_{cp}, added to a member shall satisfy Equation 6.150 (Art. 6.10.12):

$$L_{cp} \geq \frac{d}{6.0} + 3 \qquad (6.150)\ [A6.10.12.1\text{-}1]$$

where
L_{cp} = length of the cover plate (ft)
d = total depth of steel section (in.)

Additionally, the following requirements should also be satisfied:

1. Partial length welded cover plates shall not be used on flanges thicker than 0.8 in. for nonredundant load path structures subjected to repetitive loadings that produce reversal of stress in the flange.
2. The maximum thickness of a single cover plate on a flange shall not be greater than two times the thickness of the flange to which it is attached.
3. Multiple cover plates are *not* permitted.
4. Cover plates may either be wider or narrower than the flange to which they are attached.

Designer should be aware that cover plates are available in certain incremental thicknesses as follows (AISC 2011); trial plate thicknesses should be chosen accordingly:

1/32-in. increments to 1/2 in.
1/16-in. increments from 1/2 in. to 1 in.

www.EngineeringEBooksPdf.com

6.11 FATIGUE AND FRACTURE CONSIDERATIONS

6.11.1 General

The fatigue phenomenon was introduced in Section 1.4.1.3. A discussion on loading for fatigue was presented in Section 3.9. LRFD Art. 3.6.1.4 presents specifics related to fatigue loading. Readers are urged to read these sections first to gain a good understanding of various aspects related to design of steel superstructures for fatigue presented herein. To summarize, consider the following:

1. The fatigue load shall be one design truck or axles thereof as specified in Art. 3.6.1.2.2, but with a constant spacing of 30 ft (instead of 14 ft) between the two 32 kip axles.
2. The dynamic load allowance as specified in Art. 3.6.2 (15 percent for fatigue and fracture limit states) shall be applied to the fatigue load.
3. Lane load is not to be considered for the fatigue load.
4. The frequency of the fatigue load shall be taken as the single-lane average daily truck traffic ($ADTT_{SL}$) as discussed in Section 3.9.4. This frequency shall be applied to all components of the bridge, even to those located under lanes that carry a lesser number of trucks.
5. The value of $ADTT_{SL}$ should be obtained from reliable sources, in consultation with traffic engineers. Research suggests that the *ADT*, including all vehicles, that is, trucks and cars, is physically limited to 20,000 vehicles per lane per day under normal conditions (LRFD Art. C3.6.1.4.2). In the absence of project-specific data/study, this limit value of traffic should be considered when estimating the ADTT (see Example 3.16).
6. The number of stress-range cycles, *N*, can be determined from Equation 3.59 and illustrated by Example 3.17.

6.11.2 Classification of Fatigue

Fatigue can be classified as

1. Load-induced fatigue
2. Distortion-induced fatigue

These two effects are caused differently. Load-induced fatigue relates to the force effects due to live load stress range. Load-induced fatigue is covered under Art. 6.6.1.2. The distortion-induced fatigue, on the other hand, results from poor or improper detailing. For example, fatigue cracking has been found to occur due to strains not normally calculated in the design process. This type of fatigue often occurs in the web near a flange at a welded connection plate for a cross frame where a rigid load path has not been provided to adequately transmit the force in the transverse member from the web to the flange. The following discussion is limited to load-induced fatigue.

For simple-span superstructures, the stress range is simply the live load stress from the critical design truck location. For continuous structures, the stress range should be calculated for the critical location of the design truck on adjacent or remote spans. The stress range for continuous spans is determined as the sum of the absolute values of the maximum live load stresses when the design truck is on the span under consideration and the maximum live load stresses when the truck is on all adjacent or remote spans.

6.11.3 Design for Load-Induced Fatigue

6.11.3.1 Design Considerations

A discussion on design considerations for fatigue design is provided by LRFD Commentary C6.6.1.2.1, which is summarized here. As noted earlier, only the live load plus dynamic load

www.EngineeringEBooksPdf.com

allowance effects (i.e., cyclical loading) need to be considered for calculating the stress range cycle for fatigue design of a steel superstructure; permanent loads do not contribute to the stress range. Tensile stresses can cause fatigue cracks to propagate. For this reason, fatigue design criteria are considered for components detail subject to effective stress cycles in tension and/or stress reversal. If a component or detail is subject to stress reversal, fatigue is to be considered no matter how small the tension component of the stress cycle is because a flaw in the tensile residual stress zone could still be propagated by small tensile component of the stress. Residual stresses need not be considered in investigating fatigue.

For design purposes, Fatigue Limit State I load combination (fatigue and fracture load combination related to infinite fatigue-induced life) is considered because this is the loading that causes the largest stress range that a component detail is expected to experience often enough to propagate a crack. A design consideration ensues when the tensile component of the stress range cycle resulting from this load combination exceeds the compressive stress due to the unfactored permanent loads, there is a net tensile stress in the component or at the detail under consideration, and therefore fatigue must be considered. However, if the tensile stress component of the stress range does not exceed the compressive stress due to the unfactored permanent loads, there is no net tensile stress; in this case, the net stress is compressive and a fatigue crack would not propagate beyond a heat-affected zone.

Cross frames and diaphragm connecting adjacent girders in steel superstructures are components that have fatigue-prone detailing. These components are stressed when one girder deflects with respect to the adjacent girder connected by the diaphragm or cross frame. The sense of stress is reversed when the design truck is positioned over the adjacent girder. Because it is the total stress range that produces fatigue, the effects of trucks in different transverse positions usually create the largest stress range in bracing members.

6.11.3.2 Design Criteria

For load-induced fatigue considerations, each detail is required to satisfy Equation 6.151:

$$\eta\gamma(\Delta f) \leq \phi(\Delta F)_n \tag{6.151}$$

where

η = load modifier
γ = load factor
(Δf) = force effect specified in LRFD Table 3.4.1-1 for the fatigue load combination
ϕ = resistance factor
$(\Delta F)_n$ = nominal fatigue resistance as specified in Art. 6.6.1.2.5 (ksi)

For the fatigue limit state, $\eta = 1.0$ and $\phi = 1.0$, so Equation 6.151 can be expressed as Equation 6.152:

$$\eta\gamma(\Delta f) \leq (\Delta F)_n \tag{6.152} \text{ [A6.6.1.2.2-1]}$$

6.11.3.3 Detail Categories

Construction of steel bridge superstructures involves many different types of connections (viz., bolted and welded) and detailing (viz., direction of stress with respect to the direction of weld or the bolt lines). Depending on the type and location of these connections and detailing, they are subjected to different levels and types of stress range. For the convenience of designers and fabricators, various components and details susceptible to load-induced fatigue are divided into eight categories, called *detail categories*, by fatigue resistance; these are identified by letters A, B, B′, C, C′, D, E, and E′. They are summarized in Tables A6.3-1 through A6.3-11 and A6.4 (see at the end of this chapter) and provide the following information:

www.EngineeringEBooksPdf.com

Tables 6.A.3-1 through 6.A.3-11 (one continuous table) provide information on nine sections for the following types of connections:

Section 1: Plain material away from any welding
Section 2: Connected material in mechanically fastened material
Section 3: Welded joints joining components of built-up members
Section 4: Welded stiffener connections
Section 5: Welded joints transverse to the direction of primary stress
Section 6: Transversely loaded welded attachments
Section 7: Longitudinally loaded welded attachments
Section 8: Miscellaneous attachments
Section 9: Miscellaneous attachments

In Section 6, *transversely* signifies that the direction of applied stress is perpendicular to the longitudinal axis of the detail. Likewise, *longitudinally* in Section 7 signifies that the direction of the applied stress is parallel to the longitudinal axis of the detail.

In each of the aforementioned sections, the following information is provided:

1. Column 1: Description of detail/joint
2. Column 2: Each detail/joint categories is assigned one of the eight types: (A), (B), (B′), (C), (C′), (D), (E), and (E′), A being the best and (E′) the worst
3. Each detail type is assigned a detail category constant, A (ksi) (Table 6.2)
4. Threshold, $(\Delta F)_{TH}$ (ksi), for infinite fatigue life resistance for each detail category (also summarized in Table 6.3)
5. Potential crack initiation point for a detail/joint
6. Illustrative examples of detail/joint

As stated in LRFD Art. C6.6.1.2.3, "in design process, the fatigue considerations for Detail Categories A through B′ rarely, if ever, govern. Nevertheless, Detail Categories A through B′ have been included for completeness. Investigation of components and details with a fatigue resistance based on Detail Categories A through B′ may be appropriate in unusual cases."

The concept and calculation of 75-year single-lane average daily truck traffic ($ADTT_{SL}$) was discussed earlier in Section 3.9.4. Depending on the $ADTT_{SL}$, a component or detail should be

TABLE 6.2
Detail Category Constant

Detail Category	Constant, A Times 10^8 (ksi)
A	250.0
B	120.0
B′	61.0
C	44.0
C′	44.0
D	22.0
E	11.0
E′	3.9
M 164 (A325) bolts in axial tension	17.1
M 253 (A490) bolts in axial tension	31.5

Source: From *AASHTO LRFD Bridge Design Specifications*, Copyright © 2012 by American Association of State Highway and Transportation Officials, Washington, DC. Used by permission.

www.EngineeringEBooksPdf.com

TABLE 6.3
CAFTs, $(\Delta F)_{TH}$

Detail Category	Threshold, $(\Delta F)_n$ (ksi)
A	24.0
B	16.0
B′	12.0
C	10.0
C′	12.0
D	7.0
E	4.5
E′	2.6
M 164 (A325) bolts in axial tension	31.0
M 253 (A490) bolts in axial tension	38.0

Source: From *AASHTO LRFD Bridge Design Specifications*, Copyright © 2012 by American Association of State Highway and Transportation Officials, Washington, DC. Used by permission.

TABLE 6.4
75-Year ($ADTT_{SL}$) Equivalent to Infinite Life

Detail Category	75-Years ($ADTT_{SL}$) Equivalent to Infinite Life (Trucks/Day)
A	530
B	860
B′	1035
C	1295
C′	745
D	1875
E	3530
E′	6485

Source: From *AASHTO LRFD Bridge Design Specifications*, Copyright © 2012 by American Association of State Highway and Transportation Officials, Washington, DC. Used by permission.

designed for *infinite life* or *finite life*. The required decision-making information for this purpose is obtained from Table 6.4 that lists 75 yrs ($ADTT_{SL}$) equivalent to infinite life corresponding to each detail category. The significance of this information is that where the design stress range calculated using Fatigue I Limit State load combination is less than $(\Delta F)_{TH}$, the detail would, theoretically, provide infinite life. On the other hand, if the projected 75-year single-lane average daily truck traffic ($ADTT_{SL}$) is *less than or equal to* that listed in Table 6.4 for the component or detail under consideration, that component or detail shall be designed for finite life.

Orthotropic components and details are to be designed to satisfy the requirements of their respective detail categories as summarized in Table 6.A.4 which is formatted as follows:

Column 1: Description of detail
Column 2: Illustrative example of the detail
Column 3: Description of the condition of detail
Column 4: Fatigue category of detail
Column 5: Allowable design level (1, 2, or 3, as specified in Art. 9.8.3.4: Analysis of Orthotropic Decks).

www.EngineeringEBooksPdf.com

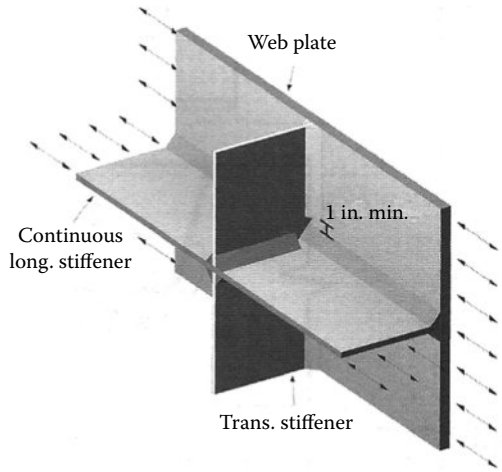

FIGURE 6.47 A weld detail where the longitudinal stiffener is continuous and has stress that is parallel to the primary stress. It is interrupted by a transverse stiffener. A 1-in. gap is provided between the toes of the intersecting welds to reduce constraint (LRFD Figure C6.6.1.2.4-1). (From *AASHTO LRFD Bridge Design Specifications*, Copyright © 2012 by American Association of State Highway and Transportation Officials, Washington, DC. Used by permission.)

6.11.3.4 Detailing to Reduce Constraint

Detailing constitutes a very important phase of both design and fabrication. The objective should be to design joints so as to avoid brittle fracture-prone details. Welded structures should be detailed to avoid conditions that create highly constrained joints and crack-like geometric discontinuities that are susceptible to constraint-induced fracture. Because of its specific nature, this form of brittle fracture is referred to as *constraint-induced* brittle fracture that can occur without any perceptible fatigue crack growth and without warning.

Art. 6.6.1.2.4 (Detailing to Reduce Constraint) specifies that welds that are parallel to primary stress but interrupted by intersecting members shall be detailed to allow a minimum gap of 1 in. between the weld toes, the idea being to avoid intersecting welds. An attachment parallel to primary stress (e.g., a longitudinal stiffener) is less prone to fatigue if it is continuous and transverse attachment is discontinuous (Figure 6.47). Art. C6.6.1.2.4 provides recommended guidelines for common joints to avoid such details.

6.11.3.5 Fatigue Resistance

Art 6.6.1.2.5 specifies expression for calculating the nominal fatigue resistance for details/components depending on the fatigue limit state. For fatigue I limit state and infinite life, the nominal resistance, $(\Delta F)_n$, is to be taken as given by Equation 6.153:

$$(\Delta F)_n = (\Delta F)_{TH} \qquad (6.153)\ [A6.6.1.2.5\text{-}1]$$

For Fatigue II Limit State and finite life, the nominal resistance is to be taken as given by Equation 6.154:

$$\left(\Delta F\right)_n = \left(\frac{A}{N}\right)^{\frac{1}{3}} \qquad (6.154)\ [A6.6.1.2.5\text{-}2]$$

where

$$N = (365)(75)n(ADTT)_{SL} \qquad (6.155)\ [6.6.1.2.5\text{-}3]$$

www.EngineeringEBooksPdf.com

A = detail category constant taken from Table 6.2
N = number of cycles of stress range (see Example 3.17)
n = number of stress range cycles per truck passage taken from Table 3.22
$(ADTT)_{SL}$ = single lane ADTT as specified in Art. 3.6.1.4 (see Example 3.16)
$(\Delta F)_{TH}$ = constant-amplitude fatigue threshold (CAFT) taken from Table 6.3 (ksi)

Equation 6.154 states that nominal fatigue resistance is inversely proportional to the cube root of the number of stress cycles, N. Equation 6.154 can also be expressed in terms of the CAFT, A and $(\Delta F)_n$, as Equation 6.156:

$$N = \frac{A}{(\Delta F)_n^3} \tag{6.156}$$

It can be seen from Equation 6.156 that if the live load stress range is reduced by half, then fatigue life increases by a factor of 2^3 or 8. Conversely, if the live load stress range is doubled, then the fatigue life is reduced to one-eighth (or divided by 8). Figure 6.48, called S-N diagram, gives a relationship between the stress range (S) and the number of stress cycles, N for all detail categories listed in Table 6.A.3.

Sometimes, a detail involves loaded discontinuous plate elements connected with a pair of fillet welds or partial joint penetration groove welds on opposite sides of the plate normal to the direction of primary stress (Figure 6.49). The fatigue resistance for the base metal and the weld metal in such details shall be determined from Equation 6.157:

$$(\Delta F)_n = (\Delta F)_n^c \left(\frac{0.65 - 0.59\left(\frac{2a}{t_p}\right) + 0.72\left(\frac{w}{t_p}\right)}{t_p^{0.167}} \right) \le (\Delta F)_n^c \tag{6.157) [A6.6.1.2.5-4}$$

where
$(\Delta F)_n^c$ = nominal fatigue resistance for detail category C (ksi)
$2a$ = length of the nonwelded root face in the direction of the thickness of the loaded plate (in.). For fillet welded connections, the quantity $(2a/t_p)$ shall be taken as 1.0
t_p = thickness of the loaded plate
w = leg size of the reinforcement or contour fillet, if any, in the direction of the thickness of the loaded plate (in.)

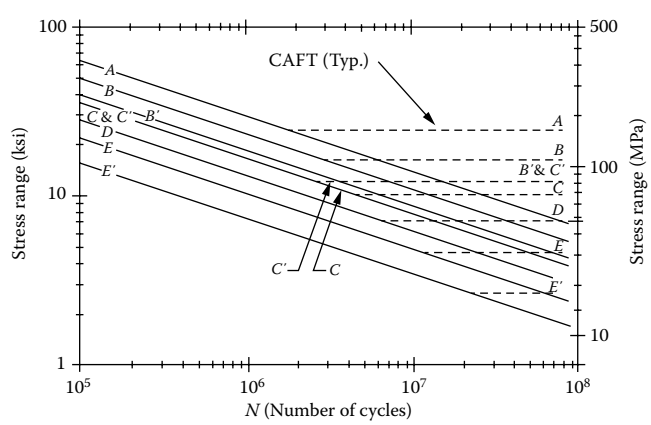

FIGURE 6.48 Stress range (S) versus the number of cycles (N) (LRFD Figure C6.6.1.2.5-1). CAFT = constant-amplitude fatigue threshold. (From *AASHTO LRFD Bridge Design Specifications*, Copyright © 2012 by American Association of State Highway and Transportation Officials, Washington, DC. Used by permission.)

www.EngineeringEBooksPdf.com

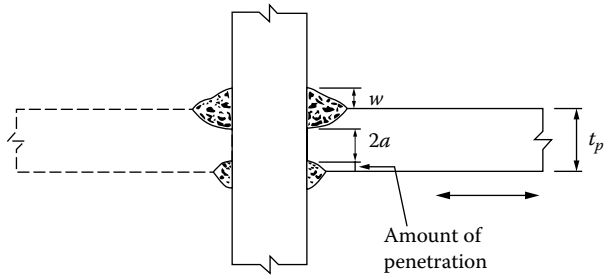

FIGURE 6.49 Loaded discontinuous plate element connected by a pair of partial joint penetration groove welds. (From *AASHTO LRFD Bridge Design Specifications*, Copyright © 2012 by American Association of State Highway and Transportation Officials, Washington, DC. Used by permission.)

6.12 DESIGN OF NONCOMPOSITE SLAB–STEEL GIRDER SUPERSTRUCTURES

For all bridges, loads (and their effects, viz, moments and shears) are calculated separately into two categories: permanent loads (dead loads) and live loads. Permanent loads are further divided in two categories: (1) dead load of structural components (e.g., deck and girders, traffic barriers) denoted as w_{DC} and (2) dead load due to the FWS denoted as w_{WD}; this is necessary because different load factors apply to them (1.25 and 1.5, respectively, for w_{DC} and w_{DW} for the Strength I Limit State).

For computing the force effects from vehicular live loads on bridges, approximate methods specified in Section 4 of LRFD Specifications (live load distribution factors for bending moment and shear specified in Art. 4.6.2.2.2 and 4.6.2.2.3) and discussed in Chapter 4 would be used. As specified in Art. 4.6.2.2.1, the distribution of live load specified in Art. 4.6.2.2.2 and 4.6.2.2.3 can be used if the following six conditions are satisfied:

1. Width of deck is constant.
2. Unless otherwise stated, the number of beams is not less than four.
3. Beams are parallel and have approximately the same stiffness.
4. Unless stated otherwise, the roadway part of the overhang, d_e, does not exceed 3 ft.
5. Curvature in plan is less than the limit specified in Art. 4.6.1.2.4 (this article limits the arc span divided by the girder radius to 0.06 radians or 3.44 degrees).
6. Cross section (s) is constant with one of the cross sections shown in LRFD Table 4.6.2.2.1.1 (see this table in Chapter 4 appendix).

The aforementioned six conditions are satisfied for bridges in both Examples 6.2 and 6.10.

Of necessity, as in any other structural design problem, a trial sections must be first chosen to proceed with calculations required to satisfy the many provisions of LRFD Specifications. A few trials are always required before a satisfactory section can be found. Even before selecting a trial section, it is necessary to design the deck slab, which requires selecting the girder spacing as the design depth of the deck slab depends on the spacing of girders. A minimum design depth of deck slab of 7½ in. is usually provided; greater design depth would be required in corrosive environment, for which increased cover is required. For short-span slab–girder superstructures, a girder spacing of 7–10 ft is commonly used. For Example 6.2, a girder spacing of 7 ft 6 in. has been selected arbitrarily; the design of the deck slab for this bridge was presented in Chapter 5.

Example 6.2 is presented as follows to illustrate the LRFD provisions for designing a noncomposite slab–steel girder superstructure. The design of concrete deck of this bridge was presented as Example 5.3 and is not repeated here. All calculations are presented in a step-by-step format to demonstrate compliance with all LRFD provisions (notably Art. 6.10), which have been discussed in the preceding paragraphs.

www.EngineeringEBooksPdf.com

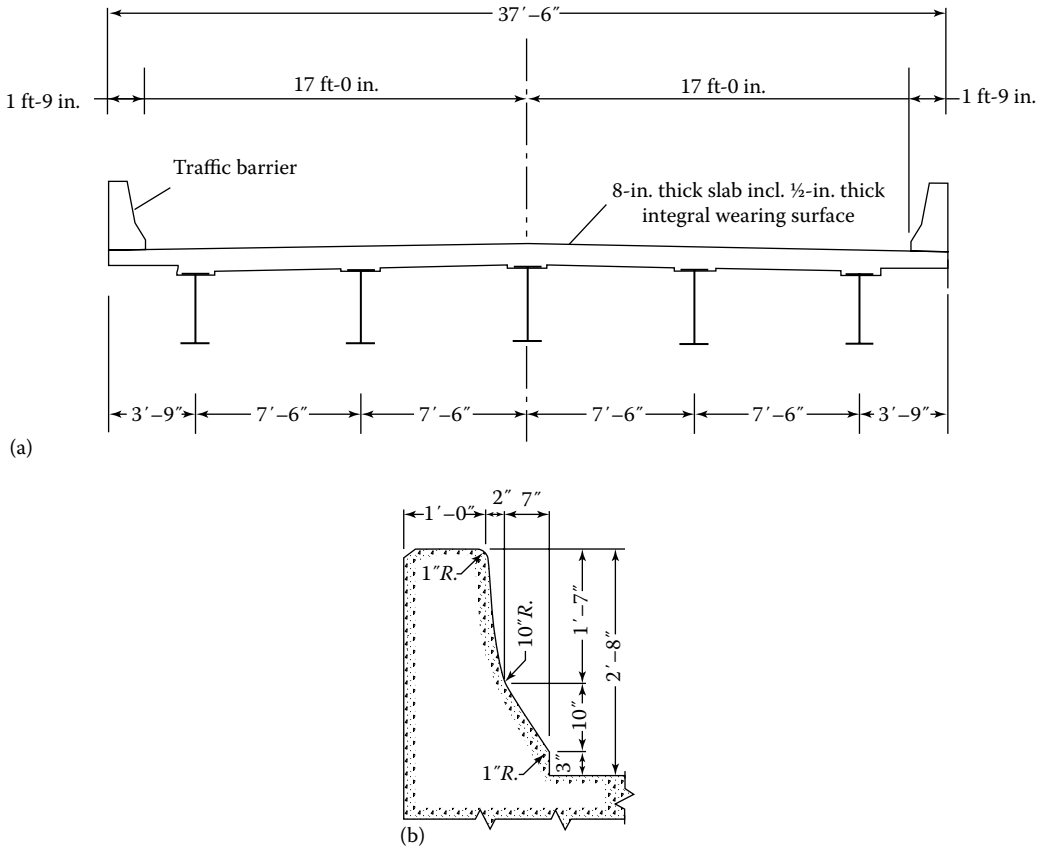

FIGURE 6.50 (a) Typical bridge cross section and (b) cross section of traffic barrier.

Example 6.2

Prepare a preliminary design of a simple-span, noncomposite two-lane bridge for a span of 50 ft on a rural interstate highway. The preliminary bridge cross section is shown in Figure 6.50a.

Solution

Assumptions

The following assumptions/data would be used for this two-lane bridge:

Span, L = distance between center-to-center bearings = 50 ft.
Slab-thickness including 1/2 in integral wearing surface = 8 in.
Structural depth of slab = 8 − 0.5 = 7.5 in.
FWS = 25 lb/ft^2.
Center-to-center girder spacing = 7 ft 6 in.
Girder size: trial size—W33 × 118 grade M 270/50W, F_y = 50 ksi, F_u = 70 ksi.
(Other sizes were tried and were rejected as either under-designed or overdesigned. Calculations are presented for W33 × 118 as the final trial size).
Unshored construction would be used.
The bridge has no skew.
As specified in LRFD Art. 4.6.2.2.1 and discussed in Section 4.3, the dead load of concrete traffic barriers, which will be cast after the deck hardens, would be distributed equally to all

www.EngineeringEBooksPdf.com

girders (exterior and interior). This assumption is used in this example. However, designers, at their discretion, may choose to distribute the dead load of traffic barriers to only the exterior girders and none of it to the interior girders; this option is not followed in this book.

Load and Resistance Design (LRFD) Parameters

For structural design based on the LRFD philosophy, the following parameters as specified in LRFD Specifications will be used.

Load Modifiers

$$\eta = \eta_D \eta_R \eta_I \qquad (1.69)\ [A1.3.2.1\text{-}1]$$

For this example, the bridge is assumed to be a typical, conventional bridge. Therefore, the following values of load modifiers will be used:

η_D = a factor related to ductility = 1.0.
η_R = a factor related to redundancy = 1.0.
η_I = a factor related to operational classification = 1.0.
Therefore, $\eta = (1.0)(1.0)(1.0) = 1.0$.

Strength Reduction Factors (Section 6.9/Art. 6.5.4.2)

1. Strength limit state	ϕ
Flexure	1.0
Shear	1.0
2. Service limit state	1.0
3. Fatigue limit state	
Fatigue I	1.0
Fatigue II	1.0

Limit States Considered

The structural design of the superstructure presented herein would be checked for Strength I Limit State. No permit vehicle is specified in this example, so Strength II Limit State is not checked. The Strength IV Limit State relates to very high dead-to-live load force effect ratios, which is not the case in this example and, therefore, not checked.

Wind load checks are not presented in this example; therefore, load combinations Strength III Limit State and Strength V Limit State are not checked.

Extreme event checks are not performed in this example.

Service I and Service III Limit States are not directly related to steel girder and, therefore, not checked in this example.

Live load deflection check would be performed as specified in Art. 2.5.2.6.2 using the live load portion of Service II load combination (Art. 6.10.4.2.1).

Load Combinations and Load Factors

The following load combination specified in AASHTO LRFD Art. 3.4.1 would be used in this example. Only the maximum permanent load factors γ_p (from AASHTO Table 3.4.1-2) would be used here because uplift is not a concern in this bridge geometry. In case potential for uplift at the end abutments exists, the minimum permanent load factors specified in the table should be used in the strength load combinations when checking for uplift.

The following load combinations are obtained directly from LRFD Table 3.4.1-1:

1. Strength I Limit State

$$U = \eta[1.25DC + 1.5DW + 1.75(LL + IM) + 1.0WA + 1.0FR + (0.5 \text{ or } 1.2)TU + \gamma_{TG}TG + \gamma_{SE}SE]$$

The forces *WA* (water load and stream pressure), *FR* (friction load), *TU* (force effects due to uniform temperature), *TG* (force effects due to temperature gradient), and *SE* (force effect due

www.EngineeringEBooksPdf.com

to settlement) in the aforementioned load combination equation are not relevant to this design example and therefore dropped from the aforementioned equation (also dropped from load combinations equations for other limit states) resulting in the following load combination equation that would be used in this example:

$$U = \eta[1.25DC + 1.5DW + 1.75(LL + IM)]$$

2. Service II Limit State $\eta[1.00DC + 1.00DW + 1.30\ (LL + IM)]$
3. Fatigue Limit States
Fatigue I $1.5(LL + IM)$
Fatigue II $0.75(LL + IM)$
where LL is the HL-93 vehicular live load as specified in Art. 3.6.1.4.1.

Dynamic Load Allowance (Section 3.8.3, Table 3.18/Art. 3.6.2.1)

Fatigue and fracture limit state $IM = 0.15$
All other limit sates $IM = 0.33$

Structural Design of the Bridge Superstructure

The structural design of this bridge consists of three parts:

1. Design of deck slab
2. Design of a typical interior girder
3. Design of a typical exterior girder

Design of deck slab for this bridge is presented in Example 5.3. Calculations for the design of a typical interior girder are presented as follows; these are followed by design calculations for a typical exterior girder. All calculations are presented step-by-step.

Design of a Typical Interior Girder
Calculation of Unfactored Loads on a Typical Interior Girder

a. *Permanent loads*:

Slab including 1/2 in. thick integral wearing surface $= \left(\frac{8}{12}\right)(1)(1)(0.15) = 0.10$ kip/ft

Tributary width of deck slab contributory to each girder = 7.5 ft
Dead load due to the deck slab = (0.10) (7.5) = 0.75 kip/ft (1)
Flange width of a W33 × 118 = 11.5 in., assume 12 in. (for preliminary calculations)
Depth of haunch = 2 in. (assumed)

Weight of concrete haunch $= \left(\frac{2.0}{12}\right)\left(\frac{12}{12}\right)(0.15) = 0.025$ kip/ft (2)

Weight of steel girders, cross frames, and details = 0.20 kip/ft (3)
Calculate the dead weight of the traffic barriers. The cross-sectional area of the traffic barriers, A, is (see Figure 6.50b):

$$A = \left(\frac{1}{144}\right)\left[\left(\frac{12+14}{2}\right)(19) + \left(\frac{14+21}{2}\right)(10) + (21)(3)\right] = 3.36806\ \text{ft}^2$$

Self-weight of the traffic barriers = (3.36806) (1.0) (0.15) = 0.505 kip/ft
Dead load of the two traffic barriers is distributed equally to all five girders.
Dead load due to two traffic barriers = 2(0.505)/5 = 0.202 kip/ft (4)
Dead load due to the FWA at 25 lb/ft^2 = (0.025)(1)(7.5) = 0.188 (5)
Permanent load on the girder, w_{DC1} = Items 1, 2, and 3 = 0.75 + 0.025 + 0.20 = 0.975 kip/ft
Permanent load on the girder, Item 4, w_{DC2} = 0.202 kip/ft
Permanent load on the girder, Item 5, w_{DW} = 0.188 kip/ft

www.EngineeringEBooksPdf.com

Total dead load on a typical interior girder:

$$w_D = w_{DC1} + w_{DC2} + w_{DW}$$

$$= 0.975 + 0.202 + 0.188$$

$$= 1.365 \text{ kip/ft}$$

The dead load of 1.365 kip/ft would be used to calculate mid-span deflection of the interior girder due to the dead load, which would be used to determine the required camber.

Calculate maximum moments and shear in the span (unfactored loads).

Maximum moment due to w_{DC1}: $M_{DC1} = \dfrac{w_{DC}L^2}{8} = \dfrac{(0.975)(50)^2}{8} = 304.7$ kip-ft

Maximum moment due to w_{DC1}: $M_{DC2} = \dfrac{w_{DC}L^2}{8} = \dfrac{(0.202)(50)^2}{8} = 63.1$ kip-ft

Maximum moment due to w_{DW}: $M_{DW} = \dfrac{w_{DW}L^2}{8} = \dfrac{(0.188)(50)^2}{8} = 58.8$ kip-ft

Maximum shear due to dead load w_{DC1}, $V_{DC1} = \dfrac{w_{DC1}L}{2} = \dfrac{0.975(50)}{2} = 24.4$ kip

Maximum shear due to dead load w_{DC2}, $V_{DC2} = \dfrac{w_{DC2}L}{2} = \dfrac{0.202(50)}{2} = 5.1$ kip

Maximum shear due to w_{DW}, $V_{DW} = \dfrac{w_{DW}L}{2} = \dfrac{0.188 \times (50)}{2} = 4.7$ kip

b. *Maximum moments due to live load*:

1. Moment due to design truck:

   For L = 50 ft (>40.27 ft), the truck load governs over tandem (see Example 3.9):

   Due to the design truck, $M_{truck} = 18L - 280 + \dfrac{392}{L} = 18(50) - 280 + 392/50 = 628$ kip-ft

   Dynamic load allowance = 0.33 (design truck load only)

$$M_u(1 + IM) = 628\ (1 + 0.33) = 835 \text{ kip-ft}$$

2. Moment due to lane load (refer to Example 3.66):

   The influence line ordinate is: $\dfrac{ab}{L} = \dfrac{(25-2.335)(25+2.335)}{50} = 12.391$ ft

$$M_{lane} = (0.64)\left(\frac{1}{2}\right)(L)\left(\frac{ab}{L}\right)$$

$$= (0.64)(0.5)(50)(12.391) = 198.3 \text{ kip-ft}$$

   Total moment due to live load = 835 + 198.3 = 1033.3 kip-ft

   Live load distribution factor would be applied to 1033.3 kip-ft

c. *Maximum shear due to live load*:

1. Due to design truck:

   The reaction at the left support is obtained from Equation 3.25 for x = 0:

$$V_x = \frac{72}{L}(L - x - 9.33)$$

   For L = 50 ft > 26 ft, truck load governs over the tandem (see Example 3.12).

$$R_L = \frac{72}{50}(50 - 0 - 9.33) = 58.6 \text{ kip}$$

www.EngineeringEBooksPdf.com

Dynamic load allowance = 0.33

$$V_{Truck} = 58.60\ (1 + 0.33) = 77.94 \text{ kip}$$

2. Due to lane load:

$$\text{Max shear due to lane load} = w_L\left(\frac{L}{2}\right)$$

$$= 0.64\frac{(50)}{2} = 16 \text{ kip}$$

Total maximum shear due to live load:

$$V_L = V_{Truck} + V_{Lane} = 77.94 + 16 = 93.94 \text{ kip}$$

Live load distribution factor for shear would be applied to V_L = 93.94 kip

Calculate Live Load Distribution Factors for the Interior Girder

The superstructure of the bridge conforms to type "(a)" in AASTOLRFD Table 4.6.2.2.1.1 (cast-in-place deck over steel girders). Check the applicability criteria:

$3.5 \le S \le 16.0$	$S = 7.5$ ft, OK
$4.5 \le t_s \le 12.0$	$t_s = 7.5$ in., OK
$20 \le L \le 240$	$L = 50$ ft, OK
$N_b \le 4$	$N_b = 5$, OK
$10{,}000 \le K_g \le 7{,}000{,}000$	

$$K_g = n\left(I + Ae_g^2\right)$$

where

n = modular ratio = 8 for $f_c' = 4$ ksi
I = moment of inertia of steel girder (W33 × 118) and = 5900 in.^{4}
$e_g = 0$ (assumed for noncomposite section)
$K_g = 8\ (5900 + 0) = 47{,}200$ in.^{4}
$10{,}000 \le (K_g = 47{,}200) \le 7{,}000{,}000$ $K_g = 47{,}200$ in.^{4}, OK (calculations to follow)

The range of applicability is satisfied.

Number of design lanes: N_L
Clear roadway width for design lanes: w

w = overall bridge width − 2(width of the traffic barrier)

= 37.5 − 2(1.75)

= 34.00 ft

$$N_L = \frac{w}{12} = \frac{34.00}{12} = 2.83 < 3$$

Use the integer part of 2.83, and use $N_L = 2$ design lanes.

www.EngineeringEBooksPdf.com

1. *Live load distribution factor for moment*

   Case 1. One design lane loaded

$$g_{mi1} = 0.06 + \left(\frac{S}{14}\right)^{0.4}\left(\frac{S}{L}\right)^{0.3}\left(\frac{K_g}{12.0Lt_s^3}\right)^{0.1}$$

$$= 0.06 + \left(\frac{7.5}{14}\right)^{0.4}\left(\frac{7.5}{50}\right)^{0.3}\left(\frac{47,200}{(12.0)(50)(7.5)^3}\right)^{0.1}$$

$$= 0.06 + (0.779)(0.566)(0.845)$$

$$= 0.43$$

   Case 2. Two design lanes loaded

$$g_{mi2} = 0.075 + \left(\frac{S}{9.5}\right)^{0.6}\left(\frac{S}{L}\right)^{0.2}\left(\frac{K_g}{12.0Lt_s^3}\right)^{0.1}$$

$$= 0.075 + \left(\frac{7.5}{9.5}\right)^{0.6}\left(\frac{7.5}{50}\right)^{0.2}\left(\frac{47,200}{(12.0)(50)(7.5)^3}\right)^{0.1}$$

$$= 0.075 + (0.868)(0.684)(0.845)$$

$$= 0.577 > 0.43$$

   Therefore, $g_{mi2} = 0.577$ governs.

2. *Live load distribution factor for shear*

   Check the range of applicability criteria.

   The range of applicability criteria for shear for type (a) superstructure is the same as those for the moment checked earlier (except for the term K_g that is not required). Therefore, the applicability criteria are satisfied.

   Case 1. One design lane loaded:

$$g_{vi1} = 0.36 + \frac{S}{25.0} = 0.36 + \frac{7.5}{25} = 0.66$$

   Case 2. Two or more design lanes loaded:

$$g_{vi2} = 0.2 + \frac{S}{12} - \left(\frac{S}{35}\right)^2$$

$$= 0.2 + \left(\frac{7.5}{12}\right) - \left(\frac{7.5}{35}\right)^2$$

$$= 0.779 > 0.66$$

$$g_{vi2} = 0.779 \text{ governs}$$

3. *Live load distribution factor for fatigue*

   As discussed in Section 3.9.2, for fatigue limit state, only the design truck is placed in one lane with the distance between the two 32 kip axle loads equal to a fixed 30 ft (instead of 14 ft); lane load is ignored for fatigue limit state considerations. Multiple presence factor is not applied when checking for fatigue. Therefore, live load distribution

www.EngineeringEBooksPdf.com

factor for fatigue is obtained by dividing the live load factors for moment and shear for the one lane loaded case by $m = 1.2$.

The moment due to one lane loaded case was determined as 0.43. Therefore,

$$g_{mi1,fat} = \frac{g_{mi1}}{m} = \frac{0.43}{1.2} = 0.358$$

The shear due to one lane loaded case was determined as 0.66. Therefore,

$$g_{vi1,fat} = \frac{g_{vi1}}{m} = \frac{0.66}{1.2} = 0.55$$

4. *Live load distribution factor for deflection*
   Live load distribution factor for deflection is same for interior and exterior girders because it is assumed that all lanes are loaded and all girders deflect equally. For the two lanes loaded case, the multipresence factor, $m = 1.0$.

$$g_{\Delta} = m\left(\frac{Number\ of\ lanes}{Number\ of\ girders}\right) = 1.0\left(\frac{2}{5}\right) = 0.4$$

Calculate Design Loads (Factored Loads)

The following unfactored loads were calculated earlier:

$$M_{DC} = M_{DC1} + M_{DC2} = 304.7 + 63.1 = 367.8 \text{ kip-ft}, \quad V_{DC} = V_{DC1} + V_{DC2} = 24.4 + 5.1 = 29.5 \text{ kip}$$

$$M_{DW} = 58.8 \text{ kip-ft}, \quad V_{DW} = 4.7 \text{ kip}$$

$$M_{(L+I)} = 1033.3 \text{ kip-ft}, \quad V_{L+I} = 93.94 \text{ kip}$$

Apply load factors to unfactored loads to calculate factored loads. The following unfactored loads were calculated earlier. Apply live load distribution factors to live load moment and shear.

Bending moment: $g_{mi} = 0.577$

Maximum live load plus impact moment in the interior girder = (0.577)(1033.3) = 596.2 kip-ft

Factored Loads: Bending Moments

$$M_u = \Sigma\eta_i\gamma_i M_i$$

$$\eta_i = \eta_D\eta_R\eta_I \text{ (Art. 1.3.2.1)}$$

Select Load Modifiers

Ductility, $\eta_D = 1.0$ (Art. 1.3.3).

Redundancy, $\eta_R = 1.0$ (Art. 1.3.4)

Importance, $\eta_I = 1.0$

Therefore, $M_u = \eta\Sigma\gamma_i M_i$

$$M_U = 1.0\ [1.25M_{DC} + 1.5M_{DW} + 1.75(M_{LL+IM})]$$

$$= 1.0\ [1.25(304.7 + 63.1) + 1.5(58.8) + 1.75(596.2)]$$

$$= 1591.3 \text{ kip-ft}$$

www.EngineeringEBooksPdf.com

Select the girder size. Calculate the required value of the plastic section modulus, Z_x, assuming that the girder is fully braced.

$$Z_{x,reqd} = \frac{M_u}{F_y} = \frac{1591.3(12)}{50} = 382 \text{ in.}^3$$

Try a W33 × 118, Z_x = 415 in^3 (AISC 2011). Assume that the compression flange of the girder is fully braced.

$$\phi_b M_n = \phi_b Z_x F_y$$
$$= 1.0(415)(50)$$
$$= 20{,}750 \text{ kip-in.} = 1729 \text{ kip-ft}$$

$$\phi_b M_n = 1729 \text{ kip-ft} > M_u = 1593.1 \text{ kip-ft, OK}$$

Therefore, W33 × 118 is adequate for the strength limit state.

Check Compliance for Section Properties (Art. 6.7.3, 6.10.2)
The section properties of W33 × 118, obtained from AISC (2011), are as follows:

$$A = 34.7 \text{ in.}^2, \quad d = 32.9 \text{ in.}, \quad t_w = 0.55 \text{ in.}, \quad b_f = 11.5 \text{ in.},$$
$$t_f = 0.74 \text{ in.}, \quad I_x = 5900 \text{ in.}^4, \quad S_x = 359 \text{ in.}^4, \quad Z_x = 415 \text{ in.}^4$$

Web thickness to be not less than 0.25 in.

$$t_w = 0.55 \text{ in.} > 0.25 \text{ in., OK}$$

$$D = d - 2t_f = 32.9 - 2(0.74) = 31.42 \text{ in.}$$

$$\frac{D}{t_w} = \frac{31.42}{0.55} = 57.13 < 150, \text{ OK}$$

$$\frac{b_f}{2t_f} = \frac{11.5}{2(0.74)} = 7.77 \le 12, \text{ OK}$$

$$b_f = 11.5 \text{ in.} \ge \frac{D}{6} = \frac{32.9 - 2(0.74)}{6} = 5.24, \text{ OK}$$

$$t_f \ge 1.1 t_w$$

$$0.74 \ge 1.1(0.55) = 0.61 \text{ in., OK}$$

For handling, check if $0.1 \le I_{yc}/I_{yt} \le 10$.
where

I_{yc} = moment of inertia of compression flange about the vertical axis of the web
I_{yt} = moment of inertia of tension flange about the vertical axis of the web

For a rolled section, $I_{yc} = I_{yt}$; therefore, $I_{yc}/I_{yt} = 1.0$

$$0.1 \le 1.0 \le 10, \text{ OK}$$

www.EngineeringEBooksPdf.com

Check for Flange Stresses and Member Bending Stresses (Art. 6.10.1.6)
Lateral bending stresses in continuously braced flanges are taken equal to zero. However, such is not the case here; compression flange is not braced when concrete is being poured.

Constructibility: (Art. 2.5.3 and 6.10.3)

1. General: Art. 6.10.13.1
   Constructibility issues include, but are not limited to, consideration of deflection, strength of steel and concrete, and stability during critical stage of construction. Local buckling resistance and LTB resistance of the compression flange during construction will be checked to comply with LRFD Art. 6.10.8.2.2 and 6.10.8.2.3, respectively. Lateral support to the compression flange provided to the stay-in-place forms is ignored in this check. However, it is assumed that limited lateral support to compression flange would be provided by the hardened concrete.
2. Flexure: Art. 6.10.3.2
   The trial section W33 × 118 would not have any local buckling issues. However, calculations are provided for illustrative purposes.
   λ_f = slenderness ratio for the compression flange = $\dfrac{b_{fc}}{2t_{fc}}$

$$\lambda_f = \frac{b_{fc}}{2t_{fc}} = \frac{11.5}{2(0.74)} = 7.77$$

$$\lambda_{pf} = 0.38\sqrt{\frac{E}{F_{yc}}}$$

$$= 0.38\sqrt{\frac{29{,}000}{50}} = 9.2 \qquad \text{(A6.10.8.2.2-4)}$$

$$\lambda_{rf} = 0.56\sqrt{\frac{E}{F_{gc}}}$$

$$= 0.56\sqrt{\frac{29{,}000}{50}} = 13.49 \qquad \text{(A6.10.8.2.2-5)}$$

$$\lambda_f = 7.77 \le \lambda_{pf} = 9.2$$

Therefore,

$$F_{nc} = R_h R_b F_{yc} \qquad \text{(A6.10.8.2.2-1)}$$

where
R_b = web-shedding factor (Art. 6.10.1.10.2)
R_h = hybrid factor (Art. 6.10.1.10.1)

Check if the web satisfies the following (refer to LRFD Commentary C.10.6.1.10.2):

$$\frac{2D}{t_w} \le \lambda_{rw} \qquad \text{(A6.10.1.10.2-2)}$$

$$\frac{2D}{t_w} = \frac{2(31.42)}{0.55} = 114.25$$

www.EngineeringEBooksPdf.com

λ_{rw} = limiting slenderness ratio for a noncompact web

$$\lambda_{rw} = 5.7\sqrt{\frac{E}{F_{yc}}} = 5.7\sqrt{\frac{29{,}000}{50}} = 137.27$$

$$\frac{2D}{t_w} = 114.25 < \lambda_{rw} = 137.27$$

Therefore, $R_b = 1.0$.

For rolled shapes, $R_h = 1.0$ (Art. 6.10.1.10.1).

$$F_{yc} = 50 \text{ ksi.}$$

Therefore, $F_{nc} = R_h R_b F_{yc} = (1.0)(1.0)(50) = 50$ ksi.

At the strength limit state, discretely braced flanges are required to satisfy provisions of Art. 6.10.8.1.1:

$$f_{bu} + \frac{1}{3} f_\ell \le \phi_f F_{nc} \qquad (6.62)\ [A6.10.8.1.1\text{-}1]$$

where

f_{bu} = largest value of the compressive stress throughout the unbraced length under consideration, calculated without consideration of flange lateral bending (ksi) (Art. 6.10.1.6)

f_ℓ = flange lateral bending stress as specified in Art. 6.10.1.7 (ksi)

F_{nc} = nominal flexural resistance of a compression flange (ksi)

Calculate f_{bu}, f_ℓ, and F_{nc}

For service loads II,

$$M_u = \eta[1.0DC + 1.0DW + 1.3(M_{LL+IM})]$$

$$= (1.0)[1.0(304.7 + 63.1) + 1.0(58.8) + 1.3(596.2)$$

$$= 1201.7 \text{ kip-ft}$$

$$f_{bu} = \frac{M_u}{S_x} = \frac{(1201.7)(12)}{359} = 40.17 \text{ ksi}$$

The flange lateral bending stress, f_ℓ, is very small for this example and ignored. It is caused by the wind load for which calculations are provided later for design of diaphragms.

Calculate F_{nc}.

Lateral-Torsional Buckling Resistance

L_p = limiting unbraced length to achieve the nominal flexural resistance of $R_b R_h F_{yc}$ under uniform bending (in.)

$$= 1.0 r_t \sqrt{\frac{E}{F_{yc}}} \qquad (6.73)\ [A6.10.8.2.3\text{-}4]$$

www.EngineeringEBooksPdf.com

L_r = limiting unbraced length to achieve the onset of nominal yielding in either flange under uniform bending with a consideration of compression residual stress effects (in.)

$$= \pi r_t \sqrt{\frac{E}{F_{yr}}} \qquad (6.74)\ [A6.10.8.2.3\text{-}5]$$

F_{yc} = specified minimum yield strength of compression flange (ksi)
F_{yr} = compression flange stress at the onset of nominal yielding within the cross section, including residual stress effects, but not including compression flange-lateral bending, and is the smaller of $0.7F_{yc}$ and F_{yw} but not less than $0.5F_{yc}$ (ksi)
r_t = effective radius of gyration for LTB (Equation 6.27/A6.10.8.2.3-9) (in.)

Calculate r_t.

$$r_t = \frac{b_{fc}}{\sqrt{12\left(1+\frac{1}{3}\frac{D_c t_w}{b_{fc} t_{fc}}\right)}} \qquad (6.27)\ [A6.10.8.2.3\text{-}9]$$

For a W33 × 118, b_{fc} = 11.5 in., t_{fc} = 0.74 in., $D_c = D/2$ = 31.42/2 = 15.71 in., t_w = 0.55 in.

$$r_t = \frac{11.5}{\sqrt{12\left(1+\frac{1}{3}\frac{(15.71)(0.55)}{(11.5)(0.74)}\right)}} = 2.87 \text{ in.}$$

$$L_p = 1.0 r_t \sqrt{\frac{E}{F_{yc}}} = 1.0(2.87)\sqrt{\frac{29{,}000}{50}} = 69.1 \text{ in.}$$

$$L_r = \pi r_t \sqrt{\frac{E}{F_{yr}}} = \pi(2.87)\sqrt{\frac{29{,}000}{0.7(50)}} = 260 \text{ in.}$$

Try bracings at one-fifth points, $L_b = \frac{50}{5} = 10 \text{ ft} = 120 \text{ in.}$

$$F_{nc} = C_b\left[1-\left(1-\frac{F_{yr}}{R_h F_{yc}}\right)\left(\frac{L_b - L_p}{L_r - L_p}\right)\right] R_b R_h F_{yc} \le R_b R_h F_{yc}$$

$$= 1.0\left[1-\left(1-\frac{0.7F_{yc}}{1.0F_{yc}}\right)\left(\frac{120-69.1}{260-69.1}\right)\right](1.0)(1.0)(50) \le 50 \text{ ksi}$$

$$= 46.00 \text{ ksi} < 50 \text{ ksi, OK} \qquad (6.71)\ [A6.10.8.2.3\text{-}2]$$

$$M_u = 1.25 M_{DC} = 1.25(367.8) = 460 \text{ kip-ft}$$

$$f_u = \frac{M_u}{S_x} = \frac{460(12)}{359} = 15.38 \text{ ksi} \ll F_{nc} = 46.00 \text{ ksi}$$

Note that in the aforementioned calculations, C_b = 1.0 has been conservatively assumed equal to 1.0, which is valid for uniform moment, which is not the case here. For the present case, $C_b > 1.0$. Exact value of C_b can be determined from Equation 6.25 if necessary.

www.EngineeringEBooksPdf.com

Since, f_c = 15.38 ksi ≪ F_{nc} = 46.00 ksi, increase the bracing interval. Try bracings at quarter points, that is, at 50/4 = 12.5 ft or L_b = 150 in. L_p = 69.1 in. as before:

$$F_{nc} = C_b\left[1-\left(1-\frac{F_{yr}}{R_hF_{yc}}\right)\left(\frac{L_b-L_p}{L_r-L_p}\right)\right]R_bR_hF_{yc} \le R_bR_hF_{yc}$$

$$= 1.0\left[1-\left(1-\frac{0.7F_{yc}}{1.0F_{yc}}\right)\left(\frac{150-69.1}{256.8-69.1}\right)\right](1.0)(1.0)(50) \le 50 \text{ ksi}$$

$$= 43.64 \text{ ksi} < 50 \text{ ksi, OK.} \qquad (6.71)\ [A6.10.8.2.3\text{-}2]$$

$$f_c = 15.38 \text{ ksi} \ll F_{nc} = 43.64 \text{ ksi, OK}$$

$$\phi_f F_{nc} = 1.0(43.64) = 43.64 \text{ ksi}$$

$$f_{bu} + \frac{1}{3}f_\ell = 40.17 + 0 = 40.17 \text{ ksi} < \phi_f F_{nc} = 43.64 \text{ ksi, OK.}$$

The aforementioned calculations (f_c = 15.38 ksi < F_{nc} = 43.64 ksi) would suggest that a girder with a smaller section modulus, S_x, might be adequate. However, it is noted that plastic section modulus, Z_x = 415 in³ for the selected W-shape (W33 × 118), is only slightly larger than $Z_{x,reqd}$ = 403 in³. Therefore, the girder section need not be revised.

Provide lateral bracings at quarter points, that is, at 12 ft 6 in. intervals. These would be again considered later for wind bracings.

Check for Shear (Art. 6.10.9.2)

Generally speaking, for rolled wide flange beams such as one used in this example, shear is not a matter of concern. However, all calculations are provided for completeness:

$$V_u \le \phi_v V_n \qquad (6.75)\ [A6.10.9.1\text{-}1]$$

$$V_n = V_{cr} = CV_p \qquad (6.76)\ [A6.10.9.2\text{-}1]$$

$$V_p = 0.58F_yDt_w \qquad (6.77)\ [A6.10.9.2\text{-}2]$$

where

V_u = shear due to factored loads
V_{cr} = critical buckling resistance
V_p = plastic shear resistance
C = critical buckling coefficient (from Equations 6.80 through 6.82 as applicable and k = 5 for unstiffened webs)

For a W33 × 118,

$$D = d - 2t_f = 32.9 - 2(0.74) = 31.42 \text{ in.}$$

$$t_w = 0.55 \text{ in.}$$

$$\frac{D}{t_w} = \frac{31.42}{0.55} = 57.13$$

$$1.12\sqrt{\frac{Ek}{F_{yw}}} = 1.12\sqrt{\frac{29{,}000(5)}{50}} = 60.31 > \frac{D}{t_w} = 57.13$$

www.EngineeringEBooksPdf.com

Therefore, $C = 1.0$.

$$V_p = 0.58F_yDt_w$$
$$= 0.58(50)(31.42)(0.55)$$
$$= 501 \text{ kip}$$
$$\phi_v V_p = 1.0(501) = 501 \text{ kip}$$

Strength I Limit State

$$V_u = 1.0[1.25DC + 1.5DW + 1.75(LL + IM)]$$
$$= 1.0[1.25(29.4) + 1.5(4.7) + 1.75(93.94)]$$
$$= 208.2 \text{ kip}$$
$$\phi_v V_p = 501 \text{ kip} > V_u = 208.2 \text{ kip, OK}$$

Fatigue and Fracture Limit State: Art. 6.6.1.2 and 6.10.5

Check compliance for load-induced fatigue requirements (Art. 6.6.1.2 and 6.10.5.1, 6.6.1).

Allowable fatigue stress range depends on the frequency of load cycles as discussed in Section 3.9.4 (Art. 6.6.1.2.1).

ii. Determine the frequency of truck loads on the bridge
For a rural interstate highway, the number of vehicles per lane per day = 20,000 (LRFD C3.6.1.4.2):

$$ADT = 20{,}000 \text{ per lane per day}$$

Fraction of trucks in traffic on a rural interstate = 0.20 (Table 3.20):

$$ADTT = 0.2(\text{ADT}) = 0.2(20{,}000)(2 \text{ lanes}) = 8000 \text{ trucks/day}$$

For two lanes, fraction of truck traffic in a single lane, $p = 0.85$ (Table 3.21)

$$ADTT_{SL} = 0.85(8000) = 6800 \text{ trucks per day}$$

iii. Determine the allowable fatigue stress range

1. For detailing purposes, the design component (the steel girder) is assumed as uncoated weathering steel, which falls in Category B Case 1.2, Table A6.3-1 (LRFD Table 6.6.1.2.3-1, noncoated weathering steel base metal with rolled or cleaned surfaces and detailed in accordance with FHWA [1989]). The listed CAFT value, $(\Delta F)_{TH}$, corresponding to this detail category for infinite fatigue life is

$$(\Delta F)_{TH} = 16 \text{ ksi}$$

2. The calculated $(ADTT)_{SL}$ = 6800 trucks per day far exceeds 860 trucks per day (75-year $(ADTT)_{SL}$ equivalent to infinite life) as listed in Table 6.4. Therefore, Fatigue I Limit State load combination would be used, with $\gamma = 1.5$.

   For fatigue loading, only one truck is placed on the bridge as explained in Section 3.9.2. The live load moment due to the fatigue loading is determined from Equation 3.41 (Chapter 3):

$$M_{fat} = \frac{72x}{L}\left(L - x - 11.78\right) - 112 \tag{3.41}$$

www.EngineeringEBooksPdf.com

For L = 50 ft, x = 25 ft (at midspan),

$$M_{fat} = \frac{72(25)}{50}(50-25-11.78)-112$$
$$= 363{,}92 \text{ kip-ft}$$

Apply the following modifiers to M_{fat}.
IM = 0.15; multiply by 1.15
Live load distribution factor for fatigue, $g_{mi1,\,fat}$ = 0.358
Load factor for fatigue I limit state, γ = 1.5

$$M_{ftt1} = 1.5(363.92)(1.15)(0.358) = 224.74 \text{ kip-ft}$$

Calculate the live load stress range:

$$f = \frac{M_{fat\,I}}{S_x} = \frac{224.74(12)}{359} = 7.51\text{ksi} < (\Delta F)_{TH} = 16.0 \text{ ksi, OK.}$$

Since the live load stress range (f = 7.51 ksi) is smaller than the constant amplitude fatigue threshold value ($(\Delta F)_{TH}$ = 16 ksi), infinite fatigue life is OK, and check for finite fatigue life is not warranted.

Fatigue I Limit State shear loads are much smaller than the factored shear in Strength I Limit State. For this noncomposite superstructure using rolled w-shapes, fatigue is not a matter of concern. However, calculations for fatigue loads are provided for completeness.

Maximum shear due to fatigue loads is calculated from the following (Chapter 3):

$$V_{fat} = 72 - \frac{1312}{L} = 72 - \frac{1312}{50} = 45.76 \text{ kip}$$

IM = 0.15, distribution factor for fatigue, $g_{vi1,fat}$ = 0.55

$$V_{fat1} = 1.5[V(LL + IM)(g_{i1,fat})] = 1.5[45.76(1 + 0.15)(0.55)] = 43.42 \text{ kip}$$

$$\phi_v V_{cr} = 501 \text{ kip} \gg V_{fat} = 43.42 \text{ kip, OK}$$

Fracture: Special Requirements for Webs: Art. 6.10.5.2
Check that

$$V_u \le \phi_v V_{cr} \qquad (6.42)\ [A6.10.5.3.1]$$

where
V_u = shear in the web at the section under consideration due to unfactored permanent loads plus the factored fatigue load
V_{cr} = shear-buckling resistance determined from Equation 6.43 (A6.10.9.3.3-1)

$$V_u = V_{DC} + V_{DW} + 1.5(V_{fat+im})(g_{vi1,fat})$$
$$= 29.4 + 4.7 + 43.42 = 77.52 \text{ kip}$$
$$\phi_v V_{cr} = 501 \text{ kip} \gg V_u = 77.52 \text{ kip, OK}$$

Service Limit State (Art 6.5.2, A6.10.4)
Art. 6.10.4.1: Compliance with Art. 2.5.2.6 is required.

1. Optional live load deflection control:
Since no deflection criteria are specified, optional deflection criteria (Art. 2.6.2.6.2) will be used in this example.

www.EngineeringEBooksPdf.com

Allowable deflection due to vehicular load, $\Delta_{LL} = \dfrac{span}{800} = \dfrac{50(12)}{800} = 0.75$ in.

Art. 3.6.1.3.2: Calculated deflection will be taken as the larger of the following as discussed in Section 2.6.3:

1. Deflection due to design truck alone. Dynamic load allowance will be applied to this deflection.
2. Deflection due to 25 percent of the deflection due to the design truck *plus* deflection due to lane load. Dynamic load allowance is not applied to the deflection due to the lane load.

Calculate Deflection due to Vehicular Live Load

Live load deflections would be computed for the governing loading conditions—separately for the design truck and lane (Figure 6.51)—by the usual methods of computing deflections. Formulas for relevant load cases given in AISC Manual of Steel Construction (AISC 2011) would be used (see discussion in Section 2.6.6). Referenced formulas used in calculations are taken from Chapter 2. For the noncomposite beams used in this example, the moment of inertia, *I*, of the steel section would be used for calculating deflections.

Deflection due to Design Truck

As discussed in Section 2.6.6, in the case of the design truck loading, it is difficult, although theoretically possible, to determine the exact positions of the three axles that will result in maximum deflection. As a practical matter, however, the maximum deflection in the girder would be computed by placing the middle 32 kip load at the midspan, and the other two loads (8-kip and 32-kip loads) at 14 ft from the midspan, one on the left and the other on the right side of the midspan (Figure 6.52). This load case can be split into two separate cases as shown in AISC (2011):

a. Load Case 7 for the centrally placed point load
b. Load Case 8 for point loads placed off the midspan

For the centrally placed point load *P* (Load Case 7), the maximum deflection occurs at the center that can be calculated from Equation 2.2:

$$\Delta_c = \frac{PL^3}{48EI} \tag{2.2}$$

where

Δ_c = deflection at midspan due to point load
L = span
E = modulus of elasticity
I = moment of inertia

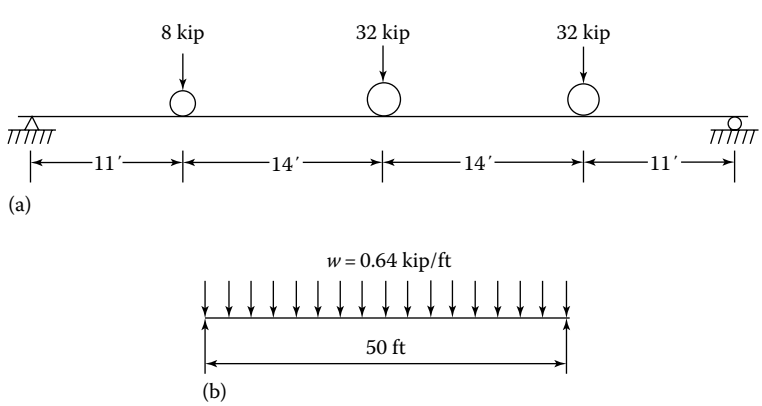

FIGURE 6.51 HL-93 live loads: (a) design truck and (b) lane load.

www.EngineeringEBooksPdf.com

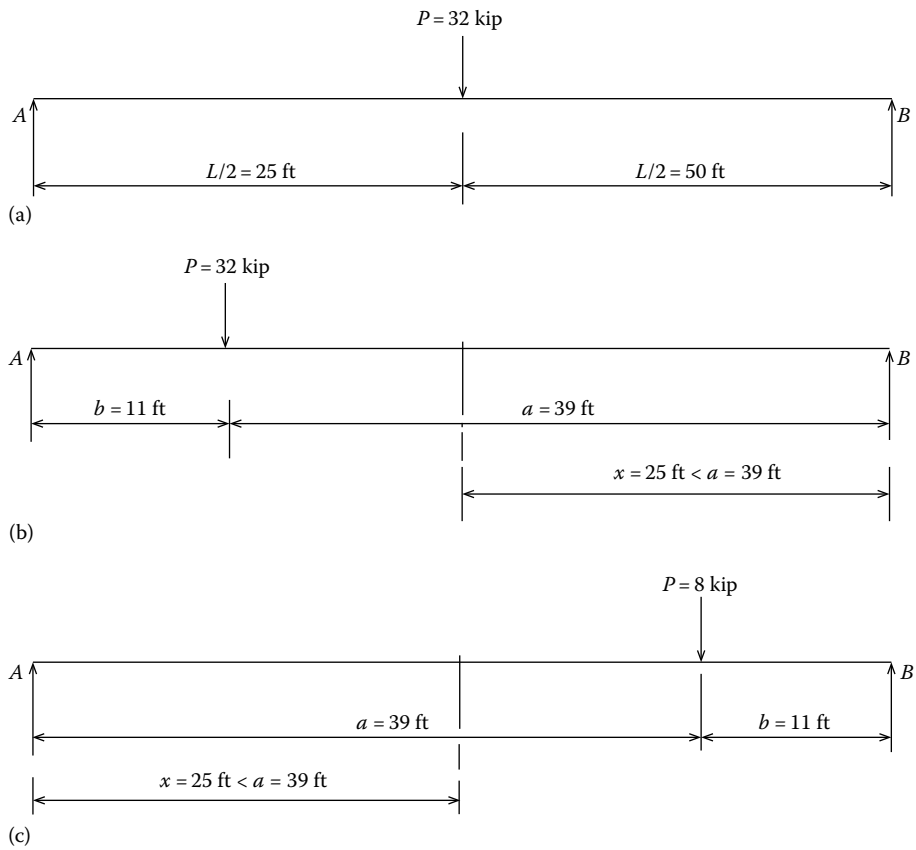

FIGURE 6.52 (a) Point load at midspan, (b) point load off midspan, x measured from the right support, B, and (c) point load off midspan, x measured from the left support, A.

The axle loads should be multiplied by $(1 + IM) = (1 + 0.33) = 1.33$ to account for dynamic allowance. The resulting axle loads are as follows:

$$P_1 = P_2 = 32(1.33) = 42.56 \text{ kip}$$

$$P_3 = 8(1.33) = 10.64 \text{ kip.}$$

Substitute $P = 42.56$ kip, $L = 50$ ft, $E = 29{,}000$ ksi, and $I = 5900$ in.^{4} in Equation 2.2. The deflection at the midspan is

$$\Delta_c = \frac{42.56(50)^3(12)^3}{48(29{,}000)(5{,}900)} = 1.12 \text{ in.}$$

For the remaining axle loads that are placed off-center on the span, Load Case 8 would be used.

For a point load P placed at a distance a from the left support, the deflection at a distance x (when $x < a$) from the left support can be calculated from Equation 2.3:

$$\Delta_x = \frac{Pbx\left(L^2 - b^2 - x^2\right)}{6EIL} \tag{2.3}$$

www.EngineeringEBooksPdf.com

Equation 2.3 is used to calculate deflections due to the two off-center point loads (the 10.56 kip and 42.56 kip loads, including *IM*). Substitute $P = P_2 + P_3 = 42.56 + 10.56$ kip, $x = 25$ ft, $b = 11$ ft, $E = 29{,}000$ ksi, $I = 5900$ in.^{4}, and $L = 50$ ft in Equation 2.3R. The deflection at the midspan ($x = 25$ ft) is as follows:

$$\Delta_{x=25\text{ ft}} = \frac{(42.56+10.64)(11)(25)\left[(50)^2-(11)^2-(25)^2\right]}{6(29{,}000)(5{,}900)(50)}(12)^3 = 0.86 \text{ in.}$$

Total deflection due to the design truck, $\Delta_c + \Delta_{x=25\text{ ft}} = 1.12 + 0.86 = 1.98$ in.

Distribution factor for live load deflection = 0.4 (computed earlier)

Maximum deflection in the girder = (0.4)(1.98) = 0.79 in.

Deflection Due to Lane Load

For the case of lane loading (uniform load), the maximum deflection is calculated from Equation 2.9 (Case 1, AISC 2011):

$$\Delta_{lane} = \frac{5wL^4}{384EI} \tag{2.9}$$

where

$w = 0.64$ kip/ft

L = span = 50 ft

Substituting these values along with $E = 29{,}000$ ksi and $I = 5900$ in.^{4} in Equation 2.9R, the maximum deflection due to lane load is as follows:

$$\Delta_{lane.max} = \frac{5(0.64)(50)^4(12)^3}{384(29{,}000)(5{,}900)} = 0.53 \text{ in.}$$

$$0.25\Delta_{truck} + \Delta_{lane} = 0.25(1.98) + 0.53 = 1.03 \text{ in.}$$

Apply live load distribution factor for live load = 0.4.

$$(0.4)(0.25\Delta_{truck} + \Delta_{lane}) = 0.4(1.03) = 0.4 \text{ in.}$$

$$\Delta_{truck} = 0.79 \text{ in.} > (0.25\Delta_{truck} + \Delta_{lane}) = 0.4 \text{ in.}$$

Therefore, $\Delta_{truck} = 0.79$ in controls.

Allowable live load deflection, $\Delta_{allowable} = \dfrac{L}{800} = \dfrac{50\times 12}{800} = 0.75 \text{ in.} \approx 0.79 \text{ in., OK.}$

Optional Criteria for Span-to-Depth Ratio (Art. 2.5.2.6.3)

The owner may invoke the minimum girder depth equal to 0.033*L* as specified in Table 2.5 (LRFD Table 2.5.2.6.3-1). For this example,

$$0.033(50)(12) = 19.8 \text{ in.} < d = 32.9 \text{ in., OK}$$

Span-to-depth ratio is satisfied.

2. Permanent Deformations (Art. 6.10.4.2)

The purpose of this check is to prevent objectionable permanent deflections due to expected severe traffic loadings that would impair rideability. For noncomposite sections, compliance with Equation 6.43 (A6.10.4.2.2-3) is required:

$$f_f + \frac{f_\ell}{2} \le 0.8R_hF_{yf} \tag{6.43} \text{ [A6.10.4.2.2-3]}$$

www.EngineeringEBooksPdf.com

f_f = flange stress at the section under consideration due to Service II load calculated without consideration of flange lateral bending
f_ℓ = flange lateral buckling stress at the section under consideration due to Service II loads determined as specified in Art. 6.10.1.6 (ksi)
≈ 0 for wide flange section

For Service II load, the maximum moment is as follows:

$$M_u = \eta[1.0M_{DC} + 1.0M_{DW} + 1.3(M_{LL+IM})]$$

$$= (1.0)[1.0(304.7 + 63.1) + 1.0(58.8) + 1.3(596.2)]$$

$$= 1202 \text{ kip-ft}$$

$$f_f = \frac{M_u}{S_x} = \frac{1202(12)}{359} = 40.18 \text{ ksi}$$

$$0.8R_hF_{yf} = 0.8(1.0)(50) = 40 \text{ ksi}$$

$$f_f = 40.18 \text{ ksi} \approx 0.8R_hF_{yf} = 40 \text{ ksi, OK}$$

The slight overstress of 0.18 ksi is considered inconsequential.

Strength Limit State: Art. 6.10.6
Check for compliance for strength limit state as specified in Art. 6.10.6.

1. Art. 6.10.6.2.1: Composite sections in positive flexure:
   Not applicable for this noncomposite steel slab–girder bridge.
2. Art. 6.10.6.2.3 and 6.10.8: Composite sections in negative flexure and noncomposite sections:
   Satisfied as calculated earlier.
3. Art. 6.10.1.8: Net section in flexure:
   Not applicable; the W33 × 118 used for this bridge because it does not have any splices.
4. Art. 6.10.1.10: Flange-strength reduction factors:
   Automatically satisfied for W33 × 118 rolled shape used in this bridge

Diaphragms and Cross Frames
Diaphragms and cross frames need to be provided to comply with Art. 6.7.4. Refer to Section 2.4.3.2 for a discussion pertaining to requirements for diaphragms and cross frames.

Art, 6.7.4.2 specifies that diaphragms *or* cross frames for rolled beams and plate girders be as deep as practicable, but as a minimum should not be shallower than one-half of the beam depth for rolled beams and not shallower than ¾th of the beam depth for plate girders. Intermediate diaphragms or cross frames should be provided at nearly uniform spacing for efficiency in structural design and constructibility and/or to allow for simplified methods of analysis for calculation of flange lateral bending stresses.

Intermediate Diaphragms
Intermediate diaphragms are designed to transmit lateral loads due to wind to the girders and then to the bearings at the abutments. As calculated earlier, intermediate diaphragms are provided at quarter points, that is, at 12 ft-6 in. intervals. These diaphragms are oriented perpendicular to the girders and provided contiguously in between all girders so that the girders and diaphragms together form a simple frame in a horizontal plane supporting a deck on top. The whole system so constructed forms a stiff *horizontal diaphragm* that resists horizontal forces acting transversely to the bridge superstructure and transmits them to the abutments through the bearings. However, this seemingly simple system (horizontal diaphragm) is not amenable to simple mathematical analysis.

www.EngineeringEBooksPdf.com

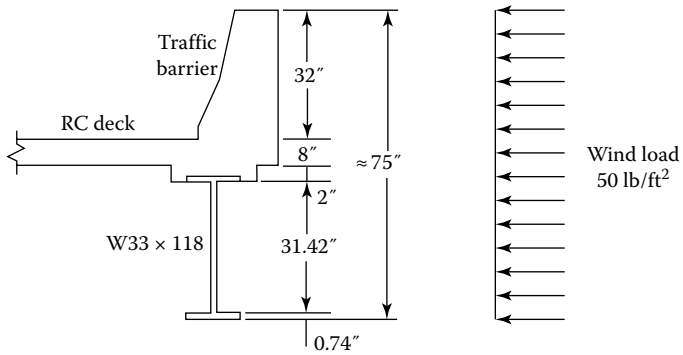

FIGURE 6.53 Wind loading on the superstructure.

A uniform wind load of WS = 50 lb/ft² (wind load on superstructure, Art. 3.8.1.2, LRDF Table 3.8.1.2.1-1) is assumed for design of diaphragms (Figure 6.53). This horizontal force is assumed to act normal to superstructure over its entire height (= height of parapet + deck + girder).

Conservatively, the lateral forces transmitted to intermediate and end diaphragms are calculated on tributary area basis. It is assumed that the wind load acting on the bottom half of the girder is transmitted to the bottom flange; the wind force acting over the remainder of the height is transmitted to the top flange of the girder.

Wind Loads on Intermediate Diaphragms

Lateral wind load distribution on the girders is analyzed as specified in LRFD Art. 4.6.2.7. The wind force W applied to the flanges of the exterior girders is determined from the following equation:

$$W = \frac{\eta_i \gamma P_D d}{2} \qquad \text{(LRFD C4.6.2.7.1-1)}$$

where

W = factored wind force per unit length applied to the flange (kip/ft)
P_D = design horizontal wind pressure, ksf, (Art. 3.8.1)
d = depth of member
γ = load factor as specified in LRFD Table 3.4.1-1 for the particular group loading combination
η_i = load modifier relating to ductility, redundancy, and operational importance as specified in Art. 1.3.2.1

Depth of girder, d = 32.9 in., P_D = 50 lb/ft², load modifier for WS, η_i = 1.0, γ = 1.4 (LRFD Table 3.4.1-1)

$$W_{bot} = \frac{\gamma P_D d}{2} = \frac{1.4(0.050)(32.9)}{2(12)} = 0.096 \text{ kip/ft}$$

Tributary length for an intermediate diaphragm = L_b = 12.5 ft = 150 in.

Lateral force transmitted from the bottom flange of the girder to diaphragm,

$$P_{w,bot} = 0.096(12.5) = 1.2 \text{ kip}$$

Maximum wind moment on the loaded flange is

$$M_w = \frac{WL_b^2}{10} \qquad \text{(LRFD C4.6.2.7.1-2)}$$

www.EngineeringEBooksPdf.com

$$M_w = \frac{0.096(12.5)^2(12)}{10} = 18 \text{ kip-in.}$$

For a W33 × 118, $S_y = 32.6$ in.^{3}

Flange lateral-bending stress: $f_\ell = \frac{M_w}{S_x} = \frac{18}{32.6} = 0.55$ ksi (very small)

Contributory height for the top flange of the girder, $d_{w,top} = 32 + 8 + 2 + 0.5(32.9) = 58.45$ in.

$$W = \gamma P_D d = \frac{1.4(0.050)(58.45)}{(12)} = 0.341 \text{ kip/ft}$$

Lateral force transmitted from the top flange of the girder to diaphragm is

$$P_{w,top} = 0.341(12.5) = 4.26 \text{ kip}$$

Therefore, total lateral force, F_{uDi}, transmitted to an intermediate diaphragm is

$$F_{uDi} = P_{w,bot} + P_{w,top} = 1.2 + 4.26 = 5.46 \text{ kip}$$

The intermediate diaphragm must be able to resist an axial force of 5.46 kip.

Select a channel section for the diaphragms. A channel section is preferred for easy constructibility and simplicity of (bolted) connections to the girders. The depth of the diaphragm should be not less than half the girder depth. For a W33 × 118, $d = 32.9$ in., $0.5d \approx 16.5$ in. Try an MC18 × 42.7 Gr. 50, $d = 18$ in. > 16.5 in., OK. The section properties of an MC18 × 42.7 are (obtained from AISC 2011):

$$d = 18 \text{ in.}, \quad A = 12.6 \text{ in.}^2, \quad t_w = 0.45 \text{ in.}, \quad T = 15.125 \text{ in.}, \quad r_x = 6.64 \text{ in.}, \quad r_y = 1.07 \text{ in.}$$

Calculate the nominal compressive resistance of an MC18 × 42.7 as specified in Art. 6.9.3 and 6.9.4. Assume it as a secondary member having pin-ended connections at both ends.

$$P_n = \left[(0.658)^{\left(\frac{P_o}{P_e}\right)} \right] P_o \qquad \text{(A6.9.4.1.1-1)}$$

For a secondary compression member, $\frac{k\ell}{r} \le 140$. (Art. 6.9.3)

For the MC18 × 42.7, ℓ = center to center spacing of girders = 7 ft 6 in. = 90 in.

$$\frac{k\ell}{r_s} = \frac{k\ell}{r_y} = \frac{1.0(90)}{1.07} = 84.1 < 140, \text{ OK}$$

where r_s = radius of gyration about the axis normal to the plane of buckling = r_y

Calculate elastic flexural-buckling resistance, P_e (Art. 6.9.4.1):

$$P_e = \frac{\pi^2 E A_g}{\left(\frac{k\ell}{r_s}\right)^2} = \frac{\pi^2(29{,}000)(12.6)}{(84.1)^2} = 510 \text{ kip} \qquad \text{(A6.9.4.1.2-1)}$$

$$P_o = Q F_y A_g$$

www.EngineeringEBooksPdf.com

where Q = slender element reduction factor as specified in Art. 6.9.4.1. Check if the channel MC18 × 42.7 is composed of nonslender plate elements. Check the b/t ratio of the web.

$$\frac{b}{t} = \frac{T}{t_w} = \frac{15.125}{0.45} = 33.16$$

Check if

$$\frac{b}{t} \le k\sqrt{\frac{E}{F_y}}$$

From LRFD Table 6.9.4.2.1-1, for channel sections, k = 1.49:

$$k\sqrt{\frac{E}{F_y}} = 1.49\sqrt{\frac{29{,}000}{50}} = 35.88$$

$$\frac{b}{t} = 33.16 \le 35.88$$

Therefore, the channel MC18 × 42.7 is composed of nonslender elements, so Q = 1.0 (Art. 6.9.4.2.1):

$$P_o = QF_yA_g = 1.0(50)(12.6) = 630 \text{ kip}$$

$$\frac{P_o}{P_e} = \frac{630}{510} = 1.235$$

$$P_n = \left[(0.658)^{\left(\frac{P_o}{P_e}\right)}\right]P_o \qquad \text{(A6.9.4.1.1-1)}$$

$$P_n = \left[(0.658)^{\left(\frac{630}{510}\right)}\right](630) = 376 \text{ kip}$$

$$P_r = \phi_c P_n = 0.9(376) = 338.4 \text{ kip} > F_{uD} = 5.46 \text{ kip, OK}$$

Therefore, provide MC18 × 42.7 for intermediate diaphragms at 12 ft-6 in. on center. These diaphragms will also serve as lateral bracings at 12 ft-6 in. on center (L_b = 12 ft-6 in.).

Wind Loads on End Diaphragms

Each end diaphragm is required to transmit half of the wind load (*WS*) acting on the superstructure.

Total wind force on the superstructure,

$$w = w_{bot} + w_{top} = 0.0963 + 0.341 \approx 0.44 \text{ kip/ft}$$

Length of the superstructure, L = 50 ft

Wind force to be transmitted by the end diaphragm: F_{uDe}:

$$F_{uDe} = \frac{wL}{2} = \frac{0.44(50)}{2} = 11.0 \text{ kip}$$

Axial resistance of MC18 × 42.7 (calculated earlier), P_r = 338.4 kip > F_{uDe} = 11.0 kip

www.EngineeringEBooksPdf.com

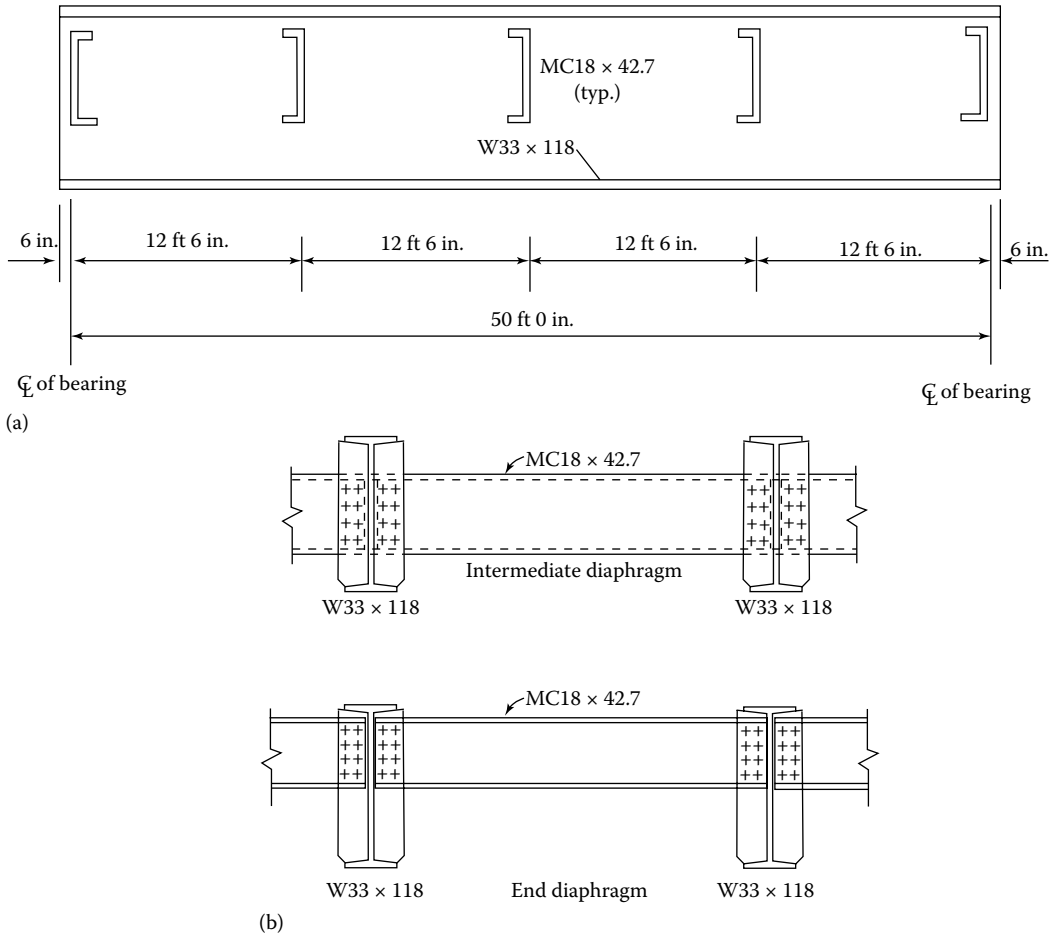

FIGURE 6.54 Location of intermediate and end diaphragms. (a) Elevation of girder showing end diaphragms. (b) Diaphragms bolted to girders.

Therefore, provide MC18 × 42.7 for the end diaphragms (Figure 6.54). This has the same size and length as the intermediate diaphragms, an advantage that results in repetitive detailing cost savings.

Dead Load Camber

Calculate maximum deflections of the interior beams due to the dead load.

a. Maximum dead load deflection in the interior beam

$$\text{Total dead load, } w_D = w_{DC1} + w_{DC2} + W_{DW}$$
$$= 0.975 + 0.202 + 0.188$$
$$= 1.365 \text{ kip/ft}$$

$$\Delta_{D,max} = \frac{5w_D L^4}{384EI}$$
$$= \frac{5(1.365)(50)^4(12)^3}{384(29{,}000)(5{,}900)} = 1.12 \text{ in.}$$

Provide a camber of 1 1/8 in. in all interior beams.

www.EngineeringEBooksPdf.com

Design of a Typical Exterior Girder
Loads on a Typical Exterior Girder (Unfactored Loads)

a. *Permanent loads*:
Since dead weight of traffic barriers is assumed distributed equally to all girders (interior and exterior), the tributary width of deck slab for the exterior girder is also the same as that for the interior girder (7.5 ft), and the permanent load (w_{DC1} and w_{DC2}) on the exterior girder is the same as that on a typical interior girder. Therefore, from the calculations for the interior girders,

$$w_{DC} = w_{DC1} \text{ and } w_{DC2} = 0.975 + 0.202 = 1.177 \text{ kip/ft}$$

The bottom width of the traffic barrier = 21 in. = 1.75 ft
Tributary width contributing FWS to the exterior girder = 7.5 − 1.75 = 5.75 ft

$$w_{DW} = (0.025)(5.75)(1.0) = 0.144 \text{ kip/ft}$$

$$\begin{aligned}\text{Total dead load on the girder} &= w_{DC} + w_{DW}\\ &= 1.177 + 0.144\\ &= 1.321 \text{ kip/ft}\end{aligned}$$

The dead load of 1.308 kip/ft would be used to calculate midspan deflection of the exterior girder due to the dead load, which would be used to determine the required camber.

Calculate Maximum Moments and Shear in the Span (Unfactored Loads)

Maximum moment due to w_{DC1}:

$$M_{DC1} = \frac{w_{DC}L^2}{8} = \frac{(0.975)(50)^2}{8} = 304.7 \text{ kip-ft}$$

Maximum moment due to w_{DC1}:

$$M_{DC2} = \frac{w_{DC}L^2}{8} = \frac{(0.202)(50)^2}{8} = 63.1 \text{ kip-ft}$$

Maximum moment due to w_{DW}:

$$M_{DW} = \frac{w_{DW}L^2}{8} = \frac{(0.144)(50)^2}{8} = 45.0 \text{ kip-ft}$$

Maximum shear due to dead load w_{DC1}:

$$V_{DC1} = \frac{w_{DC1}L}{2} = \frac{0.975(50)}{2} = 24.4 \text{ kip}$$

Maximum shear due to dead load w_{DC2}:

$$V_{DC2} = \frac{w_{DC2}L}{2} = \frac{0.202(50)}{2} = 5.1 \text{ kip}$$

Maximum shear due to w_{DW}:

$$V_{DW} = \frac{w_{DW}L}{2} = \frac{0.144 \times (50)}{2} = 3.6 \text{ kip}$$

www.EngineeringEBooksPdf.com

Note: The aforementioned force effects are the same as those for the interior girders, except the force effect of *DW*, which is slightly smaller for the exterior girder. This slight difference (4.7 kip *vs.* 3.6 kip) is insignificant for practical purposes. Therefore, force effects due to permanent loads on the interior girder would be used also for the design of the exterior girder.

Live Load Distribution Factors for the Exterior Girders

a. *Distribution factor for bending moment*
Check the range of applicability: $-1.0 \le d_e \le 5.5$ ft
where d_e = distance between the edge of curb and the center line of the exterior web of the exterior girder.

As shown in Figure 6.55a, distance between the outside edge of the traffic barrier and the centerline of the web of the exterior girder = 3.75 ft, and the width of the bottom of the traffic barrier = 1.75 ft. Therefore, distance d_e is determined to be

$$d_e = 3.75 - 1.75 = 2.0 \text{ ft}$$

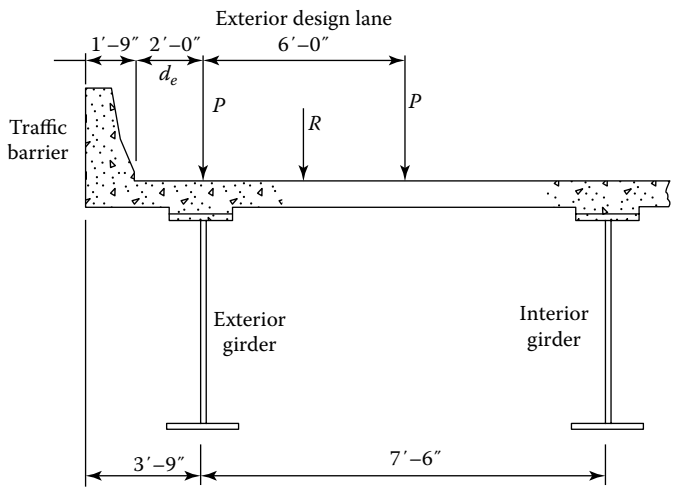

d_e is the horizontal distance from the center line of the exteroir web of the exterior beam at the deck level to the interior edge of curb or traffic barrier (Art. 4.6.2.2.1)

(a)

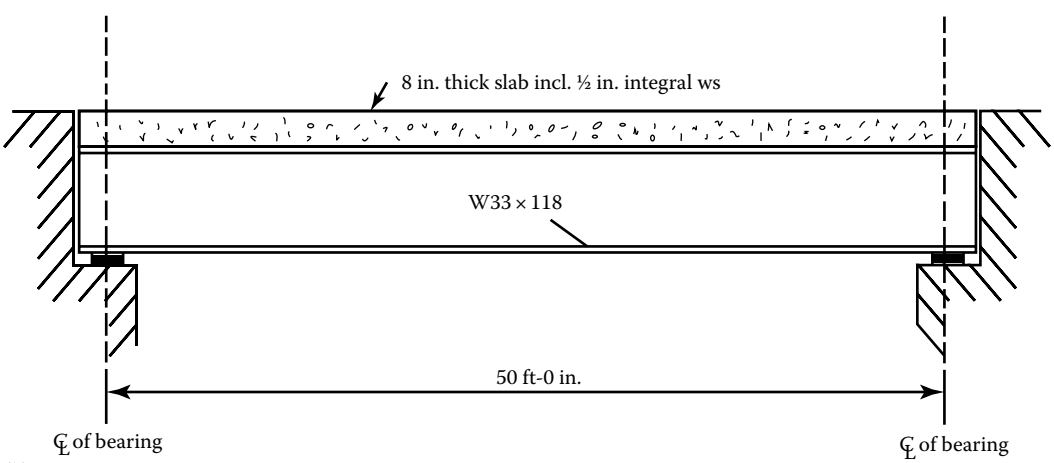

(b)

FIGURE 6.55 (a) Distance d_e for Example 6.2. (b) Sketch of the elevation of the noncomposite bridge.

www.EngineeringEBooksPdf.com

Case 1. One design lane loaded: Use lever rule. From Figure 6.55a,

$$R_e = \frac{R(4.5)}{7.5} = 0.6$$

Multiple presence factor = 1.2

$$g_{mi1} = 1.2(0.6) = 0.72$$

Case 2. Two or more design lanes loaded: $g = e(g_{interior})$

$$e = 0.77 + \frac{d_e}{9.1} = 0.77 + \frac{2.0}{9.1} = 0.99$$

$$g_{me2} = 0.99(0.577) = 0.571$$

b. *Distribution factor for shear*

Case 1. One design loaded: Use lever rule.

$$g_{ev1} = 0.72 \text{ (as calculated earlier)}$$

Case 2. Two or more design lanes loaded: $g = e(g_{interior})$

$$e = 0.6 + \frac{d_e}{10} = 0.6 + \frac{2.0}{10} = 0.8$$

$$g_{ev2} = 0.8(0.779) = 0.623$$

Special Analysis for Exterior Girders: Art. 4.6.2.2.2d

Art. 4.6.2.2.2d specifies that in beam–slab bridge cross sections with diaphragm or cross frames, the distribution factor for the exterior girder *shall* not be taken to be less than that which would be obtained by assuming that the cross-section deflects and rotates as a rigid cross section. Under this assumption, the distribution factor for the exterior girder is required to be determined from LRFD Equation C4.4.2.2.2d as discussed in Section 4.8, and illustrated by examples in Chapter 4. In this design example, partial-depth diaphragms (not full-depth diaphragms or cross frames) have been provided at the ends as well as intervals of 12 ft 6 in. This type of framing plan is not considered to provide significant rigidity to the cross section. Accordingly, the special analysis method is not used here.

Table 6.5 presents a summary of live load distribution factors for bending moment and shear in both interior and exterior girders; the governing values of distribution factors for both interior and exterior girders are shown bold-faced. It is, therefore, concluded that

1. The distribution factor for live bending moment in the exterior girder (0.72) is greater than that for the interior girder (0.577). Therefore, the factored live load moment in the exterior girder would be larger than that in the interior girder.
2. The distribution factor for live load shear in the interior girder (0.779) is larger than that for the exterior girder (0.72). Therefore, the factored live load shear in the exterior girder would be smaller than that in the interior girder.

Based on the aforementioned statement, the exterior girder would be checked for the Strength I Limit State-bending moment. Other limit states are automatically satisfied.

Strength Limit State: Art. 6.10.6

The following unfactored loads were calculated earlier:

$$M_{DC} = 367.8 \text{ kip-ft}, \quad V_{DC} = 29.4 \text{ kip}$$

www.EngineeringEBooksPdf.com

TABLE 6.5
Summary of Live Load Distribution Factors

	One Design Lane Loaded	Two or More Design Lanes Loaded
Bending Moment		
Interior girder	0.43	0.577
Exterior girder	**0.72**	0.571
Shear		
Interior girder	0.66	**0.779**
Exterior girder	0.72	0.462

$$M_{DW} = 40.9 \text{ kip-ft}, \quad V_{DW} = 3.3 \text{ kip}$$

$$M_{(L+I)} = 1033.3 \text{ kip-ft}, \quad V_{L+I} = 93.94 \text{ kip}$$

Apply load factors to unfactored loads to calculate factored load, and live load distribution factors to live load moment and shear.

Bending moment: $g_{mi} = 0.72$

Max *LL* moment in the exterior girder = (0.72)(1033.3) = 744.0 kip-ft

Factored Loads: Moments

$$M_u = \Sigma\eta_i\gamma_i M_i$$

$$\eta_i = \eta_D\eta_R\eta_I \text{ (Art. 1.3.2.1)}$$

Select Modifiers: Same as for the interior girders.

Ductility, $\eta_D = 1.0$ (Art. 1.3.3).

Redundancy, $\eta_R = 1.0$ (Art. 1.3.4)

Importance, $\eta_I = 1.0$ (Art. 1.3.5)

Therefore, $M_u = \eta\Sigma\gamma_i M_i = (1.0)\Sigma\gamma_i M_i$

$$M_u = 1.0\ [1.25M_{DC} + 1.5M_{DW} + 1.75(M_{LL+im})]$$

$$= 1.0\ [1.25(367.8) + 1.5(45.0) + 1.75(744.0)]$$

$$= 1829.3 \text{ kip-ft}$$

Select the girder size. Calculate the required value of the plastic section modulus, Z_x, assuming the girder as fully braced.

$$Z_{x,reqd} = \frac{M_u}{F_y} = \frac{1829.3(12)}{50} = 439 \text{ in.}^3$$

For the selected W33 × 118, $Z_x = 415$ in.$^3 < Z_{reqd} = 439$ in.^{3}, ng.

Therefore, W33 × 118 for the exterior girder is not adequate for the strength limit state. Instead, try a W33 × 130 for which $Z_x = 467$ in.$^3 > Z_{x,reqd} = 439$ in.^{3}

Therefore, use W33 × 130 for the exterior girders. All checks and calculations performed earlier for the interior girder (W33 × 118) should be repeated for W33 × 130.

Alternatively, W33 × 130 may be used for both the interior as well as exterior girders. The required calculations for the suggested W33 × 130 are left as an exercise for readers.

Figure 6.55b shows the sketch of elevation of the bridge as designed.

www.EngineeringEBooksPdf.com

6.13 COMPOSITE SLAB–STEEL BEAM SUPERSTRUCTURES

6.13.1 Introduction to Composite Construction

Example 6.2 was presented to illustrate design of a noncomposite slab–steel beam superstructure. Although LRFD Specifications do not prohibit construction of noncomposite bridges per se, the practice is not encouraged because noncomposite construction is uneconomical. It is common practice to design and build slab-beam type of superstructures using composite construction.

Reference is made to Figure 6.2 that shows a cross section of slab–steel beam superstructure that consists of a concrete slab supported by steel I-beams. In composite slab–girder superstructures, the construction is such that the deck slab acts compositely with the steel beams. Composite construction implies that the hardened concrete slab and the supporting steel beams (or prestressed concrete beams when used) act in unison; that is, there is no slip (relative movement) at the interface between the slab and the supporting beams/girders. In the case of composite steel beams, interfacial resistance is provided by the shear connectors welded to the top flanges of the beams and embedded in the slab (discussed in Section 6.10.10 and Example 6.1). The result is that the steel beams alone support the dead load of the deck slab while the concrete is curing. Once the deck hardens, the superimposed dead loads and live loads are carried by the composite action of slab–girder unit. This allows use of beams of relatively shallower cross sections as compared to those required for noncomposite construction. By contrast, in noncomposite construction, the deck simply rests on girders; the girders alone carry the entire load (permanent as well as transient) acting on the superstructure. As discussed in Chapter 5, in the case of prestressed concrete composite beams, interfacial resistance is provided by the stirrups projecting from the top of the beams and embedded in the slab.

Noncomposite and composite sections were defined in Section 6.7. A detailed discussion of analysis of composite sections follows.

6.13.2 Flexural Strength of Composite Sections

6.13.2.1 Stress Distribution in Composite Beams in Positive Flexure

In a beam subjected to flexure, the position of neutral axis defines the types of stresses above and below it. When subjected to positive flexure, the stresses above the neutral axis are designated as compressive and those below it as tensile. Under elastic conditions, stress distribution in the beam is assumed to be linear: maximum at the extreme fibers, varying linearly to zero at the neutral axis. This neutral axis is referred to as *elastic neutral axis* (or simply *neutral axis*). At ultimate load conditions, this linear stress distribution is not valid. Instead, the stress distribution is assumed to be rectangular: stresses in all fibers above and below the neutral axis equal the strength of the material, compressive and tensile, respectively, and the neutral axis corresponding to this state of stress distribution is referred to as *plastic neutral axis* (PNA).

The concept of plastic moment of a steel section in flexure was introduced in Section 1.3.2. The PNA of a steel section can be easily determined from the principle of force equilibrium when the entire section has attained a rectangular stress distribution equal to the yield stress, F_y. This topic is well covered in text on steel design and is not discussed here. The method of determining the PNA of a composite section is discussed in the following sections.

To determine the flexural strength, M_p, of composite section, it is necessary to locate the position of PNA in the composite section. Figure 6.56 shows the cross sections of a composite beam isolated from the bridge cross section of Figure 6.2. Theoretically, the PNA can have any position in the beam depending on the compressive strength of concrete and yield strength of steel. To introduce the concept of plastic stress distribution in composite beams, three arbitrarily selected

www.EngineeringEBooksPdf.com

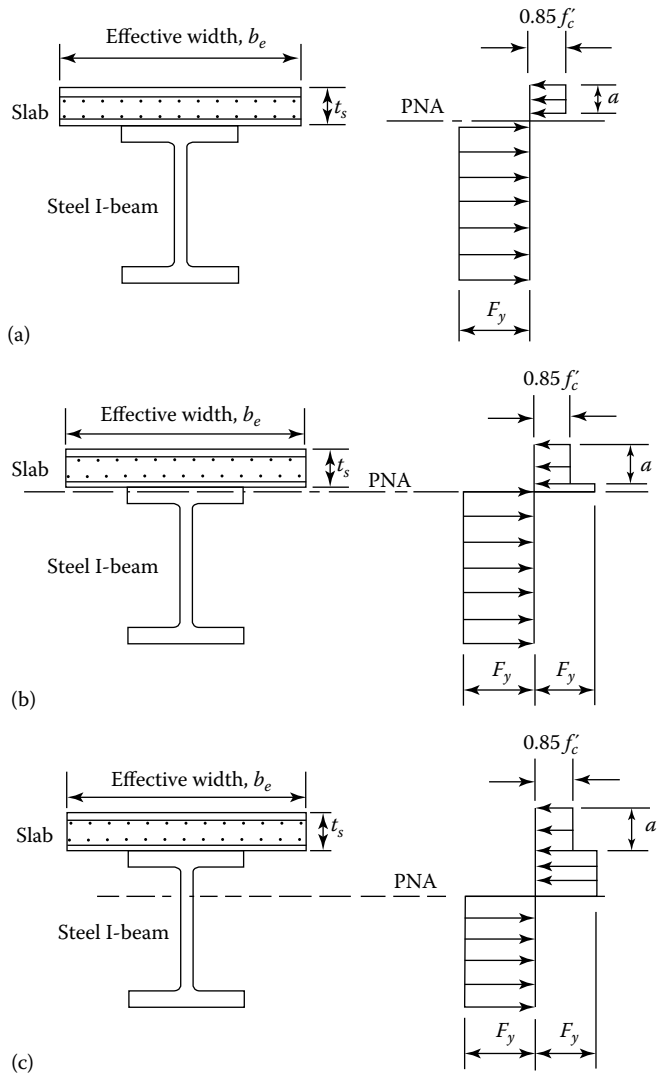

FIGURE 6.56 Concept of plastic stress distribution in composite beams: (a) PNA in concrete slab, (b) PNA in the compression flange, and (c) PNA in the web.

positions of PNA in the composite cross section are shown in Figure 6.56 as follows, along with the corresponding state of stress distribution:

1. PNA in the slab
2. PNA in the top flange of the steel beam
3. PNA in the web

All elements in the cross section (except the haunch, which is ignored) contribute resistances (forces) that resist the applied bending moment. These include concrete slab, longitudinal slab reinforcement (i.e., the reinforcement bars placed parallel to the longitudinal axis of the steel girder), and the steel girder (its flanges and the web). The magnitude of the element resistance is determined as stress at

www.EngineeringEBooksPdf.com

ultimate conditions *times* the element cross-sectional area. The stresses in elements are assumed to have reached their ultimate strength values as follows:

1. Stress in concrete slab:
   a. If the element lies above the PNA, the stress in it is assumed to be equal to the compressive strength of concrete, $0.85f'_c$.
   b. If the element lies below the PNA, the stress in it is assumed to be zero (because concrete in tension is assumed to have cracked and, therefore incapable of resisting any force).
2. Stresses in slab reinforcement: Only the longitudinal reinforcement at the top and the bottom of the slab is considered; the slab reinforcement oriented transverse to the longitudinal axis of the beam is ignored as it does not contribute any resistance in the longitudinal direction.
   a. If the PNA lies above the top layer of longitudinal reinforcement, stresses in both layers of longitudinal reinforcement are assumed to be equal to their yield strength in tension, F_{yr}.
   b. If the PNA lies somewhere between the top and the bottom longitudinal layers of reinforcement, then the stress in the upper longitudinal reinforcement layer is assumed to be equal to F_{yr} in compression; that in the layer below the PNA is assumed to be equal to F_{yr} in tension.
   c. If the PNA lies below the bottom longitudinal reinforcement layer, then the stresses in both longitudinal reinforcement layers are assumed to be equal to F_{yr} in compression.
   d. If the PNA lies at the centroid of a layer of longitudinal reinforcement, the stress in the bars of that layer is assumed to be zero.
3. Stress in steel:
   a. If the element lies above the PNA, the stress in it is assumed to be equal to the yield strength in compression, F_y.
   b. If the element lies below the PNA, the stress is assumed to be equal to the yield strength in tension, F_y.
4. Concrete in tension and in the haunch area is ignored.

Based on the aforementioned assumptions, stress distributions, consistent with the selected positions of the PNA in Figure 6.56, are shown as follows:

1. In Figure 6.56a, the PNA lies in the slab. Therefore, the stress in slab concrete above the PNA is shown as compressive ($=0.85f'_c$), the stress in the concrete below the PNA is zero, and the stress in the steel section is tensile ($=F_y$).
2. In Figure 6.56b, the PNA lies in the top flange of the steel section. Therefore, the stress in the entire slab is compressive ($=0.85f'_c$); the stress in the steel section above the PNA (only a portion of the top flange) is compressive ($=F_y$), and the stress in the steel section below the PNA (a portion of the top flange, the web and the bottom flange) is tensile ($=F_y$).
3. In Figure 6.56c, the PNA lies in the web of the steel section. Therefore, the stress in the entire slab is compressive ($=0.85f'_c$); the stress in the steel section above the PNA (the top flange and a portion of the web) is compressive ($=F_y$), and the stress in the steel section below the PNA (a portion of the web and the bottom flange) is tensile ($=F_y$).

Note that in all three cases of Figure 6.56 discussed previously, stresses in the slab reinforcement are not shown (intentionally) for the sake of simplicity. But, the slab reinforcement does influence the position of the PNA in the composite cross section in that it contributes a force equal to its area times the yield strength (A_rF_{yr}). Typically, a reinforced concrete deck slab is provided with four layers of reinforcement: two layers of bars perpendicular to each other near the top and two layers of bars perpendicular to each other near the bottom. Of these four layers, only the two layers of bars

www.EngineeringEBooksPdf.com

(one near the top and the other near the bottom) that are oriented parallel to the longitudinal axes of the beams are considered as contributing to the forces that resist bending of the composite beam. At the ultimate conditions, the stresses in these bars are considered to be at their yield strength level, so the magnitude of the axial forces in these reinforcing bars equals their cross-sectional areas (A_s) times the yield strength (F_{yr}). The nature of forces in the bars in these two reinforcing layers depends on their location relative to the PNA. For analytical purposes, it would be assumed that these reinforcement forces would be compressive if the bars are located above the PNA and tensile if the bars are located below the PNA. In case the centroid of bars is located in the plane of the PNA, their contribution to flexural resistance would be ignored. Transverse reinforcing bars (i.e., oriented perpendicular to the longitudinal axis of steel girder), both near the top and the bottom, which serve to resist moments caused due to the transverse bending of the slab, do *not* contribute to the forces that are considered in locating the PNA.

6.13.2.2 Stress Distribution in Composite Beams in Negative Flexure

In simply supported spans, a composite beam is in positive flexure. In such cases, depending on the location of the PNA, the deck slab (partly or wholly) is in compression and the steel girder (partly or wholly) in tension. In continuous spans, a portion of the composite beam (near interior supports) would be in negative flexure. In that case, depending on the location of PNA, the deck slab (partly or wholly) would be in *tension*, and the steel beam (partly or wholly) would be in *compression*. When calculating the plastic moment strength, M_p, of a composite section in negative flexure, it is assumed that

1. Portion of concrete slab located above the PNA (which is in tension) is cracked and does not contribute any strength
2. Concrete below the PNA is in compression (stress = 0.85 f_c')
3. The longitudinal slab reinforcement bars in the top and bottom layers contribute forces, tensile or compressive, respectively, depending on the location of these bars, above or below the PNA
4. Concrete in tension and in the haunch area is ignored
5. Stresses in steel portion of the composite section may be tensile (if above the PNA) or compressive (if below the PNA), each being equal to F_y

6.13.2.3 Locating Plastic Neutral Axis of a Composite Section in Positive Flexure

The first step in determining the plastic moment strength, M_p, of a composite beam involves determination of the position of the PNA in the cross section, which is determined from the principle of equilibrium of horizontal forces (compressive and tensile) acting on the composite beam cross section: the compressive forces equal the tensile forces or that there is no net axial force, which can be stated by Equation 6.158:

$$\sum F_x = 0 \tag{6.158}$$

The plastic moment strength, M_p, of the composite beam is obtained by taking moments of all cross-sectional element forces acting on the cross section about the PNA.

In a composite section, the PNA may lie in the deck slab or in the steel beam, which depends on the following parameters:

1. Effective width b_e of the slab
2. Compressive strength of concrete, f_c'
3. Area (A_r) and grade of steel reinforcement (F_{yr}) in the slab
4. Yield strength (F_y) of girder steel. F_y may be the same for the entire steel cross section, or it might be different for flanges and the webs as in the case of hybrid girders as discussed in Section 6.6.

www.EngineeringEBooksPdf.com

6.13.3 Effective Flange Width

The *effective width* of the flange (b_s) is a key parameter for calculating the plastic moment strength, M_p, of a composite beam. Flexural stresses are distributed across the deck of composite and monolithic flexural members by in-plane shear stresses. Due to corresponding shear deformations, plane sections do not remain plane, and longitudinal stresses in the deck are not uniform, a phenomenon called *shear lag*. The effective flange width is the width of the deck over which the assumed uniform stress distribution results in the same deck force and member moments as calculated from elementary beam theory assuming plane sections remain plane, as would be produced by the nonuniform stress distribution.

For determining the cross-section stiffness for analysis and for determining the flexural resistances, the effective flange width of a beam in composite or monolithic construction is taken as its tributary width perpendicular to the axis of the member (LRFD Art. 4.6.2.6.1). Accordingly, the effective flange width in composite beam and/or stringer systems or in chords of composite deck trusses may be taken as follows:

1. *Interior beams*: One-half the distance to the adjacent beam or stringer on each side of the component.
2. *Exterior beams*: One-half the distance to the adjacent beam or stringer plus full overhang width.
3. In cases where a structurally continuous concrete barrier is present and is included in the structural analysis, the deck overhang width used for the analysis as well for checking the structural resistances of composite beam may be extended as given in Equation 6.159:

$$\Delta w = \frac{A_b}{2t_s} \qquad (6.159)\ [A4.6.2.6.1\text{-}1]$$

where
A_b = cross sectional area of the concrete barrier
t_s = thickness of the deck slab

(*Commentary*: This aforementioned assumption for the effective width of the flange for a concrete–steel composite beam is a deviation from the pre-2007-AASHTO practice, which specified the effective width as follows:

For interior beams:

1. One-fourth of the effective span length
2. Twelve times the average depth of the slab, plus greater of the web thickness or one-half the width of top flange
3. Average spacing of the adjacent beams

For exterior beams:

The effective width may be taken as one-half the effective width of the adjacent interior beam, plus the least of the following:

1. One-eighth of the effective span length
2. 6.0 times the average depth of the slab, plus the greater of one-half of the web thickness or one-quarter of the width of the top flange of the basic girder
3. The width of the overhang

www.EngineeringEBooksPdf.com

This revision of the previous specification is based on a study by Chen et al. (2005) that demonstrated that there was no significant relationship between the effective width and the slab thickness as implied by previous specification.)

6.13.4 AASHTO Procedure for Determining the Plastic Neutral Axis and Plastic Moment Strength of a Composite Section: LRFD Appendix D6, Art. D6.1

The AASHTO LRFD procedure for locating the PNA of a composite beam cross section is based on the principles of force equilibrium as stated by Equation 6.158 (described in LRFD: *Appendix D6: Fundamental Calculations for Flexural Members*, Art. D6.1: Plastic Moment). The axial forces in various elements of the cross section are determined as products of the cross-sectional area of the element and the stress ($0.85f_c'$ times the compressive strength of concrete or yield strength of steel, F_y, as applicable). Figure 6.57 shows the cross section of a composite steel girder bridge superstructure (shown in Figure 6.2) and the element forces acting on it. These element forces are defined as follows (assuming a nonhybrid steel beam so the f_y is same for flanges and the web):

P_s = compressive force in the slab = $0.85f_c'b_st_s$.
P_{rt} = compressive or tensile force in the top slab reinforcement = $A_{rt}F_{yr}$.
P_{rb} = compressive or tensile force in the bottom slab reinforcement = $A_{rb}F_{yr}$.
P_c = compressive or tensile force in the top (or compression) flange of the steel girder = A_cF_y.
P_w = compressive or tensile force in the web of steel girder = A_wF_y.
P_t = compressive or tensile force in the bottom (or tension) flange of steel girder = A_tF_y.

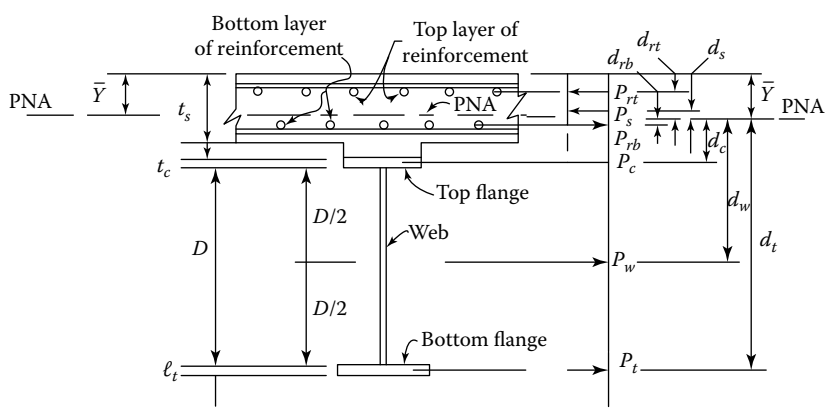

FIGURE 6.57 Element forces on a composite steel girder cross section in positive flexure. PNA is shown to lie in the slab between the top and bottom layers of reinforcement. *Note*: P_s, compressive force in the slab = $0.85f_c'b_et_s$; P_{rt}, compressive or tensile force in the top slab reinforcement = $A_{rt}F_{yr}$; P_{rb}, compressive or tensile force in the bottom slab reinforcement = $A_{rb}F_{yr}$; P_c, compressive or tensile force in the top (or compression) flange of the steel girder = A_cF_y; P_w, compressive or tensile force in the web of steel girder = A_wF_y; P_t, compressive or tensile force in the bottom (or tension) flange of steel girder = A_tF_y, where f_c', compressive strength of concrete; b_e, effective width of the flange of composite section; t_s, thickness of concrete slab; A_{rt}, total area of reinforcement in the top layer of the slab contained in the effective width; A_{rb}, total area of reinforcement in the bottom layer of the slab contained in the effective width; A_c, area of top (compression) flange of steel girder; A_w, area of the web of steel girder; A_t, area of the bottom (tension flange of steel girder); F_{yr}, yield strength of reinforcing steel; F_y, yield strength of steel girder (for hybrid girders, the yield strength of flanges and the web may be different).

www.EngineeringEBooksPdf.com

where

f'_c = compressive strength of concrete
b_s = effective width of the flange of composite section
t_s = thickness of concrete slab
A_{rt} = total area of reinforcement in the top layer of the slab contained in the effective width
A_{rb} = total area of reinforcement in the bottom layer of the slab contained in the effective width
A_c = area of top (compression) flange of steel girder
A_w = area of the web of steel girder
A_t = area of the bottom (tension flange of steel girder)
F_{yr} = yield strength of reinforcing steel
F_y = yield strength of steel girder (for hybrid girders, the yield strength of flanges and the web may be different)

The six element forces listed previously are assumed to act at the centroids of respective elements as follows:

1. P_{rt} acts at the center of the top layer of reinforcement.
2. P_{rb} acts at the center of the bottom layer of reinforcement.
3. P_s acts at the geometric center of the portion of the slab in compression.
4. P_c acts at the centroid of the compression flange (top flange) of the steel section.
5. P_w acts at the centroid of the web.
6. P_t acts at the centroid of the tension flange (bottom flange) of the steel section.

Location of PNA in a composite beam is not always obvious (as it is in beams of homogeneous materials having cross sections that are symmetrical about the axis of bending). In such cases, the PNA may be located by an iterative process by assuming the location of PNA anywhere in the composite cross section. The correct location of PNA is known when the equilibrium of horizontal forces acting on the cross section is satisfied (Equation 6.158). For analytical purposes, it is convenient to assume that PNA is located at any of the following seven locations as shown in Table 6.6.

The plastic moment strength of the composite section, M_p, can be determined by following basic steps:

1. Assume the location of the PNA in the given cross section, and calculate element forces.
2. Determine the location of the PNA from Equation 6.158, that is, calculate $\overline{Y}$, the distance of the PNA from the top fibers of the section. A few iterations may be required.

TABLE 6.6
Various Cases for Determination of PNA in a Composite Beam Cross Section

Case No.	Location of PNA
Case I	In the web of steel girder
Case II	In the top flange of steel girder
Case III	In the concrete deck, below the bottom layer of reinforcement, P_{rb}
Case IV	In the concrete deck, at the level of bottom layer of reinforcement, P_{rb}
Case V	In the concrete deck, between the top and bottom layers of reinforcement
Case VI	In the concrete deck, at the level of P_{rt}
Case VII	In the concrete deck, above the level of P_{rt}

Note: The possibility of the PNA lying in the bottom flange of a steel girder is not considered as one of the seven cases listed in Table 6.5 as it is practically impossible.

www.EngineeringEBooksPdf.com

3. Determine the centroids of all element forces (from principles of statics).
4. Calculate moments about the PNA due to all of the element forces.
5. The plastic moment strength of the composite beam is the algebraic sum of moments due to all element forces.

Expressions for the locations of PNA in cross section of a composite beam in positive flexure for the seven cases listed in Table 6.6 are given in Table 6.7 (and in Table 6.8 for a composite beam in negative flexure). Element forces and their locations in the composite beam cross section are also shown in Tables 6.7 and 6.8. These expressions are given in terms of the six cross-sectional element forces described previously. Also listed in Tables 6.7 and 6.8 are the corresponding values of the plastic moment strength, M_p. Element forces, compressive or tensile, appearing in these expressions act at the centroids (i.e., at the mid-depths) of the respective elements; forces in reinforcement are assumed to act at their respective centers. Moment due to an element force is obtained as the element force times its distance from the PNA as listed in Table 6.8. Algebraic sum of the moments due to all element forces taken about the PNA gives the plastic moment strength of the composite section.

Note that in the equations for M_p given in Tables 6.7 and 6.8, the distance d is measured from the PNA to the element force. All element forces, dimensions, and distances are to be taken as positive.

Analyzing a composite beam cross section for all seven cases listed in Table 6.6 is a monotonous, cumbersome, time-consuming exercise. Fortunately, it is usually not necessary to analyze/investigate all seven cases for locating the PNA. In this context, the following observations are made:

1. The possibility of the PNA lying in the slab, between the top and bottom layers of reinforcement (i.e., between P_{rt} and P_{rb}), is a real one. This is because the slab contributes a significant amount of compression force in Equation 6.158, which represents equilibrium of forces acting on the composite cross section. Therefore, one should always start with this assumption to determine the location of the PNA (see Example 6.3).
2. Of the seven possible PNA positions, Cases VI and VII, though theoretically possible, are merely academic and not likely to occur in practical cases. This is because the locations of the PNA defined by these cases would result in rather small values of the compression forces (the area of concrete above the top layer of reinforcement is relatively small), which would not balance the relatively large tensile force contributed by the elements of the steel girder. Therefore, only Cases I through V are investigated in the examples in this chapter.
3. The forces in the longitudinal reinforcement may be ignored (for expediency) so that $P_{rt} = P_{rb} = 0$. This assumption is conservative and considerably simplifies the expressions for the seven cases of Table 6.6 and has been used in the examples in this chapter. Contribution of the longitudinal slab reinforcement to the plastic moment strength of a composite section (in positive flexure) may be considered at the option of the designer; however, it does not appreciably change the plastic moment strength of the composite beam.

Expressions listed in Tables 6.7 and 6.8 can be derived from the principles of statics. Consider, for example, Case V of Table 6.7. When the PNA lies in the slab (Figure 6.57), only a portion of the slab (which is above the PNA) is in compression. If the depth of the PNA is equal to $\bar{Y}$ ($< t_s$, the thickness of the slab) from the top of slab, then the compressive strength of slab of depth $\bar{Y}$ can be expressed as given by Equation 6.160:

$$P_{s1} = 0.85 f_c' b_s \bar{Y} \tag{6.160}$$

$$\text{Moment of } P_{s1} \text{ about PNA} = \frac{P_{s1}\bar{Y}}{2} = \frac{0.85 f_c' b_s \left(\bar{Y}\right)^2}{2} \tag{6.161}$$

www.EngineeringEBooksPdf.com

TABLE 6.7
Calculation of $\bar{Y}$ and M_p for Sections in Positive Flexure

Case	PNA	Condition	$\bar{Y}$ and M_p
I	In web	$P_t + P_w \geq P_c + P_s + P_{rb} + P_{rt}$	$\bar{Y} = \frac{D}{2}\left[\frac{P_t - P_c - P_s - P_{rt} - P_{rb}}{P_w} + 1\right]$ $M_p = \frac{P_w}{2D}\left[\bar{Y}^2 + (D - \bar{Y})^2\right] + \left[P_s d_s + P_n d_{rt} + P_{rb} d_{rb} + P_c d_c + P_t d_t\right]$
II	In top flange	$P_t + P_w + P_c \geq P_s + P_{rb} + P_{rt}$	$\bar{Y} = \frac{t_c}{2}\left[\frac{P_w + P_t - P_s - P_n - P_{rb}}{P_c} + 1\right]$ $M_p = \frac{P_c}{2t_c}\left[\bar{Y}^2 + (t_c - \bar{Y})^2\right] + \left[P_s d_s + P_n d_{rt} + P_{rb} d_{rb} + P_w d_w + P_t d_t\right]$
III	Concrete deck, below P_{rb}	$P_t + P_w + P_c \geq \left(\frac{c_{rb}}{t_s}\right)P_s + P_{rb} + P_{rt}$	$\bar{Y} = (t_s)\left[\frac{P_c + P_w + P_t - P_{rt} - P_{rb}}{P_s}\right]$ $M_p = \left(\frac{\bar{Y}^2 P}{2t_s}\right) + \left[P_{rt} d_{rt} + P_{rb} d_{rb} + P_c d_c + P_w d_w + P_t d_t\right]$
IV	Concrete deck, at P_{rb}	$P_t + P_w + P_c P_{rb} \geq \left(\frac{c_{rb}}{t_s}\right)P_s + P_{rt}$	$\bar{Y} = c_{rb}$ $M_p = \left(\frac{\bar{Y}^2 P_s}{2t_s}\right) + \left[P_{rt} d_{rt} + P_c d_c + P_w d_w + P_t d_t\right]$
V	Concrete deck, above P_{rb} below P_{rt}	$P_t + P_w + P_c + P_{rb} + P_{rt} \geq \left(\frac{c_{rt}}{t_s}\right)P_s$	$\bar{Y} = (t_s)\left[\frac{P_{rb} + P_c + P_w + P_t - P_{rt}}{P_s}\right]$ $M_p = \left(\frac{\bar{Y}^2 P_s}{2t_s}\right) + \left[P_{rt} d_{rt} + P_{rb} d_{rb} + P_c d_c + P_w d_w + P_t d_t\right]$

www.EngineeringEBooksPdf.com

VI	Concrete deck, at P_{rt}	$P_t + P_w + P_c + P_{rb} \geq \left(\frac{c_{rb}}{t_s}\right)P_s + P_{rt}$	$\overline{Y} = c_{rt}$ $M_p = \left(\frac{\overline{Y}^2 P_s}{2t_s}\right) + \left[P_{rb}d_{rb} + P_c d_c + P_w d_w + P_t d_t\right]$
VII	Concrete deck, above P_{rt}	$P_t + P_w + P_c + P_{rb} + P_{rt} < \left(\frac{c_n}{t_s}\right)P_s$	$\overline{Y} = (t_s)\left[\frac{P_{rb} + P_c + P_w + P_t + P_{rt}}{P_s}\right]$ $M_p = \left(\frac{\overline{Y}^2 P_s}{2t_s}\right) + \left[P_{rt}d_{rt} + P_{rb}d_{rb} + P_c d_c + P_w d_w + P_t d_t\right]$

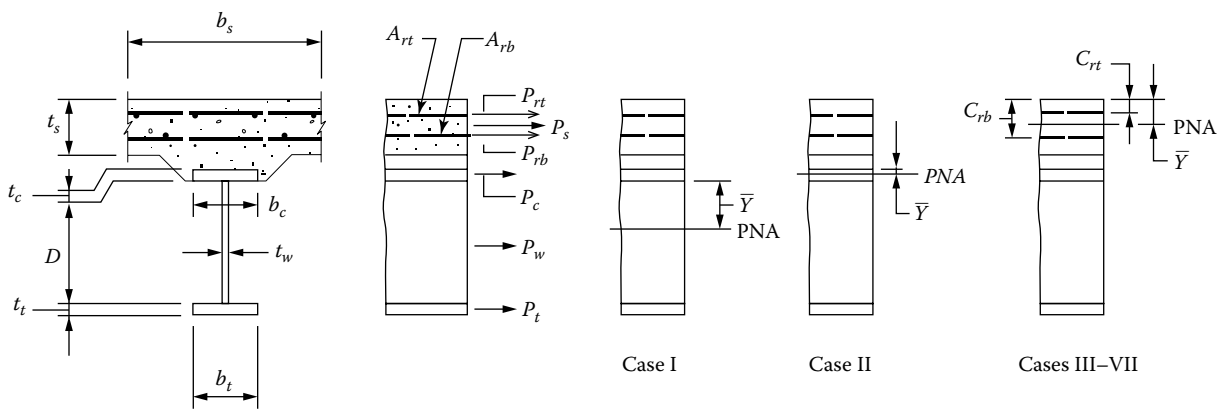

Source: From *AASHTO LRFD Bridge Design Specifications*, Copyright © 2012 by American Association of State Highway and Transportation Officials, Washington, DC. Used by permission.

www.EngineeringEBooksPdf.com

TABLE 6.8
Calculation of $\bar{Y}$ and M_p for Sections in Negative Flexure

Case	PNA	Condition	$\bar{Y}$ and M_p
I	In web	$P_c + P_w \geq P_t + P_{rb} + P_{rt}$	$\bar{Y} = \frac{D}{2}\left[\frac{P_c - P_t - P_{rt} - P_{rb}}{P_w} + 1\right]$ $M_p = \frac{P_w}{2D}\left[\bar{Y}^2 + (D - \bar{Y})^2\right] + \left[P_n d_{rt} + P_{rb} d_{rb} + P_c d_c + P_t d_t\right]$
II	In top flange	$P_c + P_w + P_t \geq P_{rb} + P_{rt}$	$\bar{Y} = \frac{t_c}{2}\left[\frac{P_w + P_c - P_{rt} - P_{rb}}{P_t} + 1\right]$ $M_p = \frac{P_t}{2t_t}\left[\bar{Y}^2 + (t_t - \bar{Y})^2\right] + \left[P_n d_{rt} + P_{rb} d_{rb} + P_w d_w + P_c d_c\right]$

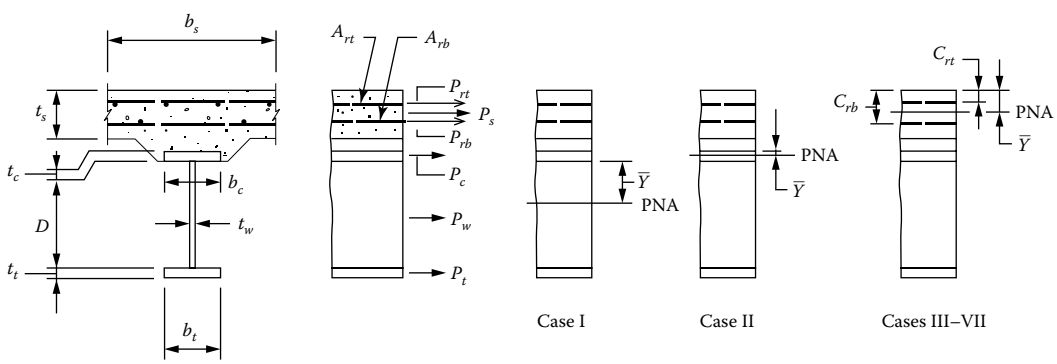

Source: From *AASHTO LRFD Bridge Design Specifications*, Copyright © 2012 by American Association of State Highway and Transportation Officials, Washington, DC. Used by permission.

Multiply both the numerator and the denominator of the right-hand side expression of Equation 6.161 by the slab thickness, t_s; the result is Equation 6.162:

$$\text{Moment of } P_s \text{ about PNA} = \frac{0.85 f_c' b_s t_s \left(\bar{Y}\right)^2}{2t_s} \tag{6.162}$$

If the entire slab were in compression, its contribution to compressive force could be determined from Equation 6.163:

$$\text{Compressive strength of entire deck slab, } P_s = 0.85 f_c' b_s t_s \tag{6.163}$$

Note that there is no contribution to P_s from concrete in the haunch.

Substitution for the quantity $0.85 f_c' b_s t_s$ from Equation 6.163 to Equation 6.162 yields Equation 6.164:

$$\text{Moment of } P_s \text{ about PNA} = \frac{\bar{Y}^2 P_s}{2t_s} \tag{6.164}$$

The right-hand side term of Equation 6.164 appears as the first term for expressions for the plastic moment strength, M_p, for Case V in Table 6.7 (last column), which represents the moment due to

www.EngineeringEBooksPdf.com

compression force in concrete (P_s) taken about the PNA. Sum of moments due to the remaining element forces are determined from Equation 6.165:

$$M_{p,elements} = \sum F_{element}\left(d_{element}\right) \tag{6.165}$$

Various terms in Equation 6.165 are shown in Figure 6.58 and in Table 6.9.

Thus, the plastic moment strength of the composite girder, M_p, for Case V is obtained as the algebraic sum of moments given by Equation 6.164 and Equation 6.165 as expressed by Equation 6.166:

$$M_p = \left(\frac{\overline{Y}^2 P_s}{2t_s}\right) + \left[P_{rt}d_{rt} + P_{rb}d_{rb} + P_c d_c + P_w d_w + P_t d_t\right] \tag{6.166}$$

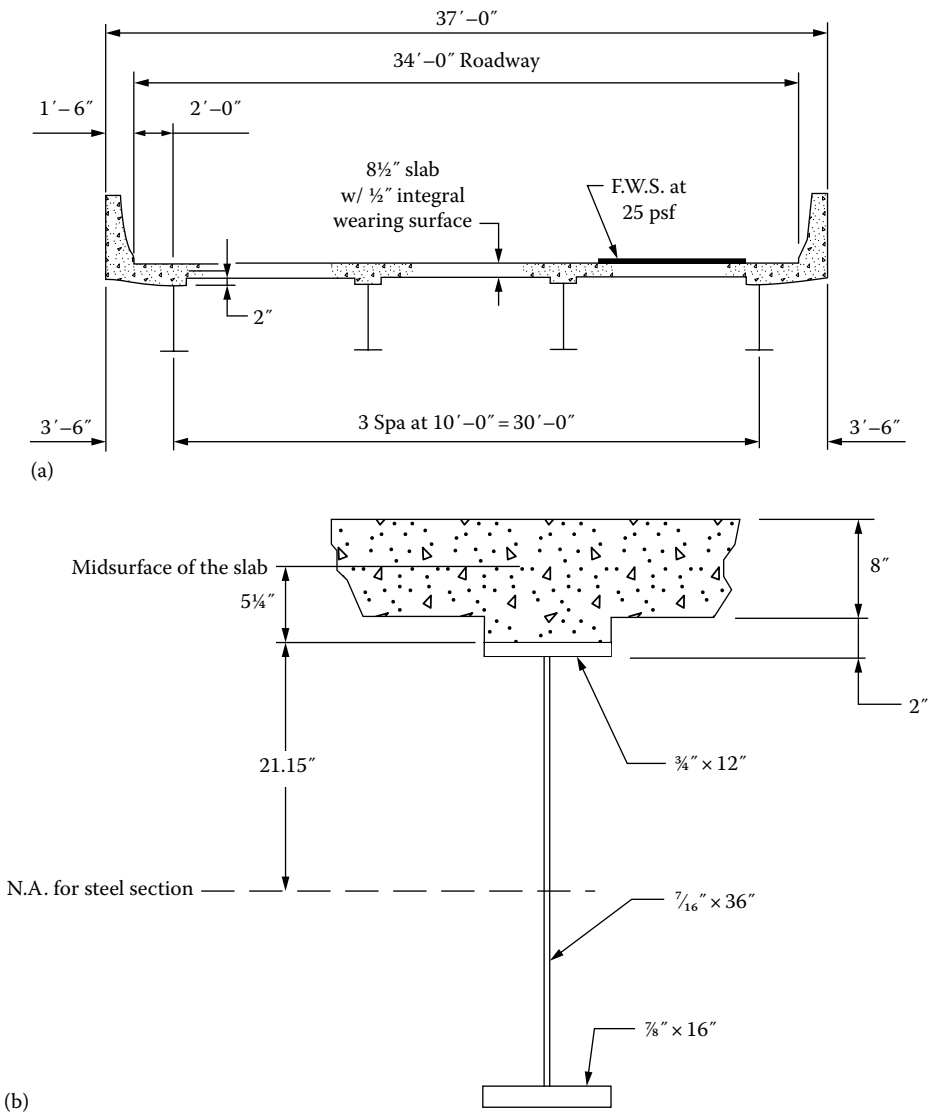

FIGURE 6.58 Concrete deck-steel girder bridge superstructure for Example 6.3. (a) Bridge cross section and (b) composite girder details (slab reinforcement not shown).

www.EngineeringEBooksPdf.com

TABLE 6.9
Element Forces, Locations, and Moments in Composite Beam Cross Section

Element Force	Distance from PNA	Moment about PNA
Top reinforcement, P_{rt}	d_{rt}	$P_{rt}d_{rt}$
Bottom reinforcement, P_{rb}	d_{rb}	$P_{rb}d_{rb}$
Top flange of steel beam, P_c	d_c	$P_c d_c$
Web, P_w	d_w	$P_w d_w$
Bottom flange of steel beam, P_t	d_t	$P_t d_t$

Equation 6.166 is listed as the value of plastic moment strength in the last column of Table 6.7 for Case V.

Expressions presented in Table 6.7 are applicable to composite girder in a simple span and in segments of positive flexure in a continuous span. In the negative flexure segment of a composite beam, the deck concrete would be in tension and assumed cracked; therefore, it does not contribute any tensile stress resultant for force equilibrium (i.e., $P_s = 0$), but the contribution of top and bottom layers of reinforcement present in the slab (P_{rt} and P_{rb}) must be considered. However, because of relatively small contribution of these forces, the PNA would be either in the web (Case I) or in the top flange (Case II) of the steel girder. In both cases, portions of cross sections above the PNA would be in *tension*; those below the PNA would be in *compression*.

Expressions for the location of PNA and the corresponding value of plastic moment strength, M_p, for the composite cross section in the negative flexure segment of a beam are listed in Table 6.8. The contribution of slab reinforcement to nominal moment strength of the section in negative flexure should be considered. The nature of forces (tensile or compressive) in elements of the steel beam changes when the applied moment changes from positive to negative (e.g., over supports of a continuous composite beam). Top flange, which is in compression when in positive flexure, goes in tension when in negative flexure. Likewise, the bottom flange, which is in tension when in positive flexure, goes in compression when in negative flexure. The same is true of the web. A portion of the web that is in compression when the moment is positive goes in tension when the moment becomes negative, and a portion of the web that is in tension when the moment is positive goes in compression when the moment is negative. Typically, the nominal moment strength of a composite section is smaller in negative flexure as compared to that in positive flexure, mainly because contribution to plastic moment strength from the slab is lost when it cracks in tension.

For preliminary design of a composite section in positive flexure, it may be expedient to ignore the contribution of longitudinal slab reinforcement, in which case P_{rt} and P_{rt} is each equal to zero. With this assumption, the PNA in the positive flexure segment of a beam would lie either in the deck slab or in the girder. Two separate cases can be considered on the basis of the following:

1. If the compressive strength of slab were greater than the axial tensile yield strength of steel girder, the PNA would lie in the slab. In that case, the concrete below the PNA, being in tension, is assumed to have cracked, and its contribution to plastic moment strength is ignored.
2. If the compressive strength of slab were smaller than the axial tensile strength of steel, the PNA would lie in the steel girder, either in the top flange or in the web. In this case, a portion of the flange or the entire flange and a portion of the web would be under compressive stress equal to F_y, and the portion of the girder below the PNA would be under tensile stress equal to F_y.

www.EngineeringEBooksPdf.com

6.13.5 Examples on Determination of Plastic Moment Strength, M_p

Several examples are presented as follows to clarify and illustrate applications of the procedure for determining the plastic moment strength, M_p, discussed in the preceding section. Different values of compressive strength of concrete (f'_c) and yield strength of steel (F_y) have been used in these examples to understand computational complexities involved and influence of these parameters on the plastic moment strength, M_p.

Examples 6.3 (f'_c = 4500 psi and F_y = 36 ksi) and 6.4 (f'_c = 4500 psi and F_y = 50 ksi) demonstrate application of the previous principles for determining the location of the PNA of a composite girder in positive flexure and its plastic moment strength, M_p. For simplicity, contribution of longitudinal slab reinforcement has been intentionally ignored in both these examples. Example 6.5 takes into account the force contribution from top and bottom longitudinal slab reinforcement to the nominal strength of a composite section. Example 6.6 presents calculations for the nominal moment strength of the composite section of Example 6.4 but in negative flexure.

Example 6.3: Determination of Plastic Moment Strength of Composite Section (Slab Reinforcement Ignored)

Calculate the plastic moment strength, M_p, of the composite girder shown in Figure 6.58. The bridge has a simple span of 80 ft. The 8 in. thick (excluding the integral wearing surface) deck slab is cast from a 4500 psi concrete; the girder is fabricated from A36 steel. Ignore the presence of steel reinforcement in the slab.

Solution

The effective width of the slab is assumed to be equal to its tributary width, TW (LRFD Art. 4.6.2.1):

$$b_s = TW = \text{center-to-center adjacent girders} = 10 \text{ ft} = 120 \text{ in.}, \quad f'_c = 4.5 \text{ ksi}$$

The compressive force, P_s, due to the concrete deck slab is

$$P_s = 0.85 f'_c b_s t_s = (0.85)(4.5)(120)(8) = 3672 \text{ kip}$$

The tensile yield strength of steel girder, T, having a cross-sectional area A_s is

$$T = F_y A_s$$

$$A_s = 36\left[(0.75)(12) + \left(\frac{7}{16}\right)(36) + \left(\frac{7}{8}\right)(16)\right] = 38.75 \text{ in.}^2$$

$$T = F_y A_s = 36(38.75) = 1395 \text{ kip} < 3672 \text{ kip}$$

Because $T < P_s$, the PNA lies in the slab. This is because the horizontal shear at the slab–girder interface cannot exceed the tensile strength of steel girder. Assume that the plastic neutral lies at a distance of $\bar{Y}$ below the top of the slab. Then, equating the compression resultant in the slab concrete and the tension resultant in steel girder, we have

$$P_s = T$$

$$0.85 f'_c b_s \bar{Y} = T$$

$$\bar{Y} = \frac{T}{0.85 f'_c b_s} = \frac{1395}{0.85(4.5)(120)} = 3.04 \text{ in.} < t_s = 8 \text{ in.}$$

$\bar{Y} < t_s$; therefore, the assumption that the PNA lies in the slab is valid.

www.EngineeringEBooksPdf.com

Alternatively, the PNA can be located using the LRFD formulas for Cases I through V listed in Table 6.7 (LRFD Table D6.1-1) as follows. Calculate the strengths of various elements in the cross section of the composite girder. In the following calculations, the contribution from slab reinforcement is ignored. Therefore,

$$P_{rt} = P_{rb} = 0.$$

The compression strength of the deck slab is

$$P_s = 3672 \text{ kip (calculated earlier)}$$

Tensile strength of top flange of steel girder is

$$P_c = (0.75)(12)(36) = 324 \text{ kip}$$

Tensile strength of web of steel girder is

$$P_w = \left(\frac{7}{16}\right)(36)(36) = 567 \text{ kip}$$

Tensile strength of bottom flange of steel girder is

$$P_t = \left(\frac{7}{8}\right)(16)(36) = 504 \text{ kip}$$

(*Check*: Total tensile yield strength of girder, $T = P_c + P_w + P_t = 324 + 567 + 504 = 1395$ kip, is much smaller than the compression strength of slab, 3672 kip. Because the compression and tensile forces must be equal in the cross section, it is obvious that only a portion of the slab (not its entire depth) should be in compression. In other words, PNA lies *inside* the slab.)

Check the following five conditions for location of the PNA as specified in LRFD Specifications (Table 6.7), and determine the location of PNA using the process of elimination.

Commentary: As explained earlier, one could start by checking Case V first and get the desired result. However, calculations are provided for all cases for illustrative purposes, starting with Case I.

Case I: PNA in the web

$$P_t + P_w \geq P_c + P_s + P_{rb} + P_{rt}$$

$$504 + 567 \ngeq 324 + 3672 + 0 + 0$$

$$1071 \ngeq 3996$$

Therefore, the PNA does not lie in the web.

Case II: PNA in the top flange

$$P_t + P_w + P_c \geq P_s + P_{rb} + P_{rt}$$

$$504 + 567 + 324 \ngeq 3672 + 0 + 0$$

$$1395 \ngeq 3672$$

Therefore, the PNA does not lie in the top flange.

www.EngineeringEBooksPdf.com

Case III: PNA in the slab, below P_{rb} (bottom slab reinforcement)

$$P_t + P_w + P_c \geq \left(\frac{c_{rb}}{t_s}\right)P_s + P_{rb} + P_{rt}$$

From Figure 6.58, c_{rb} = 6.5 in. = distance from the top of slab to the centroid of bottom slab reinforcement or 1.5 in. from the bottom of the slab (assumed).

$$504 + 567 + 324 \ngeq \left(\frac{6.5}{8.0}\right)(3672) = 2983.5$$

$$1395 \ngeq 2983.5$$

Therefore, the PNA is not below the P_{rb} level in the slab.

Case IV: PNA to be in the slab at the P_{rb} level (bottom slab reinforcement)

$$P_t + P_w + P_c + P_{rb} \geq \left(\frac{c_{rb}}{t_s}\right)P_s + P_{rt}$$

$$504 + 567 + 324 + 0 \ngeq 2983.5 + 0 = 2983.5 \text{ kip}$$

$$1395 \ngeq 2983.5$$

Therefore, the PNA is not at the P_{rb} level in the slab.

Case V: PNA to be in the slab above the P_{rb} and below P_{rt} (i.e., between the bottom layer and the top layer of longitudinal reinforcement)

$$P_t + P_w + P_c + P_{rb} + P_{rt} \geq \left(\frac{c_{rb}}{t_s}\right)P_s$$

where c_{rt} = 2.5 in. = distance from the top of slab to the centroid of top slab reinforcement (assumed).

$$504 + 567 + 324 + 0 + 0 > \left(\frac{2.5}{8.0}\right)3672 + 0$$

$$1395 > 1147.5$$

Because the left-hand side term (1395 kip) is *greater* than the right-hand side term (1147.5 kip), it indicates that the PNA lies *inside* the slab and is located *above* the P_{rb}. Thus, Case V governs, and, consequently, Case VI (PNA inside the slab, located *at* the P_{rt} level) and Case VII (PNA inside the slab, located *above* the P_{rt} level) are not investigated. Let $\bar{Y}$ be the distance of the PNA from the top of the slab. For Case V,

$$\bar{Y} = t_s\left[\frac{P_{rb} + P_c + P_w + P_t - P_{rt}}{P_s}\right] = (8.0)\left(\frac{1395}{3672}\right) = 3.04 \text{ in. (see Figure 6.59)}$$

which is the same as calculated earlier. The plastic moment strength, M_p, of the girder can be obtained by summing up the moments of various element forces about the PNA. These distances of various element forces measured from the PNA are as follows (Figure 6.59):

$$P_c = 324 \text{ kip}, d_c = 8 + 2 - \frac{1}{2}\left(\frac{3}{4}\right) - 3.04 = 6.585 \text{ in.}$$

www.EngineeringEBooksPdf.com

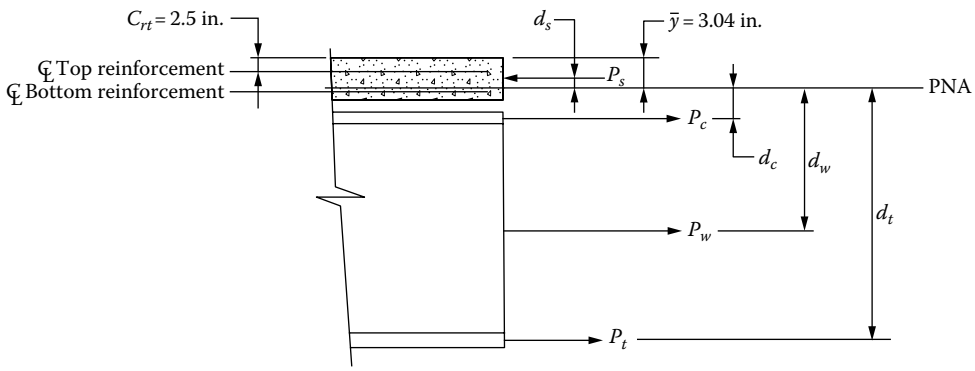

FIGURE 6.59 Element forces for computing plastic moment capacity (reinforcement forces have been ignored).

$$P_w = 567 \text{ kip}, d_w = 8 + 2 + \left(\frac{1}{2}\right)(36) - 3.04 = 24.96 \text{ in.}$$

$$P_t = 504 \text{ kip}, d_t = 8 + 2 + 36 + \left(\frac{1}{2}\right)\left(\frac{7}{8}\right) - 3.04 = 43.4 \text{ in.}$$

$$P_s = 3672 \text{ kip (calculated earlier)}$$

Therefore, the plastic moment strength, M_p, of the girder is

$$M_p = \left(\frac{\bar{Y}^2 P_s}{2t_s}\right) + \left(P_{rt}d_{rt} + P_{rb}d_{rb} + P_c d_c + P_w d_w + P_t t_t\right)$$

$$= \frac{(3.04)^2(3672)}{2(8)} + [0 + 0 + (324)(6.585) + (567)(24.96) + (504)(43.4)]$$

$$= 2{,}121 + 2{,}134 + 14{,}152 + 21{,}874$$

$$= 40{,}281 \text{ k-in.} = 3{,}357 \text{ kip-ft}$$

Commentary: The previous calculations demonstrate that Case V governs for the position of the PNA. Therefore, one could have started with Case V, obviating the need for investigating other cases. See Example 6.6.

Example 6.4: Determination of Plastic Moment Strength, M_p, of Composite Section (Longitudinal Slab Reinforcement Ignored)

Calculate the plastic moment strength, M_p, of the composite girder described in Example 6.3. Ignore the contribution of longitudinal steel reinforcement in the slab. Assume f'_c = 4.5 ksi, F_y = 50 ksi for the steel girder.

Refer to Figure 6.58 for details of bridge cross section and the details of the girder cross section. All data remain the same as in Example 6.3, except that F_y = 50 ksi (instead of 36 ksi in Example 6.3).

www.EngineeringEBooksPdf.com

Solution

The compressive strength of the concrete deck slab is based on the effective width of the slab, which is taken equal to the tributary width of the slab, TW = 10 ft = 120 in. (see Example 6.3) and the compressive strength of concrete (f_c' = 4.5 ksi).

$$P_s = 0.85 f_c' b_s t_s = (0.85)(4.5)(120)(8) = 3672 \text{ kip}$$

The tensile yield strength of steel is F_y = 50 ksi. Therefore, the tensile yield strength of steel girder, T, having a cross-sectional area A_s is

$$T = F_y A_s$$

$$A_s = \left[(0.75)(12) + \left(\frac{7}{16}\right)(36) + \left(\frac{7}{8}\right)(16) = 38.75 \text{ in.}^2\right]$$

$$T = F_y A_s = 50(38.75) = 1937.5 \text{ kip} < 3672 \text{ kip}$$

Because $T < P_s$, PNA lies in the slab. This is because the horizontal shear at the slab–girder interface cannot exceed the tensile strength of steel girder. Assume that the PNA lies at a distance of $\bar{Y}$ below the top of the slab. Then,

$$C = T$$

$$0.85 f_c' b_s \bar{Y} = T$$

$$\bar{Y} = \frac{A_s F_y}{0.85 f_c' b_s} = \frac{1937.5}{0.85(4.5)(120)} = 4.22 \text{ in.} < t_s = 8 \text{ in.}, \text{ OK (Figure 6.59)}$$

$\bar{Y} < t_s$; therefore, the assumption that the PNA lies below the top of slab is satisfied.

Alternatively, the PNA can be located using the formulas listed in Table 6.8 (LRFD Table D6.1-1) as follows. Calculate the strengths of various elements in the cross section of the composite girder. If the presence of slab reinforcement is ignored, then

$$P_{rt} = P_{rb} = 0$$

$$P_s = 3672 \text{ kip (calculated earlier)}$$

Tensile strength of top flange of steel girder is

$$P_c = (0.75)(12)(50) = 450 \text{ kip}$$

Tensile strength of web of steel girder is

$$P_w = \left(\frac{7}{16}\right)(36)(50) = 787.5 \text{ kip}$$

Tensile strength of bottom flange of steel girder is

$$P_t = \left(\frac{7}{8}\right)(16)(50) = 700 \text{ kip}$$

www.EngineeringEBooksPdf.com

(*Check*: Total tensile yield strength of girder is $T = P_c + P_w + P_t = 450 + 787.5 + 700 = 1937.5$ kip. The compression strength of slab is $P_s = 3672$ kip. Because the compression strength of the slab is much greater than the tensile force in the steel girder, it is obvious that PNA would lie in the slab.)

Check the following five conditions for location of the PNA. Although we could have started with Case 5 (assuming PNA in the slab) and determined the location of PNA in one step, calculations for Cases I through V are presented as follows:

Case I: PNA in the web

$$P_t + P_w \geq P_c + P_s + P_{rb} + P_{rt}$$

$$700 + 787.5 \ngeq 450 + 3672 + 0 + 0$$

$$1487.5 \ngeq 4122$$

Therefore, the PNA is not in the web.

Case II: PNA in the top flange

$$P_t + P_w + P_c \geq P_s + P_{rb} + P_{rt}$$

$$700 + 787.5 + 450 \ngeq 3672 + 0 + 0 = 3672 \text{ kip}$$

$$1937.5 \ngeq 3672$$

Therefore, the PNA is not in the top flange.

Case III: PNA in the slab, below P_{rb} (bottom slab reinforcement)

$$P_t + P_w + P_c \geq \left(\frac{C_{rb}}{t_s}\right) P_s + P_{rb} + P_{rt}$$

where c_{rb} = distance from the top of slab to the centroid of bottom slab reinforcement or 1.5 in. from the bottom of the slab = 6.5 in.

$$700 + 787.5 + 450 \ngeq \left(\frac{6.5}{8.0}\right)(3672) + 0 + 0 = 2983.5 \text{ kip}$$

$$1937.5 \ngeq 2983.5 \text{ kip}$$

Therefore, PNA is not located below the P_{rb} level in the slab.

Case IV: PNA in the slab at the P_{rb} (bottom slab reinforcement)

$$P_t + P_w + P_c + P_{rb} \geq \left(\frac{C_{rb}}{t_s}\right) P_s + P_{rt}$$

$$700 + 787.5 + 450 + 0 \ngeq 2983.5 + 0$$

$$1937.5 \ngeq 2983.5 \text{ kip}$$

Therefore, PNA is not at the P_{rt} level in the slab.

www.EngineeringEBooksPdf.com

Case V: PNA in the slab above the P_{rb} and below the P_{rt}:

$$P_t + P_w + P_c + P_{rb} + P_{rt} \geq \left(\frac{C_{rb}}{t_s}\right) P_s$$

Form the given cross section, c_{rt} = 2.5 in. = distance from the top of slab to the centroid of top slab reinforcement. Thus,

$$700 + 787.5 + 450 + 0 + 0 > \left(\frac{2.5}{8}\right)(3672)$$

$$1937.5 \text{ kip} > 1147.5 \text{ kip}$$

Because the left-hand side term in Case V is *greater* than the right-hand side term, the PNA lies in the slab above the P_{rb} and below the P_{rt}. Consequently, Case VI (PNA in slab at the level of P_{rt}) and Case VII (PNA in slab above the P_{rt} level) are not investigated. Let $\bar{Y}$ be the distance of the PNA from the top of the slab. Then,

$$\bar{Y} = \left[\frac{P_c + P_w + P_c}{P_s}\right] = 8\left(\frac{1937.5}{3672}\right) = 4.22 \text{ in. (Figure 6.60)}$$

The previous value of $\bar{Y}$ is the same as calculated earlier. The nominal plastic strength of the girder, M_p, can be obtained by summing up the moments of various element forces about the PNA as shown in Figure 6.60. These distances measured from the PNA are as follows:

$$P_c = 450 \text{ kip}, d_c = 8 + 2 - \frac{1}{2}\left(\frac{3}{4}\right) - 4.22 = 5.405 \text{ in.}$$

$$P_w = 787.5 \text{ kip}, d_c = 8 + 2 - \frac{1}{2}(36) + 4.22 = 23.78 \text{ in.}$$

$$P_t = 700 \text{ kip}, d_c = 8 + 2 + 36 + \frac{1}{2}\left(\frac{7}{8}\right) - 4.22 = 42.22 \text{ in.}$$

$$P_s = 3672 \text{ kip (calculated earlier)}$$

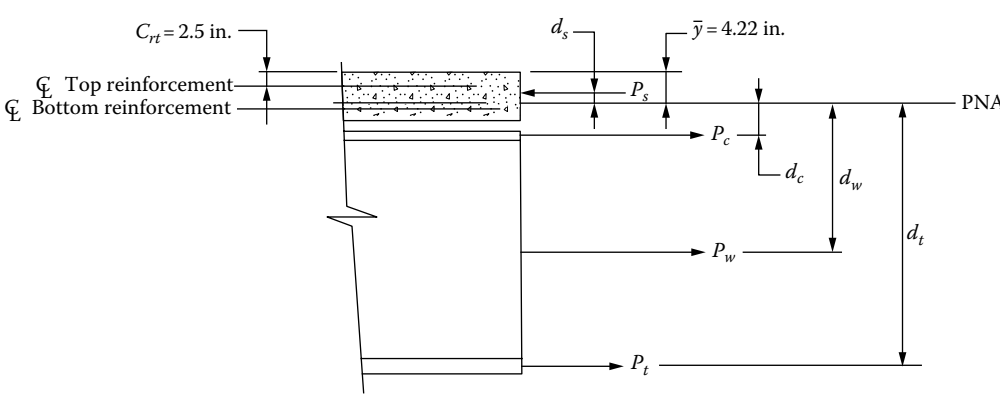

FIGURE 6.60 Element forces for computing plastic moment capacity (longitudinal reinforcement forces have been ignored).

www.EngineeringEBooksPdf.com

Therefore, the plastic moment strength of the composite girder, M_p, is

$$M_p = \left(\frac{\bar{Y}^2 P_s}{2t_s}\right) + \left(P_c d_c + P_w d_w + P_t t_t\right)$$

$$= \frac{(4.22)^2(3672)}{2(8)} + \left[(450)(5.405) + (787.5)(23.78) + (700)(42.22)\right]$$

$$= 4{,}087 + 2{,}432 + 18{,}727 + 29{,}554$$

$$= 54{,}800 \text{ k-in.} = 4{,}567 \text{ kip-ft}$$

Commentary: The previous calculations demonstrate that Case V governs for the position of the PNA. Therefore, one could have started with Case V, obviating the need for checking other cases. See Example 6.5.

Example 6.5: Determination of Plastic Moment Strength of Composite Section Considering the Strength Contribution of the Slab Reinforcement

Calculate the plastic moment strength, M_p, of the composite girder described in Example 6.4 (f'_c = 4.5 ksi and F_y = 50 ksi). The contribution of longitudinal slab reinforcement (Grade 60) shown in Figure 6.60 to moment strength must be accounted for. What is the percentage increase in the plastic moment strength of the composite beam as a result of contribution by the slab reinforcement?

Note: Refer to Figure 6.58 for the bridge and girder cross sections referred to in this example. Details of composite beam cross section and deck slab reinforcement are shown in Figure 6.61.

Solution

First, check that slab reinforcement satisfies the following empirical design requirements (LRFD Art. 9.7.2.5: Reinforcement Requirements).

Four layers of isotropic reinforcement are provided (Figure 6.61) in this empirically design deck slab. Reinforcement is provided in each face of the slab with the outermost layers placed in the direction parallel to the effective flange width (i.e., perpendicular to the longitudinal axis of the girder) and placed as close to the outside surfaces as permitted by the cover requirements. The required minimum reinforcement is 0.18 in.^{2} for each top layer and 0.27 in.^{2} for each bottom layer. The spacing of bars is not to exceed 18 in. Reinforcing steel shall be Grade 60 or better.

Details of the Grade 60 reinforcement provided:

Each top layer: $A_{s,reqd}$ = 0.18 in.^{2}/ft.

$$A_{s,provided} = \text{No. 5 at 18 in. o.c.} = 0.21 \text{ in.}^2\text{, OK.}$$

Each bottom layer: $A_{s,reqd}$ = 0.27 in.^{2}/ft

$$A_{s,provided} = \text{No. 5 at 12 in. o.c.} = 0.31 \text{ in.}^2\text{, OK.}$$

Maximum spacing = 18 in., OK.

Slab reinforcement is adequate.

Calculate the area of reinforcement in each layer contained in the effective width of the slab. Of the four layers of reinforcement in the slab, only the longitudinally placed reinforcement will

www.EngineeringEBooksPdf.com

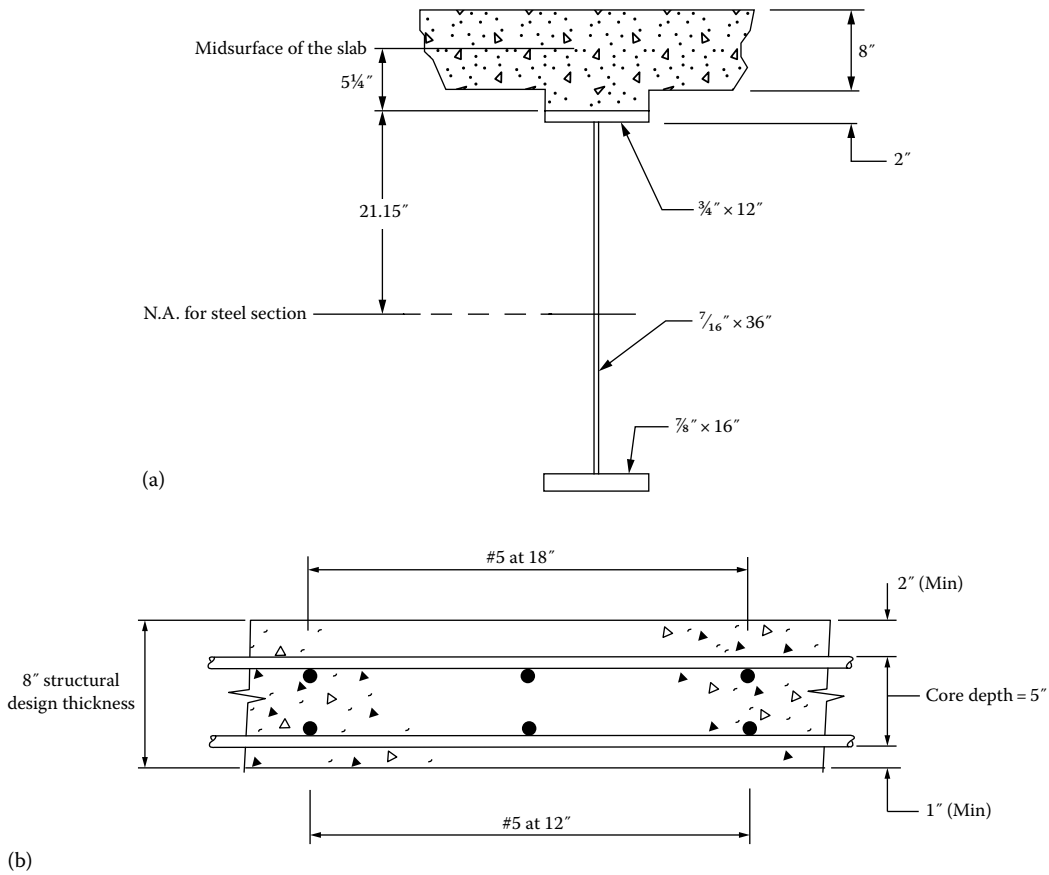

FIGURE 6.61 (a) Cross section of composite beam, (b) deck slab reinforcement details. (Courtesy of AISI.)

be considered, that is, No. 5 at 12 in. on center in the top layer and No. 5 at 12 in. on center in the bottom layer. For Grade 60 reinforcement, F_{yr} = 60 ksi

Effective width, b_s = 10 ft = 120 in.
Top layer: A_{rt} = 0.21 (10) = 2.1 in.^{2}
Bottom layer: A_{rb} = 0.31 (10) = 3.1 in.^{2}

Calculate axial forces in longitudinal reinforcing bars:

Top bars: $P_{rt} = A_{rt}F_{yr}$ = 2.1(60) = 126 kip
Bottom bars: $P_{rb} = A_{rb}F_{yr}$ = 3.1(60) = 186 kip

The position of plastic neutral axis is unknown at this stage, so it must be guessed. Let us assume that it lies in the slab somewhere between the top and bottom layers of reinforcement. This assumption corresponds to Case V in Table 6.7. Check the following condition:

$$P_t + P_w + P_c + P_{rb} + P_{rt} \geq \left(\frac{C_{rt}}{t_s}\right) P_s$$

www.EngineeringEBooksPdf.com

The following values were determined in Example 6.4:

$$P_t = 700 \text{ kip}$$

$$P_w = 787.5 \text{ kip}$$

$$P_c = 450 \text{ kip}$$

$$P_s = 3672 \text{ kip}$$

$$c_{rt} = 2.5 \text{ in.}$$

Substitution of the previous values in the previous equation yields

$$700 + 787.5 + 450 + 126 + 186 \geq \left(\frac{2.5}{8.0}\right)(3672)$$

$$2249.5 \text{ kip} > 1147.5 \text{ kip.}$$

The previous inequity is valid. Therefore, the PNA lies in the slab, in between the P_{rt} (the top layer of reinforcement) and the P_{rb} (the bottom layer of reinforcement) as assumed. Its position is calculated from the expression for $\bar{Y}$ corresponding to Case V in Table 6.6.

$$\bar{Y} = t_s\left[\frac{P_{rb} + P_c + P_w + P_t - P_{rt}}{P_s}\right]$$

$$= (8.0)\left[\frac{186 + 450 + 787.5 + 700 - 126}{3672}\right]$$

$$= 4.35 \text{ in. from the top of slab (Figure 6.62).}$$

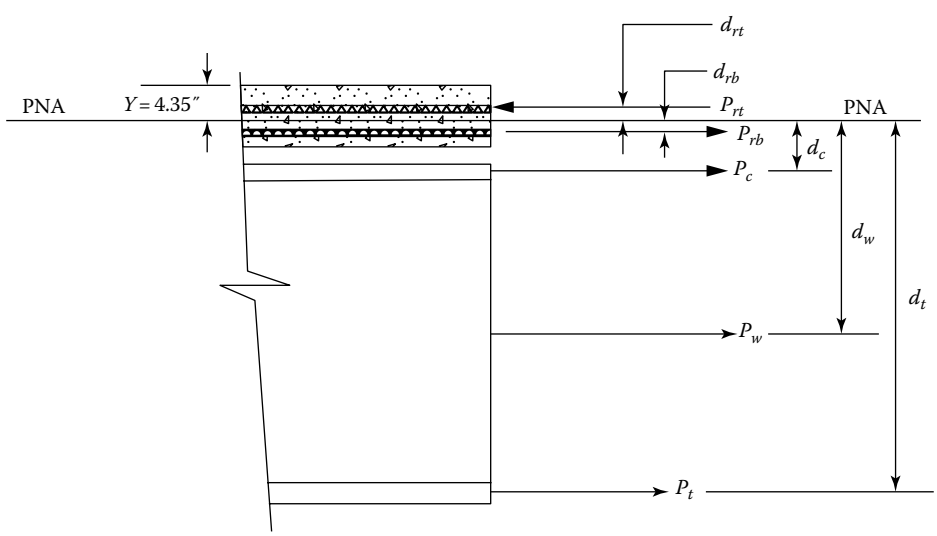

FIGURE 6.62 Element forces acting on the composite section for computing the plastic moment strength of the composite girder.

www.EngineeringEBooksPdf.com

Calculate distances of various element forces acting on the composite section from the PNA:

$$P_{rt} = 126 \text{ kip}, \quad d_{rt} = 4.35 - 2.5 = 1.85 \text{ in.}$$

$$P_{rb} = 186 \text{ kip}, \quad d_{rb} = 6.5 - 4.354 = 2.15 \text{ in.}$$

$$P_c = 450 \text{ kip}, \quad d_c = 8 + 2 - \frac{1}{2}\left(\frac{3}{4}\right) - 4.354 = 5.28 \text{ in.}$$

$$P_w = 787.5 \text{ kip}, \quad d_w = 8 + 2 + \frac{1}{2}(36) - 4.354 = 23.65 \text{ in.}$$

$$P_t = 700 \text{ kip}, \quad d_t = 8 + 2 + 36 + \frac{1}{2}\left(\frac{7}{8}\right) - 4.354 = 42.09 \text{ in.}$$

$$P_s = 3672 \text{ kip (calculated earlier)}$$

The previous forces and their distances from the PNA are shown in Figure 6.62. Calculate the plastic moment strength, M_p, of the composite section. From Table 6.6 for Case V, the plastic moment strength is calculated as follows:

$$\begin{aligned} M_p &= \left(\frac{\bar{Y}^2 P_s}{2t_s}\right) + P_{rt}d_{rt} + P_{rb}d_{rb} + P_c d_c + P_w d_w + P_t d_t \\ &= \left(\frac{(4.35)^2(3{,}672)}{2(8.0)}\right) + \left[(126)(1.85) + (186)(2.15) + (450)(5.28) \right. \\ &\qquad \left. + (787.5)(23.65) + (700)(42.09)\right] \\ &= 4{,}343 + 233 + 400 + 2{,}376 + 18{,}624 + 29{,}463 \\ &= 55{,}439 \text{ kip-in.} \approx 4{,}620 \text{ kip-ft} \end{aligned}$$

The plastic moment strength of the composite section without contribution from the slab reinforcement was calculated as 4567 kip-ft in Example 6.4.

Percentage increase in plastic moment strength $= \dfrac{4620 - 4567}{4567}(100) = 1.16$ percent

Thus, there is hardly any increase in the nominal moment strength of the composite section, M_p, as a result of contribution from the longitudinal slab reinforcement. As such, it is justified to ignore the contribution of the longitudinal slab reinforcement to the plastic moment strength of a composite beam.

Example 6.6: Determination of Plastic Moment Strength of a Composite Section in Negative Flexure

Calculate the plastic moment strength of the composite beam section of Example 6.5 assuming that it is subjected to negative flexure. All other data remain the same as in Example 6.5. Contribution of the reinforcement forces must be considered in computing the plastic moment strength in negative flexure. Composite beam cross section and slab reinforcement details are shown in Figure 6.61.

www.EngineeringEBooksPdf.com

Solution

Assume that the PNA lies in the steel section and the entire deck slab is in tension. Because the composite beam section is in negative flexure, the deck slab is in tension and is assumed to have cracked and, hence, ineffective in contributing to the flexural resistance. Therefore,

$$P_s = 0$$

Contribution of the reinforcement forces will be considered in computing the plastic moment strength in negative flexure.

Check the condition for Case I (Table 6.8), which assumes that the PNA lies in the web.

$$P_c + P_w \geq P_t + P_{rb} + P_{rt}$$

From Example 6.5, we obtain the following value of element forces:

$$P_c = 450 \text{ kip}$$

$$P_w = 787.5 \text{ kip}$$

$$P_t = 700 \text{ kip}$$

$$P_{rb} = 186 \text{ kip}$$

$$P_{rt} = 126 \text{ kip}$$

$$450 + 787.5 \geq 700 + 186 + 126$$

$$1237.5 \geq 1012 \text{ kip}$$

The previous inequity is valid; therefore, the PNA lies in the web. From Table 6.8 (Case 1), the PNA is located at a distance of

$$\begin{aligned}\bar{Y} &= \left(\frac{D}{2}\right)\left[\frac{P_t - P_c - P_{rt} - P_{rb}}{P_w} + 1\right] \\ &= \left(\frac{36}{2}\right)\left[\frac{700 - 450 - 126 - 186}{787.5} + 1\right] \\ &= 16.583 \text{ in. from the top of the web}\end{aligned}$$

The calculated position of the PNA and various element forces are shown in Figure 6.63.

Various element forces and their distances from the PNA are as follows:

$$P_{rt} = 126 \text{ kip}, \quad d_{rt} = 16.583 + 2 + 8 - 2.5 = 24.083 \text{ in.}$$

$$P_{rb} = 186 \text{ kip}, \quad d_{rb} = 16.583 + 2 + 8 - 6.5 = 20.083 \text{ in.}$$

$$P_w = 787.5 \text{ kip}, \quad d_w = 36/2 - 16.583 = 1.417 \text{ in.}$$

$$P_t = 450 \text{ kip}, \quad d_t = 16.583 + (1/2)(3/4) = 16.958 \text{ in.}$$

$$P_c = 700 \text{ kip}, \quad d_c = 36 - 16.583 + (1/2)(7/8) = 19.855 \text{ in.}$$

www.EngineeringEBooksPdf.com

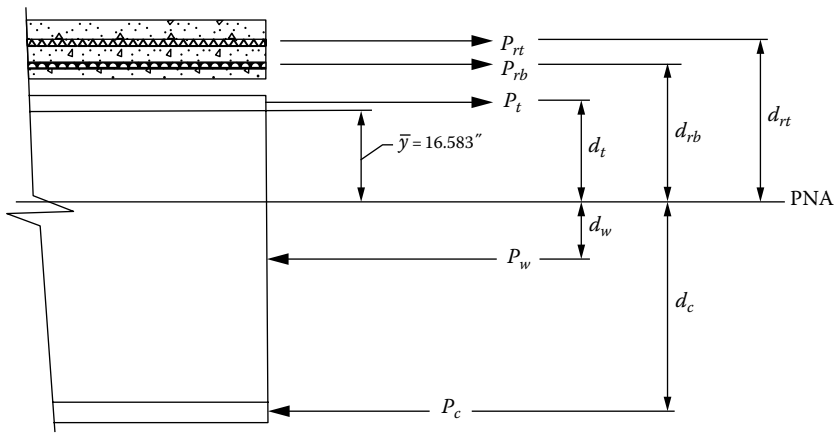

FIGURE 6.63 Element forces for computing plastic moment strength in negative flexure.

The nominal moment strength of the composite is calculated as

$$M_p = \left(\frac{P_w}{2D}\right)\left[\bar{Y}^2 + \left(D - \bar{Y}\right)^2\right] + \left(P_{rt}d_{rt} + P_{rb}d_{rb} + P_t d_t + P_c d_c\right)$$

$$= \left(\frac{787.5}{2(36)}\right)\left[(16.583)^2 + (36 - 16.583)^2\right]$$

$$+ \left[(126)(24.083) + (186)(20.083) + (450)(16.958) + (700)(19.855)\right]$$

$$= 7{,}131.4 + 3{,}034.5 + 3{,}735.4 + 7{,}631.1 + 13{,}898.5$$

$$= 35{,}431 \text{ kip-in.} = 2{,}953 \text{ kip-ft}$$

Commentary:

1. The plastic moment strength of the composite beam section in negative flexure is 2953 kip-ft as compared with 4620 kip-ft in positive flexure or only 63.53 percent of plastic moment strength in positive flexure.
2. The accuracy of the location of the PNA can be verified by checking the equilibrium of horizontal forces as follows:

Tensile forces: P_{rt} = 126 kip

P_{rb} = 186 kip

P_t = 450 kip

P_{wt} = (7/16)(16.583)(50) = 362.8 kip

Compressive forces: P_{wc} = (7/16)(36 − 16.583)(50) = 424.7 kip

P_c = 700 kip

$\sum F_{element}$ = 126 + 186 + 450 + 362.8 − 424.7 − 700 = 0.1 kip ≈ 0, checks.

www.EngineeringEBooksPdf.com

Example 6.7: To Check the Adequacy of a Composite Section to Carry Design Loads

Figure 6.58 shows the cross section of a single-span concrete deck–steel girder bridge spanning 75 ft on an urban highway. The 8½ in. thick deck slab, which includes 1/2 in. thick integral wearing surface, is cast from 4500 psi concrete. The deck is supported by four steel girders of A36 steel, built to act compositely with deck slab using 4 in. long, 3/4 in. diameter headed shear studs (F_y = 50 ksi, F_u = 60 ksi) welded to the girder. Check if the interior girder is adequate to carry Strength Limit I design loads. Assume the dead weight due to stay-in-place forms (to support concrete during construction), cross frames, and detailing as 200 lb/ft of girder length. Ignore the contribution of the slab reinforcement to the nominal strength of the girder.

Solution

Commentary: This example bridge was used in Example 3.1 to calculate dead load bending moments in the interior girder and in Example 4.9 (Chapter 4) to calculate live load distribution factors and bending moment for Strength I Limit State. The same bridge is used in Example 6.4 to calculate the plastic moment strength, M_p, of the composite girder. This example presents calculations to check if the composite steel girder is adequate to carry the Strength I Limit State loads in flexure.

The following unfactored bending moments due to gravity loads were calculated in previous examples as noted:

Example 3.1: Dead load moments in girders:

$$M_{DC} = 1118 \text{ kip-ft}$$

$$M_{DW} = 176.0 \text{ kip-ft}$$

Example 4.6: Live load moment:

Total bending moment due to live load:

$$M_{LL+IM} + M_{Lane} = 1878.3 \text{ kip-ft}$$

Calculated distribution factor for the live load:

Case 2: Two or more lanes loaded (governs): $DF = 0.733$

Apply the distribution factor to live load moment:

$$(M_{design\ LL})(DF) = (1878.3)(0.733) = 1377 \text{ kip-ft } (LL + IM)$$

Calculate the design bending moment for Strength Limit State I. From the previous information,

$$M_{dead\ load} = 1112.3 \text{ kip-ft } (DC)$$

$$M_{dead\ load} = 175.8 \text{ kip-ft } (DW)$$

$$\text{Strength Limit State I: } U = 1.25\ (DC) + 1.5(DW) + 1.75(M_{LL+IM})$$

$$M_u = 1.25(1118) + 1.5(176.0) + 1.75\ (1377)$$

$$= 4071 \text{ kip-ft}$$

From Example 6.4, M_p = 4567 kip-ft

Strength reduction factor for flexure, ϕ_f = 1.0 (Section 6.9/Art. 6.5.4.2)

From Example 6.4, the depth of PNA from the top of concrete deck, D_p = 4.22 in.

www.EngineeringEBooksPdf.com

Total depth of composite section, D_t = slab thickness + thickness of haunch including top flange + depth of the web + thickness of bottom flange

$$= 8 + 2 + 36 + 0.875$$

$$= 46.875 \text{ in.}$$

$$0.1D_t = 0.1(46.875) = 4.69 \text{ in.}$$

$$D_p = 4.22 \text{ in.} < 0.1\ D_t\ (=4.69 \text{ in.})$$

Therefore,

$$M_n = M_p$$

$$= 4567 \text{ kip-ft} \qquad (6.54)\ [A6.10.7.1.2\text{-}1]$$

$$\phi_f M_n = 1.0(4567) = 4567 \text{ kip-ft}$$

$$M_u = 4071 \text{ kip-ft} < \phi_f M_n = 4567 \text{ kip-ft, OK}$$

Therefore, the composite section is adequate to support the loads in flexure.

6.13.5.1 Yield Moment of Noncomposite Sections: LRFD Art. 6.2.1

The concept of yield moment of steel sections, M_y, was introduced in Section 1.3.2. As a review, consider an I-shaped beam subjected to positive flexure (Figure 6.64). As the load on the beam is increased, both moment and stresses increase proportionally. Figure 6.64a shows loading when the flexural stress in the extreme fibers is less than the yield stress, F_y. As the load is increased, the moment and stress also increase proportionally. A stage is reached when the stresses in the extreme fibers (top and bottom) reach stresses equal to the yield stress, F_y, as shown in Figure 6.64b; the moment corresponding to this state of stress is called the *yield moment*, M_y. The stress distribution in both cases is linear, maximum (equal to F_y) at the extreme fibers and zero at the neutral axis; the stresses in fibers away from the neutral axis remain below F_y. As the load (and hence the moment) is further increased, the stresses in the extreme fibers continue to remain at the F_y level, but stresses in the beam section away from the extreme fibers continue to increase until $f = F_y$ (Figure 6.64c); at this stage, the state of stress is no longer linear. With increasing load, the stresses in the interior of the section continue to increase until the entire section attains a stress $f = F_y$, compressive above the neutral axis and tensile below the neutral axis; the state of stress at this stage is rectangular, and the corresponding value of moment is referred to as the plastic moment, M_y.

For a section that is symmetrical about the axis of bending, both extreme fibers attain yield stress simultaneously. But for a section that is unsymmetrical about the axis of bending, the two extreme fibers do not attain yield stress simultaneously; in this case, the extreme fibers closest to the neutral axis attain the yield stress first (referred to as *first yielding*). These extreme fibers may be in compression or tension depending on whether the section is in positive or negative flexure. Accordingly, the yield moment, M_y, of a noncomposite section is taken as the smaller of the following two values at the strength limit state:

1. Moment required to cause nominal first yielding in the compression flange, M_{yc}.
2. Moment required to cause nominal first yielding in the tension flange, M_{yt}.

Flange lateral bending in all types of sections and web yielding in hybrid sections is to be disregarded in this calculation.

6.13.5.2 Yield Moment of Composite Sections in Positive Flexure: LRFD Art. D6.2.2

The determination of yield moment for a noncomposite section discussed in the previous section is a trivial, straightforward exercise. But the determination of yield moment for a composite section,

www.EngineeringEBooksPdf.com

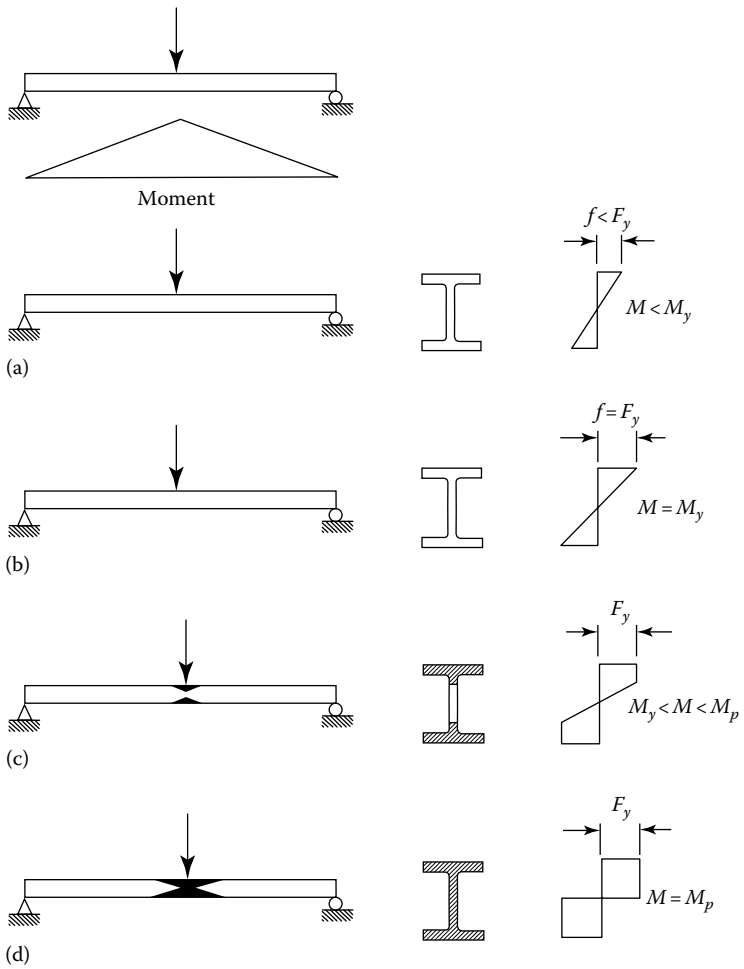

FIGURE 6.64 Concept of yield and plastic moment of a beam section. (a) $f < F_y$ in the extreme fibers, varying linearly to zero at the neutral axis, $M < M_y$, (b) bending stress in the extreme fibers of the beam at the point of maximum moment, $f = F_y$, varying linearly to zero at the neutral axis, $M = M_y$, (c) partial cross section with $f = F_y$, varying linearly to zero at the neutral axis, so that $M_y < M < M_p$, and (d) bending stress $f = F_y$ in the entire cross section, resulting in rectangular stress distribution, so that $M = M_p$. (Adapted from Segui, W.T., *Steel Design*, 5th ed., Cengage Learning, Stamford, CT, 2013.)

although conceptually simple, is computationally time-intensive and cumbersome. The difficulty arises from the fact that stresses in a composite section must necessarily be calculated in three stages. When the deck concrete is wet, the factored moment due to its dead weight must be resisted by the noncomposite section (steel section alone). At this stage, the stresses in the steel section are fairly low, much below the yield stress level. Only after the deck concrete cures (hardens), the composite action comes into play. Thereafter, additional loads are resisted by the composite section of the girder. What is more, the stresses due to the remainder of permanent load (viz., dead weight of traffic barriers, FWS) and stresses due to the live load need to be calculated using different properties of the composite section as follows (see discussion in Section 6.7.2):

1. For the factored moment due to the remainder of the permanent load, the stresses need to be calculated using the *long-term section properties* of the composite section.
2. The stresses due to the live load are to be calculated using the *short-term section properties* of the composite section.

www.EngineeringEBooksPdf.com

Art. D6.6.2 suggests the following procedure for calculating the yield moment of a composite section in flexure:

1. Calculate the moment M_{D1} caused by the factored permanent load applied before concrete hardens or composite action takes place. Apply this moment to the steel section.
2. Calculate the moment M_{D2} caused by the remainder of the factored permanent load. Apply this moment to the long-term composite section.
3. Calculate the additional moment, M_{AD} (this value is unknown and needs to be calculated), which must be applied to the short-term composite section to cause nominal yielding in either steel flange from Equation 6.167:

$$F_{yf} = \frac{M_{D1}}{S_{NC}} + \frac{M_{D2}}{S_{LT}} + \frac{M_{AD}}{S_{ST}} \qquad (6.167)\ [\text{AD}6.2.2\text{-}1]$$

   Note that the three quantities on the right-hand side of Equation 6.167 represent elastic stresses that can be calculated from the following familiar flexural formula:

$$f = \frac{M_c}{I} \qquad (6.168)$$

   In Equation 6.167, all quantities are known except M_{AD}.
4. The yield moment is the sum of the total permanent load and additional moments as expressed by Equation 6.169:

$$M_y = M_{D1} + M_{D2} + M_{AD} \qquad (6.169)\ [\text{AD}6.2.2\text{-}2]$$

   where
   F_{yf} = yield strength of the flange (50 ksi for Grade 50 steel)
   S_{NC} = noncomposite section modulus (in.^{3})
   S_{ST} = short-term composite section modulus (in.^{3})
   S_{LT} = long-term composite section modulus (in.^{3})
   M_{D1}, M_{D2}, and M_{AD} = moments as defined previously
   M_y is to be taken as the smaller of the values calculated for the compression flange (M_{yc}) or the tension flange (M_{yt})

As discussed in Section 6.7.3, the short-term and long-term section moduli are calculated by considering transformed area of the deck slab within the effective width of the flange as follows:

For calculating the short-term section properties, the effective width of flange, b_s, is divided by the modular ratio, n (values listed in Table 4.4).
For calculating the long-term section properties, the effective width of flange, b_s, is divided by the three times the modular ratio, that is, $3n$.

Example 6.8 illustrates the previously discussed procedure.

Example 6.8: Yield Moment of a Composite Section in Positive Flexure

Figure 6.65 shows the cross section of a concrete deck–steel girder superstructure spanning 75 ft on an urban highway. The 8½ in. thick deck slab, which includes 1/2 in. integral wearing surface, is cast from 4500 psi concrete. The deck is supported by four steel girders (Grade 50W) built to act compositely with deck using 4 in. long, 3/4 in. diameter headed shear studs. The girders are spaced at 10 ft on centers. All girders have identical cross sections. Assume the dead weight due

www.EngineeringEBooksPdf.com

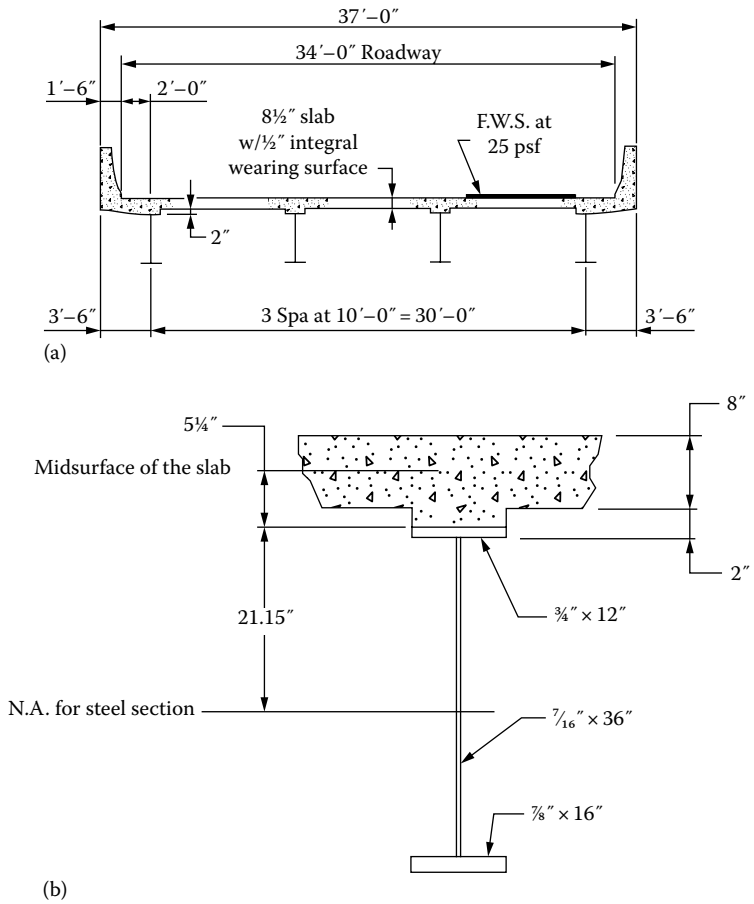

FIGURE 6.65 Concrete deck-steel girder bridge cross section for Example 6.8 (a) bridge cross section and (b) details of girder cross section.

to stay-in forms (to support concrete during construction), cross frames, and detailing as 200 lb/ft of girder length and dead weight of FWS as 25 lb/ft^2 of the deck. Determine the yield moment, M_y, of the composite cross section of a typical girder of this bridge.

Solution

Note: The bridge described in this example is the same bridge as used in Examples 3.1 and 6.3. Moments used for calculations in this example are taken from Example 3.1. Calculations for determining the yield moment are shown step-by-step as follows:

Step 1. Calculate the section properties of the noncomposite section. First, determine the neutral axis and the moment of inertia of the noncomposite section. Distance y is measured from the bottom flange.

All calculations are shown in Table 6.10.

$$\bar{y}_b = \frac{\Sigma Ay}{\Sigma A} = \frac{638.66}{38.75} = 16.48 \text{ in.}$$

$$I_{NC} = \Sigma\left[A\left(y-\bar{y}\right)^2 + I_o\right] = 7576.1 + 1702.3 = 9278 \text{ in.}^4$$

Total depth of girder = 0.875 + 36.0 + 0.75 = 37.625 in.

www.EngineeringEBooksPdf.com

TABLE 6.10
Calculations for Locating Neutral Axis and the Moment of Inertia of Noncomposite Section

Component	Dimensions	A, in.^{2}	y, in.	Ay, in.^{3}	$(y-\bar{y})$, in.	$A(y-\bar{y})^2$, in.^{4}	I_o, in.^{4}
Top flange	3/4 × 12	9.0	37.25	335.25	20.77	3882.5	0.4
Web	7/16 × 36	15.75	18.875	297.28	2.395	90.3	1701
Bot. flange	7/8 × 16	14.0	0.4375	6.13	−16.043	3603.3	0.9
Σ		38.75		638.66		7576.1	1702.3

The section moduli for the top and bottom of noncomposite section (steel section) are as follows:

$$S_{NC}^{t} = \frac{9278}{37.625-16.48} = 439 \text{ in.}^3$$

$$S_{NC}^{b} = \frac{9278}{16.48} = 563 \text{ in.}^3$$

where
S_{NC}^{t} = section modulus of the noncomposite section at the top
S_{NC}^{b} = section modulus of the noncomposite section at the bottom

Step 2. Calculate the section properties of the short-term composite section: $n = 8$. All calculations are shown in Table 6.11.

$$\bar{y}_b = \frac{\Sigma Ay}{\Sigma A} = \frac{5783}{158.75} = 36.43 \text{ in.}$$

$$I_{NC} = \Sigma\left[A\left(y-\bar{y}\right)^2 + I_o\right] = 27{,}989 + 2{,}342 = 30{,}331 \text{ in.}^4$$

Total depth of composite girder = 0.875 + 36.0 + 2.0 + 8 = 46.875 in.

The section moduli for the top and bottom of short-term composite section are as follows:

$$S_{ST}^{t} = \frac{30{,}323}{46.875-36.43} = 2904 \text{ in.}^3 \ \left(\text{top of deck}\right)$$

TABLE 6.11
Calculations for Locating Neutral Axis and the Moment of Inertia of the Short-Term Composite Section: $n = 8$

Component	Dimensions	A, in.^{2}	y, in.	Ay, in.^{3}	$\left(y_b-\bar{y}_b\right)$, in.	$A\left(y_b-\bar{y}_b\right)^2$, in.^{4}	I_o, in.^{4}
Slab	(120/8) × 8	120.0	42.875	5145	6.445	4,985	640
Top flange	3/4 × 12	9.0	37.25	335	0.82	6	~0
Web	7/16 × 36	15.75	18.875	297	17.555	4,854	1701
Bot. flange	7/8 × 16	14.0	0.4375	6	36.00	18,144	1.0
Σ		158.75		5783		27,989	2342

www.EngineeringEBooksPdf.com

TABLE 6.12
Calculations for Locating Neutral Axis and the Moment of Inertia of the Long-Term Composite Section: 3*n* = 24

Component	Dimensions	A, in.^{2}	y, in.	Ay, in.^{3}	$(y_b - \bar{y}_b)$, in.	$A(y_b - \bar{y}_b)^2$, in.^{4}	I_o, in.^{4}
Slab	(120/24) × 8	40.0	42.875	1715	12.995	6,755	213
Top flange	3/4 × 12	9.0	37.25	335	7.37	489	~0
Web	7/16 × 36	15.75	18.875	297	−11.005	1,907	1701
Bot. flange	7/8 × 16	14.0	0.4375	6	−29.4425	12,136	1.0
Σ		78.75		2353		21,287	1915

$$S_{ST}^{t} = \frac{30,331}{37.625 - 36.43} = 25,382 \text{ in.}^3 \text{ (top of steel)}$$

$$S_{ST}^{b} = \frac{30,331}{36.43} = 833 \text{ in.}^3 \text{ (bottom of steel)}$$

S_{ST}^{t} = section modulus of the short-term composite section at the top (top of deck or flange)
S_{ST}^{b} = section modulus of the short-term composite section at the bottom

Step 3. Calculate the section properties of the long-term composite section: 3*n* = 24. Calculations are shown in Table 6.12.

$$\bar{y}_b = \frac{\Sigma Ay}{\Sigma A} = \frac{2353}{78.75} = 29.88 \text{ in.}$$

$$I_{NC} = \Sigma\left[A\left(y_b - \bar{y}\right)^2 + I_o\right] = 21,287 + 1915 = 23,202 \text{ in.}^4$$

Total depth of composite girder = 0.875 + 36.0 + 2.0 + 8 = 46.875 in.

The section moduli at the top and bottom of long-term composite section are as follows:

$$S_{LT}^{t} = \frac{23,202}{46.875 - 29.88} = 1365 \text{ in.}^3 \text{ (top of deck)}$$

$$S_{LT}^{t} = \frac{23,202}{37.625 - 29.88} = 2996 \text{ in.}^3 \text{ (top of steel)}$$

$$S_{LT}^{b} = \frac{23,202}{29.88} = 777 \text{ in.}^3 \text{ (bottom of steel)}$$

S_{LT}^{t} = section modulus of the long-term composite section at the top (top of deck or flange)
S_{LT}^{b} = section modulus of the long-term composite section at the bottom

Step 4. Calculate the factored moments, M_{D1} and M_{D2}. From Example 3.1, the following values of unfactored moments are obtained:

Moment permanent loads acting on the noncomposite section,

$$M_{DC1} = 993.52 \text{ kip-ft}$$

www.EngineeringEBooksPdf.com

Moment due to permanent loads acting on the long-term composite section,

$$M_{DC2} = 124.45 \text{ kip-ft}$$

Moment due to the FWS acting on the long-term composite section,

$$M_{DW} = 176.0 \text{ kip-ft}$$

$$M_{D1} = M_{DC1} = 993.52 \text{ kip-ft}$$

$$M_{D2} = M_{DC2} + M_{DW} = 124.45 + 176.0 = 300.45 \text{ kip-ft}$$

The factored moments are as follows:

$$\gamma_p M_{D1} = 1.25(993.52) = 1242 \text{ kip-ft}$$

$$\gamma_p M_{D2} = 1.5(300.45) = 451 \text{ kip-ft}$$

Step 5. Calculate the yield moment, M_y.

The maximum stress in the composite girder occurs first in the bottom of steel section. Apply Equation 6.167 for the bottom fibers. For Grade 50W steel, $F_{yf} = 50$ ksi. Thus,

$$F_{yf} = \frac{M_{D1}}{S_{NC}} + \frac{M_{D2}}{S_{LT}} + \frac{M_{AD}}{S_{ST}} \qquad (6.167)\ [AD6.2.2\text{-}1]$$

$$50 = \frac{(1242)(12)}{563} + \frac{(451)(12)}{777} + \frac{M_{AD}(12)}{833}$$

$$50 = 26.47 + 6.96 + \frac{M_{AD(12)}}{833}$$

whence $M_{AD} = 1150$ kip-ft

Apply Equation 6.169 to determine M_y.

$$M_y = M_{D1} + M_{D2} + M_{AD} \qquad (6.169)\ [AD6.2.2\text{-}2]$$

$$M_y = 1242 + 451 + 1150 = = 2843 \text{ kip-ft}$$

6.13.5.3 Yield Moment of Composite Sections in Negative Flexure: LRFD Art. D6.2.3

For composite sections in negative flexure, the procedure described in the preceding section is to be followed, except that the composite section for both the long-term and the short-term moments shall consist of the steel section and the longitudinal slab reinforcement within the effective width of the concrete deck. Because the deck concrete is assumed cracked when it is subjected to negative flexure, the deck slab concrete sectional area does not contribute to the section properties; thus, S_{ST} and S_{LT} have the same values. Also, M_{yt} is taken with respect to either the tension flange or the longitudinal reinforcement, whichever yields first.

6.13.5.4 Yield Moment of Composite Sections with Cover Plates: LRFD Art. D6.2.4

In a composite girder, the flanges of steel section might have cover plates attached to them. In simple-span composite girders, the bottom flange in the middle segments is usually beefed up by attaching a cover plate. This helps to resist the large moments that occur at the midspan. In simple spans, the moments taper off toward the supports, becoming zero at the supports. In the regions of smaller moments, the girder can resist the moments without contribution from the cover plates. In continuous spans, girders might be cover plated in the regions of larger moments (at the midspan and at supports).

www.EngineeringEBooksPdf.com

In both cases, the result of such a design is an economical section. In this case, M_{yc} or M_{yt} is taken as the smallest value of moment associated with nominal first yielding based on either the flange under consideration or any of the cover plates attached to that flange, whichever yields first. Flange lateral bending in all types of sections and web yielding in hybrid sections are to be disregarded in this calculation.

6.13.6 Depth of the Web in Compression: LRFD Art. D6.3

6.13.6.1 Depth of the Web in Compression in the Elastic Region (D_c): LRFD Art. D6.3.1

A portion of the web in I-sections subjected to flexure is subjected to compression, which makes it prone to buckling. In noncomposite sections, half of web depth is in compression. In composite sections, the depth of the web in compression depends on the magnitude of the moment that varies with span.

Art. 6.10.6.2.3 defines the slenderness limit for a noncompact web in terms of the depth of the web in compression in the elastic range, D_c, by Equation 6.52 (A6.10.6.2.3-1). A web with a slenderness ratio exceeding this limit is termed slender.

For composite sections in positive flexure, Art. D6.3.1 defines the depth of the web in compression in the elastic range, D_c, as the depth over which the algebraic sum of the stresses in the steel (i.e., noncomposite section), long-term and short-term composite sections from the dead and live loads plus impact, is compressive.

For composite sections, D_c is determined by the procedure described herein. The procedure requires determination of loads $DC1$, $DC2$, DW, and $LL + IM$, from which moments M_{D1}, M_{D2}, and M_{LL+IM} can be computed. From these moments, the elastic stresses in the top and the bottom flanges of the steel section can be computed individually from conventional flexural formula ($f = M/S$, where S = section modulus). The sum of the elastic stresses, compressive at the top, f_c, and tensile at the bottom, f_t, respectively, can be expressed by the following expressions:

$$f_c = \frac{M_{D1}}{S_{NC}^t} + \frac{M_{D2}}{S_{LT}^t} + \frac{M_{LL+IM}}{S_{ST}^t} \tag{6.170}$$

$$f_t = \frac{M_{D1}}{S_{NC}^b} + \frac{M_{D2}}{S_{LT}^b} + \frac{M_{LL+IM}}{S_{ST}^b} \tag{6.171}$$

where M_{LL+IM} = moment due to live load plus impact; other terms were defined earlier.

In equations 6.170 and 6.171, the superscripts t and b associated with section moduli (S_{NC}, S_{LT}, and S_{ST}) refer, respectively, to top and bottom fibers.

The elastic stress distribution being linear, the depth of the girder to the zero stress (location of elastic neutral axis), is determined from proportionality; the depth of the web in compression in the elastic range, D_c, is obtained by deducting the thickness of the top flange from the depth to the zero stress so computed. This computation can be expressed as Equation 6.172:

$$D_c = \left(\frac{-f_c}{|f_c| + f_t}\right) d - t_{fc} \geq 0 \qquad \text{(6.172) [AD6.3-1]}$$

where

d = depth of steel section

f_c = sum of the compressive flange stresses caused by the different loads, that is, $DC1$ (the permanent load acting on the noncomposite section), $DC2$ (the permanent load acting on the long-term composite section), DW (the wearing surface load), and $LL + IM$ acting on their respective sections (ksi). f_c is to be taken as negative when in compression. Flange lateral bending stress is to be disregarded in this calculation

f_t = sum of tension-flange stresses caused by different loads (ksi). Flange lateral bending stress is to be disregarded in this calculation

t_{fc} = thickness of flange in compression

www.EngineeringEBooksPdf.com

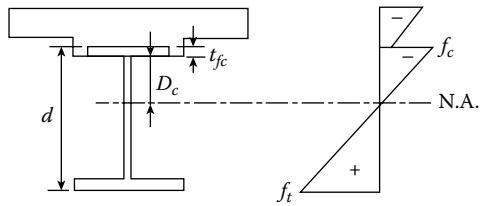

FIGURE 6.66 Elastic distribution of stress in a composite section in positive flexure. (Reprinted with permission from American Association of State Highway and Transportation Officials [AASHTO], Washington, DC.)

Note that the first term on the right-hand side of Equation 6.172 represents the depth of elastic neutral axis from the top of the compression flange; deducting the thickness of the compression flange, t_{fc}, from this depth gives the depth of the web in compression, D_c. The distribution of elastic stresses in the composite section is shown in Figure 6.66.

Art. D6.3.1 clarifies that Equation 6.172 only needs to be employed for checking web bend-buckling at the service limit state and for computing the hybrid factor, R_b, at the strength limit state for sections in which web longitudinal stiffeners are required based on Art. 6.10.2.1.1 (see discussion in Section 6.10.2.1.2).

Example 6.9 illustrates the previously described procedure.

Example 6.9: Depth of Web in Compression in the Elastic Range

For the bridge and the girder described in Example 6.8, calculate the depth of the girder web in compression in the elastic range. The unfactored moment due to live load plus impact is 1377 kip-ft.

Solution

Note: The moments M_{D1} and M_{D2} are taken as determined in Example 6.8. The value of M_{LL+IM} = 1377 kip-ft is taken from Example 4.9 for the same bridge.

Since the stresses are in the elastic range, the compressive and tensile stresses in the top and the bottom flanges, respectively, can be determined from the conventional flexure formula, Equation 6.168.

From Example 6.8, we obtain the values of M_{D1} and M_{D2} as follows:

$$M_{D1} = 993.52 \text{ kip-ft}$$

$$M_{D2} = 300.45 \text{ kip-ft}$$

The factored live load plus impact moment is

$$M_{LL+IM} = 1377 \text{ kip-ft}$$

The stresses in the girder are computed from Equations 6.173 and 6.174 as follows:

1. The stress due to the factored moment M_{D1} is determined using the properties of the non-composite section.
2. The stress due to the factored moment M_{D2} is determined using the properties of the long-term composite section.
3. The stress due to the factored moment M_{LL+IM} is determined using the properties of the short-term composite section.

www.EngineeringEBooksPdf.com

Using the values of section moduli calculated in Example 6.8, the maximum compressive stress in the top flange is computed from Equation 6.170:

$$\begin{aligned} f_c &= \frac{M_{D1}}{S_{NC}^t} + \frac{M_{D2}}{S_{LT}^t} + \frac{M_{LL+IM}}{S_{ST}^t} \\ &= \frac{993.52(12)}{439} + \frac{300.45(12)}{2996} + \frac{1{,}377(12)}{25{,}382} \\ &= 27.16 + 1.20 + 0.65 \\ &= 29.00 \text{ ksi} \end{aligned}$$

The maximum compressive stress in the bottom flange is computed from Equation 6.171:

$$\begin{aligned} f_t &= \frac{M_{D1}}{S_{NC}^b} + \frac{M_{D2}}{S_{LT}^b} + \frac{M_{LL+IM}}{S_{ST}^b} \\ &= \frac{993.52(12)}{563} + \frac{300.45(12)}{777} + \frac{1377(12)}{833} \\ &= 21.18 + 4.64 + 19.84 \\ &= 45.66 \text{ ksi} \end{aligned}$$

(**Note:** The notations f_c (compressive stress in the top flange) and f_t (tensile stress in the bottom flange) used earlier are consistent with the AASHTO LRFD notations. In other examples in this chapter, the stresses in the top and the bottom flange are denoted, respectively, by f_t and f_b.)

The depth of the steel section, $d = 0.75 + 36 + 0.875 = 37.625$ in.

Substituting the previous values of stresses in Equation 6.172, we obtain

$$\begin{aligned} D_c &= \left(\frac{-f_c}{|f_c| + f_t}\right) d - t_{fc} \geq 0 \\ &= \left(\frac{-(-29.00)}{29.00 + 45.66}\right)(37.625) - 0.75 = 13.86 \geq 0 \end{aligned}$$

Depth of the web in compression in the elastic range, $D_c = 13.86$ in.

It is important to recognize that the previous example is presented purely for illustrative purposes and to impress upon the fact that Equation 6.172 is *not* applicable here. Art. D6.3.1 presents an important commentary (CD6.3.1) regarding applicability of Equation 6.172, which states that Equation 6.172 is never intended for composite sections in positive flexure when the web satisfies the requirement of Art. 6.10.2.1.1 (see Section 6.10.2.2.1) such that longitudinal stiffeners are not required. This can be checked from Equation 6.7 (A6.10.2.1.1-1):

$$\frac{D}{t_w} = \frac{36.0}{0.4375} = 82.29 < 150$$

Because the web of the girder in this example satisfies with the requirements of Art. 6.10.2.1.1, Equation 6.172 need not be checked for depth of the web in compression in the elastic range.

6.13.6.2 Depth of the Web in Compression at Plastic Moment (D_{cp}): LRFD Art. D6.3.2

Section 6.13.4 presented a discussion of determining the depth of PNA in composite sections in positive flexure. Various possible cases for location of PNA are listed in Table 6.6; equations for

www.EngineeringEBooksPdf.com

locating the PNA in corresponding cases are listed in Table 6.7. For a given case, the depth of the web in compression at the plastic moment, D_c, can be easily determined once the PNA is located.

It must be noted that of all the seven cases listed in Table 6.5, the web of the beam in a composite section would be in compression only in Case 1 (PNA in web). In the remainder of the six cases (Cases II through VII), the PNA is located anywhere above the top flange or in the top flange of the steel section, so the web would not be in compression at all, and $D_{cp} = 0$. Likewise, for a composite section in negative flexure, a portion of the web would be in compression only in Case I in Table 6.8; for all other cases of composite sections in negative flexure, the entire web would be in tension and $D_{cp} = 0$.

Art. D6.3.2 presents the following equations for the depth of the web in compression for composite sections in positive and negative flexure. These equations are essentially the same as those listed in Tables 6.7 and 6.8 albeit in different formats.

1. For composite section in positive flexure when the PNA is in the web,

$$D_{cp} = \frac{D}{2}\left(\frac{F_{yt}A_t - F_{yc}A_c - 0.85f_c'A_s - F_{yrs}A_{rs}}{F_{yw}A_w} + 1\right) \qquad (6.173)\ [AD6.3.2\text{-}1]$$

where
A_c = area of compression flange (in.^{2})
A_{rs} = area of the longitudinal reinforcement within the effective deck width (in.^{2})
A_s = area of concrete deck (in.^{2})
A_t = area of tension flange (in.^{2})
A_w = area of the web (in.^{2})
D_{cp} = depth of the web in compression at the plastic moment (in.)
F_{yrs} = specified minimum yield strength of the longitudinal reinforcement (ksi)

2. For composite section in negative flexure when the PNA is in the web,

$$D_{cp} = \frac{D}{2A_wF_{yw}}\left(F_{yt}A_t + F_{yw}A_w + F_{yrs}A_{rs} - F_{yc}A_c\right) \qquad (6.174)\ [AD6.3.2\text{-}2]$$

3. For noncomposite sections, where

$$F_{yw}A_w \geq \left|F_{yc}A_c - F_{yt}A_t\right| \qquad (6.175)\ [AD6.3.2\text{-}3]$$

D_{cp} is to be taken as follows:

$$D_{cp} = \frac{D}{2A_wF_{yw}}\left(F_{yt}A_t + F_{yw}A_w - F_{yc}A_c\right) \qquad (6.176)\ [AD6.3.2\text{-}4]$$

For all other noncomposite sections, D_{cp} is to be taken as equal to D. This means that the entire web, along with the compression flange, is in compression; the PNA lies at the junction of the web and the tension flange.

6.14 DESIGN OF COMPOSITE SLAB-GIRDER SUPERSTRUCTURES

Example 6.2 presented the design of typical simple-span, noncomposite slab–girder superstructure. Various calculations presented in Example 6.2 are also required for the design of composite slab–steel girder superstructure. Additionally, calculations are required for short-term and long-term

www.EngineeringEBooksPdf.com

section properties of the composite section to account for creep and for the design of shear connectors that are required to develop composite action.

Of necessity, as in Example 6.2 (and in any other structural design problem), a trial section of the girder must be selected first to proceed with calculations required to satisfy the many provisions of LRFD Specifications for flexure. A few trials are always required before a satisfactory girder section can be found. This exercise becomes more difficult when built-up girders, often with cover plates, must be used for longer spans for which the rolled sections might not serve the purpose.

Before selecting a trial section, it is necessary to design the deck slab, which requires a priori the knowledge of the girder spacing as the design depth of the deck slab depends on the spacing of girders. A minimum design depth of deck slab of 7½ in. is usually provided; greater design depth would be required in corrosive environment, for which increased cover is required. For common short-span slab–girder superstructures, a girder spacing of 7–10 ft is commonly used; the greater the spacing of the girders, the larger the depth of the girders. In the following example, a girder spacing of 7 ft 6 in has been arbitrarily selected.

The very nature of structural design requires a trial-and-error procedure. Because of the many variables involved in design (strength of concrete, thickness of deck slab, size and spacing of girders, to name a few), a unique design solution is impossible. To achieve an acceptable design, a few trials must be made, and the most efficient of these must be selected. In the following example, two trials of the rolled girder sizes are shown to get a sense of the trial-and-error procedure and to also help in decision making to select the new trial girder size. Complete calculations are provided for both trial sizes.

Example 6.10: Design of a Composite Slab–Steel Girder Superstructure

Figure 6.67 shows the cross section and plan of a two-lane, simple composite slab–girder bridge having a center-to-center span of 50 ft. Design the superstructure of this bridge.

Solution

Calculation of section properties: The cross section of composite section is shown in Figure 6.68.

Assumptions

The following assumptions/data would be used for this two-lane bridge:

Span, L = center-to-center distance of bearings = 50 ft
Slab-thickness including 1/2-in. integral wearing surface = 8 in.
$f_c' = 4$ ksi

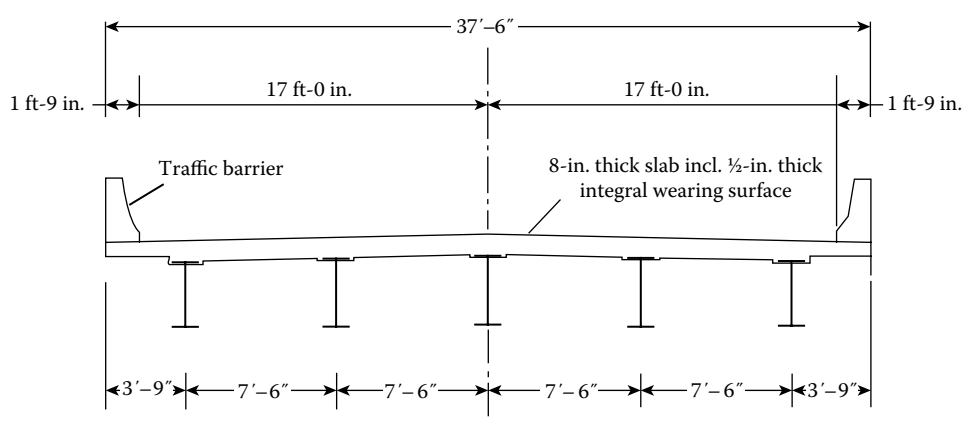

FIGURE 6.67 Cross section and plan of the composite bridge of Example 6.10.

www.EngineeringEBooksPdf.com

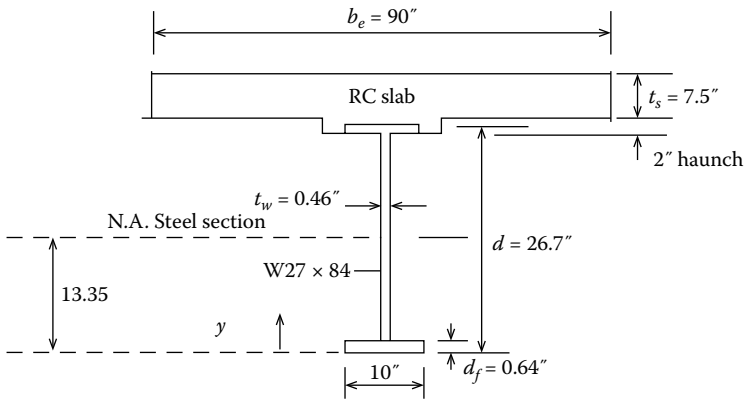

FIGURE 6.68 Cross section of composite girder for Example 6.10.

Structural depth of slab = 8 − 0.5 = 7.5 in.
FWS = 25 lb/ft^2
Center-to-center girder spacing = 7 ft 6 in.
Girder size: Trial size: W27 × 84 Grade M 270/50W, F_y = 50 ksi, F_u = 70 ksi

Note: A W27 × 84 has been selected as the first trial size (a shallower wide flange section compared to the W33 × 118 used for the noncomposite section for the same span length in Example 6.2). Calculations later showed that W27 × 84 did not satisfy LRFD requirements. As a result, a second trial size, a W330 × 90, was selected which was found to be satisfactory and finally selected for proposing the design. Calculations are presented for both trial sections for illustrative purposes.

Dead load of traffic barriers is equally distributed to all five girders.
Unshored construction would be used.
The bridge has no skew.

As specified in LRFD Art. 4.6.2.2.1 and discussed in Section 4.3, the dead load of concrete traffic barriers, which will be cast after the deck hardens, would be distributed equally to all girders (exterior and interior). This assumption is used in this example. However, designers, at their discretion, may choose to distribute the dead load of traffic barriers to only the exterior girders, and none of it to the interior girders; this option is not followed in this book.

Solution

Trial girder section: W27 × 84. Its section properties, found in AISC Steel Construction Manual (AISC 2011), are as follows:

$$A = 24.7 \text{ in.}^2, \quad d = 26.7 \text{ in.}, \quad t_w = 0.46 \text{ in.}, \quad b_f = 10 \text{ in.},$$
$$t_f = 0.64 \text{ in.}, \quad I_x = 2850 \text{ in.}^4, \quad S_x = 213 \text{ in.}^3, \quad Z_x = 244 \text{ in.}^3$$

Load and Resistance Design Parameters

For structural design based on the LRFD philosophy, the following parameters as specified in LRFD Specifications will be used.

Load Modifiers

$$\eta = \eta_D \eta_R \eta_I \qquad (1.69)\ [A1.3.2.1\text{-}1]$$

www.EngineeringEBooksPdf.com

For this example, the bridge is assumed to be a typical, conventional bridge. Therefore, the following values of load modifiers will be used:

η_D = a factor related to ductility = 1.0
η_R = a factor related to redundancy = 1.0
η_I = a factor related to operational classification = 1.0

Therefore, $\eta = (1.0)(1.0)(1.0) = 1.0$

Strength Reduction Factors (Section 6.9/Art. 6.5.4.2)

1. Strength limit state	ϕ
Flexure	1.0
Shear	1.0
2. Service limit state	1.0
3. Fatigue limit state	
Fatigue I	1.0
Fatigue II	1.0

Limit States Considered

The structural design of the superstructure presented herein would be checked for Strength I Limit State. No permit vehicle is specified in this example, so Strength II Limit State is not checked. The Strength IV Limit State relates to very high dead-to-live load force effect ratios, which is not the case in this example and, therefore, not checked.

Wind load checks are not presented in this example; therefore, load combinations Strength III Limit State and Strength V Limit State are not checked.

Extreme event checks are not performed in this example.

Service I and Service III Limit States are not directly related to steel girder and, therefore, not checked in this example.

Live load deflection check would be performed as specified in Art. 2.5.2.6.2 using the live load portion of Service II Limit State load combination (Art. 6.10.4.2.1).

Load Combinations and Load Factors

The following load combination specified in AASHTO LRFD Art. 3.4.1 would be used in this example. Only the maximum permanent load factors γ_p (from AASHTO Table 3.4.1-2) would be used here because uplift is not a concern in this bridge geometry. In case potential for uplift at the end abutments exists, the minimum permanent load factors specified in the table should be used in the strength load combinations when checking for uplift.

The following load combinations are obtained directly from LRFD Table 3.4.1-1:

1. Strength I Limit State

$$U = \eta[1.25DC + 1.5DW + 1.75(LL + IM) + 1.0WA + 1.0FR + (0.5 \text{ or } 1.2)TU + \gamma_{TG}TG + \gamma_{SE}SE]$$

The forces *WA* (water load and stream pressure), *FR* (friction load), *TU* (force effects due to uniform temperature), *TG* (force effects due to temperature gradient), and *SE* (force effect due to settlement) in the previous load combination equation are not relevant to this design example and therefore dropped from the previous equation (also dropped from load combinations equations for other limit states) resulting in the following load combination equation that would be used in this example:

$$U = \eta[1.25DC + 1.5DW + 1.75(LL + IM)]$$

2. Service II Limit State $\eta[1.00DC + 1.00DW + 1.30\ (LL + IM)]$

www.EngineeringEBooksPdf.com

3. Fatigue Limit States

Fatigue I 1.5(*LL* + *IM*)
Fatigue II 0.75(*LL* + *IM*)

where *LL* is the HL-93 vehicular live load as specified in Art. 3.6.1.4.1.

Dynamic Load Allowance (Section 3.8.3, Table 3.18/Art. 3.6.2.1)
Fatigue and fracture limit state $IM = 0.15$
All other limit states $IM = 0.33$

Structural Design of the Bridge Superstructure
The structural design of this bridge consists of three parts:

1. Design of deck slab
2. Design of a typical interior girder
3. Design of a typical exterior girder

Part 1. Design of Deck Slab
The design of the deck slab for this bridge is presented in Example 5.3.

Part 2: Design of a Typical Interior Girder
Calculations for the design of a typical interior girder are presented as follows; these are followed by design calculations for a typical exterior girder. All calculations are presented in a step-by-step format.

Unfactored Loads on a Typical Interior Girder
Permanent loads: *DC*1 due to permanent loads

Slab including 1/2 in. thick integral wearing surface $= \left(\frac{8}{12}\right)(1)(1)(0.15) = 0.10 \text{ kip/ft}^2$

Tributary width of deck slab contributory to each girder = 7.5 ft
Dead load due to the deck slab = (0.10)(7.5) = 0.75 kip/ft (1)
Self-weight of girder W27 × 84 = 0.084 kip/ft (2)
Flange width of W27 × 84, $b_f = 10.0$ in.
Depth of haunch = 2 in. (assumed)
Weight of concrete haunch $= \left(\frac{2.0}{12}\right)\left(\frac{10}{12}\right)(0.15) = 0.020$ kip/ft (3)
Weight of steel girders, cross frames, and details = 0.10 kip/ft (4)

Calculate the dead weight of the traffic barriers. The cross-sectional area of the traffic barriers, *A*, is as follows (see Figure 6.50b):

$$A = \left(\frac{1}{144}\right)\left[\left(\frac{12+14}{2}\right)(19) + \left(\frac{14+21}{2}\right)(10) + (21)(3)\right] = 3.368 \text{ ft}^2$$

Self-weight of the traffic barriers, *DC*2 = (3.368)(1.0)(0.15) = 0.505 kip/ft

Dead load of the two traffic barriers is distributed equally to all five girders
Dead load due to two traffic barriers = 2(0.505)/5 = 0.202 kip/ft (5)
Dead load due to the FWS at 25 lb/ft², *DW* = (0.025)(1)(7.5) = 0.188 (6)
w_{DC1} = sum of Items 1 through 4 = 0.75 + 0.084 + 0.02 +0.10 = 0.954 kip/ft
Permanent load on the girder, Item 5, $w_{DC2} = 0.202$ kip/ft
Permanent load on the girder, Item 6, $w_{DW} = 0.188$ kip/ft

Total dead load on a typical interior girder:

$$\begin{aligned} w_D &= w_{DC1} + w_{DC2} + w_{DW} \\ &= 0.954 + 0.202 + 0.188 \\ &= 1.344 \text{ kip/ft} \end{aligned}$$

where
w_{DC1} = dead load component that acts on noncomposite section
w_{DC2} = dead load component that acts on long-term composite section
w_{DC1} = dead load component due to wearing surface that acts also on the long-term composite section but has $\gamma_p = 1.5$

www.EngineeringEBooksPdf.com

The previous dead load values would be used to calculate midspan deflection of the interior girder, which would be used to determine the required camber.

Calculate maximum moments and shear in the span (unfactored loads)

Maximum moment due to w_{DC1}:

$$M_{DC1} = \frac{w_{DC1}L^2}{8} = \frac{(0.954)(50)^2}{8} = 298.1\,\text{kip-ft}$$

Maximum moment due to w_{DC2}:

$$M_{DC2} = \frac{w_{DC2}L^2}{8} = \frac{(0.202)(50)^2}{8} = 63.1\,\text{kip-ft}$$

Maximum moment due to w_{DW}:

$$M_{DW} = \frac{w_{DW}L^2}{8} = \frac{(0.188)(50)^2}{8} = 58.8\ \text{kip-ft}$$

Maximum shear due to dead load w_{DC1}:

$$V_{DC1} = \frac{w_{DC1}L}{2} = \frac{0.954(50)}{2} = 23.85\ \text{kip}$$

Maximum shear due to dead load w_{DC2}:

$$V_{DC2} = \frac{w_{DC2}L}{2} = \frac{0.202(50)}{2} = 5.05\ \text{kip}$$

Maximum shear due to w_{DW}:

$$V_{DW} = \frac{w_{DW}L}{2} = \frac{0.188 \times (50)}{2} = 4.7\ \text{kip}$$

Maximum moments due to live load

1. Moment due to design truck: See Examples 3.5 and 3.20
   For L = 50 ft (>40.27 ft), the truck load governs over tandem (see Example 3.9).
   Due to the design truck, $M_{truck} = 18L - 280 + \frac{392}{L} = 18(50) - 280 + \frac{392}{50} = 628$ kip-ft
   Dynamic load allowance = 0.33 (design truck load only)

   $$M_u(1 + IM) = 628\ (1 + 0.33) = 835\ \text{kip-ft}$$

2. Moment due to lane load: See Example 3.6
   The influence line ordinate is $\frac{ab}{L} = \frac{(25-2.335)(25+2.335)}{50} = 12.391\,\text{ft}$

   $$M_{lane} = (0.64)\left(\frac{1}{2}\right)(L)\left(\frac{ab}{L}\right)$$
   $$= (0.64)(0.5)(50)(12.391) = 198.3\ \text{kip-ft}$$

   Total moment due to live load, M_{LL} = 835 + 198.3 = 1033.3 kip-ft
   Live load distribution factor would be applied to M_{LL} = 1033.3 kip-ft.

www.EngineeringEBooksPdf.com

Maximum shear due to live load

1. Shear due to design truck:
   The reaction at the left support is obtained from Equation 3.25 for $x = 0$:

$$V_x = \frac{72}{L}(L - x - 9.33)$$

For L = 50 ft >26 ft, truck load governs over the tandem (see Example3.12).

$$R_L = \frac{72}{50}(50 - 0 - 9.33) = 58.6 \text{ kip}$$

Dynamic load allowance = 0.33

$$V_{Truck} = 58.6\ (1 + 0.33) = 77.94 \text{ kip}$$

2. Due to lane load:

$$\text{Max shear due to lane load} = w_L\left(\frac{L}{2}\right)$$

$$= 0.64\left(\frac{50}{2}\right) = 16 \text{ kip}$$

Total maximum shear due to live load:

$$V_L = V_{Truck} + V_{Lane} = 77.94 + 16 = 93.94 \text{ kip}$$

Live load distribution factor for shear would be applied to V_L = 93.94 kip.

Live Load Distribution Factors for the Interior Girder

The superstructure of the bridge conforms to type "(a)" in LRFD Table 4.6.2.2.1.1 (cast-in-place deck over steel girders). Check the applicability criteria:

$3.5 \le S \le 16.0$	$S = 7.5$ ft, OK
$4.5 \le t_s \le 12.0$	$t_s = 7.5$ in., OK
$20 \le L \le 240$	$L = 50$ ft, OK
$N_b \le 4$	$N_b = 5$, OK
$10{,}000 \le K_g \le 7{,}000{,}000$	

$$K_g = n\left(I + Ae_g^2\right)$$

where
n = modular ratio = 8 for f'_c = 4 ksi
I = moment of inertia of steel girder (W27 × 84) = 2,850 in.^{4}
e_g = girder eccentricity = $0.5d + t_h - t_f + 0.5t_s$
= 0.5(26.7) + 2 − 0.64 + 3.75 = 18.46 in.
K_g = 8 [2,850 + 24.7(18.46)^2] = 90,136 in.^{4}
10,000 ≤ (K_g = 90,136) ≤ 7,000,000

The range of applicability is satisfied.

www.EngineeringEBooksPdf.com

Number of design lanes: N_L

Clear roadway width for design lanes: w

$$w = \text{Clear bridge width} - 2(\text{width of the traffic barrier})$$
$$= 37.5 - 2(1.75)$$
$$= 34.00 \text{ ft}$$

$$N_L = \frac{w}{12} = \frac{34.00}{12} = 2.83 < 3$$

Use the integer part of 2.83, and use $N_L = 2$ design lanes

Live Load Distribution Factor for Bending Moment

Case 1. One design lane loaded

$$g_{mi1} = 0.06 + \left(\frac{S}{14}\right)^{0.4}\left(\frac{S}{L}\right)^{0.3}\left(\frac{K_g}{12.0Lt_s^3}\right)^{0.1}$$
$$= 0.06 + \left(\frac{7.5}{14}\right)^{0.4}\left(\frac{7.5}{50}\right)^{0.3}\left(\frac{90{,}136}{(12.0)(50)(7.5)^3}\right)^{0.1}$$
$$= 0.06 + (0.779)(0.566)(0.902)$$
$$= 0.458$$

Case 2. Two design lanes loaded

$$g_{ml2} = 0.075 + \left(\frac{S}{9.5}\right)^{0.6}\left(\frac{S}{L}\right)^{0.2}\left(\frac{K_g}{12.0Lt_s^3}\right)^{0.1}$$
$$= 0.075 + \left(\frac{7.5}{9.5}\right)^{0.6}\left(\frac{7.5}{50}\right)^{0.2}\left(\frac{90{,}136}{(12.0)(50)(7.5)^3}\right)^{0.1}$$
$$= 0.075 + (0.868)(0.684)(0.902)$$
$$= 0.611 > 0.458$$

Therefore, $g_{mi} = 0.611$ governs.

Live Load Distribution Factor for Shear

Check the range of applicability criteria.

The range of applicability criteria for shear for type "(a)" superstructure is the same as those for the moment checked earlier (except for the term K_g that is not required). Therefore, the applicability criteria are satisfied.

Case 1. One design lane loaded:

$$g_{vi1} = 0.36 + \frac{S}{25.0} = 0.36 + \frac{7.5}{25} = 0.66$$

www.EngineeringEBooksPdf.com

Case 2. Two or more design lanes loaded:

$$g_{vi2} = 0.2 + \frac{S}{12} - \left(\frac{S}{35}\right)^2$$

$$= 0.2 + \left(\frac{7.5}{12}\right) - \left(\frac{7.5}{35}\right)^2$$

$$= 0.779 > 0.66$$

$$g_{vi2} = 0.779 \text{ governs}$$

Live Load Distribution Factor for Fatigue

As discussed in Section 3.9.2, for fatigue limit state, only the design truck is placed in one lane with the distance between the two 32 kip axle loads a fixed 30 ft (instead of 14 ft); lane load is ignored for fatigue limit state considerations. Multiple presence factor is not applied when checking for fatigue. Therefore, live load distribution factor for fatigue is obtained by dividing the live load factors for moment and shear for the one lane loaded case by 1.2.

The moment due to one lane loaded case was determined as 0.458. Therefore,

$$g_{mi1,fat} = \frac{g_{mi1}}{m} = \frac{0.458}{1.2} = 0.382$$

The shear due to one lane loaded case was determined as 0.66. Therefore,

$$g_{vi1,fat} = \frac{g_{vi1}}{m} = \frac{0.66}{1.2} = 0.55$$

Live Load Distribution Factor for Deflection

Live load distribution factor for deflection is the same for interior and exterior girders because it is assumed that all lanes are loaded and all girders deflect equally. For two lanes loaded, the multipresence factor, $m = 1.0$.

$$g_{\Delta} = m\left(\frac{\text{Number of lanes}}{\text{Number of girders}}\right) = 1.0\left(\frac{2}{5}\right) = 0.4$$

Design Loads (Factored Loads)

The following unfactored loads were calculated earlier:

$$M_{DC1} = 298.1 \text{ kip-ft}, \quad V_{DC1} = 23.89 \text{ kip}$$

$$M_{DC2} = 63.1 \text{ kip-ft}, \quad V_{DC2} = 5.05 \text{ kip}$$

$$M_{DW} = 58.8 \text{ kip-ft}, \quad V_{DW} = 4.7 \text{ kip}$$

$$M_{(L+IM)} = 1033.3 \text{ kip-ft}, \quad V_{L+I} = 93.94 \text{ kip}$$

Apply load factors to unfactored loads to calculate factored loads, and live load distribution factors to live load moment and shear.

www.EngineeringEBooksPdf.com

Bending moment: $g_{mi2} = 0.611$

$$\text{Design live load plus impact moment} = g_{mi}\,(M_{LL+IM})$$
$$= (0.611)(1033.3)$$
$$= 631.34 \text{ kip-ft}$$

Shear: $g_{vi2} = 0.779$

$$\text{Design live load plus impact shear} = g_{vi2}\,(V_{LL+IM})$$
$$= (0.779)(93.94)$$
$$= 73.2 \text{ kip}$$

Loads for Strength I Limit State

Factored loads: Moments

$$M_u = \Sigma\eta_i\gamma_i M_i$$

$$\eta_i = \eta_D\eta_R\eta_I \text{ (Art. 1.3.2.1)}$$

Select Load Modifiers

Ductility, $\eta_D = 1.0$ (Art. 1.3.3).
Redundancy, $\eta_R = 1.0$ (Art. 1.3.4)
Importance, $\eta_I = 1.0$ (Art. 1.3.5)

Therefore, $M_u = \eta\Sigma\gamma_i M_i$

$$M_u = 1.0\,[1.25M_{DC} + 1.5M_{DW} + 1.75(M_{LL+IM})]$$
$$= 1.0\,[1.25(361.2) + 1.5(58.8) + 1.75(631.34)]$$
$$= 1645 \text{ kip-ft}$$

Factored Loads: Shear

$$V_{DC} = V_{DC1} + V_{DC2} = 23.89 + 5.05 = 28.9 \text{ kip}$$

$$V_u = 1.0\,[1.25V_{DC} + 1.5V_{DW} + 1.75(V_{LL+IM})]$$
$$= 1.0\,[1.25(28.9) + 1.5(4.7) + 1.75(73.2)]$$
$$= 171.3 \text{ kip}$$

Plastic Strength of Composite Section

Ignore contribution from longitudinal reinforcement (for simplicity).

Effective width of the slab (flange), b_s = center-to-center of girders = 7 ft 6 in. = 90 in.

Maximum compressive force in the slab:

$$P_s = 0.85f_c'b_st_s$$
$$= 0.85(4.0)(90)(7.5) = 2295 \text{ kip}$$

Maximum compressive force in the steel section,

$$P_{steel} = A_{steel}F_y = 24.7(50) = 1235 \text{ kip}$$

www.EngineeringEBooksPdf.com

Since $P_s > P_{steel}$, the PNA must lie in the slab. Let $\bar{Y}$ be the depth of PNA below the top of the deck slab. Then, the compressive force in the slab is

$$P_s = 0.85 f'_c b_s \bar{Y}$$

For horizontal equilibrium, we must have

$$0.85 f'_c b_s \bar{Y} = 1235 \text{ kip}$$

$$0.85(4)(90)\,\bar{Y} = 1{,}235$$

whence $\bar{Y} = 4.04$ in.

Alternatively, using LRFD Table D6.1-1, Case V, $\bar{Y}$ can be determined from the following expression:

$$\bar{Y} = (t_s)\frac{P_{rb} + P_c + P_w + P_t - P_{rt}}{P_s}$$

Since contribution from longitudinal reinforcement is ignored,

$$P_{rb} = P_{rt} = 0$$

$$P_{steel} = P_c + P_w + P_t = 1235 \text{ kip}$$

$$P_s = 2295 \text{ kip}$$

Consequently,

$$\bar{Y} = (7.5)\frac{0 + 1235 - 0}{2295} = 4.04 \text{ in.}$$

With reference to Figure 6.69,

$$\text{Lever arm} = 7.5 - 0.5(4.04) + 2.0 - 0.64 + 0.5(26.7)$$
$$= 20.19 \text{ in.}$$

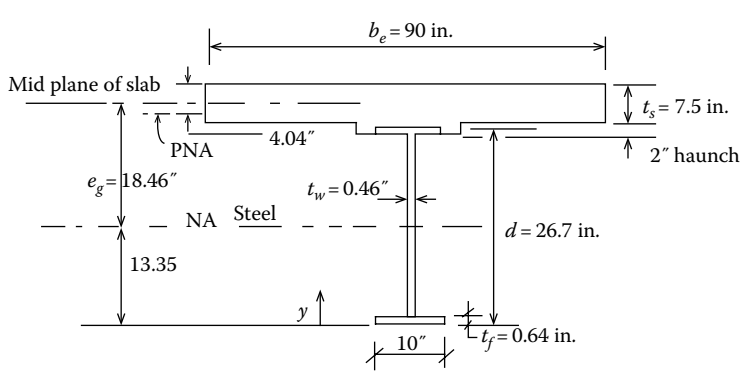

FIGURE 6.69 Determination of PNA and the plastic moment strength of composite section.

www.EngineeringEBooksPdf.com

Take moment of P_s about P_{steel},

$$\phi_m M_n = 1.0(1235)(20.19)$$
$$= 24{,}935 \text{ kip-in.}$$
$$= 2078 \text{ kip-ft}$$

$$M_u \leq \phi_m M_n$$

$$1645 \text{ kip-ft} \leq 2078 \text{ kip-ft, OK}$$

Check the ductility requirement (Art. 6.10.7.3)

$$D_p \leq 0.42 D_t$$

Overall depth of composite section, $D_t = t_s + t_h + d - t_f$

$$= 7.5 + 2.0 + 26.7 - 0.64$$

$$= 35.56 \text{ in.}$$

$$0.4D_t = 0.42(35.56) = 14.94 \text{ in.}$$

$$D_p = \bar{Y} = 4.04 \text{ in.} \leq 14.94 \text{ in., OK}$$

Check member properties: (Art. 6.10.1.1)

Check Compliance for Section Properties (Art. 6.7.3, 6.10.2)

The section properties of W27 × 84 are as follows:

$$A = 24.7 \text{ in.}^2, \quad d = 26.7 \text{ in.}, \quad t_w = 0.46 \text{ in.}, \quad b_f = 10.0 \text{ in.}, \quad t_f = 0.64 \text{ in.},$$
$$I_x = 2850 \text{ in.}^4, \quad S_x = 213 \text{ in.}^4,$$

Web thickness to be not less than 0.25 in.

$$t_w = 0.46 \text{ in.} > 0.25 \text{ in., OK}$$

$$D = 26.7 - 2(0.64) = 25.42 \text{ in.}$$

$$b_f \geq \frac{D}{6}$$

$$10.0 \geq \frac{25.42}{6} = 4.24 \text{ in. OK}$$

$$\frac{D}{t_w} \leq 150$$

$$\frac{D}{t_w} = \frac{25.42}{0.46} = 55.26 \leq 150, \text{ OK}$$

$$\frac{b_f}{2t_f} \leq 12$$

www.EngineeringEBooksPdf.com

$$\frac{b_f}{2t_f} = \frac{10.0}{2(0.64)} = 7.81 \leq 12, \text{ OK}$$

$$t_f \geq 1.1t_w$$

$$0.64 \geq 1.1(0.46) = 0.51 \text{ in., OK}$$

$$b_{fc} = \frac{L}{85} \text{ (Art. 6.10.3.4)}$$

$$10.0 \geq \frac{50(12)}{85} = 7.06, \text{ OK}$$

For handling, check if $0.1 \leq I_{yc}/I_{yt} \leq 10$ (A6.10.2.2.4)

where
I_{yc} = moment of inertia of compression flange about the vertical axis of the web
I_{yt} = moment of inertia of tension flange about the vertical axis of the web

For a rolled section, $I_{yc} = I_{yt}$; therefore, $I_{yc}/I_{yt} = 1.0$.

$$0.2 \leq 1.0 \leq 10, \text{ OK}$$

Constructibility
Check the resistance of girders during construction.

1. General: Art. 2.5.3 and 6.10.3.1
   Check the resistance of girders (W27 × 84) during construction. Ensure that the compression flanges of the girders are adequately braced to preclude the possibility of LTB while the deck concrete is wet and the section acts as noncomposite. Nominal yielding or reliance on post-buckling resistance is not permitted during construction.
   a. Local buckling: Art. 6.10.3.2.1
      The rolled W27 × 84 would not have any local buckling issues during construction.
   b. Flexure: Art. 6.10.3.2 and 6.10.8
      Check compliance with Art. 6.10.8.2.1: Compression Flange Flexural Resistance.

Compression flange flexural resistance should be checked for local buckling and LTB using the appropriate value of the nominal flexural resistance of the compression flange, F_{nc}, as specified in Art. 6.10.8.2.2 and 6.10.8.2.3.

1. *Art. 6.10.8.2.2: Local buckling resistance*
   The rolled wide flange section would not have any local buckling issues. However, calculations are provided for illustrative purposes.

$$\lambda_f = \frac{b_f}{2t_f} = \frac{10}{2(0.64)} = 7.81$$

$$\lambda_{pf} = 0.38\sqrt{\frac{E}{F_{yc}}}$$

$$= 0.38\sqrt{\frac{29{,}000}{50}} = 9.15$$

$$\lambda_f = 7.81 \leq \lambda_{pf} = 9.15, \text{ OK}$$

www.EngineeringEBooksPdf.com

Therefore,

$$F_{nc} = R_b R_h F_{yc}$$

where

R_b = web-shedding factor (Art. 6.10.1.10.2)
R_h = hybrid factor (Art. 6.10.1.10.1)

The web-shedding factor, R_b, is determined as specified in Art. 6.10.1.10.2. The section is composite and it is in positive flexure and satisfies the requirements of Art. 6.10.2.1.1 (web without longitudinal stiffeners:

$$\frac{D}{t_w} = \frac{25.42}{0.46} = 55.26 \leq 150, \text{ OK}$$

Therefore, R_b = 1.0. For rolled shapes, R_h = 1.0 (Art. 6.10.1.10). Therefore,

$$F_{nc} = R_b R_h F_{yc} = (1.0)(1.0(50) = 50 \text{ ksi}$$

2. *Art. 6.10.8.2.3: LTB resistance*
The compression flange is not laterally braced, and the section acts as noncomposite when deck concrete is being poured. Check LTB resistance of the compression flange for this construction condition. Calculate L_p and L_r, and select a suitable length of bracing interval, L_b; then calculate F_{nc} from Equation 6.73 (A 6.10.8.2.3-2).

L_p = limiting unbraced length to achieve the nominal flexural resistance of $R_b R_h F_{yc}$ under uniform bending, in.

$$= 1.0 r_t \sqrt{\frac{E}{F_{yc}}} \qquad (6.75)\ [A6.10.8.2.3\text{-}4]$$

L_r = limiting unbraced length to achieve the onset of nominal yielding in either flange under uniform bending with a consideration of compression residual stress effects (in.)

$$= \pi r_t \sqrt{\frac{E}{F_{yr}}} \qquad (6.76)\ [A6.10.8.2.3\text{-}5]$$

F_{yc} = specified minimum yield strength of compression flange
F_{yr} = compression flange stress at the onset of nominal yielding within the cross section, including residual stress effects, but not including compression flange-lateral bending, which is the smaller of $0.7F_{yc}$ and F_{yw} but not less than $0.5F_{yc}$
r_t = effective radius of gyration for LTB (Equation 6.27 [A6.10.8.2.3-9])

Calculate r_t.

$$r_t = \frac{b_{fc}}{\sqrt{12\left(1 + \frac{1}{3}\frac{D_c t_w}{b_{fc} t_{fc}}\right)}} \qquad (6.27)\ [A6.10.8.2.3\text{-}9]$$

For a W27 × 84, b_{fc} = 10.0 in., t_{fc} = 0.64 in., $D_c = D/2$ = 25.42/2 = 12.71 in., t_w = 0.46 in.

$$r_t = \frac{10.0}{\sqrt{12\left(1 + \frac{1}{3}\frac{(12.71)(0.46)}{(10.0)(0.64)}\right)}} = 2.53 \text{ in.}$$

www.EngineeringEBooksPdf.com

$$L_p = 1.0r_t\sqrt{\frac{E}{F_{yc}}} = 1.0(2.53)\sqrt{\frac{29{,}000}{50}} = 60.93 \text{ in.} \approx 61 \text{ in.}$$

$$L_r = \pi r_t\sqrt{\frac{E}{F_{yr}}} = \pi(2.53)\sqrt{\frac{29{,}000}{0.7(50)}} = 228.79 \text{ in.} \approx 229 \text{ in.}$$

Try bracings at quarter points, $L_b = \frac{50}{4} = 12.5 \text{ ft} = 150 \text{ in.}$

Note: These braces would be temporary: to be kept in place until the deck concrete hardens, following which they may be removed. Continuous lateral support to compression flanges would be provided by the composite action after the concrete hardens. Calculate F_{nc} (Equation 6.71 [A6.10.8.2.3-2]) and then calculate f_{bu} (Equation A6.10.3.2.1-2).

$$F_{nc} = C_b\left[1-\left(1-\frac{F_{yr}}{R_hF_{yc}}\right)\left(\frac{L_b-L_p}{L_r-L_p}\right)\right]R_bR_hF_{yc} \le R_bR_hF_{yc}$$

$$= 1.0\left[1-\left(1-\frac{0.7F_{yc}}{1.0F_{yc}}\right)\left(\frac{150-61.0}{229-61.0}\right)\right](1.0)(1.0)(50) \le 50 \text{ ksi}$$

$$= 42.05 \text{ ksi} < 50 \text{ ksi, OK.} \qquad (6.73)\ [A6.10.8.2.3\text{-}2]$$

Note that in the previous calculations, $C_b = 1.0$ has been conservatively assumed equal to 1.0, which is valid for only uniform moment, which is not the case here. For the present case, $C_b > 1.0$. Exact value of C_b can be determined from Equation 6.25 (A6.10.8.2.3-7) if necessary. A value $C_b > 1.0$ would result in $F_{nc} > 42.05$ ksi.

Calculate the load effect under construction. The flange lateral-bending stress, f_ℓ, is negligible for the rolled wide flange shape and is ignored.

$$M_u = 1.25M_{DC} = 1.25(298.1) = 372.63 \text{ kip-ft}$$

$$f_u = \frac{M_u}{S_x} = \frac{372.63(12)}{213} = 21.00 \text{ ksi} \ll F_{nc} = 42.05 \text{ ksi}$$

$$f_{bu} + \frac{1}{3}f_\ell = 21.00 + 0 = 21.00 \text{ ksi} < \phi_f F_{nc} = (1.0)(42.05) = 42.05 \text{ ksi, OK.}$$

Provide lateral bracings at quarter points, that is, at 12 ft 6 in. intervals. These would be again considered later for wind bracings.

Check compliance with Equation 6.32 (A6.10.1.3.2-3) to ensure that theoretical web bend-buckling would not occur during construction.

$$f_{bu} \le \phi F_{crw}$$

where F_{crw} is computed from Equation A6.10.1.9.1-1.

$$F_{crw} = \frac{0.9Ek}{\left(\frac{D}{t_w}\right)^2} \text{ but not to exceed } R_hF_y \text{ or } F_{yw}/0.7$$

$$k = \text{bend-buckling coefficient} = \frac{9}{\left(\frac{D_c}{D}\right)^2}$$

www.EngineeringEBooksPdf.com

For W27 × 84 rolled section, $D_c = 0.5D$, so $D_c/D = 0.5$

$$k = \frac{9}{(0.5)^2} = 36$$

$$F_{crw} = \frac{0.9(29{,}000)(36)}{\left(\frac{25.42}{0.46}\right)^2} = 308 \text{ ksi} > R_h F_{yc} = (1.0)(50) = 50 \text{ ksi}$$

So, $F_{crw} = 50$ ksi

$$f_{bu} = 21.0 \text{ ksi} < F_{crw} = 50 \text{ ksi, OK}$$

3. *Check for shear (Art. 6.10.9.2, Art. 6.10.10.3): Shear strength of unstiffened webs*
Generally speaking, for rolled wide flange beams such as the one used in this example, shear is not a matter of concern. However, all calculations are provided for completeness.

$$V_u \le \phi_v V_n \qquad (6.77)\ [A6.10.9.1\text{-}1]$$

$$V_n = V_{cr} = CV_p \qquad (6.78)\ [A6.10.9.2\text{-}1]$$

$$V_p = 0.58F_y Dt_w \qquad (6.79)\ [A6.10.9.2\text{-}2]$$

where
V_u = shear due to factored loads
V_{cr} = critical buckling resistance
V_p = plastic shear resistance
C = critical buckling coefficient (from Equations 6.78 through 6.80 as applicable and $k = 5$ for unstiffened webs)

$$V_p = 0.58F_{yw}Dt_w$$
$$= 0.58(50)(25.42)(0.46)$$
$$= 339 \text{ kip}$$

Calculate the critical buckling coefficient, C. For a W27 × 84, $D = 25.42$ in, $t_w = 0.46$ in.

$$\frac{D}{t_w} = \frac{25.42}{0.46} = 52.26$$

$$1.12\sqrt{\frac{Ek}{F_{yw}}} = 1.12\sqrt{\frac{29{,}000(5)}{50}} = 60.31 > \frac{D}{t_w} = 52.26$$

Therefore, $C = 1.0$.

$$V_n = V_{cr} = CV_p = (1.0)(339) = 339 \text{ kip}$$

$$\phi_v V_{cr} = 1.0(339) = 339 \text{ kip}$$

$$1.25V_{DC1} = 1.25\ (23.85) = 29.81 \text{ kip} < 339 \text{ kip, OK}$$

www.EngineeringEBooksPdf.com

4. *Deck placement: Art. 6.10.3.4*
   Sections that are composite in the final condition but are noncomposite during construction (as in this example) must be checked for flexure during various stages of construction as specified in Art. 6.10.3.2. For the 50 ft short span bridge in this example, the entire deck would be cast in one operation. Therefore, staged construction need not be considered. Calculations demonstrating compliance with Art. 6.10.3.2 have been provided earlier.
   Service Limit State: Art. 6.10.4
   a. Elastic deformation: Provisions of Art. 2.5.2.6 are applied.

Service Limit State (Art 6.5.2, A6.10.4)
Art. 6.10.4.1: Compliance with 2.5.2.6 is required.

1. Optional live load deflection control:
   Since no deflection criteria are specified, optional deflection criteria (Art. 2.6.2.6.2) will be used in this example.
   Allowable deflection due to vehicular load, $\Delta_{LL} = \frac{span}{800} = \frac{50(12)}{800} = 0.75$ in.
   Art. 3.6.1.3.2: Calculated deflection will be taken as the larger of the following as discussed in Section 2.6.3:
   a. Deflection due to design truck alone. Dynamic load allowance will be applied to this deflection.
   b. Deflection due to 25 percent of the deflection due to the design truck *plus* deflection due to lane load. Dynamic load allowance is not applied to the deflection due to the lane load.

Calculate Deflection due to Vehicular Live Load
Live load deflections would be computed for the governing loading conditions—separately for the design truck and the lane load (Figure 6.51)—by the usual methods of computing deflections. Formulas for relevant load cases given in AISC Steel Construction Manual (AISC 2011) would be used (see discussion in Section 2.6.6). Referenced formulas used in calculations are taken from Chapter 2. For the noncomposite beams used in this example, the moment of inertia, I, of the steel section would be used for calculating deflections.

Deflection due to Design Truck
As discussed in Section 2.6.6, in the case of the design truck loading, it is difficult, although theoretically possible, to determine the exact positions of the three axles that will result in maximum deflection. As a practical matter, however, the maximum deflection in the girder would be computed by placing the middle 32 kip load at the midspan and the other two loads placed at 14 ft apart, one on each side of the midspan (Figure 6.52). This loading condition can be split into two separate cases (AISC 2011) as shown in Figure 6.52:

1. Load Case 7 for the centrally placed point load
2. Load Case 8 for point load placed off the midspan

For the centrally placed point load P (Load Case 7), the maximum deflection occurs at the center that can be calculated from Equation 2.2:

$$\Delta_c = \frac{PL^3}{48EI} \tag{2.2}$$

where
Δ_c = deflection at midspan due to point load
L = span
E = modulus of elasticity
I = moment of inertia

www.EngineeringEBooksPdf.com

The axle loads should be multiplied by (1 + *IM*) = (1 + 0.33) = 1.33 to account for dynamic allowance. The resulting axle loads are as follows:

$$P_1 = P_2 = 32(1.33) = 42.56 \text{ kip}$$

$$P_3 = 8(1.33) = 10.64 \text{ kip.}$$

Substitute P = 42.56 kip, L = 50 ft, E = 29,000 ksi, and $I = I_c$ = 9757 in.^{4} in Equation 2.2 (calculations for I_c are shown later).

$$\Delta_c = \frac{42.56(50)^3(12)^3}{48(29,000)(9,757)} = 0.68 \text{ in.}$$

For the remaining axle loads that are placed off center on the span, Load Case 8 would be used.

For a point load P placed at a distance a from the left support, the deflection at a distance x (when $x < a$) from the left support can be calculated from Equation 2.3:

$$\Delta_x = \frac{Pbx\left(L^2 - b^2 - x^2\right)}{6EIL} \tag{2.3}$$

Equation 2.3R is used to calculate deflections due to the two off-center point loads (the 10.64 and 42.56 kip loads, which include impact). Substitute $P = P_2 + P_3$ = 42.56 + 10.64 kip, x = 25 ft, b = 11 ft, E = 29,000 ksi, I = 5900 in.^{4} and L = 50 ft in Equation 2.3.

$$\Delta_{x=25\text{ ft}} = \frac{(42.56+10.64)(11)(25)\left[(50)^2-(11)^2-(25)^2\right]}{6(29,000)(9,757)(50)}(12)^3 = 0.52 \text{ in.}$$

Total deflection due to the design truck, $\Delta_c + \Delta_{x=25\text{ ft}}$ = 0.68 + 0.52 = 1.20 in.

Distribution factor for live load deflection = 0.4 (computed earlier)

Maximum deflection in the girder due to the design truck = (0.4)(1.20) = 0.48 in.

Deflection due to Lane Load

For the case of lane loading (uniform load), the maximum deflection is calculated from the following (Case 1, AISC 2011):

$$\Delta_{lane} = \frac{5wL^4}{384EI} \tag{2.9}$$

where

$$w = 0.64 \text{ kip/ft}$$

$$L = \text{span} = 50 \text{ ft}$$

Substituting these values along with E = 29,000 ksi and I_c = 9757 in.^{4} in Equation 2.9R, the maximum deflection due to lane load is

$$\Delta_{lane.max} = \frac{5(0.64)(50)^4(12)^3}{384(29,000)(9,757)} = 0.32 \text{ in.}$$

Apply the live load distribution factor to deflection due to lane load:

$$\Delta_{lane.max} = (0.4)(0.32) = 0.13 \text{ in.}$$

$$(0.25\Delta_{truck} + \Delta_{lane}) = 0.25(0.48) + 0.13 = 0.25 \text{ in.} < \Delta_{truck} = 0.48 \text{ in.}$$

Therefore, Δ_{truck} = 0.48 in governs.

www.EngineeringEBooksPdf.com

Allowable live load deflection,

$$\Delta_{allowable} = \frac{L}{800} = \frac{(50)(12)}{800} = 0.75 \text{ in.} > 0.48 \text{ in., OK.}$$

Optional Criteria for Span-to-Depth Ratio (Art. 2.5.2.6.3)
The owner may invoke the minimum girder depth ratios as specified in LRFD Table 2.5.2.6.3-1. Check if the span-to-depth ratio is satisfied. For this example,

i. Overall depth of composite section:
Overall depth of composite section, D_t = 35.56 in. (computed earlier)
Minimum depth of composite section = $0.04L = 0.04(50)(12) = 24$ in.

$$D_t = 35.56 \text{ in} > 0.04L = 24 \text{ in., OK}$$

ii. Depth of the I-beam portion of composite beam:

$$d = 26.7 \text{ in.}$$

$$0.033(50)(12) = 19.8 \text{ in.} < d = 26.7 \text{ in., OK}$$

Span-to-depth ratio is satisfied.

2. Permanent deformations (Art. 6.10.4.2)
The purpose of check is to prevent objectionable permanent deflections due to expected severe traffic loadings that would impair rideability. For composite sections, compliance with the following (A6.10.4.2.2-3) is required:

$$f_f + \frac{f_\ell}{2} \leq 0.95R_hF_{yf} \qquad (6.43)\ [A6.10.4.2.2\text{-}3]$$

f_f = flange stress at the section under consideration due to Service II loads calculated without consideration of flange lateral bending (ksi)
f_ℓ = flange lateral buckling stress at the section under consideration due to Service II loads determined as specified in Art. 6.10.1.6 (ksi)
≈ 0 for the rolled section

Therefore, $f_f = 0.95(1.0)(50) = 47.5$ ksi
For Service II load, the maximum moment is

$$M_u = \eta[1.0M_{DC} + 1.0M_{DW} + 1.3(LL + IM)]$$

$$= 1.0[1.0M_{DC} + 1.0M_{DW} + 1.3(LL + IM)]$$

$$M_{DC1} = 298.1 \text{ kip-ft}$$

$$M_{DC2} + M_{DW} = 63.1 + 58.8 = 121.9 \text{ kip-ft}$$

$$1.30M_{LL+IM} = 1.30(631.34) = 821 \text{ kip-ft}$$

Calculate the short-term and the long-term section properties of the composite section. These section properties are computed with reference to Figures 6.70 and 6.71 (datum is selected at the bottom of the steel section).

www.EngineeringEBooksPdf.com

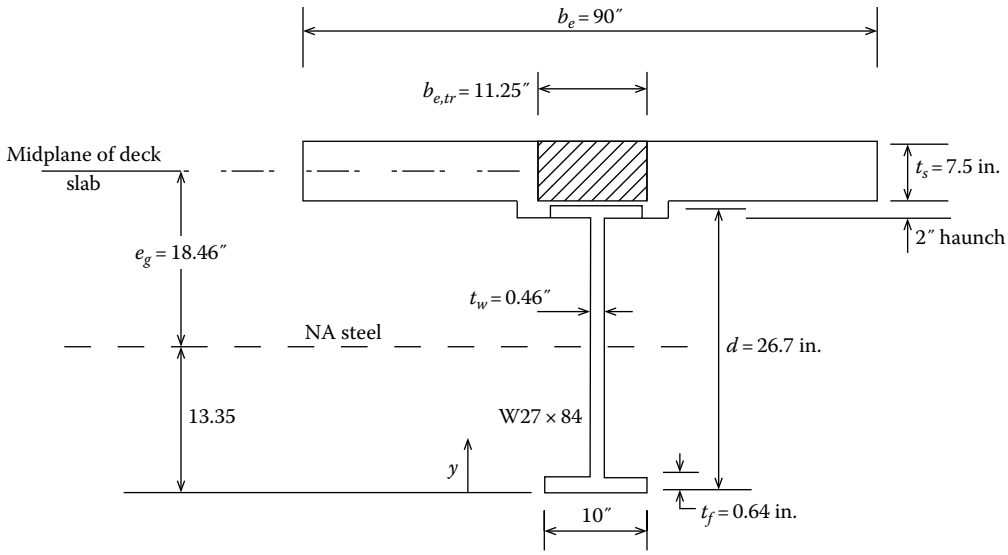

FIGURE 6.70 Computation of short-term properties of composite section.

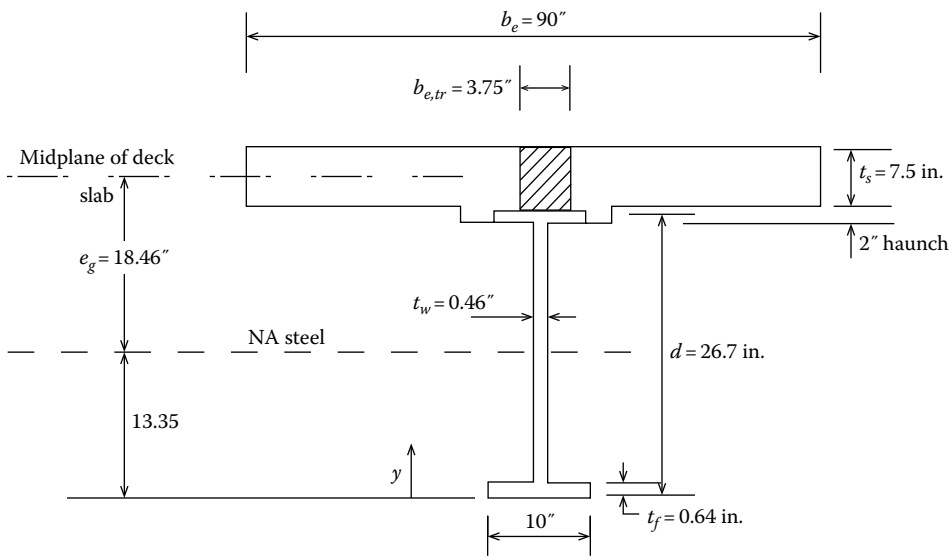

FIGURE 6.71 Computation of long-term properties of composite section.

Effective width, b_s = center-to-center spacing of girders = 7.5 ft = 90 in.
For f'_c = 4 ksi, n = 8 (Table 6.13)

$$\bar{y}_b = \frac{\Sigma A y_b}{\Sigma A} = \frac{3014}{109.08} = 27.63 \text{ in.}$$

$$I_c = 6511 + 3246 = 9757 \text{ in.}^4$$

$$S_{ST}^t = \frac{9757}{|27.63 - 26.7|} = 10{,}491 \text{ in.}^3 \text{ (top of steel)}$$

www.EngineeringEBooksPdf.com

TABLE 6.13
Short-Term Composite Section Properties: $n = 8$

Component	A, in.^{2}	y_b, in.	Ay_b, in.^{3}	$(y_b - \bar{y}_b)$, in.	$A(y_b - \bar{y}_b)^2$, in.^{4}	I_o, in.^{4}
Slab (90/8) × 7.5	84.38	31.81	2684	4.18	1474	396
Girder W27 × 84	24.70	13.35	330	14.28	5037	2850
Σ	109.08		3014		6511	3246

TABLE 6.14
Long-Term Composite Section Properties: $3n = 24$

Component	A, in.^{2}	y_b, in.	Ay_b, in.^{3}	$(y_b - \bar{y}_b)$, in.	$A(y_b - \bar{y}_b)^2$, in.^{4}	I_o, in.^{4}
Slab (90/24) × 7.5	28.13	31.38	895	8.62	2090	132
Girder W27 × 84	24.70	13.35	330	3.51	304	2850
Σ	52.83		1225		2394	2982

$$S_{ST}^b = \frac{9757}{27.63} = 353 \text{ in.}^3 \text{ (bottom of steel)} \quad \text{(Table 6.14)}$$

$$\bar{y}_b = \frac{\Sigma A y_b}{\Sigma A} = \frac{1225}{52.83} = 23.19 \text{ in.}$$

$$I_c = 2394 + 2982 = 5376 \text{ in.}^4$$

$$S_{LT}^t = \frac{5376}{|26.7 - 23.19|} = 1532 \text{ in.}^3 \text{ (top of steel)}$$

$$S_{LT}^b = \frac{5376}{23.19} = 232 \text{ in.}^3 \text{ (bottom of steel)}$$

Calculate flange stresses as follows:

For M_{DC1}, use noncomposite section properties.
For M_{DC2} and M_{DW}, use long-term section properties.
For $1.3M_{LL+IM}$, use short-term properties.

Compressive stress (f_c) in the top flange of composite section:

$$f_c = \frac{298.1(12)}{213} + \frac{121.9(12)}{1{,}532} + \frac{821(12)}{10{,}491}$$

$$= 16.79 + 0.95 + 0.94 = 18.68 \text{ ksi}$$

$$f_f = 47.5 \text{ ksi} > f_c = 18.68 \text{ ksi, OK}$$

Tensile stress (f_t) in the bottom flange of composite section:

$$f_t = \frac{298.1(12)}{213} + \frac{121.9(12)}{232} + \frac{821(12)}{353}$$

$$= 16.79 + 6.31 + 27.91 = 51.01 \text{ ksi} > f_f = 47.5 \text{ ksi, ng.}$$

www.EngineeringEBooksPdf.com

Discussion: The aforementioned computations show that the section W27 × 84 is *not* adequate to resist permanent deformations since the tensile stress in the bottom flange (= 51.01 ksi) exceeds the permitted flange stress value of 47.5 ksi. Therefore, the proposed design must be modified.

Several options may be used to find an acceptable girder size. One option is reducing the spacing of girders. This would reduce the loads to be carried by the interior girders and thereby reduce the stresses in girder flanges. Another option is to use a cover plate in the middle segment of W27 × 84, which would increase section modulus of the steel section and thereby reduce flange stresses.

Yet another option is to select a wide flange section with depth d greater than that of W27 × 84 (d = 26.7 in.), which would have a larger moment of inertia and larger values of section moduli than those of W27 × 84; this would also result in lower flange stresses. This later option is used in this example. The next economical wide flange section, a W30 × 90, with a greater depth (d = 29.5 in.) is selected for the second trial with the expectation that its greater depth would result in larger values of the section moduli and consequent reduction in the elastic stresses.

The following calculations are similar to those presented earlier for the W27 × 84 trial girder. With the exception of a slight increase in the girder weight (from 84 to 90 lb/ft), there is no change in other design parameters. An increase of 6 lb/ft in the permanent load would hardly make any change in the design loads. Therefore, in the following calculations, the permanent design loads are kept the same as those in the first trial.

Because the section properties of W30 × 90 are different than those of previous trial wide flange section (W27 × 84), the longitudinal stiffness parameter, K_g, must be recalculated; this would result in a slight change in live load distribution factors for bending moment and fatigue (but not for shear and deflection). Consequently, the factored live load bending moment would need to be recalculated.

Revised Trial Section: W30 × 90

Since the previous trial section (W27 × 84) did not pass the checks for *permanent deformation*, it is advisable to first check the adequacy of the revised trial section, W30 × 90, for the same before making other checks. The live load distribution factors for bending moment must be calculated first (it is required to compute the service live load moment that depends on the live load distribution factor for bending moment).

Section properties of W30 × 90:

$$A = 26.3 \text{ in.}^2, \quad d = 29.5 \text{ in.}, \quad t_w = 0.47 \text{ in.}, \quad b_f = 10.4 \text{ in.}, \quad t_f = 0.61 \text{ in.},$$

$$I_x = 3610 \text{ in.}^4, \quad S_x = 245 \text{ in.}^3$$

Calculate Live Load Distribution Factors for the Interior Girder

The superstructure of the bridge conforms to type "(a)" in LRFD Table 4.6.2.2.1.1 (cast-in-place deck over steel girders). Check the applicability criteria:

$3.5 \le S \le 16.0$	$S = 7.5$ ft, OK
$4.5 \le t_s \le 12.0$	$t_s = 7.5$ in., OK
$20 \le L \le 240$	$L = 50$ ft, OK
$N_b \le 4$	$N_b = 5$, OK
$10{,}000 \le K_g \le 7{,}000{,}000$	

$$K_g = n\left(I + Ae_g^2\right)$$

where

n = modular ratio = 8 for f'_c = 4 ksi

I = moment of inertia of steel girder (W30 × 90) = 3610 in.^{4}

e_g = girder eccentricity = $0.5d + t_h - t_f + 0.5t_s$

= 0.5(29.5) + 2 − 0.61 + 3.75 = 19.89 in.

$$K_g = 8\ [3610 + 26.3(19.89)^2] = 112{,}117 \text{ in.}^4$$

$$10{,}000 \le (K_g = 112{,}117) \le 7{,}000{,}000$$

The range of applicability is satisfied.

www.EngineeringEBooksPdf.com

Live Load Distribution Factor for Bending Moment

Case 1. One design lane loaded:

$$g_{mi1} = 0.06\left(\frac{5}{14}\right)^{0.4}\left(\frac{S}{L}\right)^{0.3}\left(\frac{K_g}{12.0Lt_s^3}\right)^{0.1}$$

$$= 0.06 + \left(\frac{7.5}{14}\right)^{0.4}\left(\frac{7.5}{50}\right)^{0.3}\left(\frac{112{,}117}{(12.0)(50)(7.5)^3}\right)^{0.1}$$

$$= 0.06 + (0.779)(0.566)(0.922)$$

$$= 0.467$$

Case 2. Two design lanes loaded:

$$g_{mi2} = 0.075 + \left(\frac{5}{9.5}\right)^{0.6}\left(\frac{S}{L}\right)^{0.2}\left(\frac{K_g}{12.0Lt_s^3}\right)^{0.1}$$

$$= 0.075 + \left(\frac{7.5}{9.5}\right)^{0.6}\left(\frac{7.5}{50}\right)^{0.2}\left(\frac{112{,}117}{(12.0)(50)(7.5)^3}\right)^{0.1}$$

$$= 0.075 + (0.868)(0.684)(0.922)$$

$$= 0.622 > 0.467$$

Therefore, $g_{mi2} = 0.622$ governs.

Live Load Distribution Factor for Shear

Check the range of applicability criteria.

The range of applicability criteria for shear for type (a) superstructure is the same as those for the moment checked earlier (except for the term K_g that is not required). Therefore, the applicability criteria are satisfied.

Case 1. One design lane loaded:

$$g_{vi1} = 0.36 + \frac{S}{25.0} = 0.36 + \frac{7.5}{25} = 0.66$$

Case 2. Two or more design lanes loaded:

$$g_{vi2} = 0.2 + \frac{S}{12} - \left(\frac{S}{35}\right)^2$$

$$= 0.2 - \left(\frac{7.5}{35}\right) - \left(\frac{7.5}{35}\right)^2$$

$$= 0.779 > 0.66$$

$$g_{vi2} = 0.779 \text{ governs}$$

Live Load Distribution Factor for Fatigue

As discussed in Section 3.9.2, for fatigue limit state, only the design truck is placed in one lane with the distance between the two 32 kip axle loads equal to a fixed 30 ft (instead of 14 ft); lane

www.EngineeringEBooksPdf.com

load is ignored for fatigue limit state considerations. Multiple presence factor is not applied when checking for fatigue. Therefore, live load distribution factor for fatigue is obtained by dividing the live load factors for moment and shear for the one lane loaded case by 1.2.

The distribution factor for moment due to one lane loaded case was determined as 0.467. Therefore,

$$g_{mi1,fat} = \frac{g_{mi1}}{m} = \frac{0.467}{1.2} = 0.389$$

The distribution factor for shear due to one lane loaded case was determined as 0.66. Therefore,

$$g_{vi1,fat} = \frac{g_{vi1}}{m} = \frac{0.66}{1.2} = 0.55$$

Live Load Distribution Factor for Deflection

Live load distribution factor for deflection is same for interior and exterior girders because it is assumed that all lanes are loaded and all girders deflect equally. For two lanes loaded, the multi-presence factor, $m = 1.0$.

$$g_{\Delta} = m\left(\frac{Number\,of\,lanes}{Number\,of\,girders}\right) = 1.0\left(\frac{2}{5}\right) = 0.4$$

Permanent Deformations (Art. 6.10.4.2)

The purpose of this check is to prevent objectionable permanent deflections due to the expected severe traffic loadings that would impair rideability. For composite sections, compliance with the following (A6.10.4.2.2-3) is required:

$$f_f + \frac{f_\ell}{2} \le 0.95R_hF_{yf} \qquad (6.43)\ [A6.10.4.2.2\text{-}3]$$

f_f = flange stress at the section under consideration due to Service II load calculated without consideration of flange lateral bending (ksi)

f_ℓ = flange lateral buckling stress at the section under consideration due to Service II loads determined as specified in Art. 6.10.1.6 (ksi)

≈ 0 for the rolled section

For Service II load, the maximum moment is

$$M_u = \eta[1.0M_{DC} + 1.0M_{DW} + 1.3(LL + IM)]$$

$$= 1.0[1.0M_{DC} + 1.0M_{DW} + 1.3(LL + IM)]$$

$$M_{DC1} = 298.1 \text{ kip-ft}$$

$$M_{DC2} + M_{DW} = 63.1 + 58.8 = 121.9 \text{ kip-ft}$$

Calculate bending moment in the girder with the revised governing distribution factor for bending moment, $g_{mi2} = 0.622$.

Unmodified live load bending moment in the girder, $M_{LL+IM} = 1033.3$ kip-ft

Apply live load distribution factor for bending moment:

Live load bending moment in the girder = $(M_{LL+IM})(0.622) = (1033.3)(0.622) = 642.71$ kip-ft

$$1.30M_{LL+IM} = 1.30(642.71) = 833.5 \text{ kip-ft}$$

www.EngineeringEBooksPdf.com

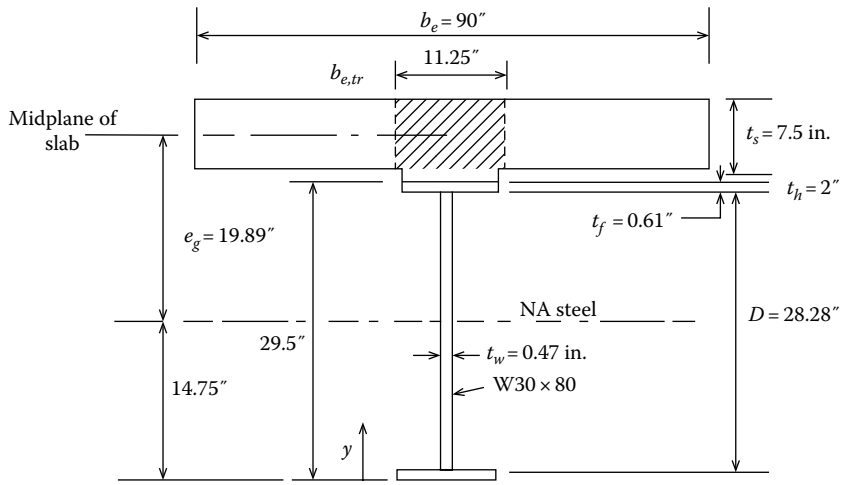

FIGURE 6.72 Computation of short-term properties of composite section.

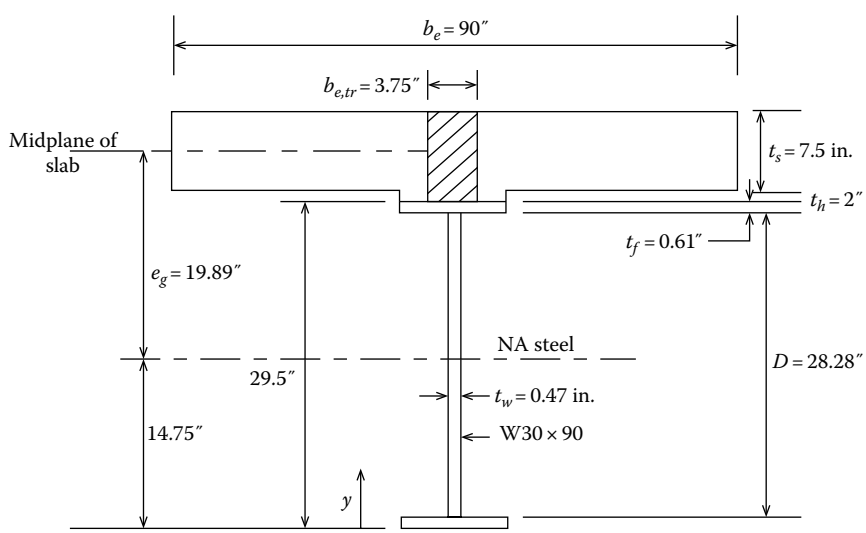

FIGURE 6.73 Computation of long-term properties of composite section.

Calculate the short-term and long-term section properties of the composite section. These section properties are computed with reference to Figures 6.72 and 6.73 (datum is selected at the bottom of the steel section).

Effective width, b_e = center-to-center spacing of girders = 7.5 ft = 90 in.

For f'_c = 4 ksi, n = 8 (Table 6.15)

$$\bar{y}_b = \frac{\Sigma A y_b}{\Sigma A} = \frac{3310}{110.68} = 29.91\,\text{in.}$$

$$I_c = 7932 + 4006 = 11{,}938 \text{ in.}^4$$

$$S^t_{ST} = \frac{11{,}938}{29.91 - 29.5} = 29{,}117 \text{ in.}^3 \text{ (top of steel)}$$

www.EngineeringEBooksPdf.com

TABLE 6.15
Short-Term Composite Section Properties: $n = 8$

Component	A, in.^{2}	y_b, in.	Ay_b, in.^{3}	$(y_b - \bar{y}_b)$, in.	$A(y_b - \bar{y}_b)^2$, in.^{4}	I_o, in.^{4}
Slab (90/8) × 7.5	84.38	34.64	2922	4.73	1888	396
Girder W30 × 90	26.30	14.75	388	15.16	6044	3610
Σ	110.68		3310		7932	4006

TABLE 6.16
Long-Term Composite Section Properties: $3n = 24$

Component	A, in.^{2}	y_b, in.	Ay_b, in.^{3}	$(y_b - \bar{y}_b)$, in.	$A(y_b - \bar{y}_b)^2$, in.^{4}	I_o, in.^{4}
Slab (90/24) × 7.5	28.13	34.64	974	9.62	2603	132
Girder W30 × 90	26.30	14.75	388	10.27	2774	3610
Σ	54.43		1362		5377	3742

$$S_{ST}^b = \frac{11{,}938}{29.91} = 399 \text{ in.}^3 \text{ (bottom of steel)} \quad (\text{Table 6.16})$$

$$\bar{y}_b = \frac{\Sigma A y_b}{\Sigma A} = \frac{1362}{54.43} = 25.02 \text{ in.}$$

$$I_c = 5377 + 3742 = 9119 \text{ in.}^4$$

$$S_{ST}^t = \frac{9119}{29.5 - 25.02} = 2035 \text{ in.}^3 \text{ (top of steel)}$$

$$S_{ST}^b = \frac{9119}{25.02} = 364 \text{ in.}^3 \text{ (bottom of steel)}$$

Calculate stresses in flanges as follows:

For M_{DC1}, use noncomposite section properties.
For M_{DC2} and M_{DW}, use long-term section properties.
For $1.3M_{LL+IM}$, use short-term properties.

Compressive stress (f_c) in the top flange of composite section:

$$f_c = \frac{298.1(12)}{245} + \frac{121.9(12)}{2{,}035} + \frac{835.5(12)}{29{,}117}$$

$$= 14.6 + 0.72 + 0.34 = 15.66 \text{ ksi}$$

$$f_f = 47.5 \text{ ksi} > f_c = 15.66 \text{ ksi, OK}$$

www.EngineeringEBooksPdf.com

Tensile stress (f_t) in the bottom flange of composite section:

$$f_t = \frac{298.1(12)}{245} + \frac{121.9(12)}{364} + \frac{835.5(12)}{399}$$

$$= 14.6 + 4.02 + 25.13 = 43.75 \text{ ksi} < f_f = 47.5 \text{ ksi, OK.}$$

So, the revised section, W30 × 90, satisfies the flange stress requirements. Compliance with the remaining LRFD provisions is checked as follows.

Design Loads
Both permanent and live loads are the same as before.

Calculate Design Loads (Factored Loads)
The following unfactored loads were calculated earlier:

$$M_{DC1} = 298.1 \text{ kip-ft}, \quad V_{DC1} = 23.85 \text{ kip}$$

$$M_{DC2} = 63.1 \text{ kip-ft}, \quad V_{DC2} = 5.05 \text{ kip}$$

$$M_{DW} = 58.8 \text{ kip-ft}, \quad V_{DW} = 4.7 \text{ kip}$$

$$M_{(L+IM)} = 1033.3 \text{ kip-ft}, \quad V_{L+I} = 93.94 \text{ kip}$$

Apply load factors to unfactored loads to calculate factored loads. The following unfactored loads were calculated earlier. Apply live load distribution factors to live load moment and shear.

Bending moment: $g_{mi} = 0.622$
Max *LL* moment in the interior girder = (0.622)(1033.3) = 642.71 kip-ft
Shear: $g_{vi2} = 0.779$

$$V_{L+IM} = (0.779)(93.94) = 73.18 \text{ kip}$$

Calculate Loads for Strength I Limit State

Factored Loads: Moments

$$M_u = \Sigma\eta_i\gamma_i M_i$$

$$\eta_i = \eta_D\eta_R\eta_I \text{ (Art. 1.3.2.1)}$$

Select Load Modifiers

Ductility, $\eta_D = 1.0$ (Art. 1.3.3).
Redundancy, $\eta_R = 1.0$ (Art. 1.3.4)
Importance, $\eta_I = 1.0$ (Art. 1.3.5)

Therefore, $M_u = \eta\Sigma\gamma_i M_i$

$$M_u = 1.0\ [1.25M_{DC} + 1.5M_{DW} + 1.75(M_{LL+IM})]$$

$$= 1.0\ [1.25(361.2) + 1.5(58.8) + 1.75(642.71)]$$

$$= 1664 \text{ kip-ft}$$

www.EngineeringEBooksPdf.com

Factored Loads: Shear

$$V_u = 1.0\ [1.25V_{DC} + 1.5V_{DW} + 1.75(V_{LL+IM})]$$

$$= 1.0\ [1.25(28.9) + 1.5(4.7) + 1.75(93.94)]$$

$$= 207.57 \text{ kip} \approx 208 \text{ kip}$$

Plastic Strength of Composite Section

Ignore contribution from longitudinal reinforcement (for simplicity).

Effective width of flange = center to center of girders = 7 ft 6 in. = 90 in.

Maximum compressive force in the slab:

$$P_s = 0.85f'_c b_s t_s$$

$$= 0.85(4.0)(90)(7.5) = 2295 \text{ kip}$$

Maximum compressive force in the steel section:

$$P_{steel} = A_{steel}F_y = (26.3)(50) = 1315 \text{ kip}$$

Since $P_s > P_{steel}$, the PNA must lie in the slab. Let $\bar{Y}$ be the depth of PNA below the top of the deck slab. Then, the compressive force in the slab is

$$P_s = 0.85f'_c b_s \bar{Y}$$

For horizontal equilibrium, we must have

$$0.85f'_c b_s \bar{Y} = 1315 \text{ kip}$$

$$0.85(A)(90)\bar{Y} = 1315$$

whence $\bar{Y}$ = 4.3 in.

Alternatively, using LRFD Table D6.1-1, Case V, $\bar{Y}$ can be determined from the following expression:

$$\bar{Y} = (t_s)\frac{P_{rb} + P_c + P_w + P_t - P_{rt}}{P_s}$$

Since contribution from longitudinal reinforcement is ignored,

$$P_{rb} = P_{rt} = 0$$

$$P_{steel} = P_c + P_w + P_t = 1315 \text{ kip}$$

$$P_s = 2295 \text{ kip}$$

Consequently,

$$\bar{Y} = (7.5)\frac{0 + 1315 - 0}{2295} = 4.3 \text{ in.}$$

Referring to Figure 6.74,

$$\text{Lever arm} = 14.75 + 2 - 0.61 + 7.5 - 0.5(4.3)$$

$$= 21.49 \text{ in.}$$

www.EngineeringEBooksPdf.com

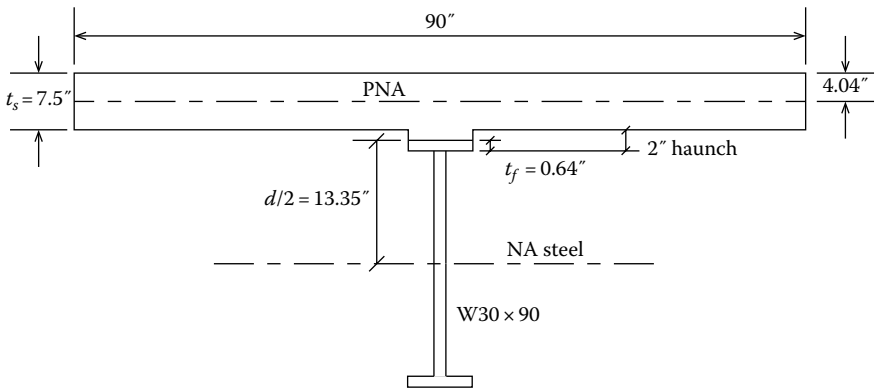

FIGURE 6.74 Determination of PNA and the plastic moment strength of composite section.

$$\phi_m M_n = 1.0(1315)(24.19)$$

$$= 28{,}259 \text{ kip-in.}$$

$$= 2355 \text{ kip-ft}$$

$$M_u \leq \phi_m M_n$$

$$1664 \text{ kip-ft} \leq 2355 \text{ kip-ft, OK}$$

Check the Ductility Requirement (Art. 6.10.7.3)

$$D_p \leq 0.4D_t$$

Overall depth of composite section, $D_t = t_s + t_h + d - t_f$

$$= 7.5 + 2.0 + 29.5 - 0.61$$

$$= 38.39 \text{ in.}$$

$$0.4D_t = 0.42(38.39) = 16.12 \text{ in.}$$

$$D_p = \bar{Y} = 4.3 \text{ in.} \leq 16.12 \text{ in., OK.}$$

Check Member Properties: (Art. 6.10.1.1)

Check compliance for section properties (Art. 6.7.3, 6.10.2)
The section properties of W30 × 90 are as follows:

$$A = 26.3 \text{ in.}^2, \quad d = 29.5 \text{ in.}, \quad t_w = 0.47 \text{ in.}, \quad b_f = 10.4 \text{ in.}, \quad t_f = 0.61 \text{ in.},$$

$$I_x = 3610 \text{ in.}^4, \quad S_x = 245 \text{ in.}^3$$

Web thickness to be not less than 0.25 in.

$$t_w = 0.47 \text{ in.} > 0.25 \text{ in., OK}$$

$$b_f \geq \frac{D}{6}$$

www.EngineeringEBooksPdf.com

$$D = d - 2t_f = 29.5 - 2(0.61) = 28.28 \text{ in.}$$

$$10.4 \geq \frac{28.28}{6} = 4.71 \text{ in. OK}$$

$$\frac{D}{t_w} \leq 150$$

$$\frac{D}{t_w} = \frac{28.28}{0.47} = 60.17 \leq 150, \text{ OK}$$

$$\frac{b_f}{2t_f} \leq 12$$

$$\frac{b_f}{2t_f} = \frac{10.4}{2(0.61)} = 8.52 \leq 12, \text{ OK}$$

$$t_f \geq 1.1t_w$$

$$0.61 \geq 1.1(0.47) = 0.52 \text{ in., OK}$$

$$b_{fc} = \frac{L}{85} \text{ (Art. 6.10.3.4)}$$

$$10.4 \geq \frac{50(12)}{85} = 7.06, \text{ OK}$$

For handling, check if $0.1 \leq I_{yc}/I_{yt} \leq 10$

where

I_{yc} = moment of inertia of compression flange about the vertical axis of the web
I_{yt} = moment of inertia of tension flange about the vertical axis of the web

For a rolled section, $I_{yc} = I_{yt}$; therefore, $I_{yc}/I_{yt} = 1.0$

$$0.1 \leq 1.0 \leq 10, \text{ OK}$$

Constructibility
Check the resistance of girders during construction.

1. General: Art. 2.5.3 and 6.10.3.1
   Check the resistance of girders (W30 × 90) during construction. Ensure that the compression flanges of the girders are adequately braced to preclude the possibility of LTB while the deck concrete is wet and the section acts as noncomposite. Nominal yielding or reliance on post-buckling resistance is not permitted during construction.
2. Local buckling: Art. 6.10.3.2.1
   The rolled W30 × 99 would not have any local buckling issues during construction.
3. Flexure: Art. 6.10.3.2 and 6.10.8
   Check compliance with Art. 6.10.8.2.1: Compression-flange flexural resistance
   Compression flange flexural resistance should be checked for local buckling and LTB using the appropriate value of the nominal flexural resistance of the compression flange, F_{nc}, as specified in Art. 6.10.8.2.2 and 6.10.8.2.3.

www.EngineeringEBooksPdf.com

4. *Art. 6.10.8.2.2: Local buckling resistance*
The rolled wide flange section would not have any local buckling issues. However, calculations are provided for illustrative purposes.

$$\lambda_f = \frac{b_f}{2t_f} = \frac{10.4}{2(0.61)} = 8.52$$

$$\lambda_{pf} = 0.38\sqrt{\frac{E}{F_{yc}}} = 0.38\sqrt{\frac{29{,}000}{50}} = 9.15$$

$$\lambda_f = 8.52 \le \lambda_{pf} = 9.15$$

Therefore, $F_{nc} = R_b R_h F_{yc}$

where
R_b = web-shedding factor (Art. 6.10.1.10.2)
R_h = hybrid factor (Art. 6.10.1.10.1)

The web-shedding factor, R_b, is determined as specified in Art. 6.10.1.10.2. The section is composite and it is in positive flexure and satisfies the requirements of Art. 6.10.2.1.1 (web without longitudinal stiffeners):

$$\frac{D}{t_w} = \frac{28.28}{0.47} = 60.17 \le 150, \text{ OK}$$

Therefore, R_b = 1.0. For rolled shapes, R_h = 1.0 (Art. 6.10.1.10). Therefore,

$$F_{nc} = R_b R_h F_{yc} = (1.0)(1.0(50) = 50 \text{ ksi}$$

5. *Art. 6.10.8.2.3: LTB resistance*
The compression flange is not laterally braced, and the section acts as noncomposite when deck concrete is being poured. Check LTB resistance of the compression flange for this construction condition. Calculate L_p and L_r, and select a suitable value of bracing interval, L_b; then calculate F_{nc} from LRFD Equation 6.10.8.2.3-1.
L_p = limiting unbraced length to achieve the nominal flexural resistance of $R_b R_h F_{yc}$ under uniform bending

$$= 1.0 r_t \sqrt{\frac{E}{F_{yc}}} \qquad (6.75)\ [A6.10.8.2.3\text{-}4]$$

L_r = limiting unbraced length to achieve the onset of nominal yielding in either flange under uniform bending with a consideration of compression residual stress effects (in.)

$$= \pi r_t \sqrt{\frac{E}{F_{yr}}} \qquad (6.76)\ [A6.10.8.2.3\text{-}5]$$

F_{yc} = specified minimum yield strength of compression flange (ksi)
F_{yr} = compression flange stress at the onset of nominal yielding within the cross section, including residual stress effects, but not including compression flange-lateral bending,
= smaller of $0.7F_{yc}$ and F_{yw} but not less than $0.5F_{yc}$
r_t = effective radius of gyration for LTB (Equation 6.27 [A6.10.8.2.3-9])

www.EngineeringEBooksPdf.com

Calculate r_t.

$$r_t = \frac{b_{fc}}{\sqrt{12\left(1+\frac{1}{3}\frac{D_c t_w}{b_{fc} t_{fc}}\right)}} \qquad (6.27)\ [A6.10.8.2.3\text{-}9]$$

For a W30 × 90, $b_{fc} = 10.4$ in., $t_{fc} = 0.61$ in., $D_c = D/2 = 28.28/2 = 14.14$ in., $t_w = 0.47$ in.

$$r_t = \frac{10.4}{\sqrt{12\left(1+\frac{1}{3}\frac{(14.14)(0.47)}{(10.4)(0.61)}\right)}} = 2.58 \text{ in.}$$

$$L_p = 1.0 r_t \sqrt{\frac{E}{F_{yc}}} = 1.0(2.58)\sqrt{\frac{29{,}000}{50}} \approx 62.0 \text{ in.}$$

$$L_r = \pi r_t \sqrt{\frac{E}{F_{yr}}} = \pi(2.58)\sqrt{\frac{29{,}000}{0.7(50)}} \approx 233 \text{ in.}$$

Try bracings at quarter points, $L_b = \frac{50}{4} = 12.5 \text{ ft} = 150 \text{ in.}$

Note: These braces would be temporary; to be kept in place until the deck concrete hardens, following which they may be removed. Continuous lateral support to compression flanges would be provided by the composite action after the concrete hardens. Calculate F_{nc} (Equation 6.71 [A6.10.8.2.3-2]) and then calculate f_{bu} (Equation A6.10.3.2.1-2).

$$F_{nc} = C_b\left[1-\left(1-\frac{F_{yr}}{R_h F_{yc}}\right)\left(\frac{L_b - L_p}{L_r - L_p}\right)\right] R_b R_h F_{yc} \le R_b R_h F_{yc}$$

$$= 1.0\left[1-\left(1-\frac{0.7F_{yc}}{1.0F_{yc}}\right)\left(\frac{150-62.0}{233-62.0}\right)\right](1.0)(1.0)(50) \le 50 \text{ ksi}$$

$$= 42.28 \text{ ksi} < 50 \text{ ksi, OK.} \qquad (6.71)\ [A6.10.8.2.3\text{-}2]$$

Note that in the previous calculations, $C_b = 1.0$ has been conservatively assumed equal to 1.0, which is valid for only the uniform moment, which is not the case here. For the present case, $C_b > 1.0$. Exact value of C_b can be determined from Equation 6.25 if necessary.

Calculate the load effect under construction. The flange lateral-bending stress, f_l, is negligible for the rolled wide flange shape and is ignored.

$$M_u = 1.25 M_{DC} = 1.25(298.1) = 372.63 \text{ kip-ft}$$

$$f_u = \frac{M_u}{S_x} = \frac{372.63(12)}{245} = 18.25 \text{ ksi} \ll F_{nc} = 42.28 \text{ ksi}$$

Flange lateral bending stress, f_ℓ, for a rolled section is negligible and is ignored.

$$f_{bu} + \frac{1}{3} f_\ell = 42.05 + 0 = 42.05 \text{ ksi} < \phi_f F_{nc} = (1.0)(42.05) = 42.05 \text{ ksi, OK.}$$

Provide lateral bracings at quarter points, that is, at 12 ft 6 in. intervals. These would be again considered later for wind bracings.

www.EngineeringEBooksPdf.com

Check compliance with Equation 6.32 (A6.10.1.3.2-3) to ensure that theoretical web bend-buckling would not occur during construction.

$$f_{bu} \leq \phi F_{crw}$$

where F_{crw} is computed from Equation A6.10.1.9.1-1.

$F_{crw} = \dfrac{0.9\,Ek}{\left(\dfrac{D}{t_w}\right)^2}$ but not to exceed R_hF_y or $F_{yw}/0.7$

k = bend-buckling coefficient = $\dfrac{9}{\left(\dfrac{D_c}{D}\right)^2}$

For W30 × 90 rolled section, $D_c = 0.5D$, so $D_c/D = 0.5$

$$k = \frac{9}{(0.5)^2} = 36$$

$$F_{crw} = \frac{0.9(29{,}000)(36)}{\left(\dfrac{28.28}{0.47}\right)^2} = 260 \text{ ksi} > R_hF_{yc} = (1.0)(50) = 50 \text{ ksi}$$

$$\frac{F_{yw}}{0.7} = \frac{50.0}{0.7} = 71.43 \text{ ksi} > 50 \text{ ksi}$$

So, F_{crw} = 50 ksi

$$F_{bu} = 18.25 \text{ ksi} < F_{crw} = 50 \text{ ksi, OK}$$

6. *Check for shear (Art. 6.10.9.2, Art. 6.10.10.3): Shear strength of unstiffened webs*
Generally speaking, for rolled wide flange beams such as one used in this example, shear is not a matter of concern. However, all calculations are provided for completeness.

$$V_u \leq \phi_v V_n \qquad (6.77)\ [A6.10.9.1\text{-}1]$$

$$V_n = V_{cr} = CV_p \qquad (6.78)\ [A6.10.9.2\text{-}1]$$

$$V_p = 0.58F_yDt_w \qquad (6.79)\ [A6.10.9.2\text{-}2]$$

where

V_u = shear due to factored loads
V_{cr} = critical buckling resistance
V_p = plastic shear resistance
C = critical buckling coefficient (from Equations 6.78 through 6.80 as applicable and k = 5 for unstiffened webs)

$$\begin{aligned} V_p &= 0.58F_{yw}Dt_w \\ &= 0.58(50)(28.28)(0.47) \\ &= 385 \text{ kip} \qquad (6.79)\ [A6.10.9.2\text{-}2] \end{aligned}$$

Calculate the critical buckling coefficient, C. For a W30 × 90, D = 28.28 in, t_w = 0.47 in.

$$\frac{D}{t_w} = \frac{28.28}{0.47} = 60.17$$

www.EngineeringEBooksPdf.com

$$1.12\sqrt{\frac{Ek}{F_{yw}}} = 1.12\sqrt{\frac{29{,}000(5)}{50}} = 60.31 > \frac{D}{t_w} = 60.17$$

Therefore, $C = 1.0$.

$$V_n = V_{cr} = CV_p = (1.0)(385) = 385 \text{ kip}$$

$$\phi_v V_{cr} = 1.0(385) = 385 \text{ kip}$$

$$1.25V_{DC1} = 1.25\ (23.85) = 29.81 \text{ kip} < 385 \text{ kip, OK}$$

7. *Deck placement: Art. 6.10.3.4*
   Sections that are composite in the final condition but are noncomposite during construction (as in this example) must be checked for flexure as specified in Art. 6.10.3.2 during various stages of construction. For the 50 ft short-span bridge in this example, the entire deck would be cast in one operation. Therefore, staged construction need not be considered. Calculations demonstrating compliance with Art. 6.10.3.2 have been provided earlier.

Service Limit State (Art 6.5.2, 6.10.4)

Art. 6.10.4.1: Compliance with 2.5.2.6 is required.

Optional live load deflection control:

Since no deflection criteria are specified, optional deflection criteria (Art. 2.6.2.6.2) will be used in this example.

Allowable deflection due to vehicular load, $\Delta_{LL} = \frac{span}{800} = \frac{50(12)}{800} = 0.75$ in.

Art. 3.6.1.3.2: Calculated deflection will be taken as the larger of the following as discussed in Section 2.6.3:

1. Deflection due to design truck alone. Dynamic load allowance will be applied to this deflection.
2. Deflection due to 25 percent of the deflection due to the design truck *plus* deflection due to lane load. Dynamic load allowance is not applied to the deflection due to the lane load.

Calculate Deflection due to Vehicular Live Load

Live load deflections would be computed for the governing loading conditions—separately for the design truck and lane (Figure 6.51)—by the usual methods of computing deflections. Formulas for relevant load cases given in AISC Steel Construction Manual (AISC 2011) would be used (see discussion in Section 2.6.6). Referenced formulas used in calculations are taken from Chapter 2. For the noncomposite beams used in this example, the moment of inertia, I, of the steel section would be used for calculating deflections.

Deflection due to the Design Truck

As discussed in Section 2.6.6, in the case of the design truck loading it is difficult, although theoretically possible, to determine the exact positions of the three axles that will result in maximum deflection. As a practical matter, however, the maximum deflection in the girder would be computed by placing the middle 32 kip load at the midspan, and the other two loads placed 14 ft apart, one on each side of the midspan (Figure 6.52). This loading case can be split into two separate cases (AISC 2011):

1. Load Case 7 for the centrally placed point load
2. Load Case 8 for point load placed off the midspan

www.EngineeringEBooksPdf.com

For the centrally placed point load P (Load Case 7, Figure 6.52a), the maximum deflection occurs at the center that can be calculated from the following:

$$\Delta_c = \frac{PL^3}{48EI_c} \tag{2.2}$$

where
Δ_c = deflection at midspan due to point load
L = span
E = modulus of elasticity
I_c = moment of inertia of composite section

Substitute P = 32 kip, L = 50 ft, E = 29,000 ksi, and I_c = 11,938 in.^{4} in Equation 2.2R. The deflection at the midspan is

$$\Delta_c = \frac{32(50)^3(12)^3}{48(29,000)(11,938)} = 0.42 \text{ in.}$$

For the remaining axle loads that are placed off-center on the span, Load Case 8 would be used:

$$\Delta_x = \frac{Pbx\left(L^2 - b^2 - x^2\right)}{6EIL} \tag{2.3}$$

For the 32 kip load left of the midspan, measure all distances from the right support B so a = 39 ft, b = 11 ft, x = 25 ft < a = 39 ft. The deflection at the span due to this 32 kip load is calculated from Equation 2.3R:

$$\Delta_{x=25\,ft} = \frac{32(11)(25)[(50)^2 - (11)^2 - (25)^2]}{6(29,000)(11,938)(50)}(12)^3 = 0.26 \text{ in.}$$

For the 8 kip load right of the midspan, measure all distances from the left support A so a = 39 ft, b = 11 ft, x = 25 ft < a = 39 ft. The deflection at the span due to this 8 kip load is calculated again from Equation 2.3R:

$$\Delta_{x=25\,ft} = \frac{8(11)(25)[(50)^2 - (11)^2 - (25)^2]}{6(29,000)(11,938)(50)}(12)^3 = 0.06 \text{ in.}$$

Total deflection due to the design truck, Δ_c = 0.42 + 0.26 + 0.06 = 0.74 in.

Apply dynamic load allowance (1 + 0.33) and distribution factor for live load deflection (= 0.4, computed earlier).

Maximum deflection in the girder, Δ_{truck} = (0.74)(1.33)(0.4) = 0.40 in.

Deflection Due to Lane Load

For the case of lane loading (uniform load), the maximum midspan deflection is calculated from Equation 2.9 (Case 1, AISC 2011):

$$\Delta_{lane} = \frac{5wL^4}{384EI_c} \tag{2.9}$$

where
w = 0.64 kip/ft
L = span = 50 ft

www.EngineeringEBooksPdf.com

$$\Delta_{lane.max} = \frac{5(0.64)(50)^4(12)^3}{384(29{,}000)(11{,}938)} = 0.26 \text{ in.}$$

Apply live load distribution factor for live load (= 0.4). The maximum midspan deflection due to the lane load is as follows:

$$\Delta_{lane} = (0.26)(0.4) = 0.10 \text{ in.}$$

Compare deflections (Art. 3.6.1.3.1):

$$0.25\Delta_{truck} + \Delta_{lane} = 0.25(0.40) + 0.10 = 0.20 \text{ in.} < \Delta_{truck} = 0.40 \text{ in.}$$

$$\Delta_{truck} = 0.40 \text{ in. (the larger value governs)}$$

Allowable live load deflection, $\Delta_{allowable} = \frac{L}{800} = \frac{50 \times 12}{800} = 0.75 \text{ in.} > 0.40 \text{ in., OK.}$

Optional Criteria for Span-to-Depth Ratio (Art. 2.5.2.6.3)
The owner may invoke the minimum girder depth equal to $0.033L$ as specified in Chapter 2, Table 2.5 (LRFD Table 2.5.2.6.3-1). For this example,

$$0.033(50)(12) = 19.8 \text{ in.} < d = 32.9 \text{ in., OK}$$

Span-to-depth ratio is satisfied.

a. *Optional criteria for span-to-depth ratio (Art. 2.5.2.6.3)*
   The owner may invoke the minimum girder depth ratios as specified in LRFD Table 2.5.2.6.3-1. Check if the span-to-depth ratio is satisfied. For this example,
   i. Overall depth of composite section:
      Overall depth of composite section, $D_t = 38.39$ in. (computed earlier)
      Minimum depth of composite section = $0.04L = 0.04(50)(12) = 24$ in.

$$D_t = 38.39 \text{ in} > 0.04L = 24 \text{ in., OK}$$

   ii. Depth of the I-beam portion of composite beam:

$$d = 29.5 \text{ in.}$$

$$0.033(50)(12) = 19.8 \text{ in.} < d = 29.5 \text{ in., OK}$$

Optional criteria for span-to-depth ratio is satisfied.

Strength Limit State: Check for Shear (Art. 6.10.9.2)
Generally speaking, for rolled wide flange beams such as one used in this example, shear is not a matter of concern. However, all calculations are provided for completeness.

$$V_u \le \phi_v V_n \qquad (6.77)\ [A6.10.9.1\text{-}1]$$

$$V_n = V_{cr} = CV_p \qquad (6.78)\ [A6.10.9.2\text{-}1]$$

www.EngineeringEBooksPdf.com

$$V_p = 0.58F_yDt_w \qquad (6.79)\ [A6.10.9.2\text{-}2]$$

where
V_u = shear due to factored loads
V_{cr} = critical buckling resistance
V_p = plastic shear resistance
C = critical buckling coefficient (from Equations 6.80 through 6.82 as applicable and $k = 5$ for unstiffened webs)

For a W30 × 90, $\phi_v V_{cr} = 1.0(385) = 385$ kip (calculated earlier)

Strength I Limit State load combination:

$$V_u = 1.0[1.25DC + 1.5DW + 1.75(LL + IM)]$$

$$= 1.0[1.25(29.4) + 1.5(4.7) + 1.75(93.4)]$$

$$= 208.\ 2 \text{ kip}$$

$$\phi_v V_{cr} = 385 \text{ kip} > V_u = 208.2 \text{ kip, OK}$$

Fatigue and Fracture Limit State: Art. 6.6.1.2 and 6.10.5
The number of shear studs required will be calculated separately for

a. Fatigue limit state
b. Strength limit state

a. Shear Connectors Required to Satisfy Fatigue Limit State

Check compliance for load-induced fatigue requirements (Art. 6.6.1.2 and 6.10.5.1, 6.6.1)

Allowable fatigue stress range depends on the frequency of load cycles as discussed in Section 3.9.4 (Art. 6.6.1.2.1).

1. Determine the frequency of truck loads on the bridge.
   For a rural interstate highway, the number of vehicles per lane per day = 20,000 (LRFD C3.6.1.4.2)

   $$ADT = 20{,}000 \text{ per lane per day}$$

   Fraction of trucks in traffic on a rural interstate = 0.20 (Table 3.20)

   $$ADTT = 0.2(ADT) = 0.2(20{,}000)(2 \text{ lanes}) = 8000 \text{ trucks/day}$$

   For two lanes, fraction of truck traffic in a single lane, $p = 0.85$ (Table 3.21)

   $$ADTT_{SL} = 0.85(8000) = 6800 \text{ trucks/day}$$

2. Determine allowable fatigue stress range
   For detailing purposes, the design component (the steel girder) is assumed as uncoated weathering steel, which falls in Category B Case 1.2, Table 6.A.3-1 (LRFD Table 6.6.1.2.3-1, noncoated weathering steel base metal with rolled or cleaned surfaces and detailed in accordance FHWA [1989]). For this detail category, the listed CAFT value, $(\Delta F)_{TH}$, corresponding to this detail category for infinite fatigue life is as follows:

   $$(\Delta F)_{TH} = 16 \text{ ksi}$$

   Therefore, the nominal fatigue resistance, $(\Delta F)_n = (\Delta F)_{TH} = 16$ ksi

www.EngineeringEBooksPdf.com

3. The calculated $(ADTT)_{SL}$ = 6800 trucks per day far exceeds 860 trucks/day (75-year $(ADTT)_{SL}$ equivalent to infinite life) as listed in Table 6.3. Therefore, Fatigue I Limit State load combination would be used, with $\gamma = 1.5$.

   For fatigue loading, only one truck is placed on the bridge as explained in Section 3.9.2. The live load moment due to the fatigue loading is determined from the following (Chapter 3):

$$M_{fat} = \frac{72x}{L}\left(L - x - 11.78\right) - 112 \tag{3.41}$$

For L = 50 ft, x = 25 ft (at midspan),

$$M_{fat} = \frac{72(25)}{50}\left(50 - 25 - 11.78\right) - 112$$
$$= 363{,}92 \text{ kip-ft}$$

Apply the following modifiers to M_{fat}.

IM = 0.15; multiply by 1.15
Live load distribution factor for fatigue, $g_{mi1,fat} = 0.389$
Load factor for Fatigue I limit state, $\gamma = 1.5$
$M_{ftt1} = 1.5(363.92)(1.15)(0.389) = 244.2$ kip-ft

Calculate the live load stress range:

$$f = \frac{M_{fat\,I}}{S_x} = \frac{244.2(12)}{245} = 12.00 \text{ ksi} < \left(\Delta F\right)_{TH} = 16.0 \text{ ksi, OK.}$$

Since the live load stress range (f = 12.00 ksi) is smaller than the constant amplitude fatigue threshold value ($(\Delta F)_{TH}$ = 16 ksi), infinite fatigue life is OK, and check for finite fatigue life is not warranted.

Fatigue I Limit State shear loads are much smaller than the factored shear in Strength I Limit State. For this composite superstructure using rolled wide flange shapes, fatigue is not a matter of concern. However, calculations for fatigue loads are provided for completeness.

Maximum shear due to fatigue loads is calculated from Equation 3.42:

$$V_{fat} = 72 - \frac{1312}{L} = 72 - \frac{1312}{50} = 45.76 \text{ kip}$$

IM = 0.15, distribution factor for fatigue, $g_{vi1,fat} = 0.55$

$$V_{fat1} = \gamma[V(LL + IM)(g_{i1,fat})] = 1.5[45.76(1 + 0.15)(0.55)] = 43.42 \text{ kip}$$

$$\phi_v V_{cr} = 385 \text{ kip} \gg V_{fat} = 43.42 \text{ kip, OK}$$

a. Fracture: special requirements for webs, Art. 6.10.5.2
Check that

$$V_u \le \phi_v V_{cr} \tag{6.44} \text{ [A6.10.5.3-1]}$$

where
V_u = shear in the web at the section under consideration due to unfactored permanent loads plus the factored fatigue load
V_{cr} = shear buckling resistance determined from Equation 6.43 (A6.10.9.3.3-1)

www.EngineeringEBooksPdf.com

$$V_u = V_{DC} + V_{DW} + 1.5(V_{fat+im})(g_{vi1,fat})$$

$$= 29.4 + 4.7 + 43.42 = 77.52 \text{ kip}$$

$$\phi_v V_{cr} = 385 \text{ kip} \gg V_u = 77.52 \text{ kip, OK}$$

Calculate fatigue resistance of 4 in. high, 3/4 in. diameter headed shear studs. First check the height-to-diameter ratio of the stud.

$$\frac{h}{d} = \frac{4}{0.75} = 5.33 > 4, \text{ OK}$$

Because the number of trucks (6800) is greater than 960, the fatigue resistance of the shear connector is controlled by the infinite life criterion as determined from the following:

$$Z_r = 5.5d^2$$

$$= 5.5(0.75)^2$$

$$= 3.09 \text{ kip} \qquad (6.89) \text{ [A6.10.10.2-1]}$$

Based on $Z_r = 3.09$ kip, pitch p of shear studs at $0.1L$ intervals along the span would be determined from the following:

$$p \le \frac{nZ_r I}{V_f Q} \qquad (6.102)$$

Calculate the range of shear, V_r, at $0.1L$ intervals along the span due to HL-93 truck. Design value of range of shear, V_f, would be calculated later from values of V_r. Note that for determining the force effects due to fatigue, the distance between the two rear 32 kip axles of HL-93 truck (herein after referred to as *fatigue* truck) is maintained at a constant distance of 30 ft (instead of 14 ft); lane load is not to be used for this purpose (Art. 3.6.1.4.1). Method of influence lines is used to determine maximum positive and maximum negative shear at $0.1L$ intervals; these values are determined for half span only.

Range of shear force at $x = 0$ ft from the left support.

Figure 6.75 shows the influence line for maximum shear at the support (same as the influence line for reaction at the left support).

From the influence line,

$$V_{max}^{+} = \text{Reaction at A}$$

$$= \sum P_i y_i$$

$$= 32(1+0.4) + 8(0.12) = 45.76 \text{ kip}$$

$$V_{max}^{-} = 0$$

Range of shear, $V_r = V_{max}^{+} - V_{max}^{-} = 45.76 - 0 = 45.76$ kip

6. Range of shear force at $x = 0.1L = 0.1(50) = 5.0$ ft from the left support.
   Figure 6.76 shows the influence line for shear at $x = 5.0$ ft from the left support.

www.EngineeringEBooksPdf.com

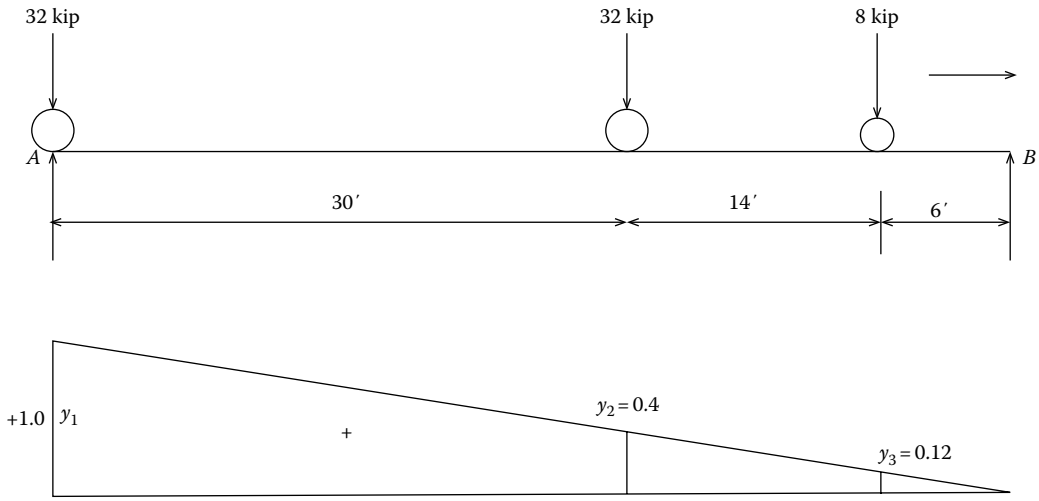

FIGURE 6.75 Influence line for maximum live load shear due to fatigue truck at the left support.

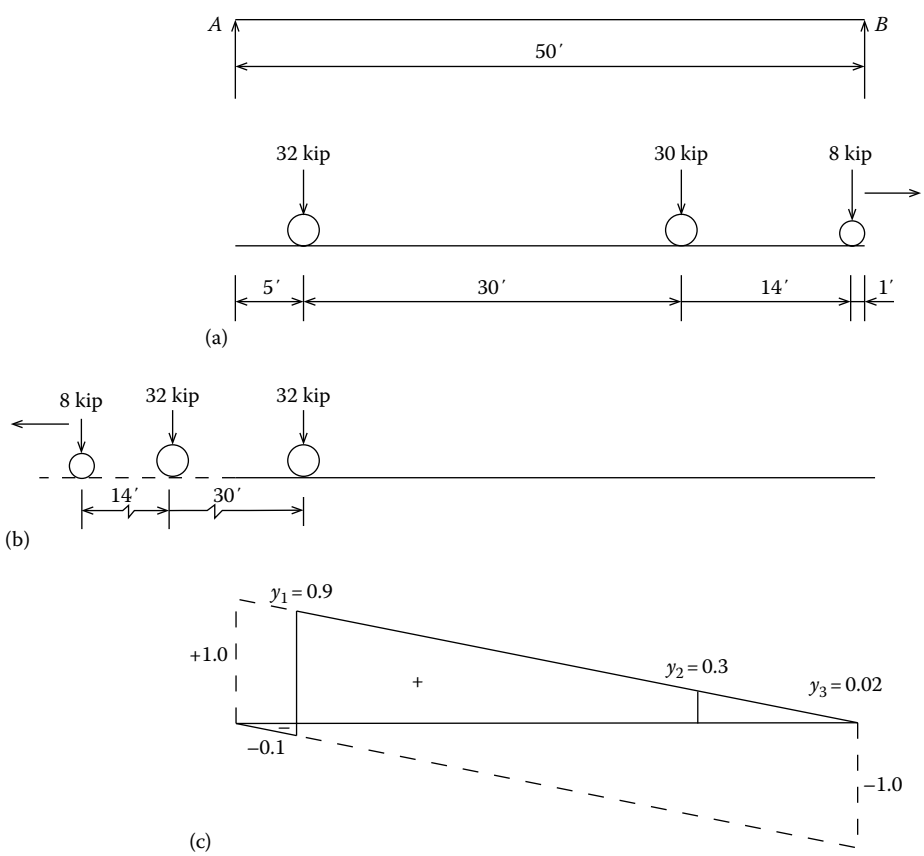

FIGURE 6.76 Influence line for shear at $x = 0.1L = 5.0$ ft from the left support. Position of the fatigue truck (a) maximum positive shear, (b) maximum negative shear, and (c) influence line.

www.EngineeringEBooksPdf.com

From the influence line,

$$V_{max}^{+} = \sum P_i y_i$$

$$= 32(0.9 + 0.3) + 8(0.02) = 38.56 \text{ kip}$$

$$V_{max}^{-} = \sum P_i y_i = 32(-0.1) = -3.2 \text{ kip}$$

Range of shear, $V_r = V_{max}^{+} - V_{max}^{-} = 38.56 - (-3.2) = 41.76$ kip

7. Range of shear force at $x = 0.2L = 0.2(50) = 10$ ft from the left support.
   Figure 6.77 shows the influence line for shear at $x = 10$ ft from the left support.
   From the influence line,

$$V_{max}^{+} = \sum P_i y_i$$

$$= 32(0.8 + 0.2) + 8(0.0) = 32.0 \text{ kip}$$

$$V_{max}^{-} = \sum P_i y_i = 32(-0.2) = -6.4 \text{ kip}$$

Range of shear, $V_r = V_{max}^{+} - V_{max}^{-} = 32.0 - (-6.4) = 38.4$ kip

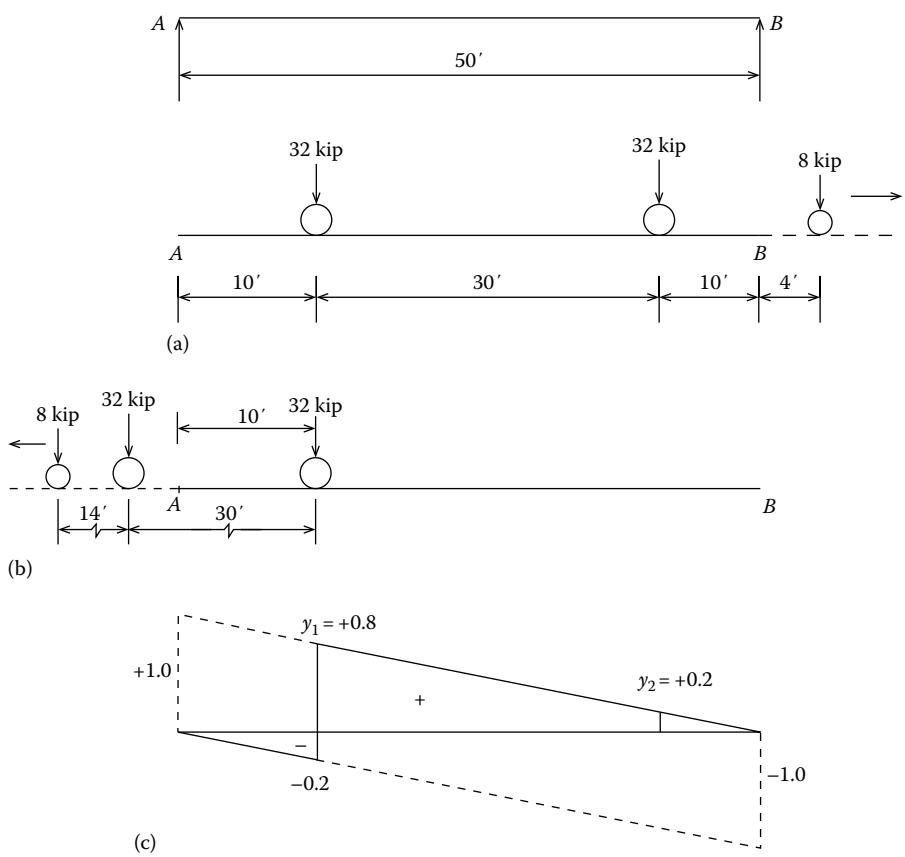

FIGURE 6.77 Influence line for shear at $x = 0.2L = 10$ ft from the left support. Position of the fatigue truck (a) for maximum positive shear and (b) for maximum negative shear, and (c) influence line.

www.EngineeringEBooksPdf.com

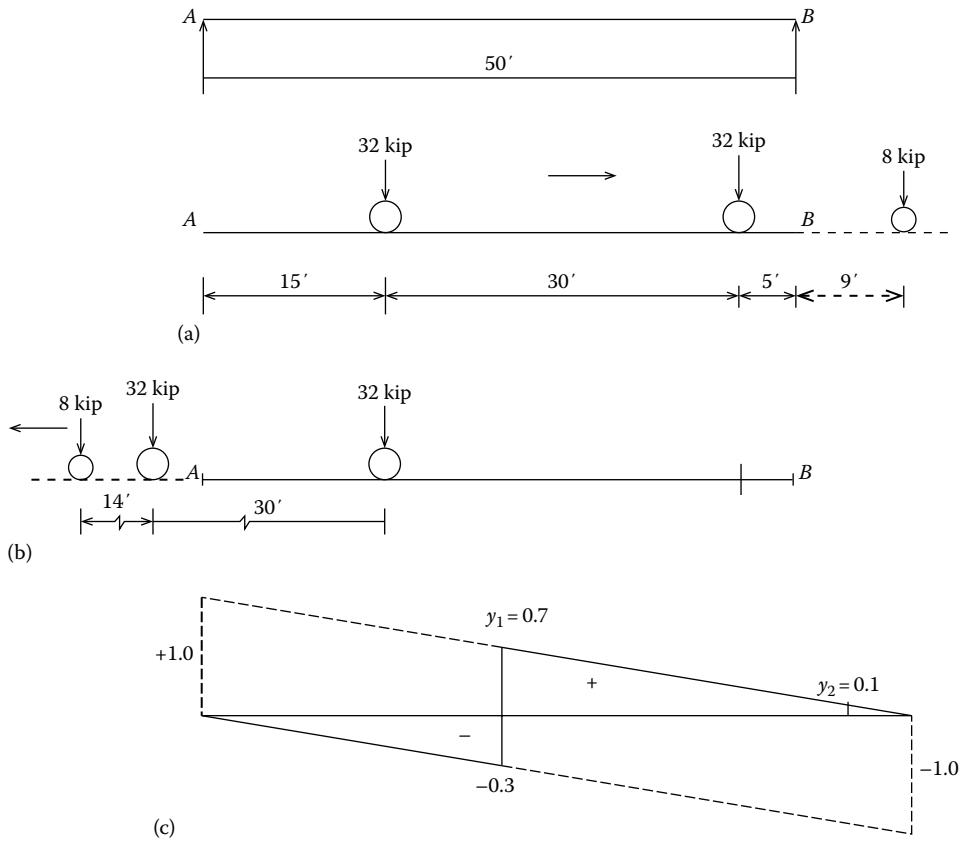

FIGURE 6.78 Influence line for shear at $x = 0.3L = 15$ ft from the left support. Position of the fatigue truck for (a) maximum positive shear, (b) maximum negative shear, and (c) influence line.

8. Range of shear force at $x = 0.3L = 0.3(50) = 15$ ft from the left support.
   Figure 6.78 shows the influence line for shear at $x = 15$ ft from the left support.
   From the influence line,

$$V_{max}^{+} = \sum P_i y_i$$

$$= 32(0.7 + 0.1) + 8(0.0) = 25.6 \text{ kip}$$

$$V_{max}^{-} = \sum P_i y_i = 32(-0.3) = -9.6 \text{ kip}$$

   Range of shear, $V_r = V_{max}^{+} - V_{max}^{-} = 25.6 - (-9.6) = 35.2$ kip
9. Range of shear force at $x = 0.4L = 0.4(50) = 20$ ft from the left support.
   Figure 6.79 shows the influence line for shear at $x = 20$ ft from the left support.
   From the influence line,

$$V_{max}^{+} = \sum P_i y_i$$

$$= 32(0.6) + 8(0.32) = 21.67 \text{ kip}$$

$$V_{max}^{-} = \sum P_i y_i = 32(-0.4) = -12.8 \text{ kip}$$

   Range of shear, $V_r = V_{max}^{+} - V_{max}^{-} = 21.76 - (-12.8) = 34.56$ kip

www.EngineeringEBooksPdf.com

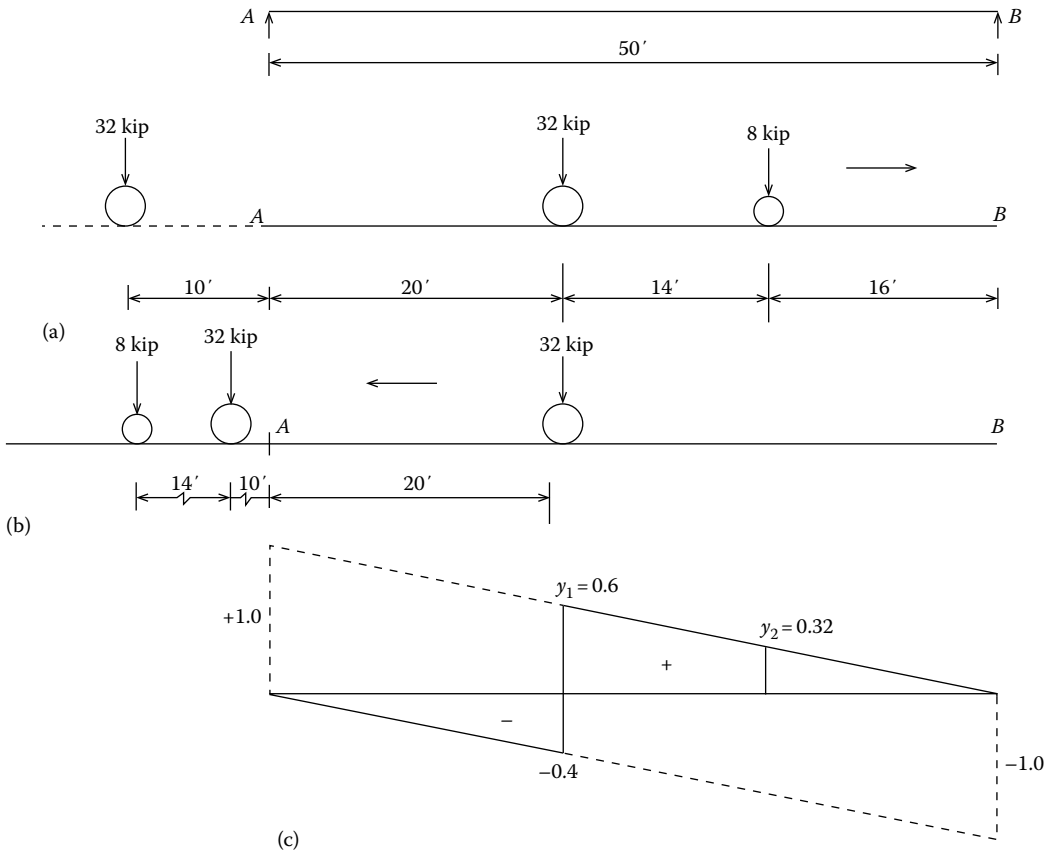

FIGURE 6.79 Influence line for shear at $x = 0.4L = 20$ ft from the left support. Position of the fatigue truck (a) maximum positive shear, (b) maximum negative shear, and (c) influence line.

10. Range of shear force at $x = 0.5L = 0.5(50) = 25$ ft from the left support.
    Figure 6.80 shows the influence line for shear at $x = 25$ ft from the left support.
    From the influence line,

$$V_{max}^{+} = \sum P_i y_i$$

$$= 32(0.5) = 16.0 \text{ kip}$$

$$V_{max}^{-} = \sum P_i y_i = 32(-0.5) = -16.0 \text{ kip}$$

Range of shear, $V_r = V_{max}^{+} - V_{max}^{-} = 16.0 - (-16.0) = 32.0$ kip

The aforementioned values of range of shears are unfactored shear values.

Apply the live load distribution factor for fatigue (calculated earlier)

$$DF_{fat} = 0.55 \text{ lane}$$

www.EngineeringEBooksPdf.com

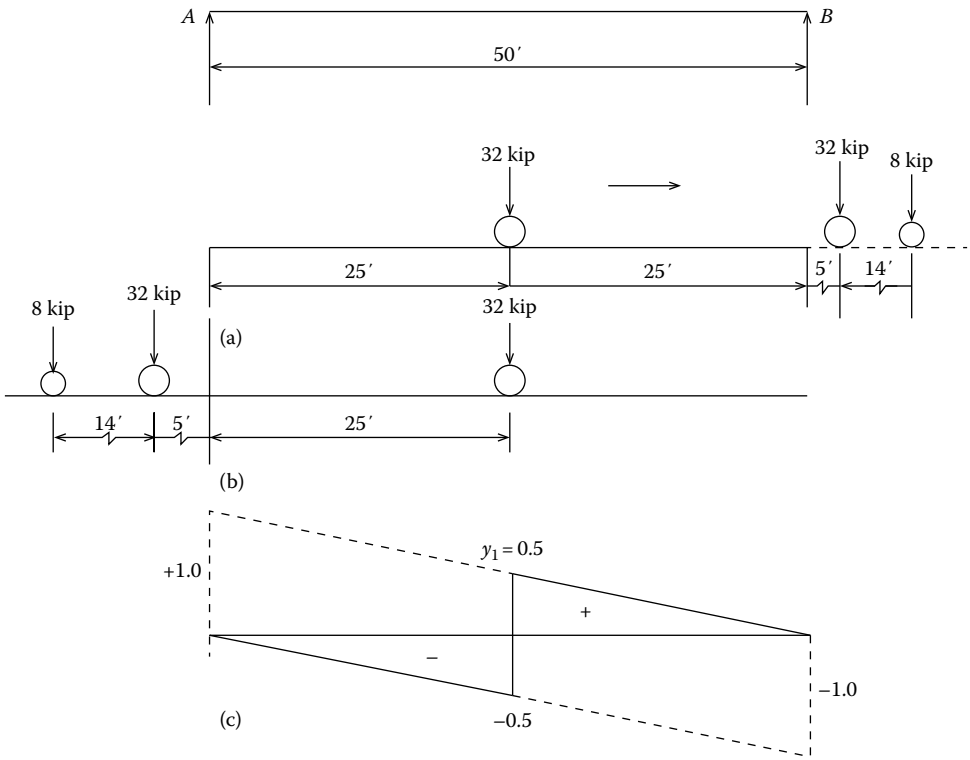

FIGURE 6.80 Influence line for shear at $x = 0.5L = 25$ ft from the left support. Position of the fatigue truck for (a) maximum positive shear, (b) maximum negative shear, and (c) influence line.

The design value of the range of shear, V_f, is obtained by multiplying the unfactored value of the range of shear (V_r) by the following factors:

1. $1 + IM = 1.15$
2. Distribution factor for fatigue, $DF_{fat} = 0.55$
3. Load factor for Fatigue Limit State I = 1.5

$$V_f = (V_r)(1.15)(0.55)(1.5) = 0.95V_r$$

Moment of inertia of the short term composite section, $I_c = 11{,}938$ in.^{4} (calculated earlier)

Q = first moment of the transformed area of slab (A_{tr}) taken about the neutral axis of the short-term composite section.

Effective width of slab, $b_e = 90$ in., $n = 8$, $t_s = 7.6$ in.

$$A_{tr} = \frac{(90)(7.5)}{8} = 84.38 \text{ in.}^2$$

The neutral axis of the short-term composite section is located at 29.91 in. from the bottom of the steel section.

Distance of neutral axis of the short-term composite section from the top of slab,

$$y_{comp}^{top} = D_t - y_b$$

$$= 38.39 - 29.91 = 8.48 \text{ in.}$$

$$Q = 84.38[8.48 - 0.5(7.5)] = 399.1 \text{ in.}^3$$

Moment of inertia of short-term composite section, $I_{c,SH} = 11{,}938$ in.^{4} (computed earlier)

www.EngineeringEBooksPdf.com

Calculate pitch, p, for short-term composite section near the support from Equation 6.102.

$$V_f = 0.95V_r = 0.474(45.76) = 43.4 \text{ kip}$$

Try one shear connector per transverse section, $n = 1$. For a 3/4 in. diameter headed shear connector, $Z_r = 3.09$ kip.

$$p \le \frac{nZ_rI}{V_fQ} \tag{6.102}$$

$$p \le \frac{nZ_rI}{V_fQ} = \frac{(1)(3.09)(11{,}938)}{(43.4)(399.1)} = 2.13 \text{ in.}$$

$$p = 2.13 \text{ in.} < 6d_s = 6(0.75) = 4.5 \text{ in, ng.}$$

where d_s = diameter rrof the headed shear connector.

The calculated spacing of $p = 2.13$ in., with one shear stud per transverse section, is too small. Try three shear studs per transverse section of the short-term composite section: $n = 3$.

$$p \le \frac{nZ_rI}{V_fQ} = \frac{(3)(3.09)(11{,}938)}{(43.4)(398.3)} = 6.4 \text{ in.}$$

$$(6d_s = 4.5 \text{ in.}) < (p = 6.4 \text{ in.}) < 24 \text{ in., OK}$$

Calculate pitch for other points along the span (at 0.1L intervals). Pitch p for various 0.1L intervals, as calculated from the following expression, is shown in Table 6.17 (values are rounded off to one decimal place).

$$p = \frac{(3)(3.09)(11{,}938)}{(V_f)(399.1)} = \frac{277.3}{V_f}$$

The pitch for various intervals along the span varies from 6.4 in. near the support to approximately 9 in. near the midspan. The pitch at 0.3L is computed to be 8.3 in. Therefore, provide three shear studs per transverse section at various spacings along the span as follows:

1. Provide the first two rows of shear studs at 4 in. from the end of the girder	0 ft–8 in.
2. 30 spacings at 6 in. o.c.	15 ft–0 in.
3. 14 spacings at 8 in. o.c.	9 ft–4 in.
Total distance to midspan	25 ft–0 in.

TABLE 6.17
Pitch of Shear Connectors at Various Intervals along the Span

x form Left Support, ft (at 0.1L Intervals)	Unfactored Shear Force Range, V_r, kip	Design Shear Range, $V_f = 0.95_r$, kip	Pitch, $p \le \frac{nZ_rI}{V_fQ} = \frac{227.3}{V_f}$, in.
0.0	45.76	43.5	6.4
5.0	41.76	39.7	7.0
10.0	38.4	36.5	7.6
15.0	35.2	33.4	8.3
20.0	34.56	32.8	8.5
25.0	32.0	30.4	9.1

Note: The variation in spacing (pitch) of shear connectors (three in a row) along the span is plotted in Figure 6.81a.

www.EngineeringEBooksPdf.com

The total number of spacings for half span = 46
Total number of stud shear connectors for half span is 46(3) = 138
Total number of shear connectors required for full span is 138(2) − 3 = 273
This total number of shear connectors (273) should be compared with that required to satisfy Strength Limit State I requirements (calculations follow), and the *larger* of the two numbers of shear connectors so determined should be provided.

b. Strength Limit State: Shear Connectors Requirements
Determine P_{1p}, the compressive strength of concrete slab:
The effective width of the slab, b_e, equals the center-to-center spacing of girders.
b_e = center-to-center of beams = 7.5 ft = 90 in., t_s = 7.5 in.

$$f'_c = 4.0 \text{ ksi}$$

Therefore, $P_{1p} = 0.85 f'_c b_e t_s = (0.85)(4.0)(90)(7.5) = 2295$ kip
Determine P_{2p}, the axial tensile yield strength of steel section.

$$P_{2P} = F_{yc} b_{fc} t_{fc} + F_{yw} d_w t_w + F_{yt} b_{ft} t_{ft}$$

In the present example, $F_{yw} = F_{yt} = F_{yc} = F_y = 50$ ksi. Therefore, $P_{2P} = A_s F_y$
Calculate the cross-sectional area of W30 × 90, $A_s = 26.3$ in.^{2}
Therefore, $P_{2P} = F_y A_s = (50)(26.3) = 1315$ kip $< P_{1P} = 2295$ kip
Therefore, $P_{2P} = 1315$ kip (smaller value) governs. Determine the nominal shear strength, Q_n, of a 3/4 in. diameter headed shear connector.

$$Q_n = 0.5 A_{sc} \sqrt{f'_c E_c} \le A_{sc} F_u \qquad (6.116)\ [A6.10.10.4.3\text{-}1]$$

The cross-sectional area of a ¾ in. diameter shear connector is

$$A_{sc} = \frac{\pi d^2}{4} = \frac{\pi (0.75)^2}{4} = 0.442 \text{ in.}^2$$

The modulus of elasticity of concrete is given by

$$\begin{aligned} E_c &= 33{,}000 (w)^{1.5} \sqrt{f'_c} \text{ ksi} \\ &= 33{,}000 (0.145)^{1.5} \sqrt{4.0} \text{ ksi} \\ &= 3{,}644 \text{ ksi} \end{aligned} \qquad (6.117)$$

Substitution for f'_c and E_c in the previous equation yields

$$\begin{aligned} Q_n &= 0.5 A_{sc} \sqrt{f'_c E_c} \\ &= 0.5 (0.442) \sqrt{(4.0)(3644)} \\ &= 26.68 \text{ kip} \end{aligned}$$

For shear connectors, $F_u = 60$ ksi (Art. 6.4.4). Therefore,

$$A_{sc} F_u = (0.442)(60) = 26.52 \text{ kip} < 26.88 \text{ kip}$$

Use $Q_n = 26.52$ kip (the *smaller* value governs)

www.EngineeringEBooksPdf.com

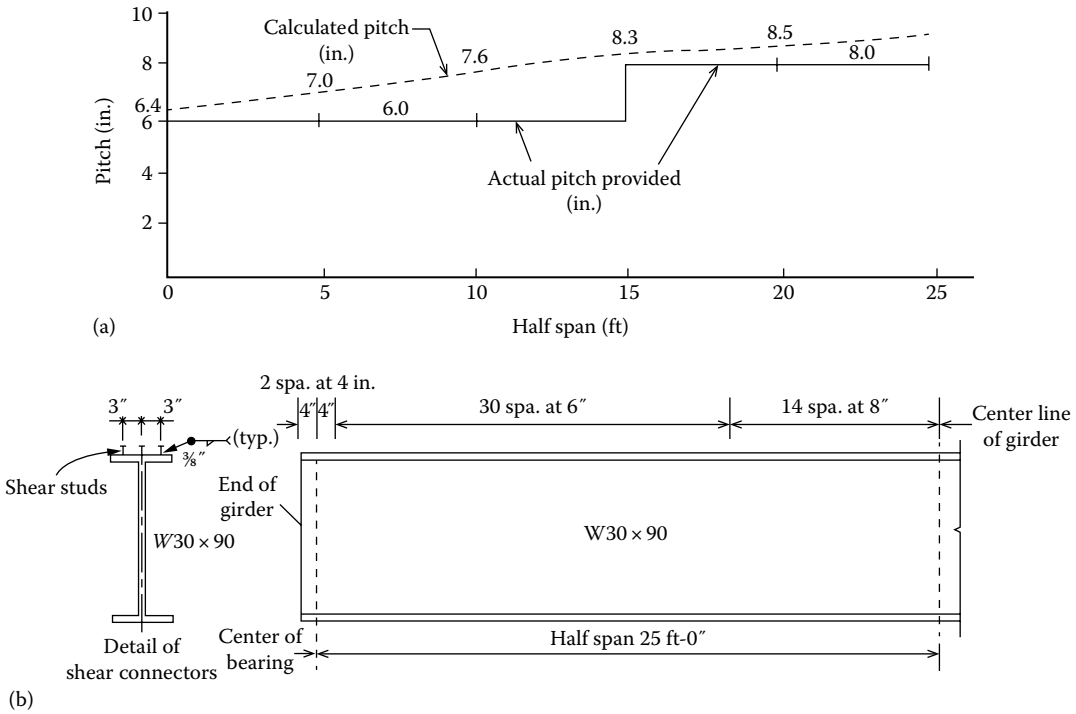

FIGURE 6.81 (a) Pitch of shear studs along the span, (b) lay out of shear studs for the girder (details shown for the left half span, the other half is symmetrical.)

With a strength reduction factor, $\phi_{SC} = 0.85$ for shear connectors, the factored shear resistance of the headed shear stud is (Art. 6.5.4.2)

$$Q_r = \phi_{SC} Q_n = 0.85(26.52) = 22.54 \text{ kip} \qquad (6.103)\ [A6.10.10.4.1\text{-}1]$$

The number of 3/4 in. diameter headed shear studs required for the half span is

$$n = \frac{P_{2p}}{Q_r} = \frac{1315}{22.54} = 59 \qquad (A6.10.10.4.1\text{-}2)$$

Total number of shear connectors for the entire span = 2(59) = 118 studs.

The number of shear connectors required to satisfy Strength I Limit State is 118 (governs)

The number of headed shear studs required to satisfy Strength Limit State I (118 studs) is smaller than the number of stud shear connectors required to satisfy the fatigue limit state (273 studs). Therefore, provide a total of 273 stud shear connectors as calculated earlier. The layout of shear connectors is shown in Figure 6.81b.

Placement requirements stated in Section 6.10.10.8.2 must be complied with. Transverse spacing of stud shear connectors should conform to the following requirements:

1. The center-to-center spacing of stud shear connectors transverse to the longitudinal axis of the girder should not be closer than four stud diameters (3 in. for ¾ in. diameter studs).
2. The clear distance between the edge of the top flange and the edge of the nearest stud shear connector shall be not less than 1 in. This requires a minimum flange width, b_f, of at least 2 × 3 + 2 × 1 = 8 in. The flange width of W30 × 90 is 10.4 in. > 10 in., OK

www.EngineeringEBooksPdf.com

Dimensions and Detail Requirements

i. *Diaphragms and cross frames: Art. 6.7.4*
Refer to Example 6.2: Design of noncomposite bridge. The bridge in this example has the same span (50 ft) and cross section as in the present example. Provide the same diaphragms as in Example 6.2. Provide MC18 × 42.7 M270 Grade 50W for the end diaphragms (Figure 6.54). This has the same size and length as the intermediate diaphragms, an advantage that results in repetitive detailing cost savings.

ii. *Compression flange lateral support until deck concrete hardens*
Provide lateral bracings (MC18 × 42.7 M270 Grade 50W) at 12 ft 6 in. intervals as computed earlier.

iii. *Dead load camber*
Deflection due to permanents loads (dead loads)
The permanent loads are as follows (computed earlier):

Dead load due to the slab, girder, etc., w_{DC1} = 0.954 kip/ft
Dead load due to traffic barriers, w_{DC2} = 0.202 kip/ft
Dead load due to the wearing surface, w_{DW} = 0.188 kip/ft

The midspan deflection of the interior girder would be calculated using the moment of inertia of noncomposite girder for deflection due to W_{DC1} and the moment of inertia of the long-term composite section for deflection due to W_{DC2} and w_{DW}.

$$\Delta_D = \frac{5(0.954)(50)^4(12)^3}{384(29{,}000)(3{,}610)} + \frac{5(0.202+0.188)(50)^4(12)^3}{384(29{,}000)(9{,}119)}$$

$$= 1.28 + 0.21 \text{ in.}$$

$$= 1.49 \text{ in.} \approx 1.50 \text{ in.}$$

Provide a dead load camber of 1.5 in. for all interior girders.

Design of a Typical Exterior Girder

Loads on a Typical Exterior Girder (Unfactored Loads)

1. *Permanent loads*
Since dead weight of traffic barriers is assumed distributed equally to all girders (interior and exterior), and the tributary width of deck slab for the exterior girder is also the same as that for the interior girder (7.5 ft), the permanent load (w_{DC1} and w_{DC2}) on the exterior girder is the same as that on a typical interior girder. Therefore, from the calculations for the interior girders, the permanent loads are as follows:

Dead load due to the slab, girder, etc., w_{DC1} = 0.954 kip/ft
Dead load due to traffic barriers, w_{DC2} = 0.202 kip/ft
Dead load due to the wearing surface, w_{DW}, to be carried by the exterior girder would be recalculated because of the presence of the traffic barrier that occupies a width of 1.75 ft (equal to the bottom width of the traffic barrier = 21 in.) of the tributary width of 7.5 ft.
The bottom width of the traffic barrier = 21 in. = 1.25 ft
Tributary width contributing FWS to the exterior girder = 7.5 − 1.75
= 5.75 ft

$$w_{DW} = (0.025)(5.75)(1.0) = 0.144 \text{ kip/ft}$$

These permanent loads would be used to calculate midspan deflection of the exterior girder due to the dead load, which would be used to determine the required camber.

www.EngineeringEBooksPdf.com

Maximum Moments and Shear in the Span (Unfactored Loads)

Maximum moment due to w_{DC1}:

$$M_{DC1} = \frac{w_{DC}L^2}{8} = \frac{(0.954)(50)^2}{8} = 298.1\,\text{kip-ft}$$

Maximum moment due to w_{DC1}:

$$M_{DC2} = \frac{w_{DC}L^2}{8} = \frac{(0.202)(50)^2}{8} = 63.1\,\text{kip-ft}$$

Maximum moment due to w_{DW}:

$$M_{DW} = \frac{w_{DW}L^2}{8} = \frac{(0.144)(50)^2}{8} = 45.0\ \text{kip-ft}$$

Maximum shear due to dead load w_{DC1}:

$$V_{DC1} = \frac{w_{DC1}L}{2} = \frac{0.954(50)}{2} = 23.85\ \text{kip}$$

Maximum shear due to dead load w_{DC2}:

$$V_{DC2} = \frac{w_{DC2}L}{2} = \frac{0.202(50)}{2} = 5.1\,\text{kip}$$

Maximum shear due to w_{DW}:

$$V_{DW} = \frac{w_{DW}L}{2} = \frac{0.144 \times (50)}{2} = 3.6\ \text{kip}$$

Note: The previous force effects are the same as those for the interior girders, except the force effect due to *DW*, which is slightly smaller for the exterior girder than for the interior girder. This slight difference (4.7 kip *vs*. 3.6 kip) is insignificant for practical purposes. Therefore, force effects due to permanent loads on the interior girder would be used also for the design of the exterior girder.

2. *Live Load*

Live Load Distribution Factors for the Exterior Girders

a. Distribution factor for bending moment
Check the range of applicability: $-1.0 \le d_e \le 5.5$ ft
where d_e = distance between the edge of curb and the center line of the exterior web of the exterior girder.
Referring to Figure 6.82,
Distance between the outside face of the traffic barrier and the center line of the web of the exterior girder = 3.75 ft.
Width of the bottom of the traffic barrier = 1.75 ft. Therefore, distance d_e is determined to be

$$d_e = 3.75 - 1.75 = 2.0\ \text{ft}$$

$$-1.0 \le 2.0 \le 5.5\ \text{ft, OK}$$

www.EngineeringEBooksPdf.com

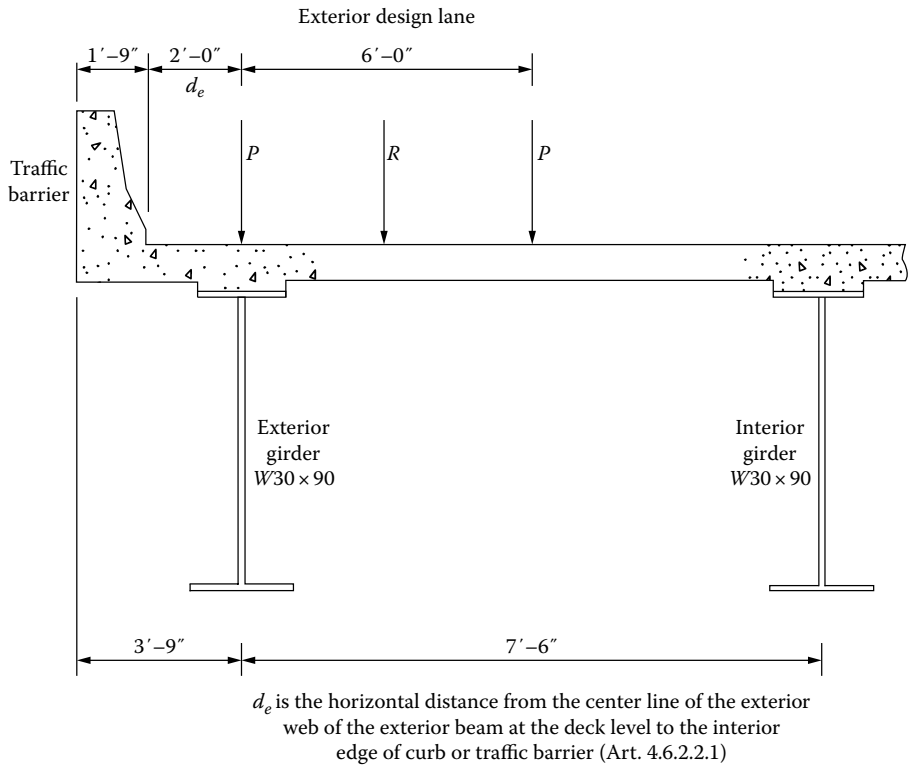

FIGURE 6.82 Lever rule for live load distribution factor for the exterior girder: one design lane loaded.

Case 1. One design lane loaded: Use lever rule. From Figure 6.82,
Distance between the center of the exterior truck lane and the centerline of the first interior girder = 3.75 + 7.5 − 1.75 − 2.0 − 3.0
= 4.5 ft

$$R_e = \frac{R(4.5)}{7.5} = 0.6\,R$$

Multiple presence factor, $m = 1.2$

$$g_{mi1} = 1.2(0.6) = 0.72$$

Case 2. Two or more design lanes loaded: $g = e(g_{interior})$

$$e = 0.77 + \frac{d_e}{9.1} = 0.77 + \frac{2.0}{9.1} = 0.99$$

$$g_{me2} = 0.99(0.622) = 0.62 < g_{mi1} = 0.72$$

Therefore, $g_{mi1} = 0.72$ (governs)

b. *Distribution factor for shear*
Case 1. One design lane loaded: Use lever rule.

$$g_{ev1} = 0.72 \text{ (calculated earlier for } g_{mi1})$$

www.EngineeringEBooksPdf.com

Case 2. Two or more design lanes loaded: $g = e(g_{interior})$

$$e = 0.6 + \frac{d_e}{10} = 0.6 + \frac{2.0}{10} = 0.8$$

$$g_{ev2} = 0.8(0.779) = 0.623$$

Special Analysis for Distribution Factors for the Exterior Girders
Art. 4.6.2.2.2d specifies that in beam–slab bridge cross sections with diaphragm or cross frames, the distribution factor for the exterior girder *shall* not be taken to be less than that which would be obtained by assuming that the cross section deflects and rotates as a rigid cross section. Under this assumption, the distribution factor for the exterior girder is required to be determined from LRFD Equation C4.4.2.2.2d as discussed in Chapter 4, Section 4.8 (Examples 4.3 and 4.4). In this design example, partial-depth diaphragms (not full-depth diaphragms or cross frames) have been provided at the ends as well as at intervals of 12 ft 6 in. This type of framing plan is not considered to provide significant rigidity to the cross section. Accordingly, the special analysis method is not used here.

Discussion: Quite likely, the special analysis (LRFD Art. 4.6.2.2.2d) may result in a higher live load distribution factor for bending moment in the exterior girder than that calculated using the approximate analysis. This would result in a larger live load bending moment (M_{LL+IM}) in the exterior girder than that in the interior girder and, consequently, a larger value of the design moment, M_u, which may require a larger girder size than W30 × 90 used for the interior girder. Fortunately, in the present case, the nominal strength of the composite girder (ϕM_n = 2355 kip-ft) is about 41.5 percent greater than the strength limit state-bending moment (M_u = 1664 kip-ft); therefore, the composite section with W30 × 90 would still be adequate.

Table 6.18 presents a summary of live load distribution factors for bending moment and shear in both interior and exterior girders; the governing values of these factors are shown bold-faced. The following are observed:

1. The governing distribution factor for live load bending moment in the exterior girder (0.72) is *greater* than that for the interior girder (0.622). Therefore, the factored live load moment in the exterior girder would be *greater* than that in the interior girder.
2. The distribution factor for live load shear in the exterior girder (0.72) is *smaller* than that for the interior girder (0.779). Therefore, the factored live load shear in the exterior girder would be *smaller* than that in the interior girder. Therefore, further check for shear is not required.

Important Note: It is required that "regardless of the method of analysis used, i.e., approximate or refined, exterior girders of multibeam bridges shall not have less resistance than an interior beam" (Art. 4.6.2.2.1). This requirement is so specified because if and when a bridge is widened (a real possibility that should always be considered in design), the exterior beam becomes an interior beam. For this reason, Art. 2.5.7.2.1 explicitly specifies that "unless future widening is virtually inconceivable, the load carrying capacity of exterior beams shall not be less than the load carrying capacity of an interior beam."

Therefore, the exterior girder will be checked for compliance with LRFD provisions pertaining to the bending moment limit states. Other limit states are automatically satisfied.

TABLE 6.18
Summary of Live Load Distribution Factors

	One Design Lane Loaded	Two or More Design Lanes Loaded
Bending Moment		
Interior girder	0.467	**0.622**
Exterior girder	**0.72**	0.62
Shear		
Interior girder	0.66	**0.779**
Exterior girder	**0.72**	0.623

www.EngineeringEBooksPdf.com

Strength Limit State

From previous calculations for the interior girder,

$$M_{DC1} = 298.1 \text{ kip-ft}$$

$$M_{DC2} = 63.1 \text{ kip-ft}$$

$$M_{DW} = 58.8 \text{ kip-ft}$$

Governing live load distribution factor for bending moment in the exterior girder, $g_{ie1} = 0.72$

$$M_{LL+IM} = 1033.3 \text{ kip-ft}$$

Design live load moment for the exterior girder = $M_{LL+IM}(g_{ie1}) = 1033.3(0.72) = 744$ kip-ft

Factored Loads: Bending Moment

$$M_u = \Sigma\eta_i\gamma_i M_i$$

$$\eta_i = \eta_D\eta_R\eta_I \text{ (Art. 1.3.2.1)}$$

Select Load Modifiers

Ductility, $\eta_D = 1.0$ (Art. 1.3.3).
Redundancy, $\eta_R = 1.0$ (Art. 1.3.4)
Importance, $\eta_I = 1.0$ (Art. 1.3.5)

Therefore, $M_u = \eta\Sigma\gamma_i M_i$

$$M_{DC} = M_{DC1} + M_{DC2} = 298.1 + 63.1 = 361.2 \text{ kip-ft}$$

$$M_u = 1.0\ [1.25M_{DC} + 1.5M_{DW} + 1.75(M_{LL+IM})]$$

$$= 1.0\ [1.25(361.2) + 1.5(58.8) + 1.75(744)]$$

$$= 1841.7\text{-ft}$$

Plastic strength of the composite section, $\phi M_n = 2355$ kip-ft > $Mu = 1841.7$ kip-ft, OK

Permanent Deformation

$$M_{DC1} = 298.1 \text{ kip-ft}$$

$$M_{DC2} = 63.1 \text{ kip-ft}$$

$$M_{DW} = 58.8 \text{ kip-ft}$$

$$M_{DC2} + M_{DW} = 63.1 + 58.8 = 121.9 \text{ kip-ft}$$

$$1.30M_{LL+IM} = 1.30(744) = 967.2 \text{ kip-ft}$$

The short-term and long-term section properties of the composite section were computed earlier.

Short-Term Composite Section Properties: n = 8

$$S_{ST}^{t} = 29{,}117 \text{ in.}^3 \text{ (top of steel)}$$

$$S_{ST}^{b} = 399 \text{ in.}^3 \text{ (bottom of steel)}$$

Long-Term Composite Section Properties: 3n = 24

$$S_{LT}^{t} = 2035 \text{ in.}^3 \text{ (top of steel)}$$

$$S_{LT}^{b} = 364 \text{ in.}^3 \text{ (bottom of steel)}$$

www.EngineeringEBooksPdf.com

Calculate stresses in flanges as follows:

For M_{DC1}, use noncomposite section properties.
For M_{DC2} and M_{DW}, use long-term section properties.
For $1.3M_{LL+IM}$, use short-term properties.

Compressive stress (f_c) in the top flange of composite section:

$$f_c = \frac{298.1(12)}{245} + \frac{121.9(12)}{2{,}035} + \frac{967.2(12)}{29{,}117}$$

$$= 14.6 + 0.72 + 0.40 = 15.72 \text{ ksi}$$

$$f_f = 47.5 \text{ ksi} > f_c = 15.72 \text{ ksi, OK}$$

Tensile stress (f_t) in the bottom flange of composite section:

$$f_t = \frac{298.1(12)}{245} + \frac{121.9(12)}{364} + \frac{967.2(12)}{399}$$

$$= 14.6 + 4.02 + 29.09 = 47.71 \text{ ksi} > f_f = 47.5 \text{ ksi}$$

The tensile stress (f_t) in the bottom flange of composite section, 47.71 ksi, is less than 0.5 percent over the permitted value of f_f = 47.5 ksi. In view of this negligible overstress condition, the use of W30 × 90 steel section is considered acceptable. In case, this overstress condition is found unacceptable, a larger girder for the exterior girder should be considered. For the present case, use W30 × 90 for the exterior girder (same as for the interior girder). The use of the same girder size for both interior and exterior girders is preferable for ease of fabrication, connections, and overall construction considerations.

Dead Load Camber

Calculate maximum deflection of the exterior beams due to the permanent loads.

Dead load due to the slab, girder, etc., w_{DC1} = 0.954 kip/ft
Dead load due to traffic barriers, w_{DC2} = 0.202 kip/ft
w_{DW} = 0.144 kip/ft

The midspan girder deflection of the exterior girder would be calculated using the moment of inertia of noncomposite girder for deflection due to w_{DC1} and the moment of inertia of the long-term composite section for deflection due to w_{DC2} and w_{DW}. Note that the section properties of the exterior girders are the same as those of the interior girders.

$$\Delta_D = \frac{5(0.954)(50)^4(12)^3}{384(29{,}000)(3{,}610)} + \frac{5(0.202+0.144)(50)^4(12)^3}{384(29{,}000)(9{,}119)}$$

$$= 1.28 + 0.18 \text{ in.} = 1.46 \text{ in.} \approx 1.50 \text{ in.}$$

Provide a dead load camber of 1.5 in. for both exterior girders (same as for the interior girders).

Provide a Camber of 1.5 in. for All Girders

Diaphragms and Cross Frames

Diaphragms and cross frames need to be provided to comply with Art. 6.7.4. Refer to Section 2.4.3.2 for a discussion pertaining to requirements for diaphragms and cross frames.

Art. 6.7.4.2 specifies that diaphragms *or* cross frames for rolled beams and plate girders be as deep as practicable, but as a minimum should not be shallower than one-half the beam depth for rolled beams and not shallower than ¾ of the beam depth for plate girders. Intermediate diaphragms or cross frames should be provided at nearly uniform spacing for efficiency in structural design and constructibility and/or to allow for simplified methods of analysis for calculation of flange lateral bending stresses.

www.EngineeringEBooksPdf.com

Intermediate Diaphragms

Intermediate diaphragms are designed to transmit lateral loads due to wind to the girders and then to the bearings at the abutments. As calculated earlier, intermediate diaphragms are provided at quarter points, that is, at 12 ft–6 in intervals. These diaphragms are oriented perpendicular to the girders and provided contiguously in between all girders so that the girders and diaphragms together form a simple frame in a horizontal plane supporting a deck on top. The whole system so constructed forms a stiff *horizontal diaphragm* that resists horizontal forces acting transversely to the bridge superstructure and transmits them to the abutments through the bearings. However, this seemingly simple system (horizontal diaphragm) is not amenable to simple mathematical analysis.

A uniform wind load of WS = 50 lb/ft^2 (wind load on superstructure, Art. 3.8.1.2, LRDF Table 3.8.1.2.1-1) is assumed for design of diaphragms (Figure 6.83). This horizontal force is assumed to act normal to superstructure over its entire height (= height of traffic barrier + deck + girder).

Conservatively, the lateral forces transmitted to intermediate and end diaphragms are calculated on tributary area basis. It is assumed that the wind load acting on the bottom half of the girder is transmitted to the bottom flange; the wind force acting over the remainder of the height is transmitted to the top flange of the girder.

Wind Loads on Intermediate Diaphragms

Lateral wind load distribution on the girders is analyzed as specified in LRFD Art. 4.6.2.7 and discussed in Section 4.17.2 (Chapter 4). The wind force W applied to the flanges of the exterior girders is determined from the following:

$$W = \frac{\eta_i \gamma P_D d}{2} \qquad (4.39)\ [\text{AC}4.6.2.7.1\text{-}1]$$

where

W = factored wind force per unit length applied to the flange (kip/ft)
P_D = design horizontal wind pressure, ksf (Art. 3.8.1)
d = depth of member
γ = load factor as specified in LRFD Table 3.4.1-1 for the particular group loading combination
η_i = load modifier relating to ductility, redundancy, and operational importance as specified in Art. 1.3.2.1

Depth of girder (W30 × 90), d = 29.5 in., P_D = 50 lb/ft^2, load modifier for WS, η_i = 1.0, γ = 1.4 (LRFD Table 3.4.1-1)

$$W_{bot} = \frac{\gamma P_D d}{2} = \frac{1.4(0.050)(29.5)}{2(12)} = 0.086 \text{ kip/ft}$$

Tributary length for an intermediate diaphragm = L_b = 12.5 ft = 150 in.

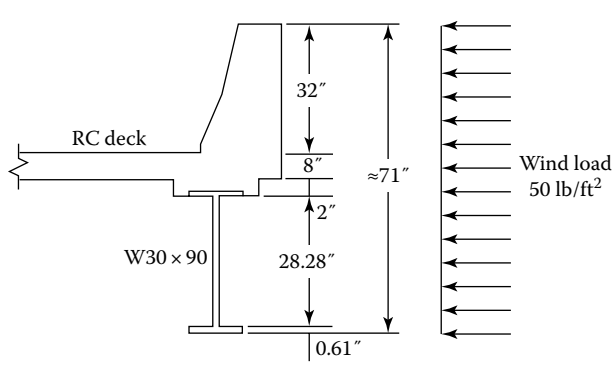

FIGURE 6.83 Wind loading on the superstructure.

www.EngineeringEBooksPdf.com

Lateral force transmitted from the bottom flange of the girder to diaphragm is as follows:

$$P_{w,bot} = 0.086\ (12.5) = 1.08 \text{ kip}$$

Maximum wind moment on the loaded flange is determined from the following,

$$M_w = \frac{WL_b^2}{10} \qquad (4.40)\ [AC4.6.2.7.1\text{-}2]$$

$$M_w = \frac{0.086(12.5)^2(12)}{10} = 16.13 \text{ kip-in.}$$

For a W30 × 90, $S_y = 22.1$ in.^{3}

Flange lateral-bending stress, $f_\ell = \dfrac{M_w}{S_x} = \dfrac{16.13}{22.1} = 0.73$ ksi (very small)

The actual value of the flange lateral-bending stress would be much smaller than the calculated value of 0.73 ksi because the girders are composite and are not free to deflect laterally.

Contributory height for the top flange of the girder, $d_{w,top} = 32 + 8 + 2 + 0.5(29.5) = 56.75$ in. ≈ 57 in.

$$W = \gamma P_D d = \frac{1.4(0.050)(57)}{(12)} = 0.333 \text{ kip/ft}$$

Lateral force transmitted from the top flange of the girder to diaphragm is

$$P_{w,top} = 0.333(12.5) = 4.16 \text{ kip}$$

Therefore, total lateral force, F_{uDi}, transmitted to an intermediate diaphragm is

$$F_{uDi} = P_{w,bot} + P_{w,top} = 1.08 + 4.16 = 5.24 \text{ kip}$$

The intermediate diaphragm must be able to resist an axial force of 5.24 kip.

Select a channel section for the diaphragms. A channel section is preferred for easy constructibility and simplicity of (bolted) connections to the girders. The depth of the diaphragm should be not less than half the girder depth. For a W30 × 90, $d = 29.5$ in., $0.5d = 14.75$ in. Try an MC18 × 42.7 Gr. 50, $d = 18$ in. > 14.75 in., OK. The section properties of an MC18 × 42.7 are as follows (obtained from AISC 2011):

$d = 18$ in., $A = 12.6$ in.^{2}, $t_w = 0.45$ in., $T = 15.125$ in., $r_x = 6.64$ in., $r_y = 1.07$ in.

Calculate the nominal compressive resistance of an MC18 × 42.7 as specified in Art. 6.9.3 and 6.9.4. Assume it as a secondary member having pin-ended connections at both ends.

$$P_n = \left[(0.658)^{\left(\frac{P_o}{P_e}\right)}\right]P_o \qquad (A6.9.4.1.1\text{-}1)$$

For a secondary compression member, $\dfrac{k\ell}{r} \le 140$. (Art. 6.9.3)

For the MC18 × 42.7, ℓ = center-to-center spacing of girders = 7 ft 6 in. = 90 in.

$$\frac{k\ell}{r_s} = \frac{k\ell}{r_y} = \frac{1.0(90)}{1.07} = 84.1 < 140, \text{ OK}$$

where r_s = radius of gyration about the axis normal to the plane of buckling = r_y.

Calculate elastic flexural-buckling resistance, P_e (Art. 6.9.4.1)

$$P_e = \frac{\pi^2 E A_g}{\left(\dfrac{k\ell}{r_s}\right)^2} = \frac{\pi^2(29{,}000)(12.6)}{(84.1)^2} = 510 \text{ kip} \qquad (A6.9.4.1.2\text{-}1)$$

$$P_o = QF_yA_g$$

www.EngineeringEBooksPdf.com

where Q = slender element reduction factor as specified in Art. 6.9.4.2. Check if the channel MC18 × 42.7 is composed of nonslender plate elements. Check the b/t ratio of the web:

$$\frac{b}{t} = \frac{T}{t_w} = \frac{15.125}{0.45} = 33.16$$

Check if

$$\frac{b}{t} \le k\sqrt{\frac{E}{F_y}}$$

From LRFD Table 6.9.4.2.1-1, for channel sections, k = 1.49.

$$k\sqrt{\frac{E}{F_y}} = 1.49\sqrt{\frac{29{,}000}{50}} = 35.88$$

$$\frac{b}{t} = 33.16 \le 35.88$$

Therefore, the channel MC18 × 42.7 is composed of non-slender elements, so Q = 1.0 (Art. 6.9.4.2.1).

$$P_o = QF_yA_g = 1.0(50)(12.6) = 630 \text{ kip}$$

$$\frac{P_o}{P_e} = \frac{630}{510} = 1.235$$

$$P_n = \left[(0.658)^{\left(\frac{P_o}{P_e}\right)}\right]P_o \qquad \text{(A6.9.4.1.1-1)}$$

$$P_n = \left[(0.658)^{\left(\frac{630}{510}\right)}\right](630) = 376 \text{ kip}$$

$$P_r = \phi_c P_n = 0.9(376) = 338.4 \text{ kip} > F_{uD} = 5.19 \text{ kip, OK}$$

Therefore, provide MC18 × 42.7 for intermediate diaphragms at 12 ft-6 in. on center. These diaphragms will also serve as lateral bracings at 12 ft-6 in. on center (L_b = 12 ft-6 in.).

Wind Loads on End Diaphragms

Each end diaphragm is required to transmit half the wind load (WS) acting on the superstructure.

Total wind force on the superstructure is

$$w = w_{bot} + w_{top} = 0.086 + 0.333 = 0.42 \text{ kip/ft}$$

Length of the superstructure, L = 50 ft

Wind force to be transmitted by the end diaphragm, F_{uDe}:

$$F_{uDe} = \frac{wL}{2} = \frac{0.42(50)}{2} = 10.5 \text{ kip, OK.}$$

Axial resistance of MC18 × 42.7 (calculated earlier), P_r = 338.4 kip > F_{uDe} = 10.5 kip

Therefore, provide MC18 × 42.7 for the end diaphragms (Figure 6.84). This has the same size and length as the intermediate diaphragms, an advantage that results in repetitive detailing cost savings.

Figure 6.85 shows the sketch of the composite steel girder bridge superstructure as designed.

www.EngineeringEBooksPdf.com

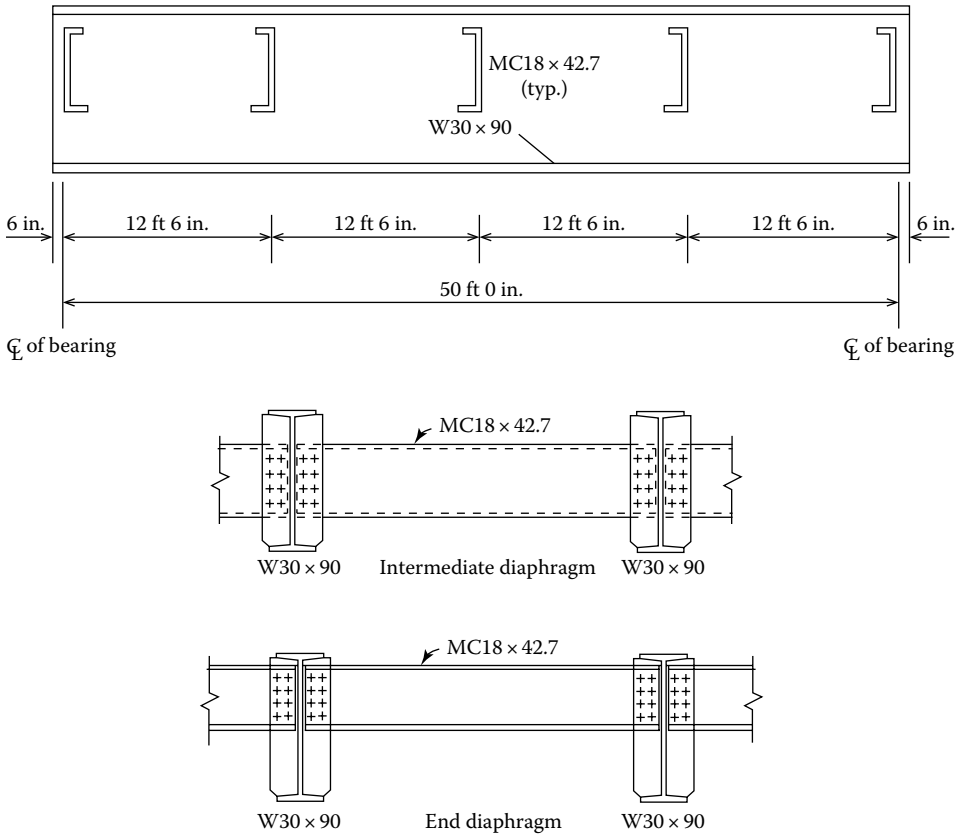

FIGURE 6.84 Location of intermediate and end diaphragms. (a) Elevation of girder showing end diaphragms. (b) Diaphragms bolted to girders.

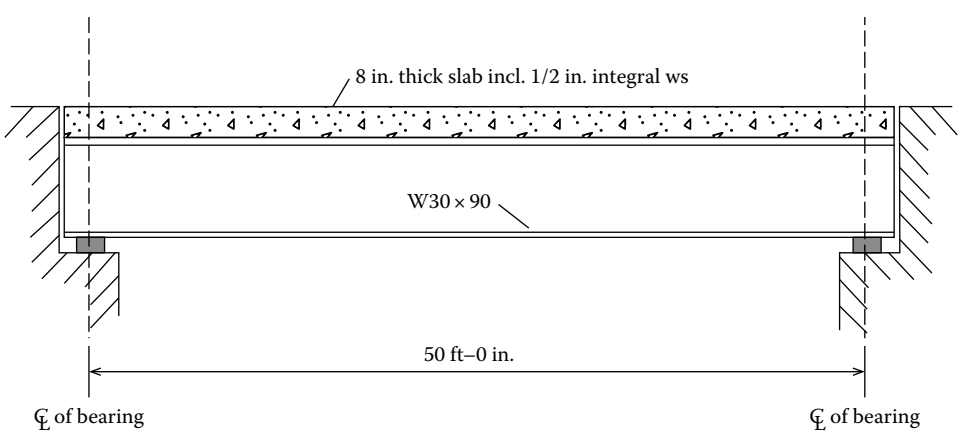

FIGURE 6.85 Design sketch of the composite steel girder bridge of Example 6.10.

www.EngineeringEBooksPdf.com

6.A APPENDIX

TABLE 6.A.1
Minimum Mechanical Properties of Structural Steel by Shape, Strength, and Thickness (AASHTO LRFD 2012 Table 6.4.1-1)

AASHTO designation	M270M/M 270 Grade 36	M 270M/M 270 Grade 50	M 270M/M 270 Grade 50S	M 270M/M 270 Grade SOW	M 270M/M 270 Grade HPS 50W	M270M/M 270 Grade HPS 70W	M 270M/M 270 Grade HPS 100W	
Equivalent ASTM designation	A709/A709M Grade 36	A709/A709M Grade 50	A709/A709M Grade SOS	A709/A709M Grade 50W	A709/A709M Grade HPS 50W	A709/A709M Grade HPS 70W	A709/A709M Grade HPS 100W	
Thickness of plates, in.	Up to 4.0 incl.	Up to 4.0 incl.	Not applicable	Up to 4.0 incl.	Up to 4.0 incl.	Up to 4.0 incl.	Up to 2.5 incl.	Over 2.5 to 4.0 incl.
Shapes	All groups	All groups	All groups	All groups	Mot applicable	Not applicable	Not applicable	Not applicable
Minimum tensile strength, F_u, ksi	58	65	65	70	70	85	110	100
Specified minimum yield point or specified minimum yield strength, F_y, ksi	36	50	50	50	50	70	100	90

Source: From *AASHTO LRFD Bridge Design Specifications*, Copyright © 2012 by American Association of State Highway and Transportation Officials, Washington, DC. Used by permission.

Notes: HPS, high performance steel; W, weldable.

www.EngineeringEBooksPdf.com

TABLE 6.A.2
Minimum Mechanical Properties of Pins, Rollers, and Rockers by Size and Strength

AASHTO designation with size limitations	M 169 4.0 in. in dia. or less	M 102M/M 102 to 20.0 in. in dia.	M 102M/M 102 to 20.0 in. in dia.	M 102M/M 102 to 10.0 in. in dia.	M 102M/M 102 to 20.0 in. in dia.
ASTM designation grade or class	A10S Grades 1016–1030 incl.	A66S/A668M Class C	A668/A668M Class D	A668/A668M Class F	A668/A668M Class G
Specified minimum yield point, F_y, ksi	36	33	37.5	50	50

Source: From *AASHTO LRFD Bridge Design Specifications*, Copyright © 2012 by American Association of State Highway and Transportation Officials, Washington, DC. Used by permission.

www.EngineeringEBooksPdf.com

TABLE 6.A.3-1
Detail Categories for Load-Induced Fatigue

Description	Category	Constant A (ksi^3)	Threshold $(\Delta F)_{TH}$ ksi	Potential Crack Initiation Point	Illustrative Examples
Section 1—Plain material away from any welding					
1.1 Base metal, except noncoated weathering steel, with rolled or cleaned surfaces. Flame-cut edges with surface roughness value of 1000 μ-in. or less, but without reentrant corners.	A	250×10^8	24	Away from all welds or structural connections	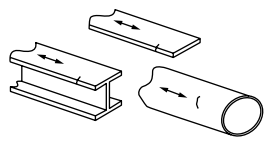
1.2 Noncoated weathering steel base metal with rolled or cleaned surfaces designed and detailed in accordance with FHWA (1989). Flame-cut edges with surface roughness value of 1000 μ-in. or less, but without reentrant corners.	B	120×10^8	16	Away from all welds or structural connections	
1.3 Member with reentrant corners at copes, cuts, block-outs, or other geometrical discontinuities made to the requirements of AASHTO/AWS D1.5, except weld access holes.	C	44×10^8	10	At any external edge	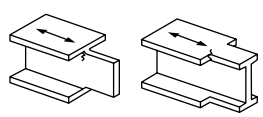
1.4 Rolled cross sections with weld access holes made to the requirements of AASHTO/AWS D1.5, Art. 3.2.4.	C	44×10^8	10	In the base metal at the reentrant corner of the weld access hole	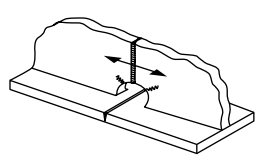
1.5 Open holes in members (Brown et al. 2007).	D	22×10^8	7	In the net section originating at the side of the hole	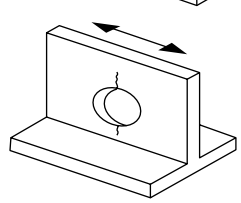
Section 2—Connected material in mechanically fastened joints					
2.1 Base metal at the gross section of high-strength bolted joints designed as slip-critical connections with pretensioned high-strength bolts installed in holes drilled full size or subpunched and reamed to size—e.g., bolted flange and web splices and bolted stiffeners. (*Note*: See Condition 2.3 for bolt holes punched full size.)	B	120×10^8	16	Through the gross section near the hole	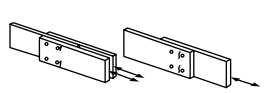

www.EngineeringEBooksPdf.com

TABLE 6.A.3-2
Detail Categories for Load-Induced Fatigue

Description	Category	Constant A (ksi^3)	Threshold $(\Delta F)_{TH}$ ksi	Potential Crack Initiation Point	Illustrative Examples
Section 2—Connected material in mechanically fastened joints (continued)					
2.2 Base metal at the net section of high-strength bolted joints designed as bearing-type connections but fabricated and installed to all requirements for slip-critical connections with pretensioned high-strength bolts installed in holes drilled full size or subpunched and reamed to size. (*Note*: See Condition 2.3 for bolt holes punched full size.)	B	120×10^8	16	In the net section originating at the side of the hole	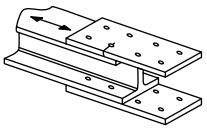
2.3 Base metal at the net section of all bolted connections in hot dipped galvanized members (Huhn and Valtinat 2004); base metal at the appropriate section defined in Condition 2.1 or 2.2, as applicable, of high-strength bolted joints with pretensioned bolts installed in holes punched full size (Brown et al. 2007); and base metal at the net section of other mechanically fastened joints, except for eyebars and pin plates, e.g., joints using ASTM A307 bolts or non-pretensioned high-strength bolts.	D	22×10^8	7	In the net section originating at the side of the hole or through the gross section near the hole, as applicable	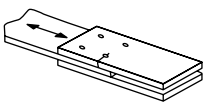
2.4 Base metal at the net section of eyebar heads or pin plates. (*Note*: For base metal in the shank of eyebars or through the gross section of pin plates, see Condition 1.1 or 1.2, as applicable.)	E	11×10^8	4.5	In the net section originating at the side of the hole	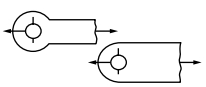
Section 3—Welded joints joining components of built-up members					
3.1 Base metal and weld metal in members without attachments built up of plates or shapes connected by continuous longitudinal complete joint penetration groove welds back-gouged and welded from the second side, or by continuous fillet welds parallel to the direction of applied stress.	B	120×10^8	16	From surface or internal discontinuities in the weld away from the end of the weld	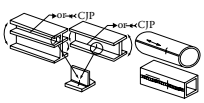
3.2 Base metal and weld metal in members without attachments built up of plates or shapes connected by continuous longitudinal complete joint penetration groove welds with backing bars not removed, or by continuous partial joint penetration groove welds parallel to the direction of applied stress.	B′	61×10^8	12	From surface or internal discontinuities in the weld, including weld attaching backing bars	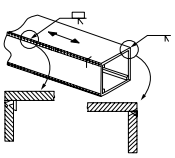

www.EngineeringEBooksPdf.com

TABLE 6.A.3-3
Detail Categories for Load-Induced Fatigue

Description	Category	Constant A (ksi^3)	Threshold $(\Delta F)_{TH}$ ksi	Potential Crack Initiation Point	Illustrative Examples
Section 3—Welded joints joining components of built-up members (continued)					
3.3 Base metal and weld metal at the termination of longitudinal welds at weld access holes made to the requirements of AASHTO/AWS D1.5, Art. 3.2.4 in built-up members. (*Note*: Does not include the flange butt splice.)	D	22×10^8	7	From the weld termination into the web or flange	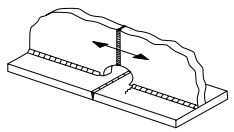
3.4 Base metal and weld metal in partial length welded cover plates connected by continuous fillet welds parallel to the direction of applied stress.	B	120×10^8	16	From surface or internal discontinuities in the weld away from the end of the weld	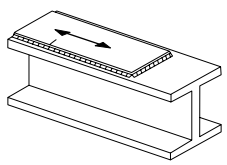
3.5 Base metal at the termination of partial length welded cover plates having square or tapered ends that are narrower than the flange, with or without welds across the ends, or cover plates that are wider than the flange with welds across the ends:				In the flange at the toe of the end weld or in the flange at the termination of the longitudinal weld or in the edge of the flange with wide cover plates	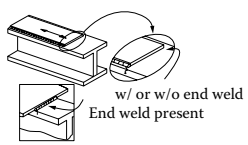
Flange thickness ≤ 0.8 in.	E	11×10^8	4.5		
Flange thickness > 0.8 in.	E′	3.9×10^8	2.6		
3.6 Base metal at the termination of partial length welded cover plates with slip-critical bolted end connections satisfying the requirements of Art. 6.10.12.2.3.	B	120×10^8	16	In the flange at the termination of the longitudinal weld	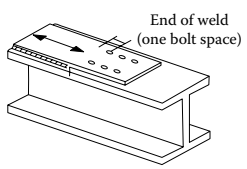
3.7 Base metal at the termination of partial length welded cover plates that are wider than the flange and without welds across the ends.	E′	3.9×10^8	2.6	In the edge of the flange at the end of the cover plate weld	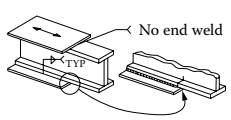

www.EngineeringEBooksPdf.com

TABLE 6.A.3-4
Detail Categories for Load-Induced Fatigue

Description	Category	Constant A (ksi^3)	Threshold $(\Delta F)_{TH}$ ksi	Potential Crack Initiation Point	Illustrative Examples
Section 4—Welded stiffener connections					
4.1 Base metal at the toe of transverse stiffener-to-flange fillet welds and transverse stiffener-to-web fillet welds. (*Note*: Includes similar welds on bearing stiffeners and connection plates.)	C′	44×10^8	12	Initiating from the geometrical discontinuity at the toe of the fillet weld extending into the base metal	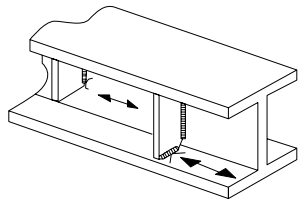
4.2 Base metal and weld metal in longitudinal web or longitudinal box-flange stiffeners connected by continuous fillet welds parallel to the direction of applied stress.	B	120×10^8	16	From the surface or internal discontinuities in the weld away from the end of the weld	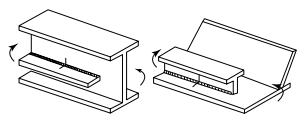
4.3 Base metal at the termination of longitudinal stiffener-to-web or longitudinal stiffener-to-box flange welds:					
With the stiffener attached by fillet welds and with no transition radius provided at the termination:				In the primary member at the end of the weld at the weld toe	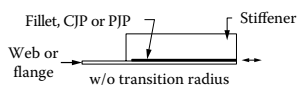
Stiffener thickness < 1.0 in.	E	11×10^8	4.5		
Stiffener thickness ≥ 1.0 in.	E′	3.9×10^8	2.6		
With the stiffener attached by welds and with a transition radius R provided at the termination with the weld termination ground smooth:					
$R \geq 24$ in.	B	120×10^8	16		
24 in. > $R \geq 6$ in.	C	44×10^8	10	In the primary member near the point of tangency of the radius	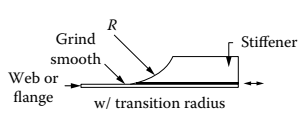
6 in. > $R \geq 2$ in.	D	22×10^8	7		
2 in. > R	E	11×10^8	4.5		

www.EngineeringEBooksPdf.com

TABLE 6.A.3-5
Detail Categories for Load-Induced Fatigue

Description	Category	Constant A (ksi^3)	Threshold $(\Delta F)_{TH}$ ksi	Potential Crack Initiation Point	Illustrative Examples
Section 5—Welded joints transverse to the direction of primary stress					
5.1 Base metal and weld metal in or adjacent to complete joint penetration groove welded butt splices, with weld soundness established by NDT and with welds ground smooth and flush parallel to the direction of stress. Transitions in thickness or width shall be made on a slope no greater than 1:2.5 (see also Figure 6.13.6.2-1).				From internal discontinuities in the filler metal or along the fusion boundary or at the start of the transition	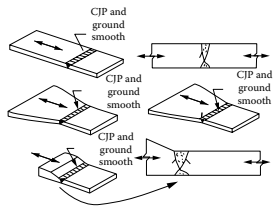
$F_y < 100$ ksi	B	120×10^8	16		
$F_y \geq 100$ ksi	B′	61×10^8	12		
5.2 Base metal and weld metal in or adjacent to complete joint penetration groove welded butt splices, with weld soundness established by NDT and with welds ground parallel to the direction of stress at transitions in width made on a radius of not less than 2 ft with the point of tangency at the end of the groove weld (see also Figure 6.13.6.2-1).	B	120×10^8	16	From internal discontinuities in the filler metal or discontinuities along the fusion boundary	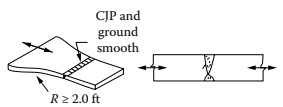
5.3 Base metal and weld metal in or adjacent to the toe of complete joint penetration groove welded T or corner joints, or in complete joint penetration groove welded butt splices, with or without transitions in thickness having slopes no greater than 1:2.5 when weld reinforcement is not removed. (*Note*: Cracking in the flange of the "T" may occur due to out-of-plane bending stresses induced by the stem.)	C	44×10^8	10	From the surface discontinuity at the toe of the weld extending into the base metal or along the fusion boundary	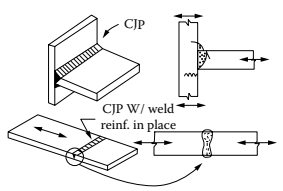

(Continued)

www.EngineeringEBooksPdf.com

TABLE 6.A.3-5 (*Continued*)
Detail Categories for Load-Induced Fatigue

Description	Category	Constant A (ksi^3)	Threshold $(\Delta F)_{TH}$ ksi	Potential Crack Initiation Point	Illustrative Examples
5.4 Base metal and weld metal at details where loaded discontinuous plate elements are connected with a pair of fillet welds or partial joint penetration groove welds on opposite sides of the plate normal to the direction of primary stress.	C as adjusted in Equation 6.6.1.2.5-4	44×10^8	10	Initiating from the geometrical discontinuity at the toe of the weld extending into the base metal or initiating at the weld root subject to tension extending up and then out through the weld	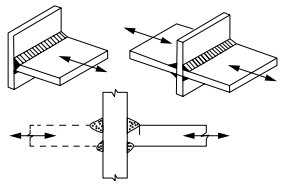

TABLE 6.A.3-6
Detail Categories for Load-Induced Fatigue

Description	Category	Constant A (ksi^3)	Threshold $(\Delta F)_{TH}$ ksi	Potential Crack Initiation Point	Illustrative Examples
Section 6—transversely loaded welded attachments					
6.1 Base metal in a longitudinally loaded component at a transversely loaded detail (e.g., a lateral connection plate) attached by a weld parallel to the direction of primary stress and incorporating a transition radius R with the weld termination ground smooth.				Near point of tangency of the radius at the edge of the longitudinally loaded component or at the toe of the weld at the weld termination if not ground smooth	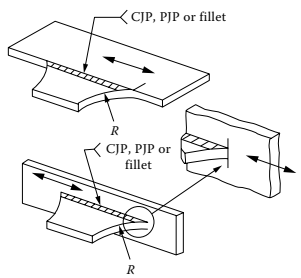
$R \geq 24$ in.	B	120×10^8	16		
24 in. $> R \geq 6$ in.	C	44×10^8	10		
6 in. $> R \geq 2$ in.	D	22×10^8	7		
2 in. $> R$	E	11×10^8	4.5		
For any transition radius with the weld termination not ground smooth	E	11×10^8	4.5		
(*Note*: Condition 6.2, 6.3 or 6.4, as applicable, shall also be checked.)					

www.EngineeringEBooksPdf.com

TABLE 6.A.3-7
Detail Categories for Load-Induced Fatigue

Description	Category	Constant A (ksi^3)	Threshold $(\Delta F)_{TH}$ ksi	Potential Crack Initiation Point	Illustrative Examples
Section 6—Transversely loaded welded attachments (continued)					
6.2 Base metal in a transversely loaded detail (e.g., a lateral connection plate) attached to a longitudinally loaded component of equal thickness by a complete joint penetration groove weld parallel to the direction of primary stress and incorporating a transition radius R, with weld soundness established by NDT and with the weld termination ground smooth:					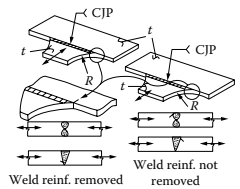
With the weld reinforcement removed:					
$R \geq 24$ in.	B	120×10^8	16	Near points of tangency of the radius or in the weld or at the fusion boundary of the longitudinally loaded component or the transversely loaded attachment	
24 in. $> R \geq 6$ in.	C	44×10^8	10		
6 in. $> R \geq 2$ in.	D	22×10^8	7		
2 in. $> R$	E	11×10^8	4.5		
With the weld reinforcement not removed:				At the toe of the weld either along the edge of the longitudinally loaded component or the transversely loaded attachment	
$R \geq 24$ in.	C	44×10^8	10		
24 in. $> R \geq 6$ in.	C	44×10^8	10		
6 in. $> R \geq 2$ in.	D	22×10^8	7		
2 in. $> R$	E	11×10^8	4.5		
(*Note*: Condition 6.1 shall also be checked.)					

(Continued)

www.EngineeringEBooksPdf.com

TABLE 6.A.3-7 (*Continued*)
Detail Categories for Load-Induced Fatigue

Description	Category	Constant A (ksi^3)	Threshold $(\Delta F)_{TH}$ ksi	Potential Crack Initiation Point	Illustrative Examples
6.3 Base metal in a transversely loaded detail (e.g., a lateral connection plate) attached to a longitudinally loaded component of unequal thickness by a complete joint penetration groove weld parallel to the direction of primary stress and incorporating a weld transition radius R, with weld soundness established by NDT and with the weld termination ground smooth:				At the toe of the weld along the edge of the thinner plate In the weld termination of small radius weld transitions At the toe of the weld along the edge of the thinner plate	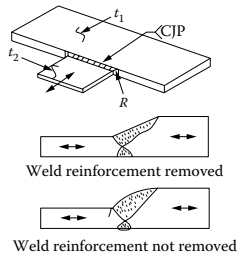
With the weld reinforcement removed:					
$R \geq 2$ in.	D	22×10^8	7		
$R < 2$ in.	E	11×10^8	4.5		
For any weld transition radius with the weld reinforcement not removed	E	11×10^8	4.5		
(*Note*: Condition 6.1 shall also be checked.)					

www.EngineeringEBooksPdf.com

TABLE 6.A.3-8
Detail Categories for Load-Induced Fatigue

Description	Category	Constant A (ksi³)	Threshold $(\Delta F)_{TH}$ ksi	Potential Crack Initiation Point	Illustrative Examples
Section 6—Transversely loaded welded attachments (continued)					
6.4 Base metal in a transversely loaded detail (e.g., a lateral connection plate) attached to a longitudinally loaded component by a fillet weld or a partial joint penetration groove weld, with the weld parallel to the direction of primary stress (*Note*: Condition 6.1 shall also be checked.)	See Condition 5.4				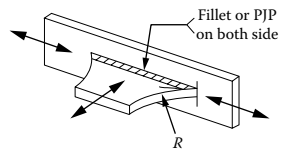
Section 7—Longitudinally loaded welded attachments					
7.1 Base metal in a longitudinally loaded component at a detail with a length L in the direction of the primary stress and a thickness t attached by groove or fillet welds parallel or transverse to the direction of primary stress where the detail incorporates no transition radius:				In the primary member at the end of the weld at the weld toe	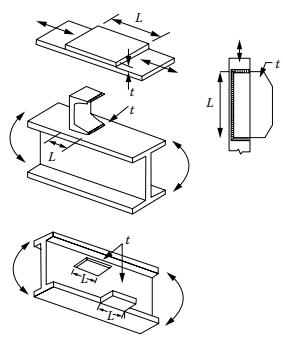
$L < 2$ in.	C	44×10^8	10		
2 in. $\leq L \leq 12t$ or 4 in	D	22×10^8	7		
$L > 12t$ or 4 in.					
$t < 1.0$ in.	E	11×10^8	4.5		
$t \geq 1.0$ in.	E′	3.9×10^8	2.6		
Section 8—Miscellaneous					
8.1 Rib to deck weld—one-sided 80 percent (70 percent min) penetration weld with root gap ≤ 0.02 in. prior to welding Allowable Design Level 1, 2, or 3	C	44×10^8	10	See figure	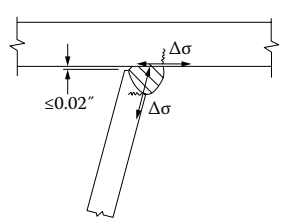
8.2 Rib splice (welded)—single groove butt weld with permanent backing bar left in place. Weld gap > rib wall thickness Allowable Design Level 1, 2, or 3	D	22×10^8	7	See figure	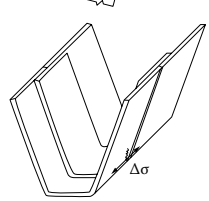

www.EngineeringEBooksPdf.com

TABLE 6.A.3-9
Detail Categories for Load-Induced Fatigue

Description	Category	Constant A (ksi^3)	Threshold $(\Delta F)_{TH}$ ksi	Potential Crack Initiation Point	Illustrative Examples
Section 8—Miscellaneous (continued)					
8.3 Rib splice (bolted)—base metal at gross section of high strength slip critical connection Allowable design level 1, 2, or 3	B	120×10^8	16	See figure	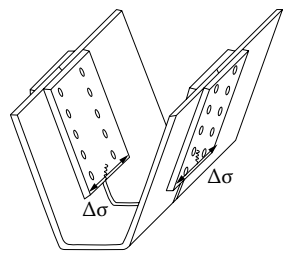
8.4 Deck plate splice (in plane)—transverse or longitudinal single groove butt splice with permanent backing bar left in place Allowable design level 1, 2, or 3	D	22×10^8	7	See figure	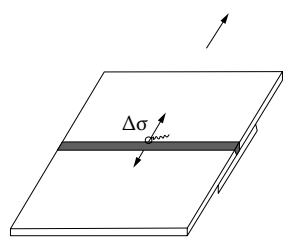
8.5 Rib to FB weld (rib)—rib wall at rib to FB weld (fillet or CJP) Allowable design level 1, 2, or 3	C	44×10^8	10	See figure	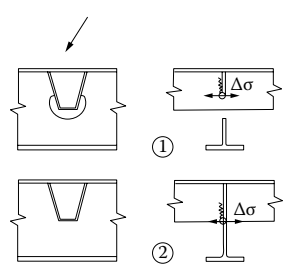

www.EngineeringEBooksPdf.com

TABLE 6.A.3-10
Detail Categories for Load-Induced Fatigue

Description	Category	Constant A (ksi³)	Threshold $(\Delta F)_{TH}$ ksi	Potential Crack Initiation Point	Illustrative Examples
8.6 Rib to FB weld (FB web)—FB web at rib to FB weld (fillet, PJP, or CJP) Allowable design level 1 or 3	C (see Note 1)	44×10^8	10	See figure	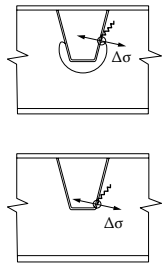
8.7 FB Cutout—base metal at edge with "smooth" flame cut finish as per AWS D1.5 Allowable design level 1 or 3	A	250×10^8	24	See figure	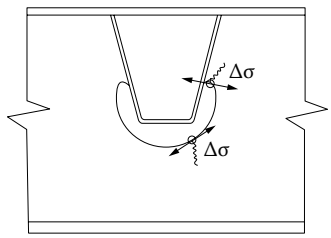
8.8 Rib wall at cutout—rib wall at rib to FB weld (fillet, PJP, or CJP) Allowable design level 1 or 3	C	44×10^8	10	See figure	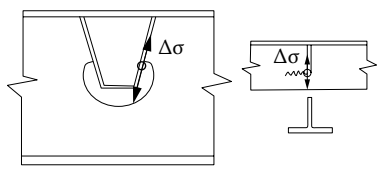
8.9 Rib to deck plate at FB Allowable design level 1 or 3	C	44×10^8	10	See figure	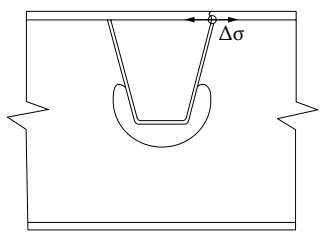

Note 1: Where stresses are dominated by in-plane component at fillet or PJP welds, Equation 6.6.1.2.5-4 shall be considered. In this case, Δf should be calculated at the mid-thickness and the extrapolation procedure as per Art. 9.8.3.4.3 need not be applied.

Section 9—Miscellaneous

9.1 Base metal at stud-type shear connectors attached by fillet or automatic stud welding		44×10^8	10	At the toe of the weld in the base metal	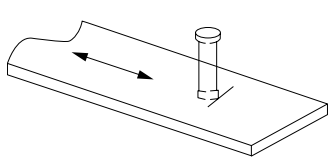

www.EngineeringEBooksPdf.com

TABLE 6.A.3-11
Detail Categories for Load-Induced Fatigue

Description	Category	Constant A (ksi^3)	Threshold $(\Delta F)_{TH}$ ksi	Potential Crack Initiation Point	Illustrative Examples
Section 9—Miscellaneous					
9.2 Nonpretensioned high-strength bolts, common bolts, threaded anchor rods, and hanger rods with cut, ground, or rolled threads. Use the stress range acting on the tensile stress area due to live load plus prying action when applicable.				At the root of the threads extending into the tensile stress area	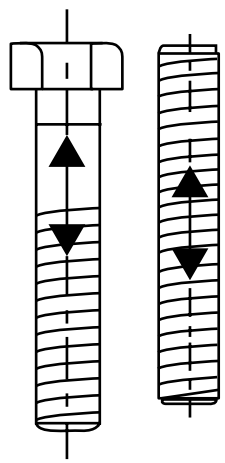
(Fatigue II) Finite Life	E′	3.9×10^8	N/A		
(Fatigue I) Infinite Life	D	N/A	7		

Source: From *AASHTO LRFD Bridge Design Specifications*, Copyright © 2012 by American Association of State Highway and Transportation Officials, Washington, DC. Used by permission.

www.EngineeringEBooksPdf.com

TABLE 6.A.4
Orthotropic Fatigue Details (LRFD Table 6.6.1.2.3-3)

Detail	Illustrative Example	Description of Condition	Fatigue Category Detail	Allowable Design Level
Rib to deck weld	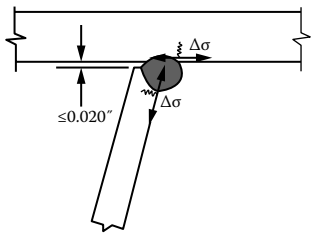	One-sided 80 percent (70 percent min) penetration weld with root gap ≤0.02 in. prior to welding.	C	1, 2, or 3
Rib splice (welded)	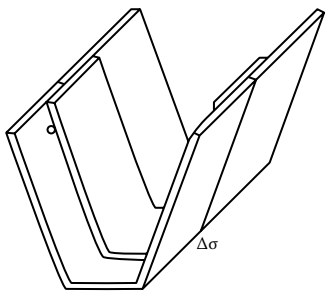	Single groove butt weld with permanent backing bar left in place. Weld gap > rib wall thickness.	D	1, 2, or 3
Rib splice (bolted)	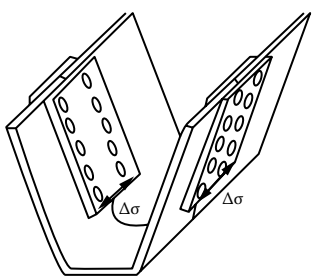	Base metal at gross section of high-strength slip-critical connection.	B	1, 2, or 3
Deck plate splice (in plane)	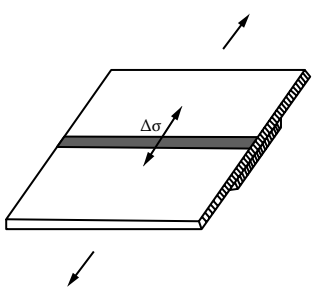	Transverse or longitudinal single groove butt splice with permanent backing bar left in place.	D	1, 2, or 3

(*Continued*)

www.EngineeringEBooksPdf.com

TABLE 6.A.4
Orthotropic Fatigue Details (LRFD Table 6.6.1.2.3-3)

Detail	Illustrative Example	Description of Condition	Fatigue Category Detail	Allowable Design Level
Rib to FB weld (rib)	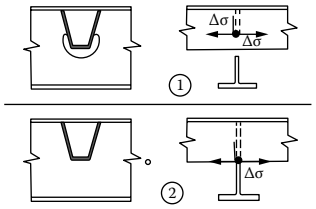	Rib wall at rib to FB weld (fillet or CJP).	C	1, 2, or 3
Rib to FB weld (FB web)	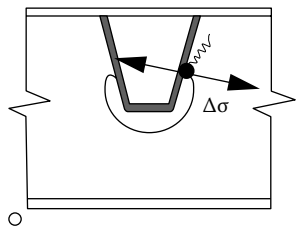	FB web at rib to FB weld (fillet, PJP, or CJP).	C (see Note 1)	1 or 3
	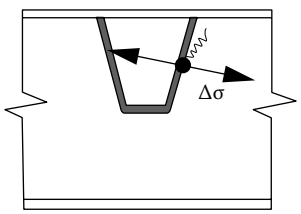			
FB cutout	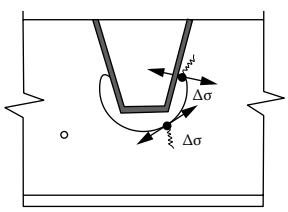	Base metal at edge with smooth flame-cut finish as per AWS D1.5.	A	1 or 3
Rib wall at cutout	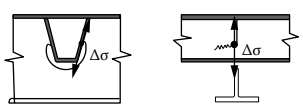	Rib wall at rib to FB weld (fillet, PJP, or CJP).	C	1 or 3
Rib to deck plate at FB	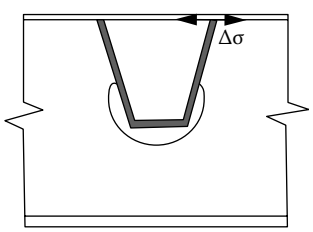		C	1 or 3

Source: From *AASHTO LRFD Bridge Design Specifications*, Copyright © 2012 by American Association of State Highway and Transportation Officials, Washington, DC. Used by permission.

Note: Where stresses are dominated by in-plane component at fillet or PJP welds, Equation 6.6.1.2.5-4 shall be considered. In this case, Δf should be calculated at the mid-thickness and the extrapolation procedure as per Art. 9.8.3.4.3 need not be applied.

www.EngineeringEBooksPdf.com

REFERENCES

AASHTO. 2012. *AASHTO LRFD Bridge Design Specifications*, American Association of State Highway and Transportation Officials, Washington, DC.

AASHTO. 2014. *Standard Specifications for Transportation Materials and Methods of Sampling and Testing*, 34th Edition, American Association of State Highway and Transportation Officials, Washington, DC.

AISC. 1963. *Design Manual for Orthotropic Steel Deck Bridges*, American Institute of Steel Construction (AISC), New York.

AISC. 2011. *Steel Construction Manual*, American Institute of Steel Construction, Chicago, IL.

ASCE-AASHTO. 1968. "Design of hybrid steel beams, Report of Subcommittee on Hybrid Beams and Girders, Joint ASCE-AASHTO Committee on Flexural Members of the Committee on Metals of Structural Division, C. G. Schilling, Chairman", *ASCE Journal of the Structural Division*, 94 (ST6), 1397–1426.

ASCE-AASHTO. 1978. "Theory and design of longitudinally stiffened plate girders, Task Committee on Longitudinally Stiffened Plate Girders of the ASCE-AASHTO Committee on Flexural Members of the Committee on Metals of Structural Division, Andrew Lilly, Chairman", *ASCE Journal of the Structural Division*, 104 (ST4), 697–716.

ASTM. 2014. *Annual Book of ASTM Standards*, ASTM International, West Conshohocken, PA.

Bleich, F. 1952. *Buckling of Metal Structures*, McGraw-Hill Book Company, New York.

Breen, F.L. 1972. Load factor design of W-beams, in *Four Design Examples, Load Factor Design of Steel Highway Bridges*, T.J. Moon, Y.I. Gonulsen, and A.P. Bezzone, ed., AISI Pub. 123(PSB010), American Iron and Steel Institute (AISI), New York.

Brown, J.D., Lubitz, D.J., Cekov, Y.C., and Frank, K.H. 2007. *Evaluation of Influence of Hole Making Upon the Performance of Structural Steel Plates and Connections*, Report No. FHWA/TX-07/0-4624-1, University of Texas at Austin, Austin, TX.

Chen, S.S., Aref, A.J., Ahn, I.-S, Chiewanichakorn, Carpenter, J.A., Nottis, A., and Kalpakidis, I. 2005. *Effective Slab Width for Composite Steel Bridge Members*, NCHRP Report 543, National transportation Research Board, National Research Council, Washington, DC.

Cooper, P.B. 1967. "Strength of longitudinally stiffened plate girders", *ASCE Journal of the Structural Division*, 93 (ST2), Proc. Paper 5211, 419–451.

Englekirk, R. 1994. *Steel Structures*, John Wile & Sons, New York.

FHWA. 1989. *Technical Advisory on Uncoated Weathering Steel in Structures*, FHWA Technical Advisory, Federal Highway Administration, Washington, DC, October 3.

Fisher, J.W. 1984. *Fatigue and Fracture in Steel Bridges*: *Case Studies*, John Wiley & Sons, New York.

Hopkins, H.J. 1970. *A Span of Bridges*, Praeger, New York.

Huhn, H. and Valtinet, G. 2004. "Bolted connections with hot dip galvanized steel members with punched holes," *Proceedings of the ECCS/AISC Workshop, Connections in Steel Structures V: Innovative Steel Connections*, June 3–5, 2004, European Convention for Constructional Steelwork/American Institute of Steel construction, Amsterdam.

Johnston, B.G., Lin, F.-J., and Galambos, T.V. 1986. *Basic Steel Design*, Prentice-Hall, Englewood Cliffs, NJ.

Kayser, J.R. 1988. The effects of corrosion on the reliability of steel girder bridges, PhD thesis, Department of Civil Engineering, University of Michigan, Ann Arbor, MI.

Kayser, J.R. and Nowak, A.S. 1987. Evaluation of corroded steel bridges, in *ASCS Bridges and Transportation Line Structures*, pp. 35–46.

Kayser, J.R. and Nowak, A.S. 1989. Capacity loss due to corrosion in steel-girder bridges, *ASCE Journal of Structural Engineering*, 115 (6), 1525–1537.

Leet, K.M. 1988. *Fundamental of Structural Analysis*, McMillan and Co., New York, 1988.

McCormac, J.C. 1992. *Structural Steel Design*, Prentice-Hall, Upper Saddle River, NJ.

McGuire, W. 1968. *Steel Structures*, Prentice-Hall, Englewood Cliffs, NJ.

Moiseiff, L.S. and Lienhard, F. 1941. "Theory of elastic stability applied to structural design", *Transactions of the American Society of Civil Engineers*, 106, 1052.

NTSB. 1968. Collapse of U.S. 35 highway bridge, Point Pleasant, West Virginia, December 15, 1967, A Report, National Transportation Safety Board (NTSB), Washington, DC, October 4, 1968.

O'Connor, C. 1971. *Design of Bridge Superstructures*, John Wiley & Sons, New York.

Ollgaard, J.G., Slutter, R.G., and Fisher, J.W. 1971. "Shear strength of shear connectors in lightweight and normal concrete", *AISC Engineering Journal*, American Institute of Steel Construction, Chicago, IL, 8 (2), 55.

Salmon, C.G., Johnson, J.E., and Malhas, F.A. 2009. *Steel Structures: Design and Behavior*, 5th ed., Prentice-Hall, Upper Saddle River, NJ.

www.EngineeringEBooksPdf.com

Segui, W.T. 2013. *Steel Design*, 5th ed., Cengage Learning, Stamford, CT.

Simpson, C.V.J. 1970. "Modern long-span bridge construction in Western Europe," *Proceedings of the Institute of Civil Engineers*, London.

Steinman, D.B. and Watson, S.R. 1957. *Bridges and Their Builders*, Dover Publications, New York.

Taly, N. 1998. *Design of Modern Highway Bridges*, McGraw Hill Co., New York.

Timoshenko, S.P. and Gere, J.M. 1961. *Theory of Elastic Stability*, 2nd ed., McGraw-Hill Book Company, New York.

Trotsky, M.S. 1967. *Orthotropic Bridges—Theory and Design*, The James F. Lincoln Arc Welding Foundation, Cleveland, OH.

Vincent, G.S. 1969. Tentative criteria for load and resistance factor design of steel bridges, AISI Bulletin No. 15, American Iron and Steel Institute, New York.

White, D.W. and Grubb, M.A. 2005. Unified resistance equations for design of curved and tangent steel bridge I-girders, *Proceedings of the 2005 TRB Bridge Engineering Conference*, Transportation Research Board, Washington, DC.

Wolchuck, R. 1990. *Design Manual for Orthotropic Steel Plate Deck Bridges*, American Institute of Steel Construction (AISC), Chicago, IL.

www.EngineeringEBooksPdf.com

Index

A

AASHO, *see* American Association of State Highway Officials (AASHO)
AASHTO LRFD Specifications
braking force, 251–255
centrifugal force, 248–251
commentary to, 67
deck superstructure types, 436–437
diaphragms and cross-frames, 93–94
DLA, 193–196
earthquake forces, 273
effective ice crushing strengths, 260
format, of load and resistance relationship, 56–63
highway bridge design, 65
highway bridges, historical review, 64–65
interims, 65–66
live load deflection, 99–100
multiple presence factors, 216–218
notional model (*see* Notional live load model)
probabilistic basis of, 18–19
safety factors, probabilistic determination of, 44–52
scope of, 66–67
seismic design (*see* Seismic design)
shear connectors, 752–754
single-span bridges, seismic analysis of, 298
thermal gradient forces, 335–336
tire contact area, 245–247
TSL consideration, 94–95
unidirectional thermal movements, 327
vehicular collision forces, 255–256
Absolute maximum bending moments, simple spans
HS20 truck
approximate method, 170–171
exact and approximate methods, 171–173
HL-93 loading, 169–170
influence line, 169–170
left to right positions, 175–176
limiting span lengths, 174–175
right to left positions, 176–178
influence lines, 161–164
permit vehicles, 178–183
ACI 318 Code, 14, 59, 461
Active lateral earth pressure
coefficient calculation, 312
definition, 309
Adjacent prestressed concrete box superstructures, 85–86
integral concrete deck/transverse posttensioning, 85–86
AISC, *see* American Institute of Steel Construction (AISC)
Allowable stress design (ASD), 1, 5
American Association of Highway and Transportation Officials (AASHTO) Standard Specifications
diaphragm
reinforced and prestressed concrete superstructures, 92
steel girder bridge superstructures, 92
live load model
lane loading, 134–135
truck loads, 131–134
American Association of State Highway Officials (AASHO), 64
American Institute of Steel Construction (AISC), 16
American Railway Engineers Association (AREA), 97, 133
American Society of Civil Engineers (ASCE), 130
Approximate strip model, slab-type bridges
cast-in-place solid slab, 430
equivalent strip width, 430–431
exterior trip/edge strip, 430–433
permanent load effects, 431
traffic barriers, 431
voided slab-type bridges, 430
ASCE, *see* American Society of Civil Engineers (ASCE)
ASD, *see* Allowable stress design (ASD)
At-rest lateral earth pressure
coefficient calculation, 312
definition, 309
Average daily traffic (ADT), 206
Average daily truck traffic (ADTT), 206, 218

B

Backfill materials, 313–316
Barrier walls, *see* Traffic railing
Bascule bridge, 80
Bay Area Rapid Transit System (BART), San Francisco, 615–616, 622
Bearing pads, 121
Bearing stiffeners, 765
axial resistance, 772–773
design requirements, 770–772
Bending moment
AASHTO Type BIII-48 precast-prestressed adjacent box beams, 383
cast-in-place multicell concrete box beam, 383
exterior girder, 375–377, 379–380
exterior longitudinal beams, 440
four-lane superstructure, 383, 392
interior beams, 438–439
with corrugated steel planks, 439
with wood decks, 437
longitudinal beams, skewed supports, 441
precast-prestressed concrete I-girders, 383
slab-beam-type superstructures
elastic neutral axis determination, 371–373
longitudinal stiffness parameter, 368–370
slab–steel beam bridge, 383
three-lane superstructure, 383
torsionally stiff superstructures
closed, thin-walled, rectangular sections, 373–375
one design lane loaded, 373
stocky open sections, 373

www.EngineeringEBooksPdf.com

thin-walled open sections, 373
two/more design lanes loaded, 373
transverse beams, 441
two-lane slab-beam bridge, 382–390
Bicycle bridges, 210–211
Braking force, 251–255
Bridge esthetics, 107
Bridge frequency–human discomfort relationship, 212
Bridge load components, parameters of, 56
Bridge type, size, and location (TSL), 94–95
Bridge width, 95
BT-72 precast prestressed concrete girder bridge, 630

C

Cable-stayed bridges, 78–79, 356
Calibration procedure, 52–55
California permit load, 157
Canadian interprovincial load vehicles, 147
Capacity design method, 5; *see also* Plastic design method
Cast-in-place concrete multicell box girder, 84–85
Cast-in-place RC T-beam bridge, 85
Central limit theorem (CLT), 37–39
Centrifugal force
AASHTO LRFD Specifications, 248–251
multiple presence factors, 217, 249
single-span curved bridge, 250–251
Channel shear connectors, 742, 744
fatigue shear strength, 745–746
nominal shear strength, 752
City and suburban bridges, 130
CLT, *see* Central limit theorem (CLT)
Collapse mechanism, 6
Columbus Drive bascule bridge, Chicago, 80
Commercial vehicular loads
exclusion vehicles, 144–146
legal loads, 140–144
permit loads, 156–158
Composite slab–steel beam superstructures, 704–705
cross section and plan, 848
deck slab design
cross section, 589–590
empirical method, 590–592
depth of the web in compression
elastic range, 844–846
plastic moment, 846–847
effective flange width, 814–815
exterior girder design
dead load camber, 899
diaphragms and cross frames, 899
factored loads, 898
live load distribution factors, 895–897
section properties, 898–899
strength limit state, 898
unfactored loads, 894–895
wind loads, 900–903
flexural strength, 810–813
interior girder design
factored loads, 855–856, 873–874
fatigue limit state, 883–892
live load distribution factors, 853–855, 868–870
plastic strength, 856–858, 874–875
section properties, 858–863, 871–872, 875–880
service limit state, 863–868, 880–882
shear connectors (*see* Shear connectors)
strength limit state, 882–883
unfactored loads, 851–853
plastic moment strength
deck slab reinforcement, 830–833
determination steps, 816–817
negative flexure, 833–835
without longitudinal slab reinforcement, 822–830
plastic neutral axis
locations, 816
negative flexure, 820–821
positive flexure, 817–819, 821
yield moment
cover plates, 843–844
negative flexure, 843
positive flexure, 837–843
Composite steel box girder bridges, 694, 696–697
Concrete bridges
AASHTO LRFD Bridge Construction Specifications, 455–456
aesthetics, 449
Alvord Lake Bridge, San Francisco, 449
barrier walls (*see* Traffic railing)
coefficient of thermal expansion, 458
compressive strength, 456–458
concrete mix characteristics, 456–457
corrosion
concrete cover, 453–455
protective requirements, 454–455
reinforcing bars, 452–454
treated reinforcing steel, 453
cracking moment, 486–488
creep, 458–459
deck (*see* Deck)
deck overhang (*see* Deck overhangs)
deck slab design table
design moments, 682
elastic coefficients, 686
prestressing tendons, stress limits, 688
reinforcing bars, cross-sectional areas, 684
spacing of bars, slab reinforcement, 685
tensile stress limits, 689
elastic modulus, 459–461
fatigue limit states (*see* Fatigue limit state)
flexure design (*see* Flexural design)
high-strength concrete and bridge span capabilities
AASHTO-PCI Type IV girder, 462, 465
cast-in-place decks, 462–463
simple-span bridge, 462, 464
simple-span prestressed concrete girder bridges, 462, 465
two-span continuous box girder bridge, 462, 464
lightweight concrete, 456
maximum reinforcement, 485
minimum reinforcement, 486–487
nonprestressed tensile reinforcement, 500–501
normal-weight concrete, 456
reinforced concrete T-beams (*see* Reinforced concrete T-beam superstructures)
reinforcing steel (*see* Reinforcing steel)
rupture modulus, 461–462
service limit state
camber, 491
cracked reinforced concrete section, 488–490

www.EngineeringEBooksPdf.com

deflection, 490–491
deformations, 490
shear strength
LRFD procedures, 495–497
near supports, 494
nominal shear resistance, 494–495
section design model, 493–494
shear stress, 499–500
strut-and-tie model, 493
tensile capacity, longitudinal reinforcement, 500
transverse reinforcement, 497–499
shrinkage, 459
slab precast, prestressed concrete bridges (*see* Slab-precast, prestressed concrete bridges)
strength limit state, 471–473
W/C ratio, 457–458
Concrete deck over steel girders, live load distribution factors
absolute maximum live load deflection, 397
applicability range, 390
cross section, 390–391
elastic section properties, 390–392
skew correction factors, 396
Concrete girder bridges with concrete decks, 328–329
Constant depth superstructures, 101
Constructibility requirements, 106
interior girder, noncomposite slab–steel beams, 792–795
I-shaped flexural members
continuously braced tension/compression flanges, 726
critical stages of construction, 726
dead load deflections, 717
discretely braced compression flanges, 723–726
discretely braced tension flanges, 726
flange lateral bending stress, 719–720
flowchart, 708
LTB (*see* Lateral-torsional-buckling (LTB))
moment gradient modifier, 720–723
Construction loads, 130
jacking forces, 121
posttensioning forces, 121
service limit state, 120–121
strength limit states, 120
Continuously braced tension/compression flanges, 726
Cooper E-72 loading, 134
County road bridges, 130
Cover plates, 776
Cracking moment, 486–488
Creep force, 338
Crevice corrosion, 700
Curved steel plate girder railroad bridge, 693
Curved steel superstructures, 102

D

Dam Point cable-stayed bridge, Jacksonville, Florida, 258
DBE, *see* Design basis earthquake (DBE)
Dead loads
deck slab, 124
deflections, 102–103
interior girder, noncomposite slab–steel beams, 805
I-shaped flexural members, 717
exterior girder, composite slab–steel beams, 899
girders, 124–125
structural analysis, 356
underestimation, 122
unit weights of materials, 122–123
Deck overhangs
live loads, 215–216
slab–steel girder superstructure
bending moment, 605, 608
cross section, 605
empirical design method, 605
factored flexural resistance, 607–608
permanent loads, 605–607
reinforcement requirements, 609–611
strength I limit state load combination, 604
Decks
cantilever slabs, 507–508
composite action, 505–507
cover requirements, 504
cross section of, 503, 505
edge support requirements, 507
empirical design method
applicability criteria, 508–509
design of overhang, 511
effective length, 509–511
force effects calculation, 512–513
internal arching action, 508
longitudinal components, 508
reinforcement requirements, 510–511
stay-in-place formwork, 512
vs. traditional design method, 513–514
skewed, 507
structural thickness, 503–504
traditional design method, 513–514
W/C ratio, 505
Deck slab design
applicability criteria, 581
dead loads, 124
elastic coefficients, 686
empirical method, 579–580, 588
fatigue and fracture limit state, 589
live load force effects, 582–584
live loads, 214–215
maximum live load moments, 547
permanent loads, 581–582
prestressing tendons, stress limits, 688
reinforcement requirements, 581
cracking moment, 585
deck top, 586–587
distribution steel, 586
factored moment, 584
shrinkage and temperature reinforcement, 585–586, 588
strength reduction factor, 587–588
traditional methods, 588–589
reinforcing bars, cross-sectional areas, 684
spacing of bars, slab reinforcement, 685
strength reduction factor, 584
tensile stress limits, 689
Deflections
AREA specifications, 97
ASCE Committee, 98–99
dead load, 102–103
deflection-to-span ratios, 97–98
depth-to-span ratios, 97–98
constant depth superstructure, 101
curved steel superstructure, 102

www.EngineeringEBooksPdf.com

highway bridges, 97–98
railroad bridges, 97–98
live load
AASHTO LRFD criteria, 99–100
HL-93 live load (*see* HL-93 live loads)
orthotropic plate decks, 101
principles, 100
steel, aluminum, and/or concrete vehicular bridges, 100–101
wood construction, 101
serviceability criteria, 97
Delta frame steel bridges, 697–698
Depth of the web in compression, composite slab–steel beams
elastic range, 844–846
plastic moment, 846–847
Design basis earthquake (DBE), 284
Design lane, 95
Design philosophies
general design concepts, 1
limit states
concepts of, 8–13
load and resistance factor design, 14
load factor design, 14
strength design, 14
strength *vs.* serviceability, 13–14
structure classification, 9
LFD, 15
LRFD (*see* Load and resistance factor design (LRFD))
strength design concept, 14–15
structural design, 1
Diaphragm action, 91
Diaphragms
AASHTO LRFD Specifications, 92–94
AASHTO Standard Specifications, 92
bridge structures, 91–92
building structures, 91
definition, 91
exterior girder, composite slab–steel beams, 899
interior girder, noncomposite slab–steel beams, 801–805
Differential shrinkage, 338
Discretely braced compression flanges, 723–726
Discretely braced tension flanges, 726
Distortion-induced fatigue, 777
Double-deck Cypress Viaduct, 274
Downdrag forces, 324
Ductility and ductile behavior, 59–62
Dynamic load allowance (DLA)
AASHTO LRFD Specifications, 193–196
application exceptions, 197
definition, 185
Hwang and Nowak study
midspan deflection *vs.* time, 189, 194
slab–girder-type bridge cross sections, 189–190
static and dynamic live load responses, 189, 191–192
truck body model, 190
truck weights *vs.* dynamic load factor, 189, 193
vehicle configurations, 187, 189
natural frequency–span relationship, 186–187
OHBDC, 187–188
simple span, live load effects, 159
worldwide research, 193, 195
Dynamic loads, 185

E

Eads Bridge, St. Louis, MO, 75
Earth pressure
active lateral earth pressure coefficient, 312
assumptions, determining methods, 310
at-rest lateral earth pressure coefficient, 312
backfill material, selection of, 313–316
basement walls, 308
bridge abutments, 308
equivalent-fluid method, 313
external and internal stability, 311
functional parameters, 308–309
log spiral method, 311
passive lateral earth pressure coefficient, 313
Rankine's and Coulomb's theory, 311
seismic events, 324
surcharge loads
downdrag, 324
line load, 318–319
live load, 319–323
point load, 317–318
strip loads, 317, 319
uniform loads, 316
Earthquake forces
AASHTO bridge design specifications, 272–273
design response spectrum, 273, 276
determination of
elastic seismic forces, 276–277
Newton's second law of motion, 275
extreme event I load combination, 298
fundamental periods of vibration
multimode spectral analysis method, 308
single-mode spectral analysis method, 305–307
load cases, longitudinal and lateral directions, 297
seismic design
acceleration coefficients, 280–283
conventional bridges, 277
DBE, 284
design response spectrum, 285–293
elastic seismic response coefficient, 278–280
nonconventional bridges, 277
operational classification, 293–294
response modifications factors, 294–296
site class characterization, 278
single-span bridges
AASHTO LRFD provisions, 298
minimum design connection force, 300
minimum seat width requirements, 299
Seismic Zone 1, 300–301
Seismic Zone 2, 303–304
Seismic Zones 3 and 4, 304–305
East Bay Bridge, San Francisco, 301–302
Effective flange width, composite slab–steel beams, 814–815
Effective ice crushing strength, 260–261
Elastic behavior
AISC specifications, 5
compressive strength, 4
and inelastic material behavior, 63–64
typical stress–strain curve, 2
yield strengths, 2, 4

www.EngineeringEBooksPdf.com

Elastic seismic response coefficient, 276, 278–280
Elastic stresses, 712
Empirical design method
  applicability criteria, 508–509
  composite slab–steel girder bridge, 590–592
  design of overhang, 511
  effective length, 509–511
  force effects calculation, 512–513
  internal arching action, 508
  longitudinal components, 508
  reinforcement requirements, 510–511
  stay-in-place formwork, 512
End diaphragms, 91
End transverse stiffeners, 765
Endurance limit, 13; *see also* Fatigue limit state
Envelopes for moments and shear
  bridge cross section and framing plan, 219
  dead load, 220
  dead load moments, 220–222
  dead load shears, 224–226
  design live load moments, 223–224
  fatigue load moments, 230–232
  fatigue load shear, 232–235
  HS20 truck shears, 226
  live load moments, 222–223
  negative lane load shear, 228
  positive lane load shear, 227
  total factored moments, 238–239
  total factored shears, 242–243
  total live load moments, 223, 236–237
  total unfactored positive and negative live load shear, 228–229
  unfactored design live load shear, 229–230, 240–241
Equivalent-fluid method, 313
Exclusion trucks
  force effects
    centerline moments, 149
    negative moments at 0.4L, 149
    negative moments at support, 150
    negative shear, 151
    positive moments at 0.4L, 150
    positive shear, 151
  schematics, 144
Exclusion vehicles
  AASHTO Standard live load model
    moment ratio, 154
    shear ratio, 155
  grandfather clauses, U.S. Congress, 146
  HL-93 live load model
    moment ratio, 153
    shear ratio, 154
  schematics, 144–145
Extended bridge formula vehicles
  force effects
    centerline moments, 149
    negative moments at 0.4L, 149
    negative moments at support, 150
    negative shear, 151
    positive moments at 0.4L, 150
    positive shear, 151
  schematics, 148
Exterior girder design
  composite slab–steel beams
    dead load camber, 899
    diaphragms and cross frames, 899
    factored loads, 898
    live load distribution factors, 895–897
    section properties, 898–899
    strength limit state, 898
    unfactored loads, 894–895
    wind loads, 900–903
  live load distribution factors
    bending moment, 375–377, 379–380
    concrete deck over steel girders, 393–396
    diaphragms, 375
    four-lane superstructure, 383
    lever rule, 361, 386
    shear, 375, 377–380, 383, 389
    three-lane steel plate girder bridge, 413–415
    two-lane precast-prestressed adjacent box beam superstructure, 404–405
  noncomposite slab–steel beams
    factored loads, 809
    live load distribution factors, 807–809
    strength limit state, 808–809
    unfactored loads, 806–807
  reinforced concrete T-beam superstructures
    bending moment, 578
    live load distribution factors, 578–579
Extreme event limit states, 111–112

F

Factored loads
  composite slab–steel beams
    exterior girder design, 898
    interior girder design, 855–856, 873–874
  noncomposite slab–steel beams
    exterior girder design, 809
    interior girder design, 790–791
Fatigue and fracture limit states, 111, 796–797
Fatigue design life, 742
Fatigue failure, 12
Fatigue limit state, 12–13
  $ADTT_{SL}$, 206–209
  bending moment, 199–202
  concrete flexural members, 491
  flexure design
    compression-controlled, 477–478
    rectangular stress distribution, 478–479
    reinforced and prestressed concrete bridge, 476–477
    reinforcing steel and surrounding concrete, 477
    tension-controlled, 477–478
  headed shear studs, 755–762
  interior girder, 641, 660–662
  interior girder, composite slab–steel beams, 883–892
  live load distribution factors, 382, 389–390
    concrete deck over steel girders, 397
    three-lane steel plate girder bridge, 416
    two-lane precast-prestressed adjacent box beam superstructure, 403–404
  magnitude and configuration, 198–199
  maximum shear, 202–206
  number of stress cycles, 209–210

www.EngineeringEBooksPdf.com

reinforced concrete T-beam superstructures, 572–576
shear connectors, 744
stress limits
live load force effect, 492
prestressing tendons, 492
reinforcing bars, 492
welded/mechanical splices, 492–493
Fatigue requirements, I-shaped beams
flowchart, 710
stiffened webs, 728–729
Fiber-reinforced polymer (FRP) superstructure systems, 89–90
Flange lateral bending stress, 719–720
Flange proportion, 715–716
Flange-strength reduction factors, 712–714
Flexural design
composite slab–steel beams, 810–813
elastic shortening, 649–650
factored flexural resistance, 657
girder end, 647–649
highway bridges, 473–476
I-shaped flexural members
compact sections in positive flexure, 730–731
discretely braced flanges, 734
ductility requirements, 732
lateral-torsional buckling resistance, 736
local buckling resistance, 734–736
noncompact sections, 731–732
at midspan, 647
nominal flexural resistance
factored flexural resistance, 484
flanged sections, 484–485
nonprestressed concrete members, 479–481
prestressed concrete members
bonded tendons, 481–483
unbonded tendons, 483–484
nominal moment capacity, 656–657
prestressing force estimation, 643–645
prestress loss and effective prestress, 651–655
prestress losses, 649
reinforcing materials, 479
service and fatigue limit states
compression-controlled, 477–478
rectangular stress distribution, 478–479
reinforced and prestressed concrete bridge, 476–477
reinforcing steel and surrounding concrete, 477
tension-controlled, 477–478
strand pattern, 645–647
time-dependent losses, 650–651
Florida Department of Transportation standard beams, 613, 615, 617
Footprint area, *see* Tire contact area
Frictional forces, 338

G

Galvanic corrosion, 699–700
Gantor Bridge, Switzerland, 451
Gaussian distribution, 26–37
General corrosion, 699
General Specifications for Railway and Highway Bridge Combined over the Wisconsin River at Kilburn City, Wisconsin, 131
General Specifications for Steel and Iron Bridges and Viaducts, 131
Gradually applied load, 185
Gravity loads, 109
dead loads, 122–123
deck slab, 124
girders, 124–125
live loads (*see* Live loads)
Grillage method, 429–430

H

Half skew, 380
Half skewed bridges, 96
Haunch, 125
Headed shear studs, 742–743
fatigue shear strength, 745
nominal shear strength, 751–752
HL-93 live loads
design truck
continuous composite girder, 105
middle 32-kip load, 103–104
noncomposite girder, 104
two-point loads, 105
lane load, 103, 106
HL-93 loading, *see* Notional live load model
Horizontal diaphragms, 91
Horizontal framing, 121
Horizontal ice forces, 261–262
Horizontally curved bridges, 94
Horizontal wind pressure, 265–266
HS20 truck load
absolute maximum bending moment, simple spans
approximate method, 170–171
exact and approximate methods, 171–173
HL-93 loading, 169–170
influence line, 169–170
left to right positions, 175–176
limiting span lengths, 174–175
right to left positions, 176–178
schematics, 148
H15 truck load, 132
H20 truck load, 132
Hwang and Nowak DLA study
midspan deflection *vs.* time, 189, 194
slab–girder-type bridge cross sections, 189–190
static and dynamic live load responses, 189, 191–192
truck body model, 190
truck weights *vs.* dynamic load factor, 189, 193
vehicle configurations, 187, 189
Hybrid factor, 713
Hybrid steel girders, 702–703

I

Ice loads
effective ice crushing strength, 260–261
failure modes, 260
floes, 260
horizontal force, 261–262
piers, 259–260
transverse force, 262–263

www.EngineeringEBooksPdf.com

Impact loads, 185
Influence line diagrams, 159
  longitudinal beams, 184–185
  simple and cantilevered spans
    bending moment, 162
    HL-93 loading, 169–170
    reactions, 161–162
    shear, 163–164
Interior girder design
  composite slab–steel beams
    factored loads, 855–856, 873–874
    fatigue limit state, 883–892
    live load distribution factors, 853–855, 868–870
    plastic strength, 856–858, 874–875
    section properties, 858–863, 871–872, 875–880
    service limit state, 863–868, 880–882
    shear connectors (*see* Shear connectors)
    strength limit state, 882–883
    unfactored loads, 851–853
  live load distribution factors
    concrete deck over steel girders, 392–393
    multicell, cast-in-place, concrete box girder superstructure, 406–409
    three-lane steel plate girder bridge, 412, 416
    two-lane precast-prestressed adjacent box beam superstructure, 402–403
    wide flange (W-Shape) steel girders, 384–390
  noncomposite slab–steel beams
    constructibility, 792–795
    dead load deflection, 805
    diaphragms, 801–805
    factored loads, 790–791
    fatigue and fracture limit state, 796–797
    flange stresses, 792
    lateral-torsional buckling resistance, 793–795
    live load distribution factor, 788–790
    section properties, 791
    service limit state, 797–801
    shear, 795–796
    strength limit state, 801
    unfactored loads, 786–788
  slab-precast, prestressed concrete bridges
    camber, 676–677
    dead loads, 642
    deflection, 677–681
    design loads/factored loads, 640
    end and transfer point at release, 658–660
    fatigue limit states, 641, 660–662
    flexural design, 644–655
    live load, 637–638
    live load distribution factors, 638–640
    noncomposite girder, 643
    reinforcement limits, 657–658
    service limit state, 641
    shear (*see* Shear strength)
    span-to-depth ratio, 681
    strength limit state, 641
    unfactored loads, 635–637
Intermediate diaphragms, 91–92
Intermediate transverse stiffeners, 764
Internal stiffeners, 766
Iron bridge, Coalbrookdale, England, 692
I-shaped flexural members
  constructibility requirements
    continuously braced tension/compression flanges, 726
    critical stages of construction, 726
    dead load deflections, 717
    discretely braced compression flanges, 723–726
    discretely braced tension flanges, 726
    flange lateral bending stress, 719–720
    flowchart, 708
    LTB (*see* Lateral-torsional-buckling (LTB))
    moment gradient modifier, 720–723
  cover plates, 776
  elastic stresses, 712
  fatigue requirements
    flowchart, 710
    stiffened webs, 728–729
  flange proportion, 715–716
  flange-strength reduction factors
    hybrid factor, 713
    unbraced length, 712
    web load-shedding factor, 713–714
  flexural resistance
    compact sections in positive flexure, 730–731
    discretely braced flanges, 734
    ductility requirements, 732
    lateral-torsional buckling resistance, 736
    local buckling resistance, 734–736
    noncompact sections, 731–732
  minimum metal thickness, 714–715
  service limit state
    elastic deformations, 727 (*see also* Deflections)
    flange stresses, 727–728
    flexural stresses, 727
    flowchart, 709
  shear connectors
    channel shear connectors (*see* Channel shear connectors)
    fatigue loading, 744–746
    fatigue shear strength, 748–751
    headed shear connectors (*see* Headed shear studs)
    LRFD provisions, 752–754
    nominal shear strength, 751–752
    permanent load contraflexure, 752
    pitch, 746–748
    role of, 741–742
    size and number, 743
    types, 742–743
  shear resistance
    steel girders, 737–738
    stiffened web, 741
    unstiffened web, 739–740
  stiffeners (*see* Stiffeners)
  strength limit state
    design requirements, 729–730
    flowchart, 711
  unbraced length, 712
  web proportion limits, 715
I-35W Mississippi River Bridge, Minneapolis, 122

www.EngineeringEBooksPdf.com

L

Lake Alvord Bridge, San Francisco Park, California, 450
Lateral force resisting systems (LFRS), 91
Lateral loads, 109
braking force, 251–255
creep forces, 338
earth pressure (*see* Earth pressure)
ice loads
effective ice crushing strength, 260–261
failure modes, 260
floes, 260
horizontal force, 261–262
piers, 259–260
transverse force, 262–263
posttensioning forces, 338
seismic forces (*see* Earthquake forces)
settlement forces, 338
shrinkage forces, 338
temperature-induced forces, 325
thermal gradient forces, 327, 332–334
AASHTO LRFD provisions, 335–336
axial extension, 337
flexural deformation, 338
internal stresses, 338
nonlinear temperature variation, 334–335
vehicular collision forces, 255–256
vessel collision forces, 256–259
wind loads
aerodynamic vibrations, 264–265
components, 265
estimation, 268–270
horizontal wind pressure, 265–266
velocity *vs.* height, 266–268
wind pressure on live load, 271–272
wind pressure on structure, 270–271
Lateral-torsional-buckling (LTB)
braced lengths, 719
compression flanges, 717–719, 736
interior girder, noncomposite slab–steel beams, 793–795
Legal loads, 140–144
LFD, *see* Load factor design (LFD)
Lift bridge, 81
Limit state function, 39–40
Line load, 318–319
Live load distribution factors, 357–358
AASHTO Type BIII-48 precast-restressed adjacent box beams, 383
approximate methods
distribution factor concept, 358–360
short- and medium-span bridge, 358
bending moment (*see* Bending moment)
cast-in-place multicell concrete box beam superstructure, 383
composite slab–steel beams
exterior girder design, 895–897
interior girder design, 853–855, 868–870
concrete deck over steel girders
absolute maximum live load deflection, 397
applicability range, 390
cross section, 390–391
elastic section properties, 390–392
exterior girder, 393–396
fatigue limit state, 397
interior girder, 392–393
skew correction factors, 396
constant deck width and parallel girders, 363–364
correction factors, 444
deflection limit state, 382
exterior girders
bending moment, 375–377, 379–380
diaphragms, 375
four-lane superstructure, 383
girder cross section, 383–384
heavy loads combined with traffic loads, 421
interior beams with wood decks, 437
lever rule
curved I-girder bridges, 362
definition, 360
notional model, 362
precast units, 362
slab-beam type superstructure, 361–362
moving load, 353
multicell, cast-in-place, concrete box girder superstructure, 406–409
multiple loaded lanes
design/traffic lane, 365
wheel loads, 366
noncomposite slab–steel beams
exterior girder design, 807–809
interior girder design, 788–790
refined methods, 357–358
reinforced concrete T-beams, 579
single-span concrete deck steel girder bridge, 417–420
slab over precast-prestressed concrete girders, 397–400
slab-precast, prestressed concrete bridges
applicability criteria, 638–639
bending moment, 639
deflection, 640
fatigue, 640
shear, 639
slab-WF steel beam bridge, 383–384
stiffened plate, 357
supporting girders, 357
three-lane steel plate girder bridge
absolute maximum live load deflection, 416
applicability range, 409
centroid of steel, 411–412
exterior girder, 413–415
interior girder, 412
properties, 411
skew correction factors, 415–416
typical cross section, 409–410
three-lane superstructure, 383
transverse floor beams, 421
two-lane precast-prestressed adjacent box beam superstructure, 401–103
uniform load, 353
varying deck width and splayed girders, 364
Live loads
AASHO Standard Specifications, 133
absolute maximum bending moment, simple spans
HS20 truck, 167–178
influence lines, 160–164, 169–170
moving concentrated loads, 164–167
permit vehicles, 178–183

www.EngineeringEBooksPdf.com

ASCE categories, 130
box culverts, top slabs of, 214–215
Cooper E-72 loading, 133–134
deck overhangs, 215–216
decks, 214–215
deflection
AASHTO LRFD criteria, 99–100
HL-93 live load (*see* HL-93 live loads)
orthotropic plate decks, 101
principles, 100
steel, aluminum, and/or concrete vehicular bridges, 100–101
wood construction, 101
deflection considerations, 214
HS20 truck, 175–178
influence lines, longitudinal beams, 184–185
lane load model, 134–135
longitudinal beams
design, 212–214
influence lines, 184–185
longitudinal girders supporting bridge deck, 218
maximum shear, 183–184
moments and shear, envelopes for
bridge cross section and framing plan, 219
dead load, 220
dead load moments, 220–222
dead load shears, 224–226
design live load moments, 223–224
fatigue load moments, 230–232
fatigue load shear, 232–235
HS20 truck shears, 226
live load moments, 222–223
negative lane load shear, 228
positive lane load shear, 227
total factored moments, 238–239
total factored shears, 242–243
total live load moments, 223, 236–237
total unfactored positive and negative live load shear, 228–229
unfactored design live load shear, 229–230, 240–241
multiple presence factors, 216–218
notional model
exclusion vehicles, 144–148
lane load configuration, 136, 138
legal loads, 140–144
permit loads, 156–158
tandem load configuration, 138
truck load configuration, 136–137
permit trucks, 178–183
reinforced concrete T-beam superstructures
bending moment, 542
distribution factors, 544–546
shear, 542–544
road rollers, 131
slab-precast, prestressed concrete bridges
maximum shear, 637–638
minimum moment, 637
surcharge loads, 319–323
truck load model, 134
vehicular loads
continuous spans, 160
dynamic effects (*see* Dynamic load allowance (DLA))
simple spans, 158–159
Load and resistance factor design (LRFD)
AASHTO LRFD Specifications
bridge design, 18–19
format, of load and resistance relationship, 56–63
probabilistic basis of, 18
calibration of, 55–56
design philosophies, 1
equation of sufficiency, 56
highway bridges, in United States, 16–18
limit states design philosophy, 14
vs. plastic design method, 64
safe and unsafe combinations of, 39
safety factors, probabilistic determination of
AASHTO LRFD criteria, 44–52
AISC LRFD criteria, 40–44
calibration, of load and resistance factors, 55–56
calibration procedure, 52–55
limit state function, 39–40
statistical nature of
CLT, 37–39
Gaussian distribution, 26–37
normal and lognormal distributions, 19–26
normal convergence theorem, 37–39
normal curve of errors, 21
normal/Gaussian distribution, 26–37
probability, 19–26
random variables, 19–26
steel buildings, in United States, 16
strength design, 14–16, 64
structural design philosophies, 1, 15–16
Load combinations, 115–116
Load factor design (LFD), 1, 14–15, 64
Load factors
construction loads
jacking forces, 121
posttensioning forces, 121
service limit state, 120–121
strength limit states, 120
load combinations, 115–116
Load-induced fatigue, slab–steel beam bridges
$ADTT_{SL}$, 779–780
constraint-induced fracture, 781
cross frames and diaphragms, 778
design criteria, 778
detail categories
connected material in mechanically fastened joints, 906–907
longitudinally loaded welded attachments, 914
miscellaneous attachments, 914–917
orthotropic fatigue details, 918–919
plain material away from any welding, 906
transversely loaded welded attachments, 911–914
welded joints joining components of built-up members, 908
welded joints transverse to the direction of primary stress, 910–911
welded stiffener connections, 909
nominal fatigue resistance, 781–782
stress range cycle, 778, 782
Lognormal distribution, 38–39
Long combination vehicles (LCVs), 140

www.EngineeringEBooksPdf.com

Longitudinal girders supporting bridge deck, 218
Longitudinal stiffeners
arrangement schemes, 765–766
schematics, 765
section properties, 774–776
web bend-buckling resistance, 767
Long-span bridges, 73
LRFD, *see* Load and resistance factor design (LRFD)
LTB, *see* Lateral-torsional-buckling (LTB)

M

Maillart's Salginatobel Bridge, Switzerland, 450
Maximum considered earthquakes (MCEs), 284
Medium-span bridges, 73
Minimum metal thickness, 714–715
Modified Texas Transportation Institute (TTI) formula vehicles
force effects
centerline moments, 149
negative moments at 0.4L, 149
negative moments at support, 150
negative shear, 151
positive moments at 0.4L, 150
positive shear, 151
schematics, 147
Moment gradient modifier, 720–723
Mononabe–Okabe (M-O) analysis, 324
Movable bridges, 73
Muller-Breslau principle, 161
Multibeam superstructures
future widening, 106
lateral wind load distribution
forces and bending moments, 423–424
load path, 422–423
seismic load distribution
design criteria, 425
earthquake load distribution, 425
load path, 424–425
Multimode spectral analysis method, 308
Multiple presence factors, 216–218, 249
Multispan bridge, 73–74
Multi-span welded delta-frame bridge, 698

N

National Cooperative Highway Research Program (NCHRP), 65
National Transportation Safety Board (NTSB), 122
National Truck Weight Advisory Committee (NTWAC) special hauling vehicles
force effects
centerline moments, 149
negative moments at 0.4L, 149
negative moments at support, 150
negative shear, 151
positive moments at 0.4L, 150
positive shear, 151
schematics, 146
NCHRP, *see* National Cooperative Highway Research Program (NCHRP)
Nebraska Department of Transportation I-shaped girders, 613, 615, 618
New River Gorge Arch Bridge, WVA, 76–77
Noncomposite slab–steel beam superstructures, 704
conditions, load calculations, 783
exterior girder design
factored loads, 809
live load distribution factors, 807–809
strength limit state, 808–809
unfactored loads, 806–807
girder spacing, 783
interior girder design
constructibility, 792–795
dead load deflection, 805
diaphragms, 801–805
factored loads, 790–791
fatigue and fracture limit state, 796–797
flange stresses, 792
lateral-torsional buckling resistance, 793–795
live load distribution factor, 788–790
section properties, 791
service limit state, 797–801
shear, 795–796
strength limit state, 801
unfactored loads, 786–788
limit states, 785–786
load combinations, 785–786
load modifiers, 785
preliminary bridge cross section, 784
strength reduction factors, 785
yield moment, 837
Normal bridges, 95–96
Notional live load model
vs. AASHTO Standard live load model
moment ratio, 155
shear ratio, 156
equivalent uniform load, 153–154
exclusion vehicles, 144–148
family of three loads, 152–153
HL-93 design live load, 152–153
HTL57, 152–153
lane load configuration, 136, 138
legal loads, 140–144
permit loads, 156–158
tandem load configuration, 138
truck load configuration, 136–137
weigh-in-motion (WIM) data, 140
Number of stress cycles, 209–210

O

Ontario Highway Bridge Design Code (OHBDC), 54, 187–188
Open steel/precast concrete box superstructures, 83–84
Operational classification, 293–294
Orthotropic steel bridges, 691–694

P

Passive lateral earth pressure
coefficient calculation, 313
definition, 310
Pedestrian loads
bicycle bridges, 210–211
bridge frequency–human discomfort relationship, 212

www.EngineeringEBooksPdf.com

sidewalks, 210
significance, 210
Pennsylvania Department of Transportation I-shaped girders, 613, 615
Pennsylvania permit load, 157
Perception of failure, 10
Performance function, 39–40
Permanent loads, 109, 114, 117
Permit loads, 156–158, 178–183
Pitting corrosion, 699
Plastic design method
collapse mechanism, 6
ductility, 5
inelastic design method, 5
vs. LFD, 64
vs. LRFD, 64
plastic analysis, 5
plastic hinge, 6
plastic moment, 7–8
vs. strength design, 64
stress–strain curve, 3, 6
Plastic hinge, 6
Plastic moment strength, composite slab–steel beams
deck slab reinforcement, 830–833
determination steps, 816–817
interior girder design, 856–858, 874–875
negative flexure, 833–835
without longitudinal slab reinforcement, 822–830
Plate girder bridge, 691, 693
Point load, 317–318
Posttensioning forces, 338
Precast concrete superstructures with shear keys
channel sections, 86–87
double-T girders, 87–88
single-T girders, 87–88
Prestressed concrete girder bridge
cross section, 128
dead loads, 129
Prestressed I-beams/bulb-T girders, 87, 89
Prestressed steel
alloy steel bars, 467–468
elastic modulus, 469
properties, 468
relaxation, 470–471
stress-relieved seven-wire compacted strands, 468–469
stress-relieved seven-wire standard strands, 468–469
stress–strain curves, 469–470
wires, 467–468
Probability of failure, 42, 46–51

Q

Quebec Bridge, Canada, 122

R

Rail transit loads, 247
Random variables, linear functions of
product of, 38–39
sum of, 37–38
Rankine's lateral earth pressures, 313
Redundancy, 62–63
The Reichenau Bridge, 451
Reinforced concrete T-beam superstructures
beams/girders design, 539
decks design, 539
deck slab design (*see* Deck slab design)
deformations
and camber, 553–555
design lane, 559
design truck, 556–559
lane load, 559
live load deflection, 556
vehicular live load, 556
exterior girder design
bending moment, 578
live load distribution factors, 578–579
shear, 579
factored loads, 547
fatigue limit state, 572–576
interior T-beam, 541
live load
bending moment, 542
distribution factors, 544–546
shear, 542–544
load modifier selection, 547
monolithic cast feature, 539
permanent loads, 541–542
vs. prestressed concrete superstructures, 539
reinforcement requirement
centroid distance, 548
minimum reinforcement, 551–553
minimum web width, 548
rectangular section analysis, 547
service limit state, 576–577
shear
critical section, location of, 559–560
design truck, 566
factored loads, 563
influence line, 560
live load, 561–563, 566
midspan, 566
nominal shear resistance, 563–564
permanent loads, 561
transverse reinforcement, 564–566
stirrups spacing
critical section, 566–567
design truck, 568–569
dynamic load allowance and live load distribution factor, 569–570
influence lines, 567–568
layout of, 570
shear demand, 568–569
tensile capacity, longitudinal reinforcement, 570–573
trial cross section of, 539–541
Reinforcing steel
reinforcing bars
identification marks, 465, 467
protrusion profiles, 465–466
yield strengths, 462
Reliability index concept
AASHTO LRFD criteria
development of, 44–46
specifications of, 51–52

www.EngineeringEBooksPdf.com

AISC LRFD criteria, development of, 40–43
and probability of failure, 46–51
Resistance factors
concrete bridges, 471–473
slab–steel beam bridges, 706–707
Resonant loads, 185
Response modifications factors, 294–296
Right bridge, 96

S

Safety index, 42; *see also* Reliability index concept
Save (Sava) I Bridge, Belgrade, Yugoslavia, 693, 695
SD, *see* Strength design (SD)
Section design model, 493–494
Section properties
composite slab–steel beams
exterior girder design, 898–899
interior girder design, 858–863, 871–872, 875–880
longitudinal stiffeners, 774–776
noncomposite slab–steel beams, 791
transverse stiffeners, 768–770
Seismic design
acceleration coefficients, 280–283
conventional bridges, 277
DBE, 284
design response spectrum, 285–293
elastic seismic response coefficient, 278–280
nonconventional bridges, 277
operational classification, 293–294
response modifications factors, 294–296
site class characterization, 278
Seismic earth pressure, 310, 324
Seismic force resisting system (SFRS), 425
Serviceability criteria, 97
Serviceability limit state
cracking, phenomenon of, 10–12
deflection limits, 10
excess vibration, 10
permanent deformations, 10–11
vs. strength limit states, 13–14
Service limit state
concrete bridges
camber, 491
cracked reinforced concrete section, 488–490
deflection, 490–491
deformations, 490
construction loads, load factors for, 120
interior girder design
composite slab–steel beams, 863–868, 880–882
noncomposite slab–steel beams, 797–801
I-shaped flexural members
elastic deformations, 727 (*see also* Deflections)
flange stresses, 727–728
flexural stresses, 727
flowchart, 709
load combination, 110–111
Settlement force, 338
Shear connectors
channel shear connectors, 742, 744
fatigue shear strength, 745–746
nominal shear strength, 752
fatigue loading, 744–746
fatigue shear resistance, 744–746
headed shear studs, 742–743
fatigue shear strength, 745
nominal shear strength, 751–752
interior girder, composite slab–steel beams
fatigue limit state, 883–892
strength limit state, 892–893
LRFD provisions, 752–754
nominal shear strength, 748–751
permanent load contraflexure, 752
pitch, 746–748
role of, 741–742
size and number, 743
strength, 751–752
types, 742–743
Shear strength
anchorage zone requirement, 673–674
available longitudinal force, 672–673
component calculation, 666
concrete bridges
LRFD procedures, 495–497
near supports, 494
nominal shear resistance, 494–495
section design model, 493–494
shear stress, 499–500
strut-and-tie model, 493
tensile capacity, longitudinal reinforcement, 500
transverse reinforcement, 497–499
concrete calculation, 666–667
confinement reinforcement, 674
critical section, 662–663
dead load, 663–664
factored interface shear force, 669–670
hold-down forces, 674–676
interior girder, noncomposite slab–steel beams, 795–796
live load, 664–666
longitudinal reinforcement requirement, 671
minimum area of interface shear reinforcement, 670–671
nominal interface shear resistance, 670
reinforcement, 666–669
Shear stress range, 742
Shored construction, 705
Short-span bridges, 73
Showa Bridge, Niigata, Japan, 300
Simple-span concrete deck–steel girder bridge
cross section, 126
dead loads
deck slab, 126, 129
girders, 127
traffic barriers, 127
Single-lane average daily truck traffic ($ADTT_{SL}$), 206–209, 218, 777
Single-mode spectral analysis method, 305–307
Single-span bridges
longitudinal stiffness parameter, 369–370
seismic analysis
AASHTO LRFD provisions, 298
minimum design connection force, 300
minimum seat width requirements, 299
Seismic Zone 1, 300–301
Seismic Zone 2, 303–304
Seismic Zones 3 and 4, 304–305

www.EngineeringEBooksPdf.com

Single-span concrete deck steel girder bridge, 417
Single-span highway bridge, 74
Single-span, two-lane curved, slab–girder bridge, 250–251
Skewed bridges, 95–97
Skewed decks, 507
Slab-beam bridge
  bending moment
    elastic neutral axis determination, 371–373
    longitudinal stiffness parameter, 368–370
    modular ratio, 370–371
    noncomposite construction, 368–369
    one design lane loaded, 367–368
    span length, 367
    St. Venant torsion constant, 371–372
    two/more design lanes loaded, 367–368
  lever rule, 361–362
  load path, 355–356, 422
Slab-girder type superstructures, modular ratio, 370
Slab over precast-prestressed concrete girders, 397–400
Slab-precast, prestressed concrete bridges
  AASHTO-PCI solid and voided slabs, 612–613, 615
  AASHTO-PCI standard precast sections, 612, 614–615
  BT-72 girder, 630
  compressive stresses, 618
  concentric prestressing, 618–620, 623, 626
  constant eccentricity, 623–626
  cross section, 614, 618
  curvilinear tendon profile, 627–628
  draped tendon, 626–627
  flexural strength, 618
  high-strength concrete, 612
  interior girder design (*see* Interior girder design)
  live load
    maximum shear, 637–638
    minimum moment, 637
  multicell box girders, 615, 617, 623
  nonprestressed steel, 617
  pretensioned and posttensioned girders, 628
  segmental box beams, 615, 617, 624–625
  segmental construction methods, 611
  singlepoint harped tendon, 626–627
  strand patterns, 627, 629, 631
  stress limits, 630
  tensile stress limits, 630
  T-shapes, 614–615, 619
  two-point harped tendon, 626–627
Slab–steel beam bridges, 81, 83, 121
  AASHTO LRFD Specification, 73, 78
  composite sections (*see* Composite slab–steel beam superstructures)
  composite steel box girder bridges, 694, 697
  construction considerations, 700–701
  corrosion
    cause of, 697
    forms of, 699–700
  crevice corrosion, 700
  deck overhang
    bending moment, 605, 608
    cross section, 605
    empirical design method, 605
    factored flexural resistance, 607–608
    live load, 607
    permanent loads, 605–607
  delta frame steel bridges, 697–698
  diaphragm, 93–94
  distortion-induced fatigue, 777
  galvanic corrosion, 699–700
  general corrosion, 699
  hybrid girders, 702–703
  I-section flexural members
    constructibility requirements, 708, 716–726
    cover plates, 776
    elastic stresses, 712
    fatigue requirements, 710, 728–729
    flange proportion, 715–716
    flange-strength reduction factors, 712–714
    flexural resistance, 730–736
    minimum metal thickness, 714–715
    service limit state, 709, 727–728
    shear connectors (*see* Shear connectors)
    shear resistance, 737–741
    stiffeners (*see* Stiffeners)
    strength limit state, 711, 729–730
    web proportion limits, 715
  load-induced fatigue
    $ADTT_{SL}$, 779–780
    constraint-induced fracture, 781
    cross frames and diaphragms, 778
    design criteria, 778
    detail categories, 778–780
    nominal fatigue resistance, 781–782
    stress range cycle, 778, 782
  mechanical properties, 701–702
  modular ratio, 370
  noncomposite sections (*see* Noncomposite slab–steel beam superstructures)
  orthotropic steel bridges, 691–694
  pitting corrosion, 699
  plate girder bridge, 691, 693
  resistance factors, 706–707
  with sidewalk, 692
  stress corrosion, 700
  unshored construction, 706
  without sidewalk, 692
Slab-type bridges
  approximate strip model
    cast-in-place solid slab, 430
    equivalent strip width, 430–431
    exterior trip/edge strip, 430–433
    interior strip, 430
    permanent load effects, 431
    traffic barriers, 431
    voided slab-type bridges, 430
  contiguous prestressed box beam and slab deck, 427, 430
  deflection
    crack under service loads, 435
    live load deflections, 434
    long-term, 435
  grillage method, 429–430
  hollow slab bridge, 426
  influence surfaces, 429
  lateral deflection, 427–429
  load-carrying mechanism, 427
  plate action, 427, 429
Snow loads, 263
Specialized hauling vehicle (SHV), 143–144

www.EngineeringEBooksPdf.com

Specifications for Design of Highway Bridges, 133
Spread box beam superstructures, 83–84
Standard normal distribution function, 68–69
Standard skewed bridges, 96
Standard Specifications of the Phoenix Bridge Company for Steel and Iron Railway and Highway Structures, 131
State of Alaska permit loads, 158
Static load, 185
Steel girder bridge superstructures, 92–94
Steel girder bridges with concrete decks
  thermal movements, contour maps of, 330–331
Steel through truss bridge, 699
Steel truss bridge, 75
Stiffeners
  bearing stiffeners, 765
    axial resistance, 772–773
    design requirements, 770–772
  longitudinal stiffeners
    arrangement schemes, 765–766
    schematics, 765
    section properties, 774–776
    web bend-buckling resistance, 767
  transverse stiffeners
    arrangement schemes, 766
    design requirements, 767
    end stiffeners, 765
    intermediate stiffeners, 764
    section properties, 768–770
Straight line design, 1
Strength design (SD)
  limit states design philosophies, 8
  LFD, 14–15, 64
  LRFD, 14–16, 64
  vs. plastic design method, 64
  strength design concept, 14–15
  structural design philosophies, 1
Strength limit state
  composite slab–steel beams
    exterior girder design, 898
    interior girder design, 882–883
  concepts of, 9
  concrete bridges, 471–473
  construction loads, load factors for, 120
  headed shear studs, 762–763
  HS20 truck loading, 178
  I-shaped flexural members
    design requirements, 729–730
    flowchart, 711
  load combination, 110–112
  noncomposite slab–steel beams
    exterior girder design, 808–809
    interior girder design, 801
  vs. serviceability limit states, 13–14
  shear connectors, 748–751
Stress corrosion, 700
Stringers, 73
Strip loads, 317, 319
Structural analysis
  concrete decks, 426–427
    slab–steel beam bridge, 426, 428
    T-beam bridge, 426, 428
  dead load, 356
  deck systems analysis
    equivalent strips, 433, 445
    force effects calculation, 433–434
  designer needs, 353
  factored loads, 354
  interior girder, 402
  live loads (*see* Live loads)
  load path, 354–356, 422
  multibeam bridges
    lateral wind load distribution, 422–424
    seismic load distribution, 424–426
  refined analysis, 421–422
  skew angle, correction factors, 380–382
  slab-girder bridge, 354
  slab-type bridges (*see* Slab-type bridges)
  unfactored live loads, 354
Structural design philosophies, 1; *see also* Design philosophies
  concept, 14–15
  on elastic behavior, 2–5
  fundamentals of, 2–8
  on inelastic behavior, 5–8
  LFD, 15
  LRFD, 15–16
Strut-and-tie model, 493
Struve Slough Bridge, Watsonville, 274
Substructure, 73
Sunshine Skyway Bridge, Florida
  protective islands and dolphins, 258
Superimposed deformations, 325–338
Surcharge loads
  downdrag, 324
  line load, 318–319
  live load, 319–323
  point load, 317–318
  strip loads, 317, 319
  uniform loads, 316
Suspension bridge, 79

T

Tacoma Narrows Bridge, 78–79
Tacoma Narrows suspension bridge, 264–265
Target reliability index, 43–44
Temperature-induced forces, 325
Thermal gradient forces, 327, 332–334
  AASHTO LRFD provisions, 335–336
  axial extension, 337
  flexural deformation, 338
  internal stresses, 338
  nonlinear temperature variation, 334–335
Thermally induced stress, 326
Three-lane steel plate girder bridge
  absolute maximum live load deflection, 416
  applicability range, 409
  centroid of steel, 411–412
  fatigue limit state, 416
  properties, 411
  skew correction factors, 415–416
  typical cross section, 409–410
Three-span, cantilevered Whisky Creek Bridge, California, 703
Three-span, slant-leg Whitebird Canyon Bridge, 694, 697

www.EngineeringEBooksPdf.com

Tire contact area
AASHTO LRFD Specifications, 245–247
point load *vs.* distributed load, 235, 244
Torsionally stiff superstructures
closed, thin-walled, rectangular sections, 373–375
closed thin-walled sections, 374
one design lane loaded, 373
stocky open sections, 373
thin-walled open sections, 373
two/more design lanes loaded, 373
Total live load, 159
Traditional design method, 513–514
Traffic lane, 95
Traffic railing
design forces
extreme-event limit state, 592
nomenclature, 594–595
test levels, 593
vehicle rollover force, effective height of, 593–594
flexural resistance, 598–603
yield line analysis, 595–597, 603–604
Transformed effective width of flange, 705
Transient loads, 109, 114–115; *see also* Pedestrian loads; Vehicular live loads
Transportation Research Board (TRB), 65
Transverse ice force, 262–263
Transverse stiffeners
arrangement schemes, 766
design requirements, 767
end stiffeners, 765
intermediate stiffeners, 764
section properties, 768–770
Trapezoid skewed bridges, 96, 380
TRB, *see* Transportation Research Board (TRB)
Turkstra's rule, 114
Turner trucks
force effects
centerline moments, 149
negative moments at 0.4L, 149
negative moments at support, 150
negative shear, 151
positive moments at 0.4L, 150
positive shear, 151
schematics, 148
Two-lane precast-prestressed adjacent box beam superstructure
live load distribution factors, 401
exterior girder, 404–405
fatigue limit state, 403–404
Two-lane reinforced concrete slab bridge
cross section, 514–515
dead load, 515–516
edge beam design
bending moment, 536
cracking, 537–538
dead load, 535–536
reinforcement, 537–538
shear, 536–537
elevation, 514–515
interior strip design
cracking, 523–525
deformation, 528–534
design lanes, 517–519
distribution reinforcement, 525
fatigue moment, 526–527
minimum reinforcement, 522–523
shear strength, 534
shrinkage and temperature reinforcement, 526
strength limit state, 519–522
stresses, 528
live load, 516–517
minimum thickness, 515
Typical Specifications for the Fabrication and Erection of Steel Highway Bridges, 131

U

Ultimate strength design method, 14
Unbraced length, 712
Unfactored loads
composite slab–steel beams
exterior girder design, 894–895
interior girder design, 851–853
noncomposite slab–steel beams
exterior girder design, 806–807
interior girder design, 786–788
Unidirectional thermal movements, 327–331
Uniform surcharge loads, 316
Union Pacific Railroad Overpass, Cheyenne, Wyoming, 765
Unshored construction, 130, 706
U.S. Department of Transportation (USDOT), 66
Utility-cum-pedestrian bridge, 80

V

Vehicular collision forces, 255–256
Vehicular live loads
commercial loads (*see* Commercial vehicular loads)
continuous spans, 160
dynamic effects (*see* Dynamic load allowance (DLA))
pedestrian loads, 210–212
simple spans, 158–159
Vertical diaphragms, 91
Vessel collision forces, 256–259

W

Washington state standard I-shaped girders, 616
Web load-shedding factor, 713–714
Web proportion limits, 715
Wind loads
aerodynamic vibrations, 264–265
components, 265
estimation, 268–270
exterior girder, composite slab–steel beams, 900–903
horizontal wind pressure, 265–266
velocity *vs.* height, 266–268
wind pressure on live load, 271–272
wind pressure on structure, 270–271
Wind pressure on live load, 271–272
Wind pressure on structure, 270–271
Working stress design (WSD), 1, 5

Y

Yield moment, 7
composite slab–steel beams, 837–844
noncomposite slab–steel beams, 837
reinforcing steel, 462

www.EngineeringEBooksPdf.com